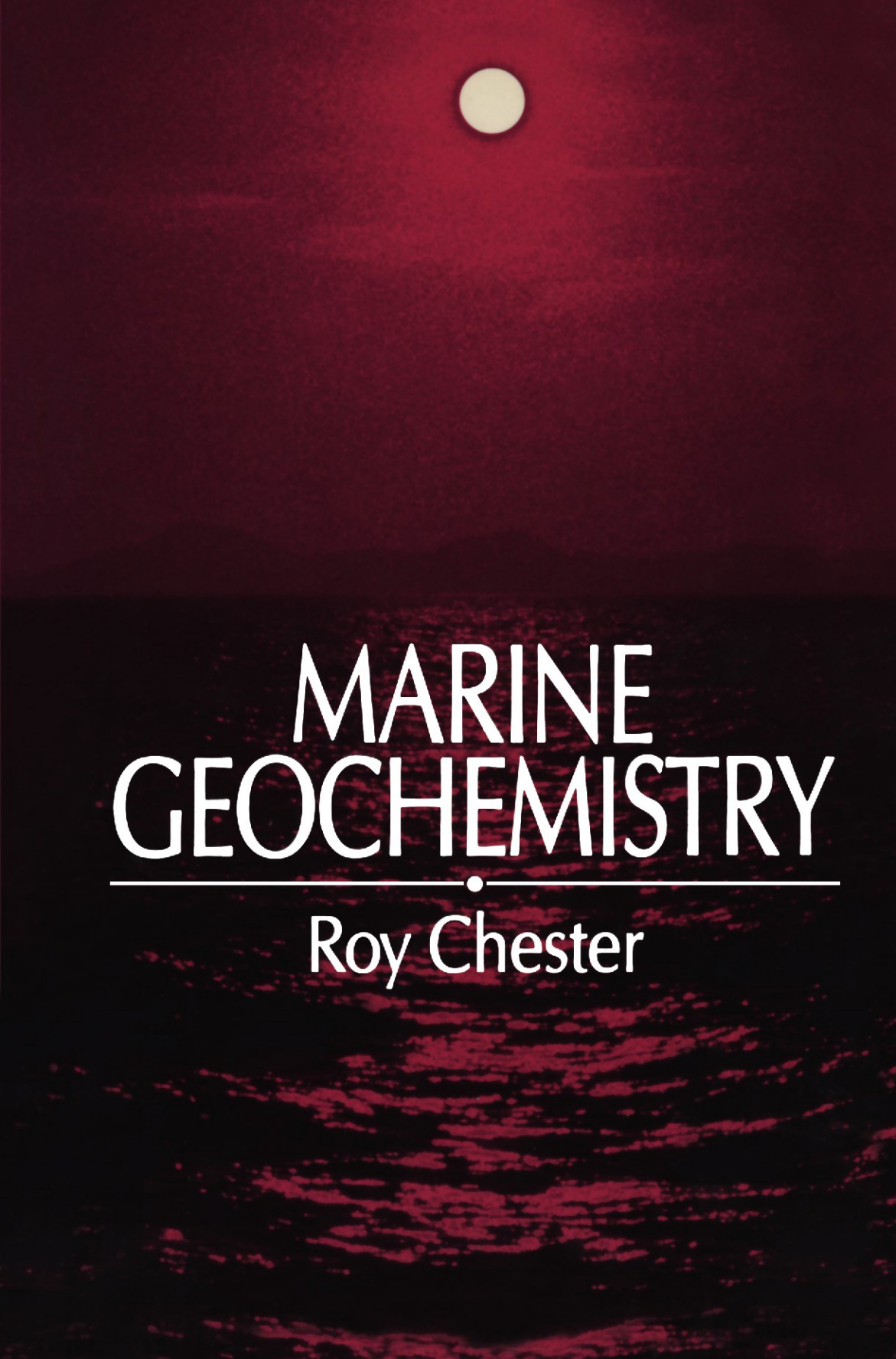

MARINE GEOCHEMISTRY

Roy Chester

MARINE GEOCHEMISTRY

TITLES OF RELATED INTEREST

Cathodoluminescence of geological materials
D. J. Marshall

Chemical fundamentals of geology
R. Gill

Deep marine environments
K. Pickering *et al.*

Elements of dynamic oceanography
D. Tolmazin

Experiments in physical sedimentology
J. R. L. Allen

Image interpretation in geology
S. Drury

Karst geomorphology and hydrology
D. C. Ford & P. W. Williams

Mathematics in geology
J. Ferguson

Neptune's domain
M. Glassner

Perspectives on a dynamic Earth
T. R. Paton

Petroleum geology
F. K. North

Petrology of the sedimentary rocks
J. T. Greensmith

A practical approach to sedimentology
R. C. Lindholm (ed.)

Principles of physical sedimentology
J. R. L. Allen

Sedimentary structures
J. Collinson & D. Thompson

Sedimentology: process and product
M. R. Leeder

Soils of the past
G. Retallack

Volcanic successions
R. A. F. Cas & J. V. Wright

MARINE GEOCHEMISTRY

Roy Chester

Department of Earth Sciences, University of Liverpool

London
UNWIN HYMAN
Boston Sydney Wellington

Published by the Academic Division of
Unwin Hyman Ltd
15/17 Broadwick Street, London W1V 1FP

Allen & Unwin Inc.,
8 Winchester Place, Winchester, Mass. 01890, USA

Allen & Unwin (Australia) Ltd,
8 Napier Street, North Sydney, NSW 2060, Australia

Allen & Unwin (New Zealand) Ltd in association with
the Port Nicholson Press Ltd, Compusales Building,
75 Ghuznee Street, Wellington 1, New Zealand

First published in 1990

British Library Cataloguing in Publication Data

Chester, Roy
Marine geochemistry.
1. Oceans. Chemical composition & chemical properties
I. Title
551.46'.01

ISBN-13:978-94-010-9490-0 e-ISBN-13:978-94-010-9488-7
DOI:10.1007/978-94-010-9488-7

Library of Congress Cataloguing-in-Publication Data

Chester, R. (Roy), 1936–
Marine geochemistry/Roy Chester.
p. cm.
Includes bibliographies and index.

1. Chemical oceanography. 2. Marine sediments. 3. Geochemistry.
I. Title.
GC111.2.C47 1989 89–5735
551.46'01 – dc20 CIP

Typeset in 10 on 12 point Times by Columns of Reading

Preface

The past two or three decades have seen many important advances in our knowledge of the chemistry, physics, geology and biology of the oceans. It has also become apparent that in order to understand the manner in which the oceans work as a 'chemical system', it is necessary to use a framework which takes account of these interdisciplinary advances. *Marine geochemistry* has been written in response to the need for a single state-of-the-art text that addresses the subject of treating the sea water, sediment and rock reservoirs as a unified system. In taking this approach, a process-orientated framework has been adopted in which the emphasis is placed on identifying key processes operating within the 'unified ocean'. In doing this, particular attention has been paid to making the text accessible to students from all disciplines in such a way that future advances can readily be understood.

I would like to express my thanks to those people who have helped with the writing of this volume. In particular, I wish to put on record my sincere appreciation of extremely helpful suggestions made by Professor John Edmond, FRS. In addition, I thank Dr S. Rowlatt for his comments on the sections covering the geochemistry of oceanic sediments, and Dr G. Wolff for his invaluable advice on the organic geochemistry of biota, water and sediments. It is a great pleasure to acknowledge the help of Dr K. J. T. Murphy, who gave so freely of his time at all stages in the preparation of the text. I also thank all those authors who have kindly allowed their diagrams and tables to be reproduced in the book. Many other people have influenced the way in which my thoughts have developed over the years, and to these friends and colleagues I owe a great debt of gratitude.

I would like to thank Unwin Hyman for their understanding during the preparation of the volume; Roger Jones for helping to develop the idea in the beginning, and Andy Oppenheimer, whose patience in handling the manuscript has known no bounds.

Finally, I would like to express my gratitude to my wife Alison, for all the devoted support she has given me during the writing of this book and at all other times.

R. Chester
Liverpool

Acknowledgements

We are grateful to the following individuals and organizations who have kindly given permission for the reproduction of copyright material (figure numbers in parentheses):

Figure 3.1 © 1970 American Association for the Advancement of Science; Geological Society of America (3.2, 13.1a, 15.5b); Figures 3.3, 6.1a and Worksheet 7.1a,b reproduced by permission of Unesco, © Unesco 1981; Academic Press (3.5a, 3.5b(i), 3.5b(ii), 3.5b(v), 3.7, 4.3a, 5.1b, 8.1, 8.2, 8.6, 9.2b(i), 9.2b(iii), 9.3, 9.4, 11.4, 13.5, 14.6, 15.6, 16.7, 17.1, Tables 5.1, 11.1, 13.5, 15.3, Worksheets 8.1a, 14.2(i)); Pergamon Press (3.5b(iii), 3.6, 4.1, 6.3, 7.1a, 7.1b(i), 7.1c(i), 7.3, 7.5, 9.2a, 10.3, 11.2, 11.5c, 11.5d, 11.7–9, 13.3a, 14.1, 14.5, 14.8a, 15.1, 15.9c, 16.3b, 16.4–6, 16.10, Tables 4.13, 15.2, Worksheets 7.3(i-iii), 14.4ii(b); Elsevier Science Publishers (3.5b(iv), 4.7b, 5.2, 9.5, 9.7, 10.2, 11.3, 11.5a, 11.5b, 11.5e, 12.1, 12.5, 13.3b, 13.4, 14.2, 14.7, 15.2, 16.2, 16.3a, 16.12, 17.2, Worksheets 3.1(i, ii), 14.3(i, ii)); Plenum Publishing (11.6a, 15.10, Tables 3.6, 3.10); Kluwer Academic Publishers (4.2a-b, 4.3b, 8.7); Figures 4.4, 4.6, 8.4, 15.4, 16.8 © American Geophysical Union; Figures 4.5, 7.2, 7.4, 13.2b © 1979 John Wiley & Sons, Inc; Springer-Verlag (4.7a, 4.8, 8.5, 14.3); Academic Press and Geological Society of America (5.1a); I.A.H.S. (6.1b); SCOPE/UNEP (6.1c, 6.2, 12.2); Tables 6.13, 6.14 © CRC Press, Inc; Figure 7.1b(ii) reproduced by permission of Macmillan Publishing Company, © 1979 J.G. Weihaupt; Figure 7.1c(ii) reproduced by permission of Prentice-Hall, Inc, © 1987; Worksheet 7.2(i-iii) reproduced by permission from *Nature* **314**, 526, © 1985 Macmillan Magazines Ltd; Worksheet 8.2(i) © 1974 Munksgaard International Publishers Ltd; Academic Press and Geochemical Research Association (Japan) (8.3); Figure 9.1 reproduced by permission from *Nature* **282**, 677, © 1979 Macmillan Magazines Ltd; Figure 9.2b(ii) reproduced by permission of Prentice-Hall, Inc, © 1970; G. Wolff (Worksheet 9.1); CHIMIA (9.8); Figure 10.1 © CRC Press, Inc and Elsevier; Aberdeen University Press (10.4); Figure 11.1 reproduced by permission from *Nature* **303**, 225, © 1983 Macmillan Magazines Ltd; American Society of Limnology and Oceanography, Inc (11.6b, 11.6c, 14.4); U.S. National Academy of Science (12.3, 12.4, Table 12.2); Figures 13.1b, 15.5a reproduced by permission of Prentice-Hall, Inc, © 1982; Oxford University Press (13.2a); Worksheet 14.1(i) © 1981 John Wiley & Sons, Inc; Figures 14.8b, 15.9a, 15.9b and Worksheets 14.4(i), 14.4(iia) reproduced by permission of American Journal of Science; Blackwell Scientific Publications (15.3); D.S. Cronan and S.A. Moorby (15.7); University of Rhode Island (15.8); Figure 16.9a reproduced by permission from *Nature* **326**, 244, © 1987 Macmillan Magazines Ltd; Figure 16.9b reproduced by permission from *Nature* **326**, 278, © 1987 Macmillan Magazines Ltd; Figure 16.11 © 1973 American Association for the Advancement of Science.

This book is dedicated with affection and gratitude
to Dr G. D. Nicholls, an innovative geochemist,
and a fine teacher who has the truly rare gift of
being able to inspire his students

Contents

Symbols and concentration units

1 General symbols

All symbols used in the present work are defined at the appropriate place in the text, which can be found by reference to the index at the end of the volume.

2 Units

The units defined below, and the symbols by which they are identified, are confined to a general list of those most commonly used in the present work; other units will be defined where necessary in the text itself. It must be noted that a number of traditional units have been retained as a matter of policy throughout the work because they are still widely used in the current as well as in the past literature; e.g. the litre has been employed as a unit volume although IAPSO have recommended that for high precision measurements of volume it be replaced by the cubic decimetre (dm^3). For a detailed treatment of the use of SI units in oceanography see the IAPSO recommendations published by Unesco (1985).

Length
SI unit = metre
nm, nanometre = 10^{-9} m
μm, micrometre = 10^{-6} m
mm, millimetre = 10^{-3} m
cm, centimetre = 10^{-2} m
m, metre
km, kilometre = 10^{3} m

Weight or mass
SI unit = kilogram
pg, picogram = 10^{-12} g
ng, nanogram = 10^{-9} g
μg, microgram = 10^{-6} g
mg, milligram = 10^{-3} g
g, gram
kg, kilogram = 10^{3} g
t, ton/tonne = 10^{6} g

Volume
SI unit = cubic metre
dm^3, cubic decimetre = 10^{-3} m^3 = 1 litre
m^3, cubic metre
µl, microlitre = 10^{-6} l
ml, millilitre = 10^{-3} l
l, litre

Time
SI unit = second
s = second
min = minute
h = hour
d = day
yr = year
Ma = million years = 10^6 yr

*Concentration**
The SI unit for the amount of a substance is the mole. However, the most commonly used concentration for particulates and sediments is still mass per unit mass; e.g.

µg g^{-1} = ppm = parts per million
ng g^{-1} = ppb = parts per billion

A number of systems are currently in common use for expressing the concentration of solutes in sea water.

(a) The concentrations can be expressed in units of mass per unit volume or per unit mass of sea water: e.g. g kg^{-1} or mg kg^{-1} for major components, or ng dm^{-3} or ng kg^{-1} of sea water for trace elements; however, trace element concentrations are still often expressed in terms of mass l^{-1}. Examples of such concentrations are

µg l^{-1} = 10^{-6} g l^{-1} (or dm^{-3}, or kg^{-1})
ng l^{-1} = 10^{-9} g l^{-1} (or dm^{-3}, or kg^{-1})
pg l^{-1} = 10^{-12} g l^{-1} (or dm^{-3}, or kg^{-1})

(b) The most usual practice now is to use the mole as the unit of concentration for solutes in sea water. Examples of concentrations are

µmol l^{-1} = 10^{-6} mol l^{-1} (or dm^{-3}, or kg^{-1})
nmol l^{-1} = 10^{-9} mol l^{-1} (or dm^{-3}, or kg^{-1})
pmol l^{-1} = 10^{-12} mol l^{-1} (or dm^{-3}, or kg^{-1})

(c) Traditionally, the concentrations of the nutrients have often been expressed as μg-at l^{-1}, where

μg-at l^{-1} = μg-atoms l^{-1} = μg/atomic weight l^{-1}

The atmospheric concentrations of particulate elements given in the text are expressed in the form

μg m^{-3} of air = 10^{-6} g per cubic metre of air
ng m^{-3} of air = 10^{-9} g per cubic metre of air

Radioactivity
SI unit = Bq m^{-3} (becquerels per cubic metre) or Bq kg^{-1}
dpm = disintegrations per minute
Ci = curie; 1 Ci = 3.7×10^{10} Bq

3 Some data that are useful for flux calculations

Areas†
Area of the oceans = $361\,110 \times 10^3$ km^2
  Area of the Atlantic Ocean (to ~ 80°S) = $98\,013 \times 10^3$ km^2
    Area of the North Atlantic = $52\,264 \times 10^3$ km^2
    Area of the South Atlantic = $45\,749 \times 10^3$ km^2
  Area of the Indian Ocean (to ~ 70°S) = $77\,700 \times 10^3$ km^2
    Area of the northern Indian Ocean = $12\,482 \times 10^3$ km^2
    Area of the southern Indian Ocean = $65\,218 \times 10^3$ km^2
  Area of the Pacific Ocean (to ~80°S) = $176\,888 \times 10^3$ km^2
    Area of the North Pacific = $81\,390 \times 10^3$ km^2
    Area of the South Pacific = $95\,498 \times 10^3$ km^2
Area of the continents = $148\,904 \times 10^3$ km^2

River transport
River inflow into the North Atlantic Ocean = 11 405 km^3 yr^{-1}
River inflow into the South Atlantic Ocean = 7946 km^3 yr^{-1}
River inflow into the northern Indian Ocean = 3247 km^3 yr^{-1}
River inflow into the southern Indian Ocean = 2354 km^3 yr^{-1}
River inflow into the North Pacific Ocean = 7678 km^3 yr^{-1}
River inflow into the South Pacific Ocean = 4459 km^3 yr^{-1}
Total river inflow to all oceans ≃ 37 400 km^3 yr^{-1}

Atmospheric transport
The area of the marine atmosphere is equal to the total area of the oceans; however, the atmospheric volume used for calculating atmospheric deposition fluxes depends on the scale height to which a component is dispersed, usually between about 3 and 5 km – see Section 6.2.

References

Baumgartner, A. & E. Reichel 1975. *The world water balance.* Amsterdam: Elsevier.
Unesco 1985. Unesco Tech. Pap. Mar. Sci., no. 32. Paris: Unesco.

* *Note on the use of concentration units.* The concentration of dissolved elements is usually expressed in the text in the most widely used mole form. However, since it is still common practice for many authors to use the μg/ng g^{-1} form for the expression of concentrations in particulates and sediments, the convention has been retained here. This does not present problems in the evaluation of elemental distribution pattern (or of the processes that control them) in either sea water or sediments. However, the approach adopted in the text is to follow a global 'source–sink' journey, and in order to simplify and standardize assessments of the transport of elements from sea water to the sediment reservoir, mole concentrations have been converted to mass concentrations in water column/sediment surface flux calculations.

† Taken mainly from Baumgartner & Reichel (1975).

1 Introduction

The fundamental question underlying marine geochemistry is 'How do the oceans work as a chemical system?' At present, that question cannot be fully answered. However, the past two decades or so have seen a number of 'quantum leaps' in our understanding of some aspects of marine geochemistry. Three principal factors have made these leaps possible: (a) advances in sampling and analytical techniques; (b) the development of theoretical concepts; and (c) the setting up of large-scale international oceanographic programmes (e.g. DSDP, MANOP, HEBBLE, GEOSECS, TTO, VERTEX, GOFS, SEAREX), which have extended the marine geochemistry database to a global ocean scale.

1.1 Setting the background: a unified 'process-orientated' approach to marine geochemistry

Oceanography attracts scientists from a variety of disciplines, including chemistry, geology, physics, biology and meteorology. A knowledge of at least some aspects of marine geochemistry is an essential requirement for scientists from all these disciplines and for students who take courses in oceanography at any level. The present volume has therefore been written with the aim of bringing together these recent advances in marine geochemistry in a form that can be understood by all those scientists who use the oceans as a natural laboratory and not just by marine chemists themselves. However, one of the major problems involved in doing this is to provide a coherent global ocean framework within which marine geochemistry can be described in a manner that not only can readily relate to the other oceanographic disciplines but also can accommodate future advances in the subject. To develop such a framework, it is necessary to explore some of the basic concepts that underlie marine geochemistry.

Geochemical balance calculations show that a number of elements that could not have come from the weathering of igneous rocks are present at the Earth's surface. It is now generally accepted that these elements, which are termed the **excess volatiles**, have originated from the degassing of the Earth's interior. The excess volatiles, which include H and O (combined as H_2O), C, Cl, N, S, B, Br and F, are especially abundant in the atmosphere and the oceans. It is believed, therefore, that both the atmosphere and the oceans were generated by the degassing of the

Earth's interior. In terms of global cycling, Mackenzie (1975) suggested that sedimentary rocks are the product of a long-term titration of primary igneous-rock minerals by acids associated with the excess volatiles, a process that can be expressed as

$$\text{Primary igneous-rock minerals} + \text{Excess volatiles} \rightarrow \text{Sedimentary rocks} + \text{Oceans} + \text{Atmosphere.} \quad (1.1)$$

As this reaction proceeds, the seawater reservoir is continuously subjected to material fluxes, which are delivered along various pathways from external sources. The oceans are therefore a **flux-dominated** system. However, sea water is not a static reservoir in which the material has simply accumulated over geological time, otherwise it would have a very different composition from that which it has at present; for example, the material supplied over geological time far exceeds the amount now present in sea water. Further, the composition of sea water has not changed markedly over very long periods of time. Rather than acting as an accumulator, therefore, the flux-dominated seawater reservoir can be regarded as a reactor. It is the nature of the reactions that take place within the reservoir, i.e. the manner in which it responds to the material fluxes, which defines the composition of sea water via an input → internal reactivity → output cycle.

Traditionally, there have been two schools of thought on the overall nature of the processes that operate to control the composition of sea water. In the **equilibrium ocean** concept, a state of chemical equilibrium is presumed to exist between sea water and sediments via reactions that are reversible in nature. Thus, if the supply of dissolved elements to sea water were to increase, or decrease, the equilibrium reactions would change in the appropriate direction to accommodate the fluctuations. In the **steady-state ocean** concept, it is assumed that the input of material to the system is balanced by its output, i.e the reactions involved proceed in one direction only. In this type of ocean, fluctuations in input magnitudes would simply result in changes in the rates of the removal reactions, and the concentrations of the reactants in sea water would be maintained. At present, the generally held view supports the steady-state ocean concept. Whichever theory is accepted, however, it is apparent that the oceans must be treated as a **unified input–output type of system**, in which materials stored in the sea water, the sediment and the rock reservoirs interact, sometimes via recycling stages, to control the composition of sea water.

It is clear, therefore, that the first requirement necessary to address the question 'How do the oceans work as a chemical system?' is to treat the sea water, sediment and rock reservoirs as a unified system. It is also apparent that one of the keys to solving the question lies in understanding

the nature of the chemical, physical and biological processes that control the composition of sea water, since this is the reservoir through which the material fluxes flow in the input → internal reactivity → output cycle. In order to provide a **unified ocean** framework within which to describe the recent advances in marine geochemistry in terms of this cycle, it is therefore necessary to understand the nature and magnitude of the fluxes that deliver material to the oceans (the input stage), the reactive processes associated with the throughput of the material through the seawater reservoir (the internal reactivity stage), and the nature and magnitude of the fluxes that take the material out of sea water into the sinks (the output stage).

The material that flows through the system includes inorganic and organic components in both dissolved and particulate forms, and a wide variety of these components will be described in the text. However, in order to avoid falling into the trap of not being able to see the wood for the trees in the morass of data, it is essential to recognize the importance of the processes that affect constituents in the source-to-sink cycle. Rather than taking an element-by-element 'periodic table' approach to marine geochemistry, the treatment adopted in the present volume will therefore involve a **process-orientated** approach, in which the emphasis will be placed on identifying the key processes that operate within the cycle. The treatment will include both natural and anthropogenic materials, but is is not the intention to offer a specialized overview of marine pollution. This treatment does not in any way underrate the importance of marine pollution. Rather, it is directed towards the concept that it is necessary first to understand the natural processes that control the chemistry of the ocean system, since it is largely these same processes that affect the cycles of the anthropogenic constituents.

Since the oceans were first formed, sediments have stored material, and thus have recorded changes in environmental conditions. However, the emphasis in the present volume is largely on the role that the sediments play in controlling the chemistry of the oceans. The diagenetic changes which have the most immediate effect on the composition of sea water take place in the upper few metres of the sediment column. For this reason attention will be focused on these surface deposits, and the role played by sediments in palaeooceanography will only be touched upon briefly.

In order to rationalize the process-orientated approach, special attention will be paid to a number of individual constituents, which can be used to elucidate certain key processes that play an important role in controlling the chemical composition of sea water. In selecting these process-orientated constituents it was necessary to recognize the flux-dominated nature of the seawater reservoir. The material fluxes that reach the oceans deliver both dissolved and particulate elements to sea

water. However, it was pointed out above that the amount of dissolved material in sea water is not simply the sum of the total amounts brought to the oceans over geological time. This was highlighted in the last century by Forchhammer (1865) when he wrote: 'Thus the quantity of the different elements in sea water is not proportional to the quantity of elements which river water pours into the sea, but is inversely proportional to *the facility with which the elements are made insoluble by general chemical or organo-chemical actions in the sea*' [my italics]. According to Goldberg (1963), this statement can be viewed as elegantly posing the theme of marine chemistry, and it is this 'facility with which the elements are made insoluble', and so are removed from the dissolved phase, which is central to our understanding of many of the factors that control the composition of sea water. This was highlighted more recently by Turekian (1977). In one of the most influential geochemical papers published in recent years, this author formally posed a question that had attracted the attention of marine geochemists for generations, and may be regarded as another expression of Forchhammer's statement, i.e. 'Why are the oceans so depleted in trace metals?' Turekian concluded that the answer lies in the role played by particles in the sequestration of reactive elements during every stage in the transport cycle from source to marine sink.

Ultimately, therefore, it is the transfer of dissolved constituents to the particulate phase, and the subsequent sinking of the particulate material, that is responsible for the removal of the dissolved constituents from sea water to the sediment sink. However, it must be stressed that, although dissolved $\rightarrow$ particulate transformations are the driving force behind the removal of most elements to the sediment sink, the transformations themselves involve a wide variety of biogeochemical processes. For example, Stumm & Morgan (1981) identified a number of chemical reactions and physicochemical processes that are important in setting the chemical composition of natural waters. These included acid–base reactions, oxidation–reduction reactions, complexation reactions between metals and ligands, adsorption processes at interfaces, the precipitation and dissolution of solid phases, gas–solution processes, and the distribution of solutes between aqueous and non-aqueous phases. The manner in which reactions and processes such as these, and those specifically assocated with biota, interact to control the composition of sea water will be considered throughout the text. For the moment, however, they can simply be grouped under the general term **particulate $\leftrightarrow$ dissolved** reactivity. The particulate material itself is mainly delivered to the sediment surface via the down-column sinking of large-sized organic aggregates as part of the oceanic **global carbon flux**. Thus, within the seawater reservoir, reactive elements undergo a continuous series of dissolved $\leftrightarrow$ particulate transformations, which are coupled with the

transport of biologically formed particle aggregates to the sea bed. Turekian (1977) aptly termed this overall process **the great particle conspiracy**. In the flux-dominated ocean system the manner in which this conspiracy operates to clean up sea water is intimately related to the oceanic throughput of externally transported, and internally generated, particulate matter. Further, it is apparent that several important aspects of the manner in which this **throughput cycle** operates to control the inorganic and organic compositions of both the seawater reservoir and the sediment sink can be assessed in terms of the oceanic fates of reactive trace elements and organic carbon.

Many of the most important thrusts in marine geochemistry over the past few years have used tracers to identify the processes that drive the system, and to establish the rates at which they operate. These tracers will be discussed at appropriate places in the text. However, the **tracer approach** has also been adopted in a much broader sense in the present volume in that special attention will be paid to the trace elements and organic carbon in the source/input → internal reactivity → sink/output transport cycle. Both stable and radionuclide trace elements (e.g. the use of the 'time clock' Th isotopes as both transport and process indicators) are especially rewarding for the study of reactivity within the various stages of the cycle, and organic carbon is a vital constituent with respect to both the oceanic biomass and the down-column transport of material to the sediment sink.

To interpret the source/input → internal reactivity → sink/output transport cycle in a coherent and systematic manner, a three-stage approach will be adopted, which follows the cycle in terms of a **global journey**. In Part I, the movements of both dissolved and particulate components will be tracked along a variety of transport pathways from their original sources to the point at which they cross the interfaces at the land/sea, air/sea and rock/sea boundaries. In Part II, the processes that affect the components within the sea water reservoir will be described. In Part III, the components will be followed as they are transferred out of sea water into the main sediment sink, and the nature of the sediments themselves will be described. However, the treatment is mainly concerned with the role played by the sediments as marine sinks for material that has flowed through the sea water reservoir. In this context, it is the processes that take place in the upper few metres of the sediments which have the most immediate effect on the composition of sea water. For this reason attention will be restricted mainly to the uppermost sediment sections, and no attempt will be made to evaluate the status of the whole sediment column in the history of the oceans.

The steps involved in the three-stage global journey are illustrated schematically in Figure 1.1. This is not meant to be an all-embracing representation of reservoir interchange in the ocean system, but is simply

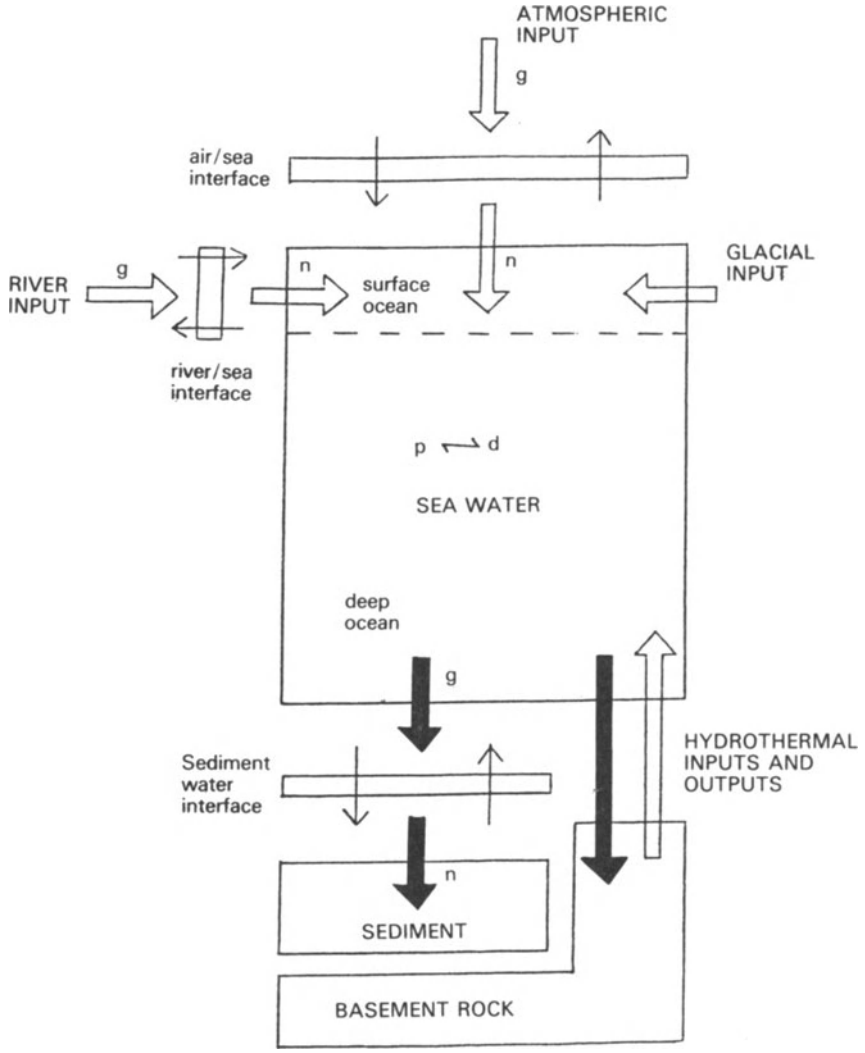

Figure 1.1 A schematic representation of the source/input → sea water internal reactivity → sink/output global journey. The large open arrows indicate transport from material sources, and the large filled arrows indicate transport into material sinks; relative flux magnitudes are not shown. The small arrows indicate only that the strengths of the fluxes can be changed as they cross the various interfaces in the system; thus, g and n represent gross and net inputs or outputs, respectively. Material is brought to the oceans in both particulate and dissolved forms, but is transferred into the major sediment sink mainly as particulate matter. The removal of dissolved material to the sediment sink therefore usually requires its transformation to the particulate phase. This is shown by the p ⇌ d term. However, the intention here is simply to indicate that internal particulate/dissolved reactivity occurs within the seawater reservoir, and it must be stressed that a wide variety of chemical reactions and physicochemical processes are involved in setting the composition of the water phase – see text. For convenience coastal zones are not shown.

intended to offer a general framework within which to describe the global journey. By directing the journey in this way, the intention is therefore to treat the sea water, sediment and rock phases as integral parts of a unified ocean system.

The volume has been written for scientists of all disciplines. To contain the text within a reasonable length, a basic knowledge of chemistry, physics, biology and geology has been assumed and the fundamental principles in these subjects, which are readily available in other textbooks, have not been reiterated here. However, since the volume is deliberately designed with a multidisciplinary readership in mind, an attempt has been made to treat the more advanced chemical and physical concepts in a generally descriptive manner, with appropriate references being given to direct the reader to the original sources. However, one of the major aims of marine geochemistry in recent years has been to model natural systems on the basis of theoretical concepts. To follow this approach it is necessary to have a more detailed understanding of the theory involved, and for this reason a series of Worksheets have been included in the text. Some of these Worksheets are used to describe a number of basic geochemical concepts; for example, those underlying redox reactions and the diffusion of solutes in interstitial waters. In others, however, the emphasis is placed on modelling a variety of geochemical systems using, where possible, actual examples from the literature sources; for example, the topics covered include a sorptive equilibrium model for the removal of trace metals in estuaries, a stagnant film model for the exchange of gases across the air/sea interface, and a variety of models designed to describe solid phase–dissolved phase interactions in sediment interstitial waters.

Overall, therefore, the intention is to provide a unifying framework, which has been designed to bring a state-of-the-art assessment of marine geochemistry to the knowledge of a varity of ocean scientists in such a way that allows future advances to be understood within a meaningful context.

References

Forchhammer, G. 1865. On the composition of sea water in the different parts of the ocean. *Phil. Trans. R. Soc. Lond.* **155,** 203–62.

Goldberg, E.D. 1963. The oceans as a chemical system. In *The sea,* M.N. Hill (ed.), Vol. 2, 3–25. New York: Interscience.

Mackenzie, F.T. 1975. Sedimentary cycling and the evolution of the sea water. In *Chemical oceanography*, J.P. Riley & G. Skirrow (eds), Vol. 1, 309–64. London: Academic Press.

Stumm, W. & J.J. Morgan 1981. *Aquatic chemistry*. New York: Wiley.

Turekian, K.K. 1977. The fate of metals in the oceans. *Geochim. Cosmochim. Acta* **41,** 1139–44.

PART I

THE GLOBAL JOURNEY: MATERIAL SOURCES

2 The input of material to the ocean reservoir

The World Ocean may be regarded as a planetary dumping ground for material that originates in other geospheres, and to understand marine geochemistry it is necessary to evaluate the composition, flux rate and subsequent fate of the material that is delivered to the ocean reservoir.

2.1 The background

The major natural sources of the material that is injected into sea water are the continental crust and the oceanic crust. Primary material is mobilized directly from the continental crust mainly by low-temperature weathering processes and high-temperature volcanic activity. In addition, secondary (or pollutant) material is mobilized by a variety of anthropogenic 'weathering' processes, which often involve high temperatures. The various types of material released on the continents during both natural and anthropogenic processes include particulate, dissolved and gaseous phases, which are then moved around the surface of the planet by a number of transport pathways. The principal routes by which continentally mobilized material reaches the World Ocean are via fluvial, atmospheric and glacial transport. However, the relative importance of these pathways varies considerably in both space and time. For example, atmospheric transport is strongest in low latitudes, where aeolian dust can be carried to the sea surface in the form of intermittent pulses. However, material is dispersed throughout the atmosphere over the whole ocean and is present, albeit sometimes at low concentrations, at all marine locations. Fluvial transport also delivers material to very large areas of the World Ocean. However, glacial transport is much restricted in scope.

Water in the form of ice can act as a major mechanism for the physical mobilization of material on the Earth's surface. The magnitude of the transport of this material depends on the prevailing climatic regime. At present, the Earth is in an interglacial period and large-scale ice sheets are confined to the polar regions. Even under these conditions, however, glacial processes are a major contributor of material to the oceans. For example, Garrels & Mackenzie (1977) estimated that at present $\sim 20 \times 10^{14}$ g yr^{-1} of crustal products are delivered to the World Ocean by glacial transport, of which $\sim$ 90% is derived from Antarctica. Thus,

ice transport is second only to fluvial run-off in the global supply of material to the marine environment. From the point of view of marine geochemistry, however, glacial transport is less important than either fluvial or atmospheric transport in the supply of material to the oceans on a global scale. There are two principal reasons for this:

(a) Glacial transport is at present largely restricted to the polar regions, and so does not have the same global importance as either fluvial or atmospheric transport. For example, although ice-rafted material has been found in marine sediments from many areas, glacial marine sediments are largely confined to the polar regions around Antarctica, where they form a ring of sediment, and to areas in the Arctic Ocean (see Figure 13.5a).
(b) Water is the main agency involved in chemical weathering, and during glacial processes this water is locked in a solid form. As a result, there is a general absence of chemical weathering in the polar regions and therefore little release of elements into the soluble phase.

In general, therefore, glacial material does not make a significant global contribution to the dissolved pool of elements in sea water. It has been suggested, however, that one way in which glacially transported material can contribute to this dissolved pool is by the leaching of elements from fine-grained rock flour by sea water. In this context, Schutz & Turekian (1965) suggested that such a process might account for enrichments in Co, Ni and Ag in waters of intermediate depth south of 68°S. In general, however, it may be concluded that the effects resulting from the transport of material to the World Ocean by glacial processes are largely confined to the polar regions. The principal transport pathways that supply material derived from the continental crust to the oceans are therefore river run-off and atmospheric deposition.

Material is also supplied to the oceans from processes that affect the oceanic crust. These processes involve low-temperature weathering of the ocean basement rocks, mainly basalts, and high-temperature water–rock reactions associated with hydrothermal activity at spreading ridge centres. This hydrothermal activity, which can act as a source of some components and a sink for others, is now known to be of major importance in global geochemistry; for example, in terms of primary inputs it dominates the supply of dissolved manganese to the oceans. Although the extent to which this type of dissolved material is dispersed about the ocean is not yet clear, hydrothermal activity must still be regarded as a globally important mechanism for the supply of material to the seawater reservoir.

On a global scale, therefore, the main pathways by which material is brought to the oceans are: (a) river run-off, which delivers material to the

surface ocean at the land/sea boundaries; (b) atmospheric deposition, which delivers material to all regions of the surface ocean; and (c) hydrothermal activity, which delivers material to deep and intermediate waters above the sea floor. The manner in which these principal pathways operate is described individually in the next three chapters, and this is then followed by an attempt to estimate the relative magnitudues of the material fluxes associated with them.

References

Garrels, R.M. & F.T. Mackenzie 1971. *Evolution of sedimentary rocks.* New York: Norton.

Schutz, D.F. & K.K. Turekian 1965. The distribution of cobalt, nickel and silver in ocean water profiles around Pacific Antarctica. *J. Geophys. Res.* **70,** 5519–28.

3 The transport of material to the oceans: the river pathway

Much of the material mobilized during both natural crustal weathering and anthropogenic activities is dispersed by rivers, which transport the material towards the land/sea margins. In this sense, rivers may be regarded as the carriers of a wide variety of *chemical signals* to the World Ocean. The effect that these signals have on the chemistry of the ocean system may be assessed within the framework of three key questions (see e.g. Martin & Whitfield 1983): (1) What is the quantity and chemical composition of the dissolved and particulate material carried by rivers? (2) What are the fates of these materials in the estuarine mixing zone? (3) What is the ultimate quantity and composition of the material that is exported from the estuarine zone and actually reaches the open ocean? These questions will be addressed in this chapter, and in this way river-transported materials will be tracked on their journey from their source, across the estuarine (river/ocean) interface, through the coastal receiving zone and out into the open ocean.

3.1 Chemical signals transported by rivers

3.1.1 Introduction

River water contains a large range of inorganic and organic components in both dissolved and particulate forms. However, a note of caution must be introduced before any attempt is made to assess the strengths of the chemical signals carried by rivers, especially with respect to trace elements. In attempting to describe the processes involved in river transport, and the strengths of the signals that they generate, great care must therefore be taken to assess the validity of the databases used. 'Modern', i.e. post-1975, trace element data have now started to appear in the literature and, where available, these will be used in the discussion of river-transported chemical signals.

3.1.2 The sources of dissolved and particulate material found in river waters

Water reaches the river environment either directly from the atmosphere

or indirectly from surface run-off, underground water circulation and the discharge of waste solutions. The sources of the dissolved and particulate components that are found in the river water include rock weathering, the decomposition of organic material, wet and dry atmospheric deposition and, for some rivers, pollution. The source strengths are controlled by a number of complex, often interrelated, environmental factors which operate in an individual river basin; these factors include rock lithology, relief, climate, the extent of vegetative cover and the magnitude of pollutant inputs.

The various factors that are involved in setting the composition of river water are considered in the following sections, and to do this it is convenient to use a framework in which the **dissolved** and the **particulate** components are considered separately.

3.1.3 Major and trace elements: the dissolved river signal

3.1.3.1 Major elements The major element composition of rivers entering the principal oceans is given in Table 3.1, together with that of sea water. From the average river and seawater compositions given in this table it can be seen that there are a number of differences between these two types of surface water. The most important of these are that in river water there is a general dominance of **calcium** and **bicarbonate**, whereas in sea water **sodium** and **chloride** are the principal dissolved components contributing to the total ionic, i.e. salt, content. However, the major element composition of river water is much more variable than that of sea water, and some idea of the extent of this variability can be seen from the data in Table 3.1. Maybeck (1981) has ranked the global order of variability for the major dissolved constituents of river water as follows: $Cl^- > SO_4^{2-} > Ca^{2+} = Na^+ > Mg^{2+} > HCO_3^- > SiO_2 > K^+$. The major factors that control these variations are discussed below.

There are a number of types of water on the Earth's surface, which can be distinguished from each other on the basis of both their total ionic content (**salinity**) and the mutual proportions in which their various ions are present (**ionic ratios**). Gibbs (1970) employed variations in both parameters to identify a number of end-member surface waters. The cations that characterize the two principal water types are Ca^{2+} for **fresh water** and Na^+ for **highly saline waters**, and Gibbs (1970) used variations in these two cations to establish compositional trends in world surface waters – see Figure 3.1a. He also demonstrated that the same general trends could be produced using variations in the principal anions in the two waters, i.e. HCO_3^- for fresh water and Cl^- for highly saline waters – see Figure 3.1b. By displaying the data in these two forms, Gibbs (1970) was able to produce a framework which could be used to characterize three end-member surface waters – see Figure 3.1c. These end-member waters were defined as follows:

Table 3.1 The major element composition of rivers draining into the oceans[a] (units, mg l^{-1})

Element	Atlantic	Indian	Arctic	Pacific	World average river water	Sea water
Na^+	4.2	8.5	8.8	5.2	5.3	10733
K^+	1.4	2.5	1.2	1.2	1.5	399
Ca^{2+}	10.5	21.6	16.1	13.9	13.3	412
Mg^{2+}	2.5	5.4	1.3	3.6	3.1	1294
Cl^-	5.7	6.8	11.8	5.1	6.0	19344
SO_4^{2-}	7.7	7.9	15.9	9.2	8.7	2712
HCO_3^-	37	94.9	63.5	55.4	51.7	142
SiO_2^{3-}	9.9	14.7	5.1	11.7	10.7	-
TDS[b]	78.9	154.9	123.7	105.3	101.6	-

[a] Data from Martin & Whitfield (1983), and Riley & Chester (1971).

[b] TDS = total dissolved solids.

(a) A **precipitation- or rain-dominated** end-member, in which the total ionic content is relatively very low, and the Na/(Na + Ca) and the Cl/(Cl + HCO_3^-) ratios are both relatively high. Conditions that favour the formation of this end-member are low weathering intensity and low rates of evaporation.

(b) A **rock-dominated** end-member, which is characterized by having an intermediate total ionic content and relatively low Na/(Na + Ca) and Cl/(Cl + HCO_3^-) ratios. This end-member is formed under conditions of high weathering intensity and low rates of evaporation.

(c) An **evaporation–crystallization** end-member, which has a relatively very high total ionic content and also relatively high Na/(Na + Ca) and Cl/(Cl + HCO_3^-) ratios. Conditions that favour the formation of this end-member are high weathering intensity and high rates of evaporation.

Gibbs (1970) was therefore attempting to classify surface waters on the basis of the predominance of the principal external sources of the major ionic components, i.e. precipitation and rock weathering, and the operation of internal processes, such as evaporation and precipitation. However, the diagrams he produced have received considerable criticism. For example, Feth (1971) suggested that the Pecos River, which was identified by Gibbs (1970) as belonging to the evaporation–crystallization end-member, has acquired its *major* increase in total dissolved salts from

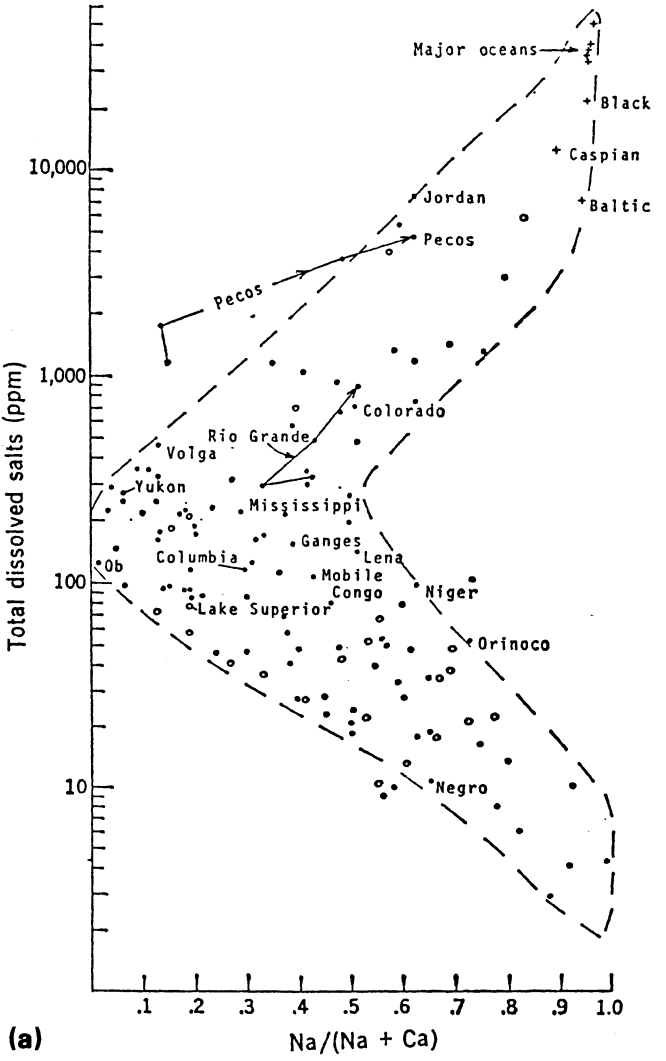

Figure 3.1 Processes controlling the composition of surface waters (from Gibbs 1970). (**a**) Variations in the weight ratio Na/(Na + Ca) as a function of total dissolved salts.

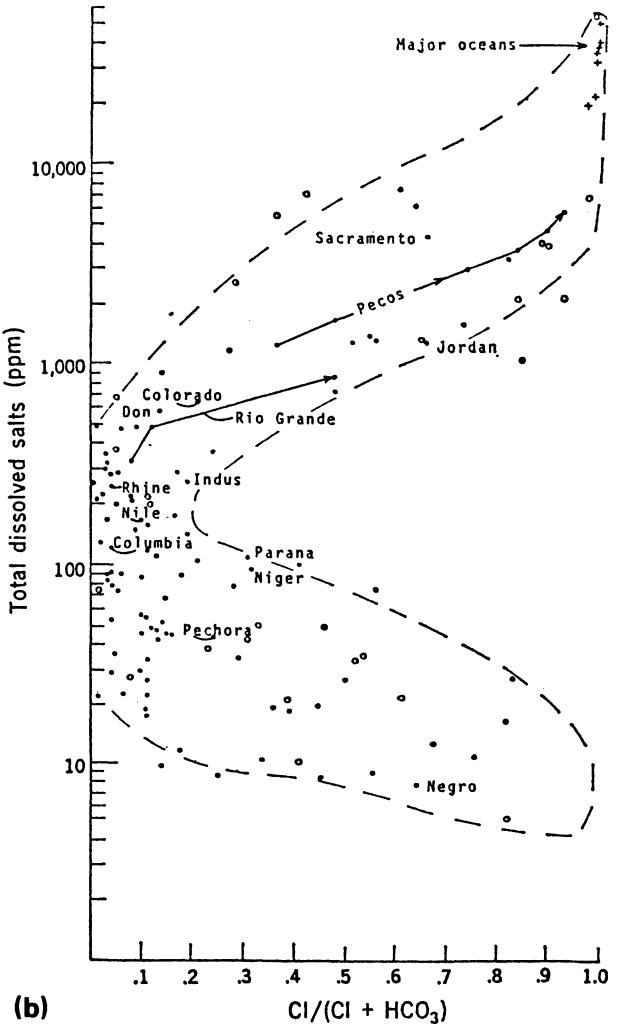

Figure 3.1b Variations in the weight ratio $Cl/(Cl + HCO_3^-)$ as a function of total dissolved salts.

the inflow of groundwater brines; thus, it should perhaps be termed an evaporite end-member. Stallard & Edmond (1983) also demonstrated that the Amazon Basin rivers, which have relatively high total salt contents, have arisen primarily via the weathering of evaporites and carbonates.

Stallard & Edmond (1981) also cast doubt on the existence of the rain-dominated end-member in the rivers of the Amazon Basin. By using

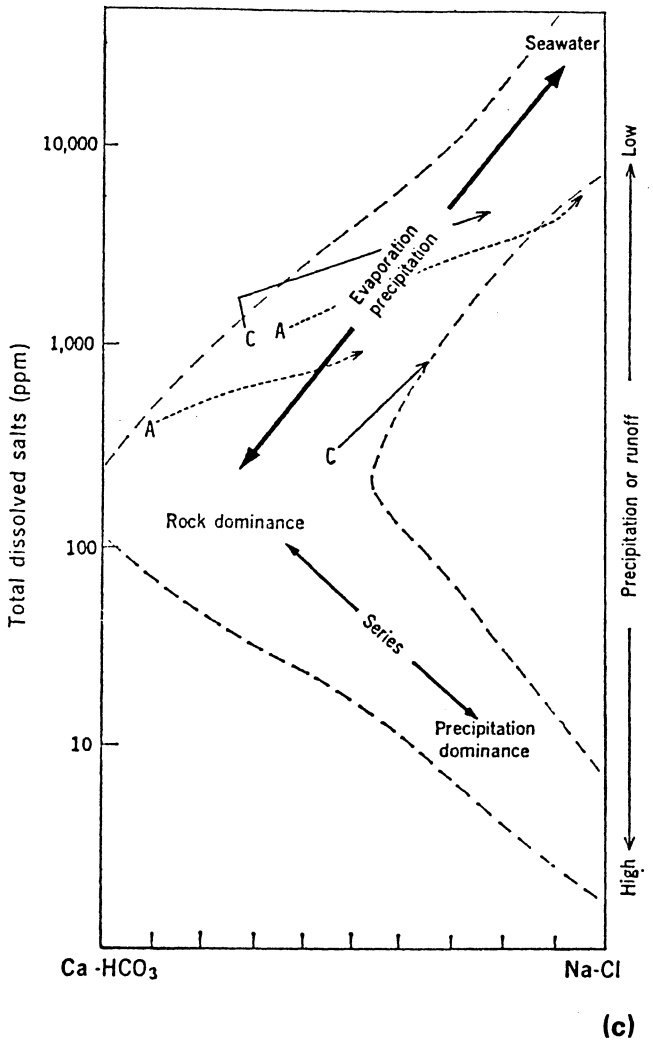

Figure 3.1c Diagrammatic representation of the processes controlling end-member water compositions. See text for explanation.

chloride as a marine reference element, the authors were able to define the **cyclic salt** background for the Amazon surface waters, and drew the following conclusions from their data. (a) Only Na^+, Mg^{2+} and SO_4^{2-}, after Cl^- the next three most abundant ions in sea water, exhibited significant cyclic contributions in any of the rivers in the basin. For a near-coastal river the cyclic source was dominant, and for one other river cyclic Na contributed ~ 50% to the surface water. However, for all other

rivers, the cyclic Na and Mg was found to be minor compared to inputs from weathering. (b) For the near-coastal river, ~ 15% of the Ca and K had a cyclic origin, but for all other rivers less than ~ 3% of the Ca and K had a marine origin. These estimates are considerably lower than those made by Gibbs (1970), who proposed that ~ 80% of the Na, K, Mg and Ca in the dilute lowland rivers of the Amazon Basin are cyclic. These conclusions were confirmed in a later publication in which Stallard & Edmond (1983) concluded that it is rock weathering, and not precipitation input, which controls the major cation chemistry of the lowland rivers of the Amazon Basin, i.e. the rivers are *not* precipitation-dominated. Thus, the very existence of the rain-dominated river end-member was challenged.

It is apparent, therefore, that, in the division of surface waters into the three end-members, the status of the rain-dominated and the evaporation–crystallization types must be seriously questioned. Nevertheless, there is no doubt that there are considerable variations in the total ionic content of river waters. This can be illustrated with respect to a number of individual river types (see Table 3.2), and in a general way the variations can be related to the Gibbs classification.

(a) Rivers with relatively small total ionic contents can be found (i) in catchments draining thoroughly leached areas of low relief where the rainfall is small, e.g. in some tropical regions of Africa and South America, and (ii) in catchments that drain the crystalline shields, e.g. those of Canada, Africa and Brazil. For example, very 'pure' waters, with total ionic contents of ~ 19 mg l^{-1}, are found on the Canadian Shield – see Table 3.2. It is waters such as these that

Table 3.2 Average major element concentrations of rivers draining different catchment types[a] (units, mg l^{-1})

	Rivers draining Canadian Shield	Mackenzie River; 'rock-dominated' end-member	Colorado River; 'evaporation - crystallization' end-member
Na^+	0.60	7.0	95
K^+	0.40	1.1	5.0
Ca^{2+}	3.3	33	83
Mg^{2+}	0.7	10.4	24
Cl^-	1.9	8.9	82
SO_4^{2-}	1.9	36.1	270
HCO_3^-	10.1	111	135
TIC[b]	18.9	207	694

[a] Data from Maybeck (1981).
[b] TIC = total ionic content.

will have their major ion composition most influenced by precipitation, even if they are not rain-dominated.

(b) As rock weathering becomes increasingly more important, the total ionic content of the river water increases. The Mackenzie River, which drains sedimentary and crystalline formations, is an example of a river having a rock-dominated water type. The average total ionic content of the Mackenzie River water is $\sim$ 200 mg l^{-1}, which is about an order of magnitude higher than that of the Canadian Shield rivers, and the concentration of Ca^{2+} exceeds that of Na^{+} by a factor of 4.7 – see Table 3.2.

(c) Some river waters have relatively high total ionic contents and high Na/(Na + Ca) ratios. The Colorado River is an example of this type and has a total ionic content of $\sim$ 700 mg l^{-1} and a Na^{+} concentration slightly in excess of Ca^{2+} – see Table 3.2. It is probable, however, that the major ion composition of this river has been influenced more by the input of saline underground waters draining brine formations than by evaporation–crystallization processes.

Maybeck (1981) took a global overview of the extent to which the three end-member waters are found on the Earth's surface. He concluded that the precipitation-dominated end-member (even if it exists at all) and the evaporation–crystallization (or evaporite) end-member together make up only around 2% of the world's river waters, and that in fact $\sim$ 98% of these surface waters are rock-dominated types.

Because the vast majority of the world's river waters belong to the rock-dominated category it is the extent to which the major rock-forming minerals are weathered, i.e. the influence of the **chemical composition** of the source rocks, that is the principal factor controlling the concentrations of the major ions in the waters. This can be illustrated with respect to varations in the major ion composition of rivers that drain a number of different rock types – see Table 3.3. From this table it can be seen, for example, that sedimentary rocks release greater quantities of Ca^{2+}, Mg^{2+}, SO_4^{2-} and HCO_3^{-} than do crystalline rocks. Maybeck (1981) assessed the question of the chemical denudation rates of crustal rocks and concluded that: (a) chemical denudation products originate principally from sedimentary rocks, which contribute $\sim$ 90% of the total products, $\sim$ 66% being derived from carbonate deposits; and (b) the relative rates at which the rocks are weathered follows the overall sequence evaporites $\gg$ carbonate rocks $\gg$ crystalline rocks, shales and sandstones. However, these are general trends, and in practice the extent to which a crustal terrain is weathered depends on a complex of interrelated topographic and climatic factors.

Clear relations between the catchment geology and water chemistry have been demonstrated for a number of large river basins. For example,

Table 3.3 Major ion composition of rivers draining different rock types[a] (units, mg l^{-1})

	Plutonic and highly metamorphic rocks	Volcanic rocks	Sedimentary rocks
Na^+	Lithological influence displaced by oceanic influence		
K^+	1.0	1.5	1.0
Ca^{2+}	4.0	8.0	30
Mg^{2+}	1.0	3.0	8.0
Cl^-	Lithological influence displaced by oceanic influence		
SO_4^{2-}	2.0	6.0	25
HCO_3^-	15.0	45	100
TIC[b]	30	70	175

[a] Data from Maybeck (1981).
[b] TIC = total ionic content.

Stallard & Edmond (1981, 1983, 1987) assessed the influence of geology and weathering environment on the dissolved constituents in the rivers of the Amazon catchment. In doing this, they identified a number of water types on the basis of their **total cation concentration** (TZ^+) and were able to relate them to the general geology–morphology relationships of their catchments.

(a) Rivers with total cation concentrations in the range $0 < TZ^+ < 200$ μeq l^{-1} drain the most intensely weathered materials formed in transport-limited regimes; i.e. regimes in which the weathering rate exceeds the transport rate, where thick highly leached soils are developed. These rivers are enriched in silica relative to other major species, and also have cation ratios that are similar to those in the substrate rocks.

(b) Rivers with total cation concentrations in the range $200 < TZ^+ < 450$ μeq l^{-1} drain siliceous terrains and are also rich in silica relative to other dissolved species. The highest TZ^+ values in this range are found for rivers draining weather-limiting siliceous terrains; i.e. regimes in which weathered material is removed as fast as it is produced. In the Amazon catchment these rivers tend to have a cation load that is preferentially enriched in Na relative to K, and in Ca relative to Mg, compared to the catchment rocks.

(c) Rivers with total cation concentrations in the range $450 < TZ^+ < 3000$ μeq l^{-1} drain marine sediments or red beds with high cation concentrations arising from the presence of carbonates, reduced shales and minor evaporites. These river waters have relatively high concentrations of Ca and Mg, high alkalinity and, for rivers draining reduced shales and minor evaporites, high SO_4^{2-}.

(d) Rivers with total cation concentrations in the range $TZ^+ > 3000$ $\mu eq\ l^{-1}$ drain massive evaporites, and are rich in Na and Cl.

The Amazon study provides a modern database for the major dissolved species composition of surface waters. However, the relatively simple relationships between the major species found in the Amazon waters are probably *not* reflected in global surface waters, at least to the same degree. One reason for this is that the Amazon Basin lies within the humid tropics, where the environmental conditions favour the formation of cation-depleted solids in geologically short time periods. However, the rock composition–water chemistry relationships have also been demonstrated for other large rivers, e.g. the Mackenzie River, which is an example of a large unpolluted system in a temperature region (see e.g. Reeder *et al.* 1972), and the relationships found for the Amazon do appear to be generally similar to those found for other rivers (see e.g. Holland 1978).

It is apparent, therefore, that river waters can be characterized on the basis of their major ionic constituents. The total concentrations, and mutual proportions, of these constituents are regulated by a variety of interrelated parameters. However, rock weathering is the principal control on the dissolved major element chemistry of the vast majority of the world's rivers, with regional variations being controlled by the lithological character of the individual catchment. The dissolved solid loads transported by rivers are correlated with mean annual run-off (see e.g. Walling & Webb 1987), and although the *concentrations* of dissolved solids decrease with increasing run-off, as a result of a dilution effect, the *flux* of dissolved solids increases.

3.1.3.2 Trace elements The sources that supply the major constituents to river waters (e.g. rock weathering, atmospheric deposition, pollution) also release trace elements into surface waters. Although relatively few reliable analyses have been reported for these trace constituents, a number of modern data sets have become available over the past few years and a summary of some of these is given in Table 3.4. The table includes the data set produced by Yeats & Bewers (1982). These authors made a compilation of the concentrations of dissolved trace elements in a number of major rivers and found, perhaps surprisingly, that there was a reasonable agreement between them. This led them to suggest that many of the observed differences in the composition of river water are probably a consequence of temporal variability, rather than being a result of major compositional variations. However, the factors that control the distributions of dissolved trace elements in large river systems are considerably less well understood than those that govern the major constituents. The geology of a river catchment will obviously impose a fundamental

Table 3.4 Recent data on the concentrations of some dissolved elements in river water

	Data source																		
Element	1	2	3	4	5	6	7	8	9	10	11	12	13	14	15	16	17	18	19
Fe ($\mu g\ l^{-1}$)	55	20-75	5-60	-	-	130	-	4.9	30	-	-	-	30	-	-	-	125	40	40
Mn ($\mu g\ l^{-1}$)	6.3	-	-	-	-	8.3	-	10	-	-	-	-	19	-	-	-	12	8.2	8.2
Al ($\mu g\ l^{-1}$)	64	-	-	-	-	36	-	-	-	-	-	-	40	-	-	-	224	50	50
Cd ($ng\ l^{-1}$)	111	9-25	11-25	25-38	-	-	-	90	-	-	-	390	-	-	-	-	200	-	50[a]
Cu ($\mu g\ l^{-1}$)	2.5	1.1-1.4	1.0-1.3	1.0-1.3	1.5	0.3	-	1.9	-	-	1.1	6.3	1.8	-	-	-	4.8	1.5	1.5
Ni ($\mu g\ l^{-1}$)	1.5	0.7-0.9	0.7-1.3	0.23	0.29	-	-	1.6	-	0.5	-	-	-	-	-	-	2.1	0.5	0.5
Pb ($\mu g\ l^{-1}$)	-	0.09-0.2	0.08-0.2	-	-	-	-	-	-	-	-	-	-	-	-	-	-	0.1	0.1
Zn ($\mu g\ l^{-1}$)	8.6	6-7	6-7	-	-	-	-	10	-	-	-	54	-	-	-	0.39	21	30	0.39
Cr ($\mu g\ l^{-1}$)	-	-	-	-	-	-	0.7	-	-	-	-	-	-	-	-	-	-	1.0	1.0
Co ($\mu g\ l^{-1}$)	0.15	-	-	-	-	-	-	-	-	-	-	-	0.06	-	-	-	0.14	0.2	0.2
Ge ($ng\ l^{-1}$)	-	-	-	-	-	-	-	-	-	-	-	-	-	8.1	-	-	-	-	-
Sn ($ng\ l^{-1}$)	-	-	-	-	-	-	-	-	-	-	-	-	-	-	1.4	-	-	-	-
V ($\mu g\ l^{-1}$)	-	-	-	-	-	-	-	-	-	-	-	-	-	-	-	-	-	1.0	1.0

1. St. Lawrence river (Yeats & Brewers 1982).
2. Gota river (Danielsson et al. 1983).
3. Nodre river (Danielsson et al. 1983).
4. Changjiang river (Edmond et al. 1985).
5. Amazon river (Boyle et al. 1982).
6. Zaire river (Maybeck 1978).
7. St. Lawrence estuary (Campbell & Yeats 1984).
8. Mississippi river (Trefry & Presley 1976).
9. Rhine river (Eisma 1975).
10. Amazon river (Sclater et al. 1976).
11. Amazon river (Boyle et al. 1977b).
12. Rhine river (Duinker & Kramer 1977).
13. Amazon river (Gibbs 1972, 1977).
14. Average inorganic Ge; remote, clean rivers (Froelich et al. 1985).
15. Geometric average 45 rivers (Byrd & Andreae 1968).
16. Average S. American and N. American rivers (Shiller & Boyle 1985) .
17. Average of the data set given by Yeats & Brewers 1982 .
18. Average global river water (Martin & Whitfield 1983).
19. Average used in present work for flux calculations; [a] - an attempt to estimate a global average for Cd assuming a Cd concentration of 200 ng l^{-1} for run-off from N. America and Europe (~ 10% global run-off) and a concentration of 30 ng l^{-1} for the remaining run-off.

constraint on the amounts of trace elements available for mobilization and transport. Despite this, some of the data available suggest that the relatively clear-cut rock–water chemistry relationships found for the major constituents do not universally apply to the trace elements. For example, in their study of the Mackenzie River system, Reeder *et al.* (1972) were unable to find any clear relationships between the distributions of Ni, Cu and Zn and rock lithology, thus giving an indication that factors in addition to relatively simple rock–water chemistry relationships control the concentrations of dissolved trace elements in river waters. These factors are related to the dissolved–particulate speciation of the elements and are influenced by the nature of the weathering solutions. The leaching mechanisms involved in the weathering of continental rocks are controlled mainly by carbonic acid and organic acids produced by biological activity, and to a lesser extent by mineral acids; the latter being enhanced in areas which receive acid rain. If organic acid leaching predominates, the solubility of many trace elements will be increased both as a result of the formation of complexes with organic ligands and by the stabilization of metal-containing colloids by organic material (GESAMP 1987). For example, Windom & Smith (1985) gave data showing that the concentrations of dissolved Fe, Zn, Pb and Cd in river water increase as the concentration of dissolved organic carbon increases. Further evidence that factors other than simple rock–water relationships affect the dissolved concentrations of trace elements in rivers has also been provided by Shiller & Boyle (1985), who reported one of the few modern studies carried out with the aim of providing reliable data for dissolved trace metals in rivers on a quasi-global scale. The authors applied well tested modern analytical techniques to the determination of dissolved Zn in a number of rivers draining both pristine and anthropogenically influenced catchments. The data reported by these authors, some of which are given in Table 3.4, showed that, in river systems which have suffered relatively little anthropogenic perturbation, dissolved Zn concentrations are typically only $\sim$ 390 ng l^{-1}, whereas in systems influenced by anthropogenic inputs the concentrations are one to two orders of magnitude higher (see Table 3.4). One of the most significant findings to emerge from the study was that in the pristine rivers there was evidence of a degree of dependence between the dissolved Zn concentrations and the pH (acidity) of the waters, alkaline rivers being depleted in dissolved Zn relative to acidic systems. The authors concluded that this pH dependence did not reflect source rock composition, but was more likely to be chemical in nature, resulting from the adsorption of Zn onto, or its desorption from, suspended particulate matter. Fluvial dissolved Zn concentrations were therefore thought to be controlled by reversible adsorption–desorption reactions; however, since the concentration of dissolved organic carbon is related to pH, the

increased trace element concentrations associated with decreasing pH could be due to complexation with organic matter. A dependence of dissolved trace element concentrations on pH has also been suggested for Be in river waters by Measures & Edmond (1983), who showed that the mobility of the element was a strong function of pH, with acid streams (pH < 6) being strongly enriched with dissolved Be compared to alkaline carbonate rivers in which the element had been flocculated or adsorbed onto particulate matter. Higher dissolved Fe concentrations are also found in rivers with relatively high pH values. However, the rock–water chemistry relationship can also exert a control on the fluvial concentrations of trace elements. For example, Measures & Edmond (1983) reported data showing that, in addition to the pH dependence described above for Be, there was also a first-order separation between streams draining siliceous rocks (^{9}Be > 9 ng l^{-1}) and those draining uplifted Andean belts dominated by marine sediments (^{9}Be < 9 ng l^{-1}). The rock–water chemistry relationship was also demonstrated in a recent study reported by Froelich *et al.* (1985). These authors presented data on the concentrations of inorganic Ge in 56 rivers, which included seven of the largest in the world. Germanium concentrations averaged ~ 8 ng l^{-1} in 'clean' rivers, compared to ~ 136 ng l^{-1} in polluted systems, which again demonstrates the effect that anthropogenic inputs can have on fluvial trace element levels. The inorganic Ge exhibited a silicon-like behavioiur pattern during continental weathering and the average naturally weathered fluvial flux carried a Ge : Si atom ratio signal of ~ 0.7×10^{-6}, which is close to that in average continental granites. However, this rock–water chemistry relation was perturbed in rivers that had suffered contaminant inputs, where the Gi : Si ratios could be up to 10 times higher than the natural background. The effects of anthropogenic inputs on the concentrations of trace elements in river waters has also been demonstrated for dissolved Sn by Byrd & Andreae (1986); these authors reported that the concentrations of dissolved Sn ranged from as low as ~ 0.2 ng l^{-1} in pristine rivers to as high as ~ 500 ng l^{-1} in very polluted systems, with an average concentration of 1.3 ng l^{-1} in global river water.

It may be concluded, therefore, that the concentrations of many dissolved trace elements in river waters are influenced by several factors. These include: (a) geology of the river catchment; (b) chemical constraints within the aqueous system itself, chiefly particulate–dissolved equilibria, which can involve both inorganic and organic suspended solids (including biota) and are influenced by factors such as pH and the concentrations of complexing ligands; and (c) anthropogenic inputs.

3.1.4 Major and trace elements: the particulate river signal

In the present context, river particulate material (RPM) refers to solids carried in suspension in the water phase, i.e. the suspended sediment

load. RPM consists of a variety of components dispersed across a spectrum of particle sizes. These components include the following: primary aluminosilicate minerals, e.g. feldspars, amphiboles, pyroxenes, micas; secondary aluminosilicates, e.g. the clay minerals; quartz; carbonates; hydrous oxides of Al, Fe and Mn; and various organic components. In addition to the discrete oxides and organic solids, many of the individual suspended particle surfaces are coated with hydrous Mn and Fe oxides and/or organic substances.

The mineral composition of RPM represents that of fairly homogenized soil material from the river basin and as a result each river tends to have an individual RPM mineral signature. This was demonstrated in a recent study reported by Konta (1985) who gave data on the distributions of crystalline minerals in RPM from 12 major rivers. The results of the study may be summarized as follows.

(a) Clay minerals, or sheet silicates, were the dominant crystalline components of the RPM, although the distributions of the individual minerals differed. Mica–illite minerals were the principal sheet silicates present and were found in all the RPM samples. Kaolinite was typically found in higher concentrations in RPM from tropical river systems where weathering intensity is relatively high, e.g. the Niger and the Orinoco. Chlorite was found in highest concentrations in kaolinite-poor RPM, and tended to be absent in RPM from rivers in tropical or subtropical areas of intense chemical weathering. Montmorillonite was found only in RPM from some tropical and subtropical rivers.
(b) Significant quantities of quartz were present in RPM from all the rivers except one.
(c) Other crystalline minerals found as components of RPM included acid plagioclase, potassium feldspar and amphiboles.
(d) Calcite and/or dolomite were reported in RPM from seven of the rivers, but it was not known if these minerals were detrital or secondary in nature.

The crystalline components of RPM are therefore dominated by the clay minerals, and the distribution of these minerals reflects that in the basin soils, which itself is a function of source rock composition and weathering intensity. As a result, the clays in RPM have a general latitudinal dependence; e.g. kaolinite has its highest concentrations in RPM from tropical regions. This imposition of latitudinal control on the distribution of clay minerals in soils is used in Section 15.1.1 to trace the dispersion of continentally derived solids throughout the oceans. However, the mineral composition of RPM is also dependent on particle size. For example, the size distribution of RPM transported by the

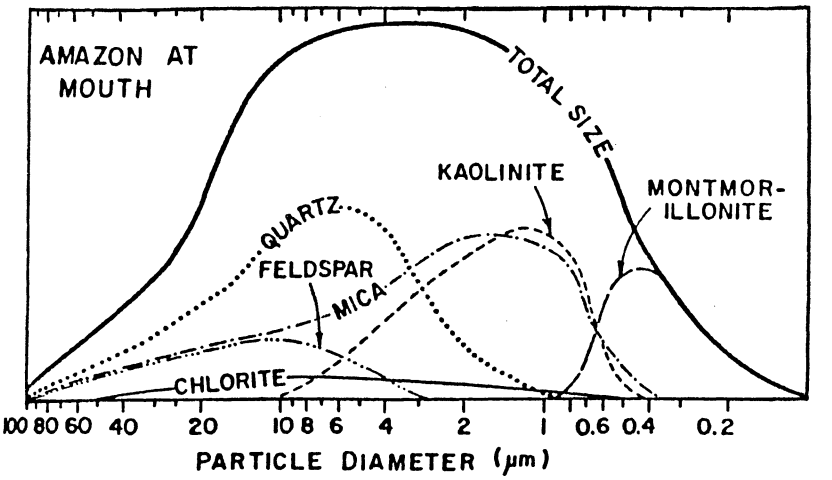

Figure 3.2 The size distribution of mineral phases transported by the Amazon River (from Gibbs 1977).

Amazon is illustrated in Figure 3.2, and demonstates that, whereas quartz and feldspar are found mainly in the > 2 μm diameter fraction, mica and the clay minerals, kaolinite and montmorillonite, are concentrated in the < 2 μm fraction. This mineral size fractionation has important consequences for the 'environmental reactivity' of elements transported via RPM, and this topic is considered below when elemental partitioning among the various components of the solids is discussed. For a first look, however, the chemical composition of RPM will be described in terms of the total samples.

Martin & Maybeck (1979) have provided an estimate of the global chemical composition of the total samples of river particulate material. This estimate was based on the determination of 49 elements in RPM from a total of 20 of the world's major rivers, and since there are considerably fewer problems involved in the analysis of particulate than of dissolved trace elements, it provides a generally reliable compositional database for RPM. Highly polluted river systems were excluded from the study, and the findings therefore refer to RPM that has its composition controlled largely by natural processes. Under these conditions the RPM is mainly derived from the surface soil cover following the mechanical and chemical weathering of the surficial parent rocks. A partial data set for the chemical composition of RPM is given in Table 3.5, in order to indicate the variability between suspended solids in different rivers. On the basis of data such as these, Martin & Maybeck (1979) were able to identify a number of important trends in the chemistry of RPM.

(a) For individual river systems the concentrations of the major

Table 3.5 The concentrations of some elements in RPM from selected individual rivers[a]

River	Element ($\mu g\ g^{-1}$)									
	Al	Fe	Ca	Mn	Ni	Co	Cr	V	Cu	Zn
Amazon	115000	55000	16000	1030	105	41	193	232	266	426
Colorado	43000	23000	34000	430	40	17	82	-	-	-
Zaire	117000	71000	8400	1400	74	25	175	163	-	400
Ganges	77000	37000	26500	1000	80	14	71	-	30	163
Garonne	118000	58000	19500	1700	33	39	255	150	51	874
Mackenzie	78000	36500	35800	600	22	14	85	-	42	126
Mekong	112000	56000	5900	940	99	20	102	175	107	300
Niger	156000	92000	3300	650	120	40	150	180	60	-
Nile	98000	108000	40000	-	-	-	-	-	39	93
St. Lawrence	78000	48500	23000	700	-	-	270	-	130	350

[a] Data from Martin & Maybeck (1979).

elements in the RPM are not usually highly variable. For trace elements, the variations are much larger; however, they do not exceed one order of magnitude, and are much smaller than those found between different rivers.

(b) Inter-river, i.e. geographical, variability in the composition of RPM differs considerably from one element to another. On the basis of the coefficient of variation (s/x) in the RPM, the elements were divided into a number of groups: (i) those which are most consistent ($s/x < 0.2$), e.g. Si, Th and the rare earths Ce, Eu, La, Sm and Yb; (ii) those which exhibit slight variability ($s/x = 0.2$–0.35), e.g. Al, Fe, K, Hf, Sc, Ta and U; (iii) those which exhibit moderate variability ($s/x = 0.35$–0.70), e.g. Ag, Cr, Mg and Na; (iv) those which are highly variable ($s/x > 0.70$), e.g. Ca, Cs, Cu, Li, Mo, Ni, Pb, Sr and Zn.

The variability for some of the major elements in the RPM can be related to climatic–weathering intensity conditions in the river catchments. Many *tropical* rivers have large areas in their drainage basins in which the rate of mechanical erosion is generally low, and the RPM originates mainly from highly developed soil material that has undergone chemical weathering, i.e. transport-limited regimes. The RPM in this type of river is enriched in those elements which are generally relatively insoluble during chemical weathering, e.g. Al, Ti and Fe, and is depleted in the more soluble elements, which are leached into the weathering solutions,

e.g. Na and Ca. In contrast, many *temperate* and *arctic* rivers have drainage basins in which mechanical erosion can greatly exceed chemical weathering, i.e. weathering-limited regimes. As a result, the parent material of the RPM in these rivers is either original rock debris or poorly weathered soils. Relative to the world average RPM, that found in temperate and arctic rivers tends to be depleted in Al, Ti and Fe, and enriched in Na and Ca, and its overall composition is closer to that of fresh rock than the RPM from tropical rivers.

It is apparent, therefore, that there is a considerable variability in the concentrations of some elements in RPM from different rivers, even when the material is derived from mainly natural sources. Nonetheless, the data for RPM given in Table 3.5 do offer an indication of chemical composition of the crust-derived solid material that is brought to the ocean margins by river transport. A more complete data set for the chemical composition of RPM is given in Table 3.6, together with the compositions of the continental rock and soil source materials and dissolved river constituents.

Up to this point we have described the elemental chemistry of RPM in terms of **total sample** composition. However, it was pointed out above that RPM consists of a variety of individual components, which are present in a range of particle sizes. The elements in suspended particulates, and also in deposited sediments, are partitioned between these individual host components, some of which can bind them more strongly than others. In this respect, it is important to make a fundamental distinction between two genetically different element–host associations: (a) elements associated with the crystalline mineral matrix (the **detrital** or **residual** fraction), which are in an environmentally immobile form and have their concentrations largely fixed at the site of weathering; and (b) elements associated with non-crystalline material (the **non-detrital** or **non-residual** fraction), which are in environmentally mobile forms and have their concentrations modified by dissolved $\leftrightarrow$ particulate reactivity. A number of elemental associations are usually identified within the non-detrital fraction itself, e.g. an exchangeable fraction, a carbonate-associated fraction, a metal oxide-associated fraction, an organic matter-associated fraction. A variety of techniques have been used to establish the partitioning of elements among these host components, and one of the most common involves the sequential leaching of the primary sample with a number of reagents that are designed progressively to take into solution elements associated with the individual hosts. Such sequential leaching techniques are open to a number of severe criticisms (see e.g. Chester 1988), not the least of which is that the host fractions identified are operationally defined in terms of the technique used, and so are not necessarily analogues of natural binding fractions. However, when the various constraints on their use are

Table 3.6 The average compositions of crustal rocks, soils, and dissolved and particulate river material

	Continents		Rivers	
	Rock ($\mu g\ g^{-1}$)	Soils ($\mu g\ g^{-1}$)	Dissolved ($\mu g\ l^{-1}$)	Particulate ($\mu g\ g^{-1}$)
Ag	0.07	0.05	0.3	0.07
Al	69300	71000	50	94000
As	7.9	6	1.7	5
Au	0.01	0.001	0.002	0.05
B	65	10	18	70
Ba	445	500	60	600
Br	4	10	20	5
Ca	45000	15000	13300	21500
Cd	0.2	0.35	0.02	(1)
Ce	86	50	0.08	95
Co	13	8	0.2	20
Cr	71	70	1	100
Cs	3.6	4	0.035	6
Cu	32	30	1.5	100
Er	3.7	2	0.004	(3)
Eu	1.2	1	0.001	1.5
Fe	35900	40000	40	48000
Ga	16	20	0.09	25
Gd	6.5	4	0.008	(5)
Hf	5	-	0.01	6
Ho	1.6	0.6	0.001	(1)
K	24400	14000	1500	20000
La	41	40	0.05	45
Li	42	25	12	25
Lu	0.45	0.4	0.001	0.5
Mg	16400	5000	3100	11800
Mn	720	1000	8.2	1050
Mo	1.7	1.2	0.5	3
Na	14200	5000	5300	7100
Nd	37	35	0.04	35
Ni	49	50	0.5	90
P	610	800	115	1150
Pb	16	35	0.1	100
Pr	9.6	-	0.007	(8)
Rb	112	150	1.5	100
Sb	0.9	1	1	2.5
Sc	10.3	7	0.004	18
Si	275000	330000	5000	285000
Sm	7.1	4.5	0.008	7
Sr	278	250	60	150
Ta	0.8	2	< 0.002	1.25
Tb	1.05	0.7	0.001	1.0
Th	9.3	9	0.1	14
Ti	3800	5000	10	5600
Tm	0.5	0.6	0.001	(0.4)
U	3	2	0.24	3
V	97	90	1	170
Y	33	40	-	30
Yb	3.5	-	0.004	3.5
Zn	127	90	30	250

[a] Data from Martin & Whitfield (1983); after Martin & Maybeck (1979).

recognized, sequential leaching techniques can provide important data on the manner in which elements are partitioned in materials such as suspended river particulates, sediments and aerosols.

A number of studies have been carried out on the partitioning of elements in RPM. Outstanding among these are the pioneer investigations reported by Gibbs (1973, 1977) on suspended particulates from the Amazon and Yukon rivers. These two rivers were selected because they are large, relatively unpolluted systems representative of the major rivers that have their catchments in tropical (Amazon) and subarctic (Yukon) land masses and drain a wide variety of rock types. In both studies, Gibbs gave data on the partitioning of a number of elements in river-transported phases. To do this, he distinguished between: elements in *solution* (1), and those associated with *particulates* in an ion-exchange phase (2), a precipitated metallic oxide coating phase (3), an organic matter phase (4), and a crystalline (detrital or residual) phase (5). A summary of the partitioning data reported by Gibbs (1973) is given in Table 3.7. A number of general conclusions can be drawn from these data.

(a) The fraction of the total amounts of the metals transported in solution ranges from $< 1\%$ for Fe to $\sim 17\%$ for Mn, but solution transport is not dominant for any of the metals.
(b) The partitioning signatures of Fe, Mn, Ni, Cu, Co and Cr are

Table 3.7 The percentage partitioning of elements in RPM[a]

River transport phase	Element					
Amazon River	Fe	Ni	Co	Cr	Cu	Mn
Solution	0.7	2.7	1.6	10.4	6.9	17.3
Ion exchange	0.02	2.7	8.0	3.5	4.9	0.7
Metal oxide coating	47.2	44.1	27.3	2.9	8.1	50
Organic matter	6.5	12.7	19.3	7.6	5.8	4.7
Crystalline matrix	45.5	37.7	43.9	75.6	74.3	27.2
Yukon River						
Solution	0.05	2.2	1.7	12.6	3.3	10.1
Ion exchange	0.01	3.1	4.7	2.3	2.3	0.5
Metal oxide coating	40.6	47.8	29.2	7.2	3.8	45.7
Organic matter	11.0	16.0	12.9	13.2	3.3	6.6
Crystalline matrix	48.2	31.0	51.4	64.5	87.3	37.1

[a] Data from Gibbs (1973).

similar in RPM from both the tropical and the subarctic river systems.

(c) Cu and Cr are transported mainly in the crystalline particulate phase.

(d) Mn is principally transported in association with the precipitated metal oxide particulate phase.

(e) Most of the total amounts of Fe, Ni and Co are partitioned between the precipitated metal oxide and crystalline particulate phases.

(f) The non-crystalline carrier phases represent the particulate metal fraction which is most readily available to biota, and the most important of these carriers are the metal oxide coatings.

(g) There is a particle size–concentration relationship for a number of elements in the RPM, with concentrations of Mn, Fe, Co, Ni and Cu all increasing dramatically with decreasing particle size.

The general RPM solid-state partitioning trends reported by Gibbs (1973, 1977) for the Amazon and Yukon have subsequently been confirmed for other rivers. For example, Tessier *et al.* (1980) found that metal oxide coatings, together with organic phases, are the most important non-crystalline trace metal particulate carriers in the Yamaska and St. Francois rivers (Canada). These authors also reported that when metals are supplied to the waters from anthropogenic sources they are captured by non-crystalline particualte phases, especially the metal oxide and organic host fractions, which results in a decrease in the proportions of most metals held in the crystalline matrix.

It may be concluded, therefore, that in river systems that receive their supply of trace elements mainly from natural sources, crystalline, metal oxide and organic host fractions are the principal metal carriers. It is the non-crystalline phases that are the most readily environmentally available, and the proportions of particulate trace metals associated with these phases generally increase in river systems that receive inputs from pollutant sources. The various total element, solid-state partitioning, mineral and particle size data for RPM can be combined to develop the general concept that rivers transport two different types of suspended solids: (a) a **trace element-poor**, large-sized ($\gtrsim 2$ μm diameter) fraction that consists mainly of crustal minerals such as quartz and the feldspars, a large proportion of the trace elements in this fraction being in crystalline solids and generally environmentally immobile; (b) a **trace element-rich**, small-sized ($\lesssim 2$ μm diameter), surface-active fraction that consists largely of clay minerals, organic matter and iron and manganese oxide surface coatings, a large proportion of the trace elements in this fraction being associated with non-crystalline carriers (e.g. oxide coatings and organic phases) and environmentally available. It must be stressed that there is no sharp division between these two fractions, but the distinction

between them is extremely important both (a) from the point of view of differential transport, i.e. the small-sized material can be carried for a longer period in suspension, and (b) because it is the small-sized, non-crystalline, environmentally available trace elements that undergo the dissolved ↔ particulate equilibria that play such an important role in controlling the river → estuarine → coastal sea → open ocean transport–deposition cycles of many elements and in regulating the composition of sea water. The non-residual elements can undergo changes between the various solid-state carrier phases themselves. All of these particulate ↔ dissolved and solid-state changes are sensitive to variations in environmental parameters (e.g. the concentrations of particulate material and complexing ligands, redox potential, pH), so that during the global transportation cycle the mobile surface-associated elements can undergo considerable speciation migration.

3.1.5 Organic matter and nutrients

3.1.5.1 Dissolved organic carbon (DOC) A compilation of DOC concentration data for a number of rivers is given in Table 3.8, from which it is apparent that the concentrations range from as low as < 0.5 mg l^{-1} to as high as 50 mg l^{-1}. According to Mantoura & Woodward (1983) these data reveal a catchment-related pattern in the DOC concentrations, with low values being found in rivers draining glacial or alpine environments, and the highest values occurring in rivers draining swamp regions. Intermediate values, lying between ~ 2 and ~ 10 mg l^{-1}, have been

Table 3.8 The concentrations of DOC in some rivers[a]

River	DOC (mg l^{-1})
North Dawes (Alaska)	0.5
Alpine streams	1.5 - 5
Amazon (Brazil)	2.0 - 6.3
Mississippi (USA)	3.4 - 6.0
Severn (UK)	3.1 - 7.8
Missouri (USA)	1.9 - 9.0
Ems-Dollart (Holland)	7 - 18
Yukon (USA)	16
Sopchoppy (USA)	6 - 52
Satilla (USA)	25 - 30

[a] Data compilation from Mantoura & Woodward (1983).

reported for a number of major rivers, including the Amazon, the Mississippi, the Mackenzie and the Columbia. The weighted global average river-water concentration of DOC is 5.75 mg l^{-1} (Ertel *et al.* 1986).

The DOC found in river waters originates mainly from three general sources: (a) soils, where the organic matter is derived from plant and animal material via microbial activity; (b) fluvial production; and (c) anthropogenic inputs. In non-polluted river systems the DOC pool thus contains organic matter synthesized and degraded in both the terrestrial (allochthonous) and aqueous (autochthonous) environments. According to Ertel *et al.* (1986) between ~ 40 and ~ 80% of fluvial DOC consists of combined humic substances, which are generally considered to be refractory material that can escape degradation in the fluvial–estuarine environment and so reach the ocean. Ertel *et al.* (1986) gave data on the humic and fulvic acid components of the DOC humic fraction in the Amazon River system. Both these components contain lignin (a phenolic polymer unique to vascular plants) and appear to be formed from the same allochthonous source material, but they differ in the extent to which they have suffered biodegradation in the soil, fulvic acids being more oxidized than humic acids. In the Amazon system the fulvic acids do not undergo reactions with suspended particles and behave in a conservative manner. In contrast, humic acids can be adsorbed onto particle surfaces and can also undergo flocculation in the estuarine environment (see Secs 3.2.5 & 3.2.6). In view of this, Ertel *et al.* (1986) suggested that humic acids may not contribute carbon, or lignin, to the oceans, and that it is fulvic acids which represent the major proportion of the DOC input to sea water. The autochthonous DOC includes potentially very labile (metabolizable) biochemical material, such as proteins and carbohydrates, and less labile components, such as lipids and pigments; much of this labile material is likely to be degraded in the river or estuarine system and so will not escape into the open ocean (see also the refractory–labile classification of POC below).

3.1.5.2 Particulate organic carbon (POC) POC concentrations in river waters also vary, but generally appear to be in the range ~ 1 to ~ 2.5 mg l^{-1}, although higher values are found in streams draining swamps and saltmarshes and in those rivers which receive relatively large inputs of sewage and industrial wastes. Few data exist on the detailed chemical composition of fluvial POC. However, in a recent study Degens & Ittekkot (1985) attempted to differentiate between stable (non-metabolizable) and labile (metabolizable) fractions of river-transported POC. This is an important distinction because, while the stable fractions will survive microbial attack, the labile fraction can be lost within rivers, estuaries and the sea. Degens & Ittekkot (1985) used carbohydrates and amino acids,

which are comparatively labile in character, as indicators of degradable POC, and concluded that between ~ 5 and ~ 30% of the POC carried by the world's rivers is labile in character. In a subsequent paper, Ittekot (1988) calculated that on a global basis ~ 35% of the fluvial POC is labile and so has the potential to become oxidized. The remainder of the POC, which is highly degraded in character, can escape to the oceans and so represents a signficant source of organic carbon to marine sediments.

3.1.5.3 The nutrients Nitrate, phosphates and silicate in river water are each derived from different sources.

PHOSPHATES Phosphorus is present in river waters in dissolved and particulate forms. The dissolved phosphorus is mainly orthophosphate (principal species HPO_4^{2-}), together with dissolved organic phosphate and, in polluted systems, polyphosphate. According to Maybeck (1982) the global average river-water concentration of total dissolved phosphorus is 28 $\mu g\ l^{-1}$, and that of total particulate phosphorus is 530 $\mu g\ l^{-1}$, of which 320 $\mu g\ l^{-1}$ is in an inorganic form and 210 $\mu m\ l^{-1}$ is in an organic form. The sources of dissolved phosphate (PO_4^{3-}) in river waters include the weathering of crustal minerals (e.g. aluminium orthophosphate, apatite) and anthropogenic inputs (e.g. from the oxidation of urban and agricultural sewage and the breakdown of polyphosphates used in detergents). Dissolved phosphorus is removed during biological production, and is often considered to be the limiting nutrient in river systems. In addition, however, the concentrations of dissolved inorganic phosphorus in river waters are significantly affected by chemical processes involved in mineral–water equilibria, e.g. those involving adsorption onto phases such as clay minerals and ferric hydroxides.

NITRATE Nitrate (NO_3^-), which originates mainly from soil leaching, terrestrial run-off (including that from fertilized soils) and waste inputs, is the most abundant stable inorganic species of nitrogen in well oxygenated waters, but dissolved organic nitrogen may dominate in humid tropical and subarctic rivers. River water also contains particulate nitrogen, which is mainly biological in origin. The average concentration of total dissolved nitrogen in a wide range of unpolluted river systems has been estimated by Maybeck (1982) to be 375 $\mu g\ l^{-1}$, of which 115 $\mu g\ l^{-1}$ is present as dissolved inorganic species (very largely nitrate) and 260 $\mu g\ l^{-1}$ is in the form of dissolved organic species. Fewer data are available for the concentration of particulate nitrogen in river water, but Maybeck (1981) estimated a value of ~ 560 $\mu g\ l^{-1}$ as a global river average. Biological reactions dominate the transfer of inorganic dissolved nitrogen to the particulate phase.

SILICATE Dissolved reactive silicate is present in river waters almost exclusively as silicic acid (H_4SiO_4), and is derived mainly from the weathering of silicate and aluminosilicate minerals; i.e. unlike nitrogen and phosphorus, anthropogenic sources play a relatively minor role in the supply of dissolved silicon to rivers. Dissolved silicon is a major constituent of river water, making up ~ 10% of the total dissolved solids, and its global average concentration has been estimated to be 4.85 mg l^{-1} (Maybeck 1979). Silicon is also present in river water in a variety of particulate forms, which include inorganic minerals (e.g. quartz, aluminosilicates) and biological material (e.g. the opaline skeletons of diatoms).

3.1.6 Pollutant inputs

In addition to the mainly natural processes that have been discussed above, the input of pollutants, via industrial and domestic wastes, can exert a significant influence on the dissolved major and trace element compositions of some river waters, especially those of northern Europe and the United States. There are many examples of this in the literature, but a survey carried out on the Rhine will serve as an illustration. This river rises in the Swiss Alps, where it receives its water from a series of catchments that are relatively free from human influence, and subsequently flows through very heavily populated and industrialized areas before reaching the land/sea boundary. Zorbrist & Stumm (1981) presented compositional data which indicated that at the present time the concentrations of dissolved constituents in the waters of the High Rhine are smaller than those in the waters of the Lower Rhine. Their findings are illustrated in Figure 3.3, and show the extent to which pollution affects the dissolved species and varies from one component to another. At one extreme, the pollutant inputs have little or no influence on silicic acid and bicarbonate, but at the other extreme more than 90% of the sodium and chloride are anthropogenically derived. For the other constituents studied the effects of pollution lie between these two extremes.

Many other investigations have also revealed the influence that pollutant emissions have on river waters. For example, Van Bennekon & Salomons (1981) concluded that the global annual river discharge of nitrogen has been increased by a factor of about five, and that of phosphorus by a factor of about four, as a result of anthropogenic inputs. The sulphate content of river waters has also been markedly raised due to pollution of the atmosphere, and in some rivers the original content has been doubled by inputs from this source (Maybeck 1981). The concentrations of some trace elements, especially those of the toxic heavy metals, can also suffer extreme perturbations from pollutant discharges in some rivers. Such discharges can increase the concentrations of metals

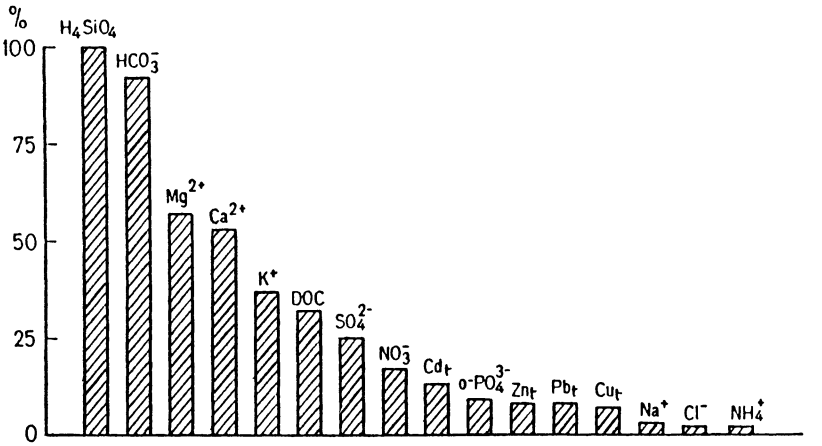

Figure 3.3 Components in 'pristine' Rhine river water as a percentage of the recent composition of the water (from Zorbrist & Stumm 1981).

such as Zn, Cd and Pb by factors as high as 500, and these may be even higher when acidic mine wastes drain into the rivers.

3.1.7 Relationships between the dissolved and particulate transport of elements in rivers

Material is transported by rivers in both dissolved and particulate forms, and in order to distinguish between the two phases Martin & Maybeck (1979) used the concept of a **dissolved transport index** (DTI), which expresses the amount of an element transported in solution as a percentage of its total (i.e. particulate + dissolved) transport. DTIs were calculated for a large range of elements found in river waters; however, it must be stressed that much of the dissolved trace element data used were suspect. Further, the DTIs reported by Martin & Maybeck (1979) are *global* averages and, since wide geographic variations can be found between individual rivers, the reliability of the values is probably no better than around ± 20%. Despite these constraints, a number of general trends could be identified from the investigation. For example, the elements transported by rivers could be divided into groups on the basis of their DTIs, and these are listed in Table 3.9. From this table it can be seen that elements exhibiting two extreme behaviour patterns can be distinguished. (a) Elements having DTIs in the range ~ 90 to ~ 50% are carried mainly in solution by rivers; these include Na, Ca, Cl and S. (b) Elements with DTIs < 1% are transported almost exclusively in a particulate form; these include Al and Fe. Other elements have

Table 3.9 The Dissolved Transport Index (DTI) in global river water (ranked in decreasing order)[a]

90-50%	Br, I, S, Cl, Ca, Na, Sr
50-10%	Li, N, Sb, As, Mg, B, Mo, F, Cu, Zn, Ba, K
10-1%	P, Ni, Si, Rb, U, Co, Mn, Cr, Th, Pb, V, Cs
1-0.1%	Ga, Tm, Lu, Gd, Ti, Er, Nd, Ho, La, Sm, Tb, Yb, Fe, Eu, Ce, Pr, Al

[a] Data from Martin & Maybeck (1979).

dissolved–particulate transport behaviour patterns that lie between these two extremes.

3.1.8 Chemical signals carried by rivers: summary

(a) Rivers transport large quantitites of both dissolved and particulate components, and in this sense they may be regarded as carriers of a wide variety of chemical signals to the land/sea margins.

(b) The dissolved major element composition of river water is mainly controlled by the chemical composition of the source rock that is weathered in the catchment region. However, these relatively simple rock–water chemistry relationships do not have the same degree of control on the dissolved trace element composition of river water, which appears to be strongly influenced by chemical constraints within the aqueous system itself; e.g. particulate–dissolved equilibria which involve both organic and biological particles, and which are influenced by factors such as pH and the concentrations of complexing ligands. Anthropogenic inputs can also influence the concentrations of trace metals in some river systems.

(c) The chemical composition of RPM from different rivers systems shows considerable variation, some of which may be due to climate-induced weathering intensity differences in catchment regions. Crystalline (residual), metal oxide and organic host fractions are the principal particulate trace metal carrier phases in rivers that receive their trace elements mainly from natural sources.

(d) There is a catchment-related pattern in the fluvial transport of POC and DOC by rivers, the highest concentrations being found in rivers draining swamp regions and the lowest in those flowing over glacial and alpine environments.

We have now tracked the transport of fluvial material to the river/ocean interface. However, before reaching either the coastal receiving zone or the open regions of the sea itself, the river-transported material must pass

through the estuarine environment. This environment can act as a filter, with the result that the fluvial signals can be severely modified before they are finally exported from the continents. The nature of these estuarine modifications is considered in the next section.

3.2 The modification of river-transported signals at the land/sea interface: estuaries

3.2.1 Introduction

Fairbridge (1980) defined as estuary as 'an inlet of the sea reaching into a river valley as far as the upper limit of the tidal rise'. This definition allows three distinct estuarine sections to be distinguished: (a) a marine (or lower) estuary, which is in connection with the sea; (b) a middle estuary, which is subject to strong sea water–fresh water mixing; and (c) an upper (or fluvial) estuary, which is characterized by freshwater inputs but which is subjected to daily tidal action. Estuaries are therefore zones in which sea water is mixed with, and diluted by, fresh water. These two types of water have different compositions (see Table 3.1), and as a result estuaries are very complex environments in which the boundary conditions are extremely variable in both space and time. As a result, river-transported signals are subjected to a variety of physical, chemical and biological processes in the estuarine mixing zone. From this point of view, estuaries can be thought of as acting as **filters** of the river-transported chemical signals, which can often emerge from the mixing zone in a form that is considerably modified with respect to that which entered the system (see e.g. Schink 1980). This concept of the estuarine filter is based on the fact that the mixing of the two very different end-member waters will result in the setting up of strong physicochemical gradients in an environment that is subjected to continuous variations in the supply of both matter and energy. It is these gradients which are the driving force behind the filter.

In the present section an attempt will be made to understand how estuaries work as chemical and physical biological filters. However, before doing this it is necessary to draw attention to three important points.

(a) The estuarine filter is selective in the manner in which it acts on different elements; for example, some dissolved species are simply diluted in an estuary and then carried out to sea, whereas others undergo reactions that lead to their addition to, or removal from, the dissolved phase.
(b) The effects of the filter can vary widely from one estuary to another, so that it is difficult to identify global estuarine processes.
(c) It is necessary to take into account the status of an estuary before any attempt is made to extrapolate its dynamics onto an ocean-wide scale.

Because of their environmental significance as material traps, estuaries require careful management, and as a result they have been the subject of considerable scientific interest over the past two or three decades. However, much of this interest has inevitably been directed towards relatively small urban estuarine systems, which are often highly perturbed by anthropogenic activities. Investigations of this type have provided invaluable insights into estuarine processes, but many of the estuaries themselves have little relevance on a natural global ocean scale. More recently, attempts have been made to study the chemical dynamics of major estuaries, such as those of the Amazon, the Zaire and the Changjiang (Yangtze) rivers. It is the processes operating on the river signals in these large systems which will have a major influence on the chemistry of the oceans, and in attempting to assess the importance of estuarine processes on fluvial signals it is therefore necessary to distinguish between such globally relevant estuaries and those which have a much more limited local effect. However, it must be stressed that an approach which concentrates only on large river–estuarine systems also has important limitations. For example, Holland (1978) has pointed out that the combined run-off of the 20 largest rivers in the world accounts for only ~ 30% of the total global river run-off; further, these rivers drain the wettest areas of the globe. Thus, although processes operating in globally relevant estuaries may provide a better understanding of the effects that the estuarine filter has on the fluxes of material that reach the oceans, the fluxes themselves will be biased and may not represent truly global values.

3.2.2 The estuarine filter: the behaviour of elements in the estuarine mixing zone

The estuarine filter operates on dissolved and particulate material, which flows through the system, and it can both modify and trap fluvially transported components within the mixing zone. The modification of the signals takes place via a number of physical, chemical and biological processes that involve dissolved ↔ particulate speciation changes. The equilibria involved can go in either direction, i.e. particulate material can act either as a **source** of dissolved components, which are released into solution, or as a **sink** for dissolved components, which are removed from solution. Since all the water in an estuary is eventually flushed out, usually on a timescale of days or weeks, it is only the **sediment** that can act as an internal (i.e. estuarine) sink for elements that are brought into the system by river run-off. However, the sediments are not a static reservoir within the estuarine system, but are in fact subjected to a variety of physical, biological and chemical processes (e.g. bioturbation, diagenesis), which can result in the recycling of deposited components back into the water compartment. These recycling processes include:

(a) the chemically driven diffusion of components from interstitial waters; (b) the physically driven flushing out of interstitial waters into the overlying water column; and (c) the tidal resuspension of surface sediments, and sometimes their transfer from one part of an estuary to another. The sediments themselves therefore play a significant biogeochemical role in estuaries, and according to Bewers & Yeats (1980) they can therefore be regarded as acting as a third end-member in estuarine mixing processes, i.e. in addition to river water and sea water.

The physicochemical processes that control the estuarine filter must therefore be considered to operate in terms of a framework involving particulate–dissolved recycling associated with three estuarine end-members, i.e. river water, sea water (which may consist of more than one component end-member) and sediments. This is illustrated in a very simplified diagrammatic form in Figure 3.4 in terms of the estuarine modification of the river signal. Within this framework the estuarine filter operates on the fluvial flux as it flows through the system. The filter does

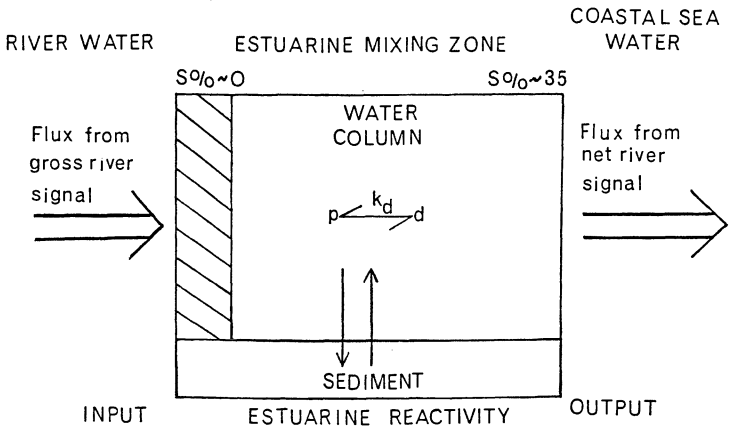

Figure 3.4 Simplified schematic representation of the modification of a river-transported signal in the estuarine environment. p $\xleftrightarrow{k_d}$ d Indicates particulate–dissolved reactivity associated with physical, chemical and biological processes in the estuarine mixing zone. In natural waters the equilibrated partitioning of an element between dissolved and particulate phases can be described by a conditional partition coefficient k_d, $k_d = X/C$, where X is the concentration of the exchangeable element on the particulate phase and C is the concentration of the element in the dissolved phase – see Worksheet 3.1. ↑↓ Indicates two-way exchange of components between the water and sediment phases. □ Indicates the low-salinity zone of enhanced particulate–dissolved reactivity. For a discussion of gross and net river fluxes, see Section 6.1.

not, however, affect all fluvially transported chemical signals, and for this reason it is necessary as a first step to establish whether or not estuarine reactivity has actually taken place.

3.2.3 The identification of estuarine reactivity: the 'mixing graph' approach

One of the principal processes that modifies a river-transported chemical signal in an estuary is the physical mixing of fresh and saline waters of markedly different compositions along salinity (and other property) gradients. In the absence of any biogeochemical processes (reactivity) that lead to the addition or removal of a component, the physical mixing of the end-member waters would result in a linear relationship between the concentrations of a component and the proportions in which the two waters have undergone mixing (the salinity gradient), providing, that is, that the compositions of the end-members remain constant over a time approximating to the estuarine flushing time, and that there are no other sources or sinks for the components. This physical mixing relationship offers a useful baseline for assessing the effects that reactive biogeochemical processes have on the distribution of a component in an estuary. The technique most commonly employed for this utilizes **mixing graphs** or **mixing diagrams**. In these diagrams, the concentrations of a component in a suite of samples (usually including the end-member waters) is plotted against a conservative index of mixing, i.e. a component whose concentrations in estuarine waters are controlled only by physical mixing. Salinity is the most widely used conservative index of mixing, although other parameters (e.g. chlorinity) can also be employed for this purpose.

Mixing diagrams have most commonly been applied to dissolved components, and the theoretical relationships involved are illustrated in Figure 3.5a. If the distribution of a dissolved component is controlled only by physical mixing processes its concentrations in a suite of estuarine waters along a salinity gradient will tend to fall on a straight line, the **theoretical dilution line** (TDL), which joins the concentrations of the two end-members of the mixing series; under these conditions its behaviour is described as being **conservative** or non-reactive. In contrast, when the component is involved in estuarine reactions that result in its addition to, or its loss from, the dissolved state its concentrations will deviate from the TDL, and its behaviour is termed **non-conservative** or reactive. For such a component the dissolved concentration data will lie above the TDL if it is added to solution, and below the TDL if it is removed from solution – see Figure 3.5a. Non-conservative behaviour therefore induces curvature in an estuarine mixing graph as concentrations deviate from the TDL. This curvature may be restricted to certain ranges of salinity, and can thus allow a geochemist to identify the specific estuarine zone in which the reactions take place.

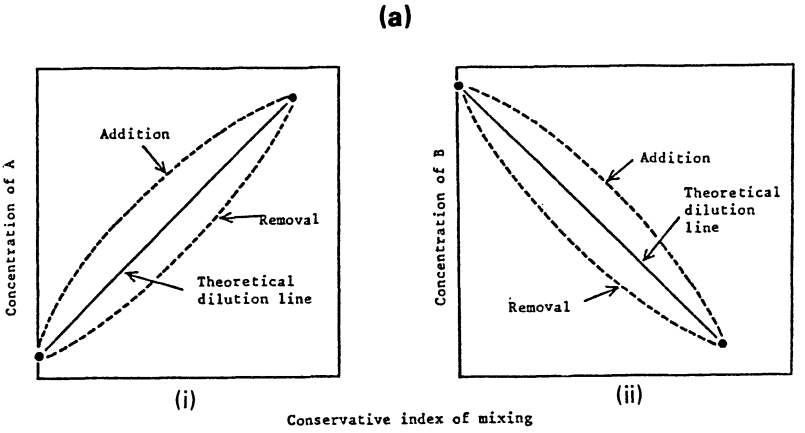

Figure 3.5 The behaviour of dissolved elements in estuaries. (a) Estuarine mixing graphs for (i) a component whose concentration is higher in sea water than in river water, and (ii) a component whose concentration is higher in river water than in sea water (from Liss 1976).

The mixing diagram is a relatively simple concept for describing the behaviour of a dissolved component during estuarine mixing, but in practice it suffers from a number of fundamental problems. For example, although it is generally easy to identify conservative behaviour, deviations from the TDL are more difficult to interpret since they may result from factors other than estuarine reactivity; e.g. from the input of non-end-member waters.

There have been various attempts to rationalize the interpretation of estuarine mixing graphs. For example, Boyle *et al.* (1974) derived a mathematical relationship for the variation of the flux of a dissolved component with salinity in an estuary. In doing this they developed a general model for mixing processes between river and ocean water in which definitive criteria were established for the identification of non-conservative behaviour among dissolved components. In this model it was assumed that the concentration of a dissolved component is a continuous, single-valued function of salinity, and the following relationship was developed for the variation of the flux of the dissolved component with salinity:

$$\frac{dQ_c}{dS} = -Q_w(S - S_r)\frac{d^2C}{dS^2} \tag{3.1}$$

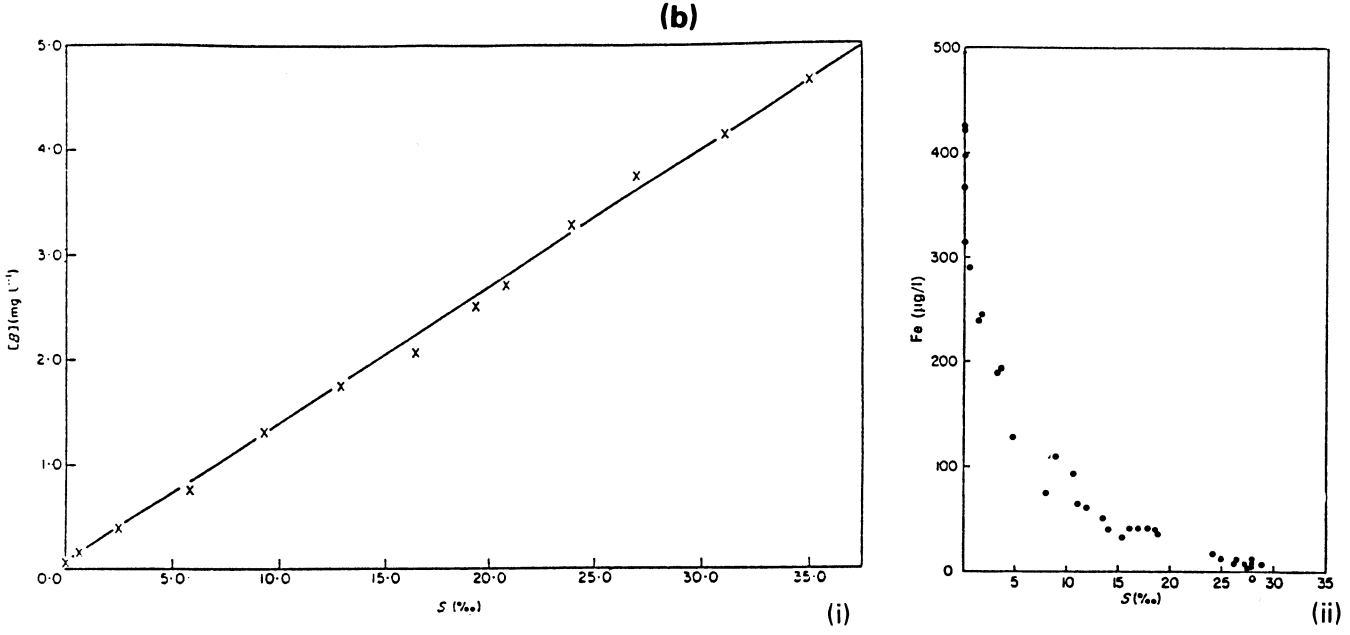

Figure 3.5b Estuarine mixing graphs and estuarine profiles for a series of representative dissolved elements. (i) Conservative behaviour of dissolved B in the Tamar estuary (from Liddicoat *et al.* 1983). (ii) Non-conservative behaviour of dissolved Fe in the Beaulieu estuary showing removal at low salinity (from Holliday & Liss 1976). (iii) Non-conservative behaviour of dissolved Ba in the Changjiang estuary showing addition to solution in the mid-salinity range (modified from Edmond *et al.* 1985). (iv) Non-conservative behaviour of dissolved Cu in the Savannah estuary showing additions at both low and high salinities (from Windom *et al.* 1983). Closed and open circles indicate data for different surveys. Broken curve indicates general trend of mixing curve only. (v) Non-conservative behaviour of dissolved Mn in the Tamar estuary showing both removal (low salinity) and addition (mid-range salinities) (modified from Knox *et al.* 1981). △ = Mn(II), ○ = total Mn; open symbols denote surface concentrations; closed symbols denote bottom concentrations.

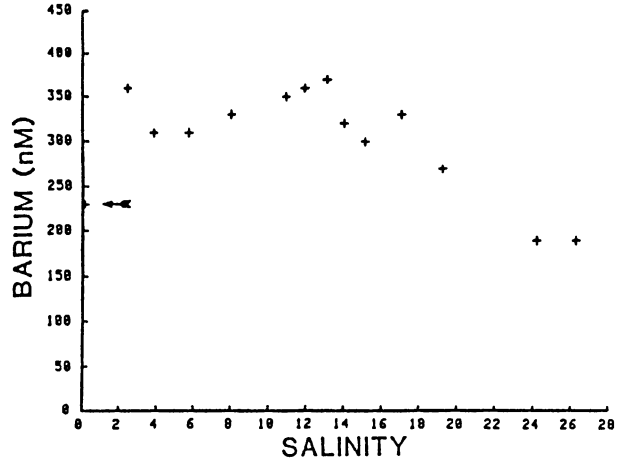
BARIUM (nM)
SALINITY
(iii)

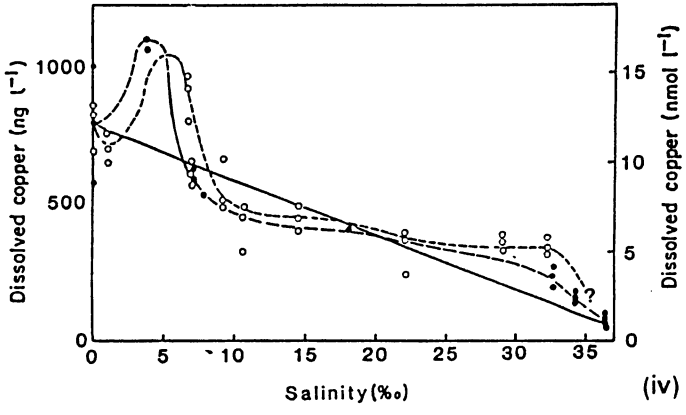
Dissolved copper (ng l⁻¹)
Dissolved copper (nmol l⁻¹)
Salinity(‰)
(iv)

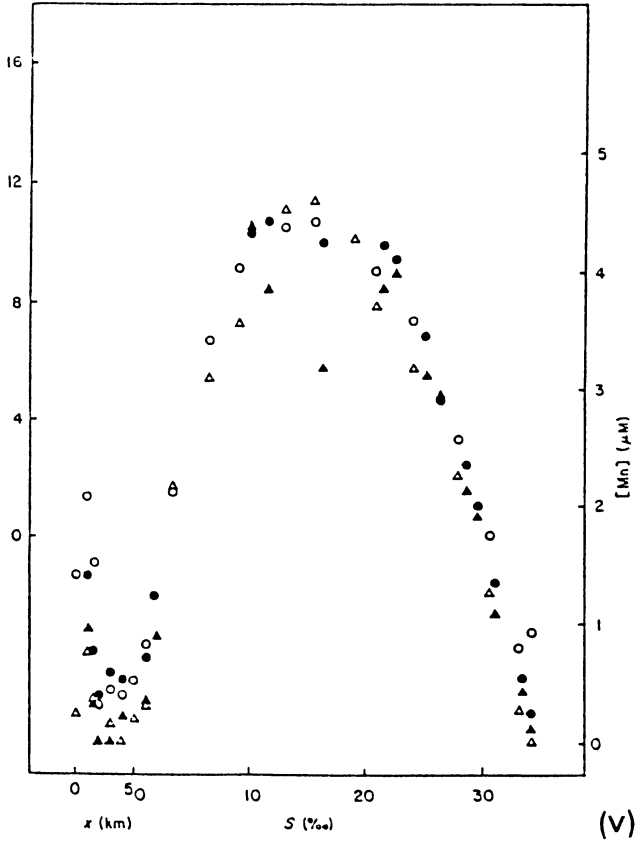
[Mn] (μM)
x (km)
S (‰)
(v)

where Q_w is the flux of the river water, Q_c is the flux of the dissolved component transported by the river water, S_r is the salinity of the fluvial end-member, S is the salinity at a given isohaline surface and C is the concentration of the dissolved component at the same isohaline surface.

For conservative behaviour there is no gain or loss of the dissolved component during mixing, and hence

$$\frac{dQ_c}{dS} = 0 = \frac{d^2C}{dS^2} \tag{3.2}$$

and the plot of the concentration of the dissolved component against salinity will be a straight line.

For non-conservative behaviour, the second derivative d^2C/dS^2 will not be equal to zero, and the plot of the concentration of the dissolved component against salinity will be a curve described by Equation 3.1.

This explicit formulation of the mixing process, i.e. of $C(S)$, shows that over straight-line segments of the mixing curve simple two-end-member dilution processes are taking place, and that to establish non-conservative behaviour curvature must be domonstrated. By applying the model to various examples of the estuarine behaviour of dissolved components, the authors were able to demonstrate that previous examples of non-conservative 'curvature' behaviour could, in fact, be shown to fit to straight-line segments on the mixing curve. This was interpreted as resulting from the introduction of a third end-member component, i.e. in addition to the river and sea water end-members, into the mixing processes. This third end-member can be a tributary stream. However, more commonly it is coastal or shelf water of intermediate salinity. For example, it was demonstrated that in the Mississippi estuary there is mixing between three end-members: Mississippi River water, shelf water of intermediate salinity and open Gulf water of high salinity. In situations such as this, the mixing between river water and sea water must therefore be interpreted in terms of two end-member sea waters, each of which can produce different straight-line relationships, which when combined can, under some circumstances, appear as curvature on the mixing diagram. The 'straight-line segment' approach to mixing diagrams outlined by Boyle *et al.* (1974) therefore offers a mathematical model for the interpretation of estuarine mixing processes.

Unless strict constraints are imposed, the mixing graph procedure can be both insensitive and imprecise. Nonetheless, it has been used as an important first step in assessing the direction, if any, in which the estuarine filter has affected a river-transported signal, and in this respect a number of different estuarine behaviour patterns can be identified.

3.2.3.1 Conservative behaviour Some elements appear to behave in a

conservative manner in all estuarine situations. These include the major dissolved components which contribute to the salinity of sea water, e.g. Na^+, K^+, Ca^{2+} and SO_4^{2-}. Boron, another major element, also seems to behave conservatively in many estuaries (see e.g. Fanning & Maynard 1978). Liddicoat *et al.* (1983) demonstrated this for the Tamar estuary (UK), and concluded that the dissolved boron in the estuarine waters was derived almost entirely from sea water. The mixing graph for boron in the Tamar is illustrated in Figure 3.5b(i), and provides an excellent example of conservative behaviour during estuarine mixing.

3.2.3.2 Non-conservative behaviour Mixing graphs that demonstrate that a component behaves in a non-conservative manner in estuaries can have a variety of forms, which can indicate the gain or loss of the dissolved component, and can sometimes also identify the zone in which the estuarine reactivity has taken place. A number of different types of estuarine mixing graphs are described below.

(a) **Removal of dissolved components.** For these components estuarine concentrations fall below the TDL. An example of this type of mixing graph is illustrated for iron in Figure 3.5b(ii), from which it is evident that the removal of dissolved iron has taken place largely in the low-salinity region.

(b) **Addition of dissolved components.** For these components estuarine concentrations lie above the TDL. An example of this is provided by the behaviour of Ba in the Changjiang (Yangtze) estuary – see Figure 3.5b(iii). A more complex mixing graph showing the addition of dissolved components has been reported by Windom *et al.* (1983) for the behaviour of copper in the Savannah estuary (US). This graph is illustrated in Figure 3.5b(iv) and indicates that there are additions to the fluvial Cu at both low ($\lesssim$ 5‰) and high ($\gtrsim$ 20‰) salinities.

(c) **Combined addition and removal.** This type of estuarine profile has been identified for dissolved managanese in the Tamar estuary (UK) by Knox *et al.* (1981). The estuarine profile is illustrated in Figure 3.5b(v), and shows that dissolved Mn is removed from solution at low salinities, but is added to solution at mid-range salinities (see also Sec. 3.2.7).

It is apparent, therefore, that if sufficient constraints are applied mixing graphs can be used to identify: (a) whether or not a dissolved component has undergone estuarine reactivity; (b) the direction, i.e. gain or loss, in which the dissolved component has been affected; and (c) the general estuarine region (e.g. low-, mid-range, or high-salinity zones) over which the reactivity has been most effective. However, the mixing graph suffers

from one very fundamental limitation. That is, it does not provide information on *why* the component behaves in the way it does or on the *nature* of biogeochemical reactions that have caused the estuarine reactivity. In order to know how the estuarine filter operates it is therefore necessary to understand the nature of the reactive processes that occur in the mixing zone.

Biogeochemical reactivity in natural waters is controlled by a number of physicochemical parameters, which include pH, redox potential, salinity, and the concentrations of complexing ligands, nutrients, organic components and particulate matter. All these parameters undergo major variations in estuaries, as a result of which a variety of dissolved ↔ particulate transformations are generated in the mixing zone. These transformations are driven by physical, chemical and biological factors, and include (a) sorption at the surfaces of suspended particles, (b) precipitation, (c) flocculation–aggregation and (d) uptake via biological processes. In general, the extent to which the transformations occur depends on the nature and concentrations of both the particulate and the dissolved components in the mixing zone.

3.2.4 Estuarine particulate matter (EPM)

3.2.4.1 The classification of EPM On the basis of the general scheme proposed by Salomons and Forstner (1984), the following classes of estuarine particulates can be identified.

(a) **River transported or fluvial particulates.** These solids, which are transferred across the river/estuarine boundary, include crustal weathering products (e.g. quartz, clay minerals), precipitated oxyhydroxides (principally those of iron and manganese), terrestrial organic components (e.g. plant remains, humic materials) and a variety of pollutants (e.g. fly ash, sewage).

(b) **Atmospherically transported particulates.** The transfer of material across the atmosphere/estuarine boundary can be important in some estuaries. The atmospheric components involved in this transfer include crustal weathering products and pollutants such as fly ash.

(c) **Ocean-transported particulates.** Particulate matter transferred across the ocean/estuarine boundary includes biogenous components of marine origin (e.g. skeletal debris, organic matter) and inorganic components (e.g. those originating in coastal sediments or formed in the marine water column).

(d) **Estuarine-generated particulates.** This type of particulate material has an internal source and includes inorganic and organic flocculants and precipitates, and both living and non-living particulate organic matter. Of the various processes that lead to the formation of

estuarine particulates, (i) flocculation, (ii) precipitation and (iii) the biological production of organic matter are especially important.

Flocculation is a process that causes smaller particles (colloids or semi-colloids) to increase in size and form larger units, and has been described in detail by Potsma (1967) and Drever (1982). In estuaries, where the mixing of saline and fresh water leads to an increase in ionic strength, flocculation affects both organic and inorganic components; these include river-transported clay mineral suspensions, colloidal species of iron and dissolved organics (such as humic material). The aggregation of particles into larger sizes can also take place via biological mediation; e.g. through the production of faecal pellets by filter-feeding organisms (see Sec. 3.2.7).

Various types of precipitation processes occur in estuaries; of these, heterogeneous precipitation in the presence of particle clouds (e.g. in turbidity maxima) are especially important in the removal of dissolved Mn, and other metals, from solution.

The estuarine biomass is formed as a result of primary production, which is related to factors such as the supply of nutrients and the turbidity of the waters. According to the estimate made by Williams (1981), the global internal estuarine photosynthetic production is $\sim 5.2 \times 10^{14}$ g yr^{-1}, which is $\sim 1.5\%$ of the total marine production if a figure of 3.6×10^{16} g yr^{-1} is used for the latter (Sec. 9.2.2.2). Rivers transport $\sim 2 \times 10^{14}$ g yr^{-1} of carbon into estuaries, which is the same order of magnitude as that resulting from primary production. However, according to Reuther (1981), much of this imported carbon is refractory, i.e. resistant to microbial attack, and so does not enter into recycling within the estuarine system.

3.2.4.2 The distribution of EPM The physical processes that control the distribution of EPM involve water circulation patterns, gravitational settling and sediment deposition and resuspension. All these processes, together with primary production, combine to set up the particle regime in an estuary.

Estuarine circulation patterns exert a fundamental influence on the processes that control the distribution of EPM. A number of characteristically different types of estuary can be distinguished on the basis of water circulation patterns (see Fig. 3.6), and these are described below in relation to the manner in which they constrain estuarine particle regimes, and therefore influence estuarine reactivity.

The most commonly occurring estuaries are of the positive type, i.e. loss from evaporation at the surface is less than the input of fresh water from rivers. The basic factor that determines the type of circulation in an estuary of this type is the part played by tidal currents (inflow of sea water) in relation to river flow (inflow of fresh water), and in a general

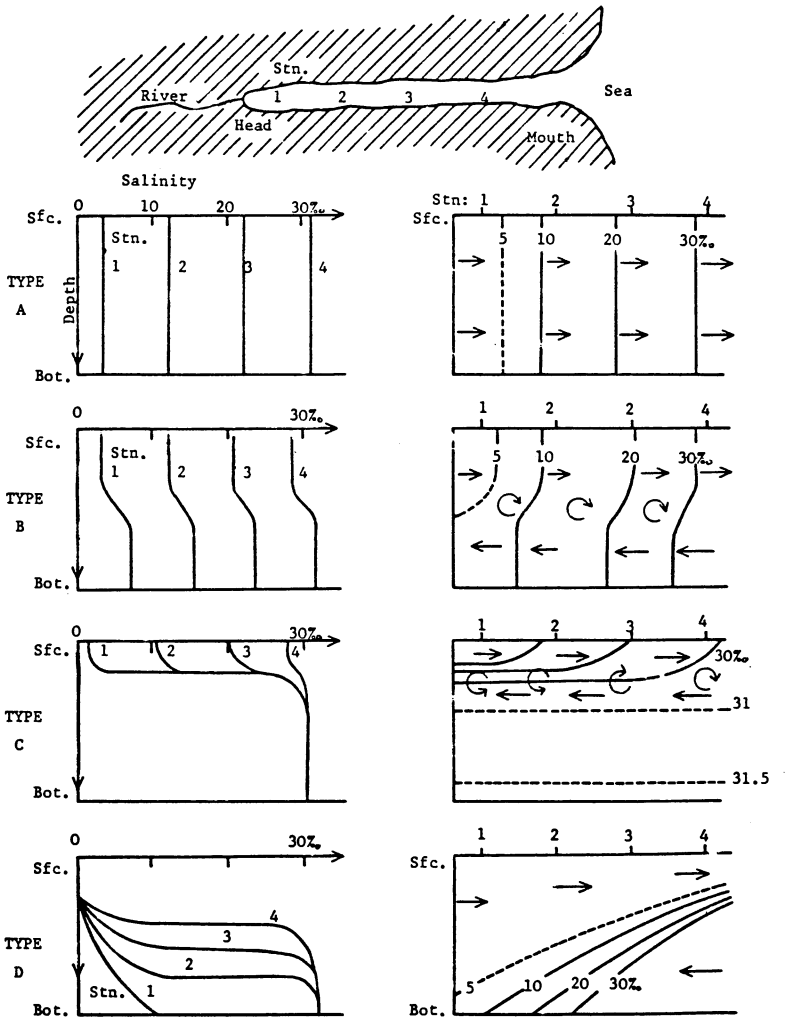

Figure 3.6 Salinity–depth profiles and longitudinal salinity sections in estuaries displaying different water circulation patterns (from Aston 1978; after Pickard and Emery 1982). Type A, a salt wedge estuary; type B, a highly stratified estuary; type C, a partially stratified estuary; type D, a vertically well mixed estuary.

way the type of circulation developed can be related to the dominance of one of these two water flow regimes.

In some estuaries the river flow is dominant. Under these conditions the less dense river water forms an upper layer over the more dense saline water, and the estuary becomes stratified. There are a number of types of stratified estuaries.

SALT WEDGE ESTUARY When the circulation is almost completely dominated by river flow, a **salt wedge** estuary can be formed. As the name implies, the salt water in this type of estuary extends into the river as a wedge under the freshwater outflow. A characteristic of the salt wedge circulation pattern is that the outflowing water remains fresh up to the mouth of the river. There is also a steep density gradient between the fresh water and saline water, which prevents mixing between the two water layers until the river flow attains a critical velocity. This velocity is not attained in a salt wedge estuary.

HIGHLY STRATIFIED ESTUARY A second type of well developed vertical stratification, but one in which the saline layer is not confined to a wedge shape, can be formed in some estuaries. These estuaries are termed **highly stratified**, or are referred to as having a two-layer flow. Like the salt wedge type, the river flow in a highly stratified estuary is large relative to the tidal flow and there is still a two-layer stratification. Now, however, the velocity of the seaward-flowing river water is sufficient to cause internal waves to break at the saline/fresh water interface. This results in the mixing of saline water from below into the upper freshwater layer, a process termed **entrainment**. This is a one-way process only and, in contrast to a salt wedge type of circulation, it results in the salinity of the upper water layer increasing as it moves seawards.

Both Meade (1972), and later Potsma (1980), have pointed out that the distribution of suspended particulate matter in an estuary is largely controlled by the dynamics of the water circulation pattern. According to these authors, most of the suspended particulate material in both salt wedge and highly stratified estuaries is of a fluvial origin and is transported seawards in the upper water layer. The suspended matter does not thereafter enter the estuarine cycle proper.

PARTIALLY STRATIFIED ESTUARY As tidal forces become more important, an estuary will begin to oscillate. In a **partially stratified** (or partially mixed) estuary, there is still a two-layer structure developed with fresh water at the surface overlying saline water at depth. However, in this situation there is vertical mixing between the mainly inflowing bottom water and the mainly outflowing surface water. This mixing takes place through eddy diffusion, which, unlike entrainment, is a two-way process,

i.e. salt water is mixed upwards and fresh water is mixed downwards, with the result that a layer of intermediate salinity is formed. In this type of estuary there are also longitudinal variations in salinity in both the upper and lower layers, and undiluted fresh water is found only at the head of the estuary.

In the partially stratified estuary, the lower-water landward flow is strong enough to move suspended material up the estuary to the head of the salt intrusion. This may include both fluvial material that has settled from the upper layer and marine material that has been transported landwards. A **turbidity maximum**, or particle cloud, may be developed at the head of the salt intrusion in the region where suspended solids can be transported from both up- and downstream directions. Such a turbidity maximum, which is a region of concentration of suspended material, is an important site for dissolved ↔ particulate interactions. In some estuaries very high concentrations (up to several hundred grams of sediment per litre) have been reported near the bed. This so-called **fluid mud**, which is built up of material sinking from the overlying turbidity maximum during neap tides, can undergo resuspension and restricted transport on spring tides.

VERTICALLY WELL MIXED ESTUARY Under certain estuarine conditions tidal flow can become completely dominant. For example, in some estuaries, which usually have a small cross section, a strong tidal flow can exceed the river flow and the velocity shear on the bottom may be of sufficient magnitude for turbulence to mix the water column completely. These estuaries are termed homogeneous or **fully mixed** estuaries and, since there is no appreciable river flow, the suspended particulates are concentrated in the nearshore region. However, there is some doubt as to whether *completely* homogeneous estuaries actually exist in nature.

It is apparent, therefore, that the nature and strength of the circulation patterns in an estuary will exert a strong control on the suspended particle regime and can lead, in the case of the partially stratified type, to the development of zones of relatively high suspended solid concentrations (turbidity maxima), which are major sites for physical, chemical and biological reactions between particulate and dissolved species. It is in these zones, therefore, that the estuarine filter is especially active. Estuarine circulation also affects the residence time of the water in estuaries. This varies from a few days to a few months, and according to Duinker (1986) it increases with the increasing extent of vertical mixing; thus, residence times generally increase in the sequence salt wedge < stratified < partially mixed < well mixed estuarine types.

3.2.5 The concentration and nature of dissolved material in estuaries

For many dissolved components, the concentrations in river water exceed those in sea water (see Table 3.10), and as a result the initial **concentrations** of the dissolved components in estuaries are regulated by the extent to which the end-member waters have undergone mixing. The nature or **speciation** of the dissolved components is also affected by the

Table 3.10 The concentrations of dissolved elements in river and sea waters[a]

	RIVERS		OCEAN	
	Dissolved $\mu g\ l^{-1}$	Particulate $\mu g\ g^{-1}$	Water $\mu g\ l^{-1}$	Deep sea clays $\mu g\ g^{-1}$
Ag	0.3	0.07	0.04	0.1
Al	50	94,000	0.5	95,000
As	1.7	5	1.5	13
Au	0.002	0.05	0.004	0.003
B	18	70	4,440	220
Ba	60	600	20	1,500
Br	20	5	67,000	100
Ca	13,300	21,500	412,000	10,000
Cd	0.02	(1)	0.01	0.23
Ce	0.08	95	0.001	100
Co	0.2	20	0.05	55
Cr	1	100	0.3	100
Cs	0.035	6	0.4	5
Cu	1.5	100	0.1	200
Er	0.004	(3)	0.0008	2.7
Eu	0.001	1.5	0.0001	1.5
Fe	40	48,000	2	60,000
Ga	0.09	25	0.03	20
Gd	0.008	(5)	0.0007	7.8
Hf	0.01	6	0.007	4.5
Ho	0.001	(1)	0.0002	1
K	1,500	20,000	380,000	28,000
La	0.05	45	0.003	45
Li	12	25	180	45
Lu	0.001	0.5	0.0002	0.5
Mg	3,100	11,800	1.29×10^6	18,000
Mn	8.2	1,050	0.2	6,000
Mo	0.5	3	10	8
Na	5,300	7,100	1.077×10^7	20,000
Nd	0.04	35	0.003	40
Ni	0.5	90	0.2	200
P	115	1,150	60	1,400
Pb	0.1	100	0.003	200
Pr	0.007	(8)	0.0006	9
Rb	1.5	100	120	110
Sb	1	2.5	0.24	0.8
Sc	0.004	18	0.0006	20
Si	5,000	285,000	2,000	283,000
Sm	0.008	7	0.0005	7.0
Sr	60	150	8,000	250
Ta	< 0.002	1.25	0.002	1.0
Tb	0.001	1.0	0.0001	1.0
Th	0.1	14	0.01	10
Ti	10	5,600	1	5,700
Tm	0.001	(0.4)	0.0002	0.4
U	0.24	3	3.2	2.0
V	1	170	2.5	150
Y	-	30	0.0013	32
Yb	0.004	3.5	0.0008	3
Zn	30	250	0.1	120

[a] Data from Martin and Whitfield (1983).

water mixing. It is the speciation of an element between particulate, colloidal and dissolved (e.g. ion pairs, and both inorganic and organic complexes) forms, rather than its total concentration, that controls its environmental reactivity. Competitive complexing between the principal inorganic ligands (e.g. Cl^-, SO_4^{2-}, CO_3^{2-}, OH^-), the organic (e.g. humic material) ligands and particulate matter is the main factor that controls the nature of the inorganic species in natural waters. This topic is considered in more detail in Section 11.6.2, with respect to sea water. However, elemental speciation is also important in the estuarine mixing zone.

From the point of view of the behaviour of both dissolved and particulate elements during estuarine mixing, three of the most important physico-chemical differences between the river and seawater end-members are those associated with the following parameters: ionic strength (salinity), which varies from zero in the river end-member to 0.7 M in the marine end-member; (b) ionic composition and the concentrations of complexing ligands – for example, in river water the most important ions are calcium and bicarbonate, whereas sea water is dominated by sodium and chloride; (c) pH – river waters can be either acidic or alkaline, with pH values that are usually in the range ~ 5 to ~ 8. Thus, in some estuaries the pH of the river end-member may be similar to that of the seawater end-member (average pH ~ 8.2). However, river waters are usually more acidic than sea water, with the result that under many estuarine conditions there is a pH gradient, which increases with increasing salinity – see Figure 3.7a. The gradient will, however, depend on the actual pH of the two end-member waters, and the estuarine behaviour patterns of some elements (e.g. Mn) with respect to particulate–dissolved partitioning will differ depending on, among other factors, the pH regime. Changes in parameters such as those identified above will affect the speciation of elements as the two end-member waters undergo estuarine mixing.

pH and P_e are often considered to be the **master variables** in natural waters (see Worksheet 14.1). P_e is a convenient way of expressing the equilibrium redox potential, which is an important parameter in estuarine chemistry, since in estuaries elements can be exposed to reducing conditions in both the water column and sediment interstitial waters, and under some estuarine conditions sulphide complexing must also be taken into account in speciation modelling. However, even with a knowledge of the master variables, there are many uncertainties involved in understanding the speciation of elements in any natural waters, and these are magnified when the mixed-water estuarine system is considered. Despite the various difficulties involved there have been attempts to investigate the speciation of elements in the estuarine mixing zone. For example, Mantoura *et al.* (1978) used a multi-element, multi-ligand interaction

model to predict metal–humic complexation changes which occur on the mixing of fresh and saline waters. The data obtained from this study will serve to illustrate a number of factors that affect metal speciation across the fresh water/saline water interface.

(a) The speciation of dissolved trace metals in river waters is principally governed by the hydrogen ion activity, the carbonate alkalinity and the concentrations of dissolved organics, such as humic acids. These

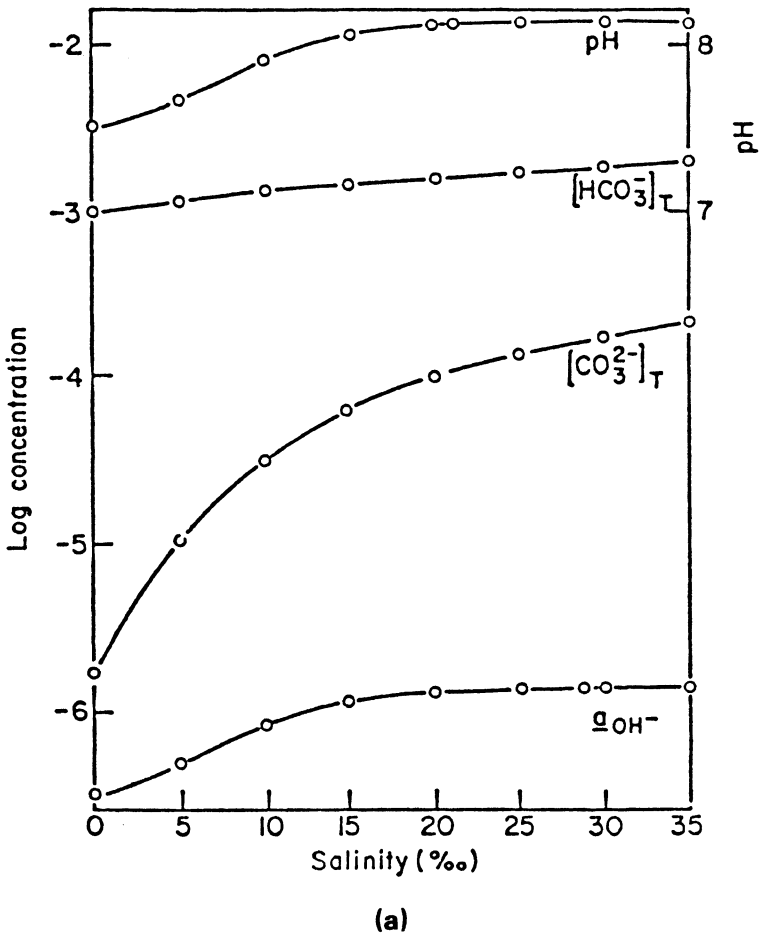

Figure 3.7 Speciation in estuaries (from Mantoura *et al.* 1978). (a) Variations in a number of water parameters along an estuarine section.

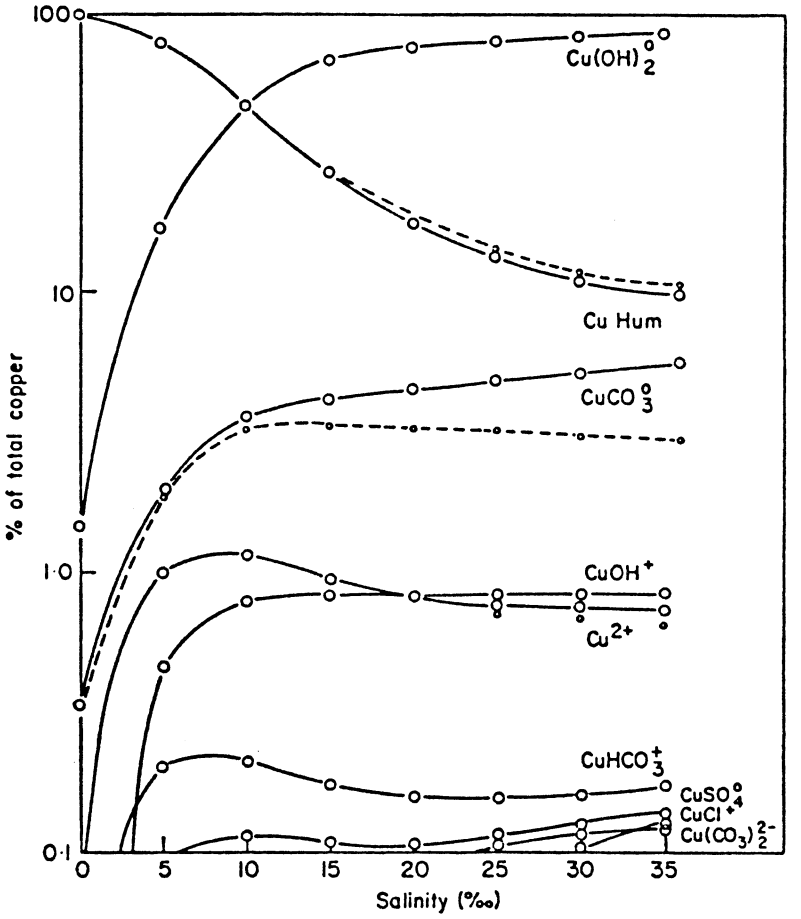

(b)

Figure 3.7b Equilibrium speciation of Cu as a function of salinity in a model estuary.

parameters vary considerably between river and sea water (see e.g. Fig. 3.7a), with the result that the speciation environment changes on the mixing of the two end-member waters.

(b) Humic acids can exert a significant influence on the speciation of some metals in river waters, especially at low pH values. For example, the model used by Mantoura *et al.* (1978) predicted that > 90% of the Cu and Hg in river water is complexed by humic material. In general, the order of increasing binding strength of the metals to humic materials followed the Irving–Williams series, i.e. Mg < Ca = Cd < Mn < Co < Zn < Ni < Cu < Hg.

(c) There is a decrease in humic complexed material with an increase in

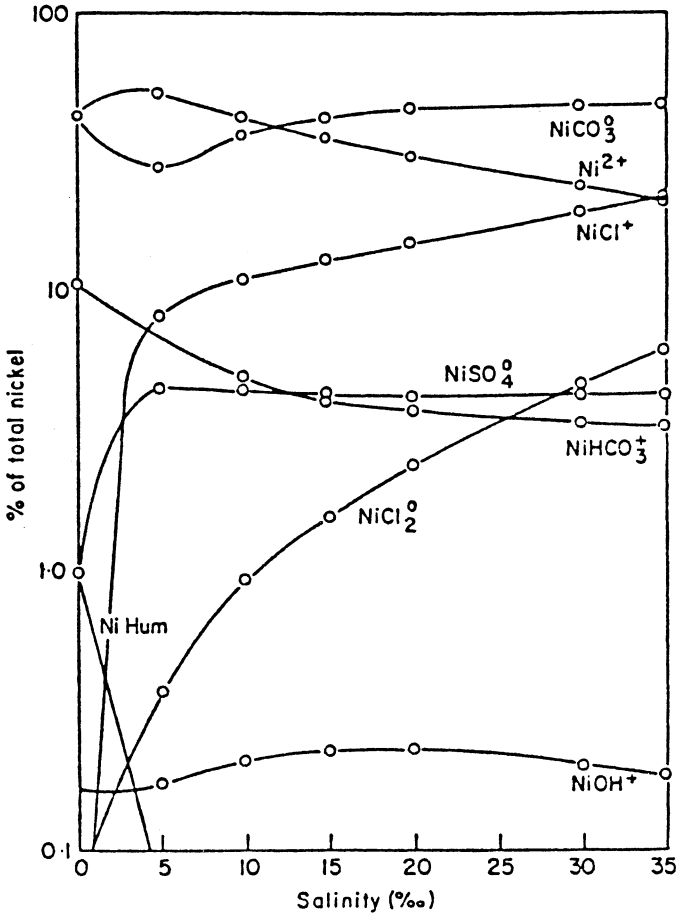

Figure 3.7c Equilibrium speciation of Ni as a function of salinity in a model estuary.

salinity, such as would be encountered in estuarine mixing. This decrease, which is rapid for Mg, Ca, Zn, Cd, Mn and Co but less rapid for Cu and Hg, is mainly the result of competition for the humic ligands from Ca and Mg, which can utilize > 90% of their complexing capacity (see also Sec. 3.2.6).

(d) In waters having salinities > 10‰, chloro species are significant (> 5%) for all the metals except Cu and Co. Some estuarine speciation changes are illustrated for Cu and Ni in Figures 3.7b and c, respectively.

These various speciation relationships are related to the estuarine

reactivity of elements in Section 3.2.6 in terms of the Sholkovitz model. However, for a more detailed treatment of the fundamental concepts involved in chemical speciation in estuarine waters the reader is referred to the review presented by Dyrssen & Wedborg (1980), which covers the binding of trace metals with both inorganic and organic ligands and also includes complexing in anoxic waters.

At this stage, therefore, it may be concluded that during the mixing of fresh and saline waters there is competition for dissolved trace elements between various complexing agents, such as those described above, and between these agents and the suspended particulate matter that is present in the resulting estuarine 'soup'.

3.2.6 Dissolved ↔ particulate interactions in estuaries

The concentrations of both complexing agents and particulate matter undergo large variations during estuarine mixing. However, it is only particulate matter that can be trapped in the mixing zone and this is coupled to dissolved material via particulate ↔ dissolved equilbria.

Processes that are involved in the addition or removal of dissolved components in the estuarine soup include the following:

(a) Flocculation, adsorption, precipitation and biological uptake, which result in the **removal** of components from the dissolved phase and their transfer to the particulate phase. It is these processes which can result in the retention of components in estuaries via particulate trapping.
(b) Desorption from particle surfaces and the breakdown of organics, which result in the **addition** of components to the dissolved phase. This will result in the flushing out of the components if they remain in the dissolved phase.
(c) Complexation and chelation reactions with inorganic and organic ligands, which **stabilize** components in the dissolved phase. These components will also be flushed out of an estuary with the water mass.

The manner in which these different types of processes can be linked to (i) the kind and concentration of EPM, and (ii) the speciation of dissolved components can be described in terms of a number of experimental approaches that have been used to model estuarine chemistry.

Laboratory studies designed to investigate chemical reactions in estuarine waters tend to be of two types: (a) those involving the mixing of end-member waters and the characterization of the reaction products formed, and (b) those attempting to study individual reaction processes, such as adsorption – desorption, by experimentally varying the controlling

parameters (e.g. pH, ionic strength).

A number of laboratory studies on the chemical reactions taking place in estuaries have involved the artificial mixing of both filtered and non-filtered samples of the fresh and saline end-member waters (see e.g. Coonley *et al.* 1971, Duinker & Nottling 1977). This is often referred to as the **product approach**, and perhaps the most significant advances in our understanding of estuarine chemistry to emerge from this approach are those which have been reported by Sholkovitz and his coworkers.

The **Sholkovitz model** (Sholkovitz 1978) was an attempt to make a quantitative prediction of the reactivity of trace metals in the estuarine mixing zone. The model is based on the following assumptions. (a) A fraction of the dissolved trace metals in river water exist as colloids in association with colloidal forms of humic acids and hydrous iron oxides. (b) In the estuarine mixing zone the removal of the metals takes place via the flocculation of these colloids and/or their subsequent adsorption onto humic acids and hydrous iron oxide flocs. (c) The extent to which this removal takes place in the estuarine soup is determined by competition for the trace metals by seawater anions, humic acids and hydrous iron oxides, in the presence of seawater cations.

The Sholkovitz model was then tested in a variety of experiments using the product approach resulting from the mixing of river and seawater end-members. One of the most significant findings to emerge from the product approach experiments was the importance of the role played by the rapidly flocculating humic fraction in the formation of metal humates (see Sec. 3.2.5 for a review of the effect of humic material on the speciation of elements in river water). The importance of the flocculation of humics and hydrous iron oxides was demonstrated by Sholkovitz & Copland (1981), who carried out an investigation into the fates of dissolved Fe, Cu, Ni, Cd, Co and humic acids following the artificial mixing of river and sea water. Although they restricted their experimental work to the filtered water of a single organic-rich river, the River Luce (UK), they were able to demonstrate the effects that resulted from the flocculation of fluvial-transported colloids by the seawater cations encountered on estuarine mixing. In this process, Ca^{2+} was found to be the main coagulating, i.e. colloid destabilizing, agent. On the basis of the River Luce data, the authors concluded that the extent of this flocculation removal (expressed as a percentage of the dissolved concentration) varied from *large* (e.g. Fe $\sim$ 80%, humic acids $\sim$ 60%, Cu $\sim$ 40%), to *small* (e.g. Ni and Cd $\sim$ 15%), to essentially *nothing* (e.g. Co and Mn $\sim$ 3%). However, Sholkovitz & Copland (1981) pointed out that their findings, based on the organic-rich river water, should not be applied *a priori* to estuaries in general. For example, Hoyle *et al.* (1984) showed that dissolved rare-earth elements (REE) were flocculated in association with Fe–organic matter colloids when water from the River Luce was mixed

with sea water; however, REE removal did not occur when the river end-member used in the experiments was organic-poor in character. In addition to the cationic destabilization of fluvially transported colloidal humic substances, organic complexes can stabilize some dissolved elements in solution; for example, Waslenchuk & Windom (1978) concluded that the conservative transport of dissolved As in estuaries from the southeastern USA results from the stabilization of the element by organic complexes.

In practice, estuarine dissolved ↔ particulate reactions depend on a number of variables. Several of these were considered by Salomons (1980) in a series of interlinked laboratory experiments in which the influence of pH, chlorinity and the concentration of suspended material on the adsorption of Zn and Cd was assessed under estuarine conditions. Three important conclusions regarding the nature of the competition for trace metals in the estuarine mixing zone can be drawn from this study.

(a) The adsorption of both metals increased with increasing pH over the experimental range (pH 7.0–8.5).
(b) The adsorption of Cd, and to a lesser extent that of Zn, decreased with increasing chlorinity, probably as a result of competition from the chloride ion for the complexation of the metals, thus keeping them in solution (see Sec. 3.2.5).
(c) The adsorption of both elements increased with increasing turbidity, i.e. with an increase in the concentration of suspended matter. This apparently occurred to the extent that the suspended matter was able to compete effectively with chloride ions for metal complexation.

Extrapolated to real estuarine situations the latter two findings mean that the effectiveness of suspended particulate matter for the capture of dissolved Cd and Zn decreases as salinity increases, but that this effect can be overridden when the concentrations of the suspended particulates are relatively high, e.g. in the presence of a turbidity maximum, which can act as a zone of enhanced adsorption (Salomons & Forstner 1984). A model designed to describe adsorption in the presence of a turbidity maximum in the estuarine environment is summarized in Worksheet 3.1.

The studies described above have focused largely on the removal of trace elements from solution onto particulate matter. In contrast, other laboratory experiments have shown that some elements can be added to the dissolved state via desorptive release from particulate matter during estuarine mixing (see e.g. Kharkar *et al.* 1968, Van der Weijden *et al.* 1977). However, this desorptive release does not apparently affect all elements. For example, Li *et al.* (1984) added radiotracer spikes to experiments in which river and sea water were mixed and concluded that Co, Mn, Cs, Cd, Zn and Ba will be desorbed from river suspended

WORKSHEET 3.1
A SIMPLE SORPTIVE EQUILIBRIUM MODEL FOR THE REMOVAL OF TRACE METALS IN A LOW-SALINITY TURBID REGION OF AN ESTUARY
(after Morris 1986)

A variable fraction of the river influx of many dissolved trace metals is removed from solution in the low-salinity, high-turbidity, estuarine mixing zone. The equilibrated partitioning of a trace metal between the dissolved and particulate phases in natural waters can be described by the term $K_d = X/C$, where K_d is a conditional partition coefficient, X is the concentration (w/v) of exchangeable metal on the particulate phase, and C is the dissolved metal concentration (w/v). To set up his sorptive equilibrium model, Morris (1986) made the following assumptions: (a) the diffusion of solutes from the estuary to the very-low-salinity region (< 0.2%) is minor so that the river can be considered to be the only significant source of dissolved metal; and (b) the salinity-related changes in the conditional partition coefficient are negligible. The problems involved in describing the removal of the river influx of dissolved trace metals in the turbid low-salinity estuarine mixing zone can therefore be simplified to a consideration of the change in sorptive equilibrium, at constant K_d, induced by adding suspended particulates to the river water. Under these conditions, the mass balance for the conservation of a trace metal, for unit volume of river water, can be written:

$$C_R + X_R P_R + X_S P_S = C + X(P_R + P_S) \quad (1)$$

where C_R and C are the equilibrated dissolved metal concentrations (w/v) in the river water and the turbidized water, respectively; X_R and X are the equilibrated exchangeable metal concentrations (w/w) on the particles in the river water and the turbidized water, respectively; X_S is the exchangeable metal concentration (w/w) on the added particulate load; P_R is the suspended particulate load (w/w) carried by the river and P_S is the additional suspended particulate load (w/v). Substituting $X_R = K_d C_R$ and $X = K_d C$ into Equation 1, and introducing a term $\alpha = X_S/X$, yields:

$$C/C_R = (1 + K_d P_R)/[1 + K_d P_S(1 - \alpha)] \quad (2)$$

Equation 2 therefore predicts the change in dissolved metal concentration induced by adding particles to river water as a function of the particle load, the added particulate load, and α (the fraction of the exchangeable metal on the added particles relative to ultimate equilibration). For sorptive removal to occur, the added particles must have a lower concentration of exchangeable metal than the particles in the turbidized water, i.e. $\alpha < 1$.

Morris (1986) considered how the predicted concentration ratio (C/C_R) within the zone of removal varies with K_d, P_R and α. The relationship for K_d is illustrated in Figure (i), and shows how the predicted concentration ratio (C/C_R) varies with K_d for additions of suspended particulate load (P_S) ranging from 0 to 1000 mg l^{-1}, with a representative depletion factor of $\alpha = 0.90$, and a river suspended particulate load (P_R) = 5 mg l^{-1}. The curves illustrate that at constant P_R and α, the degree of removal for any P_S value increases (i.e. the ratio (C/C_R) decreases) with increasing K_d, the most sensitive changes being in the K_d range 1×10^3 to 1×10^6 mg l^{-1}. The

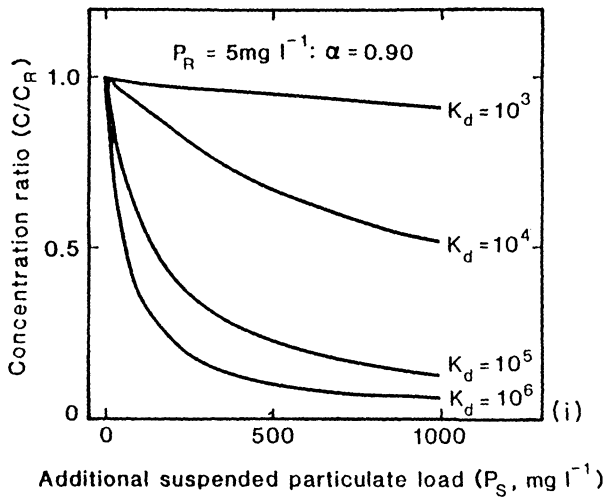

Figure (i) The influence of the partition coefficient (K_d) on the sorptive uptake of fluvial dissolved constituents in the very-low-salinity, high-turbidity estuarine region (from Morris 1960).

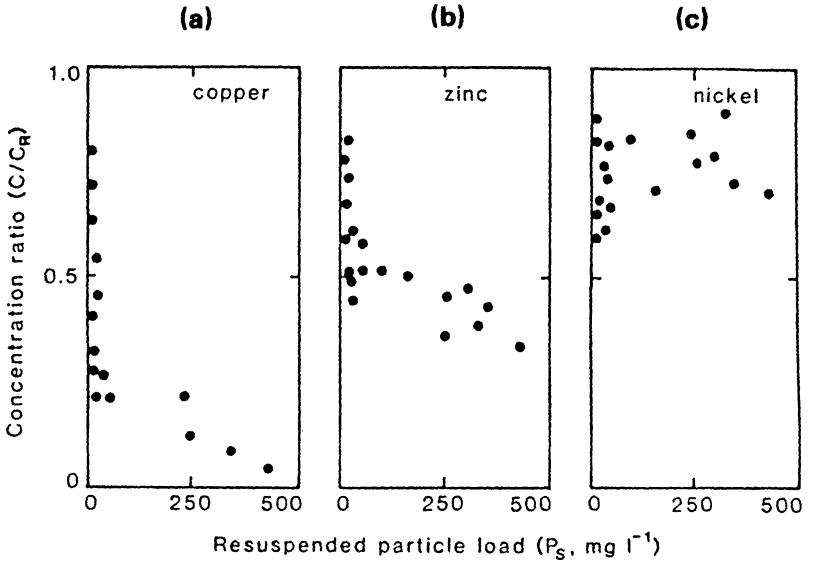

Figure (ii) Variations in the concentration ratio (C/C_R) for dissolved Cu, Zn and Ni with changes in suspended particulate load (P_S) in the very-low-salinity, high-turbidity zone in the Tamar estuary (UK) (from Morris 1986).

extent of removal is also sensitive to changes in P_R and α. Morris (1986) then used data from the Tamar and plotted the concentration ratio (C/C_R) against the resuspended particulate load (P_S) for Cu, Zn and Ni. The results are illustrated in Figures (ii)(a), (b) and (c), and show that for Cu and Zn the data correspond with the form of the relationship predicted by the model.

From the equilibrium sorption model it may be predicted that for elements with K_d values higher than $\sim 1 \times 10^3$ there will be significant removal in the turbid waters. Data in the literature indicate that K_d values in river water can generally exceed this value, and Morris (1986) therefore concluded that sorptive removal is potentially an important feature of the behaviour of trace metals in moderately to highly turbid estuaries.

particulate material on estuarine mixing, whereas Fe, Sn, Bi, Ce and Hg will undergo removal by adsorption.

The findings deduced from laboratory studies can be used to interpret estuarine mixing diagrams. This can be illustrated with respect to the study reported by Windom *et al.* (1983), who carried out an investigation of the estuarine behaviour of copper in the Savannah and Ogeechee estuaries (USA). The field survey data showed that Cu behaved in a non-conservative manner, with additions to the dissolved fluvial load being found in both estuaries. The additions occurred at both low (< 5‰) and high (> 20%) salinities, with a possible removal taking place at intermediate salinities (see Fig. 3.5b(iv)). The addition of Cu to the dissolved phase at the two ends of the estuarine salinity range implied that the element was being released from suspended particulate matter and/or bottom sediments. In order to distinguish between these two potential release mechanisms the authors carried out a series of experiments in which Ogeechee river water was mixed with mid-shelf sea water in various proportions before filtration and analysis of the samples. This series of experiments, in which only the water and its suspended particulate matter were used, thus eliminated any effects that would have arisen from the release of Cu from bottom sediments. The results revealed that, following an initial release of Cu at low salinities, the element behaved in an essentially conservative manner over the salinity range ~ 8 to ~ 34‰. The authors concluded, therefore, that the addition of Cu to solution at salinities < 5‰ was due to its release from suspended particulate matter, but that the addition at salinities > 20‰ was a result of its mobilization from bottom or resuspended sediment.

It may be concluded that mixing graphs can be used to establish whether or not a dissolved component has suffered reactivity in the estuarine mixing zone, and laboratory experiments can be employed to interpret the processes involved; although it must be remembered that such experiments never fully reproduce the complex estuarine situation. Despite this constraint, laboratory experiments have led to at least a first-

order understanding of some of the processes, e.g. competition for dissolved components from complexing ligands and particulate material, which control particulate ↔ dissolved equilibria in the estuarine soup. However, perhaps the single most important finding to emerge from all this work is that both the mixing graphs and the laboratory experiments have shown that some elements can, under different conditions, behave differently in the mixing zone. This reinforces the concept that for many elements there is no such thing as a global estuarine behaviour pattern. For this reason it is necessary to look at the behaviour of components in a number of individual estuaries. With this in mind, an attempt will be made in the following section to summarize the behaviour patterns of some components in the estuarine mixing zone, and to relate these to both non-biological and biological controls; in doing this attention will be focused, where possible, on the large globally important estuarine systems.

3.2.7 The behaviour of individual components in the estuarine mixing zone

3.2.7.1 Total particulate material At the present day much of the particulate material that enters estuaries is trapped within the system. For example, only ~ 8% of the particulate matter entering the upper zone of the Scheldt estuary is exported to the North Sea (Duinker *et al.* 1979); more than 90% of the RPM carried by the Mississippi is deposited in the delta (Trefry & Presley 1976); more than 95% of the suspended solids in the Amazon settle out within the river mouth (Milliman *et al.* 1975); over the entire St. Lawrence system (i.e. upper estuary, lower estuary, gulf) ~ 90% of the particulate input is held back (Bewers & Yeats 1977). Overall, therefore, it would appear that ~ 90% of RPM reaching the land/sea margins is retained in estuaries.

3.2.7.2 Iron and manganese Iron and manganese are extremely important elements in aquatic geochemical processes because their various oxide and hydroxide species act as scavengers for a variety of trace metals. However, the processes that control the estuarine chemistries of the two elements are different.

IRON Iron is present in natural waters in a continuum of species ranging through true solution, colloidal suspension and particulate forms. Most determinations of dissolved iron given in the literature refer to species that have passed through a 0.45 μm filter, and this definition will be used here.

Dissolved iron in river water is mainly present as hydrous Fe(III) oxides, which are stabilized in colloidal dispersion by high-molecular-

weight humic acids (see e.g. Boyle *et al.* 1977a, Sholkovitz *et al.* 1978, Hunter 1983). Humic material is affected by speciation changes on the mixing of fresh and saline waters (see Sec. 3.2.5), and the dominant mechanism for the removal of iron to the particulate state appears to be the flocculation of mixed iron oxide–humic matter colloids of fluvial origin, which undergo electrostatic and chemical destabilization during estuarine mixing, partly as a result of neutralization of colloid charges by marine cations. The coagulative removal of iron therefore takes place at low salinities, and a typical estuarine mixing graph for iron is given in Figure 3.5b(ii).

Figueres *et al.* (1978) summarized the behaviour of iron in estuaries and found that in 15 out of the 16 systems considered fluvial dissolved iron was removed during estuarine mixing; expressed in terms of the fluvial input, the removal ranged from ~ 70 to ~ 95%. This pattern has been confirmed with respect to the major estuaries, e.g. those of the Amazon, the Zaire and the Changjiang, which will have the greatest influence on oceanic chemistry. It may be concluded, therefore, that iron is one of the few elements for which a **global behaviour pattern**, i.e. removal at low salinities, has been almost unambiguously demonstrated for the estuarine environment.

MANGANESE In contrast to iron, the distribution patterns for manganese in estuaries are variable and both gains and losses of dissolved manganese, and even conservative behaviour, have been reported in the literature. These variations can be related to the aqueous chemistry of the element.

Manganese is a redox-sensitive element which is biogeochemically reactive in the aqueous environment, and it readily undergoes transformations between the dissolved and particulate phases in response to physicochemical changes. Much of the dissolved manganese supplied by rivers is in the reduced Mn(II) state, and this can undergo oxidative conversion to particulate Mn(IV) as the physicochemical parameters change on the mixing of fresh and saline waters. The oxidation of Mn(II) is autocatalytic, the product being a solid manganese dioxide phase whose composition depends on the reaction conditions, i.e. it is heterogeneous. The process is pH-dependent and also proceeds faster in the presence of a particulate phase that is able to adsorb the Mn(II), e.g. in the presence of a turbidity maximum. In estuarine waters, therefore, it is redox-driven processes involving dissolved $\leftrightarrow$ particulate reactions that play the dominant role in the chemistry of manganese. These redox reactions also continue after the deposition of Mn(IV) particulates in the bottom sediments. Many estuarine sediments are reducing at depth so that the Mn(IV) solids can become reduced during diagenesis, thus releasing

Mn(II) into the interstitial waters and setting up a concentration gradient with respect to the overlying water column, which usually contains smaller concentrations of dissolved manganese. Dissolved Mn migrates up this gradient and, if the upper sediments are reducing, it may escape into the overlying water column, either directly or during the tidal resuspension of bottom material. If the upper sediments are oxic, much of the dissolved Mn will be reprecipitated as Mn(IV) hydrous oxides. However, Mn in this form can also enter the water column during resuspension processes, and this has been demonstrated for the St. Lawrence by Sundby *et al.* (1981). These authors showed that the manganese enrichment in the sediment surface layers was not uniform, but occurred mostly on discrete, small-sized (0.5–4 μm), Mn-enriched particles. These particles were also found in the water column, including the upper waters, and it was suggested that they can become caught up in the estuarine circulation pattern and, as a consequence of their small size, some may escape into the open ocean. This, therefore, provides a potential mechanism for the leaking or particulate manganese from the estuarine system.

Under certain estuarine conditions manganese can behave in a conservative manner. This was demonstrated for the Beaulieu estuary (UK) by Holliday & Liss (1976). Here, there was no evidence for the removal of dissolved manganese from solution, a situation that may be attributed to the low concentration of suspended solids and the rapid freshwater replacement time in the estuary (Mantoura & Morris 1983). In many estuaries, however, dissolved manganese shows pronounced non-conservative behaviour patterns. These patterns can be of different types, but that reported by Knox *et al.* (1981) for the Tamar (UK) will serve to illustrate the behaviour of the element in an estuary where a turbidity maximum is present and where the bottom sediments are in a reduced condition. The principal features of the dissolved Mn profile in this estuary are (a) a decrease in the concentrations of dissolved manganese at low salinities and (b) a broad increase at higher, mid-estuarine, salinities (see Fig. 3.5b(v)). Essentially, this profile can be interpreted in terms of a fluvial input of Mn(II), which is strongly removed from solution by the oxidative precipitation of Mn(IV) at the turbidity maximum that is present in the low-salinity region of the Tamar estuary. This turbidity maximum removes a large quantity of the fluvially transported Mn(II) before it can enter the estuary proper, and in order to account for the mid-estuarine Mn(II) increase, the authors proposed that in this region interstitial waters from anoxic sediments had been swept into the overlying water column. Under these conditions, therefore, the redox-driven production of Mn(II) took place in the sediment reservoir. Different behaviour patterns of dissolved Mn, in which the production of Mn(II) takes place in the water column, have been reported for other estuaries, e.g. those of the Rhine

and Scheldt (Duinker *et al.* 1979).

It may be concluded, therefore, that profiles of dissolved manganese in estuarine surface waters are controlled by the fluvial input of dissolved Mn(II), the oxidative conversion of the dissolved Mn(II) to particulate Mn(IV), and the reduction and resolubilization of Mn(IV) in either the water column or the sediment compartments. However, owing to inter-estuarine variations in the parameters that control the redox-driven cycling of manganese, the element does not appear to exhibit a global estuarine mixing pattern. In many estuaries it appears that dissolved Mn is *removed* from solution, but this is not a universal feature especially in large river–estuarine systems. For example, Edmond *et al.* (1985) reported that in the Changjiang estuary dissolved manganese appears to *increase* up to a salinity of ~ 12‰, beyond which it behaves conservatively.

3.2.7.3 Barium There is now a considerable body of evidence in the literature which suggests that there may be a common pattern in the behaviour of barium during estuarine mixing. This involves the desorption of the element from particulate matter at low salinities, often followed by conservative behaviour across the rest of the mixing zone (see e.g. Fig. 3.5b(iii)). Significantly, this estuarine production of barium has been reported for large river–estuarine systems, such as those of the Amazon (Boyle 1976), the Mississippi (Hanor & Chan 1977), the Zaire (Edmond *et al.* 1978) and the Changjiang (Edmond *et al.* 1985); in the latter system the fluvial flux of dissolved barium was increased by 25% following the estuarine production of the element.

3.2.7.4 Boron A number of authors have suggested that boron can be removed from solution during estuarine mixing (see e.g. Liss & Pointon 1973). Fine-grained suspended material, especially illite-type clays, are thought to adsorb the boron from solutions, a process that is enhanced as salinity increases. However, Fanning & Maynard (1978) reported data showing that boron behaves conservatively in both the Zaire and Madalena river plumes (see also Fig. 3.5b(i)), thus casting doubt on the concept that the inorganic adsorption of the element onto suspended solids at the fresh water/saline water interface is a globally significant geochemical process.

3.2.7.5 Aluminium Several studies carried out on the behaviour of dissolved aluminium in small river–estuarine systems have indicated removal of the element at low salinities, either via flocculation, sorption onto resuspended sediment particles or precipitation with silica (see e.g. Hosokawa *et al.* 1970, Hydes & Liss 1977, Sholkovitz 1978, Macklin & Aller 1984). A consensus of the data in the literature therefore appears to indicate that the Al delivered to the oceans by fluvial sources may be

largely removed in the estuarine and coastal zones before it can reach the open ocean (see e.g. Orians & Bruland 1985), the removal apparently varying between ~ 20 and ≳ 50% of the fluvial flux. It must be stressed, however, that few data exist on the behaviour of dissolved Al in the estuaries of large rivers. Van Bennekon & Jager (1978) carried out a preliminary study in the Zaire plume and reported that in this tropical system, which is characterized by low suspended solids and high dissolved organic matter loads and a short residence time of the water in the low-salinity region, there was a production of dissolved aluminium with maximum values at ~ 5‰. The authors concluded, however, that it is not possible to predict a global estuarine behaviour pattern for dissolved aluminium since variations in the concentrations and type of suspended solids, the amount and type of dissolved organics and the residence time of the water in different salinity regions must all be taken into account when assessing the fate of the element.

3.2.7.6 The nutrients A variety of behaviour patterns, involving both chemical and biological controls, have been described in the literature for nitrogen, phosphorus and silicon in estuaries (see e.g. GESAMP 1987). Much of the earlier work on the estuarine behaviour of the nutrients was confined to smaller, often polluted estuaries. In order to assess the effects that the major, globally important, rivers have on the fluxes of nutrients to the World Ocean it is necessary to understand the basic principles which govern nutrient geochemistry in the estuarine system. However, Kaul and Froelich (1984) drew attention to the fact that these principles are not well understood, and in order to rectify this the authors modelled estuarine nutrient chemistry in a simple pristine system (the Ochlockonee River and Bay, USA). Using a combination of a variety of standard estuarine models, they were able to describe mathematically the long-term (14-month) profiles of silica, phosphate and nitrate by deconvoluting them into three component functions: linear mixing, removal by biological productivity and regeneration. The model provided quantitative estimates of the subsequent fluxes of the nutrients to the ocean, and the results may be summarized as follows.

(a) Around 29% of the dissolved fluvial silica flux is removed in the estuary by biological mechanisms; however, all of this silica is regenerated within the estuary and quantitatively released back into the water column. As a result, the flux of silica out of the estuary is virtually identical to the fluvial flux, that is, little of the silica is trapped in estuarine sediments.
(b) Around 80% of the 'dissolved-reactive' phosphate, about one-third of which enters the system in a particle-associated form and is released after deposition in sediments, undergoes biological removal

in the estuary, but most of this is regenerated so that, like silica, $\simeq$ 100% of the fluvial phosphate enters the oceans.

(c) A mass balance could not be constructed for nitrate since most of it enters and escapes the system in unmeasured forms: for example, as ammonia, or via denitrification to N_2 and N_2O.

(d) The authors concluded, therefore, that estuaries are **geochemical transformers** that enhance the reactive fluvial phosphate flux to the oceans by releasing particulate phosphate, and that pass the fluvial silica flux virtually unaltered.

The investigation reported by Kaul and Froelich (1984) provided data that could be extrapolated to globally-important river systems, and a number of studies have been carried out on the behaviour of the nutrients in such systems. These can be illustrated with reference to the Amazon (Edmond *et al.* 1981), Changjiang (Edmond *et al.* 1985) and Zaire (Van Bennekon *et al.* 1978) estuarine systems.

In the Amazon, the remineralization of the labile fraction of particulate organic material in a depositional zone above the estuary results in increases in dissolved nitrate and phosphate, which yield concentrations that are $\sim$ 75% above their fluvial inputs. Data reported for the Amazon plume during a *summer* diatom bloom (Edmond *et al.* 1981) showed that photosynthetic activity commenced when suspended particulates had decreased to $\lesssim$ 10 mg l^{-1}, which occurred at a salinity of $\sim$ 7‰, thus making sufficient light available for primary production to be initiated. The diatom bloom occurred over the salinity range $\sim$ 7 to $\sim$ 15‰, and here there was complete depletion of dissolved nitrate and phosphate and a 25% depletion in dissolved silica. The underlying salt wedge became enriched in nutrients remineralized from this sinking planktonic material, and mass-balance calculations showed that: (a) almost all the organic carbon and phosphorus is remineralized in the salt wedge or at the sediment surface; (b) the remineralization of fixed nitrogen is only partial, with $\sim$ 50% being transformed into forms other than nitrate or nitrite; and (c) only a minor part of the silica is dissolved so that the rest must be transferred to the sediment sink as diatoms. These various processes affect the net fluxes of the nutrients to the ocean.

(a) Nitrate and phosphate are added to the fluvial input above the estuary.

(b) Phosphate is little affected by the estuarine processes, since planktonic uptake and remineralization are in approximate balance.

(c) Only $\sim$ 50% of the fixed nitrogen can escape as nitrate or nitrite.

(d) Around 20% of the fluvial-transported silica appears to be trapped in the sediments as diatom tests. However, in a subsequent paper, DeMaster *et al.* (1983) estimated that only $\sim$ 4% of the fluvial silica flux accumulates on the Amazon shelf as biogenic opal.

The seasonal effect on nutrient distributions in the Amazon plume is evident from data collected under *winter* conditions of very much reduced biological activity. These data, which are described in Edmond *et al.* (1985), indicated that although phosphate concentrations increased at low salinities, probably as a result of desorption from particulate material, both nitrate and silica are essentially conservative over the salinity range ~ 3 to ~20‰.

In the Changjiang estuary high concentrations of suspended particulates are maintained up to a salinity of $\gtrsim$ 20‰, and as a result summer plankton blooms are found only on the inner shelf, at salinities greater than this, where the concentrations of suspended material do not suppress biological activity. Edmond *et al.* (1985) have given data on the seasonal behaviour of nutrients in the Changjiang estuary. In the *summer* months both silica and nitrate behaved conservatively out to salinities of ~ 18 to ~ 20‰, but showed some depletion beyond this in the presence of plankton blooms, thus indicating biological removal. In *winter*, however, when there is no significant photosynthetic activity, both nutrients behaved in a conservative manner over the entire salinity range of the mixing zone. This was an important conclusion with regard to the estuarine behaviour of silica, since it showed that despite very high concentrations of suspended matter there was no significant removal by processes associated with particulates. In *summer* phosphate was almost completely depleted at salinities > 18‰, suggesting that this, rather than nitrate, is the limiting nutrient in the system. However, in the *winter* there was an increase in dissolved phosphate at low salinities ($\lesssim$ 5‰), indicating an extensive desorption of phosphate from suspended material.

In the Zaire estuary the nutrient relationships are somewhat different from those found in the Amazon and Changjiang systems, since photosynthetic activity in the Zaire does not occur at salinities $\lesssim$ 30‰, and even here the water is still relatively turbid and *in situ* production remains low (Cadee 1978). According to the data provided by Van Bennekon *et al.* (1978), silica in the estuary is conservative out to the salinities at which phytoplankton blooms occur, again indicating a lack of interaction with particulate matter, beyond which the concentrations decrease due to biological uptake. Phosphate profiles showed maximum concentrations at salinities of ~ 10‰, due partly to desorption from suspended material, followed by uptake at higher salinities as a result of biological removal. Nitrate had a similar profile, but the addition to the fluvial source at lower salinities mainly arose from the mixing of subsurface sea water, with higher nitrate concentrations, into the surface waters.

There are major differences between the Amazon and Zaire plumes; for example, in the Amazon plume *in situ* production is one order of magnitude higher than in the adjacent ocean, whereas in the Zaire plume the values are about the same as outside. Cadee (1978) has suggested a

number of reasons for this, one of which is related to the suspended sediment regime. In the Amazon $\gtrsim$ 95% of the suspended material in the surface waters settles out within the river mouth before the salinities reach $\sim$ 3‰, whereas in the Zaire particulate matter remains in suspension up to higher salinity levels. For example, at salinities of 10‰ suspended solid levels in the Zaire of $\sim$ 15 mg l^{-1} have been reported, compared to $\sim$ 1 mg l^{-1} for the Amazon. In the Amazon system, therefore, plankton blooms reach their maximum development at salinities $<$ 10‰ where development is favoured by the low turbidity of the waters and nutrient concentrations that are still relatively high. In contrast, in the Zaire plume, the blooms develop at much higher salinities, by which time dilution of the river-transported nutrients by nutrient-poor sea water has produced levels too low to give rise to major blooms.

In terms of the major, non-polluted estuaries the following general nutrient dynamics can therefore be outlined. Nutrients are carried by fluvial transport in both dissolved and particulate forms, and the dissolved load can be increased by the remineralization of labile particulate nutrients within the estuary. When sufficient dissolved nutrients are available, biological uptake is controlled by the availability of light and the turbidity of the water. Thus, the distribution of suspended material appears to be the controlling variable on the onset of large-scale biological productivity (see e.g. Milliman & Boyle 1975). Once biological activity takes place, e.g. via the production of diatom blooms, nutrients are removed from solution and the sinking of planktonic debris containing nutrients in a particulate form can lead to either (a) their remineralization in the saline layer and their subsequent transport out to sea where, when the flow is debouched onto open shelves, they can lead to an increase in nutrients in bottom waters and can sustain coastal productivity following upwelling, or (b) their trapping in the bottom sediment. Although the picture is by no means totally clear yet, there is evidence that some nutrients may exhibit a globial behaviour pattern. For example, the following tentative conclusions can be drawn as regards the changes affecting the fluvial fluxes of silica in pristine, i.e. unpolluted, estuaries. Silica can undergo biological uptake, but much of this appears to be remineralized and only a relatively small fraction (less than $\sim$ 20% and perhaps $\lesssim$ 5%) of the total dissolved fluvial flux of silica which enters natural estuarine systems appears to be buried in bottom sediments. Mass balance calculations show that much of the fluvial silica can escape the estuarine system and be delivered to the oceans; for example, DeMaster *et al.* (1983) estimated that $\sim$ 95% of the silica supplied by the Amazon River escapes the continental shelf to yield a net flux to the Atlantic Ocean of $\sim 4.7 \times 10^{13}$ g yr^{-1}. In polluted estuaries enriched in nitrate and phosphate, however, the situation is different.

3.2.7.7 Organic carbon

PARTICULATE ORGANIC CARBON (POC) In attempting to assess the fate of fluvial POC (and DOC) in the estuarine and coastal zones it is necessary to distinguish between a labile and a refractory fraction (see Sec. 9.2). The total fluvial flux of POC has been estimated to be 2.31×10^{12} g yr^{-1}, and according to Ittekkot (1988) ~ 35% of this (i.e. 81×10^{12} g yr^{-1}) is labile and may undergo oxidative destruction in estuaries and the sea. The remaining 65% (i.e. $\sim 150 \times 10^{12}$ g yr^{-1}) is refractory and can escape to the ocean environment to be accumulated in sediments.

DISSOLVED ORGANIC CARBON (DOC) Data for the behaviour of DOC during estuarine mixing are somewhat contradictory. Evidence is available from both laboratory experiments and field surveys which suggests that at least some fractions of fluvial DOC can be removed in estuaries and coastal waters by processes such as flocculation, adsorption onto particulates and precipitation (see e.g. Sieburth & Jensen 1968, Sholkovitz 1978, Menzel 1974, Schultz & Calder 1976, Hunter & Liss 1979). These removal mechanisms would lead to the non-conservative behaviour of DOC at the land/sea margins. However, this was challenged by Mantoura & Woodward (1983). These authors reported data derived from a large-scale, two-and-a-half-year survey of the distribution, variability and chemical behaviour of DOC in the Severn estuary and Bristol Channel (UK), a system selected because of its relatively long water residence times (100–200 days) and its particle-rich waters, both of which would favour the *in situ* detection of any of the DOC removal processes. However, the survey revealed that even under these conditions DOC behaved in a conservative manner in the estuary. If such conservative non-reactivity is characteristic of the behaviour of DOC in *major*, i.e. globally significant, estuaries it will have extremely important implications for both the fluxes of DOC to the oceans (see e.g. Sec. 6.1.4) and the origins of the material in the deep water oceanic DOC pool (see Sec. 9.2.2).

3.2.7.8 Trace metals There is considerable scatter in the data for the behaviour of a number of trace elements in estuaries. Both conservative and non-conservative behaviour patterns have been reported for individual dissolved trace metals in different estuarine systems, and these patterns are obviously dependent on local conditions. For example, there is considerable evidence that trace metals such as Zn, Cu, Cd, Pb and Ni *can* exhibit non-conservative patterns during estuarine mixing, and Campbell & Yeats (1984) showed that ~ 50% of the dissolved Cr was removed at low salinities in the St. Lawrence estuary; at salinities > 5‰ the element behaved conservatively. However, Danielsson *et al.* (1983) gave data on the distributions of dissolved Fe, Pb, Cd, Cu, Ni and Zn in the Gota River estuary (Sweden), a relatively unpolluted salt wedge

system, and demonstrated that the processes which remove dissolved trace metals from solution did not operate very effectively in the system. The result of this was that, apart from iron, the metals behaved in an essentially conservative manner during estuarine mixing. Balls (1985) used salinity versus concentration plots to demonstrate the conservative behaviour of Cu and Cd in the Humber estuary (UK). It is apparent, therefore, that the non-conservative behaviour of some trace metals is not a universal feature of the estuarine environment. Further, even when non-conservative behaviour has been identified for trace metals it may involve either the loss of, or the production of, dissolved species. For example, Duinker & Notling (1977, 1978) showed that fluvial dissolved Fe, Cu, Zn and Cd are removed in the Rhine estuary. However, the Rhine is a relatively small, heavily polluted system and the removal processes that operate there do not appear to be typical of those in large non-polluted rivers systems. Thus, Byrd & Andreae (1986) showed that, although dissolved Sn can behave in a non-conservative manner in polluted estuaries, mixing zone reactions have little effect on the element under most estuarine conditions. From the point of view of the influence that estuarine reactivity has on the trace metal chemistry of the World Ocean, it is therefore perhaps most sensible to concentrate on the behaviour of trace metals in the large estuarine systems. Although data on this topic are still relatively scarce, it is worthwhile summarizing the findings of a number of recent studies.

Boyle *et al.* (1982) concluded that Cu, Cd and Ni are usually unreactive during the mixing of river and sea water in the Amazon plume, a low organic and high particulate system. In contrast, Edmond *et al.* (1985) reported that in the Changjiang estuary Ni was desorbed from particulate matter at low salinities, then behaved conservatively at values above 8‰; however, Cu and Be behaved in a conservative manner over the entire mixing zone in the same estuary. Moore & Burton (1978) described the distribution of dissolved Cu in the Zaire estuary, and although trends in the data were not very clear there was a suggestion that Cu was desorbed at intermediate salinities. Both Boyle *et al.* (1982) and Edmond *et al.* (1985) have provided evidence that Cd undergoes desorption at low salinities in the Amazon and Changjiang estuaries, respectively. Measures & Edmond (1983) showed how dissolved Be can behave differently in different estuarine systems. (a) In the Amazon system the element was removed dramatically in the early stages of mixing (up to a salinity of ~ 15‰) and then behaved in a conservative manner. (b) In the Zaire system there was removal of Be at the onset of mixing followed by only minor non-conservative behaviour out to a salinity of ~ 28‰, after which there was a sharp drop in concentration (coincident with the onset of diatom growth), followed by conservative mixing out to open-ocean salinities. (c) In contrast, in the Changjiang estuary Be exhibited

approximately conservative behaviour; in this system, the high alkalinity of the river water had induced the flocculation or adsorption of the element from solution, with the result that dissolved concentrations were exceptionally low. Thus, it appears that, with the exception of iron, which is universally removed from solution (see above), there are few common trends in the conservative/non-conservative behaviour patterns of trace metals in estuaries. However, when non-conservative behaviour does occur, low-salinity **desorption**, i.e. gain to solution, followed by essentially conservative behaviour appears to be an important process in the behaviour of Ba, Mn, Ni and Cd in major estuarine systems.

The behaviour of elements in the estuarine mixing zone can also be dependent on speciation. For example, Froelich *et al.* (1985) found that although inorganic Ge follows silica and can behave in a non-conservative way in estuaries, monomethyl and dimethyl species of the element exhibited conservative behaviour patterns. Speciation differences can also affect the estuarine behaviour of other elements, such as Cu – see Section 3.2.5 for a description of these species-related estuarine behaviour patterns.

3.2.8 The estuarine modification of river-transported signals: summary

(a) Estuaries, which are located at the land/sea margins, exhibit large property gradients and can be regarded as acting as filters of river-transported chemical signals. This filter acts mainly via dissolved–particulate reactivity. This reactivity can be mediated by both physicochemical and biological processes, and is dependent on a range of interrelated factors which include: the physical regime of an estuary, the residence time of the water, primary production, pH, differences in composition between the end-member waters, and the concentrations of suspended particulate material, organic and inorganic ligands and nutrients. However, the effects of the filter can vary widely from one estuary to another, and it is difficult to identify global estuarine processes.

(b) The estuarine filter is also selective in the manner in which it acts on individual elements. Some dissolved elements are simply diluted on the mixing of river and sea water (conservative behaviour), whereas others undergo estuarine dissolved–particulate reactions, which lead to their addition to, or removal from, the dissolved phase (non-conservative behaviour).

(c) Particulate elements that are added to the dissolved phase (e.g. by desorption, biological degradation) increase the fluvial flux and can be carried out of the estuarine environment during tidal flushing. In contrast, elements that are added to the particulate phase (e.g. by adsorption, flocculation, biological uptake) can be trapped in the bottom sediments; however, processes such as sediment resuspension

and diagenetic release followed by the flushing out of interstitial waters can recycle these elements back into the water phase.

(d) The dissolved–particulate reactivity can take place over a number of estuarine regions. (i) Physicochemically mediated particulate–dissolved reactions are especially intense at the low-salinity region where the initial mixing of the fresh and saline end-member waters takes place. Here, processes such as flocculation (e.g. Fe) and particle adsorption–precipitation (e.g. Mn) are active in the removal of elements from solution, the latter being enhanced in the presence of a turbidity maximum. (ii) Primary production, which involves the biologically mediated generation of particulate matter and the removal of nutrients from solution, is controlled largely by the availability of nutrients and the turbidity of the waters, and tends to reach a maximum at mid- and high-salinity ranges where the concentrations of particulate matter (turbidity) decrease and where nutrients are present in sufficient quantity to initiate production.

(e) Around 90% of the particulate matter transported into estuaries via the fluvial flux is trapped in the estuarine environment under present-day conditions.

(f) With the exception of iron, which is removed at low salinities, few dissolved elements exhibit a global estuarine behaviour pattern. For example, dissolved Cu has been shown to exhibit either conservative or non-conservative behaviour (including both addition to and removal from solution) in different estuaries. However, recent evidence has suggested that desorption at low salinities, followed by conservative behaviour over the rest of the mixing zone, is an important process in the behaviour of Ba, Mn, Ni and Cd in major estuarine systems.

References

Aston, S.R. 1978. Estuarine chemistry. In *Chemical oceanography*, J.P. Riley & R. Chester (eds), Vol. 7, 361–440. London: Academic Press.

Balls, P.W. 1985. Copper, lead and cadmium in coastal waters of the western North Sea. *Mar. Chem.* **15,** 363–78.

Bewers, J.M. & P.A. Yeats 1977. Oceanic residence times of trace metals. *Nature* **268,** 595–8.

Bewers, J.M. & P.A. Yeats 1980. Behaviour of trace metals during estuarine mixing. In *River inputs to ocean systems*, J.-M. Martin, J.D. Burton & D. Eisma (eds), 103–15. Paris: UNEP/Unesco.

Boyle, E.A. 1976. The marine geochemistry of trace metals. *Thesis*, MIT-WHOI, Cambridge, Mass.

Boyle, E.A., R. Collier, A.T. Dengler, J.M. Edmond, A.C. Ng & R.F. Stallard 1974. On the chemical mass-balance in estuaries. *Geochim. Cosmochim. Acta* **38,** 1719–28.

Boyle, E.A., J.M. Edmond & E.R. Sholkovitz 1977a. The mechanism of iron removal in estuaries. *Geochim. Cosmochim. Acta* **41,** 1313–24.

Boyle, E.A., S.S. Huested & B. Grant 1982. The chemical mass balance of the Amazon plume – II. Copper, nickel and cadmium. *Deep-Sea Res.* **29,** 1355–64.

Boyle, E.A., F.R. Sclater & J.M. Edmond 1977b. The distribution of dissolved copper in the Pacific. *Earth Planet. Sci. Lett.* **37,** 38–54.

Byrd, J.T. & M.O. Andreae 1986. Geochemistry of tin in rivers and estuaries. *Geochim. Cosmochim. Acta* **50,** 835–45.

Cadee, G.C. 1978. Primary production and chlorophyll in the Zaire river, estuary and plume. *Neth. J. Sea Res.* **12,** 368–81.

Campbell, J.A. & P.A. Yeats 1984. Dissolved chromium in the St. Lawrence estuary. *Estuar. Coastal Shelf Sci.* **19,** 513–22.

Chester, R. 1988. The storage of metals in sediments. In *Workshop on metals and metalloids in the hydrosphere*, Bochum 1987, Unesco Int. Hydrol. Programme, in press.

Coonley, L.S., E.B. Baker & H.D. Holland 1971. Iron in the Mullica River and Great Bay, New Jersey. *Chem. Geol.* **7,** 51–64.

Danielsson, L.G., B. Magnusson, S. Westerlund & K. Zhang 1983. Trace metals in the Gota River estuary. *Estuar. Coastal Shelf Sci.* **17,** 73–85.

Degens, E.T. & V. Ittekkot 1985. Particulate organic carbon: an overview. In *Transport of carbon and minerals in major world rivers*, Part 3, E.T. Degens, S. Kempe & R. Herrera (eds), 7–27. Mitt.Geol.–Palont. Inst. Univ. Hamburg, SCOPE/UNEP, Sonderband 58.

DeMaster, D.J., G.B. Knapp & C.A. Nittrover 1983. Biological uptake and accumulation of silica on the Amazon continental shelf. *Geochim. Cosmochim. Acta* **47,** 1713–23.

Drever, J.L. 1982. *The geochemistry of natural waters*. Englewood Cliffs, NJ: Prentice-Hall.

Duinker, J.C. 1986. Formation and transformation of element species in estuaries. In *The importance of chemical 'speciation' in environmental processes*, M. Bernhard, F.T. Brinckman & P.J. Sadler (eds), 365–84. Berlin: Springer-Verlag.

Duinker, J.C. & C.J.M. Kramer 1977. An experimental study on the speciation of dissolved zinc, cadmium, lead and copper in Rhine River and North Sea water, by differential pulsed anodic stripping voltammetry. *Mar. Chem.* **5,** 207–28.

Duinker, J.C. & R.F. Notling 1977. Dissolved and particulate trace metals in the Rhine Estuary and the Southern Bight. *Mar. Pollut. Bull.* **8,** 65–71.

Duinker, J.C. & R.F. Notling 1978. Mixing, removal and mobilization of trace metals in the Rhine Estuary. *Neth. J. Sea Res.* **12,** 205–23.

Duinker, J.C., R. Wollast & G. Billen 1979. Behaviour of manganese in the Rhine and Scheldt estuaries. II. Geochemical cycling. *Estuar. Coastal Shelf Sci.* **9,** 727–38.

Dyrssen, D. & M. Wedborg 1980. Major and minor elements, chemical speciation in estuarine waters. In *Chemistry and biochemistry of estuaries*, E. Olausson & I. Cato (eds), 71–120. New York: Wiley.

Edmond, J.M., E.A. Boyle, D. Drummond, B. Grant & T. Mislick 1978. Desorption of barium in the plume of the Zaire (Congo) River. *Neth. J. Sea Res.* **12,** 324–8.

Edmond, J.M., E.A. Boyle, B. Grant & R.F. Stallard 1981. Chemical mass balance in the Amazon plume I: the nutrients. *Deep-Sea Res.* **28,** 1339–74.

Edmond, J.M., A. Spivack, B.C. Grant, H. Ming-Hui, C. Zexiam, C. Sung & Z. Xiushau 1985. Chemical dynamics of the Changjiang estuary. *Cont. Shelf Res.* **4,** 17–36.

Eisma, D. 1975. Dissolved iron in the Rhine estuary and the adjacent North Sea. *Neth. J. Sea Res.* **9,** 222–30.

Ertel, J.R., J.I. Hedges, A.H. Devol, J.E. Richey & M. Ribeiro 1986. Dissolved humic substances of the Amazon River system. *Limnol. Oceanogr.* **31,** 739–54.

REFERENCES

Fairbridge, R.W. 1980. The estuary: its identification and geodynamic cycle. In *Chemistry and biochemistry of estuaries*, E. Olausson & I. Cato (eds), 1–36. New York: Wiley.

Fanning, K.A. & V.I. Maynard 1978. Dissolved boron and nutrients in the mixing plumes of major tropical rivers. *Neth. J. Sea Res.* **12,** 345–54.

Feth, J.H. 1971. Mechanisms controlling world water chemistry: evaporation–crystallization processes. *Science* **172,** 870–2.

Figueres, G., J.M. Martin & M. Maybeck 1978. Iron behaviour in the Zaire estuary. *Neth. J. Sea Res.* **12,** 329–37.

Froelich, P.N. 1988. Kinetic control of dissolved phosphate in natural rivers and estuaries: a primer on the phosphate buffer mechanism. *Limnol. Oceanogr.* **33,** 649–68.

Froelich, P.N., G.A. Hambrick, M.O. Andreae & R.A. Mortlock 1985. The geochemistry of inorganic germanium in natural waters. *J. Geophys. Res.* **90,** 1133–41.

GESAMP 1987. *Land/sea boundary flux of contaminants from rivers.* Paris: Unesco.

Gibbs, R.J. 1970. Mechanisms controlling world river water chemistry. *Science* **170,** 1088–90.

Gibbs, R.J. 1972. Water chemistry of the Amazon river. *Geochim. Cosmochim. Acta* **36,** 1061–6.

Gibbs, R.J. 1973. Mechanisms of trace metal transport in rivers. *Science* **180,** 71–3.

Gibbs, R.J. 1977. Transport phases of transition metals in the Amazon and Yukon rivers. *Bull. Geol. Soc. Am.* **88,** 829–43.

Hanor, J.S. & L.A. Chan 1977. Non-conservative behaviour of barium during mixing of Mississippi River and Gulf of Mexico waters. *Earth Planet. Sci. Lett.* **37,** 242–50.

Holland, H.D. 1978. *The chemistry of the atmosphere and oceans.* New York: Wiley Interscience.

Holliday, L.M. & P.S. Liss 1976. The behaviour of dissolved iron, manganese and zinc in the Beaulieu Estuary. *Estuar. Coastal Shelf Sci.* **4,** 349–53.

Hosokawa, I.O., F. Ohshima & N. Kondo 1970. On the concentration of the dissolved chemical elements in the estuary of the Chikugogawa River. *J. Oceanogr. Soc. Jap.* **26,** 1–5.

Hoyle, J., H. Elderfield, A. Gledhill & M. Grieves 1984. The behaviour of the rare earth elements during mixing of river and sea waters. *Geochim. Cosmochim. Acta* **48,** 148–9.

Hunter, K.A. 1983. On the estuarine mixing of dissolved substances in relation to colloid stability and surface properties. *Geochim. Cosmochim. Acta* **47,** 467–73.

Hunter, K.A. & P.S. Liss 1979. The surface charge of suspended particles in estuarine and coastal waters. *Nature* **282,** 823–5.

Hydes, D.J. & P.S. Liss 1977. The behaviour of dissolved Al in estuarine and coastal waters. *Estuar. Coastal Shelf Sci.* **5,** 755–69.

Ittekkot, V. 1988. Global trends in the nature of organic matter in river suspensions. *Nature* **332,** 436–8.

Kaul, L.W. & P.N. Froelich 1984. Modelling estuarine nutrient geochemistry in a simple system. *Geochim. Cosmochim. Acta* **48,** 1417–33.

Kharkar, D.P. & K.K. Turekian 1968. Stream supply of dissolved Ag, Mo, Sb, Se, Cr, Co, Rb, and Cs to the oceans. *Geochim. Cosmochim. Acta* **32,** 285–98.

Knox, S., D.R. Turner, A.G. Dickson, M.I. Liddicoat, M. Whitfield & E.I. Butler 1981. Statistical analysis of estuarine profiles: application to manganese and ammonium in the Tamar estuary. *Estuar. Coastal Shelf Sci.* **13,** 357–71.

Konta, J. 1985. Mineralogy and chemical maturity of suspended matter in major rivers sampled under the SCOPE/UNEP Project. In *Transport of carbon and minerals in major*

world rivers, Part 3, E.T. Degens, S. Kempe & R. Herrera (eds), 569–92. Mitt.Geol.-Palont. Inst. Univ. Hamburg, SCOPE/UNEP, Sonderband 58.

Li, Y.-H., L. Burkhard & H. Teroaka 1984. Desorption and coagulation of trace elements during estuarine mixing. *Geochim. Cosmochim. Acta* **48,** 1879–84.

Liddicoat, M.I., D.R. Turner & M. Whitfield 1983. Conservative behaviour of boron in the Tamar Estuary. *Estuar. Coastal Shelf Sci.* **17,** 467–72.

Liss, P.S. 1976. Conservative and non-conservative behaviour of dissolved constituents during estuarine mixing. In *Estuarine chemistry*, J.D. Burton & P.S. Liss (eds), 93–130. London: Academic Press.

Liss, P.S. & M.J. Pointon 1973 Removal of dissolved boron and silicon during estuarine mixing of sea and river waters. *Geochim. Cosmochim. Acta* **37,** 1493–8.

Macklin, J.E. & R.C. Aller 1984. Dissolved Al in sediments and waters of the East China Sea: implications for authigenic mineral formation. *Geochim. Cosmochim. Acta* **48,** 281–98.

Mantoura, R.F.C. & A.W. Morris 1983. Measurement of chemical distributions and processes. In *Practical procedures for estuarine studies*, A.W. Morris (ed.), 101–38. Plymouth: IMER.

Mantoura, R.F.C. & E.M.S. Woodward 1983. Conservative behaviour of riverine dissolved organic carbon in the Severn Estuary: chemical and geochemical implications. *Geochim. Cosmochim. Acta* **47,** 1293–309.

Mantoura, R.F.C., A. Dickson & J.P. Riley 1978. The complexation of metals with humic materials in natural waters. *Estuar. Coastal Shelf Sci.* **6,** 387–408.

Martin, J.-M. & M. Maybeck 1979. Elemental mass balance of material carried by major world rivers. *Mar Chem.* **7,** 173–206.

Martin, J.-M. & M. Whitfield 1983. The significance of the river input of chemical elements to the ocean. In *Trace metals in sea water*, C.S. Wong, E. Boyle, K.W. Bruland, J.D. Burton & E.D. Goldberg (eds), 265–96. New York: Plenum.

Maybeck, M. 1978. Note on dissolved elemental contents of the Zaire River. *Neth. J. Sea Res.* **12,** 293–5.

Maybeck, M. 1979. Concentrations des eaux fluviales en elements majeurs et apports en solution aux oceans. *Rev. Geol. Dyn. Geogr. Phys.* **21,** 215–46.

Maybeck, M. 1981. Pathways of major elemens from land to ocean through rivers. In *River inputs to ocean systems*, J.-M. Martin, J.D. Burton & D. Eisma (eds), 18–30. Paris: UNEP/Unesco.

Maybeck, M. 1982. Carbon, nitrogen and phosphorus transport by world rivers. *Am. J. Sci.* **282,** 401–50.

Meade, R.H. 1972. Transport and deposition of sediments in estuaries. *Geol. Soc. Am. Mem.* **133,** 91–120.

Measures, C.I. & J.M. Edmond 1983. The geochemical cycle of ^{9}Be: a reconnaissance. *Earth Planet. Sci. Lett.* **66,** 101–10.

Menzel, D.W. 1974. Primary productivity, dissolved and particulate organic matter, and the sites of oxidation of organic matter. In *The sea*, E.D. Goldberg (ed.), Vol. 5, 659–78. New York: Wiley Interscience.

Milliman, J.D. & E.A. Boyle 1975. Biological uptake of dissolved silica in the Amazon River estuary. *Science* **189,** 995–7.

Milliman, J.D., C.P. Summerhayes & H.T. Barreto 1975. Oceanography and suspended matter of the Amazon River, February–March 1973. *J. Sed. Petrol.* **45,** 189–206.

Moore, R.M. & J.D. Burton 1978. Dissolved copper in the Zaire estuary. *Neth. J. Sea Res.* **12,** 355–7.

Morris, A.W. 1986. Removal of trace metals in the very low salinity region of the Tamar Estuary, England. *Sci. Total Environ.* **49,** 297–304.

REFERENCES

Orians, K.J. & K.W. Bruland 1985. Dissolved aluminium in the central North Pacific. *Nature* **316,** 427–9.

Pickard, G.L. & W.J. Emery 1982. *Descriptive physical oceanography*. Oxford: Pergamon Press.

Potsma, H. 1967. Sediment transport and sedimentation in the estuarine environment. In *Estuaries*, G.H. Lauff (ed.) 158–9. Am. Assoc. Adv. Sci., Publ. no. 83.

Potsma, H. 1980. Sediment transport and sedimentation. In *Chemistry and biochemistry of estuaries*, E. Olausson & I. Cato (eds), 153–86. New York: Wiley.

Reeder, S.W., B. Hitchon & A.A. Levinson 1972. Hydrogeochemistry of the surface waters of the Mackenzie River drainage basin, Canada – I. Factors controlling inorganic composition. *Geochim. Cosmochim. Acta* **36,** 825–65.

Reuther, J.H. 1981. Chemical interactions involving the biosphere and fluxes of organic material in estuaries. In *River inputs to ocean systems*, J.-M. Martin, J.D. Burton & D. Eisma (eds), 239–42. Paris: UNEP/Unesco.

Riley, J.P. & R. Chester 1971. *Introduction to marine chemistry*. London: Academic Press.

Salomons, W. 1980. Adsorption processes and hydrodynamic conditions in estuaries. *Environ. Technol. Lett.* **1,** 356–65.

Salomons, W. & U. Forstner 1984. *Metals in the hydrosphere*. Berlin: Springer-Verlag.

Schultz, D.J. & J.A. Calder 1976. Organic $^{13}C/^{12}C$ variations in estuarine sediments. *Geochim. Cosmochim. Acta* **40,** 381–5.

Sclater, F.R., E.A. Boyle & J.M. Edmond 1976. On the marine geochemistry of nickel. *Earth Planet. Sci. Lett.* **31,** 119–28.

Shiller, A.M. & E. Boyle 1985. Dissolved zinc in rivers. *Nature* **317,** 49–51.

Shink, D. 1981. Behaviour of chemical species during estuarine mixing. In *River inputs to ocean systems*, J.-M. Martin, J.D. Burton & D. Eisma (eds), 101–2. Paris: UNEP/Unesco.

Sholkovitz, E.R. 1978. The flocculation of dissolved Fe, Mn, Al, Cu, Ni, Co and Cd during estuarine mixing. *Earth Planet. Sci. Lett.* **41,** 77–86.

Sholkovitz, E.R. & D. Copland 1981. The coagulation, solubility and adsorption properties of Fe, Mn, Cu, Ni, Cd, Co and humic acids in a river water. *Geochim. Cosmochim. Acta* **45,** 181–9.

Sholkovitz, E.R., E.A. Boyle & N.B. Price 1978. The removal of dissolved humic acids and iron during estuarine mixing. *Earth Planet. Sci. Lett.* **40,** 130–6.

Sieburth, J.M. & A. Jensen 1968. Studies on algal substances in the sea. I. Gelbstoff (humic materials) in terrestrial and marine waters. *J. Exp. Mar. Biol. Ecol.* **2,** 174–80.

Stallard, R.F. & J.M. Edmond 1981. Geochemistry of the Amazon 1. Precipitation chemistry and the marine contribution to the dissolved load at the time of peak discharge. *J. Geophys. Res.* **86,** 9844–58.

Stallard, R.F. & J.M. Edmond 1983. Geochemistry of the Amazon 2. The influence of geology and weathering environment on the dissolved load. *J. Geophys. Res.* **88,** 9671–88.

Stallard, R.F. & J.M. Edmond 1987. Geochemistry of the Amazon 3. Weathering chemistry and limits to dissolved inputs. *J. Geophys. Res.* **92,** 8293–302.

Sundby, B., N. Silverburg & R. Chesselet 1981. Pathways of manganese in an open estuarine system. *Geochim. Cosmochim. Acta* **45,** 293–307.

Tessier, A., P.G.C. Campbell & M. Bisson 1980. Trace metal speciation in the Yamaska and St. Francois Rivers (Quebec). *Can. J. Earth Sci.* **17,** 90–105.

Trefry, J.H. & B.J. Presely 1976. Heavy metal transport from the Mississippi River to the Gulf of Mexico. In *Marine pollutant transport*, H.L. Windom & R.A. Duce (eds), 39–76. Lexington, Mass: Lexington Books.

Van Bennekon, A.J. & J.E. Jager 1978. Dissolved aluminium in the Zaire River plume. *Neth. J. Sea Res.* **12,** 358–67.

Van Bennekon, A.J. & W. Salomons 1981. Pathways of nutrients and organic matter from land to ocean through rivers. In *River inputs to ocean systems*, J.-M. Martin, J.D. Burton & D. Eisma (eds), 33–51. Paris: UNEP/Unesco.

Van Bennekon, A.J., G.W. Berger, W. Helder & R.T.P. De Vries 1978. Nutrient distribution in the Zaire Estuary and river plume. *Neth. J. Sea Res.* **12,** 296–323.

Van der Weijden, C.H., M.J.H.L. Arnoldus & C.J. Meurs 1977. Desorption of metals from suspended material in the Rhine estuary. *Neth. J. Sea Res.* **11,** 130–45.

Walling, D.E. & B.W. Webb 1987. Material transport by the world's rivers: evolving perspectives. In *Water for the future: hydrology in perspective*, IAHS Publ. no. 164, 313–29.

Waslenchuk, D.C. & H.L. Windom 1978. Factors controlling the estuarine chemistry of arsenic. *Estuar. Coastal Shelf Sci.* **7,** 455–62.

Williams, P.J. 1981. Primary productivity and heterotrophic activity in estuaries. In *River inputs to ocean systems*, J.-M. Martin, J.D. Burton & D. Eisma (eds), 243–9. Paris: UNEP/Unesco.

Windom, H.L. & R. Smith 1985. Factors influencing the concentration and distribution of trace metals in the South Atlantic Bight. In *Oceanography of the Southeastern U.S. continental shelf*, L.P. Atkinson, D.W. Menzel & K.A. Bush (eds), 141–152. Washington, D.C.: AGU.

Windom, H.L., G. Wallace, R. Smith, N. Dudek, M. Maeda, R. Dulmage & F. Storti 1983. Behaviour of copper in southeastern United States estuaries. *Mar. Chem.* **12,** 183–94.

Yeats, P.A. & J.M. Bewers 1982. Discharge of metals from the St. Lawrence River. *Can. J. Earth Sci.* **19,** 982–92.

Zorbrist, J. & W. Stumm 1981. Chemical dynamics of the Rhine catchment area in Switzerland, extrapolation to the 'pristine' Rhine river input to the ocean. In *River inputs to ocean systems*, J.-M. Martin, J.D. Burton & D. Eisma (eds), 52–63. Paris: UNEP/Unesco.

4 The transport of material to the oceans: the atmospheric pathway

The trophosphere is a reservoir in which particles have a relatively short residence time, usually in the order of days for those with radii in the range ~ 0.1 to ~ 10 μm, and from which they are removed at about the same rate as they enter. The particles carried in the marine atmosphere have a different genetic history from those transported to the oceans via river run-off, one of the most important differences being that they do not undergo trapping, or modification, in the estuarine *filter* at the land/sea margins. At the present time, estuaries act as an effective trap for river-transported solids, holding back ~ 90% of RPM (see Sec. 6.1.2). Potentially, therefore, the atmosphere is perhaps the most important pathway for the long-range transport of particulate material directly to open-ocean areas. This has become increasingly apparent over the past two decades. For example, Delany *et al.* (1967) concluded that the land-derived material in equatorial North Atlantic deep-sea sediments deposited to the east of and on the Mid-Atlantic Ridge has been derived wholly from wind transport. Such long-range transport, spanning several thousand kilometres, has also been found over the Pacific Ocean, and Blank *et al.* (1985) estimated that almost all of the non-biogenic material in deep-sea sediments in the Central North Pacific is essentially aeolian in origin. In addition to supplying material to sediments the atmospheric components can have a pronounced effect on the chemistry of the oceanic mixed layer. However, atmospheric material has to be transferred across an interface before it is introduced into the ocean system; this is the air/sea interface (or microlayer), which is involved in the exchange of particulate and gaseous phases between sea water and the atmosphere.

4.1 Material transported via the atmosphere: the marine aerosol

4.1.1 Introduction

A suspension of solid and liquid material in a gaseous medium is usually referred to as an **aerosol**. Prospero *et al.* (1983) defined a number of aerosol types on the basis of their compositions and sources, and a summary of their classification is given in Table 4.1. It is important to

Table 4.1 The classification of aerosols on the basis of their composition or sources[a]

1.	**NATURAL AEROSOLS**	
	1.1	Sea spray residues
	1.2	Windblown mineral dust
	1.3	Volcanic effluvia
	1.4	Biogenic materials
	1.5	Smoke from the burning of land biota
	1.6	Natural gas-to-particle conversion products
2.	**ANTHROPOGENIC AEROSOLS**	
	2.1	Direct anthropogenic particle emissions.
	2.2	Products from the conversion of anthropogenic gases.

a. Based on Prospero et al. (1983).

stress at this stage that the components making up the world aerosol originate from two different kinds of processes: (a) the direct formation of particles (e.g. during crustal weathering, sea-salt generation, volcanic emissions), and (b) the indirect formation of particles in the atmosphere itself by chemical reactions and by the condensation of gases and vapours. A generalized relationship between the processes responsible for the generation of aerosol particles and their size spectra is illustrated in Figure 4.1. In this figure, the particles are divided into two broad groups, **fine** particles ($d < 2$ μm) and **coarse** particles ($d > 2$ μm), and there are three size maxima, two in the fine class and one in the coarse class. The maxima in the *fine* mode relate to two particle populations: (a) those in the Aitken nuclei range, and (b) those in the accumulation range. **Aitken nuclei** originate predominantly from combustion processes, which are chiefly anthropogenic but also include volcanic emissions and forest fires, and also from some non-combustion processes. Particles in the **accumulation** mode are thought to result primarily from the coagulation of Aitken nuclei into larger aggregates. In contrast, particles in the *coarse* mode have been formed by mechanical action, which can involve both low-temperature processes (e.g. the generation of crustal dusts and sea salts) and high-temperature processes (e.g the formation of industrial fly-ash).

The particle size of the marine aerosol has been described by Junge (1972), who identified five classes of size-related components in a North Atlantic aerosol. These are (a) particles with diameters > 40 μm, (b) sea spray particles, (c) mineral dust particles, (d) tropospheric background particles and (e) particles with diameters < 0.06 μm. The nature of the

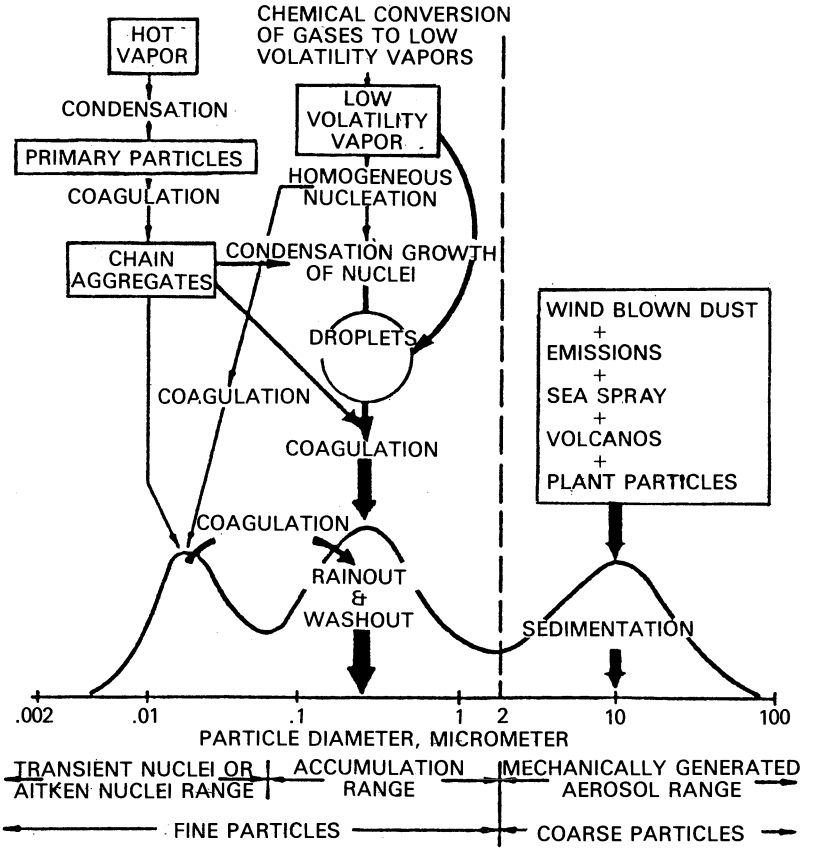

Figure 4.1 Schematic representation of the processes involved in the generation and removal of atmospheric particles (from Whitby 1977).

tropospheric background material has been the subject of much speculation, but it is generally thought that an aerosol of fairly uniform composition, dominated by sulphate, is present over ~ 85% of the troposphere. If the very small particles ($d < 0.06$ μm) are excluded, the marine aerosol can therefore be regarded as being composed of the tropospheric background material upon which is superimposed continental dust (the mineral aerosol), sea spray (the sea-salt aerosol) and the large-sized component (consisting of biological material, pollutants such as 'cokey balls', and giant sea spray particles).

Close to the source, the composition of a specific aerosol component, such as mineral dust, will be closely related to that of the parent material. However, during their residence time in the atmosphere both coarse and fine particles can undergo physical and chemical modifications, and the

character of an aerosol will change with increasing distance from the source; for example, the concentration falls off, the particle size distribution is altered and the chemical composition tends to become more uniform. As a consequence aerosols are the end-product of a complex series of processes and are therefore not static components, but are best regarded in terms of a **dynamic aerosol continuum** (Prospero *et al.* 1983). The physical and chemical composition of the marine aerosol is therefore extremely variable in both space and time, and the aerosol characteristics are governed by a combination of processes that are involved in the generation, conversion, transport and removal of particles. In the following sections the marine aerosol will therefore be discussed in terms of this general generation–conversion–transport–removal framework.

4.1.2. The transport of aerosols within the troposphere

Most of the continentally derived material (both natural and anthropogenic) that contributes to the world aerosol is initially injected into the planetary boundary layer of the atmosphere. This is the layer in which the direct influence of the underlying surface is felt, and it has a height of $\sim$ 1000 to $\sim$ 1500 m over the land and $\sim$ 300 to $\sim$ 600 m over the sea (Hasse 1983). The upper surface of the boundary layer is defined by an inversion, which inhibits the transfer of material to the upper atmosphere (Prospero 1981). According to Prospero (1981), the primary transport path by which material generated close to the continents, i.e. within tens to hundreds of kilometres, reaches the sea surface may be via this marine boundary layer. Over longer distances, however, the major transport path is probably via the free troposphere above the marine boundary layer. Thus, at remote marine regions much of the continentally derived aerosol in the boundary layer will have been transferred from the overlying atmosphere, and as a consequence the rate of exchange between the free troposphere and the boundary layer itself will affect the distance an aerosol component can be transported. ^{210}Pb (half-life 22 years), which is supplied to the atmosphere from the radioactive decay of ^{222}Rn (half-life 3.8 days) that escapes from soils, can be used as a tracer for the dispersal of these continentally derived components in the marine atmosphere (see e.g. Turekian & Graustein 1989). It must also be remembered that, since most collections of the marine aerosol are made in the boundary layer, they are probably not representative of the concentrations at high levels in the troposphere.

The transport of aerosols within the troposphere takes place via the major wind systems, which operate on a global scale. For simplicity it is convenient to describe atmospheric circulation in terms of a meridional three-cell model. In this model the circulation in each hemisphere can be related to the presence of three cells of alternating belts of easterly and

westerly zonal winds, the cells being separated by pressure zones. This is illustrated with respect to the Northern Hemisphere in Figure 4.2a. The three pressure zones are: (a) the equatorial low-pressure belt or trough, originally termed the 'Doldrums' but now referred to as the Inter-Tropical Convergence Zone (ITCZ); (b) the subtropical high-pressure belt (~ 30°N), an area of dry sinking air characterized by calms and often called the 'Horse Latitudes': and (c) the low-pressure belt at ~ 60°N. The

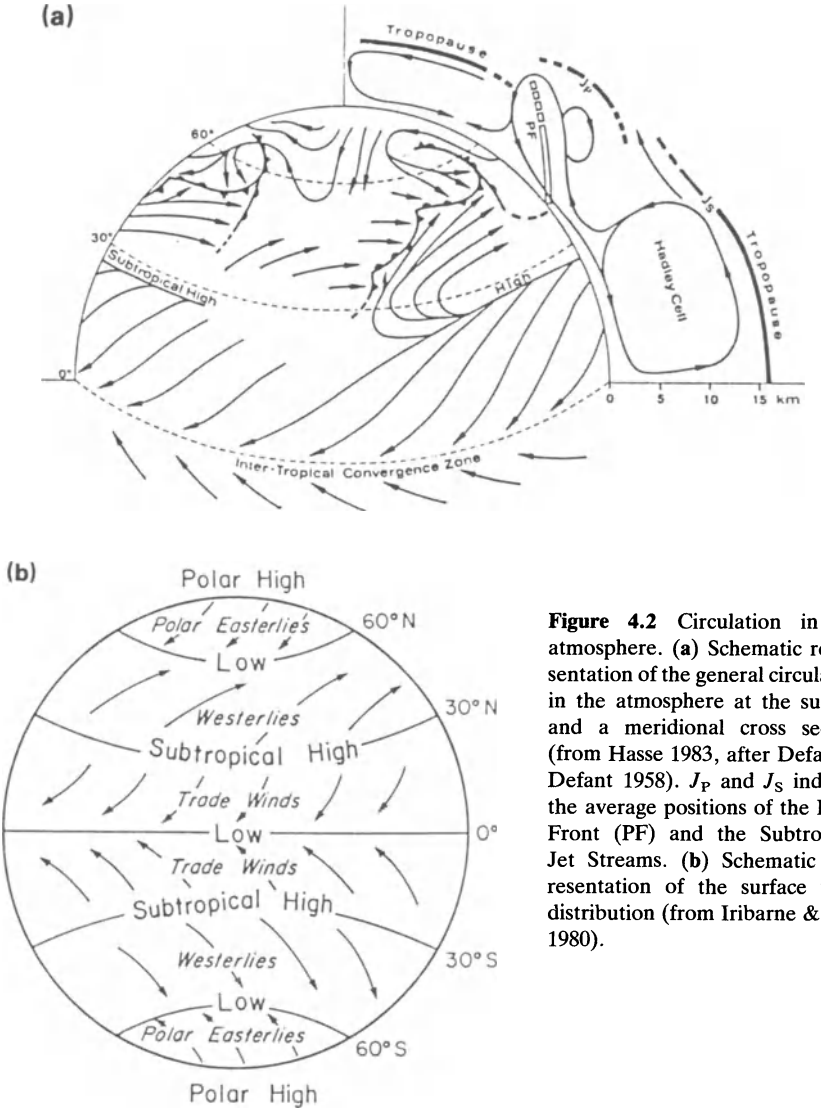

Figure 4.2 Circulation in the atmosphere. (**a**) Schematic representation of the general circulation in the atmosphere at the surface and a meridional cross section (from Hasse 1983, after Defant & Defant 1958). J_P and J_S indicate the average positions of the Polar Front (PF) and the Subtropical Jet Streams. (**b**) Schematic representation of the surface wind distribution (from Iribarne & Cho 1980).

main features of the circulation lying between these zones are illustrated in Figure 4.2b and are described in very general terms below.

(a) In the Hadley cell operating between the equatorial low-pressure and subtropical high-pressure belts, the prevailing zonal winds are northeasterly or southeasterly, and are termed the **trades**; the Northeast Trades in the Northern Hemisphere and the Southeast Trades in the Southern Hemisphere. These trades are directionally quite stable and have relatively constant velocities, in the range $\sim$ 16 to $\sim$ 32 km h^{-1}. The trades converge at the ITCZ. In some regions (e.g. India, South-East Asia and China) the trade-wind pattern can be modified by the development of a **monsoon** system. Here there is seasonal reversal of wind direction in which trans-equatorial westerlies replace the regular trade-wind easterlies. These monsoons can result in the transfer of air across the Equator and so can initiate the inter-hemispheric exchange of aerosol components.

(b) The circulation in the temperate or mid-latitude Ferrel cell, which lies between the subtropical high-pressure belt at $\sim$ 30°N and the low-pressure belt at $\sim$ 60°N, has a prevailing zonal wind that is westerly in direction. However, the **westerlies** are not as directionally stable as the trades and exhibit considerable variability in both space and time. Further, they have a greater force than the trades, and are sometimes referred to as the 'upper westerlies' since their force increases with altitude to reach a maximum at $\sim$ 12 km. Cores of high-speed winds are embedded in the westerlies, the two main types of being the Subtropical Jet Stream and the Polar Front Jet Stream, both of which are important for the transport of aerosols in the mid-latitudes.

(c) A third or polar cell is found to the north of the low-pressure belt located at $\sim$ 60°N. Here, the winds are the **polar easterlies**, although the atmospheric circulation system is extremely complex.

Aerosols are dispersed about the surface of the planet by these various zonal wind systems and by transfer between them. However, such transfer tends to be inhibited by the various pressure belts. Another factor that restricts the long-range transport of aerosols is their relatively short residence time in the troposphere, usually in the order of a few days to a few weeks, compared with the timescale required for inter-hemispheric transfer, probably in the order of 3–12 months. Despite this, the inter-hemispheric transfer of aerosols can take place; for example, when the ITCZ is shifted across the Equator, or when it is absent during the development of some monsoon systems. Like much of our knowledge of large-scale aerosol transport, the details of inter-hemispheric transfer

have been elucidated using data derived from atmospheric nuclear test programmes. For example, Peirson & Cambray (1970) identified nuclear debris that had remained in the troposphere for as long as 90 days, and had been transferred from the Southern to the Northern Hemisphere in the southwest monsoon over the Indian Ocean. It is probable, therefore, that at least a small fraction of the tropospheric aerosol may remain in the air long enough to undergo inter-hemispheric transfer and so become part of the background aerosol.

4.1.3 Sources of material to the marine atmosphere

The particulate and gaseous material suplied to the atmosphere can originate from either natural or anthropogenic sources, and when considering the elemental chemistry of both of these it is useful to distinguish between *low*-temperature and *high*-temperature generation processes. This is important because the forms in which the elements are present in the atmosphere, i.e. their speciation, can be strongly dependent on the temperature at which they were released from their parent hosts. Some of the more important sources of material to the world atmosphere are listed below.

4.1.3.1 Natural sources

THE EARTH'S CRUST The Earth's surface can supply both particulate and gaseous components to the atmosphere. The generation of particulate crustal material involves a low-temperature mechanical mobilization of surface deposits by wind erosion, and these products are an important component of many marine aerosols.

THE OCEANS Like the crust, the surface of the ocean can supply material to the atmosphere in both particulate and gaseous forms. Particulate material is formed during the low-temperature generation of sea salts by mechanical action. Volatilization from the sea surface, in the form of a sea-to-air gaseous flux, can also be a source for some volatile components (see Sec. 8.2).

VOLCANIC ACTIVITY Volcanoes can release particulate material, e.g. ash, together with gaseous phases formed from high-temperature volatilization processes. These gaseous phases may undergo condensation reactions, which can result in the enrichment of the particulate material in some volatile elements.

THE BIOSPHERE The supply of material to the atmosphere from the biosphere occurs through the high-temperature burning of vegetation, and by the emisson of particulate and vapour phases from plant surfaces and soils.

OUTER SPACE Extraterrestrial sources provide a small, but interesting, supply of material to the atmosphere. This extraterrestrial material includes micro-meteorites (cosmic spherules) and a number of cosmic-ray-produced radioactive or stable nuclides (see Sec. 15.4).

4.1.3.2 Anthropogenic sources There are a wide variety of anthropogenic processes that release both particulate and gaseous material into the atmosphere. These include fossil fuel burning, mining and the processing of ores, waste incineration, the production of chemicals, agricultural utilization, and numerous other industrial and social activities.

4.1.3.3 Source strengths Particle emission source strengths of some of the processes listed above are given in Table 4.2. The data are presented in terms of natural and man-made emissions, and each of these is subdivided into **direct** and **particle conversion** generation processes. A number of points must be considered when any attempt is made to evaluate these data.

(a) The data are average values, based on a number of wide-ranging estimates. This is illustrated by the inclusion of two data sets for the direct production of natural particles; however, for the purpose of making general comparisons, the data set provided by Prospero *et al.* (1983) will be used here.
(b) The emission of natural particles considerably exceeds that from anthropogenic processes, especially for direct particle production.
(c) For anthropogenic emissions, particle conversion from gases exceeds that from direct production by an order of magnitude; however, direct production dominates the natural emission of particles. In total (i.e. anthropogenic + natural) direct particle production yields $\sim 810 \times 10^{12}$ g yr^{-1} and conversion from gases results in $\sim 750 \times 10^{12}$ g yr^{-1}. It is apparent, therefore, that on a global scale the two processes have about the same magnitude. Sulphates are the principal particles derived from gas conversion, and $\sim 535 \times 10^{12}$ g yr^{-1} are produced in the atmosphere from a combination of natural and anthropogenic processes. This is similar in magnitude to sea-salt production ($\sim 500 \times 10^{12}$ g yr^{-1}), and sulphates and sea salts make up $\sim$ 70% of the particulate material in the atmosphere, with sea salts being dominant over the oceans.
(d) A number of the particle sources are localized in nature (e.g. those arising from industrial and volcanic activity), whereas others (e.g. those associated with sea-salt generation and crustal weathering) have a more global significance.
(e) The most important sources for the *direct* production of particles to the atmosphere are low-temperature processes involved with both

the generation of sea salts from the **ocean** surface and the weathering mobilization of crustal material from the **land** surface; however, the sea salts are recycled from an internal (i.e. oceanic) source, whereas crustal weathering products are transported to the oceans from external (i.e. non-oceanic) sources. As a result, continental weathering processes represent the single largest external source for the direct production of particles to the marine atmosphere. Components arising from the crustal and oceanic sources, together with sulphates and to a lesser extent nitrates (both of which are important oxidative end-members of the atmospheric sulphur and nitrogen cycles), can therefore dominate the marine aerosol, and their distributions are considered in the following sections. However, although crustal material (mainly alumino-silicates), sea salts and sulphates can dominate the marine aerosol, they can be present in intimate mixtures rather than as individual components (see e.g. Andreae *et al.* 1986).

4.1.4. The principal components of the marine aerosol

4.1.4.1 The mineral aerosol over the World Ocean Particulate material in the form of continental dust is mobilized into the atmosphere mainly by wind erosion. The process is strongly dependent on the nature of the surface cover in the source (or catchment) area, which itself is dependent on the prevailing geological, weathering and general climatic regimes. In regions having loose surface deposits, e.g. desert and arid land areas, there is a readily available reservoir of particulate material that is susceptible to wind erosion and transport during dust storm events. According to Prospero *et al.* (1989), however, the best correlation between dust storm frequency and aridity is found in those regions that have an annual rainfall between ~ 100 and ~ 200 mm, and not in hyper-arid regions, which may be essentially blown out with respect to particles of the size that can undergo wind deflation. Prospero *et al.* (1989) concluded, therefore, that as a result of this, the most important regions for the production of soil dust are probably those that are undergoing a transition from moist to arid conditions. In contrast to the conditions found in arid regions, surface covers of forest, grassland and snow or ice will considerably reduce the production rates of atmospheric dusts. Most mineral dust present in the atmosphere is produced from surface soils. However, in addition to the low-temperature mobilization of this surface material into the atmosphere, high-temperatue volcanic activity can generate particles that form part of the mineral aerosol. This volcanic activity is a sporadic source, but at the time of large-scale eruptions (e.g. that of Mount St. Helens) very large quantities of material can be injected into the atmosphere.

Junge (1979) estimated the magnitude of the inputs to the global

tropospheric dust cycle, and a summary of the data is given in Table 4.3a. Two important conclusions can be drawn from these data. (a) The Northern Hemisphere has a higher tropospheric dust burden than the Southern Hemisphere, mainly as a result of the larger area of land mass in the northern latitudes. (b) The Sahara Desert plays an extremely important role in the Northern Hemisphere dust cycle. However, more recent estimates have also indicated the importance of the Asian arid lands as sources for dust transported to the oceans in the Northern Hemisphere. A summary of some of these recent estimates is given in Table 4.3b. It is apparent from this table that the dust flux to the western North Pacific ($\sim 300 \times 10^{12}$ g yr^{-1}), much of which originates from Asian desert sources, has a similar magnitude to that for Saharan dust transported to the tropical North Atlantic. On the basis of the more recent data, the global dust source strength is $\sim$ (800–1100) $\times 10^{12}$ g yr^{-1}; however, there is still considerable uncertainty in the estimates.

A large amount of data are now available for the concentrations of mineral aerosols in the marine atmosphere, and some of these are reviewed below in terms of the major oceans.

THE ATLANTIC OCEAN AND SURROUNDING WATERS In many ways the Atlantic Ocean and its surrounding waters provide a classical example of the factors that control the distributions of the mineral aerosol over marine areas. The reason for this is that the Atlantic is a relatively narrow

Table 4.2 Estimates of the global emissons of particulate material to the atmosphere (units, 10^{12} g yr^{-1})

Source	Global production[a]		
	1	2	3
Man-made			
Direct particle production	30		
Particles formed from gases			
Converted sulphates	200		
Others	50		
Total man-made	280		200
Natural			
Direct particle production			
Forest fires	5	36	
Volcanic emissions	25	10	
Vegetation		75	
Crustal weathering-(mineral dust)	250	500	
Sea salt	500	1000	
Particles formed from gases			
Converted sulphates	335		
Others	135		
Total natural	1250		
Overall total	1530		

[a] 1, Prospero et al. (1983); 2, Nriagu (1979); 3, Lantzy & Mackenzie (1979).

Table 4.3 The global tropospheric dust cycle

A. After Junge (1979).

Tropospheric region	Dust burden (10^{12} g)	Source strength (10^{12} g yr^{-1})
Northern hemisphere[a]	3.0[b]	150[c]
Southern hemisphere[a]	1.0[b]	50[c]
Total troposphere[a]	4.0[b]	200[c]
Sahara plume	1.2-4.0	60-200
Total troposphere[d]	3.2-12.0	130-800

a These estimates disregard special production in deserts, particularly the Saharan plume in the North Atlantic.
b Estimated uncertainty factor about ± 2.
c Source strength calculated from dust burden, assuming an aerosol residence time of 1 week. Estimated uncertainty factor about ± 3.
d After application of uncertainty factors b and c.

B. After Prospero (1981), and Prospero et al. (1989).

Ocean Region	Deposition rate 10^{-6} g cm^2 yr^{-1}	10^{12} g yr^{-1}
North Atlantic; north of trades	82	12
North Atlantic trades	-	100-400
South Atlantic	85	18- 37
Indian Ocean	450	336
North Pacific		
Western N. Pacific	5000	300
Central and eastern N. Pacific	11-62	30
South Pacific	5-64	18
Entire Pacific		350
All Oceans (minimum - maximum)		816-1135

elongated ocean, which encompasses all the major wind systems and also has a wide variety of particle catchment sources on its surrounding land masses. The latitudinal effects that these parameters exert on the transport of mineral aerosols can be illustrated in terms of an Arctic–North Atlantic–South Atlantic–Antarctic transect. Mineral aerosol dust loadings along this transect are listed in Table 4.4, from which it can be seen that there is a broad pattern in the data, with a general increase in the dust loadings towards lower latitudes in both hemispheres.

Table 4.4 Mineral aerosol loadings on an Arctic–Atlantic–Antarctic transect

Oceanic region	Mineral aerosol concentration ($\mu g\ m^{-3}$ of air)
Arctic	Variable; haze episodes
North Atlantic; westerlies	~ 0.1 - ~ 2.5
North Atlantic; north east trades	< 1.0 - > 10^3
South Atlantic; south east trades	~ 0.1 - ~ 1.0
South Atlantic; westerlies	< 0.1
Antarctic	< 0.01

The **Arctic polar regions** are remote, but the atmosphere is less pristine than might be expected because it is subjected to seasonal injections of **Arctic haze**, which bring in a mixture of both mineral and pollutant components from distant sources such as Eurasia, the eastern USA and central Europe. Reported concentrations of mineral aerosol over the Arctic therefore show considerable variation, depending on whether sampling has taken place in background air or in a haze episode.

In the general region of the **North Atlantic westerlies** ($\sim$ 65 to $\sim$ 40°N) mineral aerosol concentrations are probably $< 0.5\ \mu g\ m^{-3}$ of air, rising to $\sim 2.5\ \mu g\ m^{-3}$ of air closer to the land masses. The westerlies transport aerosols generated in the US–European pollution belt, but the forest–grass surface cover in the catchment inhibits the large-scale mobilization of crustal material.

The most striking feature in the distribution of the mineral aerosol over the Atlantic is the very high concentrations found in the **Northeast Trades** off the coast of West Africa. These winds transport crustal material originating in the Sahara Desert, and estimates of the Saharan dust burden carried over the Atlantic vary in the range $(60–400) \times 10^{12}\ g\ yr^{-1}$ (see e.g. Schultz *et al.* 1980, Prospero *et al.* 1989). The offshore transport of this Saharan dust takes place mainly above the trade wind inversion in the 'Harmattan'. Mineral aerosol concentrations in the Atlantic Northeast Trades are among the highest found over the World Ocean and can reach values $> 10^3\ \mu g\ m^{-3}$ of air. However, the concentrations can be extremely variable. For example, at Sal Island, off the coast of West Africa, the mineral aerosol varied over the range 10–180 $\mu g\ m^{-3}$ of air during a three-month period in 1974 (Savoie & Prospero 1977). The variations are due to outbreaks, or **pulses**, of Saharan dust-carrying air. The effect of these pulses was apparent in the data reported by Chester *et al.* (1984a), who found mineral aerosol concentrations in the Northeast Trades off West Africa to range between $< 1\ \mu g\ m^{-3}$ of air in quiet

periods and ~ 700 μg m^{-3} of air in dust storm outbreaks. Dust pulses can therefore be thought of as imposing intermittent concentration increases onto the background aerosol, and this is illustrated below with respect to the Pacific mineral aerosol (see Fig. 4.3a). Saharan dust can be transported all the way across the Atlantic, and even further west (see e.g. Delany *et al.* 1967). It may be concluded, therefore, that there is a **dust envelope** over the North Atlantic in the area underlying the Northeast Trades, i.e. between ~ 30°N and ~ 5°N (see e.g. Chester *et al.* 1979). The limits of the area over which the Saharan dust is transported vary seasonally, with a southerly shift in the dust envelope being evident in the winter months (Prospero 1968).

Across the Equator in the Atlantic **Southeast Trades** the mineral aerosol concentrations fall off dramatically, and although few reliable data are available it would appear that in the region lying between the Equator and ~ 40°S the loadings are generally $\lesssim$ 1 μg m^{-3} of air (see e.g. Prospero 1979, Chester *et al.* 1984a). It is apparent, therefore, that the desert regions of southern Africa do not act as massive mineral aerosol reservoirs supplying material to the Southeast Trades (see e.g. Chester *et al.* 1971).

Further south, the mineral aerosol concentrations continue to decrease, to reach values in the **South Atlantic westerlies** which are about an order of magnitude lower than those in the Atlantic Southeast Trades (see e.g. Chester *et al.* 1984a).

In the pristine air over the snow-covered **Antarctic plateau** aerosol concentrations are extremely low, ranging from < 0.004 μg m^{-3} of air (winter) to ~ 0.01 μg m^{-3} of air (summer); and in both seasons mineral components make up less than ~ 5% of the total aerosol population.

THE MEDITERRANEAN SEA The Mediterranean Sea is confined to a narrow latitudinal band, but it has contrasting aerosol-generation catchments on its opposite shores. Thus, it is bordered in the north by nations having a variety of economies, ranging from industrial to agricultural, and in the south by the North African desert belt. There is also volcanic activity in the region. Aerosols are transported into the Mediterranean from all the surrounding land masses, and as a result the concentration of mineral dust can exhibit considerable variation. For example, Chester *et al.* (1984b) showed that incursions of Saharan dust could be identified in the lower troposphere over the Tyrrhenian Sea. The mineral dust concentrations in these pulses (average, 25 μg m^{-3} of air) were an order of magnitude higher than those in the 'European background' air (average, 1.4 μg m^{-3} of air). However, pulses of this kind are intermittent, and make it difficult to identify an average mineral aerosol loading for the Mediterranean.

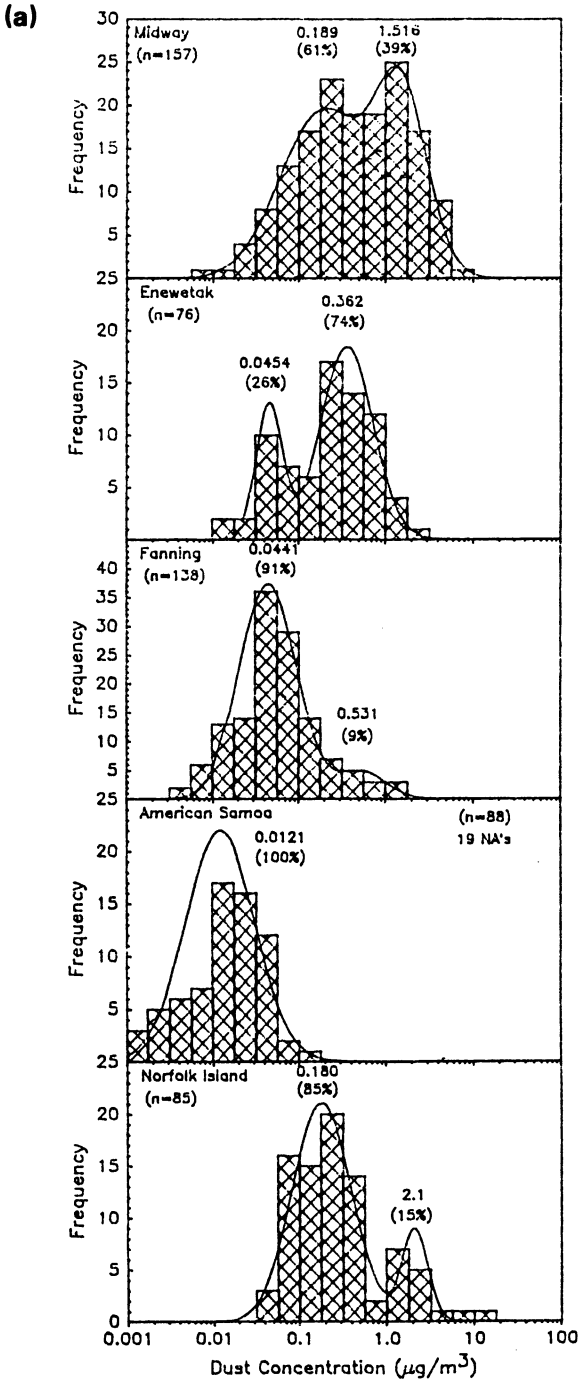

Figure 4.3a Tropospheric mineral dust concentrations. (a_m) Frequency distributions of mineral aerosol concentrations over the Pacific Ocean (from Prospero *et al.* 1989). The mineral aerosols for the Midway and Enewetak Island sites in the North Pacific show a bimodal distribution, the lower mode representing the background aerosol and the upper mode representing dust pulses from Asian desert sources. In contrast, the aerosol frequency distributions for the American Samoa and Norfolk Island sites in the South Pacific, and for the Fanning Island site in the North Pacific, are essentially unimodal and represent background aerosol only. (The locations of the island sites are shown in Fig. 4.3b.)

(b)

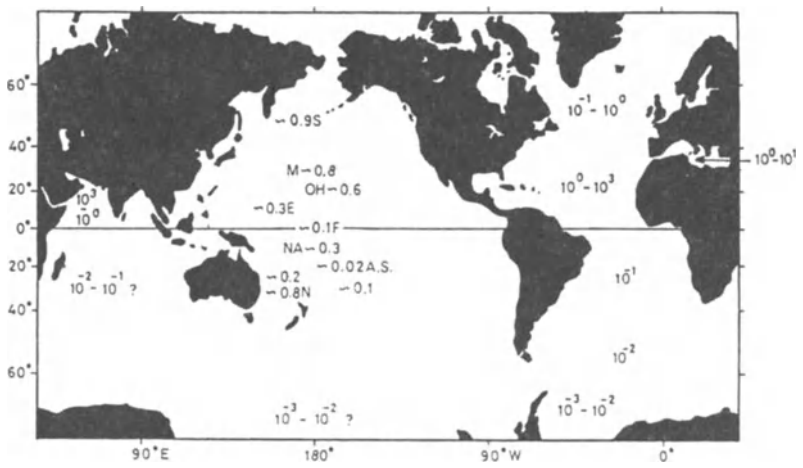

Figure 4.3b Tropospheric mineral aerosol concentrations over the World Ocean (units, μg m^{-3} of air) (from Chester 1986). For most regions order-of-magnitude ranges are given, but mean values are listed for the Pacific Ocean where long-term collections have been made on island stations. The island stations indicated are: S, Shemya; M, Midway; Oh, Oahu; F, Fanning; NA, Nauru; A.S., American Samoa; N, Norfolk.

THE INDIAN OCEAN The desert and arid regions surrounding the northern Indian Ocean are a highly productive source of mineral aerosols. For example, over the northern Arabian Sea an average loading of 16 μg m^{-3} of air was reported by Chester *et al.* (1985); however, individual values ranged between 4 and 250 μg m^{-3} of air, clearly demonstrating the transport of pulses of dust from the desert regions of Iran–Makran and Rajasthan. The effect of this desert material decreases with distance from the source; for example, in the Bay of Bengal, Goldberg & Griffin (1970) reported an average aerosol loading (mainly mineral dust) of 7 μg m^{-3} of air. Further south the decrease continues, and Prospero (1979) found an average of mineral aerosol concentration of 3 μg m^{-3} of air over the Indian Ocean in the region 7°N to 15°S. However, relatively few data are available for the concentrations of mineral aerosols over the remote regions of the Indian Ocean.

THE PACIFIC OCEAN It is only in the last few years that data have become available on the nature of the Pacific aerosol. These data have been obtained from the SADS and SPAN networks set up as part of the SEAREX Programme.

(a) **The North Pacific.** The SEAREX Asian Dust Study (SADS) was initiated in 1981, and involved the collection of aerosol samples at seven island stations in the North Pacific; a number of the SADS stations are identified in Figure 4.3. The mineral aerosol over this oceanic region is dominated by material supplied from the Asian deserts, and the initial SADS data, which were described by Uematsu *et al.* (1983), revealed two main trends in its distribution. (i) There was a decreasing concentration gradient away from the Asian mainland, the highest dust concentrations being found in the high- and mid-latitude belt lying between ~ 50°N and ~ 20°N, with an average mineral aerosol loading for the three island stations in this belt (Shemya, Midway and Oahu) of 0.79 μg m^{-3} of air. The loading decreased to an average of 0.26 μg m^{-3} of air at Enewetak (~ 11°N) and fell even further at Fanning Island close to the Equator, which had an average of 0.07 μg m^{-3} of air. (ii) There was a well defined seasonal variability in the transport of mineral dust over the North Pacific, with concentrations in the period February to June being an order of magnitude higher than those for the rest of the year. This seasonal pattern is similar to that of the frequency of dust storms in Asia, which exhibit a maximum in the spring.

(b) **The South Pacific.** A general picture of the distribution of mineral dust over the South Pacific can be obtained from the SPAN (SEAREX South Pacific Aerosol Network) data (Uematsu *et al.* 1985); a number of the SPAN island stations are identified in Figure 4.3b. Between the Equator and ~ 15°S, at the Nauru and Fanning Island stations, mineral aerosol loadings have an average of ~ 0.23 μg m^{-3} of air. Further south, in the band extending from ~ 15°S to ~ 25°S, the loadings decrease considerably and have an average of 0.01 μg m^{-3} of air. The lowest concentrations of mineral aerosol found at any of the Pacific stations were found at American Samoa, and the range here (< 0.003 to 0.14 μg m^{-3} of air) included values as low as those reported over the pristine Antarctic continent. The highest concentrations of mineral aerosol in the South Pacific were found at Norfolk Island (average, 0.79 μg m^{-3} of air). This station is the closest to the Australian mainland and the loadings probably reflect an input of dust from this continental source.

It may be concluded that mineral aerosol loadings over the Pacific vary over at least an order of magnitude. The dominant feature in the distribution of the mineral aerosol over this ocean is the seasonal input of dust pulses that originate in Asian dust storms. The effect of the pulses can be seen in concentration versus frequency diagrams for the mineral aerosol collected at the Pacific stations. A set of these diagrams is illustrated in Figure 4.3a. From this figure it can be seen that, with the

exception of that for Fanning Island, all the mineral aerosols for the North Pacific show a bimodal distribution, the lower mode representing the background aerosol and the upper mode representing perturbations to the background from aerosols associated with the Asian dust events. In contrast, aerosol frequency distributions for the South Pacific stations, and the samples collected at Fanning Island, are essentially unimodal and may be regarded as being background aerosol.

Mineral aerosol fluxes to the Pacific were given in Table 4.3, from which it is evident that the dust flux to the western North Pacific, mainly from Asian desert sources, is similar in magnitude to that transported to the tropical North Atlantic from the Sahara Desert.

THE WORLD OCEAN: SUMMARY Following Chester (1986) the main features in the distribution of mineral aerosols over the World Ocean may be summarized as follows.

(a) There is a mineral aerosol or dust veil present over all oceanic areas; however, the concentrations of material in the veil vary over several orders of magnitude in both space and time, ranging from $\lesssim 10^{-3}$ μg m^{-3} of air in the remote South Pacific to $> 10^{3}$ μg m^{-3} of air in the Atlantic Northeast Trades off the coast of West Africa.
(b) Desert and arid regions are the principal source reservoirs for mineral aerosols in the atmosphere, and because these regions tend to be concentrated into specific belts they impose a general latitudinal control on the distribution of the mineral dust over marine areas. In the Atlantic the highest concentrations of the mineral aerosol are found at low latitudes (0–35°N), which reflects the influence of the North African deserts to the west, whereas in the Pacific the highest concentrations are located at mid-latitudes (20–50°N), reflecting the influence of the Asian deserts to the north.
(c) A very important feature of the supply of material from the desert areas is that the mineral aerosol is often transported over the oceans in the form of pulses, which are related to dust storm outbreaks on land. These pulses can bring relatively large quantities of mineral aerosol to the sea surface, and because of their intermittent nature they can impose short-term non-steady-state conditions on the upper water column. The pulses can also result in the transport of relatively large particles, e.g. with diameters of tens of micrometres, to open-ocean regions far from the land masses.

The general distribution of the mineral aerosol over the World Ocean is shown in Figure 4.3b.

4.1.4.2 The sea-salt aerosol over the World Ocean The sea surface

provides a vast reservoir for the generation of aerosols, and sea salt is the largest component of the particulate matter that is cycled through the atmosphere. According to Berg and Winchester (1978), the bursting of bubbles produced by the trapping of air in surface water by breaking waves, or whitecaps, is the chief mechanism for the formation of particulate matter in the marine atmosphere, and the mechanism has been described in detail by Blanchard (1983). However, sea spray produced by the direct shearing of droplets from wave crests may play a role in the generation of sea salts (see e.g. Lai & Shemdin 1974, Koga 1981).

Sea salts have particle sizes ranging from < 0.2 μm to > 200 μm in diameter, with a distinct maximum in number distribution below a diameter of 2 μm. However, more than 90% of the sea-salt aerosol mass is located in giant particles having a median mass diameter (MMD) between 2 and 20 μm, and McDonald *et al.* (1982) have shown that large and giant particles dominate the deposition of sea salts, even though they are present in the air in only relatively low numbers.

The concentration of sea salt in the marine atmosphere varies with both windspeed and altitude. In general, it appears that for winds between 5 and 35 m s^{-1}, the sea-salt concentration increases exponentially with windspeed, and at lower velocities the salt concentration falls off rapidly since few bubbles are produced by the sea under these conditions. However, the relationship between salt generation and windspeed is complex, and variations in salt concentration of a factor of more than 2 can occur at a given windspeed. Estimates of the global sea-salt production rate vary by an order of magnitude, the two most often quoted in the literature being 10^{15} g yr^{-1} (Eriksson 1959) and 10^{16} g yr^{-1} (Blanchard 1963). However, Blanchard (1983) believes that when the complexities of making such estimates are considered, a difference of a factor of 10 is not surprising. However, the most recent estimate for the global flux of atmosphere sea salt is at the higher end of the previous estimates, i.e. $1–3 \times 10^{16}$ g yr^{-1} (Erickson & Duce 1988).

Erickson *et al.* (1986) have produced global distribution maps of the concentration of atmospheric sea salts at 15 m above the ocean surface. The maps for the summer and winter concentrations are illustrated in Figure 4.4. The data generally support previous findings, and a number of overall conclusions can be drawn from the maps. (a) The high-latitude regions of both hemispheres usually have higher atmospheric sea-salt concentrations than do the low latitudes. (b) The strong uniform surface winds in the Southern Hemisphere at high latitudes result in high, and relatively constant, atmospheric sea-salt concentrations in both winter and summer periods. (c) The high-latitude winds in the Northern Hemisphere vary seasonally, and the atmospheric sea-salt concentrations exhibit a difference of a factor of 3 between winter and summer periods.

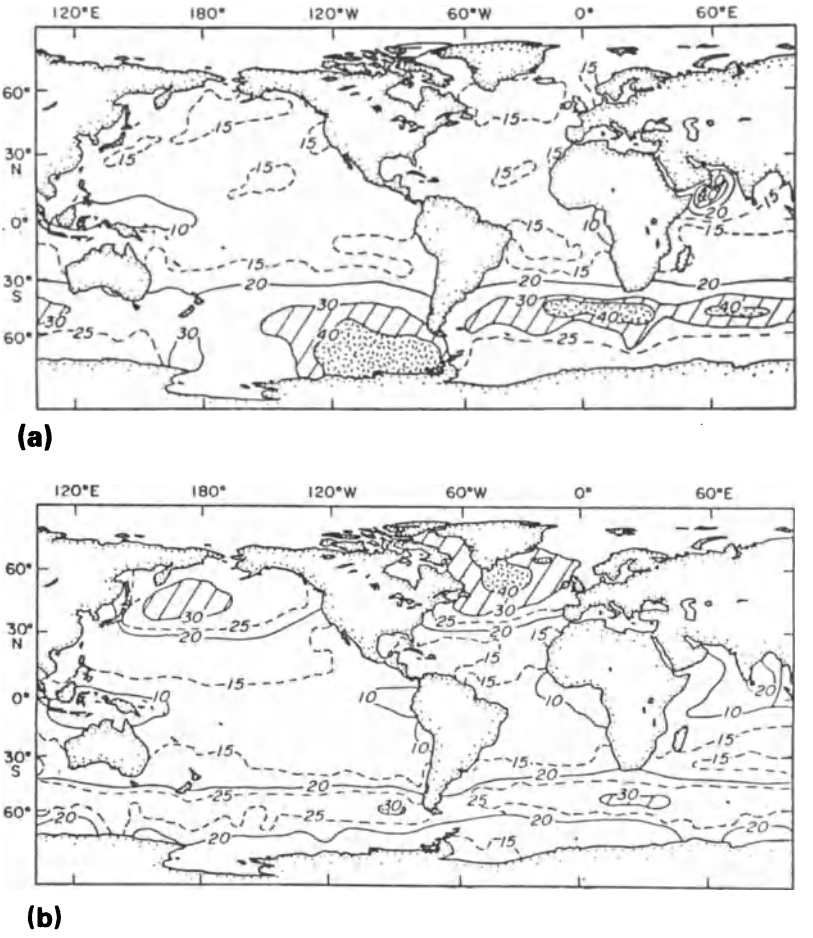

Figure 4.4 Sea-salt concentrations over the World Ocean (from Erickson *et al.* 1986); the isopleths are lines of constant sea-salt concentration in μg m^{-3} of air. (**a**) Sea-salt concentrations during the boreal summer (June–August). (**b**) Sea-salt concentrations during the boreal winter (December–February).

The overall distribution of the sea-salt aerosol differs from that of the mineral aerosol in that the highest sea-salt concentrations occur at high latitudes in areas of relatively strong winds, whereas the highest mineral aerosol concentrations are found in low-latitude areas off desert and arid regions (see Table 4.5).

4.1.4.3 The sulphate aerosol over the World Ocean Sulphates, such as $(NH_4)_2SO_4$, are an important constituent of the tropospheric background

Table 4.5 Concentrations of sea-salt and mineral aerosols in the lower marine troposphere[a]

Oceanic region	Arithmetic mean concentration ($\mu g\ m^{-3}$ of air)	
	Mineral aerosol	Sea-salt aerosol
North Atlantic; 22°-64°N	1.30	6.71
North Atlantic; 0°-28°N	36.6	11.2
South Atlantic; 5°-35°S	1.35	9.06
South Atlantic; 5°-35°S including Cape of Good Hope	1.22	11.3
Pacific; 28°N-40°S	0.58	8.44
Mediterranean Sea	4.57	6.98
Indian Ocean; 15°S-7°N	7.20	3.52

a Data from Prospero (1979).

aerosol. Sulphates from both natural and pollutant sources can be transported into the marine atmosphere from the continents. In addition, sulphates can be generated from the sea surface, either directly during the formation of sea salts or indirectly from gas-to-particle conversion reactions. The SO_4^{2-} : Na^+ ratio in sea water (0.25) has been used to estimate the sea-salt-associated sulphate in marine aerosols; thus, for ratios in excess of the seawater value, the non-sea-salt sulphate component is usually referred to by convention as **excess sulphate**.

Varhelyi & Gravenhorst (1983) compiled a comprehensive database on the distribution of sulphates over the World Ocean from which a number of trends can be identified; the data are summarized in a very general form in Table 4.6. (a) The total sulphate aerosol concentrations range within about an order of magnitude, with the highest values occurring near the continents. (b) The highest individual total sulphate concentrations are found over the Mediterranean Sea, with intermediate values over the North Atlantic and the lowest concentrations over the rest of the World Ocean. (c) Concentrations of sea-salt-associated sulphates are rather uniform, and although some variations are found, SO_4^{2-} values are generally in the range 0.6–1.2 $\mu g\ m^{-3}$ of air. (d) Excess sulphate concentrations decrease in the order Mediterranean Sea $\gg$ North Atlantic $>$ rest of World Ocean, and are responsible for much of the variation in the distribution of total sulphate in the marine aerosol.

It is apparent, therefore, that in the marine atmosphere there is a background of sea-salt-associated sulphate upon which is superimposed varying amounts of non-marine, or excess, sulphate. Evidence for the origin of sulphates in the marine atmosphere has been provided from

Table 4.6 The sulphate aerosol over the World Ocean (units, μg m^{-3} of air)[a]

Ocean area	Total sulphate	Sea-salt sulphate	Excess sulphate
Mediterranean	3.1	0.2	2.9
North Atlantic	0.5 - 0.8	0.2 - 0.4	0.3 - 0.4
Other areas	0.3 - 0.6	0.2 - 0.4	0.1 - 0.2

[a] Data from Varhelyi & Gravenhorst (1983).

their particle size distributions (for a discussion of the element–particle size relationships see Sec. 4.1.5.1). For example, Bonsang *et al.* (1980) reported that sulphates associated with large marine aerosol particles (diameter > 2.5 μm) are characterized by having Na : SO_4^{2-} ratios close to that of sea water, indicating that they have a marine origin from the generation of sea salts. In contrast, SO_4^{2-} : Na ratios in the aerosols increased sharply on smaller particles, to reach values 2–20 times greater than those for sea water on particles having diameters less than < 0.6 μm. The excess sulphate in these marine aerosols is therefore present on submicrometre-sized particles, i.e. those in the accumulation mode (see Sec. 4.1), which are probably formed via gas-to-particle conversions. It would appear, therefore, that much of the excess sulphate in the marine aerosol has a gas precursor, which is most likely to be SO_2. In addition, substantial amounts of non-sea-salt sulphates in the marine aerosol can be derived directly from soil material (see e.g. Savoie *et al.* 1987).

Over the continents particulate sulphates can be formed from precursor SO_2 that has an anthropogenic source and these can be transported to marine areas. In some remote regions, however, the excess sulphate is not associated with continentally transported material. For example, Bonsang *et al.* (1980) found that over such remote regions there was a good correlation between the concentrations of excess sulphate and SO_2, and concluded that both components have a common marine origin. They were also able to show that concentrations of SO_2 in the marine atmosphere increased as the primary production of the surface waters increased, implying that biological processes play a role in the origin of the SO_2. This raises a problem, however, since according to Nguyen & Bonsang (1979) SO_2 cannot emanate directly from sea water. To overcome this, Bonsang *et al.* (1980) suggested that dimethyl sulphide (DMS), formed during biological production, could be a major source of SO_2 to the marine atmosphere (see also Nguyen *et al.* 1983) and

subsequent studies confirmed that DMS is by far the most predominant volatile sulphur compound emitted to the atmosphere from the sea surface. (For a detailed discussion of this topic see Andreae (1986).) Once in the atmosphere, the DMS can undergo a number of oxidation reactions, but various lines of evidence suggest that SO_2 is the major oxidation product, and from the model constructed by Andreae (1986) to represent conditions in the tropical and subtropical marine atmosphere it would appear that DMS is, in fact, the major source of non-sea-salt, i.e. excess, sulphur in the marine atmosphere.

It may be concluded, therefore, that over some continentally influenced marine regions sulphates formed via gas-to-particle conversion (e.g. from anthropogenically produced SO_2), together with soil-derived sulphates, can be transported into the atmosphere. However, over most of the open-ocean surface, sea water itself is the only significant source of directly formed sulphate particles. Even so, this source cannot account for all the particulate sulphate in the marine aerosol and the excess sulphate, which is present largely on submicrometre-sized particles, is now thought to have formed mainly from the gas-to-particle conversion of SO_2, much of which has originated from DMS emitted to the atmosphere following assimilatory biological reduction processes associated with the marine biomass.

4.1.4.4 Organic carbon in the marine aerosol The atmosphere is a primary pathway for the transport of some types of organic substances to the oceans. The organic components in the atmosphere may be divided into particulate organic matter (POM), for which the organic carbon fraction is termed POC, and vapour-phase organic material (VOM), for which the organic carbon fraction is referred to as VOC. The principal sources for both POM and VOM in the atmosphere are vegetation, soils, the marine and freshwater biomass, forest burning and a variety of anthropogenic activities; to these must be added the *in situ* production of some organic substances within the atmosphere itself. The sinks for all these organics can be related to the mechanisms that remove them from the atmosphere. For VOM four removal mechanisms are important: conversion to POC, dry deposition, wet deposition and transformation to inorganic gaseous products. The removal of POM is dominated by wet and dry deposition. In addition, the oxidation of POM to inorganic gaseous products, e.g. CO_2, can result in its loss from the atmosphere.

The distributions and kinds of organic substances in the atmosphere have been described by Duce *et al.* (1983b), and the following discussion is based largely on the data given in that review.

PARTICULATE ORGANIC MATTER (POM) Particulate organic aerosols can be produced in two ways, either directly as particles or as a result of gas-to-

particle conversions, and the resultant POM can be divided into non-viable and viable species.

Most data for **non-viable POM** in the atmosphere is confined to measurements of POC, although information is now becoming available on individual organic compounds. The concentration of POC in the lower marine troposphere is usually ~ 0.5 μg m^{-3} of air, and although concentrations may be somewhat lower in the Southern Hemisphere than in the Northern Hemisphere, the present database is too small to confirm this trend. A large fraction of the POC is present on small particles; for example, Hoffman & Duce (1977) showed that 80% of the POC in marine air sampled at Bermuda, Hawaii and Samoa was present on particles with diameters < 2 μm. Data on the origin of the POC in the marine atmosphere have come from a variety of sources. For example, Chesselet *et al.* (1981) employed carbon isotopes to demonstrate that the small-sized POC is derived from a continental source, whereas the large-sized POC has a marine origin.

The **viable POM** species in aerosols include fungi, bacteria, pollen, algae, yeasts, moulds, mycoplasma, viruses, phages, protozoa and nematodes, and a number of these have been identified in marine air. For example, Delany *et al.* (1967) noted the presence of various marine organisms, freshwater diatoms and fungi in aerosols collected at Barbados (North Atlantic) in the path of the Northeast Trades. Folger (1970) reported the presence of phytoliths, freshwater diatoms, fungi, insect scales and plant tissue in the atmosphere over the North Atlantic. Various insects have also been found in marine air samples, and the atmosphere offers a pathway by which some plant and animal species can colonize remote islands.

VAPOUR-PHASE ORGANIC MATTER (VOM) Vapour-phase organics have varying degrees of chemical reactivity, and their atmospheric lifetimes therefore vary over a wide timescale. In addition to methane, which can remain in the atmosphere for between four and seven years, a large range of vapour-phase organic compounds, which have considerably shorter lifetimes (~ 1 to ~ 100 days), are present in marine air. For a detailed inventory of these non-methane vapour-phase organics see Duce *et al.* (1983b), Gagosian (1986) and Section 8.2.

In addition to natural organic material, the atmosphere is important in the transport of pollutant organics to the oceans; these include DDT* residues and PCBs* (see e.g. Goldberg 1975). Air–sea exchange is a critical link in this transport process, and differences in chemical properties of individual heavy synthetic organics can affect the mechanism by which they are transferred to the ocean surface and their reactivity in sea water. For a review of this topic, and for comprehensive data on

* DDT is a (complex) mixture containing mainly *p,p'*-dichlorodiphenyltrichloroethane and PCBs are polychlorinated biphenyls. They are used as insecticides.

synthetic vapour-phase organics, the reader is referred to Duce *et al.* (1983b) and Atlas & Giam (1986).

In terms of global cycles, the oceans provide a major sink for some atmospheric organic material, and although the data are still sparse, several attempts have been made to estimate the global tropospheric burdens of organic matter. For example, Duce (1978) calculated that the non-methane global VOC burden is $\sim 50 \times 10^{12}$ g, and the total POC burden has been estimated to be $\sim (1\text{–}5) \times 10^{12}$ g, of which $\sim 90\%$ is on particles with diameters < 1 μm (see e.g. Duce *et al.* 1983b). In addition, the total amount of organic carbon cycling through the troposphere each year has been put at $\geqslant 800 \times 10^{12}$ g (see e.g. Duce 1978, Robinson 1978, Zimmerman *et al.* 1978). A number of first-order estimates have been made of the source–sink relationships of POM and VOM in the marine atmosphere. Thus, Williams (1975) calculated a wet deposition flux of carbon of $\sim 2.2 \times 10^{14}$ g yr^{-1} to the ocean surface, which is somewhat smaller than that of $\sim 10 \times 10^{14}$ g yr^{-1} estimated by Duce & Duursma (1977), although both are within the same order of magnitude. The dry deposition flux of organic material (carbon) to the oceans has been put at $\sim 6 \times 10^{12}$ g yr^{-1} (Duce & Duursma 1977). Thus, although it would appear that wet deposition is more important than dry fall-out in the fluxes of organic material (POC = POM × 0.7) to the sea surface, all the estimates should be treated with great caution. Further complications to the assessment of the fluxes of organic material to the ocean arise because the sea surface itself can act as a source, as well as a sink, for both POM and VOM through processes such as gas exchange and bubble bursting (see Secs 4.1.4.2 & 8.2). For example, Duce (1978) calculated that $\sim 14 \times 10^{12}$ g yr^{-1} of organic carbon is produced by the ocean surface, with $\sim 90\%$ being found on particles > 1 μm in diameter. However, even when recycling is taken into account, it would appear that on the basis of the estimate given by Williams (1975) for the oceanic wet deposition flux of carbon ($\sim 2.2 \times 10^{14}$ g yr^{-1}), the input of organic material to the ocean surface is greatly in excess of the output from the marine source. The overall result of this is that the oceans act as a major sink for atmospheric organic material (Duce *et al.* 1983b).

The atmospheric transport of a number of individual terrestrially derived organic compounds to the ocean surface is considered in Section 14.1.

4.2 The chemistry of the marine aerosol

4.2.1 Elemental composition

The concentrations of many particulate elements in the marine atmosphere vary over several orders of magnitude (see Table 4.7), and at any specific location the concentrations are dependent on a number of factors. These include the efficiency with which its host components are mobilized into,

Table 4.7 The concentration ranges of some elements in the marine aerosol

Element	Estimated concentration range [a] (ng m^{-3} of air)
Al	1 - 10^4
Fe	1 - 10^4
Mn	0.1 - 10^2
Cu	0.1 - 10^1
Zn	0.1 - 10^2
Pb	0.1 - 10^2

[a] Approximate values only.

transported through and removed from the atmosphere, and the extent to which the aerosol containing the components has been aged.

According to Berg & Winchester (1978) the composition of the marine aerosol resembles that expected from the mixing of finely divided materials from large-scale sources. The main sources of material to the atmosphere have been described in Section 4.1.3, and a source–control relationship offers a convenient framework within which to describe the chemistry of the marine aerosol.

One of the most widely used methods of relating an element in an aerosol to its source is by employing a source indicator, or marker, which is derived predominantly from one specific source. In order to assess the enrichment of an element relative to a source it is common practice to define the excess, i.e. non-source fraction, in terms of an **enrichment factor** (EF), which is calculated with respect to an equation of the type:

$$EF_{source} = (E/I)_{air}/(E/I)_{source} \qquad (4.1)$$

in which $(E/I)_{air}$ is the ratio of concentrations of an element E and the indicator element I in the aerosol, and $(E/I)_{source}$ is the ratio of their concentrations in the source material.

The two most important sources for the low-temperature generation of particulate matter to the marine atmosphere are the Earth's crust and the ocean surface.

4.2.1.1 The crustal aerosol Aluminium is the most commonly used indicator element for the crustal source and although there are problems involved in selecting a composition for the source (or precursor) material, that of the average crustal rock is frequently used for the calculation of

EF_{crust} values, according to the equation:

$$EF_{crust} = (E/Al)_{air}/(E/Al)_{crust} \quad (4.2)$$

in which $(E/Al)_{air}$ is the ratio of the concentrations of an element E and Al in the aerosol, and $(E/Al)_{crust}$ is the ratio of their concentrations in average crustal rocks.

Because of the various constraints involved in the calculation, EF_{crust} values should only be treated as order-of-magnitude indicators of the crustal source. Thus, values close to unity are taken as an indication that an element has a mainly crustal origin, and those > 10 are considered to indicate that a substantial portion of the element has a non-crustal origin.

Rahn (1976) and Rahn *et al.* (1979) have tabulated the EF_{crust} values for some 70 elements in over a hundred samples from the world aerosol, and a geometric mean for the whole population gives a first approximation of the most typical value for each element. These geometric means are plotted in Figure 4.5, from which it can be seen that over half the elements have EF_{crust} values which range between 1 and 10, indicating that they are present in the aerosol in roughly crustal proportions. These are termed the crustal or **non-enriched elements** (NEE). The remaining elements have EF_{crust} values in the range 10 to $\sim 5 \times 10^3$, and their concentrations in the aerosol are not crust-controlled. These are referred to as the enriched or **anomalously enriched elements** (AEE).

The NEE will amost always retain their character in all aerosols. However, it is important to stress that the degree to which an AEE is actually enriched can vary considerably as the mutual proportions of the various components in an aerosol change. Data to illustrate this are given in Table 4.8, which lists the EF_{crust} values for several elements from a variety of marine locations. These data show, for example, that EF_{crust} values of the AEE Cu, Pb and Zn can vary between < 10 and > 100. Thus, under certain conditions the EF_{crust} values of the AEE can indicate that they are present in crustal proportions. Some of the factors that control the source strengths, and so the EF_{crust} values, of both the NEE and the AEE in the marine aerosol can be illustrated with respect to the distributions of Fe and Cu in the Atlantic atmosphere. The average Al, Cu and Fe concentrations, and EF_{crust} values for Fe and Cu, from a number of aerosol populations sampled on a north–south Atlantic transport are listed in Table 4.9. Iron is a crustal element, and the Fe EF_{crust} values are all < 10 and exhibit little variation between the populations. In contrast, Cu is an AEE in the world aerosol, but Cu EF_{crust} values in the Atlantic aerosol vary considerably. In most of the populations in fact, they are > 10. However, the average Cu EF_{crust} values fall in the aerosol collected over the Straits of Gibraltar and reach a maximum of around unity in the Northeast Trades population, which

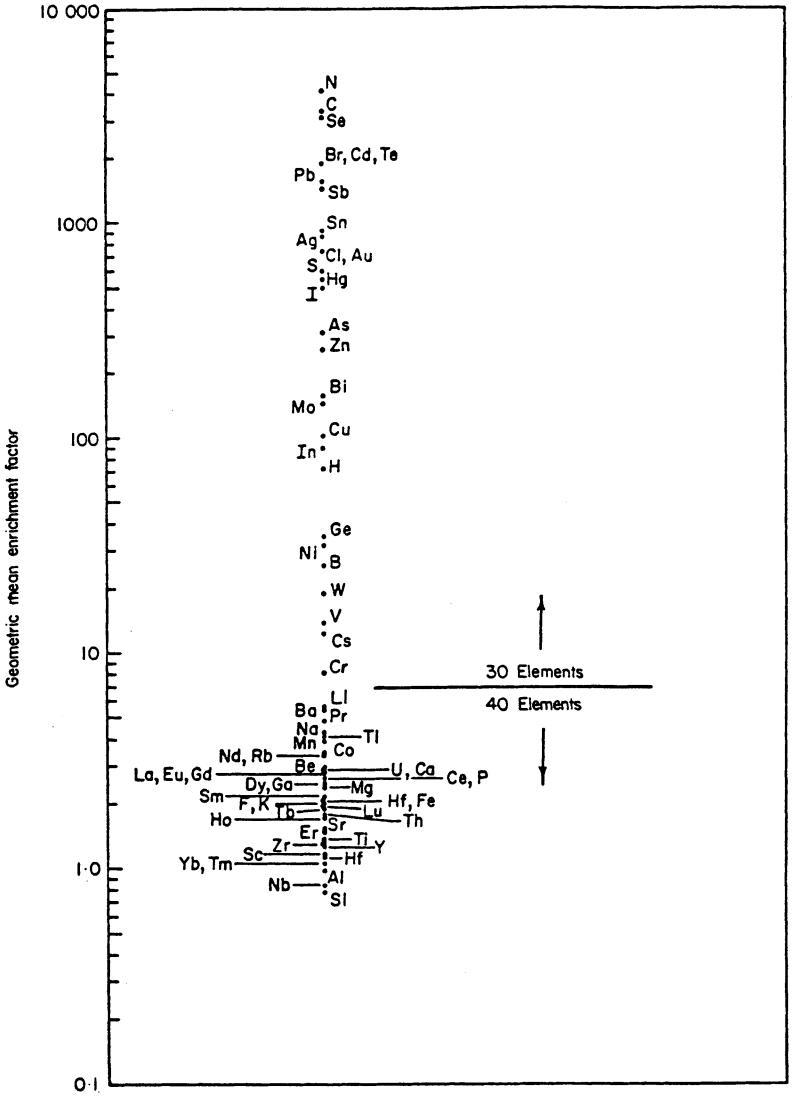

Figure 4.5 Geometric mean EF_{crust} values for elements in the world aerosol (from Rahn *et al.* 1979).

Table 4.8 EF_{crust} values for some anomalously enriched crustal elements in marine aerosols

Element	EF_{crust}			
	North Atlantic; westerlies[a]	Bermuda (N. Atlantic)[b]	Enewetak (N. Pacific)[c]	North Atlantic northeast trades[d]
Cu	120	9.6	3.2	1.2
Zn	110	26	~14	3.8
Pb	2200	170	40	9.1
Cd	730	570	130	9.4

[a] Data from Duce et al (1975).
[b] Data from Duce et al. (1976).
[c] Data from Duce et al. (1983a)
[d] Data from Murphy (1985).

Table 4.9 Average concentrations and EF_{crust} values for Al, Fe and Cu in Atlantic aerosols[a]

Oceanic region	Element				
	Al	Fe		Cu	
	Conc. (ng m^{-3} of air)	Conc. (ng m^{-3} of air)	EF_{crust}	Conc. (ng m^{-3} of air)	EF_{crust}
North Atlantic					
Westerlies	48	36	1.2	1.0	30
Straits of Gibraltar	827	626	1.1	2.4	8.2
Northeast trades	5925	3865	1.0	4.5	1.2
South Atlantic					
Southeast trades	17	13	1.2	0.30	44
Westerlies	2.7	2.6	1.8	0.29	225

[a] Data from Murphy (1985).

was sampled off the coast of West Africa, where pulses of Saharan dust-laden air are common – see Section 4.1.4.1. It is apparent, therefore, that although Cu is classified as an AEE in the world aerosol (average Cu EF_{crust} value ~ 100), under some conditions crustal material can become the dominant source of the element and can completely mask the non-crustal components. It may be concluded, therefore, that although the atmospheric concentrations of the NEE (e.g. Fe) vary considerably, their

EF_{crust} values remain relatively constant. In contrast, both concentrations and EF_{crust} values of the AEE vary, the latter being lowered by increases in the input of crustal material.

4.2.1.2 The sea-salt aerosol In order to assess the importance of the sea surface as a source for the marine aerosol, Na can be used as the marine indicator element, and the precursor source composition is assumed to be that of bulk sea water. The EF_{sea} is then calculated according to the equation:

$$EF_{sea} = (E/Na)_{air}/(E/Na)_{sea\ water} \quad (4.3)$$

in which $(E/Na)_{air}$ is the ratio of the concentrations of an element E and Na in the aerosol, and $(E/Na)_{sea\ water}$ is the ratio of their concentrations in *bulk* sea water.

A selection of EF_{sea} values for aerosols for a number of marine regions is given in Table 4.10. The regions are ranked on the basis of their

Table 4.10 EF_{sea} values for a number of elements in the marine aerosol[a]

Element	EF_{sea}		
	North Atlantic	North Pacific Hawaii	North Pacific Enewetak
K	1.3	1.1	1.3
Mg	0.9	1.0	1.1
Al	1×10^6	3×10^5	1×10^5
Co	8×10^3	$<1 \times 10^3$	1×10^3
Cu	6×10^4	7×10^3	3×10^3
Fe	4×10^7	6×10^5	3×10^4
Mn	4×10^5	8×10^3	2×10^4
Pb	5×10^5	5×10^5	3×10^4
V	9×10^3	4×10^2	2×10^2
Zn	2×10^6	6×10^5	1×10^5
Sc	1×10^5	-	4×10^4

Mo	U.K. coastal aerosol	N. Atlantic westerlies	Atlantic north east trades	Atlantic south east trades	South Atlantic westerlies
	116	20	13	9.5	1.4

[a] Data for Mo from Chester et al. (1984); data for all other elements from Weisel et al. (1984).

distance from the major continental trace metal sources, and so represent increasingly more pristine marine environments. The elements in the table can be divided into three general groups.

(a) **Group 1** contains K and Mg. For these two elements there is little inter-site variation in their EF_{sea} values, which are all around unity and indicate that the elements have a predominantly oceanic source at all locations.
(b) **Group 2** contains Mo. This element has EF_{sea} values that range up to ~ 100 close to the continents but fall to around unity in the remote South Atlantic westerlies. This indicates that in remote areas bulk sea water can be a significant source for this element (see e.g. Chester *et al.* 1984a).
(c) **Group 3** contains Al, Fe, Mn, Co, V, Cu, Pb and Zn. For these elements there is a progressive decrease in their EF_{sea} values towards the more pristine oceanic environments. However, even at the remote sites the elements are still enriched, by factors ranging up to 600 000, relative to bulk sea water.

From their EF_{sea} values, therefore, it would appear that the ocean is not a significant source for the elements in group 3 above, even in areas remote from the influence of other sources. However, the calculation of the EF_{sea} values present problems that are considerably more complex than those associated with EF_{crust} values. These problems involve the selection of a composition for the oceanic precursor material, and the most serious of them arises in response to the nature of the processes involved in the generation of sea-salts. During the bursting of bubbles, which is the principal mechanism in sea-salt formation, part of the sea surface microlayer can be skimmed off to be incorporated into the salt particles. This microlayer can contain concentrations of many trace metals, which are enhanced up to 10^3–10^7 times relative to bulk sea water (see Sec. 4.2). As a result, considerable fractionation of these trace metals can take place during the formation of sea salts, so that **bulk** sea water is not their immediate oceanic source. A number of attempts have been made to evaluate a more realistic source composition for material generated from the sea surface by relating the material directly to the microlayer itself. One of these involves the collection and analysis of bubble-produced sea salts using the Bubble Interfacial Microlayer Sampler (BIMS) (see e.g. Fasching *et al.* 1974, Piotrowicz *et al.* 1979). In a recent study, Weisel *et al.* (1984) carried out a series of BIMS experiments in the open-ocean western North Atlantic. During these experiments bubbles were artificially generated from water depths ranging from immediately below the surface to 1 m down, and the sea-salt particles formed were collected on filters and subsequently analysed for a

series of elements. The net concentration of each element on the bubble-generated sea salts was then used, together with its North Atlantic surface seawater concentration, to calculate a BIMS EF_{sea} value. The geometric BIMS EF_{sea} means for all bubble depths for the elements studied are given in Table 4.11, and on this basis, following Weisel *et al.* (1984), the elements can be divided into two broad groups.

Table 4.11 BIMS EF_{sea} values determined over the North Atlantic Ocean[a]

Element	BIMS EF_{sea}
K	1.0
Mg	1.0
Al	5×10^3
Co	6×10^2
Cu	8×10^2
Fe	1×10^4
Mn	1×10^3
Pb	4×10^3
V	1×10^2
Zn	2×10^4

[a] Data from Weisel et al. (1984).

(a) **Group 1** contains K and Mg. These two elements have average BIMS EF_{sea} values of unity, just as they did in the bulk aerosol (see above). That is, these elements, together with Na, retain their original bulk seawater ratios on the bubble-generated salts.

(b) **Group 2** contains Al, Fe, Mn, Co, V, Cu, Zn, Pb and Sc. These elements have relatively high BIMS EF_{sea} values, ranging from 10 for Sc to 20 000 for Zn, and apparently undergo fractionation at the sea surface.

Despite the very real difficulties inherent in assessing the fractionation of elements at the air/sea interface, the BIMS EF_{sea} data provide at least a first approximation of the degree to which such fractionation has taken place. Further, by making the assumption that the BIMS EF_{sea} values found for the North Atlantic apply globally, Weisel *et al.* (1984) introduced the important concept of a **relative oceanic enrichment factor** (REF_{sea}), which is the aerosol EF_{sea} value (calculated with respect to bulk sea water) divided by the BIMS EF_{sea} value. The REF_{sea} values therefore directly related the enrichment of an element in a marine

aerosol to the fractionation that occurs at the sea surface, and so should offer a more realistic assessment of the ocean as a source material. The REF_{sea} values should approach unity if the sea surface is a significant source for an element, and this is evaluated with respect to a number of marine aerosol populations in Table 4.12. In this table, the BIMS EF_{sea} values are expressed as a percentage of the EF_{sea} value (i.e. that obtained using bulk sea water), and the REF_{sea} values are also given. From these various data it can be seen that for Al, Co, Mn and Pb the BIMS EF_{sea} values are $< 10\%$ of the EF_{sea} values, and for these elements the sea surface is a trivial source even at the remote site (Enewetak). For V, Cu and Zn, however, the BIMS EF_{sea} values are $> 20\%$ of the EF_{sea} values for the Enewetak population, indicating that at some remote sites the sea surface becomes a non-trivial source for these elements; this was confirmed by Arimoto *et al.* (1987) for aerosols at the remote Samoa (South Pacific) site. However, extreme caution must be exercised when attempting to interpret the enrichment of elements on sea salts. One reason for this is that particles deposited onto the sea surface from the atmosphere can be recycled back into the air during sea-salt production. For example, Settle & Patterson (1982) showed that much of the Pb in the sea-salt aerosol may have originated from Pb-rich atmospheric particles that have been recycled from the microlayer. Recycling of this kind makes it difficult to estimate the true *net* flux of elements from the ocean surface to the atmosphere. Another factor that can complicate the assessment of fluxes of elements from the sea surface is the formation of particulate components from gaseous emissions, since these will have a

Table 4.12 Sea surface sources of elements in marine aerosol populations

Element	North Atlantic		North Pacific			
			Hawaii		Enewetak	
	BIMS EF_{sea} as a % of aerosol EF_{sea}	REF_{sea}	BIMS EF_{sea} as a % of aerosol EF_{sea}	REF_{sea}	BIMS EF_{sea} as a % of aerosol EF_{sea}	REF_{sea}
Al	0.5	200	1.6	6	5	20
Co	0.75	133	6	17	6	17
Mn	0.25	400	12	8	5	20
Cu	1.3	75	11	8.75	27	3.75
V	1.1	90	25	4	50	2
Zn	1	100	3	30	20	5
Pb	0.80	125	0.80	125	10	7.5

a original data from Weisel et al. (1984).

small particle, and not a sea-salt particle, size. For example, Mosher *et al.* (1987) gave data on the distribution of Se in the Pacific atmosphere. Although the element is concentrated on particles with an MMD of 1.5 μm, the authors concluded that the enrichment of the element on marine aerosols is a sea surface phenomenon and can be explained by the gas-to-particle conversion of a natural vapour-phase flux generated by biologically mediated reactions associated with primary production. The ocean-to-atmosphere vapour-phase selenium flux was estimated to be $\sim (5\text{–}8) \times 10^9$ g yr^{-1}, $\sim 40\%$ of which is derived from the highly productive upwelling waters of the equatorial and subpolar zones. This natural ocean-to-atmosphere Se flux is of the same order of magnitude as the total anthropogenic emissions of atmospheric Se, i.e. $\sim 7 \times 10^9$ g yr^{-1}, thus demonstrating the important role played by sea surface recycling in the atmospheric budget of Se. Such sea surface-derived gas precursors are also significant in the production of aerosol nitrate and sulphate (Sec. 4.1.4.3).

4.2.1.3 The enriched aerosol There are a number of processes that can supply the AEE to the atmosphere, and many of these are associated with some form of high-temperature generation (see Sec. 4.1.1). However, unlike the low-temperature processes involved in the production of crustal and oceanic particulate material, the high-temperature processes do not in general have readily identifiable indicator elements that can be determined on a routine basis. It is not usual, therefore, to calculate enrichment factors for these high-temperature processes, and although their presence is indicated by the fraction that is in excess of those accounted for by the EF_{crust} and REF_{sea} values, other approaches must be employed for their actual identification. Two such approaches applicable to the marine aerosol will be discussed here; these involve the particle size distribution and the solid-state speciation of the elements in the aerosol.

THE PARTICLE SIZE DISTRIBUTION OF ELEMENTS IN THE MARINE AEROSOL The particle size of an element in the atmosphere is controlled by the manner in which it is incorporated into its host component, which, in turn, is a function of its source. The overall particle size–source relationships have been illustrated in Figure 4.1, from which two general populations can be identified. The coarse particles are in the **mechanically generated** range and have diameters $\gtrsim 2$ μm. These include the crustal and sea-salt components, and during their formation these particles acquire their elements directly from the precursor material. In contrast, the fine particles are in the **Aitken nuclei** or **accumulation** range and have diameters $\lesssim 2$ μm. Those in the accumulation range are formed by processes such as condensation and gas-to-particle conversions, and

elements associated with them can be acquired from the atmosphere itself. For example, during high-temperature processes (such as volcanic activity, fossil fuel combustion, waste incineration and the processing of ore materials) some elements can be volatilized from the parent material in a vapour phase. They can be removed from this vapour phase via condensation and gas-to-particle processes during which the elements may be adsorbed onto the surfaces of the ambient aerosols. The processes are size-dependent because, in general, small particle condensation nuclei will have a large ratio of surface area to volume (see e.g. Rahn 1976). As a result, many of the elements released during high-temperature processes become associated with small particles in the accumulation range, i.e. with diameters $\lesssim 1$ to 0.1 μm – see Figure 4.1.

Because of the different processes involved in the generation of their host particles, elements having a crustal or an oceanic source should be present in association with larger ($\gtrsim 1$ μm diameter) aerosols, whereas those having a high-temperature source should be found on smaller ($\lesssim 1$ μm diameter) aerosols. There are also differences in the particle size distributions of the mechanically generated crustal and sea-salt aerosols. The particle size distribution of an element in an aerosol population should therefore offer an insight into its source. This has been demonstrated in a number of studies. For example, Figure 4.6 illustrates the mass particle size distributions of: (a) ^{210}Pb, which can be used as an example of an element that has a mass predominantly associated with submicrometre-sized particles typical of many high-temperature-generated pollutant-derived elements; (b) Al, which is typical of crust-derived elements; and (c) Na, which is typical of sea-salt-derived elements. From data such as these, three general conclusions can be drawn regarding the particle size distribution of elements in the marine aerosol.

(a) Sea-salt-associated elements have most of their total mass on particles with MMDs in the range ~ 3–7 μm; these elements include Na, Ca, Mg and K.
(b) Crust-derived elements have most of their total mass on particles with MMDs in the range ~ 1–3 μm; these elements include the NEE Al, Sc, Fe, Co, V, Cs, Ce, Rb, Eu, Hf and Th.
(c) Elements associated with high-temperature sources (mainly anthropogenic) have most of their total mass on particles with MMDs $\lesssim 0.5$ μm; these elements include the AEE Pb, Zn, Cu, Cd and Sb.

However, it must be stressed that the particle size characteristics of some elements in an aerosol can change as the source influence changes. For example, it was shown in Section 4.2.1.1 that under certain circumstances some of the AEE can be crust-controlled, and here their size distribution will be dominated by particles with MMDs in the ~ 1–3 μm crustal range.

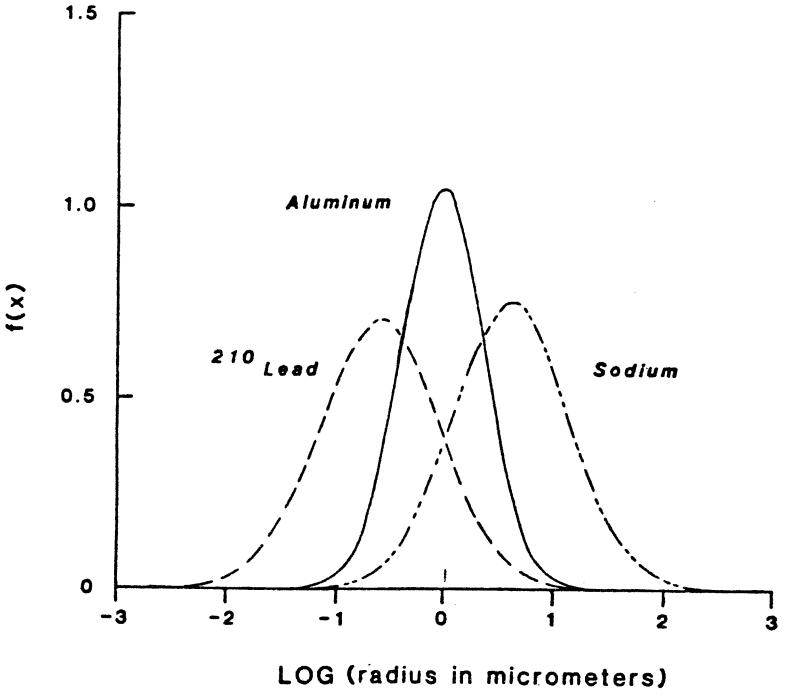

Figure 4.6 Mass size distributons of ^{210}Pb, Al and Na in aerosols from the marine atmosphere (from Arimoto & Duce 1986).

In remote areas, a number of trace elements can have a significant sea surface source, and these will be concentrated on particles having MMDs in the ~ 3–7 μm sea-salt range. Such particle size variations resulting from changes in the dominance of anthropogenic, crustal and sea-salt soures for the AEE (e.g. Cu and Zn) have been demonstrated by Duce *et al.* (1983a) for aerosols collected at Enewetak (North Pacific). It may be concluded, therefore, that in an aerosol population the particle size distributions of elements between the three size classes, together with EF data for the individual size classes, can be used to establish the predominance of their anthropogenic, crustal and sea-salt sources.

THE SOLID-STATE SPECIATION OF ELEMENTS IN THE MARINE AEROSOL The partitioning of elements among the components of an aerosol, i.e. their solid-state speciation, can reveal information on their sources. This can be illustrated with respect to two recent studies carried out on the speciation of elements in urban and crustal aerosol end-members. As an example of a pollution-dominated (high-temperature-generated) urban

aerosol, Lum *et al.* (1982) used a sample of urban particulate material (UPM) collected at St. Louis (USA). For the crustal (low-temperature-generated) aerosol, Chester *et al.* (1986) used a series of soil-sized particulates collected in the Atlantic Northeast Trades off the coast of West Africa. The speciation schemes employed in the two studies were generally similar, and the partitioning signatures of a number of elements in the two end-member aerosols are illustrated in Figures 4.7a and b.

The partitioning signatures for some elements differ considerably between the urban and crustal aerosol end-members. These differences follow two principal trends.

(a) This trend is related to the manner in which the refractory nature of some of the elements changes. Although both Al and Fe have smaller percentages of their total concentrations in the refractory fraction of the UPM than in the crustal aerosol, they still retain their overall refractory nature in the urban material. However, Pb, Cr, Zn, Cu and Cd all have substantially smaller proportions of their total concentrations in the refractory fraction of the UPM than in that of the crustal material. This is most apparent for Cu and Zn, both of which fall from being ~ 80% refractory in the crustal aerosol to ~ 15% in the UPM.

(b) The second trend lies in the manner in which the loosely bound nature of some of the elements varies. For Al, Fe and Cr, < 5% of their total concentrations are held in this association in both aerosol

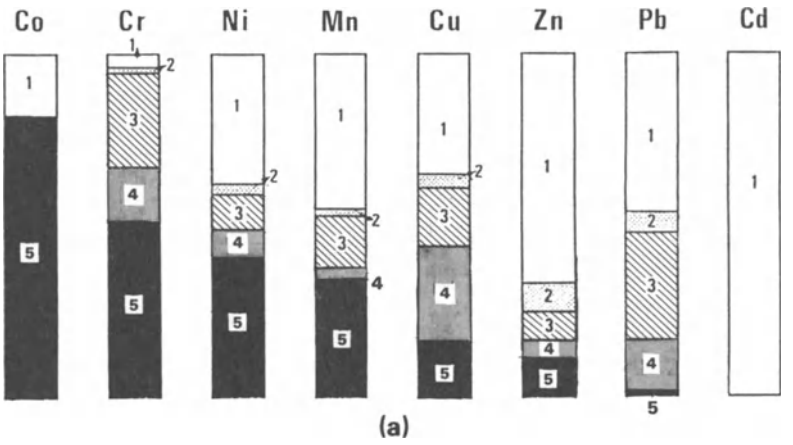

Figure 4.7 The partitioning of elements in aerosols. (**a**) High-temperature-generated aerosols (modified from Salomons & Forstner 1984; original data from Lum *et al.* 1982). 1, Exchangeable (or loosely held) association. 2, Surface oxide and carbonate association. 3, Oxide association. 4, Organic association. 5, Residual, or refractory, association.

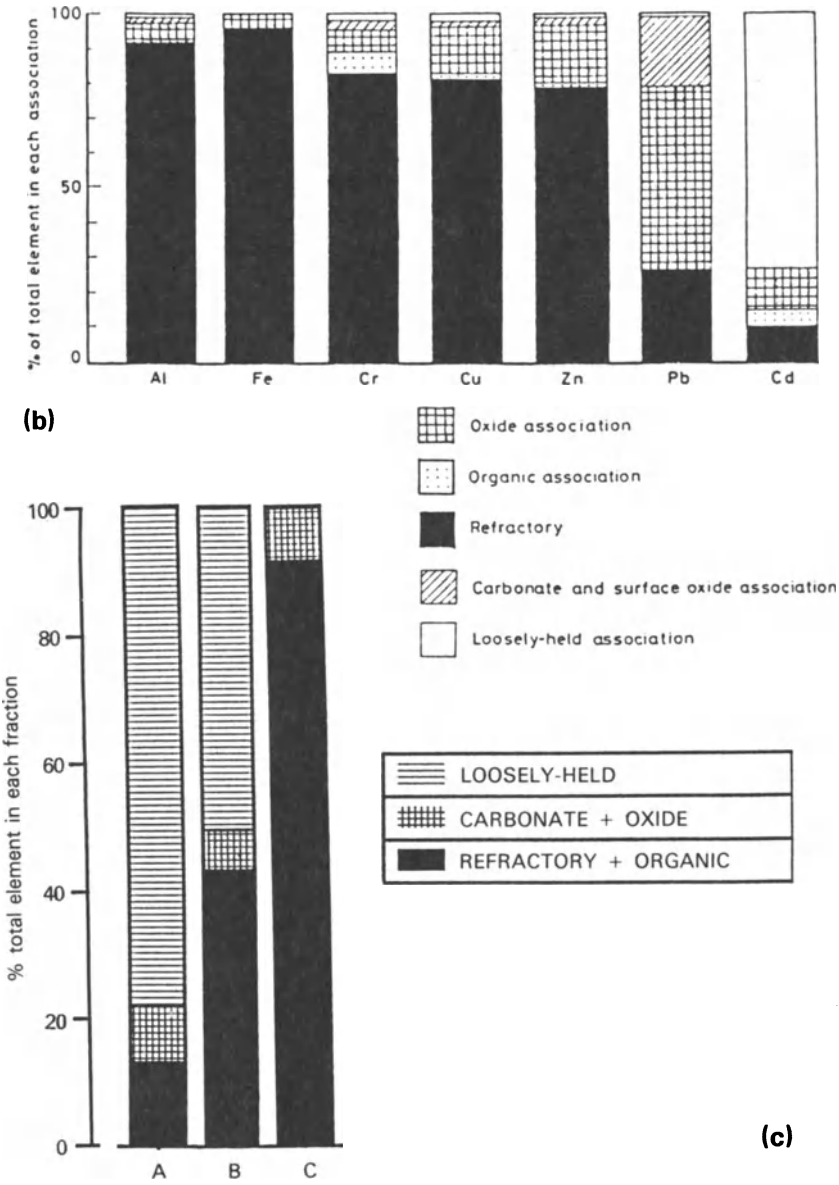

Figure 4.7 (**b**) Low-temperature-generated crustal aerosols (from Chester *et al.* 1986). (**c**) The speciation signatures of Zn in aerosols from the North Atlantic (adapted from data in Chester *et al.* 1988). A, Aerosols collected at Liverpool, representative of a European coastal urban-dominated population. B, Aerosols collected around Cape Verde, representative of a mixed North Atlantic population. C, Aerosols collected in the Atlantic northeast trades, representative of a crust-dominated population. Note how the proportion of the loosely bound Zn decreases in the sequence urban-dominated > mixed > crust-dominated aerosols.

end-members. However, there are relatively very large increases in the percentages of Cu, Zn, Pb and Cd in loosely bound associations in the UPM. This effect is strongest for Zn, which has only ~ 5% of its total concentration in a loosely bound association in the crustal material compared to ~ 65% in the UPM.

It is, therefore, the more volatile elements (e.g. Cd, Pb, Zn, Cu) that become increasingly 'loosely bound' in character in the urban relative to the crustal aerosol end-member. This is entirely consistent with the release of these elements into the vapour phase during high-temperature processes and their subsequent uptake onto ambient particle surfaces. The extent to which the volatile elements are in loosely bound associations varies with the degree to which the end-member aerosols are mixed in the marine atmosphere. This was demonstrated by Chester *et al.* (1988), who provided data on the speciation of a number of elements in the North Atlantic aerosol. These authors applied a three-stage sequential leaching technique to a series of filter-collected atmospheric particulates and showed that the loosely bound nature of Zn, Pb and Cu decreased on a north–south transect from the European coast to the Northeast Trades off West Africa. The speciation signature for Zn is illustrated in Figure 4.7c, from which it can be seen that the loosely bound fraction of the element decreases away from the European pollutant sources, clearly demonstrating the value of speciation techniques as element source indicators in the marine aerosol.

4.2.2. Elemental source strengths

Recently there have been a number of attempts to estimate the global source strengths of elements to the atmosphere. There are large uncertainties involved in making these estimates and they should be treated at best as no more than approximations. Nonetheless, a number of overall trends in elemental atmospheric source strengths can be identified from the pubished estimates.

Lantzy & Mackenzie (1979) compiled data on the natural and anthropogenic global source of elements released into the atmosphere, and derived an **atmospheric interference factor** (AIF) calculated according to the equation:

$$\text{AIF} = (E_a/E_n) \times 100 \qquad (4.4)$$

in which E_a is the total anthropogenic emission of an element E, and E_n is its total natural emission. Thus, an AIF of 100 indicates that the anthropogenic flux of an element is equal to its natural flux. The data for the global atmospheric source strengths, and the AIF values, for the various elements are listed in Table 4.13. The elements in this table fall

into three main groups. (a) Al, Ti, Fe, Mn and Co have AIF values < 100, and for these elements natural fluxes dominate their supply to the atmosphere. (b) Cr, V and Ni have AIF values in the range 100–500, i.e. their anthropogenic fluxes are in excess of their natural fluxes, but only by factors of less than 5. (c) Sn, Cu, Cd, Zn, As, Se, Mo, Hg and Pb have AIF values in the range 500 to 35 000, and for these elements the atmospheric fluxes from anthropogenic sources greatly exceed those from natural sources. However, it must be remembered that the influx of anthropogenic components to the atmosphere is in the proportion ~ 90% to the Northern Hemisphere and only ~ 10% to the Southern Hemisphere (Robinson & Robbins 1971).

Weisel *et al.* (1984) have also estimated the global source strengths of a number of elements to the atmosphere. The data set, which is given in Table 4.14, is of interest because it offers a more detailed breakdown of some of the individual sources; for example, it includes the ocean surface as a potential source. From these data it is apparent that > 90% of the

Table 4.13 Natural and anthropogenic sources of atmospheric emissions[a] (units, 10^8 g yr^{-1})

Element	Continental Dust Flux	Volcanic Dust Flux	Volcanic Gas Flux	Industrial Particulate Emissions	Fossil Fuel Flux	Total Emissions (industrial, fossil fuel)	Atmospheric[b] Interference Factor (%)
Al	356,500	132,750	8.4	40,000	32,000	72,000	15
Ti	23,000	12,000	-	3,600	1,600	5,200	15
Sm	32	9	-	7	5	12	29
Fe	190,000	87,750	3.7	75,000	32,000	107,000	39
Mn	4,250	1,800	2.1	3,000	160	3,160	52
Co	40	30	0.04	24	20	44	63
Cr	500	84	0.005	650	290	940	161
V	500	150	0.05	1,000	1,100	2,100	323
Ni	200	83	0.0009	600	380	980	346
Sn	50	2.4	0.005	400	30	430	821
Cu	100	93	0.012	2,200	430	2,630	1,363
Cd	2.5	0.4	0.001	40	15	55	1,897
Zn	250	108	0.14	7,000	1,400	8,400	2,346
As	25	3	0.10	620	160	780	2,786
Se	3	1	0.13	50	90	140	3,390
Sb	9.5	0.3	0.013	200	180	380	3,878
Mo	10	1.4	0.02	100	410	510	4,474
Ag	0.5	0.1	0.0006	40	10	50	8,333
Hg	0.3	0.1	0.001	50	60	110	27,500
Pb	50	8.7	0.012	16,000	4,300	20,300	34,583

[a] from Lantzy and Mackenzie (1979).

[b] interference factor = (total emissions/continental + volcanic fluxes) x 100.

Al, Fe, Mn and Co in atmospheric particulates have natural sources and are supplied by the injection of crustal dust, and that ~ 80% of the K and Mg are associated with the generation of sea salts. The authors used BIMS REF_{sea} values, rather than those calculated using bulk sea water, to assess the importance of the ocean surface as a source for metals. On the basis of the mean BIMS data it can be estimated that ~ 24% of the V, ~ 23% of the Cu and as much as 69% of the Pb released to the atmosphere from *natural* processes can have an oceanic source. Of the elements considered by Weisel *et al.* (1984), only Cu has a volcanic source, which contributes $\gtrsim 5\%$ of its natural atmospheric input. However, volcanic sources dominate the natural release of As (see e.g. Walsh *et al.* 1979a, b), and may be significant in the release of Cd (Nriagu 1979). From the data presented by Weisel *et al.* (1984) vegetation does not appear to be an important source for the elements in Table 14.4, although Nriagu (1979) estimated that vegetative release can be important in the atmospheric cycles of some elements, contributing, for example, ~ 20% of the Zn released naturally into the atmosphere.

Table 4.14 Global source strengths for atmospheric trace metals[a] (units, 10^9 g yr^{-1})

	Natural				Anthropogenic	
Element	Ocean[b] (mean)	Crust	Volcanoes	Vegetation	Fossil fuel	Others
Al	200	20000	700	40	2000	2000
Co	0.2	7	0.1	0.04	0.9	2
Cu	5	10	6	0.9	2	50
K	30000	6000	200	100	200	200
Fe	50	10000	300	20	2000	4000
Mg	100000	3000	80	20	300	200
Mn	7	200	9	5	8	400
Pb	8	3	0.4	0.2	4	400
Sc	0.0005	7	0.2	0.002	0.8	0.4
V	10	30	0.7	0.2	20	2
Zn	8	80	10	10	80	200
Cd	0.4	0.05	0.1	0.05	0.2	5

[a] Data from Weisel et al. (1984); except Cd, which is from Buat-Menard (1983).

[b] Based on BIMS EF_{sea} data for all bubble depths.

It may be concluded that on the basis of the data available at present, the *natural* inputs of some NEE elements (e.g. Al, Fe, Mn, Co and Sc) are dominated by the injection of crustal material into the atmosphere, and that those of other elements (e.g. Na, K, Mg and possibly some trace metals) are dominated by the generation of sea salts. The release of elements into the atmosphere via volcanic activity and vegetative processes may be significant in the natural fluxes of some elements, but they are difficult to quantify at present. In the past, however, volcanic sources may have been more important in the release of some AEE to the atmosphere. For example, Patterson & Settle (1987) have estimated that although at present both crustal dust and volcanic sources, which have roughly equal source strengths, are negligible compared to industrial inputs, the two natural sources were dominant in pre-industrial Holocene times when the atmospheric Pb reservoir was only ~ 1% of its present size. In the Holocene, therefore, volcanic activity was the source of around half of the Pb in the atmosphere. Although the sea surface may be important in the release of V, Cu, Zn and Pb to the atmosphere by natural processes, it can be seen from the data in Table 4.14 that at present the natural sources of the AEE are dwarfed on a global scale by their anthropogenic inputs, and it is only in regions remote enough from the influence of these inputs that the ocean source may become significant (see Sec. 4.1.5.1). Further, it must be remembered that elements released from the sea surface have been recycled into the air, and do not take part in the *net* input of elements to the oceans from the atmosphere.

4.2.3 Geographic variations in the elemental composition of the marine aerosol

It was pointed out in Section 4.1.5.1 that the concentrations of many elements in the marine atmosphere vary over several orders of magnitude from one region to another. The reasons for these variations can now be assessed in the light of the factors discussed above. The overall composition of the marine aerosol is controlled by the extent to which components derived from the various sources are mixed together in the atmosphere. A considerable amount of data are now available on the concentrations of elements in marine aerosols from a wide variety of environments, and a compilation of some of the more recent data is given in Table 4.15. In this table the marine locations are arranged in an increasing order of remoteness from the primary, i.e. non-oceanic, sources. The principal trends in atmospheric concentrations that emerge from this data set can be summarized as follows.

(a) The highest concentrations of the AEE are found over coastal seas that are relatively close to the continental anthropogenic sources.
(b) The highest concentrations of the NEE are found over regions close

Table 4.15 Concentration (1) and EF values (2) of trace metals in marine aerosols

		Coastal seas; close to pollution sources				Coastal seas and open ocean; close to crust sources								Open ocean									
Conc. units; m^3 of air		North[a] Sea		Keil[b] Bight		Western[c] Med.		Eastern[d] Med.		N.Atlantic[e] (northeast trades)		N.Arabian[f] Sea		Tropical[g] N.Atlantic		N.Atlantic[h] (Bermuda)		N.Atlantic[e] westerlies		S.Atlantic[e] westerlies		N.Pacific[i] (Enewetak)		S.Pacific[j] (Samoa)	
		1	2	1	2	1	2	1	2	1	2	1	2	1	2	1	2	1	2	1	2	1	2	1	2
Al	ng	159	1.0	394	1.0	324	1.0	915	1.0	5925	1.0	1184	1.0	160	1.0	140	1.0	48	1.0	2.7	1.0	21	1.0	0.72	1.0
Fe	ng	330	3.0	369	1.4	-	-	570	0.9	3865	1.0	908	1.1	100	0.9	94	1.0	36	1.1	2.6	1.4	17	1.2	0.21	0.4
Sc	pg	82	1.9	-	-	-	-	-	-	-	-	-	-	35	0.8	20	0.5	-	-	-	-	5	0.9	0.04	0.2
Mn	ng	21	11	15	3.3	-	-	12	1.1	65	1.0	15	1.1	2.2	1.2	1.2	0.7	1.7	3.1	0.11	3.5	0.29	1.2	0.005	0.6
Ni	ng	10	69	4	11	-	-	-	-	6.6	1.2	3.9	3.6	0.64	4.4	0.08	0.6	0.51	12	0.02	8.1	-	-	-	-
Co	pg	360	7	-	-	-	-	-	-	2100	1.2	670	1.9	80	1.6	-	-	50	3.4	10	12	8	1.3	0.37	1.7
Cr	ng	4.5	23	-	-	-	-	1.6	1.4	10	1.4	4.3	3.0	0.43	2.2	0.28	1.6	0.49	8.4	0.17	52	0.09	3.5	-	-
V	ng	12	46	9.7	15	-	-	-	-	15	1.5	-	-	0.54	2.1	-	-	1.0	13	0.03	6.8	0.08	2.3	-	-
Cu	ng	-	-	7.7	29	-	-	4.9	8.0	4.5	1.1	3.2	4.0	0.79	7.4	0.90	10	1.0	31	0.29	161	0.045	3.2	0.013	27
Zn	ng	153	1132	57	170	-	-	-	-	16	3.2	4.3	4.3	4.4	32	3.2	27	7.5	184	1.8	784	0.17	9.5	0.07	114
Cd	ng	-	-	-	-	1.9	2413	-	-	0.12	8.3	0.05	17	-	-	0.19	558	0.11	943	0.02	3048	0.004	78	-	-
Se	ng	1.5	15466	1.6	6657	-	-	-	-	-	-	-	-	0.43	4405	0.13	1522	-	-	-	-	0.13	10148	0.09	20491
Sb	pg	2900	7600	-	-	-	-	-	-	-	-	-	-	110	286	30	89	-	-	-	-	4.0	79	0.20	116
Pb	ng	147	6082	53	885	40	812	7.4	53	6.9	7.7	2.9	16	9.9	407	3.5	164	6.0	882	0.97	2364	0.12	38	0.016	146

[a] Cambray et al. (1975)
[b] Schneider (1987)
[c] Dulac et al. (1987)
[d] Saydam (1981)
[e] Murphy (1985)
[f] Sanders (1983)
[g] Buat-Menard & Chesselet (1979).
[h] Duce et al. (1976)
[i] Duce et al. (1983a)
[j] Arimoto et al. (1987)

to the continental arid land and desert sources.

(c) The concentrations of both the AEE and the NEE decrease with remoteness from the continental sources, and for those regions for which sufficient data are available the general rank order is coastal seas > North Atlantic > North Pacific > South Pacific.

(d) The EF_{crust} values are highest in aerosols from the coastal seas, but those for the Samoa aerosol are higher than those for the less remote Enewetak aerosol, which suggests that the residence times of the small-sized AEE-containing anthropogenic particles are longer than those of the larger NEE-containing mineral particles.

The various data in Table 4.15 offer an indication of the concentrations of elements in the marine atmosphere. These elements are available for deposition at the sea surface. However, before entering the ocean system proper they have to cross the air/sea interface, and the characteristics of this important transition zone are described in the next section.

4.3 Material transported via the atmosphere: the air/sea interface and the sea surface microlayer

From the point of view of aerosol chemistry, the recycling of components is perhaps the most important process taking place at the air/sea interface. However, this interface is also the site of a very specialized marine environment, the sea surface **microlayer**, at which a number of other geochemically important processes occur.

Surface-active organic materials are found on the surfaces of all natural water bodies, including the oceans. These organic materials, which are usually of a biological origin but can also include man-made substances (e.g. petroleum products), sometimes manifest themselves as visible slicks. However, even in the absence of such slicks the sea surface is covered by a thin organic film. This thin film, or microlayer, forms a distinct ecosystem and is an extremely important feature of the ocean reservoir. The thickness of the microlayer has been variously reported to extend from that of a monomolecular layer to several hundred micrometres, but since it is notoriously difficult to sample it is usually operationally defined in terms of the device used to collect it. Recently, a new surface microlayer sampler, the Self-Contained Underway Microlayer Sampler (SCUMS), which is designed to provide real-time information on iterfacial chemical and biological components, has been described by Carlson *et al.* (1985). In practice, however, most collection techniques retrieve samples that are considerably diluted with underlying bulk sea water.

The microlayer is the site across which the atmosphere–ocean system

interacts, i.e. where the sea 'breathes', and it has unique chemical, physical and biological properties, which are very different from those of the underlying sea water. Although there have been a number of major reviews of the microlayer (see e.g. MacIntyre 1974, Liss 1975, Duce & Hoffman 1976, Hunter & Liss 1981, Lion & Leckie 1981a, b, Seiburth 1983), our conceptual understanding of this marine phenomenon is still somewhat hazy and is continually evolving. There is, for example, controversy over the organic composition of the microlayer. Lion & Leckie (1981a) have pointed out that most of the organics that have been reported to occur in the microlayer fall into two categories of surface-active material: type 1, e.g. fatty acids, alcohols and lipids; and type 2, which consists of proteinaceous substances. Carbohydrates, insoluble hydrocarbons and chlorinated hydrocarbons are also found in the microlayer. Originally, it was thought that in the absence of petroleum pollution sea surface films consisted mainly of simple surfactants of type 1 (see e.g. Garrett 1967), but this was thrown into doubt when it was found that type 2 materials were perhaps dominant (see e.g. Baier 1970, 1972). More recently, however, it has been suggested that a third, humic-type, material makes up a large proportion of the organics in the microlayer. A large fraction of the dissolved organic material (DOM) in sea water is uncharacterized (see Sec. 9.2.3.2) but is known to contain surface-active material, such as humic and fulvic acids (much of which originates from planktonic exudates). Hunter & Liss (1981) suggested that surfactants in the microlayer consist to a large extent of polymeric material arising mainly from that part of the uncharacterized DOM that is surface-active. Seiburth (1983) reviewed the available data on the organic composition of the microlayer and concluded that carbohydrates account for $\sim$ 33% of the DOC in surface films, proteins $\sim$ 13% and lipids $\sim$ 3% (ratios that are similar to those in materials released from algal cultures), the remainder being thought to consist of condensed humic substances.

In the light of findings such as these, a different view of the microlayer is now beginning to emerge in the literature. By re-examining the original concepts, Seiburth (1983) proposed that substances such as carbohydrates, proteins, lipids and condensed humics, in both dissolved and colloidal forms, are advected through the mixed layer to adsorb on the 'solid' air/sea interface where they form a microlayer (or surface film), which may be described in terms of a loose hydrated gel of intertangled macromolecules, both free and condensed, which is colonized by bacteria.

This then is the nature of the organic 'soup' that is present at the sea surface, and it is apparent from the various data given in the literature that relative to bulk sea water the microlayer is enhanced in a variety of substances. These include total suspended solids, particulate and dissolved organic carbon, organic and inorganic phosphorus, particulate

Table 4.16 Order-of-magnitude trace metal enrichments in the sea surface microlayer relative to bulk sea water[a]

Element	Microlayer enrichment; no observable surface slick[b]	Microlayer enrichment; slick or foam samples[b]
Pb	2 - 10^1	10^3 - 10^7
Cu	2 - 10^1	10^2 - 10^5
Fe	<1 - 10^1	10^2 - 10^6
Ni	1 - 2	10^5
Zn	1.5 - 3	10^2 - 10^4

[a] Data from Lion & Leckie (1981a).

[b] Approximate values only.

and dissolved forms of nitrogen (excluding nitrate), bacteria and other micro-organisms, pollutants (such as DDT and PCBs) and trace metals. The enrichment of trace metals in the microlayer has been demonstrated by many workers (see e.g. Szekielda *et al.* 1972, Eisenreich *et al.* 1978, Pojasek & Zajicek 1978, Pattenden *et al.* 1981, Hardy *et al.* 1985a, b). These enrichments are found mainly in the organic and particulate microlayer fractions, but not in the dissolved inorganic fractions. Lion & Leckie (1981a) summarized the various data given in the literature for the enhancement of trace metals in the microlayer (see Table 4.16) and drew a number of overall conclusions.

(a) The enhancement of trace metals in the microlayer is not a consistent phenomenon.
(b) The frequency and degree of enhancement increase with the presence of observable organic surface slicks.
(c) The relative amounts of both organically associated and particulate trace metals (PTMs) are higher in the microlayer than in bulk sea water, although the degree of enhancement varies widely.

It may also be concluded that the concentrations of elements such as Pb, Zn, Cu, Cd and Fe are higher in microlayer samples from polluted than from non-polluted coastal waters (see e.g. Hardy *et al.* 1985b). The question that then arises is 'What process, or processes, cause(s) these microlayer enrichments?' To address this question it is useful to refer to the model outlined by Lion & Leckie (1981b) – see Figure 4.8. The principal features in this model can be described as follows. Trace metals are enhanced in the organic and particulate fractions of the microlayer (see above), e.g. by preferential transport via processes such as bubble

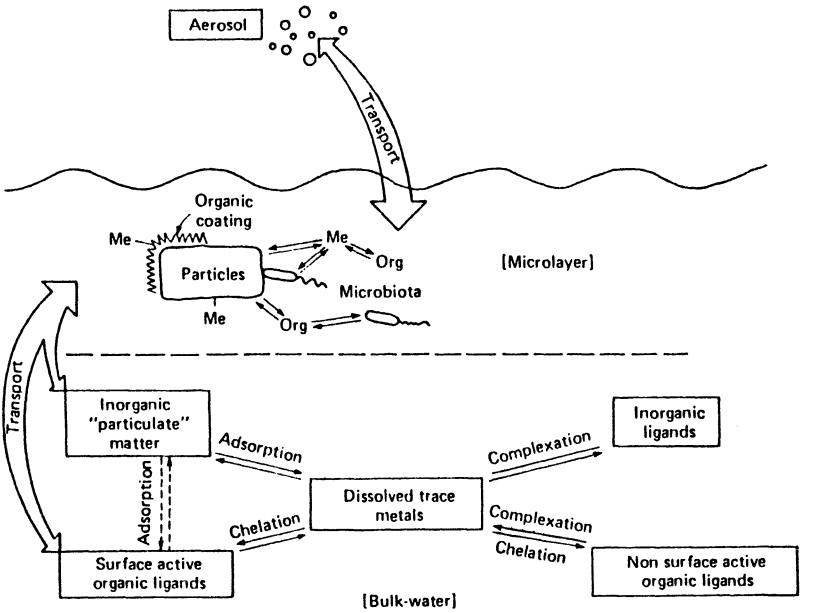

Figure 4.8 Schematic representation of the alternatives for the fates of trace metals at the air/sea interface (from Lion & Leckie 1981b). The trace metals may be thought of as competing with each other, and with the major marine cations, for adsorption sites and for available complexing ligands. At equilibrium, the results of interactions of this type will reflect the differing aqueous chemistries (including speciation) of the various trace metals.

flotation. However, dissolved inorganic forms of trace metals can also be transported into the microlayer, e.g. by turbulent mixing, where the enhancement of particulate matter and dissolved organic ligands provides the conditions for *in situ* adsorption and complexation. These various processes therefore combine to produce an enrichment of organically bound and particulate trace metals in the microlayer environment.

The question of the residence times of trace metals in the microlayer has been considered by a number of authors, and in one of the most recent studies Hardy *et al.* (1985a) used laboratory-derived data to set up a model designed to predict the behaviour of the metals in the microlayer under various conditions of biotic enhancement, windspeed and atmospheric PTM deposition rates. Mean predicted residence times for PTMs in the microlayer were in the range 1.5–15 h before they entered the water column.

The various components, including dissolved gases, that are concentrated in the microlayer are available for exchange across the air/sea interface and, in particular, the enhancement of trace metals in the microlayer can have an important effect on the chemistry of the marine aerosol. For example, it was shown in Section 4.1.5 that during the formation of sea salts by bubble bursting part of the microlayer can be

skimmed off and transferred into the atmosphere. The microlayer is therefore the region in which aerosols are both deposited from the atmosphere into the sea and are injected from the sea into the atmosphere, i.e. it is a site of recycling.

On the basis of the brief discussion outlined above it may therefore be concluded that the microlayer is a complex and reactive environment that forms the interface separating the sea from the atmosphere.

4.4 The atmospheric pathway: summary

(a) A mineral 'dust veil' is present over all the oceans, but the concentrations of material in it vary over several orders of magnitude, ranging from $\gtrsim 10^3$ μg m^{-3} of air off desert regions to $\lesssim 10^{-3}$ m^{-3} of air in remote oceanic areas.

(b) The global dust source strength is ~ 100 to ~ 800 g yr^{-1}; however, much of the mineral aerosol from desert sources is delivered to the marine atmosphere in the form of intermittent pulses.

(c) The particulate elements in the marine aerosol have three principal sources: the Earth's crust, the ocean surface and anthropogenic (mainly high-temperature) processes. The elements associated with each of these sources have characteristic particle size spectra in the aerosol: anthropologically derived elements have most of their total mass on particles with MMDs < 0.5 μm, crust-derived elements have most of their mass on particles with MMDs in the range ~ 1–3 μm, and sea-salt-associated elements have most of their mass on particles with MMDs in the range ~ 3–7 μm.

(d) The concentrations of many particulate elements in the marine atmosphere vary over several orders of magnitude, the highest concentrations being found close to the continental (crustal and anthropogenic) sources, and the lowest in remote pristine regions.

(e) Atmospherically transported particulates have to cross the air/sea interface before entering the bulk ocean. This interface is the site of the sea surface microlayer, which is an organic-rich, particle-rich and trace metal-rich zone, and is one of the most reactive environments in the oceans.

References

Andreae, M.O. 1986. The ocean as a source of atmospheric sulfur compounds. In *The role of air–sea exchange in geochemical cycling*, P. Buat-Menard (ed.), 331–62. Drodrecht: Reidel.

Andreae, M.O., R.J. Carlson, F. Bruynseels, H. Storm, R. van Grieken & W. Maenhaut

1986. Internal mixtures of sea salt, silicates, excess sulfate in marine aerosols. *Science* **232,** 1620–3.

Arimoto, R. & R.A. Duce 1986. Dry deposition and the air/sea exchange of trace elements. *J. Geophys. Res.* **91,** 2787–92.

Arimoto, R., R.A. Duce, B.J. Ray, A.D. Hewitt & J. Williams 1987. Trace elements in the atmosphere of American Samoa: concentrations and deposition to the tropical South Pacific. *J. Geophys. Res* **92,** 8465–79.

Atlas, S. & C.S. Giam 1986. Sea–air exchange of high molecular weight synthetic organic compounds. In *The role of air–sea exchange in geochemical cycling*, P. Buat-Menard (ed.), 295–329. Dordrecht: Reidel.

Baier, R.E. 1970. Surface quality assessment in natural bodies of water. *Proc. 13th Conf. Great Lakes Res.*, 114–27. Int. Assoc. Great Lakes Res.

Baier, R.E. 1972. Organic films on natural waters: their retrieval, identification, and modes of elimination. *J. Geophys. Res.* **77,** 5062–75.

Berg, W.W. & J.W. Winchester 1978. Aerosol chemistry of the marine atmosphere. In *Chemical oceanography*, J.P. Riley & R. Chester (eds), Vol. 7, 173–231. London: Academic Press.

Blanchard, D.C. 1963. Electrification of the atmosphere by particles from bubbles. In *Prog. Oceanogr.* **1,** 71–202.

Blanchard, D.C. 1983. The production, distribution, and bacterial enrichment of the sea-salt aerosol. In *Air-sea exchange of gases and particles*, P.S. Liss & W.G.N. Slin (eds), 407–54. Dordrecht: Reidel.

Blank, M., Leinen, M. & J.M. Prospero 1985. Major Asian aeolian inputs indicated by the mineralogy of aerosols and sediments in the western North Pacific. *Nature* **314,** 84–6.

Bonsang, B., B.C. Nguyen, A. Gaudry & G. Lambert 1980. Sulfate enrichment in marine aerosols owing to biogenic gaseous sulfur compounds. *J. Geophys. Res.* **85,** 7410–16.

Buat-Menard, P. 1983. Particle geochemistry in the atmosphere and oceans. In *Air–sea exchange of gases and particles*, P.S. Liss & W.G.N. Slin (eds), 455–532. Dordrecht: Reidel.

Buat-Menard, P. & R. Chesselet 1979. Variable influence of the atmospheric flux on the trace metal chemistry of oceanic suspended matter. *Earth Planet. Sci. Lett.* **42,** 399–411.

Carlson, A.J., J.L. Cantey & J.J. Cullen 1988. Description of and results from a new surface microlayer sampling device. *Deep-Sea Res.* **35,** 1205–13.

Cambray, R.S., D.F. Jefferies & G. Topping 1975. *An estimate of the input of atmospheric trace elements into the North Sea and the Clyde Sea (1972–73).* UK Atomic Energy Authority, Harwell, Rep. AERE-R7733.

Chesselet, R., M. Fontugne, P. Buat-Menard, U. Ezat & C.E. Lambert 1981. The origin of particulate organic carbon in the marine atmosphere as indicated by its stable carbon isotope composition. *Geophys. Res. Lett.* **8,** 345–8.

Chester, R. 1986. The marine mineral aerosol. In *The role of air–sea exchange in geochemical cycling*, P. Buat-Menard (ed.), 443–76. Dordrecht: Reidel.

Chester, R., H. Elderfield & J.J. Griffin 1971. Dust transported in the northeast and southeast trade winds of the Atlantic Ocean. *Nature* **233,** 93–134.

Chester, R., A.G. Griffiths & J.M. Hirst 1979. The influence of soil-sized atmospheric particulates on the elemental chemistry of the deep-sea sediments of the northeastern Atlantic. *Mar. Geol.* **32,** 141–54.

Chester, R., F.J. Lin & K.J.T. Murphy 1988. A scheme for the determination of elemental speciation in filter-collected aerosols. In preparation.

Chester, R., K.J.T. Murphy, J. Towner & A. Thomas 1986. The partitioning of elements in crust-dominated aerosols. *Chem. Geol.* **54,** 1–15.

REFERENCES

Chester, R., E.J. Sharples & K.J.T. Murphy 1984a. The distribution of particulate Mo in the Atlantic aerosol. *Oceanol. Acta* **7,** 441–50.

Chester, R., E.J. Sharples & G.S. Sanders 1985. The concentration of particulate aluminium and clay minerals in aerosols from the northern Arabian Sea. *J. Sed. Petrol.* **55,** 37–41.

Chester, R., E.J. Sharples, G.S. Sanders & A.C. Saydam 1984b. Saharan dust incursion over the Tyrrhenian Sea. *Atmos. Environ.* **18,** 929–35.

Defant, A. & F. Defant 1958. *Physikalische Dynamik der Atmosphere.* Frankfurt: Akademie Verlagsgesellschaft.

Delany, *et al.* 1967. Airborne dust collected at Barbados. *Geochim. Cosmochim. Acta* **31,** 885–909.

Duce, R.A. 1978. Speculations on the budget of particulate and vapor phase non-methane organic carbon in the global troposphere. *Pure Appl. Geophys.* **116,** 244–73.

Duce, R.A. & E.K. Duursma 1977. Inputs of organic matter to the ocean. *Mar. Chem.* **5,** 319–39.

Duce, R.A. & G.L. Hoffman 1976. Atmospheric vanadium transport to the ocean. *Atmos. Environ.* **10,** 989–96.

Duce, R.A., R. Arimoto, B.J. Ray, C.K. Unni & P.J. Harder 1983a. Atmospheric trace metals at Enewetak Atoll: I. Concentrations, sources and temporal variability. *J. Geophys. Res.* **88,** 5321–42.

Duce, R.A., G.L. Hoffman & W. Zoller 1975. Atmospheric trace metals at remote Northern and Southern hemisphere sites: pollution or natural? *Science* **187,** 59–61.

Duce, R.A., G.L. Hoffman, B.J. Ray, J.S. Fletcher, G.T. Wallace, J.L. Fasching, S.R. Piotrowicz, P.R. Walsh, E.J. Hoffman, J.M. Miller & J.L. Heffter 1976. Trace metals in the marine atmosphere: sources and fluxes. In *Marine pollutant transfer*, H.L. Windom & R.A. Duce (eds), 77–120. Lexington, Mass: Lexington Books.

Duce, R.A., V.A. Mohnen, P.R. Zimmerman, D. Grosjean, W. Cautreels, R. Chatfield, R. Jaenicke, J.A. Ogren, E.D. Pellizzari & G.T. Wallace 1983b. Organic material in the global troposphere. *Rev. Geophys. Space Phys.* **21,** 921–52.

Dulac, F., P. Buat-Menard, M. Arnold, U. Ezat & D. Martin 1987. Atmospheric input of trace metals to the Western Mediterranean Sea. I. Factors controlling the variability of atmospheric concentrations. *J. Geophys. Res.* **92,** 8437–53.

Eisenreich, S.J., A.W. Elzerman & D.E. Armstrong 1978. Enrichment of micronutrients, heavy metals and chlorinated hydrocarbons in wind-generated lake foam. *Environ. Sci. Technol.* **12,** 413–22.

Erickson, D.J. & R.A. Duce 1988. On the global flux of atmospheric sea salt. *J. Geophys. Res.* **93,** 14079–88.

Erickson, D., J.I. Merrill & R.A. Duce 1986. Seasonal estimates of global atmospheric sea-salt distributions. *J. Geophys. Res.* **91,** 1067–72.

Eriksson, E. 1959. The yearly circulation of chloride and sulphate in nature. Meteorological, geochemical, pedological implications. Part I. *Tellus* **11,** 317–403.

Fasching, J.L., R.A. Courant, R.A. Duce & S.R. Piotrowicz 1974. A new surface microlayer sampler utilizing the bubble microtome. *J. Rech. Atmos.* **8,** 649–52.

Folger, D.W. 1970. Wind transport of land-derived mineral, biogenic and industrial matter over the North Atlantic. *Deep-Sea Res.* **17,** 337–52.

Gagosian, R.B. 1986. The air–sea exchange of particulate organic matter: the sources and long-range transport of lipids in aerosols. In *The role of air–sea exchange in geochemical cycling*, P. Buat-Menard (ed.), 409–42. Dordrecht: Reidel.

Garrett, W.D. 1967. The organic chemical composition of the ocean surface. *Deep-Sea Res.* **14,** 221–7.

Goldberg, E.D. 1975. Marine pollution. In *Chemical oceanography*, J.P. Riley & G. Skirrow (eds), Vol. 3, 39–89. London: Academic Press.

Goldberg, E.D. & J.J. Griffin 1970 The sediments of the northern Indian Ocean. *Deep-Sea Res.* **17,** 513–37.

Hardy, J.T., C.W. Apts, E.A. Crecelius & N.S. Bloom 1985a. Sea-surface microlayer metals enrichments in an urban and rural bay. *Estuar. Coastal Shelf Sci.* **20,** 299–312.

Hardy, J.T., C.W. Apts, E.A. Crecelius & G.W. Fellingham 1985b. The sea-surface microlayer: fate and residence times of atmospheric metals. *Limnol. Oceanogr.* **30,** 93–101.

Hasse, L. 1983. Introductory meteorology and fluid mechanics. In *Air–sea exchange of gases and particles*, P.S. Liss & W.G.N. Slin (eds), 1–51. Dordrecht: Reidel.

Hoffman, E.J. & R.A. Duce 1977. Organic carbon in marine atmospheric particulate matter: concentrations and particle size distributions. *Geophys. Res. Lett.* **4,** 449–52.

Hunter, K.A. & P.S. Liss 1981. Organic sea surface films. In *Marine organic chemistry*, E.K. Duursma & R. Dawson (eds), 259–98. Amsterdam: Elsevier.

Iribarne, J.V. & H.-R. Cho 1980. *Atmospheric physics.* Dordrecht: Reidel.

Junge, C.E. 1972. Our knowledge of the physico-chemistry of aerosols in the undisturbed marine environment. *J. Geophys. Res.* **77,** 5183–200.

Junge, C. 1979. The importance of mineral dust as an atmospheric constituent. In *Saharan dust*, C. Morales (ed.), 243–66. New York: Wiley.

Koga, M. 1981. Direct production of droplets from breaking wind waves – its observation by a multicolored overlapping exposure photography technique. *Tellus* **33,** 552–63.

Lai, R.J. & O.H. Shemdin 1974. Laboratory study of the generation of spray over water. *J. Geophys. Res.* **79,** 3055–63.

Lantzy, R.J. & F.T. Mackenzie 1979. Atmospheric trace metals: global cycles and assessment of man's impact. *Geochim. Cosmochim. Acta* **43,** 511–25.

Lion, L.W. & J.O. Leckie 1981a. The biogeochemistry of the air–sea interface. *Annu. Rev. Earth Planet. Sci.* **9,** 449–86.

Lion, L.W. & J.O. Leckie 1981b. Chemical speciation of trace metals at the air–sea interface: the application of an equilibrium model. *Environ. Geol.* **3,** 293–314.

Liss, P.S. 1975. Chemistry of the sea surface microlayer. In *Chemical oceanography*, J.P. Riley & G. Skirrow (eds), Vol. 3, 193–243. London: Academic Press.

Lum, K.R., J.S. Betteridge & R.R. Macdonald 1982. The potential availability of P, Al, Cd, Co, Cr, Fe, Mn, Ni, Pb and Zn in urban particulate matter. *Environ. Technol. Lett.* **3,** 57–62.

McDonald, R.L., C.K. Unni & R.A. Duce 1982. Estimation of atmospheric sea salt dry deposition: wind speed and particle size dependence. *J. Geophys. Res.* **87,** 1246–50.

MacIntyre, F. 1974. Chemical fractionation and sea-surface microlayer processes. In *The sea*, E.D. Goldberg (ed.), Vol. 5, 245–99. New York: Interscience.

Mosher, B.W., R.A. Duce, J.M. Prospero & D.L. Savoie 1987. Atmospheric selenium: geographical distribution and ocean to atmosphere flux in the Pacific. *J. Geophys. Res.* **92,** 13277–87.

Murphy, K.J.T. 1985. The trace metal chemistry of the Atlantic aerosol. *Ph.D. Thesis*, University of Liverpool.

REFERENCES

Nguyen, B.C. & B. Bonsang 1979. The ocean as a source and sink for natural and anthropogenic sulfur compounds. *XVIIth Assembl. Gen. Union Geodes. Int.*, Canberra, Australia, 1–15 December 1979.

Nguyen, B.C., B. Bonsang & A. Gaudry 1983. The role of the ocean in the global atmospheric sulfur cycle. *J. Geophys. Res.* **88,** 10903–14.

Nriagu, J.O. 1979. Global inventory of natural and anthropogenic emissions of trace metals to the atmosphere. *Nature* **279,** 409–11.

Pattenden, N.J., R.S. Cambray & K. Playford 1981. Trace and major elements in the sea-surface microlayer. *Geochim. Cosmochim. Acta* **45,** 93–100.

Patterson, C.C. & D.M. Settle 1987. Magnitude of lead flux to the atmosphere from volcanoes. *Geochim. Cosmochim. Acta* **51,** 657–81.

Peirson, D.H. & R.S. Cambray 1970. Transfer of nuclear debris from southern to northern troposphere during 1968. *J. Geophys. Res.* **75,** 1760–5.

Piotrowicz, S.R., R.A. Duce, J.L. Fasching & C.P. Weissel 1979. Bursting bubbles and their effect on the sea-to-air transport of Fe, Cu, and Zn. *Mar. Chem.* **7,** 307–24.

Pojasek, R.B. & O.T. Zajicek 1978. Surface microlayers and foams – source and metal transport in aquatic systems. *Water Res.* **12,** 7–11.

Prospero, J.M. 1968. Atmospheric dust studies on Barbados. *Am. Meteorol. Soc. Bull.* **49,** 645–52.

Prospero, J.M. 1979. Mineral and sea salt aerosol concentrations in various oceanic regions. *J. Geophys. Res.* **84,** 725–31.

Prospero, J.M. 1981. Eolian transport to the World Ocean. In *The sea*, C. Emiliani (ed.), Vol. 7, 801–74. New York: Interscience.

Prospero, J.M., R.W. Charlson, V. Mohnen, R. Jeanicke, A.C. Delany, J. Moyers, W. Zoller & K. Rahn 1983. The atmospheric aerosol system: an overview. *Rev. Geophys. Space Phys.* **21,** 1607–29.

Prospero, J.M., M. Uematsu & D.L. Savoie 1989. Mineral aerosol transport to the Pacific Ocean. In *Chemical oceanography*, J.P. Riley & R. Chester (eds), Vol. 10, In press. London: Academic Press.

Rahn, K.A. 1976. *The chemical composition of the atmospheric aerosol.* Tech. Rep., Grad. School Oceanogr., Univ. Rhode Is., Kingston, RI.

Rahn, K.A., R.D. Borys, G.E. Shaw, L. Schutz & R. Jaenicke 1979. Long-range impact of desert aerosol on atmospheric chemistry: two examples. In *Saharan dust*, C. Morales (ed.), 243–66. New York: Wiley.

Robinson, E. 1978. Hydrocarbons in the atmosphere. *Pure Appl. Geophys.* **116,** 327–84.

Robinson, E. & R.D. Robbins 1971. *Emissions, concentrations, and fate of particulate atmospheric pollutants.* Publ. 4067, Am. Petrol. Inst., Washington, DC.

Salomons, W. & U. Forstner 1984. *Metals in the hydrosphere.* Berlin: Springer-Verlag.

Sanders, G.S. 1983. Metals in marine atmospheric particles. *Ph.D. Thesis*, University of Liverpool.

Savoie, D.L. & J.M. Prospero 1977. Aerosol concentration statistics for the northern tropical Atlantic. *J. Geophys. Res.* **82,** 5954–64.

Savoie, D.L., J.M. Prospero & R.T. Nees 1987. Nitrate, non-sea-salt sulphate, and mineral aerosol over the northwestern Indian Ocean. *J. Geophys. Res.* **92,** 933–42.

Saydam, A.C. 1981. The elemental chemistry of Eastern Mediterranean atmospheric particulates. *Ph.D. Thesis*, University of Liverpool.

Schneider, B. 1987. Source characterization for atmospheric trace metals over Kiel Bight. *Atmos. Environ.* **21,** 1275–83.

Schultz, L., R. Jaenicke & H. Pietrek 1980. *Saharan dust transport over the North Atlantic*

Ocean. Geol. Soc. Am. Spec. Paper, no. 186, 87–100.

Seiburth, J. McN. 1983. Microbiological and organic-chemical processes in the surface and mixed layers. In *Air–sea exchange of gases and particles*, P.S. Liss & W.G.N. Slin (eds), 121–72. Dordrecht: Reidel.

Settle, D.M. & C.C. Patterson 1982. Magnitudes and sources of precipitation and dry deposition fluxes of industrial and natural leads to the North Pacific at Enewetak. *J. Geophys. Res.* **87,** 8857–69.

Szekielda, K.M., S.L. Kupferman, V. Klemas & D.F. Polis 1972. Element enrichment in organic films and foams associated with aquatic frontal systems. *J. Geophys. Res.* **77,** 5278–82.

Turekian, K.K. & W.C. Graustein 1989. Lead-210 in the SEAREX program: an aerosol tracer across the Pacific. In *Chemical oceanography*, J.P. Riley & R. Chester (eds), Vol. 10. London: Academic Press.

Uematsu, M., R.A. Duce, J.M. Prospero, L. Chen, J.I. Merrill & R.L. McDonald 1983. Transport of mineral aerosol from Asia over the North Pacific Ocean. *J. Geophys. Res.* **88,** 5343–52.

Uematsu, M., R.A. Duce, T. Patterson & J.M. Prospero 1985. Spatial distribution of mineral aerosol over the southwest Pacific Ocean. *SEAREX News* **8,** 34–8.

Varhelyi, G. & G. Gravenhorst 1983. Production rate of airborne sea-salt sulfur deduced from chemical analysis of marine aerosols and precipitation. *J. Geophys. Res.* **88,** 6737–51.

Walsh, P.R., R.A. Duce & J. Fasching 1979a. Tropospheric arsenic over marine and continental regions. *J. Geophys. Res.* **84,** 1710–18.

Walsh, P.R., R.A. Duce & J.L. Fasching 1979b. Considerations of the enrichment, sources and fluxes of arsenic in the troposphere. *J. Geophys. Res.* **84,** 1719–26.

Weisel, C.P., R.A. Duce, J.L. Fasching & R.W. Heaton 1984. Estimates of the transport of trace metals from the ocean to the atmosphere. *J. Geophys. Res.* **89,** 11607–18.

Whitby, K.T. 1977. The physical characteristics of sulphur aerosols. *Atmos. Environ.* **12,** 135–59.

Williams, P.J. 1975. Biological and chemical aspects of dissolved organic material in sea water. In *Chemical oceanography*, J.P. Riley & G. Skirrow (eds), Vol. 2, 301–63. London: Academic Press.

Zimmerman, P.R., R.B. Chatfield, J. Fishman, P.J. Crutzen & P.L. Hanst 1978. Estimates on the production of CO and H_2 from the oxidation of hydrocarbon emissions from vegetation. *Geophys. Res. Lett.* **5,** 679–82.

5 The transport of material to the oceans: the hydrothermal pathway

The upper part of the igneous oceanic basement (Layer 2 of the oceanic crust), which overlies the sediment column (Layer 1 of the oceanic crust), is composed predominantly of basaltic lavas and their intrusive equivalents. These basalts are by far the commonest rock type found on the sea bed, and the chemical compositions of a number of marine basalts are given in Table 5.1. These basaltic lavas can interact with sea water over a wide range of temperatures and timespans. In very general terms, the reactions can be classifed into three types: (a) those involving hydrothermal activity, either at high temperature at depth in the crust at the centres of sea-floor spreading or at intermediate temperatures on the ridge flanks; (b) those associated with the low-temperature weathering of basalt that has been exposed to sea water for relatively long periods of time, either at the sea floor or within the upper part of the basement; and (c) those involving the extrusion of hot lava directly onto the sea bed.

5.1 Hydrothermal activity: high-temperature sea water–basalt reactions

The most dramatic manifestation of sea water–rock interaction has only been identified over the last two decades or so. This was the discovery that sea water convecting through newly generated oceanic crust at ridge-divergent plate boundaries during sea-floor spreading can play an important role in controlling the chemical mass balance of the oceans. Various lines of geological and geophysical evidence have now established that sea-floor spreading is the dominant process in the formation of the ocean basins. In this process, new oceanic crust (or lithosphere) is formed from molten rock (magma) at the spreading centres on the mid-ocean ridge system – see Figure 5.1a. The pre-existing, i.e. older, basalt sequences are porous, and fault and large transform fractures are found at both fast- and slow-spreading ridges. In these regions cold sea water penetrates this higly permeable pre-existing crust around the centres, sometimes to a depth of several kilometres, where it undergoes heat-driven circulation and comes into contact with the zones of active magma

Table 5.1 Elemental composition of oceanic basalts[a]

(a) Major element composition (wt% oxides)

	Oceanic island basalts		Mid-Atlantic Ridge basalts	
	Average tholeiitic basalt	Average alkalic basalt	Tholeiitic basalt	High alumina basalt
SiO_2	49.36	46.46	50.47	48.13
TiO_2	2.50	3.01	1.04	0.72
Al_2O_3	13.94	14.64	15.93	17.07
Fe_2O_3	3.03	3.37	0.95	1.17
FeO	8.53	9.11	7.88	8.65
MnO	0.16	0.14	0.13	0.13
MgO	8.44	8.19	8.75	10.29
CaO	10.30	10.33	11.38	11.26
Na_2O	2.13	2.92	2.60	2.39
K_2O	0.38	0.84	0.10	0.09
H_2O (total)	-	-	0.59	0.29
P_2O_3	0.26	0.37	0.11	0.10

(b) Minor element composition ($\mu g\ g^{-1}$)

	Oceanic alkali basalts	Oceanic tholeiitic basalts	Basalts; Mid-Atlantic Ridge	Basalts; Mid-Indian Ocean Ridge	Basalt; Tonga Island Arc
Fe	82600	76800	63616	68282	54008
Mn	1084	1239	-	-	-
Cu	36	77	87	90	51
Ni	51	97	123	242	25
Co	25	32	41	73	30
Ga	22	17	18	20	13
Cr	67	297	292	347	75
V	252	292	289	340	230
Ba	498	14	12	-	14
Sr	815	130	123	131	115

[a] From original data sources listed by Riley & Chester (1971), and Chester & Aston (1976). The central ocean areas are dominated by tholeiitic pillow basalts of layer 2A, which are generated at the spreading ridges and which are moved away during sea-floor spreading so that their ages increase with increasing distance from the ridge crests.

intrusion. During this process the sea water undergoes drastic changes in composition to form high-temperature hydrothermal solutions, which emerge through the sea-floor venting system as hot springs that mix with the overlying sea water.

Elderfield (1976) made a distinction between geothermal and hydrothermal solutions. During the formation of **geothermal solutions** thermal transfer takes place between the circulating water and the heat source, but there is no chemical transfer between the two. These geothermal solutions can then extract, i.e. leach, chemical components from the rocks or sediments with which they come into contact as they circulate, with the result that they become mineralized in character. In contrast, **hydrothermal solutions** are involved in both thermal and chemical transfer from the heat source. During the chemical transfer the degassing of the

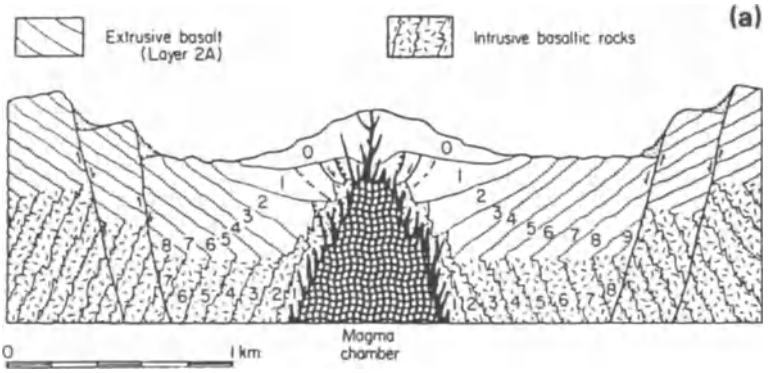

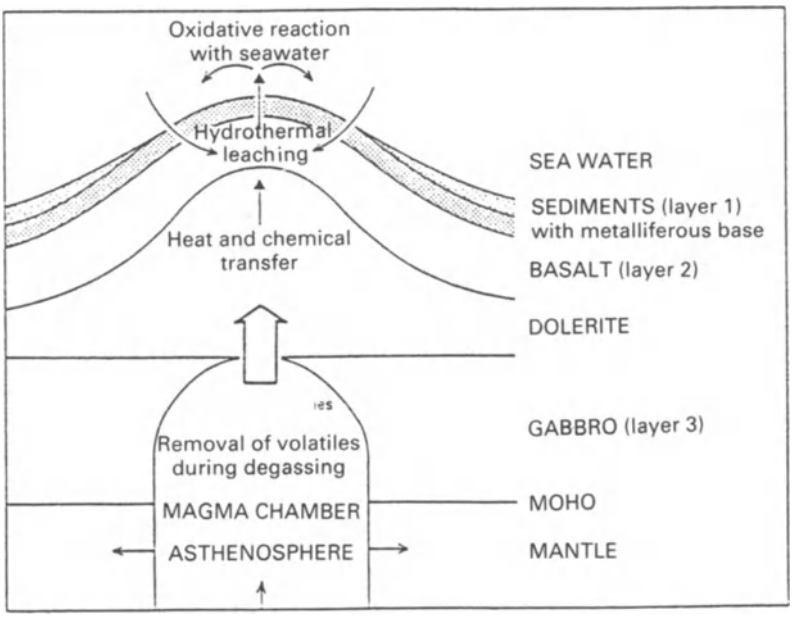

Figure 5.1 High-temperature hydrothermal activity at the spreading centres. (**a**) Preliminary structural model of the inner rift valley in the Famous area (Mid-Atlantic Ridge) showing the location of the magma chamber in relation to the generation of basalts (from Jones 1978; after Moore *et al.* 1974). Relative ages of the basalts are indicated by the numbers 0–9, with 0 being the youngest. (**b**) The generation of hydrothermal solutions: the East Pacific Rise model (from Elderfield 1976). Sea water penetrates the porous rock at the spreading ridge centre and circulates through the underlying crust. During this process the sea water undergoes both thermal and chemical transfer from the magma heat source, and also leaches elements from the rocks and sediments with which it comes into contact before re-entering the seawater reservoir via a series of venting systems as mineralized solutions.

mantle can release volatiles such as Hg, As, Ce and B, and gases such as non-radiogenic ^{3}H. In addition to this chemical transfer from the heat source, hydrothermal solutions can also become mineralized by leaching metals from rocks and sediments as they circulate. This type of hydrothermal solution is generated at the East Pacific Rise (EPR), and the general features of the EPR hydrothermal model are illustrated in Figure 5.1b.

It is now known that large-scale hydrothermal activity is a ubiquitous concomitant to the production of new oceanic crust at the centres of the mid-ocean ridges (Edmond *et al.*, 1982), as was first predicted by Elder (1965). The process has far-reaching implications for Earth science, and such is its global extent that it has been estimated that the entire ocean circulates through the high-temperature ridge axial zone, and so undergoes reaction with fresh basalt, to emerge via the hydrothermal venting system every 8–10 Ma. The dramatic effect that the venting of these high temperature hydrothermal solutions can have on the chemistry of sea water is illustrated in Figure 5.2, which shows the increase in dissolved Mn around a vent system at the TAG site on the Mid-Atlantic Ridge. Because of the importance of basalt–sea water interactions

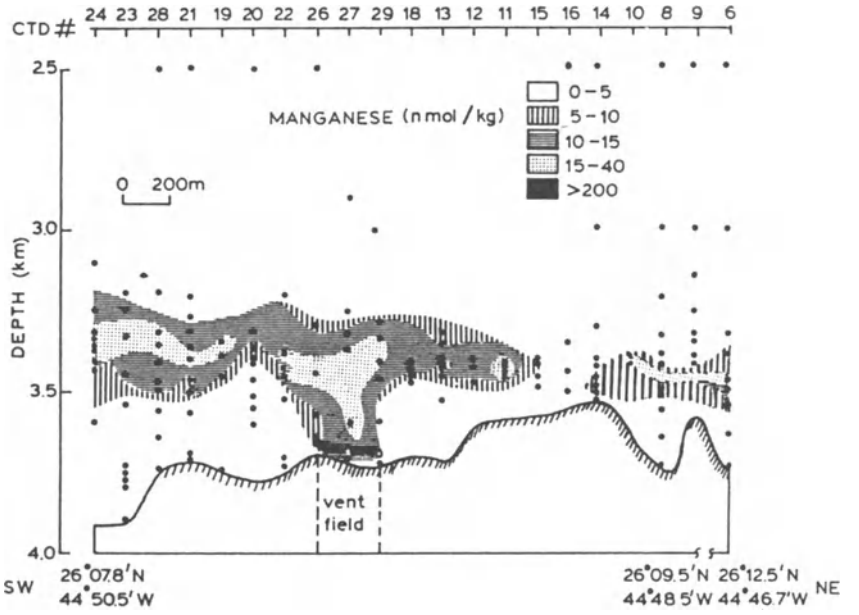

Figure 5.2 SW-NE transect for total reactive Mn at the TAG hydrothermal system on the Mid-Atlantic Ridge (from Klinkhammer *et al.* 1986). Total reactive Mn is the Mn extracted from unacidified seawater samples by oxine after adjustment of the pH to 9, and represents mainly the dissolved fraction of the element.

associated with venting systems such as this, oceanic rock is now recognized as a major reservoir in global geochemistry.

Recent confirmation of the existence of the hydrothermal solutions has been provided by photographic and visual (submersible dives) sightings of the venting of hot springs onto the sea floor at various spreading centres. These sightings have also shown the presence of specialized biological communities around the hot springs. These include dense beds of clams, mussels and giant vestimentiferan tubeworms, for which the primary food source is chemosynthetic bacteria; this is an example of chemical, as opposed to photosynthetic, production. For a detailed description of the biology of hydrothermal vent systems, the reader is referred to the volume edited by Childers (1988).

Following the formation of new crust, factors such as the deposition of sediments limit the access of sea water and so hinder the circulation in the basalt layer. Wolery & Sleep (1976) have estimated that on fast-spreading ridges hydrothermal activity stops after 6–14 Ma and that on slow-spreading ridges it ceases after 11–19 Ma. Thompson (1983) defines these periods as the **active** phases of hydrothermal activity, during which new crust is continually exposed to circulating sea water and convection is vigorous and rapid. A **passive** phase continues on the flanks of the ridges, in the absence of the formation of new crust, and there is evidence that considerable convective circulation of sea water through Layer 2 continues for periods up to 50–70 Ma.

Hydrothermal activity at the spreading centres, during which the circulating sea water comes into contact with newly generated oceanic crust, leads to the production of high-temperature ($\approx$ 350°C), acidic, reducing solutions, which are eventually mixed with ambient sea water that has a much lower initial temperature ($\sim$ 2°C). During the sea water–rock reaction the composition of the original sea water is considerably modified with respect to both major and minor constituents, gases (e.g. ^{3}He and other rare gases, methane, hydrogen, carbon monoxide, carbon dioxide) and the isotopic ratios of various elements (e.g. O, Sr, Nd). The location of the zone in which the high-temperature hydrothermal solutions, rich in H_2S, mix with O_2-rich ambient sea water is critical in determining the composition of the hot-spring water that vents at the sea surface. To date, two general types of hydrothermal 'plumbing' systems have been identified with respect to the temperature at which fluids are debouched onto the sea floor.

LOW-TEMPERATURE SYSTEMS Hot springs found at the Galapagos Ridge, East Pacific (spreading rate $\sim$ 3.5 cm yr^{-1}), are an example of a low-temperature hydrothermal system. Thompson (1983) described four active vents in the region, which were named Clambake, Dandelions, Garden of Eden and Oyster Beds after the benthic communities

associated with them. Water flows on to the sea bed from these vents at a rate of 2–10 l s^{-1}, and has temperatures in the range 6–17°C. The chemistry of the Galapagos hydrothermal solutions has been described by Edmond *et al.* (1979). The authors found that there was a negative magnesium–temperature relationship in the vented fluids, and since experimental laboratory data had shown that magnesium is completely removed from solution during basalt–sea water reactions (Bischoff & Dickson 1975), they extrapolated the Mg–temperature relationship to zero concentration, which gave an intercept at ~ 350°C. Thus, by assuming that Galapagos vent solutions were a simple mixture of two end-members, i.e. a hot hydrothermal solution and cold sea water, they were able to demonstrate that the original hydrothermal fluid had a temperature of ~ 350°C and that it had mixed with sea water at depth within the venting system. During the mixing of hydrothermal solutions and sea water some elements form insoluble phases (e.g. sulphides, oxides), i.e. they behave non-conservatively, whereas others are unaffected by the mixing process, i.e. they are conservative. Edmond *et al.* (1979) then extrapolated the concentration–temperature gradients for a number of conservative elements and so were able to estimate the composition of the 350°C hydrothermal end-member; the results are given in Table 5.2. These data were the first of their kind and led to the very important conclusion that, for some elements, fluxes into and out of the crestal ridge zone are comparable with, or greater than, those for river transport. It was also shown that the non-conservative elements (e.g. Cu, Ni, Cd, Se, V and Cr) were removed by the formation of insoluble phases at intermediate temperatures during the mixing process, and the authors concluded that the elements were extracted not only from the hydrothermal solutions but also from the sea water end-member. For these elements, therefore, it was not possible to obtain concentration data for the 350°C end-member.

In the Galapagos system, therefore, reactions between sea water and hydrothermal solutions take place at depth within the venting system, leading to the precipitation of sulphide-forming metals below the sea surface. That is, only the last phases of hydrothermal fractionation occur on the sea bed in the Galapagos Rift Valley.

HIGH-TEMPERATURE SYSTEMS A variety of hydrothermal vents are located on the East Pacific Rise (EPR; spreading rate 6 cm yr^{-1}) at 21°N. These include (a) inactive vents, (b) warm springs of the Galapagos type, which discharge clear milky white plumes and are sometimes referred to as **white smokers**, and (c) hot springs. The hot springs emit black plumes through tall (up to 10 m high) chimneys composed predominantly of the sulphides of Fe, Zn and Cu. These high-temperature systems are termed **black smokers**, the colour arising from the precipitation of fine-grained

Table 5.2 Chemical composition of the high-temperature (350°C) hydrothermal end-member solution[a]

Component		Galapagos vents	21°N EPR vents	Sea water
Li	(μmol kg^{-1})	1142-689	820	28
K	(mmol kg^{-1})	18.8	25.0	10.1
Rb	(mmol kg^{-1})	20.3-13.4	26.0	1.32
Mg	(mmol kg^{-1})	0	0	52.7
Ca	(mmol kg^{-1})	40.2-24.6	21.5	10.3
Sr	(μmol kg^{-1})	87	90	87
Ba	(μmol kg^{-1})	42.6-17.2	95-35	0.145
Mn	(μmol kg^{-1})	140-360	610	0.002
Fe	(μmol kg^{-1})	+	1800	-
Si	(μmol kg^{-1})	21.9	21.5	0.160
SO_4^{2-}	(mmol kg^{-1})	0	0	28.6
H_2S	(mmol kg^{-1})	+	6.5	0

[a] Data from Edmond et al. (1982). Data for the Galapagos vents is extrapolated to the 350°C end-member, the ranges resulting from different composition versus heat trends. Data for the EPR vents are based on direct observation of the high-temperature end-members.

\+ Non-conservative in subsurface mixing.

\- Seawater concentration not accurately known.

sulphides as sea water is entrained in the plumes emitted from the chimneys, a process that took place at depth within the Galapagos white smoker venting system. The black smokers debouch high-temperature (~ 350°C), acidic, reducing, sulphide- and metal-rich hydrothermal solutions directly onto the sea floor where they are rapidly mixed with ambient sea water.

The presence of high-temperature black smokers on the EPR allowed the pristine hydrothermal end-member to be sampled directly. The data obtained for this hydrothermal end-member have been reported by Edmond *et al.* (1982) and Von Damm *et al.* (1983). The data obtained for the EPR high-temperature fluids, which are summarized in Table 5.2, essentially confirm the validity of the extrapolated Galapagos hydrothermal end-member composition, and thus establish a general chemical uniformity in the solutions produced during the reactions of sea water with newly formed basaltic crust at high temperature at the centres of sea-floor spreading. It can be seen from the data in Table 5.2 that the high-temperature hydrothermal end-member has very special characteristics; thus, relative to sea water it is completely depleted in Mg and SO_4^{2-}, and is enriched in H_2S, Mn, Rb, Ca, Ba, K and Si. The Mg is removed by

precipitation as sepiolite, which is formed in the altered basalt. During this process H^+ ions are generated, which make the solutions more acidic, so releasing elements from the basalts and keeping certain elements (e.g. Fe, Mn, Zn and Cu) in solution. Hydrothermal activity is also a sink for sulphate, e.g. by the precipitation of calcium sulphate, which is subsequently reduced by ferric iron in the basalts to give rise to a sulphide-dominated system (see e.g. Martin & Whitfield 1983); for a detailed discussion of the fate of sulphate during hydrothermal mixing see McDuff & Edmond (1982).

A more detailed investigation of the hot springs in the 12°N EPR hydrothermal system was carried out by Von Damm *et al.* (1985a). Four hydrothermal fields were sampled, all of which vented high-temperature fluids, with the maximum temperatures being ~ 350°C. The four hydrothermal smoker fields were designated National Geographic Smoker (NGS; venting solution exit temperature 273°C), Ocean Bottom Seismometer (OBS; venting solution exit temperature 350°C), South West (SW; venting solution exit temperature 355°C) and Hanging Garden (HG; venting solution exit temperature 351°C). The major ion data for the end-member venting solutions was consistent with the estimates made on the hot springs from the Galapagos Spreading Centre low-temperature venting system (see Table 5.3), and may be summarized as follows. (a) Li (up to ~ 50), K (~ 2.5), Rb (~ 25), Be ($\gtrsim 10^3$), Ca (up to ~ 2) and Ba (up to $> 10^2$) were enriched in the hydrothermal fluids; the figures in parentheses refer to the approximate enrichment over ambient seawater concentrations. (b) Sr and Na exhibit both enrichments and depletions in the hydrothermal fluids relative to sea water. (c) Mg is depleted in the venting fluids relative to sea water, and is assumed to reach zero concentration in the hydrothermal end-member. There are difficulties in the estimation of the hydrothermal end-member concentrations of many trace metals because of their precipitation as sulphides, which can be formed at depth in the system, in the chimney structures and in the hydrothermal plume itself; however, Mn, which rarely forms a sulphide, is an exception to this. The calculated high-temperature hydrothermal end-member concentrations of Mn, Fe, Co, Cu, Zn, Ag, Cd and Pb are given in Table 5.3. All these elements are enriched in the venting solutions relative to ambient sea water. However, one of the most striking features of the 21°N EPR data is that there are considerable variations in the end-member concentrations of the trace metals at the various venting sites. Von Damm *et al.* (1985a) identified a number of factors that might contribute to variations of this type.

(a) Differences in rock type; e.g. glasses react with sea water more rapidly than more crystalline forms.

Table 5.3 Chemical compositions of the individual high-temperature (~ 350°C) hydrothermal end-member venting solutions at 21°N on the EPR[a]

Component	Hydrothermal smoker field[b]				Sea Water
	NGS	OBS	SW	HG	
Li (μmol kg^{-1})	1033	891	899	1322	26
Na (m kg^{-1})	510	432	439	433	464
K (m kg^{-1})	25.8	23.2	23.2	23.9	9.79
Rb (μmol kg^{-1})	31	28	27	33	1.3
Be (nmol kg^{-1})	37	15	10	13	0.02
Mg (m kg^{-1})	0	0	0	0	52.7
Ca (m kg^{-1})	20.8	15.6	16.6	11.7	10.2
Sr (μmol kg^{-1})	97	81	83	65	87
Ba (μmol kg^{-1})	>15	>7	>9	>10	0.14
Al (μmol kg^{-1})	4	5.2	4.7	4.5	0.005
Mn (μmol kg^{-1})	1002	960	699	878	<0.001
Fe (μmol kg^{-1})	871	1664	750	2429	<0.001
Co (nmol kg^{-1})	22	213	66	227	0.03
Cu (μmol kg^{-1})	<0.02	35	9.7	44	0.007
Zn (μmol kg^{-1})	40	106	89	106	0.01
Ag (nmol kg^{-1})	<1	38	26	37	0.02
Cd (nmol kg^{-1})	17	155	144	180	1
Pb (nmol kg^{-1})	183	308	194	359	0.01
pH	3.8	3.4	3.6	3.3	7.8
Alk (meq)	-0.19	-0.40	-0.30	-0.50	2.3
NH_4 (m kg^{-1})	<0.01	<0.01	<0.01	<0.01	<0.01

[a] Data from Von Damm et al. (1985a).

[b] See text for details of smoker fields.

(b) Differences in temperature of the hydrothermal solutions at depth in the system.
(c) Differences in the residence times, or flow rates, of the water in the fissure system; an increased residence time implying an increase in the time over which the water can react with the rock.
(d) Differences in the depth at which the sea water–basalt reaction takes place, which affect the path length of the hydrothermal cell.
(e) Differences in the age of the hydrothermal systems; i.e. in older systems the water is flowing through rocks that have already undergone considerable leaching.

It was not possible to resolve the relative importance of these factors in the EPR system, but they serve to illustrate how the trace element composition of venting fluids can be influenced by local conditions. Further, the venting solutions can become enriched in some elements by entrainment into the hydrothermal plume if the elements have themselves

been enriched in the surrounding bottom waters by other processes.

From studies of low- and high-temperature venting fluids it has become apparent that the mass flux from hydrothermal systems occurs at high temperature. Originally, it was thought that high-temperature venting systems were more common on ridges formed at fast ($\sim$ 9–18 cm yr^{-1}) to intermediate ($\sim$ 5–9 cm yr^{-1}) spreading rates, but were fairly rare on those formed at slow ($\sim$ 1–5 cm yr^{-1}) rates; an exception being those found at the Reykjanes Ridge and other 'hotspot'-influenced ridges. Recently, however, Rona *et al.* (1986) have reported finding the first black smokers on a slow-repeating ridge in the TAG hydrothermal field on the Mid-Atlantic Ridge (MAR). Deposits of massive sulphides were found in association with the venting system in this region.

The hydrothermal systems described above are associated with spreading ridge crests where the sedimentation rates are low and where the venting fluids debouch into sea water, via chimneys, directly from the fissure systems. Under some conditions, however, the spreading axis can be buried under a blanket of sediment. One example of this is found in the Red Sea where the axis is covered by marine evaporites. Another example of this kind of hydrothermal system, which has been described by Von Damm *et al.* (1985b), is located in the Guaymas Basin in the Gulf of California. North of the vent fields at 21°N, the EPR extends into the Gulf of California, and the spreading regime changes from a mature, open-ocean, sediment-starved type to an early opening, continental rifting type. An increase in sedimentation rate is associated with this change, and as a result the Guaymas Basin spreading axis is covered with a thick blanket of biogenous sediment that is rich in organic carbon derived from the highly productive overlying waters. The high-temperature (up to 315°C) Guaymas Basin venting solutions have a composition that is strikingly different from those characteristic of the sediment-starved, open-ocean systems, such as that found at 21°N on the EPR (see Table 5.4). In particular, whereas the venting solutions at 21°N on the EPR are rich in the ore-forming elements (Fe, Mn, Cu, Zn, Pb, Co and Cd), have an acidic pH (3.3–3.8) and have low concentrations of ammonium, those from the Guaymas Basin are depleted in the ore-forming elements, have a more alkaline pH (5.9) and contain ammonium as a major ion. Von Damm *et al.* (1985b) concluded that the Guaymas Basin venting solutions were formed as the result of a two-stage reaction process in which the hydrothermal solutions first reacted with the underlying basalt to produce a primary solution similar in composition to those found at the 21°N EPR sites, which then subsequently reacted with the biogenous sediments overlying the intrusion zone. During this second stage the pH of the primary hydrothermal solutions is raised by the dissolution of carbonate and by the thermocatalytic cracking of plankton carbon. As a result, sulphides are precipitated from the ascending solutions at depth in the

Table 5.4 Chemical compositions of the Guaymas Basin and the 21°N EPR high-temperature hydrothermal venting solutions[a]

Component	Guaymas Basin solutions	21°N EPR solutions	Sea water
Li (μmol kg^{-1})	630-1076	891-1322	26
Na (mmol/kg^{-1})	475-513	432-510	463
K (mmol/kg^{-1})	37.1-49.2	23.2-25.8	9.79
Rb (μmol kg^{-1})	57-86	27-33	1.3
Be (nmol kg^{-1})	12-91	10-37	0.02
Mg (mmol/kg^{-1})	0	0	52.7
Ca (mmol/kg^{-1})	26.6-41.5	11.7-20.8	10.2
Sr (μmol kg^{-1})	160-253	67-97	87
Ba (μmol kg^{-1})	>7->24	>7->15	0.14
Al (μmol kg^{-1})	0.9-7.9	4.0-5.2	0.005
Mn (μmol kg^{-1})	128-236	699-1002	<0.001
Fe (μmol kg^{-1})	17-180	750-2429	<0.001
Co (nmol kg^{-1})	<5	22-227	0.03
Cu (μmol kg^{-1})	<0.02-1.1	<0.02-44	0.007
Zn (μmol kg^{-1})	0.1-40	40-106	0.01
Ag (nmol kg^{-1})	<1-230	<1-38	0.02
Cd (nmol kg^{-1})	<10-46	17-180	1
Pb (nmol kg^{-1})	<20-652	183-359	0.01
pH	5.9	3.3-3.8	7.8
Alk	2.8-10.6	-0.19- -0.50	2.3
NH_4 (mmol/kg^{-1})	10.7-15.6	<0.01	<0.01

[a] Data from Von Damm et al. (1985b).

sediment column, and the Guaymas Basin is thus a site of the active formation of a **sediment-hosted** massive sulphide deposit. The authors concluded that sediment-covered hydrothermal systems are probably not quantitatively important for the formation of oxidized metal-rich sediments.

High-temperature reactions can also take place between basalt and sea water when hot lava is extruded directly onto the sea bed. Bonatti (1965) has classified these submarine volcanic eruptions into two general types: (a) a quiet type, in which the reaction between sea water and lava is essentially prevented by the instantaneous formation of a thin crust of glass; (b) a more violent or explosive type, in which the lava is shattered on contact with sea water and the large surface area then available allows considerable hydration of the glass. In the explosive, **hyaloclastic**, eruption there is reaction between the basalt and sea water, with the result that new minerals, such as palagonite, smectites and zeolites are formed, and elements such as Ca, Na, K, Si, B, Mn, Zn and Cu are released into solution.

5.2 Hydrothermal activity: low-temperature sea water–basalt reactions

The upper 2–3 km of Layer 2 of the oceanic basement is a zone of chemical reaction between sea water and the crust as it moves away from the spreading centres. The extent to which an oceanic basalt undergoes low-temperature weathering reactions is a function of its age, i.e. of the time it has spent in contact with sea water, which is related to its distance from the generation centres. The low-temperature sea water–basalt reactions can take place both at the sea floor (as evidenced from dredged basalts) and at depth within Layer 2 of the oceanic crust (as evidenced from drilled basalts). Basalt–sea water reactions on the ocean floor take place in the presence of large volumes of water under oxidizing conditions. At depth within Layer 2, however, the rocks are in contact with much smaller volumes of water. In general, both field and laboratory experimental data indicate that the deeper basalts have undergone alteration, following reaction with sea water, in much the same way as surface basalts, although the reactions involved do not appear to have proceeded to the same extent.

Basalts dredged from the sea floor have invariably undergone some degree of reaction with sea water at the cold ambient bottom temperatures, and are often termed **weathered basalts**. During these low-temperature reactions, which have been reviewed by Honnerez (1981) and Thompson (1983b), new mineral phases are formed and chemical transfer takes place between the rocks and sea water. Volcano glass and bulk rock can be affected in different ways, but a number of general conclusions can be drawn regarding the low-temperature alteration of oceanic basalts (see e.g. Honnerez 1981)

(a) The oxidation and hydration of basalt is a ubiquitous phenomenon.
(b) During basalt–sea water reactions there is often an uptake of K, Cs, Rb, B, Li and ^{18}O by the basalt (i.e. the rock acts as a *sink*, and the elements are usually incorporated into mineral phases formed during the alteration processes), and a loss of Ca, Mg and Si (i.e. the rock acts as a *source*).
(c) Fe, Mn, Na, Cu, Ba and Sr exhibit no clear patterns, although the low-temperature weathering of basalt may provide a source for Fe and Mn to sea water (Elderfield 1976).
(d) Al, Ti, Y, Zr and the heavy rare earths show little or no change following sea water–basalt reactions.
(e) Low-temperature alteration of the oceanic crust is a major sink for U, and according to Bloch (1980) may account for ~ 50% of the total amount of U supplied to the oceans at the present day.

5.3 The hydrothermal pathway: summary

(a) The oceanic crust is a major reservoir in global geochemistry. To bring this reservoir on-line, a number of different types of reactions occur between sea water and the basalts of Layer 2.
(b) These sea water reactions take place at a variety of temperatures and rock : water ratios, and can act as either source or sink terms in the marine budgets of some components.
(c) The most dramatic hydrothermal activity is found at the spreading ridge centres where cold sea water circulates through hot, newly formed, basaltic crust. In this process, the composition of the sea water undergoes extensive changes before emerging at the sea bed in the form of white smoker or black smoker hot springs.

In the present chapter attention has been confined to the effects of hydrothermal activity on sea water, and the magnitude of the fluxes involved are discussed in Section 6.3. However, the effects that hydrothermal processes have on marine geochemistry are much wider than this. In particular, the hydrothermal activity of spreading centres results in the formation of a series of mineral precipitates and in the generation of a unique type of deep-sea sediment. The chemical dynamics involved in the formation of the hydrothermal precipitates are discussed in Section 15.3.2.4 in terms of a sequential precipitation model, and the generation of the hydrothermal sedimentary deposits is covered in Section 16.6.2. In this way, the full spectrum of hydrothermal activity in the oceans will be placed in a global marine context.

References

Bischoff, J.L. & F. Dickson 1975. Seawater–basalt interaction at 200°C and 500 bars: implications for origin of sea floor heavy metal deposits and regulation of seawater chemistry. *Earth Planet. Sci. Lett.* **25,** 385–97.

Bloch, S. 1980. Some factors controlling the concentration of uranium in the World Ocean. *Geochim. Cosmochim. Acta* **44,** 373–7.

Bonatti, E. 1965. Palagonite, hyaloclastites and alteration of volcanic glass in the ocean. *Bull. Volcanol.* **28,** 257–69.

Childers, J.J. 1988. Hydrothermal vents. A case study of the biology and chemistry of a deep-sea hydrothermal vent of the Galapagos Rift. J.J. Childers (ed.), *Deep-Sea Res.* **35,** 1677–1849.

Chester, R. & S.R. Aston 1976. The geochemistry of deep-sea sediments. In *Chemical oceanography*, J.P. Riley & R. Chester (eds), Vol. 6, 281–390. London: Academic Press.

Edmond, J.M., C.I. Measures, R.E. McDuff, L.H. Chan, R. Collier, B. Grant, L.I. Gordon & J.B. Corliss. 1979. Crest hydrothermal activity and the balance of the major

and minor elements in the ocean; the Galapagos data. *Earth Planet. Sci. Lett.* **46,** 1–18.
Edmond, J.M., K.L. Von Damm, R.E. McDuff & C.I. Measures 1982. Chemistry of hot springs on the East Pacific Rise and their effluent dispersal. *Nature* **297,** 187–91.
Elder, J.W. 1965. Physical processes in geothermal areas. In *Terrestrial heat flow,* Am. Geophys. Union Monogr. no. 8, W.H.K. Lee (ed.), 211–39.
Elderfield, H. 1976. Hydrogenous material in marine sediments: excluding manganese nodules. In *Chemical oceanography,* J.P. Riley & R. Chester (eds), Vol. 5, 137–215. London: Academic Press.

Honnerez, J. 1981. The aging of the oceanic crust at low temperature. In *The sea,* C. Emillani (ed.), Vol. 7, 525–87. New York: Interscience.

Jones, E.J.W. 1978. Sea floor spreading and the evolution of the ocean basins. In *Chemical oceanography,* Vol. 4, J.P. Riley & R. Chester (eds), 1–74. London: Academic Press.

Kinkhammer, G., H. Elderfield, M. Grieves, P. Rona & T. Nelson. 1986. Manganese geochemistry near high temperature vents in the Mid-Atlantic Ridge rift valley. *Earth Planet. Sci. Lett.* **80,** 230–40.

McDuff, R.E. & J.M. Edmond 1982. On the fate of sulphate during hydrothermal circulation at mid-ocean ridges. *Earth Planet. Sci. Lett.* **57,** 117–32.
Martin, J.-M. & M. Whitfield 1983. The significance of the river input of chemical elements to the ocean. In *Trace metals in sea water,* C.S. Wong, E. Boyle, K.W. Bruland, J.D. Burton & E.D. Goldberg (eds), 265–96. New York: Plenum.
Moore, J.G., H.S. Fleming and J.D. Phillips 1974. Preliminary model for extrusion and rifting at the axis of the Mid-Atlantic Ridge, 36°48′ north. *Geology* **2,** 437–40.

Riley, J.P. & R. Chester 1971. *Introduction to marine chemistry.* London: Academic Press.
Rona, P.A., G. Klinkhammer, T.A. Nelson, J.H. Trefry & H. Elderfield 1986. Black smokers, massive sulphides and vent biota at the Mid-Atlantic Ridge. *Nature* **321,** 33–7.

Thompson, G. 1983. Hydrothermal fluxes in the ocean. In *Chemical oceanography.* J.P. Riley & R. Chester (eds), Vol. 8, 270–337. London: Academic Press.

Von Damm, K.L., J.M. Edmond, B. Grant, C.I. Measures, B. Walden & R.F. Weiss 1985a. Chemistry of submarine hydrothermal solutions at 21°N, East Pacific Rise. *Geochim. Cosmochim. Acta* **49,** 2197–220.
Von Damm, K.L., J.M. Edmond, C.I. Measures & R. Grant 1985b. Chemistry of submarine hydrothermal solutions at Guaymas Basin, Gulf of California. *Geochim. Cosmochim. Acta* **49,** 2221–37.
Von Damm, K.L., B. Grant & J. Edmond 1983. Preliminary report on the chemistry of hydrothermal solutions at 21° north, East Pacific Rise. In *Hydrothermal processes at seafloor spreading centres,* P.A. Rona, K. Bostrom, L. Laubier & K.L. Smith (eds), 369–90. New York: Plenum.

Wolery, T.J. & N.H. Sleep 1976. Hydrothermal circulation and geochemical flux at mid-ocean ridges. *J. Geol.* **84,** 249–76.

6 The transport of material to the oceans: relative flux magnitudes

In the preceding chapters we have considered the three principal primary pathways by which material is transported to the World Ocean at the present day, i.e. river run-off, atmospheric deposition and hydrothermal exhalations. The magnitudes of the fluxes associated with each of these transport pathways are discussed below.

6.1 River fluxes to the oceans

6.1.1 Introduction

The flux of material transported by a river reflects a complex interaction between hydrological and chemical factors in the catchment system, and it must be stressed that there are considerable uncertainties associated with all fluvial flux estimates. To make global flux estimations, average concentrations of constituents in individual river systems are often used, e.g. in scaling-up procedures, but there are problems in assessing the extent to which the average values are meaningful. For example, concentrations of constituents in river water can be affected by a number of factors associated with variations in river flow. These include: **long-term** (e.g. annual) temporal variations at individual sampling stations, and spatial variations between individual stations; **short-term** fluctuations, e.g. those in response to storm events; fluctuations due to **rare events**, such as those brought about by severe drought and catastrophic flooding; and **seasonal** variations in biological production. Further, the scaling-up of a single river data set to a global ocean scale, even if the average concentrations used are representative of that river system, can bias flux estimates because hydrological, climatic and lithological controls on the composition of river water vary widely from one river catchment to another. One way of overcoming this difficulty is to use data from major river systems. However, this approach also has problems since the aggregate run-off from the 20 largest rivers in the world accounts for only $\sim 30\%$ of the global run-off. It may therefore be more reasonable to select rivers on the basis of particular catchment regimes rather than on the basis of size (see e.g. GESAMP 1987). Despite these difficulties, however, it is still potentially rewarding to take a first look at the magnitude of fluvial fluxes to the oceans.

When the magnitude of the river-transported signal is considered it is necessary to distinguish between gross and net fluxes. In the present context, the following general definitions are adopted. (a) **Gross fluxes** are those transported by rivers to the marine boundary, which is taken here as the estuarine mixing zone. (b) **Net fluxes** are those which are transported out of the estuarine mixing zone in an offshore direction and so are discharged into coastal seas. The simplest way of estimating gross fluvial fluxes, and the one adopted here, involves a scaling-up procedure, which can be represented by equations such as

$$RF_g = X_d Q + X_p M_p \tag{6.1}$$

where X_d is the average dissolved content of an element X in river water, Q is the annual river-water discharge to the oceans (usually assumed to be 37 400 km^3 yr^{-1}), X_p is the average content of river particulate material (RPM) and M_p is the river particulate discharge to the oceans (usually assumed to be 15.5×10^{15} g yr^{-1}). For net fluxes, it is necessary to take account of the processes that occur in estuaries, and this is discussed below in relation to dissolved and particulate trace elements.

6.1.2 The gross and net fluvial fluxes of total suspended material

6.1.2.1 Gross flux There have been various attempts to quantify the average global discharge of river suspended sediment to the land/ocean margins, and these have been reviewed by Walling & Webb (1987). Two of the most recent comprehensive assessments of the magnitudes of gross fluvial suspended load fluxes have been made by Holeman (1968) and Milliman & Meade (1983). A summary of the two data sets is given in Table 6.1, and several features in the river sediment discharge pattern are illustrated in Figure 6.1a.

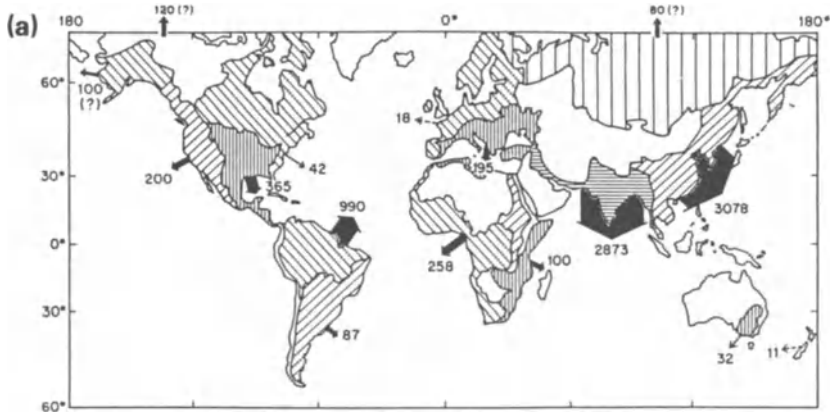

Figure 6.1 General trends in fluvial discharges of suspended and dissolved material to the ocean margins. (**a**) Discharge of suspended sediment (from Milliman 1981); units in millions of metric tons (Mt).

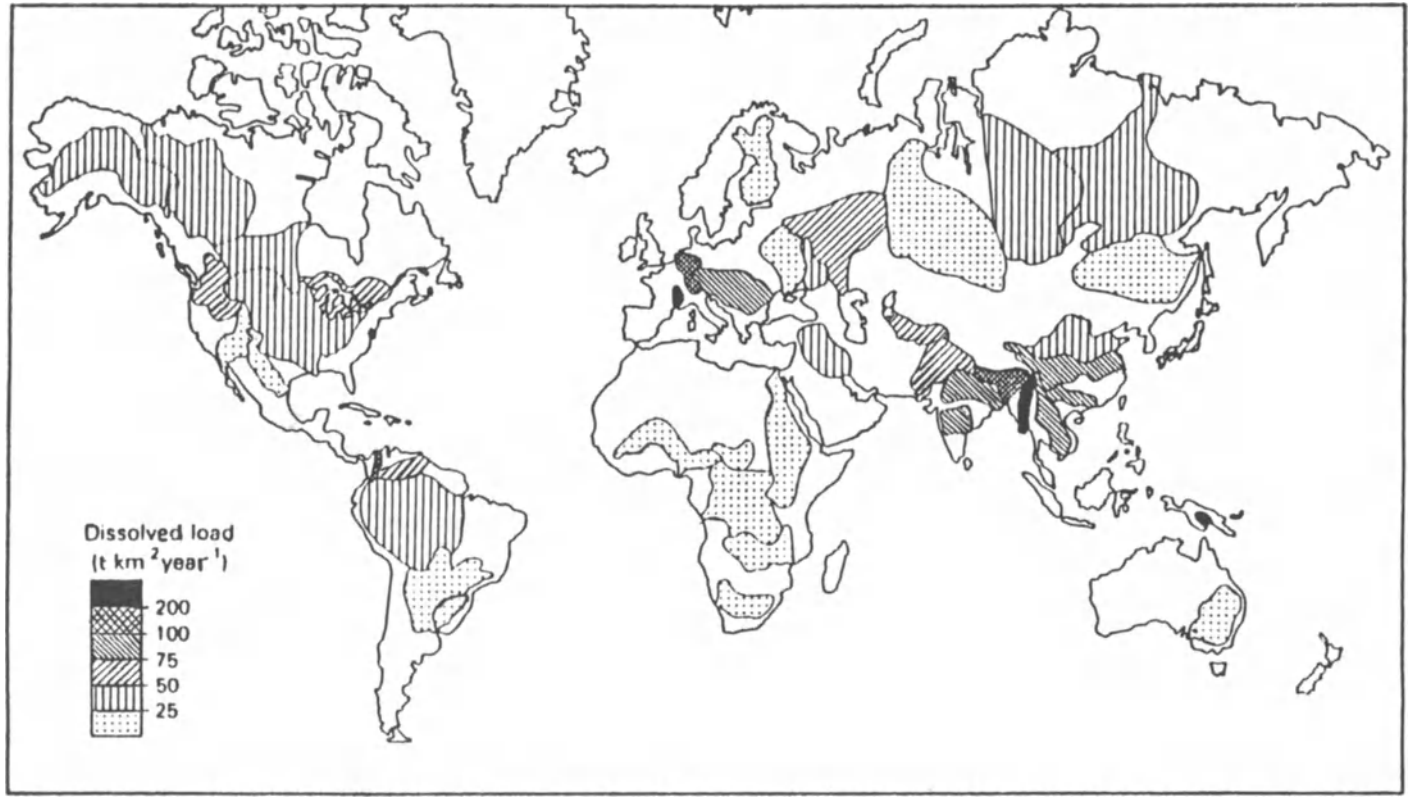

(b)

Figure 6.1b Discharge of total dissolved solutes (from Walling & Webb 1987).

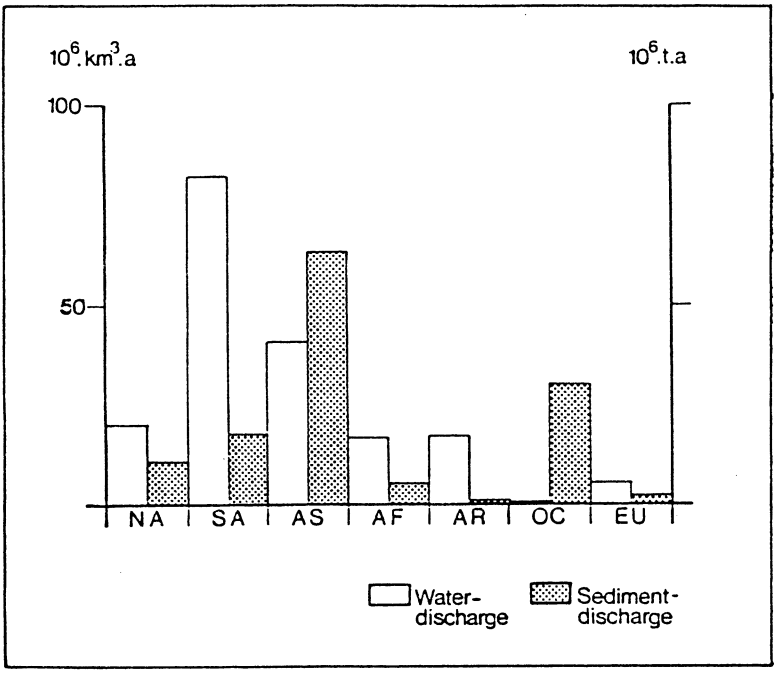

(c)

Figure 6.1c Relative fluvial suspended sediment and water discharges from the continents (from Degens & Ittekkot 1985). NA, North America; SA, South America; AS, Asia; AF, Africa; AR, Arctic USSR; OC, Oceania; EU, Europe.

It can be seen from the data in Table 6.1 that there are a number of significant differences between the two RPM discharge estimates. From the point of view of global discharges to the World Ocean the most important of these can be summarized as follows.

(a) The Milliman & Meade (1983) estimate for the annual discharge of river sediment from Asia is less than half of that given by Holeman (1968). There is no doubt that these Asian rivers carry the highest sediment loads of any of the world's streams. However, over much of the Asian continent the sediment yield is in fact relatively small and the discrepancy between the two discharge estimates probably arose because Holeman (1968) did not take account of this in the scaling-up procedure used in calculating his average estimate of the Asian sediment discharge.
(b) The estimate given by Milliman & Meade (1983) for sediment discharge from the Amazon, which is based on more recent

Table 6.1 The river discharge of suspended sediment to the oceans: gross flux estimates[a]

(a) Suspended sediment discharge from major rivers

River	Annual suspended sediment discharge ($\times 10^6$ t yr^{-1})	
	1	2
Hwang Ho (China)	1890	1080
Ganges (India)) Brahmaputra (Bangladesh))	2180	1670
Yangtze (China)	502	478
Indus (Pakistan)	440	100
Amazon (Brazil)	364	900
Mississippi (USA)	349	210
Irrawaddy (Burma)	300	265
Mekong (Thailand)	170	160
Red (N. Vietnam)	410	-
Nile (Africa)	111	0
Zaire (Africa)	64	43
Niger (Nigeria)	4	40
St. Lawrence (Canada)	4	4

(b) Suspended sediment discharge in the oceans by rivers from the continents

Continental region	Drainage area (10^6 km^2)		Sediment discharge (10^6 t yr^{-1})		Sediment yield (t km^{-2} yr^{-1})	
	1	2	1	2	1	2
N+C America	20.48	17.50	1780	1462	87	84
S America	19.20	17.90	1090	1788	57	97
Europe	9.2	4.61	290	230	32	50
Eurasian Arctic	-	11.17	-	84	-	8
Asia	26.6	16.88	14480	6349	543	380
Africa	19.7	15.34	490	530	25	35
Australia	5.1	2.20	210	62	41	28
Large Pacific Islands	-	3.00	-	3000	-	1000

[a] Data set 1 from Holeman (1968), data set 2 from Milliman & Meade (1983).

measurements, is considerably higher than that listed by Holeman (1968) and, according to the later estimates, the Amazon now ranks third among the world's rivers for the discharge of sediment to the land/ocean boundary.

(c) Holeman (1968) did not take into account the large islands of the western Pacific in making his global estimate of river sediment discharge.

Despite constraints imposed by uncertainties in the database, it is still possible to identify a number of general features in the geographical distributions of river suspended sediment loads (i.e. excluding bedload, which probably makes up ~ 10% of the total sediment load) and their discharges to the land/ocean boundaries.

(a) Most rivers have average suspended sediment loads in the range $\sim 10^2$ to 10^3 mg l^{-1} (Milliman 1981).
(b) Mountain rivers have sediment yields that, on average, are around three times greater than those of plains rivers (Dedkov & Mozzherin 1984).
(c) The suspended loads transported to the ocean margins annually can vary over three orders of magnitude from one river to another (e.g. from the 1890×10^{12} g yr^{-1} for the Hwang Ho, to the 4×10^{12} g yr^{-1} for the St. Lawrence (estimates from Holeman 1968), and much of the suspended sediment delivered to the oceans is carried by a relatively small number of major rivers.
(d) Overall, a large proportion of the total river suspended sediment discharged annually to the land/ocean boundary originates from the Asian continent. On the basis of the Holeman (1968) data set, the Asian river suspended sediment input accounts for $\sim$ 80% of the total discharge to the World Ocean, and still remains at $\sim$ 50% in the revised estimates given by Milliman & Meade (1983), which include discharges from the Pacific islands.
(e) There are a number of estimates in the literature for the total annual transport of river sediment to the ocean margins. In general, these appear to lie in the range $\sim 13.5 \times 10^{15}$ g yr^{-1} (Milliman & Meade 1983) to $\sim 18.3 \times 10^{15}$ g yr^{-1} (Holeman 1968), with that of $\sim 15.5 \times 10^{15}$ g yr^{-1} given by Martin & Maybeck (1979) lying between the two.

6.1.2.2 Net flux Processes operating in the estuarine environment severely modify the gross RPM flux delivered to the land/sea margins and according to Judson (1968) it is probable that at the present time $\sim$ 90% of the particulate material transported by rivers is trapped in estuaries (see Sec. 3.2.7). If this estimate of $\sim$ 90% for the estuarine removal of suspended particulates is applied to the global estimate of $\sim 15.5 \times 10^{15}$ g yr^{-1} for the discharge of RPM (see Sec. 6.1) it would result in a *net* global river-transported flux of $\sim 1.55 \times 10^{15}$ g yr^{-1}. This is very close to the esimate of $\sim 1.26 \times 10^{15}$ g yr^{-1} for the global flux of particulate material to the ocean made independently by Bewers & Yeats (1977). A compilation of the gross particulate fluxes of some major elements is given in Table 6.2.

6.1.3 The gross and net fluvial fluxes of total dissolved material
According to Maybeck (1979) the total dissolved load transported to the oceans by rivers is $\sim 3.7 \times 10^{15}$ g yr^{-1}, which is around 25% of the suspended sediment load (using the estimate of $\sim 15.5 \times 10^{15}$ g yr^{-1} given above), although it falls to around 20% if bedload is included in the particulate river load. Like the suspended sediment yields, there are

patterns in the fluvial discharge of total solutes to the oceans. This was highlighted by Walling & Webb (1987), who produced a map showing the generalized global pattern of fluvial total solute yields – see Figure 6.1b. Global total solute discharge patterns reflect the combined influences of factors such as the magnitude of the river run-off, the catchment lithology and the climatic regime. Walling & Webb (1987) identified a number of general features in the global river discharge of total solutes that can be related to these run-off, geological and climatic controls.

(a) The large dissolved solute discharge values for Asian rivers result from their high run-off, which promote enhanced transport.
(b) The relatively high loads for European rivers reflect the predominance of sedimentary strata, including limestones, in their catchments.
(c) Generally low dissolved loads are found for the rivers of Africa and Australia, which are a consequence of the presence of ancient basement rocks, with a low weathering susceptibility, in their catchments.
(d) The extremely high dissolved solute loads for Burma (the Irrawaddy River) and Papua New Guinea (the Fly and Putari Rivers) reflect a combination of high run-off, the availability of sedimentary rocks in the catchment regions and tropical temperatures, which enhance chemical weathering.

A comparison of fluvial water and sediment discharges from the continents is illustrated in Figure 6.1c.

To apply equations such as Equation 6.1 to dissolved components, it is necessary to have reliable data on their concentrations in river water. Data of this kind have been available for some time for a number of dissolved major components in river water, and the gross fluvial fluxes for several of these are given in Table 6.2, together with their gross particulate fluxes. Some dissolved elements exhibit unambiguous conservative behaviour in the estuarine mixing zone. For these elements, which include those major components contributing to the salinity of sea water, the gross river fluxes will not be markedly changed during estuarine mixing, and those listed in Table 6.2 can be assumed to represent the net fluxes.

6.1.4 The gross and net fluvial fluxes of dissolved and particulate trace elements

6.1.4.1 Gross fluxes Much of the concentration data in the literature for particulate elements in river water have been of an acceptable quality for some time. However, it was pointed out in Section 3.1.3 that it is only recently that reliable data have become available on the concentrations of

Table 6.2 Gross fluvial fluxes of some dissolved and particulate major elements to the ocean margins[a] (units, g yr^{-1})

Element	Dissolved flux	Particulate flux
B	46.5×10^9 (1)	9.3×10^{12} (3)
Br	743×10^9 (2)	77.5×10^9 (3)
Ca	481×10^{12} (1)	345×10^{12} (3)
Cl	245×10^{12} (1)	-
Cs	1.3×10^9 (2)	93×10^9 (3)
F	3.1×10^{12} (1)	-
K	70×10^{12} (1)	310×10^{12} (3)
Li	94×10^9 (1)	0.39×10^{12} (3)
Mg	129×10^{12} (1)	209×10^{12} (3)
Mo	19×10^9 (2)	47×10^9 (3)
Na	131×10^{12} (2)	110×10^{12} (3)
Rb	32×10^9 (1)	1.55×10^{12} (3)
Sr	2.3×10^{12} (1)	2.3×10^{12} (3)

[a] (1) Based on data from Thompson (1983a).
(2) Based on data from Martin & Maybeck (1979).
(3) Calculated from data given by Martin & Maybeck (1979).

dissolved trace elements in river water, and even these data are still limited to a relatively small number of elements. In order to estimate order-of-magnitude gross fluxes of river-transported trace elements, an attempt has therefore been made to apply Equation 6.1 to a 'modern' database. To illustrate the concepts involved, attention has been limited to a number of process-orientated elements, which are used in Chapter 11 to describe the factors that control the distributions of trace elements in sea water. To make these gross flux estimates, data for the particulate phase were taken from Martin & Whitfield (1983), and for the dissolved phase the average global river-water concentration given in column 19 of Table 3.4 was used. The gross river fluxes obtained in this manner are listed in Table 6.3, together with those estimated by Yeats & Bewers (1982). These authors concluded that, in general, their flux estimates for individual rivers (expressed as ranges in Table 6.3) showed a remarkable degree of similarity, despite the fact that the river catchments involved: (a) varied from tropical to subarctic; (b) included both polluted and unpolluted rivers; and (c) had a wide range of suspended matter loads.

6.1.4.2 Net fluxes The data given in Table 6.3 are for *gross* river-transported fluxes, i.e. those which enter the estuarine mixing zone. Processes operating in estuaries can modify both the dissolved and particulate phases in the river-water inputs, and as a result the strengths

Table 6.3 Gross fluvial fluxes of some dissolved and particulate trace elements to the ocean margins (units, 10^{12} g yr^{-1})

Element	Dissolved gross flux		Particulate gross flux	
	1	2	3	4
Al	1.9	-	1460	1500
Fe	1.5	0.16-2.2	745	730
Mn	0.31	0.25-0.63	16	17
Ni	0.019	0.011-0.057	1.4	1.5
Co	0.0075	0.0026-0.0065	0.31	0.32
Cr	0.037	-	1.55	-
V	0.037	-	2.6	-
Cu	0.056	0.061-0.088	1.55	1.6
Pb	0.0037	-	1.55	-
Zn	0.015	-	3.9	5.4
Cd	0.0015	0.0028-0.0043	0.016	0.026-0.03

1 Scaled up from the average global dissolved river concentration given in Table 3.4, column 19; assuming a global river discharge of 37 400 km^3 yr^{-1}.

2 and 4 Data from Yeats & Bewers (1982).

3 Scaled up from the average composition and RPM given by Martin & Whitfield (1983); assuming a total river particulate discharge load of 15.5 x 10^{15} g yr^{-1}.

of the river-transported signals entering an estuary can be very different from those which are exported to the ocean (see Sec. 3.2).

It was shown above that ~ 90% of the particulate material transported by rivers is trapped in estuaries at the present time. It is apparent, therefore, that the gross river particulate fluxes given in Table 6.3 must be strongly reduced in order to derive *net* fluxes for the export of particulate components from estuaries. In order to offer a first look at these net fluxes, the gross particulate fluxes have been reduced by a global factor of 90%; the data are listed in Table 6.4, together with those derived by Bewers & Yeats (1977) from the St. Lawrence experiment (see below).

Various attempts have been made over the past few years to estimate net river fluxes of dissolved trace elements from their gross fluxes by taking account of estuarine processes. For example, the **zero-salinity end-member** approach has been adopted in several investigations. This is an attempt to estimate the chemical composition of river water that has actually passed through the estuarine filter and reached coastal waters. Although there are a number of problems associated with this approach, it can still produce useful data. The zero-salinity end-member or, as it is sometimes called, the effective river end-member, can be identified from

Table 6.4 Net fluvial fluxes of some particulate elements to the oceans (units, 10^{12} g yr^{-1})

Element	Particulate flux	
	1	2
Al	146	-
Fe	75	111
Mn	1.6	2.4
Ni	0.14	0.036
Co	0.03	0.017
Cr	0.155	-
V	0.26	-
Cu	0.155	0.036
Pb	0.155	-
Zn	0.39	0.018
Cd	0.0016	0.00008

1 Gross fluvial flux from Table 6.3, assuming an estuarine retention of 90% of RPM.

2 Data from Bewers & Yeats (1977).

Footnote to **Table 6.4.** The estimate of particulate and dissolved fluvial transport reported by Bewers & Yeats (1979) for the St. Lawrence was an attempt to assess the magnitude of the fluxes across regions of the adjacent marginal sea. The relative importance of the particulate transport was in the following order (ratio of dissolved to particulate flux given in parenthesis): Fe (0.01); Mn (0.15); Co (0.43); Ni (1.4); Cu (2.5); Zn (9.0); Cd (90). Recently, Windom *et al.* (1989; *Mar. Chemistry*, 27, 283–97) have attempted to estimate the cross-shelf fluxes of series of land-derived particulate elements across the southeastern U.S. continental shelf. They concluded that in this region the relative importance of particulate cross-shelf transport follows the following order (ratio of dissolved to particulate flux given in parenthesis): Fe (0.19) > Mn (2.6) > Pb (3.7) > Co (10) > Zn (20) > Ni (240) > Cd (370) Cu > (730).

either estuarine or, under suitable conditions, coastal water data. A number of workers have used the estuarine mixing model outlined by Boyle *et al.* (1974) (see Sec. 3.2.3) to evaluate an effective river end-member by extrapolating linear element : salinity ratios back to a zero-salinity intercept. For example, Edmond *et al.* (1985) used this approach to evaluate the *net* river fluxes to the ocean from the Changjiang River and also quoted similar data for the Amazon; these data, together with those from some other rivers, are listed in Table 6.5. The application of the zero-salinity end-member approach for estimating the net fluvial input to coastal waters can be illustrated by two examples, selected to identify inputs from contrasting river catchments. These are (a) the US eastern seaboard (Bruland & Franks 1983) and (b) the North Sea (Kremling

Table 6.5 Net fluvial fluxes of some dissolved trace elements to the oceans

Element	Zero-salinity end-member		Global net fluvial flux to oceans (10^{12} g yr^{-1})			
	North Sea ($\mu g l^{-1}$)[a]	US eastern seaboard ($\mu g l^{-1}$)[b]	Estimated from zero-salinity end-member; US eastern seaboard[c]	Estimated from St. Lawrence estuary data[d]	Estimated from Amazon data[e]	Estimated from Changjiang data
Mn	7.6	6.2	0.23	0.35	-	-
Ni	9.4	1.2	0.05	0.05	0.014	0.010
Cu	5.8	1.2	0.05	0.09	0.07	0.05
Zn	-	1.0	0.04	0.16	-	-
Cd	0.65	0.12	0.0046	0.0075	0.00045	0.0012
Be	-	-	-	-	0.00007	0.00006
Ba	-	-	-	-	3.1	1.9

[a] Data from Bruland & Franks (1983).
[b] Data from Kremling (1985).
[c] Data scaled-up from column 2.
[d] Data from Bewers & Yeats (1977).

1985); data for the two zero-salinity end-members are given in Table 6.5. It can be seen from this table that the concentrations of dissolved Ni, Cu and Cd in the North Sea zero-salinity end-member are higher than those for the US eastern seaboard end-member. This probably reflects a combination of different estuarine processes in the two areas, together with a stronger pollutant influence from rivers draining into the North Sea.

The zero-salinity end-member approach yields estimates of the *net* flux of components from individual river-estuarine systems. These can then be extrapolated onto a global scale by some form of scaling-up procedure. Any attempt to extrapolate the effects of local estuarine removal processes to such a global scale will inevitably be fraught with very considerable uncertainty. Despite this, Bewers & Yeats (1977) used data obtained from a mass-balance study carried out in the St. Lawrence river to make such a net global flux estimate. To do this, the authors scaled up the St. Lawrence data by taking account of global discharges of both river water and particulate material, thus correcting, for example, for the low suspended load in the St. Lawrence system. The net fluvial World Ocean fluxes for the dissolved trace metals given by these authors are summarized in Table 6.5. It is of interest to compare the net global fluxes for dissolved trace metals estimated from the St. Lawrence experiment with those scaled up from the zero-salinity end-member and effective river concentration estimates. The zero-salinity end-member concentration that was identified by Kremling (1985) for rivers discharging into the North Sea has apparently been affected by local river pollution. However, that derived by Bruland & Franks (1983) for rivers draining the US eastern seaboard had a composition more similar to that of global river water. The data given by Bruland & Franks (1983) can therefore be scaled up to a global framework, and the net flux calculated in this way is given in Table 6.5. In addition, the Changjiang and Amazon fluxes have been scaled up to global estimates and these are also listed in Table 6.5. This table therefore offers a number of recent estimates of the *net* fluxes of dissolved components transported to the oceans via river run-off. Considering that these estimates have been derived by applying different approaches to data from a variety of river systems, there is a surprisingly good measure of agreement between them for some of the dissolved elements. By combining the data in Table 6.5 with those from a variety of other sources, it is possible to make a first-order estimate of the net fluvial fluxes of a number of dissolved and particulate elements to the World Ocean, and these are listed in Table 6.6. It should be pointed out that for some elements, e.g. Cd, the net dissolved fluxes exceed the gross fluxes, a situation that will arise when estuarine processes lead to the addition of dissolved components from the particulate phase.

Table 6.6 Estimates of net global fluvial fluxes of some dissolved and particulate elements to the World Ocean (units, 10^{12} g yr^{-1})

Element	Dissolved flux[a]	Particulate flux[b]
Al	~ 0.95	~ 146
Fe	~ 0.30	~ 75
Mn	~ 0.30	~ 1.6
Ni	~ 0.03	~ 0.14
Co	~ 0.0075	~ 0.03
Cr	~ 0.0185	~ 0.155
V	~ 0.037	~ 0.26
Cu	~ 0.06	~ 0.155
Pb	~ 0.0037	~ 0.155
Zn	~ 0.025	~ 0.39
Cd	~ 0.0031	~ 0.0016

[a] Dissolved fluxes estimated as follows:

Co, V, Pb	Gross fluxes only - see Table 6.3.
Zn, Mn	Based on the average of the net global flux estimates (Table 6.5) derived from the US eastern seaboard zero salinity end-member, the St. Lawrence estuary data (Table 6.5) and the gross flux data in Table 6.3.
Cu, Cd, Ni	Based on the average of the net global flux estimates (Table 6.5) from the US eastern seaboard zero-salinity end-member, the St. Lawrence estuary data (Table 6.5), the Amazon River (Table 6.5) and the Changjiang River data (Table 6.5) and the gross flux data in Table 6.3.
Al	Gross flux from Table 6.3, reduced for an estuarine retention of 50% (see e.g. Maring & Duce 1987).
Fe	Gross flux from Table 6.3, reduced for an estuarine retention of 80% (see e.g. Figueres et al. 1978).
Cr	Gross flux from Table 6.3, reduced for an estuarine retention of 50% (see e.g. Campbell & Yeats 1984).

[b] All net particulate fluxes are from Table 6.4.

6.1.5 The gross and net fluvial fluxes of organic carbon and the nutrients

6.1.5.1 Organic carbon The database for the transport of organic carbon by rivers has been greatly expanded recently by the SCOPE/UNEP project *Transport of carbon and minerals in major world rivers*, and the results have been reviewed by Degens & Ittekkot (1985), who also estimated annual river fluxes of organic carbon to the ocean margins. The magnitudes of the carbon fluxes, expressed in relation to the major continental drainage regions, are illustrated graphically in Figure 6.2. For POC transport the river drainage areas are ranked Asia > North America > South America > Oceania > Africa > Europe, and for DOC transport the order is South America > Asia > Arctic > North America > Africa > Europe > Oceania. The SCOPE/UNEP data were also used to update estimates of organic carbon fluxes to the total *global* ocean. From these data the gross global DOC flux was given as (4.2–5.7) $\times$ 10^{14} g yr^{-1}. According to Mantoura & Woodward (1983), DOC can behave conservatively in the estuarine mixing zone, which on the basis of their estimate can result in a global *net* DOC flux to the oceans of ~ 5 $\times$ 10^{14} g yr^{-1}. The SCOPE/UNEP estimate for the gross fluvial POC flux was ~ (1.1–2.5) $\times$ 10^{14} g yr^{-1}. Using the same database, Ittekkot (1988)

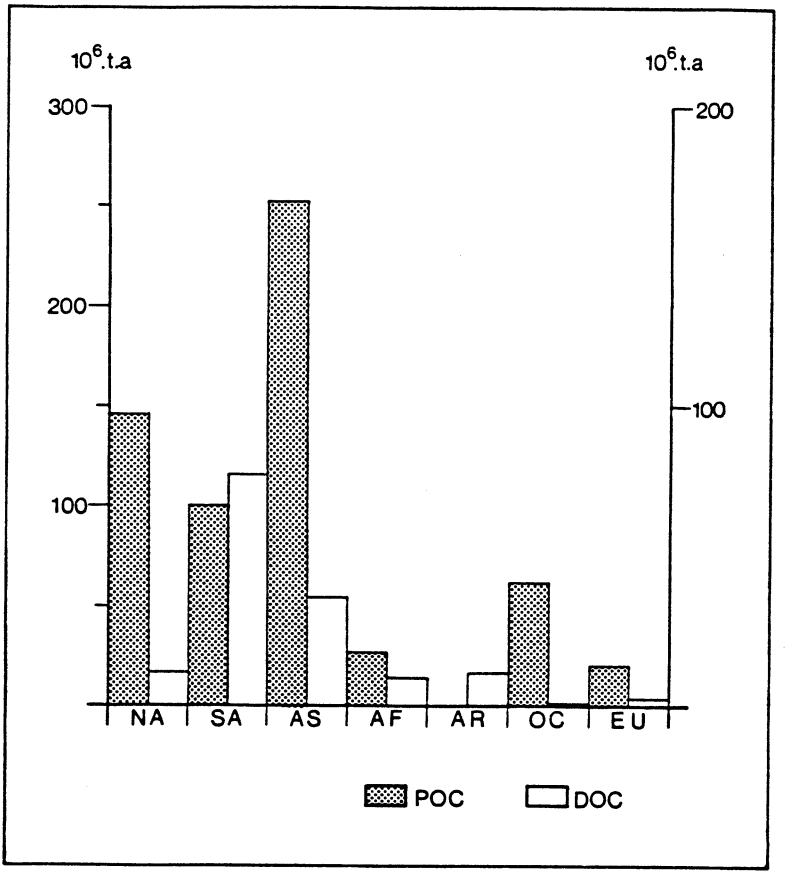

Figure 6.2 Annual fluvial inputs of particulate organic carbon (POC) and dissolved organic carbon (DOC) from the continents (from Degens & Ittekkot 1985). NA, North America; SA, South America; AS, Asia; AF, Africa; AR, Arctic USSR; OC, Oceania; EU, Europe.

calculated an average global value of $\sim 2.31 \times 10^{14}$ g yr^{-1} for the gross fluvial POC flux, and estimated that $\sim$ 65% of this is highly refractory and so can escape the estuarine environment as a *net* POC flux, which is taken up by marine sediments, mainly in tropical and subtropical seas.

6.1.5.2 The nutrients Natural gross fluvial nutrient fluxes to the land/sea margins have been estimated to be as follows: $\sim$ (14–15) $\times 10^{12}$ g yr^{-1} for total dissolved nitrogen and $\sim 21 \times 10^{12}$ g yr^{-1} for particulate nitrogen (Van Bennekon & Salomons 1981, Maybeck 1982); $\sim 1 \times 10^{12}$ g yr^{-1} for total dissolved phosphorus and $\sim 20 \times 10^{12}$ g yr^{-1} for total particulate phosphorus (Maybeck 1982); and 181×10^{12} g yr^{-1} for dissolved silicon (GESAMP 1987). A number of authors have estimated the gross anthropogenic fluvial nutrient fluxes and these are in the ranges $\sim$ (7–35) $\times 10^{12}$ g yr^{-1} for dissolved nitrogen, and $\sim$ (0.6–3.75) $\times 10^{12}$ g yr^{-1} for dissolved phosphorus (GESAMP 1987). It is apparent, therefore, that the

anthropogenic fluxes of the dissolved nutrients are at least of the same order as, and may in fact exceed, those from natural sources. Net fluvial fluxes for the nutrients are difficult to estimate. However, the nutrients are extensively involved in biological, chemical and physical processes both in the estuarine and coastal sea zones which can severely restrict their transport to the open ocean, for example, by trapping in sediments. It may be concluded, therefore, that the nutrients required to support primary production in the open ocean are supplied mainly by upwelling processes, or by vertical turbulent mixing (GESAMP 1987).

6.2 Atmospheric fluxes to the oceans

In order to estimate the *net* flux of a component from the atmosphere to the ocean it is necessary to know (a) its burden in the air, (b) the rate at which it is deposited onto the sea surface and (c) the extent to which it is recycled back into the atmosphere.

ATMOSPHERIC BURDEN To determine the atmospheric burden of a component in a slice of the atmosphere (e.g. a 1 m^2 column), data must be available on its concentration per unit of air (e.g. $\mu g\ m^{-3}$) and the height to which it is dispersed, i.e. the scale height. The global atmospheric concentrations of many elements vary over one to three orders of magnitude, and are often geographically dependent. Because of this, the assessment of the atmospheric burdens of elements has often been restricted to a local scale. However, as more reliable data have become available, it has been possible to make first-approximation estimates of the global atmospheric burdens of some elements (see e.g. Walsh *et al.* 1979). In making these estimates it is assumed that the atmosphere is in a steady state, i.e. the rate of input of the component is equal to its rate of output, and the global burden (C_T) of the component is then computed from an equation of the type

$$C_T = C_0 A S \tag{6.2}$$

in which C_0 is the surface concentration of an element ($g\ m^{-3}$ of air), A is the surface area of the atmosphere (m^2) and S is the scale height, i.e. the height to which the atmospheric component is dispersed (usually assumed to be between $\sim$ 3000 and $\sim$ 5000 m).

RATE OF DEPOSITION The deposition of aerosols from the atmosphere is controlled by a combination of dry (gravitational settling and turbulent diffusion) and wet (precipitation scavenging) processes.

The **dry removal** of particles from the atmosphere is a *continuous* process that is affected by a number of factors, which include windspeed and particle size. For example, McDonald *et al.* (1982) showed that the

dry deposition of sea salts was dominated by large particles (MMD > 10 μm), which accounted for ~ 70% of the total salt deposition although they made up only ~ 13% of the total mass. Dry deposition is therefore especially important for large particles.

Wet deposition is the removal of substances from the atmosphere by precipitation scavenging, a process that is *random* in time. In the most general sense, wet deposition rates depend on the concentration of a component in rain and the total amount of that rain which falls onto a surface. Data are now available on the elemental composition of rain at a number of marine locations, and a representative selection of these is given in Table 6.7. It can be seen from these data that, as was the case for particulates, the concentrations of the AEE in the rain are higher in samples taken close to the major continental sources of pollution than they are in those from the more remote areas. However, there are problems when rain concentrations are used in the estimation of trace metal wet deposition rates. One of the principal reasons for this is that concentration of the metals in the rain can change during the course of a rainfall event; for example, some trace metals can have higher

Table 6.7 Concentrations of elements in precipitation over marine regions (units, μg l^{-1})

	North Sea[a]	Bay of Bengal[b]	Bermuda[c]	N. Pacific[d] (Enewetak)	S. Pacific[e] (Samoa)
Na	19000	14000	3400	1100	2500
Mg	-	1600	490	170	270
K	-	1400	160	39	88
Ca	-	1700	310	50	75
Cl	32000	25000	6800	2000	4700
Br	-	-	-	7.1	12
Al	105	-	-	2.1	16
Fe	84	30	4.8	1.0	0.42
Mn	<12	-	0.27	0.012	0.020
Sc	0.010	0.016	-	0.00023	-
Th	-	0.12	-	0.00091	-
Co	0.17	0.95	-	-	-
I	-	-	-	1.2	0.021
V	3.7	-	-	0.018	-
Zn	35	100	1.15	0.052	1.6
Cd	-	-	0.06	0.0021	-
Cu	15	-	0.66	0.013	0.021
Pb	-	-	0.77	0.035	0.014
Ag	-	-	-	0.0056	-
Se	-	-	-	0.021	0.026

[a] Cambray et al. (1975).
[b] Mahadevan et al. (1982).
[c] Jickells et al. (1984).
[d] Arimoto et al. (1985).
[e] Arimoto et al. (1987).

concentrations in the early, relative to the later, precipitation. There are also variations in the efficiencies with which aerosols of different particle sizes are scavenged by rain; however, at remote sites, where the number of particles in the air is relatively low, rain may scavenge aerosols of different sizes with nearly equal efficiencies (see e.g. Arimoto *et al.* 1985).

Washout factors, or scavenging ratios, are often employed to determine the degree to which a component is removed from the air by rain. The washout actor (WF) is calculated from an equation of the type

$$\mathrm{WF} = C_r/C_a \tag{6.3}$$

in which C_r is the concentration of a component in the rain and C_a is its concentration in low-level air; sometimes an air density term is included in the equation. WF values for the most commonly studied elements lie in the range $\sim 10^2$ to $\sim 10^3$.

EXTENT OF RECYCLING The recycling of particulate components across the sea surface can occur during the generation of sea salts. Data are now available on the degree to which some elements are fractionated at the ocean surface with respect to bulk sea water (see Sec. 4.2.1.2), and for these the extent of recycling across the air/sea interface can be estimated with some degree of certainty. For example, Arimoto *et al.* (1985) used a combination of aerosol, rain and seawater data to estimate that at Enewetak (North Pacific) the percentage of wet deposition associated with recycled sea salts can be substantial; values for individual elements included 15% (Zn), 30% (V) and 48% (Cu). Clearly, recycling must be taken into account when estimates are made of the *net* deposition fluxes of some elements to the sea surface from the atmosphere.

Buat-Menard (1983) concluded that, in general, the net atmospheric fluxes of the AEE (small particle size) to the sea surface are primarily due to *wet* deposition over most marine areas, but that *dry* deposition is signficant for sea salt and mineral aerosols (large particle size). The data available in the literature tend to confirm these overall trends, although the situation is by no means absolutely clear. For example, at Enewetak, flux data (corrected for sea surface recycling) showed that, although wet deposition exceeded dry deposition for Pb, V, Cd and Se, this was not the case for Cu and Zn. Further, at Enewetak, wet deposition was more important than dry deposition for Fe, although for Al dry deposition was an order of magnitude higher than wet removal.

Many of the early models used to estimate the input of elements to the sea surface were inevitably somewhat crude, and total atmospheric deposition fluxes (F) were often calculated from an equation of the general type

$$F = CV \tag{6.4}$$

in which C is the mean atmospheric concentration of an element and V is the global deposition velocity. The simplest way of estimating the global deposition velocity of an element is by assuming that all deposition takes place by rain scavenging, which cleans the atmosphere around 40 times per year; see, for example, the model described by Bruland *et al.* (1974). In more complex models, attempts were made to take account of the actual deposition rates of elements to the sea surface, either by assuming a total deposition rate (see e.g. Buat-Menard & Chesselet 1979) or by taking individual account of wet and dry deposition rates (see e.g. Duce *et al.* 1976). Recently, more advanced 'wet and dry' flux deposition models have become available. For example, Arimoto *et al.* (1985) determined the gross and net atmospheric fluxes of a series of crustal and enriched elements to the sea surface at Enewetak. The findings are of particular interest because the models take account of sea surface recycling, and thus offer an estimate of the true *net* deposition of the elements to the ocean surface from the atmosphere. Advanced models of this type were subsequently applied to the Samoa (South Pacific) aerosol (Arimoto *et al.* 1987). The data sets provided by Arimoto *et al.* (1985, 1987) therefore represent the best available estimates of the net deposition of trace metals to the sea surface.

A summary of some of the data given in the literature for the fluxes of trace elements to the sea surface is given in Table 6.8. With the exception of the data sets for Enewetak and Samoa, most of the calculations do not take account of sea surface recycling, with the result that the fluxes, especially those for the AEE, will tend to be overestimated. Further, the fluxes have been obtained by different methods. Despite constraints such as these, however, a strong geographical trend can be identified from the data in Table 6.8, indicating that the strengths of the air-to-sea fluxes decrease by orders of magnitude as the degree of remoteness of a site from the major aerosol sources increases. For example, this trend is well developed for Pb, for which the atmospheric input from the North Atlantic westerlies is over 50 times greater than that from the South Pacific westerlies.

It is clear that the atmosphere provides an important pathway for the transport of trace metals to the oceans. The subsequent fate of the elements will depend on a number of factors. The initial constraint on the behaviour of atmospherically transported trace metals in the mixed layer will be imposed by the extent to which they are solubilized in sea water. This is important since the physical state (i.e. particulate or dissolved) of the metals affects both their subsequent involvement in the biogeochemical cycles and their residence times in sea water.

There are considerable problems involved in the experimental study of

Table 6.8 Atmospheric fluxes of trace metals to the sea surface (units, ng cm^{-2} yr^{-1})

	New York Bight[a]	North Sea[b]	Western Med[c]	South Atlantic Bight[d]	Bermuda[e]	North Atlantic; north-east trades[f]	Tropical North Atlantic[g]	Tropical North Pacific; total net deposition[h]	South Pacific; total net deposition[i]	North Atlantic[j]; westerlies	North Pacific; westerlies	South Pacific[j]; easterlies
Al	6000	30000	5000	2900	3900	97000	5000	1200	132 - 1800	-	-	-
Sc	-	5	1	-	0.6	-	1.1	0.18	0.06	-	-	-
V	-	480	-	-	5	-	17	7.8	-	-	-	-
Cr	-	210	49	-	9	111	14	-	-	-	-	-
Mn	-	920	-	60	45	570	70	9.0	3.6	-	-	-
Fe	5700	25500	5100	5900	3000	48000	3200	560	47 - 337	-	-	-
Co	-	39	3.5	-	1.2	12	2.7	-	0.25	-	-	-
Ni	-	260	-	390	3	67	20	-	-	-	-	-
Cu	-	1300	96	220	30	48	25	8.9	4.4 - 7.9	-	-	-
Zn	1400	8950	1080	750	75	152	130	67	5.8 - 2.4	-	-	-
As	-	280	54	45	3	-	-	-	-	-	-	-
Se	-	22	48	-	3	-	14	4.2	0.8	-	-	-
Ag	-	-	3	-	-	-	0.9	-	-	-	-	-
Cd	30	43	13	9	4.5	-	5	0.35	-	-	-	-
Sb	-	58	48	-	1.0	-	3.5	-	-	-	-	-
Au	-	-	0.05	-	-	-	0.1	-	-	-	-	-
Hg	-	-	5	24	-	-	2.1	-	-	-	-	-
Pb	3900	2650	1050	660	100	32	310	7.0	1.4 - 2.8	170	50	3
Th	-	4	1.2	-	-	-	0.9	0.61	0.036	-	-	-

[a] Duce et al. (1976).
[b] Cambray et al. (1975).
[c] Arnold et al. (1982).
[d] Windom (1981).
[e] Duce et al. (1976).
[f] Chester et al. (1979).
[g] Buat-Menard & Chesselet (1979).
[h] Arimoto et al. (1985).
[i] Arimoto et al. (1987).
[j] Settle and Patterson (1982).

the solubility of trace elements from aerosols deposited at the sea surface. Chester & Murphy (1988) reviewed this topic and identified a number of variables that must be considered in such laboratory experiments. These variables include the following:

(a) The presence of suspended particulates and dissolved organic material in the experimental sea water; e.g. the particulates can scavenge elements released from the aerosols and so decrease the real solubility values, and dissolved organics may coat the aerosol particles with an electronegative surface layer, which can trap elements and make them less soluble.
(b) The length of time the aerosols are allowed to react with the sea water; e.g. it has been estimated that the residence time of a particle in the upper $\sim$ 100 m of the water column is $\sim$ 100 h (Maring & Duce 1987), but most aerosol solubility experiments employ leaching times of only a few hours or even less.
(c) The aerosol deposition mode; e.g. the exposure of aerosols directly to sea water will only simulate dry deposition, and to model wet deposition it is necessary to employ leaching solutions with the composition and pH of rain water.
(d) The nature of the aerosols used in the experiments; e.g. the solid-state speciation of the AEE is very different in aerosols from urban-dominated and crust-dominated populations, and this can affect the solubilities of the elements in both the dry and wet deposition modes.
(e) The effects of photoreduction on the solution chemistry of some elements; e.g. Sunda *et al.* (1983) demonstrated that the photoreduction of solid Mn(IV) oxide phases to dissolved Mn(II) can occur in sea water.

Chester & Murphy (1988) concluded, therefore, that it is necessary to give a strict operational definition of the conditions used in aerosol sea water solubility experiments before the results can be extrapolated to the real marine environment. With this constraint in mind it is possible to evaluate a number of the aerosol sea water solubility studies described in the literature.

Walsh & Duce (1976) simulated the dry deposition of aerosols to the sea surface, and reported that $\sim$ 70% of the V in filter-collected aerosols taken at Rhode Island (US) was rapidly solubilized, i.e. within < 2 min of the exposure of the filters to sea water. Most of this V was non-crustal (probably anthropogenic) in origin, and during the solubilization experiments the V EF_{crust} values of the particulates fell from > 25 to $\sim$ 10 after 1 or 2 min contact with sea water. This early work suggested, therefore, that the manner in which an element is partitioned between crustal and non-crustal components of an aerosol exerts a major control on its fate in sea water.

This partitioning control was also very apparent in the study carried out by Hodge *et al.* (1978), who simulated the dry deposition of both crustal (Baja California) and urban (Southern California) aerosols to sea water, using a leaching time of 3 h. A summary of their solubility data is given in Table 6.9a, from which it can be seen that there are considerable differences in the solubilities of a number of the elements between the two aerosol populations. For example, Pb, Zn and Cu were solubilized to a much greater extent from the polluted aerosols, in which they had relatively high EF_{crust} values, than from the dust-rich samples, in which the enrichment factors were lower. These trends can be related in a general way to the partitioning of the elements among the aerosol components (see Sec. 4.2.1.3). The most potentially mobile (i.e. soluble) elements will be those held in a loosely bound form, and the most immobile (i.e. insoluble) elements will be those present in the refractory fractions. In the pollutant end-member described in Section 4.2.1.3, relatively large amounts of the total concentrations of Pb ($\sim$ 46%), Zn ($\sim$ 67%) and Cu ($\sim$ 37%) are in a loosely bound form, but in the crustal end-member $< 5\%$ of their total concentrations are present in this fraction. The greater release of the elements from the polluted aerosols on contact with sea water is therefore entirely consistent with their solubilization from particle surfaces and from specific compounds with which they become associated during high-temperature volatilization processes. In contrast to Pb, Zn and Cu, cadmium is found mainly in loosely held forms in both the pollutant and the crustal end-member aerosols and so will be relatively soluble from both types. The general relationships between the solid-state partitioning and the sea water solubilities of elements have been confirmed by Chester *et al.* (1988).

Maring & Duce (1987) provided data showing that the sea water leaching time affected the solubility of Al from North Pacific aerosols. The element had a bimodal solubility, with $\sim$ 5–6% of the total Al being solubilized in $<$ 6 h and an additional $\sim$ 3–4% being released within $\sim$ 60 h. The authors suggested that this bimodal solubility was related to two forms of Al in the aerosols: the more soluble fraction represented Al that had already been weathered in the soil profile, and the less soluble fraction represented Al removed from the aluminosilicate matrix within sea water. Dissolved organic matter in sea water had little effect on the solubility of the Al, but experiments using artificial rain water (simulated wet deposition) showed that in solutions at pH 5.5 the rate of solubilization, and perhaps the total quantity of Al solubilized, increased relative to those found for sea water at pH 8.

From these studies it may be concluded that there are difficulties in attempting to model long-time seawater solubilities (e.g. to approach the 100 h particle residence time in the mixed layer), and in any case it is unlikely that atmospherically deposited particles will retain their original

Table 6.9 The solubility of atmospherically transported trace metals in sea water (**a**) The solubility of atmospheric trace metals in sea water from anthropogenic-rich and crust-rich aerosols (% total element)[a]

Atmospheric population	Al	Fe	Mn	Ni	Co	Cr	V	Ag	Zn	Cu	Pb	Cd
Anthropogenic-rich[b]												
Mean concentration (ng m^{-3} of air)	900	610	11	11	<0.4	<1.6	13	<0.05	25	16	560	0.25
Mean % soluble in sea water	0.56	1.1	47	47	25	12.5	31	80	68	28	39	84
Mean EF_{crust}	1.0	0.99	1.0	14	1.5	1.5	9.0	-	33	26	4148	16
Dust-rich[c]												
Mean concentration (ng m^{-3} of air)	3380	2100	46	2.8	<0.5	4.0	<11	<0.03	18	20	150	0.20
Mean % soluble in sea water	0.09	0.19	34	28	20	10	18	67	24	14.5	13	80
Mean EF_{crust}	1.0	0.91	1.2	0.92	0.49	0.99	2.0	-	6.2	8.4	296	25

[a] Data taken from Hodge et al. (1978).
[b] Southern California.
[c] Baja California.

Table 6.9b The seawater solubilities of elements from aerosols over various marine regions (% total element)[a]

Element	Coastal regions; aerosol dominated by anthropogenic sources	Coastal regions; aerosol dominated by crustal sources	Open-ocean 'mixed-source' aerosols
Al	5	< 5	5
Fe	7.5	< 7.5	7.5
Mn	45	<20	35
Ni	50	<25	40
Co	25	<20	22.5
Cr	12.5	<10	10
V	30	<20	25
Cu	30	< 5	30
Pb	50	< 5	30
Zn	70	< 5	45
Cd	85	-	80

[a] Data from various sources quoted in text; values are rounded-off first-order estimates and are only approximate.

identity as discrete particles in the upper water column following their deposition to the sea surface. For example, the aerosols may be coated with organics, they may be taken out of solution onto the surfaces of other suspended particulates, or they may enter the gut of filter-feeding organisms where the pH can be very much lower than in sea water. Experimental sea water solubilities will therefore only reflect the initial fate of an atmospherically transported element in the mixed layer, and it must be remembered that their subsequent biogeochemical fates will be affected by a variety of complex processes.

Despite the various constraints that it is necessary to impose on aerosol seawater solubility studies, a number of trends can be identified from the published data. For example, Crecelius (1980) divided the atmospherically transported elements into a number of groups on the basis of their solubilities in sea water. A modified version of this classification, in which the number of elements has been increased in the light of more recent studies, is given below.

(a) **Very soluble elements** (> 90% of the total concentration soluble in sea water). This group includes Na, Br and Cs. These are sea-salt

elements, and should be soluble in sea water from all marine aerosols.

(b) **Relatively soluble elements** (20–90% of the total concentration soluble in sea water). This group includes Cd, Zn, As, Se, Co, Sb, Cr, Ag, Mn, V and Pb. These elements have a variety of sources in the marine aerosol, and in general the solubilities will increase as the proportion of anthropogenic material increases in the particulates. Cadmium and Mn are an exception to this, and their solubilities appear to be largely independent of the aerosol source.

(c) **Slightly soluble and insoluble elements** (< 10% of the total concentrations soluble in sea water). This group includes Al, Fe, Sc, Ce, La, Hf, Yb, Pa and Lu. These elements are usually non-enriched, i.e. they have a predominantly crustal origin, and will be relatively insoluble from all marine aerosols.

By taking all the available data into consideration, Chester & Murphy (1988) made very crude estimates of the solubility of elements from aerosols deposited to the sea surface, and these are listed in Table 6.9b. The data are given in terms of three characteristically different oceanic environments, selected to illustrate how the solubility of an element from an aerosol is dependent on its source. A number of overall trends can be identified from the data in this table.

(a) In coastal regions where anthropogenic inputs are highest, very significant fractions of the AEE are soluble in sea water.

(b) For those coastal and open-ocean regions in which desert-derived crustal dusts dominate the aerosol population, and in which EF_{crust} values for all elements (i.e. including the AEE) are relatively low, considerably smaller amounts of the relatively soluble elements will enter the dissolved phase on contact with sea water. In these areas, however, the deposition fluxes of the atmospheric elements can be relatively very high, so that the soluble fractions may become significant, especially in those regions that receive dust pulses (see Sec. 4.1.4.1).

(c) Over open-ocean regions the solubilities of elements from aerosols will depend on the extent to which components from various sources, e.g. anthropogenic and crustal, are mixed together in the total particle population. The estimates for the solubilities of elements from these mixed aerosols given in Table 6.9b represent an attempt to assess average values from the published data.

It must be stressed, however, that the aerosol solubility data given in Table 6.9b should be regarded as no more than first-order approximations.

6.3 Hydrothermal fluxes to the oceans

Attempts to assess the global impact of basalt–sea water reactions on the chemistry of the World Ocean are still in their infancy, but in recent years progress has been made towards developing frameworks within which the various fluxes involved can be evaluated. One such framework was adopted by Thompson (1983a). In this, four types of basalt–sea water reactions were classified in terms of their temperature and water : rock ratios, and the fluxes associated with each one was then estimated using a combination of field data and experimental observations. In making the estimates the author assessed the changes in composition of the basalt samples, relative to their precursor material, as a function of age to calculate an **annual mass exchange** for individual components. **Fluxes** were then derived from these mass exchange data by making a series of assumptions about the total volume of basalt that undergoes reaction with sea water. The four types of basalt–sea water reactions are described below.

(a) **Those involving surface basement rocks:** low temperature, high sea water : rock ratios. These reactions are typical of those that occur at the surface when the basalt basement is in contact with sea water. Thompson (1983b) made use of various rock–sea water reaction data to calculate the annual mass exchange rates for this type of basalt–sea water reaction. In order to calculate annual fluxes from these exchange rates, the following assumptions were made: (i) new crust is formed at a rate of 2.94 $km^2\ yr^{-1}$ to a depth of 6 km; (ii) the upper 10 m of this crust ($\sim$ 0.1%) is involved in exchange reactions, which are mimicked by experimental high water : rock ratios; and (iii) the exchange reactions last for 80 Ma. The surface basement rock fluxes derived from these various data are given in Table 6.10.

(b) **Those involving deeper basement rocks:** low temperature, low water : rock ratios. These reactions take place within the basement away from the centres of sea-floor spreading. They are apparently not very different from those that affect surface basalts, but they occur over a much shorter period. Thompson (1983b) used basalt–sea water reaction data obtained at two Deep Sea Drilling Project (DSDP) sites to calculate mass chemical exchanges, and to estimate the fluxes from these it was assumed that 500 m of the crust were involved in the exchange and that it was complete in 3 Ma. The fluxes derived in this manner are given in Table 6.10.

(c) **Those taking place at the mid-ocean ridge flanks:** medium temperatures, medium water : rock ratios. These reactions are thought to be typical of those occurring during the so-called passive hydrothermal

Table 6.10 Hydrothermal fluxes between sea water and oceanic rock[a]

	Flux (10^{14} g yr^{-1})				Flux (10^{10} g yr^{-1})			
	Si	Ca	Mg	K	B	Li	Rb	Ba
CASE A								
Surface basement	-0.006	-0.045	-0.03	+0.013	+0.45	+0.44	+0.14	+0.43
Deeper basement	-0.52	-0.082	-0.26	+0.09	+2.69	+2.42	+1.37	+2.73
Ridge flanks	-0.2	-0.47	-0.11	+0.22	+5.12	+3.7	+4.23	+1.1
Ridge axis	-0.87	-1.3	+1.87	-0.49	(-)0[b]	-111	-20.5	-46
Total net basement flux	-1.6	-1.9	+1.47	-0.17	+8.26	-104.54	-14.76	-41.74
River flux	-1.99	-4.88	-1.33	-0.47	-47.0	-9.4	-3.2	-137.3
Net basement flux as a % of river flux	80.4	38.9	110.5	23.0	17.6	1112	461	30.4
CASE B								
Surface basement	-0.006	-0.045	-0.03	+0.013	+2.45	+0.44	+0.14	+0.43
Deeper basement	-0.52	-0.082	-0.26	+0.09	+2.69	+2.42	+1.37	+2.73
Ridge flanks	-0.2	-0.47	-0.11	+0.22	+5.12	+3.7	+4.23	+1.1
Ridge axis	-0.087	-0.13	+1.0	-0.049	(-)0[b]	-11.1	-2.05	-4.6
Total net basement flux	-0.82	-0.73	+0.6	+0.27	+8.26	-4.54	+3.69	-0.34
River flux	-1.99	-4.88	-1.33	-0.74	-47.0	-9.4	-3.2	-137.3
Net basement flux as a % of river flux	41.2	14.9	45.1	36.5	17.6	48.3	115.3	0.2

[a] After Thompson (1983a).
[b] Boron is not found in Galapagos vent fluids.
\+ = gained by rock (rock sink).
\- = gained by sea water (source for sea water).

circulation phase, where the temperature of the water decreases away from the ridge crests. Thompson (1983b) again used DSDP data for the calculation of this type of mass chemical exchange, and to derive the associated fluxes it was assumed that the reactions affect the upper 200 m of the crust (~ 3% of the new crust) for a period of 3 Ma. The fluxes calculated on this basis are given in Table 6.10.

(d) **Those taking place at the mid-ocean ridge axes:** high temperature, low water : rock ratios. These are associated with the dramatic venting of hydrothermal solutions at the spreading centres during the active phase of hydrothermal activity. The first attempt to estimate global

fluxes from this type of hydrothermal venting was made by Edmond *et al.* (1979). To do this the authors extrapolated the currently best available data, which were obtained from the low-temperature Galapagos Spreading Centre (GSC) system, to determine the composition of the 350°C high-temperature hydrothermal end-member and combined this with global heat flux data estimated from hydrothermal ^{3}He : transported heat ratios to derive global hydrothermal fluxes for those elements that behaved in a conservative manner during the mixing of hydrothermal solutions and sea water. A summary of the ridge crest hydrothermal flux data obtained from the GSC system is given in Table 6.10, together with those for fluvial fluxes. However, a number of authors (see e.g. Wolery 1979, Hart & Strudigel 1982) have suggested that the GSC-derived fluxes may be too high, perhaps even by an order of magnitude. For this reason, Thompson (1983b) used two approaches in assessing the magnitude of the hydrothermal ridge crest fluxes: *case A*, in which the fluxes derived by Edmond *et al.* (1979a) were used directly; and *case B*, in which the fluxes were reduced by an order of magnitude (except that for Mg, which was reduced by only 45%). The resulting flux data are given in Table 6.10.

Hydrothermal activity can act as either a source or a sink term in marine geochemistry, and it is apparent from the various factors discussed above that the type of basalt–sea water reaction that takes place is mainly a function of the temperature and the water : rock ratio at the contact site. The magnitudes of the hydrothermal fluxes, relative to those from river inputs, are discussed in the following section.

6.4 Relative mangitudes of the primary fluxes to the oceans

In the three preceding sections an attempt has been made to estimate the net fluxes of material delivered to the oceans from the major global-scale primary sources. These sources are river run-off, atmospheric deposition and hydrothermal exhalations; although it must also be remembered that hydrothermal activity can also act as a sink for some dissolved components as well as a source for others.

For many years it was thought that the oceans were a fluvially dominated system. However, this view has changed dramatically over the past few years as the importance of hydrothermal activity at the spreading ridges has become increasingly recognized. A general comparison between the relative importance of the combined hydrothermal fluxes (i.e. high- and low-temperature processes) and fluvial fluxes can be made using the data in Table 6.10 (which employs the case A and case B

approach outlined in Sec. 6.3), together with other findings given in the literature (see e.g. Edmond *et al.* 1979, 1982, 1985, Honnorez 1983, Measures & Edmond 1983). The low-temperature GSC data used in these general flux comparisons were extrapolated to estimate the composition of the high-temperature venting fluid. Such an extrapolation could only be applied to elements that behaved conservatively in the hydrothermal system, and so excluded the ore-forming metals. Subsequently, however, data have been obtained for black smoker hydrothermal systems, which vent high-temperature fluids directly to the sea water. For example, Von Damm *et al.* (1985) made a detailed study of a series of high-temperature venting fluids in the 21°N EPR region (see Sec. 5.1). The data obtained allowed estimates to be made of the hydrothermal injection of the ore-forming metals (e.g. Mn, Fe, Co, Cu, Zn, Cd and Pb) to the oceans; this was not possible for the GSC since a large proportion of the metals was precipitated at depth within the crust (see Sec. 5.1). A more detailed comparison between high-temperature ridge crest hydrothermal and fluvial fluxes can therefore be made using the data provided by Von Damm *et al.* (1985), and this is presented in Table 6.11. However, it must

Table 6.11 Relative magnitudes of high-temperature (~ 350°C) ridge crest hydrothermal and fluvial fluxes (moles yr^{-1})[a]

Component	Hydrothermal flux (21°N EPR)	Fluvial flux
Li	1.2 ---> 1.9 x 10^{11}	1.4 x 10^{10}
Na	-8.6 ---> 1.9 x 10^{12}	6.9 x 10^{12}
K	1.9 ---> 2.3 x 10^{12}	1.9 x 10^{12}
Rb	3.7 ---> 4.6 x 10^{9}	5.0 x 10^{6}
Be	1.4 ---> 5.3 x 10^{6}	3.3 x 10^{7}
Mg	-7.5 x 10^{12}	5.3 x 10^{12}
Ca	2.4 ---> 15 x 10^{11}	1.2 x 10^{13}
Sr	-3.1 ---> + 1.4 x 10^{9}	2.2 x 10^{10}
Ba	1.1 ---> 2.3 x 10^{9}	1.0 x 10^{10}
SiO_2	2.2 ---> 2.8 x 10^{12}	6.4 x 10^{12}
Al	5.7 ---> 7.4 x 10^{8}	6.0 x 10^{10}
Mn	1.0 ---> 1.4 x 10^{11}	4.9 x 10^{9}
Fe	1.1 ---> 3.5 x 10^{11}	2.3 x 10^{3}
Co	3.1 ---> 32 x 10^{6}	1.1 x 10^{8}
Cu	0 ---> 6.3 x 10^{9}	5.0 x 10^{9}
Zn	5.7 ---> 15 x 10^{9}	1.4 x 10^{10}
Ag	0 ---> 5.4 x 10^{6}	8.8 x 10^{7}
Cd	2.3 ---> 26 x 10^{6}	-
Pb	2.6 ---> 5.1 x 10^{7}	1.5 x 10^{8}
As	0 ---> 6.5 x 10^{7}	7.2 x 10^{8}
Se	0 ---> 1.0 x 10^{7}	7.9 x 10^{7}

[a] Data from Von Damm et al. (1985).

be stressed that there are still difficulties in estimating the *net* hydrothermal fluxes of these metals from the EPR system because an unknown proportion of them may have been lost in the formation of the venting chimneys and in the black smoker precipitates that are debouched into sea water.

One of the main problems in estimating the global ocean importance of hydrothermal exhalations lies in assessing the extent to which they are dispersed away from the venting centres. Edmond *et al.* (1982) combined data on the distributions of hydrothermally derived sediments and ridge-produced ^{3}He to demonstrate that the dispersal of hydrothermal solutions is controlled by the global oceanic circulation at mid-water depths. Manganese can also be used as a hydrothermal tracer. For example, Klinkhammer (1980) used dissolved Mn profiles to show the existence of hydrothermal vents on the EPR. He also reported anomalously high dissolved Mn concentrations in the bottom waters of the Guatemala Basin ~1000 km from the crest of the EPR. Hydrographic evidence suggested that this anomaly is a hydrothermal signal, thus providing evidence of the dispersal of hydrothermal solutions over large distances. However, the extent to which the dispersal takes place may be controlled by the topography of the ridge where the venting systems are found. In this context, Klinkhammer *et al.* (1985) employed dissolved Mn as a tracer for hydrothermal activity on the Mid-Atlantic Ridge between 11°N and 26°N, and found that the plumes were confined to the rift valley and did not spill over into the adjacent deep ocean basins. Clearly, therefore, the dispersal of hydrothermal plumes can vary considerably, depending on local conditions, and as a result of ridge geometry the solutions may be dispersed over much greater distances in the Pacific than in the Atlantic (see Sec. 11.5).

The general findings that can be derived from hydrothermal–fluvial flux comparisons of the type given in Tables 6.10 and 6.11 can be summarized as follows:

(a) Both Li and Ba are leached from basalts at high temperatures, and although the rock acts as a sink at low temperatures the amounts released during ridge crest hydrothermal activity are sufficient to make basalt–sea water reactions a net source of the two elements to sea water. For Li, the net basalt–sea water flux is about 10 times the river flux (case A) and about 60% of it at the lower estimate (case B); for Ba the basalt–sea water flux is about the same as the river flux (case A), but for case B it constitutes $< 1\%$ of the river input.
(b) Both K and Rb are leached from basalt at high temperatures; for example, for case A, hydrothermal activity supplies about seven times as much Rb to the oceans as does river run-off. However, the two elements are taken out of solution during low-temperature

weathering processes to the extent that for case B the basalt–water reactions act as a net sink for both elements.

(c) The venting of hydrothermal solutions delivers at least an order-of-magnitude more Mn to sea water than does river transport (see e.g. Collier & Edmond 1984, and Table 6.11).

(d) Oceanic rock is a source for Si and Ca in reactions that take place at both high and low temperatures. For Si the net basalt–sea water flux makes up between 80% (case A) and ~ 40% (case B) of the river input; for Ca it comprises between ~ 40% (case A) and ~ 15% (case B) of the river supply.

(e) Hydrothermal ridge crest activity is a sink for Mg, but during low-temperature weathering the rock acts as a source for the element. However, in net terms basalt–sea water reactions are still a major sink for Mg since the amount released during low-temperature processes is only ~ 20% of that taken up in hydrothermal activity at the ridge crests (case A) or ~ 40% (case B). Even at the lower (case B) estimate the basalt–sea water sink accounts for ~ 50% of the river flux transported to the oceans, which is close to the amount required to balance the oceanic magnesium budget according to the mass-balance calculation made by Drever (1974) (see also Sec. 17.2). Hydrothermal processes therefore act as a sink for Mg, the quantity removed from sea water being of the same order of magnitude as that carried in by rivers.

(f) Beryllium is strongly enriched in hydrothermal fluids relative to ambient sea water and the hydrothermal flux has been estimated to be as much as ~ 50% of that delivered to the deep ocean by rivers, after correction for an estuarine retention of > 80% (Measures & Edmond 1983).

(g) It is evident that, in addition to Mn, large amounts of other ore-forming metals, such as Fe, Zn, Cu and Pb, are leached from the crust during hydrothermal activity (see Table 6.11), although they are mainly precipitated on mixing with sea water either in the vents or on the sea floor.

It is apparent, therefore, that although there are uncertainties over the estimates of the primary net fluxes involved, hydrothermal activity is an important source or sink term in oceanic chemistry. However, there are considerable problems inherent in estimating both the magnitudes of the hydrothermal fluxes and the extent to which they are dispersed about the oceans. For example, the global hydrothermal fluxes from ridge crest hot spring venting systems have been estimated from the oceanic budget of ^{3}He, which has its only significant source in the mantle, and there is considerable evidence that the major source of the ^{3}He is, in fact, derived from these axial systems and not from the low-temperature circulation

associated with ridge flank systems. As Von Damm *et al.* (1985) have pointed out, estimates of the global hydrothermal heat flux that accompanies the ^{3}He injection are within the range of estimates for the total anomaly in conductive heat loss; however, this heat loss includes not only the young crust of the ridge axial zone but also the older crust of the flanks, and current estimates suggest that only about one-sixth of the total convective heat loss is from the young crust. Thus, there are differences in the geophysical and geochemical estimates of the global ridge crest hydrothermal flux, and therefore in the effect that the flux has on the geochemical cycle of the oceans. These geochemical–geophysical inconsistencies are particularly evident in estimates of the ridge crest hydrothermal sources for K and B. For example, Spivack & Edmond (1987) showed that flux estimates based on the ^{3}He flux and the average B enrichment in hydrothermal fluids yielded a high-temperature hydrothermal flux that was nine times higher than that based on mass-balance calculations utilizing the B concentrations in fresh basaltic glass and crustal generation rates. This discrepancy was similar to that found for K (Von Damm *et al.* 1985) and that for ^{3}He itself. According to Spivack & Edmond (1987) it suggests either that the process of crustal generation is not fully understood or that basalts that have previously been enriched in B and K by low-temperature alteration processes (which are sinks for both elements) have been involved in the high-temperature reactions. In addition to the problems discussed above, much of the controversy regarding the magnitude of hydrothermal fluxes has surrounded the question of the actual areal extent, and therefore the global importance, of the present-day hydrothermal systems. For example, it was first thought that the black smoker type of venting systems were confined to fast-spreading ridges, e.g. those found on the EPR. It was pointed out in Section 5.1, however, that more recently the first black smokers have been identified on a slow-spreading area of the Mid-Atlantic Ridge (Rona *et al.* 1986). Further, Klinkhammer *et al.* (1985) identified buoyant Mn-rich plumes associated with these black smokers, which gave rise to large Mn anomalies 380 m above the sea floor. These plumes were similar to those found over the EPR black smoker region, and clearly indicate the ocean-wide important of high-temperature hydrothermal venting systems.

On the basis of our present knowledge, therefore, it is still very difficult to assess the relative strengths of the primary sources of most of the trace elements in sea water, especially those which may have a significant hydrothermal source. Despite this constraint, a number of authors have attempted to make very general comparisons between the strengths of the fluvial and atmospheric fluxes for some dissolved trace elements. These two fluxes are of special interest because they both deliver material directly to the surface ocean, where it can become involved in biogeochemical reactions in the particle-rich, biologically active, euphotic

zone. In order to discuss the fluvial–atmospheric source comparison it is convenient to divide the ocean into coastal and open-ocean waters, since the source signals to the two regions vary considerably in strength.

COASTAL REGIONS There have been a number of attempts to evaluate the relative contributions made by fluvial and atmospheric transport to the total trace metal budgets in the coastal zone. A number of these have been summarized by Windom (1981) and Buat-Menard (1983), and some of the relevant data are given in Table 6.12a. Because most of the particulate matter transported by rivers is trapped in the estuarine environment (see Sec. 6.1.2), Windom (1981) confined his fluvial fluxes to the dissolved phase. However, the atmospheric fluxes that he presented were for the total aerosol population. In order to make the comparison between the fluvial and atmospheric inputs more viable, the sea water-soluble fractions of the atmospheric inputs have been calculated on the

Table 6.12 Relative fluvial and atmospheric fluxes to some coastal oceanic regions[a]

(a) Ratio of total atmospheric flux to fluvial flux.

Element	South Atlantic Bight	New York Bight[a]	North Sea[a]	Western Mediterranean[b]
Fe	5.8	6.4	1.7	-
Mn	0.6	-	0.8	-
Cu	1.9	-	1.9	-
Ni	1.7	-	1.3	-
Pb	9.5	20	6.8	6.2
Zn	2.3	3.1	1.9	0.8
Cd	2.7	3.1	1.1	-
As	2.1	1.0	1.7	-
Hg	22	-	2.1	0.8

[a] Data from Windom (1981). [b] Data from Buat-Menard (1983).

(b) Estimated fluvial and soluble atmospheric fluxes to the South Atlantic Bight (units, 10^6 g).

Element	Fluvial flux[a]	Total atmospheric flux[a]	Soluble atmospheric flux[c]	Ratio: soluble atmospheric flux to fluvial flux
Fe	950	5500	413	0.43
Mn	91	57	26	0.29
Cu	110	210	63	0.57
Ni	220	370	185	0.85
Pb	65	620	310	4.8
Zn	310	710	497	1.6
Cd	3	8	6.8	2.3

[a] Data from Windom (1981). [c] Solubility data from Table 6.9.

basis of the solubilities to be expected from polluted aerosols of the type thought to be deposited over the coastal zones identified; these data are given in Table 6.12b. Even after making this correction, it is apparent that the atmospheric fluxes of Pb, Zn and Cd exceed their fluvial fluxes, and that for Ni the two fluxes are similar. In coastal regions, therefore, solubilization from atmospheric particulates can play a substantial role in governing the dissolved trace metal burden of the surface sea waters.

THE OPEN OCEAN Chester & Murphy (1988) made an estimate of the relative magnitudes of the fluvial and atmospheric sources of a series of dissolved elements to the World Ocean. To make the comparison viable both the fluvial and atmospheric fluxes were expressed in terms of a supply to the sea surface ($\mu g\ cm^{-2}\ yr^{-1}$). To make these estimates the following data were used. (i) For the fluvial inputs the authors employed net global-scale fluxes, calculated using data derived from a combination of the average river-water concentrations given in Table 3.4 and the independently obtained estuarine effluxes listed in Table 6.6, assuming that the total global run-off was spread in an even layer over the World Ocean; the net fluxes are reproduced in Table 6.13. (ii) For the atmospheric inputs it was assumed that the deposition fluxes given in the literature for the tropical North Atlantic, the North Pacific and the South Pacific (Table 6.8) offered a representative cross section of those affecting all marine regions, and a weighted average deposition obtained from them was extrapolated to the whole ocean surface; this was then adjusted for the average sea water solubility of the elements from marine aerosols, to yield the effective dissolved atmospheric flux. The atmospheric fluxes obtained in this way are reproduced in Table 6.13. Collier & Edmond (1984) also made a general comparison between fluvial and atmospheric oceanic inputs of a number of components, and some of their data are included in Table 6.13.

From this first order comparison it can be seen that for Al, Mn and Cu the dissolved fluvial fluxes to the global ocean surface exceed those from the atmosphere by an order of magnitude. For Zn and Pb, however, the dissolved atmospheric fluxes dominate the input to the surface ocean. The fluxes given in Table 6.13 are for the global ocean. However, the concentrations of elements, and therefore their deposition fluxes to the sea surface, vary both temporally and spatially in the marine atmosphere. These varitions can range over several orders of magnitude, and in an attempt to take account of them Chester & Murphy (1988) calculated atmospheric deposition fluxes on a regional basis. Fluvial fluxes were also estimated in this way, and the data are listed in Table 6.14. From this table, it can be seen that atmospheric deposition has the most influence on the surface waters of the North Atlantic, and the least on those of the

Table 6.13 Net fluvial and atmospheric fluxes to the global sea surface[a] (units, μg cm^{-2} yr^{-1})

Element	Net global fluvial dissolved flux		Net global total atmospheric input		Estimated average sea water solubility from aerosols	Net global dissolved atmospheric flux
	Chester & Murphy (1988)	Collier & Edmond (1984)	Chester & Murphy (1988)	Collier & Edmond (1984)		
Al	0.27	0.13-0.67	1.85	0.27-5.4	5%	0.088
Fe	0.085	<0.73	1.0	1.12-3.35	7.5%	0.075
Mn	0.085	0.093	0.021	0.016-0.044	35%	0.0074
Ni	0.0082	0.0035	<0.02	0.003	40%	<0.008
Co	0.0021	-	0.00068	-	22.5%	0.00015
Cr	0.0052	-	<0.014	-	10%	<0.0014
V	0.010	-	<0.010	-	25%	<0.0028
Cu	0.018	0.019	0.010	0.00064 - 0.0095	30%	0.0033
Pb	0.001	-	0.074	-	30%	0.022
Zn	0.0079	<0.0065	0.055	0.022-0.013	45%	0.025
Cd	0.00088	0.00022	<0.00096	0.0023	80%	<0.00077

[a] From Chester & Murphy (1988).

South Pacific. In terms of open-ocean areas, therefore, it is the North Atlantic that receives the highest input of trace metals from the atmosphere. Under these extreme conditions the dissolved atmospheric fluxes for Mn, Ni, Co, Cr, V and Cu are all an order of magnitude less than their dissolved fluvial fluxes. For Al, Fe and Cd the two fluxes are the same order of magnitude, but for Zn and Pb the atmospheric fluxes are dominant.

The fluxes given in Table 6.13 and 6.14 are essentialy very crude. In addition, they do not include data for hydrothermal inputs, and even when such data do become available their global impact will be difficult to establish. However, hydrothermal exhalations have their principal effects on mid-depth waters, and in view of this the flux estimates given in the tables do allow a number of generalities to be made regarding the supply of elements to open-ocean *surface* waters. These generalities are

Table 6.14 Atmospheric dissolved versus fluvial dissolved inputs to regions of the World Ocean[a] (units, μg cm^{-2} yr^{-1})

Element	Oceanic region					
	North Atlantic		North Pacific		South Pacific	
	Fluvial dissolved flux[b]	Atmospheric dissolved flux	Fluvial dissolved flux	Atmospheric dissolved flux	Fluvial dissolved flux	Atmospheric dissolved flux
Al	0.56	0.25	0.24	0.09	0.12	0.0066
Fe	0.18	0.24	0.076	0.062	0.038	0.0035
Mn	0.18	0.025	0.076	0.004	0.038	0.0013
Ni	0.017	0.008	0.0074	-	0.0037	-
Co	0.0044	0.00061	0.0019	0.00004	0.0009	0.000006
Cr	0.011	0.0014	0.0047	-	0.0023	-
V	0.022	0.0043	0.0094	0.0017	0.0047	-
Cu	0.037	0.0075	0.016	0.0021	0.0079	0.0013
Pb	0.0022	0.093	0.0009	0.0022	0.0005	0.0004
Zn	0.016	0.059	0.0071	0.029	0.0035	0.0026
Cd	0.0018	0.0016	0.0008	0.00023	0.0004	-

[a] From Chester & Murphy (1988).

[b] No attempt has been made to adjust the North Atlantic fluvial flux for European and N. American anthropogenic inputs.

illustrated below with reference to a selection of process-orientated elements. These elements, which have been selected to illustrate specific processes that control the distributions of components in the water column, are described in detail in Chapter 11. At this stage, however, it is useful to introduce the concepts of scavenging-type and nutrient-type elements, since their distributions in the water column are controlled by different source inputs.

THE SCAVENGING TYPE ELEMENTS The scavenging-type elements have vertical distribution profiles in the oceans, exhibiting a surface enrichment and a subsurface depletion. It is the scavenging-type elements that should therefore retain the most identifiable open-ocean surface water fingerprints from atmospheric deposition, and this is illustrated below for Al, Mn and Pb.

(a) **Aluminium.** On a whole-ocean basis, the supply of dissolved Al from atmospheric sources makes up ~ 30% of the fluvial flux using the estimate provided by Chester & Murphy (1988). On a regional basis,

atmospheric deposition yields between ~ 45% (North Atlantic) and ~ 5.5% (South Pacific) of the fluvial flux. However, the estimates were based on an estuarine retention of 50% of the gross river flux, and according to data summarized by Maring & Duce (1987) a large fraction, perhaps even most, of the dissolved Al that does escape the estuarine zone is lost via the deposition of biogenic silica to coastal sediments. The authors conclude, therefore, that the fluvial supply of dissolved Al has *little* effect on the dissolved Al in open-ocean waters. As a result, atmospheric deposition must be invoked as the principal source for dissolved Al in the surface waters of the open ocean. Orians & Bruland (1985) have shown that surface water concentrations of dissolved Al in the North Atlantic are around eight times higher than in the North Pacific and relate this to an atmospheric source. From the data in Table 6.14, it would appear that the atmospheric deposition of dissolved Al to the North Atlantic is about four times higher than that to the North Pacific. However, intermittent dust pulses (see Sec. 4.1.4.1), which bring in large quantities of crustal material to the region underlying the Northeast Trades, may raise the average input of dissolved Al to the North Atlantic (see e.g. Kremling 1985). For example, on the basis of data given by Prospero (1981) it is clear that over parts of the tropical North Atlantic the deposition of mineral dust could lead to a dissolved Al input of ~ 1 to ~ 6 $\mu g\ m^{-2}\ yr^{-1}$. Orians & Bruland (1985) demonstrated that at a total atmospheric flux of 3.6 $\mu g\ m^{-2}\ yr^{-1}$ and a seawater solubility of 5% from mineral particles, the input of dissolved Al (0.18 $\mu g\ m^{-2}\ yr^{-1}$) (cf. the estimate of 0.09 in Table 6.13) is consistent with the levels in the surface waters. Maring & Duce (1987) also concluded that the dissolution of Al from atmospheric particles constituted the major source of dissolved Al in the open-ocean North Pacific. However, Measures *et al.* (1984) have suggested that fluvial inputs of dissolved Al may predominate in the tropical eastern Pacific, and have pointed out that considerably more work is required before the mechanisms that control the distribution of Al in the oceans are fully understood. It may be concluded, therefore, that the supply of dissolved Al to open-ocean surface waters is at least strongly influenced by the atmospheric deposition of mineral aerosols and the subsequent dissolution of Al into sea water.

(b) **Manganese.** On a whole-ocean basis, the surface water dissolved atmospheric Mn flux makes up between ~ 8 and ~ 9% of the dissolved fluvial flux. On a regional basis, however, the atmospheric dissolved Mn flux rises to ~ 14% of the fluvial run-off in the North Atlantic. There is no doubt that rivers supply dissolved Mn to the coastal regions, but some lines of evidence suggest that only a small fraction of this Mn is advected to open-ocean regions in the North

Atlantic. For example, Kremling (1983) showed that dissolved Mn, and certain other elements, exhibited a very sharp decrease in concentration at the shelf edge off northwest Europe and do not reach open waters. Statham & Burton (1986) therefore concluded that the importance of fluvial inputs of dissolved Mn to the open ocean must be considered to be uncertain. These authors carried out a survey of dissolved Mn in the North Atlantic and reported that the highest concentrations in surface waters were found in those latitudes that receive large inputs of Saharan dust. This led them to suggest that atmospheric inputs are the most significant source of dissolved Mn to the surface waters in these areas. Data to support this conclusion have been provided by Kremling (1985), who carried out a survey of total dissolvable Mn (TDM) in surface waters collected on a north–south Atlantic transect and showed the presence of elevated concentrations in the region lying between ~ 10°N and ~ 30°N (see Fig. 6.3), which was assumed to arise from dissolution of Mn from Saharan dust deposition to the sea surface. However, atmospheric sources do not always dominate the supply of dissolved Mn to the mixed layer. For example, Landing & Bruland (1987) found that in the North Pacific surface water concentrations of dissolved Mn were elevated in a salinity maximum associated with the North Pacific Equatorial Current, and suggested that this resulted from advection from the eastern boundary of the ocean where dissolved Mn can be supplied from reducing shelf sediments, i.e. a secondary recycled oceanic source. In the central gyre, however, there was evidence for an aeolian input of dissolved Mn, and Klinkhammer & Bender (1980) concluded that desorption from atmospherically deposited mineral particles is the most important overall source of dissolved Mn to the surface waters in the Pacific.

(c) **Lead.** It can be seen from Table 6.13 that the input of Pb to the surface ocean is dominated by atmospheric deposition. This is apparent in the surface water distribution of Pb between the major

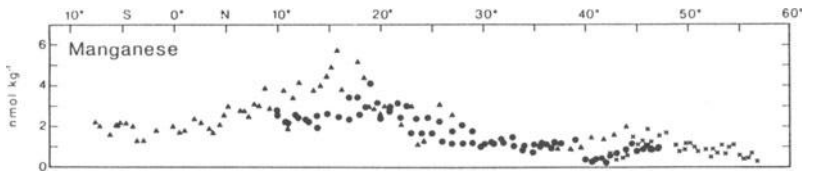

Figure 6.3 Total dissolvable manganese (TDM) concentrations as a function of latitude in Atlantic surface waters (from Kremling 1985). The figure shows the elevated concentrations of TDM between 10°N and 20°N, which result from the dissolution of Mn from atmospherically transported particulates. The data are from two different cruises and variations in the TDM concentrations probably reflect variations in the input strength of the atmospheric particulate flux, e.g. in response to dust pulses.

oceans, which strongly reflects the magnitude of the atmospheric inputs; e.g. concentrations in the mixed layer of the North Atlantic are two to three times higher than those in the North Pacific. Further, in the North Pacific the highest concentrations of dissolved Pb are found in the central gyre, which can only be explained in terms of an atmospheric input (see Sec. 11.4).

THE NUTRIENT-TYPE ELEMENTS The nutrient-type elements have vertical profiles that exhibit a surface depletion and a subsurface enrichment, and are maintained by the involvement of the elements in biological recycling processes. For this type of element, therefore, the atmospheric fingerprints will be more difficult to identify in open-ocean surface waters because of surface water uptake in biological processes and supply from below by upwelling. This is demonstrated below with respect to copper.

(a) **Copper.** Copper is not strictly a nutrient-type element since it also undergoes scavenging in deep waters. However, it does exhibit a surface depletion characteristic of the nutrient-type elements and will serve to illustrate the processes that affect a nutrient-type element in open-ocean surface waters. Dissolved Cu can be supplied to open-ocean surface waters by a variety of transport mechanisms; these include river run-off, advection from shelf waters following release from bottom sediments, atmospheric deposition, and upwelling following regeneration from biological material. There have been a number of attempts to deconvolute these various dissolved Cu source signals. For example, Boyle *et al.* (1981) showed that dissolved Cu is significantly enriched in coastal, relative to open-ocean, waters, and concluded that this arises because much of the dissolved Cu injected into the shelf regions from both river run-off and diffusion from sediments can be prevented from escaping to the open ocean by being caught in a coastal nutrient trap. Some of the Cu does escape, however, and can be advected for considerable distances into open-ocean waters. However, the remobilization of elements from shelf sediments may be sporadic in nature, and Bruland (1980) concluded that direct horizontal transport from coastal regions was not an important source for Cu, and a series of other elements, in the open-ocean North Pacific. The author suggested, therefore, that the main sources for these elements to the open-ocean surface waters were atmospheric deposition and vertical mixing with deep water, and he attempted to estimate the magnitudes of the fluxes associated with the two supply mechanisms. The data for Cu, Zn, Ni and Cd are given in Table 6.15. It can be seen from this table that the two fluxes vary in importance from one element to another. (i) For Cd and Ni, the atmospheric flux is around an order of magnitude less than the upwelling flux. For these two elements, therefore, although atmos-

Table 6.15 Atmospheric and vertical mixing fluxes of some trace elements to the surface waters of the eastern North Pacific[a] (units, nmol cm^{-2} yr^{-1})

Element	Atmospheric flux	Vertical mixing flux
Cd	0.018	0.14
Zn	0.40	0.15
Ni	0.043	0.80
Cu	0.16	0.21
Pb[b]	0.18	-0.01

[a] Data from Bruland (1980).

[b] Pb is enriched in surface waters relative to deep water and thus has a negative vertical mixing term.

pheric deposition is the principal *primary* surface water source, it is overwhelmed by Ni and Cd supplied from below by upwelling. (ii) For Cu the two fluxes are approximately equal. (iii) For Zn, the atmospheric flux exceeds the upwelling flux by a factor of around 3. It may be concluded, therefore, that although atmospheric deposition may be the principal primary source of the nutrient-type elements to open-ocean surface waters, the actual concentrations of the elements can be severely modified, and sometimes completely dominated, by secondary sources arising from the upwelling flux.

6.5 Relative magnitudes of the primary fluxes to the oceans: summary

(a) The major primary sources of both particulate and dissolved components to the oceans on a global scale are river run-off, atmospheric deposition and hydrothermal exhalations, with glacial sources being predominant in some polar regions.

(b) Of the major primary sources, river run-off and atmospheric deposition deliver their loads to the surface ocean: rivers to the ocean margins, and the atmosphere to the whole ocean surface. On a global basis, fluvial sources are generally greater than those resulting from atmospheric deposition, although there are some exceptions to this (e.g. atmospheric deposition dominates the input of Pb to almost the whole surface ocean). However, retention in the estuarine and coastal zones can mean that the direct input of some fluvially transported components to the open ocean is less than that from atmospheric deposition. This atmospheric deposition retains its

strongest surface water fingerprints for the scavenging-type elements.

(c) Hydrothermal activity can act as a source for some components and a sink for others. When it acts as a source, hydrothermal activity delivers components to mid-depth and bottom waters, and although the extent to which these components are globally dispersed is not yet known with certainty it is now recognized that for some elements hydrothermal inputs can match, and sometimes exceed, fluvial inputs.

We have now identified the principal primary sources that supply material to the World Ocean, and have described the pathways along which the material travels in order to enter the sea water reservoir. In the following sections, we will describe the physical and chemical nature of this reservoir, and discuss the mechanisms that keep it in motion.

References

Arimoto, R., R.A. Duce, B.J. Ray, A.D. Hewitt & J. Williams 1987. Trace elements in the atmosphere of American Samoa: concentrations and deposition to the tropical South Pacific. *J. Geophys. Res.* **92,** 8465–79.

Arimoto, R., R.A. Duce, B.J. Ray & C.K. Unni 1985. Atmospheric trace elements at Enewetak Atoll: transport to the ocean by wet and dry deposition. *J. Geophys. Res.* **90,** 2391–408.

Arnold, M., A. Seghaier, D. Martin, P. Buat-Menard & R. Chesselet 1982. Geochimie de l'aerosol marin au-dessus la Mediterranee occidentale. *CIESM J. Etud. Pollut. Mar. Mediterr.* **VI,** 27–37.

Bewers, J.M. & P.A. Yeats 1977. Oceanic residence times of trace metals. *Nature* **258,** 595–8.

Boyle, E.A., R. Collier, A.T. Dengler, J.M. Edmond, A.C. Ng & R.F. Stallard 1974. On the chemical mass-balance in estuaries. *Geochim. Cosmochim, Acta* **38,** 1719–28.

Boyle, E.A., S.S. Huested & S.P. Jones 1981. On the distribution of copper, nickel and cadmium in the surface waters of the North Atlantic and North Pacific Ocean. *J. Geophys. Res.* **86,** 8048–66.

Bruland, K.W. 1980. Oceanographic distributions of cadmium, zinc, nickel and copper in the North Pacific. *Earth Planet. Sci. Lett.* **77,** 176–98.

Bruland, K.W. & R.P. Franks 1983. Mn, Ni, Zn and Cd in the western North Atlantic. In *Trace metals in sea water*, C.S. Wong, E. Boyle, K.W. Bruland, J.D. Burton & E.D. Goldberg (eds), 395–414. New York: Plenum.

Bruland, K.W., K. Bertine, M. Koide & E.D. Goldberg 1974. History of metal pollution in southern California coastal zone. *Environ. Sci. Technol.* **8,** 425–31.

Buat-Menard, P. 1983. Particle geochemistry in the atmosphere and oceans. In *Air–sea exchange of gases and particles*, P.S. Liss & W.G.N. Slinn (eds), 455–532. Dordrecht: Reidel.

Buat-Menard, P. & R. Chesselet 1979. Variable influence of the atmospheric flux on the trace metal chemistry of oceanic suspended matter. *Earth Planet. Sci. Lett.* **42,** 399–411.

Cambray, R.S., D.F. Jeffries & G. Topping 1975. *An estimate of the input of atmospheric trace elements into the North Sea and the Clyde Sea (1972–73).* UK Atomic Energy

Authority, Harwell, Rep. AERE-R7733.
Campbell, J.A. & J.M. Yeats 1984. Dissolved Cr in the St. Lawrence estuary. *Estuar. Coastal Shelf Sci.* **19,** 513–22.
Chester, R. & K.J.T. Murphy 1988. Metals in the marine atmosphere. In *Heavy metals in the marine environment*, R. Furness & P. Rainbow (eds), in press. Boca Raton, Florida: CRC Press.
Chester, R., A.G. Griffiths & J.M. Hirst 1979. The influence of soil-sized atmospheric particulates on the elemental chemistry of the deep-sea sediments of the North Eastern Atlantic. *Mar. Geol.* **32,** 141–54.
Chester, R., F.J. Lin, A. Berry & K.J.T. Murphy 1988. The solubility of aerosol trace metals in sea water following dry mode deposition. In preparation.
Collier, R.W. & J.M. Edmond 1984. The trace element geochemistry of marine biogenic particulate matter. *Prog. Oceanogr.* **13,** 113–99.
Crecelius, E.A. 1980. The solubility of coal fly ash and marine aerosols in sea water. *Mar. Chem.* **8,** 245–50.

Dedkov, A.P. & V.I. Mozzherin 1984. *Eroziya i stok Nanosov na Zemle. Izdatatelstova Kazanskogo Universiteta.*
Degens, E.T. & V. Ittekkot 1985. Particulate organic carbon: an overview. In *Transport of carbon and minerals in major world rivers*, Part 3, E.T. Degens, S. Kempe & R. Herrera (eds), 7–27. Mitt.Geol.-Palont. Inst. Univ. Hamburg, SCOPE/UNEP, Sonderband 58.
Drever, J.I. 1974. The magnesium problem. In *The sea*, E.D. Goldberg (ed.), Vol. 5, 337–57. New York: Interscience.
Duce, R.A., G.L. Hoffman, B.J. Ray, I.S. Fletcher, G.T. Wallace, J.L. Fasching, S.R. Piotrowitcz, P.R. Walsh, E.J. Hoffman, J.M. Miller & J.L. Heffter 1976. Trace metals in the marine atmosphere: sources and fluxes. In *Marine pollutant transfer*, H. Windom & R.A. Duce (eds), 77–119. Lexington: Heath.

Edmond, J.M., C.I. Measures, R.E. McDuff, L.H. Chan, R. Collier, B. Grant, L.I. Gordon & J.B. Corless 1979. Crest hydrothermal activity and the balance of the major and minor elements in the ocean; the Galapagos data. *Earth Planet. Sci. Lett.* **46,** 1–18.
Edmond, J.M., A. Spivack, B.C. Grant, H. Ming-Hui, C. Zexiam, C. Sung & Z. Xiushau 1985. Chemical dynamics of the Changjiang estuary. *Cont. Shelf. Res* **4,** 17–30.
Edmond, J.M., K.L. Von Damm, R.E. McDuff & C.I. Measures 1982. Chemistry of hot springs on the East Pacific Rise and their effluent dispersal. *Nature* **297,** 187–91.

Figueres, G., J.M. Martin & M. Maybeck 1978. Iron behaviour in the Zaire estuary. *Neth. J. Sea Res.* **12,** 327–37.

GESAMP 1987. *Land/sea boundary flux of contaminants from rivers.* Paris: Unesco.

Hart, S.R. & H. Strudigel 1982. The control of alkalis and uranium in seawater by ocean crust alteration. *Earth Planet. Sci. Lett.* **58,** 202–12.
Hodge, V., S.R. Johnson & E.D. Goldberg 1978. Influence of atmospherically transported aerosols on surface ocean water composition. *Geochem. J.* **12,** 7–20.
Holeman, J.N. 1968. The sediment yield of major rivers of the world. *Water Resour. Res.* **4,** 734–47.
Honnorez, J. 1983. Basalt–seawater exchange: a perspective from an experimental viewpoint. In *Hydrothermal processes at seafloor spreading centres*, P.A. Rona, K. Bostrom, L. Laubier & K.L. Smith (eds), 117–98. New York: Plenum.

Ittekkot, V. 1988. Global trends in the nature of organic matter in river suspensions. *Nature* **332,** 436–8.

Jickells, T., A.H. Knapp & T.M. Church 1984. Trace metals in Bermuda rainwater. *J. Geophys. Res.* **89,** 1423–8.

Judson, S. 1986. Erosion of the land (What's happening to our continents?). *Amer. Scientist* **5,** 514–16.

Klinkhammer, G.P. 1980. Observations of the distribution of manganese over the East Pacific Rise. *Chem. Geol.* **29,** 211–26.

Klinkhammer, G.P. & M.L. Bender 1980. The distribution of manganese in the Pacific Ocean. *Earth Planet. Sci. Lett.* **46,** 361–84.

Klinkhammer, G.P., P. Rona, M. Greaves & H. Elderfield 1985. Hydrothermal manganese plumes in the Mid-Atlantic Ridge rift valley. *Nature* **314,** 727–31.

Kremling, K. 1983. Trace metal fronts in European shelf waters. *Nature* **303,** 225–7.

Kremling, K. 1985. The distribution of cadmium, copper, nickel, manganese and aluminium in surface waters of the open Atlantic and European shelf area. *Deep-Sea Res.* **32,** 531–55.

Landing, W.M. & K.W. Bruland 1987. The contrasting biogeochemistry of iron and manganese in the Pacific Ocean. *Geochim. Cosmochim. Acta* **51,** 29–43.

McDonald, R.L., C.K. Unni & R.A. Duce 1982. Estimation of atmospheric sea salt dry deposition: wind speed and particle size dependence. *J. Geophys. Res.* **87,** 1246–50.

Mahadevan, T., S. Sadasivan & U.C. Mishra 1982. Chemical composition of precipitation in tropical marine atmosphere around Indian subcontinent. *Sci. Total Environ.* **24,** 275–85.

Mantoura, R.F.C. & E.M.S. Woodward 1983. Conservative behaviour of riverine dissolved organic carbon in the Severn Estuary: chemical and geochemical implications. *Geochim. Cosmochim. Acta* **47,** 1293–309.

Maring, H.B. & R.A. Duce 1987. The impact of atmospheric aerosols on trace metal chemistry in open ocean surface waters. 1. Aluminium. *Earth Planet. Sci. Lett.* **84,** 381–92.

Martin, J.-M. & M. Maybeck 1979. Elemental mass balance of material carried by major world rivers. *Mar. Chem.* **7,** 173–206.

Martin, J.-M. & M. Whitfield 1983. The signficance of the river input of chemical elements to the ocean. In *Trace metals in sea water*, C.S. Wong, E. Boyle, K.W. Bruland, J.D. Burton & E.D. Goldberg (eds), 265–96. New York: Plenum.

Maybeck, M. 1979. Concentrations des eaux fluviales en elements majeurs et apports en solution aux oceans. *Rev. Geol. Dyn. Geogr. Phys.* **21,** 215–46.

Maybeck, M. 1982. Carbon, nitrogen and phosphorus transport by world rivers. *Am. J. Sci.* **282,** 401–50.

Measures, C.I. & J.M. Edmond 1983. The geochemical cycle of ^{9}Be: a reconnaissance. *Earth Planet. Sci. Lett.* **66,** 101–10.

Measures, C.I., B. Grant, M. Khadem, D.S. Lee & J.M. Edmond 1984. Distribution of Be, Al, Se and Bi in the surface waters of the western North Atlantic and Caribbean. *Earth Planet. Sci. Lett.* **71,** 1–12.

Milliman, J.D. 1981. Transfer of river-borne particulate material to the oceans. In *River inputs to ocean systems*, J.-M. Martin, J.D. Burton & D. Eisma (eds), 5–12. Paris: UNEP/Unesco.

Milliman, J.D. & R.H. Meade 1983. World-wide delivery of river sediment to the oceans. *J. Geol.* **91,** 1–21.

Orians, K.J. & K.W. Bruland 1985. Dissolved aluminium in the central North Pacific. *Nature* **316,** 427–9.

REFERENCES

Prospero, J.M. 1981. Eolian transport to the World Ocean. In *The sea* C. Emiliani (ed.), Vol. 7, 801–74. New York: Interscience.

Rona, P.A., G. Klinkhammer, T.A. Nelson, J.H. Trefry & H. Elderfield 1986. Black smokers, massive sulphides and vent biota at the Mid-Atlantic Ridge. *Nature* **321,** 33–7.

Settle, D.M. & C.C. Patterson 1982. Magnitudes and sources of precipitation and dry deposition fluxes of industrial and natural lead to the North Pacific at Enewetak. *J. Geophys. Res.* **87,** 8857–69.

Spivack, A.J. & J.M. Edmond 1987. Boron isotope exchange between seawater and the oceanic crust. *Geochim. Cosmochim. Acta* **51,** 1033–43.

Statham, P.J. & J.D. Burton 1986. Dissolved manganese in the North Atlantic Ocean, 0–35°N. *Earth Planet. Sci. Lett.* **79,** 55–65.

Sunda, W.G., S.A. Huntsman & G.R. Harvey 1983. Photoreduction of manganese oxides in seawater and its geochemical and biological implications. *Nature* **301,** 234–6.

Thompson, G. 1983a. Hydrothermal fluxes in the ocean. In *Chemical oceanography*, J.P. Riley & R. Chester (eds), Vol. 8, 270–337. London: Academic Press.

Thompson, G. 1983b. Basalt–seawater interaction. In *Hydrothermal processes at seafloor spreading centres*, P.A. Rona, K. Bostrom, L. Laubier & K.L. Smith (eds), 225–78. New York: Plenum.

Van Bennekon, A.J. & W. Salomons 1981. Pathways of nutrients and organic matter from land to ocean through rivers. In *River inputs to ocean systems*, J.-M. Martin, J.D. Burton & D. Eisma (eds), 33–51. Paris: UNEP/Unesco.

Von Damm, K.L., J.M. Edmond, B. Grant, C.I. Measures, B. Walden & R.F. Weiss 1985. Chemistry of submarine hydrothermal solutions at 21°N, East Pacific Rise. *Geochim. Cosmochim. Acta* **49,** 2197–220.

Walling, D.E. & D.W. Webb 1987. Material transport by the world's rivers: evolving perspectives. In *Water for the future: hydrology in perspective*, IAHS Publ. no. 164, 313–29.

Walsh, P.R. & R.A. Duce 1976. The solubilization of anthropogenic atmospheric vanadium in sea water. *Geophys. Res. Lett.* **3,** 375–8.

Walsh, P.R., R.A. Duce & J.L. Fasching 1979. Considerations of the enrichment, sources and fluxes of arsenic in the troposphere. *J. Geophys. Res.* **84,** 1719–26.

Windom, H.L. 1981. Comparison of atmospheric and riverine transport of trace elements to the continental shelf environment. In *River inputs to ocean systems*, J.-M. Martin, J.D. Burton & D. Eisma (eds), 360–9. Paris: UNEP/Unesco.

Wolery, T.J. 1979. Sea water–ocean crust hydrothermal chemistry: some theoretical considerations. *EOS,* **60,** 863.

Yeats, P.A. & J.M. Bewers 1982. Discharge of metals from the St. Lawrence River. *Can. J. Earth Sci.* **19,** 982–92.

PART II

THE GLOBAL JOURNEY: THE OCEAN RESERVOIR

7 Descriptive oceanography: water column parameters

In the previous chapters, the various kinds of material that are brought to the oceans have been tracked along their transport pathways to the point where they cross the interfaces separating the sea from the other planetary reservoirs. Once they have entered the ocean reservoir these materials are subjected to a variety of physical, chemical and biological processes, which combine to control the composition of both the *sea water* and the *sediment* phases within it.

7.1 Introduction

In order to provide a framework within which to discuss the physical, chemical and biological oceanic processes, it is necessary first to describe the nature of the water itself, in terms of some of its fundamental properties, and then to define the circulation mechanisms that keep it in motion. This circulation controls the physical transport of water masses, and their associated dissolved and particulate constituents, from one part of the oceanic system to another in the form of **conservative** signals. Superimposed on these are **non-conservative** signals, which arise from the involvement of the constituents in the major biogeochemical cycles that operate within the World Ocean. Components are incorporated into bottom sediments mainly by the sinking of particulate material, and there is a continual movement of particulate components through the oceans. In order to understand how this throughput operates, a simple oceanic box model will be constructed. This will then be used, together with a variety of other approaches, as a framework within which to describe the oceanic distributions of a number of parameters that have proved especially rewarding for understanding the nature of the biogeochemical cycles in the sea; these parameters include dissolved oxygen and carbon dioxide, the nutrients, and both dissolved and particulate organic carbon. By means of this approach, the throughput of materials in the oceans will be described in relation to organic matter, suspended particulates and dissolved trace metals as they are transported to the interface that separates the water column from the sediment sink.

7.2 Some fundamental properties of sea water

7.2.1 Introduction

The three fundamental properties of sea water that are of most interest to marine geochemists are **salinity** and **temperature**, which can be used to characterize water masses and which, together with pressure, fix the density of sea water, and **density** itself, which fixes the depth to which a water mass will settle and so drives thermohaline circulation. Each of these properties will be described individually below. However, it must be remembered that they are interlinked, and the equation of state of sea water is a mathematical expression of the relationship between the temperature, pressure, salinity and density of sea water; it is used, for example, for the calculation of the density of sea water from the other parameters. Recently, a new International Equation of State of Seawater has been adopted, which is consistent with the definition of 'practical salinity' (see e.g. Millero *et al.* 1980, Unesco 1981); this equation of state is given in Worksheet 7.1.

WORKSHEET 7.1
THE INTERNATIONAL EQUATION OF STATE OF SEAWATER, 1980
(from Unesco 1981)

The equation of state of sea water is a mathematical expression that can be used to calculate the density of sea water from measurements of temperature, pressure and salinity, or from other parameters derived from these. The expression adopted by the Unesco/ICES/IAPSO Joint Panel on Oceanographic Tables and Standards as the International Equation of State of Seawater gives the density of sea water (ρ, kg m^{-3}) as a function of practical salinity (S), temperature (t, °C) and applied pressure (p, bar) in the form:

$$\rho(S, t, p) = \frac{\rho(S, t, 0)}{1 - p/K(S,t,p)}$$

where $\rho(S, t, 0)$ is the One Atmosphere International Equation of State, 1980, and $K(S, t, p)$ is the secant bulk modulus, the full definitions of which are given below.

The One Atmosphere International Equation of State of Seawater, 1980

Definition

The density (ρ, kg m^{-3}) of sea water at one standard atmosphere ($p = 0$) is to be computed from the practical salinity (S) and the temperature (t, °C) with the following equation:

$$\begin{aligned}\rho(S, t, 0) &= \rho_w + (8.244\,93 \times 10^{-1} - 4.0899 \times 10^{-3}t \\ &+ 7.6438 \times 10^{-5}t^2 - 8.2467 \times 10^{-7}t^3 + 5.3875 \times 10^{-9}t^4)S \\ &+ (-5.724\,66 \times 10^{-3} + 1.0227 \times 10^{-4}t - 1.6546 \times 10^{-6}t^2)S^{3/2} \\ &+ 4.8314 \times 10^{-4}S^2\end{aligned}$$

where ρ_w, the density of the Standard Mean Ocean Water (SMOW) taken as pure water reference, is given by

$$\begin{aligned}\rho_w &= 999.842\,594 + 6.793\,952 \times 10^{-2}t - 9.095\,290 \times 10^{-3}t^2 \\ &+ 1.001\,685 \times 10^{-4}t^3 - 1.120\,083 \times 10^{-6}t^4 \\ &+ 6.536\,332 \times 10^{-9}t^5\end{aligned}$$

The One Atmosphere International Equation of State of Seawater, 1980 is valid for practical salinity from 0 to 42 and temperature from − 2 to 40°C.

The High Pressure International Equation of State of Seawater, 1980

Definition

The density (ρ, kg m^{-3}) of seawater at high pressure is to be computed from the practical salinity (S), the temperature (t, °C) and the applied pressure (p, bar) with the following equation:

$$\rho(S, t, p) = \frac{\rho(S, t, 0)}{1 - p/K(S, t, p)}$$

where $\rho(S, t, 0)$ is the One Atmosphere International Equation of State, 1980, given above, and $K(S, t, p)$ is the secant bulk modulus given by

$$K(S, t, p) = K(S, t, 0) + Ap + Bp^2$$

where

$$\begin{aligned}K(S, t, 0) &= K_w + (54.6746 - 0.603\,459t + 1.099\,87 \times 10^{-2}t^2 \\ &- 6.1670 \times 10^{-5}t^3)S + (7.944 \times 10^{-2} + 1.6483 \times 10^{-2}t \\ &- 5.3009 \times 10^{-4}t^2)S^{3/2}\end{aligned}$$

$$\begin{aligned}A &= A_w + (2.2838 \times 10^{-3} - 1.0981 \times 10^{-5}t - 1.6078 \times 10^{-6}t^2)S \\ &+ 1.910\,75 \times 10^{-4}S^{3/2}\end{aligned}$$

$$B = B_w + (-9.9348 \times 10^{-7} + 2.0816 \times 10^{-8}t + 9.1697 \times 10^{-10}t^2)S$$

The pure water terms K_w, A_w and B_w of the secant bulk modulus are given by

$$\begin{aligned}K_w &= 19\,652.21 + 148.4206t - 2.327\,105t^2 + 1.360\,477 \times 10^{-2}t^3 \\ &- 5.155\,288 \times 10^{-5}t^4\end{aligned}$$

$$\begin{aligned}A_w &= 3.239\,908 + 1.437\,13 \times 10^{-3}t + 1.160\,92 \times 10^{-4}t^2 \\ &- 5.779\,05 \times 10^{-7}t^3\end{aligned}$$

$$B_w = 8.509\,35 \times 10^{-5} - 6.122\,93 \times 10^{-6}t + 5.2787 \times 10^{-8}t^2$$

The High Pressure International Equation of State of Seawater, 1980 is valid for practical salinity from 0 to 42, temperature from − 2 to 40°C and applied pressure from 0 to 1000 bar.

7.2.2 Salinity

Salinity is a measure of the degree to which the water in the oceans is salty, and is a function of the weight of total solids dissolved in a quantity of sea water. The major ions in sea water, i.e. those which make a significant contribution to salinity, are listed in Table 7.1, and although the total salt content can vary, these constituents are always, or almost always, present in the same relative proportions. This **constancy of composition** of sea water has extremely important implications for oceanographers.

Historically, there have been a number of definitions of salinity. According to an International Commission set up in 1899 salinity was defined as 'the weight of inorganic salts in one kilogram of sea water, when all bromides and iodides are replaced by an equivalent quantity of chlorides, and all carbonates are replaced by an equivalent quantity of oxides'. In theory, perhaps the most simple direct method for the measurement of salinity is to evaporate the water to dryness and weigh the salt residue. In practice, however, gravimetric methods are tedious

Table 7.1 The major ions of sea water[a]

Ion	g kg^{-1} at S = 35°/oo
Cl^-	19.354
SO_4^{2-}	2.712
Br^-	0.0673
F^-	0.0013
B	0.0045
Na^+	10.77
Mg^{2+}	1.290
Ca^{2+}	0.4121
K^+	0.399
Sr^{2+}	0.0079

[a] Data from Wilson (1975).

and time-consuming, and in order to design a routine method for the determination of salinity the Commission made use of the concept of constancy of composition, which implies that it should be possible to use any of the major constituents as an index of salinity. It can be seen from Table 7.1 that chloride ions make up ~ 55% of the total dissolved salts in sea water, and reliable methods for the determination of chloride, using chemical titration with silver nitrate, were available at the time the Commission met. Chlorides, iodides and bromides have similar properties, and all of them react with silver nitrate to appear as chlorides in the titration.

An investigation was therefore made between **salinity** (S, ‰) and **chlorinity** (Cl, ‰); the latter being defined as 'the mass in grams of chlorine equivalent to the mass of halogens contained in one kilogram of sea water'. To examine the relationship, the salinities of nine sea waters were determined using an accurate gravimetric method. The chlorinities of the waters were then measured by titration, and the following relationship between salinity and chlorinity was established:

$$S(‰) = 1.805Cl(‰) + 0.030 \tag{7.1}$$

This is termed **chlorinity salinity**, and was used for many years as the working definition of salinity.

However, the position began to change with the introduction of the conductimetric salinometer, and a new investigation was carried out into the interrelations between the *measured* parameters (e.g. chlorinity, conductivity ratio, refractive index) and the *derived* parameters (e.g. salinity, specific gravity) of sea water. The data were assessed by a Unesco Joint Panel, and on the basis of the relationship between chlorinity and the conductivity ratio a new equation for salinity was recommended:

$$S(‰) = 1.806\,55Cl(‰) \tag{7.2}$$

This is termed **conductivity salinity**, and the equation can be used to determine salinity from the chlorinity obtained by the titration method.

However, the increasing use, and greater convenience, of high-precision electrical conductivity measurements has meant that chlorinity titration is now no longer the preferred method for the determination of salinity. In the light of this, the Joint Panel proposed a method for the determination of salinity from conductivity ratios, using a polynomial that relates salinity to the conductivity ratio R determined at 15°C at one standard atmosphere pressure:

$$\begin{aligned} S(‰) = {} & -0.089\,96 + 28.2970R_{15} + 12.808\,32R_{15}^2 \\ & - 10.678\,69R_{15}^3 + 5.986\,24R_{15}^4 - 1.323\,11R_{15}^5 \end{aligned} \tag{7.3}$$

where R_{15} is the conductivity ratio at 15°C, and is defined as the ratio of the conductivity of a seawater sample to that of one having an S(‰) of 35‰ at 15°C under a pressure of one standard atmosphere. Tables are available for the conversion of R_{15} values into salinity, and a second polynomial has been provided to permit the conversion of conductivity ratios measured at other temperatures. Salinities determined from these polynomials are termed **practical salinities**. Practical salinity is based on conductivity ratios and has no dimension, and terms such as ‰ have been abandoned to be replaced with $S = 2$ to $S = 42$; i.e. the range over which practical salinities are valid. However, it is still useful for many purposes to use the old ‰ values (see e.g. Duinker 1986).

The major elements that contribute to salinity are described as being **conservative,** i.e. their concentration ratios remain constant, and their total concentrations can only be changed by physical processes. This is an operationally valid concept and it does appear that there are no significant variations in the ratios of sodium, potassium, sulphate, bromide and boron to chlorinity in sea water. However, variations have been found in the ratios of calcium, magnesium, strontium and fluoride to chlorinity (for a detailed review of the major elements in sea water – see Wilson (1975)). Despite the fact that the major elements are more or less conservative in sea water there are conditions under which their concentration ratios can vary considerably. Situations under which these atypical conditions can be found include those associated with estuaries and land-locked seas, anoxic basins, the freezing of sea water, the precipitation and dissolution of carbonate minerals, submarine volcanism, admixture with geological brines and evaporation in isolated basins.

Under *most* conditions, therefore, the major elements in sea water may be regarded as being present in almost constant proportions. However, the total salt content (S, ‰) can vary. This is due to the operation of a number of processes. Those which *decrease* salinity include the influx of fresh water from precipitation (rainfall), land run-off and the melting of ice; and those which *increase* salinity include evaporation and the formation of ice (Bowden 1975). A number of general trends can be identified in the distribution of salinity in the surface ocean.

(a) Salinity in surface ocean waters usually ranges between ~ 32‰ and ~ 37‰.
(b) Higher values are found in some semi-enclosed, mid-latitude seas where evaporation greatly exceeds precipitation and run-off. Examples of this are found in the Mediterranean Sea (range 37–39‰), and the Red Sea (range 40–41‰).
(c) In coastal waters run-off can result in a decrease in surface salinities.

The processes that cause the major variations in salinity occur at the

surface of the ocean, and the most rapid variations are usually found within a few hundred metres or so of the air/sea interface. Regions in the water column over which rapid salinity changes take place are termed **haloclines** (see Fig. 7.1a). Since there are no sources or sinks for salt in the deep layers of the ocean, the salinity derived at the surface can only be changed by the mixing of different water types with different initial salinities (see Sec. 7.3.4). In these deep water layers, variations in salinity are smaller than those found at the surface. However, different water masses have individual 'salinity signatures', and these are extremely important in relation to deep water circulation processes (see Sec. 7.3.3).

7.2.3 Temperature

Both horizontal and vertical temperature variations are found in the ocean. The main horizontal variations occur in the surface region, with temperatures ranging from ~ 28°C in the equatorial zones to as low as ~ − 2°C in the polar seas. There is also a vertical temperature stratification in the water column, with the warm surface layer being separated from the main body of the colder deep ocean by the **thermocline**. There are thus three main temperature zones in the vertical ocean.

(a) **The surface ocean.** Here, the waters are heated by solar energy and the heat is mixed down to a depth of around 100–200 m, with the temperatures reflecting those of the latitude at which the water is found.

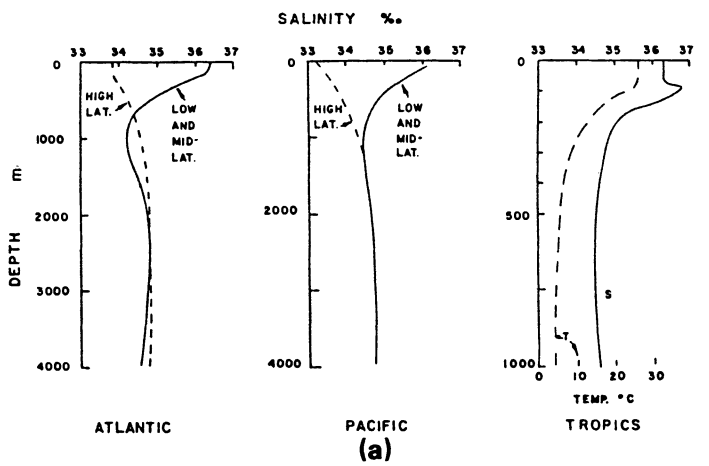

Figure 7.1 The salinity, temperature and density structure of the oceans. (a) Depth distribution of salinity (from Pickard & Emery 1982).

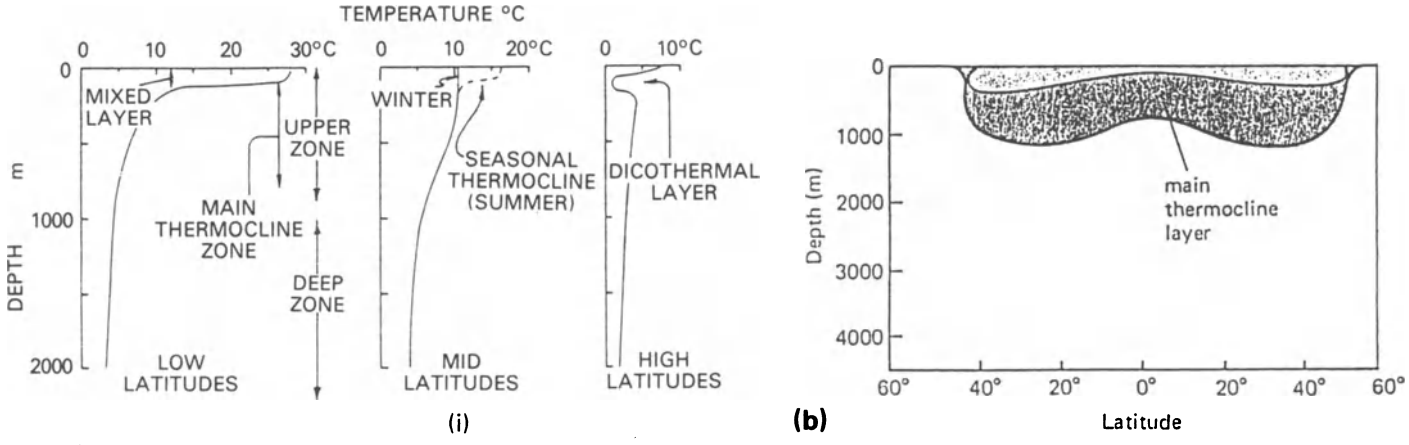

Figure 7.1b (i) Depth distribution of temperature (from Pickard & Emery 1982). (ii) Schematic representation of the thermocline (after Weihaupt 1979).

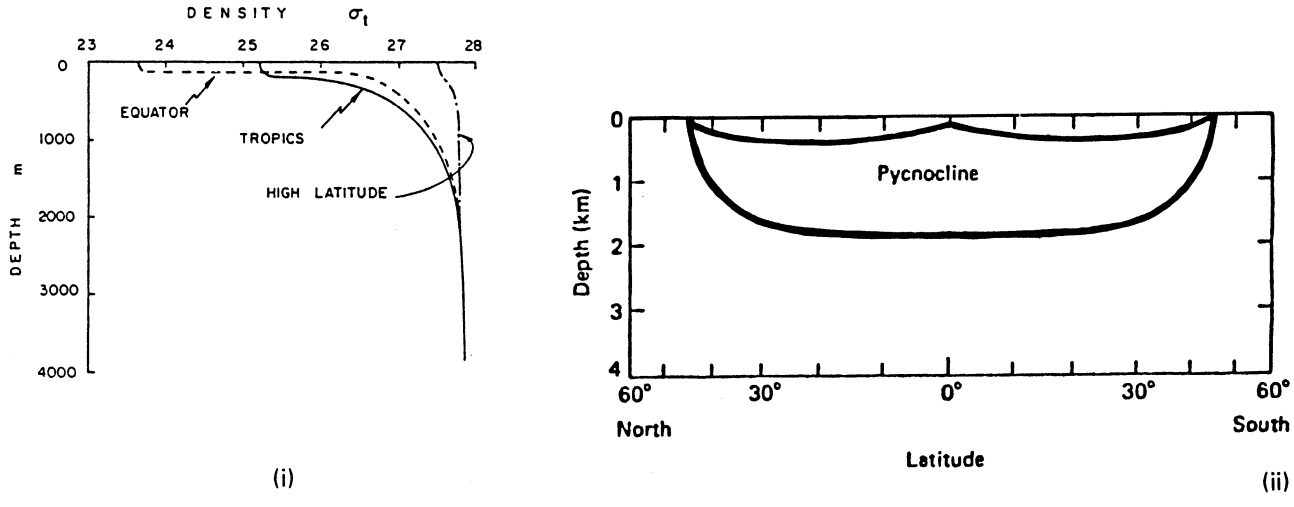

(c)

Figure 7.1c (i) Depth distribution of density (from Pickard and Emery 1982). (ii) Schematic representation of the pycnocline (after Gross 1977).

(b) **The thermocline.** Below the surface, or mixed, layer, the temperatures decrease rapidly with depth through a zone (the thermocline) that extends from the base of the surface layer down to as deep as ~ 1000 m in some places. A permanent **main thermocline** is found at low and mid-latitudes in all the major oceans, but it is absent at high latitudes. This main thermocline is usually less than 1000 m thick and its top is located at shallower depths in the equatorial than in the mid-latitude regions. Seasonal thermoclines are also found in parts of the ocean.

(c) **The deep ocean.** Under the base of the thermocline the deep ocean extends to the bottom of the water column. The waters here are cold, most being at ~ 5°C, and although the temperature falls towards the bottom (to ~ 1°C) the rate of decrease is very much slower than that found in the thermocline. A generalized vertical temperature profile in the oceans, showing these various zones, is illustrated in Figure 7.1b.

If a sample of sea water is brought to the surface from depth without exchanging heat with its surroundings, the temperature will fall as a result of adiabatic cooling and so will be lower than the *in situ* temperature. The temperature that it would have at the surface under atmospheric pressure is termed the **potential temperature** (θ). Since θ is not a function of depth it is a more useful parameter than *in situ* temperature for characterizing water masses and vertical motion in the oceans. Potential temperature is now calculated using *in situ* temperature and the equation of state (see Sec. 7.2.1 and Worksheet 7.1).

7.2.4 Density

The density (ρ) of sea water is a function of temperature, salinity and pressure, and the equation of state is a mathematical expression used to calculate the density from measurements of these parameters. The density of sea water exceeds that of pure water owing to the presence of dissolved salts, and the densities of most surface sea waters lie in the range 1024–1028 kg m^{-3}. However, since the values always start with 1000, it is common practice to shorten them by introducing the quantity

$$\sigma_{s,t,p} = \rho_{s,t,p} - 1000 \tag{7.4}$$

This is the *in situ* density, where subscript s,t,p indicates a function of salinity, temperature and pressure. Thus, the *in situ* density is the density of a sea water sample with the observed salinity and temperature, and the pressure found at the location of the sample. However, the effect of pressure on density can often be ignored in descriptive oceanography, and for convenience atmospheric pressure is used, and the quantity

$$\sigma_t = \rho_{s,t,0} - 1000 \tag{7.5}$$

is employed. This is termed 'sigma-tee', and seawater densities are most often quoted as σ_t values. Since these σ_t values are a function of only temperature and salinity, they can therefore be plotted onto temperature–salinity diagrams, which can then be used in the identification of water masses. Alternatively, potential density can be used on potential temperature–salinity diagrams, potential density (ρ_e) being the quantity

$$\sigma_\theta = \rho_{s,\theta,0} - 1000 \tag{7.6}$$

θ is the potential temperature (see above). Lines of equal density in vertical or horizontal ocean sections are termed **isopycnals**, and isopycnal surfaces, or horizons, are often used in tracer circulation–distribution studies since they are the preferred surfaces along which lateral mixing takes place (see Sec. 7.5).

There is a vertical density stratification in the water column, with densities increasing with depth. The most dramatic change in density with depth is found in the upper water layer. In equatorial and mid-latitude regions there is a shallow layer of low-density water under the surface, below which the density increases rapidly. This zone of rapidly increasing density is termed the **pycnocline**, and it is an extremely important oceanographic feature since it acts as a barrier to the mixing of the low-density surface ocean and the high-density deep ocean. The pycnocline is formed in response to the combined rapid vertical changes in salinity (the halocine) and temperature (the thermocline). However, it was pointed out above that the thermocline is absent in high-latitude waters, and the pycnocline is not developed here either – see Figure 7.1c. As a result, the water column at high latitudes is less stable than it is at lower latitudes, and in the absence of the mixing barrier the sinking of dense cold surface water can take place; it is this gravity-mediated sinking that is the driving force behind thermohaline circulation in the oceans (see Sec. 7.3.3).

7.3 Oceanic circulation

7.3.1 Introduction

The oceanic water column distributions of many dissolved constituents (e.g. the trace elements) are controlled by a combination of a **transport process** signal, associated with oceanic circulation, and a **reactive process** signal, associated with the major biogeochemical cycles. In order to evaluate the overall factors that control the distributions of the dissolved constituents in sea water it is therefore necessary to be able to distinguish between the effects of the two signals, i.e. to extract reactive process information from the transport process, or advective, background. With this in mind, transport processes associated with oceanic circulation patterns will be described in the present section, the aim being simply to

provide the basic information that is needed to interpret the reactive processes acting on dissolved constituents. This is especially relevant to the factors that control the distributions of the trace elements, a topic considered in Chapter 11. The processes that control the motions of the water in the ocean system are complex. However, within the present context it is only necessary to consider the most general features of oceanic circulation.

In the oceans, waters undergo both horizontal and vertical movements. The principal forces driving these movements are **wind** and **gravity**, and the resultant circulation patterns are modified by the effects of factors such as the rotation of the Earth, the topography of the sea bed and the positions of the land masses that form the ocean boundaries. Two basic types of circulation dominate the movement of water in the oceans. In the **surface ocean** the currents are wind-driven, and move in mainly horizontal flows at relatively high velocities. In the **deep ocean** circulation is largely driven by gravity (density changes) and the resultant thermohaline currents, which can have a vertical as well as a horizontal component, flow at relatively low velocities.

7.3.2 Surface water circulation

Circulation in the upper layer of the ocean is driven mainly by the response of the surface water to the movement of the wind in the major atmospheric circulation cells, and is constrained by the shape of the ocean basins. The currents that are generated across the air/sea interface decrease in strength downwards to fade away at relatively shallow depths, usually around 100 m. In terms of the major circulation patterns, the way in which the surface ocean responds to wind movement can be evaluated in terms of the two major wind systems, i.e. the trades and the westerlies. In average terms, the trades move diagonally from the east towards the Equator in low latitudes, and the westerlies move diagonally from the west away from the Equator at mid-latitudes. The principal result of these wind movements, combined with the constraint imposed by the shape of the ocean basins, is that in each hemisphere a series of large anticyclonic water circulation cells, termed **gyres**, are set up in subtropical and high-pressure regions. These gyres, which are the dominant feature of the surface water circulation system, are illustrated in Figure 7.2; note that the water circulates clockwise in the Northern Hemisphere and anticlockwise in the Southern Hemisphere, with the result that there is **divergence** around the Equator.

Boundary currents are developed on the landward sides of the gyres as the land masses are encountered. These currents are more intense on the western sides of the ocean basins, and the western boundary currents (e.g the Gulf Stream and the Kuroshio in the Northern Hemisphere; and the Brazil and Agulhas Currents in the Southern Hemisphere) are narrow

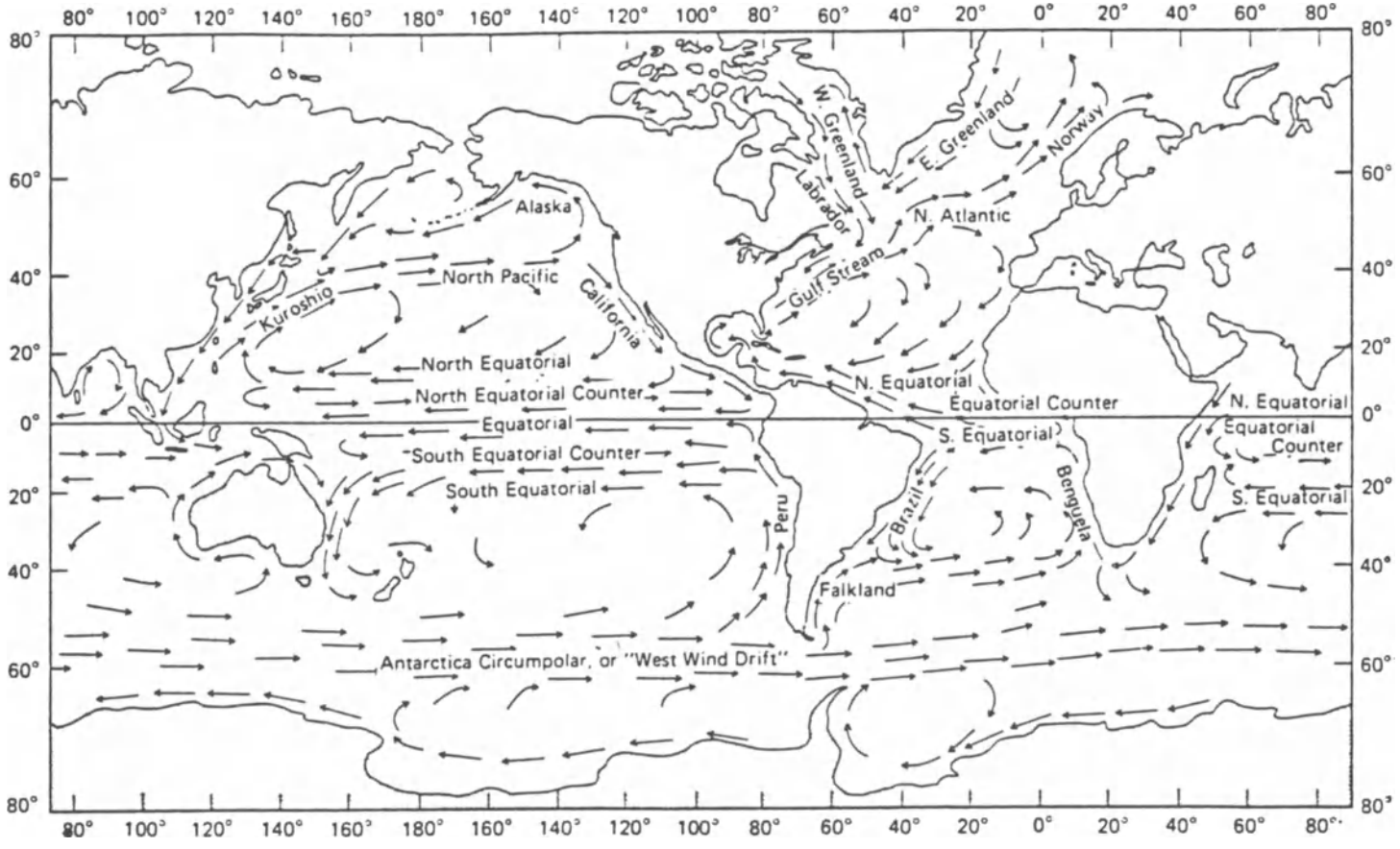

Figure 7.2 Surface water circulations in the World Ocean (from Stowe 1979). Note the central gyre systems.

and fast-flowing, and form a sharp break between coastal and open-ocean waters. In contrast, the return flows on the eastern sides of the gyres are less intense and more diffuse in nature.

The main northern and southern gyre flows in the Atlantic and the Pacific are separated by the **equatorial countercurrents**. These are particularly well developed in the Pacific; for example, the strong subsurface Cromwell Current has been traced for over 12 000 km. In the Atlantic, the countercurrents are less intense on the eastern than on the western side of the ocean, and there is an important link between the North and South Atlantic surface waters on the western side where part of the South Equatorial Current crosses the Equator to join the North Equatorial Current – see Figure 7.2. At their southern edges the South Atlantic, South Pacific and Indian Ocean gyres open out into the Antarctic and are bounded by the Circumpolar, or **West Wind Drift**, Current – see Figure 7.2. A circumpolar current of this type is not, however, found at high latitudes in the Northern Hemisphere because of the presence of the land masses there.

The Indian Ocean is a special case in that its northern land boundary is located at relatively low latitudes ($\sim$ 20°N). As a result, surface circulation in the northern Indian Ocean is strongly influenced by conditions on the surrounding land masses and is affected by the monsoon systems. During the winter months, the North Equatorial Current is developed, as it is in the Atlantic and the Pacific, but during the summer in the southwest monsoon the current is replaced by a flow in the opposite direction. Surface circulation patterns in the southern Indian Ocean are, however, similar to those in the South Atlantic and South Pacific.

In addition to the generation of surface currents, wind flow can also be responsible for vertical movement in the oceans in the form of upwelling and downwelling (sometimes termed 'Ekmann pumping'). **Upwelling** is the process by which deep water is transferred to the surface, and is extremely important in controlling primary productivity since it brings new nutrients from depth to the surface waters (see Sec. 9.1.1). This type of upwelling can occur under various conditions, but it is classically associated with the eastern boundary currents (i.e. on the western margins of the continents) in subtropical coastal regions where the wind drives the water offshore and in order to conserve volume it is replaced by subsurface water from depths of around 200–400 m. **Coastal upwelling** is found (a) on the western margins of the continents off West Africa, Peru and Western Australia, (b) off Arabia and the east coast of Asia under the influence of the monsoons, and (c) around Antarctica. **Equatorial upwelling** occurs in non-coastal, or mid-ocean, areas where it can be initiated by, for example, diverging current systems, as happens in the equatorial Pacific. In other open-ocean areas where the thermocline

acts as a mixing barrier, upwelling can take place as a result of the erosion of the thermocline by turbulence as a result of an ocean–atmospheric coupling mechanism. This turbulent vertical transport through the thermocline occurs in pulses, and can have a major effect on the output of new deep water nutrients to the euphotic zone in oligotrophic open-ocean areas (see Sec. 9.1.1).

It may be concluded, therefore, that on a global scale wind-driven circulation, modified mainly by the Coriolis effect and constrained by the shape of the ocean basins, determines the surface current patterns in the oceans. In addition, tidal currents are present everywhere in the sea, but only achieve a major importance in coastal seas and estuaries.

7.3.3 Deep water circulation

The movement of water in the deep ocean is mainly set up in response to gravity. The resultant **thermohaline circulation**, which results from the density difference between waters, is much slower than the surface circulation and involves vertical as well as horizontal motion. In the simplest sense, dense water will sink until it finds its own density level in the water column where it will then spread out horizontally along a density surface, which provides a preferred water transport horizon as well as setting up a density stratification in the oceans. Thus, if new dense water is continuously produced at the surface the displacement of subsurface water as the new water sinks will lead to the vertical and horizontal thermohaline circulation that keeps the deep ocean in motion.

Mixing between the surface and deep ocean must take place across the pycnocline, which acts as a mixing barrier. The pycnocline is well developed in tropical and temperate waters, but is less well developed, or is absent entirely, at high latitudes where the density of the cold surface waters is greater. It is here, in these high-latitude regions where the mixing barrier does not operate efficiently, that the main sites are found for the sinking of the cold dense surface water, which is responsible for the ventilation of the deep sea.

A generalized deep water circulation model was proposed by Stommel (1958), and this offers a convenient framework within which to outline the principal features in the transport of deep waters. Two primary sources of deep water are identified. Both are at high latitudes, one in the North Atlantic (the northern component) and one in the Antarctic (the southern component). The northern component deep water source is in the Norwegian Sea and off the coast of southern Greenland. Here the waters, which have a low surface temperature and a high salinity, sink to form the **North Atlantic Deep Water** (NADW). The southern component originates in the Weddell Sea where cold, dense, sub-ice water sinks to form **Antarctic Bottom Water** (ABW). The principal sources of deep water are located in the Atlantic and Antarctic, and it is possible to track

the deep water circulation path through the World Ocean from the Atlantic and Antarctic sources following the patterns suggested in Stommel's model, a characteristic feature of which is the existence of strong boundary currents on the western sides of the oceans (see Fig. 7.3).

Taking the pathway proposed in the model, the NADW spills out from the northern basins and begins its global oceanic 'grand tour'. At the start of the tour the NADW flows down the North Atlantic in the strong boundary currents at the western edge of the land masses, crosses the Equator into the South Atlantic and becomes underlain by the ABW from the southern sinking source. Deep water leaves the Atlantic–Antarctic by moving eastwards below the tip of southern Africa to enter the Indian Ocean via the Circumpolar Current. Some of the deep water circulates within the Indian Ocean, moving northwards along a western boundary current. Transport out of the ocean into the Pacific is again via the Antarctic Circumpolar Current. In the Pacific the water is moved northwards along a western boundary current through the South Pacific into the North Pacific. The overall global oceanic deep water 'grand tour' is therefore down the Atlantic (~ 80 yr), through the Antarctic into the Indian Ocean and up through the South Pacific and then the North Pacific (~ 1000 yr). Thus, the deep water of the North Pacific is the oldest in the World Ocean, and acts as a sink for other deep waters. This pathway along which the deep ocean is ventilated has an important impact on the distributions of constituents such as nutrients, trace metals and particulate matter in the ocean system, and this is discussed in subsequent sections.

Figure 7.3 Deep water circulation in the World Ocean (from Stommel 1958). Note the strong western boundary currents.

The water that sinks from the surface to the deep ocean must be replaced and in Stommel's model it is assumed that there is a uniform upwelling throughout the oceans, a process that must be distinguished from the localized (e.g. coastal) wind-driven upwelling described above. On the basis of radiotracer data, Broecker & Peng (1982) estimated that the upwelling of subsurface water occurs at a rate of ~ 3 m yr^{-1}, although somewhat higher values of ~ 5 to ~ 7 m yr^{-1} have been proposed by Bolin *et al.* (1983). In order to reach the surface, deep water has to cross the thermocline, which acts as a mixing barrier. Recent work, again using radiotracers, has demonstrated that the ventilation of the thermocline takes place particularly in the equatorial regions of the oceans from depths of at least 500 m (see e.g. Broecker & Peng 1982). Large-scale upwelling of subsurface waters also occurs at high latitudes in the Antarctic, where the thermocline mixing barrier is absent.

7.3.4 Mid-depth water circulation: water types and water masses

So far, a brief outline has been given of the circulation patterns at the upper and lower levels at the oceanic water column. It is now necessary to consider what happens in the mid-depth, or intermediate, water column, and for this the concept of a water mass will be introduced. Because there are no appreciable sinks for heat and salt in the interior of the ocean, the temperature and salinity of a water, both of which are conservative parameters, will have been fixed once it leaves the surface ocean and can only be changed by mixing with other waters having different properties. An exception to this is provided by heat transmitted through the oceanic basement, which can raise the temperature of bottom waters. Temperature and salinity are therefore very useful properties for characterizing sea waters of different origins, and a number of waters with different temperature–salinity signatures are found in vertical sections of the water column. The relationship between the temperature (T) and the salinity (S) of a water can be illustrated graphically on a *TS* diagram, or more usually now a potential temperature–salinity diagram, which is one of the most widely used diagnostic tools in physical oceanography.

A **water type** is a body of unmixed water that is defined by a single temperature and a single salinity value, and therefore plots on a *TS* diagram as a single point. Thus, the temperature and salinity of a water type do not change. Changes do occur, however, on the mixing of water types and this leads to the identification of a **water mass**, which has a range of temperatures and salinities (and other properties) and is characterized on a *TS* diagram by a *TS* curve, instead of a single point. A well defined water mass is one having a linear potential temperature–salinity relationship.

The structure of the water column can be elucidated in terms of water

masses, and this can be illustrated with respect to the Atlantic – see Figure 7.4. North Atlantic Deep Water (NADW) is formed at the northern source and sinks to the bottom to be overlain by the Atlantic Intermediate Water (AIW). The North Atlantic Deep Water (NADW) flows northwards across the Equator where it is underlain by the ABW. Surface and near-surface waters in the South Atlantic are underlain by the Antarctic Intermediate Water (AIW), which is formed by the sinking of surface water at the Antarctic convergence (~ 50°S), and extends into the North Atlantic as far as ~ 10–20°N. Between ~ 20 and ~ 40°N there is an intrusion of high-salinity Mediterranean Water, which flows east to west.

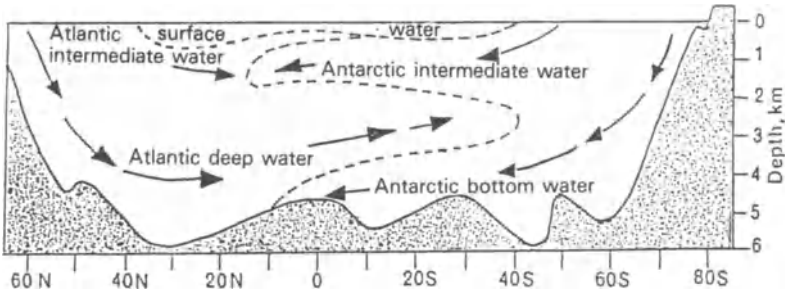

Figure 7.4 Cross section of the Atlantic from Greenland to Antarctica, with schematic representation of water masses (from Stowe 1979).

7.4 Tracers

The water column is formed of a series of water types and water masses, which sink to a level dictated by their density, displacing other waters as they do so. Since the formation of water types is a continuous process, the oceans are kept continually in motion as water circulates around the system. One of the principal thrusts in chemical oceanography over the past few years has been the use of various tracers to determine the rates at which the system operates. Tracers have also been used to elucidate the routes followed by components taking part in oceanic biogeochemical processes, and to study the rates at which the processes occur.

Conservative tracers have no oceanic sources, or sinks, and their distributions depend only on the transport of water. In contrast, **non-conservative tracers** undergo a variety of reactions within the system; these include biogeochemical cycling, radioactive decay, isotopic fractionation and exchange with the atmosphere. Tracers used to date have included temperature, salinity, dissolved oxygen, the nutrients and, more recently, trace metals, stable and radioactive isotopes and the 'Freons'.

The use of tracers such as these was considerably advanced by data obtained during GEOSECS (Geochemical Ocean Sections Study). This was particularly the case with respect to the penetration of man-made tritium and carbon-14 from the atmosphere into the thermocline and deep water, thus allowing the surface waters of the World Ocean into which they initially entered to be labelled and traced during their oceanic passage. A detailed review of the findings that emerged from GEOSECS has been compiled by Campbell (1983). A follow-up programme, TTO (Transient Tracers in the Ocean), was started in 1980 and a series of papers on the initial results was published in 1985 in *J. Geophys. Res.* **90**. Tracers are proving to be invaluable tools for oceanographers, and an excellent overview of their use in ocean studies has been provided by Broeckner & Peng (1982); this is one of the classic texts in chemical oceanography, and will serve for many years as the 'tracer Bible'. For this reason, tracers will not be treated in detail in the present volume, and only a very general summary of their applications will be given in order to relate their use to the wider aspects of marine geochemistry.

The geochemical tracers used in oceanography can be divided into three broad groups; those used to identify water masses, those used to study water transport, and those used to study geochemical processes.

7.4.1 Water mass tracers

Parameters that have been used to define water masses include temperature, salinity, dissolved oxygen, phosphate, nitrate and silica. However, dissolved oxygen, phosphate and nitrate are non-conservative tracers, i.e. their concentrations change during the residence of the water in the deep sea. Water masses originate from the mixing of water types and to unscramble the mixtures it is therefore necessary to use conservative tracers, i.e. those which are not changed by processes such as respiration or radioactive decay during their residence time in the deep sea. Tracers of this type include: (a) salinity (conductivity), (b) temperature, (c) SiO_2 and Ba, (d) the isotopes ^{2}H and ^{18}O, and (e) 'NO' and 'PO', which were introduced by Broecker (1974). For a detailed treatment of the use of these various tracers in the identification of water masses, the reader is referred to Broecker (1981), Broecker & Peng (1982) and Campbell (1983). Other types of tracers are also used for water mass studies. These include the chlorofluoromethanes (CFMs). The two most commonly measured CFMs (CCl_3F (F-11) and CCl_2F_2 (F-12)) have no known natural sources and have been increasing in concentration in the atmosphere since their commercial production started in the 1930s. The CFMs enter the ocean across the air–sea interface (see Sec. 8.2), and their concentrations in surface sea water are functions of their concentrations in the overlying atmosphere and their water solubilities, which are dependent on the temperature and salinity of the sea water.

According to Fine & Molinari (1988), the CFMs have their oceanic sources at outcrops where water masses are ventilated by the atmosphere, and as a result relatively high CFM concentrations are indicative of waters that have had recent contact with the atmosphere at the source regions and have not suffered extensive dilution by mixing with other waters having lower CFM concentrations. Thus, as the CFMs are transported from the surface into the interior of the ocean their distributions can be used to trace mixing and circulation patterns. For example, Fine & Molinari (1988) used CFMs, together with other parameters, to investigate the extent of the Deep Western Boundary Current in the North Atlantic.

7.4.2 Water transport tracers

The main emphasis on water transport in recent years has involved radioisotopes, which, for this purpose, can be classified into two types, depending on whether their distributions are influenced primarily by (a) transport in the water phase or (b) transport in the particulate phase. **Water tracers** include the following: the anthropogenically produced transient tracers ^{90}Sr (half-life, 28.6 yr), ^{137}Cs (half-life, 30.2 yr), ^{85}Kr (half-life, 10.7 yr) and the Freons; the natural steady-state tracers ^{39}Ar (half-life, 270 yr), ^{228}Ra (half-life, 5.8 yr) and ^{32}Si (half-life, 250 yr); and the mixed origin tracers ^{14}C (half-life, 5730 yr) and ^{3}He (half-life, 12.4 yr). **Particulate-phase tracers** include: ^{210}Pb (half-life, 22.3 yr), ^{228}Th (half-life, 1.9 yr), ^{210}Po (half-life, 0.38 yr) and ^{234}Th (half-life, 0.07 yr). Together, these two types of tracers yield information on ventilation and mixing in the subsurface ocean and on the origin, movement and fate of particulate matter in the system. In addition to these classical tracers, a number of individual chemical elements have recently been used to trace water mass movements. For example, Measures & Edmond (1988) used dissolved Al as a tracer for the outflow of Western Mediterranean Deep Water into the North Atlantic. Other tracers that have been used for the elucidation of circulation and mixing in the oceans include the rare-earth elements (REE) (see e.g. Elderfield 1988) and Mn (see e.g. Burton & Statham 1988). A recent example of how water circulation patterns deduced by radiotracers can aid trace element studies has been provided by Livingstone *et al.* (1985). These authors used radio-caesium distributions to define a circulation path showing that there is a direct hydrographic connection between some European Shelf waters and North Atlantic Deep Water. These data were subsequently used by Measures *et al.* (1988) to demonstrate that an enrichment of Al in surface waters north of Iceland could have originated from the European Shelf, and that convective water mass formation in this high-latitude region could result in the injection of Al-rich waters into the deep ocean.

7.4.3 Geochemical process tracers

Plotting down-column dissolved trace element concentrations against a conservative tracer, e.g. salinity or potential temperature, and interpreting the shape of the curve can provide evidence on geochemical processes; for example, a concave shape indicates deep water removal, or scavenging, of the element. However, the natural series radioisotopes are the most widely used geochemical process tracers. These isotopic clocks, which operate on timescales ranging from a few days (e.g. ^{234}Th, half-life, 24 days), through a few tens of years (e.g. ^{210}Pb, half-life, 22 yr), to several thousand years (e.g. ^{230}Th, half-life, 7.52×10^4 yr) have been employed for a wide variety of biogeochemical purposes. These include tracing the origin of atmospherically transported components (e.g. ^{210}Pb), gas exchange across the air/sea interface (e.g. ^{222}Rn), trace element scavenging in the water column (e.g. ^{230,228,234}Th), trace element down-column fluxes (e.g. ^{234}Th) and trace metal accumulation rates and bioturbation in sediments (e.g. ^{234}Th, ^{210}Pb). In addition, considerable use has been made in the past of artificial radionuclides, and this has been revived recently following the Chernobyl incident.

Tracers have provided information on a wide variety of oceanographic topics, and from the point of view of their importance to our understanding of the processes involved in marine geochemistry it is worthwhile highlighting a number of these.

(a) **Deep-sea residence time.** According to Broecker (1981) the great triumph of natural radio-carbon measurements in the oceans has been the establishment of a 1000 year timescale for the residence of water in the deep sea.

(b) **Thermocline ventilation time.** ^{14}C and ^{3}He data have been used to establish the ventilation time of the main oceanic thermocline. For example, the findings suggest that there is an upwelling flux in the equatorial regions that on a global scale is comparable to the flux of newly formed deep water.

(c) **The rates of vertical mixing.** In the more simple box models used by marine chemists it is often the practice to separate a surface ocean and a deep ocean compartment. In order to apply such models to biogeochemical processes it is necessary to have at least an approximation of the rate at which the reservoirs mix. There are various problems involved in making such approximations, but Collier & Edmond (1984) used the ^{14}C deep water residence and a deep water reservoir thickness of 3200 m to derive a mixing flux of 3.5 m yr^{-1} for the mixing rate between the surface and deep ocean (see Sec. 7.5).

(d) **The dispersion of hydrothermal solutions.** Helium isotopes have been

used to predict the mid-depth circulation of hydrothermal fluids vented at sea-floor spreading centres (see Sec. 6.4).

(e) **Oceanic biogeochemical processes.** Important advances have been made in our understanding of geochemical processes through the use of the radionuclide 'time clock' tracers. For example, Bacon & Anderson (1982) used Th isotopes to investigate particulate–dissolved exchange in the water column and demonstrated that reversible equilibria take place as the particulate matter falls to the sea bed. Other work of note includes that of Coale & Bruland (1985), who have shown that the removal rates of ^{234}Th correlate closely with primary productivity, and that non-reversible equilibria are involved in dissolved–particulate interactions on these short timescales.

(f) **Palaeo-oceanography.** Oxygen isotopes in carbonates have been used for the identification of past climatic conditions (see e.g. Broecker 1974).

(g) **Atmospheric transport.** ^{210}Pb has been employed as an atmospheric source indicator (see e.g. Schaule & Patterson 1981).

(h) **Gas exchange.** ^{222}Rn, and its disequilibrium with the parent ^{226}Rn, has been used as a gas tracer in the oceans to model air–sea exchange processes.

(i) **Sedimentary processes.** Bacon & Rosholt (1984) and Thompson *et al.* (1984) have used thorium isotopes to elucidate trace element accumulation rates in deep-sea deposits. In addition, various isotopes have been used to investigate processes such as bioturbation, and to identify sources of individual components in sediments; the latter has involved elements such as the rare earths (see e.g. Bender *et al.* 1971) and Sr isotopes (see e.g. Dasch *et al.* 1971).

(j) **The oceanic cycles of elements.** The extent to which the isotopes of an element undergo fractionation is often characteristic of specific geochemical processes, and isotopic tracers have proved to be extremely useful in elucidating the marine cycles of a number of elements. An example of this is given in Worksheet 7.2, with respect to the marine cycle of Sr.

Even from this very brief survey it is apparent that the utilization of tracers has provided invaluable insights into the processes involved in the mixing and transport of waters in the oceans, and especially into the rates at which the system operates. It is this mixing, and the subsequent transport of the waters, that controls the structure of the oceans. The transport of water during oceanic circulation also exerts a fundamental control on the distributions of both dissolved and particulate constituents in the system. This control is conservative, and compositional changes only take place as the result of the mixing of end-member waters that have different compositions acquired at their sources. Superimposed on

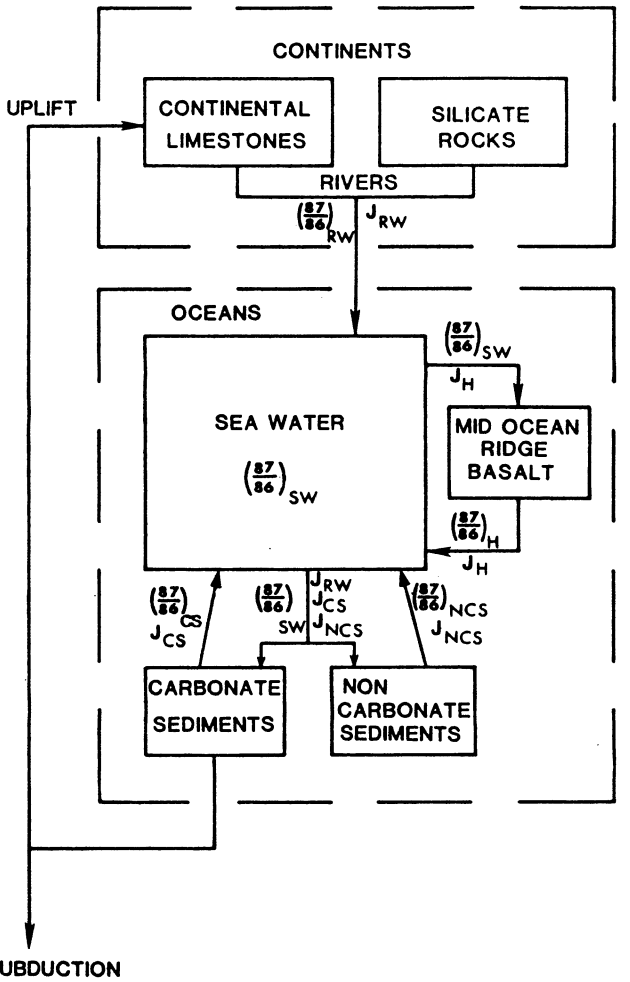

(ii)

Figure (ii) A model for the marine geochemical cycle of Sr showing the magnitudes of the fluxes, J, involved together with their associated ^{87}Sr : ^{86}Sr isotopic ratios, (87/86) (from Palmer & Elderfield 1985). At steady state, $[87]_{SW} = ([87]_{RW}J_{RW} + [87]_H J_H + [87]_{CS}J_{CS} +)/(J_{RW} + J_H + J_{CS} + J_{NCS}$ and $[86]_{SW} = ([86]_{RW} J_{RW} + [86]_H J_H + [86]_{CS}J_{CS} + [86]_{NCS}J_{NCS})/((J_{RW} + J_H + J_{CS} + J_{NCS})$, where SW = sea water, RW = river water, H = hydrothermal isotope exchange, CS = carbonate sediment pore waters and NCS = non-carbonate sediment pore waters. Magnitudes of present-day fluxes (mol yr^{-1}) are: $J_{RW} = 2.5 \times 10^{10}$, $J_{NCS} = 4.0 \times 10^8$, $J_{CS} = 3.0 \times 10^9$, $J_H = 1.2 \times 10^{10}$ or 0.38×10^{10}. ^{87}Sr ratios of present-day fluxes are: $(87/86)_{NCS} = 0.7064$, $(87/86)_{CS} = 0.7087$, $(87/86)_H = 0.7040$ and $(87/86)_{SW} = 0.70924$. Sensitivity of model to uncertainties in above values: resulting uncertainty in calculated $(87/86)_{SW}$ is 2×10^{-4} for uncertainty in J_{RW} and 1.4×10^{-4} for uncertainty in $(87/86)_H$; all other variables produce negligible uncertainties in $(87/86)_{SW}$ or are considered in the original text.

WORKSHEET 7.2
THE USE OF ISOTOPES IN THE STUDY OF THE MARINE CYCLES OF ELEMENTS

An example of how isotopic ratios can be used as 'process tracers' in marine geochemistry has been provided by Palmer & Elderfield (1985), who employed Sr isotopes to evaluate long-term variations in the compositions of sea water by modelling recent data on ^{87}Sr : ^{86}Sr variations to establish the marine geochemical cycle of the element. A Sr isotope curve was produced from dated samples showing how the ratio has varied with time over the past 75 Ma – see Figure (i).

The outstanding feature in the curve is the increase in ^{87}Sr : ^{86}Sr ratios over the past ~ 25 Ma. Sr isotopes can be fractionated during different geochemical processes, and the principal factors that were originally thought to control variations in the marine ^{87}Sr : ^{86}Sr ratio were: (a) the proportions of marine Sr derived from crustal sources (mainly granitic) and mantle sources (continental basalts and hydrothermal activity); (b) the rate at which Sr is transported from the continents to the oceans; and (c) the recycling of Sr from marine calcareous sediments. To compare the relative importance of processes such as these, a model was constructed for the marine geochemical cycle of Sr. This model incorporated the best currently available estimates of the magnitudes, and the strontium isotope ratios, associated with present-day fluxes, and is illustrated in Figure (ii).

In the model the principal flux of dissolved Sr to sea water is via river run-off, with ~ 75% originating from recycled Sr associated with the weathering of uplifted

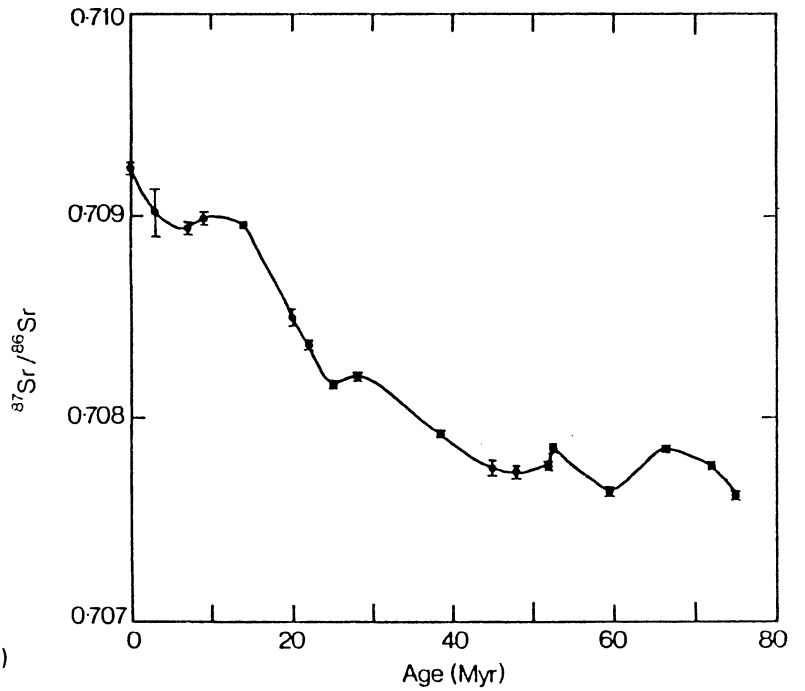

(i)

Figure (i) The marine ^{87}Sr : ^{86}Sr ratio over the past 75 Ma (after Palmer & Elderfield 1985).

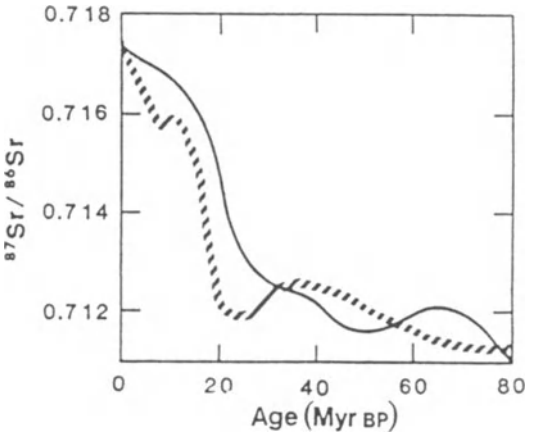

(iii)

Figure (iii) Variations in the ^{87}Sr : ^{86}Sr ratio derived from the weathering of silicate rocks; the broken curve indicates qualitative variations in glacial intensity (from Palmer & Elderfield 1985).

limestones, and the rest from silicate rocks. The other fluxes result from the diffusion of Sr from the pore waters of marine sediments (mainly carbonate-rich types), and from Sr isotope exchange between sea water and basalt during high-temperature hydrothermal activity at the ridge spreading centres. The authors then considered the effects that temporal variations in these fluxes would have on the marine ^{87}Sr : ^{86}Sr ratio. In this way, they were able to show that variations in the ratio resulting from changes in either the rates of hydrothermal activity, or in the recycling of Sr via diffusion from carbonate-rich sediments, were unable to account fully for the observed variations in the marine Sr isotopes. They concluded, therefore, that changes in the isotopic ratio of the fluvial flux must be a major control on the temporal variations in the ^{87}Sr : ^{86}Sr in sea water. Further, by modelling the various factors that can affect the Sr isotopic ratio in the fluvial flux, they concluded that the only processes that could adequately account for the temporal variations in the marine Sr isotopic ratios are changes in the ^{87}Sr : ^{86}Sr ratio derived from the weathering of silicate rocks. The changes in the Sr isotopic ratios derived from silicate rock weathering that are necessary to produce the observed marine ^{87}Sr : ^{86}Sr ratios are illustrated in Figure (iii).

The principal feature of the curve illustrated in Figure (iii) is the sharp rise in ^{87}Sr : ^{86}Sr ratios from ~ 25 Ma BP to the present day. Palmer & Elderfield (1985) pointed out that this feature correlates with two important variables in geological history. (a) It is similar to the curve for the intensity of glacial activity over the past 75 Ma, thus providing evidence to confirm an earlier suggestion that increased glacial action had an effect on the marine ^{87}Sr : ^{86}Sr ratio by exposing, and increasing the weathering rates of, ancient shield regions in terrains that have relatively high ^{87}Sr : ^{86}Sr ratios. (b) The Alpine and Himalayan orogenies occurred over the last 30 Ma and resulted in the uplift, exposure and accelerated erosion of rocks having relatively high ^{87}Sr : ^{86}Sr ratios.

The authors concluded, therefore, that although hydrothermal fluxes and carbonate recycling are extremely important in determining the *absolute* value of the marine ^{87}Sr : ^{86}Sr ratio at any one time, the principal control over the *variations* in the ratio during the past 75 Ma has been changes in the isotropic composition of the Sr derived from the weathering of silicate rocks.

this conservative circulation control is a second effect produced by the involvement of many constituents in the major biogeochemical processes that operate within the oceans, and which lead to non-conservative behaviour. It is possible therefore to make an important distinction between two genetically different types of signals in the oceans: (a) one resulting from the mixing and transport of water masses, and (b) one resulting from internal biogeochemical oceanic reactivity.

In order to gain an understanding of how these two types of signals interact to control the oceanic cycles of elements it is useful to set up ocean models designed to trace the pathways by which materials move through the system. In the followng section a simple two-box model will therefore be outlined for use as a framework within which to describe the distributions of dissolved and particulate components in the oceans.

7.5 An ocean model

7.5.1 Introduction

Mixing in the water column involves a combination of advection and diffusion. **Advection** is a large-scale transport involving the net movement of water from one point in the ocean to another. This may occur either in a horizontal direction, e.g. along a major current system, or in a vertical direction, e.g. during upwelling or sinking. Superimposed on this net water transport are the effects of turbulent mixing, or turbulent exchange; this is a more or less random mixing caused by **diffusion**, in which an exchange of properties takes place between waters by eddy, and to a much lesser extent molecular, diffusion without any overall net transport of the water itself.

There are, however, problems involved in understanding the real nature of vertical and horizontal mixing in the oceans. Some of these problems have been identified by Broecker & Peng (1982), who distinguished between **isopycnal** and **diapycnal** mixing. Isopycnal surfaces, along which potential density remains constant, are the preferred surfaces along which lateral mixing takes place. Diapycnal mixing results when water is carried in a perpendicular direction across isopycnal surfaces. In the interior of the ocean isopycnal surfaces are almost horizontal, but at high latitudes they rise towards the surface where they can outcrop. The authors suggested therefore that the concept of isopycnal and diapycnal mixing should replace that of horizontal and vertical mixing.

Although a wide variety of models are available, many marine chemists prefer to adopt a discontinuous, or **box model**, approach to gain a first-order, or perhaps even a zero-order, understanding of biogeochemical processes within the ocean system. Box models of varying complexity have been used for the interpretation of the distributions of various

components in the World Ocean, using tracer-derived data for the rates at which the system operates. The general principles involved in these models are described below.

In the *steady-state* ocean a component is removed from the system at the same rate at which it is added, i.e. the input balances the output and the concentrations at any point in the system do not change with time. To construct an oceanic model for a constituent it is therefore necessary to have data on (a) magnitude and rates of the primary input mechanisms, (b) the rates of exchange between the oceanic reservoirs involved, and (c) the magnitudes and rates of the primary output mechanisms. The *primary* inputs to the oceans are mainly via river run-off, atmospheric deposition and hydrothermal exhalations (see Chs 3–6). Exchange between oceanic reservoirs occurs through the advective transport of water during thermohaline circulation (downwelling and upwelling), by turbulent exchange and by the sinking of particulate matter from the surface to the deep ocean. Output from the system for most elements is via the burial of particulate material in sediments, although reactions of various kinds between sea water and the basement rocks can also act as sinks for some elements (see Ch. 5). In the steady-state ocean, the amount of a component entering a reservoir must balance the amount leaving. For example, if the concentration of an element in the surface ocean is to remain constant, the gain from primary inputs and upwelling must be matched by the outputs from downwelling and particle sinking (Broecker 1974). Thus, in the system as a whole, the 'through flux' of a constituent entering via the primary input mechanisms must equal the total permanently lost to the output mechanisms.

7.5.2 A simple two-box oceanic model

It was shown in Section 7.3 that different processes control the circulation in the surface ocean (wind-driven) and the deep ocean (gravity-driven). The simplest two-box model therefore divides the ocean into these two reservoirs, i.e. a **surface water reservoir** (~ 2% of the total volume of the ocean) and a **cold deep water reservoir** (~ 80% of the total volume of the ocean), which are separated by the waters of the **thermocline** (~ 18% of the total volume of the ocean). Both reservoirs are assumed to be well mixed and interconnected, and they interact via vertical mixing, i.e. the downwelling of surface water and the upwelling of deep water and the winter turnover of cooled upper layer, and via the sinking of coarse particulate matter (CPM; see Sec. 10.4) from the surface ocean.

This type of two-box model is a useful first approximation of the ocean system since the main barrier to mixing in the water column is the thermocline, which separates the two main reservoirs, the waters of which have different densities. Two other factors are also important in distinguishing between the two reservoirs: (a) two of the principal

primary input mechanisms, i.e. river run-off and atmospheric deposition, supply material to the surface ocean, and (b) the bulk of the phytoplankton and zooplankton biomass, which is involved in the oceanic cycles of many components, is found in the upper sunlit water layer of the surface reservoir (see Sec. 9.2.2.2).

A number of paremeters are used to evaluate the rate of exchange of water between the surface and deep reservoirs. A ^{14}C residence time of $\sim$ 900 yr has been proposed for the deep ocean. This means that at the rate at which deep water circulates in the World Ocean it takes $\sim$ 900 yr for water to go through the cycle of sinking at the poles, circulating through the deep ocean and returning to the surface. By rounding up the estimate to 1000 yr, Broecker & Peng (1982) calculated that the yearly volume of water exchange between the deep and surface ocean is equal to a layer $\sim$ 300 cm thick with an area equal to that of the ocean, i.e. a mixing flux of 3 m yr^{-1}. Thus, the ^{14}C data indicate that upwelling brings an amount of water to the surface equal to an ocean-wide layer of $\sim$ 300 cm. For comparative purposes, Broecker (1974) estimated that fluvial input to the ocean from continental run-off would yield a layer $\sim$ 10 cm thick if it was spread over the entire ocean.

In order to illustrate the principles involved in incorporating data of this kind into oceanic box models, a generalized two-box model that has been applied to the marine geochemical cycles of trace metals is illustrated in Figure 7.5.

7.6 Characterizing oceanic water column sections

Various parameters that characterize the water in the oceans have now been described. From the viewpoint of marine geochemistry the question that must now be addressed is 'Which of these paremeters must be measured on a semi-routine basis during the occupation of water column sections in order (a) to set the location in an oceanographic context and (b) to provide data that can be used to interpret biogeochemical processes?'

(a) To set an individual seawater section into an oceanographic context, i.e. to describe the nature of the water, it is usual to prepare vertical profiles of temperature, salinity, dissolved oxygen and the nutrients; other parameters may also be measured during individual investigations. These various parameters, either singly or in combination, can be used for purposes such as defining the depth of the mixed layer, describing the structure and location of the thermocline, and identifying the different water masses (and therefore water sources) that are cut by the section.

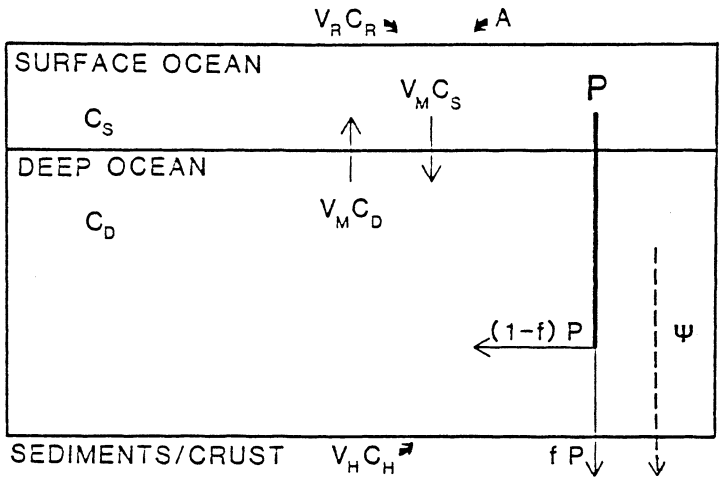

$$P = V_M(C_D - C_S) + V_R C_R + A$$

Figure 7.5 A generalized two-box ocean model applied to the marine geochemical cycles of trace elements (from Collier & Edmond 1984): P, particulate matter flux out of the surface ocean; V_R, C_R, volume and concentration of an element in river water; A, atmospheric input; C_S, C_D, dissolved concentrations of an element in the surface and deep reservoirs; f, fraction of particulate matter preserved in sediments; ψ, additional particulate matter flux due to scavenging within the deep ocean; V_H, C_H, volume and concentration of an element in hydrothermal solutions. The particulate matter flux (P) is calculated by the mass balance of all other inputs and outputs to the surface ocean reservoir.

(b) Data that are useful for the interpretation of biogeochemical processes include dissolved oxygen (to characterize redox-mediated reactions), the nutrients (to characterize the involvement of elements in biological cycles), total particulate matter (to characterize the involvement of elements in particle-scavenging reactions), chlorophyll (to characterize the standing crop and primary production), DOC and POC (to characterize the oceanic carbon cycle and global carbon flux), and a variety of the tracers listed in Section 7.4 (the choice depending on the nature of a specific investigation); however, it must be stressed that not all these parameters are measured on a purely routine basis. The use of a variety of water column parameters in a marine geochemical context is illustrated in Worksheet 7.3. Further examples of the manner in which oceanographic-related and process-related water column parameters are used in marine geochemistry

WORKSHEET 7.3
CHARACTERIZING THE WATER COLUMN FOR GEOCHEMICAL STUDIES

The distribution of 'reactive' dissolved constituents in sea water is controlled by a combination of oceanic circulation patterns and the effects of internal reactive processes. However, a large proportion of the chemical signal for these constituents can be determined by long-distance advection and the mixing of water masses of different end-member compositions, and it is therefore necessary to extract chemical information from the advective background. For trace elements one way of doing this is to relate the distribution of the element to an 'analogue' species that has a well understood distribution (see Sec. 11.1). This 'advective–chemical' approach, which combines data for a variety of water column parameters, was employed by Chan *et al.* (1977) in their study of the distribution of dissolved barium in the Atlantic

(i)

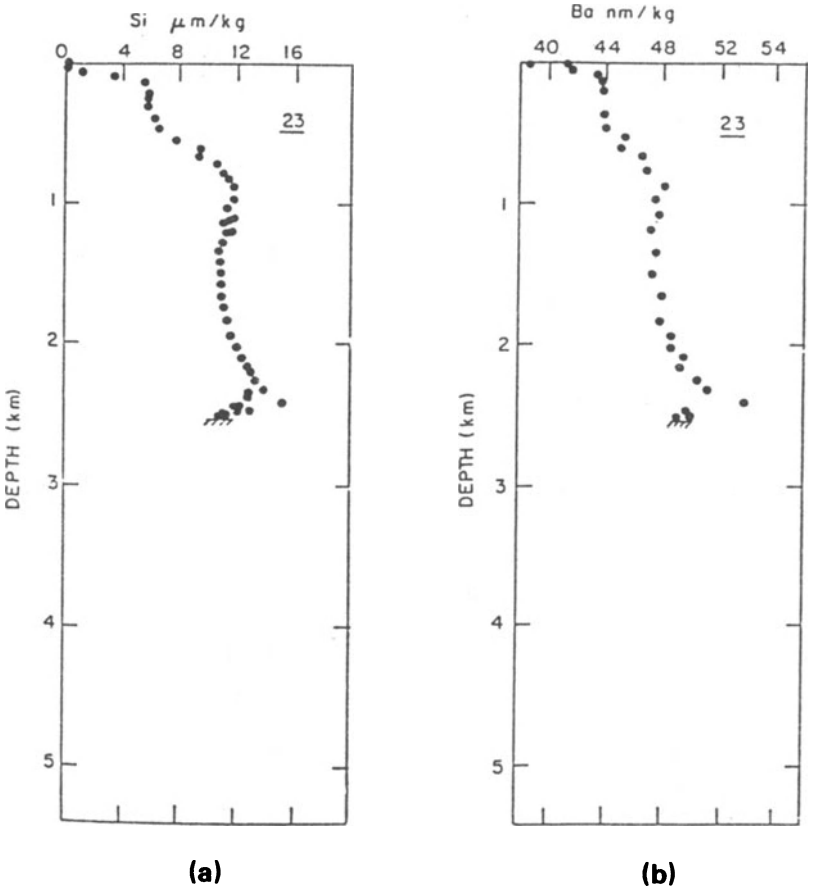

Figure (i) Profiles of Ba and Si at station 23 (from Chan *et al.* 1977).

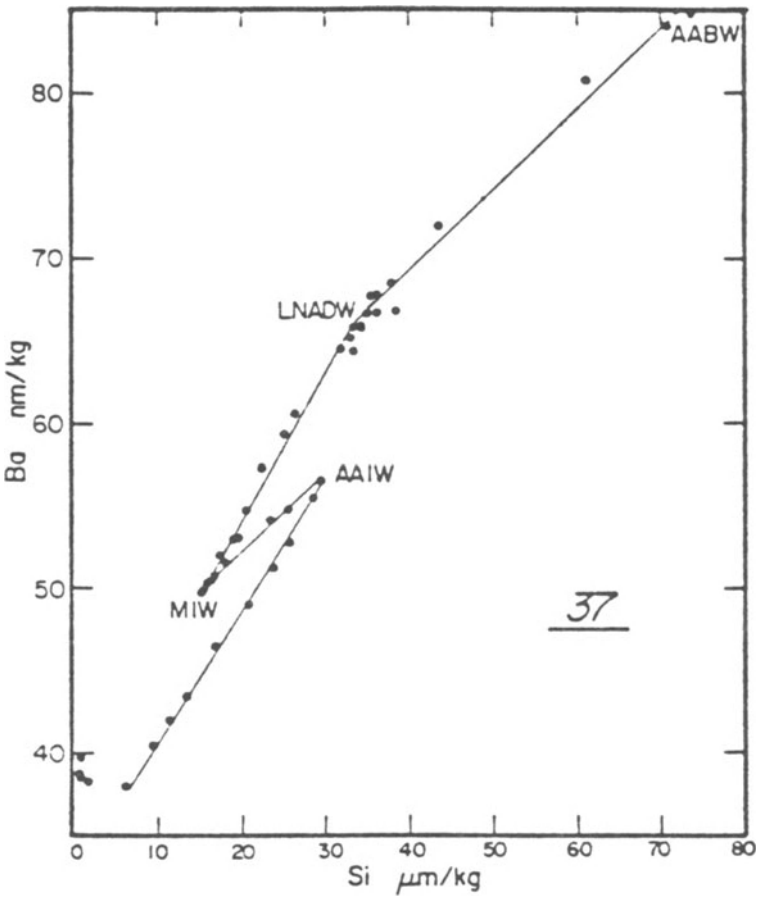

Figure (ii) Plot of Ba against Si at station 37 (from Chan *et al.* 1977).

Ocean. This study can be used to illustrate how a variety of the sea water parameters described in the text can be used both to characterize the water column and to interpret the biogeochemical controls on the distribution of trace elements in the oceans. In this context, the use of a number of these water column parameters is described below in relation to a variety of geochemical applications.

'Species analogue' interpretation of trace element data

Physical circulation is the dominant control on the distribution of dissolved Ba, and many other dissolved constituents, in the basins of the Atlantic, and in order to extract chemical information from the advective background Chan *et al.* (1977) related the distribution of the element to those of other species that have well understood distributions. The results showed that the water column distributions of barium mimic those of the refractory nutrient silicate. This relationship is illustrated in Figure (i) for a station southeast of Iceland, and shows the close correspondence between silicate and Ba.

Chan *et al.* (1977) were able to use this Ba–silicate correlation to extract chemical information from the advective background by demonstrating that the marine geochemistry of barium is dominated by its involvement in the oceanic biogeochemical cycle in which it takes part in a deep water regeneration cycle associated with a slowly dissolving refractory, non-labile, phase (mimicked by silicate), rather than a more rapidly dissolving, labile, tissue phase (mimicked by nitrate and

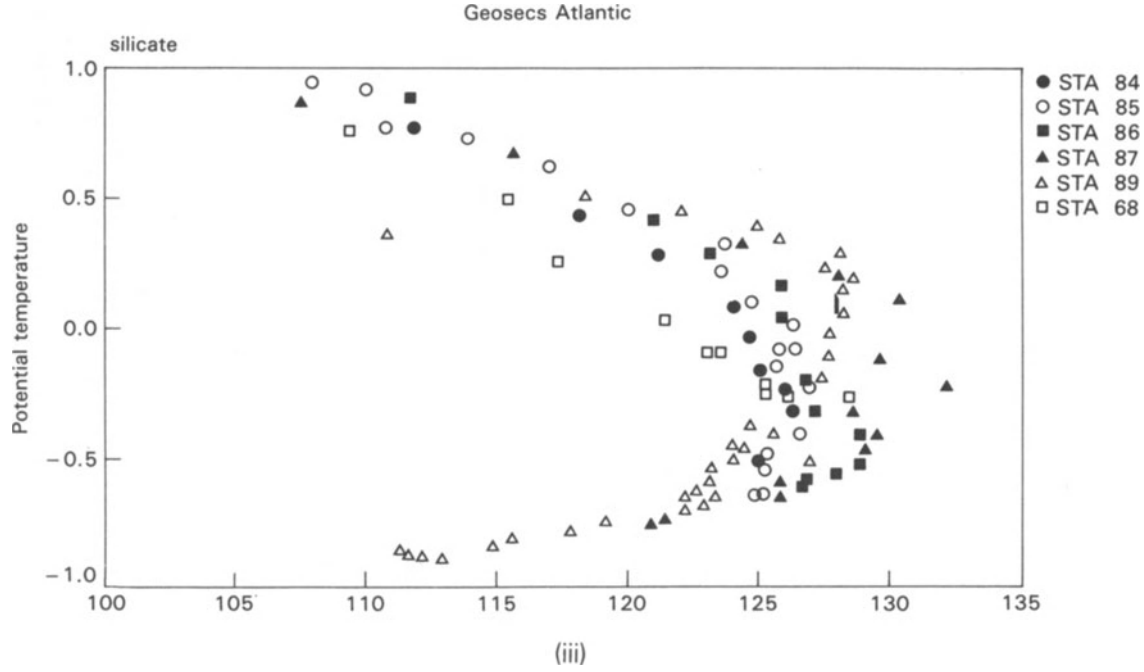

Figure (iii) Si–θ plots for stations between the South Sandwich Trench and the Atlantic Indian Ridge (84–90) and station 68 in the Argentine Basin (after Chan *et al.* 1977; not all original data points are plotted).

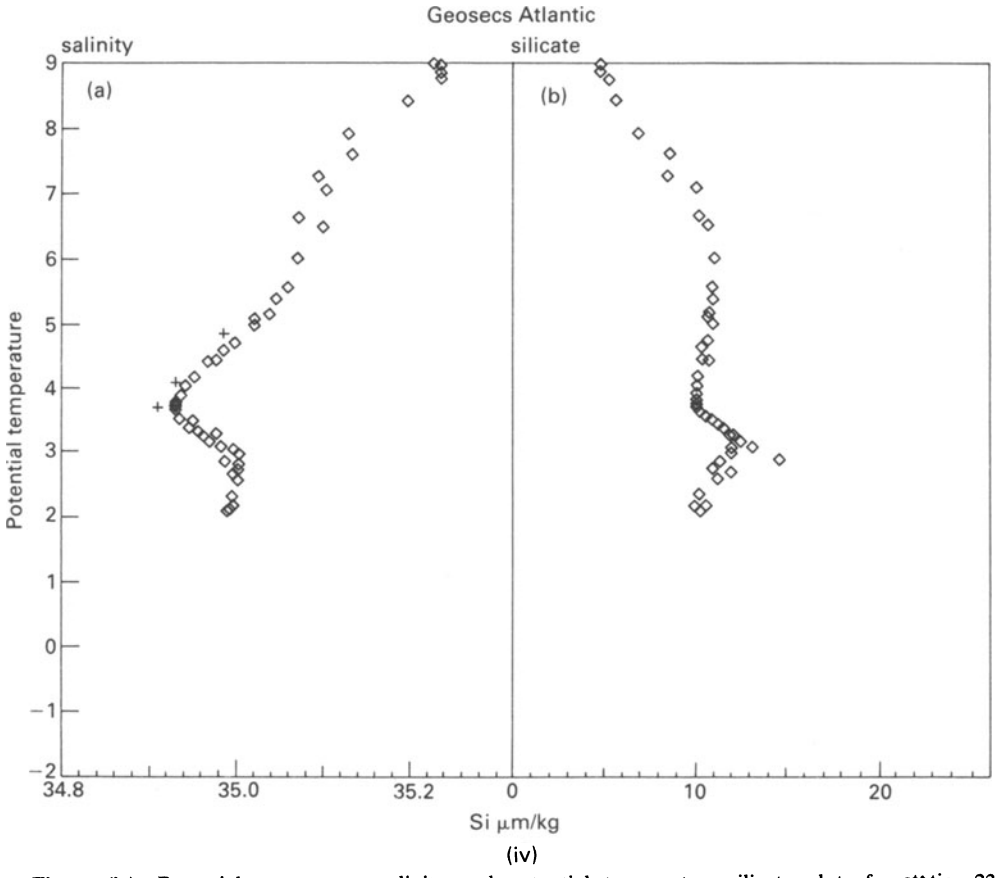

Figure (iv) Potential temperature–salinity and potential temperature–silicate plots for station 23 (from Chan *et al.* 1977).

phosphate) that is regenerated at higher levels in the water column. However, the Ba–silica relationship is not an exact one, and this can be seen in property–property diagrams for GEOSECS station 37; this is located in the western Atlantic at a site where the major water mass cores are well developed. The silica–Ba plot for this station is illustrated in Figure (ii). It is apparent that this plot consists of straight-line segments connecting end-member waters of different compositions; e.g. the Antarctic water masses are strongly enriched in silica relative to barium compared to the North Atlantic deep water. Property–property plots such as this can therefore prove extremely useful for elucidating the complex interplay between chemical and physical features in the distributions of dissolved constituents in the ocean.

In general, the oceanic distribution of Ba mimics that of silicate and further details on the physical features that affect Ba can be obtained by combining data for the element with that for silicate, which can be used to characterize water masses. Two such applications using this approach are described below.

The application of property–property plots to distinguish between water masses

Silicate is the 'analogue' for dissolved Ba, and since the silicate concentrations of water masses can differ, silicate–property plots can be used to distinguish between individual water masses. This can be illustrated in terms of silicate–potential temperature plots for the waters of a series of high-latitude South Atlantic stations. In the region around the Weddell Sea the circulation is controlled by the interaction of the warmer, more silica-rich, Circumpolar Current (CPC) water with the colder, less silica-rich, Weddell Sea Water (WSW). The relationship can be displayed on a θ–Si plot and is illustrated in Figure (iii) for deep waters from a number of stations lying between the South Sandwich Trench and the Atlantic Indian Ridge.

Information can be extracted from the type of plot shown in Figure (iii) in terms of identifying both (a) overall water mass trends and (b) variations at individual stations.

(a) The make-up of the deep water column. The waters at these high-altitude stations have a range of properties intermediate between those of the CPC and WSW end-members. The property–property plot shows a broad silicate maximum centred around ~ -0.2°C, with values which are close to those for the CPC ($\sim$ 129 μmol kg^{-1}) at stations 86 and 87. Below the silicate maximum there is clear evidence of the presence of colder, less silica-rich Weddell Sea Water (θ, -0.88; silicate, 111.5 μmol kg^{-1}), the most extreme values for the Weddell Sea Bottom Water being at station 89.

(b) Effects at individual stations. On the basis of the data for the different stations, it would appear that the influence of the CPC proper on the deep waters has its strongest effect at stations 86 and 87, but that it has a lesser effect on stations 84, 85 and 89.

Characterizing the water column

The hydrography of the Atlantic is dominated by the horizontal advection and vertical mixing of water mass cores formed at high latitudes. The formation processes in the Northern and Southern Hemispheres are different and so therefore are the physical and chemical properties of the waters produced in the two regions. In the North Atlantic the water masses are formed by the cooling and downwelling of surface waters that have tropical and subtropical origins, and the cores formed have *high salinities* and *low nutrient* concentrations. The waters are formed in a number of regions (see Sec. 7.3.3). The most extreme water types are produced in late winter in

the Norwegian and Greenland Seas via a modification of high-salinity water transported northwards through the passage around Iceland. The densest water formed in stored within deep basins, but there is a southwards return flow of waters of less extreme properties which are determined by the source depths at which they originated and vertical mixing both in the overflow regions themselves and during descent to the deep ocean floor. The main flows of these water masses are through the Denmark Strait, the Southwestern Faroe Channel and across the Wyville–Thompson Ridge between Faroe and Orkney. These water masses, together with one formed in the Labrador Sea, follow a number of complex trajectories and are then propagated southwards as a composite termed the North Atlantic Deep Water (NADW). Mediterranean Deep Water, which outflows through the straits of Gibraltar, forms an additional core that spreads across the North Atlantic and forms the upper boundary of the deep water that moves into the South Atlantic.

The great complexity of the water column, which is characteristic of the formation areas of the NADW, can be illustrated by the chemical and hydrographic data obtained for the station southeast of Iceland (station 23). These data can be used to characterize the water column in terms of water masses, and to illustrate this plots of salinity and silicate against potential temperature are shown in Figure (iv); some features of this figure should be interpreted in conjunction with Figure (i).

On the basis of these plots the characterization of the water column at station 23 can be summarized as follows. The upper part of the column is occupied by high-salinity waters of a central Atlantic origin. At $\sim$ 800 m there is an inflection in potential temperature and salinity and an increase in silicate. This, together with other properties not illustrated here (e.g. a pronounced oxygen minimum), indicates the presence of the core of the Mediterranean Intermediate Water (MIW). At depths below this there is a broad minimum in salinity and silicate (and an oxygen maximum), which shows the presence of the Labrador Sea Water. Below the salinity and silicate minima, i.e. at depths $\gtrsim$ 1600 m, the silicate values increase to reach a well defined maximum (15.2 μm kg^{-1}) at $\sim$ 2400 m, then fall off rapidly towards the bottom (11.0 μm kg^{-1}) at 2516 m. The values for potential temperature and salinity also decrease in a similar manner. These features were interpreted as representing the residual core of the Antarctic Bottom Water (AABW; high silicate, intermediate salinity) overriding the Arctic Bottom Water (ABW; low silicate, high salinity) from the Faroe Channel; i.e. the AABW has penetrated to these high latitudes in the Northern Hemisphere. The θ–S properties of the ABW at station 23 indicate that the properties of the original Norwegian Sea Water which has overflowed via the Faroe Channel have been strongly modified by mixing with warmer, more saline Atlantic waters as it flowed down the slope.

will be described later in the text when the factors controlling the elemental compositions of the sea water and the sediment reservoirs are described.

7.7 Water column parameters: summary

(a) The oceanic water column can be divided into two layers: a thin, warm, less dense surface layer that caps a thick, cold, more dense deep water layer. The two layers are separated by the thermocline and the pycnocline, which act as barriers to water mixing.
(b) Currents in the surface layer of the ocean are wind-driven, and the major features of the surface circulation are a series of large anticyclonic circulation cells, termed gyres, which have boundary currents on their landward sides.
(c) Circulation in the deep ocean is gravity-driven. Cold, relatively dense, surface water sinks at high latitudes where the pycnocline is less well developed, or is absent entirely. The main features of the bottom circulation are strong boundary currents on the western sides of the oceans. The deep water undergoes a global oceanic 'grand tour', which takes it down the Atlantic, through the Antarctic into the Indian Ocean, up through the South Pacific and into the North Pacific. As a result, the deep water of the North Pacific is the oldest in the World Ocean, and acts a sink for other deep waters.
(d) For many geochemical purposes, the ocean can be represented by a two-box model that distinguishes between (a) a warm surface water reservoir ($\sim$ 2% of the total volume of the ocean) and (b) a cold deep water reservoir ($\sim$ 80% of the total volume of the ocean). The two layers are separated by the waters of the thermocline ($\sim$ 18% of the total volume of the ocean).
(e) The structure of the oceans is controlled by the mixing and transport of water masses, and information on the processes involved, and on the rates at which they operate, can be gained by using a variety of oceanic tracers.

References

Bacon, M.P. & R.F. Anderson 1982. Distribution of thorium isotopes between dissolved and particulate forms in the deep sea. *J. Geophys. Res.* **87,** 2045–56.

Bacon, M.P. & J.N. Rosholt 1984. Accumulation rates of Th-230, Pa-231 and some transition metals on the Bermuda Rise. *Geochim. Cosmochim. Acta* **48,** 651–66.

REFERENCES

Bender, M., W.S. Broecker, V. Gornitz, U. Middel, R. Kay, S.-S. Sun & P. Biscaye 1971. Geochemistry of three cores from the East Pacific Rise. *Earth Planet. Sci. Lett.* **12,** 425–33.

Bolin, B., A. Bjorkstrom & K. Holmen 1983. The simultaneous use of tracers for ocean circulation studies. *Tellus* **35B,** 206–36.

Bowden, K.F. 1975. Oceanic and estuarine mixing processes. In *Chemical oceanography*, J.P. Riley & G. Skirrow (eds), Vol. 1, 1–41. London: Academic Press.

Broecker, W.S. 1974. *Chemical oceanography*. New York: Harcourt Brace Jovanovich.

Broecker, W.S. 1981. Geochemical tracers and oceanic circulation. In *Evolution of physical oceanography*, B.A. Warren & C. Wunsch (eds), 434–60. Cambridge, Mass.: MIT Press.

Broecker, W.S. & T.-H. Peng 1982. *Tracers in the sea.* Palisades, NY: Lamont-Doherty Geological Observatory.

Burton, J.D. & P.J. Statham 1988. Trace metals as tracers in the ocean. *Phil. Trans. R. Soc. Lond.* **325,** 127–45.

Campbell, J.A. 1983. The Geochemical Ocean Sections Study – GEOSECS. In *Chemical oceanography*, J.P. Riley & R. Chester (eds), Vol. 8, 89–155. London: Academic Press.

Chan, L.H., D. Drummond, J.M. Edmond & B. Grant 1977. On the barium data from the GEOSECS Expedition, *Deep-Sea Res.* **24,** 613–649.

Coale, K.H. & K.W. Bruland 1985. ^{234}Th : ^{238}U disequilibria within the California Current. *Limnol. Oceanogr.* **30,** 22–33.

Collier, R.W. & J.M. Edmond 1984. The trace element geochemistry of marine biogenic particulate matter. *Prog. Oceanogr.* **13,** 113–99.

Dasch, E.J., J. Dymond & G.R. Heath 1971. Isotopic analysis of metalliferous sediments from the East Pacific Rise. *Earth Planet. Sci. Lett.* **13,** 175–80.

Duinker, J.C. 1986. Formation and transformation of element species in estuaries. In *The importance of chemical 'speciation' in environmental processes*, M. Bernhard, F.E. Brinkman & P.J. Sadler (eds), 365–84. Berlin: Springer-Verlag.

Elderfield, H. 1988. The oceanic chemistry of the rare-earth elements. *Phil. Trans. R. Soc. Lond.* **35,** 105–26.

Fine, R.A. & R.L. Molinari 1988. A continuous deep western boundary current between Abaco (26.5°N) and Barbados (13°N). *Deep-Sea Res.* **35,** 1441–50.

Gross, M.G. 1977. *Oceanography – a view of the Earth.* Englewood Cliffs, NJ: Prentice Hall.

Livingstone, H.D., J.H. Swift & H.G. Ostlund 1985. Artificial radionuclide tracer supply to the Denmark Strait Overflow between 1972 and 1981. *J. Geophys. Res.* **90,** 6971–82.

Measures, C.I. & J.M. Edmond 1988. Aluminium as a tracer of the deep outflow from the Mediterranean. *J. Geophys. Res.* **93,** 591–5.

Measures, C.I., J.M. Edmond & T.D. Jickells 1986. Aluminium in the northwest Atlantic. *Geochim. Cosmochim. Acta* **50,** 1423–9.

Millero, F.J., C.-T. Chen, A. Bradshaw & K. Schleicher 1980. A new high pressure equation of state for sea water. *Deep-Sea Res.* **27,** 255–64.

REFERENCES

Palmer, M.R. & H. Elderfield 1985. Sr isotope composition of sea water over the past 75 Myr. *Nature* **314,** 526–8.

Pickard, G.L. & W.J. Emery 1982. *Descriptive physical oceanography.* Oxford: Pergamon Press.

Schaule, B.K. & C.C. Patterson 1981. Lead concentrations in the northeast Pacific: evidence for global anthropogenic perturbations. *Earth Planet. Sci. Lett.* **54,** 97–116.

Stommel, H. 1958. The abyssal circulation. *Deep-Sea Res.* **5,** 80–2.

Stowe, K.S. 1979. *Ocean Science.* New York: Wiley.

Thompson, J., M.S.N. Carpenter, S. Colley, T.R.S. Wilson, H. Elderfield & H. Kennedy 1984. Metal accumulation in northwest Atlantic pelagic sediments. *Geochim. Cosmochim. Acta* **48,** 1935–48.

Unesco 1981. Unesco Tech. Pap. Mar. Sci, no. 38. Paris: Unesco.

Weihaupt, J.G. 1979. *Exploration of the oceans. An introduction to oceanography.* New York: Macmillan.

Wilson, T.R.S. 1975. Salinity and the major elements of sea water. In *Chemical oceanography*, J.P. Riley & G. Skirrow (eds), Vol. 1, 365–413. London: Academic Press.

8 Dissolved gases in sea water

The atmosphere is the major source of gases to sea water. The atmosphere itself consists of a mixture of major, minor and trace gases, and the abundances of a number of these are given in Table 8.1. The ocean can act as either a source or a sink for atmospheric gases. The gases enter or leave the ocean via exchange across the air/sea interface, and are transported within the ocean reservoir by physical processes.

8.1 Introduction

During their residence in the sea some gases behave in a conservative manner. In contrast, other gases are reactive and take part in biological and chemical processes. Dissolved gases are important for a number of reasons, but from the point of view of marine geochemistry the most significant implications of their presence in sea water are related to the role they play in the oceanic biogeochemical cycles. In terms of global-scale processes within these cycles the two most important gases are oxygen and carbon dioxide, and attention here will therefore focus on the roles played by these two gases. Before looking at these roles in detail, however, it is necessary to review briefly the factors that control the ocean–atmosphere exchange of gases.

Table 8.1 Non-variable gases in the atmosphere[a]

Gas	Concentration (%)	Gas	Concentration (ppm)
N_2	78.084	Ne	18.18
O_2	20.946	He	5.24
CO_2	0.033	Kr	1.14
Ar	0.934	Xe	0.087
		H_2	0.5
		CH_4	2.0
		N_2O	0.5

[a] After Richards (1965).

8.2 The exchange of gases across the air/sea interface

The solubility of a gas in sea water is an important factor in controlling its uptake by the oceans; thus, the more soluble gases partition in favour of the water phase, whereas the less soluble gases partition in favour of the atmosphere. The solubilities of gases in sea water are a function of temperature, salinity and pressure. A considerable amount of very accurate data is now available on the solubilities of various gases (e.g. oxygen, nitrogen, argon) in sea water, and equations have been derived to express the dependence of the solubility values on temperature and salinity; an example of this is given in Worksheet 8.1. All gases become more soluble, at least to some degree, in water as the temperature decreases, and this has important implications for the distributions of gases in surface waters, which exhibit considerable temperature variations from the equatorial regions to the poles.

Kester (1975) drew attention to the importance of the concept of partial pressure as a useful means of representing the composition of a gaseous mixture, e.g. the atmosphere. Thus, the total pressure exerted by a mixture of gases in a volume of the mixture is the sum of the partial pressures of the individual gases. This concept of partial pressure can also be applied to gas molecules dissolved in aqueous solution, and Henry's law describes the relationship between the partial pressure of a gas in solution (P_G) and its concentration (c_G); thus

$$P_G = K_G c_G \tag{8.1}$$

where K_G is the Henry's law constant. In a very simplistic manner, therefore, the rate of transfer of a gas from the atmosphere is proportional to its partial pressures in the two reservoirs, i.e. the atmosphere (p) and the sea (P), respectively. At equilibrium, when the partial pressure of a gas is the same in both the air and the water reservoirs (i.e. $p = P$), molecules enter and leave each phase at the same rate. However, when the partial pressure of the gas in one reservoir is higher than that in the other, there will be a *net* diffusive flow of gas into or out of the sea in response to the concentration gradient across the air/sea interface.

Following Liss (1983) and Liss & Merlivat (1986), a net gas flux (F) across the air/sea interface must therefore be driven by a concentration difference (ΔC) between the air and the surface water, with the magnitude and direction of the flux being proportional to the numerical value and sign of ΔC; thus

$$F = K_{(T)w}\,\Delta C \tag{8.2}$$

WORKSHEET 8.1
THE SOLUBILITY OF GASES IN SEA WATER

Weiss (1970) derived an equation to calculate the temperature and salinity dependence of gas solubilities in sea water from moist air. Thus:

$$\ln c^* = A_1 + A_2(100/T) + A_3 \ln(T/100) + A_4(T/100) + S‰[B_1 + B_2(T/100) + B_3(T/100(^2] \quad (1)$$

where c^* is the solubility in sea water from water-saturated air at a total pressure of one atmosphere; the A's and B's are constants, the numerical values of which depend on the individual gas and the expression of the solubility; T is the absolute temperature; and $S(‰)$ is the salinity. A data set derived from Equation 1 is given in Table (i) showing how the solubility of oxygen in sea water varies with temperature and salinity. There are various ways of expressing gas solubilities, and in order to illustrate the temperature and salinity variations the values listed are given in μmol kg^{-1}.

Table (i) The solubility of oxygen in sea water[a] (units, μmol kg^{-1})

	Salinity (‰)												
T°C	0	4	8	12	16	20	24	28	31	33	35	37	39
−1	469·7	455·5	441·7	428·3	415·4	402·8	390·6	378·8	370·2	364·6	359·0	353·5	348·2
0	456·4	442·7	429·4	416·5	404·0	391·9	380·1	368·7	360·4	354·9	349·5	344·2	339·0
1	443·8	430·6	417·7	405·3	393·2	381·5	370·1	359·0	351·0	345·7	340·5	335·4	330·3
2	431·7	418·9	406·5	394·5	382·8	371·5	360·5	349·8	342·0	336·9	331·8	326·9	322·0
3	420·2	407·9	395·9	384·2	372·9	361·9	351·3	340·9	333·4	328·5	323·6	318·8	314·1
4	409·3	397·3	385·7	374·4	363·5	352·9	342·6	332·5	325·2	320·4	315·7	311·1	306·5
5	398·8	387·2	375·9	365·0	354·4	344·1	334·1	324·4	317·4	312·7	308·1	303·6	299·2
6	388·7	377·5	366·6	356·0	345·8	335·8	326·1	316·7	309·8	305·3	300·9	296·5	292·2
7	379·1	368·2	357·7	347·4	337·5	327·8	318·4	309·3	302·6	298·3	294·0	289·7	285·5
8	369·9	359·4	349·1	339·2	329·6	320·2	311·1	302·2	295·8	291·5	287·3	283·2	279·2
9	361·1	350·9	341·0	331·3	322·0	312·9	304·0	295·4	289·2	285·0	281·0	277·0	273·0
10	352·6	342·7	333·1	323·7	314·6	305·8	297·2	288·9	282·8	278·8	274·8	271·0	267·1
11	344·5	334·9	325·5	316·5	307·6	299·1	290·7	282·6	276·7	272·8	269·0	265·2	261·5
12	336·7	327·3	318·3	309·5	300·9	292·6	284·5	276·6	270·8	267·0	263·3	259·6	256·0
13	329·2	320·1	311·3	302·8	294·4	286·3	278·5	270·8	265·2	261·5	257·9	254·3	250·8
14	322·0	313·2	304·7	296·3	288·2	280·4	272·7	265·3	259·8	256·2	252·7	249·2	245·8
15	315·1	306·5	298·2	290·1	282·3	274·6	267·1	259·9	254·6	251·1	247·7	244·3	240·9
16	308·5	300·1	292·0	284·2	276·5	269·1	261·8	254·7	249·6	246·2	242·8	239·5	236·3
18	295·9	288·0	280·3	272·9	265·6	258·5	251·7	245·0	240·1	236·9	233·7	230·6	227·5
20	284·2	276·7	269·5	262·4	255·5	248·8	242·3	235·9	231·2	228·2	225·2	222·2	219·3
22	273·4	266·3	259·4	252·7	246·1	239·7	233·5	227·5	223·0	220·1	217·3	214·4	211·6
24	263·3	256·5	250·0	243·6	237·3	231·3	225·4	219·6	215·4	212·6	209·9	207·2	204·5
26	253·8	247·4	241·2	235·1	229·2	223·4	217·7	212·2	208·2	205·6	202·9	200·4	197·8
28	245·0	238·9	232·9	227·1	221·5	215·9	210·6	205·3	201·5	198·9	196·4	194·0	191·5
30	236·7	230·9	225·2	219·7	214·2	209·0	203·8	198·8	195·1	192·7	190·3	188·0	185·7
32	228·9	223·4	217·9	212·6	207·5	202·4	197·5	192·7	189·2	186·9	184·6	182·3	180·1

[a] From Kester (1975).

where ΔC is the concentration difference driving the flux (F) and the constant of proportionality $K_{(T)w}$, which links the flux and the concentration difference, has the dimensions of a velocity and may be termed the transfer coefficient, transfer velocity, or piston velocity.

The concentration difference (ΔC) can be expressed as

$$\Delta C = C_a H^{-1} - C_w \tag{8.3}$$

where C_a and C_w are the gas concentrations in the air and the water, respectively, and H is the dimensionless Henry's law constant (expressed as the ratio of the concentration of gas in air to its concentration in non-ionized form in the water, at equilibrium).

The total transfer velocity can be expressed as

$$1/K_{(T)w} = 1/\alpha k_w + 1/Hk_a \tag{8.4}$$

where k_a and k_w are the individual transfer velocities for chemically unreactive gases in the air and water phases, respectively, α is a factor that quantifies any enhancement of gas transfer in the water as a result of chemical reactions, and H is as defined in Equation 8.3. According to Liss (1983), however, it is more convenient to think in terms of the reciprocal of the transfer velocity, which is a measure of the resistance to interfacial gas exchange. In this manner, Equation 8.4 can be expressed in terms of resistance to gas exchange when $1/K_{(T)w} = R_{(T)w}$, $1/\alpha k_w = r_w$ and $1/Hk_a = r_a$; thus

$$R_{(T)w} = r_w + r_a. \tag{8.5}$$

Liss (1983) pointed out that the phase whose resistance controls the air/sea transfer of a gas can be identified from a knowledge of the magnitude of r_w and r_a. On this basis, the author divided the principal gases into two groups.

(a) Gases for which $r_a \gg r_w$. These gases generally have low H values (high water solubilities), i.e. they partition dominantly into the water phase. Gases in this group include SO_2, NH_3 and HCl.
(b) Gases for which $r_w \gg r_a$. Thus r_w is the dominant resistance to transfer. These gases generally have high H values (low water solubility) and include O_2, CO_2, CO, CH_4, CH_3I, MeI, Me_2S and the inert gases. Liss & Merlivat (1986) pointed out that the majority of gases that are important in geochemical cycling therefore fall into the (b) category.

The exchange or transfer of a gas across the air/sea interface is therefore dependent on: (a) the concentration difference across the air/sea interface, i.e. any flux must be driven by a concentration gradient and the magnitude of the diffusive flux is proportional to this gradient (the coefficient of molecular diffusion); and (b) the transfer coefficient (piston velocity). In turn, these are dependent on physical factors such as wind velocity and temperature, and on the solubilities, diffusion rates and

chemical reactivities (aqueous chemistry) of individual gases. Data are available on both the molecular diffusivities and solubilities of gases in sea water, and a summary of these data is given in Table 8.2.

The main resistance to gas transfer is concentrated in a thin layer near the air/sea interface, and a number of approaches have been used to investigate gas exchange rates across this interface. These include: (a) theoretical models of the gas transfer processes; (b) laboratory experiments designed to quantify the parameters required for the flux equations, e.g. wind tunnel experiments for investigating the dependence of transfer coefficients on windspeed; and (c) field measurements of air/sea gas fluxes or transfer coefficients. Each of these approaches is considered below.

THEORETICAL MODELS The ability to model the gas transfer process adequately is obviously important since it would permit transfer velocities to be determined from a knowledge of other parameters (e.g. windspeed), and would also allow measurements of the transfer velocity for one gas to be converted into equivalent values for another gas. Models of varying complexity have been used to describe the exchange of gases across the air/sea interface. These include the following. (i) The 'stagnant film model', in which the rate-controlling process is transport across the

Table 8.2 The solubilities and molecular diffusivities of some gases in sea water[a]

Gas	0°C		24°C	
	Solubility ($cm^3 l^{-1}$)	Diffusion coefficient ($\times 10^{-5}$ cm^2 s^{-1})	Solubility ($cm^3 l^{-1}$)	Diffusion coefficient ($\times 10^{-5}$ cm^2 s^{-1})
He	7.8	2.0	7.4	4.0
Ne	10.1	1.4	8.6	2.8
N_2	18.3	1.1	11.8	2.1
O_2	38.7	1.2	23.7	2.3
Ar	42.1	0.8	26.0	1.5
Kr	85.6	0.7	46.2	1.4
Xe	192	0.7	99	1.4
Rn	406	0.7	186	1.4
CO_2	1437	1.0	666	1.9
N_2O	1071	1.0	476	2.0

[a] Data from Broecker & Peng (1982).

stagnant film layer by molecular diffusion. (ii) The 'surface renewal model', which still retains the concept of a stagnant film, but where this film is periodically replaced by bulk sea water and the rate-determining step for gas transfer is the rate at which the film is replaced. (iii) 'Boundary-layer models', which are relatively complex models that make use of boundary-layer theories on the transfer of mass (or heat) at surfaces and apply them to gas exchange across an air/sea interface. There are various problems involved in applying any of these models to field data (see e.g. Burton *et al.* 1986). However, the classical stagnant film model (SFM) has been widely used in oceanography, and according to Broecker & Peng (1974) it does offer an adequate first-order approximation of the very complex processes that actually take place at the air/sea interface. For this reason the SFM is considered in more detail in Worksheet 8.2. In order to use the theoretical models it is necessary to have a knowledge of, among other parameters, air–sea gas transfer coefficients (k_w). These can be measured under both laboratory and field conditions.

WORKSHEET 8.2
THE STAGNANT FILM MODEL FOR GAS EXCHANGE ACROSS THE AIR/SEA INTERFACE

Following Broecker & Peng (1974, 1982), the concepts underlying the stagnant film model (SFM) can be summarized as follows. In the SFM it is assumed that the rate-limiting step to the transfer of a gas between the air and the water is molecular diffusion through a stagnant water film. The air above the film and the water below it are assumed to be well mixed, and the gas concentration at the top of the film is assumed to be in equilibrium with the air above it. If the partial pressure of the gas in the air yields a concentration of the gas at the top of the film that is different from that in the water below, then a concentration gradient is set up. Transfer of the gas through the film then results from molecular diffusion along the gradient from the high- to the low-gradient region.

The rate at which the diffusion occurs depends on a number of factors, which include the following.

(a) The rate at which the gas diffuses through sea water. A list of the molecular diffusivities of dissolved gases in sea water is given in Table 8.2, from which it can be seen that the diffusivities increase with temperature.
(b) The thickness of the film. As the thickness of the film increases, the time taken for a gas to diffuse through it also increases. The thickness of the film, and so the rate of gas exchange across it, is dependent on the degree of agitation of the sea surface by the wind; the stronger the wind, the thinner the film and the more rapid the exchange rate.
(c) The difference in the concentration of a gas between the air and the sea (disequilibrium magnitude). The larger the difference, the greater the concentration gradient and the faster the molecular diffusive transfer.

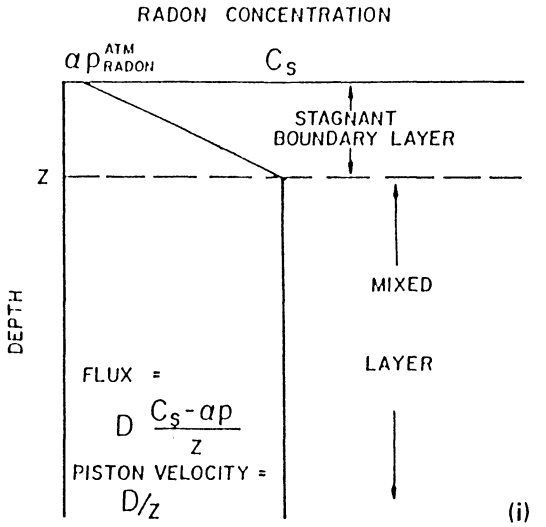

Figure (i) The stagnant boundary layer model (from Broecker & Peng 1974).

The SFM is illustrated diagrammatically in Figure (i), with reference to radon exchange. The rate of transfer of the gas between the water and the air is controlled by the thickness of the stagnant boundary layer through which the gas is transferred only by molecular diffusion. The overlying air and the underlying water are assumed to be well mixed. In the flux equation D is the molecular diffusivity of the gas, z is the thickness of the film, C_s is the concentration of the gas at the bottom of the film, α is the solubility of the gas, and p is the partial pressure of the gas in the air.

There are difficulties in applying the SFM to 'reactive' gases, such as CO_2, for which chemical, as well as physical, transport across the stagnant layer are important. For example, CO_2 can react via hydration to give, on ionization, HCO_3 and CO_3 (see Sec. 8.4.2). If this hydration were rapid enough for carbonate equilibria to be reached at all points as it crossed the film, then concentration gradients would be set up for all components in the system, i.e. not simply for dissolved CO_2, and since the net rate of transport is the sum of all the individual carbon species along the individual gradients, the overall transfer rate would be enhanced. The effect of chemical enhancement on the exchange rate for CO_2 varies with the film thickness, although the average film thickness in the sea probably lies in the region where the chemical enhancement is negligible. Under some conditions, however, the air–sea exchange of CO_2 can be enhanced by the side effects of pH variations within the film, which are dependent on the equilibria in the carbonate system.

LABORATORY MEASUREMENTS Most laboratory experiments involve the use of wind tunnels to elucidate the dependence of gas transfer coefficients on wind velocity. Liss & Merlivat (1986) summarized the available wind tunnel data on the k_w–windspeed relationship and drew the following conclusions. (i) In 'smooth surface regimes' with windspeeds up to ~ 5 m s^{-1} the water surface has only few waves and values of k_w increase only gradually. (ii) In 'rough surface regimes' with windspeeds between ~ 5 and ~ 12 m s^{-1}, waves are more common and there is a considerable increase in k_w with increasing windspeed. (iii) In 'breaking wave (bubble) regimes', which have windspeeds >10 m s^{-1}, the bubble bursting enhances gas transfer rates, which increase more strongly than in the other two regimes with increasing windspeed. In both the rough surface and breaking wave regimes, the dependence of k_w on wind velocity varies for different gases; thus, less soluble gases (e.g. O_2) show the effect of bubble enhancement on k_w at lower windspeeds than the more soluble gases (e.g. CO_2; see Table 8.2). However, there is considerable doubt as to the applicability of the laboratory experiments to real oceanic conditions, and according to Roether (1986) the transfer coefficients can only be predicted from field measurements.

FIELD MEASUREMENTS A number of field techniques are available for the measurement of k_w, and these have been summarized by Roether (1986). An example of how field data can be plugged into a theoretical model has been provided by Broecker & Peng (1974) who attempted to assess the applicability of the SFM to the exchange of gases across the ocean/atmosphere interface using radio-carbon and radon tracers to determine k_w values. Their principal findings may be summarized as follows. (i) The mean stagnant film thickness for the World Ocean was found to be between 40 ± 30 and 50 ± 30 μm, depending on the tracer technique used. The thickness appears to vary in inverse proportion to the square of the wind velocity, as predicted by Kanwisher (1963). (ii) From a knowledge of the wind velocity, mixed layer thickness and partial pressure difference between the air and the sea surface, the net transfer rate of most gases between the atmosphere and the sea can be predicted to within an accuracy of $\sim \pm 30\%$. (iii) Using the average of film layer thickness it is possible to compute the mean residence times of various gases in the atmosphere with respect to transfer to the mixed layer, and in the mixed layer with respect to transfer to the atmosphere. The average residence time for transfer from the atmosphere to the mixed sea surface layer is ~ 300 yr for gases with solubilities in the normal range (see Table 8.2); for CO_2 it is ~ 8 yr. The average residence time for transfer from the mixed layer of the sea to the atmosphere for most gases is ~ 1 month. For CO_2 the situation is more complex. The mixed layer of the ocean probably achieves chemical equilibrium with CO_2 in the atmosphere in

1.5 yr. This leads to the important conclusion that, since the replacement time of the mixed layer by mixing with underlying water is around a decade, the rate-limiting step in the removal of anthropogenic (fossil fuel) CO_2 from the atmosphere is vertical mixing within the sea, rather than gas transfer of CO_2 across the air/sea interface. Except for gases with very high solubilities (e.g. SO_2, CO_2, NO_2 – see Table 8.2) the sea is not an effective sink for anthropogenic gases, since their entry into the system would require many hundreds of years.

Once a gas is dissolved in sea water, i.e. it has diffused across the interface into the liquid phase, the processes that determine its oceanic distribution depend on the nature of the gas itself. The distribution of those gases which are generally regarded as being **non-reactive** in sea water, e.g. nitrogen and the inert gases, are controlled by physical processes and by the effects of temperature and salinity on their solubility (Kester 1975). It is usual to express variations in the non-reactive gases in terms of their percentage saturation. To do this, the observed concentration of the gas in the sea is given as the percentage of its solubility in pure water of the same temperature and salinity. Thus

$$\text{Saturation (\%)} = 100 \times G/G' \tag{8.6}$$

where G is the observed gas content in sea water, and G' is the solubility of the gas in pure water having the observed temperature and salinity (Richards 1965, Riley & Chester 1971).

Factors in addition to those described above affect the distributions of the **reactive** gases, such as oxygen and carbon dioxide, in the oceans. Although oxygen is in fact relatively chemically inert in sea water, it is involved in biological processes and these strongly affect its distribution in the water column. Carbon dioxide also takes part in biological processes, and the competing processes of photosynthesis (utilization of CO_2, liberation of O_2) and respiration (utilization of O_2, liberation of CO_2) are the cause of many of the *in situ* changes in the concentrations of the two gases in the sea. In addition, CO_2 is extremely reactive in sea water. Oxygen and carbon dioxide therefore behave in a non-conservative manner in the oceans.

All gases present in the atmosphere are found to some extent in solution in sea water. In the present context, attention will be mainly confined to those gases which play a major role in the marine biogeochemical cycles. These are chiefly oxygen and carbon dioxide; the importance of SO_2 (and other sulphur species) in the marine aerosol sulphate cycle has been discussed in Section 4.1.4.3, and the role of H_2S in redox-mediated reactions is covered in Section 11.5.6. However, before describing the factors that affect the distributions of oxygen and carbon

dioxide in the oceans, it is worthwhile briefly reviewing some of the work carried out on some of the other gases that are dissolved in sea water.

The oceans can act as a source or a sink for atmospheric gases, and air–sea exchange can play a significant role in the global geochemical cycles of some gases. A number of attempts have been made recently to evaluate the importance of this air–sea exchange in the geochemical cycles of various gases. For example, Liss (1983) used the then currently available data to draw up a compilation of the air–sea fluxes of a number of gases. Some of these data are reproduced in Table 8.3, in which the magnitudes of the fluxes indicate whether the sea surface acts as a source (sea → air) or a sink (air → sea). The magnitudes of the fluxes for some other gases are also included in the table, so that the importance of the air–sea exchange flux can be evaluated within their global cycles. For example, it can be seen that for methane (CH_4) the sea surface acts as a source; however, the sea → air flux ($\sim 10^{12}$–10^{13} g yr^{-1}) is only a few per cent of the total amount of CH_4 from natural terrestrial sources ($\sim 10^{15}$ g yr^{-1}). Methyl iodide (CH_3I) also has a flux in the sea → air direction, and the most recent data indicate that it is in the range $\sim$ (3–13) $\times 10^{11}$ g yr^{-1}. It has been estimated that a sea to air flux of some form of volatile iodine amounting to $\sim 5 \times 10^{11}$ g yr^{-1} is required to balance the global geochemical cycle of iodine, and it is apparent that the CH_3I out-of-sea flux can account for between $\sim$ 50 and 250% of this. Liss (1986) concludes, therefore, that the emissions from the sea surface are important, if not dominant, in the global geochemical cycling of iodine. The sea surface also acts as a source for atmospheric CO and H_2 (see Table 8.3), although the marine inputs amount to only $\sim$ 3% of the total CO and $\sim$ 5% of the total H_2 emitted to the atmosphere. In contrast, for some gases the sea acts as a sink. Carbon tetrachloride (CCl_4) and trichlorofluoromethane (Freon-11) are examples of such gases, and both are of special interest because anthropogenic sources dominate their inputs to the atmosphere; in fact, Freon-11 has no natural sources. Data reported by Liss & Slater (1974) for the North and South Atlantic indicated that there was a sea → air flux of $\sim 1.4 \times 10^{10}$ g yr^{-1} for CCl_4 ($\sim$ 2% of the total anthropogenic production rate at the time), with a mean undersaturation of sea water with respect to the air of $\sim$ 10%. However, a decade later data from the same region (Hunter-Smith *et al.* 1983) indicated that the air and sea water were essentially at equilibrium, thus implying that there was no net CCl_4 flux at this time. A similar situation has also been found for Freon-11. Thus, although Liss & Slater (1974) estimated that there was an air–sea Freon-11 flux of $\sim 5.4 \times 10^9$ g yr^{-1}, more recent data have indicated that there is a saturation equilibrium for the gas between the surface ocean and the atmosphere. These time changes in the air–sea flux relations for the two gases probably result from recent decreases in their release rates to the atmosphere.

Table 8.3 Net global fluxes of some gases across the air/sea interface

Gas	Global air-sea direction[a]	Flux magnitude[b]	Data source
CH_4	+	$10^{12} - 10^{13}$	c
Man-made CO_2	-	6×10^{15}	c
N_2O	+	6×10^{12}	c
$(CCl_4$	-	10^{10}	c
$(CCl_4$	=	~ 0	c
$(CCl_3F$	-	5×10^9	c
$(CCl_3F$	=	~ 0	c
CH_3I	+	$3 - 13 \times 10^{11}$	c
CO	+	$100 \pm 90 \times 10^{12}$	d
H_2	+	$4 \pm 2 \times 10^{12}$	d
Hg	+	$\sim 2 \times 10^9$	e

[a] + indicates sea ---> air flux direction,
- indicates air ---> sea flux direction,
= indicates no net flux.

[b] Units in g (of the compound, where applicable) per year.

[c] Data from Liss (1983).

[d] Data from Conrad & Seiler (1986).

[e] Data from Fitzgerald (1986).

Exchange across the air/sea interface is also important in the global cycle of mercury. For example, in a state-of-the-art review, Fitzgerald (1986) concluded that although there are many deficiencies in the database the contribution of mercury from sea surface sources ($\sim 2 \times 10^9$ g yr^{-1}) could account for ~ 30–40% of the total emissions of the element to the atmosphere.

8.3 Dissolved oxygen in sea water

The vertical and horizontal distributions of oxygen in the oceans reflect a balance between: (a) input across the air/sea interface from the atmosphere, (b) involvement in biological processes and (c) physical transport. The various factors that control the distribution of dissolved oxygen in the sea lead to a number of pronounced features in its vertical profiles. These are illustrated in Figure 8.1a, and can be summarized as follows.

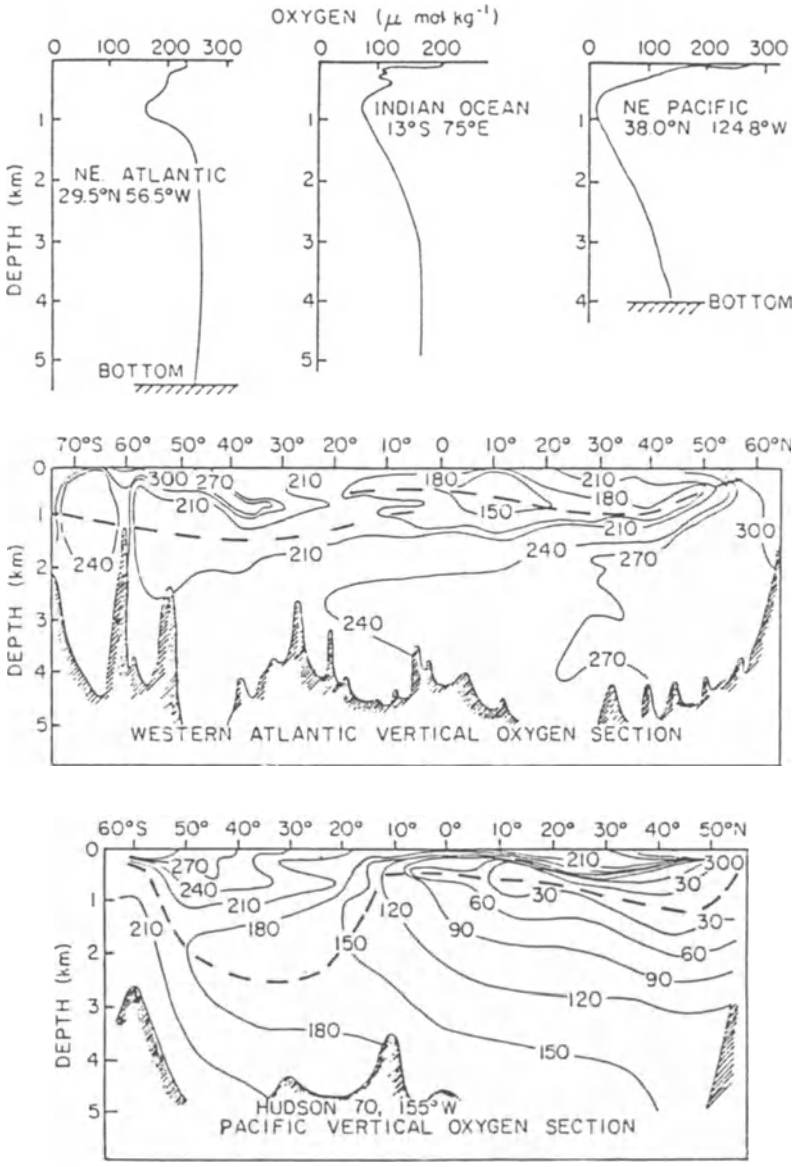

Figure 8.1 The vertical distribution of oxygen in the oceans (modified from Kester 1975), which lists the original data sources). (**a**) Vertical profiles for the Atlantic, Indian and Pacific Oceans. (**b**) Vertical section – western Atlantic. (**c**) Vertical section – central Pacific. The broken curves in (**b**) and (**c**) indicate the depth of the oxygen minimum surface.

(a) Oxygen in the surface, or mixed, layer is derived from exchange with the atmosphere so that its concentration is largely determined by its solubility in sea water, and on a global basis the concentrations of dissolved oxygen in sea water are greater in cold high-latitude waters than in those from the warmer subtropical regions. This atmospheric supply is supplemented by oxygen released during photosynthesis, a process that may be represented as

$$CO_2 + H_2O = CH_2O + O_2 \qquad (8.7)$$

where CH_2O indicates carbohydrate material (Richards 1965). However, the rate of exchange with the atmosphere is much faster than the rate at which the internal oceanic processes take place. As a result, photosynthesis does not usually lead to an excess of oxygen in the surface layer; nonetheless, the surface ocean does usually have a slight oxygen supersaturation ($\sim$ 5%), which may result from the trapping of air bubbles (Broecker 1974). Under some conditions, however, the exchange of photosynthetically produced oxygen and the atmosphere can be blocked (e.g. by a density cap formed by summer warming of the surface layer), with the result that photosynthesis can produce an oxygen saturation. For example, a summer subsurface **shallow oxygen maximum** (SOM) has been reported in a number of nutrient-poor oligotrophic marine regions (see e.g. Shulenberger & Reid 1981).

(b) Below the zone in which photosynthesis takes place there is a decrease in dissolved oxygen due to its consumption as a result of respiration and the decay of organic matter. The change in concentration at these depths may be either gentle or sharp.

(c) **Oxygen minima** are a characteristic feature in many marine areas. An *in situ* consumption of oxygen is necessary to sustain the layers, and this may arise from the oxidative decomposition of sinking detritus that has accumulated at a particular depth. Many oxygen minimum zones (OMZs) are large features, e.g. that in the eastern tropical Pacific, and although the oceanographic features leading to their formation are not fully understood, Packard *et al.* (1988) have suggested that they are formed when biological oxygen utilization exceeds the rates of oxygen replenishment via advection and diffusion. The depth of the OMZ varies from one ocean to another, being $\sim$ 300 m in the Atlantic, $\sim$ 200 m in the Pacific and $\sim$800 m in the Indian Ocean. Intense minima are especially well developed in the eastern subtropical Pacific, where they are advanced westwards off the coast of Central and South America.

(d) All *in situ* processes in the deep ocean lead to a decrease in dissolved oxygen, so that a depth depletion of the gas might be expected.

However, relatively little organic matter reaches the deep ocean, and as a result there is little consumption of oxygen. In fact, dissolved oxygen concentrations usually show a gradual increase from the base of the minimum layers to the bottom of the water column. This is a consequence of the deep water thermohaline circulation system in which oxygen-rich high-latitude surface waters sink and are transported along the global 'grand tour' (see Sec. 7.3.3). Once the oxygen has been transported to deep water it is removed from contact with the atmosphere, and it is also taken out of the euphotic zone in which photosynthetic reactions take place. Nonetheless, there is *some* oxygen utilization by animals and bacteria in deep water, and this oxygen cannot be replaced by exchange with the atmosphere or by plant activity. During the 'grand tour' therefore dissolved oxygen becomes depleted, with the overall result that concentrations decrease from the waters of the deep Atlantic to those of the deep Pacific; this is the reverse of the situation for the nutrients (see Sec. 9.1.2.2). In order to evaluate the amount of oxygen that is biologically consumed in the deep ocean the concept of **oxygen utilization** is often employed. This is a measure of the oxygen that has been utilized, rather than the amount that remains in the waters, and is based on the premise that in surface water the oxygen is present at almost equilibrium, or saturation, values with the overlying atmosphere. In contrast to surface waters, deep waters are highly undersaturated with respect to dissolved oxygen, and a measure of the amount of oxygen that has been utilized can therefore be obtained from the difference between the saturation and the observed oxygen contents. It is usual, however, to use the term **apparent oxygen utilization** (AOU) since surface water can be up to ~ 5% supersaturated with dissolved oxygen (see above). The AOU is thus a measure of the change in dissolved oxygen that has taken place after the waters have left the surface. AOU values are lowest in the Atlantic (less utilization) and highest in the Pacific (more utilization), as the deep water 'grand tour' progresses along its path, and utilization and water mass mixing take place. It must be stressed, however, that most oxygen utilization occurs in surface waters.

According to Kester (1975) ocean-scale sections of the vertical and horizontal distributions of dissolved oxygen reflect a number of major features in water circulation patterns. This is evident in the oxygen distribution diagrams given in Figures 8.1b and c, and these can be used to illustrate in a general way how dissolved oxygen can be employed for the characterizataion of water masses. In this context, Kester (1975) identified a number of features in these diagrams.

(a) Antarctic Intermediate Water can be seen as an intrusion of oxygen-rich water in both the Atlantic and Pacific Oceans, extending from the surface at ~ 50°S to ~ 800 m at ~ 20°S.
(b) North Atlantic Deep Water is evident as oxygen-rich deep water extending from ~ 0 to ~ 2000 m at ~ 60°N to an oxygen maximum at ~ 3000 m in the south equatorial Atlantic.
(c) The northward flow of North Atlantic Deep Water and Antarctic Bottom Water into the deep and Pacific gives rise to a progressive decrease in the oxygen content from south to north.
(d) Waters at intermediate depths are more deficient in oxygen in the North Pacific than in the North Atlantic.

There are some conditions in the oceans, and in other bodies of water, where the subsurface circulation, and so the supply of dissolved oxygen, is restricted. Here, the oxidative decomposition of organic matter utilizes, and can sometimes exhaust, the dissolved oxygen so that **anoxic** conditions are set up. Such anoxic conditions actually prevail in only a very small proportion of the World Ocean, examples being found in fjords, certain basins (e.g. the Gotland Basin, the Black Sea) and in deep-sea trenches (e.g the Cariaco Trench). However, there are also some open-ocean areas in which the concentrations of dissolved oxygen are reduced almost to zero values. For example, dissolved oxygen concentrations are extremely low in intermediate and deep waters north and south of the Equator in the eastern Pacific, and in the northern Indian Ocean; these are close to regions of upwelling and high primary productivity. Oxygen-deficient waters are also found in the Mediterranean Sea – see Figure 8.2.

The two common isotopes of oxygen are ^{16}O and the stable trace species ^{18}O. These isotopes are fractionated during biochemical reactions so that the organic matter has an $^{18}O : {}^{16}O$ ratio that is lower than that in sea water. The fractionation is also affected by temperature changes. For example, the $^{18}O : {}^{16}O$ ratios of carbonate shells reflect the temperature of the water in which they grew, and this has been used in evaluating past climatic changes. In addition, $^{18}O : {}^{16}O$ ratios can be used as water mass tracers; this is because surface waters can be characterized on the basis of their ^{18}O contents, which tend to be enriched at low latitudes.

8.4 Dissolved carbon dioxide in sea water: the dissolved CO_2 cycle

8.4.1 Introduction

Carbon dioxide is transferred into the biosphere via both the photosynthesis of marine plants and the formation of carbonate shells by plants

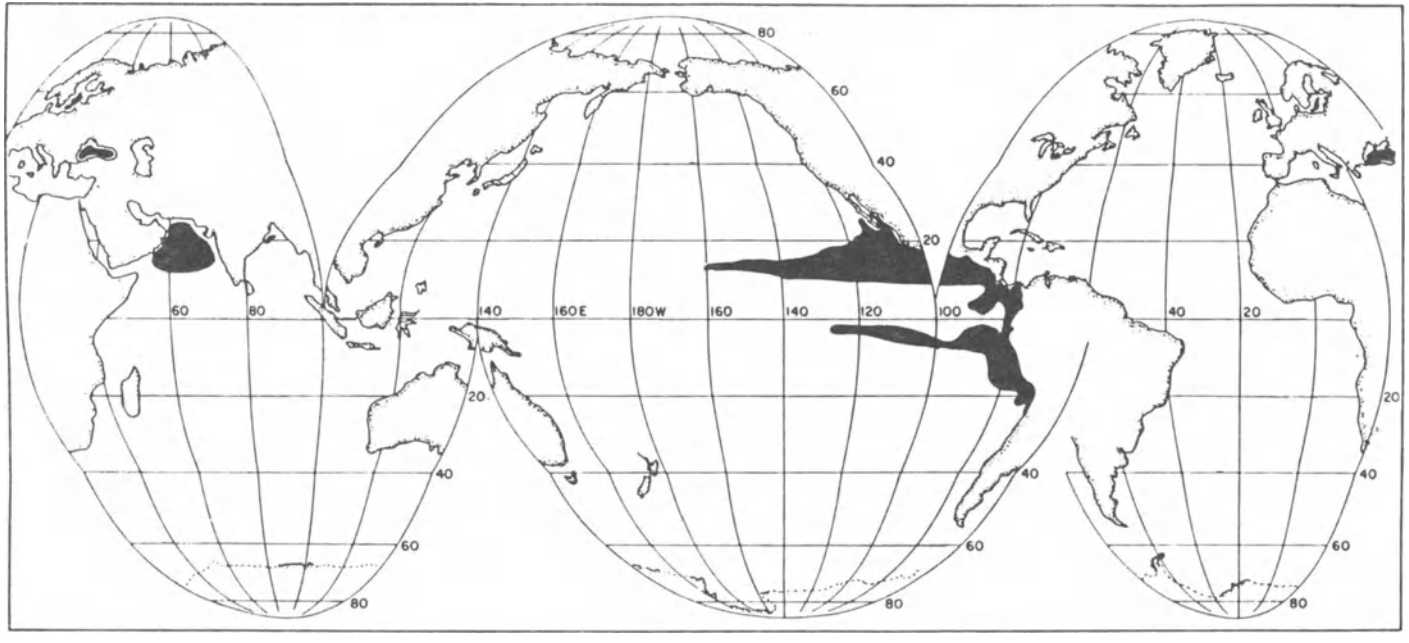

Figure 8.2 The distribution of oxygen-deficient water ($< 20\ \mu g\ atom\ l^{-1}$) in intermediate and deep waters from the World Ocean (from Deuser 1975).

and animals, and is therefore involved in the formation of both soft organic tissues and hard skeletal material. As carbon dioxide is removed from the waters by these biological reactions it is being continuously added from the atmosphere, and at greater depths in the water column it is regenerated by the oxidative destruction of organic matter and so increases in concentration below the surface. Thus, typical water column profiles of carbon dioxide show a depletion in the surface layers and an overall increase towards the base of the euphotic zone. In this respect the behaviour of carbon dioxide and oxygen may be thought of as being a mirror image of each other. However, carbon dioxide also differs from oxygen in that it is extremely chemically *reactive* in sea water, and this reactivity within the CO_2 system has a number of profound effects on the chemistry of the oceans. Perhaps the most important of these is the control it maintains on the pH of sea water. Another important feature of the reactivity of the gas in sea water is that the oceans, which contain around 53 times as much CO_2 as the atmosphere, act as a sink for excess atmospheric CO_2 and therefore as a regulator of planetary CO_2.

Carbon dioxide is taken into sea water via exchange with the atmosphere. Photosynthesis, primary production and the organic carbon cycle are covered in Section 9.3, and at this stage attention will be mainly confined to the dissolved CO_2 cycle.

8.4.2 Parameters in the seawater CO_2 system

The chemical cycle of CO_2 in the oceans is governed by a series of equilibria, which can be expressed as follows (see e.g. Skirrow 1975, Unesco 1987).

(a) The CO_2 in the atmosphere equilibrates with sea water via exchange across the air/sea interface; thus

$$CO_2(\text{gas}) \leftrightharpoons CO_2(\text{dissolved}) \tag{8.8}$$

(b) The dissolved CO_2 then becomes hydrated; thus

$$CO_2 + H_2O \leftrightharpoons \underset{\text{(carbonic acid)}}{H_2CO_3} \tag{8.9}$$

(c) The carbonic acid undergoes very rapid dissociation; thus

$$H_2CO_3 \leftrightharpoons H^+ + \underset{\text{(bicarbonate ion)}}{HCO_3^-} \tag{8.10}$$

and

$$HCO_3^- \rightleftharpoons H^+ + \underset{\text{(carbonate ion)}}{CO_3^{2-}} \tag{8.11}$$

These carbon dioxide–sea water equilibria are temperature- and pressure-dependent, and the relative proportions of the species are set by the pH of the system; transitions between the species take place in a direction that tends to maintain a constant pH, i.e. the carbonate in sea water is a buffering system. The major parameters in the sea water carbon dioxide system are therefore CO_2, H_2CO_3, HCO_3^- and CO_3^{2-}, and the total carbon dioxide content, or total inorganic carbon (ΣCO_2), is given by the sum of the concentrations (c) of all the species:

$$\Sigma CO_2 = c_{CO_2} + c_{H_2CO_3} + c_{HCO_3} + c_{CO_3}. \tag{8.12}$$

Only two of the parameters in the oceanic carbonate system can be measured directly; these are ΣCO_2 and the equilibrium partial pressure of carbon dioxide (P_{CO_2}). In this manner, therefore, P_{CO_2} is a measure of the dissolved carbon dioxide, and ΣCO_2 is a term that refers to the chemistry of the carbonate system in the oceans.

Carbon dioxide enters sea water as the atmosphere and the ocean attempt to achieve equilibrium, and in doing so it changes the chemistry of the system. Two of the keys to understanding these changes are linked to the pH and the alkalinity of the oceans.

8.4.2.1 pH Traditionally, pH has been operationally defined as

$$pH = -\log_{10} a_H \tag{8.13}$$

where a_H is the activity of the hydrogen ion. Thus, pH is the negative log of the hydrogen ion concentration, and the pH of a solution is a measure of its acidity in terms of some operational scale (see also Worksheet 14.1). In terms of modern electrochemical theory, however, the situation is much more complex than this. Precise potentiometric techniques are available for the measurement of pH, but there is disagreement over the scales that should be used for saline waters. The theoretical concepts involved in the measurement of pH have been described by Stumm & Morgan (1981) in their comprehensive text on aquatic chemistry, and the various problems inherent in the selection of pH scales for marine and estuarine waters have been reviewed by Culberson (1981), Dickson (1984) and Millero (1986). For the present purposes, however, it is sufficient to understand that, by taking the appropriate precautions, it is possible to make highly reproducible pH measurements in sea water that are normally adequate for most purposes in marine chemistry.

In sea water the equilibrium betweeen the components of the carbon dioxide system is controlled by the pH. At the pH range normally found for sea water, $> 99\%$ of the dissolved CO_2 is present in the form of carbonate (CO_3^{2-}) and bicarbonate (HCO_3^-) ions. Thus, according to

Skirrow (1975) for many purposes Equation 8.12 can be rewritten so that

$$\Sigma CO_2 = c_{HCO_3} + c_{CO_3}. \tag{8.14}$$

The pH range in normal open-ocean sea water is ~ 7.5 to ~ 8.4, and Sillen (1963) proposed that on a geological timescale this pH is controlled by chemical equilibria between the water and the common minerals of marine sediments (see Sec. 15.1.3). However, on timescales of hundreds, or thousands, of years it is changes in the equilibria between dissolved carbon dioxide, bicarbonate ion, carbonate ion and hydrogen ion that provide the principal pH-regulating system in the ocean (Skirrow 1975).

8.4.2.2 Alkalinity From the pH range given above it can be seen that sea water is slightly alkaline in character, a property that arises from the dissolution of basic minerals in sea water. The **total alkalinity** (TA) is the buffering capacity of natural waters and is equal to the charges of all the weak ions in solution (Stumm & Morgan 1981). TA is an important physicochemical property of sea water and plays a critical role in several chemical and biological processes. The reasons for this have been summarized by Burke & Atkinson (1988) as follows.

(a) HCO_3^- and CO_3^{2-} ions are the major anions of weak acids in sea water, so that changes in total positive charge resulting from alterations in the ratios of cations can be accompanied by shifts in TA ($HCO_3^- \rightarrow CO_3^{2-}$).
(b) The precipitation of calcium carbonate decreases the TA, and as a result TA is a measure of calcification and other biogeochemical processes involving species of CO_2.
(c) Net photosynthesis and respiration of biological communities change the concentration of dissolved inorganic carbon (DIC); the DIC of a water sample can therefore be calculated from its pH and TA.

Overall, alkalinity is a major factor in the oceanic carbon dioxide system; for example, changes in alkalinity affect the regulation of the ocean–atmosphere CO_2 equilibrium and the dissolution–preservation patterns of biogenic carbonates. Alkalinity is therefore one of the parameters used in assessing the status of the oceans in the global carbon cycle.

The alkalinity of sea water can be expressed in terms of the amount of strong acid necessary to bring its reaction to some standard specified end-point in a given volume of solution. Alkalinity has therefore been determined using a titrimetric technique, and historically total alkalinity (TA) has been defined as the number of equivalents of strong acid required to neutralize 1 litre of sea water to an end-point corresponding to the formation of carbonic acid from carbonate. Rakestraw (1949)

attempted to redefine the historical concept of alkalinity on a more rigorous basis by relating it to the Lowry-Brønsted definition, in which an acid is a proton donor and a base is a proton acceptor. Thus, alkalinity can be defined as the excess of bases (proton acceptors) over acids (proton donors) in sea water. The only anions of weak acids that are present at significant concentrations in sea water are the bicarbonate, the carbonate and the borate ions, and originally it was considered that it is these which contribute to the alkalinity. For the determination of alkalinity by titration with a strong acid (e.g. HCl) an end-point was therefore selected at which the bicarbonate, carbonate and borate ions are completely combined with protons to form H_2CO_3 and H_3BO_3, and the expression for the total alkalinity of sea water (in units of equivalents per litre, eq l^{-1}) was therefore commonly given as follows (see e.g. Dickson 1981):

$$TA = [HCO_3] + 2[CO_3] + [B(OH)_4] + [OH] - [H] \qquad (8.15)$$

which defines the equivalence point for an alkalinity determination at which

$$[H] = [HCO_3] + 2[CO_3] + [B(OH)_4] + [OH]. \qquad (8.16)$$

For example, the alkalinity of sea water was defined by Riley & Chester (1971) as

$$\text{Alkalinity (eq } l^{-1}) = c_{HCO_3^-} + 2c_{CO_3^{2-}} + c_{B(OH)_4} + (c_{HO} - c_H) \qquad (8.17)$$

where $c_{HCO_3^-}$, $2c_{CO_3^{2-}}$ and $c_{B(OH)_4}$ are the equilibrium concentrations of the ions (the concentrations of the doubly charge ions are multiplied by 2), and the term $(c_{HO} - c_H)$ is included to take account of the fact that the concentrations of the various anions determined by titration are greater than their equilibrium concentrations by $(c_{HO} - c_H)$ because of the reactions of the type

$$HCO_3^- + H_2O = H_2CO_3 + OH^-. \qquad (8.18)$$

The contributions made to the alkalinity of sea water by the carbonate species are termed the **carbonate alkalinity** (i.e. $c_{HCO_3^-} + 2c_{CO_3^{2-}}$), and since bicarbonate and carbonate are the dominant anions of weak acids in sea water, carbonate alkalinity $\simeq$ total alkalinity; that is, it is largely bicarbonate and carbonate ions which give sea water its alkalinity. However, various workers have drawn attention to the fact that sea water also contains a variety of other bases (such as NH_3, $Si(OH)_3O^-$, SO_4^{2-}), which will react with hydrogen ions in an alkalinity titration. In view of

this, a number of attempts have been made both to expand Equation 8.16 to take account of these other acid–base systems for the definition of total alkalinity, and to design instrumentation for its precise determination; for a detailed description of the principles underlying this modern approach to alkalinity, the reader is referred to Edmond (1970), Hansson & Jagner (1973), Dickson (1981) and Brewer *et al.* (1986).

Much of the recent data using the modern approach to alkalinity in the oceans has been generated by the GEOSECS and, more recently, the TTO programmes. In the GEOSECS programme around 6000 alkalinity measurements were made in waters from the major oceans, and the data have been described by Takahasi *et al.* (1980, 1981) and reviewed by Campbell (1983). Alkalinity in surface waters is well correlated with salinity (at a salinity of 35‰ the alkalinity is ~ 2300 eq l^{-1}), and variations in alkalinity are due mainly to differences in salinity (see e.g. Brewer *et al.* 1986). As a result, different water masses often have characteristic alkalinities, and clear linear alkalinity–salinity trends are found in all the major oceans. However, as Campbell (1983) has pointed out, processes such as the precipitation and dissolution of calcium carbonate, and the removal and regeneration of nitrate, affect alkalinity and contribute to its non-conservative behaviour.

The geographical distribution of alkalinity can be illustrated with respect to the GEOSECS data reported by Takahasi *et al.* (1980) and Campbell (1983) for the surface waters of the Atlantic Ocean lying between $\sim$ 40°S and $\sim$ 60°S – Figure 8.3. The alkalinity can be expressed as a linear function of salinity, and three clear trends are evident in the data.

(a) A warm water trend, which is defined by waters having a temperature > 10°C and probably represents the North and South Atlantic Central Waters.
(b) The Antarctic trend, which is defined by waters having a temperature of 2°C and probably represents Weddell Sea and Circumpolar Water.
(c) The sub-Antarctic transition, which forms a mixing line between the two major trends.

The alkalinity differences between the two major trends are due to differences in calcium concentrations resulting from the extraction of calcium, as $CaCO_3$, in the warm surface water, and the dissolution of $CaCO_3$ in deep water, which outcrops in the Antarctic. The GEOSECS data also provided information on the vertical distribution of alkalinity in the oceans. In general, there is a gradual increase in alkalinity with depth below the mixed layer (see Fig. 8.6b); there is also an increase in alkalinity in the deep waters of the Pacific, at the end of the 'grand tour'.

From the point of view of marine geochemistry, the two most

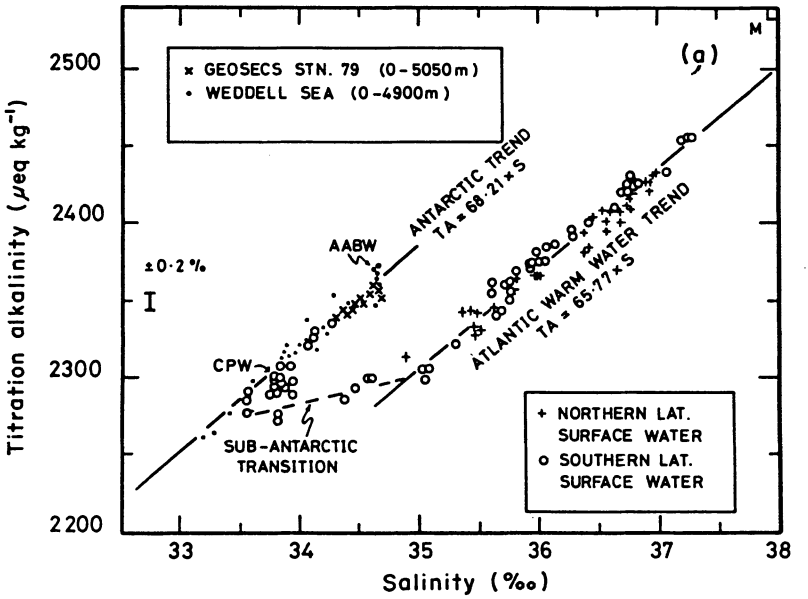

Figure 8.3 The alkalinity–salinity relationship for the Atlantic Ocean (from Campbell 1983, after Takahasi *et al.* 1980). Data are from GEOSECS stations (40°N–60°S) for water depths less than 50 m.

important features in the distribution of alkalinity in the oceans are (a) an increase in cold high-latitude relative to warm low-latitude surface water and (b) and increase in deep relative to surface waters. These variations are important because they can be related to the production and dissolution of calcium carbonate in the oceans. Thus, in warm low-latitude waters the relatively low alkalinity values probably result from the rapid growth of carbonate-secreting organisms and the associated uptake of nutrients during primary production, both of which lead to a lowering of the alkalinity. In deep waters, the increases in alkalinity reflect the presence of excess calcium, which is released as a result of the increasing extent of carbonate dissolution with depth in the water column and in the underlying sediment (see Sec. 15.2.4.1).

Any two of the four properties, i.e. P_{CO_2}, Σ_{CO_2}, pH and alkalinity, together with measurements of temperature and pressure, can be used to compute the remaining properties in the oceanic carbon dioxide system, and it is now possible to build up a general picture of how the system varies on a global basis. Variations in the oceanic CO_2 system arise in response to number of factors, which can be divided into two general types:

(a) External factors, such as temperature and pressure changes, water mass circulation, and water mixing.
(b) Internal factors, which involve material exchange within the oceanic carbon dioxide system itself.

According to Skirrow (1975) the principal effects of material exchange within the systems are those associated with the gain or loss of either carbon dioxide or calcium carbonate. The loss of CO_2 during photosynthesis, or by evasion to the atmosphere, leads to an increase in pH and a decrease in P_{CO_2} and ΣCO_2 in the surface layer. In contrast, the production of CO_2 by respiration and the oxidative destruction of organic matter leads to an increase in P_{CO_2} and ΣCO_2. It also lowers the pH of the deeper waters, making them more corrosive to calcium carbonate. As the carbonates dissolve they raise the ΣCO_2 concentration and alkalinity of the deep waters. Material exchanges involving calcium carbonate production (mainly surface waters) and dissolution (during descent down the water column) also affect the relative proportions of HCO_3^-, CO_3^{2-} and H^+.

An example of the manner in which the various parameters within the oceanic–atmospheric carbon dioxide system interact on a global scale has recently been provided by Boyle (1988) in terms of the glacial–interglacial CO_2 cycles. From ice core data it is apparent that atmospheric CO_2 levels were $\sim$ 80 ppm by volume lower during cold glacial climates than during warm interglacial times. The scenario developed by Boyle (1988) to explain this may be summarized as follows. Palaeochemical evidence has shown that the nutrients and metabolic CO_2 were shifted from intermediate waters to deeper waters during glacial times. As this redistribution was initiated, the increased deep-water-dissolved CO_2 concentrations raised the level of carbonate dissolution above that required for a steady-state input–output balance. In response to this, oceanic alkalinity then increased until steady-state dissolution rates were restored. Boyle (1988) therefore proposed that the atmospheric CO_2 decrease during cold glacial climates arose in direct response to the increased oceanic alkalinity.

8.4.3 The uptake of CO_2 by the oceans

According to Sundquist *et al.* (1979) the capacity of sea water to dissolve atmospheric CO_2 is enhanced by the capacity of the ocean system to buffer the associated changes in seawater chemistry. This buffering capacity depends on the conditions and reactions that control the partitioning of carbon within the oceans. Brewer (1983) has pointed out that the principal effect of adding CO_2 to the surface water of the oceans is to consume carbonate ion; thus

$$CO_2 + CO_3^{2-} + H_2O = 2HCO_3^-. \quad (8.19)$$

However, the reaction does not proceed completely to the right, and resistance to change occurs. This resistance, which is a function of the thermodynamics of the CO_2 system, is described by the buffer factor, or Revelle factor, and may be written

$$R = \frac{(dP_{CO_2}/P_{CO_2})_{TA,\ T,\ S}}{(dT_{CO_2}/T_{CO_2})_{TA,\ T,\ S}} \quad (8.20)$$

where T_{CO_2} is the total concentration of carbon dioxide in all its forms, P_{CO_2} is the partial pressure of carbon dioxide gas, TA is the total alkalinity, T is the temperature and S is the salinity. The buffer factor varies with temperature and has a value of ~ 10, but it changes as the level of CO_2 in the oceans rises. For example, Takahasi *et al.* (1980) showed that the values of R increase as the CO_2 content of the surface waters rise and so less CO_2 is taken up. However, the system is complex and is sensitive to the alkalinity : total CO_2 ratio, and therefore to pH. According to Brewer (1983), although it is therefore possible to predict the effects of adding CO_2 to sea water that has a constant alkalinity and chemical composition, changes in alkalinity will perturb the system. The addition of CO_2 to sea water does not alter the charge balance (Eqn 8.19), and so does not change the alkalinity. However, the dissolution of calcium carbonate does result in alkalinity changes. The CO_2 absorbed into surface sea water, and its subsequent entry into the oceanic biological and chemical systems, therefore affects the atmosphere, the water column and the sediment reservoirs.

A knowledge of the variation of P_{CO_2} in the World Ocean offers an understanding of how the atmosphere and the sea exchange on the global scale. It is useful, therefore, to assess quantitatively the way in which carbon dioxide enters and leaves the oceans, and this will be done with reference to the distribution of P_{CO_2}.

8.4.3.1 Geographical variations in the CO_2 system in surface ocean waters The distribution of P_{CO_2} in the oceans responds in a complex manner to seasonal temperature changes, water mixing and biological cycles within the surface layer of the sea. Many general features in the geographical distribution of P_{CO_2} in the World Ocean can be identified from the summer data set produced by Keeling (1968), which has been refined by the addition of other data, including those generated during GEOSECS and the TTO experiment. The overall picture reveals a complex system of P_{CO_2} highs and lows. This can be illustrated with respect to Keeling's data (see Fig. 8.4) and the situation can be summarized as follows.

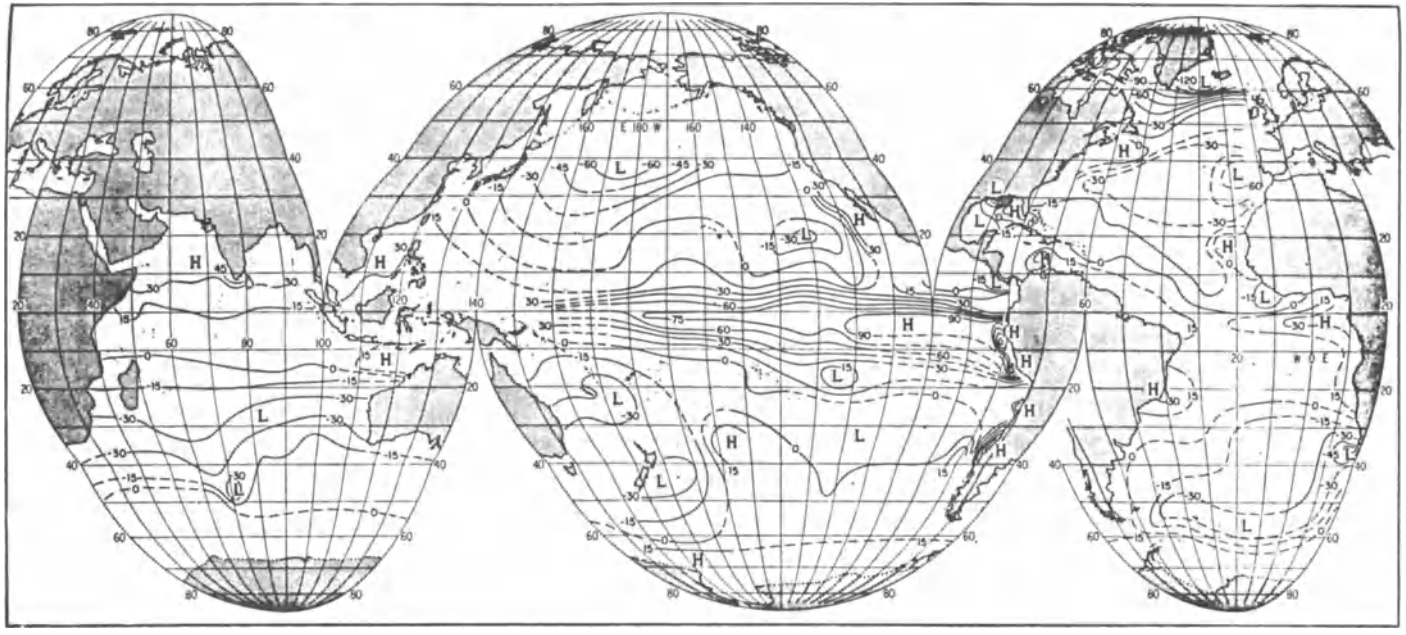

Figure 8.4 The distribution of P_{CO_2} in the World Ocean expressed as the departure in ppm from equilibrium with atmospheric CO_2 (from Keeling 1968). Most data represent summer conditions. The distribution shows a number of highs (H; positive values which imply evasion of CO_2 from the ocean to the air) and lows (L; negative values which imply invasion of CO_2 from the atmosphere to the ocean). More recently, other authors have presented data on the distribution of the sea/air CO_2 partial pressure difference ($\triangle P_{CO_2}$). Positive values indicate that the ocean is a source of CO_2, and include the equatorial waters of the Pacific and the Atlantic. These areas are strong CO_2 sources as a result of the upwelling of deep CO_2-rich waters and surface warming; a combined effect which overcomes the P_{CO_2} lowering caused by photosynthesis, although the 'source' can disappear in the equatorial Pacific during El Niño events. Negative values indicate that the ocean is a sink for CO_2, and include the northern North Atlantic and the Southern Ocean which act as sinks due to the combined effects of water cooling and photosynthesis (see, e.g., Takahashi 1989; *Oceanus* **32** (No. 2), 22–29).

(a) There are relatively large spatial variations in the distribution of P_{CO_2} in the surface waters of the World Ocean.
(b) High values of P_{CO_2} are found in pronounced belts in the equatorial regions of the Pacific, and to a lesser extent the Atlantic, where the upwelling of CO_2-rich waters and surface warming have increased the P_{CO_2}.
(c) P_{CO_2} in the equatorial zone in the Indian Ocean appears to be close to atmospheric equilibrium.
(d) Low values are found in the subtropical (and polar) gyres, where surface water cooling and biological activity have lowered P_{CO_2}; exceptions are found in areas of upwelling where CO_2-rich intermediate waters are upwelled to the surface.
(e) Localized areas where specialized conditions prevail include shallow water regions where chemical precipitation of calcium carbonate is occurring (e.g. the Bahama Banks).

This overall P_{CO_2} distribution is driven by a combination of processes, which include latitudinal changes in temperature and biological productivity, and surface water flows. Variations in P_{CO_2} in the upper oceans are particularly influenced by two important factors.

(a) **Biological primary production.** It has been suggested that the photosynthetic uptake, or 'drawdown', of CO_2 in the spring and summer, followed by regeneration in the winter, exerts a primary control on ocean surface CO_2 distributions (Brewer *et al.* 1986).
(b) **Temperature changes.** These affect the solubility of the gas in sea water and because of the relatively slow rate of exchange with the atmosphere, the heating and cooling of the ocean result in large-scale latitudinal P_{CO_2} gradients.

At high latitudes the partial pressure of carbon dioxide in the water (P_{CO_2}) is low relative to the partial pressure of the gas in the atmosphere (P_{CO_2}), to that there is a net transport, or flow, of CO_2 from the air to the sea, which leads to an increase in ΣCO_2 in the surface waters. In contrast, at low latitudes P_{CO_2} exceeds p_{CO_2}, and the net transport of the gas is from the sea surface to the atmosphere, which leads to a decrease in ΣCO_2 in the surface waters.

There is, however, considerable disagreement in the literature as to whether it is the *biological* or the *physical* factors that play the dominant role in controlling the CO_2 chemistry of the ocean system. The question was recently addressed by Brewer *et al.* (1986), who reviewed the literature on the topic and attempted a re-evaluation using new data from the TTO Atlantic Ocean experiment. A crude correction term was applied to the P_{CO_2} data to take account of the biological drawdown of CO_2 so that the residual signal should more closely approximate the

purely physical processes that affect the distribution of P_{CO_2} at the TTO stations. The data are illustrated in Figure 8.5 in the form of a three-dimensional plot, which shows CO_2 invasion 'holes' and evasion 'hills'. Brewer *et al.* (1986) pointed out that the corrected P_{CO_2} signal is similar to maps of the annual heat gain of the ocean. This similarity was thought to result from the fact that the heating and cooling of the ocean operate at a rate that is faster than that which controls the exchange of CO_2 between the atmosphere and the ocean, so that anomalies created by the heating–cooling processes persist. The correlations found are not perfect, but the signal that was revealed does offer a tantalizing glimpse of what might be possible in future experiments, e.g. those in GOFS, designed to separate more effectively the physical and biological factors controlling the distribution of P_{CO_2} in the oceans.

8.4.3.2 Vertical variations in the oceanic CO_2 Vertical profiles of the carbonate system in the sea show a number of distinctive features, the most striking being the differences between surface and deep waters; profiles of ΣCO_2, total alkalinity and P_{CO_2} and are given in Figure 8.6a, b and c, respectively.

Both ΣCO_2 and P_{CO_2} have low values in surface waters where biological activity removes CO_2 during the photosynthetic production of organic matter and takes out both CO_2 and calcium during the formation of carbonate shells. Below the surface layers ΣCO_2 and P_{CO_2} increase with depth. Here, the carbon dioxide system is affected by the regeneration of organic matter (and nutrients, i.e. the biological C pump) via oxidative destruction, which is mainly responsible for the sharp rises in ΣCO_2 and P_{CO_2}, which reach a maximum corresponding approximately to the oxygen minimum (see Sec. 8.3). Below this maximum, the values of P_{CO_2} and ΣCO_2 fall and then either fall further towards deeper water or become more or less constant with depth. In these deep waters, which are out of contact with the atmosphere, ΣCO_2 is changed by the mixing of different water masses, by the dissolution of carbonate shells, and by the decomposition of the relatively small amount of organic matter that reaches these depths. The dissolution of calcium carbonate shells, with the release of calcium, at depth in the water column is reflected in the total alkalinity profile, which also increases with depth. Overall, therefore, the shapes of the deep water profiles of the parameters of the carbonate system depend on (a) the flux of organic matter from the upper layers of the water column and its rate of oxidation, (b) the rate of dissolution of calcium carbonate, and (c) the characteristics of, and circulation patterns in, the various water masses cut by the vertical profile.

8.4.3.3 The global climatic importance of the oceanic CO_2 system: a brief overview The climatic implications of changes in the global CO_2 cycle

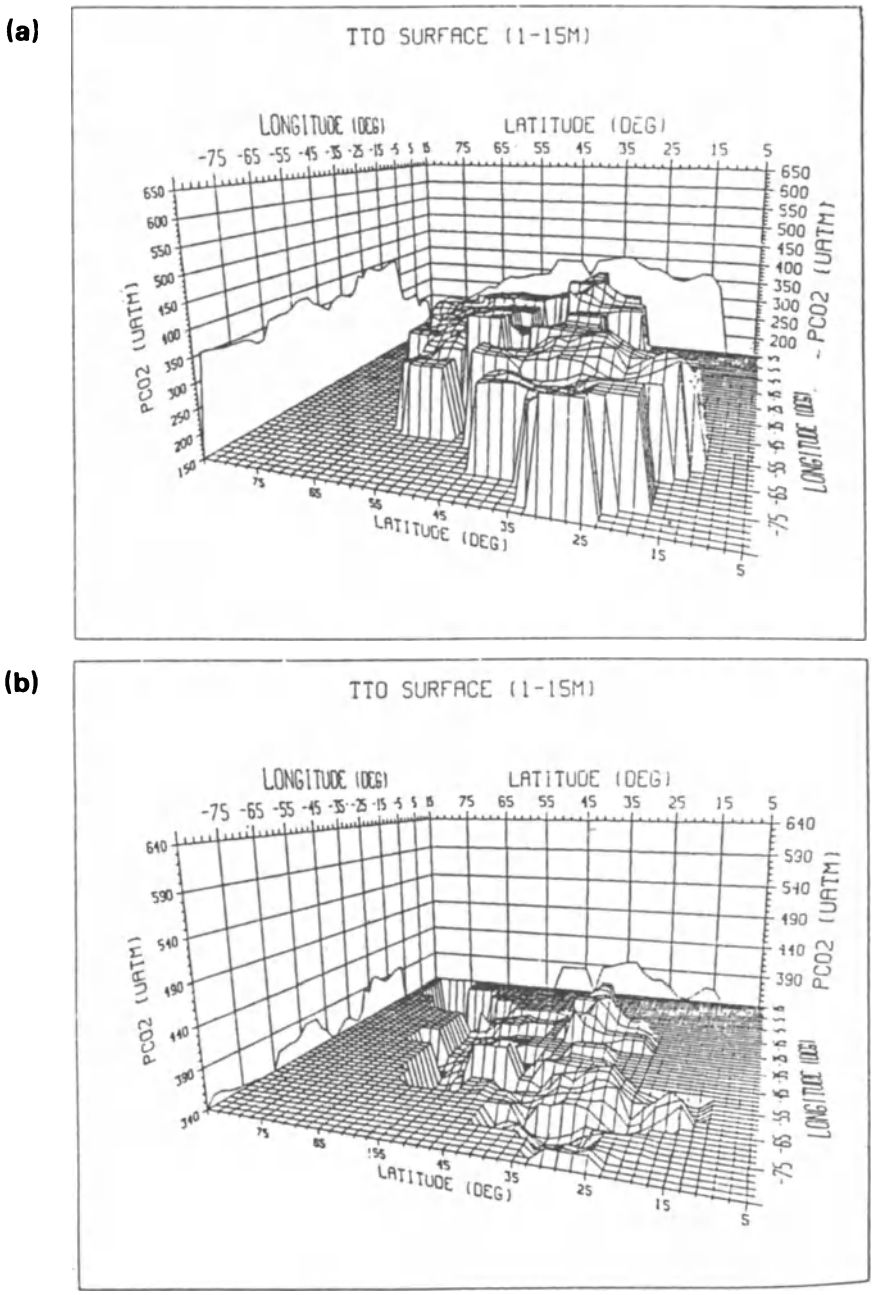

Figure 8.5 Three-dimensional perspective drawing of the North Atlantic surface water P_{CO_2} values as viewed from the US east coast (from Brewer *et al.* 1986). (**a**) The P_{CO_2} field with a floor of 150 ppm, so that the entire system is visible. (**b**) The P_{CO_2} field with a floor of 340 ppm, the atmospheric CO_2 value in 1981. Gaseous CO_2 invasion of the ocean takes place in the 'holes', and evasion is attributable to the 'hills'.

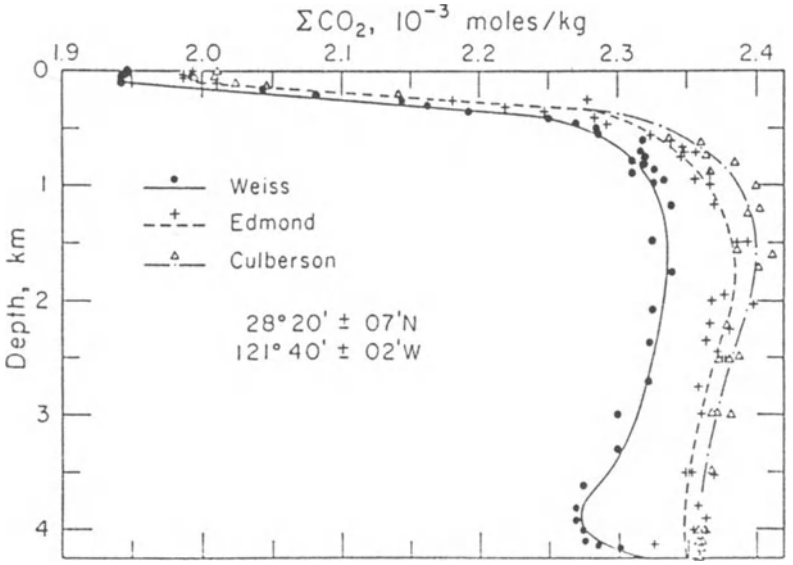

(a)

Figure 8.6 Vertical profiles of carbonate system parameters at GEOSECS Pacific Station 28°20′N, 121°W (modified from Skirrow 1975; data sources given in original publication): (**a**) ΣCO_2; (**b**) total alkalinity; (**c**) P_{CO_2}.

have attracted considerable attention in recent years. The problems involved are extremely complex and have been the subject of many meetings and countless review articles. The topic will not be covered in detail here, and only a brief overview will be given of the most general aspects of the role played by the oceans in the global CO_2 cycle. For updated reviews of the environmental effects associated with changes in the global CO_2 system the reader is referred to Siegenthaler (1986) and Trabalka & Reichle (1986), and the references therein.

When carbon dioxide enters the ocean it is utilized in photosynthesis and also takes part in a complex water chemistry. Carbon dioxide therefore has an important role in both the biological and chemical cycles that operate within the oceans. In addition, the oceans themselves are a major sink for excess CO_2 in the atmosphere, and so play a significant part in the global CO_2 budget; and, in fact, the atmospheric concentration of CO_2 is largely determined by the ocean (Siegenthaler 1986). This has become increasingly important in recent years, mainly because of the part played by CO_2 in the radiation budget of the atmosphere. Put simply, carbon dioxide allows solar radiation to pass to the Earth's surface but absorbs outgoing radiation, and so warms the atmosphere, the so-called

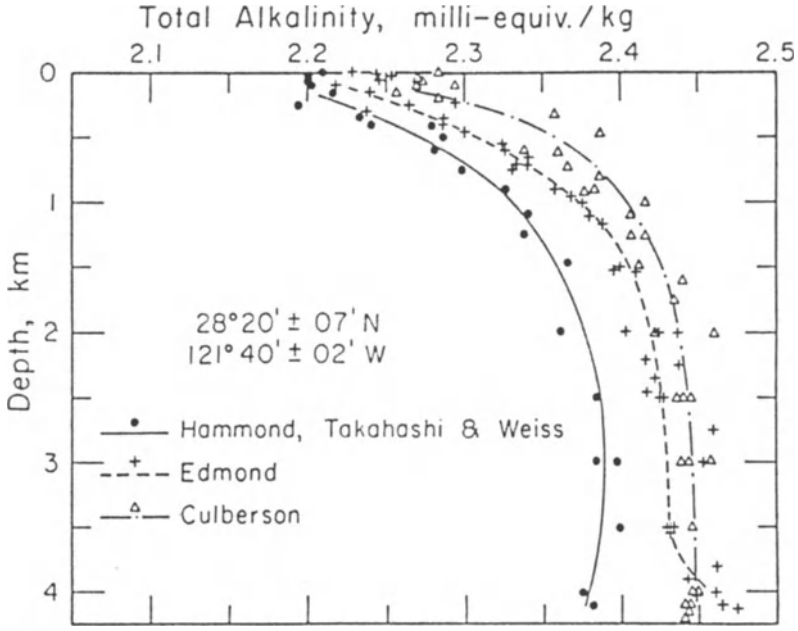

(b)

Figure 8.6b

greenhouse effect; other gases (e.g. N_2O, CH_4, the CFCs) also contribute to this. Clearly, therefore, changes in the concentration of atmospheric CO_2 can have far-reaching climatic implications and it has been suggested, for example, that they may have been a major cause of the climatic fluctuations associated with the Ice Ages (see e.g. Sarmiento & Toggweiler 1984).

On the basis of data obtained from air bubbles trapped in old polar ice it is apparent that atmospheric CO_2 levels were ~ 200 ppm during the last ice age and that there was an increase to ~ 280 ppm at ~ 10 000 yr BP. This level was then maintined to recent pre-industrial times; for example, according to Siegenthaler (1986) the levels during the 18th century were ~ 280 ppm. However, since the onset of the Industrial Revolution the CO_2 content of the atmosphere has been gradually increasing as a combined result of changes in the biosphere (e.g deforestation, land clearance), and especially from the burning of fossil fuels, so that at present the atmosphere contains ~ 20% more carbon dioxide than the pre-industrial level (see Fig. 8.7).

A considerable amount of research has been carried out in an attempt to understand the factors which caused the glacial/inter-glacial variations in atmospheric CO_2 levels. Since the oceans contain ~ 60 times as much

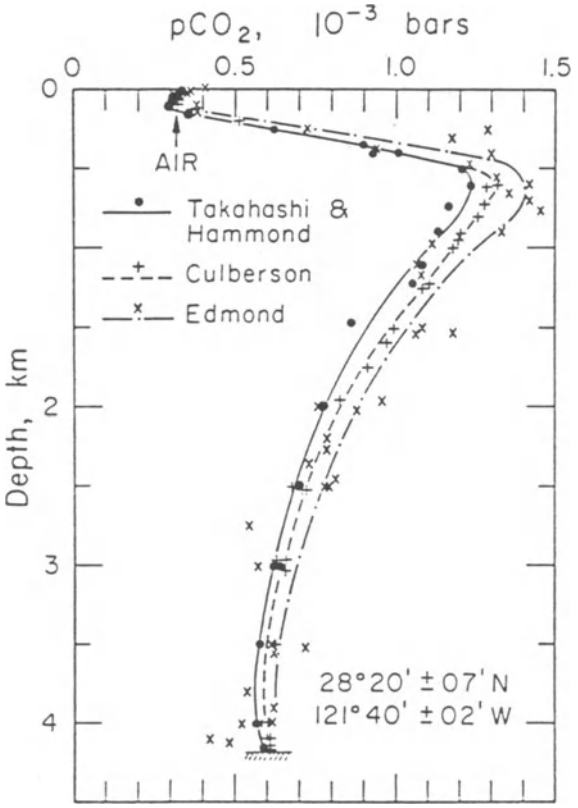
pCO2, 10⁻³ bars
0
0.5
1.0
1.5
AIR
Takahashi & Hammond
Culberson
Edmond
Depth, km
2
3
4
28°20' ± 07' N
121°40' ± 02' W

(c)

Figure 8.6c

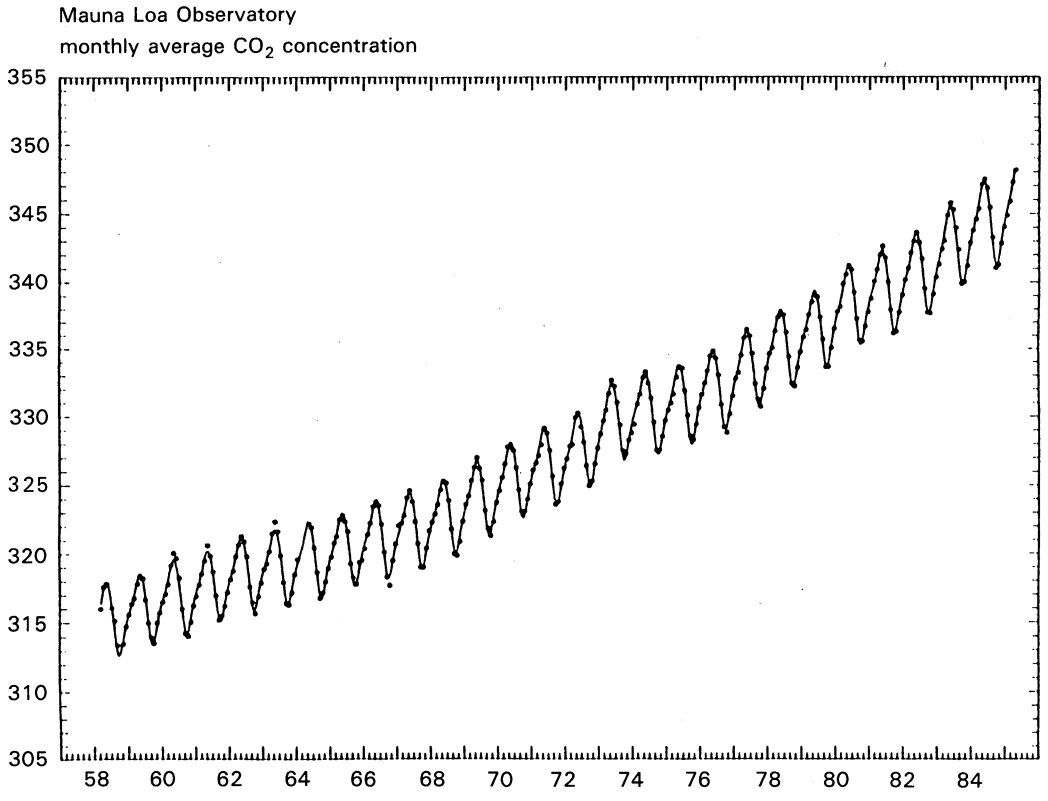

Figure 8.7 Atmospheric CO_2 concentrations (ppm) over the period 1958–1985: as measured at the Mauna Loa Observatory, Hawaii (from Siegenthaler 1985, after data from C.D. Keeling). Dots are monthly average values, smooth curve is a fit.

CO_2 as the atmosphere, atmospheric CO_2 is a slave to ocean chemistry. However, it is generally accepted that the decrease in temperature and the increase in salinity, both of which affect the solubility of CO_2 in the glacial ocean, cannot explain the glacial/inter-glacial variations in atmospheric CO_2. It is therefore necessary to invoke other changes in seawater chemistry, particularly with respect to biological activity, to explain the atmospheric variations (see e.g. Duplessey 1986). The role played by the oceanic biomass in determining atmospheric CO_2 has been extensively studied recently. For example, Broecker (1982) suggested that the concentration of phosphate in the oceans during glacial times was higher than at present, as a result of the supply of the nutrient from organic-rich sediments, that were deposited on the shelf regions during marine transgressions associated with previous interglacial periods of high sea level. The higher concentrations of phosphate during the glacial periods would have led to a greater depletion of ΣCO_2, and so of P_{CO_2}, in the surface ocean waters. This, in turn, would lead to a decrease in atmospheric CO_2 during the glacial period. The increase in phosphate during glacial times is also supported by Cd data (see e.g. Boyle & Keigwin 1982).

According to some authors, however, the rate of the CO_2 change associated with the changes in phosphate would have been too slow. For example, recent data derived from air bubbles trapped in ice cores have shown that variations of 50–100 ppm in atmospheric CO_2 may have happened during the last ice age over periods as short as ~ 100 yr (Stauffer *et al.* 1984). Such short time changes can be explained in terms of the kind of model proposed by, among other, Sarmiento & Toggweiler (1984). Using this model, it is suggested that the CO_2 changes result from variations in the nutrient levels in high-latitude waters. These waters have only a relatively small area, but are important in the atmospheric budget of CO_2, because they are in rapid exchange with large volumes of the deep-sea; for example, $\sim 75\%$ of the ocean volume interacts with the atmosphere through $\leqslant 4\%$ of the ocean's high latitude surface area (Sarmiento & Toggweiler 1984). Phosphate and nitrate are abundant in the high-latitude waters and biological activity here is governed by factors other than nutrient availability (see Sec. 9.1.2); these include changes in productivity and nutrient supply. For example, rapid vertical mixing associated with high-latitude overturning and deep-water formation, with constant biological productivity, could lead to lower surface concentrations of nutrients and consequently to a lower atmospheric CO_2 level. According to Siegenthaler (1986) this mechanism could result in changes in atmospheric CO_2 levels of the order of 50–100 ppm on a time scale of hundreds of years, which is more rapid than the changes associated with the shelf sediment theory. Sarmiento (1986) pointed out that if such changes, which suggest an extremely rapid uptake or removal of large

amounts of carbon from some reservoir (probably the oceans), were to occur today, they would have a dramatic effect on the rate of increase of fossil-fuel CO_2 in the atmosphere.

The 'high-latitude' models permit changes in productivity, but not all require such changes. For example, it was suggested above that biological productivity could in fact be held constant and that vertical water-mixing processes could yield lower atmospheric CO_2 concentrations. In a recent paper, Mix (1989) made a study of the long-term influence of productivity variations on the concentrations of CO_2 in the atmosphere. The author pointed out that atmospheric CO_2 concentrations have varied by up to 40% over the past few hundred thousand years, and concluded that because most of the exchangeable carbon resides in the deep sea, the source of the atmospheric CO_2 variations must be found here. The distribution of carbon in the ocean is linked to a number of factors; these include biological productivity, the sinking and degradation of organic matter and calcium carbonate, and oceanic circulation patterns. Mix (1989) used data for the distribution of planktonic foraminifera species in both modern and ice age sediments to evaluate spatial patterns of changes in productivity. He demonstrated that during the ice age 'new' production (see Sec. 9.1.1) was higher than at present by $\sim$ 40% for the entire Atlantic Ocean, and by $\sim$ 90% under equatorial regions, and concluded that if these changes were extrapolated to the World Ocean they would support the concept that a significant proportion of CO_2 concentration changes in the atmosphere are driven by variations in biological productivity in the oceans.

The three major reservoirs through which carbon dioxide exchanges are the atmosphere, the biosphere and the oceans. The ocean is the largest of the rapidly exchanging carbon reservoirs, and contains about 60 times as much carbon as the atmosphere, most of which is in the form of dissolved CO_2. Not all of the excess CO_2 actually enters the oceans, but since they do act as a sink for the gas much research has been directed towards predicting the environmental impact that excess CO_2 will have both on the ocean system itself and on the global climate in general. There are three stages in the uptake of excess CO_2 by the oceans.

(1) The relatively thin, well mixed surface layer will quickly establish equilibrium with CO_2 in the atmosphere.
(2) Downward mixing and the sinking of organic particles will carry the carbon to the deep sea.
(3) As the CO_2 content of the oceans rises, water masses now supersaturated with respect to carbonate minerals will become undersaturated and carbonates that are in contact with them will begin to dissolve.

The rates at which the carbon cycle operates within the oceans have been evaluated using carbon isotopes, and the rate data have been plugged into a variety of ocean–atmosphere models designed to simulate the natural conditions.

The problems involved in setting up and interpreting these models are extremely complex and will not be covered here. However, with respect to the question of how the ocean system copes with excess CO_2, the conclusions drawn by Broecker & Peng (1982) provide a useful summary of the possible consequences of an oceanic invasion of CO_2, which can be related to the various stages involved in the uptake of excess CO_2.

(a) The times required for the ocean system to equilibrate with the carbon dioxide in the atmosphere are about one year for the surface ocean, several tens of years for the main thermocline, and hundreds of years for the deep sea. Thus, the thermocline acts as a barrier for the oceanic equilibrium with atmospheric CO_2, and equilibrium between the atmosphere and the total ocean will take many centuries.
(b) The dissolution of calcite from deep-sea sediments, which raises the alkalinity, affects the bottom waters and therefore only equilibrates with the atmosphere when they are brought to the surface in a time period that requires several thousands of years. Further, the excess calcium released from the carbonates in a dissolved form will only be removed from sea water in many tens of thousands of years.

It is apparent, therefore, that the various reservoirs, or boxes, in the oceans equilibrate with the atmosphere on very different timescales, ranging up to tens of thousands of years. Broecker & Peng (1982) concluded, therefore, that as a consequence of this, carbon dioxide added to the atmosphere by man's activities over the next two centuries will have an effect on ocean chemistry even on geological timescales.

8.5 Dissolved gases in sea water: summary

(a) The oceans can act as either a source or a sink for atmospheric gases, which leave or enter the system via exchange across the air/sea interface. Attention here has been focused on oxygen and carbon dioxide, both of which play important roles in the biogeochemistry of sea water.
(b) Dissolved oxygen is released during the photosynthetic production of biological soft tissue material in the euphotic zone and is consumed during the oxidative destruction of the organic matter at greater

depths in the water column. Oxygen minima, which occur at depths ranging between ~ 200 and ~ 800 m, are found in various parts of the ocean; these are important features that can mediate redox reactions in the water column. There is relatively little consumption of dissolved oxygen in deep waters. Apparent oxygen utilization values, which are a measure of the amount of the gas that has been utilized after the waters have left the surface, follow the deep water 'global grand tour' and are lowest in Atlantic subsurface waters (less utilization) and highest in the Pacific (more utilization). Dissolved oxygen can be used to characterize water masses.

(c) Carbon dioxide is consumed during photosynthesis, during which carbon enters both the soft tissue and the hard skeletal phases of organisms, and is released during the oxidative destruction of organic matter. In addition, carbon dioxide is extremely reactive in sea water and the complex equilbria involved have a number of profound effects on the chemistry of the oceans. The manner in which the oceanic carbon dioxide system operates can be summarized as follows. Carbon dioxide is pulled down into surface sea water from the atmosphere in response to a combination of biological and physical processes, but since the charge balance is not affected this does not result in a change in the alkalinity of sea water. The air–sea fluxes of CO_2 vary with latitude, large positive net fluxes (net evasions from the ocean) being found in tropical warm water latitudes where P_{CO_2} is high, and net negative fluxes (net invasion into the ocean) occurring in colder waters where the P_{CO_2} values are low. Once it is drawn down into the surface ocean, CO_2 enters into a biological cycle and also takes part in a complex inorganic carbonate chemistry. In the biological cycle carbon dioxide is utilized to fix carbon into organic tissue by the photosynthetic activity of phytoplankton. This removal of CO_2 raises the pH, and the uptake of the nutrients, nitrate and phosphate, that occurs at the same time raises both the pH and the alkalinity of the waters, so that the biological cycle also affects the inorganic carbonate chemistry. As the organisms die, a small fraction (~ 5%) of the organic material escapes to carry the fixed CO_2 to deep waters (see Sec. 9.3). However, the vast majority of the organic tissue undergoes oxidative regeneration, with the release of CO_2 and the nutrients into waters of intermediate depths. The release of the gas lowers the pH of the waters and makes them more corrosive to calcium carbonate material. The dissolution of the carbonates alters the charge balance of the system and changes the alkalinity. As the waters of the World Ocean move along the 'grand tour' they become progressively depleted in oxygen and enriched in CO_2 and the nutrients. As a result, the dissolution

horizon below which calcium carbonate dissolves (see Sec. 15.2.4.1) shoals to shallower depths in the North Pacific relative to the North Atlantic. The calcium carbonate dissolved from sediments further increases the CO_2 content of the bottom waters and also raises the alkalinity of the system. The oceans are a major sink for excess CO_2 in the atmosphere. This excess CO_2 enters the seawater carbonate system and passes through the surface ocean, the main thermocline and the deep sea, and equilibrates with the various reservoirs on different timescales, which apparently range from tens to tens of thousands of years.

References

Boyle, E.A. 1988. Vertical oceanic nutrient fractionation and glacial/interglacial CO_2 cycles. *Nature* **331,** 55–6.

Boyle, E.A. & L.D. Keigwin 1985. Comparison of Atlantic and Pacific paleochemical records for the last 250 000 years: changes in deep ocean circulation and chemical inventories. *Earth Planet. Sci. Lett.* **76,** 135–50.

Brewer, P.G. 1983. Carbon dioxide and the oceans. In *Changing climate*, 186–215. Rep. Carbon Dioxide Assess. Comm. Washington, DC: National Academy Press.

Brewer, P.G., A.L. Bradshaw & R.T. Williams 1986. Measurement of total carbon dioxide and alkalinity in the North Atlantic Ocean in 1981. In *The changing carbon cycle. A global analysis*, J.R. Trabalka & D.E. Reichle (eds), 348–70. New York: Springer-Verlag.

Broecker, W.S. 1974. *Chemical oceanography*. New York: Harcourt Brace Jovanovich.

Broecker, W.S. 1982. Ocean chemistry during glacial times. *Geochim. Cosmochim. Acta* **46,** 1689–705.

Broecker, W.S. & T.-H. Peng 1974. Gas exchange rates between air and sea. *Tellus* **26,** 21–35.

Broecker, W.S. & T.-H. Peng 1982. *Tracers in the sea.* Palisades: Lamont-Doherty Geological Observatory.

Burke, C.M. & M.J. Atkinson 1988. Measurement of total alkalinity in hypersaline waters. *Mar. Chem.* **25,** 49–55.

Burton, J.D., P.G. Brewer & R. Chesselet (eds) 1986. *Dynamic processes in the chemistry of the upper ocean.* New York: Plenum.

Campbell, J.A. 1983. The Geochemical Ocean Sections Study – GEOSECS. In *Chemical oceanography*, J. P. Riley & R. Chester (eds), Vol. 8, 89–155. London: Academic Press.

Conrad, R. & W. Seiler 1986. Exchange of CO and H_2 between ocean and atmosphere. In *The role of air–sea exchange in geochemical cycling*, P. Buat-Menard (ed.), 269–82. Dordrecht: Reidel.

Culberson, C.H. 1981. Direct potentiometry. In *Marine electrochemistry*, M. Whitfield & D. Jagner (eds), 187–261. Chichester: Wiley.

Deuser, W.G. 1975. Reducing environments. In *Chemical oceanography*, J.P. Riley & G. Skirrow (eds), Vol. 3, 1–37. London: Academic Press.

Dickson, A.G. 1981. An exact definition of total alkalinity and a procedure for the estimation of alkalinity and total inorganic carbon from titration data. *Deep-Sea Res.* **28,** 609–23.

Dickson, A.G. 1984. pH scales and proton-transfer reactions in saline media such as sea

water. *Geochim. Cosmochim. Acta* **48,** 2299–308.
Duplessey, J.C. 1986. CO_2 air–sea exchange during glacial times: importance of deep-sea circulation changes. In *The role of air–sea exchange in geochemical cycling.* P. Buat-Menard (ed.), 249–67. Dordrecht: Reidel.

Edmond, J.M. 1970. High precision determination of titration alkalinity and the total carbon dioxide content of sea water by potentiometric titration. *Deep-Sea Res.* **17,** 737–50.

Fitzgerald, W.F. 1986. Cycling of mercury between the atmosphere and oceans. In *The role of air–sea exchange in geochemical cycling*, P. Buat-Menard (ed.), 363–408. Dordrecht: Reidel.

Hansson, I. & D. Jagner 1973. Evaluation of the accuracy of Gran plots by means of computer calculations. Application to the potentiometric titration of the total alkalinity and carbonate content in sea water. *Anal. Chim. Acta* **65,** 363–72.
Hunter-Smith, R.J., P.W. Balls & P.S. Liss 1983. Henry's law constants and the air–sea exchange of various low molecular weight halocarbon gases. *Tellus* **35,** 170–6.

Kanwisher, J. 1963. On the exchange of gases between the atmosphere and the sea. *Deep-Sea Res.* **10,** 195–207.
Keeling, C.D. 1968. Carbon dioxide in surface ocean waters. 4. Global distribution. *J. Geophys. Res.* **14,** 4543–53.
Kester, D.R. 1975. Dissolved gases other than CO_2. In *Chemical oceanography*, J.P. Riley & G. Skirrow (eds), Vol. 1, 497–589. London: Academic Press.

Liss, P.S. 1983. Gas transfer: experiments and geochemical implications. In *Air–sea exchange of gases and particles*, P.S. Liss & W.G. Slinn (eds), 241–98. Dordrecht: Reidel.
Liss, P.S. 1986. The air–sea exchange of low molecular weight halocarbon gases. In *The role of air–sea exchange in geochemical cycling*, P. Buat-Menard (ed.), 283–94. Dordrecht: Reidel.
Liss, P.S. & L. Merlivat 1986. Air–sea gas exchange rates: introduction and synthesis. In *The role of air–sea exchange in geochemical cycling*, P. Buat-Menard (ed.), 113–27. Dordrecht: Reidel.
Liss, P.S. & P.G. Slater 1974. Flux of gases across the air–sea interface. *Nature* **247,** 181–4.

Millero, F.J. 1986. The pH of estuarine waters. *Limnol. Oceanogr.* **31,** 839–47.
Mix, A.C. 1989. Influence of productivity variations on long-term atmospheric CO_2. *Nature* **337,** 541–44.

Packard, T.T., H.J. Minas, B. Coste, R. Martinez, M.C. Bonin, J. Gostan, P. Garfield, J. Chistensen, Q. Dortch, M. Minas, G. Copin-Montegut & C. Copin-Montegut 1988. Formation of the Alboran oxygen minimum zone. *Deep-Sea Res.* **35,** 1111–8.

Rakestraw, N.W. 1949. The conception of alkalinity of excess base in sea water. *J. Mar. Res.* **8,** 14–20.
Richards, F.A. 1965. Dissolved gases other than carbon dioxide. In *Chemical oceanography*, 1st edn, J.P. Riley & G. Skirrow (eds), 197–225. London: Academic Press.
Riley, J.P. & R. Chester 1971. *Introduction to marine chemistry.* London: Academic Press.
Roether, W. 1986. Field measurements of gas exchange. In *Dynamic processes in the chemistry of the upper ocean*, J.D. Burton, P.G. Brewer & R. Chesselet (eds), 117–28. New York: Plenum.

REFERENCES

Sarmiento, J.L. 1986. Three-dimensional ocean models for predicting the distribution of CO_2 between the ocean and atmosphere. In *The changing carbon cycle: a global analysis*. J.R. Trabalka & D.E. Reichle (eds), 279–94. New York: Springer-Verlag.

Sarmiento, J.L. & J.R. Toggweiler 1984. A new model for the role of the oceans in determining atmospheric pCO_2. *Nature* **303,** 621–4.

Shulenberger, E. & J.L. Reid 1981. The Pacific shallow oxygen maximum, deep chlorophyll maximum, and primary productivity, reconsidered. *Deep-Sea Res.* **28,** 901–19.

Siegenthaler, U. 1986. Carbon dioxide: its natural cycle and anthropogenic perturbation. In *The role of air–sea exchange in geochemical cycling*, P. Buat-Menard (ed.), 209–47. Dordrecht: Reidel.

Sillen, L.G. 1963. How has sea water got its present composition? *Sven. Kem. Tidskr.* **75,** 161–77.

Skirrow, G. 1975. The dissolved gases – carbon dioxide. In *Chemical oceanography*, J.P. Riley & G. Skirrow (eds), Vol. 2, 1–192. London: Academic Press.

Stauffer, B., H. Hofer, H. Oeschger, J. Schwanfer & U. Siegenthaler 1984. Atmospheric CO_2 concentrations during the last glaciation. *Ann. Glaciol.* **5,** 160–4.

Stumm, W. & J.J. Morgan 1981. *Aquatic chemistry*. New York: Wiley.

Sundquist, E.T., L.N. Plummer & T.M.L. Wigley 1979. Carbon dioxide in the ocean surface: the homogeneous buffer factor. *Science* **204,** 1203–5.

Takahasi, T., W.S. Broeker & A.E. Bainbridge 1981. The alkalinity and total carbon dioxide concentration in the world oceans. In *Carbon cycle modelling*, Scope 16, B. Bolin (ed.), 159–99. New York: Wiley.

Takahasi, T., W.S. Broecker, S.R. Werner & A.E. Bainbridge 1980. Carbonate chemistry of the surface waters of the World Ocean. In *Isotope marine chemistry*, E.D. Goldberg, Y. Horibe & K. Saruhashi (eds), 291–326. Tokyo: Uchida Rokahuho.

Trabalka, J.R. & D.E. Reichle 1986. *The changing carbon cycle. A global analysis*. New York: Springer-Verlag.

Unesco 1987. Unesco Tech. Pap. Mar. Sci., no. 51. Paris: Unesco.

Weiss, R.F. 1970. The solubility of nitrogen, oxygen and argon in water and sea water. *Deep-Sea Res.* **17,** 721–35.

9 Nutrients, organic carbon and the carbon cycle in sea water

The manner in which the carbon cycle operates in the ocean is of prime importance to marine geochemistry because the down-column transport of particulate organic carbon, i.e. the *global carbon flux*, drives the processes that control the removal of material from the water column and its incorporation into the sediment sink. The nutrient and carbon cycles are intimately interrelated, but for convenience they are considered separately in the following sections.

9.1 The nutrients in sea water

9.1.1 Introduction

Parsons (1975) defines a nutrient element as one that is functionally involved in the processes of living organisms. However, he points out that in oceanography the term has been applied almost exclusively to **nitrate**, **phosphate** and **silicate**, and attention here will be focused on the traditional nutrients.

NITROGEN NUTRIENTS Nitrogen is present in sea water as (a) molecular nitrogen, (b) fixed inorganic salts, such as nitrate nitrogen (NO_3-N), nitrite nitrogen (NO_2-N) and ammonia (NH_3-N), (c) a range of organic nitrogen compounds associated with organisms, e.g. amino acids and urea, and (d) particulate nitrogen. In order to satisfy their nitrogen requirements most phytoplankton utilize fixed nitrogen, with a preference for nitrate, nitrite and ammonia. This takes place in the euphotic zone and some of the nitrogenous nutrients are released in a soluble form within this zone. The remainder are transported out via sinking particulates, and a large fraction of these is released back into solution at depth in the water column by remineralization of the organic material, mainly via bacterial mediation, the final inorganic end-product being nitrate.

PHOSPHORUS NUTRIENTS There are a variety of forms of phosphorus in sea water. These include dissolved inorganic phosphorus (predominantly

orthosphosphate ions, HPO_4^{2-}), organic phosphorus and particulate phosphorus; however, phytoplankton normally satisfy their phosphorus requirements by direct assimilation of orthophosphate. Phosphate, like nitrate, is also released back into the water column during the oxidative destruction of organic tissues. Most of the regeneration of phosphorus probably takes place via bacterial decomposition, which leads to the formation of orthophosphates, although chemical decomposition may also occur.

Inorganic nitrate and phosphate are not the only forms of nitrogen and phosphorus that can be used by organisms for their nutritional needs, and Jackson and Williams (1985) have discussed the importance of dissolved *organic* nitrogen (DON) and phosphorus (DOP) in the nutrient economy of the ocean. The data provided by these authors showed that DON and DOP concentrations increase as those of nitrate and phosphate decrease, indicating a change in the dominant chemical form of nitrogen from nitrate to DON and of phosphorus from phosphate to DOP. The authors concluded that both DON and DOP constitute significant fractions of the oceanic nutrient pools, especially in the euphotic zone, with the labile fractions of DON and DOP being important sources of nitrogen and phosphorus for phytoplankton in oligotrophic oceanic areas. In these low-nutrient regions, where nutrients are removed by particle production, the N : P ratio changed at low phosphate concentrations, but the ratios of total dissolved nitrogen to total dissolved phosphorus (TDN : TDP) were more nearly constant.

SILICON NUTRIENTS Organisms such as diatoms and radiolarians require silicate for shell formation. Silicon is supplied to the oceans in both dissolved and particulate forms via river run-off, atmospheric deposition and glacial weathering (especially from the Antarctic), and dissolved silicon in sea water is probably present as orthosilicic acid, $Si(OH)_4$. The particulate forms of the element include a wide variety of silicate and aluminosilicate minerals, together with diatom and radiolarian shells, which contain silica in the form of opal (see Sec. 15.2.2). Silica from the skeletal or hard parts of the organisms is released back into the water column during down-column solution; this process does not appear to involve bacterial action, but it is probably aided by passage through the gut of other organisms in the food chain and expulsion as a faecal material.

When considering the major nutrients in terms of their oceanic chemistries, it is useful to distinguish silicate from nitrate and phosphate. The reason for this is that both the latter two nutrients are involved in nutrition and are incorporated into soft tissues, whereas silicate is only

employed in the building of hard skeletal parts. Nonetheless, all three nutrients are initially removed from solution by organisms, mainly phytoplankton, in the euphotic zone.

Phytoplankton take up the nutrients during photosynthetic primary production in the euphotic zone (see Sec. 9.2.2.2). The bulk of these phytoplankton are consumed by zooplankton grazers in the food web and a proportion of the nutrients are excreted, either directly in soluble forms or indirectly as faecal pellets, in the euphotic zone. The soluble excretory products become directly available for rapid assimilation by successive crops of phytoplankton. As a result of this, a quasi-steady-state will be initiated, and the balance between supply and removal processes will maintain low concentrations of the nutrients in these euphotic waters (Spencer 1975). The solid excretory products, together with other forms of detritus such as dead organisms, sediment out of the surface layers. These are replaced by new nutrients, some of which are supplied from deep water following their release from the sinking detritus. However, before the nutrients associated with the detritus can become regenerated in a form that is available to phytoplankton, the organic particulates must be remineralized by oxidative decay, a process that is mediated via bacterial attack.

One of the most important concepts to emerge in the nutrient field in recent years has been the distribution between new and regenerated production (see e.g. Dugdale & Goering 1967; Eppley & Peterson 1979). This concept is related to the way in which nutrients are supplied to the euphotic zone, and the processes involved can be illustrated with respect to nitrogen. The supply of nitrogenous nutrients required during primary production can be related to two different types of sources:

(a) A new supply to the euphotic layer from river run-off, atmospheric deposition, upwelling from deep water and nitrogen fixation; mainly in the form of nitrate.
(b) A regenerated supply from the short-term recycling processes within the euphotic layer itself; mainly in the form of ammonia, with lesser amounts of urea and amino acids, arising from the excretory activities of animals and the metabolism of heterotrophic micro-organisms, i.e. this supply is derived originally from phytoplankton via the food web.

The system is illustrated diagrammatically in Figure 9.1. Eppley & Peterson (1979) pointed out that in an ideal closed system, with steady-state standing stocks and fluxes, the cycling of nutrients through an enclosed food web could continue indefinitely. In the real ocean system, however, there is a loss of organic material from the euphotic zone to deep water, e.g. by the sinking of faecal pellets and 'marine snow' (see Sec. 10.4), and this is compensated by the input of new nutrients into the

euphotic zone. Primary production associated with the newly available nitrogen (e.g. nitrate) is termed **new production**, and that resulting from the nitrogen recycledin the euphotic zone (e.g. ammonia) is referred to as **regenerated production**. Thus, the organic matter sinking out of the euphotic zone represents the new production (Martin *et al.* 1987), i.e. the new production is that part of the primary production which is available for export, and it is this which drives the downward flux of organic matter (the global carbon flux) to deep waters (see Secs 9.3 & 10.4). New production, as a percentage of the total primary production, ranges from ~ 5% in the oligotrophic waters of the subtropical gyres to ~ 45% in coastal upwelling regions (see e.g. Bruland 1980).

Regenerated production arises from nutrients that undergo short-term recycling in the euphotic zone. In contrast, new production requires the input of new nutrients into the euphotic zone. Recently, a number of attempts have been made to evaluate the source strengths of these new nutrients to the euphotic zone. For example, Duce (1986) employed a variety of approaches to estimate the fluxes of new nutrient nitrogen and phosphorus to surface water in the Sargasso Sea (North Atlantic) and the Central North Pacific Gyre. For the supply of new nutrients to the euphotic zone, the following sources were considered: (a) a deep water flux via eddy diffusion and vertical advection; (b) atmospheric input; and, for nitrogen, (c) fixation. The findings are listed in Table 9.1 and can be summarized as follows.

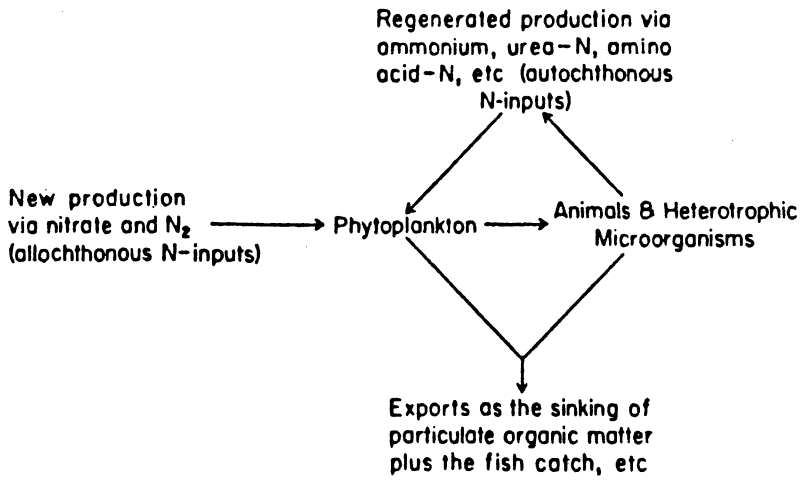

Figure 9.1 The production system of the surface ocean, illustrating the concepts of new and regenerated production (from Eppley & Peterson 1979).

Table 9.1 Source strength comparisons for 'new' nutrients in surface waters of the Sargasso Sea and the North Pacific Gyre[a]

Nutrient	Source	Flux (μmol m^{-2} d^{-1})	
		Sargasso Sea	North Pacific Gyre
Nitrogen	Vertical advection	0 - 40	10 - 22
	Eddy diffusion	22 - 210	60 - 730
	Nitrogen fixation	0.5 - 5	0.2 - 2
	Atmospheric input	26 - 54	8 - 26
	Total	50 - 310	80 - 800
Phosphorus	Vertical advection	0 - 4	2.4 - 4.8
	Eddy diffusion	1.7 - 10	5 - 50
	Atmospheric input	0.033 - 0.080	0.005 - 0.012
	Total	1.7 - 14	7 - 55

[a] Data from Duce (1986)

(a) **Nitrogen.** Within the range of the estimates, the upward flux from deep water can account for between $\sim$ 7% and $\geqslant$ 100%, and the atmospheric flux between $\sim$ 8% and $\sim$ 100%, of the input of new nitrogen to the Sargasso Sea. In the North Pacific Gyre, the deep water flux can make up between $\sim$ 9% and $\geqslant$ 100%, and the atmospheric flux between $\sim$ 1% and $\sim$ 30%, of the new nitrogen input. For nitrogen, therefore, the atmosphere might be a significant source to the euphotic layer. However, the importance of the atmospheric input of fixed nitrogen to the Sargasso Sea has been questioned on the grounds that one-dimensional advection–diffusion models of the type used to compute the input from deep water can grossly underestimate the vertical flux of nitrate across the thermocline (see e.g. Jenkins & Goldman 1985).

(b) **Phosphorus.** In contrast to nitrogen, the supply of new phosphorus to the euphotic zone in both regions is dominated by the upward flux from deep water, with the atmospheric flux accounting for a maximum of only $\sim$ 5% of the new phosphorus in the Sargasso Sea, and $<$ 1% in the Central North Pacific Gyre region.

Duce (1986), however, drew attention to the fact that there are a number of problems inherent in attempting to assess the relative magnitudes of the atmospheric and deep water fluxes of new nutrients to the euphotic zones. One of these relates to the fact that atmospheric

inputs are variable in both space and time; thus, they could be strongly affected by short-term dust pulses of the type described in Section 4.1.4.1. Another problem concerns the manner in which the deep water flux operates. Short-term bursts of nutrients can be injected into the euphotic zone during the erosion of the thermocline by turbulence, and on a global basis the fluxes associated with these bursts could be of such magnitude that the atmospheric input becomes insignificant in terms of the whole euphotic zone. However, according to the model proposed by Jenkins & Goldman (1985), the euphotic zone can be considered to be made up of two regions: (a) an upper region, which is essentially devoid of new nutrients, and in which production relies on regenerated nutrients; and (b) a lower portion, which receives new nutrients from deep water. As Duce (1986) points out, this could, in fact, make the input of new atmospheric nutrients more significant since these are delivered into surface waters.

The availability of nutrients can limit phytoplankton growth, the limiting nutrients usually being considered to be nitrate and phosphate, although silicate can limit diatom growth. It must be stressed, however, that this concept of a limiting nutrient strictly refers only to new production, since productivity can be maintained in the presence of low nutrient concentrations by recycling.

9.1.2 The distributions of nutrients in the oceans

Over the past two decades or so, the database on the distributions of nutrients in the oceans has been considerably extended by information obtained in a variety of ways. Data on the spatial distributions of the nutrients have been derived from sources such as: (a) large-scale expeditions (e.g. GEOSECS, NORPAX and TTO); (b) attempts to produce global ocean nutrient maps from other parameters, such as temperature and σ_t (e.g. the study reported by Kamykowski & Zentara (1986) using the NODC data set); and (c) remote sensing (see e.g. Traganza *et al.* 1983). Temporal variations in nutrient distributions have been studied in various specific oceanic regions (see e.g. Biggs *et al.* 1985, French *et al.* 1983). Data from sources such as these, together with older archival material, can be used to build up a general picture of the distribution of nutrients in the oceans.

Redfield (1934, 1958) showed that the concentrations of the major nutrients, such as nitrate and phosphate, in sea water change in relation to fixed concentration ratios (stoichiometry) in organisms (see Section 9.2.3.1 for a discussion of the Redfield ratios), and therefore implied that it is organisms which control the concentrations and distributions of the nutrients in sea water. As a result of this, linear relationships exist between the concentrations of dissolved nutrients. For example, nitrate and phosphate exhibit such a linear relationship in sea water (see Fig. 9.2a);

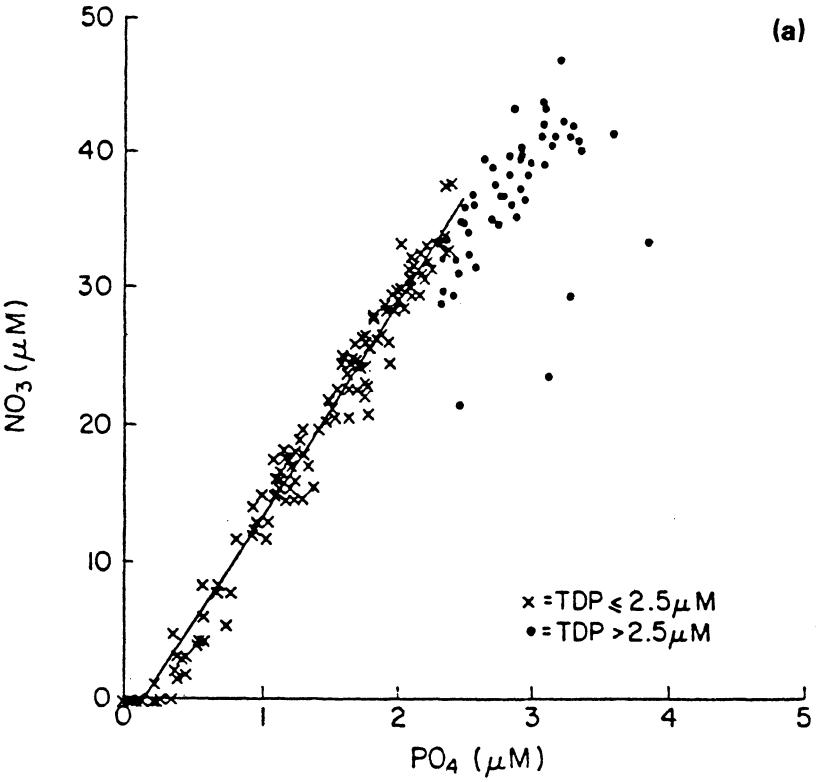

Figure 9.2 The distributions of nutrients in the oceans. (a) nitrate versus phosphate relationships (from Jackson & Williams 1985). The data are taken from water column profiles in the Pacific Ocean. The least-squares fit to a linear relationship for all data points is $[NO_3\ (\mu M)] = 13.2[PO_4\ (\mu M)] + 0.23$, $r^2 = 0.935$, $n = 186$. For samples with total dissolved phosphorus (TDP) ≤ 2.5 μM, the relationship is $[NO_3\ (\mu M)] = 15.5[PO_4\ (\mu M)] - 2.27$, $r^2 = 0.978$, $n = 134$ (full line).

however, there are two general exceptions to this. (a) In anoxic regions, in which nitrate is used in the destruction of organic matter (see Sec. 14.2.2), phosphate can increase with a corresponding increase in nitrate. (b) Nitrate concentrations can approach, and sometimes reach, zero concentrations in nutrient-starved regions which have low concentrations of phosphate (see e.g. Jackson 1988).

Three features are apparent in the overall distributions of the nutrients in various seawater environments: (a) nutrient concentrations in surface waters are higher in coastal areas and regions of upwelling; (b) deep water concentrations are considerably higher than in those of open-ocean surface waters; and (c) deep water concentrations are higher in the Pacific than in the Atlantic.

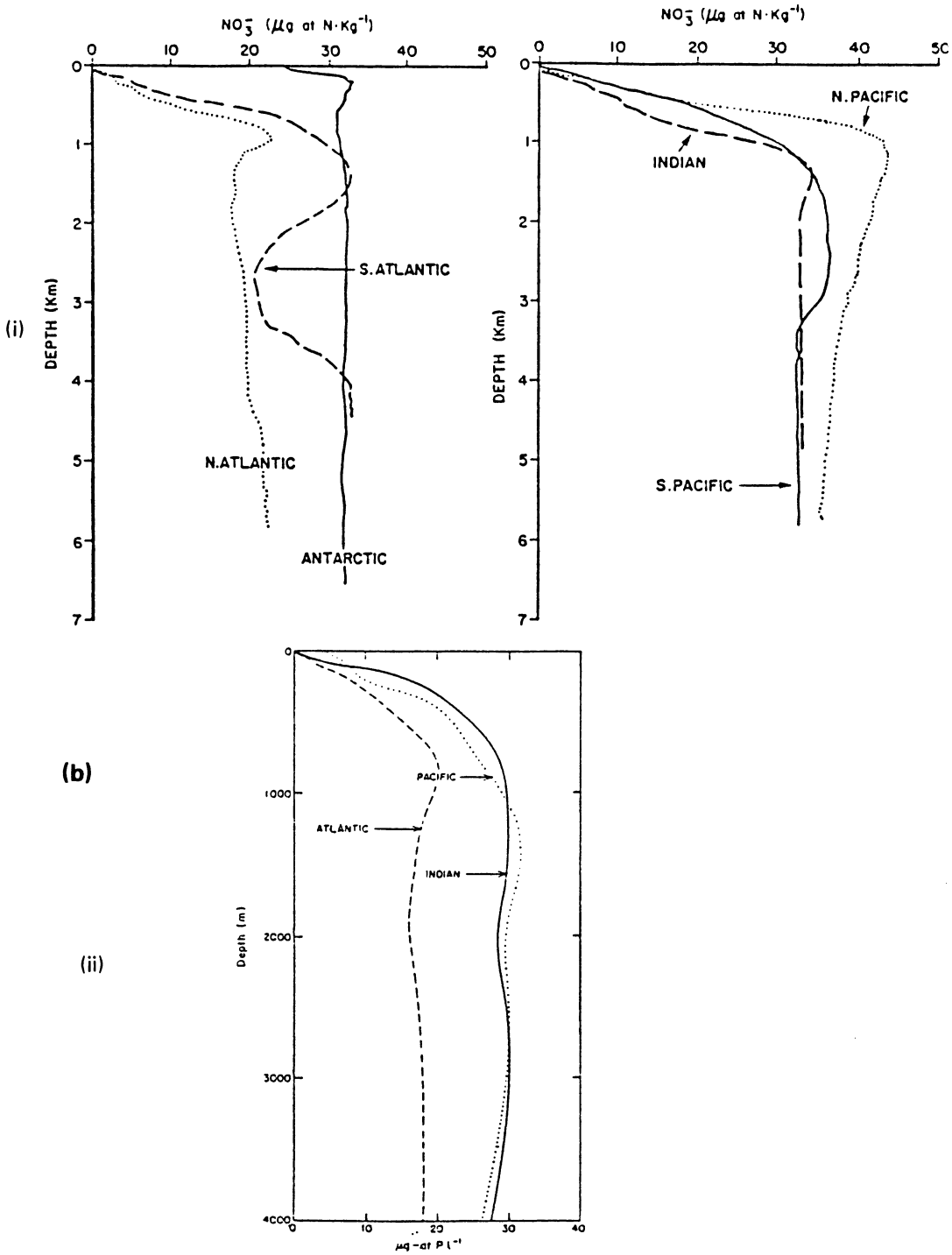

Figure 9.2b Typical vertical profiles of nutrients in the oceans: (i) nitrate (from Sharp 1983; plots constructed from GEOSECS data); (ii) phosphate (from Sverdrup *et al.* 1942).

(iii)

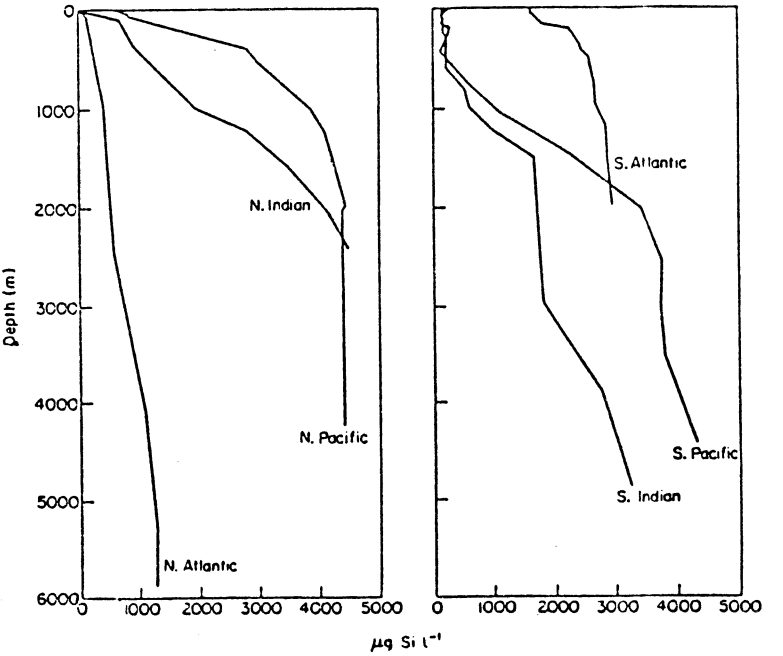

Figure 9.2b contd. Typical vertical profiles of nutrients in the oceans: silicate (from Armstrong 1965).

9.1.2.1 The water column profiles of the nutrients Nutrients are taken up in the euphotic zone and released back into sea water following the remineralization of sinking detritus, and the concentrations thus build up in deeper water from which they can be brought to the surface again via physical processes, such as upwelling and seasonal increases in the depth of the wind-mixed upper layer; the 'biological pump'. The overall effect of these processes is to generate vertical nutrient distributions that exhibit a characteristic surface water depletion–deep water enrichment profile. Such vertical water column profiles are of particular interest in marine geochemistry because when they are shown by other constituents they indicate that these have also been affected by processes associated with living organisms, i.e. they have entered the oceanic biomass cycle.

Nitrate, phosphate and silicate, for which precise analytical techniques are available, are convenient indicators of the involvement of nitrogen, phosphorus and silicon, respectively, in the oceanic nutrient cycles.

NITRATE AND PHOSPHATE Vertical water column profiles of nitrate and phosphate in the major oceans are illustrated in Figure 9.2b(i) and (ii), respectively. There are considerable similarities between the profiles of

the two nutrients, and the general features can be identified as follows. Both profiles can be subdivided into a number of layers:

(a) A surface layer in which nitrate and phosphate are heavily depleted by biological uptake.
(b) A layer in which the concentrations increase rapidly with depth due to their regeneration from the sinking biomass. Sometimes a layer of maximum concentration is found for both nutrients between ~ 500 and ~ 1500 m; this is particularly well developed in Atlantic Ocean profiles.
(c) A thick layer in which the concentrations vary little with depth.

However, within this overall pattern the individual profiles for the two nutrients differ in detail between the various oceans. This can be illustrated with respect to nitrate. The inter-oceanic variations in the depth profiles of this nutrient have been described by Sharp (1983), and can be summarized with reference to Figure 9.2b(i). The North Atlantic profile exhibits a pronounced nitrate maximum near the oxygen minimum layer, below which the concentration is generally uniform. A nitrate maximum associated with the oxygen minimum is also found in the South Atlantic, but here it is broader and deeper than in the North Atlantic, and a secondary maximum is located in the deep water. The South Pacific also has a broader, deeper, nitrate maximum than the North Pacific. The Antarctic has a very shallow nitrate maximum and a generally constant deep water value (N content 32 μg atom l^{-1}), which is characteristic of the waters of this region. In addition to variations in the detailed shapes of the nitrate profiles, concentrations also differ between the oceans. For example, the concentration of nitrate at the maximum in the North Pacific (N content ~ 45 μg atom l^{-1}) is higher by a factor of 2 than in the North Atlantic (N content ~ 22 μg atom l^{-1}) (see below).

SILICATE Although silicate is incorporated into the shells of organisms, and not their soft tissues, it still has a nutrient-type distribution profile in the water column; some typical profiles are illustrated in Figure 9.2b(iii). However, the silicate profile does differ from those of nitrate and phosphate in that its return to the water column by shell dissolution can occur at different depths from the soft tissue regeneration of the other two nutrients – see Figure 9.2. In general, the concentration of silicate increases down the water column, as a result of the dissolution of shell material, to around 1000 m, but does not usually exhibit a very distinct maximum at this depth. Below this, silicate tends to remain fairly constant to the sea bottom. Silicate is depleted in the surface layers of all the oceans, but the degree of depletion with respect to deep water

concentrations differs from ocean to ocean, with, for example, the concentration of dissolved silicate being very much higher in the North Pacific than in the North Atlantic deep waters.

9.1.2.2 The horizontal distribution and circulation of nutrients in the oceans In Section 7.1, attention was drawn to the fact that the chemical signals of non-conservative constituents in the oceans are controlled by circulation patterns that transport the constituents from one part of the sea to another and mix water masses, upon which are superimposed the effects of internal oceanic reactions arising from the involvement of the constituents in biogeochemical cycles. The nutrients provide a classical example of how this **two-fold signal control** operates. The shapes of the vertical oceanic profiles of nitrate, phosphate and silicate described above were interpreted in terms of the involvement of the nutrients with the biomass. During this, they are removed from solution into particulate phases of the biomass, including both tissue and skeletal parts of organisms, in the upper water layer and are subsequently regenerated back into solution at depth, i.e. a non-conservative signal. Recently, data have become available on the large-scale horizontal distributions of nutrients in sea water, both for general oceanic sections (see e.g. Sharp 1983 (nitrate), Tsuchiya 1985 (phosphate) and for specific isopycnal surfaces (see e.g. Kawase & Sarmiento 1985, Takahasi *et al.* 1985).

Nitrate can be used to illustrate the factors that control the horizontal distribution of a nutrient in the World Ocean. Sharp (1983) used GEOSECS data to compile latitudinal profiles through a multiple ocean basin section. The section is illustrated in Figure 9.3, and the principal feautures in the nitrate distribution are summarized below.

(a) Deep waters of the Indian and Pacific Oceans are derived partially from the North Atlantic and Antarctic sinking regions (see Sec. 7.3.3), and North Atlantic Deep Water (NADW) can be seen in the section at a depth lying between 1.5 and 4 km in the western Atlantic (isopleths for N at 16–35 μg atom kg^{-1}).
(b) Antarctic waters show little variation with depth and are the source of the Antarctic Bottom Water (ABW), which has isopleths for N of 32–33 μg atom kg^{-1}.
(c) In the western Atlantic NADW is overlain by Antarctic Intermediate Water (AIW), which appears as a distinct intrustion extending as far as ~ 30°N. Although the AIW is less distinct in the Pacific Ocean it is apparent that the source of the subsurface waters is largely in the Antarctic.
(d) Equatorial upwelling can be seen in both the Atlantic and Pacific, but it is more pronounced in the Pacific.
(e) The highest nitrate concentrations are found in the deep waters of the Pacific Ocean.

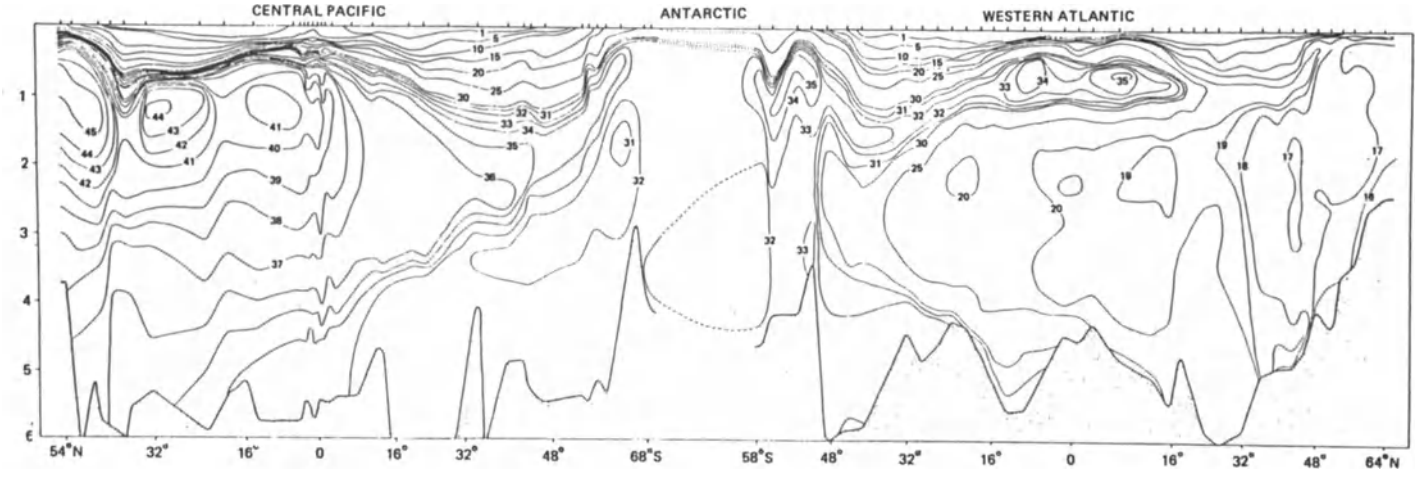

Figure 9.3 Central Pacific–Antarctic–western Atlantic oceanic section for nitrate (from Sharp 1983; section constructed from GEOSECS data); units, μg-atom N kg^{-1}, water depths in km.

The type of nutrient distribution described above can be related to deep water circulation patterns, and Broecker (1974) has suggested that the following sequence governs the nutrient build-up in the deep waters of the Pacific. The high-latitude sink waters (see Sec. 7.3.3) are depleted in nutrients by biological activity, but as they move along the global deep water circulation path some biogenic debris containing nutrients falls from the surface to deep water as particulate material, and this is supplemented by mixing with other nutrient-carrying deep waters from the Indian and Pacific Oceans. For every unit of deep water formed at the sinking sources, one unit must return to the surface by upwelling, a process that occurs over the entire ocean but tends to be more active in certain regions (see Sec. 7.3.2). This upwelled water, which is rich in nutrients, is then transported by surface currents. However, instead of following the surface circulation patterns the nutrients themselves are utilized by organisms, extracted from the water, and carried downwards via the organic particulate matter. A large fraction of these nutrients is regenerated, but some is carried to the deep sea in association with the particulate matter that escapes destruction (see Sec. 9.3). Thus, as Broecker & Peng (1982) have pointed out, the nutrients can be transported by deep currents but not by surface currents, the net result being that there is a steady push of nutrients towards the deep Pacific, which lies at the end of the transport path on the deep water global 'grand tour' (see Sec. 7.3.3). The distributions of the nutrients in the oceans are therefore controlled by an interaction, or balance, between oceanic circulation and biological activity.

It was suggested above that nutrient distributions are important in marine geochemistry because they can be used as analogues for the behaviour of other constituents, such as the trace metals, which are also involved in the major oceanic biogeochemical cycles. Thus, nitrate and phosphate can be used as analogues for elements that are taken into organic tissue phases, and silicate can be used as an analogue for elements incorporated into the skeletal parts of organisms. In this way, it is possible to distinguish between organic tissue and skeletal trace metal particulate carrier phases. This type of approach is discussed in detail in Section 11.6.3. However, it must be remembered that the distributions of nutrients differ from one part of the ocean to another. For example, in many regions biological activity is limited by phosphate and especially nitrate, which can be depleted to almost zero concentrations in some surface waters. In contrast, in regions in which there is strong vertical mixing, such as in the Antarctic, the concentrations of phosphate and nitrate can be significant at all water depths. For example, in the Antarctic, surface water phosphate concentrations are $\sim$ 70% of their deep water values, compared to only $\sim$ 10% elsewhere in the oceans. In this region, therefore, the nutrients are not depleted to near zero

concentrations, and biological activity is not limited by the availability of nutrients (see e.g. Siegnthaler & Wenk 1984).

9.1.3 The nutrients in the oceans: summary

(a) Nitrate and phosphate are involved in nutritional processes and are incorporated into the soft tissue phases of plankton, whereas silicate is only involved in building the hard skeletal parts of organisms.
(b) New nutrients are supplied to the euphotic zone by processes such as upwelling and erosion of the thermocline from below, and atmospheric deposition; these nutrients take part in new production and are transported out of surface waters via sinking particulates. Regenerated nutrients are recycled within the euphotic zone and take part in regenerated production.
(c) The vertical water column profiles of the nutrients exhibit a characteristic surface depletion–depth enrichment effect as a result of their uptake in surface waters during primary production and their release at depth following the remineralization of sinking detritus.
(d) The horizontal distribution of the nutrients is controlled by water circulation patterns, upon which are superimposed the effects of internal biogeochemical reactivity. As a result, there is a steady push of nutrients towards the deep Pacific, which lies at the end of the deep water global transport path, leading to their build-up in these waters.

9.2 Organic matter in the sea

9.2.1 Introduction

For analytical convenience, the organic matter in aquatic systems is usually divided into two fractions.

(a) The fraction passing through a 0.45 μm membrane filter includes material in true solution, together with some colloidal components, and is termed **dissolved organic matter** (DOM); its carbon content is classed as **dissolved organic carbon** (DOC).
(b) The filter-retained material is referred to as **particulate organic matter** (POM), and its carbon content is termed **particulate organic carbon** (POC).

Some authors also distinguish a third fraction, termed **volatile organic carbon** (VOC).

Estimates of the amount of organic carbon in the POC and DOC oceanic pools vary considerably. However, the values given by Williams (1975) will serve as order-of-magnitude estimates. According to this

author, the POC pool contains $\sim 3 \times 10^{16}$ g of carbon. Of this POC, $\sim 5 \times 10^{14}$ g are held in the plankton biomass and the remainder is associated with non-living detritus. On a whole-ocean scale, therefore, detrital POC dominates the total POC, but in surface waters of the euphotic zone the living POC associated with plankton and bacteria can predominate. The total POC is, however, only ~ 20 per cent of the DOC pool, which is estimated to contain $\sim 1 \times 10^{18}$ g of carbon. Thus, the DOC pool is the principal reservoir for organic carbon in the oceans.

In the following sections the composition and origin of the organic carbon in the oceans will be discussed, and an attempt will be made to synthesize the various data in terms of a marine organic carbon cycle.

9.2.2 The origins of oceanic organic matter

The organic matter in sea water can be divided into two genetic classes. That having an external source is termed **allochthonous**, and that originating in the ocean system itself, i.e. from internal sources, is referred to as **autochthonous**.

9.2.2.1 Allochthonous organic matter in the oceans This type of organic matter is brought to the oceans chiefly by river run-off and atmospheric deposition. These inputs have been discussed in Sections 3.1.5 and 4.1.4.4, respectively, and here attention will be mainly confined to the internally generated organic matter.

9.2.2.2 Authochthonous organic matter in the oceans The principal mechanism by which organic carbon is produced in the oceans is *in situ* photosynthesis by phytoplankton, which may be crudely represented by an equation of the general type

$$\underset{\text{(uptake)}}{CO_2 + H_2O} = \underset{\text{(release)}}{(CH_2O) + O_2} \qquad (9.1)$$

where CH_2O is carbohydrate. The resulting biotic carbon may form part of the POC pool, or it may enter the DOC pool through processes such as the exudation of organics by phytoplankton, excretion by zooplankton and post-death decay reactions.

Until a few years ago, little was known of the importance of photochemical reactions in the sea, apart from those involved in photosynthesis. It is now recognized, however, that such reactions can play a role in the production, transformation and destruction of organic matter in the sea and that, in particular, they can affect its oxidation in sea water. For a detailed discussion of marine photochemistry, the reader is referred to the extensive state-of-the-art reviews by Zafiriou (1983, 1986).

AUTOCHTHONOUS POC: THE LIVING POC FRACTION **Plankton** are microscopic free-floating, or weakly swimming, organisms that are distributed by ocean currents. They are subdivided into plants (phytoplankton) and animals (zooplankton). Important members of the **phytoplankton**, or marine algae, include diatoms, coccolithophores, silicoflagellates and dinoflagellates. The **zooplankton** include copepods, foraminifera, pteropods and radiolarians.

Marine autotrophs (e.g the algal biomass) are primary producers whereas marine heterotrophs (e.g. zooplankton) obtain their energy from preformed organic material. The photo-autotrophic algal biomass (phytoplankton) is the most important primary source of organic carbon in the oceans, and primary production is the intial stage in a marine food chain that subsequently involves a number of trophic levels. For example, herbivorous zooplankton (the grazers of the ocean) consume the phytoplankton (the grass of the ocean) during secondary production in which plant tissue is converted into animal tissue. These herbivorous zooplankton are, in turn, fed upon by carnivorous zooplankton and fish species (tertiary production). Over the last two or three decades there has been a change in our view of the oceanic plankton community, which has arisen from the identification of the **nanoplankton**. These are small plankton cells ($\sim$ 5–60 μm in diameter) that were largely missed by the early collection techniques, and it is now thought that small phytoplankton and small zooplankton are responsible for a large fraction of oceanic primary production and its consumption in secondary production.

The process of **photosynthesis**, in which organic compounds are synthesized from the inorganic constituents present in sea water during the growth of marine plants (phytoplankton), is usually termed **primary production**, although this is not a biochemically rigorous definition. In the process, which includes the absorption of solar energy and the assimilation of carbon dioxide, the chlorophyll-containing plants synthesize complex organic molecules from inorganic starting materials, the principal products being oxygen and food substances such as carbohydrates. It is the convention now to distinguish between *new* primary production, which arises from nutrients transported into the euphotic zone (e.g. from upwelling and atmospheric deposition), and *regenerated* production, which utilizes nutrients that are recycled within the surface layers (see Sec. 9.1.1).

Primary production in the oceans is controlled by a complex combination of physical (e.g. light, temperature), biological (e.g. growth rate) and chemical (e.g. availability of nutrients) variables. However, according to Neinhuis (1981), the availability of nutrients is probably the limiting factor in most marine systems. Under these conditions the supply of new nutrients to the euphotic layer is mainly dependent upon the instability of the water column, which results in the transport of nutrients

to the surface layers from the underlying waters by upwelling (the main source of nutrients to the euphotic zone). Under **eutrophic**, i.e. high-production, conditions, such as those found in coastal upwelling areas and in regions of divergence, the input of nutrients into surface waters is largely controlled by horizontal and vertical advection. However, in open-ocean **oligotrophic**, i.e. low-production, waters where there is a well developed thermocline, the physical transport of nutrients into the surface layer is largely via turbulent cross-thermocline vertical transport. Klein & Coste (1984) made a numerical study of the influence of unsteady dynamic atmospheric forcings on the physical entrainment of nutrients from deep water into the mixed layer as a result of the erosion of the thermocline by turbulence. They concluded that the nutrient entrainment is not driven by wind stress but is a result of a wind–surface current interaction, i.e. an ocean–atmosphere coupling. The important implication of this study to the supply of nutrients in oligotrophic waters is that the flux of the nutrients through the thermocline can take place in pulses, which have a timescale of ~ 5–10 h. These short pulses can increase the flux of nutrients into the euphotic zone considerably over short periods and so can affect the time evolution of primary production. In some regions, however, the supply of nutrients is not the dominant control on primary production. For example, in the Antarctic, where the thermocline is not developed, nutrient concentrations are significant at all water depths and biological activity is not limited by nutrient availability (see Sec. 9.1.2). Another exception is found in some turbid and eutrophic estuarine and coastal waters in which solar radiation, and not nutrient supply, can limit production (see Sec. 3.2.7). At low latitudes the surface waters are generally warm and well illuminated throughout the year, and primary production occurs at all seasons, the limiting factor being the nutrient supply. In contrast, at high latitudes production is virtually confined to the short summer season in which there are long periods of daylight. However, seasonal variations in production are highest in the mid-latitudes, where surface water temperatures show the greatest year-round fluctuations.

Photosynthesis requires light in the wavelength range 370–720 nm, and even in clear tropical waters only ~ 1% of the visible light energy penetrates to a depth of ~ 100 m. Photosynthesis is therefore generally restricted to the upper 100 m or so of the open-ocean water column, although it may, in fact, be inhibited at the surface layer itself because of the effects of high light intensity, and as a result the zone of *maximum* production is often found a few metres below the surface. Gross primary production decreases with depth, but the loss of carbon through respiration remains constant because phytoplankton respire during the hours of sunlight and darkness. The depth at which gross primary production and respiration balance is termed the **compensation depth**, and at this position net production is zero. Net primary production is positive

in the water column above the compensation depth, and this is the region referred to as the **euphotic zone**. In the aphotic zone, which lies below the compensation depth, respiration exceeds gross production and there is a net loss of organic material.

Much of our knowledge of the oceanic distribution of primary production has come from the work that Soviet scientists carried out over a decade ago (see e.g. Koblentz-Mishk *et al.* 1970). There are thought to be inadequacies in this work, and it is now being updated in the Global Ocean Flux Study (GOFS). Nonetheless, a number of useful trends can be identified from the original data, and for this purpose the geographical distribution of primary production is illustrated in Figure 9.4. Perhaps the most striking feature of this diagram is the variation in the fertility of the oceans, with large areas being almost barren (oligotrophic) whereas others are highly productive (eutrophic). It was suggested above that, on a global basis, the principal limiting factor for primary production is the availability of nutrients, and this is reflected in several of the major features in Figure 9.4.

(a) Primary production is generally greater in coastal than in open-ocean water, i.e. the so-called land-mass effect; for a detailed discussion of this phenomenon see Strickland (1965).
(b) Specific regions of high productivity (eutrophic zones) are found in areas of upwelling. It was shown in Section 9.1.2 that in the water column the concentrations of the nutrient elements are greater at depth than at the surface, where they are depleted by biological activity. During upwelling these nutrient-rich subsurface waters are brought to the surface, and so lead to an increase in primary production. High primary production is therefore found in many regions of upwelling; these include the shelves off the western margins of West Africa, Namibia (South West Africa), Peru, the western United States, western Australia, India and South East Asia. In open-ocean areas, upwelling caused by divergence leads to high primary production in a number of areas, one of the most important being the 'strip' in the equatorial Pacific. A slow upwelling of nutrient-rich water is also found around Antarctica, where it forms a thermally stable layer in the euphotic zone (Strickland 1965). This, combined with a marked land-mass effect, makes Antarctica one of the most fertile of all marine regions.
(c) Infertile, or oligotrophic, regions, i.e. those with relatively low primary production, are found where water mixing is minimal, for example where a deep permanent thermocline acts as a barrier between nutrient-rich subsurface waters and the surface layer. Areas of low productivity occur in the central oceanic gyres, which lie between ~ 10° and ~ 40° north and south of the Equator (see Sec. 7.3.2).

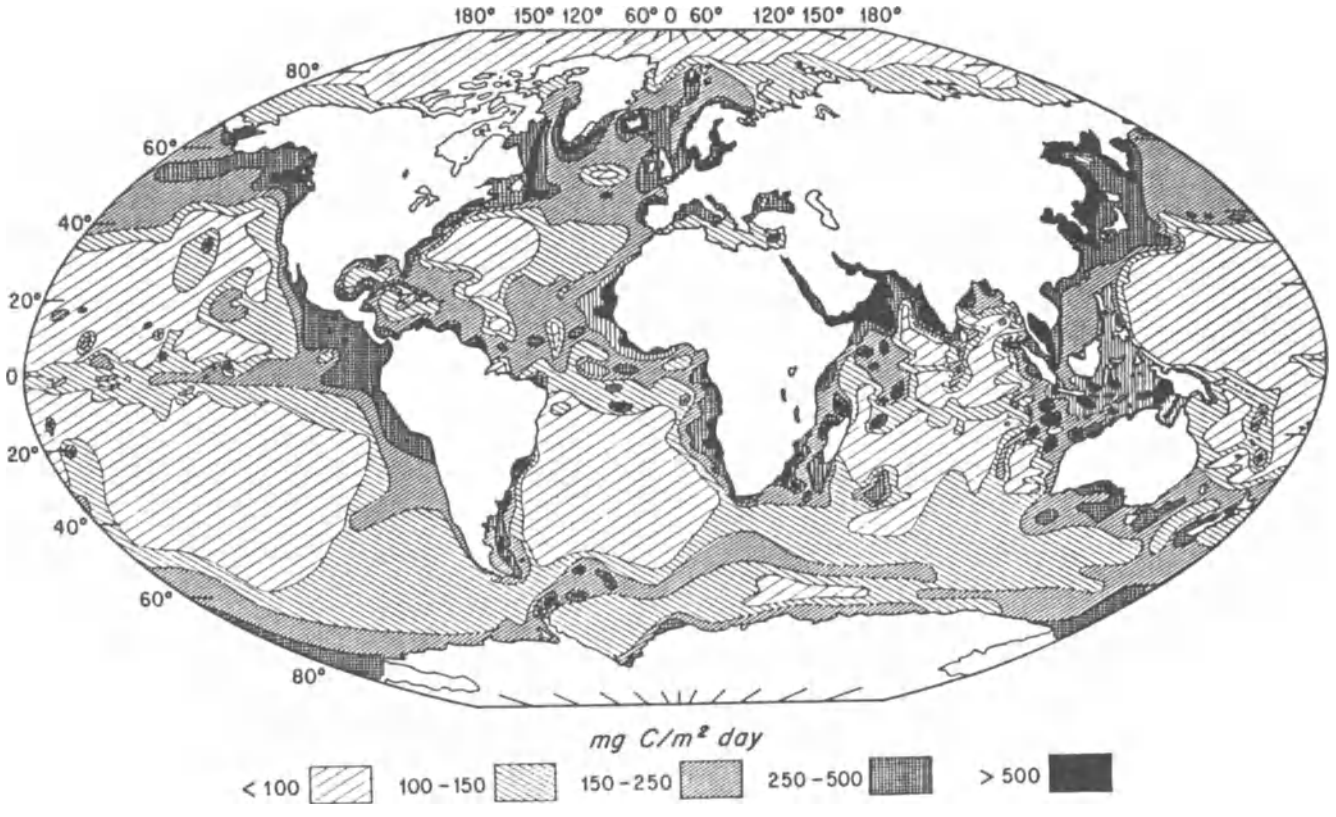

Figure 9.4 Primary production in the World Ocean (from Degens & Mopper 1976, after Koblentz-Mishk *et al.* 1968).

It is apparent from this brief description of the major trends in the distribution of primary production that the overall pattern is one of a ring of high-fertility zones around the edges of the ocean basins, particularly on the eastern margins, and a generally low fertility in their centres (except where divergence occurs). However, although this is a useful generalization it gives an oversimplistic picture, and for a more detailed discussion of the complex factors that govern primary production the reader is referred to the reviews given by Strickland (1965) and Nienhuis (1981).

There is some dispute over the assessment of the magnitude of the global primary production rate. Primary production is usually measured by the ^{14}C technique (Steeman Neilson 1952), and estimates of the global production of carbon are in the range $(1.5–1.8) \times 10^{16}$ g yr^{-1} (Williams 1975). However, Nienhuis (1981) reviewed the basis on which a number of the estimates were made, and drew attention to the fact that some authors beileve that they may be too low because it is thought that the ^{14}C technique can underestimate primary production by as much as a factor of 2 or 3. For example, De Vooys (1979) took a previous estimate of 3.1×10^{16} g yr^{-1} and corrected it to take account of uncertainties both in the ^{14}C technique and in estimates of the production of extracellular material. On this basis, he suggested that a value of 4.4×10^{16} g yr^{-1} probably affords the best estimate of the global oceanic primary production rate of carbon. Much of the criticism directed at the ^{14}C technique for the estimation of primary production came from oxygen utilization rate measurements, which required that the amount of carbon leaving the euphotic zone (new production) must be higher than had been predicted by earlier productivity measurements. The most recent estimates of primary production are therefore higher than the previous ones; for example, Williams & Druffel (1987) suggest that the global production of photosynthetically fixed carbon lies in the range $(4.0–15) \times 10^{16}$ g yr^{-1}. It was shown above that the distribution of primary production varies over the ocean surface and, in general, ~ 80% occurs in the open ocean and ~ 20% in coastal regions (see e.g. Martin *et al.* 1987).

AUTOCHTHONOUS POC: THE NON-LIVING POC FRACTION This consists mainly of dead organisms, faecal material and faecal debris, organic aggregates of various types, and other complex organic particles. In open-ocean waters much of this non-living POC is derived from phytoplankton, although the relationship between non-living POC and phytoplankton is not a simple one. Cauwet (1981) has identified four major processes that are involved in the formation of non-living POC: (a) the direct formation of detritus (e.g. organic fragments, faecal pellets); (b) the agglomeration of bacteria; (c) the aggregation of organic molecules by bubbling in the surface layers; and (d) the flocculation or adsorption of DOC onto mineral particles.

Fellows *et al.* (1981) have also suggested that bacteria, and other micro-organisms, can repackage soluble nutrients into POC. This DOC → bacteria → POC route can result in increases in POC at depth in the water column and so enhance its supply to the deep water pool (see Sec. 9.3).

AUTOCHTHONOUS DOC In general, there are three pathways by which the autochthonous POC produced in the oceans by biota can contribute to the oceanic DOC pool: (a) exudation by phytoplankton, (b) excretion by zooplankton, and (c) post-death organism decay processes. During their lifetime phytoplankton release some of their photosynthetically fixed carbon to the surrounding waters by metabolic processes. Following the death of both phytoplankton and zooplankton, decomposition occurs via the action of autolytic enzymes present in the tissues and by bacteria that have colonized the material. During these processes the DOC released into the water can include both biologically labile and refractory fractions (see Sec. 9.2.3.2). Estimates of the amount of photosynthetically fixed carbon released as extracellular products vary, but Williams (1975) concluded that a value of ~ 10% is probably representative of offshore plankton communities, which on a global scale would yield an addition of $\sim 3.6 \times 10^{15}$ g yr^{-1} to the oceanic DOC pool.

In addition to internal sources, DOC can be supplied to the oceans from external (allochthonous) terrestrial inputs. There is disagreement in the literature over the relative importance of the internal and external DOC sources. For example, Mantoura & Woodward (1983) showed that the DOC in the Severn Estuary (UK) behaved in a conservative manner (see Sec. 3.2.7.7), and pointed out that the geochemical significance of this conservative delivery of fluvial DOC is that, on a global scale, river inputs will make a significant contribution, up to as much as ~ 50%, to the oceanic DOC pool. However, other lines of evidence put the terrestial DOC contribution to the oceanic DOC pool at a much lower figure. Thus Meyers-Schulte & Hedges (1986) showed that there is an absence of lignin in open-ocean humic substances from the equatorial Pacific and on the basis of this estimated that < 10% of the oceanic DOC is terrestrial in origin; Williams & Gordon (1970) and Eadie *et al.* (1978) gave data on the $\delta^{13}C$ signature of oceanic DOC, which suggested that it originates mainly from marine-derived organic carbon; and Williams & Druffel (1987) used radio-carbon data for dissolved organic matter in the central North Pacific to conclude that the terrestially derived DOC component cannot exceed ~ 10% of the oceanic DOC.

9.2.3 The composition of oceanic organic matter

9.2.3.1 The composition of POM in the oceans The POM in the oceans consists of living organisms and dead material (**detritus**), and can

originate from both marine and terrestial sources.

Some aspects of the major element composition of organic tissue are relatively well understood. One reason for this is that the C : N : P ratios of both plant and animal tissue are fairly constant. These are often termed the **Redfield ratios**, after Redfield (1934, 1958). These ratios indicate that the major plant nutrients, phosphate and nitrate, change concentrations in sea water in a fixed stoichiometry that is the same as the N and P stoichiometry of plankton. Thus, the nutrients are removed from sea water during photosynthesis in the proportions required by the biomass. The elemental composition of phytoplankton and zooplankton is very similar, and C : N : P proportions of 106 : 16 : 1 are commonly used for their organic tissue material. These are the Redfield ratios and represent the preformed composition of the organic material that undergoes oxidative destruction in the euphotic zone according to the relationship $C : N : P - O_2 = 106 : 16 : 1 : 138$, which corresponds to the consumption of 138 moles of oxygen to produce 106 atoms of carbon, 16 atoms of nitrogen and 1 atom of phosphorus. Recently, however, it has been suggested that the accepted Redfield ratios need revision. For example, Takahasi *et al.* (1985) used a variety of chemical data from isopycnal surfaces to estimate the composition of the organic matter oxidized within the thermocline of the Atlantic and Indian Oceans, and concluded that the composition is better represented by C : N : P ratios of $122(\pm 18) : 16 : 1$. Watson & Whitfield (1985) modelled the composition of particles in the global ocean and also concluded that the original Redfield ratios should be changed, suggesting that the material leaving the euphotic zone has a composition corresponding to $C_{org} : N : P : Si : C_{inorg} = 126 : 15.7 : 1 : 23.5 : 23.0$.

The soft, i.e. non-skeletal, parts of organisms are composed mainly of proteins, carbohydrates, lipids and, in higher plants, lignins. The living biomass in the sea is dominated by phytoplankton, and the major metabolites (i.e. substances that take part in the processes of metabolism) are pigments, proteins, carbohydrates and lipids. The structures of some of the organic compounds found in plankton are illustrated in Worksheet 9.1.

PROTEINS Proteins are complex nitrogenous organic compounds built up of **amino acids**, and in the form of **enzymes** they catalyze biochemical reactions. According to Degens & Mopper (1976) the protein amino acid composition of plankton is fairly uniform from one species to another, the most abundant of these acids being glycine, alanine, glutamic acid and aspartic acid. Both phytoplankton and zooplankton release free amino acids into sea water. The free amino acid concentrations in sea water do not appear to vary with biological activity, but there is evidence that the combined amino acids may increase with plankton production (see e.g. Williams 1975).

WORKSHEET 9.1
STRUCTURES OF ORGANIC COMPOUNDS FOUND IN PLANKTON

PROTEINS

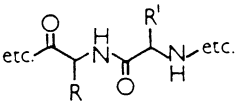

Biopolymers of amino acids e.g.

Glycine 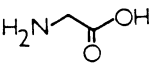

Alanine 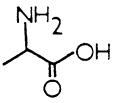

CARBOHYDRATES

e.g. Cellulose

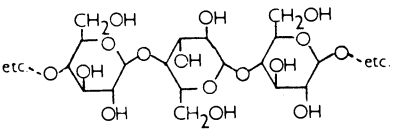

POLYSACCHARIDE

e.g. Chitin

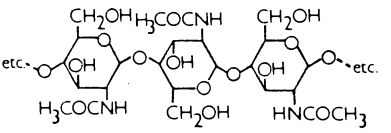

MUCOPOLYSACCHARIDE

PIGMENTS

e.g. Chlorophyll a

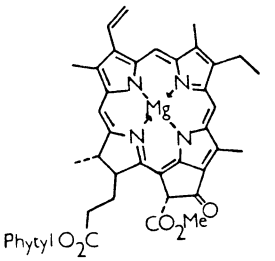

e.g. β-Carotene

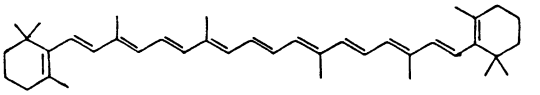

LIPIDS

Fatty acids

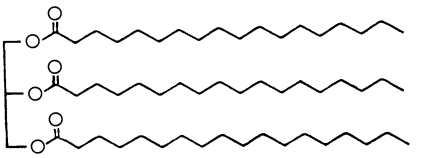

Triglycerides

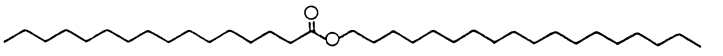

Wax esters

STEROLS

e.g. Cholesterol

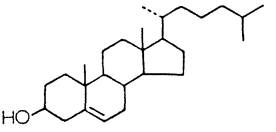

Widespread distribution in animals and plants

e.g. Dinosterol

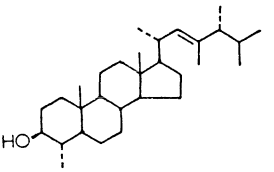

Specific to Dinoflagellate algae

CARBOHYDRATES Carbohydrates include sugars, starches and cellulose. Carbohydrates form the supporting tissues of phytoplankton and also act as energy sources; for example, catabolism of carbohydrates provides most of the energy requirement for the cell. Carbohydrates can be classified into monosaccharides, which are subdivided into pentoses (e.g. ribose) and hexoses (e.g. glucose), and disaccharides (e.g. sucrose), both of which are sugars, and polysaccharides, which include starches, cellulose and the mucopolysaccharide chitin. The general order of abundance of planktonic carbohydrates is galactose > glucose > mannose > ribose > xylose > fucose > rhamnose > arabinose (Degens & Mopper 1976); however, unlike that of protein, the carbohydrate composition of plankton varies considerably from one species to another.

LIPIDS Lipids is a general term that applies to all substances produced by organisms that are insoluble in water but can be extracted by some kind of organic solvent. Lipids include fats and waxes (simple lipids), phospholipids and glycolipids (compound lipids), sterols and some hydrocarbons. Fats, which are utilized mainly in the energy budget of organisms, are formed by the combination of glycerol and fatty acids; and waxes, which have a protective function, are formed by the combination of fatty acids with alcohols other than glycerol. Triglycerides (fatty acid

esters of glycerol) are the most abundant lipids in phytoplankton and can serve as energy store reserves, buoyancy controls and thermal or mechanical insulators; wax esters, simple esters of long-chain fatty alcohols and long-chain fatty acids, are abundant in zooplankton (Gagosian & Lee 1981). Sterols are the hormonal regulators of growth, respiration and reproduction in most marine organisms (see e.g. Kakanazawa & Teshima 1971), and may also act as membrane rigidifiers. In addition, sterols can be present as lipoproteins (e.g. cholesterol).

PIGMENTS Photosynthetic pigments, such as chlorophyll and the carotenoids, are employed by plants to absorb and transfer light energy during photosynthesis. Most phytoplankton have **chlorophyll** as their primary photosynthetic pigment, and four major chlorophylls have been identified (Chl *a*, Chl *b*, Chl *c*, and Chl *d*), with Chl *a* being the primary pigment in all oxygen-evolving organisms other than bacteria. The distribution of chlorophylla is not homogeneous throughout the water column, but is characterized by a global-scale maximum often found near the bottom of the euphotic zone in the region of the thermocline. The concentrations of chlorophylls are generally higher in euphotic waters than in those from oligotrophic regions, and chlorophyll *a* is often measured in the column as an indicator of primary production.

OTHER METABOLITES Various other organic compounds are also found in plankton. These compounds include vitamins, co-enzymes and hydrocarbons. According to Gagosian & Lee (1981), the principal hydrocarbons in algae are alkenes, together with lesser amounts of n-alkanes, branched alkanes and cyclic alkanes.

Terrestrial sources also provide a variety of dissolved and particulate organic matter to the oceans, which can eventually become incorporated into the sediment sink. This organic matter embraces a wide variety of compounds, including hydrocarbons, fatty acids, carbohydrates, fatty alcohols and sterols, natural polymers such as lignin, cutin and chitin, and possibly amino acids. Some of these compounds are exclusive to terrestrial biota. For example, lignins are complex phenolic polymers that are unique to the tissues of vascular land plants. Others can be derived from both terrestrial and marine sources, but can sometimes be distinguished from each other on the basis of their detailed chemistries. This 'biomarker' approach can be illustrated with reference to a number of compounds. For example: (a) terrestrial n-alkanes derived from plant waxes have their principal homologues in the series C_{23}–C_{35}, whereas those derived from marine plankton are dominated by homologues in the range C_{15}–C_{21}; (b) terrestrial fatty acids derived from plant waxes have homologues in the series C_{14}–C_{36}, whereas those from marine plankton

sources are generally in the range C_{12}–C_{24}.

Only a small fraction of the deep water POM, probably a few per cent, is composed of living material, the remainder being *refractory* in character. This refractory deep water POM consists of two fractions: (a) a small-sized fraction, which makes up the bulk of the POM, and (b) a large-sized fraction, consisting mainly of faecal pellets and organic debris, which is utilized in the food chain. The refractory POM is considered in more detail in Section 9.3, when the oceanic carbon cycle is described.

9.2.3.2 The composition of DOM in the oceans In a very broad sense, oceanic DOM can be divided into **labile** (i.e. biologically utilized) and **inert** (i.e. biologically and chemically refractory) fractions.

Only a small fraction, perhaps ~ 20%, of the DOM in sea water and the oceanic microlayer has been characterized and found to be labile in nature. This fraction consists mainly of compounds such as lipids, carbohydrates, amino acids, urea and pigments, which are typically associated with the biochemistry of living organisms (see Sec. 9.2.3.1). The biomass itself is probably the principal source of these labile organics, which can be introduced into the water column by processes such as exudation, excretion and the decomposition of dead organisms. In addition, soluble organic material, which can contribute to the dissolved organic pool, can be transported to the oceans via river run-off and atmospheric deposition (see Secs 3.1.5 & 4.1.4.4, respectively). The characterized fraction of the DOM also contains a number of organic pollutants, such as petroleum hydrocarbons, DDT and PCBs.

LIPIDS Various authors have given data on the concentrations of dissolved lipids, including hydrocarbons, in sea water. For example, Kennicutt & Jeffrey (1981) used a number of techniques to identify a series of compounds in the chloroform-extractable lipid fraction of dissolved organic matter in sea water, the major components being n-alkanes (C_{16}–C_{32}), pristane, phytane and fatty acid esters.

Free fatty acids constitute ~ 1–3% of the total DOM in sea water, the principal components being palmitic, oleic, myristic and stearic acids (see e.g. Ehrhardt *et al.* 1980, Kattner *et al.* 1983). In a recent study, Parrish & Wangersky (1988) gave data on the vertical profiles of a number of classes of both particulate and dissolved lipids in sea water of the Scotian Slope; the lipid classes identified were aliphatic hydrocarbons (HC), wax esters (WE), triglyceride (TG), free fatty acid (FFA), free sterol (ST), acetone-mobile polar lipid (AMPL) and phospholipid (PL). Water column profiles for some of these lipid classes, together with those for chlorophyll *a* and total particulate and dissolved lipids, are illustrated in Figure 9.5. Two important features in the vertical distributions of the lipids can be identified from profiles such as these.

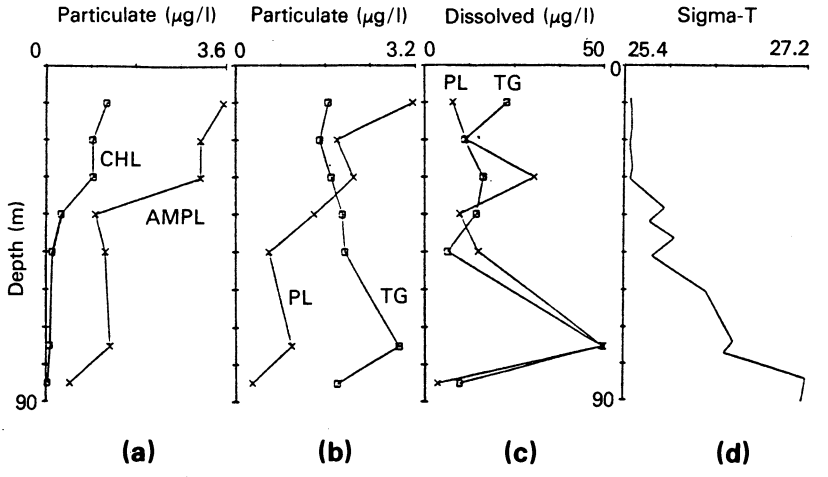

Figure 9.5 Water column profiles of lipids, chlorophyll and density over the Scotian Slope (from Parrish & Wangersky 1988). (**a**) Particulate chlorophyll *a* and acetone-mobile polar lipid (AMPL). (**b**) Particulate phospholipid (PL) and triglyceride (TG). (**c**) Dissolved phospholipid (PL) and triglyceride (TG). (**d**) Density.

(a) The distributions of a number of the particulate lipids, especially the pigment-containing AMPL, were similar to that of chlorophyll *a*. However, particulate wax esters, hydrocarbons and triglycerides did not follow the chlorophyll distribution.

(b) The most striking feature in the vertical distributions of the dissolved, and some particulate, lipids is the high concentrations of total lipids immediately above, or in the vicinity of, the pycnocline. This enhancement probably arises as a result of the large density differences at this discontinuity level, which acts as an impediment to the sinking of lipid-containing material out of the surface layer; similar enhancements have also been found for particulate chlorophyll *a*, dissolved free amino acids and carbohydrates (see e.g. Liebeziet *et al.* 1980).

Parrish & Wangersky (1988) reported that total lipid concentrations appear to be related to both biological and physical factors. Overall, however, the distributions of the dissolved and particulate lipids were not closely coupled in the waters of the Scotia Slope (see also Boehm 1980). Thus, Parrish & Wangersky (1988) concluded on the basis of their data,

which are similar to those obtained from other studies, that dissolved and particulate lipid concentrations are the result of independent processes operating on different space and time scales.

Hydrocarbons are present in all marine organisms, but usually account for only ~ 1% of the total lipids; however, the concentrations can be higher in micro-algae (Parrish 1988). The non-volatile natural hydrocarbons ($> C_{14}$) in the marine environment include saturated aliphatic hydrocarbons (e.g. n-alkanes, regular branched isoprenoids, branched alkanes), unsaturated aliphatic hydrocarbons (e.g. n-alkenes), saturated alicyclic hydrocarbons (e.g. cyclanes), unsaturated alicyclic hydrocarbons (e.g. cyclenes) and aromatic hydrocarbons (e.g. retene, perylene). The pollutants include n-alkanes, isoalkanes, cycloalkanes and aromatic compounds from oil pollution, polycyclic aromatic hydrocarbons (PAHs), polychlorinated biphenyls (PCBs), and the biocides DDT and pentachlorophenol (PCP). However, according to Parrish (1988) the latter are only present in sea water in small concentrations, which range from < 10 ng l^{-1} close to sources of pollution to $\ll 1$ ng l^{-1} in open-ocean waters. Saliot (1981) compiled a comprehensive list of the types and concentrations of natural hydrocarbons in sea water. The author concluded that the concentrations of dissolved and particulate hydrocarbons usually lie in the range 1 to 50 μg l^{-1}, with a tendency for the concentrations to increase in the surface microlayer and in inshore and productive coastal waters; the overall average concentration is probably < 10 μm l^{-1}.

The n-alkanes are the dominant constituents of natural hydrocarbons in the marine environement (Saliot 1981). The n-alkanes in sea water originate from: (a) natural internal sources, i.e. the oceanic biomass (phytoplankton, zooplankton, bacteria); (b) natural external terrestrial sources (mainly associated with higher plant metabolism; and (c) anthropogenic sources (e.g. oil pollution). These sources can sometimes be distinguished by characterizing the n-alkanes on the basis of their carbon numbers and their carbon preference index (CPI). In this context,

$$\text{CPI} = \frac{\text{Sum of odd carbon n-alkane concentrations}}{\text{Sum of even carbon n-alkane concentrations}} .$$

Thus, a CPI of 1 indicates no carbon preference (see e.g. Kennicutt & Jeffrey 1981). n-Alkanes in the range C_{17} to C_{22} are indicative of a source in phytoplankton (see e.g. Blumer 1970), whereas the heavier n-alkanes in the range C_{28} to C_{32} originate from terrestrial plants (see e.g. Eglinton & Hamilton 1963). The n-alkanes of plants and organisms generally show odd carbon preference; for example, the n-alkanes in lipids derived from terrestrial higher plants, which are in the range C_{10} to C_{40}, exhibit a strong preference for odd-numbered over even-numbered n-alkanes, with n-C_{27}, n-C_{29} and n-C_{31} being predominant (see e.g. Tissot & Welte 1984).

In contrast, the n-alkanes of oils usually have a CPI of around 1. Kennicutt & Jeffrey (1981) used these various parameters in an attempt to establish the sources of n-alkanes in sea water from the Gulf of Mexico. They found that dissolved n-alkanes, which were in the range C_{16} to C_{32}, were present in the waters in a bimodal distribution with maxima identified at C_{19}/C_{20}, which is likely to have a phytoplankton source, and at C_{32}, which is probably from a terrestrial plant source. The peaks associated with the bimodal distribution were superimposed on a low-level, steady-state, concentration of n-alkanes in the C_{22}–C_{27} range, which may have originated from oil pollution; however, no carbon preference was evident for the n-alkanes in the waters.

CARBOHYDRATES Walsh & Douglass (1966) gave data on a vertical profile of dissolved carbohydrate (DCHO) in the Sargasso Sea. The concentration of DCHO increased from 0.27 mg l^{-1} at the surface to 0.75 mg l^{-1} at a depth of 75 m. Between 350 and 1000 m there was a gradual increase in the concentrations of DCHO, followed by a decrease to around 2000 m. The concentrations of DCHO reported by these authors were considerably higher than those reported by Liebeziet *et al.* (1980) for the Sargasso Sea, but the general vertical distribution pattern was the same. The DCHO compounds identified by Liebeziet *et al.* (1980) were mainly hexoses, with a predominance of glucose and fructose. Sugugawa *et al.* (1985) have given data on a series of dissolved low-molecular-weight carbohydrates in sea water during the period of algal bloom. The compounds identified included laminaribiose, laminaritriose, glycosylglycerols, sucrose and raffinose. These low-molecular-weight carbohydrates were also identified in dinoflagellate cells, and the dissolved fractions in sea water were thought to have been derived from phytoplankton via extracellular release or cell lysis.

AMINO ACIDS Lee & Bada (1977) have given data on the dissolved free amino acids (DFAA), the dissolved combined amino acids (DCAA) and the dissolved total amino acids (DTAA) in the equatorial Pacific and the Sargasso Sea. In both environments, the concentration of DCAA was much higher than that of DFAA, and showed a maximum in the euphotic zone where the concentrations of phytoplankton and zooplankton are higher. Further, the DCAA concentrations were higher at all depths in the water column in the productive equatorial Pacific compared to the oligotrophic Sargasso Sea. Lee & Bada (1977) also found that DFAA concentrations are small and relatively invariant in the water column. However, Liebeziet *et al.* (1980) showed that there was significant variation in the concentrations of DFAA with depth in the Sargasso Sea. These authors provided data on the distributions of dissolved free amino acids (threonine, serine, glutamic acid, aspartic acid, glycine, alanine)

and carbohydrates at pycnocline boundaries in the Sargasso Sea. They found that the concentrations of both dissolved components were enriched at the upper boundaries of the pycnocline. Amino acid concentrations were low at the surface and enriched in the upper boundary of the seasonal pycnocline and within the thermocline; carbohydrate values were high at the surface and were only enriched in the upper boundary of the thermocline. The authors attributed these enhancements to increased auto- and heterotrophic activity leading to the production of dissolved organic compounds in the sharp density layer, where there is a concentration of bacteria and zooplankton that take advantage of the energy-rich compounds concentrated at the discontinuities in the water column.

HALOGENATED ORGANICS A number of organisms are known to produce halogen-containing organic compounds, with bromine rather than chlorine being the dominant halogen present. This topic has been reviewed by Fenical (1981).

DISSOLVED ORGANO-SULPHUR COMPOUNDS These compounds include those having natural sources (e.g. dimethyl sulphide (DMS), dimethyl disulphide (DMDS), carbon disulphide, methyl mercaptan (MeSH), dibenzothiophene (DBT), sulphur-containing amino acids and those derived from anthropogenic sources (e.g. DBT from oil spills, diphenylsulphone).

The description of dissolved organics in sea water given above has been confined mainly to the bulk water column. It must be stressed, however, that a considerable concentration of both dissolved and particulate organic material is found in the sea surface microlayer. For example, the total DOC is enhanced in the microlayer, relative to bulk sea water, by a factor of around 1.5 to 3, and the individual compounds contributing to this enrichment include surfactant lipids (and hydrocarbons), carbohydrates and amino acids. For a discussion of the composition of the dissolved and particulate material in the microlayer, see Section 4.3.

The bulk of the DOM in sea water has not been characterized in detail. However, it is known to be inert, i.e. it is largely refractory to biological degradation and chemical oxidation and as such it plays no part in the biological cycle. Traditionally this uncharacterized DOM has been given the name **Gelbstoff**, because of the yellow colour it imparts to sea water. Gelbstoff is not a single component, but is a complex mixture of macromolecules of humic- and lignin-type material somewhat analogous in composition to terrestial soil residues. However, Gelbstoff does not simply consist of such terrestial soil residues that have been transported from the land masses, and a significant fraction of it is in fact formed within the sea itself. Originally, it was thought that this internally formed

inert DOM was simply the residue remaining after the decomposition of phytoplankton debris. However, there now seems to be a general consensus that the humic substances in sea water are derived from reactions involving simple organic compounds produced by living organisms; these humic building blocks include amino acids, sugars, lipids, etc. The reactions involved are not yet fully understood, but since the excretion products of phytoplankton consist largely of compounds with molecular weights < 3000, this primary material must undergo further polymerization in order to form higher-molecular-weight macromolecules (Dawson & Duursma 1981). In the marine context, therefore, **humification** refers to the polymerization or condensation of low-molecular-weight compounds, which results in the formation of higher-molecular-weight substances that are presumably more stable in sea water. Detailed reviews of the humic material in sea water have been given by Williams (1975), Ogura (1977) and Skopintsev (1981).

It is apparent that much of the organic matter in sea water still remains to be identified, and the most commonly applied analytical techniques are those designed to measure organic carbon. In the following sections this component will therefore be used to describe the concentration and distribution of organic matter in the ocean system.

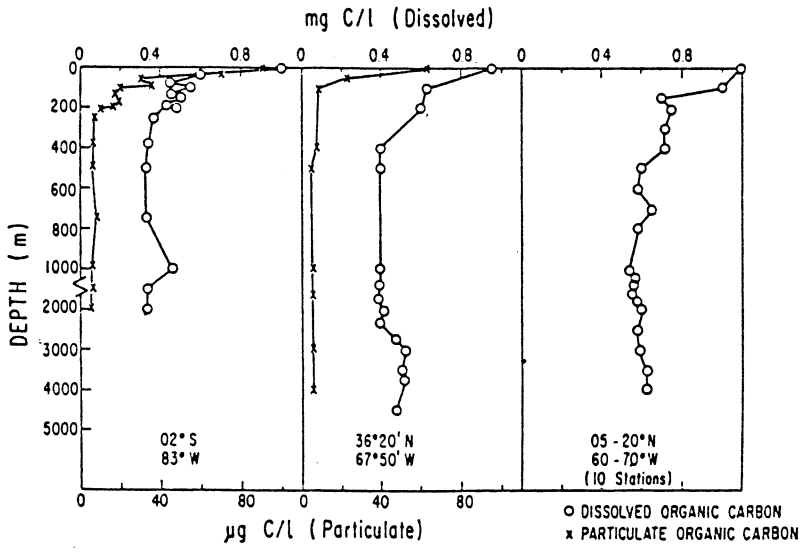

Figure 9.6 Vertical profiles of dissolved and particulate carbon in the Atlantic Ocean (from Williams 1971).

9.2.4 The distribution of organic carbon in the oceans

9.2.4.1 The distribution of POC in the oceans POC constitutes an average of ~ 20% of the TOC in sea water, and is made up of both a living fraction (mainly phytoplankton) and a non-living fraction (detritus; consisting mainly of dead organisms, faecal material and faecal debris, and organic aggregates of various types). The living POC fraction is made up largely of plankton, and in most surface waters (0 to ~ 300 m) these are the main source of POC, contributing between ~ 20% and ~ 50% of the total POC in oligotrophic waters, and up to as much as ~ 90% in highly productive waters (Mackinnon 1981). In surface waters, therefore, POC concentrations generally vary both geographically and seasonally in the same manner as does primary production, and appear to lie in the range ~ 0.03 to ~ 0.3 mg l^{-1}, with an oceanic average of ~ 0.1 mg l^{-1}. In deeper waters the POC concentrations fall, ranging from ~ 0.005 to ~ 0.03 mg l^{-1}, and have an average of ~ 0.01 mg l^{-1}. Thus, there is an overall decrease in the concentrations of POC with depth in the water column, and this is illustrated in Figure 9.6. Further, in deep waters the POC, much of which is non-living and refractory, is much less variable in concentration than it is in the surface layer. Nonetheless, variation in the concentrations of POC with depth in the water column can occur when the profile section cuts more than one water mass.

9.2.4.2 The distribution of DOC in the oceans DOC makes up on average ~ 80% of the TOC in the oceans. Williams (1975) assessed the published data on the geographic distribution of DOC in the oceans and concluded that there is no evidence of any significant, or regular, differences in the concentration patterns between the various oceans, or within their climatic zones. Thus, there is what Williams (1975) called a 'general uniformity' in the amount of dissolved organic material in the sea. However, seasonal variations in the concentrations of DOC in surface waters, and depth variations in the water column, can be superimposed on this generally uniform spatial DOC concentration pattern. For example, a general feature of the distribution of DOC in the water column is that, like those of POC, concentrations in the upper layer (0–300 m) are higher, and more variable, than those found at depth in the water column. To illustrate this overall trend, a typical DOC concentration–depth profile is illustrated in Figure 9.6. If nearshore, and especially anoxic, waters are excluded, DOC concentrations in the surface layers are usually in the range ~ 0.3 to ~ 2.4 mg l^{-1}. In contrast, deep water concentrations range from ~ 0.2 to ~ 0.8 mg l^{-1}, and have an average of ~ 0.5 mg l^{-1}.

Some recent work by Sugimura & Suzuki (1988) has, however, thrown considerable doubt on the published data for the concentrations of DOC

in sea water. These authors designed a hew high-temperature catalytic oxidation method for the determination of non-volatile DOC in sea water, and reported DOC concentrations that were considerably higher than the old values. For example, at one station in the western Pacific the new values for surface water DOC were ~ 2.5 times higher than those found using the standard persulphate oxidation procedure. The results suggest that previous methods were measuring only part of the DOC in sea water, the fraction missed probably being a high-molecular-weight material. The application of the new technique also cast doubt on the shapes of the DOC concentration–depth profiles obtained previously, which showed a generally uniform distribution (see Fig. 9.6) and did not suggest a clear relationship with apparent oxygen utilization (AOU) – see Section 8.3. Sugimura & Suzuki (1988) suggested that, because the decomposition of organic matter consumes dissolved oxygen in sea water, the DOC concentrations should be inversely related to the AOU. Their new DOC data showed that this was indeed the case (see Fig. 9.7), suggesting that the AOU is controlled by the *in situ* decomposition of DOC. The result is that the dominant consumption of oxygen once a water leaves the surface is by the oxidation of the DOC that moves with it, a relationship only picked up using the new DOC determination procedure. The new data for DOC and dissolved organic nitrogen (DON) also have other important implications. For example, Jackson (1988) has pointed out that the central tenet of nutrient cycling in the euphotic zone has been that the transport of nitrate into the zone is balanced by a loss from *particle* settling – see the description of new and regenerated production in Section 9.1.1. However, this equivalence breaks down if there is a substantial introduction of DON into the system because then the rate at which new nitrogen is introduced into the euphotic zone depends on the total dissolved nitrogen (TDN) gradient and not just on the nitrate gradient. Jackson (1988) concluded that, as a consequence of this, *particles* must be assumed to have a less important role than was first thought in nutrient (and associated trace element) cycling and transport. The author also considered the stoichiometric relationship among the nutrients in the light of the study carried out by Sugimura & Suzuki (1988). To maintain the Redfield, i.e. fixed, nutrient ratios it is necessary for the total concentrations of nitrogen and phosphorus to have the same ratio in solution and particles. This constraint must also hold for the new DON concentrations reported by Sugimura & Suzuki (1988). These data revealed that at one station in the North Pacific most nitrate production must have originated from the oxidation of TDN, and not from the remineralization of settling particles. Jackson (1988) pointed out that both nitrogen and phosphorus must have been supplied from the particles in proportions similar to the Redfield ratios, and, since this was not the main source of nitrate, most of the phosphate must have been supplied

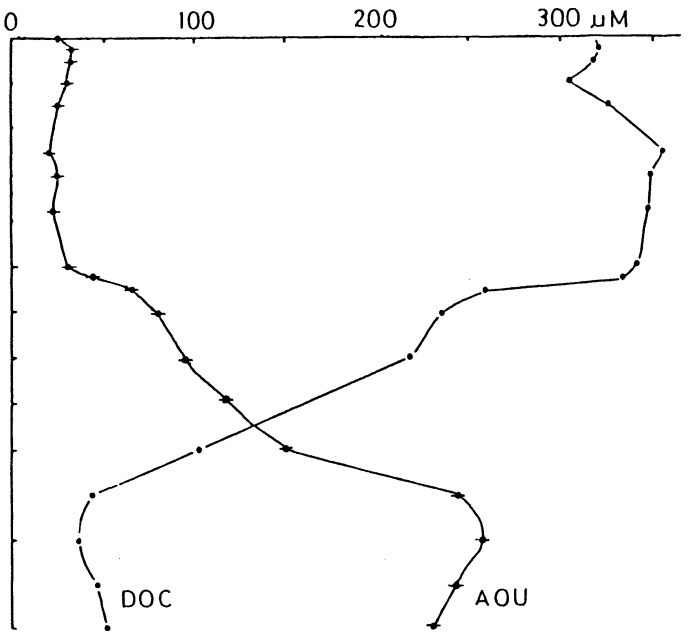

Figure 9.7 Vertical water column profiles of dissolved organic carbon (DOC) and apparent oxygen utilization (AOU) based on 'new' data (after Sugimura & Suzuki 1988: section from western North Pacific). Compare with the DOC profile in Figure 9.6; note the variation in DOC with depth, and the inverse relationship between DOC and AOU.

from a previously unidentified pool of total dissolved phosphate.

It is becoming apparent that the work reported by Sugimura & Suzuki (1988) will have profound implications for chemical oceanography. For example, the featureless nature of the vertical deep water profiles of DOC in the water column, which is now put into question by the new data, was one of the lines of evidence that led to the widely held belief that a large fraction of the oceanic DOC is inert. However, it is unlikely that the full implications of the new DOC data will be fully realized for some time yet.

9.3 The marine organic carbon cycle

The concentrations of both POC and DOC are higher, and more variable, in surface than in deep waters. Deep and surface waters may therefore be considered as two independent organic carbon reservoirs, and a two-box model approach (see Sec. 7.5) can thus be used to elucidate the main features in the marine organic carbon cycle. In order to quantify these features a knowledge of both the sizes of the two reservoirs, and the fluxes of organic carbon through them, is required. The data necessary to

define the marine organic carbon cycle are continually being refined, particularly in the light of the VERTEX programme. However, in order to grasp the fundamentals involved, the data provided by Williams (1975) still offers a useful overview of the inputs, reservoirs and losses of organic carbon within the ocean system. A summary of these data is given in Table 9.2, and the movements of organic carbon between, and within, the reservoirs, are discussed below.

It can be seen from the data in Table 9.2 that the photosynthetic fixation of CO_2 is by far the most important input of organic carbon to the sea. At first sight this may seem surprising since the living biomass makes up only a small portion of the total organic carbon in the oceans. However, most of the photosynthetic organic carbon is recycled in the upper water column (the surface reservoir) by grazing within the food web, and for many years it was thought that the organic carbon cycle in the sea followed reasonably simple pathways, which could be summarized as follows.

(1) Carbon dioxide is fixed by phytoplankton during primary production.
(2) Secondary production, involving the consumption of the phytoplankton by zooplankton, etc., and tertiary production move the fixed CO_2 along the food web.

Table 9.2 Sources, reservoirs and sinks for organic carbon in the oceans[a]

SOURCES	
Annual atmospheric input	2.2×10^{14} g
Annual fluvial input	1.8×10^{14} g
Annual net primary productivity	3.6×10^{16} g
Annual input to dissolved fraction; phytoplankton excretions	3.6×10^{15} g
resistant phytoplankton material	1.8×10^{16} g
RESERVOIRS	
Dissolved organic carbon	1.0×10^{18} g
Particulate organic carbon	3.0×10^{16} g
Plankton	5.0×10^{14} g
SEDIMENT SINKS	
Annual loss to near-shore sediments	2.7×10^{12} g
Annual loss to pelagic sediments	9.2×10^{13} g

[a] After Williams (1975).

(3) The oxidative destruction and remineralization of dead organisms at depth restores CO_2 and nutrients back into the water column, thus closing the cycle.

In fact, the cycle is not fully closed, and some of the organic carbon escapes to be added to both the DOC and POC oceanic pools. This occurs in two principal ways.

(a) Some of the photosynthetically fixed carbon, either as POC (e.g. faecal material, organic debris) or DOC, actually escapes during the tissue destruction and remineralization stage and is transported to deep water; it is this fraction that is replaced by new nutrients (see Sec. 9.1.1).
(b) An additional source to the DOC pool arises from processes such as exudation by phytoplankton, excretion by zooplankton and post-death decay processes (see Sec. 9.2.2).

It was also originally believed that all steps within the oceanic carbon cycle were biologically controlled (Fig. 9.8a), until Wangersky (1972) suggested that several important pathways within it may in fact be controlled by physical or chemical mechanisms. In this context, Williams (1975) examined the processes by which DOM can be lost from sea water and showed that, in addition to biological processes (e.g. utilization by organisms, oxidative destruction), both physicochemical and chemical mechanisms can result in the modification and/or removal of this form of organic carbon. Physicochemical removal, by which DOM is transferred to the particulate or gaseous phase, involves bubble bursting, precipitation–aggregation phenomena and organic matter–mineral adsorption reactions. For example, Kepkay & Johnson (1989) have suggested that coagulation of colloidal DOC on bubble surfaces can make ~ 5–15% of the 'inert' oceanic DOC pool available to biota via microbial respiration. Chemical modifications include those associated with the formation of inert DOM (Gelbstoff) and those resulting from some photochemical reactions. Wangersky (1972) discussed the importance of non-biological factors such as those in DOC $\leftrightarrow$ POC equilbria. Marine bacteria were believed to be the major utilizers of DOC, but since it is now known that at least some DOC can be converted to POC, this means that a fraction of the original DOC will become available to larger organisms. According to Wangersky (1972), the effect of this will be to increase the rate of organic carbon cycling, and also to make the cycle itself more complicated.

On the basis of the then currently new concepts, Wangersky (1972) outlined a revised oceanic organic carbon cycle. This is illustrated in Figure 9.8b, and essentially it involves the recycling of phytoplankton-generated organic carbon within the biological system, from which some

DOC and POC escapes to form, together with externally supplied material, the non-living organic carbon in the surface and deep water reservoirs, which is ultimately incorporated into marine sediments. There are, however, a number of steps in the cycle that are still imperfectly understood, and some of these are discussed below; recently, they have also been investigated as part of the VERTEX programme.

Organic carbon in the deep water reservoir is generally considered to be refractory in nature, i.e. to be resistant to both chemical and biological attack, and is therefore of no use for nutrition. However, there remains considerable speculation regarding the origin of this deep water organic carbon, and over the degree to which it is truly inert. Menzel (1974) suggested that the extent to which phytoplankton are decomposed in the surface region is critical in estimating the magnitude of the input of organic carbon to deep water. Most of the carbon fixed by the phytoplankton is consumed within the food web and much of the ungrazed material, together with the residues from the animal metabolism, undergoes remineralization in the surface waters and so does not escape directly from the euphotic zone in an organic form. However, the remineralization stage leaves behind a refractory residual organic material, and it is this which may then be transferred into the deep water reservoir. There have been various estimates of the amount of refractory organic material produced in the euphotic zone from phytoplankton production. For example, Menzel (1974) assumed that if *all* the phytoplankton (organic C $\sim 20 \times 10^{15}$ g yr^{-1}) are grazed, then $\sim$ 20% of the ingested material will be excreted and so become available for remineralization by bacterial degradation. This degradation was then assigned an 80% efficiency, which would yield $\sim 0.8 \times 10^{15}$ g yr^{-1} of refractory material to be added to the organic carbon pool, i.e. $\sim$ 4% of the total primary production. Of this refractory material $\sim$ 25% is DOM, giving an annual input of 0.27×10^{15} g; and $\sim$ 70% POM, yielding an annual input of 0.60×10^{15} g. Using different data, Williams (1975) arrived at an estimate of 1.8×10^{15} g yr^{-1} for the resistant material added to the DOC pool from phytoplankton. On the basis of his estimates, Menzel (1974) concluded that $\sim$ 3% of the annual phytoplankton production reaches deep-sea sediments in a particulate form; other estimates range from $\sim$ 4% to $\sim$ 12% (see e.g. Trask 1939, Datsko 1959, Bogdanov *et al.* 1971, Suess 1980, Betzer *et al.* 1984, Martin *et al.* 1987). The fate of POC produced photosynthetically in the surface ocean was considered by Martin *et al.* (1987) in terms of recent data generated for the northeast Pacific as part of the VERTEX programme. On the basis of these data, the authors estimated that global ocean primary productivity of C yields $\sim 40 \times 10^{15}$ g yr^{-1}, of which $\sim 6 \times 10^{15}$ g yr^{-1} are removed from the surface ocean via particulate sinking. However, $\sim$ 50% of this carbon is rapidly regenerated in the upper 300 m of the water column,

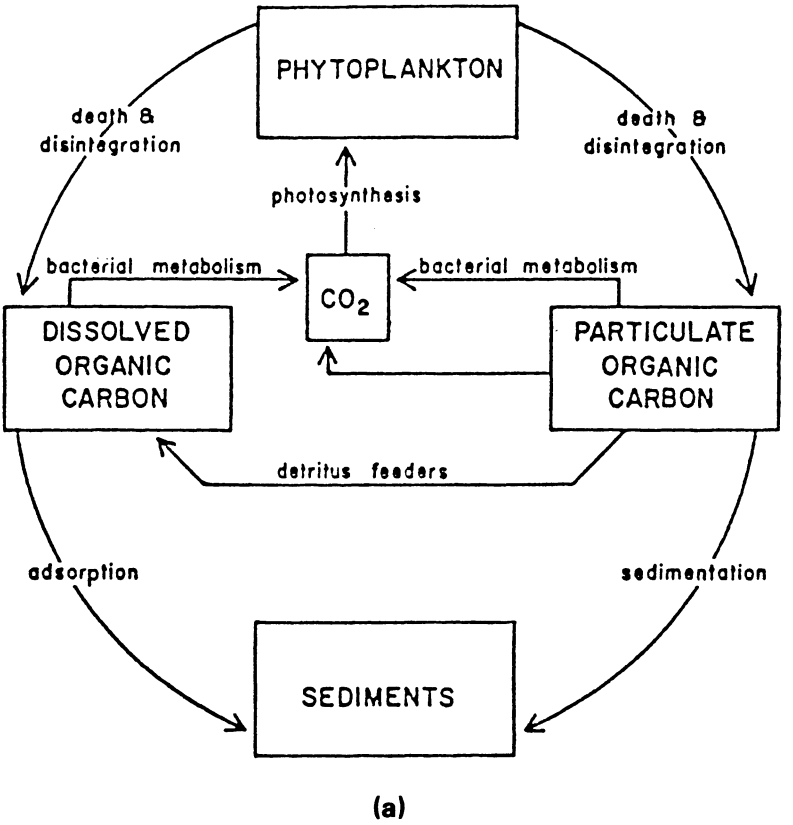

Figure 9.8a The organic carbon cycle in sea water (from Wangersky 1972): the 'old' version.

~ 75% is regenerated by 500 m and ~ 90% by 1500 m; thus, only a very small fraction of the surface-produced POC escapes to deep water. However, the POM that does escape from the surface water becomes incorporated into the global carbon flux, and has a profound importance in marine geochemistry because of the role it plays in driving the down-column transport of both dissolved and particulate material to the sea bed (see Secs. 10.4 & 12.3).

Despite the fact that the concentrations of POC in the surface ocean are considerably more variable than those at depth, variations in the absolute concentrations of POC in deep waters have been reported on both a regional and a seasonal basis. These have been related to a number of factors, some of which are discussed below.

(a) **The advective transport of POC** during the mixing of water masses. The horizontal advective transport of both inorganic and organic

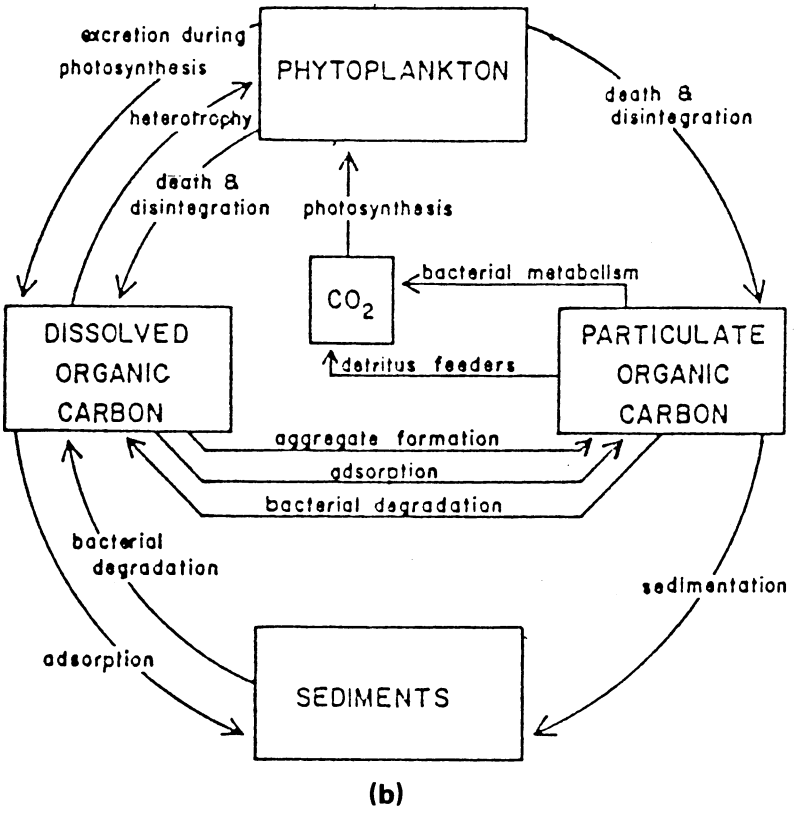

Figure 9.8b The organic carbon cycle in sea water (from Wangersky 1972): the 'new' version.

particulate matter at depth in the water column can affect the particulate fluxes in regions close to the shelf and/or slope areas, or to other particle sources.

(b) **Variations in primary production** in the euphotic zone. Several authors have attempted to model primary production and POC concentrations in open-ocean regions where horizontal particle advection is negligible (see e.g. Eppley & Peterson 1979, Suess 1980, Betzer *et al.* 1984). There is a growing body of evidence to suggest that in these open-ocean regions the concentrations of organic carbon in material that sediments down the water column is positively correlated with surface primary production. As a result, the down-column POC flux tends to vary with primary production; for example, Betzer *et al.* (1984) calculated that the POC flux varies as primary production raised to the power 1.4.

(c) **The *in situ* production of POC** in subsurface waters. Fellows *et al.*

(1981) pointed out that the *in situ* formation of POC at depth in the water column can take place by the action of micro-organisms associated with large sinking particles (see e.g. Karl & Knauer 1984).

It is apparent, therefore, that there are problems in assessing the origin of the POC found in deep waters, and over the past few years it has become evident that some of these problems arose because of the difficulties encountered in the collection of subsurface POC samples. Most of the early work involved the use of bottles to collect relatively small volumes of water for POC analysis. However, the use of large-volume collection techniques, and the deployment of sediment traps, has revealed that large organic particles are present at depth in the water column. These large particles play a significant role in down-column transport processes, and this is considered in detail in Section 10.4; however, it is important to note at this stage that these large organic aggregates, which are composed of faecal material and 'marine snow', are relatively rare and are likely to be missed when only small-volume water samples are collected.

Originally, it was generally accepted that below a transition depth lying between ~ 200 and ~ 500 m there was an overall decrease in POC (and DOC), and that here concentrations were relatively invariant at any given depth. This raised a problem, however, because if the concentrations of POC do not decrease below the transition zone, some mechanism of replenishment must be invoked to maintain an equilibrium between the utilization and accretion of POC, since organisms that require a supply of food reside and metabolize at all water depths. One of the theories proposed to explain this POC replenishment preceded the sediment trap era. In this theory, Packard (1969) suggested that the supply of POC to the food web is significantly different in surface and deep waters and he proposed that in the euphotic environment POC is supplied mainly in the form of moribund phytoplankton, whereas in deep waters the supply is largely via faecal pellets and other large-sized organic debris. Menzel (1974) also concluded that it is these faecal-type aggregates that will be consumed by deep water organisms, and that because of their rarity they will not be included in the POC concentrations listed in most studies reported in the literature. This has subsequently become apparent from sediment trap data, which has shown that around 95% of the down-column flux of POC can be associated with large faecal-type aggregates, although they account for only about 5% of the total POC present. It is probable, therefore, that there are at least two fractions of POC in deep ocean water.

(a) **A large-sized fraction**, consisting of faecal material and other organic

debris, which can be utilized in the food web and is responsible for a continuous POC flux from the surface to bottom sediments.

(b) **A small-sized fraction**, consisting of residual refractory organic matter produced in surface waters, which has a homogeneous distribution in the water column below the transition depth.

The role of the large-sized aggregates is therefore critical to an understanding of the vertical distribution of POC in the water column. The small-sized POC may have relatively invariant concentrations at depths in the water column below the transition zone. However, the vertical flux of POC, which is associated mainly with the large-sized aggregates, appears to exhibit a non-linear decrease with increasing depth (Suess 1980). Most sinking particles appear to be degraded predominantly (> 70%) in the upper ~ 1000 m of the water column, and the decrease in deeper water is relatively small, probably being less than a factor of 2 (Jahnke & Jackson 1987). However, the fact that the decrease occurs at all leads to the implications that during its passage to the sea floor the POC does undergo decomposition, fragmentation, solubilization and utilization in the food web. The sinking POM particles contain micro-organisms, and microbial decomposition via ambient bacteria has been considered to be an important mechanism controlling the POM down-column flux. However, in a recent paper Karl *et al.* (1988) disputed this, and suggested that the POM particles are, in fact, poor habitats for bacterial growth, and that the particle decomposition is carried out by microbial populations that are either free-living in the water column or are attached to suspended non-sinking particles (see also Cho & Azam 1988).

Menzel (1974) used his estimate of the amount of residual refractory organic matter produced in the surface waters to calculate the turnover time of organic matter in the oceans. Assuming an oceanic average value of 0.5 mg l^{-1} for DOC and 10 μg l^{-1} for POC in the deep water reservoir, he computed a deep water burden of 665×10^{15} g for DOC and 14×10^{15} g for POC. The input of refractory DOC to deep waters from the surface was estimated to be ~ 0.2×10^{15} g yr^{-1} (see above), which yields a turnover time of ~ 3300 yr for the refractory DOC. A number of workers have carried out ^{14}C age determinations on the DOC in the oceanic deep water layer, the most widely quoted value being that of 3500 yr given by Williams *et al.* (1969). However, some more recent values suggest that the DOC is older than this; for example, Williams & Druffel (1987) assigned an apparent age of ~ 6000 yr for deep water DOM. the age of ~ 3500 yr proposed by Williams *et al.* (1969) is very close to the value predicted by Menzel (1974) for the DOC turnover time, and, since both are greater than the mixing time of the oceans (~ 1600 yr), it would appear that the bulk of the refractory DOC is recycled several times

before being deposited in sediments. However, Dawson & Duursma (1981) pointed out that the dating gives an *average* age for unfractionated deep water DOC, and since the molecular components of DOC are diverse, and possess different origins and reactivities, it is unlikely that they are all of the same age. It may be, therefore, that some of the DOC is in fact very old and that the rest undergoes a relatively rapid oceanic turnover (see also Mantoura & Woodward 1983).

There are conflicting theories over the fate of DOC in sea water. Williams (1971) considered the relationship between the concentrations of dissolved oxygen and DOC in the region of the oxygen minima at two Pacific Ocean locations. He concluded that if the DOC was utilized by organisms over short time periods, or underwent chemical oxidation, the dissolved oxygen would all be consumed, and that if this happened on a global basis large sections of the deep oceans would become anoxic. In fact, most of the deep ocean is aerobic, which raises the question of the extent to which DOC is decomposed below the euphotic zone. In this context, Menzel & Ryther (1970) have suggested that the decomposition of DOC, and the utilization of dissolved oxygen, occur mainly in the euphotic zone. On the basis of salinity–dissolved O_2 correlations they further argued that oxygen minima are only formed in some restricted areas, such as those where upwelling takes place, and that after sinking the lateral distributions of the minima are controlled by water mass mixing. In this model, it is envisaged that the mixing takes place between waters having similar carbon, but different dissolved oxygen, concentrations, and that the DOC does not undergo decomposition in the deeper waters. In contrast, Craig (1969, 1971a, b) examined the depth distribution of the CO_2–^{14}C–^{13}C–O_2–alkalinity system in terms of a vertical advection–diffusion model, and suggested that part of the increase in the CO_2 in deep water results from an *in situ* oxidation of DOC. However, Menzel (1974) put forward a number of arguments to support the concept that the respiratory requirements of zooplankton and microplankton are sufficient to explain the measured rates of O_2 consumption in deep waters, and that it is not necessary to invoke the decomposition of DOC at these depths. The new DOC concentration data provided by Sugimura & Suzuki (1988) may help to resolve the arguments since the oceanic profiles generated by these authors showed an inverse correlation between DOC and AOU, which was interpreted as evidence for the *in situ* consumption of oxygen in subsurface water via the oxidation of DOC (see Sec. 9.2.4.2). However, until more new DOC data are reported, the situation regarding the decomposition of DOC at depth in the water column must remain unresolved.

It may be concluded that the organic carbon cycle in the oceans is complex and is not yet fully understood. Nonetheless, the cycle proposed by Wangersky (1972) still provides a useful working model to describe the

movement of organic carbon within the oceans. The principal feature in the cycle is the photosynthetic production of organic carbon in surface waters and its recycling at depth. This biologically mediated loop in the recycling of organic carbon in surface ocean waters is intimately related to the fate of the nutrient elements and involves the internal oceanic formation, and subsequent decomposition, of organic particulate matter. However, the loop is not 100% efficient, and a small fraction, perhaps $< 5\%$, of the POC formed in the surface layers escapes to deep water in the form of large-sized faecal debris and 'marine snow'. The large-sized organic aggregates are the principal driving force behind the **global carbon flux**. They also act as carrier phases for trace elements that have been removed from solution, and their down-column transport provides a mechanism for the delivery of particulate-associated constituents to the surface of the sediment reservoir. This mechanism operates on an ocean-wide scale, and it is now recognized that the operation of the global carbon flux is one of the major processes controlling both the throughput of material in the ocean system and the trace element composition of sea water.

9.4 Organic matter in the oceans: summary

(a) Organic carbon in the oceans consists of a particulate phase (POC), which makes up $\sim 20\%$ of the total organic carbon (TOC), and a dissolved phase (DOC), which constitutes $\sim 80\%$ of the TOC.
(b) The POC and DOC pools receive contributions from both internal (autochthonous) and external (allochthonous) sources.
(c) The allochthonous (terrestrial) POC transported to the oceans is mainly confined to coastal environments, and according to Parsons (1975) it may be assumed that the POC in open-ocean areas is largely autochthonous in origin. There is, however, some dispute over the origin of oceanic DOC.
(d) The principal feature in the vertical distributions of POC and DOC is that the concentrations of both components are higher, and more variable, in surface than in deep ocean waters.
(e) There is an organic carbon cycle in the oceans. Essentially, this involves the recycling of phytoplankton-generated organic carbon within the biological system, mainly in the mixed layer, from which some DOC and POC escapes by a variety of both biological and non-biological mechanisms. The POC that is exported from the mixed layer makes up $\sim 5\%$ of the photosynthetically generated carbon and is transported down the water column as the global carbon flux.

Particulate matter plays a critical role in marine geochemistry, in

removing and transporting dissolved elements, especially trace elements, via this global carbon flux. However, the total suspended matter (TSM) in sea water does not consist only of organic material, and, before reviewing the factors that control the distributions of trace elements in sea water, the overall nature of this TSM will be described in the following chapter.

References

Armstrong, F.A.J. 1965. Silicon. In *Chemical oceanography*, 1st edn, J.P. Riley & G. Skirrow (eds), Vol. 1, 409–32. London: Academic Press.

Betzer, P.R., W.J. Showers, E.A. Laws, C.D. Winn, G.R. Du Tullio & P.M. Kroopnick 1984. Primary productivity and particle fluxes on a transect of the equator at 153°W in the Pacific Ocean. *Deep-Sea Res.* **31,** 1–11.

Biggs, D.G., A.F. Amos & O. Holm-Hanson 1985. Oceanographic studies of epi-pelagic ammonium distributions: the Ross Sea ammonium flux experiment. In *Antarctic nutrient cycles, food webs*, SCAR Symp. Antarct. Biol., W.R. Seigfried, P.R. Condy & R.M. Laws (eds), 93–103. Berlin: Springer-Verlag.

Blumer, M. 1970. Dissolved organic carbon compounds in sea water: saturated and olefinic hydrocarbons and singly branched fatty acids. In *Organic matter in natural waters*, Inst. Mar. Sci. Alaska, Occas. Publ., no. 1, D.W. Hood (ed.), 153–67.

Boehm, P.D. 1980. Evidence for the decoupling of dissolved, particulate and surface microlayer hydrocarbons in northwestern Atlantic continental shelf waters. *Mar. Chem.* **9,** 255–81.

Bogdanov, Y.S., A.P. Lisitsyn & Y.A. Romankwich 1971. Organic matter in suspensions and bottom sediments of seas and oceans. In *Organic matter in recent and fossil sediments.* Moscow: Nauka.

Broecker, W.S. 1974. *Chemical oceanography.* New York: Harcourt Brace Jovanovich.

Broecker, W.S. & T.-H. Peng 1982. *Tracers in the sea.* Palisades, NY: Lamont-Doherty Geological Observatory.

Bruland, K.W. 1980. Oceanographic distributions of cadmium, zinc, nickel, and copper in the North Pacific. *Earth Planet. Sci. Lett.* **47,** 176–98.

Cauwet, G. 1981. Non-living particulate matter. In *Marine organic chemistry*, E.K. Duursma & R. Dawson (eds), 71–89. Amsterdam: Elsevier.

Cho, B.C. & F. Azam 1988. Major role of bacteria in biogeochemical fluxes in the ocean's interior. *Nature* **332,** 441–3.

Craig, H. 1969. Abyssal carbon and radiocarbon in the Pacific. *J. Geophys. Res.* **74,** 5491–506.

Craig, H. 1971a. The deep metabolism: oxygen consumption in abyssal ocean water. *J. Geophys. Res.* **76,** 5078–86.

Craig, H. 1971b. Son of abyssal carbon. *J. Geophys. Res.* **76,** 5133–9.

Datsko, V.G. 1959. *Organic matter in the southern seas of the USSR.* Izd. Akad. Nauk SSSR.

Dawson, R. & E.K. Duursma 1981. State of the art. In *Marine organic chemistry*, E.K. Duursma & R. Dawson (eds), 497–512. Amsterdam: Elsevier.

Degens, E.T. & K. Mopper 1976. Factors controlling the distribution and early diagenesis of organic matter in marine sediments. In *Chemical oceanography*, Vol. 5, J.P. Riley &

R. Chester (eds), 59–113. London: Academic Press.
De Vooys, C.G.N. 1979. Primary production in aquatic environments. In *The global carbon cycle*, SCOPE 13, 259–92. Chichester: Wiley.
Duce, R.A. 1986. The impact of atmospheric nitrogen, phosphorus, and iron species on marine biological productivity. In *The role of air–sea exchange in geochemical cycling*, P. Buat-Menard (ed.) 497–529. Dordrecht: Reidel.
Dugdale, R.C. & J.J. Goering 1967. Uptake of new and regenerated forms of nitrogen in primary productivity. *Limnol. Oceanogr.* **12,** 196–206.

Eadie, B.J., L.M. Jeffrey & W.M. Sackett 1978. Some observations on the stable carbon isotope composition of dissolved and particulate organic carbon in the marine environement. *Geochim. Cosmochim. Acta* **42,** 1265–9.
Eglinton, G. & R.J. Hamilton 1963. The distribution of alkanes. In *Chemical plant taxonomy*, T. Swain (ed.), 187–218. New York: Academic Press.
Ehrhardt, M., C. Osterroht & G. Petrick 1980. Fatty-acid methyl esters dissolved in seawater and associated with suspended particulate material. *Mar. Chem.* **10,** 67–76.
Eppley, R.W. & B.J. Peterson 1979. Particulate organic matter flux and planktonic new production in the deep ocean. *Nature* **282,** 677–80.

Fellows, D.A., D.M. Karl & G.A. Knauer 1981. Large particle fluxes and the vertical transport of living carbon in the upper 1500 m of the northeast Pacific ocean. *Deep-Sea Res.* **28,** 921–36.
Fenical, W. 1981. Natural halogenated organics. In *Marine organic chemistry*, E.K. Duursma & R. Dawson (eds), 375–93. Amsterdam: Elsevier.
French, D., M.J. Furnas & T.J. Smayda 1983. Diet changes in nitrite concentration in the chlorophyll maximum in the Gulf of Mexico. *Deep-Sea Res.* **30,** 707–22.

Gagosian, R.B. & C. Lee 1981. Processes controlling the distribution of biogenic organic compounds in seawater. In *Marine organic chemistry*, E.K. Duursma & R. Dawson (eds), 91–123. Amsterdam: Elsevier.

Jackson, G.A. 1988. Implications of high dissolved organic matter concentrations for oceanic properties and processes. *Oceanography* November, 621–3.
Jackson, G.A. & P.M. Williams 1985. Importance of dissolved organic nitrogen and phosphorus to biological nutrient cycling. *Deep-Sea Res.* **32,** 223–35.
Jahnke, R.A. & G.A. Jackson 1987. Role of sea floor organisms in oxygen consumption in the deep North Pacific Ocean. *Nature* **329,** 621–3.
Jenkins, W.J. & J.C. Goldman 1985. Seasonal oxygen cycling and primary production in the Sargasso Sea. *J. Mar. Res.* **43,** 465–91.

Kakanazawa, A. & S. Teshima 1971. *In vivo* conversion of cholesterol to steroid hormones in the spiny lobster, *Panulirus japonica. Bull. Japan. Soc. Fish.* **27,** 207–12.
Kamykowski, D. & S.-J. Zentara 1986. Predicting plant nutrient concentrations from temperature and sigma-*t* in the upper kilometer of the world ocean. *Deep-Sea Res.* **33,** 89–105.
Karl, D.M. & G.A. Knauer 1984. Vertical distribution, transport, and exchange of carbon in the northeast Pacific Ocean: evidence for multiple zones of biological activity. *Deep-Sea Res.* **31,** 221–43.
Karl, D.A., G.A. Knauer & J.H. Martin 1988. Downward flux of particulate organic matter in the ocean: a particle decomposition paradox. *Nature* **332,** 438–41.
Kattner, G., G. Gercken & K.D. Hammer 1983. Development of lipids during a spring plankton bloom in the northern North Sea. *Mar. Chem* **14,** 163–73.

Kawase, M. & J.L. Sarmiento 1985. Nutrients in the Atlantic thermocline. *J. Geophys. Res.* **90,** 8961–79.

Kennicutt, M.C. & L.M. Jeffrey 1981. Chemical and CG–MS characterization of marine dissolved lipids. *Mar. Chem.* **10,** 367–87.

Kepkay, P.E. & B.D. Johnson 1989. Coagulation on bubbles allows microbial respiration of oceanic dissolved organic carbon. *Nature* **338,** 63–5.

Klein, P. & B. Coste 1984. Effects of wind stress variability on nutrient transport into the mixed layer. *Deep-Sea Res.* **31,** 21–37.

Koblentz-Mishk, O.J., V.V. Volkovinsky & Y.G. Kabanova 1970. Plankton primary production of the world ocean. In *Scientific exploration of the South Pacific*, W.S. Wooster (ed.), 183–93. Washington DC: National Academy of Science.

Lee, C. & J.L. Bada 1977. Dissolved amino acids in the equatorial Pacific, Sargasso Sea and Biscayne Bay. *Limnol. Oceanogr.* **22,** 502–10.

Liebeziet, G., M. Bolter, I.F. Brown & R. Dawson 1980. Dissolved free amino acids and carbohydrates at pycnocline boundaries in the Sargasso Sea and related microbial activity. *Oceanol. Acta* **3,** 357–62.

Mackinnon, M.D. 1981. The measurement of organic carbon in sea water. In *Marine organic chemistry*, E.K. Duursma & R. Dawson (eds), 415–43. Amsterdam: Elsevier.

Mantoura, R.F.C. & E.M.S. Woodward 1983. Conservative behaviour of riverine dissolved organic carbon in the Severn Estuary: chemical and geochemical implications. *Geochim. Cosmochim. Acta* **47,** 1293–309.

Martin, J.H., G.A. Knauer, D.M. Karl & W.W. Broenkow 1987. VERTEX: carbon cycling in the northeast Pacific. *Deep-Sea Res.* **34,** 267–85.

Menzel, D.W. 1974. Primary productivity, dissolved and particulate organic matter and the sites of oxidation of organic matter. In *The sea*, E.D. Goldberg (ed.), Vol. 5, 659–78. New York: Wiley.

Menzel, D.W. & J.H. Ryther 1970. *Distribution and cycling of organic matter in natural waters.* Inst. Mar. Sci. Alaska, Occ. Publ. No. 1: 31–54.

Meyers-Schulte, K.J. & J.I. Hedges 1986. Molecular evidence for a terrestrial component of organic matter dissolved in ocean water. *Nature* **321,** 61–3.

Neinhuis, P.H. 1981. Distribution of organic matter in living marine organisms. In *Marine organic chemistry*, E.K. Duursma & R. Dawson (eds), 31–69. Amsterdam: Elsevier.

Ogura, N. 1977. High molecular weight organic matter in sea water. *Mar. Chem.* **5,** 535–49.

Packard, T.T. 1969. The estimation of the oxygen utilization rate in seawater from the activity of the respiratory electron transport system in plankton. *Ph.D. Thesis*, University of Washington, Seattle.

Parrish, C.C. 1988. Dissolved and particulate marine lipid classes: a review. *Mar. Chem.* **23,** 17–40.

Parrish, C.C. & P.J. Wangersky 1988. Iatroscan-measured profiles of dissolved and particulate marine lipid classes over the Scotian Slope and in Bedford Basin. *Mar. Chem.* **23,** 1–15.

Parsons, T.R. 1975. Particulate organic carbon in the sea. In *Chemical oceanography*, J.P. Riley & G. Skirrow (eds), Vol. 2, 365–83. London: Academic Press.

Redfield, A.C. 1934. On the proportions of organic derivatives in sea water and their relation to the composition of plankton. In *James Johnstone memorial volume*, 177–92. Liverpool University Press.

Redfield, A.C. 1958. The biological control of chemical factors in the environment. *Am. J. Sci.* **46,** 205–21.

Saliot, A. 1981. Natural hydrocarbons in sea water. In *Marine organic chemistry*, E.K. Duursma & R. Dawson (eds), 327–74. Amsterdam: Elsevier.

Sharp, J.H. 1983. The distributions of inorganic nitrogen and dissolved and particulate organic nitrogen in the sea. In *Nitrogen in the marine environment*, E.J. Carpenter & D.G. Capone (eds), 1–35. New York: Academic Press.

Siegenthaler, U. & T. Wenk 1984. Rapid atmosphere CO_2 variations and ocean circulation. *Nature* **308,** 624–6.

Skopintsev, B.A. 1981. Decomposition of organic matter of plankton, humification and hydrolysis. In *Marine organic chemistry*, E.K. Duursma & R. Dawson (eds), 125–77. Amsterdam: Elsevier.

Spencer, C.P. 1975. The micronutrient elements. In *Chemical oceanography*, J.P. Riley & G. Skirrow (eds), Vol. 2, 245–300. London: Academic Press.

Steeman Neilson, E. 1952. The use of radio-active carbon (C^{14}) for measuring organic production in the sea. *J. Cons. Int. Explor. Mer.* **18,** 117–40.

Strickland, J.D.H. 1965. Production of organic matter in the primary stages of the marine food chain. In *Chemical oceanography*, 1st edn, J.P. Riley & G. Skirrow (eds), Vol. 1, 477–610. London: Academic Press.

Suess, E. 1980. Particulate organic carbon flux in the oceans–surface productivity and oxygen utilization. *Nature* **288,** 260–3.

Sugimura, Y. & Y. Suzuki 1988. A high temperature catalytic oxidation method for the determination of non-volatile dissolved organic carbon in seawater by direct injection of a liquid sample. *Mar. Chem.* **24,** 105–31.

Sugugawa, H., N. Handa & K. Ohta 1985. Isolation and characterization of low molecular weight carbohydrates dissolved in seawater. *Mar. Chem.* **17,** 341–62.

Sverdrup, H.U., M.W. Johnson & R.H. Fleming 1942. *The oceans*. New York: Prentice Hall.

Takahasi, T., W.S. Broecker & S. Langer 1985. Redfield ratio based on chemical data from isopycnal surfaces. *J. Geophys. Res.* **90,** 6907–24.

Tissot, B.P. & D.H. Welte 1984. *Petroleum formation and occurrence.* Berlin: Springer-Verlag.

Traganza, E.D., V.M. Silva, D.M. Austin, W.L. Hanson & S.H. Bronsink 1983. Nutrient mapping and recurrence of coastal upwelling centres by satellite remote sensing: its implication to primary production and the sediment record. In *Coastal upwelling*, E. Suess & J. Thiede (eds), 61–83. New York: Plenum.

Trask, P. 1939. Organic content of recent marine sediments. In *Recent marine sediments*, P. Trask (ed.), 428–53. Tulsa, Okla.: American Association of Petroleum Geologists.

Tsuchiya, M. 1985. The subthermocline phosphate distribution and circulation in the far eastern equatorial Pacific Ocean. *Deep-Sea Res.* **32,** 299–313.

Walsh, G.E. & J. Douglass 1966. Vertical distribution of dissolved carbohydrate in the Sargasso Sea off Bermuda. *Limnol. Oceanogr.* **11,** 406–8.

Wangersky, P.J. 1972. The cycle of organic carbon in sea water. *Chima* **26,** 559–64.

Watson, A.J. & M. Whitfield 1985. Composition of particles in the global ocean. *Deep-Sea Res.* **32,** 1023–39.

Williams, P.J. 1975. Biological and chemical aspects of dissolved organic material in sea water. In *Chemical oceanography*, J.P. Riley & G. Skirrow (eds), Vol. 2, 301–63. London: Academic Press.

Williams, P.J. & L.I. Gordon 1970. Carbon-13 : carbon-12 ratios in dissolved and

particulate organic matter in the sea. *Deep-Sea Res.* **17,** 19–27.
Williams, P.M. 1971. The distribution and cycling of organic matter in the ocean. In *Organic compounds in aquatic environments*, S.D. Faust & J.V. Hunter (eds), 145–63. New York: Marcel Dekker.
Williams, P.M. & E.R.M. Druffel 1987. Radiocarbon in dissolved organic matter in the central North Pacific Ocean. *Nature* **330,** 246–8.
Williams, P.M., H. Oeschger & P. Kinney 1969. Natural radiocarbon activity of dissolved organic carbon in the North-East Pacific Ocean. *Nature* **224,** 256–9.

Zafiriou, O.C. 1983. Natural water photochemistry. In *Chemical oceanography*, J.P. Riley & R. Chester (eds), Vol. 8, 339–79. London: Academic Press.
Zafiriou, O.C. 1986. Atmospheric, oceanic, and interfacial photochemistry as factors influencing air–sea exchange fluxes and processes. In *The role of air–sea exchange in geochemical cycling*, P. Buat-Menard (ed.), 185–207. Dordrecht: Reidel.

10 Particulate material in the oceans

Lal (1977) estimated that the total mass of suspended material in the oceans is $\sim 10^{16}$ g, which is equivalent to an average seawater concentration of only $\sim$ 10–20 ng l^{-1}. This suspended material moves through the ocean system, but the journey it undertakes is a dynamic one and its concentration and composition are subject to continuous change as a result of processes such as aggregation, disaggregation, zooplankton scavenging, decomposition and dissolution (Gardner *et al.* 1985). As it undertakes this journey, the particle microcosm plays a vital role in regulating the chemical composition of sea water via the removal of dissolved constituents (e.g. trace elements) from solution and their down-column and lateral transport to bottom sediment sink. Indeed, such is the extent to which the behaviour of dissolved trace metals is dominated by suspended solids that Turekian (1977) referred to the phenomenon as the *great particle conspiracy*. Here, then, perhaps lies the key to Forchammer's (1865) 'facility with which the elements in sea water are made insoluble'. In the present chapter attention will be paid to the sources, distribution and composition of the *total suspended material* (TSM) in the sea, and in following this route an attempt will be made to decipher the role that the TSM plays in the major oceanic biogeochemical cycles.

10.1 The measurement and collection of oceanic total suspended matter

A number of techniques have been employed to measure the concentrations of TSM in sea water. Some of these are indirect, i.e. the concentrations of TSM are measured *in situ* in the water column, but no actual samples are collected; these techniques include those based on optical phenomena, such as light absorption (transmissometry) and light scattering (nephelometry). Other techniques involve the direct collection, and subsequent analysis, of samples of TSM, e.g. by filtration or centrifugation. In addition, one of the most important recent advances in the direct collection of TSM has come through the introduction of the sediment trap, a device that collects material as it sinks down the water column. An important advantage of this type of device is that it can retain the large-sized, relatively rare, particles that dominate the vertical TSM flux.

10.2 The distribution of total suspended matter in the oceans

Jerlov (1953) employed light scattering measurements to make one of the first major surveys of oceanic TSM. From the data obtained he was able to identify a number of overall trends in the distribution of the TSM, including the recognition of what were subsequently termed **nepheloid layers**; i.e. layers of relatively turbid water that can extend hundreds of metres above the sea bed. This work was followed by a series of investigations made by Russian scientists in the 1950s, and the results of these have been summarized by Lisitzin (1972). The next principal development came in the 1960s from work carried out by American groups, mainly at the Lamont-Doherty Geological Observatory, who used optical methods to study the oceanic distribution of TSM. One of the major findings to emerge from this work was the confirmation of the presence of the nepheloid layers in many regions of the World Ocean (see e.g. Ewing & Thorndike 1965, Eittreim *et al.* 1976, Connary & Ewing 1972). The most recent studies on the global distribution of oceanic TSM have been carried out as part of the GEOSECS and HEBBLE programmes, and down-column TSM fluxes, which have been measured by the deployment of sediment traps in many locations, are currently being assessed on an ocean-wide scale in the GOFS and VERTEX programmes.

Much of the indirect data on the distribution of oceanic TSM were obtained in the form of optical parameters. Subsequently, however, Biscaye & Eittreim (1977) converted nephelometer data from the Atlantic Ocean water into units of absolute TSM concentrations. In this way, they were able to identify a number of distinctive features in the vertical and horizontal distributions of TSM in the water column, and these are illustrated in Figure 10.1 in the form of a generalized vertical profile. From this figure it can be seen that the distribution of oceanic TSM can be described in terms of a **three-layer model** in which the main features are (a) a surface water layer, (b) a clear water minimum layer and (c) a deep water layer. This three-layer model offers a convenient framework within which to describe the distribution of TSM in the World Ocean.

10.2.1 The surface water layer

In surface waters, TSM concentrations are higher, and more variable, in coastal and estuarine regions than they are in the open ocean. This results largely from the combined effects of (a) an input of externally produced particulates via river run-off and atmospheric transport and (b) the internal generation of particulates from primary production, both of which have their strongest signals in coastal waters.

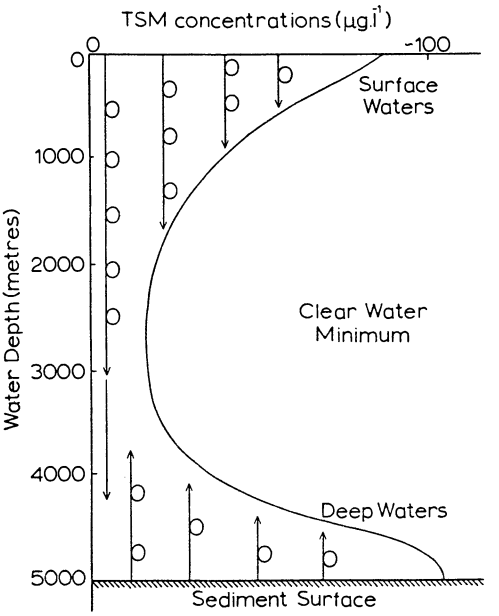

Figure 10.1 Typical oceanic TSM profile for a water column with a well developed nepheloid layer (from Chester 1982b, after Biscaye & Eittreim 1977). The curlicue arrows indicate that vertical particle settling can be affected by horizontal advective processes.

(a) Although on a global scale ~ 90% of river suspended material (RSM) is retained in estuaries (see Sec. 3.2.7), the material that does escape has a higher concentration in coastal waters. Further, some estuaries can transport **plumes** of suspended material for considerable distances out to sea in the surface water layer. For example, Gibbs (1974) reported that in periods of high discharge suspended material transported by the Amazon formed a plume, in which concentrations of TSM could exceed 5000 $\mu g l^{-1}$, extending seawards as far as ~ 100 km.

(b) Particulate organic material, including both living and dead fractions, makes up a major proportion of TSM in many surface waters of the oceans, and most of it results from the photosynthetic fixation of CO_2 during primary production. The principal features in the global distribution of this production are the 'ring' of high-fertility zones around the edges of the ocean basins, and the generally low fertility

in the central gyres, which leads to enhanced concentrations in coastal surface waters (see Sec. 9.2.2.2).

In these regions, however, the actual concentrations of TSM exhibit large temporal and spatial variations. For example, Chester & Stoner (1972) reported a range of < 100 to > 3000 $\mu g\ l^{-1}$ of TSM in a variety of coastal waters from the World Ocean. Away from the coastal regions, the lowest TSM concentrations are found in open-ocean areas of low productivity (oligotrophic zones), especially at the centres of the central gyre systems, where they can fall to values as low as < 10 $\mu g\ l^{-1}$. There are also inter-oceanic variations in the concentrations of TSM in the mixed layer. For example, Chester & Stoner (1972) reported an average TSM concentration of ~ 75 $\mu g\ l^{-1}$ for open-ocean surface waters of the Atlantic and Indian Oceans, and according to Lal (1977) concentrations in the Pacific are about two or three times lower than this.

10.2.2 The clear water minimum

This was the term used by Biscaye and Eittreim (1977) to describe the subsurface region in which there is a decrease in the concentrations of TSM. The decrease is caused by the destruction of particulate material as it sinks from surface waters, or is moved out by advective processes, and the depth at which the minimum is reached varies from one area of the ocean to another. The decrease in particulate concentrations with depth is largely due to processes that affect the organic matter (oxidative destruction) and shell fractions (dissolution) of the TSM. The overall result of these processes is a decrease in the concentrations of TSM with depth below the surface. Apart from the fact that the concentrations are lower, however, the distribution of TSM around the clear water minimum parallels that in surface waters. Thus, TSM concentrations at the clear water minimum represent the particle contribution resulting from the downward transport of material from surface waters and therefore reflect a balance between surface primary production, variable rates of particle setting and down-column particle destruction–dissolution processes. The distribution of TSM at the clear water minimum in the Atlantic Ocean is illustrated in Figure 10.2a.

10.2.3 The deep water layer

If the sinking of particulate matter from the surface reservoir were the only source of TSM to deep waters, then the concentrations of TSM would be expected to continue to fall all the way down the water column as the destructive processes continued, and the clear water minimum would not be developed. In fact, it is now known that in many oceanic areas there is an increase in TSM concentrations below the minimum, and this therefore requires an additional (i.e. non-surface water) source of

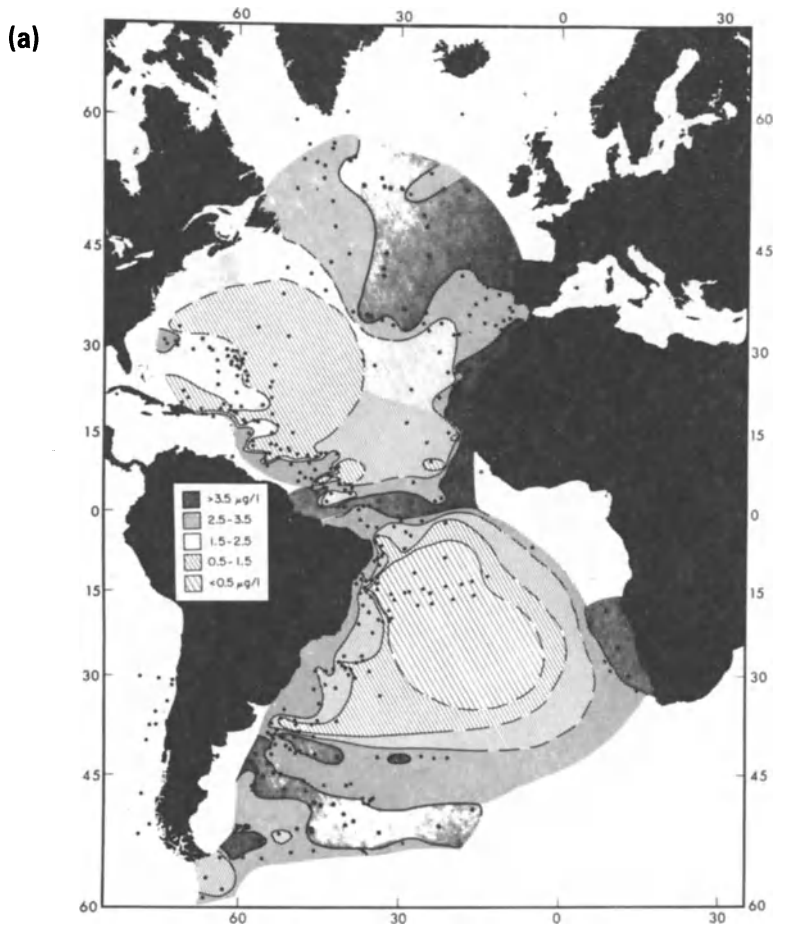

Figure 10.2 Distribution of TSM in the Atlantic Ocean (from Biscaye & Eittreim 1977). (**a**) Concentration of TSM at the clear water minimum.

particulate matter. Much of this additional source comes from the resuspension of bottom sediments into turbid nepheloid layers. In these layers the concentration of particles decreases upwards away from the sediment source, to fall away completely at the clear water minimum. However, even in deep waters there is a contribution to the TSM from particles sinking through the minimum. In order, therefore, to assess the spatial distribution of material in the nepheloid layers, Biscaye & Eittreim (1977) identified two particle popualtions below the clear water minimum.

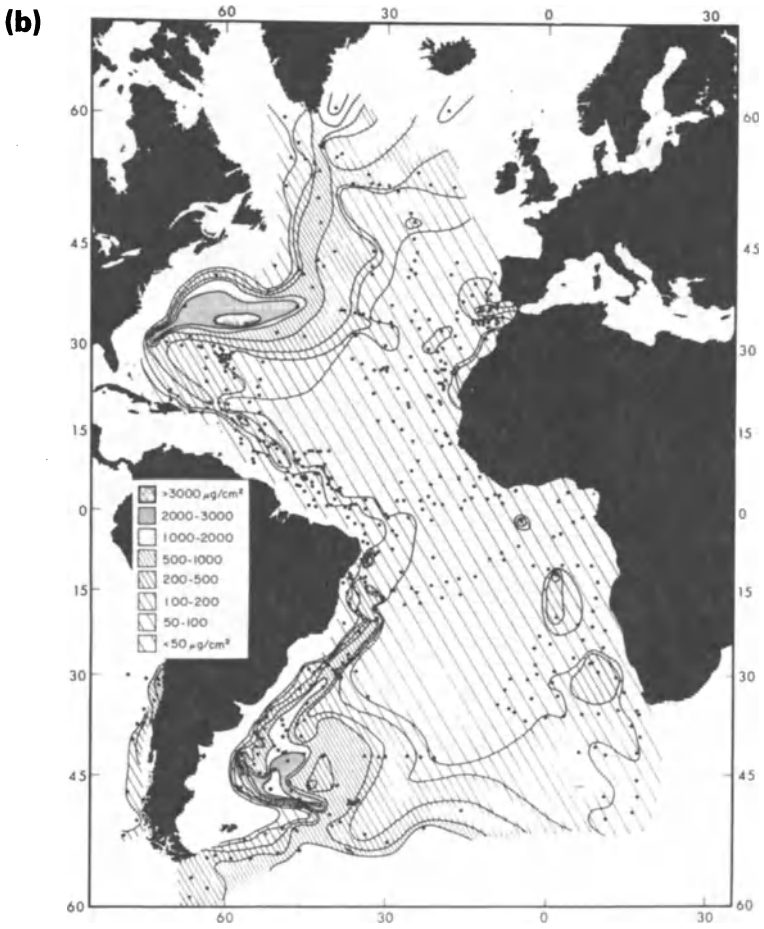

Figure 10.2b Net particulate standing crop in the deep water.

THE GROSS PARTICULATE STANDING CROP This was identified as the total TSM below the clear water minimum. There are two main features in the distribution of the gross particulate standing crop.

(a) Relatively low concentrations are found in the central portions of both the North and South Atlantic, reflecting the low surface water TSM concentrations in the main gyres.
(b) The concentrations in the western Atlantic basins are higher than those in the eastern basins, sometimes by as much as an order of

magnitude. In the western basins, the maximum TSM concentrations are coincident with the axes of the deep water boundary currents (see Sec. 7.3.3).

The distribution of the gross particulate standing crop therefore reflects the effects of two different kinds of processes, those which control the surface water distribution of TSM and those which regulate the additional supply of particulates necessary to sustain the three-layer water column model.

THE NET PARTICULATE STANDING CROP This was defined as the amount of TSM below the clear water minimum that is in excess of the clear water concentration itself. Thus, the authors were able to obtain a much clearer assessment of the deep water, or abyssal, particulate signal by excluding 'noise' from the surface-derived source. The distribution of the net particulate standing crop in Atlantic deep waters is illustrated in Figure 10.2b. On the basis of these data Biscaye & Eittreim (1977) concluded that the abyssal signal results from processes that raise particles into near-bottom waters and maintain them in suspension. These processes include supply from the continental shelves by turbidity currents and advective transport, and the direct resuspension of sediment by bottom currents. It was shown in Section 7.3.3 that a characteristic feature of deep water circulation is the existence of strong boundary currents on the western sides of the oceans, and it is these erosive boundary currents which are the most effective agents in sediment resuspension, and thus in the formation of nepheloid layers; these layers have particle concentrations that are usually in the range $\sim$ 200–500 $\mu g\ l^{-1}$. However, one problem associated with the development of nepheloid layers has been that currents with enough energy to erode the bottom, and to maintain the particles in suspension, have not been found concurrently with high concentrations of particles in the layers themselves. It has been known for some time that bottom current velocities can vary, and can include local episodes of high-speed currents. Further, data obtained from the High Energy Benthic Boundary Layer Experiment (HEBBLE) have shown that there is a high temporal and spatial variability in nepheloid layer particle concentrations, leading to the inference that strong episodic sediment-modifying events, or 'storms', have occurred on the sea bed. Such deep-sea sediment transport storms have, in fact, been identified by Gross *et al.* (1988) in the Nova Scotia Rise area of the North Atlantic. Four storms of high kinetic energy and near-bed flow were observed over a one-year period. These storms were associated with particle concentrations $> 2000\ \mu g\ l^{-1}$, and the authors suggested that the occurrence of a few of these large episodic events per year could account for most of the suspended load in the deep-sea nepheloid layer.

It may be concluded, therefore, that the spatial and temporal distributions of TSM in the oceans are controlled by the classical oceanographic parameters such as the transport of material from the continents, primary production and the major water circulation patterns. The vertical distribution of TSM in the water column can be described in terms of a three-layer model in which the main particulate sources are the surface ocean, from which particles sink downwards, and the bottom sediments, from which particles are lifted by erosive currents and moved upwards. An intermediate, or clear water minimum, layer is developed at that part of the water column where these two principal supply mechanisms have their smallest effects, the surface source trailing out downwards and the bottom source falling off upwards. In addition to these mainly vertical supply processes, the lateral advection of particles at mid-depths, e.g. from shelf sediments, can modify the simple three-layer down-column TSM profile (see Sec. 10.5).

10.3 The composition of oceanic total suspended matter

Oceanic TSM consists of a mixture of components, some of which have external sources and some of which are produced internally.

10.3.1 Externally produced components of oceanic TSM

These are formed on the continents, in estuaries, or in the air, and are transported to the oceans mainly via river run-off and atmospheric transport.

Crustal weathering products are a ubiquitous, although often minor, component of surface water TSM. The principal crust-derived minerals found in oceanic TSM are aluminosilicates (e.g. clay minerals and feldspars) and quartz. Chester *et al.* (1976) gave data on the distributions of the aluminosilicates in surface waters from a number of contrasting oceanic environments. These data showed that in the China Sea, which receives a large fluvial input, aluminosilicate (or clay) material made up an average of ~ 60% of the TSM. Krishnaswami & Sarin (1976) also reported that relatively high concentrations of particulates, and therefore aluminosilicates, were found in North and South Atlantic surface waters at high latitudes, where they probably resulted from glacial weathering. Off the coast of West Africa, where there is a relatively large aeolian input arising from dust pulses (see Sec. 4.1.4.1), Chester *et al.* (1976) found that clay accounted for ~ 10% of the total suspended solids. In open-ocean areas, however, the authors reported that land-derived aluminosilicate material made up less than ~ 5% of the TSM; this was similar to the findings of Krishnaswami & Sarin (1976), who estimated that crust-derived minerals constitute only ~ 2–3% of the TSM in most

open-ocean Atlantic surface waters. Flux calculations have shown that much of the particulate aluminium (Al_P) in these open-ocean surface waters has an atmospheric origin (see e.g. Chester 1982a), although other sources such as advective transport and bottom sediment stirring may be important at depth in the water column (see e.g. Spencer 1984, Gardner *et al.* 1985, and Sec. 10.5). The overall factors that control the distributions of aluminosilicates in surface ocean waters can be summarized as follows. The highest concentrations are found in areas where fluvial and glacial inputs are relatively high, intermediate values are observed in regions where atmospheric pulses of crustal dust are especially strong, and lowest concentrations are found in the open-ocean central gyres far from the land masses.

In addition to crustal weathering products externally produced material in oceanic TSM includes organic suspensions, flocculated metal–organic colloids and precipitated iron and manganese oxides formed in fluvial and estuarine environments.

10.3.2 Internally produced oceanic TSM components

These include biological material (tissues and shells) and inorganic precipitates, and various resuspended sediment components.

Oceanic TSM components that are produced in the biosphere include both organic matter and shell material. Particulate organic matter (POM), which is composed of living organisms (phytoplankton, zooplankton, etc.) and detritus (dead organisms, faecal debris, etc.), makes up a large fraction of the TSM found in many surface waters of the World Ocean. For example, Krishnaswami & Sarin (1976) reported that POM was the major component of TSM in Atlantic surface waters, making up an average of $\sim 50\%$ of the total solids. Chester & Stoner (1974) gave data on the concentrations of particulate organic carbon (POC) in surface waters from the North Atlantic, South Atlantic, Indian Ocean and the China Sea, and found that POM (calculated as POC $\times 2$) made up between $\sim 25\%$ and $\geqslant 80\%$ of the TSM. Clearly, therefore, organic matter is a principal component of *surface* water TSM. The factors controlling the distributions of organic matter in the oceans have been described in Section 9.2; these distributions are related to the major oceanographic parameters, and the highest concentrations are usually associated with regions of high primary production found in a ring around the major ocean basins. The shell material secreted by marine organisms consists largely of either calcium carbonate or opal (see Sec. 15.2.1). Shell carbonates can constitute between $\sim 10\%$ and $\sim 50\%$ of surface water TSM (Stoner 1974), but within this overall range there are individual trends in the distribution of calcium carbonate in surface waters. For example, Krishnaswami *et al.* (1976) were able to demonstrate that in Atlantic surface waters the highest concentrations of calcium

carbonate are associated with primary production and are found near the Antarctic convergence in the South Atlantic, near the polar front in the North Atlantic and in equatorial regions (see also Lisitzin 1972). Stoner (1974) found that opal constituted between $< 5\%$ and $> 35\%$ (with an average of $\sim 12\%$) of the surface water TSM from the Atlantic and Indian Oceans and the China Sea. Both Lisitzin (1972) and Krishnaswami *et al.* (1976) have provided evidence to show that the distribution of opaline silica in surface ocean waters is latitudinally controlled in relation to primary production. The highest concentrations are found in surface waters from latitudes south of $\sim 40°S$, and reach a maximum around Antarctica where the silica can make up as much as $\sim 80\%$ of the TSM. Less pronounced bands of opaline-rich TSM are found in the vicinity of the Equator.

Some non-biogenic components of TSM are also produced with the ocean system itself from components dissolved in sea water; these include material such as non-biogenic barite, a number of carbonates, and iron and manganese oxyhydroxides. In the lower and mid-water column, hydrothermal precipitates, consisting of minerals such as chalcopyrite, sphalerite and hydrous iron oxides (see Sec. 15.3.6), are also added to the TSM population.

In addition to the components described above, various kinds of anthropogenic material can be found in oceanic TSM. These include sewage products, nuclear components, petroleum hydrocarbons, pesticides, PCBs and other synthetic organics, and tars. The distributions of these anthropogenic components in oceanic TSM have been summarized by Chester (1984), and the wider aspects of their occurrence and fate in the marine environment have been reviewed by Preston (1989).

Data for the elemental compositions of a number of the principal components that contribute to the oceanic particulate population are given in Table 10.1. These are: (a) marine organisms, which are representative of the internally produced TSM biomass population; (b) faecal pellets, which offer an estimate of the composition of the large-sized aggregates that leave the surface waters (see Sec. 10.4); and (c) RPM and soil-sized atmospheric particulates, which represent the composition of continentally derived, i.e. external, mainly natural particulate matter transported to the ocean system. However, it must be stressed that these data are average values, and that wide variations can be found in the chemical compositions of the individual components themselves. A number of authors have provided data on the concentrations of particulate elements in surface sea water, and a compilation of some of these is given in Table 10.2. The overall chemical composition of individual TSM samples is controlled by the proportions in which the various components described above are present, and in a very general

Table 10.1 The elemental compositions of some of the principal components of oceanic TSM (units, μg g^{-1})

Element	Average; marine organisms[a]	Faecal pellets		Average; RPM[d]	Average; soil-sized aerosols[e]	Oceanic TSM[f]	
		b	c			surface water	deep water
Al	~ 160	20800	-	94000	-	3000	7500
Fe	~ 900	21600	24000	48000	52000	8800	15000
Mn	~ 10	2110	243	1050	1312	140	320
Cu	~ 30	650	226	100	157	145	200
Ni	~ 20	-	20	90	91	70	130
Co	~<1	15	3.5	20	9	5	16
Cr	~<1	-	38	100	85	125	170
V	~<3	76	-	170	145	22	-
Ba	~ 60	192	-	600	487	-	-
Sr	~ 900	1430	78	150	101	-	-
Pb	~ 20	-	34	100	465	180	570
Zn	~ 250	<20	950	250	683	640	1000
Cd	~ 5	-	-	~ 1	-	-	-
Hg	~ 0.15	-	-	-	-	16	36

[a] Data from Chester & Aston (1976).
[b] Data from Spencer et al. (1978).
[c] Data from Fowler (1977).
[d] Data from Martin & Whitfield (1983).
[e] Data from Chester & Stoner (1974).
[f] Data from Buat-Menard & Chesselet (1979).

way this is apparent from the particulate element concentration data given in Table 10.2. Thus, the concentrations are highest in surface waters from the China Sea (large river input), intermediate in the eastern margins of the North Atlantic (large aeolian input, intense primary production), and lowest in the open-ocean regions of the Atlantic and Indian Oceans (low external inputs, low primary production).

10.4 Total suspended matter fluxes in the oceans

In terms of the three-layer distribution model described in Section 10.2, it is apparent that TSM sinks through the water column from the surface layer to provide a *downward* particulate signal. This signal decreases in strength with depth, but below the clear water minimum it encounters the outriders of an *upward* particulate signal from the sea bed. In addition to these vertical signals, the water column TSM profiles can be modified by

Table 10.2 The concentrations of some particulate elements in surface sea waters from various regions (units, $\mu g\ l^{-1}$)

Element	China Sea[a]	Northeast margin; Atlantic Ocean[b]	Open ocean Atlantic Ocean[c]	Open ocean South Atlantic and Indian Oceans[d]
Al	45559	3755	78	298
Fe	-	-	222	-
Mn	778	54	3.5	9
Cu	74	43	3.6	10
Ni	-	-	1.8	-
Cr	-	-	3.1	-
V	41	14	-	6
Pb	47	19	4.5	5
Zn	149	85	16	22

[a, b] Data from Chester (1982b).

[c] Data from Buat-Menard & Chesselet (1979).

[d] Data from Wallace et al. (1977).

laterally advected particulate signals. These various signals interact, both to govern the throughput of particulate material in the ocean system and to control the net output of the material to the sediment sink. This **particulate throughput** is the key mechanism controlling the rates at which many dissolved trace metals are removed from the ocean reservoir, but before attempting to understand the way in which this 'great particle conspiracy' operates it is necessary to understand the nature of the particulate fluxes involved.

Measurements of the size distributions of the particles suspended in sea water are difficult to make, and interpretation of the data obtained presents complex problems; for a detailed discussion of this topic see Sheldon *et al.* (1972), Brun-Cottan (1971, 1986) and McCave (1975, 1984).

McCave (1984) made a detailed study of the size spectra of suspended particles in the oceans, which can be related to the three-layer model described in Section 10.1. Various authors (see e.g. Brun-Cottan 1986) have described the particle size distributions of the total particle population of oceanic TSM using the log-normal law. However, McCave (1984) showed that in terms of particle size spectra in ocean waters, the particle *number* data can nearly always be fitted by a power-law distribution over a large part of the measured range. Expressed as a

cumulative number N as a function of particle diameter d, the size distribution may be described by

$$N = kd^{-\beta} \tag{10.1}$$

where N is the number of particles with diameters $> d$. A value of $\beta = 3$ indicates equal particle *volumes* in logarithmically increasing size grades. This situation is found in mid-depth regions (i.e. the clear water minimum) where $\beta = 3$, with d in the range 1–100 μm; here, therefore, approximately equal volumes of material are found in logarithmically increasing size grades and the particle size distributions by volume are flat. However, close to the sources of particles, i.e. the surface ocean (surface layer) and the sea bed (deep water layer), the size distributions in particle volume space are not flat, but instead show a number of peaks, some of which are characteristic of the source (e.g. clay and foraminifera) and some of which are related to particle aggregation – see Figure 10.3.

Most particle production, and modification of the particle size, take place in the upper ocean. The overall distribution of small particles (as sensed by nephelometers) and large particles (as sensed by sediment traps) show a maximum in surface and bottom regions, with a broad minimum in between (cf. the three-layer model). The observed loss of peaks from the suspensions to yield flat distributions requires aggregation of material as the fine particles settle slowly down the water column; this aggregation takes place by processes such as the shear-controlled coagulation between particles of similar size, and the capture of small particles by larger biological aggregates, such as 'marine snow', which escape degradation in the upper layers of the ocean. Thus, the breakdown of larger particles as they fall from the surface waters, leading

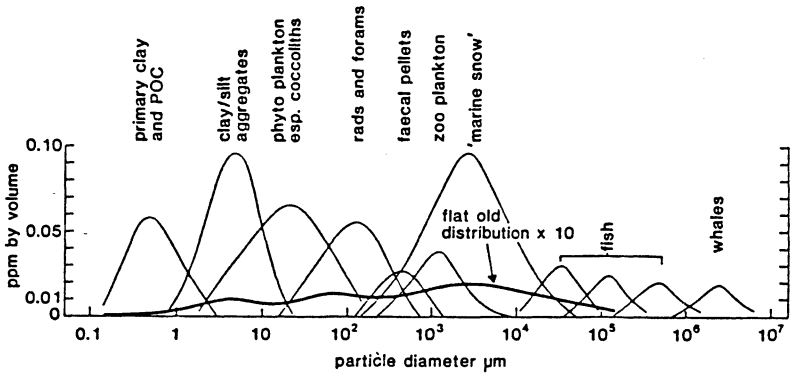

Figure 10.3 Hypothetical wide-spectrum oceanic TSM particle size distribution by volume, with suggested distributions of component particle types (from McCave 1984).

to the production of smaller particles, is matched by the formation of the larger units. The overall result of this is to produce a particle size spectrum in the oceans that is flattened in mid-water column locations. Thus, the ocean particle size distribution by volume tends to be flat at mid-depths (equivalent to a cumulative particle number distribution of $\beta = 3$) but is peaked in the nepheloid and surface layers.

The large biologically produced particles that fall from the surface zone undergo destruction in deeper waters with the release of fine, more refractory, particles, which is counterbalanced by their aggregation into larger units. This continuous cycle of aggregation and disaggregation modifies initial size distributions and produces a particle size spectrum over much of the oceans that is flattened, with no peaks that can be identified with specific particle populations.

According to McCave (1984) the size distribution of suspended particulates is a function of a number of variables, which include the source and nature of the particles, the physical and biological processes that cause their aggregation, and the age of the suspension. In practice, most of the particles suspended in sea water have diameters < 2 μm (McCave 1975), and those with diameters > 20 μm are rare (Honjo 1980). Particles are transported out of the mixed or surface layer down the water column by gravitational and Stokes settling. However, there is a growing body of evidence to suggest that there is a relatively rapid tranport of particles from the surface layers which is in excess of that predicted from Stokes' law for particles having diameters < 2 μm. This evidence for the accelerated sinking of particles has come from a number of sources. These include the measured, or inferred, down-column transit times of minerals, biogenic components, stable trace metals and radionuclides, all of which indicate that relatively large-diameter particles are required to sediment the phases out of sea water. Since most TSM is composed of particles with diameters < 2 μm, it must be assumed that this removal is preceded by the aggregation of the particles into larger units. This requirement for a 'fast' particle settling mechanism has been considered by various authors in recent years. In a benchmark paper, McCave (1975) made a theoretical study of the transport of TSM in the oceans and concluded that the principal feature in the vertical down-column flux of particles is that relatively rare, rapidly sinking, large particles contribute most of the flux, whereas more common smaller particles contribute most of the concentration. Brun-Cottan (1976) also concluded that small particles (< 5 μm diameter) might behave conservatively in the water column and undergo lateral movement in a given water mass, but that it is mainly the larger (> 50 μm diameter) particles, or aggregates, formed in surface waters that fall directly to the sea bed. In contrast, the smaller particles reach the bottom sediment by mechanisms and routes other than those which control the Stokes settling

of the larger particles. The large particles are formed by aggregation in the surface layers, and it has become apparent that the generation of faecal material by organisms is an important route by which smaller particles can undergo such aggregation into larger units, and faecal material does in fact make up a high proportion of the large-particle population. It must be stressed, however, that there is a continual break-up of the larger particles, and Cho & Azam (1988) have suggested that it is the action of free-living bacteria that gives rise to the large scale production of the small particles at the expense of the large aggregates.

It was pointed out above that the continual cycle of aggregation and disaggregation leads to the production of an oceanic particle population that has no specific size class populations within it. Nonetheless, in the context of both biogeochemical reactivity (e.g. the removal of dissolved elements by active biological uptake and passive scavenging) and particle flux transport (which is dominated by large-sized material), it is convenient to envisage the microcosm of particles as being divided into two general populations.

(a) A common, small-sized population (probably < 5 μm diameter), termed **fine particulate matter** (FPM) by Lal (1977), which undergoes large-scale horizontal transport; i.e. a suspended population (concentration $\sim$ 20–50 μg l^{-1}, sinking rate $\ll 1$ m d^{-1}), which dominates the standing stock of TSM.

(b) A rare, large-sized population, referred to as **coarse particulate matter** (CPM) by Lal (1977), which consists mainly of particle aggregates > 50 μm in diameter that undergo vertical settling; i.e. a sinking population, which is the prime carrier in down-column transport from the surface water to the ocean depths.

It is now widely recognized that faecal material (pellets and debris) makes up a significant fraction of the rain of particles from the surface layer to deep water. But faecal material is not the only type of biogenic particulate material to fall from the surface. For example, **marine snow** is a term that has been applied to relatively large amorphous aggregates of biological origin. To some extent this may be analogous to faecal material, since faecal pellets are known to be an important component of this marine snow (see e.g. Shanks & Trent 1980). However, marine snow also includes other components, and Honjo *et al.* (1984) prefer the term **large amorphous aggregates** (LAA) to describe the large-sized biogenic particles. In this terminology, therefore, LAA consist of the debris of phytoplankton and zooplankton, including faecal material, which is hydrated into a matrix of aggregates to which are attached other components, such as micro-organisms and clay particles. Shanks & Trent (1980) concluded that, like faecal pellets, marine snow can accelerate

the transport of material to the deep ocean and may in fact be the main package in which the vertial flux takes place. It is apparent, therefore, that the main flux of particulate material from the surface ocean to the sediment surface is driven by large organic aggregates, which form the main carriers of the global carbon flux; i.e. the organic matter that escapes recycling and is replaced in 'new' production (see Sec. 9.1.1). As they descend through the water column, these large aggregates drag down small-sized inorganic particles. Some of these inorganic particles are lithogenous in origin, and although they make up only a small fraction (usually $< \sim 5\%$) of the total TSM in surface water they form the main contributors of material to lithogenous pelagic clays. McCave (1984) therefore suggested the intriguing idea that 'the processes of pelagic sedimentation of lithogenic matter may be viewed as a side effect of excretion and disposal of other waste products of the ocean's biological system'.

The concept of a two-particle population in sea water has considerably advanced our understanding of how TSM is transported through the ocean reservoir. However, it has become apparent recently that the picture is more complicated than this simple two-fold particle classification would suggest. In this context, several studies have shown that the large-particle aggregates can only acount for a small fraction of the vertical flux of a number of trace metals and radio-isotopes down the water column. For example, Lal (1980) demonstrated that, although the measured sinking rate of particles based on the removal of Pu, Pb, Th and Fe from sea water is at least an order of magnitude greater than that based on the sinking of the FPM, it is also two or three orders of magnitude smaller than that derived from the sinking of the CPM. To explain this, Lal (1980) suggested that a piggy-back particle mechanism operates in the water column. In this mechanism, small particles (< 1 μm diameter), which are very active in trace metal and radionuclide scavenging, undergo impaction with the larger particles and adhere to them, probably via organic matter coatings. The large particles then carry the smaller ones down the water column by an on-and-off piggy-back mechanism. McCave (1984) also concluded that there is a scavenging of small particles by larger units in the surface and nepheloid regions of the water column, and that this is an important particle transport process. However, it must be pointed out that there are problems in using trace metal and radionuclide scavenging data to interpret particle transport rates since it is now believed that the scavenging can be of a reversible nature, i.e. the elements are not transported directly to deep water in one continuous jump – this is considered in more detail in Section 11.6.3.

The down-column flux is driven by CPM, which is composed mainly of biogenic aggregates. As a result, primary production in the euphotic layer exerts a fundamental control on the initiation of this down-column flux,

and an important thrust in marine geochemistry over the past few years has been to model the relationship between primary production at the surface and the flux of material through the interior of the ocean (see e.g. Honjo 1984). This is a complex subject, and requires further detailed clarification. At present, it does appear that the primary down-column flux is closely related to surface productivity, and that it often varies in magnitude in relation to seasonal changes in photosynthetic activity in the euphotic zone. Further, it is generally recognized that something around 95% of the organic matter produced in the surface ocean is recycled in the upper few hundred metres of the water column. However, the 5% or so of the organic matter that does escape from the surface water and is replaced in new production is largely composed of aggregates, and it is these which dominate the down-column material flux to the sediment sink. For example, Bishop *et al.* (1977) demonstrated that ~ 95% of the down-column flux of particulate material at a site in the equatorial Atlantic is associated with large faecal aggregates, although these account for < 5% of the total POC. These authors estimated that the transit times for the faecal material through a 4 km water column would be ~ 10 to ~ 15 days. During a transit of this duration, lateral displacement due to deep ocean advection in the study area would only be ~ 40 km, with the result that material deposited in the underlying sediments would reflect the oceanic variability in the surface water TSM, thus offering an explanation of the source-related clay mineral distribution patterns found in the deep-sea sediments (see Sec. 15.1.2). Further details on the sinking rates of faecal aggregates, which appear to be in the range ~ 15–800 m d^{-1}, have been summarized by Sackett (1978), and a detailed inventory of mass down-column material fluxes has been compiled by Simpson (1982). In the past it has generally been considered that the *primary* flux of particulate material through the water column is in a downward direction. Recently, however, Smith *et al.* (1989) have shown that upward fluxes of particulate organic matter, composed of positively buoyant particles, can also be significant.

In the preceding discussion, we have described the processes that control the vertical transport of oceanic TSM, and it is now necessary to consider how the components of the TSM are affected as the particles themselves are sedimented down the water column by the CPM flux.

10.5 Down-column changes in the composition of oceanic total suspended matter

The vertical transport of TSM in the water column is driven mainly by the CPM flux, and as the particulates settle they undergo considerable

modification via processes such as decomposition, aggregation–disaggregation, zooplankton grazing and dissolution. These processes dominate the changes that affect the composition of the TSM down into the clear water minimum layer. In deep water, however, the composition can be further modified by the introduction of components derived from the resuspension of bottom sediments. Thus, it is necessary to consider the effects of *two* signals, one from the sea surface and one from the sea bed, both of which affect the composition of TSM as it settles down the water column.

Many of the most recent advances in our understanding of how TSM changes in the water column have come from sediment trap experiments. Although there are still problems with the geometry of sediment traps, their prime advantage is that they are able to collect the rare large-sized material, and so allow the composition of the CPM flux to be elucidated. The distributions of trace elements in sea water are described in Chapter 11, and treatment of CPM-derived elemental fluxes will be deferred until this topic has been covered. At this stage, therefore, attention will be confined to down-column changes that affect the major components of oceanic TSM. These changes can be illustrated with reference to a number of individual studies, which have involved either filter or sediment trap collection techniques.

Feely *et al.* (1974) presented data on the composition of TSM at various water depths in the Gulf of Mexico, and their data were used by Sackett (1978) to show that the percentages of the major components in the TSM changed from ~ 85% organic and ~ 15% inorganic solids at a depth of 10 m, to ~ 34% organic matter and ~ 66% inorganic solids in the nepheloid layer. Honjo *et al.* (1982a) employed sediment traps to measure the mass down-column fluxes of biogenic particles (e.g. POM, carbonate shells and opaline shells) at four sites in the Atlantic and Pacific Oceans. At three of the sites, the contribution of biogenic material to the TSM decreased significantly with depth, accounting for 86–93% in the shallowest traps (< 1000 m) but only 40–70% in those located in deep water (> 3000 m). Further data on the changes in the nature of TSM with depth in the water column have been provided by Simpson (1982), who characterized various particle groupings in surface and deep water TSM samples from the Cape Basin (South Atlantic). The findings of the study are illustrated in Figure 10.4, and clearly demonstrate significant down-column compositional changes in the bulk TSM. For example, organic matter is dominant in the surface water sample, but is virtually absent in the deep water TSM. In contrast, the percentage of aluminosilicates increases dramatically in the deep water sample.

In general, therefore, it may be concluded that internally produced biogenic components decrease, and land-derived aluminosilicates increase, in importance as the CPM flux carries TSM down the water column.

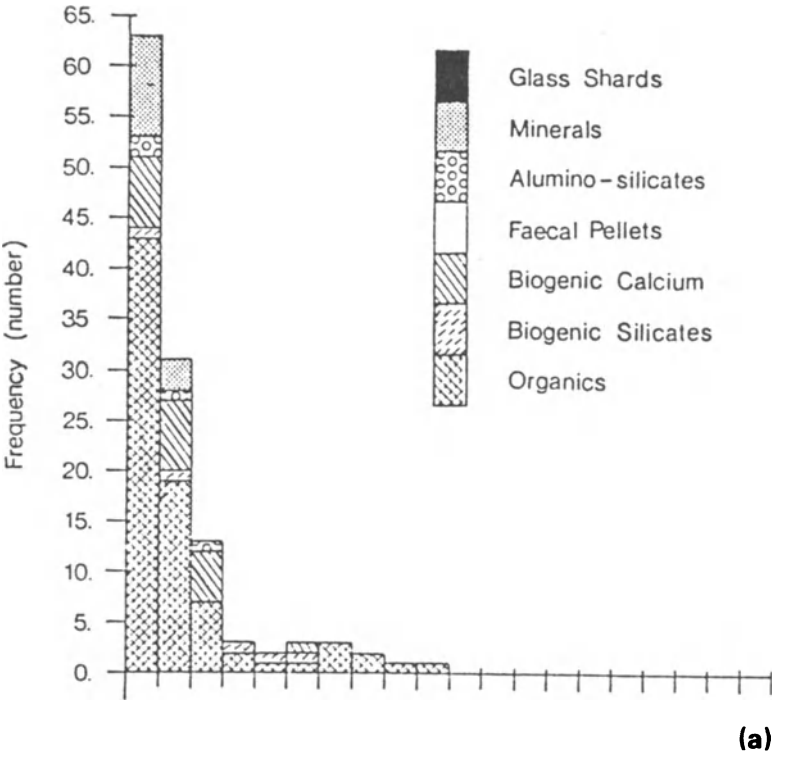

Figure 10.4 Down-column compositional changes in TSM from the Cape Basin (South Atlantic) (from Simpson 1982): (**a**) 10 m depth; (**b**) 5000 m depth.

There are a number of reasons for this, which can be related to the three-layer TSM water column distribution model, which combines downward and upward particulate signals but can also be affected by a lateral signal.

THE DOWNWARD SIGNAL Part of the decrease in the proportion of the biogenic components results from their loss as a result of the oxidative decomposition of POM and the dissolution of shell material, processes that occur both in the euphotic zone and at depth during the descent of the TSM through the water column. It is these processes which lead to the setting up of the clear water minimum zone, and they have two effects on the bulk TSM.

(a) Since biogenic components make up a large percentage of the surface water TSM, their destruction leads to a decrease in the absolute concentration of particles towards the clear water minimum zone.
(b) As these components are removed, there is an increase in the

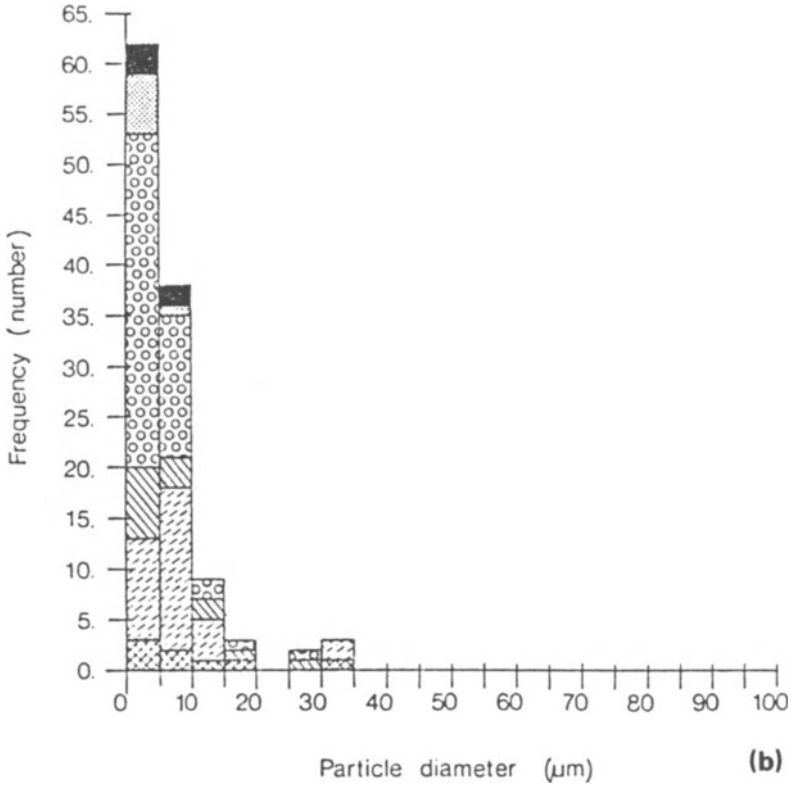

Figure 10.4b

relative proportions of the non-biogenic material, which survives to reach mid-water depths.

THE UPWARD SIGNAL The organic carbon content of most deep-sea sediments is generally quite low (< 5%; see Sec. 14.3), with the result that the resuspended particulate population is relatively rich in aluminosilicates and sometimes also in shell material. The *in situ*, i.e. non-basin-boundary, resuspended flux of bottom sediments, which results in the production of nepheloid layers, will therefore increase the proportions of non-biogenic material in bottom water TSM.

THE LATERAL SIGNAL The mixing of bottom sediment into the water column in the erosive boundary currents on the western edges of the ocean basins, and its advective transport, is now known to be a major pathway for the introduction of small-sized refractory particles into the basin interiors (see e.g. Brewer *et al.* 1980, Honjo *et al.* 1982b, Spencer

1984). The increase in the proportions of non-biogenic components at mid-water depths below the clear water minimum can therefore also result from a direct addition of fine aluminosilicate material that is transported laterally from the continental margins and is then transferred into the vertical CPM flux.

The general relationships in the processes that drive the down-column TSM flux are illustrated schematically in Figure 10.5.

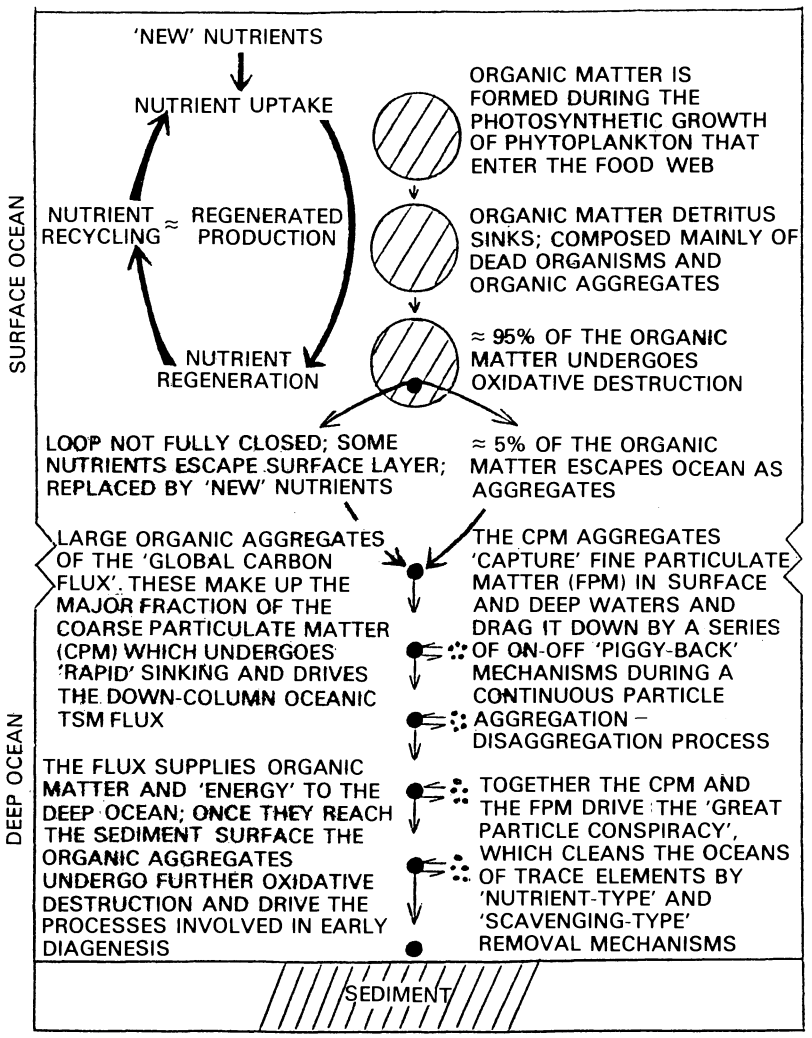

Figure 10.5 A schematic representation of the processes that drive the down-column flux of oceanic TSM.

10.6 Particulate material in the oceans: summary

(a) The vertical distribution of TSM in the water column can be described in terms of a three-layer model in which a surface layer, a clear water minimum layer and a deep water layer are distinguished. The principal mechanisms that contribute to the setting up of this model are a primary downward signal from the ocean surface, transporting mainly biogenic aggregates, and a secondary (or resuspended) upward signal from the bottom sediment, carrying mainly aluminosilicates. The two end-members in the system are therefore the **surface ocean** and the **surface sediment**. The surface ocean is the zone in which biological cycles are especially active, and it is here that biogenic solids interact with the dissolved and particulate elements transported by river run-off, atmospheric deposition and vertical mixing, and so enable them to enter the oceanic biogeochemical cycles.

(b) Oceanic TSM consists of a variety of components from both external sources (e.g. aluminosilicates and quartz) and internal sources (e.g. biological material, such as tissues and shells).

(c) There is a continual cycle of aggregation and disaggregation of oceanic TSM, which leads to the production of a particle population that has no specific size classes within it. However, from the point of view of biogeochemical reactivity is it convenient to distinguish between fine particulate matter (FPM, diameters < 5–10 μm) and coarse particulate matter (CPM, diameters > 50 μm).

(d) Much of the particulate flux to deep waters and sediments is driven by the CPM, which consists mainly of large organic aggregates. The CPM can also carry FPM to deep waters by piggy-back-type mechanisms.

In the present chapter we have described the distribution, composition and sinking characteristics of the oceanic TSM population. It is this microcosm of particles that plays a vital role in regulating the chemical composition of sea water via particulate–dissolved equilibria. In the next chapter the distributions of trace elements in the oceans will be discussed, and in doing this the TSM story will be used as a background to assess the factors that control the down-column transport of these elements. It is this vertical transport to the benthic boundary layer that eventually results in the ultimate removal of the elements into the sediment reservoir, thus initiating the final, but still complex, act in the 'great particle conspiracy', which was used as the starting point in the present chapter.

References

Biscaye, P.E. & S.T. Eittreim 1977. Suspended particulate loads and transports in the nepheloid layer of the abyssal Atlantic Ocean. *Mar. Geol.* **23,** 155–72.

Bishop, J.K.B., J.M. Edmond, D.R. Kellen, M.P. Bacon & W.B. Silker 1977. The chemistry, biology, and vertical flux of particulate matter from the upper 400 m of the equatorial Atlantic Ocean. *Deep-Sea Res.* **24,** 511–48.

Brewer, P.G., Y. Nozaki, D.W. Spencer & A.P. Fleer 1980. Sediment trap experiments in the deep North Atlantic: isotopic and elemental fluxes. *J. Mar. Res.* **38,** 703–28.

Brun-Cottan, J.C. 1971. Etude de la granulometrie des particules. Mesures effectuees avec un Coulter counter. *Cah. Oceanogr.* **23,** 193–205.

Brun-Cottan, J.C. 1976. Stokes settling and dissolution rate model for marine particles as a function of size distribution. *J. Geophys. Res.* **81,** 1601–5.

Brun-Cottan, J.C. 1986. Vertical transport of particles within the ocean. In *The role of air–sea exchange in geochemical cycling*, P. Buat-Menard (ed.), 83–111. Dordrecht: Reidel.

Buat-Menard, P. & R. Chesselet 1979. Variable influence of the atmospheric flux on the trace metal chemistry of oceanic suspended matter. *Earth Planet. Sci. Lett.* **42,** 399–411.

Chester, R. 1982a. Particulate aluminium fluxes in the eastern Atlantic. *Mar. Chem.* **11,** 1–16.

Chester, R. 1982b. The concentration, mineralogy, and chemistry of total suspended matter in sea water. In *Pollutant transfer and transport in the sea*, G. Kullenberg (ed.), 67–99. Boca Raton: CRC Press.

Chester, R. 1984. The marine mineral aerosol. In *The role of air–sea exchange in geochemical cycling*, P. Buat-Menard (ed.), 443–76. Dordrecht: Reidel.

Chester, R. & S.R. Aston 1976. The geochemistry of deep-sea sediments. In *Chemical oceanography*, J.P. Riley & R. Chester (eds), Vol. 6, 281–390. London: Academic Press.

Chester, R. & J.H. Stoner 1972. Concentration of suspended particulate matter in surface seawater. *Nature* **240,** 552–3.

Chester, R. & J.H. Stoner 1974. The distribution of Mn, Fe, Cu, Ni, Co, Ga, Cr, V, Ba, Sr, Sn, Zn and Pb in some soil-sized particulates from the lower troposphere over the World Ocean. *Mar. Chem.* **2,** 157–88.

Chester, R., D. Cross, A.G. Griffiths & J.H. Stoner 1976. The concentrations of 'aluminosilicates' in particulates from some surface waters of the World Ocean. *Mar. Geol.* **22,** M59–67.

Cho, B.C. & F. Azam 1988. Major role of bacteria in biogeochemical fluxes in the ocean's interior. *Nature* **332,** 441–3.

Connary, S.C. & M. Ewing 1972. The nepheloid layer and bottom circulation in the Guinea and Angola Basins. In *Studies in physical oceanography*, A.L. Gordon (ed.), 169–84. London: Gordon & Breach.

Eittreim, S., E.M. Thorndike & L. Sullivan 1976. Turbidity distribution in the Atlantic Ocean. *Deep-Sea Res.* **23,** 1115–27.

Ewing, M. & E. Thorndike 1965. Suspended matter in deep ocean water. *Science* **147,** 1291–4.

Feely, R.A., L. Sullivan & W.M. Sackett 1974. Light scattering measurements and chemical analysis of suspended matter in the near-bottom nepheloid layer of the Gulf of Mexico. In *Suspended solids in water*, R.J. Gibbs (ed.), 281–94. New York: Plenum.

Forchhammer, G. 1865. On the composition of sea water in the different parts of the ocean. *Phil. Trans. R. Soc. Lond.* **155,** 203–62.

Fowler, S.W. 1977. Trace elements in zooplankton particulate products. *Nature* **269,** 51–3.

Gardner, W.D., J.B. Southard & C.D. Hollister 1985. Sedimentation, resuspension and chemistry of particles in the northwest Atlantic. *Mar. Geol.* **65,** 199–242.
Gibbs, R.J. 1974. The suspended material of the Amazon shelf and tropical Atlantic Ocean. In *Suspended solids in water*, R.J. Gibbs (ed.), 203–10. New York: Plenum.
Gross, T.F., A.J. Williams & A.R.M. Nowell 1988. A deep-sea sediment transport storm. *Nature* **331,** 518–21.

Honjo, S. 1980. Material fluxes and modes of sedimentation in the mesopelagic and bathypelagic zones. *J. Mar. Res.* **38,** 53–97.
Honjo, S. 1984. Studies of ocean fluxes in time and space by bottom-tethered sediment trap arrays: a recommendation. In *Global ocean flux study*, 306–24. Washington, DC: National Academy Press.
Honjo, S., S.J. Manganini & J.J. Cole 1982a. Sedimentation of biogenic matter in the deep ocean. *Deep-Sea Res.* **29,** 609–25.
Honjo, S., D.W. Spencer & J.W. Farrington 1982b. Deep advective transport of lithogenic particles in Panama Basin. *Science* **216,** 516–18.

Jerlov, N.G. 1953. Particle distribution in the ocean. *Rep. Swed. Deep-Sea Exped.* **3,** 71–97.

Krishnaswami, S. & M.M. Sarin 1976. Atlantic surface particulates: composition, settling rates and dissolution in the deep-sea. *Earth Planet. Sci. Lett.* **32,** 430–40.
Krishnaswami, S., D. Lal & B.L.K. Somayajulu 1976. Investigations of gram quantities of Atlantic and Pacific surface particulates. *Earth Planet Sci. Lett.* **32,** 403–19.

Lal, D. 1977. The oceanic microcosm of particles. *Science* **198,** 997–1009.
Lal, D. 1980. Comments on some aspects of particulate transport in the oceans. *Earth Planet. Sci. Lett.* **49,** 520–7.
Lisitzin, A.P. 1972. *Sedimentation in the world ocean.* Soc. Econ. Paleo. Min. Spec. Publ., no. 17.

McCave, I.N. 1975. Vertical flux of particles in the ocean. *Deep-Sea Res.* **22,** 491–502.
McCave, I.N. 1984. Size spectra and aggregation of suspended particles in the deep ocean. *Deep-Sea Res.* **31,** 329–52.
Martin, J.M. & M. Whitfield 1983. The significance of the river input of chemical elements to the ocean. In *Trace elements in sea water*, C.S. Wong, E. Boyle, K.W. Bruland, J.D. Burton & E.D. Golberg (eds), 265–96. New York: Plenum.

Preston, M.R. 1989. Marine pollution. In *Chemical oceanography*, J.P. Riley (ed.), Vol. 9, 53–196. London: Academic Press.

Sackett, W.M. 1978. Suspended matter in sea water. In *Chemical oceanography*, J.P. Riley & R. Chester (eds), Vol. 7, 127–72. London: Academic Press.
Shanks, A.L. & J.D. Trent 1980. Marine snow: sinking rates and potential role in vertical flux. *Deep-Sea Res.* **27,** 137–43.
Sheldon, R.W., A. Prackash & W.H. Sutcliffe 1972. The size distribution of particles in the ocean. *Limnol. Oceanogr.* **17,** 327–40.
Simpson, W.R. 1982. Particulate matter in the oceans – sampling methods, concentration, size distribution and particle dynamics. *Oceanogr. Mar. Biol. Annu. Rev.* **20,** 119–72.
Smith, K.L, P.M. Williams & E.R.M. Druffel 1989. Upward fluxes of particulate organic matter in the deep North Pacific. *Nature* **337,** 724–26.

REFERENCES

Spencer, D.W. 1984. Aluminium concentrations and fluxes in the ocean. In *Global ocean flux study*, 206–20. Washington, DC: National Academy Press.

Spencer, D.W., P.G. Brewer, A. Fleer, S. Honjo, S. Krishnaswami & Y. Nozaki 1978. Chemical fluxes from a sediment trap experiment in the deep Sargasso Sea. *J. Mar. Res.* **36,** 493–523.

Stoner, J.H. 1974. Trace element geochemistry of particulates and waters from the marine environment. *Ph.D. Thesis*, University of Liverpool.

Turekian, K.K. 1977. The fate of metals in the oceans. *Geochim. Cosmochim. Acta* **41,** 1139–44.

Wallace, G.T., G.L. Hoffman & R.A. Duce 1977. The influence of organic matter and atmospheric decomposition on the particulate trace metal concentration in northwest Atlantic surface seawater. *Mar. Chem.* **5,** 143–70.

11 Trace elements in the oceans

Trace elements are present in sea water at concentrations that range down to picomoles per litre (pmol l^{-1}) and even lower. Such small concentrations pose extreme analytical problems, and it is only recently that these have been fully overcome. It is now known, for example, that contamination and the lack of sufficiently precise analytical techniques have led to reported concentration data that for some trace elements were too high by factors as much as 10^3. Because of this, real trends in the trace element data were sometimes totally masked by noise in the system, creating what Chester (1985) described as a 'frustration barrier', which prevented marine chemists from being able to relate trace metal distribution patterns to a consistent oceanographic framework. However, in a keynote review, Bruland (1983) pointed out that the mid-1970s had seen a quantum leap in our knowledge of the oceanic distributions of trace elements. This leap had become possible as a result of major improvements in both analytical and collection techniques, especially with regard to the elimination of sample contamination, which allowed the noise to be filtered out of the data. A selection of the new trace element concentration data in sea water is given in Table 11.1. At the same time that trace element *concentration* data were being refined, there were also advances in our understanding of the *speciation* of the elements in sea water.

11.1 Introduction

One of these key steps in the story of the new (post-1975) dissolved trace element data was the setting up of GEOSECS (Geochemical Ocean Sections Study), which was designed to provide a framework of hydrographic and geochemical measurements that could be used in the study of oceanic circulation and mixing processes. A number of oceanic water column sections were carefully selected and vertical concentration profiles of parameters such as salinity, temperature, TSM, dissolved gases and a range of radioactive and stable trace elements were measured. However, as the new, low-concentration, dissolved trace element data began to emerge, they presented marine chemists with a serious dilemma when attempts were made to interpret them. The reason for this, as

Table 11.1 A selection of 'new' data on the speciations, concentrations and types of vertical distributions of trace elements in sea water[a]

Element	Probable main species in oxygenated sea-water	Range and average concentration at 35‰ salinity†	Type of distribution
Li	Li^+	25 μmol kg^{-1}	Conservative
Be	$BeOH^+$, $Be(OH)_2^0$	4–30 pmol kg^{-1}; 20 pmol kg^{-1}	Nutrient-type and scavenging
B	H_3BO_3	0.416 mmol kg^{-1}	Conservative
C	HCO_3^-, CO_3^{2-}	2.0–2.5 mmol kg^{-1}; 2.3 mmol kg^{-1}	Nutrient-type
N	NO_3^- (also as N_2)	< 0.1–45 μmol kg^{-1}; 30 μmol kg^{-1}	Nutrient-type
O	O_2 (also as H_2O)	0–300 μmol kg^{-1}	Mirror image of nutrient-type
F	F^-, MgF^+	68 μmol kg^{-1}	Conservative
Na	Na^+	0.468 mol kg^{-1}	Conservative
Mg	Mg^{2+}	53.2 mmol kg^{-1}	Conservative
Al	$Al(OH)_4^-$, $Al(OH)_3^0$	(5–40 nmol kg^{-1}; 20 nmol kg^{-1})	Mid-depth minima
Si	H_4SiO_4	< 1–180 μmol kg^{-1}; 100 μmol kg^{-1}	Nutrient-type
P	HPO_4^{2-}, $NaHPO_4^-$, $MgHPO_4^0$	< 1–3.5 μmol kg^{-1}; 2.3 μmol kg^{-1}	Nutrient-type
S	SO_4^{2-}, $NaSO_4^-$, $MgSO_4^0$	28.2 mmol kg^{-1}	Conservative
Cl	Cl^-	0.546 mol kg^{-1}	Conservative
K	K^+	10.2 mmol kg^{-1}	Conservative
Ca	Ca^{2+}	10.3 mmol kg^{-1}	Slight surface depletion
Sc	$Sc(OH)_3^0$	8–20 pmol kg^{-1}; 15 pmol kg^{-1}	Surface depletion
Ti	$Ti(OH)_4^0$	(< 20 nmol kg^{-1})	?
V	HVO_4^{2-}, $H_2VO_4^-$, $NaHVO_4^-$	20–35 nmol kg^{-1}; 30 nmol kg^{-1}	Slight surface depletion
Cr	CrO_4^{2-}, $NaCrO_4^-$	2–5 nmol kg^{-1}; 4 nmol kg^{-1}	Nutrient-type
Mn	Mn^{2+}, $MnCl^+$	0.2–3 nmol kg^{-1}; 0.5 nmol kg^{-1}	Depletion at depth
Fe	$Fe(OH)_3^0$	0.1–2.5 nmol kg^{-1}; 1 nmol kg^{-1}	Surface depletion, depletion at depth
Co	Co^{2+}, $CoCO_3^0$, $CoCl^+$	(0.01–0.1 nmol kg^{-1}; 0.02 nmol kg^{-1})	Surface depletion, depletion at depth
Ni	Ni^{2+}, $NiCO_3^0$, $NiCl^+$	2–12 nmol kg^{-1}; 8 nmol kg^{-1}	Nutrient-type
Cu	$CuCO_3^0$, $CuOH^+$, Cu^{2+}	0.5–6 nmol kg^{-1}; 4 nmol kg^{-1}	Nutrient-type and scavenging
Zn	Zn^{2+}, $ZnOH^+$, $ZnCO_3^0$, $ZnCl^+$	0.05–9 nmol kg^{-1}; 6 nmol kg^{-1}	Nutrient-type
Ga	$Ga(OH)_4^-$	(0.3 nmol kg^{-1})	?
Ge	H_4GeO_4, $H_3GeO_4^-$	≤ 7–115 pmol kg^{-1}; 70 pmol kg^{-1}	Nutrient-type
As	$HAsO_4^{2-}$	15–25 nmol kg^{-1}; 23 nmol kg^{-1}	Nutrient-type
Se	SeO_4^{2-}, SeO_3^{2-}, $HSeO_3^-$	0.5–2.3 nmol kg^{-1}; 1.7 nmol kg^{-1}	Nutrient-type
Br	Br^-	0.84 mmol kg^{-1}	Conservative
Rb	Rb^+	1.4 μmol kg^{-1}	Conservative
Sr	Sr^{2+}	90 μmol kg^{-1}	Slight surface depletion
Y	YCO_3^+, YOH^{2+}, Y^{3+}	(0.15 nmol kg^{-1})	?
Zr	$Zr(OH)_4^0$, $Zr(OH)_5^-$	(0.3 nmol kg^{-1})	?
Nb	$Nb(OH)_6^-$, $Nb(OH)_5^0$	(≤ 50 pmol kg^{-1})	?
Mo	MoO_4^{2-}	0.11 μmol kg^{-1}	Conservative
(Tc)	TcO_4^-	No stable isotope	—
Ru	?	?	?
Rh	?	?	?
Pd	?	?	?
Ag	$AgCl_2^-$	(0.5–35 pmol kg^{-1}; 25 pmol kg^{-1})	Nutrient-type
Cd	$CdCl_4^0$	0.001–1.1 nmol kg^{-1}; 0.7 nmol kg^{-1}	Nutrient-type
In	$In(OH)_3^0$	(1 pmol kg^{-1})	?
Sn	$SnO(OH)_3^-$	(1–12, ~4 pmol kg^{-1})	High in surface waters
Sb	$Sb(OH)_6^-$	(1.2 nmol kg^{-1})	?
Te	TeO_3^{2-}, $HTeO_3^-$	?	?
I	IO_3^-	0.2–0.5 μmol kg^{-1}; 0.4 μmol kg^{-1}	Nutrient-type
Cs	Cs^+	2.2 nmol kg^{-1}	Conservative
Ba	Ba^{2+}	32–150 nmol kg^{-1}; 100 nmol kg^{-1}	Nutrient-type
La	La^{3+}, $LaCO_3^+$, $LaCl^{2+}$	13–37 pmol kg^{-1}; 30 pmol kg^{-1}	Surface depletion
Ce	$CeCO_3^+$, Ce^{3+}, $CeCl^{2+}$	16–26 pmol kg^{-1}; 20 pmol kg^{-1}	Surface depletion
Pr	$PrCO_3^+$, Pr^{3+}, $PrSO_4^+$	(4 pmol kg^{-1})	Surface depletion
Nd	$NdCO_3^+$, Nd^{3+}, $NdSO_4^+$	12–25 pmol kg^{-1}; 20 pmol kg^{-1}	Surface depletion
Sm	$SmCO_3^+$, Sm^{3+}, $SmSO_4^+$	2.7–4.8 pmol kg^{-1}; 4 pmol kg^{-1}	Surface depletion
Eu	$EuCO_3^+$, Eu^{3+}, $EuOH^{2+}$	0.6–1.0 pmol kg^{-1}; 0.9 pmol kg^{-1}	Surface depletion
Gd	$GdCO_3^+$, Gd^{3+}	3.4–7.2 pmol kg^{-1}; 6 pmol kg^{-1}	Surface depletion
Tb	$TbCO_3^+$, Tb^{3+}, $TbOH^{2+}$	(0.9 pmol kg^{-1})	Surface depletion
Dy	$DyCO_3^+$, Dy^{3+}, $DyOH^{2+}$	(4.8–6.1 pmol kg^{-1}; 6 pmol kg^{-1})	Surface depletion
Ho	$HoCO_3^+$, Ho^{3+}, $HoOH^{2+}$	(1.9 pmol kg^{-1})	Surface depletion
Er	$ErCO_3^+$, $ErOH^{2+}$, Er^{3+}	4.1–5.8 pmol kg^{-1}; 5 pmol kg^{-1}	Surface depletion
Tm	$TmCO_3^+$, $TmOH^{2+}$, Tm^{3+}	(0.8 pmol kg^{-1})	Surface depletion
Yb	$YbCO_3^+$, $YbOH^{2+}$	3.5–5.4 pmol kg^{-1}; 5 pmol kg^{-1}	Surface depletion
Lu	$LuCO_3^+$, $LuOH^{2+}$	(0.9 pmol kg^{-1})	Surface depletion
Hf	$Hf(OH)_6^0$, $Hf(OH)_5^-$	(< 40 pmol kg^{-1})	?
Ta	$Ta(OH)_5^0$	(< 14 pmol kg^{-1})	?
W	WO_4^{2-}	0.5 nmol kg^{-1}	?
Re	ReO_4^-	(14–30 pmol kg^{-1}; 20 pmol kg^{-1})	?
Os	?	?	?
Ir	?	?	?
Pt	?	?	?
Au	$AuCl_2^-$	(25 pmol kg^{-1})	?
Hg	$HgCl_4^{2-}$	(2–10 pmol kg^{-1}; 5 pmol kg^{-1})	?
Tl	Tl^+, $TlCl^0$; or $Tl(OH)_3^0$	60 pmol kg^{-1}	Conservative
Pb	$PbCO_3^0$, $Pb(CO_3)_2^{2-}$, $PbCl^+$	5–175 pmol kg^{-1}; 10 pmol kg^{-1}	High in surface waters, depleted at depth
Bi	BiO^+, $Bi(OH)_2^+$	≤ 0.015–0.24 pmol kg^{-1}	Depletion at depth

† Parentheses indicate uncertainty about the accuracy or range of concentration given.

[a] From Bruland (1983).

Boyle *et al.* (1977) pointed out, was quite simply that neither the fact that extreme precautions had been taken during the collection and analysis of the samples, nor the finding that the results were lower than previous ones, in themselves gave validity to the new data. Boyle *et al.* (1977) concluded, therefore, that, rather than accepting low trace element concentrations at face value, the validation of the data must rest on three primary criteria.

(a) The new trace element concentrations must be confirmed by inter-laboratory agreement; this was an integral part of GEOSECS.
(b) The vertical distribution profiles obtained from the new data must show smooth variations that can be related to hydrographic and chemical features displayed by conventionally measured properties, which themselves have well established distributions.
(c) The regional variations derived on the basis of the new data should be compatible with the large-scale physical and chemical circulation patterns known to operate in the ocean system. In other words, the new trace element data must be *oceanographically consistent.*

The problem therefore revolves around the overall approach that should be adopted when attempts are made to interpret the new trace metal data. According to Edmond *et al.* (1979), the local water column distributions of dissolved constituents in open-ocean waters reflect oceanic circulation patterns, with a large proportion of the chemical signal being determined by long-distance advection and the mixing of water masses of different end-member compositions. It is necessary, therefore, to extract chemical information from this advective background. This was initialy pointed out by Chan *et al.* (1977). These authors presented data on the concentration of Ba in Atlantic Ocean profiles sampled during GEOSECS, and showed the physical circulation is the dominant factor affecting the distribution of the element in the Atlantic basins. In order to extract chemical information from this background, the authors adopted the approach of relating the distribution of Ba to that of other species whose distributions in the water column are well understood. In this way, they were able to demonstrate that Ba was involved in a deep water regeneration cycle similar to those of the refractory nutrients, silicate (opal) and calcite – see Worksheet 7.3. This kind of comparison is developed more fully in Section 11.5. For the moment, however, it is important to understand that the North Atlantic is a conservative ocean with respect to *unreactive* elements that spend a relatively long time in sea water. For example, Measures *et al.* (1984) showed that this was the case for Be. However, these authors also pointed out that for *reactive* species, the North Atlantic will not be a conservative ocean. It is apparent, therefore, that the time a dissolved

trace element spends in the oceanic water column will exert a basic control on its large-scale distribution patterns. Before attempting to understand the factors that control the distributions of trace elements in sea water, it is therefore necessary to introduce the concept of oceanic residence times.

11.2 Oceanic residence times

The residence time of an element in the oceans is the average time it spends in the sea before being removed into the sediment sink. In a *steady-state* system it is assumed that the input of an element (mainly via river run-off, atmospheric deposition and hydrothermal exhalations) per unit time is balanced by its output (via sedimentation). There are a number of ways in which equations can be written to describe this relationship. For example, the residence time (τ) of an element is often calculated from the equation

$$\tau = A/(\mathrm{d}A/\mathrm{d}t) \tag{11.1}$$

where A is the total amount of the element in suspension or solution in sea water, and $\mathrm{d}A/\mathrm{d}t$ is the amount introduced or removed per unit time. In making this type of calculation it is assumed that the element is completely mixed in the system in a time that is short compared to its residence time, and that neither A nor $\mathrm{d}A/\mathrm{d}t$ change appreciably in 3–4 times this period.

Attempts have been made to estimate the residence times of elements in the oceans using the approach outlined above on the basis of *input* (e.g. Barth, 1952) and output (e.g. Goldberg & Arrhenius 1958) data. Residence time estimates based on the two techniques are given in Table 11.2. Goldberg (1965) concluded that in spite of the drastic oversimplifications involved there is a remarkable degree of agreement between the residence time estimates derived from the two techniques, and he was able to draw a number of general conclusions regarding the residence times of elements in the oceans.

(a) The values of τ span a range of six orders of magnitude, e.g. from Na (2.6×10^8 yr) to Al (100 yr), which reflect the variations in the reactivities of the elements in sea water.
(b) The longest residence times are found for the lower atomic number alkali metals and alkaline earths (excluding Be), which are characterized by a general lack of reactivity of their aqueous ions (mainly simple hydrated cations) in sea water.
(c) Intermediate residence times ($\sim 10^3$–10^4 yr) are found for trace

Table 11.2 Residence times of elements in sea water (units, yr)

Element	Goldberg[a]		Brewer[b]	Others[c-e]	MORT values[f]	Element	Goldberg[a]		Brewer[b]	Others	MORT values[f]
	River input	Sedimentation					River input	Sedimentation			
Li	1.2×10^{7}	1.9×10^{7}	2.3×10^{6}	-	5.5×10^{5}	Ga	-	-	1×10^{4}	-	1.2×10^{4}
B	-	-	1.3×10^{7}	-	0.9×10^{7}	As	-	-	5×10^{4}	-	3.2×10^{4}
F	-	-	5.2×10^{5}	-	4.8×10^{5}	Se	-	-	2×10^{4}	-	3.7×10^{4}
Na	2.1×10^{8}	2.6×10^{8}	6.8×10^{7}	-	7.4×10^{7}	Br	-	-	1×10^{8}	-	1.2×10^{8}
Mg	2.2×10^{7}	4.5×10^{7}	1.2×10^{7}	-	1.5×10^{7}	Rb	6.1×10^{6}	2.7×10^{5}	4×10^{6}	-	2.9×10^{6}
Al	3.1×10^{3}	1.0×10^{2}	1.0×10^{2}	-	3.7×10^{2}	Sr	1.0×10^{4}	1.9×10^{7}	4×10^{6}	-	4.9×10^{6}
Si	3.5×10^{4}	1×10^{4}	1.8×10^{4}	-	1.4×10^{4}	Mo	2.1×10^{6}	5×10^{5}	2×10^{5}	-	7.3×10^{5}
P	-	-	1.8×10^{5}	-	1.9×10^{4}	Ag	2.5×10^{5}	2.1×10^{6}	4×10^{4}	-	4.9×10^{3}
Cl	-	-	1×10^{8}	-	1.1×10^{8}	Cd	-	-	-	$7.7\text{-}92\times10^{3}$c	1.8×10^{4}
K	1×10^{7}	1.1×10^{7}	7×10^{6}	-	9.2×10^{6}	Sb	-	-	7×10^{3}	-	8.8×10^{3}
Ca	1×10^{6}	8×10^{6}	1×10^{6}	-	1.1×10^{6}	I	-	-	4×10^{5}	-	3.1×10^{5}
Sc	-	-	4×10^{4}	-	5.5×10^{3}	Cs	-	-	6×10^{5}	-	4.2×10^{5}
Ti	-	-	1.3×10^{4}	-	3.7×10^{3}	Ba	5×10^{4}	8.4×10^{4}	4×10^{4}	-	1.2×10^{4}
V	-	-	8×10^{4}	-	9.2×10^{4}	La	-	-	6×10^{12}	-	2.2×10^{3}
Cr	-	-	6×10^{3}	-	1.1×10^{4}	W	-	-	1.2×10^{5}	-	1.2×10^{5}
Mn	-	-	1×10^{4}	39-53c	8.9×10^{2}	Au	-	-	2×10^{5}	-	7.3×10^{4}
Fe	-	-	2×10^{2}	27-30c	1.8×10^{3}	Hg	-	-	8×10^{4}	3.5×10^{2}e	1.8×10^{4}
Co	-	-	3×10^{4}	-	9.2×10^{3}	Pb	5.6×10^{2}	2×10^{3}	4×10^{2}	-	1.1×10^{3}
Ni	1.5×10^{4}	1.8×10^{4}	9×10^{4}	$1.8\text{-}3.6\times10^{3}$c, 6×10^{3}d	1.4×10^{4}	Th	-	-	2×10^{2}	-	3.7×10^{3}
Cu	4.3×10^{4}	5×10^{4}	2×10^{4}	$4.1\text{-}6.4\times10^{3}$c, 5×10^{3}e	2.4×10^{3}	U	-	-	3×10^{6}	-	4.9×10^{5}
Zn	-	-	2×10^{4}	$0.78\text{-}1.8\times10^{4}$c	1.2×10^{2}						

[a] Goldberg (1965).
[b] Brewer (1975).
[c] Bewers & Yeats (1977).
[d] Martin & Whitfield (1983).
[e] Gill & Fitzgerald (1988).
[f] Martin & Whitfield (1983).

metals such as Zn, Mn, Co and Cu.

(d) The shortest residence times (~ 10–10^3 yr) have been calculated for elements such as Al, Ti, Cr and Fe. For these elements the residence times are less than the mixing times for oceanic water masses, and Goldberg (1965) suggested that this probably resulted from a combination of two factors. (i) The elements are transported to the oceans mainly in particulate material (i.e. they have low DTI values – see Sec. 3.1.7). (ii) They undergo generally rapid hydrolysis in solution, which leads to their uptake by particle scavenging.

It is of course obvious that any calculation of a residence time carried out using Equation 11.1 is extremely sensitive to the values used for the input and output mechanisms. This is especially true for data on the input of trace metals from their primary sources. Most calculations use only river inputs in the estimation of oceanic residence times, and even now our knowledge of these inputs for trace metals is extremely sparse (see Sec. 6.1). Further, many residence time calculations assume that the river inputs are delivered to the open ocean, i.e. they take no account of estuarine processes. Bewers & Yeats (1977) attempted to overcome this problem by using new trace metal data for *net* fluvial fluxes (see Sec. 6.1), which they combined with theories on the removal of trace metals in the coastal zone, to update the oceanic residence times of a series of trace metals. A summary of the data provided by these authors is included in Table 11.2; in general, these residence time estimates tend to be smaller than previous ones, especially for Fe and Mn.

Whitfield (1979) introduced the concept of a **mean oceanic residence time** (MORT; see Sec. 17.2), which is defined as the total quantity of an element present in the oceans divided by its input rate (from rivers) or its output rate (to the sediment). MORT values, which assume the whole ocean to be a well stirred system, are only approximate quantities since they ignore a number of important input (e.g. atmospheric deposition, hydrothermal venting) and output (e.g. atmospheric exchange, the rock sink) terms. However, they do offer an overview of the reactivities, i.e. the intensity of the particle–water interactions, of elements in the ocean system. MORT values are listed with other residence time data in Table 11.2.

The wider problems involved in the overall concept of oceanic residence times have been discussed by a number of authors. For example, Wangersky (1986) drew attention to the fact that there are probably two separate residence times for most trace metals, one for the ionic or complexed form, and another for that fraction of the metal which enters the oceans as part of the mineral matrix. Wangersky (1986) did suggest, however, that surface water residence times, combined with a deep water fall time, might have a geochemical use, providing it is recognized that **surface water residence times** are not constant on an

ocean-wide basis. For example, some trace metals will spend a shorter time in solution in the surface waters of coastal upwelling regimes than in those in the centre of a mid-ocean gyre, and even in the upwelling areas the surface water residence times will vary with the time of year and with local productivity.

Bruland (1980) also attempted to re-evaluate the residence time concept. He pointed out that for elements which are conservative in sea water the residence time can be defined as outlined above, i.e. $\tau = A/(\mathrm{d}A/\mathrm{d}t)$. These conservative elements usually have residence times that are $\gtrsim 10^6$ yr. However, the concept of oceanic residence times becomes more complex for the non-conservative elements. Dissolved elements that undergo passive particle scavenging tend to have relatively short residence times with respect to the mixing time of the ocean, and their distributions are controlled largely by their *external* inputs. For example, recent data indicate that the residence time of dissolved Al with respect to its atmospheric input, which is the major open-ocean source of the element, is ~ 100–200 yr. However, the nutrient-type elements (see Sec. 11.6.1), which are involved in an active biological removal mechanism, undergo a surface depletion and a subsurface regeneration, and this regeneration at depth implies an oceanic residence time that is long with respect to the oceanic mixing cycle (~ 1600 yr); thus, the residence times of phosphate and silicate have been estimated to be 180×10^3 and 18×10^3 yr, respectively. These elements therefore undergo numerous internal cycles within sea water prior to their final removal in the sediments. The nutrient type trace metals involved in these cycles take part in upwelling, down-column transport via organic carriers and regeneration at depth. As a result, their distributions in the oceans are virtually independent of their external points of entry, and their internal exit points are controlled mainly by *internal* oceanic processes. Bruland (1980) therefore concluded that the nutrient-type elements must have an oceanic residence time that is long with respect to the timescale of oceanic mixing, and set a lower limit of $\tau \sim 5 \times 10^3$ yr for such trace metals, e.g. Cd, Zn and Ni. Bruland (1980) then compared this τ_{min} with some of the more recent residence time estimates given in the literature. To this end, he cited the following τ values: Cd, 50×10^3 yr (input data, Boyle *et al.* 1976); Ni, 40×10^3 yr (input data, Sclater *et al.* 1976); and Ni, 6×10^3 yr (output data, Sclater *et al.* 1976). The τ for Ni based on output data is therefore close to the minimum permitted by the theory, but those estimated from input data are considerably in excess of it. Compared to the nutrient-type elements, the scavenging-type elements will have shorter residence times in sea water, and this nutrient–scavenging difference has important implications for the transport of trace element in the ocean system. For example, the nutrient-type elements, which undergo recycling and have a longer residence time, can take part in

inter-ocean transport and will tend to be enriched in the older intermediate waters of the North Pacific at the end of the oceanic 'grand tour'; thus, there is a five-fold inter-oceanic enrichment of dissolved Zn in the North Pacific compared to the North Atlantic. In contrast, scavenging-type, or particle-reactive, elements tend to be depleted in the North Pacific relative to the North Atlantic, for which the external inputs are greater; dissolved Al is an example of this, showing a 40-fold depletion in the North Pacific (Orians & Bruland 1985). This kind of inter-ocean fractionation is important in the authigenic flux of trace elements to sediments, and this is discussed in Section 16.5.

It may be concluded, therefore, that in view of the very considerable difficulties involved, the overall *trends* in the residence time characteristics of the various elements given in Table 11.2 hold in a general sense, but the actual residence time values themselves should still be regarded as being no more than speculative.

11.3 An oceanic trace metal framework

When a box model approach is adopted it is convenient to divide the ocean into a surface and deep reservoir (see Sec. 7.5), and if a system of oceanographic consistency is the principal aim of marine chemistry it must apply to trace element distributions in both reservoirs.

THE SURFACE WATER RESERVOIR The most important sources for the input of trace elements to the surface ocean reservoir are: (a) river run-off at the ocean margins; (b) atmospheric deposition, which operates to varying degrees over the entire surface ocean; (c) diffusion from shelf sediments; and (d) upwelling, which has its greatest effects in certain well defined areas of high primary production. The distributions of trace elements in the surface ocean will therefore reflect the magnitudes of the external, i.e. river and atmospheric, source term signals and the effects of surface circulation patterns, upon which are superimposed the results of internal (i.e. oceanic) processes involved in the major biogeochemical cycles.

THE DEEP WATER RESERVOIR Trace elements are supplied to this reservoir from: (a) the surface ocean, by processes such as downwelling and the settling of TSM; and (b) the deep ocean iteself, from mid-depth hydrothermal sources and diffusion from bottom sediments. Deep water trace element distributions will therefore be governed by the strengths of the source term signals and the effects of deep water circulation patterns, upon which are superimposed the involvement of the elements in the internal biogeochemical processes.

In general, therefore, there are three parameters that must be considered when any attempt is made to describe the distributions of trace elements (or other components) within the oceans. These are: **source terms**, which supply the elements; large-scale **circulation processes**, which govern the transport of both dissolved and particulate elements within the oceans; and internal **biogeochemical processes**, which involve particulate–dissolved interactions and lead, sometimes via recycling stages, to the eventual removal of the trace elements from the system. In any oceanographically consistent framework, the distributions of the trace elements must be related to all three of these parameters. In order to set up such a framework within which to evaluate the new trace element data, it is convenient to consider the *geographical* (or lateral) and the *vertical* distributions of the element separately.

In recent years new data have been reported on the concentrations of a wide range of trace elements in waters from all the major oceans, and the list of elements studied is growing all the time. A compilation of the ranges of concentrations and their averages is shown in Table 11.1. However, to attempt a 'periodic table' element-by-element description of all the trace constituents in sea water is clearly beyond the scope of this volume. Rather, the treatment adopted will concentrate on a limited number of *process-illustrating* elements (e.g. Cd, Zn, Ni, Pb, Cu, Al and Mn), which will serve as examples to illustrate the recently developed theories on the factors that control the distributions of trace elements in sea water.

In some trace element studies the seawater samples are filtered prior to analysis whereas in others bulk water samples are analysed; however, since the dissolved fraction is dominant for many trace elements, the data given in the present chapter will generally refer to the dissolved species unless otherwise stated.

11.4 Geographical variations in the distributions of trace elements in surface ocean waters

In Section 11.1 it was suggested that the distributions of trace elements in the surface ocean reservoir are controlled by the following parameters: (a) the magnitudes of the external source signals (inputs), (b) the effects of surface circulation (transport), and (c) the results of internal processes (output, trapping and recycling). The surface water concentrations of many trace elements are higher in coastal and shelf waters than they are in open-ocean waters. This is consistent with the magnitude of trace metal source strengths to surface waters, and reflects the fact that these are higher in nearshore receiving areas. However, although the signals from the primary source strength inputs are usually stronger to nearshore than

to open-ocean waters, a number of processes can act to trap elements in the coastal zone. If the trapping of the elements involves their permanent removal from solution in the coastal zone at a rate that prevents their large-scale export, and if they have a strong source direct to the open ocean, then the dissolved concentration of a trace element may be higher away from the coastal regions. The processes that trap trace elements in the coastal zone include scavenging uptake followed by deposition of the particles to the sediment, and uptake by biota involved in coastal upwelling. Both shelf sediments and upwelling associated with primary production can therefore act as traps to retain dissolved trace elements in the coastal zone. However, the two traps act in different ways. Thus, elements that have been incorporated into reducing shelf sediments can be released by diagenetically mediated diffusion and so escape into the overlying waters to be available for lateral transport. In contrast, upwelling can continually recycle the nutrient-type elements, so retaining them in the coastal zone. This zone is also important in the trapping of trace metals because a large fraction of the total, biologically driven, vertical flux of material between the surface and the deep ocean takes place near the basin margins where primary production is highest (see Secs 9.2.2.2 & 10.4). Elements can also be retained in the coastal zone by physical current regimes at the shelf edge. However, water brought to the surface by coastal upwelling can be transported into the central gyres along isopycnals without significant inputs from below (see e.g. Collier & Edmond 1984), and the interactions of the various coastal ocean–open ocean processes can be illustrated with respect to a number of recent investigations.

11.4.1 Coastal surface waters: the North Sea

An interesting example of the factors that control the distributions of Cd, Cu, Ni and Mn in surface coastal waters has been provided by Kremling (1983, 1985) for the North Sea. Samples were collected on two transects: (1) an open-ocean Atlantic–Bristol Channel–European North Sea coast transect, and (2) an open-ocean North Atlantic–northern Scottish coast–European North Sea coast transect. The most striking feature in the distributions of dissolved Cd, Cu, Ni and Mn on both transects was a sharp decrease in concentrations as the shelf/open-ocean Atlantic boundary was crossed – see Figure 11.1. This is an example of how dissolved trace elements can be retained in the coastal zone by the physical circulation regime. However, the processes maintaining the elevated metal concentrations in the shelf waters of the two transects were different, and illustrate how coastal receiving waters can be influenced by a variety of input processes.

TRANSECT 1 On this transect there was an increase in the dissolved

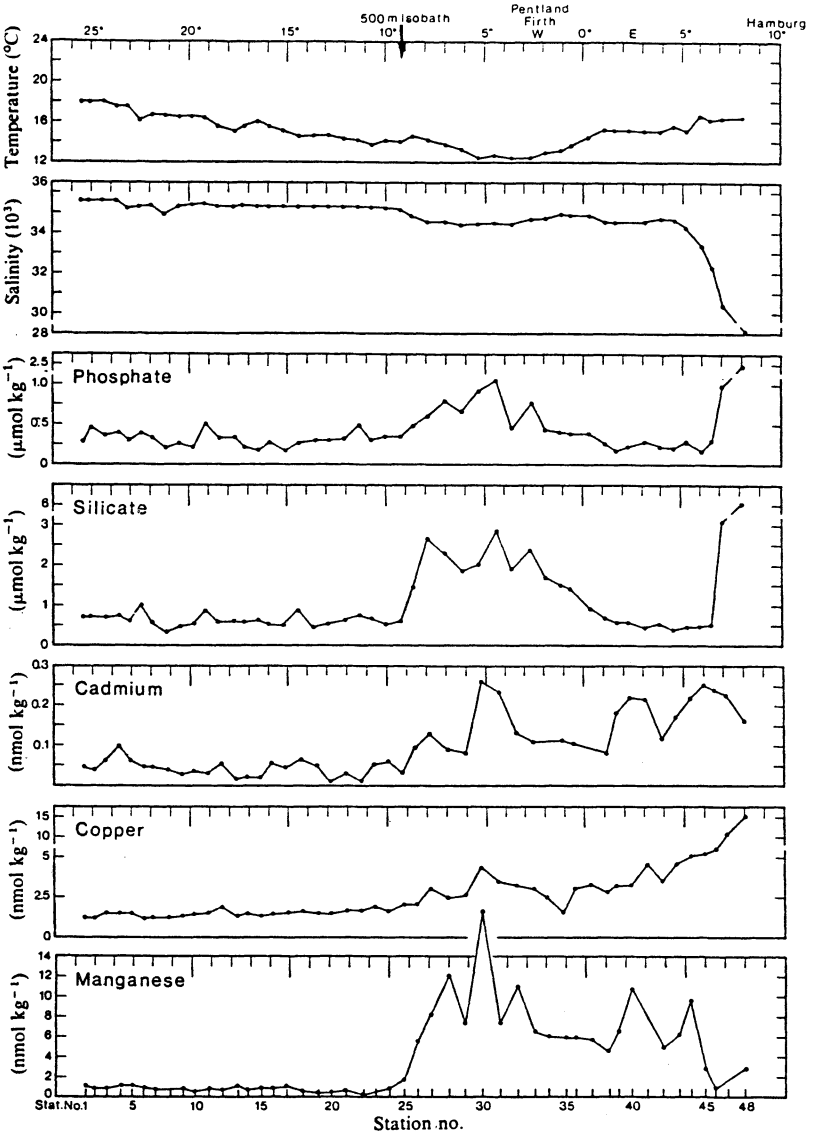

Figure 11.1 Surface water distributions of Cd, Cu, Ni, Mn and Al on an open-ocean Atlantic–European coast transect (from Kremling 1983): the shelf edge is indicated by the 500 m isobath.

concentrations of Cd, Cu, Ni and Mn in passing from the open-ocean Atlantic to the Bristol Channel, and a further increase as the North Sea European coast was approached. Kremling (1985) suggested that this transect could be considered to cross the mixing zone of two end-member waters, which could be identified as (a) the high-salinity open-ocean Atlantic water end-member, and (b) the low-salinity coastal shelf water end-member. Using the two waters as end-members of a mixing series, Kremling (1985) plotted the dissolved trace metal data from transect 1 as a function of salinity; the relationships for Mn, Cu and Cd are illustrated in Figure 11.2a. Although there was some scatter in the plots, the author extrapolated the data back to a *zero-salinity*, or river, end-member (see Sec. 6.1.4), and concluded that the mixing of the river end-member (in terms of the net estuarine output) and the open-ocean Atlantic water end-member could account for the reported dissolved distributions of Cd, Cu, Ni and Mn without having to invoke additional sources of the metals to the shelf waters.

TRANSECT 2 The edge of the shelf area on transect 2 is characterized by strong horizontal salinity gradients at **fronts**, which mark the boundary between Scottish coastal and open-ocean waters. There are also very sharp gradients in the trace metal concentrations across this boundary – see Figure 11.1. Kremling (1985) attempted to relate the elevated concentrations of dissolved Cd, Cu, Ni and Mn in the shelf region to the mixing of end-member waters. However, he reported that the concentrations of Cd, Cu and Mn, but not those of Ni, deviated strongly from the salinity mixing line; the relationships for Mn, Cu and Cd are illustrated in Figure 11.2b. These deviations from the mixing line were interpreted as indicating that Cd, Cu and Mn require a source in addition to that arising from the mixing of the low-salinity shelf and the high-salinity open-ocean water masses. Kremling (1983, 1985) rejected an atmospheric source on the grounds that this type of input would not produce trace metal distributions with such distinct boundaries. He concluded instead that the most plausible explanation for the elevated dissolved concentrations of Cd, Cu and Mn was their diagenetic remobilization, and subsequent diffusion, from partly reduced shelf sediments followed by their transport to surface waters by tidal mixing. Balls (1985) gave data for Cu and Cd concentrations in Scottish coastal waters and he too was able to identify a trace metal, salinity-associated, front to the north and northeast of Scotland. The front separated the low-salinity, trace metal-rich, coastal water from high-salinity, trace metal-poor, open-ocean water. However, Balls (1985) carried out vertical profiling of Cu and found that the concentrations decreased with depth in the water column. Since a bottom sediment source would result in an increase with depth in the water, the author concluded that freshwater inputs, and not diffusion out of

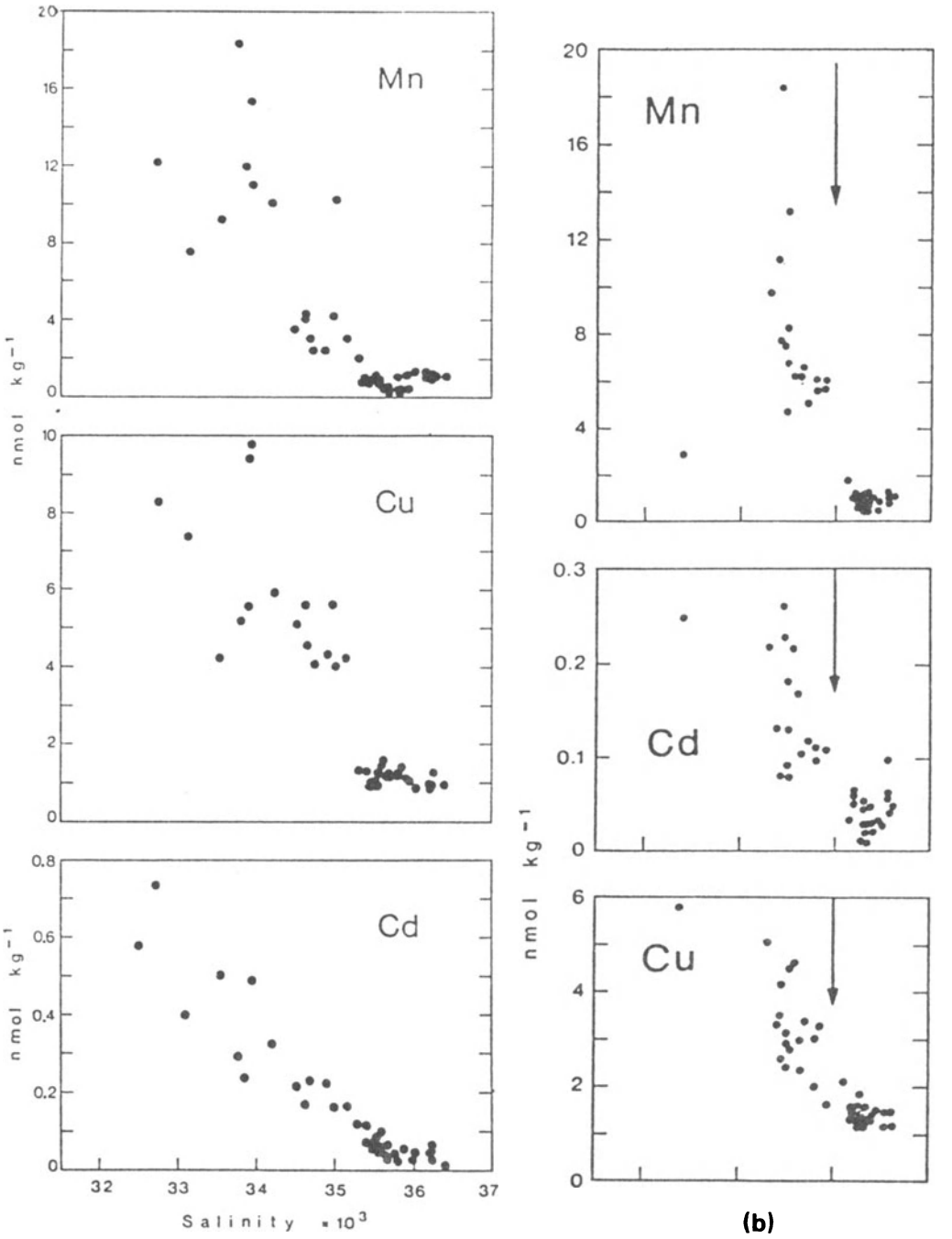

Figure 11.2 Element versus salinity relationships from Atlantic open-ocean–European coast transects (from Kremling 1985): (**a**) transect 1 (see text); (**b**) transect 2 (see text).

sediments, was the most important process maintaining the higher trace metal concentrations in the coastal waters.

11.4.2 Open-ocean surface waters: the North Pacific

It was shown in the preceding section that surface water dissolved trace element distribution profiles in coastal receiving zones are affected by variations in the source strengths of the major input mechanisms and by the rate at which the elements are scavenged from solution. A combination of these factors can impose 'fingerprints' on the concentration patterns of the trace metals, and some of these can be traced out towards the open ocean. For example, the use of mixing graphs to identify a zero-salinity end-member can, in some cases, be used to identify fluvial inputs and to establish whether or not additional inputs, such as those from the atmosphere or bottom sediments, have been imposed onto the river discharges. However, Measures *et al.* (1984) have pointed out that there is no direct method that can be used to distinguish atmospheric from fluvial trace metal inputs in *open-ocean* waters. Nonetheless, indirect 'trace metal distribution' aproaches have been used to unscramble both coastal and open-ocean surface input signals. One such approach was adopted by Schaule & Patterson (1981). In the study reported by these authors surface water samples were collected in the North Pacific on a transect that extended from off the coast of California out to the central gyre. This transect passed through a variety of oceanographic environments, which included: (a) the nutrient-rich waters of the biologically productive outer shelf region, (b) an intermediate open-ocean region, and (c) the biologically non-productive centre of the North Pacific gyre. Generalized surface water distribution profiles of the trace metals determined in the investigation are illustrated in Figure 11.3. On the basis of their distributions along this transect the trace metals can be divided into three broad groups.

COPPER AND NICKEL The distributions of Cu and Ni exhibit a negative, i.e. decreasing, horizontal surface concentration gradient away from the coastal upwelling area out towards the open ocean, and reach their lowest values around the central gyre. This type of negative coastal → open-ocean surface water concentration profile is to be expected (a) if trace metals are supplied to the coastal receiving zones by processes such as river run-off, atmospheric deposition, diffusion from sediments and shallow depth coastal upwelling, and (b) if only a fraction of the elements from these inputs subsequently escapes the coastal zone and is transported horizontally to the open ocean by advection–diffusion processes.

LEAD The concentrations of Pb in the Pacific transect exhibit a gradient

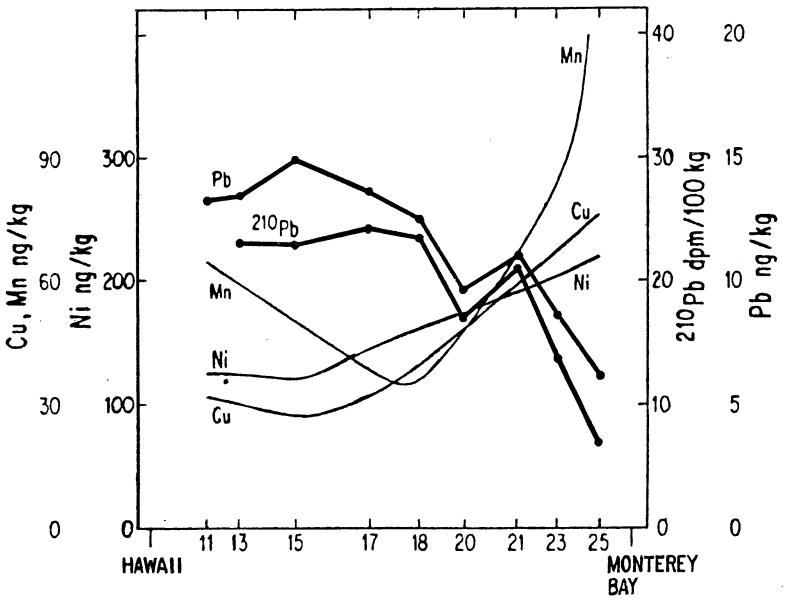

Figure 11.3 Trace element surface water distribution patterns of a North Pacific transect (from Schaule & Patterson 1981).

that is the opposite to that shown by both Cu and Ni, i.e. the lowest Pb concentrations are found in the biologically active waters of the outer shelf region and there is a general increase out towards the central gyre, in which the surface waters have about three times as much dissolved Pb as those of the shelf region. The concentrations of dissolved Pb at depth in the water column are lower than those in surface waters (see Sec. 11.5), which precludes the possibility that vertical redistribution by upwelling can be the dominant supply mechanism for Pb in the mixed layer. Schaule & Patterson (1981) concluded, therefore, that the surface water distribution of dissolved Pb had resulted from strong *external* inputs to the surface waters. However, the surface water Pb distribution pattern, with lower values in the coastal areas and higher values in the central gyre, has a concentration gradient which means that the external input into coastal waters cannot all subsequently undergo off-shelf transport by advection–diffusion to the open-ocean. The distribution of common Pb along the Pacific transect is very similar to that of ^{210}Pb, which has a predominantly aeolian input to the ocean. Both forms of Pb are subject to removal processes from surface waters, and Schaule & Patterson (1981) proposed that the distribution of Pb in the surface waters of the Pacific transect was maintained by the element having a strong

atmospheric input to both coastal and open-ocean areas, coupled with a higher rate of removal from surface waters in the coastal areas where the rates of biological activity, and so the concentrations of TSM, are higher than they are in the central gyres. The predominantly atmospheric input of Pb to the oceans is entirely consistent with the elemental source strengths discussed in Section 6.4.

MANGANESE The surface water distribution of Mn along the Pacific transect exhibits a pattern that is intermediate between those of Cu and Ni on the one hand, and Pb on the other. That is, the highest concentrations of Mn are found in the coastal waters and there is a general decrease out into the open ocean; thus, Mn exhibits a negative concentration gradient, which is similar to those of Cu and Ni – see Figure 11.3. This type of profile suggests that there must be a significant input of Mn to the coastal receiving zone (e.g. by river run-off or diffusion from bottom sediments) where much of it is removed from the surface waters, so leading to a diminished lateral transport of the element to the open ocean. In the coastal zone, therefore, it would appear that the dominant input of Mn is by fluvial transport and/or sediment diffusion, whereas that for Pb is largely atmospheric. In the open-ocean waters, however, the surface distribution of Mn differs from those of Cu and Ni in that its concentrations increase to reach higher values in the central gyre. As with Pb, this type of distribution may indicate an atmospheric input to the open-ocean North Pacific, with the lowest rate of removal from surface waters occurring in the biologically inactive central gyre. Unlike Pb, however, the input of Mn from river run-off and/or sediment diffusion in the coastal regions overshadows that from the atmosphere (see also Landing & Bruland 1980, Bruland 1983). There is no doubt, however, that in some open-ocean regions the surface waters can retain 'fingerprints' of an atmospheric input of Mn (see Sec. 6.4).

OTHER TRACE METALS Surface water profiles are also available for elements that were not studied by Schaule & Patterson (1981). From the point of view of understanding the involvement of trace metals in the biogeochemical oceanic cycles, Cd is one of the most important of these elements. Boyle *et al.* (1981) and Boyle & Huested (1983) gave data on the distribution of this element in surface waters of the North Atlantic and North Pacific oceans, and reported that the highest Cd concentrations were found in areas of equatorial upwelling (80 pmol l^{-1}) and the lowest in the non-upwelling open-ocean (< 10 pmol l^{-1}). Kremling (1985) also found that Cd was enriched in high-latitude, nutrient-rich, waters of the Atlantic relative to the oligotrophic subtropical waters. Another element that is important from the process-orientated viewpoint is Al. Orians & Bruland (1986) presented results which showed that in the North Pacific

the concentrations of dissolved Al are lowest in the eutrophic California Current (0.3–1 nmol l^{-1}) and increase westwards into the subtropical North Pacific Gyre (~ 5 nmol l^{-1}), with values in the South Pacific Gyre being five-fold lower than those in the North Pacific. The authors suggested that much of the fluvial input of dissolved Al is taken out of solution by intense scavenging in the particle-rich estuarine and highly productive coastal zones, and concluded that the increasing coastal → open-ocean horizontal concentration trends indicate that the primary source of dissolved Al to the surface ocean is via solubilization from aeolian dust following atmospheric deposition. Surface values for dissolved Al will therefore reflect the atmospheric source strength; thus, concentrations decrease in the order North Atlantic > North Pacific > South Pacific (see also Orians & Bruland 1985).

11.4.3 Geographical variations in trace elements: summary

The general patterns in the surface water distributions of a number of process-orientated trace elements in the oceans have been described above, and these can be summarized as follows.

The concentrations of many trace elements are usually higher, sometimes by orders of magnitude, in the surface waters of the coastal receiving zones than they are in open-ocean waters. This reflects the inputs from two major *primary* external sources, i.e. fluvial run-off and atmospheric deposition, both of which have stronger trace metal signals in the coastal environment. The coastal receiving zone is defined by a series of intensively active boundaries, which include the river/ocean, the air/sea, the sediment/sea water and the shelf/slope/open-ocean interfaces. Boundary processes occurring across these interfaces make the zone a region of high trace metal reactivity. Once they have reached the coastal zone, trace metals can be affected by a number of processes, the most important of which are summarized below.

(a) They can be removed into bottom sediments in association with inorganic (scavenging) and/or organic (biological) particulate matter.
(b) They can undergo recycling. This can take place in the water column, e.g. within the biological removal–upwelling cycle, or across the sediment/water or air/sea interfaces.
(c) They can be exported directly out of the coastal zone to the open ocean.

Trace elements are transported to open-ocean surface waters from the coastal receiving zones by advection and diffusion. As admixture between shelf, slope and open-ocean waters takes place there is a negative trace element concentration gradient away from the boundaries of the continents, leading to progressively smaller surface water concentrations

in the more remote oceanic areas. However, this overall lateral, physically transported, negative coastal → open-ocean concentration gradient can be modified in two principal ways.

(a) The gradient will be sharpened if the trace metal has a predominantly nearshore supply and undergoes very strong removal in the coastal zone by processes such as enhanced scavenging, nutrient trapping and retention at fronts.
(b) The direct open-ocean supply of trace elements can significantly modify the coastal → open-ocean negative concentration gradients, sometimes to the extent of totally reversing the trend. For example, an atmospheric supply coupled with a strong scavenging removal in coastal waters results in the surface water concentrations of Pb in the North Pacific being highest in the remote unproductive regions of the central gyre.

These elemental distribution patterns raise the critial question of the status of the central ologitrophic oceanic gyres in the marine cycles of the trace metals, and open up again the possibility of using inter-oceanic differences in trace element concentrations as source indicators. According to Bruland & Franks (1983) it is to be expected that trace metal concentrations in the subtropical gyres of the North Atlantic and the North Pacific, i.e. oceanographically equivalent areas, should reflect any differences in the magnitudes of the source terms in the two regions. The North Atlantic has stronger river and atmospheric input signals than does the North Pacific, with the result that the two principal external sources of trace metals to surface waters deliver greater quantities of the metals to the North Atlantic. The average concentrations of a series of trace metals in the surface waters of the subtropical gyres in the North Atlantic and North Pacific are listed in Table 11.3. From this table it can be seen that the concentrations of Mn, Cu and Pb in the surface waters of the North Atlantic Gyre are about twice as high as those in the North Pacific Gyre, thus reflecting the magnitudes of their external inputs to the two regions. However, the concentrations of Cd, Zn and Ni are essentially the same in surface waters from both gyre systems, thus suggesting that a source, or sources, in addition to those arising from river and atmospheric transport must be operating to maintain this surface water similarity. It was shown above that some elements (e.g. Cd, Ni) appear to have higher surface water concentrations in regions of upwelling. Thus, the transport of water from depth in the oceanic column would seem to be the most probable source for these elements to the mixed layer, even in the central gyres where the rate of upwelling is relatively slow.

It may be concluded, therefore, that trace element distributions in the surface ocean reflect: (a) their source strengths, i.e. the magnitudes of

Table 11.3 Concentrations of some trace metals in surface and deep waters of the subtropical central oceanic gyres (units, nmol l^{-1})

Element	North Atlantic Gyre		North Pacific Gyre	
	Surface water[a]	Deep water[b]	Surface water[a]	Deep water[b]
Cd	0.0020	0.29	0.0015	0.87
Cu	1 - 1.5	2.0	0.5	4.0
Ni	2.3	6.0	2.1	10
Zn	0.06	1.7	0.07	8.5
Pb	0.17	0.025	0.075	0.005
Mn	2.4	0.6	1.0	0.2

[a] Data from Bruland & Franks (1983).
[b] Data from Bruland & Franks (1983), Schaule & Patterson (1981) and Bruland (1983). Some data have been obtained from distribution profiles and are only approximate.

their input mechanisms from both external and internal sources; (b) their removal strengths, i.e. the magnitude of their output mechanisms; and (c) surface water circulation patterns, the effects of which are superimposed on those of both the input and the output mechanisms.

11.5 The vertical distribution of trace elements in the water column

Surface water distributions can be extremely useful in identifying the effects that source strengths have on 'fingerprinting' trace element distributions in the mixed layer. However, both the surface and the deep ocean reservoirs are zones of trace metal reactivity, and in order to assess the effects that internal oceanic processes have on trace metal distributions it is necessary to obtain data on their vertical as well as their lateral profiles. The most common approach that has been adopted to aid the interpretation of vertical profiles is to relate the distributions of individual elements to those of other species whose distributions are relatively well understood. These species include the following: (a) the *nutrients*, which can be used to assess the involvement of trace metals in both the labile and refractory stages of the oceanic biogeochemical cycles; (b) *dissolved oxygen*, to which redox-mediated reactions can be related; and (c) *particulate matter*, to which scavenging reactions and sediment resuspension can be related.

In his review paper, Bruland (1983) utilized the new data to distinguish between a number of types of vertical trace element distribution profiles in the oceans. These distributions can be summarized as follows.

11.5.1 Conservative-type vertical trace metal profiles

Elements with conservative profiles have a constant concentration relative to salinity, which results from their generally low reactivity in sea water. Trace elements with this type of profile include the hydrated cations of Rb^+ and Cs^+, and the molybdate oxyanion MoO_4^{2-}.

11.5.2 Nutrient-type vertical trace metal profiles

The characteristic features of the vertical concentration profiles of trace metals with nutrient-type profiles are (a) a depletion in surface waters and (b) an enrichment at some depth within the water column. These features arise from the involvement of the elements in the oceanic biogeochemical cycles (for a description of the nutrient cycles see Sec. 9.1). Phytoplankton utilize nutrients (phosphate, nitrate, silicate) in the euphotic zone and as they grow they extract trace elements from the water, thus leading to their depletion in these surface waters. As the organisms die and sink down the water column they undergo oxidative decay during which there is a regeneration of the nutrients, and the associated trace elements, back into solution. There is also a net flux of organic debris out of the euphotic zone (the CPM – see Sec. 10.4), which carries nutrients and trace metals to deeper waters where decomposition results in a further release of material back into solution as the organic carbon is oxidized. Bruland (1983) identified three types of nutrient-related vertical trace metal profiles.

LABILE NUTRIENT-TYPE VERTICAL TRACE METAL PROFILES The labile nutrients (phosphate, nitrate and organic carbon) are associated with the soft tissue phases of organisms, and undergo rapid regeneration in the *upper* water column. Trace metals having labile nutrient-type profiles thus have vertical distributions similar to those of phosphate and nitrate, i.e. they exhibit a surface depletion followed by a shallow water regeneration, which leads to a mid-depth concentration maximum. This type of profile is shown by dissolved Cd – see Figure 11.4a.

The oceanic distribution of dissolved Cd has been studied by a number of workers in the post-1975 period, and concentrations are reported to be in the range ~ 1–2 pmol l^{-1} in surface waters, rising to ~ 1 nmol l^{-1} at depth (see e.g. Boyle *et al.* 1976, Martin *et al.* 1976, Bruland 1980, Bruland & Franks 1983, Danielsson & Westerlund 1983, Moore 1983, Boyle & Huested 1983, Burton *et al.* 1983, Boulegue 1983, Spivack *et al.* 1983, Kremling 1983, 1985). From these various studies a reasonably detailed picture of the oceanic distribution of Cd has emerged. The predominant feature in the vertical profile of dissolved Cd is a shallow water regeneration cycle similar to those of phosphate and nitrate. In the North Pacific, for example, dissolved Cd and phosphate are linearly

correlated, at phosphate concentrations in excess of 0.2 μmol l^{-1}, by the regression:

$$[Cd] = (0.347 \pm 0.007)[P] - (0.068 \pm 0.017) \quad (\text{mean} \pm \text{s.d.}; r = 0.992)$$

where [Cd] is in units of nmol l^{-1} and [P] is in units of μmol l^{-1}. However, there are distinct regional changes in Cd–nutrient correlations (see e.g. Boyle & Huested 1983).

The similarity between the dissolved Cd and phosphate profiles (see Fig. 11.4a) suggests that there is an organic tissue Cd carrier phase produced by phytoplankton in the euphotic layer, which sinks and is decomposed mainly in the upper waters, thus releasing the Cd back into solution; the carrier-phase association is considered in more detail in Section 11.6.3.2. This type of vertical Cd distribution profile appears to be characteristic of the upper water column of all the major oceans. However, although the vertical profiles of dissolved Cd are generally similar, the deep water concentrations of the element vary considerably between the major oceans, decreasing in the order North Pacific ($\sim$ 0.8 nmol l^{-1}) > Indian Ocean ($\sim$ 0.5 nmol l^{-1}) > North Atlantic ($\sim$ 0.3 nmol l^{-1}). According to Bruland & Franks (1983), this is a consequence of the deep water circulation pattern in which the North Pacific lies at the end of the 'global grand tour' Atlantic → Indian → Pacific deep water circulation path, and so is older than the deep water in the other oceans.

REFRACTORY NUTRIENT-TYPE VERTICAL TRACE METAL PROFILES The refractory nutrients are associated with the hard skeletal parts of organisms and have a deep water regeneration. Trace metals having refractory nutrient-type profiles have vertical distributions similar to those of silicate, i.e. a surface depletion followed by a deep water regeneration, which leads to a deep water concentration maximum. Zinc is an example of a trace metal having a refractory nutrient-type profile.

Recent data on the vertical distribution of Zn in the oceanic water column have been provided by various workers, and concentrations seem to range between $\sim$ 0.05 nmol l^{-1} in surface waters and $\sim$ 9 nmol l^{-1} at depth (see e.g. Bruland *et al.* 1978, Bruland 1980, Danielsson 1980, Bruland & Franks 1983, Danielsson & Westerlund 1983, Magnusson & Westerlund 1983). In general, the vertical distribution of dissolved Zn is highly correlated with that of silicate, thus showing a strong surface depletion and a deep water enrichment; a typical dissolved Zn profile, together with that for silicate, is illustrated in Figure 11.4b. The correlation between Zn and silicate in North Pacific waters was assessed by Bruland (1980), who reported the following relationship:

$$[Zn] = (0.0535 \pm 0.0008)[Si] - (0.02 \pm 0.09) \quad \text{mean} \pm \text{s.d.}; r = 0.996)$$

where Zn is in units of nmol l^{-1} and Si is in units of μmol l^{-1}. From this type of vertical profile, in which the distribution of Zn mirrors that of silicate, it would appear that the Zn is involved in a deep regeneration cycle of the kind that affects opal (silicate) and calcium carbonate. Like those of Cd, the deep water concentrations of Zn are controlled by oceanic circulation patterns, with the highest values being found in the North Pacific deep waters at the end of the global circulation path.

COMBINED LABILE–REFRACTORY NUTRIENT-TYPE VERTICAL TRACE METAL PROFILES

Trace metals with this type of vertical profile have both a shallow water and a deep water regeneration cycle. Nickel is an example of such an element.

The vertical distribution of Ni in oceanic waters has been widely reported and concentrations appear to range from ~ 2–3 nmol l^{-1} in surface waters to ~ 12 nmol l^{-1} in the deep waters of the North Pacific (see e.g. Sclater *et al.* 1976, Bruland 1980, Danielsson 1980, Boyle *et al.* 1981, Bruland & Franks 1983, Danielsson & Westerlund 1983, Boyle & Huested 1983, Spivack *et al.* 1983, Magnusson & Westerlund 1983). Although the vertical distribution of Ni in the water column displays a nutrient-type profile, the relationship between the element and the nutrients is not as clear cut as those for either Cd (labile-type) or Zn (refractory-type). This was demonstrated by Sclater *et al.* (1976), who showed that vertical profiles of dissolved Ni in both the Atlantic and Pacific Oceans could be correlated with either phosphate (labile-type nutrient) or silicate (refractory-type nutrient) – see Figure 11.4c. The authors concluded therefore that the vertical distribution of Ni in the water column could be interpreted in terms of the incorporation of the element into both the soft tissue parts (phosphate analogue) and the hard skeletal parts (silicate analogue) of organisms, which would lead to both a shallow and a deep water regeneration stage, with each having a dissolved Ni concentration maximum. Like all nutrient-type elements, Ni has higher concentrations in the deep waters of the North Pacific than in those of the North Atlantic.

There is no doubt that the involvement of elements such as Cd, Ni and Zn in the oceanic biogeochemical cycles leads to them having nutrient-type distibutions in the water column, with the main features being the surface water depletion and the subsurface enrichment in dissolved concentrations. However, the relationships between the trace metals and the nutrients are not always simple. For example, although the correlations between some trace metals and their nutrient analogues can be described by linear equations, there is evidence that the coefficients of these equations are not globally unique and can in fact vary regionally (see e.g. Boyle *et al.* 1981, Spivack *et al.* 1983).

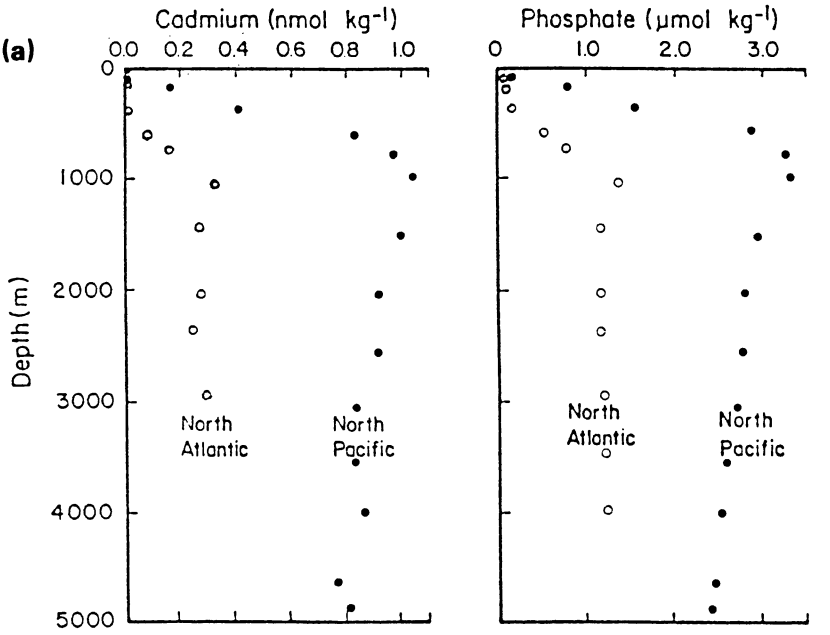

Figure 11.4a-e Vertical profiles of dissolved trace elements in the oceans (from Bruland 1983, which lists the original data sources).

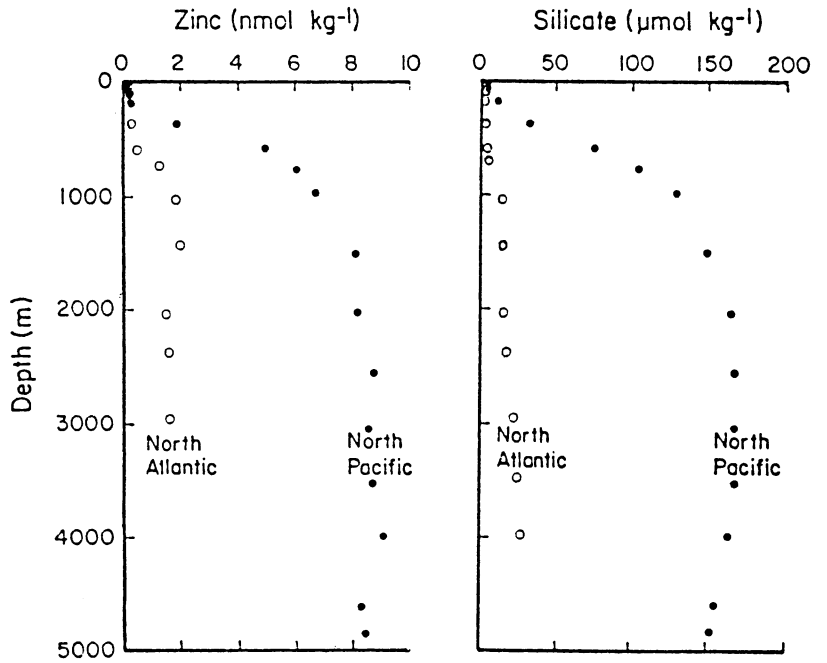

Figure 11.4b **(b)**

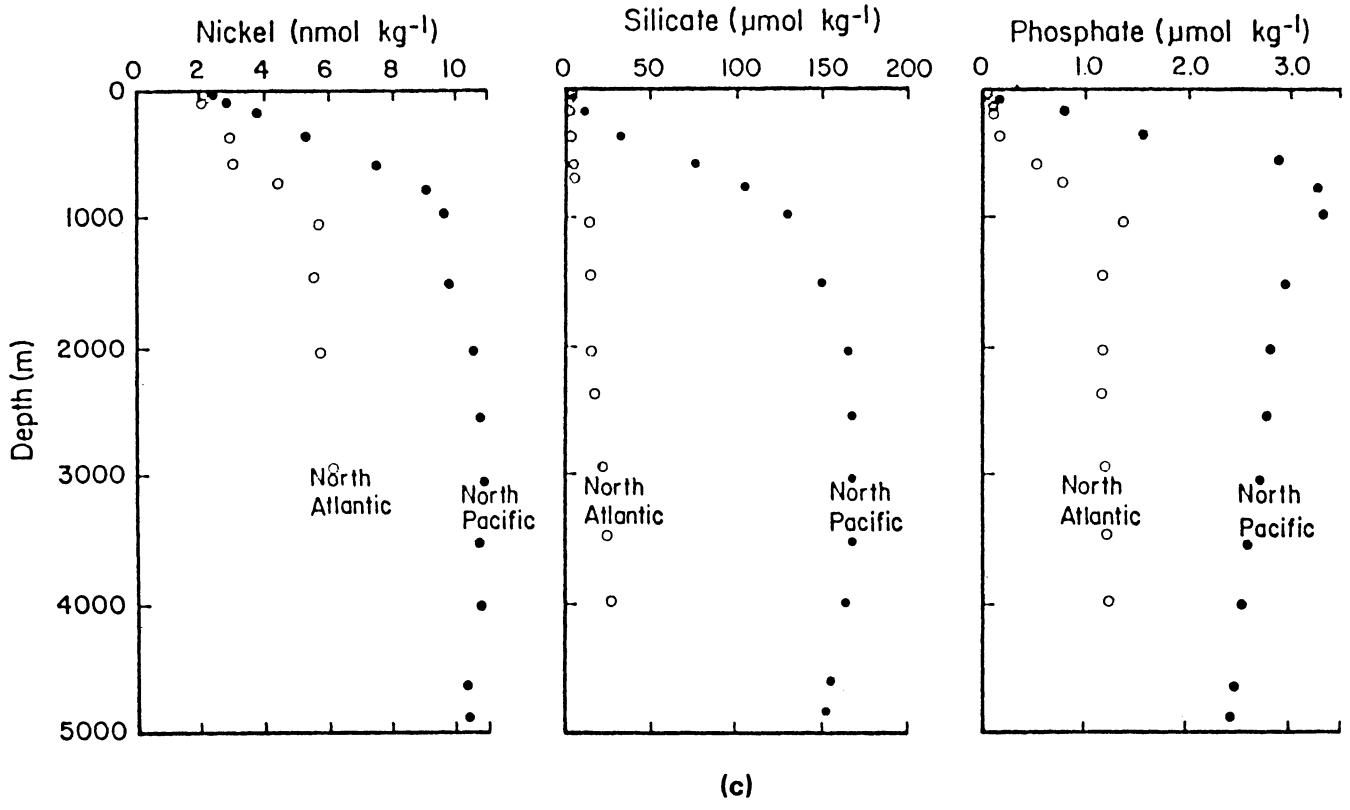
Nickel (nmol kg-1)
0
2
4
6
8
10
Silicate (µmol kg-1)
0
50
100
150
200
Phosphate (µmol kg-1)
0
1.0
2.0
3.0
Depth (m)
0
1000
2000
3000
4000
5000
North Atlantic
North Pacific
North Atlantic
North Pacific
North Atlantic
North Pacific
(c)

Figure 11.4c

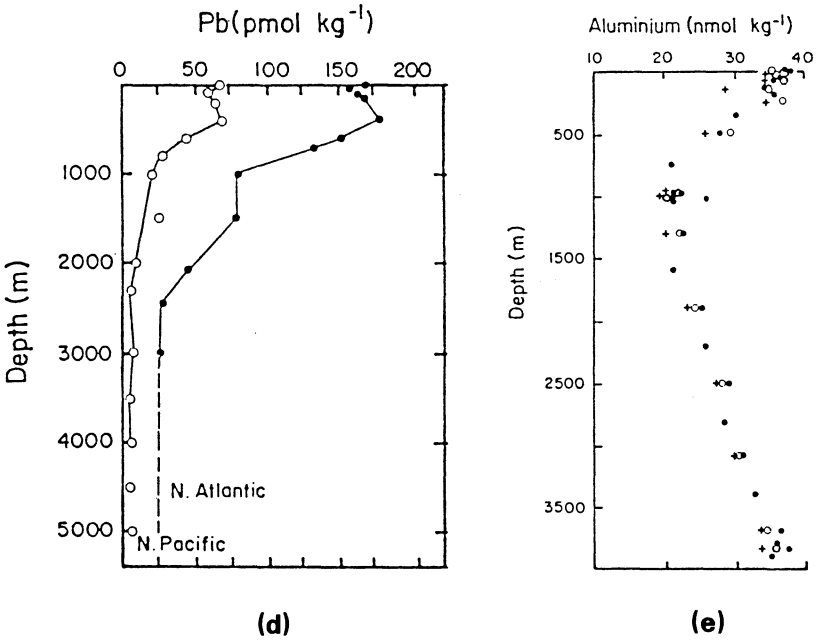

Figure 11.4d, e

11.5.3 Surface enrichment–depth depletion type of vertical trace metal profiles

Two prime requirements are necessary in order for a dissolved trace element to maintain this type of vertical oceanic profile: (a) it must be introduced mainly into surface waters, and (b) it must be removed rapidly from solution before it can be transported down the water column, i.e. its residence time must be short relative to the mixing time of the ocean. Trace elements can have a direct input to surface waters either via atmospheric transport (e.g. Pb) or by horizontal mixing into surface waters following delivery from rivers or release from shelf sediments (e.g. Mn). In addition, Bruland (1983) identified a further surface water input in which selected oxidation states, or specific chemical forms, of an element can undergo *in situ* production in surface waters followed by changes in deeper waters. For example, the production of arsenite from arsenate in the euphotic zone is a result of biologically mediated redox reactions, and this is followed by oxidation of the arsenite to arsenate at depth.

Lead is perhaps the most widely studied of the trace metals that exhibit a surface enrichment–depth depletion vertical oceanic profile. Much of our knowledge of the distribution of Pb in the marine environment has come from the pathfinding work carried out by Clair Patterson and his

group at the California Institute of Technology, Pasadena. Thanks to this work, the principal features in the oceanic distribution of Pb are now known in some considerable detail, and they may be summarized as follows.

(a) The concentrations of Pb in surface waters are higher in the North Atlantic than in the North Pacific, and in both localities they increase from the ocean margins out towards the central gyres (see Sec. 11.4).
(b) Surface water concentrations of Pb are higher than those in deep waters. This effect is most pronounced in the North Atlantic – see Figure 11.4d.
(c) Deep water concentrations of Pb in the North Atlantic, i.e. at the start of the global deep water 'grand tour', are higher than those in the North Pacific, i.e. at the end of the deep water circulation path.

This is in contrast to the distributions of the nutrient-type trace metals, which have their highest deep water concentrations in the North Pacific (see above). The factors that produce these features in the oceanic distribution of Pb have been interpeted within a general framework in which the principal input of Pb to the oceans is via the atmosphere into surface waters. The Pb is then removed relatively rapidly throughout the whole water column by scavenging reactions involving small-sized TSM. However, the atmospheric input is of a sufficient magnitude to maintain the enhanced surface water concentrations. In deep waters the residence time of dissolved Pb is short compared to the deep water circulation cycle, which, together with a stronger Atlantic than Pacific surface input signal, results in deep water Pb concentrations in the North Atlantic being higher than those in the North Pacific.

On a more detailed scale, Boyle *et al.* (1986) have shown how seasonal variations can affect the vertical distribution of Pb in the western North Atlantic. In this region, a temporal cycle operates and this may be briefly summarized as follows.

(a) The winter mixed layer accumulates aeolian-transported Pb.
(b) This Pb is depleted by scavenging during the spring bloom, prior to the formation of the seasonal thermocline.
(c) The shallow summer mixed layer is progressively enriched in Pb from aeolian sources.
(d) Following the break-up of the seasonal thermocline, a secondary autumn bloom occurs, which depletes the waters of Pb.
(e) The winter mixed layer then accumulates Pb until the spring, when the cycle begins again.

Recent evidence suggests that, although it has a more complex oceanic

chemistry, Hg shares some of the vertical distribution features common to Pb (see e.g. Gill & Fitzgerald 1988). The major input source for Hg to the oceans is atmospheric deposition, and vertical profiles of the element often exhibit a maximum within the main thermocline region. Below this maximum the Hg concentrations fall off, indicating that rapid scavenging occurs and maintains the low concentrations found in deep waters. As a result of its oceanic reactivity, Hg has a relatively short residence time in sea water, which Gill & Fitzgerald (1988) estimated to be ~ 350 yr. The distribution of Hg is of particular interest because it can be used to illustrate the importance that advection can have on the transport of elements in the oceans. According to Gill & Fitzgerald (1988) Hg is advected to the open ocean following its diagenetic release from coastal sediments. However, the authors also suggested that the element can be redistributed within the open-ocean regions themselves from advective water transport via mixing along isopycnals from areas where there is an enhanced atmospheric input to areas where the input is less strong. Thus, the authors suggested that the Hg maximum in the main thermocline in the Sargasso Sea could have originated from the isopycnal transport of Hg-enriched waters from surface outcrops at higher latitudes, thus demonstrating that horizontal transport can affect the vertical distribution of Hg in the water column.

11.5.4 Mid-depth minimum-type vertical trace metal profiles

Two examples of these profiles can be identified: those associated with a surface and deep water source, and those associated with sub-oxic waters.

PROFILES ASSOCIATED WITH A SURFACE AND DEEP WATER SOURCE These are associated with a surface water source, scavenging throughout the water column and a bottom water source. The surface enrichment–depth depletion type of profile (see above) will be significantly modified if there is also a source signal from sediments at the base of the water column; the three-layer model for the vertical distribution of TSM in the oceanic waters is an analogue for this – see Section 10.2.

Aluminium has been cited as an example of an element that can have a mid-depth minimum-type profile, which can be maintained by both surface water and deep water inputs. Al(III) has a strong tendency to hydrolyse in sea water to form particle-reactive dissolved species, and its concentration is apparently controlled by scavenging processes. Hydes (1979) derived a depth–concentration profile for dissolved Al in the North Atlantic and reported a gradual decrease in concentration from the surface waters (~ 38 nmol l^{-1}) down to ~ 1000 m (~ 22 nmol l^{-1}), followed by a steady increase to ~ 4000 m (~ 38 nmol l^{-1}) – see Figure 11.4e. To account for this type of vertical distribution, Hydes (1979) outlined the following sequence of events.

(a) Al is solubilized from the atmospheric material deposited to the North Atlantic surface water layers (see Sec. 6.2).
(b) Once the Al is brought into solution, it is scavenged by siliceous shells, leading to a decrease in dissolved Al concentrations below the surface layer. Orians & Bruland (1985) suggested that in addition to passive adsorption onto particles, e.g. in the open ocean, there is evidence that dissolved Al can be removed from solution via an active biological uptake mechanism, e.g. in confined basins such as the Mediterranean Sea.
(c) Unlike the situation for Pb (see above), the decrease in dissolved Al is, in this type of profile, balanced by an input from deep water sources, e.g. by dissolution from suspended sediment particles.

However, the vertical water column distribution of Al can be modified by advective, as well as by local source–scavenging relationships. This has recently been demonstrated for the Atlantic by Measures *et al.* (1986). One of the interesting features in the vertical distribution of Al in this ocean is that, whereas in the northwest Atlantic the profiles exhibit a surface maximum (from aeolian deposition), a mid-depth minimum and an increase in deep water, those in the northeast Atlantic do not show the deep water increase. Measures *et al.* (1986) related the different deep water Al signatures in these and other areas to the distribution of water masses in the vertical oceanic sections. Thus, they suggested that European shelf waters, which are enriched in Al having a fluvial origin, are advected into the southern Greenland Sea where they participate in the formation of Antarctic Intermediate Water, which is the major contributor to the Greenland–Scotland overflows. Thus, North Atlantic Deep Water at high latitudes in both the eastern and western basins is enriched in Al. However, although this enrichment extends south to at least 30°N in the western basin, it is not found in the eastern basin, where the circulation is more sluggish at this latitude; this therefore offers a possible explanation for the difference in the deep water Al profiles in the northwest and northeast Atlantic. According to this concept, therefore, the advection of Al-rich coastal waters to regions of convective water mass formation can result in the injection of Al-rich waters into the deep interior of the ocean, where they modify the vertical Al profile. The surface enrichment type of dissolved Al water column profile is evidently typical of areas in which there is a significant atmospheric mineral aerosol signal to the surface waters. However, the concentrations of dissolved Al differ from ocean to ocean, depending on local input source strength signals. For example, Orians & Bruland (1985, 1986) presented data which showed that, although the vertical distribution features for dissolved Al are similar in the North Atlantic and the North Pacific, the concentrations are 8–40 times lower in the central North Pacific than in

the central North Atlantic. This inter-oceanic fractionation of dissolved Al can be explained by geographical variations in the atmospheric Al sources, which are much stronger in the central North Atlantic. In some regions, however, atmospheric source strength variations can actually modify the vertical dissolved Al profile. For example, at high latitudes the atmospheric input may not be sufficient to maintain the surface maximum, and here the maximum may in fact be entirely absent, although there is still an input of dissolved Al from the bottom sediments (see e.g. Olafsson 1983). In general, however, the vertical distribution of Al in sea water is controlled by a surface atmospheric input, a deep water source (e.g. from the advection of Al-rich waters or via sediment resuspension) and intense scavenging throughout the water column.

PROFILES ASSOCIATED WITH SUB-OXIC WATERS According to Bruland (1983) this type of mid-depth minimum, which results from solubilization–precipitation reactions associated with redox changes, can be associated with the presence of subsurface, oxygen-depleted (or sub-oxic) water layers, which are found in some oceanic areas, such as the eastern tropical Pacific and the northern Indian Ocean (see Sec. 8.3). Under these conditions, mid-depth concentration minima in elemental profiles can be established when the reduced form of an element is relatively insoluble, or when it is removed from solution in association with particulate phases. Bruland (1983) used Cr(III) as an example of the reduced form of a dissolved element that is stable under sub-oxic conditions but is rapidly scavenged from the water column by particulate matter.

11.5.5 Mid-depth maxima-type vertical trace metal profiles

Two profiles of this type were described by Bruland (1983): those associated with mid-depth sources, and those associated with sub-oxic waters.

PROFILES ASSOCIATED WITH MID-DEPTH TRACE METAL SOURCES It was shown in Section 6.3 that hydrothermal activity at the spreading ridge crests can introduce major quantities of some elements directly into the water column at mid-depths, thus providing concentration maxima in vertical trace metal profiles. For example, hydrothermal inputs can cause a dramatic increase in the concentration of Mn in intermediate and deep waters; a profile of this type, taken in the vicinity of the Mid-Atlantic Ridge, is illustrated in Figure 11.5e.

PROFILES ASSOCIATED WITH SUB-OXIC WATERS Mid-depth trace metal concentration maxima can result from *in situ* redox processes, and occur when the reduced form of an element is relatively soluble in comparison with its oxidized form. Reduced species behaving in this manner include

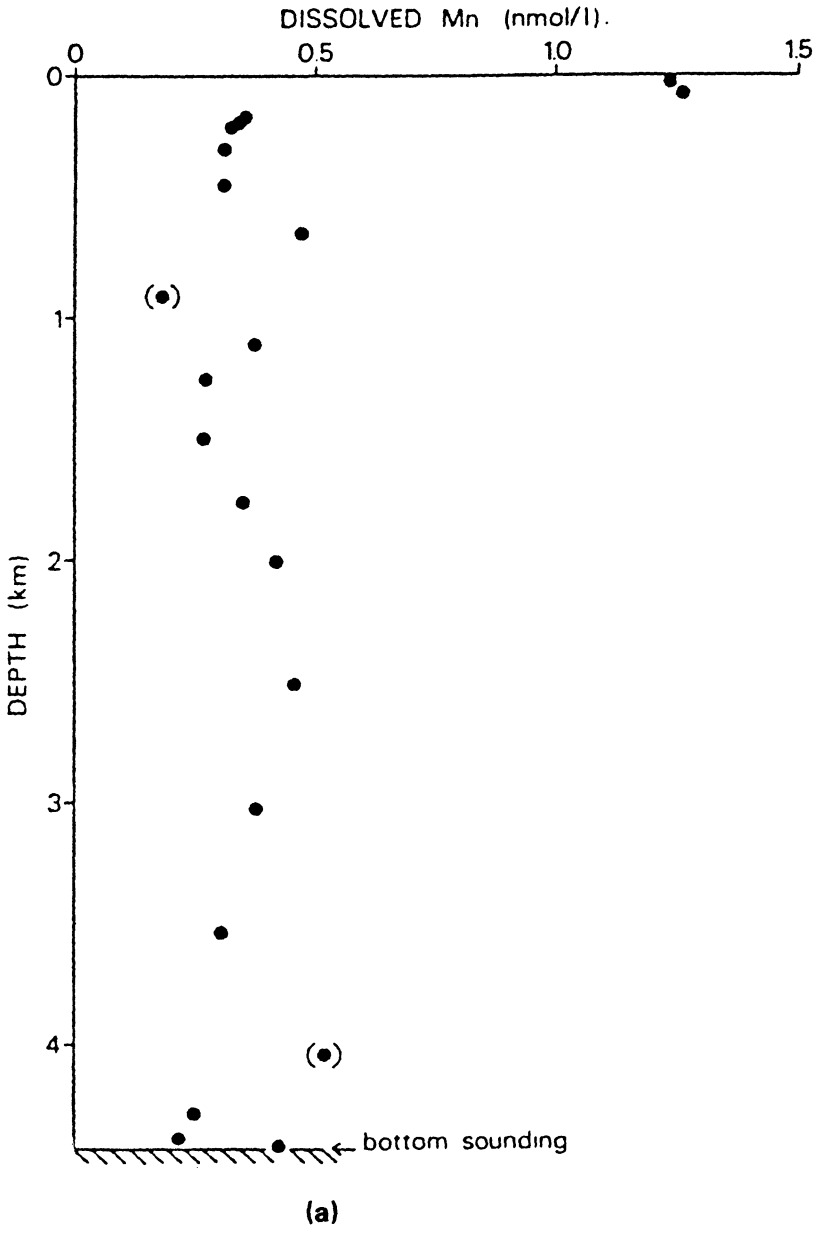

Figure 11.5 Vertical profiles of dissolved Mn in the oceans. (a) A profile from the eastern North Atlantic showing a typical distribution of dissolved Mn in the absence of intermediate and deep water sources; the principal feature is the high concentration of dissolved Mn in the mixed layer as the result of a surface input (from Statham & Burton 1986).

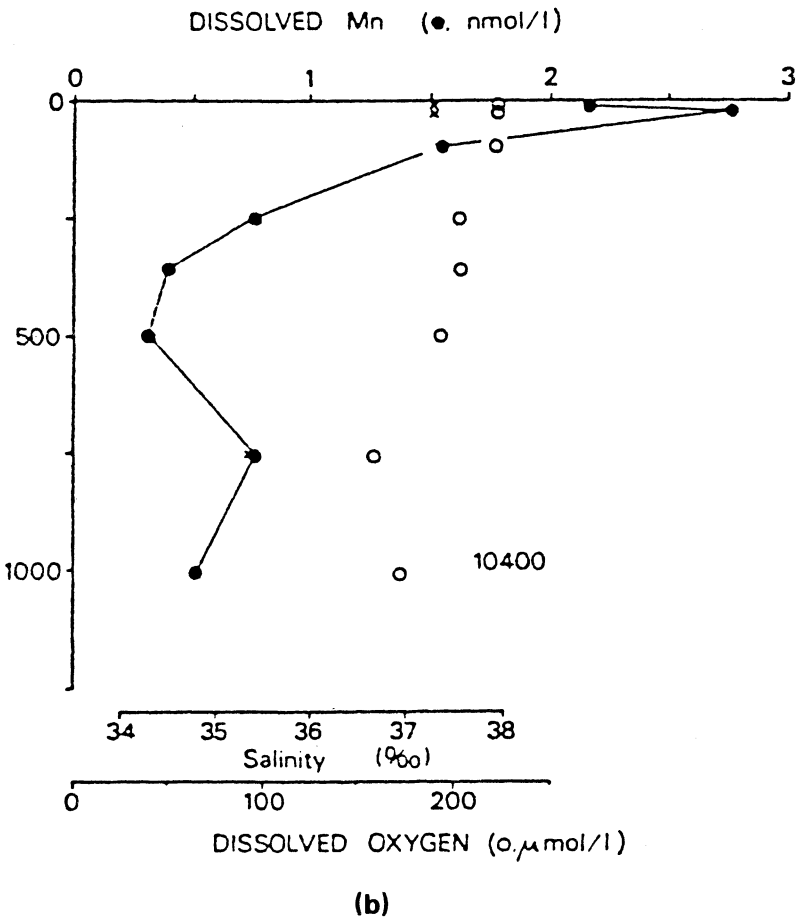

Figure 11.5b A profile from the eastern North Atlantic showing a dissolved Mn maximum in the mixed layer high-concentration region (from Statham & Burton 1986).

Mn(II) and Fe(II). For example, Klinkhammer & Bender (1980) and Murray *et al.* (1983) have reported sub-oxic Mn concentration maxima associated with an oxygen minimum zone in the Pacific Ocean – see Figure 11.5d.

11.5.6 Anoxic water-type vertical trace metal profiles

Anoxic waters can be formed in a variety of marine environments, including: (a) areas where the water circulation is restricted, e.g. in coastal inlets having a fjord-type of circulation and in deep-sea trenches; (b) at the surface exit of marine hydrothermal systems; and (c) within

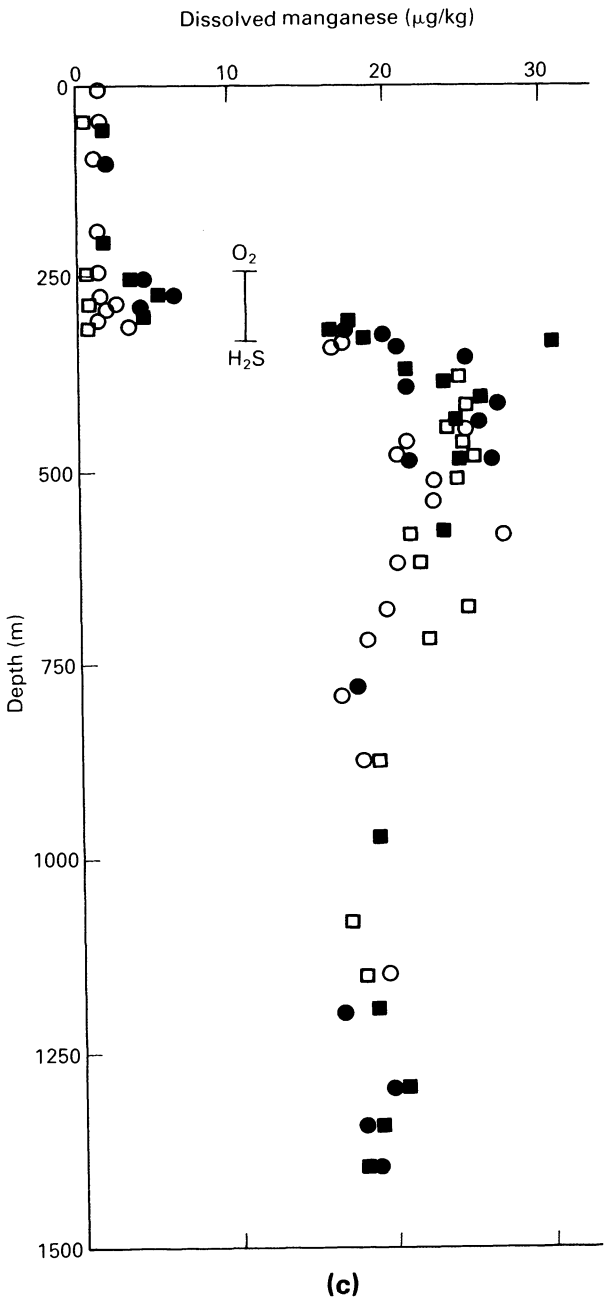

Figure 11.5c A profile from the Cariaco Trench showing an increase in dissolved Mn across the O_2/H_2S redox boundary (from Bacon *et al.* 1980).

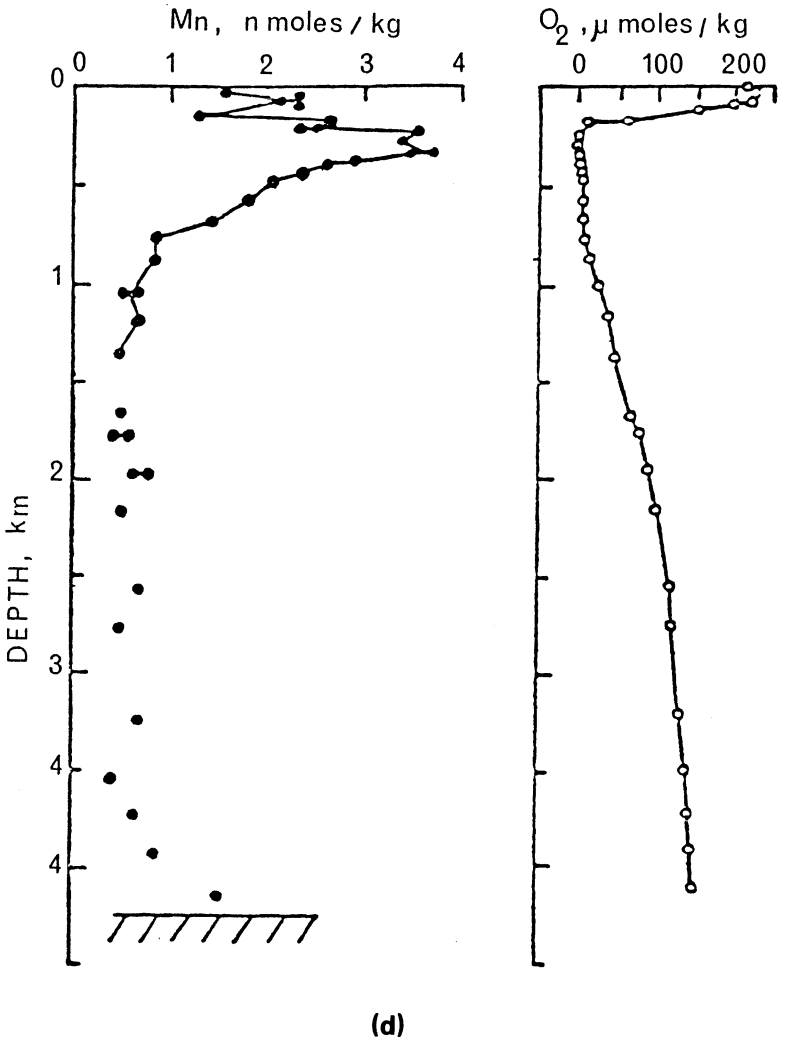

Figure 11.5d A profile from the Pacific Ocean showing an increase in dissolved Mn in the region of the oxygen minimum (from Klinkhammer & Bender 1980).

sediment interstitial waters (see e.g. Emerson *et al.* 1983). In regions of restricted water circulation, reducing conditions can be set up due to the redox couple SO_4^{2-}–H_2S. Then, as in the sub-oxic waters described above, trace metal maxima can occur when the reduced form of the element is more soluble than the oxidized form (e.g. the Mn(II) and Fe(II) forms of manganese and iron, respectively) and minima result when the reduced form is less soluble or when it is heavily scavenged (e.g. Cr(III)).

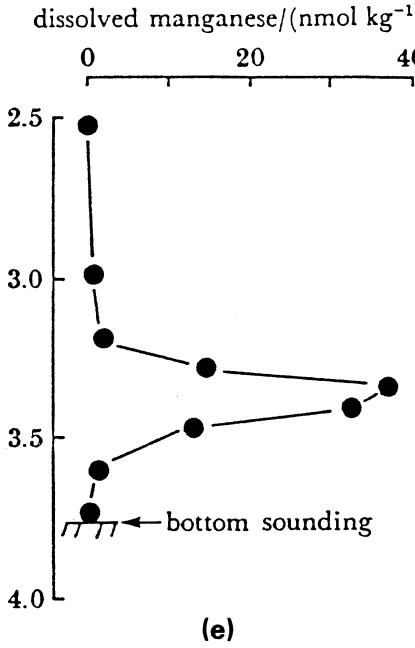

Figure 11.5e A profile from the Mid-Atlantic Ridge (26°N) showing the effect of hydrothermal inputs (from Klinkhammer *et al.* 1986).

In some regions where the water column is stratified, with anoxic conditions being developed in subsurface waters, there is a recycling of components between oxic and anoxic layers. Since there are dramatic changes in the solubilities of many trace metals at the oxic/anoxic boundary layer (or **redox front**) at the O_2/H_2S interface, this can lead to distinctive vertical trace metal profiling (see e.g. Spencer & Brewer 1971, Emerson *et al.* 1983, Kremling 1983). In a recent study, Jacobs *et al.* (1985) gave data on the behaviour of a number of metals across the O_2/H_2S interface in a permanently anoxic basin (Framvaren Fjord, Norway). The authors identified two general types of process that can occur in the presence of such an interface: (a) redox cycling at the interface, and (b) metal sulphide precipitation in the underlying sulphidic water. The data for Framvaren Fjord showed that Mn, Fe and Co were involved in an active redox cycling at the O_2/H_2S boundary, and have distribution profiles that are characterized by dissolved maxima just below the interface (type (a) behaviour). In contrast, Cu, Zn and Cd were not involved in redox cycling, but instead displayed a dramatic solubility decrease across the interface as a result of metal sulphide precipitation (type (b) behaviour). The type (b) elements are enriched in the underlying sediments, and Jacobs *et al.* (1985) therefore suggested that anoxic basins may act as traps for these elements.

Various types of vertical trace element profiles in the oceanic water

column have now been identified, and the distributions of a series of process-oriented elements have been described in terms of analogue constituents that have well established distributions in sea water. In this manner, it has been shown that the vertical profiles can provide information on the factors that control the seawater chemistry of individual components. For this purpose, the characteristic profile shapes for a wide range of elements are given in Table 11.1, although it must be stressed that the list is continually being extended as more elements are studied. So, although vertical profiles are therefore useful as process indicators, the vertical profiles of some elements can, under different conditions, exhibit 'multi-shape' profiles, which result because more than one process has affected their seawater chemistries. This can be illustrated with respect to the vertical distribution of dissolved Mn in the oceanic water column.

Dissolved Mn (Mn_d) is present in sea water in the +2 oxidation state. In oxygenated sea water the Mn(II) is thermodynamically unstable with respect to oxidation to insoluble manganese oxides (Bruland 1983). According to Burton & Statham (1988) the dominant factor that affects the aquatic geochemistry of Mn is the change of oxidation state between reducing and oxidizing environments, coupled with a marked difference in the reactivity of the element between the two oxidation states. The Mn(II) form, which is the stable oxidation state under reducing conditions, is much more soluble and geochemically mobile than the Mn(IV) state. Dissolved manganese (Mn_d) is supplied to the *surface* oceans mainly via river run-off and diffusion from shelf sediments at the basin margins, and via dissolution from atmospheric particulates over the entire sea surface. The $Mn(II)_d$ is extremely particle-reactive and is scavenged throughout the water column on a timescale of $\sim$ 10–100 yr; this form of Mn is only regenerated under reducing conditions (Bruland 1983). As a result of these input and removal processes, vertical profiles of Mn_d in a typical oceanic water column show a generally consistent overall pattern in which the concentrations are highest in the surface waters and decrease rapidly to low values, which are usually maintained to the bottom. An example of such a 'surface input–water column scavenging' vertical Mn_d profile is illustrated in Figure 11.5a. Subsurface Mn_d maxima are sometimes found within the overall high mixed layer concentration pattern. An example of such a maximum is shown in Figure 11.5b, and according to Statham & Burton (1986) features of this kind arise as a net result of input, removal, physical mixing (i.e. dynamic processes), cycling processes (such as photoreduction) and possible involvement of the element in biological systems. The typical Mn_d vertical profile can, however, be severely perturbed by subsurface sources, and a number of examples of this are described below.

(a) Mn redox recycling across the O_2/H_2S boundary, leading to an increase in Mn_d, can occur in nearshore waters with restricted circulation (e.g. the Black Sea) and in deep-sea trenches (e.g. the Cariaco Trench). An example of a vertical Mn_d profile of this type is given in Figure 11.5c.

(b) Intermediate-depth Mn_d maxima can be found in some areas at depths close to the oxygen minima (see Sec. 8.3), especially in the Pacific Ocean. Two principal processes may contribute to the setting up of this type of Mn_d maxima. One of these is the redox-mediated release of pre-scavenged Mn_d, which is solubilized from particles sinking from the surface as they reach the oxygen minima, and/or release via the decomposition of organic matter. However, various authors (see e.g. Martin & Knauer 1984, Landing & Bruland 1987) have shown that the release from particles was insufficient to account for the observed increase in Mn_d in the maxima, and have invoked the lateral off-shelf advection of Mn_d, which may have originated via redox-mediated diffusion from shelf sediments. An example of a vertical water column Mn_d profile showing an intermediate-depth concentration maximum is illustrated in Figure 11.5d.

(c) Major perturbations to the typical down-column Mn_d profiles can be found in regions of hydrothermal activity. Here, the hydrothermal inputs can cause a dramatic increase in the concentrations of Mn_d in intermediate-depth and deep waters; a profile of this type is illustrated in Figure 11.5e. Hydrothermal inputs of Mn_d have been found in both the Atlantic and the Pacific Oceans. However, Burton & Statham (1988) have pointed out that the dominant contrast between the two oceans is that in the Atlantic the ridge topography restricts the dispersal of the hydrothermal Mn plume to the rift valley. In contrast, in the Pacific hydrothermal Mn can be transported for $\sim$ 2000 km from the ridge crest venting sources (see Sec. 6.3).

By using Mn as an example, it is therefore apparent that, although the various types of vertical water column distribution profiles are useful for identifying individual processes, the profiles of some dissolved elements can be influenced by more than one biogeochemical process. In addition, it must be stressed that, although biogeochemical processes exert a strong influence on the vertical profiles of trace elements in the water column, physical advective transport can also play an important role in maintaining the shapes of the profiles.

11.6 Processes controlling the removal of trace elements from sea water

11.6.1 Introduction

If it is assumed that an element has been continually added to the oceans over geological time, then either its concentration will build up in sea water or it will be removed from the aqueous phase. The World Ocean is not thought to be in a steady-state, and although their residence times in sea water vary considerably, the trace elements are not building up to reach concentrations equal to their long-time inputs. In fact, some of the trace elements are being removed relatively fast in times of less than a hundred to a few thousand years, i.e. Forchhammer's 'facility with which the elements in sea water are made insoluble' has been operative. The question that must now be addressed is 'What are the processes that drive the facility which makes the elements insoluble'?

One of the first attempts to evaluate the processes involved in the removal of trace elements from sea water was made by Krauskopf (1956), who assessed the effects of (a) saturation precipitation, (b) adsorption onto particulate matter and (c) interactions with the biosphere on the removal of a series of elements from the ocean. His main conclusions may be summarized as follows.

(a) Saturation precipitation could only act as a potential control on the removal of Sr and Ba.
(b) Adsorption onto particulate material such as ferric hydroxide, manganese dioxide, the clay mineral montmorillonite, dried plankton and peat moss was a possible control on the removal of Zn, Cd, Pb, Bi, Cu, Hg, Ag and Mo.
(c) Interactions with the biosphere may regulate the concentrations of V, Ni and possibly also Co, W and Mo in sea water.

Krauskopf's study therefore clearly indicated the potential importance of inorganic particle adsorption and interaction with the biosphere in the removal of trace elements from sea water. Since then, many advances have been made in our understanding of both the concentrations of trace elements in sea water and the factors that control their distributions. The picture is still by no means totally clear yet, but the new data offer a better position from which to review the mechanisms that remove trace elements from the oceans, especially with respect to the evaluation of the relative importance of inorganic scavenging and biological uptake in the removal processes.

In the two preceding sections we have reviewed the lateral and vertical distributions of trace elements in the ocean system. On the basis of their lateral distributions it was possible to make a distinction between two general types of trace metals.

(a) **Type I** was exemplified by Pb. The main trend in the surface water distribution of Pb is an increase in dissolved concentrations away from the coastal regions towards the central gyres, where it reached its highest concentration. Outside the coastal waters the concentrations of Mn also increased in the central gyres, but the overall distribution of this element was complicated by a strong nearshore source.

(b) **Type II** was exemplified by Cd and Ni, which had their highest surface water concentrations in areas of upwelling and their lowest concentrations in the oligotrophic central gyres.

The reasons for the differences between the type I and type II elements became apparent when their vertical water column profiles were examined. These showed that the concentrations of Pb and Mn decreased rapidly with depth, whereas those of Cd and Ni increased with depth. Thus, if specialized conditions, such as those found in sub-oxic and anoxic waters, are ignored, then the vertial profiles of type I and type II trace metals may be considered to be essentialy maintained by two basically different biogeochemical processes, upon which the results of advective transport can be superimposed. The type I distribution is controlled by a surface input and a rapid scavenging by particulate phases throughout the water column, onto which may be superimposed the effects of other processes such as those associated with mid-depth and bottom trace metal sources; i.e. the type I element distributions are controlled by **external cycling processes**. In contrast, the type II distribution is essentially the result of the involvement of the trace metals in the major biological (nutrient) cycles, which results in a surface depletion and a subsurface enrichment in dissolved concentrations; i.e. the type II element distributions are controlled by **internal cycling processes**. This classification is by no means all-embracing and some trace elements have intermediate-type distributions (e.g. Cu). In a very general sense, therefore, vertical trace metal distributions may be considered to be controlled by either a **scavenging-type** or a **nutrient-type** mechanism, or by a combination of both, all of which involve the removal of dissolved species by some form of particulate matter.

The distinction between the scavenging-type and the nutrient-type reactions not only draws attention to the central role played by particulate matter in the removal of trace elements from sea water, but also highlights the importance of the histories of the individual particle types; thus, the internally-produced biotic particles (nutrient-type) are involved in different trace metal cycles than are the externally-produced non-biotic particles (scavenging-type). However, it will be shown later in the text that in reality the situation is not as clear-cut as this; for example, the scavenging component of marine particulate matter

has an organic nature (see Sec. 11.6.3.1). Further, it now appears that biota-generated particles may act as passive substrates for the uptake of surface-active trace elements (see Sec. 11.6.3.3). Nonetheless, for the purposes of a working hypothesis, it is still useful at this stage to categorize trace element removal mechanisms into the scavenging and nutrient-type reactions.

The importance of this particulate material in the removal of trace metals from sea water has been widely acknowledged for many years, to the extent that Turekian (1977) referred to the overall process as the 'great particle conspiracy' (see Ch. 10). However, marine geochemists are still only at a relatively early stage in their understanding of how this conspiracy works.

Particulate matter can act as either a source or a sink for trace elements dissolved in sea water. The *in situ* removal of dissolved elements onto particulate matter (i.e. their consumption) has been termed the **J-efflux**, and their *in situ* release from particulate matter (i.e. their production) has been termed the **J-flux**. It was shown in Section 10.4 that oceanic TSM can be divided into two general populations: (a) a small-sized ($\lesssim$ 5–10 μm diameter) fraction, termed the FPM; and (b) a large-sized ($\gtrsim$ 50 μm diameter) fraction, referred to as the CPM. This size classification is critical in understanding how the 'great conspiracy' operates. For example, the scavenging-type and nutrient-type mechanisms can be referred to the FPM and CPM particulate matter populations, respectively. Thus, involvement in the biological cycles introduces the nutrient-type trace elements into the large aggregated CPM population, whereas the adsorptive or scavenging removal of trace metals from sea water is dependent upon the surface area and concentration of particles, and so is dominated by the small-sized FPM population. However, this FPM sinks at very slow rates and it is the large-sized, fast-sinking, particles that deliver most of the vertical material flux in the oceans. Therefore, in order to satisfy the residence time requirements of some trace metals in the water column it is necessary to achieve a balance between the slow- and fast-sinking particles. The direct coupling between the two populations is the transfer of small particles to the large particle flux by mechanisms such as 'piggy-backing' or packaging into faecal-type material by organisms at surface and mid-depths (see Sec. 10.4), but these are not one-step processes and are best described in terms of an aggregation–disaggregation particle continuum.

It may be concluded, however, that to a first approximation trace metals can be removed from sea water by scavenging-type and nutrient-type mechanisms, and in the following sections the reactions controlling these two mechanisms will be considered in more detail. However, before attempting to do this it is necessary to understand something of the speciation of the trace metals in sea water, since this plays a vital role in

controlling the pathway that a specific trace metal will follow in its removal from the water column.

11.6.2 Trace element speciation

The speciation of dissolved components in multi-electrolyte solutions such as sea water is notoriously difficult to assess, and a full treatment of the subject will not be attempted here. Instead, attention will be focused on two questions: 'What is speciation?' and 'Why is it important to our understanding of the chemical dynamics of trace elements in sea water?'.

Speciation can be defined as the individual physicochemical forms of an element which together make up its total concentration, and the full water column separation of an element therefore involves its distributions between free ions, ion pairs, complexes (both inorganic and organic), colloids and particles. In addition, biological processes can form metastable species that have sufficiently long lifetimes to be significant components in the speciation of some elements (see e.g. Turner 1987).

According to Andreae (1986) the major processes that affect chemical speciation in sea water are solid–aqueous phase exchange, electron exchange (redox chemistry), proton exchange (acid–base chemistry) and ligand exchange (complex chemistry). This author also points out that the processes that determine the species distribution of an element can be described within the context of fundamental interactions in the bonding environment around the atom, i.e. the formation of covalent bonds, electron exchange in redox reactions, and various types of ligand exchange (complex formation, acid–base chemistry and surface interactions). A number of generalities can be identified with respect to these bonding environments.

(a) For a few elements, mainly the non-metallic and metalloid elements, the formation of covalent bonds is important in controlling species distribution in sea water.
(b) Coordination bonding chemistry (acid–base reactions, precipitation–dissolution, complex formation) dominates the species distribution of the metallic elements.
(c) Redox reactions lead to changes in electron configuration that are reflected in both covalent and coordination bonding characteristics.

Because both proton exchange (acid–base reactions) and electron exchange (redox) processes are extremely important in controlling speciation distribution, both pH and redox potential (pE) are uniquely important parameters in aqueous chemistry, and are often termed the 'master variables' of the system.

The basic concepts underlying trace element speciation in sea water have been described by Stumm & Brauner (1975). Atoms, molecules and

ions will tend to increase the stability of their outer-shell electron configurations by undergoing changes in their coordinative relationships, e.g. by acid–base, precipitation and complex formation reactions. Any combination of cations (the **central atom**) with molecules or anions (the **ligand**) contaiing unshared electron pairs (**bases**) is termed coordination (or complex formation); this can be either electrostatic, covalent or a mixture of both. In an aqueous solution, cations are coordinated with water molecules, and Stumm & Brauner (1975) distinguish between two types of complex species in sea water.

(a) In an **ion pair** (or outer-sphere species), the metal ion, the ligand or both retain the coordinated water when the complex is formed, so that the metal ion and the ligand are separated by water molecules. In an ion pair, the association between the cation and anion is largely the result of long-range electrostatic attraction.
(b) In a **complex** (or inner-sphere species), the interacting ligand is immediately next to the metal cation, and a dehydration step must precede the association reaction. In this type of species, short-range, or covalent, forces contribute towards the bonding. The number of linkages attaching ligands to a central group is known as the coordination number. When a base contains more than one ligand, and can thus occupy more than one coordination position in a complex, it is termed a multidentate (as opposed to a unidentate) ligand; complex formation with these ligands is termed chelation, and the complexes are referred to as **chelates**. Chelates are usually much more stable relative to the corresponding complexes with unidentate ligands. The order of stability of the transition metal chelates formed with ligands (especially organic ligands) follows the so-called Irving–Williams order $Mn^{2+} < Fe^{2+} < Co^{2+} < Ni^{2+} < Cu^{2+} < Zn^{2+}$.

The approaches used to date to investigate elemental speciation in natural waters can be divided into two general types, the indirect and direct approaches.

INDIRECT APPROACH TO SPECIATION The indirect approach employs theoretical equilibrium models based on thermodynamic data to calculate speciation relationships in water types of specific matrix compositions. There are a number of problems involved both in the setting up of these models and in the manner in which the data they generate are interpreted, and factors such as the use of different suites of stability constants often yield different speciation pictures. For example, Zarino & Yamamoto (1972) reported that, in the absence of organic ligands and particulate and colloidal species, ~ 90% of the inorganic Cu in sea water is present as hydroxy complexes, with only ~ 9% being in the form of

carbonate complexes; whereas Turner *et al.* (1981) calculated that ~ 79% of the Cu was present as the carbonate complex.

DIRECT APPROACH TO SPECIATION The direct methods for the determination of speciation are based on techniques such as wet chemistry (see e.g. Florence & Batley 1976, Cutter & Bruland 1984, Froelich *et al.* 1985), electrochemistry (see e.g. Nurnberg 1980) and the use of radiotracers (see e.g. Amdurer *et al.* 1983). In particular, considerable advances in metal speciation chemistry have been made using a variety of electrochemical techniques. Following Bailey *et al.* (1978) the formation of a complex in solution is part of an equilibrium process that can be represented by a series of steps, each of which can be described by an **equilibrium constant** (formation constant). The complexes usually undergo continuous breaking and remaking of the metal–ligand bonds. If the bond-breaking step is rapid, the ligand exchange reactions are also rapid, and the complex is referred to as being **labile**; in contrast, if the reactions are slow, the complex is termed **inert**. According to Nurnberg & Valenta (1983), the inorganic ligands normally abundant in sea water usually form labile mononuclear complexes with trace metals. Because of factors such as their high rate constants of formation and dissociation, these complexes are very mobile and will undergo reversible electrode processes in electrochemical determinations. This is also the situation for certain weak complexes formed between trace metals and some components of the dissolved organic matter (DOM) in sea water. In contrast, other DOM components form more stable complexes with trace metals. The reduction of these species requires a considerable overvoltage and the electrode process therefore becomes irreversible. Thus, in terms of their association–dissociation rate constants, inorganic and organic trace metal complexes can be classified electrochemically as either labile or non-labile (inert). A schematic representation of this labile/non-labile concept is illustrated in Figure 11.6a in terms of the role played by the oceans in the biogeochemical cycles of heavy metals. For a full discussion of the fundamental principles underlying electrochemical trace metal determinations the reader is referred to the volume edited by Whitfield & Jagner (1981).

It is convenient, therefore, from a biogeochemical point of view to consider some aspects of trace metal speciation in sea water within the framework of a classification that distinguishes between two general species types.

(a) Those which form kinetically very labile complexes. These species can be considered to be in thermodynamic equilibrium, and species distributions can be predicted from mathematical models.

(b) Those which are involved in the formation of very non-labile (or inert) complexes. For these, species distribution can be identified using direct techniques, which can isolate the inert complexes. Problems arise, however, for those species which are inert enough to persist in non-equilibrium but are too labile to be isolated (see e.g. Andreae 1986).

SPECIATION INVOLVING LABILE COMPLEXES This form of trace metal speciation can occur with inorganic, and also some organic, ligands. In sea water, the abundant inorganic ligands that are significant for trace metal speciation are Cl^-, OH^-, CO_3^{2-} and SO_4^{2-}. The processes involved in this speciation can be influenced by the formation of ion pairs (electrostatic attraction only) between cations and anions, and by mixed ligand complexes. Other effects that must be considered include side reactions and mixed ligand complexes. A number of workers have attempted to calculate the equilibrium speciation of dissolved components with the inorganic ligands present in sea water (see e.g. Sillen 1961, Garrels & Thompson 1962, Zarino & Yamamoto 1972, Dyrssen & Wedborg 1974, Stumm & Brauner 1975, Florence & Batley 1976, Turner *et al.* 1981), and the speciation data obtained are usually expressed as percentages of the total metal concentration.

A list of predicted trace metal species for oxygenated sea water is given in Table 11.1; the species, which are derived mainly from data provided by Stumm & Morgan (1981) and Turner *et al.* (1981), are taken from Bruland (1983). It must be stressed, however, that the speciation signatures given in the literature are often at variance with each other, e.g. as a result of different stability constant data used in the models. Despite this, two main features can be identified from the data in Table 11.1.

(a) The alkali and alkaline earth metals do not form strong complexes, and even their tendency to form ion pairs is limited, with the result that these element exist in sea water largely as *simple cations*.
(b) For the trace elements, the species are distributed between the *free ion* and *complexes* with the various ligands.

It must be pointed out that the data in the table disregard the formation of complexes with organic ligands. Despite this, Bruland (1983) suggested that the oxygenated seawater species are probably valid for most elements in the open ocean, where the concentration of dissolved organic matter is too low to contribute significantly to their speciation, Cu(II) possibly being an exception to this. Turner (1987) has pointed out that the most important conclusions to be drawn from speciation data of this kind are not usually the percentages of the individual complexes

themselves, but rather the trends in the strengths of complexation, which directly affect the biogeochemical reactivities of the elements. The most important of these are: (a) the proportion of free metal ion, which represents the *bioavailable* portion of weakly complexed metals, e.g. Cd and Pb (for a detailed discussion of the modern concepts associated with the bioavailability of elements in sea water – see Turner (1986) and Morrel (1986)); and (b) the charge distribution of the complexes, which affects their *surface interactions*. The importance of this type of elemental speciation has also been highlighted by Stumm & Brauner (1975), who pointed out that inorganic complex formation has a pronounced influence on adsorption equilibria, hydroxy, sulphato, carbonato and particularly uncharged inorganic complexes tending to be sorbed much more strongly at an interface than free metal ions.

SPECIATION INVOLVING INERT COMPLEXES WITH ORGANIC MATTER Some organic ligands can form stable complexes, or even chelates, with trace metals even though there is side reaction competition for the organic chelator from salinity components such as Ca and Mg (see e.g. Nurnberg & Valenta 1983).

A number of techniques have been used to investigate trace metal–inorganic complexes. These include the following.

(a) Indirect electrochemical techniques, in which measurements are made before and after the sample has been subjected to a number of sequential steps (e.g. those involving ion exchangers, acidification, etc.), thus providing data on operationally defined speciation fractions (see e.g. Batley & Florence 1976).
(b) Direct electrochemical techniques, in which the labile and non-labile fractions are separated by the kinetics of the analysis (see e.g. Nurnberg & Valenta 1983).
(c) Those which measure the **complexation capacity** of a water sample, i.e. the ability of the water sample to remove added trace metal from the free ion pool.

Studies have been carried out on the organic complexing of several elements in the marine environment. For example, Mackey (1983, 1985) provided evidence for the existence of organically complexed Cu, Zn, Fe, Ni, Mn and Mg in sea water. The organic complexing of elements such as Zn, Cd and Pb in sea water has also been reported by several other workers (see e.g. Florence & Batley 1976, Duinker & Kramer 1977, Imber & Robinson 1983, van den Berg 1985, Imber *et al.* 1985). As a result of studies such as these an extensive literature is now available on the organic complexing of elements in marine waters. However, various experiments with model chelators have shown that among the heavy

metals the tendency to form non-labile species decreases in the order Cu > Pb > Cd, and copper will therefore serve as an example of a trace element that can form non-labile species in sea water.

In the absence of a sufficient concentration of organic ligands, carbonate and hydroxy complexes account for more than 98% of the inorganic Cu in sea water. This situation can change, however, as the concentrations of DOM increase, and organic Cu species can form a significant part of the total dissolved Cu in some oceanic environments. The biogeochemical importance of this type of Cu speciation can be illustrated with respect to a number of recent studies.

Wood *et al.* (1983) showed that the copper complexing capacity (CuCC) of marine waters decreased in the order inner shelf > outer shelf > open ocean, and established that the trend was well correlated with the distributions of DOC and total particulate matter. The importance of organically complexed Cu in coastal sea water has also been demonstrated by van den Berg (1984), who reported that between 94 and 98% of the total dissolved Cu in Irish Sea surface waters was present in this form, and by Mills & Quinn (1984), who gave data on the distribution of dissolved organic Cu in surface waters (~ 1 m depth) from Narragansett Bay (USA) and showed that it ranged from 14 to 70% of the total Cu. Mills & Quinn (1984) also concluded that the organic Cu mixes conservatively and that the amounts entering and leaving the bay were nearly in balance. This is an extremely important conclusion, since the conservative behaviour implies that the organic complexing of Cu (and other elements) decreases the extent to which they are available for particle scavenging, which induces non-conservative behaviour. It further suggests that the conservative behaviour of the dissolved organic Cu in Narragansett Bay indicates that organic complexing may be an important factor in controlling the transport of dissolved Cu out of the estuarine environment. This topic was considered by Huizenga & Kester (1983), who gave details of a survey of the total and labile (non-organically complexed) Cu in unfiltered water samples from the northwestern Atlantic. On a shelf transect there was a linear relationship (i.e. conservative behaviour) between total Cu and salinity, with < 5% of the total Cu being in a labile form. The authors suggested that Cu may behave conservatively on the shelf because the non-labile, mainly complexed, Cu is less reactive to particle scavenging and biological uptake than is the free Cu. It is apparent, therefore, that the labile/non-labile speciation, essentially the **inorganic/organic speciation**, of Cu strongly affects the extent to which it is available for particle interactions; e.g. *organic* complexes can reduce its adsorption onto particulate surfaces. Thus, the non-labile forms of Cu are less particle-reactive than other species. As a result, the conservative/non-conservative behaviour of dissolved Cu in estuarine and shelf waters is strongly influenced by its

speciation, even to the extent that conservative behaviour can be forced upon a system when the non-labile species dominate. Labile/non-labile speciation will therefore play an important role in controlling the amounts of some elements that are sedimented from the estuarine, shelf and open-ocean water column by association with particulate matter (see also Wangersky 1986).

Labile/non-labile speciation is also extremely important in determining the behaviour of a trace element in the biosphere with respect to its uptake by phytoplankton, i.e. at the entry point into marine biological cycles. In this context, it has been known for some time that during the uptake of trace metals from sea water phytoplankton discriminate against strongly complexed, especially organic complexed, (non-labile) species, preferring to take up the fraction that is present in a free ionic, or loosely complexed labile, form. For example, Bernhard & George (1986) have suggested that biological uptake and toxicity of Cu, Cd and Zn may be related to free ion activity and to species that are labile to anodic stripping voltammetry, that is, those in electoactive forms. Thus, the **bioavailability** of trace metals is strongly influenced by their speciation in sea water. Further, the presence of organic complexing material can reduce the toxicity of a trace metal to marine organisms. It is apparent, therefore, that because only a fraction of some trace metals will undergo uptake by the phytoplankton, data on the total concentrations of the metals alone will not be sufficient to describe the organism–metal interactions. In this context, Bernhard & George (1986) concluded that, at present, anodic stripping voltammetry provides the best technique for the measurement of soluble bioavailable metal species.

Another area in which trace element speciation is important has been highlighted by the recent work on the 'hydride' elements in sea water. Andreae (1983) has pointed out that a number of metals and metalloids in the fourth, fifth and sixth main groups of the periodic table form volatile hydrides on reduction with sodium borohydride. These elements include Ge, Sn, Pb, A, Sb and Se, and an interesting feature of their marine chemistry is that some of them can be present in sea water in organometallic forms. For example, Froelich *et al.* (1983, 1985) have identified at least three forms of Ge in marine and estuarine waters, inorganic germanic acid (Ge_i), monomethylgermanium (MMGe) and dimethylgermanium (DMGe), and the authors showed that a large fraction of the oceanic Ge apparently exists in the methyl forms. The geochemical importance of these findings is that the different forms of Ge follow different geochemical pathways in the estuarine–marine environment. In general, Ge_i behaves like silica; it has a high concentration in river water, where its source is the weathering of crustal rocks, and low concentrations in sea water. In estuaries, the behaviour of Ge_i follows that of silica, and it can exhibit non-conservative behaviour following

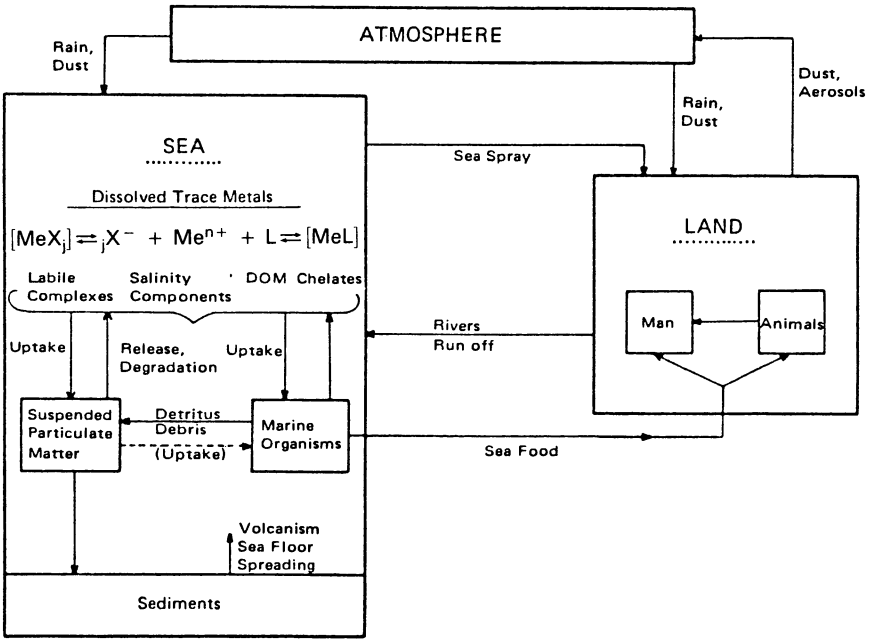
ATMOSPHERE
Rain, Dust
Rain, Dust
Dust, Aerosols
SEA
Sea Spray
Dissolved Trace Metals
$[MeX_j] \rightleftharpoons {}_jX^- + Me^{n+} + L \rightleftharpoons [MeL]$
Labile Complexes
Salinity Components
DOM Chelates
LAND
Man
Animals
Rivers Run off
Uptake
Release, Degradation
Uptake
Suspended Particulate Matter
Detritus Debris
(Uptake)
Marine Organisms
Sea Food
Volcanism Sea Floor Spreading
Sediments

(a)

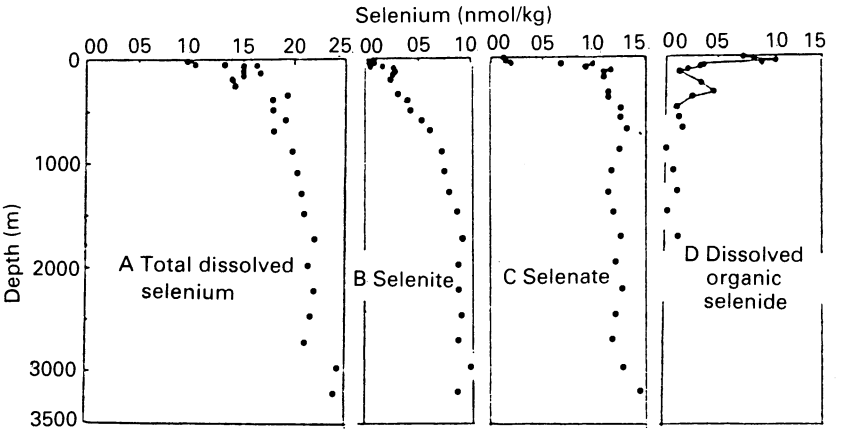
Selenium (nmol/kg)
00 05 10 15 20 25
00 05 10
00 05 10 15
00 05 10 15
0
1000
2000
3000
3500
Depth (m)
A Total dissolved selenium
B Selenite
C Selenate
D Dissolved organic selenide

(b)

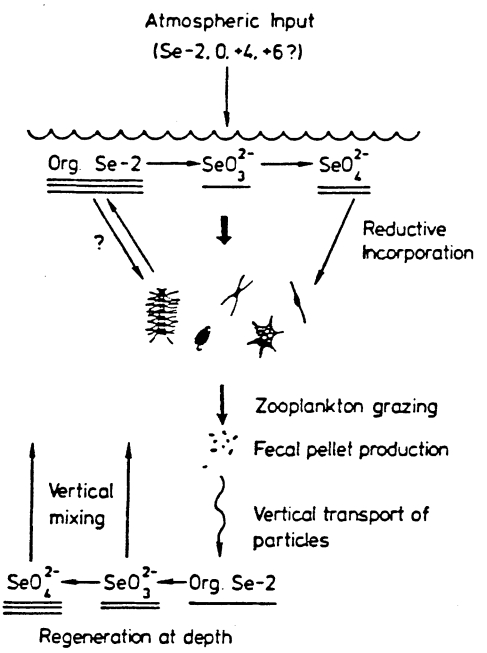

(c)

Figure 11.6 Elemental speciation in sea water. (**a**) (facing) Schematic representation of the biogeochemical cycle of heavy metals (from Nurnberg & Valenta 1983). [Me X_j] represents labile metal complexes in which Me is the metal and X is the inorganic ligand, and [MeL] represents non-labile metal chelates in which Me is the metal and L the organic ligand. (**b**) (facing) Vertical water column profiles of total dissolved selenium, selenite, selenate and organic selenide in the Pacific (from Cutter & Bruland 1984). (**c**) Schematic representation of the marine biogeochemical cycle of selenium (from Cutter & Bruland 1984). The underlining indicates the relative concentrations of selenium species in surface and deep waters. The preferential uptake of selenite in surface waters is shown by the largest of the dissolved-to-particulate arrows.

uptake by diatoms. In the oceans, the horizontal and vertical distributions of Ge_i also mimic those of silica and reflect uptake onto, and dissolution from, siliceous organisms; i.e. it is a nutrient-type element displaying a non-conservative behaviour pattern. In contrast, both MMGe and DMGe behave in a conservative manner in estuaries and in the open ocean; both species are barely detectable in river water, and in estuaries they probably have an oceanic source.

Selenium is another element that has organic and inorganic species which exhibit different biogeochemical behaviour patterns in the oceans. Cutter & Bruland (1984) have recently reviewed the oceanic chemistry of the element, and demonstrated the existence of three dissolved Se species: selenite (Se(IV)), selenate (Se(VI)) and an operationally defined organic selenide. The water column distribution of these species is illustrated in Figure 11.6b. In surface waters of the North and South Pacific organic selenide comprised ~ 80% of the total dissolved Se, with the maximum being associated with primary production. In deep waters, however, organic selenide was undetectable. In contrast to the organic Se, the selenite and selenate species exhibited nutrient-type vertical distributions and were enriched in deep waters. On the basis of their new data, the authors re-evaluated the marine biogeochemical cycle of Se. This cycle, which is illustrated in Figure 11.6c, involves the selective uptake of the element, its reductive incorporation into biogenic material, its delivery to the deep sea as particulate organic selenide via sinking detritus, and a regeneration back into the dissolved state.

Methylation is also important in the marine chemistries of As, Sb, Sn and Hg. Arsenic is present in sea water as As(V), As(III) and methylated As species. As(V) (arsenate) is the predominant dissolved As species, especially in deep water. However, in the surface layer arsenate is taken up by phytoplankton, together with phosphate, and is excreted as As(III) (arsenite) and as the methylated species methylarsenate and dimethylarsenate, the methylated species making up ~ 10% of the total As in the euphotic zone in some oceanic regions (Andreae 1986). Thus, plankton (and bacteria) can influence the speciation of As in sea water, and the speciation transformations in the euphotic zone lead to As(V) having a nutrient-type distribution in the water column. In some respects, the distribution of Sb in the water column resembles that of As, with Sb(V) predominating over Sb(III), and methylated Sb making up ~ 10% of the total antimony in surface waters. Methylated species of Sn have been identified in polluted estuarine and coastal waters; however, they are at very low concentrations in the open ocean. Toxic butyltin, like methyltin, is produced in industrial processes and it is also used as an anti-fouling agent, and these can be sources of the compound to coastal waters. According to Andreae (1986), Hg has very high stability constants with organic ligands, with the result that, in addition to forming a variety

of inorganic complexes, it can form true organometallic compounds, which have been identified in sea water. Methylmercury has been identified in some polluted coastal waters, but there is uncertainty over its concentration in the open ocean.

Redox speciation affects some elements (e.g. Mn, Fe, I, Cr, As and Se) that can exist in variable oxidation states in sea water. For example, the thermodynamically unstable Mn(II) is soluble in sea water but oxidizes to form insoluble Mn(IV) oxyhydroxides. As a result, Mn is solubilized by reduction and precipitated by oxidation, and cycling between the two species of the element, e.g. as a result of redox changes mediated by variations in dissolved oxygen, can produce the metastable form and so induce non-equilibrium behaviour in both sea water and sediment interstitial water. Chromium is another element that has a highly soluble redox state (Cr(VI)) and a very insoluble state (Cr(III)) in sea water; however, in contrast to Mn, Cr is solubilized by oxidation and precipitated by reduction. Redox changes can therefore have a strong influence on the dissolved water column distributions of both Mn and Cr; for example, there is a maximum in dissolved Mn (Mn(II)) and a minimum in dissolved Cr (Cr(VI)) associated with subsurface dissolved oxygen minima (see Sec. 8.3).

Most of the discussion of speciation discussed above has concentrated on the dissolved forms of the elements. The incorporation of the elements into particulate matter is obviously an important step, which may be regarded as contributing to the overall speciation and is, in turn, linked to their dissolved speciation state. It is this transition from the dissolved to the particulate state that controls the residence time of an element in sea water and mediates its delivery to the sediment sink, and this is considered in detail in Section 11.6.3.

It may be concluded, therefore, that speciation is important because different forms or species of the same element can behave in different ways when they enter the oceanic biogeochemical cycles. Thus, the speciation of a trace element has a strong influence on both its particle reactivity and its bioavailability, and so exerts an important control on the processes that are involved in its removal from sea water. These processes are discussed in the following section in terms of incorporation of the elements into the oceanic biogeochemical cycles that drive them on their journey through the water column.

11.6.3 The principal routes for the removal of trace elements from sea water

It was suggested in Section 11.6.1 that the mechanisms by which trace metals are removed from sea water can be classified in terms of either scavenging-type or nutrient-type processes, and each of these is considered individually below.

11.6.3.1 Scavenging-type mechanisms The adsorptive removal of trace metals occurs onto particles that sink down the water column, and Goldberg (1954) gave this removal process the general name of **scavenging**. The dissolved down-column concentration curves for scavenged elements are concave in deep water when plotted against a conservative tracer, indicating loss from the water column. The extent of this scavenging removal can be expressed in terms of a deep water scavenging residence time; a selection of these residence times is given in Table 11.4. Much of our knowledge of the scavenging of dissolved elements from sea water has been derived from the unique chemistry of the radionuclide elements, and their distributions in the oceans have allowed scavenging models to be constructed. In this respect, members of three natural radioactive decay series have proved to be useful tools for the interpretation of scavenging reactions; these are the ^{238}U series, the ^{232}Th series and the ^{235}U series. The fundamental concept behind the use of these radionuclides is the parent–daughter relationship, and the underlying rationale is that the main input of the daughter to the sea is via the *in situ* decay of its immediate radioactive parent. Thus, as Broecker & Peng (1982) have pointed out, by measuring the concentration of the parents of adsorption-prone daughters, it is possible to calculate what the production rate of the daughter should be, and by determining the actual *in situ* concentration of the daughter it is possible to establish if it is being taken out of solution by particulate matter and also, if this is the case, at what rate the process occurs.

Table 11.4 The deep water scavenging residence times of some trace elements in the oceans[a]

Element	Scavenging residence time (years)	Element	Scavenging residence time (years)
Sn	10	Mn	51 - 65
Th	22 - 33	Al	50 - 150
Fe	40 - 77	Sc	230
Co	40	Cu	385 - 650
Po	27 - 40	Be	3700
Ce	50	Ni	15850
Pa	31 - 67	Cd	177800
Pb	47 - 54	Particles	0.365

[a] Data from Balistrieri et al. (1981), Orians & Bruland (1986) and Whitfield & Turner (1987).

PROCESSES CONTROLLING REMOVAL

Following Bacon (1984), the rate of removal (R_d) of the daughter from a parcel of water is proportional to the difference in activity between the parent (A_p) and the daughter (A_d):

$$R_d = \lambda_d(A_p - A_d) \tag{11.2}$$

where λ_d is the radioactive decay constant of the daughter.

A considerable amount of work has been carried out on Th isotopes in sea water. Three isotopes of Th have been used as marine tracers: ^{230}Th (half-life 7.52×10^4 yr), and the two shorter-lived species ^{228}Th (half-life 1.91 yr) and ^{234}Th (half-life 24.1 d). Bacon & Anderson (1982) measured the three Th isotopes in sea water and found that for all of them most activity was in the dissolved form. For example, only ~ 17% of the ^{230}Th was associated with particulate matter; however, both dissolved and particulate ^{230}Th *increased* with depth in the water column.

In recent years many workers have employed radioactive disequilibrium data to interpret scavenging processes in the oceans, and a variety of scavenging models have appeared in the literature. Bacon & Anderson (1982) divided these models into three general types and then used them to identify the processes that control the scavenging of ^{230}Th in the water column; these processes have to take account of an increase in both dissolved and particulate ^{230}Th with depth in the water column. The approach adopted by Bacon & Anderson (1982) provides a useful framework within which to describe the theoretical concepts underlying trace metal scavenging in the oceans. In all three models, it is implicit that Th isotopes are supplied only by their radioactive parents dissolved in sea water, and that they are transferred to particles by adsorption, a process that is assumed to be first order with respect to the dissolved Th concentration. In the present context, the term 'particulate' Th refers to particles $\lesssim 30$ μm in diameter, which are assumed to sink at velocities of a few hundred metres per year or less.

SCAVENGING MODEL I: IRREVERSIBLE UPTAKE In this type of model it is assumed that there is an irreversible binding of the daughter radionuclide to particle surfaces, which is followed by a slow sinking of the mass of particles to the sea bed. This type of irreversible uptake assumes that the reaction site is so far out of equilibrium that the reverse, i.e. desorption, reactions are insignificant. If the suspended particulate matter has a long enough residence time in sea water, then for any isotope that is removed by scavenging, a steady-state is reached in which loss by decay is balanced by gain from uptake. A number of authors have applied this type of model, in association with advection–diffusion models, to both radioactive and stable trace metal distributions in sea water (see e.g. Craig 1974, Brewer 1975, Boyle *et al.* 1977).

Following Simpson (1982) the one dimensional vertical advection–diffusion models which assume irreversible uptake for radionuclides can be described by the following equations:

(a) Dissolved species:

$$\frac{\delta C_d}{\delta t} = K_z \frac{\delta^2 C_d}{\delta z^2} - w \frac{\delta C_d}{\delta z} + P_d - (\lambda + k_1) C_d \qquad (11.3)$$

(b) Particulate species:

$$\frac{\delta C_p}{\delta t} = K_z \frac{\delta^2 C_p}{\delta z_2} - (U_s + w) \frac{\delta C_p}{\delta z} + k_1 C_d - \lambda C_p \,. \qquad (11.4)$$

where C_d = the dissolved concentration of the nuclide,
C_p = the particulate concentration of the nuclide,
K_z = the vertical eddy diffusion coefficient,
w = the vertical advective velocity,
U_s = the particle settling velocity,
λ = the radioactive decay constant,
P_d = the rate of production of the daughter from the dissolved parent,
z = depth,
t = time,
and k_1 = the removal rate constant from solution to the particulate phase (adsorption rate coefficient).

In practice, however, such models proved to be inadequate when applied to the distribution of thorium isotopes in the water column. In terms of these Th isotopes, irreversible uptake can be described by the relationship

$$\text{Th(dissolved)} \xrightarrow{k_1} \text{Th(particulate)} \downarrow \text{S} \qquad (11.5)$$

where k_1 is the **scavenging rate constant**.

Bacon & Anderson (1982) used a mathematical treatment to apply their Th isotope data to this model and rejected it as a basis for describing the Th scavenging on the evidence of the thorium particulate/thorium dissolved (C_p/C_d) distribution. In their treatment they allowed k_1 to be fixed by the observed deep water ^{234}Th distribution. Under this constraint, it is required that the C_p/C_d value for ^{230}Th increase very sharply with depth to the extent that, for reasonable sinking velocities,

well over half the ^{230}Th would be found in the particulate form. Since this was clearly not the case (see above), the authors concluded that the simple irreversible uptake model cannot simulataneously satisfy the observed distributions of both the ^{230}Th and the ^{234}Th isotopes; i.e. since the actual particulate Th is less than the predicted value, an additional mechanisms is required to account for the loss of particulate Th from the water column. Bacon & Anderson (1982) therefore looked at other models in which the distribution of C_p/C_d is governed not only by k_1 but also by an additional transfer coefficient, which represents a loss of the particulate Th.

SCAVENGING MODEL II: IRREVERSIBLE UPTAKE WITH FAST PARTICLE REMOVAL In this model, the additional transfer coefficient for the loss of particulate Th is represented by the incorporation of rapidly sinking particles (k_2) into the down-column flux. Here, therefore, it is the small-sized particulate matter itself that is lost from the water column, e.g. by 'piggy-backing'. Thus

$$\text{Th(dissolved)} \xrightarrow{k_1} \underset{\downarrow S}{\text{Th(particulate)}} \xrightarrow{k_2} \text{Th(fast particle)} \qquad (11.6)$$

This is similar to the 'piggy-backing' model suggested by Lal (1980). However, this type of small particle–large particle 'piggy-backing' does not result in an *in situ* addition of trace metals to deep waters and so cannot account for the loss of particulate Th at depth in the water column. This was confirmed by Bacon & Anderson (1982), who showed that although model II predicted an increase in particulate Th with depth, it did not at the same time predict an increase in dissolved ^{230}Th with depth.

SCAVENGING MODEL III: REVERSIBLE EXCHANGE In this model, the additional transfer coefficient for the loss of particulate Th is by desorption from particles. Thus

$$\text{Th(dissolved)} \underset{k_{-1}}{\overset{k_1}{\rightleftarrows}} \underset{\downarrow S}{\text{Th(particulate)}} \qquad (11.7)$$

Bacon & Anderson (1982) concluded that this model is the only one that successfully predicts that there will be an increase in both dissolved and particulate ^{230}Th with depth in the water column.

From the mathematical treatment of their data Bacon & Anderson (1982) therefore concluded that although both models I and III predicted

linear increases in particulate ^{230}Th with depth, only model III was able to predict that the dissolved ^{230}Th also increases in this manner.

It was pointed out in Section 10.4 that the TSM in the oceans consisted of a small-sized (non-sinking) and a large-sized (fast-sinking) population. It is assumed that it is the fine suspended particulate population that controls the adsorption of radionuclides, and stable trace metals, from sea water. To bring about downward transport, particle aggregation into the large, fast-sinking, particle population is necessary. However, in order to satisfy residence time requirements, Bacon *et al.* (1985) have pointed out that it is also necessary for disaggregation to occur. The authors therefore envisaged a continuous exchange of material between the small and large-sized particle populations, so that before reaching the sea floor a particle may be exchanged several times between the non-sinking small population and the fast-sinking aggregated population, with the overall result that fine particles work their way down the water column at an average speed of ~ 300 to ~ 1000 m yr^{-1}. The aggregation may result from small particles 'piggy-backing' onto the larger ones (see Sec. 10.4), but the mechanism of disaggregation in the deep sea was not known at the time. However, Cho & Azam (1988) have suggested that non-sinking particles may be produced at the expense of the larger aggregates via decomposition by free-swimming bacteria at depth in the water column, thus providing a biological explanation for the down-column radionuclide transport models.

Perhaps the most important conclusion that can be drawn from the study carried out by Bacon & Anderson (1982) is that, at least to a first approximation, the suspended particulate matter in deep water exists in a state of equilibrium with respect to the exchange of Th by adsorption–desorption reactions. This can be described in terms of an equilibrium model. In the framework of models of this type, the residence time of an element with respect to its removal from the oceans by scavenging is controlled by its equilibrium partitioning between dissolved and adsorbed forms, and by the residence time of the particles with which it reacts. Thus, a knowledge of the equilibrium distribution of the element, combined with an independently determined value for the residence time of the particulate material, will yield an estimate of the scavenging rate of the element itself. This relationship can be expressed in the following manner:

$$\frac{1}{\tau_{Me}} = \frac{1}{\tau_p} \frac{[Me]_p}{[Me]_t} \qquad (11.8)$$

where τ_{Me} is the residence time of the element (metal), τ_p is the residence time of the particulate matter, and $[Me]_p$ and $[Me]_t$ are the particulate

(adsorbed) and total concentrations of the element, respectively.

The quantity $[Me]_p/[Me]_t$ can be calculated from direct field measurements, thus allowing the scavenging residence time of an element to be determined. This approach was adopted by Bacon & Anderson (1982), who concluded that on the basis of their equilibrium model the removal of Mn, Cu, Pb, Th and Pa from sea water appears to be controlled by a single population of particles with a residence time of ~ 5–10 yr in the water column. It was shown in Section 10.4 that most of the vertical flux of particulate matter from the surface to deep water is controlled by large aggregates (CPM; diameter $\geqslant 50$ μm), which have much faster sinking times than 5–10 years. However, scavenging is dominated by the small-sized population (FPM; diameter $\ll 10$ μm), which has a long residence time but can undergo accelerated settling by 'piggy-backing' onto and off the large aggregates. This, combined with reversible scavenging, yields scavenging residence times for trace metals and isotopes which lie between the residence times of the individual small- and large-particle populations. The deep water scavenging residence times of a number of metals in sea water are listed in Table 11.4.

The concept that dissolved–particulate reactions in the water column may be controlled by an equilibrium mechanism, and so lead to the possibility that marine chemists may be able to describe the reactions involved in terms of classical surface chemistry theory, was not a new one. Equilibrium models, i.e. those involving reversible uptake, had in fact been proposed by other workers to explain trace metal scavenging within the water column. For example, Balistrieri *et al.* (1981) had defined an equilibrium scavenging model, based on the principles of surface chemistry, that could be combined with field data to determine the scavenging fate of trace metals in the oceans. To do this, the quantity $[Me]_p/[Me]_t$ was calculated on the basis of equilbrium constants. Such an approach is intellectually appealing since it allows the oceanic residence times of elements to be predicted without a prior knowledge of their seawater concentrations. The results obtained by Balistrieri *et al.* (1981) strongly indicated that the scavenging component of marine particulate matter has an *organic* nature, i.e. the trace metal scavenging is controlled by organic coatings. The approach adopted by Balistrieri *et al.* (1981) is open to criticism since it may have oversimplified particle–metal interactions in the ocean. Nonetheless, it represented an important step towards the stage when trace metal scavenging in sea water can be adequately modelled.

It is now apparent that for many of the scavenging-type elements the reactions in vertical sections of the water column can be described in terms of some kind of reversible exchange mechanism. However, it has also become evident recently that the vertical seawater profiles of some trace metals can be perturbed by the effects of processes that occur at the

sediment/water interface in both coastal and open-ocean areas. For example, Bacon & Anderson (1982) showed that there was a sharp decrease in the concentration of dissolved ^{230}Th towards the sea bed, which they interpreted as resulting from an accelerated uptake of the isotope from solution onto resuspended sediment particles, which act as a sink for dissolved elements. Similar perturbations to the dissolved down-column profiles have also been reported for ^{210}Pb (see e.g. Bacon *et al.* 1976). In addition to this accelerated uptake in the benthic boundary layer (see Sec. 12.2), the dissolved forms of some trace metals are known to be preferentially removed at the ocean boundaries as a result of intensified or accelerated scavenging. Most of the non-biogenic (mainly clay) material in deep-sea sediments is small-sized, with ~ 60–70% being $\ll 2$ μm in diameter (see Sec. 13.1). The resuspension of this material at the sediment/water interface is a common feature in the distribution of oceanic TSM (see the three-layer TSM model described in Section 10.2), especially along the erosive western boundary currents where nepheloid layers are strongly developed. The particles resuspended here, which are small-sized, can then be transported laterally, thus providing a horizontal supply of TSM to supplement the vertical flux. Spencer (1984) considered the effect of this type of horizontal fine-particle flux on the distribution of particulate Al (Al_p) in the Atlantic Ocean. He demonstrated that the concentration of *fine* particulate Al decreases from the surface, where there is a substantial aeolian input, to mid-water depths. This decrease is the result of the aggregation of the fine particles (FPM) into larger units (CPM; e.g. faecal material), which sink out of the water column at a relatively fast rate and are picked up in sediment trap experiments. However, a feature of the sediment trap data was that the Al_p flux in fact *increases* with depth. To explain this, Spencer (1984) suggested that the increase resulted from an aggregation of the fine particles transported horizontally from the ocean margins, i.e. the horizontal mid-depth fine-particle flux is converted into a vertical large-particle, fast-sinking, flux by some kind of aggregation processes (e.g. from the action of mid-water zooplankton grazing).

The generation of resuspended particles at the ocean boundaries can also have an important effect on the distributions of dissolved elements in sea water. This arises because the higher concentrations of fine particles at the boundaries lead to zones of **enhanced scavenging** (cf. turbidity maxima in estuaries – see Sec. 3.2.4). Thus, processes at the ocean boundaries may act as a *source* for fine particles and as a *sink* for some dissolved elements via enhanced scavenging. Although the vertical transport of elements down the water column by incorporation into the sinking particle flux, and reference to scavenging-type and nutrient-type processes, offers a useful insight into how trace elements are removed from sea water it is evident that lateral transport into and out of the

boundary regions (e.g. along isopycnals) must also be considered in assessing the processes that control the marine cycles of the trace elements.

To summarize, the scavenging of trace elements from sea water is a complex process. The scavenging removal itself is dominated by the fine-particle population, but is then complicated by an association of the fine particles with the large-particle flux by reversible physical mechanisms (e.g. 'piggy-backing') and by reversible chemical adsorption that may tend towards an equilbrium state.

11.6.3.2 Nutrient-type mechanisms Nutrient-type distributions, i.e. surface depletion–subsurface enrichment, are displayed by those trace elements which are involved in the major oceanic biological cycles. This involvement results in the trace elements being removed from solution in the surface waters and then being transported to depth by biogenic carriers. A large fraction of the carrier material undergoes oxidative destruction below the surface layer, thus resulting in the regeneration of the dissolved species. Elements can become associated with the biogenic carriers either because they are specific to biological requirements or because they are taken up by analogy with essential elements; this can result from a lack of discrimination in the biological mechanisms or from 'mistaken identity' (see e.g. Whitfield & Turner 1987). The biogenic carriers themselves are of two types: (a) those composed of soft tissue material (**labile carriers**), and (b) those composed of hard skeletal parts (**refractory carriers**). The relative importance of these two types of biogenic trace element carriers has been assessed by Collier & Edmond (1983, 1984). These authors collected plankton samples from a variety of marine environments and subjected them to a series of leaching–decomposition experiments in order to identify the major and trace element compositions of the principal carrier phases. The elements investigated included C, N, P, Ca, Si, Fe, Mn, Ni, Cu, Cd, Al, Ba and Zn. Although the study may be criticized because the plankton collection employed nets that discriminated against small particles, the results have led to considerable advances in our understanding of the processes involved in the removal of the nutrient-type elements from sea-water.

A number of carrier phases, and types of association, are possible between trace elements and marine particulates. According to Collier & Edmond (1983) these trace element associations include: (a) those with terrigenous material scavenged by biogenic particles; (b) those involving specific biochemical processes related to metabolism; (c) those with structural skeletal materials such as calcite, opal and celestite; and (d) those with hydrous metal oxide precipitates, or organics, via active surface scavenging. The authors assessed the relative importance of these various associations, and some of the more important results of the study are summarized below.

(a) Calcium carbonate and opal were not found to be significant carriers for any of the elements studied.
(b) A phase containing Al and Fe in terrigenous ratios was present in all the plankton samples. However, this non-biogenic carrier phase made an insignificant contribution to the concentrations of the trace elements studied.
(c) The majority of the trace elements were directly associated with the non-skeletal organic phases of the plankton in three types of host associations. In order of their general ease of metal release to sea water via remineralization, these were a **very labile** association (which included the nutrient P and major fractions of the total amounts of Cd, Mn, Ni and Cu), a **moderately refractory** association (which included significant fractions of the total amounts of Cu, Ni, Cd, Ba, Mn and Zn), and a **strongly refractory** association (which included large fractions of the total amounts of Si, Al, Fe and Zn).
(d) The concentrations of trace elements in surface ocean biogenic particulate matter are not fixed in simple proportions to their surface water concentration ratios to the nutrients. To demonstrate this the authors showed that, although there are considerable variations in the surface water dissolved element : nutrient ratios (e.g. between nutrient-rich upwelling and oligotrophic waters), the particulate trace metal : carrier phase ratios are relatively constant. Thus, the trace element composition of the particulate material appears to be fixed, and limited, mainly by the properties of the organic materials involved and the metabolism of the plankton, rather than by the dissolved concentrations of the elements in the surface waters.

One of the principal aims of the investigation carried out by Collier & Edmond (1983, 1984) was to quantify the biogenic fluxes of trace elements out of the surface layer. The particulate trace element : carrier phase ratio constancy allowed the biogenic flux of each element to be predicted in terms of the major oceanic biological cycles, and Collier & Edmond (1983) used a **carrier model** to make their flux estimates. These were then compared with flux values derived from a **two-box vertical model**, which describes the dissolved distributions of the trace elements. Both of these illustrate how models can be used to elucidate the factors that control the distributions of trace elements in the ocean system, and for this reason they will be described in detail.

THE CARRIER MODEL In this model, independently derived estimates of the fluxes of major biologically cycled elements, such as C, N, P, Ca (carbonate) and Si (opal), were used, and the trace elements were coupled to these fluxes through their ratios to the major elements, which represent the biogenic carrier phases. Since extensive data were available

for P, this element was used in the model to represent the **primary flux** of organic matter. Collier & Edmond (1984) then used the following relationship to compare elemental ratios in the plankton to those in the surrounding sea water:

$$\alpha = \frac{(\text{metal/P})_{\text{plankton}}}{(\text{metal/P})_{\text{water}}}. \tag{11.9}$$

Differences in the regeneration of the nutrients and trace elements in the surface waters will result in different elemental ratios in the sinking particulates, which are given by the relationship:

$$\beta = \frac{(\text{metal/P})_{\text{sinking}}}{(\text{metal/P})_{\text{plankton}}}. \tag{11.10}$$

In these equations α represents particulate formation by primary producers, and β represents the various processes that modify the ratio before the particulate matter sinks out of the surface layer. Thus, for regeneration that takes place within the surface layer, the product $\alpha\beta$ offers a comparison between the relative enrichment, or depletion, of the particulate trace element flux with respect to the dissolved ratios. The authors employed their leaching experiment data to obtain a first-order estimate of the magnitude of β, which was calculated as the percentage of the total element *not* released by leaching to sea water, divided by the same percentage for P. Thus, β is a relative enrichment factor for the residual trace element/P ratio in the particles, and the product of the plankton sample composition and β gives an estimate of the composition of the material settling out of the surface layer. In the carrier model, the net, or 'new production', P flux out of the surface layer is coupled with the residual trace element/P ratios to calculate the down-column biogenic carrier flux. The carrier model is illustrated in Figure 11.7a.

THE TWO-BOX MODEL The two reservoirs in this model are the **surface ocean** and the **deep ocean** (see Sec. 7.5.2). The parameters used to define the model are the dissolved distributions of the elements, the mixing rates of water between the reservoirs, and the primary input and output fluxes of the elements. The particulate flux out of the surface layer (P) is then calculated to balance the sum of the other input output fluxes; thus

$$P = V_{\text{M}}(C_{\text{D}} - C_{\text{S}}) + V_{\text{R}}C_{\text{R}} + A \tag{11.11}$$

where V_{M} (3.5 m yr^{-1}) is the exchange rate between the surface and deep boxes of water with concentrations C_{S} and C_{D}, respectively; $V_{\text{R}}C_{\text{R}}$ represents the river input; and A represents the atmospheric input. The

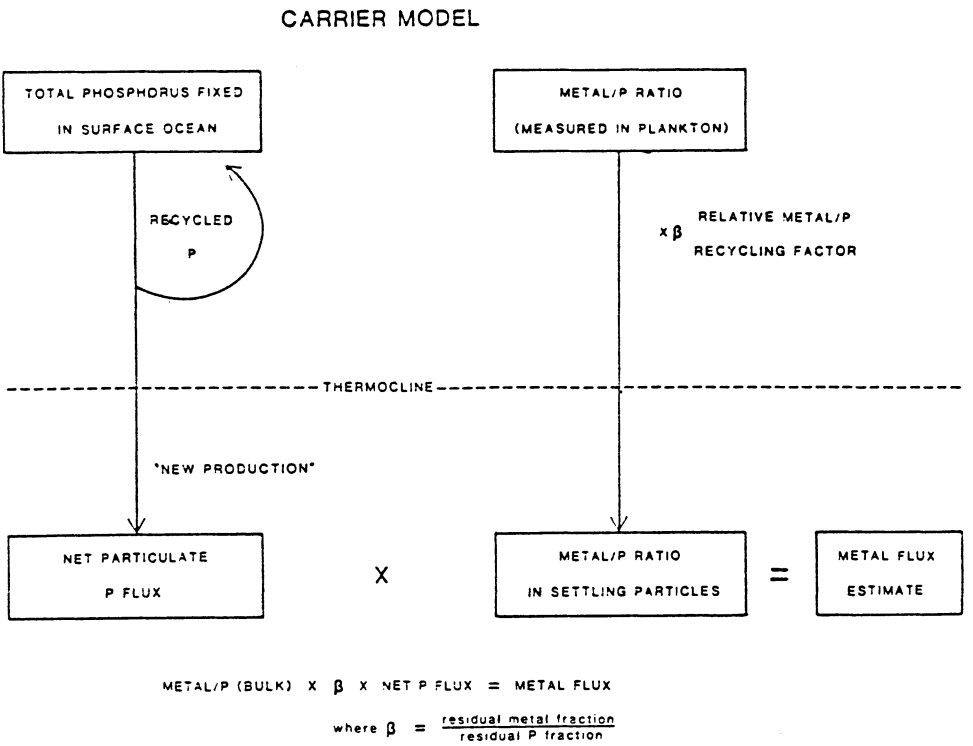

(a)

Figure 11.7 Models for the down-column transport of trace elements in the oceans (from Collier & Edmond 1984). (**a**) The carrier model. This makes use of independent predictions of the fluxes of major organically-cycled elements. Trace elements are coupled to these biogenic fluxes through their ratios to the major elements that represent the biogenic carrier phase. In the model illustrated, P is used to represent the primary flux of organic matter out of the surface layer. Independent estimates of the P flux are derived from total surface ocean carbon fixation rates. The fraction of the 'new' carbon production, i.e. that which is not recycled in the surface layer, but which actually constitutes a net flux to the deep ocean (see Sec. 9.1.1), is estimated from nitrogen flux data. The P flux associated with this net out-of-surface carbon flux is estimated using a Redfield C : P ratio of 106 : 1 (see Sec. 9.2.3.1). The resulting P flux ($\sim$ 1 μmol P $cm^{-2}yr^{-1}$) is coupled to out-of-surface fluxes of the minor element concentrations in sinking particles using β (see text) as an estimate of the residual (i.e. non-rapidly recycled) metal : P ratios, and the product of β and the plankton sample composition is used to give an estimate of the composition of the material settling out of the surface layer. This is then applied to the 'new' production estimate of the net P flux to calculate the biogenic carrier flux out of the surface ocean for each trace element.

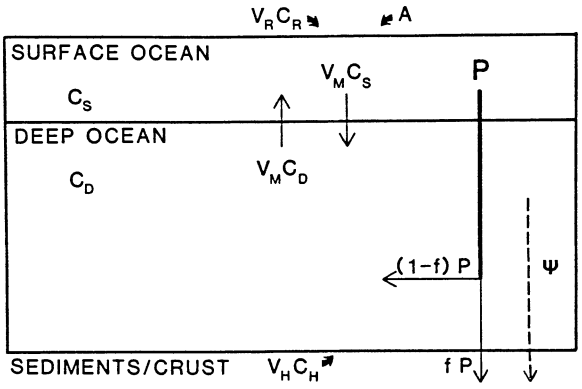

$$P = V_M(C_D - C_S) + V_RC_R + A$$

(b)

Figure 11.7b The two-box model. P, particulate matter flux out of the surface ocean; V_R, C_R, volume and concentration of an element in river water; A, atmospheric input; C_S, C_D, dissolved concentrations of an element in the surface and deep reservoirs; f, fraction of particulate matter preserved in sediments; ψ, additional particulate matter flux due to scavenging within the deep ocean; V_H, C_H, volume and concentration of an element in hydrothermal solutions. The particulate matter flux (P) is calculated by the mass balance of all other inputs and outputs to the surface ocean reservoir.

two-box model is shown diagrammatically in Figure 11.7b. Further details on both models are given in Collier & Edmond (1984).

The fluxes obtained from the two-box model may be regarded as estimates of those required to maintain the vertical gradients in the dissolved distributions of the elements. Thus, by comparing the *carrier*-phase fluxes with these *total* fluxes it was possible to make first-order assessments of the importance of biological particulates in down-column trace element fluxes. The flux estimates obtained using the two models are given in Table 11.5, and the data can be summarized as follows.

(a) The fluxes derived from the two models agree, within a factor of 2, for Cd, Ni and Cu, indicating that the data used in the carrier model are representative of the major particulate flux that maintains the

Table 11.5 Down-column flux estimates of trace metals using an organic carrier phase model and a two-box model[a] (units, ng cm^{-2} yr^{-1})

Element	Organic carrier estimate	Box model estimate
Cd	56 - 112	38
Ni	70 - 135	152
Cu	95 - 114	76 - 95
Mn	33 - 44	110
Ba	961 - 1374	5494
Zn	654 - 1635	163 - 196
Fe	1396 - 4468	1117 - 3909

[a] After Collier & Edmond (1984).

vertical flux of these elements.

(b) Mn is incorporated in plankton and released during regeneration processes. However, comparison of the magnitudes of the fluxes predicted from the models indicates that the biogenic carrier phases transport considerably less Mn out of the surface layer than do the non-biogenic carriers. Thus, the association of Mn with plankton should not have a significant effect on the dissolved distribution of the metal.

(c) The biogenic carrier flux for Ba is only sufficient to account for ~ 20–30% of the box model flux. This biogenic carrier flux for Ba includes associations with organic matter, calcium carbonate, opal and celestite, and Collier & Edmond (1983, 1984) suggested that a secondary process resulting in the formation of Ba-rich particles (such as barite) probably occurs below the surface zone of nutrient depletion.

(d) The flux predicted by the carrier model for Zn is an order of magnitude higher than that calculated by applying the dissolved distributions of the element to the two-box model. This may be the result of sample contamination in any of the values used in either model, and as a result it is not yet possible to identify with any certainty the Zn carrier phase in the oceans.

11.6.3.3 Scavenging-type versus nutrient removal mechanisms The division of trace element uptake mechanisms into scavenging-type (passive surface adsorption) and nutrient-type (active biological uptake)

classes is a useful way of describing the vertical distributions and down-column transport of some elements. However, in a recent paper, Honeyman *et al.* (1988) took a wider view of the processes that remove trace elements from sea water, and attempted to bring together recent advances in our knowledge of particle scavenging mechanisms in terms of the removal of dissolved Th from sea water.

The solids in natural aqueous systems contain surface functional groups, which can form surface complexes with solutes by coordination reactions that follow the principles of coordination chemistry. In recent years various authors have used **surface complexation models** to describe the uptake of trace elements by solid surfaces. For example, a surface complexation model is described below for the ultimate removal of elements from the oceans. For a detailed review of the application of coordination chemistry to the adsorption and transformation of trace element species at particle/water interfaces, the reader is referred to Leckie (1986). Honeyman *et al.* (1988) pointed out that two general hypotheses have been produced to account for oceanic scavenging, both of which involve marine particles. Using Th as an example, these scavenging reactions were characterized as (a) control by biological removal and (b) control by equilibrium exchange reactions. Thermodynamic scavenging models assume complete equilibrium in the system between the dissolved and particulate phases, and the equilibrium values are assumed to be constant for similar conditions regardless of reaction time relative to particle residence time (Jannasch *et al.* 1988). However, if the particle residence time is short compared to the adsorption time, an equilibrium condition may not be attained, and the system may depend on kinetic factors (see e.g. Nyffeler *et al.* 1984, Jannasch *et al.* 1988).

It is now known that the rate of transfer of dissolved Th to the particulate state is a function of particle concentration or particle residence time (see e.g. Nyffeler *et al.* 1984), i.e. the rate constants of adsorption vary with the particle concentration. Further, one of the most significant findings in recent years was that there is a correlation between dissolved Th removal rate constants and the production of particles via primary productivity (see e.g. Coale & Bruland 1985, 1987). The key to understanding the removal processes therefore lies in the fact that the adsorption of Th varies with the concentration of particles in the system. Honeyman *et al.* (1988) pointed out that this has important implications on Th fractionation since in nearshore and surface ocean waters the particle residence time is equal to, or less, than the residence time of the dissolved Th. Since particles are leaving the system the fraction of Th in the particulate phase will be less than it would be if the particles had an infinite residence time. Under these conditions, therefore, the system should not be viewed as an equilibrium system.

Honeyman *et al.* (1988) derived a series of equations to describe Th

uptake and then plotted the log value for the forward Th sorption rate constant, i.e. uptake, against the log value of the particle concentration, using data for a wide variety of oceanic environments. These included the highly productive California coastal zone, with medium particle concentrations; the low productive China shelf zone, with high particle concentrations; and the deep ocean, which is low in both biological productivity and particle concentrations. The plot is reproduced in Figure 11.8, and shows that there is a strong linear relationship between the log value of the forward sorption rate constant and the log value of the particle concentration. This particle dependence of the scavenging rate holds over seven orders of magnitude variation in particle concentration. Linear regression analysis of the data (excluding that for the Amazon) gave a slope of 0.58, and the authors described the partitioning of Th between dissolved and particulate phases by the equation:

$$\frac{A_{\text{Th, part}}}{A_{\text{Th, diss}}} = \frac{R_f(C_p)^{0.58}}{R_r + \lambda_{\text{Th}} + \lambda_{\text{part}}} \tag{11.12}$$

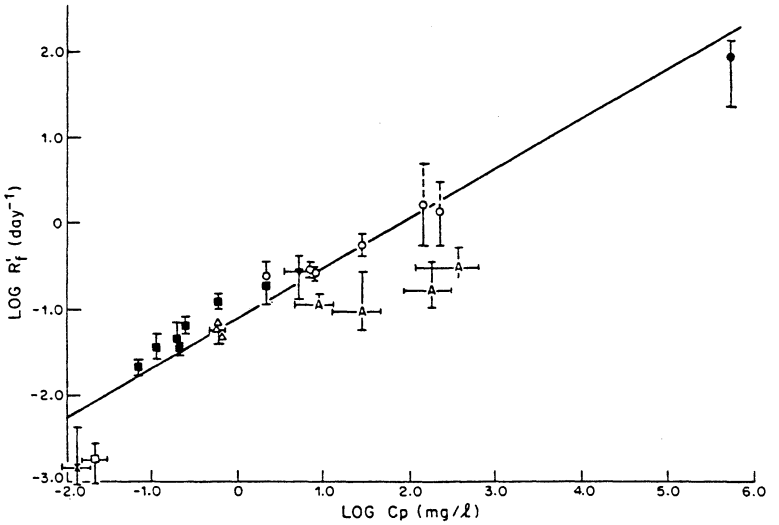

Figure 11.8 A plot of the forward sorption rate constant (log R_f) for Th versus particle concentration using field data from various oceanic regions (from Honeyman *et al.* 1988). The oceanic regions cover a wide variety of particle concentrations, particle types and primary productivity intensities: (□ and ×) deep sea; (■) surface water, California Current; (○) coastal waters, Yangtze River; (A) coastal waters, Amazon River; (△) surface waters, Funka Bay; (▼) surface waters, Narragansett Bay; (●) sediment-pore waters, Buzzards Bay. The full line represents the linear regression excluding the Amazon data.

where $A_{Th,\ part}$ and $A_{Th,\ diss}$ are the activities of particulate and dissolved Th, respectively; R_f ($= 0.079\ l^{-0.58}\ mg^{-0.58}\ d^{-1}$) is the rate constant for the transfer of Th from the dissolved to the particulate phase; R_r ($= 0.007\ d^{-1}$) is the rate constant for the reverse reaction; C_p is the mass concentration of particles (expressed in units of mg l^{-1}); and λ_{Th} and λ_{part} are the decay constants for the thorium isotope (day^{-1}) and the rate constant for particle removal (day^{-1}), respectively. Thus, the partitioning of Th depends on an interplay between the reaction rates, the particle concentration, the decay characteristics of the particular Th isotope, and the residence time of the particles in the system, which depends on the water column height, the particle concentration and the particle flux.

Trace metal removal times based on adsorption reactions are thought to be rapid, i.e. of the order of seconds, but in natural systems they appear to be of the same order as physical mixing processes, i.e. days to weeks. In order, therefore, to combine all the various features of the Th removal processes, Honeyman *et al.* (1988) suggested that the aggregation or coagulation of colloids, which is also a function of particle concentration, may play a part in controlling these slow rates. They proposed, therefore, that the constancy of the 'Th removal rate constant–particle concentration' relationship can be attributed to a Th removal mechanism that involves a combination of surface coordination reactions (based on surface coordination chemistry involving surface complex formation – see above) and colloidal particle-to-particle aggregation. This surface coordination–colloidal aggregation model implies that, although particles in a highly productive system may be of biological origin and may be supplied at a rate that is controlled by primary production, they simply serve as **new adsorptive passive substrates** for the surface-active Th. It must be stressed, however, that Honeyman *et al.* (1988) based their model on Th, and other metals may have different controlling properties. Thus, the extent to which Th can act as an analogue for other surface-active metals requires further research. Nonetheless, the model proposed by Honeyman *et al.* (1988) links microlevel adsorption reactions to macrolevel oceanic scavenging processes, and offers an explanation for the correlations found between dissolved Th removal rate constants and biological productivity.

Despite the fact that biologically produced particles may act as passive substrates for the uptake of surface-active trace metals, it is still useful to view down-column trace metal transport in terms of scavenging-type uptake, which involves inorganic (perhaps organic-coated) FPM, and nutrient-type uptake, which involves organic CPM aggregates. It is the CPM organic aggregates that dominate the down-column transport of material to the sediment sink, pulling down the FPM with them. However, once they reach the sea bed a large fraction of the organic carrier material is destroyed in open-ocean regions during oxic diagenesis,

releasing the associated trace elements back into solution, and the fraction that is buried in the sediment will continue to be degraded during sub-oxic diagenesis (see Sec. 14.2.2). As a result of processes such as this, Li (1981) has suggested that the most important mechanism for the *ultimate* removal of elements from the deep sea is adsorption onto the surfaces of fine particles. These include aluminosilicates, managanese oxides and iron oxides, and from data based on factor analyses Li (1981) showed that the following relationships exist in both ferromanganese nodules and pelagic clays.

(a) Elements such as K, Rb, Cs, Be, Sc and Ga are mainly associated with the aluminosilicate detritus.
(b) The elements associated with iron oxide phases form anions or oxyanions (e.g. P, S, Se, Te, As, B, Sn, I, Br, F, U, Pb and Hg) and hydroxide complexes of tri- and tetravalent cations (e.g. Ti, Ge, Zr, Hf, Th, Y, In, Pd and Cr).
(c) The elements associated with manganese oxides are mono- and divalent cations (e.g. Mg, Ca, Ba, Tl, Co, Ni, Cu, Zn, Bi, Ag and Cd) and oxyganions (e.g. Mo, W and Sn).

Li (1981) attempted to rationalize these relations in terms of theoretical adsorption models.

The uptake of elements onto the surfaces of particulate matter involves a distribution ratio (K_d), which is the ratio of the concentration of the element in the solid phase to that in the aqueous phase. A variety of theoretical models have been proposed to describe the inorganic adsorption of trace elements onto particulate surfaces. However, the surface complexation model (see e.g. Schindler 1975) has been most commonly used in marine chemistry, and this will serve to illustrate the general mechanisms that are thought to be involved in the ultimate removal of elements reaching the sediment surface. In this model, it is assumed that metal ions are removed by adsorption onto inorganic particulate matter at oxide surfaces covered with OH groups which act as ligands. The hydrolysis of the oxide surfaces produces hydrous oxide surface groups such as $\equiv$Si$-$OH, $\equiv$Mn$-$OH and $=$Fe$-$OH. Protonation or deprotonation results in a surface charge on the oxide surfaces, which Li (1981) represents as:

$$\equiv \mathrm{MeOH_2^+} \leftrightharpoons \equiv \mathrm{MeOH} + \mathrm{H^+} \tag{11.13}$$

$$K_{a1}^{s} = \frac{\{\mathrm{MeOH}\}[\mathrm{H^+}]}{\{\mathrm{MeOH_2^+}\}} \tag{11.14}$$

$$\equiv MeOH \leftrightharpoons MeO^- + H^+ \tag{11.15}$$

$$K^s_{a2} = \frac{\{MeO^-\}[H^+]}{\{MeOH\}} \tag{11.16}$$

where Me is the metal (e.g. Mn, Fe, Si, Al) of the solid oxides, [ ] is the concentration of species in the aqueous phase, { } is the concentration of surface species on the solid oxides, and K^s_{a1} and K^s_{a2} are acidity constants.

Li (1981) applied the surface complexation model to the observed partitioning of a series of elements between sea water and pelagic clays, and between river water and river suspended particulates. To do this, the adsorption of a cation (M^{z+}) onto a surface hydroxyl group was represented as:

$$M^{z+} + \equiv Me-OH \leftrightharpoons \equiv Me-O-M^{(z-1)+} + H^+ \tag{11.17}$$

$$^*K^s_{1(app)} = \frac{[H^+]\{Me-O-M^{(z-1)+}\}}{[M^{z+}]\{MeOH\}} \tag{11.18}$$

where the units are as for Equations 11.13–11.16, and $^*K^s_{1(app)}$ is the apparent equilibrium constant. The bond strength of a metal–oxygen bond (O–M) for various cations on silica gel has been shown to be linearly correlated with their $\log {}^*K_1$, where $^*K_1$ is the first hydrolysis constant for the reaction:

$$M^{z+} + H_2O \leftrightharpoons H-O-M^{(z-1)+} + H^+ \tag{11.19}$$

$$^*K_1 = \frac{[H^+][HOM^{(z-1)+}]}{[Mz^+][H_2O]}. \tag{11.20}$$

Schindler (1975) demonstrated that $\log {}^*K_{1(app)}$ of silica gel is also linearly correlated with $\log {}^*K_1$. Li (1981) suggested therefore that the partitioning of various *cations* between solid and liquid phases in rivers and the oceans should be positively correlated with the relative bond strength between the cations and the oxygen of the hydrous oxide surface, or with $\log {}^*K_1$. This relationship is illustrated in Figures 11.9A and C, in which the partitioning of the cations between liquid and solid phases in the ocean is plotted against $\log {}^*K_1$ values.

From this figure it can be seen that there is a general positive correlation between the two parameters for most mono- and divalent cations, i.e. the higher the $\log {}^*K_1$ values, the more the cations are partitioned towards the solid phase (surface adsorption). The tri- and

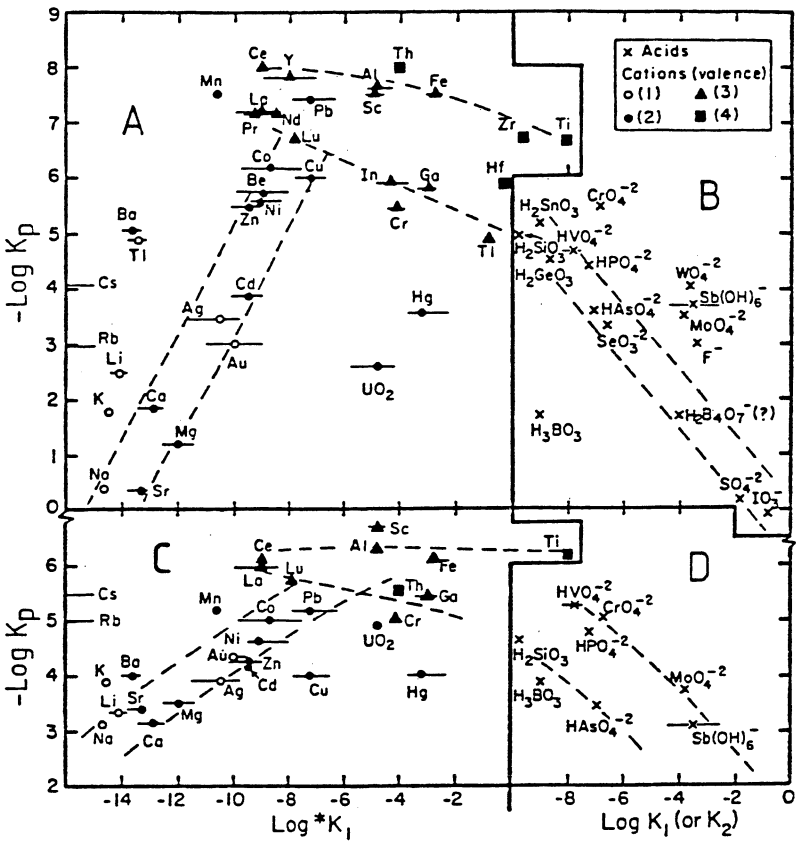

Figure 11.9 Plots of the relationship between (a, b) log K_p = log C_{op}/C_{sw} (the concentration ratio of an element in oceanic pelagic clay and sea water) and (c, d) log K_p = log C_p/C_r (the concentration of an element in river suspended particulates and river water) versus log $^*K_1$ (the first hydrolysis constant) or log K_2 (the second dissociation constant of acids) (after Li 1981).

tetra-valent cations, which usually form hydroxyl complexes in natural water, plot as a broad maximum. These are usually associated with iron oxide phases in pelagic deposits and the fact that their partitioning coefficient ratios do not increase with $^*K_1$ may be a function of the adsorption dynamics onto the iron oxide surfaces.

For undissociated acids, monovalent anions and divalent anions there is an inverse relationship between log K_1 (first dissociation constant) or log K_2 (second dissociation constant) and the partitioning coefficients for river water and sea water. This is shown in Figures 11.9B and D, and indicates that the higher the log K_1 or log K_2 values, the more the species

is partitioned to the liquid phase (less adsorption). A number of species fall outside the main correlation. These include (a) MoO_4^{2-}, WO_4^{2-} and SbO_3^-, which may be taken up in authigenic manganese phases, and (b) F^-, which may enter apatite.

Overall, therefore, Li (1981) concluded that, with the exception of those which form authigenic phases, the observed partitioning of most elements between the solid and liquid phases of river water and sea water can be adequately explained in terms of the surface complexation model, and that adsorption onto the surfaces of iron oxides, manganese oxides and clay minerals was the most important mechanism for the ultimate removal of elements from the oceans. However, Whitfield & Turner (1982) criticized the surface complexation model on a number of grounds, and proposed instead that the partitioning of elements between the solid and liquid phases in river and sea water could be better rationalized using a more simple electrostatic model; this approach is reviewed in Section 17.3.

11.7 Trace elements in sea water: summary

(a) Trace element distributions in sea water are controlled by a complex interaction between their source strengths, their removal strengths and water circulation patterns.
(b) The vertical distributions of trace elements in the water column can be related to a number of analogues. On this basis, the profiles can be divided into the following classes: (i) conservative type (unreactive), (ii) nutrient surface depletion–depth enrichment type, (iii) scavenging surface enrichment–depth depletion type, (iv) mid-depth minimum type, (v) mid-depth maximum type, and (vi) anoxic water type.
(c) Dissolved trace elements are removed in sea water by the oceanic microcosm of particles, via scavenging-type and nutrient-type mechanisms, and the subsequent settling of these particles down the water column, either directly from the surface water or indirectly following subsurface lateral advection.

The processes involved in the down-column transport of the trace elements are part of the 'great particle conspiracy', and in the next chapter an attempt will be made to assess the rate at which the conspiracy operates.

References

Amdurer, M., D. Adler & P.H. Santschi 1983. Studies of the chemical forms of trace

elements in sea water using radio tracers. In *Trace metals in sea water*, C.S. Wong *et al.* (eds), 537–62. New York: Plenum.

Andreae, M.O. 1983. The determination of the chemical species of some of the 'hydride elements' (arsenic, antimony, tin and germanium) in seawater: methodology and results. In *Trace metals in sea water*, C.S. Wong, E. Boyle, K.W. Bruland, J.D. Burton & E.D. Goldberg (eds), 1–19. New York: Plenum.

Andreae, M.O. 1986. Chemical species in seawater and marine particulates. In *The importance of chemical 'speciation' in environmental processes*, M. Bernhard, F.E. Brinckman & P.J. Sadler (eds), 301–35. Berlin: Springer-Verlag.

Bacon, M.P. 1984. Radionuclide fluxes in the ocean interior. In *Global ocean flux study*, 180–205. Washington, DC: National Academy Press.

Bacon, M.P. & R.F. Anderson 1982. Distribution of thorium isotopes between dissolved and particulate forms in the deep sea. *J. Geophys. Res.* **87,** 2045–56.

Bacon, M.P., P.G. Brewer, D.W. Spencer, J.W. Murray & J. Goddard 1980. Lead-210, polonium-210, manganese and iron from the Cariaco Trench. *Deep-Sea Res.* **27,** 119–35.

Bacon, M.P., C.-A. Huh, A.P. Fleer & W.G. Deuser 1985. Seasonality in the flux of natural radionuclides and plutonium in the deep Sargasso Sea. *Deep-Sea Res.* **32,** 273–86.

Bacon, M.P., D.W. Spencer & P.G. Brewer 1976. $^{210}Pb/^{226}Ra$ and $^{210}Po/^{210}Pb$ disequilibria in seawater and suspended particulate matter. *Earth Planet. Sci. Lett.* **32,** 277–96.

Bailey, R.A., H.M. Clarke, J.P. Ferris, S. Krause & R.L. Strong 1978. *Chemistry of the environment*. New York: Academic Press.

Balistrieri, L., P.G. Brewer & J.W. Murray 1981. Scavening residence time of trace metals and surface chemistry of sinking particles in the deep ocean. *Deep-Sea Res.* **28,** 101–21.

Balls, P.W. 1985. Copper, lead and cadmium in coastal waters of the western North Sea. *Mar. Chem.* **15,** 363–78.

Barth, T.W. 1952. *Theoretical petrology*. New York: Wiley.

Batley, G.E. & T.M. Florence 1976. Determination of the chemical forms of dissolved cadmium, lead and copper in seawater. *Mar. Chem.* **4,** 347–63.

Bernhard, M. & S.G. George 1986. Importance of chemical species in uptake, loss and toxicity of elements for marine organisms. In *The importance of chemical 'speciation' in environmental processes*, M. Bernhard, F.E. Brinckman & P.J. Sadler (eds), 385–422. Berlin: Springer-Verlag.

Bewers, J.M. & P.A. Yeats 1977. Oceanic residence times of trace metals. *Nature* **268,** 595–8.

Boulegue, J. 1983. Trace metals (Fe, Zn, Cd) in anoxic environments. In *Trace metals in sea water*, C.S. Wong, E. Boyle, K.W. Bruland, J.D. Burton & E.D. Goldberg (eds), 563–77. New York: Plenum.

Boyle, E.A. & S. Huested 1983. Aspects of the surface distributions of copper, nickel, cadmium and lead in the North Atlantic and North Pacific. In *Trace metals in sea water*, C.S. Wong, E. Boyle, K.W. Bruland, J.D. Burton & E.D. Goldberg (eds), 379–94. New York: Plenum.

Boyle, E.A., S.D. Chapnick, G.T. Shen & M.P. Bacon 1986. Temporal variability of lead in the western North Atlantic. *J. Geophys. Res.* **91,** 8573–93.

Boyle, E.A., S.S. Huested & S.P. Jones 1981. On the distribution of copper, nickel and cadmium in the surface waters of the North Atlantic and North Pacific Ocean. *J. Geophys. Res.* **86,** 8048–66.

Boyle, E.A., F. Sclater & J.M. Edmond 1976. On the marine geochemistry of cadmium. *Nature* **263,** 42–4.

Boyle, E.A., F. Sclater & J.M. Edmond 1977. The distribution of dissolved copper in the Pacific. *Earth Planet. Sci. Lett.* **37,** 38–54.

Brewer, P.G. 1975. Minor elements in sea water. In *Chemical oceanography*, J.P. Riley & G. Skirrow (eds), Vol. 1, 415–96. London: Academic Press.

REFERENCES

Broecker, W.S. & T.-H. Peng 1982. *Tracers in the sea*. Palisades, NY: Lamont-Doherty Geological Observatory.

Bruland, K.W. 1980. Oceanographic distributions of cadmium, zinc, nickel and copper in the North Pacific. *Earth Planet. Sci. Lett.* **47,** 176–98.

Bruland, K.W. 1983. Trace elements in sea water. In *Chemical oceanography*, J.P. Riley & R. Chester (eds), Vol. 8, 157–220. London: Academic Press.

Bruland, K.W. & R.P. Franks 1983. Mn, Ni, Zn and Cd in the western North Atlantic. In *Trace metals in sea water*, C.S. Wong, E. Boyle, K.W. Bruland, J.D. Burton & E.D. Goldberg (eds), 395–414. New York: Plenum.

Bruland, K.W., G.A. Knauer & J.H. Martin 1978. Cadmium in northeast Pacific waters. *Limnol. Oceanogr.* **23,** 618–25.

Burton, J.D. & P.J. Statham 1988. Trace metals as tracers in the ocean. *Phil. Trans. R. Soc. Lond.* **325,** 127–45.

Burton, J.D., W.A. Maher & P.J. Statham 1983. Some recent measurements of trace metals in Atlantic Ocean waters. In *Trace metals in sea water*, C.S. Wong, E. Boyle, K.W. Bruland, J.D. Burton & E.D. Goldberg (eds), 415–26. New York: Plenum.

Chan, L.H., D. Drummond, J.M. Edmond & B. Grant 1977. On the barium data from the Atlantic GEOSECS Expedition. *Deep-Sea Res.* **24,** 613–49.

Chester, R. 1985. Book reviews. *Chem. Geol.* **51,** 150–1.

Cho, B.C. & F. Azam 1988. Major role of bacteria in biogeochemical fluxes in the ocean's interior. *Nature* **332,** 441–3.

Coale, K.H. & K.W. Bruland 1985. ^{234}Th : ^{238}U disequilibria within the California Current. *Limnol. Oceanogr.* **30,** 22–33.

Coale, K.H. & K.W. Bruland 1987. Oceanic stratified euphotic zone as elucidated by ^{234}Th : ^{238}U disequilibria. *Limnol. Oceanogr.* **32,** 189–200.

Collier, R.W. & J.M. Edmond 1983. Plankton compositions and trace element fluxes from the surface ocean. In *Trace metals in sea water*, C.S. Wong, B. Boyle, K.W. Bruland, J.D. Burton & E.D. Goldberg (eds), 789–809. New York: Plenum.

Collier, R.W. & J.M. Edmond 1984. The trace element geochemistry of marine biogenic particulate matter. *Progr. Oceanogr.* **13,** 113–99.

Craig, H. 1974. A scavenging model for trace elements in the deep sea. *Earth Planet. Sci. Lett.* **23,** 393–402.

Cutter, G.A. & K.W. Bruland 1984. The marine biogeochemistry of selenium: a reevaluation. *Limnol. Oceanogr.* **29,** 1179–92.

Danielsson, L.-G. 1980. Cadmium, cobalt, iron, lead, nickel and zinc in Indian Ocean water. *Mar. Chem.* **8,** 199–215.

Danielsson, L.G. & S. Westerlund 1983. Trace metals in the Arctic Ocean. In *Trace metals in sea water*, C.S. Wong, E. Boyle, K.W. Bruland, J.D. Burton & E.D. Goldberg (eds), 85–95. New York: Plenum.

Duinker, J.C. & J.M. Kramer 1977. An experimental study on the speciation of dissolved zinc, cadmium, lead and copper in river Rhine and North Sea water by difference pulse anodic stripping voltammetry. *Mar. Chem.* **5,** 207–28.

Dyrssen, D. & M. Wedborg 1974. Equilibrium calculations of the speciation of the elements in sea water. In *The sea*, E.D. Goldberg (ed.), Vol. 5, 181–95. New York: Interscience.

Edmond, J.M., S.S. Jacobs, A.L. Gordon, A.W. Mantyla & R.F. Weiss 1979. Water column anomalies in dissolved silica over opaline pelatic sediments and the origin of the deep silica maximum. *J. Geophys. Res.* **84,** 7809–26.

Emerson, S., L. Jacobs & B. Tebo 1983. The behaviour of trace metals in marine anoxic waters: solubilities at the oxygen–hydrogen sulphide interface. In *Trace metals in sea water*, C.S. Wong, E. Boyle, K.W. Bruland, J.D. Burton & E.D. Goldberg (eds), 579–608. New York: Plenum.

Florence, T.M. & G.E. Batley 1976. Trace metal species in seawater. *Talanta* **23,** 179–86.
Froelich, P.N., G.A. Hambrick & M.O. Andreae 1983. Geochemistry of inorganic and methyl germanium species in three estuaries. *EOS* **45,** 715.
Froelich, P.N., G.A. Hambrick, L.W. Kaul, J.T. Byrd & O. Lecointe 1985. Geochemical behaviour of inorganic germanium in an unperturbed estuary. *Geochim. Cosmochim. Acta* **49,** 519–24.

Garrels, R.M. & M. Thompson 1962. A chemical model for sea water at 25°C and one atmosphere total pressure. *Am. J. Sci.* **260,** 57–66.
Gill, A.G. & W.F. Fitzgerald 1988. Vertical mercury distribution in the oceans. *Geochim. Cosmochim. Acta* **52,** 1719–28.
Goldberg, E.D. 1954. Marine geochemistry. I. Chemical scavengers of the sea. *J. Geol.* **62,** 249–65.
Goldberg, E.D. 1965. Minor elements in sea water. In *Chemical oceanography*, 1st edn, J.P. Riley & G. Skirrow (eds), Vol. 1, 181–95. London: Academic Press.
Goldberg, E.D. & G.O.S. Arrhenius 1958. Chemistry of Pacific pelagic sediments. *Geochim. Cosmochim. Acta* **13,** 153–212.

Honeyman, B.D., L.S. Balistrieri & J.W. Murray 1988. Oceanic trace metal scavenging: the importance of particle concentration. *Deep-Sea Res.* **35,** 227–46.
Huizenga, D.I. & D.R. Kester 1983. The distribution of total and electrochemically available copper in the northwestern Atlantic Ocean. *Mar. Chem.* **13,** 281–91.
Hydes, D.J. 1979. Aluminium in sea water: control by inorganic processes. *Science* **205,** 1260–2.

Imber, B.E. & M.G. Robinson 1983. Complexation of Zn by exudates of *Thalassiosira fluviatilis* grown in culture. *Mar. Chem.* **14,** 31–41.
Imber, B.E., M.G. Robinson, A.M. Ortega & J.D. Burton 1985. Complexation of zinc by exudates from *Skeletonema cocstatum* growth in culture. *Mar. Chem.* **16,** 131–9.

Jacobs, L., S. Emerson & J. Skei 1985. Partitioning and transport of metals across the O_2/H_2S interface in a permanently anoxic basin: Framvaren Fjord, Norway. *Geochim. Cosmochim. Acta* **49,** 1433–44.
Jannasch, H., B.D. Honeyman, L.S. Balistrieri & J.W. Murray 1988. Kinetics of trace element uptake by marine particles. *Geochim. Cosmochim. Acta* **52,** 567–577.

Klinkhammer, G.P. & M.L. Bender 1980. The distribution of manganese in the Pacific Ocean. *Geochim. Cosmochim. Acta* **46,** 361–84.
Klinkhammer, G., H. Elderfield, M. Greaves, P. Rona & T. Nelson 1986. Manganese geochemistry near high temperature vents in the Mid-Atlantic Rift valley. *Earth Planet. Sci. Lett.* **80,** 230–40.
Krauskopf, K.B. 1956. Factors controlling the concentrations of thirteen rare metals in seawater. *Geochim. Cosmochim. Acta* **12,** 61–84.
Kremling, K. 1983. Trace metal fronts in European shelf waters. *Nature* **303,** 225–7.
Kremling, K. 1985. The distribution of cadmium, copper, nickel, manganese and aluminium in surface waters of the open Atlantic and European shelf area. *Deep-Sea Res.* **32,** 531–55.

Lal, D. 1980. Comments on some aspects of particulate transport in the oceans. *Earth Planet. Sci. Lett.* **49,** 520–7.
Landing, W.M. & K.W. Bruland 1980. Manganese in the North Atlantic. *Earth Planet. Sci. Lett.* **49,** 45–56.

REFERENCES

Landing, W.M. & K.W. Bruland 1987. The contrasting biogeochemistry of iron and manganese in the Pacific Ocean. *Geochim. Cosmochim. Acta* **51,** 29–43.

Leckie, J.O. 1986. Adsorptioin and transformation of trace element species at sediment/water interface. In *The importance of chemical 'speciation' in environmental processes*, M. Bernhard, F.E. Brinckman & P.J. Sadler (eds), 237–54. Berlin: Springer-Verlag.

Li, Y.-H. 1981. Ultimate removal mechanisms of elements from the ocean. *Geochim. Cosmochim. Acta* **45,** 1659–64.

Mackey, D.J. 1983. Metal–organic complexes in sea water – an investigation of naturally occurring complexes of Cu, Zn, Fe, Mg, Ni, Cr, Mn and Cd using high-performance liquid chromatography with atomic fluorescence detection. *Mar. Chem.* **13,** 169–80.

Mackey, D.J. 1985. HPLC analyses of metal–organics in seawater – interference effects attributed to stationary-phase free silanols. *Mar. Chem.* **16,** 105–19.

Magnusson, B. & S. Westerlund 1983. Trace metals in the Skagerrak and Kategat. In *Trace metals in sea water*, C.S. Wong, E. Boyle, K.W. Bruland, J.D. Burton & E.D. Goldberg (eds), 467–73. New York: Plenum.

Martin, J.H. & G.A. Knauer 1984. VERTEX: manganese transport through the oxygen minima. *Earth Planet. Sci. Lett.* **67,** 35–47.

Martin, J.H., K.W. Bruland & W.W. Broenkow 1976. Cadmium transport in the California Current. In *Marine pollutant transfer*, H.L. Windom & R.A. Duce (eds), 159–84. Lexington, MA: Lexington Books.

Martin, J.-M. & M. Whitfield 1983. The significance of the river input of chemical elements to the ocean. In *Trace metals in sea water*, C.S. Wong, E. Boyle, K.W. Bruland, J.D. Burton & E.D. Goldberg (eds), 265–96. New York: Plenum.

Measures, C.I., J.M. Edmond & T.D. Jickells 1986. Aluminium in the northwest Atlantic. *Geochim. Cosmochim. Acta* **50,** 1423–9.

Measures, C.I., B. Grant, M. Khadem, D.S. Leee & J.M. Edmond 1984. Distribution of Be, Al, Se and Bi in the surface waters of the western North Atlantic and Caribbean. *Earth Planet. Sci. Lett.* **71,** 1–12.

Mills, G.L. & J.G. Quinn 1984. Dissolved copper and copper–organic complexes in the Narragansett Bay Estuary. *Mar. Chem.* **15,** 151–72.

Moore, R.M. 1983. The relationship between distributions of dissolved cadmium, iron and aluminium and hydrography in the central Arctic Ocean. In *Trace metals in sea water*, C.S. Wong, E. Boyle, K.W. Bruland, J.D. Burton & E.D. Goldberg (eds), 131–42. New York: Plenum.

Morrel, F.M.M. 1986. Trace metals–phytoplankton interactions: an overview. In *Biogeochemical processes at the land–sea boundary*, P. Lasserre & J.-M. Martin (eds), 177–89. Amsterdam: Elsevier.

Murray, J.W., B. Spell & B. Paul 1983. The contrasting geochemistry of manganese and chromium in the eastern tropical Pacific Ocean. In *Trace metals in sea water*, C.S. Wong, E. Boyle, K.W. Bruland, J.D. Burton & E.D. Goldberg (eds), 643–69. New York: Plenum.

Nurnberg, H.W. 1980. Features of voltammetric investigations on trace metal speciation in sea water and inland waters. *Malassia Jugosl.* **15,** 95–110.

Nurnberg, H.W. & P. Valenta 1983. Potentialities and applications of voltammetry in chemical specition of trace metals in the sea. In *Trace metals in sea water*, C.S. Wong, E. Boyle, K.W. Bruland, J.D. Burton & E.D. Goldberg (eds), 671–97. New York: Plenum.

Nyffeler, U.P., Y.-H. Li & P.S. Santschi 1984. A kinetic approach to describe trace element distribution between particles and solution in natural aquatic systems. *Geochim. Cosmochim. Acta* **48,** 1513–22.

Olafsson, J. 1983. Mercury concentrations in the North Atlantic in relation to cadmium, aluminium and oceanographic parameters. In *Trace metals in sea water*, C.S. Wong, E. Boyle, K.W. Bruland, J.D. Burton & E.D. Goldberg (eds), 475–85. New York: Plenum.

Orians, K.J. & K.W. Bruland 1985. Dissolved aluminium in the central North Pacific. *Nature* **316,** 427–9.

Orians, K.J. & K.W. Bruland 1986. The biogeochemistry of aluminium in the Pacific Ocean. *Earth Planet. Sci. Lett.* **78,** 397–410.

Schaule, B.K. & C.C. Patterson 1981. Lead concentrations in the northeast Pacific: evidence for global anthropogenic perturbations. *Earth Planet. Sci. Lett.* **54,** 97–116.

Schindler, P.W. 1975. Removal of trace metals from the oceans: a zero order model. *Thalassia Jugoslav.* **11,** 101–11.

Sclater, F.R., E. Boyle & J.M. Edmond 1976. On the marine geochemistry of nickel. *Earth Planet. Sci. Lett.* **31,** 119–28.

Sillen, L.G. 1961. The physical chemistry of sea water. In *Oceanography*, M. Sears (ed.), 549–81. Washington, DC: American Association for the Advancement of Science.

Simpson, W.R. 1982. Particulate matter in the oceans – sampling methods, concentration and particle dynamics. *Oceanogr. Mar. Biol. Annu. Rev.* **20,** 119–72.

Spencer, D.W. 1984. Aluminium concentrations and fluxes in the ocean. In *Global ocean flux study*, 206–20. Washington, DC: National Academy Press.

Spencer, D.W. & P.B. Brewer 1971. Vertial advection diffusion and redox potentials as controls on the distribution of manganese and other trace metals dissolved in waters of the Black Sea. *J. Geophys. Res.* **76,** 5877–92.

Spivack, J., S.S. Huested & E.A. Boyle 1983. Copper, nickel and cadmium in the surface waters of the Mediterranean. In *Trace metals in sea water*, C.S. Wong, E. Boyle, K.W. Bruland, J.D. Burton & E.D. Goldberg (eds), 505–12. New York: Plenum.

Statham, P.J. & J.D. Burton 1986. Dissolved manganese in the North Atlantic Ocean, 0–35°N. *Earth Planet. Sci. Lett.* **79,** 56–65.

Stumm, W. & P.A. Brauner 1975. Chemical speciation. In *Chemical oceanography*, J.P. Riley & G. Skirrow (eds), Vol. 1, 173–239. London: Academic Press.

Stumm, W. & J.J. Morgan 1981. *Aquatic chemistry*. New York: Wiley.

Turekian, K.K. 1977. The fate of metals in the oceans. *Geochim. Cosmochim. Acta* **41,** 1139–44.

Turner, D.R. 1986. Biological availability of trace elements. In *Biogeochemical processes at the land–sea boundary*, P. Lasserre & J.-M. Martin (eds), 191–214. Amsterdam: Elsevier.

Turner, D.R. 1987. Speciation and cycling of arsenic, cadmium, lead and mercury in natural waters. In *Lead, mercury, cadmium and arsenic in the environment*, SCOPE, T.C. Hutchinson & K.M. Meema (eds), 175–86. New York: Wiley.

Turner, D.R., M. Whitfield & A.G. Dickson 1981. The equilibrium speciation of dissolved components in freshwater and seawater at 25°C and 1 atm pressure. *Geochim. Cosmochim. Acta* **45,** 855–81.

van den Berg, C.M.G. 1984. Organic and inorganic speciation of copper in the Irish Sea. *Mar. Chem.* **14,** 201–12.

van den Berg, C.M.G. 1985. Determination of the zinc complexing capacity in seawater by cathodic stripping voltammetry of zinc–APDC complex ions. *Mar. Chem.* **16,** 121–30.

Wangersky, P.J. 1986. Biological control of trace metal residence time and speciation: a review and synthesis. *Mar. Chem.* **18,** 269–97.

Whitfield, M. 1979. The mean oceanic residence time (MORT) concept, a rationalization. *Mar. Chem.* **8,** 101–23.

REFERENCES

Whitfield, M. & D. Jagner (eds) 1981. *Marine electrochemistry*. New York: Wiley.

Whitfield, M. & D.R. Turner 1982. Ultimate removal mechanisms of elements from the ocean – a comment. *Geochim. Cosmochim. Acta* **46,** 1989–92.

Whitfield, M. & D.R. Turner 1987. The role of particles in regulating the composition of sea water. In *Aquatic surface chemistry: chemical processes at the particle–water interface*, W. Stumm (ed.), 457–93. New York: Wiley.

Wood, A.M., D.W. Evans & J.J. Alberts 1983. Use of an ion exchange technique to measure copper complexing capacity on the continental shelf of the southeastern United States and in the Sargasso Sea. *Mar. Chem.* **13,** 305–26.

Zarino, A. & T. Yamamoto 1972. A pH dependent model for the chemical speciation of copper, zinc and lead in seawater. *Limnol. Oceanogr.* **17,** 661–71.

12 Down-column fluxes and the benthic boundary layer

In the last two chapters we have described the distributions of particulate matter and dissolved trace elements in the oceans, and have discussed the manner in which they interact in the water column to exert a control on the elemental composition of sea water. The principal mechanism underlying this control is the removal of dissolved trace elements by the oceanic microcosm of particles via scavenging-type and nutrient-type carrier-phase associations, and the subsequent settling of these particles down the water column. These transport processes are part of the *great particle conspiracy*, and in the present chapter an attempt will be made to estimate the rate at which the conspiracy operates by assessing the magnitude of the fluxes of elements to deep waters via the particulate carriers. Following this, the journey undertaken by the particulate matter will be taken a stage further by tracking the sedimenting solids to the sediment/water interface.

12.1 Down-column fluxes

It was shown in Section 10.4 that most of the mass flux of material is carried down the water column in association with large-sized aggregates, such as faecal pellets and 'marine snow', i.e. the vertical transport is dominated by the **global carbon flux**. The strength of the flux of this biogenic debris varies with the degree of primary production in the surface waters, and the rates at which it operates have been studied by both sediment trap and radio-isotopic techniques. The general use of these radio-isotopes in dissolved–particulate equilibrium studies has been reviewed in Section 11.6.3.1, and attention at this stage will be confined largely to sediment trap work. However, before moving on to this, it is worthwhile drawing attention again to an important study which demonstrated the existence of surface layer couplings (a) between the rates of removal of dissolved elements by particulate adsorption and the rate of primary production, and (b) between the residence times of the particulates and the formation of faecal pellets. In this study, Coale & Bruland (1985) modelled the disequilibria between ^{234}Th and ^{238}U to investigate the production and scavenging rates of particulate ^{234}Th within the waters of the California Current. Using this approach, the authors were able to draw two very important conclusions.

(a) The model-derived first-order scavenging rate constant for dissolved thorium was found to be proportional to the rate of primary production, and the dissolved thorium residence times, with respect to particle scavenging, varied from ~ 200 days in oligotrophic waters to ~ 5 days in highly productive waters.
(b) The residence times of the ^{234}Th-carrying particles was a function of particle removal processes, such as the zooplankton grazing and the resultant production of faecal pellets, the particle residence times varying from ~ 2 days under intense zooplankton grazing to ~ 20 days where the zooplankton population was relatively sparse.

Much of our knowledge of the strengths of down-column, or more strictly down-column plus laterally advected, fluxes has come from the use of sediment traps, which according to Brewer *et al.* (1986) provide direct evidence of 'sediments in the making'. The down-column fluxes that carry the material forming the sediments are driven by particulate matter and in many of the field experiments the sediment traps have been deployed in relation to the three-layer model for the distribution of TSM in the water column (see Sec. 10.2); i.e. samples have been collected in the surface layer, the clear water minimum and the deep water layer. This relationship between particle collection and the three-layer model is very important because it identifies a fundamental constraint that must be placed on the interpretation of sediment trap data. That is, when attempts are made to estimate the strengths of down-column particulate fluxes it is necessary to make a distinction between the two primary sources of TSM to the water column, i.e. a *downward* flux from the surface layer and an *upward* flux from the sea bed. The overall relationship between the three-layer TSM model and the various particle fluxes is illustrated in Figure 12.1.

A survey of the sinking rates of large-sized material has been provided by Sackett (1978), and shows that the rates vary between ~ 15 m d^{-1} and ~ 860 m d^{-1}. Simpson (1982) has summarized data on the magnitude of vertical particle fluxes derived directly from sediment trap experiments; these mass fluxes appear to vary over at least two orders of magnitude, being in the range ~ 10 to ~ 10^3 mg m^{-2} d^{-1} depending on the oceanic area and the type of trap used. It may be concluded, therefore, that, although there is a 'rain' of large-sized TSM to the sea bed over the World Ocean, the mass fluxes driven by this material vary considerably in both time and space. Sediment trap experiments are capable of collecting the large-sized aggregates, which drive the down-column transport, and they have therefore played a vital role in mass particle flux studies. In view of this, a representative selection of these sediment trap experiments is described below, and the data from them is summarized in Table 12.1.

Deuser (1987) reported data on particle flux measurements taken over an eight-year period from a sediment trap deployed at 3200 m in the

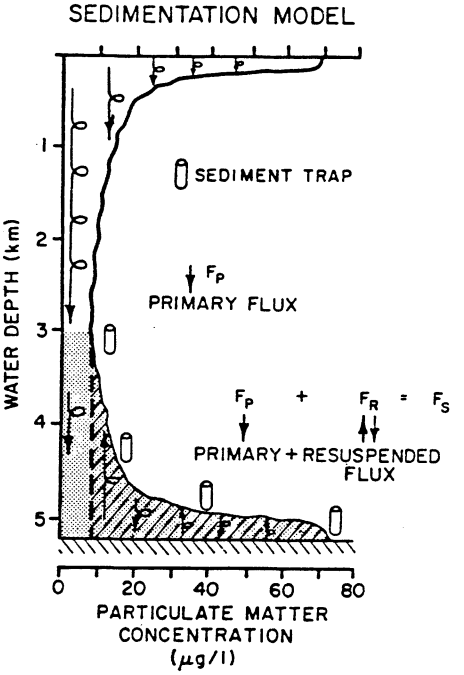

Figure 12.1 The relationship between the down-column location of sediment traps and the three-layer oceanic TSM flux model (from Gardner *et al.* 1985).

Sargasso Sea. The data are illustrated in Figure 12.2, and show both seasonal and annual variability in the magnitude of the particle flux. The seasonal variations exhibit a winter–spring maximum and a summer–autumn minimum. These features correlated well (after allowance was made for a time lag between surface and deep processes) with the mixed layer depth; the deeper the mixed layer, the greater the particle flux. The correlation is consistent with the concept that it is the mixed layer depth, or conversely the degree of stratification, that controls production by regulating the flow of nutrients to the euphotic zone; i.e. the magnitude of the particle flux is related to primary production in the overlying water. As a result, average carbon fluxes leaving the euphotic zone in eutrophic upwelling areas (> 150 mg m^{-2} d^{-1}), in which there is a plentiful external supply of nutrients, are considerably higher than those in open-ocean oligotrophic gyre areas (< 50 mg m^{-2} d^{-1}), in which the supply of nutrients is dependent on the recycling of inorganic nutrients.

Spencer *et al.* (1978) reported data from two sediment traps deployed at depths of 5367 m and 5581 m within the bottom nepheloid layer of the Sargasso Sea. Over a collection time of 75 days the mean total particle

Table 12.1 Down-column fluxes of some elements in the oceans (units, ng cm^{-2} yr^{-1})

	Al	Fe	Si	Ti	Co	V	Sc	Cu	Zn	Pb	Mn	Ca	Mg	Ba	Sr	Ni
Sargasso Sea[a]																
Primary flux	5000	5200	-	300	3.6	18	9.6	160	<5	-	500	55800	1900	46	344	-
Resuspended flux	88000	56800	-	4600	19	150	17	80	>735	-	1100	87200	32100	510	430	-
Sargasso Sea[b]																
Total flux 976m	2200	1390	15300	157	2.2	4.7	0.29	56	61	-	13	68700	1390	192	488	-
Total flux 3964m	16200	5570	54000	682	9.7	25	1.4	207	256	-	580	196000	4610	469	1330	
Off Barbados[b]																
389m	14300	6420	163000	1013	-	21	1.7	-	1132	-	106	410000	11500	-	2555	-
988m	21100	1300	177000	1492	4.0	58	4.0	47	708	-	126	330000	9170	1078	2436	-
3755m	56500	30900	266000	3157	15	102	9.6	156	665	-	646	409000	15100	1287	3092	-
5086m	65800	34500	26900	3932	20	119	12	233	849	-	831	331000	15200	9234	2259	
N.W. Atlantic[c]																
Continental slope/rise																
Site KN 58-2																
depth above bottom																
500m	116000	-	-	-	-	250	-	2800	-	-	3200	535000	48000	2800	4900	-
13m	386000	-	-	-	-	780	-	3400	-	-	1500	1180000	153000	5100	10000	-
Site DOS-2																
depth above bottom																
518m	371000	-	-	-	-	700	-	5400	-	-	5900	946000	138000	3200	7900	-
118m	754000	-	-	-	-	1400	-	7000	-	-	14000	1412000	251000	5900	10000	
Sargasso Sea[d]	-	11936	-	-	-	47	-	128	248	88	1350	-	-	-	-	58
Tropical North Atlantic[e]																
Calculated primary down-column flux	5200	14300	-	-	9	35	-	234	1040	330	240	-	-	-	-	117

[a] Data from Spencer et al. (1978).
[b] Data from Brewer et al. (1980).
[c] Data from Gardner et al. (1985).
[d] Data from Jickells et al. (1984).
[e] Data from Buat-Menard & Chesselet (1979).

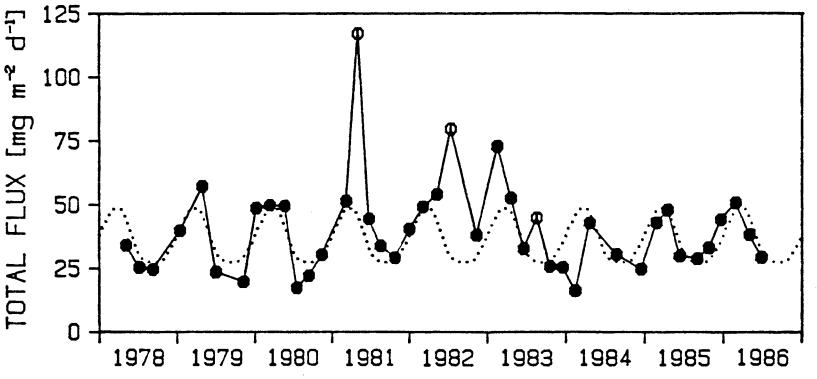

Figure 12.2 Temporal variations in particle fluxes in the deep ocean (from Deuser 1987). An eight-year record of variations in total particle flux to a sediment trap located at 3200 m in the Sargasso Sea is shown. Points represent average fluxes over two-month trap deployment periods, plotted at the period mid-points. The dotted curve represents the average timing of the winter–spring flux maximum; the three measurements indicated by open circles were not included in the calculation of the average curve.

flux was estimated to be ~ 1.68 mg cm^{-2} yr^{-1}, or ~ 46 mg m^{-2} d^{-1}. The material collected in these deep water traps consisted of ~ 50% clay, ~ 20% calcium carbonate, ~ 20% silica and ~ 5% organic matter; this is consistent with the overall decrease in the proportion of organic matter as TSM settles down the water column (see Sec. 10.5). Spencer *et al.* (1978) separated the primary down-column flux (F_p) from the resuspended flux (F_r) and concluded that of the total or gross flux (F_s) only ~ 5% of the clay, but most of the calcium carbonate and ~ 90% of the organic matter, were derived from the surface ocean and were transported downwards by the F_p term. The total, primary and resuspended fluxes for a series of elements estimated in this manner are given in Table 12.1.

Brewer *et al.* (1980) provided data on the fluxes of a wide range of elements to the deep ocean at two North Atlantic sites, one in the Sargasso Sea and one off Barbados. At the Sargasso Sea site the mass flux increased with depth from ~ 280 μg cm^{-2} yr^{-1} at 9765 m to ~ 740 μg cm^{-2} yr^{-1} at 3694 m; in contrast, at the Barbados site the flux was constant at ~ 1800 μg cm^{-2} yr^{-1} from 389 to 5085 m. However, Al increased in both concentration and flux at the two sites, and the authors used this element to normalize the concentrations of the other elements in the sediment trap material. In this manner they were able to identify the factors that controlled the chemical composition of the flux, and on this basis they divided the elements studied into three groups.

(a) A **terrigenous group**, in which the element : Al ratios were constant

with depth and were close to those in crustal material. The elements in this group were K, Ti, La, Co and ^{232}Th.

(b) A **biogenous group**, in which element : Al ratios decreased with depth. The elements in this group, i.e. Ca, Sr, Mg, Si, Ba, U, I and ^{226}Ra, are all known to be incorporated, at least to some extent, into biogenic particles such as organic matter, calcium carbonate and opal.

(c) A **scavenged group**, in which the elements were characterized by increasing element : Al ratios with depth. Mn, Cu, Fe, Sc and ^{230}Th were placed in this group. These metals are all known to be highly surface-active in sea water, as indicated by their relatively short oceanic residence times.

By applying a vertical scavenging settling model to the sediment trap data, and by assuming that the scavenging behaviour of the reactive stable elements was analogous to that of ^{230}Th, the authors were able to estimate the scavenging residence times of the stable elements to be 20 yr for Mn, 77 yr for Fe, 230 yr for Sc and 500 yr for Cu – c.t. data in Table 11.4. A summary of the down-column elemental fluxes reported by Brewer *et al.* (1980) is given in Table 12.1.

The flux data given above are mainly for sediment trap experiments at open-ocean locations. An example of how such fluxes can vary with different oceanic environments has been provided by Gardner *et al.* (1985). In this study, sediment trap arrays were used to measure both the primary and resuspended fluxes of material at two sites, one on the continental slope and one on the continental rise in the northwest Atlantic. Thus, the trap sites were located much closer to the continental margins than those in the experiments described above. The data derived from this work are summarized in Table 12.1, from which it can be seen that the primary elemental fluxes in the slope/rise areas are considerably higher than those given by other workers for the open ocean.

Temporal variation in elemental down-column fluxes has been demonstrated by Jickells *et al.* (1984). These authors carried out a two-year sediment trap experiment in the Sargasso Sea and reported data for the down-column fluxes of Cd, Cu, Mn, Ni, P, Pb, V, Zn, Al, Fe, organic carbon and total solids. On the basis of their data the authors concluded that, with the exception of Cd, the trace metal fluxes did in fact exhibit a temporal variability, which they believed was driven by the seasonal cycle of primary production in the overlying waters (see also Deuser *et al.* 1981, Deuser 1984). Jickells *et al.* (1984) found correlations between the elemental fluxes and that of organic carbon, which they concluded resulted from the consolidation of both biogenic (e.g. skeletal remains) and abiogenic (e.g. clay) particles into aggregates in the surface water and their subsequent settling down the water column. The residence times of

particulate trace metals in the surface water were estimated to be < 150 days. The total residence times (i.e. dissolved plus particulate) of the elements in the surface layer (~ 100 m) are controlled by the net rates at which they are converted to the particulate form. Elements that undergo a rapid conversion, and are not readily recycled, have the shortest residence times in the surface waters (e.g. Mn, 0.9 yr; Pb, 4 yr). In contrast, those which are mediated by phytoplankton uptake remain for a longer period in this region of the water column (e.g. Cd, 2–17 yr; Ni, 15–20 yr; P, 28 yr). A summary of the averaged trace metal down-column flux data reported by Jickells *et al.* (1984) is given in Table 12.1.

In addition to elemental and total carbon fluxes, several investigations have employed sediment traps to provide data on the down-column fates of individual organic compounds, such as lipids (including hydrocarbons), amino acids and carbohydrates. A number of the trends in the down-column fluxes of these components can be identified with reference to specific individual studies. The material is described in relation to the particulate and dissolved organic components described in Section 9.2.3.

HYDROCARBONS Matsueda & Handa (1986) gave data on the hydrocarbons collected in sediment traps at three stations in the eastern North Pacific. The hydrocarbons identified included n-alkanes in the range n-C_{15} to n-C_{32}, with the major constituent being n-C_{17}, which was thought to originate from phytoplankton. The vertical flux of the hydrocarbons tended to decrease exponentially with depth at all three stations. There were also significant changes in the composition of the hydrocarbons at two of the stations, the most striking feature being a rapid decrease in the relative abundance of n-C_{17}, which was thought to arise from biological degradation.

CARBOHYDRATES AND AMINO ACIDS The total down-column fluxes of carbohydrates appear to decrease with depth (see e.g. Wefer *et al.* 1982, Ittekkot *et al.* 1984, Liebezeit 1987). For example, Liebezeit (1987) reported data on carbohydrate fluxes in the Drake Passage. The total carbohydrate fluxes decreased from 2.6 mg m^{-2} d^{-1} at the surface to 1.2 mg m^{-2} d^{-1} at 2540 m. There were a number of interesting down-column trends in the relative proportions of the various carbohydrates. Both fucose and glucose decreased with depth, indicating that they were present in easily degradable forms. In contrast, galactose, xylose, arabinose and rhamnose increased in proportion with depth in the water column, probably as a result of their incorporation into less degradable structural compounds. Despite the overall decrease in the total carbohydrate fluxes with depth, however, the relative contribution of the carbohydrates to the total organic flux actually increased with depth, indicating that other components in the organic carbon pool are

degraded at faster rates than the carbohydrates. Ittekkot *et al.* (1984) gave data on the distributions of amino acids and amino sugars to the deep ocean in the Panama Basin. The sugars were dominated by glucose, galactose, mannose and xylose, with significant contributions from arabinose, fucose and rhamnose; and the amino acids were dominated by aspartic acid and glycine. There was an overall decrease in the fluxes of all these components with depth. However, the fluxes varied seasonally, with peaks that were associated with primary production in the surface waters. There were also differences in the seasonal distributions of the sugars and amino acids, a June–July peak flux being characterized by high amounts of arabinose and ribose within the sugars, and high amounts of aspartic acid in the amino acids. One of the most important findings of the study was that these characteristic peak-time sugar and amino acid signatures were found at all water depths, indicating a rapid vertical transport without significant decomposition. The authors suggested that ribose, in particular, could act as an indicator of the rapid transport of organic material from the surface to deep water. The study also highlighted another important feature in the down-column transport of organic components to deep waters. In this respect, the authors pointed out that the distributions of sugars and amino acids in the deep water zone (> 3000 m) is different from that observed in the bottom sediments; e.g. the concentration of amino acids in the deep water Panama trap is $\sim$ 18 mg g^{-1} compared to $\sim$ 5.5 mg g^{-1} in the bottom sediment. This led the authors to conclude that significant biochemical activity takes place in the **benthic transition layer** between the sediment surface and the deepest traps. This layer of increased biochemical activity will vary seasonally in response to the seasonal variation in the organic flux.

The data given in Table 12.1 offer some of the best presently available estimates of the down-column fluxes of elements in a variety of oceanic regions. Thus, the pathways taken by dissolved and particulate elements as they journey through the ocean system have now been followed to the point where they have reached deep waters. At this stage, they enter an extremely dynamic oceanic environment, which is termed the benthic boundary layer (BBL). Here, the 'great particle conspiracy' continues to operate, and in the following section we will describe the reactions that take place in this active oceanic layer.

12.2 The benthic boundary layer: the sediment/water interface

The point has not been reached at which the particulate material that has been transported down the water column leaves sea water and enters the sediment reservoir, a step that involves crossing the sediment/sea water

interface. This interface is the site of a number of biogeochemical reactions, which can mediate the dissolved–particulate recycling of some of the elements in the 'young' material that has been transported down the water column as part of the TSM flux. However, instead of dealing here with a single interface, i.e. the sediment/water interface, it is more useful to relate the changes that take place in bottom waters to the wider concept of the **benthic boundary layer**, because by adopting this unified approach the bottom reaction zone is extended above the top of the sediment layer and taken back into the water column itself. Before following the (sea water → sediment/sea water interface → sediment) TSM transport sequence to the sediment stage itself, we will therefore consider the processes that occur in the benthic boundary layer.

12.3 The benthic boundary layer

The benthic boundary layer (BBL) is a zone in which frictional forces result from the interaction of the deep oceanic circulation with the ocean bottom, evidenced for example in the formation of nepheloid layers, and it is one of the most dynamic environments in the entire ocean system.

The down-column transport of TSM transfers nutrients and organic carbon from the surface ocean to deep waters, and the remineralization of the carbon provides energy to the bottom benthos. Burial in the sediments removes bioactive material from the system and therefore regulates oceanic fertility (Brewer *et al.* 1986). In addition, the composition of the TSM and the magnitude of its flux play an important role in controlling the chemical environment in the bottom sediments (Dymond 1984). The reason for this is that organic carbon is the detemining factor controlling the type of redox conditions that are set up in the sediments (see Sec. 14.4). Because these redox conditions largely control the diagenetic reactions at both the sediment/sea water and the sediment/interstitial water interfaces, the POC flux to the sediments may be regarded as the driving force behind most of the diagenetic reactions occurring in marine sediments (Emmerson & Dymond 1984).

The nature and the magnitude of the particle flux to deep water have been described in Section 10.5, in which it was pointed out that in order to assess the net downward flux to the BBL it is necessary to distinguish between the primary and the resuspended fluxes that operate in this deep ocean reservoir. Data for both fluxes have been given in Table 12.1, and in order to move one step further along the TSM transport sequence it is necessary to establish how much of the net down-column flux is actually removed by, or buried in, the bottom sediment. This can be done by making use of the elegant conceptual model devised by Dymond (1984). This model is illustrated in Figure 12.3 and offers an excellent framework

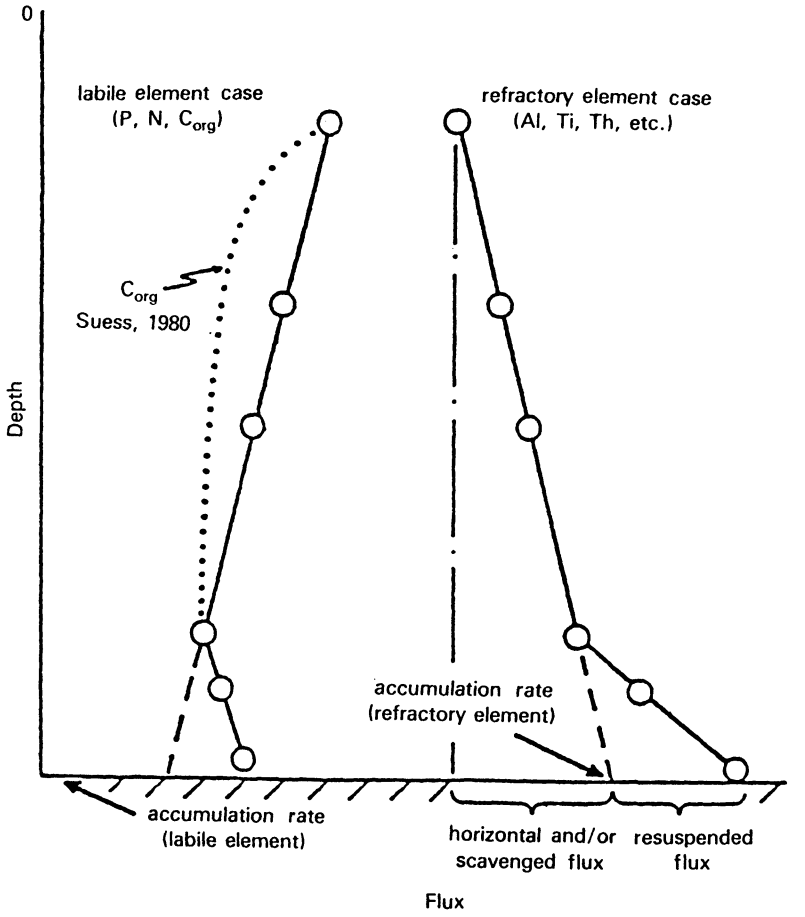

Figure 12.3 Conceptual model of particle-associated fluxes to the benthic boundary layer (from Dymond 1984).

within which to address the problem of the fate of down-column transported elements once they reach the BBL. In designing this model, Dymond (1984) made a distinction between (a) refractory, or particle reactive, elements (e.g. Al) and (b) labile elements (e.g. organic C, P, N) – cf. the scavenging-type and nutrient-type trace metal classification proposed in Section 11.6.

The particulate flux of the **refractory** elements generally increases with depth as a result of particle scavenging (i.e. the dissolved phase of the elements exhibits a depth depletion), and also perhaps from the input of an additional particle source from the ocean margins. For these refractory elements, there will also be an increase in concentration from the

secondary resuspended sediment flux since the bottom sediments are enriched in refractory material relative to the settling TSM.

In contrast, the particle flux of the **labile** elements decreases with depth, owing to processes such as particle decomposition and disaggregation, although this flux can also increase near the sea bed.

In order to obtain flux data on *net* down-column transport, Dymond (1984) constructed a flux model in which the down-column trends in settling TSM from the overlying waters were linearly extrapolated down through the resuspension zone – see Figure 12.3. He then used field data obtained from sediment trap experiments at two sites in the eastern Equatorial Pacific to compare the *down-column* fluxes with the *into-sediment* fluxes. To do this, the difference between the rates of the primary down-column flux and the sediment burial flux was assumed to be a measure of the regeneration of elements in the BBL; this is referred to as the **benthic regeneration flux** (BRF), or the benthic flux. The data set is summarized in Table 12.2, and the principal trends found can be summarized as follows.

(a) At both sites the rates at which the refractory elements undergo

Table 12.2 Particle fluxes and sediment burial fluxes at MANOP sites H and M in the eastern Equatorial Pacific[a]

	Site	Particle fluxes	Sediment burial fluxes	Benthic regeneration fluxes	% Preserved
			Refractory Elements		
Al	H	0.26	0.22 to 0.32	-0.06 to 0.04	86-124
	M	0.56	0.37 to 0.52	0.03 to 0.18	68- 94
Sc	H	4.9×10^{-5}	$5.1\text{-}7.3 \times 10^{-5}$	-0.2 to 2.4×10^{-5}	105-150
	M	10.0×10^{-5}	$7.0\text{-}9.7 \times 10^{-5}$	0.3 to 3.0×10^{-5}	89- 98
Fe	H	0.068	0.090-0.13	-0.062 to -0.022	132-189
	M	0.28	0.26 -0.36	-0.075 to 0.02	92-126
			Labile Elements		
N	H	1.2	-0.01	1.2	1
	M	1.5	-0.03	1.5	1-2
P_{total}	H	0.032	0.005-0.007	0.025-0.027	16-22
	M	0.045	0.016-0.022	0.023-0.029	36-49
P_{org}	H	0.016	-0.001	0.015	6
	M	0.026	0.004-0.005	0.021-0.022	15-19
C_{org}	H	7.4	0.07- 0.09	7.3	1
	M	11.5	0.22- 0.31	11.2- 11.3	2-3
$CaCO_3$	H	12.7	$1\text{-}2 \times 10^{-3}$	12.7	<1
	M	6.6	0.3- 0.4	6.2- 6.3	5-6
Opal	H	5.3	0.2- 0.4	4.9- 5.1	4-8
	M	9.8	0.3- 0.4	9.4- 9.5	3-4
Br	H	21×10^{-3}	0.2- 0.3	21×10^{-3}	1
	M	21×10^{-3}	0.5- 0.8	21×10^{-3}	2-4

[a] All fluxes in mmol cm^{-2} yr^{-1}. Negative benthic regeneration fluxes imply the need for a source in addition to the measure of particle fluxes. This table is from Dymond & Lyle (1984).

burial in the sediments are close to those at which they are supplied by the primary down-column flux; i.e. there is apparently little benthic cycling, or regeneration, of these elements.

(b) In contrast, the delivery of the labile elements by the primary down-column flux is considerably in excess of that required by the sediments, and in fact $\lesssim 10\%$ of these labile element down-column fluxes is preserved in the bottom deposits. Thus, for the labile elements $\sim 90\%$ of the primary down-column flux is recycled in the BBL; P is an exception to this, in that it appears to be better preserved in the sediments than the other labile components.

Dymond (1984) also gave data on the particle flux–sedimentation rate relationships for a wide range of trace metals at the same sites, and concluded that a number of particle reactive elements are accumulated in the sediments at about the same rates at which they are delivered down the water column – see Figure 12.4. Pb was an exception to this, with only $\lesssim 20\%$ of its flux to the BBL being preserved in the depositing sediment; however, this may have been because much of the Pb in the water column is of a recent anthropogenic origin, and so has not yet been integrated into the sediments, which accumulate only at slow rates.

The reactivity of a particulate element in aqueous environments is largely determined by the manner in which it is partitioned between the components of the particulate carriers (see Sec. 3.1.4), and Dymond (1984) gave data on the partitioning of a series of elements among four operationally defined, sequentially leached, particulate fractions. In this way the elements were classified as: (a) carbonate and exchangeable cations, (b) organically bound cations, (c) amorphous hydroxide-associated cations, and (d) refractory-associated cations. The partitioning data were illustrated with respect to the down-column particulate fluxes of Mn and Cu. The data for Mn showed that in the water column above the resuspension zone the element is present mainly in refractory and carbonate/exchangeable forms. The proportions of the two associations remained essentially constant, indicating that there was a continuous scavenging of Mn down the water column and a continuous horizontal addition of refractory Mn to the site. In the resuspension zone, however, $\sim 35\%$ of the total Mn was associated with amorphous hydroxides; this is the dominant association for Mn in deep-sea deposits (see Sec. 16.5) and results from sediment resuspension. For Cu the situation was different. This element had a major fraction of its flux associated with the organic host phase and the proportion of total Cu in this association increased with depth, thus highlighting the scavenging of Cu by an organic carrier phase throughout the water column. According to Dymond (1984) it is presumably this form of Cu that is regenerated at the sea floor. Data to support this were provided by Chester *et al.* (1988), who investigated the

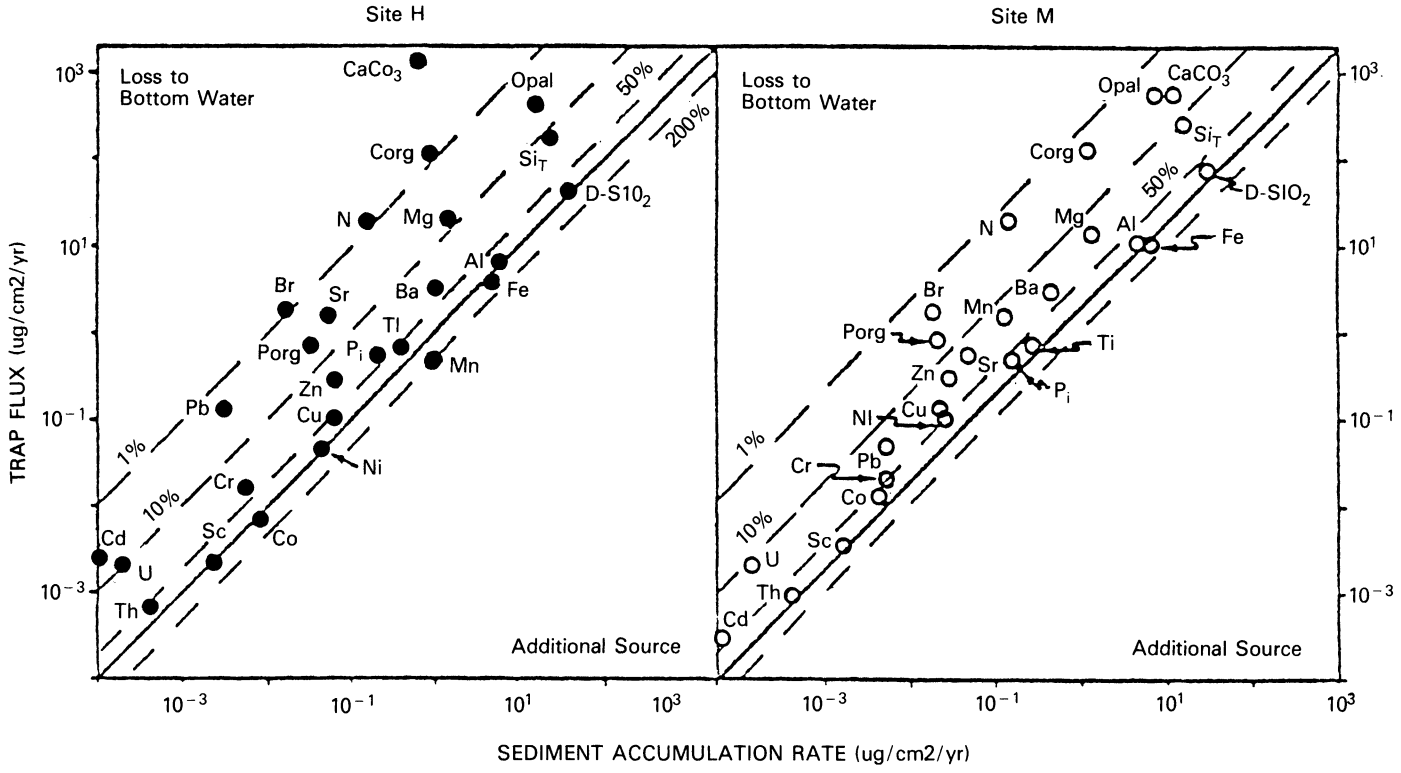

Figure 12.4 Comparison between sediment accumulation rates and measured particle fluxes at two sites in the eastern Equatorial Pacific (from Dymond 1984). The heavy line indicates equal particulate and burial fluxes; the broken lines indicate the percentage of the particle flux preserved in the sediment. P_i is inorganic P, Si is total Si, D-SiO_a is detrital silica.

solid-state speciation of Cu in surface water particulates and sediments from the Atlantic Ocean. These authors showed that, whereas on average ~ 50% of the total Cu in the surface water particulates was present in an organically associated form, this fell to ≲ 10% in the surface sediments (see Fig. 12.5); i.e. the organic form of Cu had undergone regeneration on deposition.

The resuspension of the bottom sediment has an important effect on the down-column trace metal flux profiles. This resuspended trace metal flux can be generated in a number of ways. For example, it can result from the addition of metal-rich sediment particles directly to the water column. However, the resuspended particles can themselves scavenge additional dissolved metals from the bottom water column, thus leading to a region of 'enhanced scavenging' in the resuspension zone. This could arise, for example, as metals released by the regeneration of organic particles are made available for scavenging by the resuspended material. However, an alternative mechanism to explain the increases in deep water particulate fluxes has been postulated by Walsh *et al.* (1985), who introduced the concept of a **rebound flux**. This rebound flux is thought to result from the resuspension not of well deposited sediment components, but rather of recently laid down primary flux material (see e.g. Billet *et al.* 1983). Dymond (1984) suggested that the rebound material may be similar to the organic-rich 'fluff' found over deep-sea sediments. The 'fluff' is thought to have a composition which is either essentially that of the primary flux or is intermediate between this and that of the deposited sediments. Using the modified terminology, therefore, the material in the BBL can be divided into: (a) a local primary down-column flux, (b) a local rebound flux and (c) a local, or distal, resuspended sediment flux.

12.4 Down-column fluxes and the benthic boundary layer: summary

(a) The rates at which particulate trace elements are transported down the water column vary from one oceanic region to another, and can also vary seasonally at a single site, e.g. in response to variations in the intensity of primary production in the surface waters.
(b) As they approach the sea bed the sinking particulates enter the benthic boundary layer. This layer is an oceanic region of considerable reactivity through which down-column and laterally transported TSM must pass, and perhaps be recycled, before entering the sediment reservoir.
(c) It has become clear therefore that although particulate matter is the driving force behind the reactions that control the elemental composition of sea water, the movement of both particulate and

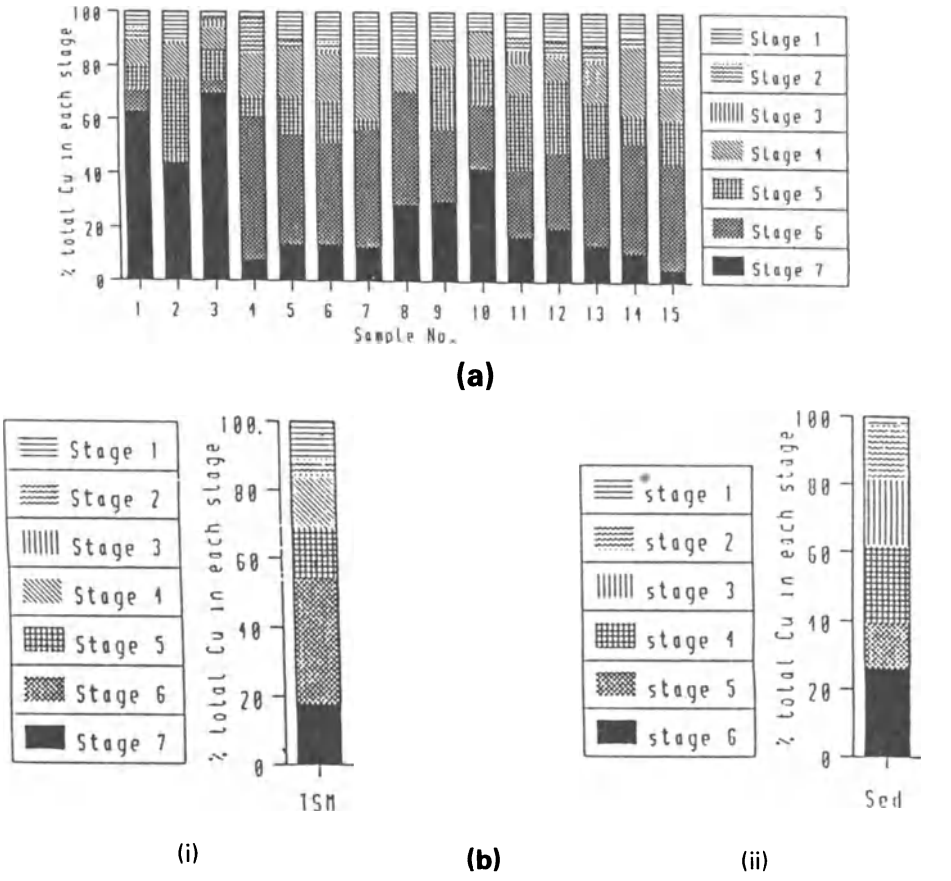

Figure 12.5 The solid-state speciation of Cu in surface water particulates (TSM) and deep-sea sediments (from Chester *et al.* 1988). (**a**) The average partitioning signatures for ΣCu in Atlantic surface seawater particulates. Samples were collected along a north–south Atlantic transect. The Cu host associations for the various stages are as follows: stage 1, loosely held or exchangeable associations; stage 2, carbonate and surface oxide associations; stage 3, easily reducible associations, mainly with 'new' oxides and oxyhydroxides of manganese and amorphous iron oxides; stage 4, humic organic associations; stage 5, moderately reducible associations, mainly with 'aged' manganese oxides and crystalline iron oxides; stage 6, refractory organic associations; stage 7, detrital or residual associations. (**b**) The average partitioning signatures for ΣCu in Atlantic deep-sea sediments. For the deep-sea sediment samples the humic and refractory organic associations were combined into one organic-associated stage. The Cu host associations are as follows: stage 1, loosely held or exchangeable associations; stage 2, carbonate and surface oxide associations; stage 3, easily reducible associations, mainly with 'new' oxides and oxyhydroxides of manganese and amorphous iron oxides; stage 4, moderately reducible associations, mainly with 'aged' manganese oxides and crystalline iron oxides; stage 5, organic associations; stage 6, detrital or residual associations. Note the differences in the solid-state speciation of Cu between the open-ocean surface water TSM (samples 4–15), in which ~ 50% of the ΣCu is held in some form of organic association, and the deep-sea sediments, in which ≲ 10% of the ΣCu is associated with organic hosts.

dissolved elements through the ocean system is not a simple one-stage journey, but rather involves a series of complex interactive recycling stages.

This complicated journey has now been followed down to the sediment/sea water interface. However, it must be stressed that even when the material has crossed this interface and has been incorporated into the bottom deposits it has not simply entered a static reservoir for the permanent storage of components extracted from the water column. On the contrary, diagenetic reactions occur within the sediment/interstitial water complex, and these can severely modify the mineral and elemental compositions of the sediments themselves. However, before looking at the reactions that occur in the sediment reservoir, it is necessary to know something of the fundamental characteristics of the oceanic sediments themselves and these are described in the next chapter.

References

Billet, D.S.M., R.S. Lampitt, A.L. Rice & R.F.C. Mantoura 1983. Seasonal sedimentation of phytoplankton to the deep-sea benthos. *Nature* **302,** 520–2.

Brewer, P.G., K.W. Bruland, R.W. Eppley & J.J. McCarthy 1986. The Global Ocean Flux Study (GOFS): status of the U.S. GOFS Program. *EOS* **67,** 827–32.

Brewer, P.G., Y. Nozaki, D.W. Spencer & A.P. Fleer 1980. Sediment trap experiments in the deep North Atlantic: isotopic and elemental fluxes. *J. Mar. Res.* **38,** 703–28.

Buat-Menard, P. & R. Chesselet 1979. Variable influences of the atmospheric flux on the trace metal chemistry of oceanic suspended matter. *Earth Planet. Sci. Lett.* **42,** 399–411.

Chester, R., A. Thomas, F.J. Lin, A.S. Basaham & G. Jacinto 1988. The solid state speciation of copper in surface water particulates and oceanic sediments. *Mar. Chem.* **24,** 261–92.

Coale, K.H. & K.W. Bruland 1985. $^{234}Th : ^{238}U$ disequilibria within the California Current. *Limnol. Oceanogr.* **30,** 22–33.

Deuser, W.G. 1984. Seasonality of particle fluxes in the ocean's interior. In *Global ocean flux study*, 221–36. Washington DC: National Academy Press.

Deuser, W.G. 1987. Variability of hydrography and particle flux: transient and long-term relationships. In *Particle flux in the ocean*, E.T. Degens, E. Izdar & S. Honjo (eds), 179–93. Mitt. Geol.-Palont. Inst. Univ. Hamburg, SCOPE/UNEP, Sonderband 62.

Deuser, W.G., E.H. Ross & R.F. Anderson 1981. Seasonality in the supply of sediment to the deep Sargasso Sea and implications for the rapid transfer of matter to the deep ocean. *Deep-Sea Res.* **28,** 495–505.

Dymond, J. 1984. Sediment traps, particle fluxes, and benthic boundary layer processes. In *Global ocean flux study*, 261–84. Washington DC: National Academy Press.

Emmerson, S. & J. Dymond 1984. Benthic organic carbon cycles: toward a balance of fluxes from particle settling and pore water gradients. In *Global ocean flux study*, 285–304. Washington DC: National Academy Press.

Gardner, W.D., J.B. Southard & C.D. Hollister 1985. Sedimentation, resuspension and chemistry of particles in the northwest Atlantic. *Mar. Geol.* **65,** 199–242.

Ittekkot, V., E.T. Degens & S. Honjo 1984. Seasonality in the fluxes of sugars, amino acids and amino sugars to the deep ocean: Panama Basin. *Deep-Sea Res.* **31,** 1071–83.

Jickells, T.D., W.G. Deuser & A.H. Knapp 1984. The sedimentation rates of trace elements in the Sargasso Sea measured by sediment trap. *Deep-Sea Res.* **31,** 1169–78.

Liebezeit, G. 1987. Particulate carbohydrate fluxes in the Bransfield Strait and Drake Passage. *Mar. Chem.* **20,** 255–64.

Matsuda, H. & N. Handa 1986. Vertical flux of hydrocarbons as measured in sediment traps in the eastern North Pacific Ocean. *Mar. Chem.* **20,** 179–95.

Sackett, W.M. 1978. Suspended matter in sea water. In *Chemical oceanography*, J.P. Riley & R. Chester (eds), Vol. 7, 127–72. London: Academic Press.

Simpson, W.R. 1982. Particulate matter in the oceans – sampling methods, concentration, size distribution and particle dynamics. *Oceanogr. Mar. Biol. Annu. Rev.* **20,** 119–72.

Spencer, D.W., P.G. Brewer, A. Fleer, S. Honjo, S. Krishnaswami & Y. Nozaki 1978. Chemical fluxes from a sediment trap experiment in the deep Sargasso Sea. *J. Mar. Res.* **36,** 493–523.

Wefer, G., E. Suess, W. Balzer, G. Liebezeit, P.J. Muller, C.A. Ungerer & W. Zenk 1982. Fluxes of biogenic compounds from sediment trap deployment in circumpolar waters of the Drake Passage. *Nature* **299,** 145–7.

PART III

THE GLOBAL JOURNEY: MATERIAL SINKS

13 Marine sediments

Marine sediments represent the major sink for material that leaves the sea water reservoir. However, before attempting to understand how this sink operates, it is necessary briefly to describe the sediments within a global ocean context.

13.1 Introduction

The sea floor can be divided into three major topological regions: the continental margins, the ocean-basin floor and the mid-ocean ridge system.

THE CONTINENTAL MARGINS These include the continental shelf, the continental slope and the continental rise. The continental shelf is the seaward extension of the land masses, and its outer limit is defined by the **shelf edge**, or break, beyond which there is usually a sharp change in gradient as the continental slope is encountered. The continental rise lies at the base of this slope. In many parts of the world both the continental slope and rise are cut by **submarine canyons**. These are steep-sided, V-shaped valleys, which are extremely important features from the point of view of the transport of material from the continents to the oceans since they act as conduits for the passage of terrigenous sediment from the shelves to deep-sea regions by processes such as turbidity flows. **Trenches** are found at the edges of all the major oceans, but are concentrated mainly in the Pacific, where they form an interrupted ring around the edges of some of the ocean basins. The trenches are long (up to $\sim$ 4500 km in length), narrow (usually $<$ 100 km wide) features that form the deepest parts of the oceans and are often associated with island arcs; both features are related to the tectonic generation of the oceans. The trenches are important in the oceanic sedimentary regime because they can act as traps for material carried down the continental shelf. In the absence of trenches, however, much of the bottom transported material is carried away from the continental rise into the deep sea.

THE OCEAN-BASIN FLOOR The ocean-basin floor lies beyond the continental margins. In the Atlantic, Indian and northeast Pacific Oceans **abyssal plains** cover a major part of the deep-sea floor. These plains are generally flat, almost featureless expanses of sea bottom composed of thick ($>$ 1000 m)

layers of sediment, and have been formed by the transport of material from the continental margins by turbidity currents, which spread their loads out on the deep-sea floor to form thick turbidite sequences. Thus, large amounts of sediment transported from the continental margins are laid down in these abyssal plains, which fringe the ocean margins in the so-called 'hemi-pelagic' deep-sea areas. The plains are found in all the major oceans, but because the Pacific is partially ringed by a trench belt that acts as a sediment trap, they are more common in the Atlantic and Indian Oceans. Because the Pacific has fewer abyssal plains than the other major oceans, **abyssal hills** are more common here, covering up to ~ 80% of the deep-sea floor in some areas. Seamounts are volcanic hills rising above the sea floor, which may be present either as individual features or in chains. Seamounts are especially abundant in the Pacific Ocean.

THE MID-OCEAN RIDGE SYSTEM This ridge system is one of the major topographic features on the surface of the planet. It is an essentially continuous feature, which extends through the Atlantic, Antarctic, Indian and Pacific Oceans for more than ~ 60 000 km, and the 'mountains' forming it rise to over 3000 m above the sea bed in the crestal areas. The topography of the ridge system is complicated by a series of large semi-parallel fracture zones, which cut across it in many areas. It is usual to divide the ridge system into crestal and flank regions. The flanks lead away from ocean basins, with a general increase in height as the crestal areas are approached. In the Mid-Atlantic Ridge the crestal regions have an extremely rugged topography with a central rift valley (~ 1–2 km deep) that is surrounded by rift mountains.

The distribution of these various topographic features is illustrated for the North Atlantic in Figure 13.1 and for the World Ocean in Figure 13.2a. The way in which these sea-bed features were formed can be related to the tectonic history of the oceans in terms of the theory of **sea-floor spreading**. In essence, this theory can be summarized as follows. The mid-ocean ridges are associated with the rising limbs of convection cells in the mantle and the sea floor 'cracks apart' at the crest regions. New crust is formed here, and as it is generated the previous crust is moved aside on either side of the crests and is lost at the edges of the oceans under zones of trenches, island arcs and young mountains associated with the descending limbs of convection cells where the ocean floor is carried back down into the mantle. Thus, the ocean floor is continually being created and destroyed in response to convection in the mantle. According to the available evidence it would appear that the spreading takes place at rates of a few centimetres per year. However, some ridges spread faster than others, allowing fast and slow spreading centres to be identified, although

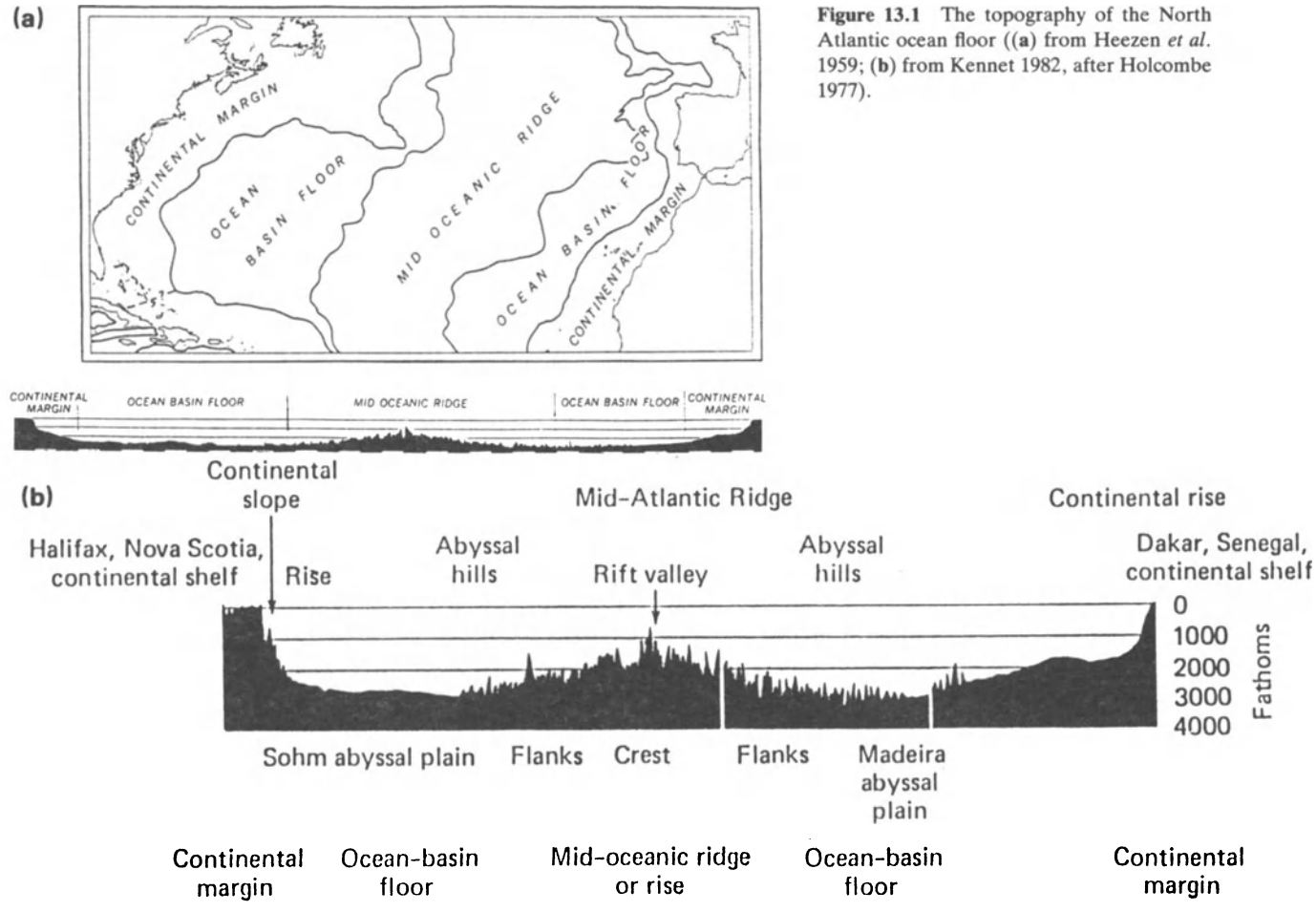

Figure 13.1 The topography of the North Atlantic ocean floor ((**a**) from Heezen *et al.* 1959; (**b**) from Kennet 1982, after Holcombe 1977).

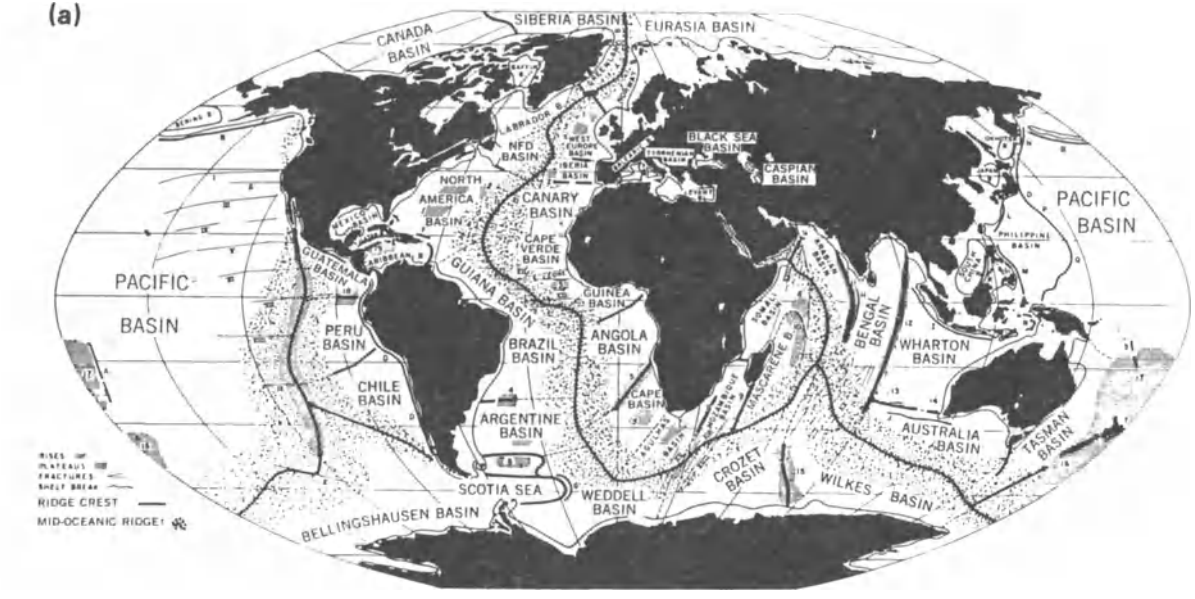

Features of the Ocean Floor

Fracture Zones:

I. Mendocino
II. Pioneer
III. Murray
IV. Molokai
V. Clarion
VI. Clipperton
VII. Galapagos
VIII. Marquesas
IX. Easter
X. Eltanin
XI. Atlantis
XII. Vema
XIII. Romanche
XIV. Chain
XV. Mozambique
XVI. Prince Edward
XVII. Malagasy
XVIII. Owen
XIX. Rodriguez
XX. Amsterdam

Plateaus:

1. Rockall Plateau
2. Azores Plateau
3. Sierra Leone Plateau
4. Rio Grande Plateau
5. Walfisch Ridge
6. Falkland Ridge
7. Agulhas Plateau
8. Mozambique Ridge
9. Madagascar Ridge
10. Mascarene Plateau
11. Chagos-Laccadive Plateau
12. Ninetyeast Ridge
13. Broken Ridge
14. Naturaliste Plateau
15. Kerguelen Plateau
16. New Zealand Plateau
17. Melanesia Plateau
18. Galapagos Plateau
19. Jamaica Plateau

Trenches:

A. Kermedec-Tonga
B. Aleutian
C. Middle America
D. Peru-Chile
E. Cayman
F. Puerto Rico
G. South Sandwich
H. Chagos
I. Java
J. Diamantina
K. Manila
L. Nansei-Shoto
M. Philippine
N. Kurile-Kamchatka
O. Japan
P. Bonin
Q. Mariana
R. Banda
S. New Hebrides
T. Hikurangi

Rises

1. Bermuda Rise
2. Corner Rise
3. Rockall Rise
4. Argentine Rise
5. Schmidt-Ott Rise
6. Madingley Rise

(b)

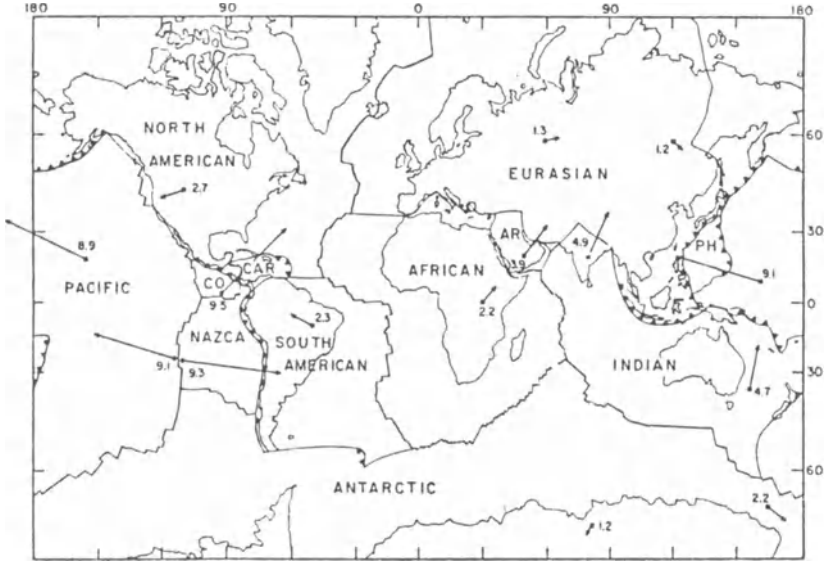

Figure 13.2 Topographic features in the oceans. (**a**) (left) The distribution of the major oceans and their principal topographic features (from Heezen & Hollister 1971). (**b**) The distribution of the principal lithospheric plates (from Parsons & Richter 1981). The principal plates are identified; the abbreviations CO = Cocos, CAR = Caribbean, AR = Arabian, PH = Philippine. Absolute plate velocities (cm yr^{-1}) are indicated at selected points. Convergent boundaries are indicated by arrow-heads that point from the subducting plate towards the non-subducting plate.

the spreading rates do not appear to have been constant with time. The slowest rates are found along parts of the Mid-Atlantic and Mid-Indian Ocean Ridges ($\sim$ 1–2.5 cm yr^{-1}), and the highest around the East Pacific Rise ($\sim$ 5 cm yr^{-1}).

One of the most important findings to emerge from these tectonic studies is that the ocean basins are relatively young on the geological timescale, and magnetic evidence, combined with sediment age data from the Deep Sea Drilling Project (DSDP), indicates that the oldest oceanic crust is around Middle Jurassic in age, i.e. it was formed $\sim$ 170 Ma ago. The concept of a dynamic ocean floor that is being generated at the ridge crests and resorbed into the mantle at the ocean edges is intimately related to the overall pattern of global tectonics. The unifying theory which brings together the various aspects of modern thinking on global structure is the **plate tectonic** concept. Put simply, it is now thought that the surface of the Earth consists of a series of thin ($\sim$ 100–150 km) plates that are continuously in motion. Six (or sometimes seven) major plates were originally identified, but additional plates have since been included (see Fig. 13.2b). The plates have boundaries between them, and Jones (1978) has classified these into three principal kinds.

(a) **Conservative boundaries**, at which the plates slide past each other without any creation or destruction of oceanic crust.
(b) **Constructive boundaries**, which are marked by the crests of the active spreading oceanic ridges where new crust is formed as the plates diverge. Thus, constructive boundaries are crust *sources*.
(c) **Destructive boundaries**, at which the plates converge and one plate moves beneath another one. These are marked by the presence of trenches, island arcs or young mountain belts. Thus, destructive margins are crust *sinks*, and the crust is lost by subduction under the trenches, where it eventually becomes sorbed back into the mantle. This is an extremely important process, because when the crust is sorbed back into the mantle it takes with it the sediment that has accumulated on the ocean floor. This has important implications for marine geochemistry because it means that the sediments deposited at the bottom of the sea, which are principal sink for much of the material poured into sea water, are eventually returned back into the global geochemical cycle.

A large part of the floor of the World Ocean is covered by sediments. The thickness of this sediment blanket varies from place to place; for example, in the Atlantic it averages > 1 km, in the Pacific it is < 1 km, and over the whole ocean it averages $\sim$ 500 m. The sediments forming this blanket are the ultimate marine sink for all the particulate components that survive destruction in the ocean reservoir. The

sediments are also the major sink for dissolved elements, although for some of these elements basement rocks can also act as a sink (see Ch. 5). Marine sediments therefore form one of the principal oceanic reservoirs.

In terms of a very simplistic model, the initial sediment in a newly formed ocean basin will be deposited onto the basalt basement as fresh crust is generated at the ridge spreading centres. This initial sediment is a hydrothermal deposit composed of metal-rich precipitates (see Secs 15.3.6 & 16.6.2), and as the ridge lies above the carbonate compensation depth (CCD; see Sec. 15.2.4.1) carbonate sediments begin to accumulate. As the basin continues to open up, the sediment surface away from the ridge falls below the CCD and clays are deposited. As sedimentation continues, the composition of the deposits is controlled by a variety of interacting chemical, physical and biological factors. Because of changes in the relative importance of these various factors as the plate on which the sediment is deposited moves through different oceanic environments (e.g. high- and low-productivity zones), the nature of the deposits forming the marine 'sediment blanket' has varied through geological times as the ocean basins evolved to their present state in response to sea-floor spreading. As a result of this sea-floor spreading, or continental drift, changes have occurred in the sizes, shapes, latitudinal distributions, water circulation patterns and depths of the ocean basins, all of which affected the patterns of sedimentation. Much of our current knowledge of the deeper parts of the oceanic sediment column has come from material collected during the DSDP. Detailed examination of the DSDP cores has shown, for example, that there have been gross changes in both the compositions and rates of accumulation of marine sediments over the past 120 million years (Davies & Gorsline 1976). During this time the depositional environments have passed through a variety of conditions leading to the preferential preservation of carbonate-rich, silica-rich, or terrigenous-rich formations, and have sometimes given rise to periods of hiatuses in which removal exceeds deposition and sediment is absent. Such hiatuses, which are found in all the oceans, probably reflect changes in current strengths and circulation patterns, and are most pronounced on the western edges of the oceans where the boundary currents are strongest (see Sec. 7.3.3). In addition to those associated with alternations in the shapes of the oceanic basins following the tectonic evolution of the oceans, changes in sediment distribution patterns are also brought about by global climatic variations, which can affect both the strengths of the external input mechanisms, which deliver material to the seawater reservoir, and the internal oceanic conditions (e.g. sea level, water temperature, current movements, primary productivity). For example, large-scale climatic changes attendant on glacial–interglacial transitions can considerably modify sedimentation patterns. The Holocene–Pleistocene transition, which markes the last transition from glacial to

interglacial conditions, is often marked in oceanic sediments by a decrease in carbonate concentrations, as a result of the rising of the CCD (see Sec. 15.2.4.1) during interglacials and its lowering during glacials, and changes in the assemblages of planktonic microfossils, which occurred mainly in response to variations in temperatures in the euphotic productive water layers.

The importance of changes in the type of deposit with depth in the oceanic sediment column will be identified where necessary in the text. However, in the present volume we are chiefly concerned with the role played by the sediments as marine sinks for components that have flowed through the seawater reservoir. The diagenetic changes, which have their most immediate effect on the composition of sea water, take place in the upper few metres of the sediment column, i.e. during early diagenesis (see Sec. 14.2), and for this reason attention will be focused mainly on the present-day sediment distribution patterns.

Marine sediments are deposited under a wide variety of depositional environments. However, it is useful at this stage to make a fundamental distinction between nearshore and deep-sea deposits, a distinction that recognizes the importance of the shelf break in dividing two very different oceanic depositional regimes.

Nearshore sediments are deposited mainly on the shelf regions under a wide variety of regimes that are strongly influenced by the adjacent land masses. As a result, physical, chemical and biological conditions in nearshore areas are much more variable than in deep-sea ones. Nearshore depositional environments include estuaries, fjords, bays, lagoons, deltas, tidal flats, the continental terrace and marginal basins.

Deep-sea sediments are usually deposited in depths of water > 500 m, and factors such as remoteness from the land-mass sources, reactivity between particulate and dissolved components within the oceanic water column, and the presence of a distinctive biomass lead to the setting up of a deep-sea environment that is unique on the planet. Because of this, deep-sea sediments, which cover more than 50% of the surface of the Earth, have very different characteristics from those found in continental or nearshore environments. Two of the most distinctive characteristics of these deep-sea sediments are (a) the particle size and (b) the rate of accumulation, of their land derived components.

(a) The land-derived fractions of deep-sea sediments are dominated by clay-sized, i.e. < 2 μm diameter, components, which usually account for $\sim$ 60–70% of the non-biogenic material in them. In contrast, material having a wide variety of particle sizes is found in nearshore sediments, and in general clay-sized components constitute a much smaller fraction of the land-derived solids – see Table 13.1.
(b) Various techniques are avaiable for the measurement of the

Table 13.1 The average content of the < 2 μm fraction in marine sediments and suspended river particulates[a]

Sediment type	Location	Wt% <2μm fraction
Pelagic sediment	Atlantic Ocean	58
	Pacific Ocean	61
	Indian Ocean	64
Shelf sediment	U.S. Atlantic coast	2
	Gulf of Mexico	27
	Gulf of California	19
	Sahul Shelf, N.W. Australia	72
Suspended river particulates	33 U.S. rivers	37

[a] Data from Griffin et al. (1968).

accumulation rates of marine sediments. These include dating by magnetic reversals, fossil assemblages and the decay of radionuclides. The radionuclide decay methods are the most commonly used, and normally involve either ^{14}C or members of the uranium, thorium and actino-uranium decay series. There are differences between the accumulation rates derived by the various techniques, and sometimes even between those obtained using the same technique. Because of this two data sets are given in Table 13.2 for the accumulation rates

Table 13.2 Accumulation rate of land-derived fractions in deep-sea sediments (units, mm/10^3 yr)

Oceanic region	Accumulation rate (mm /10^3 yr)	
	a	b
South Pacific	0.45	1.0
North Pacific	1.5	5.8
South Atlantic	1.9	6.0
North Atlantic	1.8	5.7
Indian Ocean	-	4.4

[a] Data from Goldberg & Koide (1962). Goldberg et al. (1963) and Goldberg & Griffin (1964).

[b] Data from Ku et al. (1968).

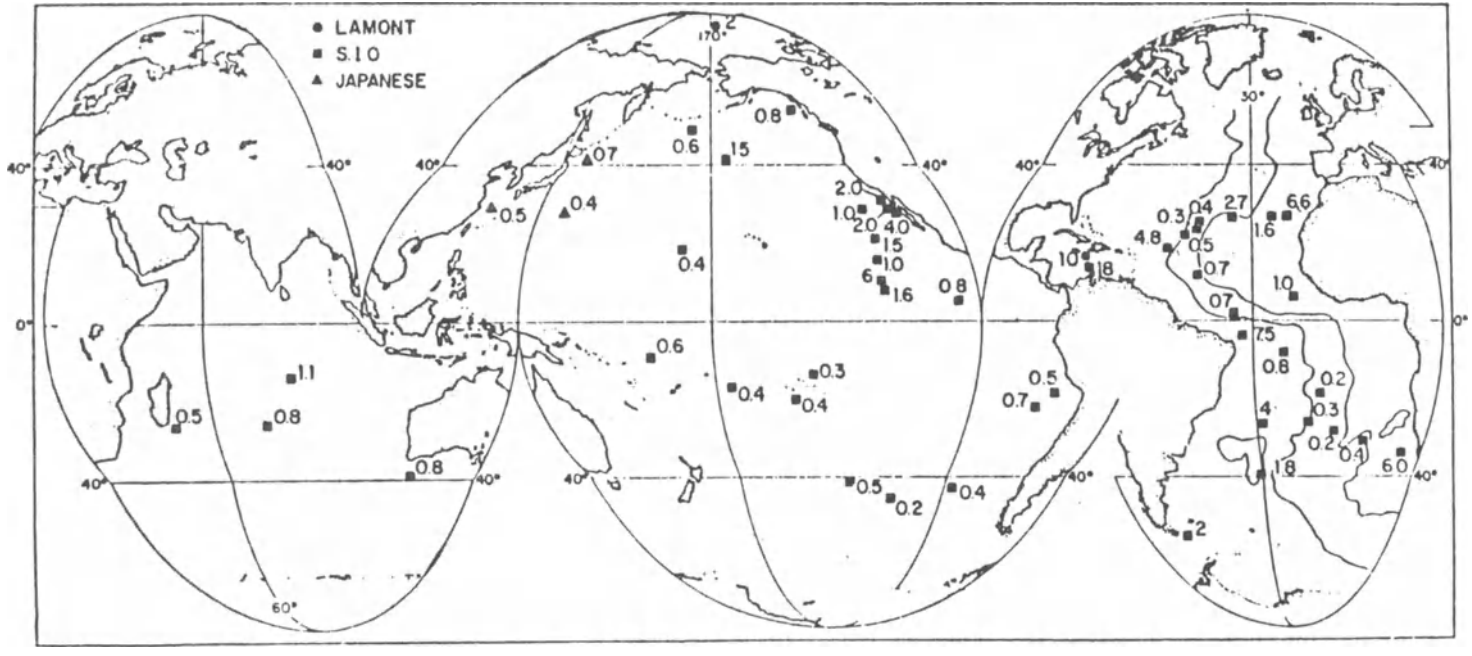

Figure 13.3 Accumulation rates of non-carbonate material in deep-sea sediments. (**a**) Accumulation rate trends, showing low values around the Mid-Atlantic Ridge (from Griffin *et al.* 1968). (**b**) Accumulation rates in the Indo-Pacific Ocean (from Bostrom *et al.* 1973).

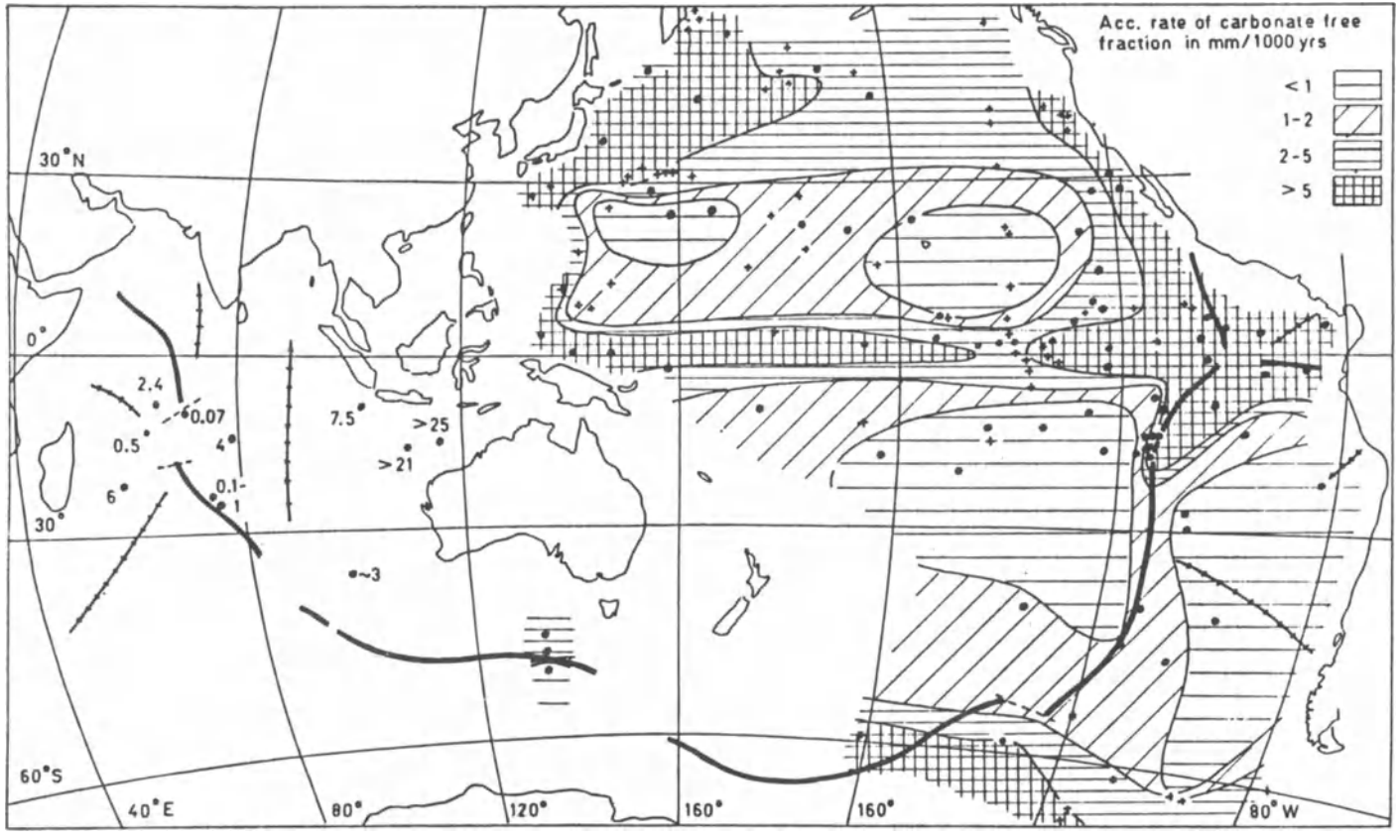
Acc. rate of carbonate free fraction in mm/1000 yrs
< 1
1-2
2-5
> 5
30°N
0°
30°
60°S
40°E
80°
120°
160°
160°
80°W
2.4
0.07
0.5
4
6
0.1-1
7.5
>25
>21
~3

(b)

of the land-derived material in deep-sea sediments. However, although there are differences between the two data sets, it is apparent that the land-derived fractions of deep-sea sediments are accumulating at a rate of the order of a few millimetres (usually < 10 mm in pelagic sediments) per 1000 years. There are, however, variations in the accumulation rates of this land-derived material within the oceans. An example of how the accumulation rates of land-derived material in deep-sea sediments vary with the environment of deposition was provided by Griffin *et al.* (1968). These authors showed that the highest accumulation rates for this material were found adjacent to the continents (hemi-pelagic areas), where they could reach values > 10 mm/10^3 yr. Away from the influence of the continents, the rates decreased to reach minimum values (~ 0.5 mm/10^3 yr) in remote open-ocean (pelagic) areas, e.g. around the Mid-Atlantic Ridge. However, Ku *et al.* (1968) reported somewhat higher values (~ 1 mm/10^3 yr) for these remote regions, and estimated the average accumulation rate for the non-carbonate fractions of deep-sea sediments to be ~ 2 mm/10^3 yr. The trends in the accumulation rate data derived by Griffin *et al.* (1968) are illustrated in Figure 13.3a. Bostrom *et al.* (1973) made a compilation of the accumulation rates of the non-carbonate fractions of Indo-Pacific deep-sea sediments, and also demonstrated that there is an overall decrease in the rates away from the land margins towards the open-ocean regions; these trends are illustrated in Figure 13.3b. Oceanic carbonate oozes usually accumulate at rates in the range 1–3 cm/10^3 yr.

It is apparent, therefore, that under present-day conditions, land-derived material is accumulating in deep-sea sediments at a rate of the order of a few millimetres per 1000 years. In contrast to deep-sea deposits, those deposited in nearshore areas have non-carbonate fractions that can accumulate at rates much greater than a few millimetres per year.

13.2 The formation of deep-sea sediments

The processes that are involved in the formation of deep-sea sediments can be linked to the manner in which material is transported to, and distributed within, the World Ocean, and by considerably simplifying the situation it is possible to distinguish between five general types of sediment transport mechanisms that operate in the deep sea.

GRAVITY CURRENTS Gravity currents transport material to the deep sea

from the shelf regions by slides, slumps and gravity flows. Of the various types of gravity flows, it is the **turbidity currents** that have the greatest influence on the movement of material from the shelf regions to the open ocean. These turbidity currents are short-lived, high-velocity, density currents that can carry vast quantities of suspended sediment off the shelves, often via submarine canyon conduits. The deep-sea deposits generated by these currents are termed **turbidites**, and they are usually made up of sand layers interbedded with pelagic deposits of smaller grain size. Proximal turbidites have been deposited relatively close to the source of the transported sediment, whereas distal types have been carried for much greater distances. Turbidite deposition is an extremely important marine sedimentary process and is thought to be responsible for the formation of features such as submarine fans on the continental rise, and the abyssal plains on the deep-sea floor.

GEOSTROPHIC DEEP-OCEAN OR BOTTOM CURRENTS Bottom currents have a significant influence on the distribution of sediment on the deep-sea floor. These currents transport material that has a finer grain size than that carried by turbidity currents, and result in the formation of features such as sediment piles and ridges. Bottom currents are most strongly developed along the western boundaries of the oceans (see Sec. 7.3.3), and it is here that nepheloid layers (layers of suspended sediment) are best developed.

MID-DEPTH CURRENTS Various kinds of TSM can be transported by advection via mid-depth oceanic circulation patterns. These include material directly released from nearshore sediments, material resuspended from deep-sea sediments at basin edges, and hydrothermal components. As well as transporting material away from the basin margins, mid-depth currents can also carry material laterally from the centres to the edges of the oceanic basins.

SURFACE AND NEAR-SURFACE CURRENTS Surface current movements, which are dominated by the gyre circulation patterns (see Sec. 7.3.2), transport the oceanic biomass, together with fine-grained land-derived material introduced to the surface ocean by river run-off, atmospheric deposition and glacial transport.

VERTICAL OR DOWN-COLUMN TRANSPORT This is the great ocean-wide carbon-driven transport process (or global ocean flux), which carries material from the surface ocean to the sea bed. During the process, the material becomes incorporated into the major oceanic biogeochemical cycles, which are involved in the down-column flux of particulate material, and play such a vital role in controlling the chemistry of the

oceans (see Secs 11.6.3.1 & 11.6.3.2). The down-column flux can also incorporate the advective mid-depth flux (see Sec. 10.5).

On the basis of these different mechanisms, important distinctions can therefore be made between the transport vectors involved in (i) *lateral* off-shelf movements, (ii) *lateral* sea-bed movements, (iii) *lateral* mid-depth movements, (iv) *lateral* sea surface movements and (v) *vertical* down-column movements.

Each of these transport vectors has a material flux associated with it which contributes material to deep-sea sediments, and a recent study reported by Grousset & Chesselet (1986) can be used both to illustrate how these transport vectors operate on a quasi-global scale and to assess the extent of any coupling between them. These authors carried out an investigation into the Holocene (10 000 yr BP) mid-ocean ridge sedimentary regime, which prevailed in the North Atlantic between ~ 45°N and ~ 65°N. The major sources of sediment to the region in the Holocene were the North American mainland and Iceland, with local mid-ocean ridge sources being generally of only minor importance. By employing a number of tracers to identify the sediment source materials and to elucidate the mechanisms by which they were transported, the authors were able to construct a first-order model for the Holocene sedimentary regime in the region. This model is illustrated in Figure 13.4, and involves the following source–flux relationships.

(a) **Source 1** was the North American mainland from which material was supplied by surface currents (Φ_s), turbidity currents (Φ_t) and aeolian transport (Φ_e). Material from this source decreased in the underlying sediments in a west-to-east direction, and it was suggested that a coupling of the aeolian transport flux into the down-column flux (Φ_v) was the principal mechanism responsible for driving this gradient.
(b) **Source 2** was Iceland, from which material was supplied via the turbidity current flux (Φ_t) and the geostrophic current flux (Φ_a). Material from this source decreased in concentration in a north-to-south direction in the underlying sediments, and it was proposed that this gradient arose from a coupling of the two fluxes that transported material from Iceland.
(c) **Source 3** was the Mid-Atlantic Ridge, but this supplied only a minor amount of sedimentary material to the region.

The two thick arrows in the flux model (Fig. 13.4), representing the down-column (Φ_v) and the geostrophic (Φ_a) fluxes, are the main pathways by which continental material was transported from the North America and Icelandic sources, respectively, and these combine to form the ridge flux (Φ_{ridge}), the ridge flux being negligible.

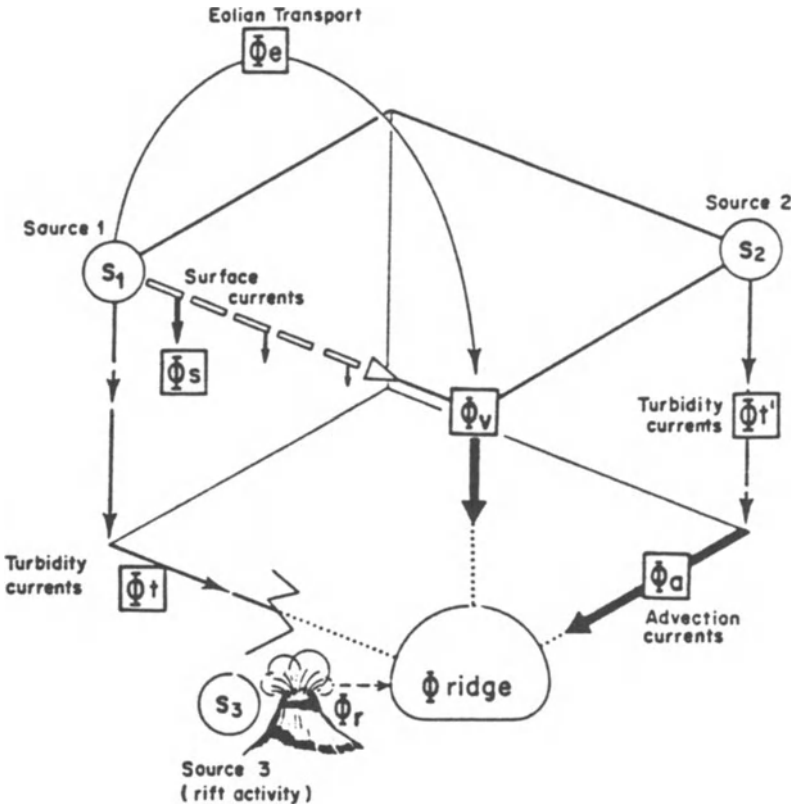

Figure 13.4 A first-order model for the mid-ocean ridge Holocene sedimentary regime in the North Atlantic (from Grousset & Chesselet 1986). The three major sediment sources are S_1, S_2 and S_3, which supply the following specific flux materials: Φ_t and Φ_t', which are fluxes associated with downslope processes; Φ_s, which is the surface current flux; Φ_a, which is the advective bottom flux; Φ_e, which is the aeolian flux; Φ_{ridge}, which is the rift flux. These are the main concepts of Φ_v (the vertical flux) and Φ_a (the advective flux).

The study reported by Grousset & Chesselet (1986) clearly demonstrates how the various mechanisms that transport land-derived material to the ocean reservoir interact on a quasi-global oceanic scale. This kind of interaction is extremely important in controlling the chemical composition of the bottom sediments. There are a number of reasons for this, and three of the more important of these are identified below.

(a) Solids derived from different continental sources may have different chemical compositions, and the extent to which they are mixed will affect the overall composition of a sediment to which they contribute.
(b) Material can be transported at varying rates by the different transport

mechanisms; for example, turbidity currents deposit material at a much faster rate than down-column settling. The accumulation rate of a sediment determines the length of time its surface is in contact with the overlying water column, and therefore influences both the degree to which the sediment components react with material dissolved in sea water and the extent to which the diagenetic sequence proceeds.

(c) The relative magnitudes of the **sea bottom** and the **vertical down-column particle fluxes** are extremely important in constraining the chemical composition of non-biogenous deep-sea sediments. There are two main reasons for this. First, the material that is initially dumped on the shelf regions has a coarser particle size, and is poorer in trace metals, than the material that escapes the coastal zone via the surface ocean; this concept was developed in Section 3.1.4. Secondly, the material that undergoes down-column transport is involved in the dissolved–particulate reactions that remove trace elements from sea water and so become a sink for additional trace elements, which are not picked up by bottom transported material. This bottom transport/down-column vertical transport trace metal fractionation is considered in more detail in Section 16.5.

13.3 A general scheme for the classification of marine sediments

A number of the parameters discussed above can be combined together to outline a general scheme for the classification of marine sediments. It must be stressed, however, that this is by no means a rigorous sediment classification, and recently several attempts have been made to produce much more detailed and lithologically consistent classifications of deep-sea sediments. Nonetheless, the simplified classification will serve its purpose, which is merely to act as a framework within which to describe the geochemistry of marine sediments. This general scheme is outlined below.

13.3.1 Nearshore sediments

Nearshore or coastal sediments are deposited on the margins of the continents under a wide variety of conditions in chemical environments that range from oxic to fully anoxic in character. The sediments include gravels, sands, silts and muds and they are composed of mixtures of terrigenous, authigenic and biogenous components; the latter is mainly shell material, but high concentrations of organic carbon are found in sediments deposited under reducing conditions. Nearshore sediments contain material having a wide variety of grain sizes, fine-grained material being found in low-energy environments and sands in high-energy

environments. Over many shelves terrigenous sediments (e.g. terrigenous muds, which accumulate at relatively high rates, e.g. > several mm yr^{-1}) are the prevalent type of deposit, but on some shelf regions carbonate deposition can predominate, e.g. on broad shallow shelves where the supply of terrigenous debris is small.

13.3.2 Deep-sea sediments

On the basis of the major transport mechanisms that supply the sediment-forming material, deep-sea deposits can be subdivided into hemi-pelagic and pelagic types.

13.3.2.1 Hemi-pelagic deep-sea sediments These sediments are deposited in areas that fringe the continents, e.g. on the abyssal plains. The land-derived material in hemi-pelagic sediments has been transported mainly by bottom processes, i.e. by the turbidity current and geostrophic bottom current fluxes described above, and much of it originated on the shelf regions. The inorganic hemi-pelagic sediments include **lithogenous clays** (or muds), **glacial marine sediments**, **turbidites** and **mineral sands**. All of these sediments can contain varying proportions of biogenous shell material. The rates of deposition of the land-derived material in hemi-pelagic deep-sea sediments can be $\gtrsim 10$ mm/10^3 yr, and they often contain as much as $\sim$ 1–5% organic carbon. The preservation of this organic carbon is a function of the extent to which the diagenetic sequence has proceeded (see Sec. 14.3 & 14.4), and hemi-pelagic clays are often grey-green in colour, indicating reducing conditions, below a thin oxidized red layer.

13.3.2.2 Pelagic deep-sea sediments These sediments accumulate in open-ocean areas. They are generally deposited in the absence of effective bottom currents, and Davies & Laughton (1972) have defined pelagic sediments as those 'laid down in deep-water under quiet current conditions'. The bulk of the material forming these deposits has settled down the water column to blanket the bottom topography with a sediment cover. Thus, pelagic sediments are formed via the vertical down-column flux identified above, and so can be differentiated from hemi-pelagic deposits, which have been formed largely from bottom transport processes. It is common practice to subdivide pelagic deep-sea sediments into inorganic and biogenous categories.

INORGANIC PELAGIC DEEP-SEA SEDIMENTS In the past these have been defined as containing < 30% biogenous skeletal remains, and as having a large fraction ($\gtrsim$ 60%) of their non-biogenous material in the < 2 μm (clay) size class. Traditionally, therefore, it is these sediments that have been known as the pelagic clays, or simply the **deep-sea clays**. The land-

derived material in all types of pelagic sediments has been in suspension for relatively long periods in the water column and is deposited at slow rates, i.e. usually a few millimetres per 1000 years. As a result, much of the organic carbon reaching the sediment surface is destroyed in the early stages of the diagenetic sequence (see Sec. 14.2.2), and the sediments usually contain only ~ 0.1–0.2% organic carbon. Pelagic clays are therefore oxidizing to a considerable depth, and often have a red colour due to the presence of ferric iron. Because of this, they have often been termed **red clays**. Some authors have further subdivided pelagic clays on the basis of the origin of their principal components, e.g. into **lithogenous** and **hydrogenous** types; for a description of these categories – see Chapter 15.

BIOGENOUS PELAGIC DEEP-SEA SEDIMENTS These sediments have been traditionally defined as containing > 30% biogenous shell remains. They are usually referred to by the term **oozes**, and are subdivided into calcareous and siliceous types.

The **calcareous oozes** contain > 30% skeletal carbonates, and are classified on the basis of the predominant organisms present into **foraminiferal ooze**, (sometimes termed ***Globigerina* ooze** after the most common of the forams), **nanofissil ooze** (or coccolith ooze) and **pteropod ooze**.

The **siliceous oozes** contain > 30% opaline silica skeletal remains, and are subdivided into **diatom oozes** and **radiolarian oozes**, depending on the principal silica-secreting organism present.

13.4 The distribution of marine sediments

The distribution of sediments in the World Ocean is illustrated in Figure 13.5. In Figure 13.5a, the sediments are classified on a general basis in which individual types of deep-sea clay are not specified. In contrast, Figure 13.5b presents an example of a classification in which the deep-sea clays are subdivided into lithogenous and hydrogenous types. A number of the principal features in the distributions of deep-sea sediments can be identified from these diagrams.

(a) Deep-sea clays and calcareous oozes are the predominant type of deep-sea deposit.
(b) The calcareous oozes cover large tracts of the open-ocean floor at water depths < 3–4 km (see Sec. 15.2.4.1).
(c) The siliceous oozes form a ring around the high-latitude ocean margins in the Antarctic and North Pacific (both diatom oozes), and are also found in a band in the Equatorial Pacific (radiolarian oozes).
(d) Exetensive deposits of glacial marine sediments are confined to a

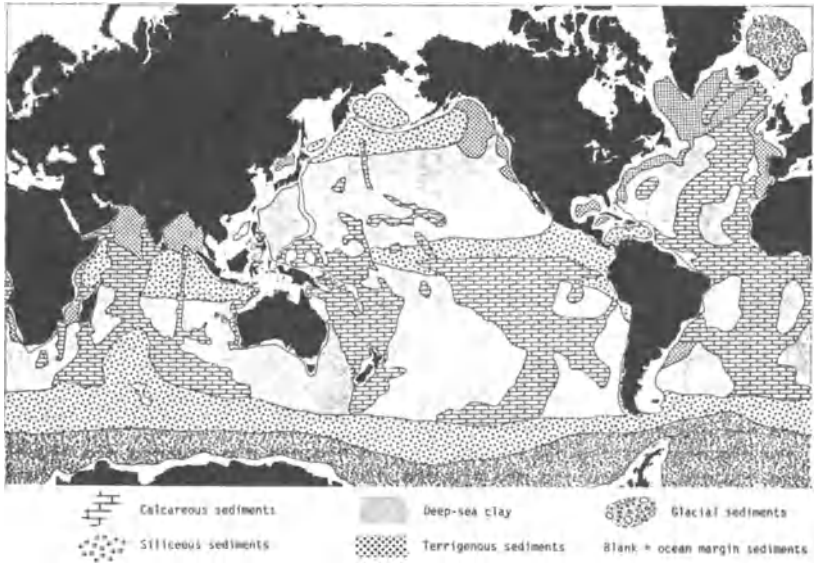

(a)

Figure 13.5 The present-day distributions of the principal types of marine sediments. (**a**) The general distribution of marine sediments (from Davies & Gorsline 1976).

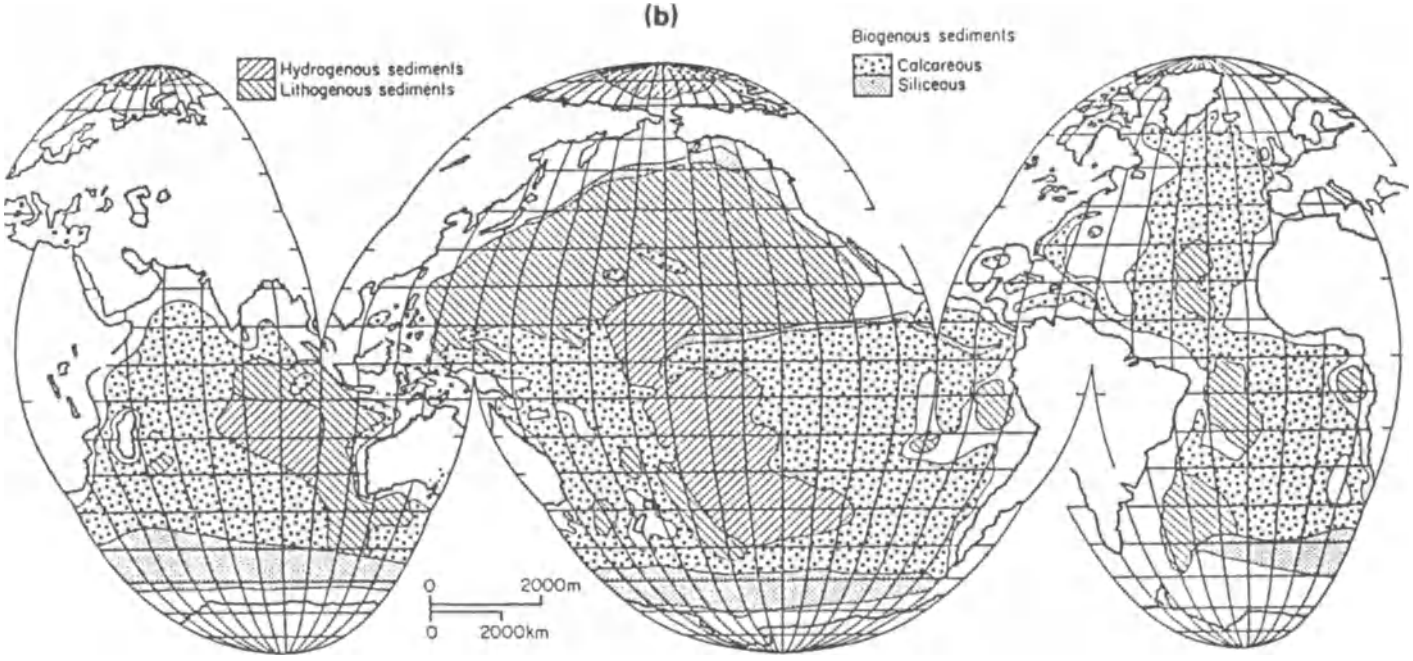

Figure 13.5b The distribution of deep-sea sediments classified on the basis of their components (from Riley & Chester 1971).

band fringing Antarctica, and to the high-latitude North Atlantic.
(e) Lithogenous clays cover a large area of the North Pacific, whereas the clays in the South Pacific are mainly hydrogenous in character.

13.5 The chemical composition of marine sediments

The material that is finally deposited in the marine sediment reservoir has undergone a complex journey before reaching its sea-bed sink. The sediments forming this reservoir respresent, if not the ultimate end-point, at least a major geological timescale halt in the global mobilization–transportation cycle. A knowledge of the chemical composition of this sediment reservoir is therefore important for an understanding of the global cycle of many elements. However, before attempting to synthesize the various factors that act together to control the chemistry of these sediments it is necessary to establish a compositional database from which to work. For this purpose, three data compilations have been prepared.

(a) The first compilation is given in Table 13.3, and lists the **overall elemental compositions** of the principal types of marine sediments, i.e. nearshore muds, deep-sea clays and deep-sea carbonates. The table also includes chemical data for the continental crust, soils, suspended river particulates and crustal aerosols, which are given so that the compositions of marine sediments can be evaluted within the global context of their principle terrestrial feeder materials.
(b) The second compilation is given in Table 13.4, and lists the **major element compositions** of the main types of deep-sea sediments.
(c) The third compilation is given in Table 13.5, and presents data showing a number of **overall trends** in the elemental compositions of a wide range of deep-sea deposits. The aim of this table is to permit compositional differences in the deposits to be evaluated within an ocean-wide framework.

From these combined databases a number of gross features in the geochemistry of marine sediments can be identified, and for this purpose it is convenient to treat the major and trace elements separately.

MAJOR ELEMENTS The major element composition of marine sediments is largely controlled by the relative proportions of the sediment-forming minerals. The principal minerals are the clays, and biogenous carbonates and opal. On the basis of the mutual proportions of these minerals the sediments can be divided into three broad types, i.e. clays, carbonate oozes and siliceous oozes. Average major element analyses for the three sediment types are given in Table 13.4, from which it can be seen that

Table 13.3 Elemental composition of marine sediments and some continental material (units, $\mu g\ g^{-1}$)

Element	Continental crust[a]	Continental soil[a]	River particulate material[a]	Crustal dust[b]	Near-shore mud[c]	Deep-sea clay[a]	Deep-sea carbonate[d]
Ag	0.07	0.05	0.07	----	----	0.1	0.0X
Al	69300	71000	94000	82000	84000	95000	20000
As	7.9	6	5	----	5	13	1.0
Au	0.01	0.001	0.05	----	----	0.003	0.00X
B	65	10	70	----	----	220	55
Ba	445	500	600	----	----	1500	190
Br	4	10	5	----	----	100	70
Ca	45000	15000	21500	----	29000	10000	312400
Cd	0.2	0.35	(1)	----	----	0.23	0.23
Ce	86	50	95	----	----	100	35
Co	13	8	20	23	13	55	7
Cr	71	70	100	79	60	100	11
Cs	3.6	4	6	----	----	5	0.4
Cu	32	30	100	47	56	200	50
Er	3.7	2	(3)	----	----	2.7	1.5
Eu	1.2	1	1.5	----	----	1.5	0.6
Fe	35000	40000	48000	48000	65000	60000	9000
Ga	16	20	25	----	----	20	13
Ge	1.5	X	----	----	----	1.2	0.1
Gd	6.5	4	(5)	----	----	7.8	3.8
Hf	5	----	6	----	----	4.5	0.41
Ho	1.6	0.6	(1)	----	----	1.0	0.8
In	0.1	----	----	----	----	0.08	0.02
K	24000	14000	20000	20000	25000	28000	2900
La	41	40	45	----	----	45	10
Li	42	25	25	----	79	45	5
Lu	0.45	0.40	0.50	----	----	0.50	0.50
Mg	16400	5000	11800	----	21000	18000	----
Mn	720	1000	1050	865	850	6000	1000
Mo	1.7	1.2	3	1.8	1	8	3
Na	14200	5000	5300	5100	40000	40000	20000
Nd	37	35	35	----	----	40	14
Ni	49	50	90	73	35	200	35
P	610	800	1150	----	550	1400	350
Pb	16	35	100	52	22	200	9
Pr	9.6	----	(8)	----	----	9	3.3
Rb	112	150	100	----	----	110	10
Se	0.05	0.01	----	----	----	4.5	0.5
Sb	0.9	1	2.5	----	----	0.8	0.15
Sc	10	7	18	----	12	20	2
Si	275000	330000	285000	----	250000	283000	32000
Sm	7.1	4.5	7.0	----	----	7.0	3.8
Sn	2	(0.1)	----	----	2	1.5	0.X
Sr	278	250	150	----	160	250	2000
Ta	0.8	2	1.2	----	----	1	0.0X
Tb	1.05	0.7	1	----	----	1	0.6
Th	9.3	9	14	----	----	10	----
Ti	3800	5000	5600	5700	5000	5700	770
Tm	0.5	0.6	(0.4)	----	----	0.4	0.1
U	3	2	3	----	----	2	----
V	97	90	170	120	145	150	20
Y	33	40	30	----	----	32	42
Yb	3.5	----	3.5	----	----	3	1.5
Zn	127	90	250	75	92	120	35
Zr	165	300	----	----	240	150	20

a Data for Ge, In, Se, Sn and Zr from a variety of sources; data for all other elements from Martin & Whitfield (1983).

b A Saharan dust population from the Atlantic Northeast Trades; data from Murphy (1985).

c Data from Wedepohl (1960).

Table 13.4 The major element composition of the principal types of deep-sea sediments[a] (units, wt.% oxides)

	Calcareous	Lithogenous clay	Siliceous	Oceanic[b] average
SiO_2	26·96	55·34	63·91	42·72
TiO_2	0·38	0·84	0·65	0·59
Al_2O_3	7·97	17·84	13·30	12·29
Fe_2O_3	3·00	7·04	5·66	4·89
FeO	0·87	1·13	0·67	0·94
MnO	0·33	0·48	0·50	0·41
CaO	0·30	0·93	0·75	0·60
MgO	1·29	3·42	1·95	2·18
Na_2O	0·80	1·53	0·94	1·10
K_2O	1·48	3·26	1·90	2·10
P_2O_5	0·15	0·14	0·27	0·16
H_2O	3·91	6·54	7·13	5·35
$CaCO_3$	50·09	0·79	1·09	24·87
$MgCO_3$	2·16	0·83	1·04	1·51
Org. C.	0·31	0·24	0·22	0·27
Org. N.	—	0·016	0·016	0·015
Total	100·0	100·0	100·0	100·0
Total Fe_2O_3	3·89	8·23	6·42	—

a Data from El Wakeel & Riley (1961).
b Weighted mean calculated on the basis of the areal coverage of the sea floor by each type of sediment: calcareous, 48.7%; lithogenous, 37.8%; siliceous, 13.5%.

aluminium is concentrated in the clays, calcium in the carbonates and silicon in the siliceous oozes. Mn and Fe are included in Table 13.4, and although they are usually present as major elements they will also be included with the trace elements because both iron and manganese phases can act as scavenging agents for dissolved metals.

TRACE ELEMENTS From the data given in Table 13.5, it is possible to establish a number of trends in the distributions of some trace elements in deep-sea sediments (see e.g. Chester & Aston 1976). These trends can be summarized as follows.

(a) In general, deep-sea carbonates are impoverished in most trace elements relative to deep-sea clays, Sr being an exception to this.

Table 13.5 The concentrations of some trace elements in deep-sea deposits (units, $\mu g\ g^{-1}$)

Trace element	Near-shore muds	Deep-sea carbonate	Atlantic deep-sea clay	Pacific deep-sea clay	Active ridge sediment	Ferro-manganese nodules
Cr	100	11	86	77	55	10
V	130	20	140	130	450	590
Ga	19	13	21	19	—	17
Cu	48	30	130	570	730	3300
Ni	55	30	79	293	430	5700
Co	13	7	38	116	105	3400
Pb	20	9	45	162	—	1500
Zn	95	35	130	—	380	3500
Mn	850	1000	4000	12500	60000	220000
Fe	69900	9000	82000	65000	180000	140580

a From Chester & Aston (1976).

(b) Certain trace elements, e.g. Cr, V and Ga, have similar concentrations in both nearshore muds and deep-sea clays (DSC).
(c) In contrast, other trace elements, e.g. Mn, Cu, Ni, Co and Pb, are enhanced in the DSC relative to nearshore muds. Thus, a fundamental oceanic fractionation between nearshore muds and deep-sea clays can be introduced for these **enriched** or **excess elements**.
(d) The excess trace elements are enhanced to a greater extent in Pacific than in Atlantic deep-sea clays.
(e) Ferromanganese nodules have particularly high concentrations of the elements that are enhanced in deep-sea clays ((c) above), but only small concentrations of the elements that are not enriched in DSC ((b) above).
(f) Metalliferous, active ridge, sediments are enhanced in elements such as Fe, Mn, Cu, Zn, Ni and Co, relative to normal DSC.
(g) Although it is not apparent from the data given in Table 13.5, a number of the early surveys carried out on the distributions of trace elements in deep-sea sediments revealed that the excess trace elements reached their highest values in deposits that had accumulated at very slow rates in areas remote from the land masses.

These various trends offer a skeleton around which to build a discussion of the factors that combine together to control the elemental composition of marine sediments. Even at this stage a number of elemental fractionation stages can be identified in the marine sediment complex. For example, there is a major fractionation of some trace metals between nearshore muds and deep-sea clays. In addition, further fractionation stages occur within the various kinds of deep-sea deposits themselves, e.g. between the ridge crest metalliferous deposits and the deep-sea clays. Thus, it begins to appear as if some kind of sequential enhancement is occurring for certain elements within marine sediments. The following chapters will be devoted to an attempt to understand how these elemental fractionations, and sequential enrichments, may have arisen. To provide a framework for this, further use will be made of the concept of chemical signals.

13.6 Chemical signals to marine sediments

Marine sediments may be thought of as having received a variety of chemical signals, or fluxes, which, in a number of combinations, have resulted in them acquiring their present composition. Two principal questions must therefore be asked in order to understand how the sediments attained this composition: (a) What is the chemical composi-

tion of the dissolved and particulate material carried by the signals themselves? (b) How can the effects of the individual signals be unscrambled in order to provide a reasonably coherent explanation for the geochemical characteristics of individual sediments, or sediment suites?

One way of addressing these questions is to identify the individual components that combine together to form marine sediments, and then to establish whether or not the *processes* by which they are formed can be related to specific **individual chemical signals**, i.e. to adopt a process-orientated approach to the problem of describing the chemical compositions of the sediments. It is possible to classify the components of marine sediments into a series of genetically different types, and a number of schemes have been proposed for this purpose. The scheme adopted in the present volume is a modification of that outlined by Goldberg (1954), which classifies the components in terms of their geospheres of origin. In the original scheme the sediment components were subdivided into a single aqueous phase, i.e. **interstitial waters**, and four solid phases, which were classified according to the origin of their component elements as **lithogenous**, **biogenous**, **hydrogenous** and **cosmogenous**. In the modified scheme employed here, however, the hydrogenous material will be subdivided into a number of different types (see Sec. 15.3.1).

13.7 Marine sediments: summary

(a) A large part of the floor of the World Ocean is covered by a blanket of sediment, which has an average thickness of $\sim$ 500 m.
(b) Nearshore sediments are deposited on the shelf region, under a wide variety of depositional environments. Deep-sea sediments are deposited seaward of the shelf, under conditions of slow accumulation, and cover more than 50% of the surface of the Earth. The deep-sea sediments are subdivided into hemi-pelagic types, which are deposited in areas fringing the continents mainly via bottom transport mechanisms, and pelagic types, which are deposited in open-ocean areas mainly via down-column transport mechanisms.
(c) Calcareous oozes cover large tracts of the open-ocean floor at water depths $\ll$ 3–4 km. Siliceous oozes from a ring around the high-latitude ocean margins.
(d) The components of marine sediments can be subdivided into an aqueous phase (interstitial water) and four solid phases, which, on the basis of their geospheres of origin, are classed as lithogenous, hydrogenous, biogenous and cosmogenous.
(e) Relative to nearshore muds, deep-sea clays contain enhanced concentrations of some trace elements, e.g. Mn, Cu, Ni, Co and Pb; these are often referred to as excess elements.

The solid sediment-forming components that make up marine sediments can be thought of as building blocks, which are stacked together in various proportions to form an individual sediment, or a suite of sediment types. However, at this stage an extremely important concept must be introduced; this is that sediments are *not* an inert reservoir, and as a result the building blocks are not simply stacked together in a way that retains their original compositions. Rather, they can be subjected to a series of *diagenetic* reactions following their deposition. Further, it is important to understand that these diagenetic reactions, which take place mainly via the medium of the interstitial waters, not only modify the compositions of pre-existing building blocks but also can supply elements that result in the formation of new blocks. In order, therefore, to be able to evaluate fully the processes involved in the formation of the sediment components, diagenesis will be described before the components themselves are considered. To do this, diagenetic reactions will be discussed in terms of the aqueous, i.e. the interstitial water, sediment phase. This will be followed by a description of the individual sediment-forming components themselves, and finally an attempt will be made to identify, and unscramble, the chemical signals that are transmitted to marine sediments.

References

Bostrom, K., T. Kraemer & S. Gartner 1973. Provenance and accumulation rates of opaline silica, Al, Ti, Fe, Mn, Cu, Ni and Co in Pacific pelagic sediments. *Chem. Geol.* **11,** 123–48.

Chester, R. & S.R. Aston 1976. The geochemistry of deep-sea sediments. In *Chemical oceanography*, J.P. Riley & R. Chester (eds), Vol. 6, 281–390. London: Academic Press.

Davies, T.A. & D.S. Gorsline 1976. Oceanic sediments and sedimentary processes. In *Chemical oceanography*, J.P. Riley & R. Chester (eds), Vol. 5, 1–80. London: Academic Press.

Davies, T.A. & A.S. Laughton 1972. Sedimentary processes in the North Atlantic. Initial reports of the Deep Sea Drilling Project, Vol. 12, 905–34. Washington DC: US Government Printing Office.

El Wakeel, S.K. & J.P. Riley 1961. Chemical and mineralogical studies of deep-sea sediments. *Geochim. Cosmochim. Acta* **25,** 110–46.

Goldberg, E.D. 1954. Marine geochemistry. Chemical scavengers of the sea. *J. Geol.* **62,** 249–55.

Goldberg, E.D. & J.J. Griffin 1964. Sedimentation rates and mineralogy in the South Atlantic. *J. Geophys. Res.* **69,** 4293–309.

Goldberg, E.D. & M. Koide 1962. Geochronological studies of deep-sea sediments by the ionium/thorium method. *Geochim. Cosmochim. Acta* **26,** 417–50.

Goldberg, E.D., M. Koide, J.J. Griffin & M.N.A. Peterson 1963. A geochronological and

sedimentary profile across the North Atlantic Ocean. In *Isotope and cosmic chemistry*, H. Craig, S.L. MIller & G.J. Wasserburg (eds), 211–32. Amsterdam: North-Holland.

Griffin, J.J., H. Windom & E.D. Goldberg 1968. The distribution of clay minerals in the World Ocean. *Deep-Sea Res.* **15,** 433–59.

Grousset, F.E. & R. Chesselet 1986. The Holocene sedimentary regime in the northern Mid-Atlantic Ridge region. *Earth Planet. Sci. Lett.* **78,** 271–87.

Heezen, B.C. & C.D. Hollister 1971. *The face of the deep*. New York: Oxford University Press.

Heezen, B.C., M. Tharp & M. Ewing 1959. The floors of the oceans. *Geol. Soc. Am. Spec. Pap.* No. 65, 1–122.

Holcombe, T.L. 1977. Ocean bottom features – terminology and nomenclature. *Geojournal* **6,** 25–48.

Jones, E.J.W. 1978. Sea-floor spreading and the evolution of the ocean basins. In *Chemical oceanography*, J.P. Riley & R. Chester (eds), Vol. 7, 1–74. London: Academic Press.

Kennet, J.P. 1982. *Marine geology*. Englewood Cliffs, NJ: Prentice Hall.

Ku, T.L., W.S. Broecker & N. Opdyke 1968. Comparison of sedimentation rates measured by paleomagnetic and ionium methods of age determination. *Earth Planet. Sci. Lett.* **4,** 1–16.

Martin, J.-M. & M. Whitfield 1983. The signficance of the river input of chemical elements to the ocean. In *Trace metals in sea water*, C.S. Wong, E.A. Boyle, K.W. Bruland, J.D. Burton & E.D. Goldberg (eds), 265–96. New York: Plenum.

Murphy, K.J.T. 1985. The trace metal chemistry of the Atlantic aerosol. *Ph.D. Thesis*, University of Liverpool.

Parsons, B. & F.M. Richter 1981. Mantle convection and the oceanic lithosphere. In *The sea*, Vol. 7, C. Emiliani (ed.), 73–117. New York: Interscience.

Riley, J.P. & R. Chester 1971. *Introduction to marine chemistry*. London: Academic Press.

Wedepohl, K.H. 1960. Spurenanalytische Untersuchungen an Tiefseetonen aus dem Atlantik. *Geochim. Cosmochim. Acta* **18,** 200–31.

14 Sediment interstitial waters and diagenesis

Interstitial waters are aqueous solutions that occupy the pore spaces between particles in rocks and sediments. In some nearshore deposits groundwater seepages can occur, and around the ridge crest areas circulating hydrothermal solutions (i.e. modified sea water) can enter the sediment column. However, for most marine sediments the interstitial fluids originated as sea water trapped from the overlying water column. The interstitial water–sediment complex is a site of intense chemical, physical and biological reactions, which can lead both to the formation of new and altered mineral phases and to changes in the composition of the waters themselves. These changes may be grouped together under the term *diagenesis*, which has been defined by Berner (1980) as 'the sum total of processes that bring about changes in a sediment or sedimentary rock subsequent to its deposition in water'. Many of the important diagenetic changes that affect marine sediments take place during *early diagenesis*, which occurs during the burial of the deposits to a depth of a few hundred metres. However, before we consider the processes that occur during early diagenesis, it is worthwhile taking an overview of the types of organic matter found in marine sediments and the manner in which they undergo long-term modification, particularly with respect to the generation of petroleum and natural gas. A great deal of information is now available on the kind of organic matter found in sediments and on the processes involved in its conversion to petroleum. The framework adopted in the brief overview given below relies heavily on the review produced by Simoniet (1978) and the comprehensive volume written by Tissot & Welte (1984), and the reader is referred to these for a more detailed treatment of the topic.

14.1 The long-term fate of organic matter in marine sediments

The organic matter found in sediments is composed of a wide range of compounds, and according to Degens & Mopper (1976) over 1000 different organic molecules had been identified in sediments at that time, and the number has grown considerably since then. For example, in the catalogue presented by Simoniet (1978) the various classes of compounds identified included: hydrocarbons, e.g. alkanes, cycloalkanes and iso-

prenoids; fatty acids; fatty alcohols, ketones and wax esters; steroids; triterpenoids; diterpenoids; tetraterpenoids; pigments; amino acids and peptides; purines and pyrimidines; carbohydrates (sugars); aromatic hydrocarbons, e.g. polynuclear aromatic hydrocarbons (PAH); natural polymers, e.g. chitin, cellulose, cutin and lignin; branched and cyclic hydrocarbons of the 'hump'; and kerogen and humates.

The organic matter in marine sediments is derived from terrestrial, marine and anthropogenic sources and is carried to the oceans via a number of transport agencies. Terrestrial (allochthonous) organics are brought to the oceans mainly via fluvial and atmospheric transport (see Secs 3.1.5 & 4.1.4.4), together with ice rafting. River run-off is the major pathway by which terrestrial material is delivered to the oceans, and much of the organic matter that accumulates in estuarine and coastal sediments is land-derived (e.g. from higher plants), and tends to be more refractory than marine-derived organic matter. For example, lignin from vascular plants remains relatively well preserved on a time scale of hundreds of years. However, much of the fluvially transported material is trapped in estuaries and coastal seas (see Sec. 3.2.7), and in recent years it has become increasingly apparent that long-range atmospheric transport is an important route for the delivery of organic material to the open ocean (see e.g. Gagosian 1986). Autochthonous organics are formed internally, largely from the photosynthetic fixation of carbon during primary production (see Sec. 9.2.2.2). In addition to the sources described above, both petroleum and natural gas can reach the marine environment by seepages. Various source markers have been used to distinguish marine from terrestrial inputs; these include n-alkanes, polycyclic aromatic hydrocarbons, n-alcohols, sterols, diterpenoids, lignins and bulk $^{13}C : {}^{12}C$ ratios.

The organic matter in marine sediments exists in a number of forms, which according to Ertel & Hedges (1985) include: (a) discrete organic particles, e.g. vascular plant debris and planktonic tissues; (b) surface films on inorganic phases, e.g. humic–clay complexes; and (c) integral components of inorganic matrices, e.g. kerogen. In addition, a number of dissolved organic components are present in the interstitial waters of the sediments. Thus, a variety of products originating in the biosphere cross the sediment/sea water interface to enter the geosphere, and once there they undergo a complex series of reactions in a sequence that follows the depth of burial of the sediment. The full sequence is in the order diagenesis (down to $\sim$ 1000 m) $\rightarrow$ catagenesis (several kilometres depth, with an increase in temperature and pressure) $\rightarrow$ metagenesis or metamorphism (Tissot & Welte 1984).

The organic matter in the upper portions of marine sediments can be divided into two general categories: (a) **hydrolysable** components (in this context, 'hydrolysable' material is that which can be converted by

hydrolysis into water-soluble substances), and (b) **non-hydrolysable** material, which makes up the bulk of the organic matter and is composed of 'humic-like' components. The formation of these two categories of organic material can be described in terms of a series of transformation reactions, which act upon the organic components. The organic material reaching the surface of marine sediments is composed largely of biogenic macromolecules, such as proteins, carbohydrates, lipids (including hydrocarbons) and lignins, together with various uncharacterized substances (see Secs 9.2.3 & 12.1). According to Tissot & Welte (1984), the most striking difference between the compositions of the organic matter in living organisms and that in surface, and near-surface, sediments is that a large proportion of the biogenic macromolecules have been lost from the sedimentary deposits. This is largely the result of bacterial activity during which the biogenic polymers (**biopolymers**), such as proteins and carbohydrates, undergo destruction. During this process water-soluble complexes containing amino acids and sugars are formed, which, together with hydrocarbons and fatty acids, are found in the upper portions of marine sediments. It is these components that comprise the free or hydrolysable content of the sediments. Most of these hydrolysable compounds are destroyed or modified at a shallow depth, especially in oxic environments, and the non-degradable residues become part of polycondensed structures (**geopolymers**), such as humic and fulvic acids, which subsequently undergo insolubilization to form 'humin'. A significant fraction of this humin is hydrolysable in young sediments, but with burial this decreases and eventually kerogen is formed. The term **kerogen** refers to the condensed macromolecular fraction of the organic matter in sediments that is insoluble in organic solvents. Kerogen can originate from either marine (plankton) or terrestrial (higher plant waxes) sources, or from a combination of both, and three different types of kerogen have been identified.

The general reaction pathway for the modification of organic matter during the complete diagenetic stage in marine sediments is therefore biopolymers → biochemical degradation → polycondensation → insolubilization → geopolymers (e.g. kerogen); thus, the overall effect is to convert *biopolymers* into *geopolymers*. In this context, therefore, the overall sequence for the full diagenesis of organic matter in sediments can be written: degraded cellular material → water-soluble complexes containing amino acids, lipids and carbohydrates → fulvic acids → humic acids → kerogen (see e.g. Nissenbaum & Kaplan 1972). However, under some extremely reducing conditions the sequence can bypass the fulvic and humic acid stages. Some of the humic material in marine sediments can also have a terrestrial source, although this type appears to be largely restricted to estuarine and coastal sea deposits.

The manner in which the sequence operates up to the stage at which

fulvic and humic acids are formed can be illustrated with respect to the diagenesis of amino acids in the upper sections of marine sediments. Various lines of evidence suggest that the concentrations of amino acids in marine sediments decrease with depth. For example, Burdige & Martens (1988) gave data on the concentrations of total hydrolysable amino acids (THAA) in anoxic rapidly accumulating sediments in an organic-rich coastal marine basin (Cape Lookout Bight, USA), and showed that they exhibited an exponential decrease with depth similar to, but at a faster rate than, that for total organic carbon. The most abundant amino acids in the sediments were aspartic acid, glutamic acid, glycine and alanine, which is a similar abundance to that in the two major sources of organic matter to the region, i.e. vascular saltmarsh plants (terrestrial) and plankton (marine). Kinetic modelling of the Cape Lookout Bight data indicated that ~ 45% of the input of amino acids to the surface sediment is remineralized in the upper ~ 40 cm, which amounted to ~ 27% of the regeneration of total organic carbon. Henrichs & Farrington (1987) estimated that THAA made up ~ 11–23% of the carbon remineralized in sediments from Buzzards Bay, USA. It may be concluded, therefore, that the mineralization of amino acids plays an important role in the regeneration of total organic carbon in nearshore sediments.

On the basis of their data, Burdige & Martens (1988) proposed a general model to describe the major processes involved in the early diagenesis of amino acids in anoxic sediments. The principal features in this model, which is illustrated in Figure 14.1, can be summarized as follows.

(a) Amino acids initially deposited in marine sediments can usually be divided into two fractions, a labile (or metabolizable) fraction, contained in proteinaceous material, and a refractory fraction, which is degraded at rates significantly slower than those at which the labile amino acids are remineralized.
(b) The decrease in the concentrations of THAA with depth is assumed to be related to the microbial utilization of the labile amino acid fraction, to produce pore-water dissolved free and dissolved combined amino acids.
(c) Individual dissolved free amino acids are metabolized to yield ammonium, methane and/or ΣCO_2 by sulphate reducers, methanogens and/or fermentative bacteria.
(d) Although the pore-water amino acids may act as intermediates in the remineralization of hydrolysable amino acids in anoxic sediments, they can also be involved in non-biological reactions (e.g. adsorption), which may result in the reincorporation of the amino acids back into the sediments as humic and/or fulvic acids, i.e. the process of geopolymerization (or humification) identified above.

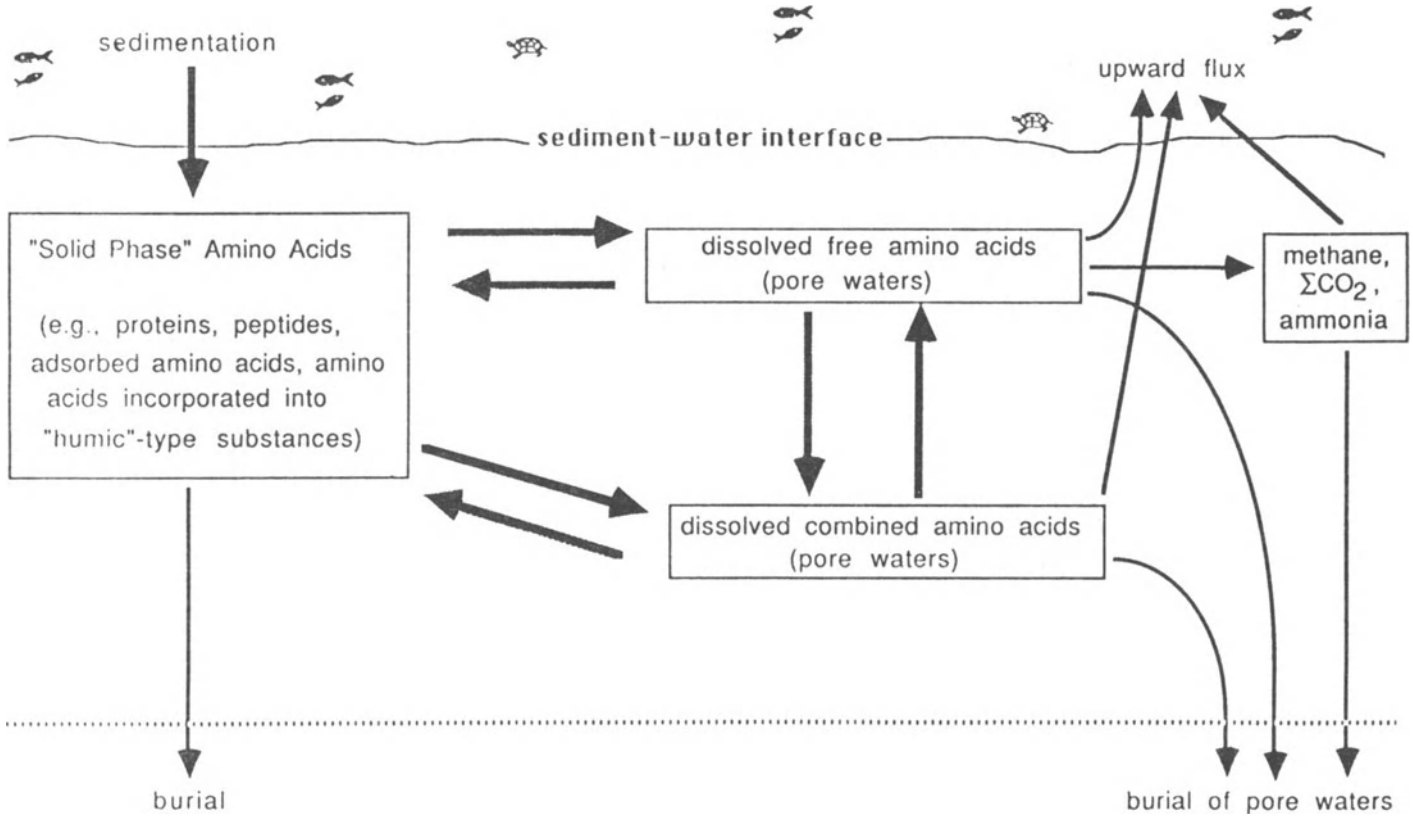

Figure 14.1 A model for the diagenesis of amino acids in anoxic marine sediments (from Burdige & Martens 1988).

Conditions can exist, however, under which the hydrolysable organic fraction does not decrease significantly with depth in the sediments. For example, Steinberg *et al.* (1987) determined amino acids and carbohydrates in recent sediments in a 'mud patch' region for the continental margin off the coast of southern New England (USA) as part of the Shelf Edge Exchange Program (SEEP) – for a full description of the various aspects of this programme see *Continental Shelf Research*, Vol. 8, 1988. An example of the amino acids found in the upper portion of one of the SEEP sediments is illustrated in Figure 14.2, showing the dominance of glycine in the sample. The total amino acid composition of the five 'mud patch' samples was similar, and there was very little decrease in their concentrations with depth in the cores. The authors suggested that this lack of a depth gradient could arise because only refractory material has reached the sediment and/or because bioturbation and resuspension have homogenized the upper sections of the cores. The study also indicated that in the SEEP region there was a considerable transport of sediment from the continental shelf to the continental slope and rise.

The overall effect of diagenesis in many marine sediments is to transform protein, carbohydrate and lignin biopolymers into geopolymers, the end-product being the formation of kerogen. However, in addition to kerogen, sediments contain an organic matter fraction that has suffered

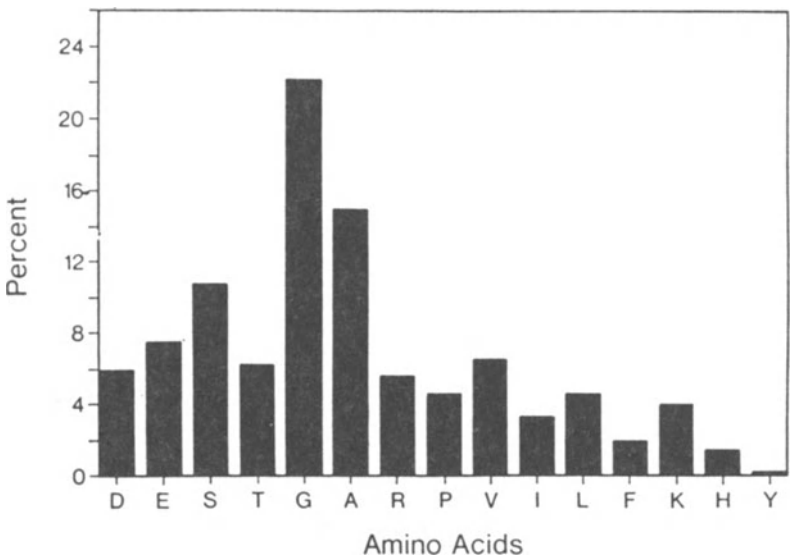

Figure 14.2 The amino acid composition of a surface sediment from the continental margin off southern New England, USA (from Steinberg *et al.* 1987). D, aspartic acid; E, glutamic acid; S, serine; T, threonine; G, glycine; A, alanine; R, arginine; P, proline; V, valine; L, leucine; I, isoleucine; F, phenylalanine; K, lysine; H, histidine; Y, tyrosine. Note the dominance of glycine in the sample.

only minor degradation. This fraction originates from high-molecular-weight lipids, including hydrocarbons, and since these molecules retain their carbon skeleton they are often termed **geochemical fossils** or **biological markers**. The n-alkanes are among the least reactive of the organic compounds, and will serve as an example of a geochemical fossil.

The n-alkanes make up the major fraction of the lipid hydrocarbons in surficial sediments, and they can have a number of origins. These include: (a) direct inputs from terrestrial, anthropogenic or marine sources; (b) diagenetic formation (e.g. from the post-depositional reduction of fatty acids); and (c) migration from deep sources. There are a number of ways in which the sources of the n-alkanes can be evaluated. The n-alkane distribution pattern in immature marine sediments is commonly characterized by the predominance of odd-carbon-number, high-molecular-weight homologues (C_{25}–C_{33}), which are typical of higher plant waxes, over light alkanes in the range C_{15}–C_{23}, which are typical of the product of marine autochthonous production, thus indicating a significant terrestrial contribution. In addition, Grimalt & Albaiges (1987) have shown that the occurrence of C_{12}–C_{22} homologues, with a strong even-carbon-number preference, is widespread in freshwater and marine sediments formed under both oxic and anoxic conditions. The authors concluded that these n-alkanes are most likely to have originated from a variety of autochthonous biological sources (e.g. micro-organisms), rather than from diagenetic processes.

According to Simoniet (1978), marine sediments found close to the continents contain n-alkanes from both terrestrial and marine sources (with terrestrial components being dominant where the continental input is strong, and marine components dominating under areas of intense primary production), whereas sediments from deep-sea regions contain n-alkanes derived predominantly from marine sources. Marine sediments from two contrasting regions provide an example of how various environmental factors act to control the origin of n-alkanes.

(a) In the SEEP region off the coast of New England (USA) the n-alkanes in the sediments are dominated by those in the range C_{21}–C_{31}, with a maximum at C_{29}, indicating a terrestrial source, and plankton-derived n-alkanes were present in only small amounts (Venkatesan *et al.* 1988).

(b) Antarctica is generally free from pollution (anthropogenic sources), and the land surface does not have a vegetative cover (terrestrial sources). However, the waters around Antarctica are highly productive, and Venkatesan & Kaplan (1987) showed that the n-alkanes (and other lipid components) in sediments from the Bransfield Strait in the Antarctic were derived principally from marine autochthonous sources.

Despite their distance from land, many deep-sea sediments do contain some terrestrially derived n-alkanes, and in this respect atmospheric transport provides a potentially important pathway for the delivery of terrestrial organics, including n-alkanes, to sediments in open-ocean regions. For example, Gagosian (1986) was able to show that at remote North and South Pacific sites the hydrocarbons in aerosols had a clear terrestrial (plant wax) signature, indicating long-range transport from the land masses. On the basis of flux data, Gagosian *et al.* (1987) concluded that atmospheric transport could have a major impact on the terrestrially derived lipid material found in deep-sea sediments. Other 'biomarkers' that have been employed for source identification in aerosols include fatty alcohols, sterols and wax esters.

Considerable advances have been made to our understanding of the long-range transport of organic material to the oceans from data produced in the SEAREX Programme. As part of this programme, a variety of organic source markers, selected to provide information on marine versus terrestrial sources, were determined in aerosols collected over the Pacific Ocean. Background aerosols from continental and coastal marine regions are dominated by a variety of biogenic lipids, and a number of these were determined in aerosols and rain samples from stations in the SEAREX network. Five compound classes of source markers were analysed in the SEAREX samples: n-alkanes, C_{23}–C_{35} (terrestrial sources); fatty alcohols, C_{21}–C_{36} (terrestrial source) and C_{13}–C_{20} (marine source); fatty acid salts, C_{19}–C_{36} (terrestrial source) and C_{13}–C_{18} (marine source). The data on these compounds have been reported by Gagosian & Peltzer (1986) and Peltzer & Gagosian (1989), and some of the principal findings are summarized below.

(a) Over the Pacific, the concentrations of the terrestrially derived and the marine-derived compounds varied independently.
(b) **Terrestrially-derived compounds**. The n-alkanes and the C_{21}–C_{36} fatty alcohols were the most abundant of these compounds, which is consistent with their predominance in the epicuticular waxes of vascular plants. In contrast, the long-chain fatty acids, which are only minor constituents of the plant waxes, were present at lower concentrations in the aerosols. There were considerable variations in the concentrations of the terrestrially derived lipids both at individual sites and between sites. However, there was an overall trend for the concentrations to be highest in mid-latitudes and lowest in the tropics.
(c) **Marine-derived compounds**. C_{13}–C_{18} fatty acid salts were the most abundant of these compounds at all the sites, with the C_{13}–C_{20} fatty alcohols being typically the least abundant of all the lipid compounds.
(d) When the various lipid homologue distributions were related to long-

range air mass trajectory analyses, a significant pattern of *regional* source marker relationships was found. For example, at Enewetak, a remote site in the North Pacific, there was a difference in the fatty alcohol distributions in aerosols collected in the dry–high dust and wet–low dust seasons. For the dry season the major homologue was C_{28} and for the wet season it was C_{30}, a difference that is indicative of a change in climate of the source regions with plants growing in tropical climates having higher-molecular-weight homologues in their epicuticular waxes than those from temperate or sub-arctic climates.

(e) The SEAREX study also highlighted the importance of transformations that affect organic material in the marine atmosphere. For example, unsaturated fatty acids, which are characteristic of marine organisms, were absent from the atmospheric samples; however, their photochemical oxidation products were identified as a major class of organic compounds in both aerosols and rain water.

(f) The total lipid content of the background marine aerosol over the Pacific was 2–20 ng m^{-3} of air.

(g) The major fluxes of the atmospherically transported organic material to the sea surface resulted from wet rather than dry deposition processes.

(h) There was evidence that some biogenic terrestrial material is protected from degradation in the marine environment to a greater extent than marine-derived material. This probably arises because the refractory terrestrial organics are protected by wax coatings and have already undergone significant degradation before reaching the sea surface.

It may be concluded, therefore, that the diagenetic preservation – destruction of organic matter in marine sediments proceeds along two general pathways, which lead to the formation of two organic fractions.

(a) **Fraction 1**. Protein, carbohydrate and lignin biopolymers are transformed into geopolymers, the end-product being the formation of the kerogen fraction.

(b) **Fraction 2**. This fraction originates from high-molecular-weight lipids, including hydrocarbons, which are retained in the sediment with only minor modification.

However, the distinction between two such fractions in sediments is far from clear, and it is apparent that, for example, lipids are incorporated into kerogen at an early stage of diagenesis (G. Wolff personal communication).

In the diagenetic zone of recent marine sediments the hydrocarbons consist of biogenic methane and lipid hydrocarbons. At greater depth of

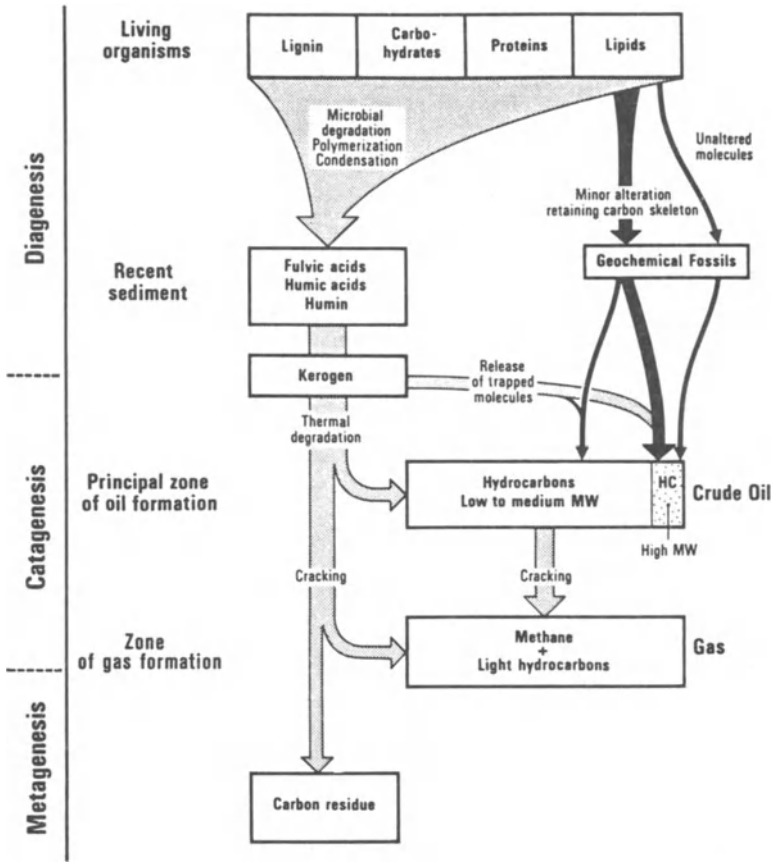

Figure 14.3 Stages in the diagenesis, catagenesis and metagenesis of organic matter in sediments (from Tissot & Welte 1984).

14.2.2 The diagenetic sequence

Diagenetic processes in sediments are driven by redox reactions that are mediated by the decomposition of organic carbon, and some of the basic concepts involved in sedimentary redox processes are described in Worksheet 14.1.

It is now generally recognized that there is a diagenetic sequence of catabolic processes in sediments, the nature of which depends on the particular oxidizing agent that 'burns' the organic matter. As sedimentary organic matter is metabolized it donates electrons to several oxidized components in the interstitial water–sediment complex, and when oxygen is present it is the preferred electron acceptor. However, during the diagenetic sequence the terminal electron-accepting species alter as the

burial, as the temperature increases, catagenesis follows diagenesis and at an early stage low- to medium-molecular-weight geogenetic hydrocarbons are generated from the thermal breakdown of kerogen, which involves the cracking of large molecules to yield small molecules, to form crude oil. In the zone of catagenesis, which is also the principal zone of petroleum formation, there are therefore two types of hydrocarbons, those which are 'directly inherited' and those which are 'newly formed' from kerogen. Tissot & Welte (1984) addressed the question of which of these two types of hydrocarbons is the principal source for petroleum. They concluded that although hydrocarbons that are directly inherited from organisms are found in crude oils, the bulk of the hydrocarbons in the oils have been newly formed at depth from the thermal degradation of kerogen. At a later stage in catagenesis, both the remaining kerogen and the previously formed oil undergo an increased cracking of carbon–carbon bonds, which leads to the formation of light hydrocarbons and methane (Simoniet 1978).

At still greater depths of burial in the sediment column the deposits enter the zone of metagenesis. Here, both the temperature and the pressure are greatly increased and the organic matter consists of methane and a carbon residue.

The various stages in the diagenesis–catagenesis–metagenesis sequence are illustrated in Figure 14.3.

We have now taken a very broad overview of the general processes that affect organic matter following its deposition to the sediment surface. We must now return to look in more detail at the fate of organic matter during early diagenesis.

14.2 Early diagenesis in marine sediments

14.2.1 Introduction

Many of the chemical changes that take place during early diagenesis are redox-mediated, i.e. they depend on the redox environment in the sediment–interstitial water–sea water system. In turn, this redox environment is largely controlled by the degree to which organic carbon is preserved, or undergoes decomposition, in the sediment complex. Most marine environments are oxic, and as a result $\gtrsim 90\%$ of the organic carbon that reaches the deep-sea floor via the particle flux is oxidized close to the sediment/water interface. This process occurs largely via catabolic microbial reactions that are involved in the breakdown of organic molecules to simple molecules or inorganic species. Berner (1980) has derived equations to describe diagenesis and these are given in Worksheet 14.4 in the context of the diagenesis of Mn in marine sediments.

WORKSHEET 14.1
REDOX REACTIONS IN SEDIMENTS

Aqueous solutions do not contain free protons and free electrons. However, according to Stumm & Morgan (1981) it is possible to define the relative proton and electron activities in these solutions. Acid–base processes involve the transfer of protons, and pH, which can be written

$$pH = -\log_{10} a_{H+} \tag{1}$$

measures the relative tendency of a solution to accept or transfer protons. The activity of a hypothetical hydrogen ion is high at low pH and low at high pH, and pH is a master variable in acid–base equilibria.

In a similar manner, it is also possible to define a convenient parameter to describe redox intensity. Redox reactions involve the transfer of electrons, and pe, which can be written

$$pe = -\log_{10} a_{e-} , \tag{2}$$

measures the relative tendency of a solution to accept or transfer electrons. A high pe indicates a relatively high tendency for oxidation, and pe is a master variable in redox equilibria.

An oxidation–reduction reaction is termed a *redox* reaction, and can be written as two half-reactions in which a reduction is accompanied by an oxidation in terms of a redox couple. To illustrate this, Drever (1982) used the reduction of Fe^{3+} by organic matter, represented by (C). Thus:

$$4\ Fe^{3+} + (C) + 2\ H_2O \rightarrow 4\ Fe^{2+} + CO_2 + 4\ H^+ . \tag{3}$$

In this equation neither molecular oxygen nor electrons are shown explicity. The equation can be broken down into two half-reactions, one involving only Fe and the other only C. Thus:

$$4\ Fe^{3+} + 4\ e^- \rightarrow 4\ Fe^{2+} \tag{4}$$

in which Fe^{3+} undergoes reduction to Fe^{2+}, and

$$(C) + 2\ H_2O \rightarrow CO_2 + 4\ H^+ + 4\ e^- \tag{5}$$

in which the organic matter undergoes oxidative destruction to yield CO_2. It must be remembered, however, that these do not represent complete chemical reactions since aqueous solutions do not contain free electrons.

The half-reaction concept can be related to measurements in electrochemical half-cells, and allows another parameter to be introduced into redox chemistry. This parameter is E_h, in which the electron activity is expressed in volts, the h subscript indicating that the E_h value is expressed relative to the standard hydrogen electrode, which is used as a zero reference. The relative activity of electrons in a solution can therefore be expressed in units of electron activity (pe), which is a dimensionless

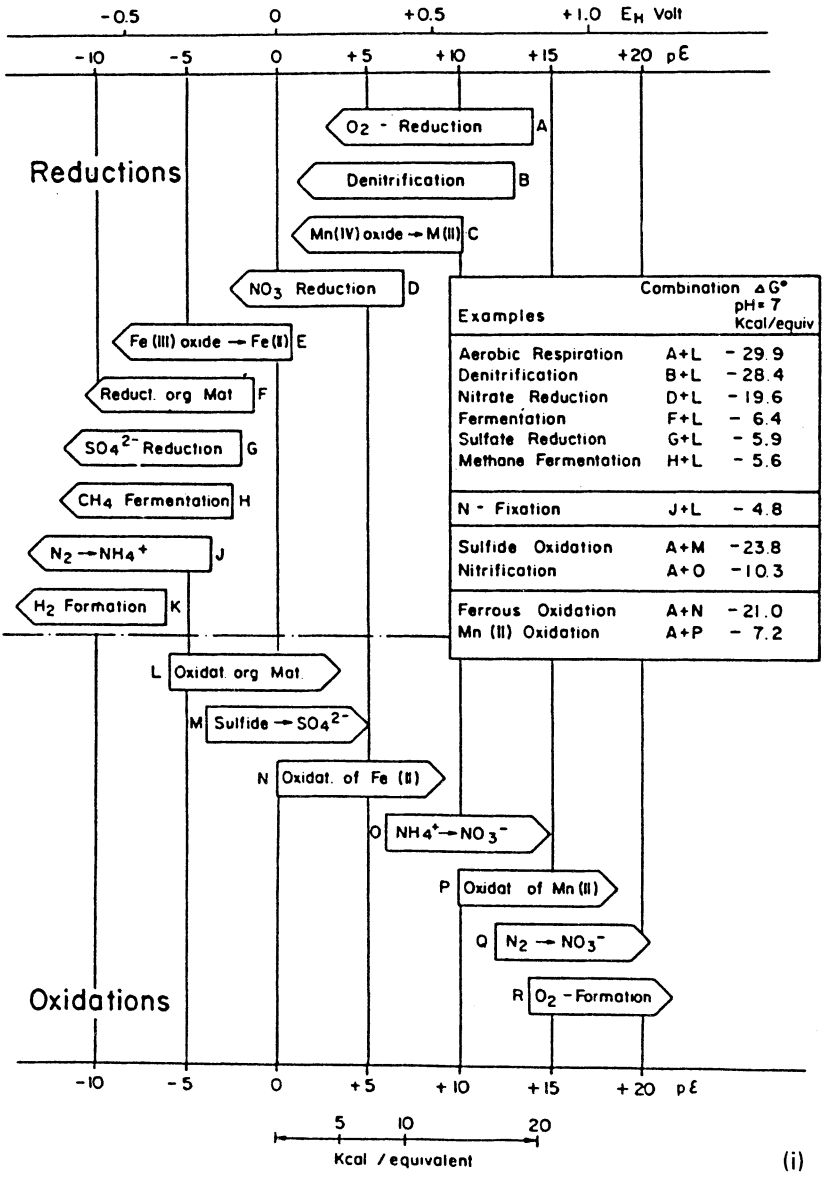

Figure (i) The microbially mediated diagenetic sequence in sediments (from Stumm & Morgan 1981).

quantity, or in volts (E_h), and the relation between pe and E_h is given by:

$$pe = \frac{F}{2.3RT} E_h \quad (6)$$

where F is Faraday's constant, R is the gas constant and T is the absolute temperature; at 25°C $E_h = 0.059pe$. Electrode-measured E_h values in oxidizing natural waters are difficult to relate to a specific redox pair, and both Stumm & Morgan (1981) and Drever (1982) have pointed out that it is important to distinguish between electrode-measured E_h and E_h calculated from the activities of a redox pair.

In the present text the general concept of *redox conditions* will be used, in which positive E_h (redox potential) values indicate oxidizing conditions and negative values indicate reducing conditions; i.e. half-reactions of high E_h are oxidizing, and those of low E_h are reducing. Thus, a half-reaction with a lower E_h will undergo oxidation when combined with a half-reaction of higher E_h. This reaction combination can be used to describe redox-mediated diagenetic reactions in sediments.

E_h conditions in sediments are controlled mainly by the decomposition of photosynthetically produced organic matter by non-photosynthetic bacteria, and are constrained by the rate of supply of the organic matter (primary production) and the rate at which it accumulates (sedimentation rate). This bacterial decomposition of organic mater is driven by a sequence of reactions that switch to a successive series of oxidants, or electron acceptors, which represent lower pe levels. During the reaction sequence, in which the organic matter is decomposed by micro-organisms, the organisms acquire energy for their metabolic requirements.

Only a relatively few elements (C, N, O, S, Fe and Mn) are predominant participants in aquatic redox processes. The overall relationships that involve these elements in the microbially mediated redox sequence have been summarized diagrammatically by Stumm & Morgan (1981); their scheme is reproduced in Figure (i) in which the energy yields associated with the various processes in the diagenetic sequence are given in the form of reaction combinations which are initiated at various E_h and pe values. For example, the first stage in the sequence involves the oxidation of organic matter by dissolved oxygen (A + L), with successive reactions following the decreased pe and E_h levels. The full 'diagenetic sequence', and the sedimentary environments associated with the various stages in the sequence, are discussed in detail in the text. Examples of the diagenetic succession are given in the box, in Figure (i), from which it can be seen, for example, that there is a tendency for the more energy-yielding reactions to take precedence over those which are less energy-yielding. Thus, the sequence begins with aerobic respiration (A + L), followed by denitrification (B + L), etc.

oxidants are consumed in order of decreasing energy production per mole of organic carbon oxidized. Thus, as oxygen is exhausted, microbial organisms switch to a succession of alternative terminal electron acceptors in order of decreasing thermodynamic advantage (see e.g. Froelich *et al.* 1979, Kahnke *et al.* 1982, Galoway & Bender 1982, Wilson *et al.* 1985). Using the schemes outlined by, among others, Froelich *et al.* (1979) and Berner (1980), the general **diagenetic sequence** in marine sediments can be outlined in the following general way.

AEROBIC METABOLISM Aerobic organisms can use **dissolved oxygen** from the overlying or interstitial waters to 'burn' organic matter. The organic matter that undergoes early diagenesis can be considered to have the Redfield composition (see Sec. 9.2.3.1), i.e. $(CH_2O)_{106}(NH_3)_{16}(H_3PO_4)$. The oxidation of organic matter by aerobic organisms can therefore be represented by a general equation such as that proposed by Galoway & Bender (1982):

$$5\ (CH_2O)_{106}(NH_3)_{16}(H_3PO_4) + 690\ O_2 \rightarrow 530\ CO_2 + 80\ HNO_3 + 5\ H_3PO_4 + 610\ H_2O. \qquad (14.1)$$

The CO_2 released during this reaction can lead to carbonate dissolution, and the ammonia can be oxidized to nitrate, a process termed **nitrification**. Under oxic conditions most of the remains of dead animals and plankton are apparently destroyed at this stage in the diagenetic sequence. For example, according to Bender & Heggie (1984), > 90% of the organic carbon that reaches the deep-sea floor is oxidized by O_2. Oxygen may therefore be regarded as he *primary* oxidant involved in the destruction of organic matter, and in a closed system reaction 14.1 (**oxic diagenesis**) will continue until sufficient oxygen has been consumed to drive the redox potential low enough to favour the next most efficient oxidant. Thus, as dissolved oxygen becomes depleted, organic matter decomposition can continue using O_2 from *secondary* oxidant sources (**sub-oxic diagenesis**).

ANAEROBIC METABOLISM Anaerobic metabolism takes over when the content of dissolved oxygen falls to very low levels, or becomes entirely exhausted, and a series of secondary oxidants are utilized. These secondary oxidants include nitrate, MnO_2, Fe_2O_3 and sulphate.

(a) **Nitrate**. According to Berner (1980), when the dissolved oxygen levels fall to ~ 5% of their concentration in aerated waters the decomposition of organic matter can occur using oxygen from nitrate, a reaction that can be represented as follows:

$$5\ (CH_2O)_{106}(NH_3)_{16}(H_3PO_4) + 472\ HNO_3 \rightarrow 276\ N_2 + 520\ CO_2 + 5\ H_3PO_4 + 886\ H_2O. \qquad (14.2a)$$

This process is termed **denitrification**. In the reaction given above it is assumed that all organic nitrogen released is in the form of ammonia, which is then oxidized to molecular nitrogen by the reaction:

$$5\ NH_3 + 3\ HNO_3 \rightarrow 4\ N_2 + 9\ H_2O. \qquad (14.2b)$$

However, this is not the only possible pathway, and Froelich *et al.* (1979) have pointed out that the fate of the nitrogen has important consequences in diagenesis with respect to the sequence in which the secondary oxidants are used. These authors suggested that if all the nitrogen goes to N_2 then the use of nitrate as a secondary oxidant overlaps with that of MnO_2, but that if the nitrogen is released as ammonia and is not oxidized to N_2 then MnO_2 is apparently reduced before nitrate.

The use of the other secondary oxidants can be illustrated by reactions of the type described by Froelich *et al.* (1979).

(b) **Manganese oxides**

$$(CH_2O)_{106}(NH_3)_{16}(H_3PO_4) + 236\ MnO_2 + 472\ H^+ \rightarrow 236\ Mn^{2+} + 106\ CO_2 + 8\ N_2 + H_3PO_4 + 336\ H_2. \quad (14.3)$$

(c) **Iron oxides**

$$(CH_2O)_{106}(NH_3)_{16}(H_3PO_4) + 212\ Fe_2O_3 + 848\ H^+ \rightarrow 424\ Fe^{2+} + 106\ CO_2 + 16\ NH_3 + H_3PO_4 + 530\ H_2O. \quad (14.4)$$

(d) **Sulphate**

$$(CH_2O)_{106}(NH_3)_{16}(H_3PO_4) + 55\ SO_4 \rightarrow 106\ CO_2 + 16\ NH_3 + 55\ S^{2-} + H_3PO_4 + 106\ H_2O. \quad (14.5)$$

(e) Following sulphate reduction, biogenic methane can be formed by two possible reaction pathways, which may be generalized as:

$$CH_3COOH \rightarrow CH_4 + CO_2 \quad \text{acetic acid formation} \quad (14.6a)$$

or

$$CO_2 + 8\ H_2 \rightarrow CH_4 + 2\ H_2O \quad CO_2 \text{ reduction.} \quad (14.6b)$$

Thus, diagenesis proceeds in a general sequence in which the oxidants are utilized in the order: oxygen > nitrate ≥ manganese oxides > iron oxides > sulphate. In this diagenetic sequence it is assumed that in marine sediments O_2, NO_3^-, MnO_2, Fe_2O_3 (or FeOOH) and SO_4^{2-} are the only electron acceptors, and that organic matter (represented by the Redfield composition) is the only electron donor. Furthermore, it is assumed that the oxidants are limiting, i.e. each reaction proceeds to completion before the next one starts. However, the diagenetic processes are not always sequential; for example, although it is usually thought that sulphate reduction precedes methane formation, Oremland & Taylor

(1978) believe that the two processes can occur simultaneously, i.e. they are not mutually exclusive.

The rates at which a number of bioactive components are buried tracks surface water productivity, and for organic carbon the burial is enhanced by low bottom water oxygen concentrations. It is now thought that about half of the organic carbon reaching the sea bed is highly labile and is degraded at the sediment surface within a few months (Smith & Baldwin 1984), the remainder, which is more refractory, being degraded over a few decades (Emmerson & Dymond 1984). To put the importance of the various sequential diagenetic processes in context, Bender & Heggie (1984) concluded that $\lesssim 10\%$ of the organic carbon flux in deep-sea sediments is oxidized by the secondary oxidants, the vast majority being oxidized by dissolved oxygen at the sediment surface. However, the secondary oxidants are involved in the destruction of a large fraction of the organic matter that does escape the primary oxidation, and therefore although they are relatively unimportant in the recycling of organic matter at the sea floor, they are critical in regulating the burial of organic matter in the sediments themselves.

14.2.3 Diagenetic environments

As diagenesis proceeds a number of end-member sedimentary environments are set up, which Berner (1980) was able to relate to a **diagnetic zone** sequence.

(1) **Oxic** environments are those in which the interstitial waters of the sediments contain measurable dissolved oxygen, and diagenesis occurs via aerobic metabolism. Under these conditions little organic matter is preserved in the sediments, and in terms of the reactions given above the diagenetic sequence has proceeded only to reaction 14.1 in oxic environments.

(2) **Anoxic** environments are those in which the sediment interstitial waters contain no measurable dissolved oxygen, i.e. diagenesis here has to proceed via the secondary oxidants through anaerobic metabolism. The anoxic environments were subdivided into a number of types.

(2.1) **Non-sulphidic post-oxic** environments. These environments, which contain no measurable dissolved sulphides, are common in many deep-sea sediments, and are perhaps more often referred to in the literature as **sub-oxic** environments. The condition necessary to set up this type of sedimentary environment is a supply of organic carbon sufficient that diagenesis can proceed beyond the oxic stage. Under these conditions, nitrate, manganese oxides and iron oxides are used as secondary oxidants, but the sequence does not reach the stage at which sulphate is utilized for this purpose. In sub-oxic

sediments, therefore, there is a relatively large, but still limited, supply of metabolizable organic matter, and the diagenetic sequence has proceeded to reactions 14.2–14.4 given above.

(2.2) **Sulphidic** environments. These result when the diagenetic sequence has reached the stage at which the bacterial reduction of dissolved sulphate takes place with the production of H_2S and HS^-. If a sufficient supply of metabolizable organic matter is available, sulphate reduction can be a common feature in marine sediments as a result of the relatively high concentration of sulphate in both sea water and marine sediment interstitial waters. In practice, however, constraints on the supply and preservation of organic matter mean that sulphate reduction is largely restricted to nearshore sediments. In sulphate environments the diagenetic sequence has now proceeded to reaction 14.5.

(2.3) **Non-sulphidic methanic** environments. In some sediments that contain a relatively large amount of metabolizable organic matter the diagenetic reactions can pass through the stage at which oxygen, nitrate, manganese oxides, iron oxides and sulphate are sequentially utilized. Continued decomposition of organic matter results in the formation of dissolved methane, e.g. by reactions 14.6a and 14.6b.

The general diagenetic sequence outlined earlier, in which the various oxidants are consumed in the order oxygen > nitrate ≥ manganese oxides > iron oxides > sulphate, leads therefore to the setting up of a series of diagenetic zones in sediments. The sedimentary environments associated with these zones give rise to an environmental succession and, depending on the amount of available organic matter, any sediment can pass through each of these environments during deposition and burial (Berner 1981). This happens in the general order oxic → anoxic non-sulphidic (sub-oxic) → anoxic sulphidic → anoxic non-sulphidic (methanic), and sets up a *vertical* diagenetic zone sequence in sediments. The determining factors controlling the extent to which the **diagenetic zone sequence** proceeds are the magnitude of the flux of organic matter to the site of deposition (which is dependent on the degree of primary production in the overlying waters) and the rate at which the sediment accumulates; together, these two factors largely determine the amount of organic carbon preserved in a sediment, and thus the extent to which it is available to consume the various oxidants.

14.3 Organic matter in sediments

The extent to which organic matter is preserved in a sediment is critical in determining how far the diagenetic sequence progresses. However, there

are considerable variations in the organic matter content of marine sediments, and these are described below in terms of their depositional environments.

NEARSHORE SEDIMENTS These deposits, which accumulate at relatively fast rates, usually contain ~ 1–5% organic carbon, but the concentrations can be considerably higher in sediments deposited in anoxic basins and under areas of high primary production; for example, Calvert & Price (1970) reported that organic-rich diatomaceous muds on the Namibian shelf contained up to ~ 25% organic carbon.

DEEP-SEA SEDIMENTS Heath *et al.* (1977) carried out a survey of the distribution of organic carbon in deep-sea sediments, and showed that its concentrations vary from ~ 5% in reduced hemi-pelagic sediments deposited close to the continental margins to $\lesssim 0.1\%$ in most oxic pelagic (red) clays. There was a general correlation between the organic carbon content and the accumulation rate of a sediment, and a regression line obtained from a log–log plot of organic carbon accumulation rate versus sedimentation rate yielded the relationship (organic carbon accumulation rate) = $0.01(\text{sedimentation rate})^{1.4}$.

14.4 Redox environments and diagenesis in marine sediments

14.4.1 Redox environments

Truly anoxic waters, where sediments are *initially* deposited under anoxic conditions, prevail over only a small area of the oceans (see Sec. 8.3). The vast majority of environments at the sea floor are therefore oxidizing, and there is usually a layer of oxic material at the sediment surface. However, as a result of the consumption of the dissolved oxygen in the interstitial waters, the sediments can become reducing, and ultimately anoxic, at depth as the diagenetic sequence proceeds and the oxic/anoxic, or redox, boundary is an extremely important chemical feature. The depth at which the oxic/anoxic change occurs depends largely on a combination of the magnitude of the down-column carbon flux, by which the carbon is *supplied*, and the sediment accumulation rate, by which it is *buried*. For example, according to Muller & Mangini (1980) a bulk sedimentation rate of $\lesssim$ 1–4 cm/10^3 yr is necessary for the deposition of an oxygenated sedimentary column. Thus, the thickness of the surface sediment oxic layer will tend to increase from nearshore to pelagic regions as the accumulation rate decreases. An example of how the thickness of the oxic surface layer in deep-sea sediments varies have been provided by Lyle (1983) for a series of hemi-pelagic deposits from the eastern Pacific. The **redox boundary**, which is indicative of the change

between oxidizing (positive redox potential) and reducing (negative redox potential) conditions in sediments is often accompanied by a colour change, which is generally from red-brown (oxidized) to grey-green (reduced). The depth of the colour transition in the sediments from the eastern tropical Pacific is illustrated in Figure 14.4, and Lyle (1983) was able to identify a number of general features in the distribution of the brown oxic surface layer which can be qualitatively related to primary productivity in the overlying euphotic layer. For example, a very thin brown layer (< 2 cm) is found (a) on the continental margin, where upwelling results in a high surface productivity, and (b) in a westward-extending tongue around the Equator, which lies below the zone of equatorial upwelling. In contrast, the tongue of sediment having a brown layer > 1 m in thickness at ~ 5°N results from the transport of low productive surface water into the area by the North Equatorial Countercurrent.

It is apparent, therefore, that there are a range of redox environments in marine sediments, which can be expressed, on the basis of the increasing thickness of the surface oxic layer, in the following general sequence.

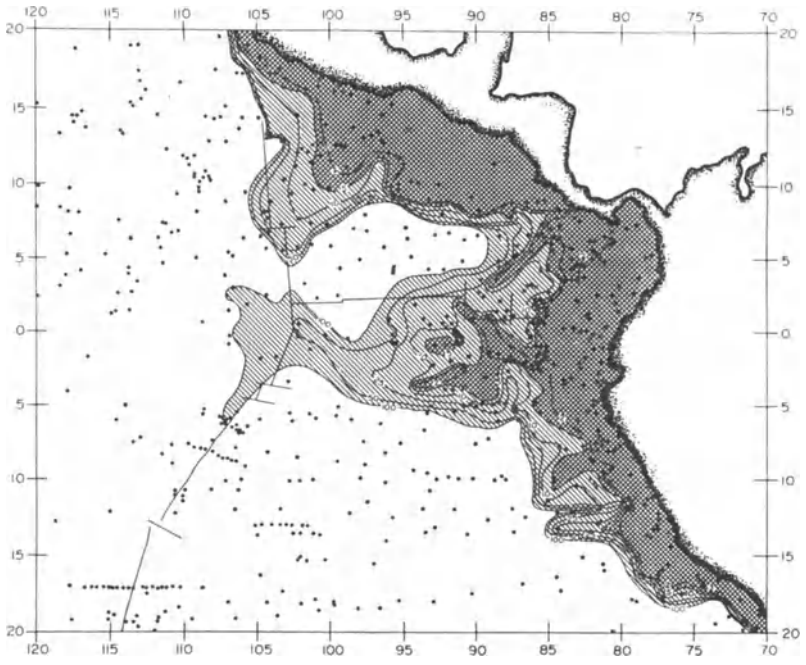

Figure 14.4 Variations in the thickness (in cm) of the surface oxic layer in sediments from the eastern Pacific (from Lyle 1983).

(a) **Anoxic sediments**. These are usually found in coastal areas, or in isolated basins and deep-sea trenches. They have organic carbon contents in the range ~ 5 to $\gtrsim 10\%$, and are reducing throughout the sediment column if the redox boundary is found in the overlying waters.
(b) **Nearshore sediments**. These sediments, which usually have organic carbon contents of $\lesssim 5\%$, accumulate at a relatively fast rate and become anoxic at shallow depths so that the brown oxic layer is usually no more than a few centimetres in thickness.
(c) **Hemi-pelagic sediments**. These have intermediate sedimentation rates, and organic carbon contents that are typically around 2%. The thickness of the oxic layer in these deposits ranges from a few centimetres up to around a metre.
(d) **Pelagic sediments**. These are deposited at very slow rates and have organic carbon contents that are usually only ~ 0.1–0.2%. In these sediments the oxic layer extends to depths well below one metre, and often to several tens of metres.

14.4.2 Diagenesis in marine sediments

It was pointed out above that early diagenesis in sediments follows a *vertical* zone sequence. On the basis of the premise that the total metabolic activity within the upper layers of marine sediments depends on the supply of organic carbon, and the rate at which it is preserved, it is apparent that there is also a *lateral*, i.e. nearshore → hemi-pelagic → pelagic, diagenetic zone sequence. In a general sense, therefore, diagenesis in marine sediments can be interpreted in terms of (a) depths in the sediment and (b) distance of the sediment from shore. Diagenesis in the various sedimentary environments found in this lateral sequence is considered below.

DIAGENESIS IN NEARSHORE SEDIMENTS In terms of the lateral sequence the extreme nearshore diagenetic environment is represented by the anoxic sediment end-member. Although anoxic waters are rare, they are a very special diagenetic environment because the sediments associated with them actually deposited under anoxic conditions, rather than becoming anoxic at shallow depths, and the oxic/anoxic boundary can occur in the water column above the sediments (e.g. in parts of the Black Sea), which sets up a specialized water chemistry. Anoxic conditions can also be set up in deep-sea trenches. In the sediments deposited in these anoxic environments diagenesis can progress through all the stages of the vertical sequence outlined above to reach the methanic stage. For example, methane, which is a terminal product of the anaerobic degradation of organic matter, can be generated in anoxic sediments found in both deep-sea trenches (e.g. the Cariaco Trench) and in nearshore regions (e.g. in

Sannich Inlet, British Columbia). In other types of nearshore sediments that are not deposited under an anoxic or intermittently anoxic water column, the extent to which the reactions involved in early diagenesis proceed is dependent on local environmental conditions. For example, diagenesis can be affected by factors such as bioturbation and bottom stirring, which tend to be unimportant in anoxic regions where there is usually an absence of both benthic fauna and erosive currents. A characteristic feature of many nearshore muds is that the surface oxic layer is very thin, and in the anoxic sediments below diagenesis often progresses to the sulphate reduction stage. Both anoxic and normal nearshore sediments contain a wide variety of authigenic minerals. These include iron sulphides, such as the polysulphide pyrite (FeS_2) and its diamorph marcasite (FeS_2); the metastable iron sulphides mackenawite and griegite; glauconite; chamosite; various carbonates (including those of iron and manganese); and iron and manganese oxides. Manganese minerals, e.g. mixed manganese carbonates, manganese sulphide (MnS), manganese phosphate ($Mn_3(PO_4)_2$), are sometimes prominent among the authigenic phases. For a detailed description of these minerals the reader is referred to Calvert (1976).

DIAGENESIS IN HEMI-PELAGIC SEDIMENTS As the thickness of the surface oxic layer increases out into open-ocean areas the extent to which the diagenetic sequence progresses decreases, and this can be traced through hemi-pelagic to truly pelagic environments. Froelich *et al.* (1979) made a study of early diagenesis in sub-oxic hemi-pelagic sediments from the eastern Equatorial Atlantic. The cores investigated typically had a light tan-coloured surface layer $\sim$ 35 cm in thickness, with a low organic carbon content (0.2–0.5%), underlain by a dark olive green terrigenous sediment, which had a higher organic carbon content ($\sim$ 0.5 to $>$ 1%). The authors gave data on a number of constituents in the interstitial waters of the sediments, and their findings can be summarized as follows.

(a) Dissolved nitrate concentrations increased from those of the ambient bottom water to a maximum, then decreased linearly to approach zero at approximately the depth of the tan–olive green lithological transition.
(b) Dissolved Mn^{2+} concentrations were very low at the surface but began to increase at a depth lying between the nitrate maximum and the nitrate zero.
(c) Dissolved Fe^{2+} concentrations were under the detection limit to a depth below the nitrate zero, then began to increase.
(d) Sulphate concentrations never differed detectably from those of the ambient bottom water, i.e. there was no indication that the sediments had entered the sulphate reduction zone.

Froelich *et al.* (1979) interpreted their data in terms of the general vertical depth zone diagenetic model, which is related to the sequential use of oxidants for the destruction of organic carbon, and they were able to identify a number of distinct zones in the sediments. The sequence is illustrated in Figure 14.5, and the individual zones are described below.

(a) **Zone 1**. This is the interval over which oxygen is being consumed during the destruction of organic matter (diagenetic reaction 14.1). During this process the ammonia is oxidized to nitrate.
(b) **Zones 2 and 5**. Below the nitrate maximum, nitrate diffuses downwards, the linearity of the gradient suggesting that nitrate is

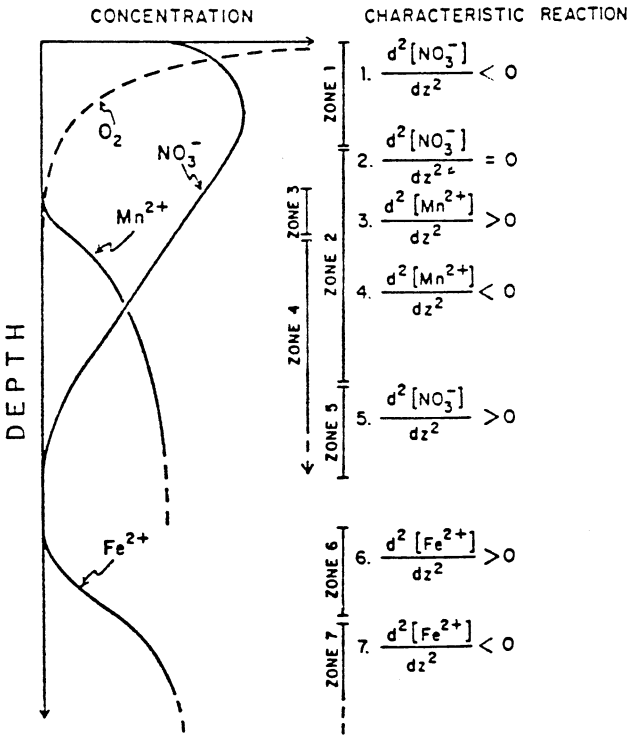

Figure 14.5 Schematic representation of diagenetic zones and trends in interstitial-water profiles during the sub-oxic diagenesis of marine sediments (from Froelich *et al.* 1979).

neither consumed nor produced in this zone. The downward diffusing nitrate is reduced by denitrification (diagenetic reaction 14.2) at the depth of the nitrate zero in zone 5.

(c) **Zones 3 and 4**. These overlap with zones 2 and 5. Zone 4 is the interval over which organic carbon is oxidized by managanese oxides (diagenetic reaction 14.3) to release dissolved Mn^{2+} into the interstitial waters. This then diffuses upwards to be oxidatively converted to solid MnO_2 at the top of the diffusion gradient in zone 3. This reduction–oxidation cycling results in the setting up of a 'sedimentary manganese trap'.

(d) **Zones 6 and 7**. Zone 7 is the region over which organic carbon oxidation takes place via oxygen formed during the reduction of ferric oxides (diagenetic reaction 14.4). Fe^{2+} is released into solution, and diffuses upwards to be consumed near the top of zone 7 and in zone 6.

This keynote investigation therefore provided clear evidence of how the diagenetic sequence operates in hemi-pelagic sediments, and demonstrates that the oxidants are, in fact, consumed in the predicted sequence, i.e. oxygen > nitrate ≃ manganese oxides > iron oxides > sulphate (although the sulphate reduction stage was not reached in these sediments).

DIAGENESIS IN PELAGIC SEDIMENTS As the thickness of the surface oxidizing layer continues to increase, the diagenetic sequence can be traced as far as the least extreme oceanic end-member. This is represented by pelagic sediments, in which the surface oxic layer can extend downwards for several tens of metres. Wilson *et al.* (1985) gave data on the interstitial water constituents of a pelagic deep-sea sediment (Station 10552) from the northeastern Atlantic which had an accumulation rate of ~ 0.42 cm/10^3 yr. The interstitial water profiles for the sediment showed that: (a) dissolved oxygen was present throughout the interval sampled (0–2 m); (b) nitrate concentrations increased downwards, i.e. there was no evidence of the consumption of nitrate as a secondary oxidant; (c) no detectable dissolved Mn^{2+} was present; and (d) there was no evidence of sulphate reduction. The diagenetic sequence in this sediment had therefore not progressed beyond the stage at which oxygen is consumed for the degradation of organic matter (diagenetic reaction 14.1), and there was little mobilization of the redox-sensitive elements.

Wilson *et al.* (1985) also provided information on the interstitial water chemistry of a mixed layer pelagic–turbidite sediment. This sediment (Station 10554) consisted of a thin (≲ 10 cm) upper light brownish grey layer of pelagic material, underlain by a turbidite sequence made up of an upper light brownish grey unit and a lower green unit. The sediment had an overall accumulation rate of ~ 10 cm/10^3 yr. The organic carbon

content was ~ 0.6% in the surface layer and rose to ~ 1.6% around the top of the green layer. The interstitial water chemistry of the sediment at this site was considerably more complex than that of the exclusively pelagic deposit at Site 10552, the major trends being as follows.

(a) Dissolved oxygen fell off rapidly with depth in a linear manner to approach zero close to the surface of the green layer.
(b) Nitrate concentrations also decreased in a continuous linear fashion, from a near-surface maximum to approach zero at a depth slightly greater than that for oxygen, although traces of both oxygen and nitrate were found in the green layer.
(c) Dissolved Mn^{2+} was found in solution below the top of the green layer.
(d) There was no evidence of sulphate reduction.

It was apparent, therefore, that in the turbidite layer of the mixed sediment the diagenetic sequence had progressed considerably further than in the pure pelagic sediment, and had in fact reached the nitrate ≃ manganese oxide reduction stage. However, the main point of interest was that there were two distinct colour units *within* the turbidite layer itself, the upper brownish grey layer, which appeared to be oxic now, and the lower green layer, which still remained anoxic. On the basis of the linearity of the dissolved interstitial water profiles of both oxygen and nitrate, and the fact that they approach zero around the top of the green layer (which is coincident with a sharp rise in the concentration of organic carbon in the sediment), Wilson *et al.* (1985) concluded that the colour change represents a **downward-moving oxidation front**, the rate of movement of which is controlled by the rates of diffusion oxygen and nitrate from the bottom water to the front itself. In terms of this concept, therefore, the upper brown turbidite layer is a zone in which the metabolizable organic carbon has already been oxidized as the front moved downwards. Under normal steady-state diagenesis, the oxic/anoxic colour change (or redox) boundary migrates *upwards* at the same rate as the sediment accumulates, so as to remain at a *constant* depth below the sediment/water interface. However, the progressive *downward* migration of the turbidite oxidation front is not a steady-state process; rather it implies that there is a continuing readjustment of the redox profile after the deposition of an organic-rich unit which was initially at the pelagic sediment surface. Almost all the diagenetic changes in the upper part of the mixed pelagic–turbidite sediment occur in two zones, one close to the sediment/water interface and one close to the top of the green layer (the migrating oxidation front). The concept of a secondary subsurface maximum in metabolic activity has important consequences, implying that even a relatively infrequent deposition of organic-rich units can have a

major effect on the redox state of the host sediment column. Thus, the differences in the redox profiles of the pelagic and mixed pelagic–turbidite deep-sea sediments are not due primarily to differences in total metabolic activity, but rather to differences in how the activity is distributed within the sediment column.

Thin trace metal-rich layers are found in a number of deep-sea sediments at, or just below, the glacial–Holocene transition, where there was a change from relatively rapid glacial sediment accumulation with reducing conditions at shallow depths to a more slowly accumulating Holocene depositional regime. The elements Mn, Ni, Co, Fe, P, V, Cu, Zn and U can be enriched in the vicinity of the layers. Wilson *et al.* (1986a, b) and Wallace *et al.* (1988) have proposed that the locus of formation of the layers is coincident with the present day oxic/post-oxic redox boundary, and can be explained in terms of the concept of a progressive oxidation front moving into the sediments following the change from glacial to interglacial conditions, with the depth of the oxidant penetration from sea water hovering around a near-fixed depth and being balanced by the reductant counterflux of Mn^{2+} and Fe^{2+} from the reducing sediments below.

Although attention in this volume is mainly concentrated on the role played by early diagenesis in present-day sediments (see Sec. 13.1), the identification of downward-migrating non-steady state diagenetic fronts associated with the deposition of turbidite sequences also has wider implications for seawater/sediment chemistry, especially from the point of view of the response of the oceans to climatic changes. For example, turbidite deposition on the Madeira Abyssal Plain may reflect global climatic changes associated with glaciations and sea level fluctuations (see e.g. Weaver & Kuijpers 1983), and thus their modification by downward-migrating digenetic fronts provides an example of how the present oceans respond to the past climatic changes. In this respect, the Atlantic Ocean may still be recovering from late Quarternary climatic changes (Wallace *et al.*, 1988; T.R.S. Wilson, Pers. Comm.).

14.5 Diagenesis: summary

(a) Early diagenesis in marine sediments follows a general pattern in which a series of oxidants are utilized for the destruction of organic carbon in the following general sequence: oxygen > nitrate ≃ manganese oxides > iron oxides > sulphate.
(b) The diagenetic sequence passes through each of the oxidant utilization stages successively in a down-column direction, thus setting up a *vertical* gradient.
(c) The extent to which the diagenetic sequence proceeds depends

largely on the rate of supply of organic carbon to the sediment surface, and the rate at which it is buried. Both of these parameters generally decrease away from the ocean margins towards the open ocean, thus setting up a *lateral* gradient in the diagenetic sequence. As a consequence of this, the diagenetic stage reached drops progressively from (i) nearshore anoxic sediments (methanic stage), to (ii) nearshore sediments having a thin oxic layer of a few millimetres (sulphate reduction stage), to (iii) hemi-pelagic deep-sea sediments having an oxic layer of a few centimetres (nitrate $\simeq$ manganese oxide, iron oxide reduction stages), to (iv) truly pelagic deep-sea sediments, in which diagenesis does not progress beyond the stage at which oxygen is consumed for organic carbon degradation.

During diagenesis elements are mobilized into solution and so can migrate through the interstitial waters. Some of these elements (together with those already present in the interstitial waters) are incorporated into newly formed or altered minerals. However, a fraction of the elements can escape capture in this way, and so be released into the overlying sea water. In the next section, therefore, the wider aspects of diagenetic mobilization will be considered in relation both to the depletion–enrichment of elements in interstitial waters and to the potential fluxes of the elements to the oceanic water column.

14.6 Interstitial-water inputs to the oceans

14.6.1 Introduction

Analyses of interstitial waters were carried out as long ago as the last century (see e.g. Murray & Irvine 1895). However, until recently data for the chemistry of interstitial water have suffered from a number of major uncertainties. According to Sayles (1979) these arise from: (a) sampling procedures, such as temperature-induced artifacts inherent in the water extraction techniques; (b) imprecise analytical techniques (especially for trace elements); and (c) a lack of detail close to the sediment/sea water interface, a region where a number of important reactions take place. Because of factors such as these, much of the early interstitial-water data must be regarded as being unreliable. In order to rectify some of these uncertainties, Sayles (1979) carried out a study of the composition of interstitial waters collected using *in situ* techniques from the upper 1–2 m of a series of sediments from the North and South Atlantic on a marginal–central ocean transect. A number of trends could be identified from the data obtained on this transect.

(a) The interstitial waters were almost always *enriched* in Na^+, Ca^{2+} and

WORKSHEET 14.2
SOME BASIC CONCEPTS RELATING TO THE BEHAVIOUR OF CHEMICAL SPECIES IN THE SEDIMENT/INTERSTITIAL WATER COMPLEX

Interstitial waters are the medium through which elements migrate during diagenetic reactions. In sediments the interstitial-water properties change very much more rapidly in the vertical than in the horizontal direction, with the result that the changes can often be described by one-dimensional models. The transport of solutes through interstitial waters takes place by convection, advection and diffusion. In the context used here *advection* refers to transport by the physical movement of the water phase, and *diffusion* refers to migration of a chemical species throught the water as a result of a gradient in its concentration (or chemical potential). Diffusion in an aqueous solution can be described mathematically by Fick's laws, which, for one dimension, may be written as follows (see e.g. Berner 1980):

(a) First law

$$J_i = D_i \frac{\partial c_i}{\partial x} \tag{1}$$

(b) Second law

$$\frac{\partial c_i}{\partial t} = D_i \frac{\partial^2 c_i}{\partial x^2} . \tag{2}$$

Here J_i is the diffusion flux of component i in mass per unit area per unit time, c_i is the concentration of component i in mass per unit volume, D_i is the diffusion coefficient of i in area per unit time, and x is the direction of maximum concentration gradient; the minus sign in the first law indicates that the flux is in the opposite direction to the concentration gradient. Fick's first law is applied to calculations that involve steady-state systems, and the second law is applied to non-steady-state systems. However, before Fick's laws can be applied directly to sediments it is necesssary to take account of the nature of the sediment–interstitial water complex. Interstitial waters are dispersed throughout a sediment and the rate of diffusion of a solute through them is less than that in water alone, i.e. as predicted by Fick's laws, because of the solids present (the porosity effect) and because the diffusion path has to move around the grains; the term *tortuosity* (θ) is used to describe the ratio of the length of the sinuous diffusion path to its straight-line distance (Berner 1980). Tortuosity is usually determined indirectly from measurements of electrical resistivity of sediments and of the interstitial waters separated from them, using the relationship

$$\theta^2 = \phi F \tag{3}$$

where ϕ is the porosity and F is the *formation factor* ($F = R/R_0$, where R is the electrical resistivity of the sediment and R_0 is the resistivity of the interstitial water alone). Formation factors in marine sediments usually appear to lie in the range ~ 1 to ~ 10, so that the *effective diffusion coefficient* (D') in a sediment will be less than

in the solution alone by a factor of up to ~ 10. The effective diffusion coefficient can be calculated from the relationship

$$D' = \frac{D\phi}{\theta^2} \tag{4}$$

where D is the diffusion coefficient in solution, ϕ is the porosity and θ is the tortuosity.

A detailed treatment of how to apply Fick's laws directly to sediments is given in Berner (1980), and for a comprehensive mathematical treatment of migrational processes and chemical reactions in interstitial waters the reader is referred to the 'benchmark' publication by Lerman (1977).

Examples in the text

Gieskes (1983) has pointed out that if it is assumed that only vertical transport through interstitial waters is important, then the flux of a chemical constituent can be described by the equation

$$J_b = -pD_b \frac{\partial c}{\partial z} + puc \tag{5}$$

where J_b is the mass flux, p is the porosity, z is the depth coordinate in centimetres (positive downwards), u is the interstitial-water velocity relative to the sediment/water interface in $cm_b\ s^{-1}$ (i.e. the advection rate), c is the mass concentration in mol cm_p^{-3} and D_b is the diffusion coefficient in the bulk sediment (the subscript b indicates that concentrations and distances are measured over the bulk sediment (i.e. solids and interstitial waters) and the subscript p indicates the interstitial water phase only).

The mass balance of the solute is given by

$$\frac{\partial pc}{\partial t} = \frac{\partial}{\partial z}(J_b) + R \tag{6}$$

where R is a chemical source–sink term, i.e. the reaction rate (mol $cm_b^{-3}\ s^{-1}$).

If the interstitial-water density and the solid density do not change in a given depth horizon, then

$$\frac{\partial p}{\partial t} = \frac{\partial pu}{\partial z} \tag{7}$$

and Equation 6 becomes

$$p\frac{\partial c}{\partial t} = \frac{\partial}{\partial z}\left(pD_b \frac{\partial c}{\partial z}\right) - pu\frac{\partial c}{\partial z} + R \tag{8}$$

and when steady state exists, this becomes

$$0 = \frac{\partial}{\partial z}\left(pD_b \frac{\partial c}{\partial z}\right) - pu\frac{\partial c}{\partial z} + R\,. \tag{9}$$

According to Gieskes (1983) if conditions (e.g. sedimentation rates, temperature gradients) have been stable during relatively recent times (the last 10–12 Ma), then

the steady-state assumption is valid for pelagic sediments, which have accumulation rates of ~ 20 m Ma^{-1}. The author then considered how a concentration–depth gradient, such as that illustrated in Figure (i), could be explained.

Gieskes (1983) considered the factors that might control the concentration–depth relationship in the dissolved Ca profile illustrated in Figure (i) and related them to changes in three variables. These variables were diffusion (D_b), reaction rate (R) and advection (u); i.e. the profiles were interpreted within a *diffusion–advection–reaction* framework. To illustrate this approach, three cases were considered.

Case (i), in which the rate of diffusion varies; i.e. $R = 0$, $D_b = f(z)$ and $u = 0$. Under these conditions, there is no reaction and no significant contribution from advection. Thus, only a gradual decrease in D_b with depth could then explain the increased curvature with depth in the otherwise conservative profile.

Case (ii), in which the reaction rate varies; i.e. $R \neq 0$, D_b is constant and $u = 0$.

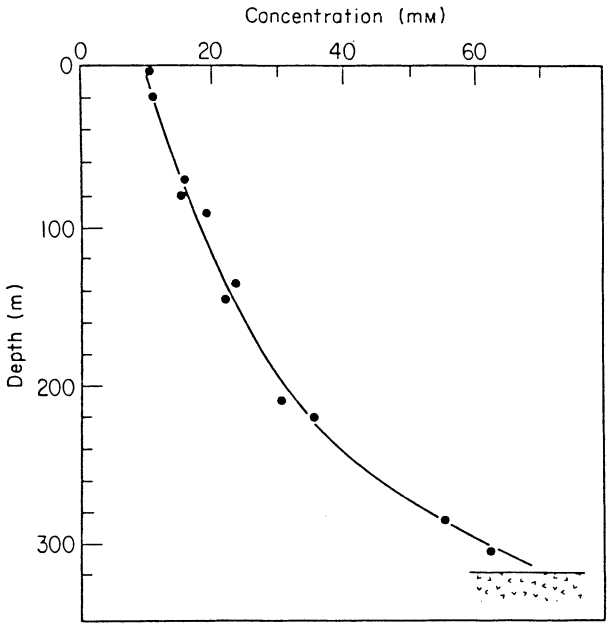

Figure (i) Concentration–depth profile of dissolved Ca in interstitial waters of a DSDP core (from Gieskes 1983).

Thus, the profile implies a removal of calcium from solution, notwithstanding the significant source term for dissolved Ca at the lower boundary.

Case (iii), in which the advection rate is not zero; i.e. $R = 0$, D_b is constant and $u \neq 0$. Thus, under these conditions of no reaction and constant diffusion coefficient, the curvature in the profile would be caused by the relatively large advective term.

Gieskes (1983) then considered two types of Ca–Mg interstitial-water concentration–depth profiles. In the first type, there are linear correlations between ΔCa and ΔMg, i.e. $R = 0$. Using data that included information on porosity, and diffusion coefficients (evaluated from a knowledge of formation factors; see above), a solution of Equation 9 assuming $R = 0$ indicated that the depth profiles of Ca and Mg could be explained in terms of conservative behaviour (i.e. transport through the interstitial water column alone and no reaction), with the boundary conditions being fixed by concentrations in the underlying basalts and the overlying sea water. In the second type, there are non-linear correlations between ΔCa and ΔMg, which implies reaction in the sediment column; i.e. $R \neq 0$. Under these conditions, derivatives of Equation 9 must be evaluated geometrically from the concentration–depth profiles in order to model the data. These two types of Ca–Mg profiles are described in the text.

HCO_3^-, and *depleted* in K^+ and Mg^{2+} relative to sea water. In addition, SO_4^{2-} was slightly enriched at most stations.

(b) The extent of these depletions or enrichments varied from element to element. For example, the enrichments in Na^+ were relatively small, and although the concentration increased with depth the gradient was only gradual. In contrast, the other major cations had interstitial-water distribution profiles that were characterized by sharp gradients in the upper 15–30 cm of the sediments with only a limited change at greater depths.

(c) The concentrations of Mg^{2+}, K^+, Ca^{2+} and HCO_3^- in the interstitial waters all exhibited a pronounced geographical variability, with the highest concentrations being found in waters from the marginal sediments and the lowest in those from the central ocean areas.

It may be concluded therefore that, relative to sea water, the interstitial fluids of oceanic sediments are generally enriched in calcium, sodium and bicarbonate and are depleted in potassium and magnesium. Some of the processes causing these interstitial-water enrichments and depletions are discussed below, and a number of the basic concepts relating to the behaviour of chemical species in interstitial water are discussed in Worksheet 14.2.

The transport of dissolved material in interstitial waters takes place by convection and diffusion. When the sediment thickness is less than ~ 150 m, convective processes can move the water through the deposits, but as the sediment thickness increases diffusive transport becomes dominant. The

external boundary conditions acting on the interstitial water–sediment 'sandwich' are therefore set by (a) the basalt basement below and (b) the water column above, which supplies the fluids that are trapped in the depositing sediments. The signals transmitted through interstitial waters therefore reflect the compositions of the overlying sea water and the underlying basalt, and are modified by *in situ* diagenetic processes within the sediment sandwich itself. The elemental composition of the interstitial waters themselves is therefore controlled by a number of interrelated factors, which include: (a) the nature of the original trapped fluid, usually sea water; (b) the nature of the transport processes, i.e. convection of diffusion; (c) reactions in the underlying basement, including both high- and low-temperature basalt–sea water interactions; (d) reactions in the sediment column; and (e) reactions across the sediment/water interface. Together, the reactions taking place in the sea water–sediment sandwich–basalt complex can involve both the release and the uptake of dissolved components. As a result, changes are produced in the composition of the interstitial waters relative to the parent sea water, and **diffusion gradients** wil be set up under which the components will migrate from high- to low-concentration regions. Under these constraints the interstitial waters can act as either a sink or a source for dissolved components. In contrast, under some conditions the compositions of the interstitial water and sea water will not differ significantly and concentration gradients will be absent.

14.6.2 Interstitial waters in marine sediments

14.6.2.1 Major elements The formation of interstitial-water gradients can be illustrated with respect to calcium and magnesium. Concentration gradients, showing increases in calcium and decreases in magnesium with depth, have been reported in the interstitial waters of many deep-sea sediments. The theories advanced to explain the existence of these gradients include: (a) the formation of dolomite or high-magnesium calcite during the dissolution and recrystallization of shell carbonates, which would account for the interstitial-water gains in calcium and losses in magnesium; and (b) the adsorption of magnesium onto opal phases, which would result in a decrease in magnesium in the interstitial waters of siliceous sediments. However, in addition to changes in magnesium and calcium there is often a decrease in $\delta^{18}O$ values in the interstitial waters, and according to Lawrence *et al.* (1975) this cannot be explained by reactions involving either carbonate or opaline diagenesis. Instead, these authors proposed that the changes in $\delta^{18}O$ values result from reactions taking place during the alteration either of the basalts of the basement or of volcanic material dispersed throughout the sediment column. The problem was addressed by Gieskes (1983), who identified two types of

calcium–magnesium profiles in the interstitial waters from 'long-core' oceanic sediments and linked them to reactions involving interstitial waters and volcanic rocks, either in the basalt basement or in the sediment column itself, or in both.

REACTIONS INVOLVING BASEMENT ROCKS In the interstitial waters of some sediments there is a linear Ca versus Mg correlation down to the base of the sediment column, i.e. gains in Ca are matched by losses in Mg. Gieskes (1983) classified the behaviour of the two elements under these conditions as *conservative*, and suggested that their distributions in the interstitial waters are controlled largely by their transport through the sediment column following reactions in the basement basalts, which act as a sink for magnesium and a source for calcium; i.e. the sediment sandwich itself is mainly unreactive, at least with respect to calcium and magnesium. An example of a DSDP core in which calcium and magnesium behave conservatively in the interstitial waters is given in Figure 14.6a. It can be seen from this figure that although calcium and magnesium have not been affected by reactions in the sediment layer, such diagenetic reactions have affected the interstitial-water profiles of other constituents in a manner that reflects the types of processes involved. For example: (a) the maximum in the strontium concentrations probably results from the recrystallization of carbonates in the nanofossil ooze, during which new mineral phases are formed that have lower strontium concentrations than the parent material; (b) potassium concentrations decrease with depth, probably as a result of the uptake of the element during the formation of potassium feldspar; (c) the sulphate profile shows a decrease with depth, indicating that there has been sulphate reduction within the sediment column.

REACTIONS INVOLVING BOTH BASEMENT ROCKS AND DISPERSED VOLCANIC MATERIAL In the interstitial waters of some deep-sea sediments there is a non-linear correlation between Ca and Mg, and the behaviour of the elements was classified as *non-conservative*. Under these conditions, Gieskes (1983) assumed that reactions controlling the interstitial-water distributions of the two elements had occurred both in the underlying basalt basement and in the sediment column. The sediment reactions were thought to have taken place mainly between the interstitial waters and dispersed volcanic material, and to have led to the addition of calcium and the removal of magnesium from the fluids. An example of the non-conservative behaviour of calcium and magnesium in the interstitial waters of sediments from a DSDP site is illustrated in Figure 14.6b, from which it can be seen that other constituents have also suffered diagenetic modifications. For example, variations in the $\delta^{18}O$ (see e.g. Lawrence *et al.* 1975) and the $^{87}Sr : {}^{86}Sr$ ratios (see e.g. Hawkesworth &

Elderfield 1978) in the interstitial waters indicate that exchange has taken place between volcanic material and the fluids. This DSDP site is located on the Bellinghausen Abyssal Plain, and is of particular interest because it contains a **silicification front** in the sediment column. At this front the conversion of biogenic opal-A to opal-CT (porcellanite) occurs, together with other diagenetic changes in the sediment–interstitial water complex that can affect mineral phases such as carbonates and volcanic material. In addition to being zones of diagenetic reaction, silicification fronts, at which the silica minerals are recrystallized, cause a decrease in the porosity of the sediment, thus acting as what Gieskes (1983) termed 'diffusion barriers'.

Other types of specialized reactions that bring about changes in the composition of interstitial waters, such as those associated with evaporite deposits and high-temperature hydrothermal activity, have been reviewed by Manheim (1976) and Gieskes (1983).

In addition to acting as a site for diagenetic reactions that exert a control on the composition of the sediments, interstitial waters play a significant role in processes that take place at the sediment/water interface and so affect the compositions of both the sediments and the overlying sea water. Data provided by Sayles (1979) showed that the reactions that control the fluxes of Mg^{2+}, Ca^{2+}, K^{+} and HCO_3^{-} across the sediment/sea water interface occur mainly in the top $\sim$ 30 cm of the sediment column, accounting for between 70 and 90% of the total fluxes. Only sodium had a deep sediment source. It may be concluded, therefore, that fluxes across the sediment/water interface that are based on data from the uppermost portions of the sediment column should give the most realistic assessment of those actually occurring in nature. Sayles (1979) calculated total diffusive fluxes of a number of elements across the interface and found that they varied geographically, being higher in the marginal than in the central areas of the Atlantic. To derive global fluxes the results were therefore weighted for high- and low-flux areas and the data obtained are listed in Table 14.1. To put the magnitude of these fluxes in context, they may be compared to those arising from fluvial run-off.

(a) For magnesium and potassium the interstitial waters act as a *sink*, with between $\sim$ 60% and $\sim$ 95% of the river input of magnesium, and between $\sim$ 84% and $\sim$ 100% of potassium, being balanced by diagenetic uptake in the sediments.
(b) For calcium, sodium and bicarbonate, the interstitial waters act as a *source* to sea water and augment the river supply by between $\sim$ 40% and $\sim$ 52% for calcium, between $\sim$ 30% and $\sim$ 48% for sodium, and between $\sim$ 24% and $\sim$ 29% for bicarbonate. Relative to the river

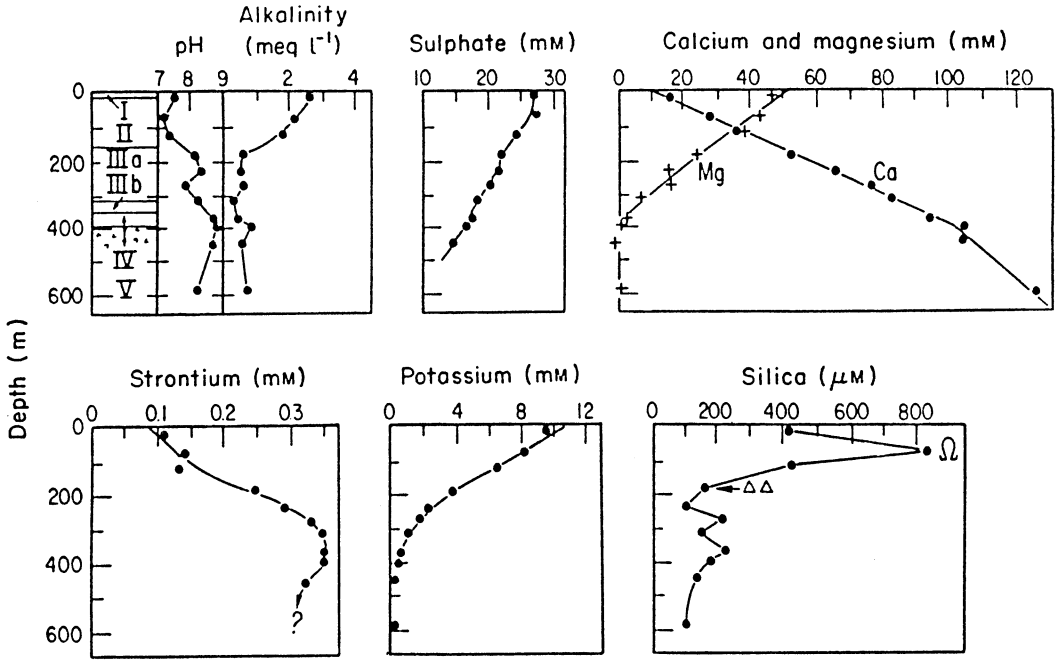

Figure 14.6 Interstitial-water profiles in sediments in DSDP sites (from Gieskes 1983). (**a**) Conservative behaviour of calcium and magnesium. (**b**) Non-conservative behaviour of calcium and magnesium.

Concentration–depth profiles at DSDP site 446 (24°42′N, 132°47′E). Lithology: I, brown terrigenous mud and clay; II, pelagic clay and ash, siliceous; IIIa, mudstone, clay stone, siltstone, sandstone; IIIb, calcareous clay and mudstones, turbidites; IV, calcareous claystones, glauconite, mudstones; V, basalt sills and intrusions.

(a)

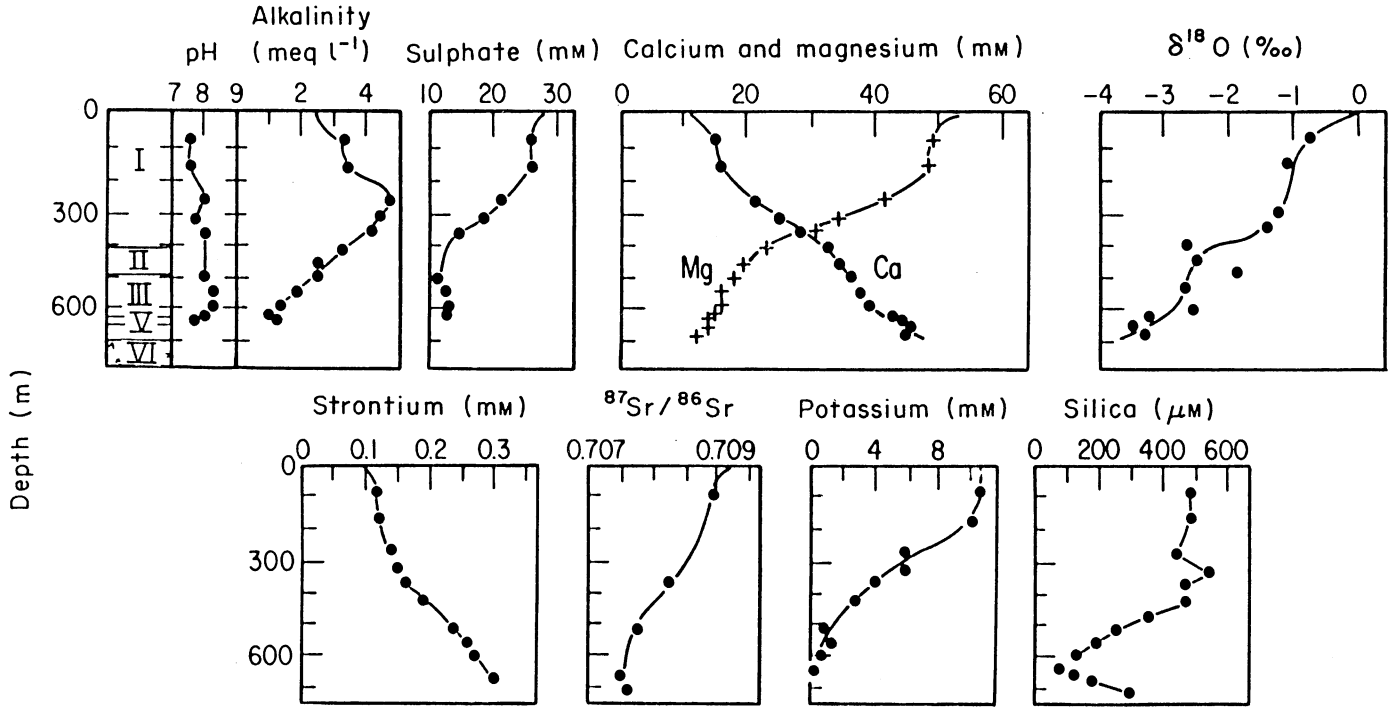

Concentration–depth profiles at DSDP site 323 (63°41′S, 98°00′W). Lithology: I, clay, silt, diatom ooze; II, chert and claystone; III, claystone; IV, nanno chalk; V, zeolitic clay; VI, basalt.

(b)

Table 14.1 Total diffusive fluxes of a number of components across the sediment/water interface[a]

Component	Flux (10^{14} meq yr^{-1})						River input (10^{14} meq yr^{-1})	Diffusive flux ÷ River input	
	Ocean margin		Central ocean		Total				
	L	A	L	A	L	A		L	A
Na^+	+16	+24	+11	+20	+27	+44	90	+0.30	+0.48
Mg^{2+}	-38	-66	-28	-38	-66	-104	110	-0.60	-0.94
Ca^{2+}	+54	+75	+43	+50	+97	+125	240	+0.40	+0.52
K^+	-7.6	-10	-8.3	-9.6	-16	-20	19	-0.84	-1.05
HCO_3^-	+43	+58	+33	+35	+76	+93	320	+0.24	+0.29

[a] Data from Sayles (1979); L and A indicate values derived from linear (L) and analytical (A) curve fit extrapolations to the sediment interface; + = release to oceans, - = loss to the oceans.

inputs these fluxes are smaller than those for magnesium and potassium, but they are still significant in terms of marine budgets. However, Sayles (1979) demonstrated that when the uptake of magnesium and potassium is calculated from the estimated fluxes across the sediment/sea water interface their concentrations would be in excess of those actually found in the sediments. He concluded, therefore, that the interstitial-water fluxes for magnesium and potassium may have been overestimated by as much as 50%, but that despite this they would still be of importance in the marine cycles of the two elements.

14.6.2.2 Trace elements In recent years new data for trace elements in interstitial waters have begun to appear in the literature, and these can be used to assess the fates of the elements in the interstitial water–sediment system. The fate of an element is intimately related to its post-depositional mobility, since in order to be added to the interstitial water from solid sediment phases it must first be solubilized to the dissolved state during diagenetic reactions. The elements that are concentrated in interstitial water relative to sea water can follow one of two general pathways; they can either be released into the sea water, or they can be reincorporated into sediment components. Thus, it is necessary to introduce the concept of a *net* interstitial water flux, which, in this context, is the flux that escapes reaccumulation and is directly added to sea water.

Several studies can throw light on the extent to which these net, or out-of-sediment, fluxes operate. In one of these, Hartmann & Muller (1982) gave data on the mean concentrations of Mn, Cu, Zn and Ni in the interstitial waters of a series of oxic pelagic sediments (siliceous oozes, clays and calcareous oozes) from the central Pacific – a summary of their data is given in Table 14.2. All the trace metals were enriched in the interstitial waters relative to ambient sea bottom water and, with the exception of Zn, they had their highest concentrations near to the sediment surface (0–2 cm depth). As a result of the interstitial-water > seawater concentration differences, diffusive fluxes will be set up to transport the dissolved metals across the sediment/water interface. Hartmann & Muller (1982) made lower limit estimates of the magnitudes of these fluxes from the upper 2 cm of the sediments and these are listed in Table 14.2, together with estimates of the rates at which the elements accumulate in the deposits.

A similar type of study was carried out by Callendar & Bowser (1980) on the interstitial-water chemistry of Mn and Cu in nodule-rich pelagic sediments from the northeastern Equatorial Pacific. The distribution of Mn in the interstitial waters varied with depth in the sediments studied, but that of Cu showed a regular pattern with the highest concentrations being in the waters from the upper 10 cm of the sediments. The authors used their data to calculate diffusive interstitial-water fluxes, and the

Table 14.2 Average concentrations of Mn, Cu, Zn and Ni in interstitial waters from central Pacific clays, siliceous oozes and carbonate oozes, together with enrichments relative to ambient sea water and their fluxes into the sediments[a]

	Depth within sediment column	Mean concentration in interstitial waters ($\mu g\ l^{-1}$)	Mean enrichment factor relative to sea water	Diffusive flux from sediments ($\mu g\ cm^{-2}\ yr^{-1}$)	Rates of accumulation to sediments ($\mu g\ cm^{-2}\ yr^{-1}$)
Mn	0-2cm	3,7±2,2	18,6	0,18	0,3-0,7
	2-38cm	3,6±3,2	15,2		
	38-973cm	2,8±2,4	12,2		
Cu	0-2cm	4,8±2,4	28,4	0,23	0,01-0,06
	2-38cm	2,1±1,5	12,4		
	38-973cm	0,9±0,6	5,4		
Zn	0-2cm	17,3±20,7	3,2	0,58	0,01-0,02
	2-38cm	19,9±20,3	3,7		
	38-973cm	19,6±17,2	3,6		
Ni	0-2cm	2,2±2,2	4,6	0,08	0,01-0,02
	2-38cm	1,4±1,1	3,0		
	38-973cm	1,1±0,9	2,3		

[a] Data from Hartmann & Muller (1982).

Table 14.3 Interstitial water concentration, diffusive fluxes and accumulation rates of Mn and Cu in northeast Equatorial Pacific Ocean sediments[a]

Sediment	Manganese			Copper		
	Concentration 0-2cm ($\mu g\ l^{-1}$)	Mean diffusion flux from sediments ($\mu g\ cm^{-2}\ yr^{-1}$)	Mean rate of accumulation in sediments ($\mu g\ cm^{-2}\ yr^{-1}$)	Concentration 0-2cm ($\mu g\ l^{-1}$)	Mean diffusion flux from sediments ($\mu g\ cm^{-2}\ yr^{-1}$)	Mean rate of accumulation in sediments ($\mu g\ cm^{-2}\ yr^{-1}$)
Terrigenous mud	1,5	0,28	2,55	11,5	0,72	0,038
Pelagic clay	1,2-11	0,015	1,06	5-9	0,31	0,06
Siliceous ooze	0,07-< 0,7	0,025	0,18	1-3	0,17	0,015
Calcareous ooze	3,0	0,12	0,20	14	0,78	0,012

[a] Data from Callender & Bowser (1980).

findings are given in Table 14.3. Callendar & Bowser (1980) concluded that Cu is mainly transported to the sediments in association with a biogenic carrier phase (see also Sawlan & Murray 1983, and Sec. 11.6.3.2), and that the interstitial-water profiles are maintained by its rapid release in surficial sediments and its uptake onto solid phases at depth. The rapid release from surficial sediments results in a diagenetic flux of Cu across the sediment/water interface. The authors used the calculated diffusive flux rates and net sediment accumulation rates to estimate that the regeneration of Cu from these deposits is $> 90\%$; i.e. most of the sedimentary flux of Cu to the sea floor is returned as dissolved Cu via a diagenetic flux across the sediment/water interface. This was in contrast to the behaviour of Mn. Manganese is transported down the water column following particle scavenging reactions (see Sec. 11.6.3.1), and although it undergoes diagenetic remobilization much of the resultant diffusive flux is taken up by sediment components and so becomes trapped before it can cross the sediment/sea water interface in a dissolved form. For example, Callender & Bowser (1980) estimated that $< 10\%$ of the Mn in the pelagic clays and siliceous oozes which they studied undergoes diagenetic transport into the overlying sea water. Unlike Cu, therefore, most of the remobilizied Mn is trapped with the sediments, a conclusion similar to that reached by Hartmann & Muller (1982).

The remobilization and recycling of trace elements in the sediment–interstitial water–sea water complex is intimately related to the diagenetic environment under which the sediment is deposited, and this can be summarized in terms of the findings of a number of recent investigations.

PELAGIC SEDIMENTS These are oxic to considerable depths (see Sec. 14.4.1), and surface enrichments do not appear to be a characteristic feature of the distributions of Mn, Fe, Ni and Cd in their interstitial waters. However, dissolved Cu does show a concentration maximum at or near the sediment/water interface. This can be illustrated by data provided by Klinkhammer *et al.* (1982) for sediments collected at MANOP site S in the central Equatorial Pacific. These sediments were oxic down to 30 cm, and their interstitial-water profiles are shown in Figure 14.7a. The authors derived a model in which it was assumed that in oxic sediments the destruction of organic matter is accomplished by dissolved oxygen, i.e. early diagenesis is analogous to oxidation in the overlying water column and interstitial water near the sediment/sea water interface is a continuum of ambient bottom waters. Nickel and Cd are nutrient-type elements that have reasonably well defined metal-nutrient relationships in sea water (see Sec. 11.5), and their interstitial-water concentrations in the oxic sediments at site S could be adequately predicted by the model from the interstitial-water nutrient concentrations. The most striking feature of the dissolved Cu profile reported by Klinkhammer *et al.* (1982), and confirmed in other pelagic cores by Sawlan & Murray (1983), is the presence of a concentration maximum near to the sediment/sea water interface (see Fig. 14.7a). The diagenetic model could not, however, be applied to the concentrations of Cu in the interstitial waters because the amount of this element released at the interface was considerably in excess of that predicted by the decomposition of organic debris on the basis of the metal–nutrient data; a second model was therefore constructed to describe the regeneration of Cu in the sediments. The models used by Klinkenhammer *et al.* (1982) are described in Worksheet 14.3.

HEMI-PELAGIC SEDIMENTS These are in a reducing condition below a relatively thin oxic surface layer (see Sec. 14.4.1), and their interstitial waters tend to show large concentration gradients in the distributions of Mn, Ni and Cu. This can be illustrated by the data provided by Klinkhammer *et al.* (1982) for sediments collected at MANOP site C in the central Equatorial Pacific (see Fig. 14.7b); see also the variety of profiles given by Sawlan & Murray (1983). At site C there is a sharp increase in the dissolved concentrations of Mn in the interstitial waters below 9 cm. This is characteristic of *sub-oxic* pore waters and results from the utilization and solubilization of Mn oxides in the diagenetic sequence. Above 9 cm, however, the dissolved Mn concentrations are lower and relatively constant, i.e. the concentration maximum does not extend through the oxic layer to the sediment/water interface. These upper oxidized portions of deep-sea sediments often exhibit an increase in solid-phase manganese, and it is generally accepted that this arises from the

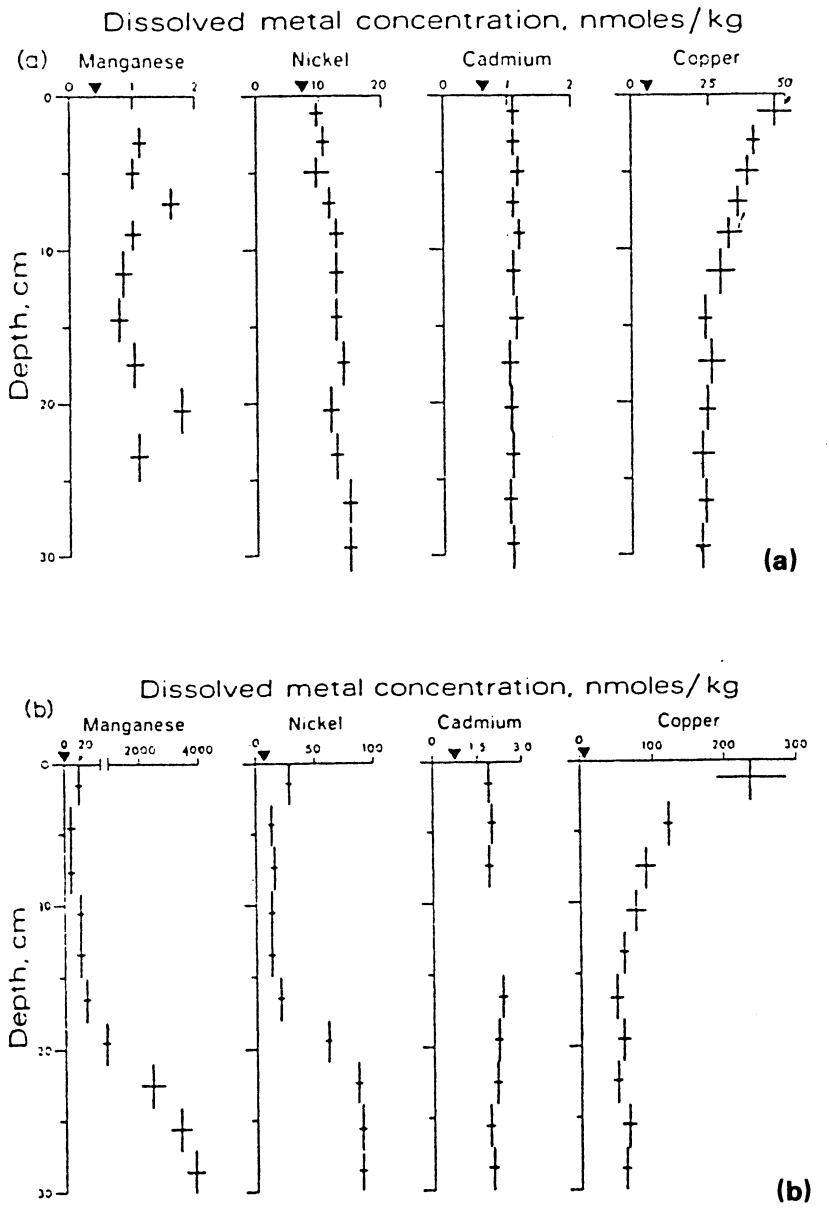

Figure 14.7 Interstitial-water profiles of dissolved trace metals (from Klinkhammer *et al.* 1982). (**a**) Profiles from a sediment that was in an oxic conditions down to 30 cm: MANOP site S, central Equatorial Pacific. (**b**) Profiles from a sediment that was in a sub-oxic condition below an oxic surface layer: MANOP site C, central Equatorial Pacific.

WORKSHEET 14.3
MODELS FOR THE REGENERATION OF TRACE METALS IN OXIC SEDIMENTS

Klinkhammer *et al.* (1982) reported data on the concentrations of Ni, Cd and Cu in bottom waters and oxic sediment interstitial waters at MANOP site S in the central Equatorial Pacific, and used these to set up diagenetic models. A characteristic feature of the metal interstitial-water profiles at the oxic site (S) is that the steepest concentration gradient is found across the sediment/sea water interface, which implies that most metal regeneration in these oxic sediments takes place across this interface. The concentration–depth profiles are maintained by a combination of the regeneration and the interaction between the dissolved metals and the sediment below the interface. Ni and Cd exhibit little tendency to react with sediment components under these conditions, with the result that their interstitial water profiles are monotonic at site S and are generated by the burial of surficial pore water. In contrast, Cu is readily taken up by sediment components, which leads to an exponential decrease in interstitial-water dissolved Cu concentrations with depth – see Figure (i).

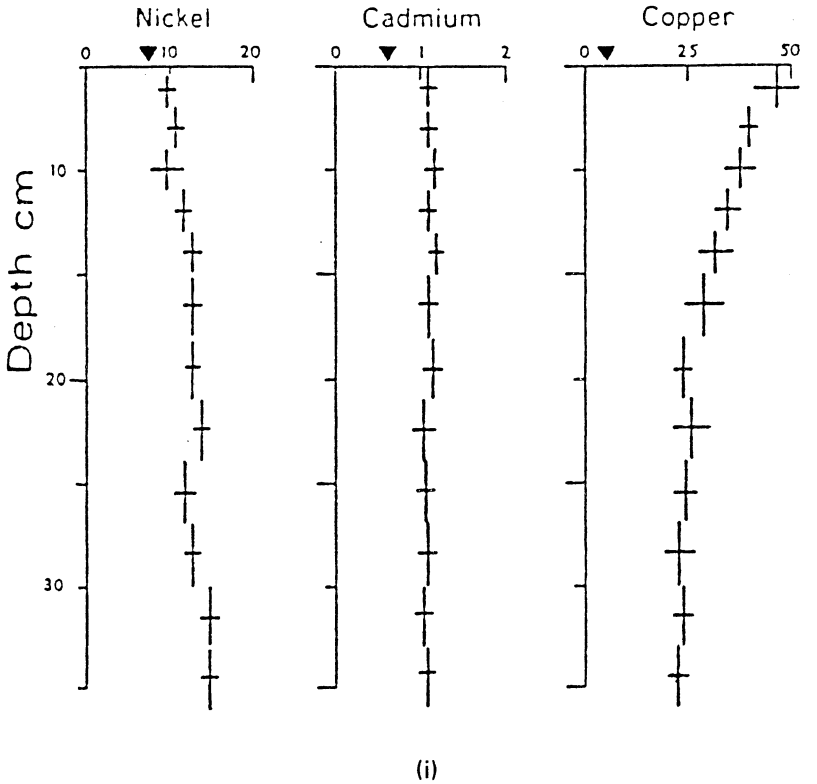

(i)

Figure (i) Dissolved metal concentrations in the interstitial waters of oxic sediments at MANOP site S (nmol l^{-1}). Arrow heads indicate bottom water concentrations.

Ni and Cd regeneration

Under conditions of oxic diagenesis the degradation of organic matter in surface sediments utilizes dissolved oxygen, and Klinkhammer *et al.* (1982) assumed that in the simplest case early oxic diagenesis on the sea floor is analogous to oxidation in the overlying water column, i.e. a 'continuum model'. Ni and Cd are nutrient-type elements in sea water so that under oxic conditions it should be possible to predict the Ni and Cd concentrations in the surficial interstitial waters from the interstitial nutrient concentrations. To set up a model for this, Klinkhammer *et al.* (1982) assumed that both the metals and the nutrients are lost from the sediment/sea water interface by diffusion only, so that the flux of a metal M across the interface is related to the corresponding flux of a nutrient N by a proportionality constant M/N. Thus

$$D_M \left(\frac{dM}{dz} \right)_{z=0} = \frac{M}{N} D_N \left(\frac{dN}{dz} \right)_{z=0} . \qquad (1)$$

By assuming a linear concentration gradient across the interface, Equation 1 reduces to the relationship

$$\frac{M}{N} = \frac{(M_0 - M_{BW})D_M}{(N_0 - N_{BW})D_N} . \qquad (2)$$

In the water column Ni mimics silica and Cd is related to nitrate, and using data from the literature the appropriate diffusion coefficient ratios (D) were calculated to be $D_{Cd}/D_{NO_3} = 0.36$ and $D_{Ni}/D_{Si} = 0.68$. M_0 and M_{BW} are metal concentrations in the top interstitial-water interval and bottom sea water, and N_0 and N_{BW} are the corresponding nutrient concentrations. A comparison of the results obtained from Equation 2 with the ratios found in sea water is a test of continuity. Klinkhammer *et al.* (1982) made such a comparison and the data from site S are reproduced in Table (i), and strongly support the 'continuum model'.

Table (i) Metal/nutrient ratios (Ni/Si and Cd/NO_3) at site S calculated from Equation 2 compared with those observed in general sea water and bottom water at the site[a]

	$(M/N)_{site\ S}$ x 10^5	$(M/N)_{SW}$ x 10^5	$(M/N)_{BW}$ x 10^5
Ni	3.2	3.3	5.3
Cd	3.3	2.3	1.8

[a] From Klinkhammer et al. (1982).

Cu regeneration

Cu is readily taken up by sediment components, which leads to an exponential decrease in interstitial-water dissolved Cu concentrations with depth. In addition, dissolved Cu is released into sea water at the interface. However, the amount of Cu released in this way is considerably greater than that which would be predicted from the decomposition of organic material consisting of plankton. Thus, the model developed for Ni and Cd is inappropriate for Cu. Klinkhammer *et al.* (1982)

therefore assumed that the interstitial-water dissolved Cu profiles are sustained by scavenging from the water column combined with vigorous recycling at the interface and uptake into the sediment. The authors then attempted to model the interstitial-water dissolved Cu profile in the following manner.

The shape of the interstitial-water dissolved Cu profile at site S (see Fig. (i)) shows a concentration gradient that indicates diffusion upwards (into sea water) and downwards (into the sediment) from the interface, and the negative curve suggests an uptake by the sediment at depth. The authors concluded that the simplest model consistent with this type of profile was a steady-state approach in which the Cu is controlled by diffusion and first-order removal, which can be represented by the equation:

$$D\frac{\partial^2 C}{\partial z^2} - kC = 0\,. \tag{3}$$

The solution of Equation 3 for a one-layer sediment is given by

$$C = \frac{C_1 \sinh[R(h - z)] + C_2 \sinh(Rz)}{\sinh(Rh)} \tag{4}$$

where $R = (k/D)^{1/2}$, C is the concentration predicted at depth z, C_1 and C_2 are the concentrations at the upper ($z = 0$) and lower ($z = h$) boundaries, D is the diffusion coefficient corrected for porosity, tortuosity and temperature ($D = 1.4 \times 10^{-6}\text{cm s}^{-1}$), and k is the reaction constant in s^{-1}. Values for k were calculated using a best-fit approach. The authors modelled their data to a depth of ~ 15 cm in the sediment,

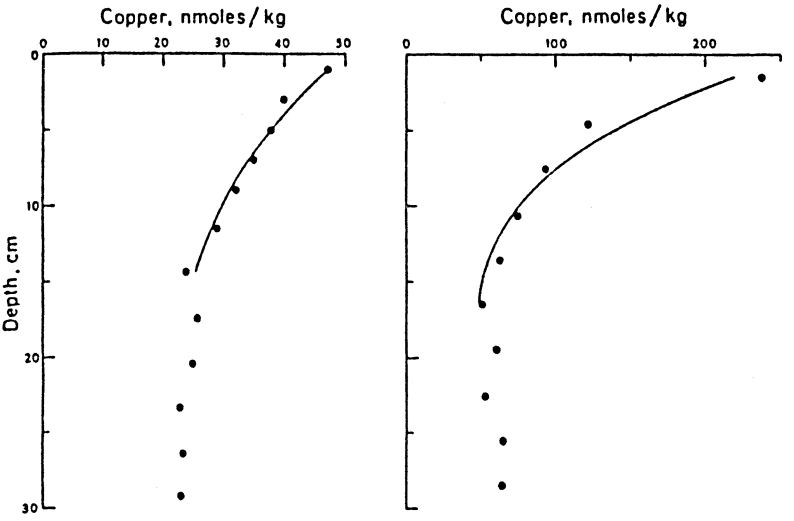

(ii)

Figure (ii) Dissolved Cu interstitial-water profiles in the oxic sediments at site S. Filled circles are the measured concentrations in the interstitial waters. The full curve indicates the curve derived from Equation 4 using the following parameters: C_1 = 47 nmol kg^{-1}, C_2 = 26 nmol kg^{-1}, h = 13 cm and k = 0.17 yr^{-1}.

below which there is little variation. The results for site S are illustrated in Figure (ii). It is apparent from Figure (ii) that there is very good agreement between the predicted and observed dissolved Cu interstitial-water profiles, i.e. the profiles are adequately explained by the remobilization of Cu at the interface and its removal into the sediment below.

reprecipitation trapping of the solubilized Mn under the oxic conditions. The distribution of Ni in the interstitial waters generally follows that of Mn, i.e. there is no surface maximum, and the subsurface maximum occurs at a similar depth to that of Mn probably as a result of its release from the Mn oxides. There is, however, a surface maximum in the interstitial-water Cu profiles, with the concentrations at the surface usually being considerably higher than those in pelagic sediment interstitial waters. This surface maximum leads to a diffusive flux out of the sediment – see below.

HIGHLY REDUCING SHELF SEDIMENTS In these sediments the upper oxic zone is either confined to the top few centimetres or absent altogether. Sawlan & Murray (1983) gave data on the distributions of a number of elements in the interstitial waters from shelf sediments of this kind. They reported that in these sub-oxic environments elevated dissolved Mn concentrations can be found at or near the sediment/water interface. These sediments, with their high coretop dissolved Mn concentrations, represent a window to the bottom water through which Mn can diffuse, thus reinforcing the status of shelf sediments for the supply of dissolved Mn to sea water (see Sec. 11.4). In contrast, Cu did not show the surface enrichments reported for the pelagic and hemi-pelagic sediment interstitial waters, and the concentrations were generally similar to those in ambient sea water, i.e. there was no concentration gradient to drive an out-of-sediment flux, such as was found for the pelagic and hemi-pelagic sediments.

A summary of some of the flux data provided by both Klinkhammer *et al.* (1982) and Sawlan & Murray (1983) is given in Table 14.4.

It may be concluded that elemental fluxes through interstitial waters are driven by diagenetic reactions involving the destruction of organic carbon and so are linked to the diagenetic sequence. As a result, some elements are released close to the surface during oxic diagenesis when organic carbon is destroyed by dissolved oxygen, while others are released at depth when secondary oxidants, such as Mn oxides, are utilized for the destruction of the organic matter. It has become evident from the various studies described above that the position at which the

Table 14.4 Diffusive fluxes of some elements from deep-sea sediments

Sediment type	Diffusive flux ($\mu g\ cm^{-2}\ yr^{-1}$)				Data source
	Cu	Mn	Ni	Cd	
Oxic pelagic	0.12	0.0008	~0.002	~0.002	a
Pelagic red clay	0.18	-	-	-	b
Hemi-pelagic	0.38	-	-	-	b

[a] Data from Klinkhammer et al. (1982).

[b] Data from Sawlan & Murray (1983).

elements are released can be critical in controlling their subsequent fate in the sediment–interstitial water system. The elements released into the interstitial waters can migrate in either upward or downward directions, and the shapes of the concentration profiles are often diagnostic of the flux direction. This can be illustrated with respect to the interstitial-water distributions of Cu and Mn.

COPPER In the interstitial waters of both pelagic and hemi-pelagic sediments dissolved Cu can have its maximum concentrations at or near the sediment surface, and the shapes of the dissolved Cu profiles reported by Klinkhammer *et al.* (1982) (see Fig. 14.7) indicate both upward and downward diffusion from the sediment/sea water interface.

(a) **Downward diffusion**. The decrease in dissolved Cu below the interface indicates downward diffusion and the removal of the element into the solid sediment phases, i.e. the downward-transported Cu is trapped in solid sediment material either at or near the sediment surface or at depth within the sediment column. According to various estimates, from at least half (Sawlan & Murray 1983) to most (Klinkhammer *et al.* 1982) of the Cu in hemi-pelagic and pelagic deep-sea sediments has an oxic diagenetic origin and is supplied by downward diffusion.

(b) **Upward diffusion.** Because of the position of the dissolved Cu maximum at the sediment/sea water interface, the dissolved Cu transported upwards will drive a diffusive flux into the overlying sea water. Klinkhammer *et al.* (1982) estimated this flux to be $\sim$ 1800 nmol $cm^{-2}/10^3$ yr at MANOP site S and $\sim$ 6600 nmol $cm^{-2}/10^3$ yr at MANOP site C. The authors concluded that the Cu must be released from a very thin layer at the top of the sediment, which they estimated should have a Cu content of $\sim$ 2500–5000 $\mu g\ g^{-1}$. Since concentrations of this kind are not picked up in sediment analysis, the

thin layer is probably present as 'fluff' (see Sec. 12.3), from which it was suggested that the Cu is recycled to sea water around nine times before it is eventually buried in the sediment. The out-of-sediment diffusive fluxes derived by Klinkhammer *et al.* (1982) are given in Table 14.4. Sawlan & Murray (1983) modelled their interstitial-water data and estimated that the diffusive flux of dissolved Cu into sea water represented around 75% of the total Cu delivered to the sediments. They also calculated that at least 50% of the total Cu in hemi-pelagic sediments had a diagenetic origin from the into-sediment flux. It may be concluded, therefore, that a large fraction of the Cu remobilized in sediments can, under some conditions, diffuse into the overlying sea water. This out-of-sediment diffusive Cu flux can impose a 'fingerprint' on the water column profile of dissolved Cu. For example, Boyle *et al.* (1977) calculated that on the basis of water column profiles in the Pacific there must be a strong general flux of dissolved Cu from the sediment surface into the water column; this flux will, of course, include Cu taken into solution in the benthic boundary layer, as well as that which is remobilized in the sediment and then escapes across the interface. Boyle *et al.* (1977) applied a diffusion–advection model to estimate that the out-of-sediment dissolved Cu flux should have a magnitude of ~ 0.16 μg cm^{-2} yr^{-1}, which is equivalent to an ocean-wide flux of $\sim 0.51 \times 10^{12}$ g yr^{-1}. Using an approach based on the down-column transport of Cu in the North Atlantic, and the rate at which it accumulates in the underlying sediments, Chester (1981) showed that there was a regeneration of Cu at the depositional surface which would amount to a flux of ~ 0.17 μg cm^{-2} yr^{-1}, or to an ocean-wide flux of $\sim 0.55 \times 10^{12}$ g yr^{-1} (see Table 14.5). Both of the latter flux values are close to those derived from interstitial-water concentration gradients, and so offer independent verification of the order-or-magnitude release of dissolved Cu from pelagic sediments.

MANGANESE In strongly reducing shelf sediments, with the sub-oxic zone lying near the surface, the dissolved Mn concentration maxima are found close to the sediment/sea water interface, and the Mn can escape into sea water through these windows. In hemi-pelagic sediments, however, dissolved interstitial-water Mn usually has its highest concentrations at depth in the sediments as a result of the utilization of Mn oxides for the destruction of organic carbon in the sub-oxic zone; other elements, such as Ni, Co, Cu and Zn, which are associated with the oxides, can also be released in this zone. The shape of the dissolved Mn profiles in the interstitial waters (see e.g. Fig. 14.7b) characteristically exhibits a decrease in concentration in the oxic zone, indicating a removal of the element into the sediment phases. This is confirmed by the distribution of

solid-phase Mn in the sediments, and it has been known for many years that Mn profiles in deep-sea sediments often display higher concentrations in the oxic layers close to the surface than at depth.

The reactions involved in the diagenesis of Mn can be related to interstitial-water phase–solid phase changes, and can be expressed in a simple form as:

$$Mn^{2+}(\text{soluble}) \underset{\text{reduction}}{\overset{\text{oxidation}}{\rightleftharpoons}} MnO_x(\text{solid hydrous oxide}) \qquad (14.7)$$

where x is generally less than 2. This reaction governs the diagenetic mobility of Mn in sediments, and the general conditions that control both the solid-phase and dissolved Mn can be described in terms of the model proposed by Lynn & Bonatti (1965). In essence, this can be summarized as follows. Manganese oxides (**first generation**) are deposited at the sediment surface and are subsequently buried below the redox boundary where they are reduced. This results in the production of dissolved Mn^{2+}, which then diffuses upwards, along a concentration gradient in the interstitial water, and is oxidized and precipitated in the upper sediment layer as hydrous Mn oxides (**second generation**). As sedimentation proceeds, the second-generation oxides are again carried down into the reducing zone and the cycle starts again. The overall result of the Mn recycling is the trapping of solid-phase Mn in a narrow zone at the redox boundary. This general pattern of Mn behaviour was refined by Froelich *et al.* (1979) in their classic paper on the diagenetic sequence in deep-sea sediments. In the **Froelich model** it is proposed that, when the sequence reaches the stage at which manganese oxides are utilized to provide dissolved oxygen for the oxidation of organic matter, the reduction, mobilization and upward diffusion of Mn^{2+} are initiated. Thus, the reduction–mobilization provides a mechanism for the stripping of Mn from the sediments as they accumulate, and the upward diffusion provides a mechanism for transporting it back into oxic layers where it is subsequently redeposited following oxidation to MnO_2. With further sediment accumulation the new MnO_2 passes into the zone where it is used as an oxidant and is again remobilized. This leads to the setting up of the sedimentary Mn trap, which can give rise to Mn-rich bands, or **spikes**, in some types of sediment (see Sec. 14.4.2). Froelich *et al.* (1979) proposed that the depth of the Mn spike is controlled by the balance of oxygen diffusing downwards and Mn^{2+} diffusing upwards. In a steady-state system the concentration of Mn in the spike will increase until the sedimentary input of reactive Mn is balanced by the efficiency of reduction and remobilization. Thus, such a steady-state system would display the highly concentrated Mn spike near the top of the dissolved Mn^{2+} gradient. The Froelich model is illustrated diagrammatically in Figure 14.8a. This general type of steady-state Mn diagenesis has also

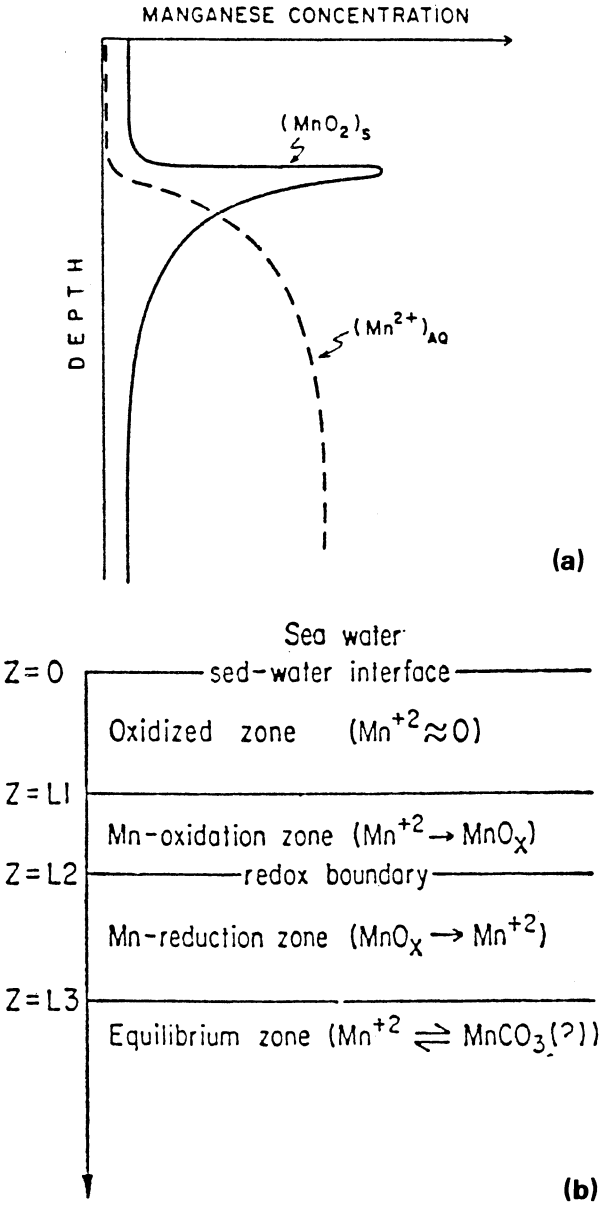

Figure 14.8 Manganese diagenesis in sediments under steady-state conditions. (**a**) Schematic representation of dissolved (AQ) and solid-phase (S) Mn profiles in a hypothetical steady-state sediment sysem (from Froelich *et al.* 1979). (**b**) Schematic representation of the zonation of marine sediments with respect to Mn diagenesis (from Burdige & Gieskes 1983).

been described in another model, which was proposed by Burdige & Gieskes (1983). In the **Burdige–Gieskes model** the sedimentary column is divided into four distinct zones.

(a) **Oxidized zone**. This is the zone in which first-generation Mn oxides accumulate, and the concentration of dissolved Mn^{2+} is essentially zero.
(b) **Manganese oxidation zone**. In this zone the dissolved Mn^{2+} profile increases with depth and is concave upwards as a result of the diffusion of Mn^{2+} from below across the redox boundary and its consumption by oxidation in the zone. The oxidation product is a solid hydrous Mn oxide, so that there is an increase in this component with depth. The **redox boundary** separates zones 2 and 3. This boundary is the depth in the sediment below which Mn^{2+} is favoured over solid Mn oxide phases.
(c) **Manganese reduction zone**. As solid Mn oxides are buried below the redox boundary they undergo reduction, e.g. as the diagenetic sequence switches to the secondary oxidants. Mn^{2+} is released into the interstitial waters and the Mn^{2+} profiles are concave downwards. Thus, dissolved Mn^{2+} increases with depth, whereas solid Mn decreases.
(d) **Equilibrium zone**. Here dissolved Mn reaches a maximum and may in fact decrease with depth perhaps due to the formation of some kind of Mn carbonate.

The main features in the Burdige–Gieskes model are illustrated diagrammatically in Figure 14.8b and a mathematical treatment of the model is given in Worksheet 14.4. Both Froelich *et al.* and Burdige & Gieskes (1983) successfully applied their steady-state Mn diagenesis models to field situations and were able to identify the presence of Mn spikes in deep-sea sediments displaying an upper oxic zone separated from a lower reducing zone by a redox boundary. However, Pederson *et al.* (1986) showed that the diagenesis of Mn in such sediments need not always take place under steady-state conditions. These authors gave data on the distribution of solid-phase and interstitial-water Mn in a hemi-pelagic core from the East Pacific Rise. The interstitial-water Mn^{2+} profile showed a negative concave-upward form and there was an enrichment of solid-phase Mn in the near-surface layer, two features characteristic of hemi-pelagic sediments. However, the solid-phase and water-phase Mn were in disequilibrium, indicated by the fact that there was no concentration gradient for dissolved Mn in the upper 5 cm of the core in the region over which the solid-phase Mn increased in concentration. The authors concluded that the increase in solid-phase Mn in the top 5 cm could not therefore be supplied by an upward diffusion of

WORKSHEET 14.4
THE BURDIGE-GIESKES MODEL FOR THE STEADY-STATE DIAGENESIS OF Mn IN MARINE SEDIMENTS

Burdige & Gieskes (1983) outlined a steady-state pore water–solid phase diagenetic model for Mn in marine sediments. The model has been described qualitatively in the text, and can also be used to illustrate how *diagenetic equations* are used. The Burdige–Gieskes steady-state diagenetic model, which involves a series of Mn reaction zones, is illustrated in Figure (i).

The derivation of the diagenetic equations used to translate this into a quantitative mathematical model is summarized below.

Burdige & Gieskes (1983) presented a mathematical treatment of their Mn 'zonation model' using the steady-state diagenetic equations given by Berner (1980):

$$D_b \frac{\partial^2 C_p}{\partial z^2} - w \frac{\partial C_p}{\partial z} + R(z) = 0 \tag{1}$$

$$- w \frac{\partial C_s}{\partial z} - \frac{\phi}{1 - \phi} R(z) = 0 \tag{2}$$

where D_b is the bulk sediment diffusion coefficient (identical with Berner's D_s term), C_p is the concentration of Mn in the pore waters, C_s is the concentration of Mn in the solid phase, w is the sedimentation rate, ϕ is the porosity and $R(z)$ is a rate expression for either oxidation or reduction. The term $\phi/(1 - \phi)$, which has units

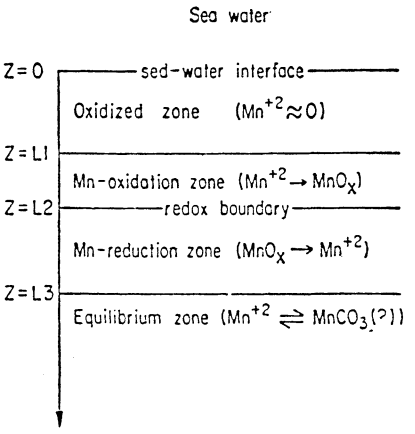

Figure (i) Manganese steady-state diagenetic zonation model (from Burdige & Gieskes 1983).

$cm^3_{pore\ water}/cm^3_{dry\ sed}$, is used to convert Mn concentrations between the solid and liquid phases.

With respect to the Mn model the following assumptions are implicit in the diagenetic equations.

(a) Steady-state diagenesis operates.
(b) Vertical gradients are much more important than horizontal gradients, to the extent that the latter can be ignored.
(c) Diffusion in pore waters occurs via molecular processes, i.e. the diffusion follows Fick's laws.
(d) Porosity and diffusion coefficients are constant with depth.
(e) Advection is constant and equal to the sedimentation rate.
(f) Solid-phase diffusion can be neglected.
(g) The supply of solid Mn to the sediment surface is constant with time.
(h) Adsorption of Mn^{2+} can be neglected.
(i) Bioturbation can be neglected since in most marine sediments it will be above the oxidation (or reducing) zone.

The authors also drew attention to two other factors, which are detailed below.

D_b differs from the free ion diffusion in sea water (D) because of tortuosity effects due to the presence of sediment particles, and D_b can be related to D by the following equation:

$$D_b = D/\phi F \tag{3}$$

where F is a 'formation factor', which is measured as the ratio of the bulk sediment resistivity to the pore-water resistivity (see Worksheet 14.3).

In Equations 2 and 3 $R(x)$ is the rate expression for either oxidation or reduction. In the presence of an abundant surface area (such as that of a sediment), Mn precipitation–oxidation is a pseudo-first-order process, so that

$$R_{ox}(z) = k_{ox}C_p \tag{4}$$

and Equation 5 should therefore be an appropriate rate expression for oxidation under these conditions in which the reaction product is assumed to be a hydrous oxide (MnO_x – see text). The authors assumed that whatever the mechanism involved, the rate of Mn reduction will be proportional to the amount of solid Mn available (which is presumed to be all hydrous oxide). Thus, $R_{red}(z)$ can be expressed as

$$R_{red}(z) = k_{red}C_s\ . \tag{5}$$

Combining the rate expressions with Equations 1 and 2, the following set of equations was obtained:

(a) For the oxidizing zone ($L_1 \leqslant z \leqslant L_2$)

$$D_b \frac{\partial^2 C_p^{ox}}{\partial z^2} - w \frac{\partial C_p^{ox}}{\partial z} - k_{ox}C_p^{ox} = 0 \tag{6}$$

$$- w \frac{\partial C_s^{ox}}{\partial z} + \frac{\phi}{1-\phi} k_{ox}C_p^{ox} = 0 \tag{7}$$

(b) For the reducing zone ($L_2 \leq z \leq L_3$)

$$D_b \frac{\partial^2 C_p^{red}}{\partial z^2} - w \frac{\partial C_p^{red}}{\partial z} + \frac{1-\phi}{\phi} k_{red} C_s^{red} = 0 \tag{8}$$

$$- w \frac{\partial C_s^{red}}{\partial z} - k_{red} C_s^{red} = 0 \tag{9}$$

By defining a series of boundary conditions the solutions to Equations 6 to 9 were given as

$$C_p^{ox} = A \sinh[\alpha(z - L_1)] \tag{10}$$

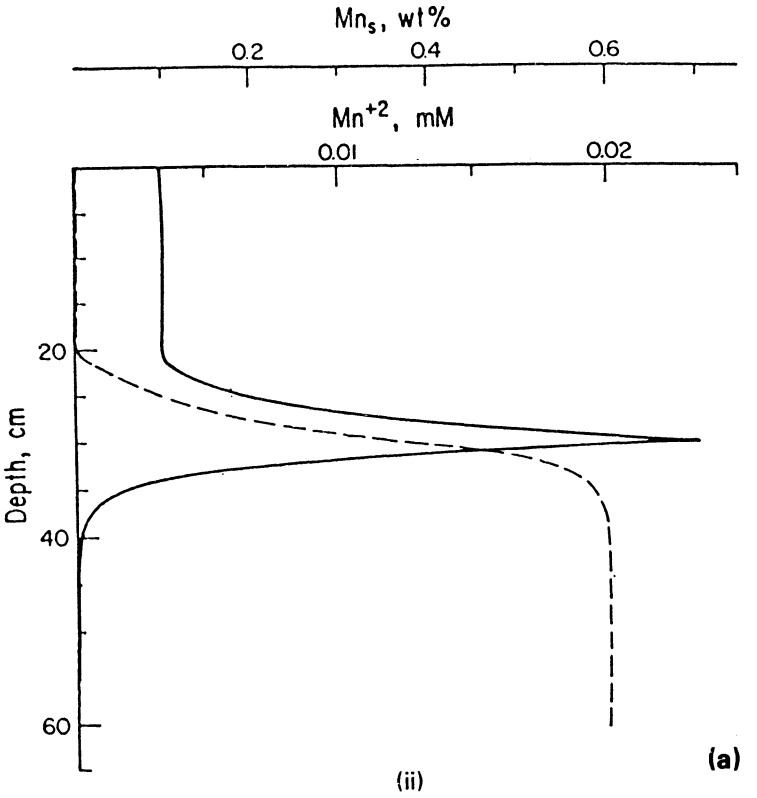

Figure (ii) Theoretical models for Mn diagenesis in marine sediments. (a) Model for porewater (broken curve) and solid-phase (full curve) Mn profiles (from Burdige & Gieskes 1983). Profiles predicted from Equations 10 to 19 using the following parameters: D_b = 71.6 cm^2 yr^{-1}, w = 3 cm/10^3 yr, ϕ = 0.8, ρ = 2.6 cm^{-3} of sediment, L_1 = 20 cm, L_2 = 30 cm, C_s^o = 0.1 wt.%, k_{ox} = 5 yr^{-1}, and k_{red} = 1.50 × 10^{-3} yr^{-1}.

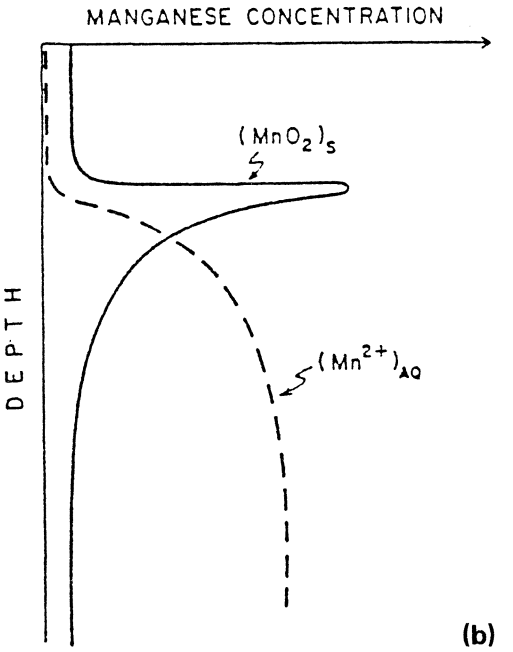

Figure (ii) (b) Schematic representation of model predicted by Froelich *et al.* (1979).

$$C_p^{red} = G - \frac{1-\phi}{\phi}\frac{Ew^2}{k_{red}D_b}\exp[-\beta(z-L_2)] \tag{11}$$

$$C_s^{ox} = C_s^o \cosh[\alpha(z - L_1)] \tag{12}$$

$$C_s^{red} = E \exp[-\beta(z - L_2)] \tag{13}$$

where

$$\alpha = (k_{ox}/D_b)^{1/2} \tag{14}$$

(assuming $4D_b k_{ox} \gg w^2$, i.e. advection in pore waters is negligible compared to diffusion) and

$$\beta = k_{red}/w \tag{15}$$

$$L_{ox} = L_2 - L_1 \tag{16}$$

$$A = \frac{C_s^o(1-\phi)w}{\phi\alpha D_b} \tag{17}$$

$$E = C_s^o \cosh(\alpha L_{ox}) \tag{18}$$

$$G = A[\sinh(\alpha L_{ox}) + \alpha/\beta \cosh(\alpha L_{ox})] \tag{19}$$

There are two unknowns (k_{ox} and k_{red}) in the equation, which can be used for a least-squares fit of the equations to actual data.

By inserting typical parameters for marine sediments into the equations the authors derived model profiles for the diagenesis of dissolved and solid-phase Mn. These are illustrated in Figure (ii) (a), and show close agreement with the diagrammatic representation suggested by Froelich *et al.* (1979) – see Figure (ii) (b).

The Mn post-depositional migration associated with this model may be summarized as follows (see text for detailed explanation). As the sediments are buried below the redox boundary, solid Mn oxides are reduced to Mn^{2+}, which diffuses upwards along the concentration gradient to be oxidized and reprecipitated. With further sedimentation, these reprecipitated oxides are again brought to the reducing zone to be redissolved, with the net result being the Mn trap at the narrow zone at the redox boundary.

Burdige & Gieskes (1983) also applied their equations to solid and porewater data from two cores in the eastern Equatorial Atlantic and obtained very good fits to the data obtained.

dissolved Mn^{2+} and its precipitation close to the sediment surface. Instead, they proposed that at present a precipitation of dissolved Mn is taking place below the enriched horizon. This was thought to be due to non-steady diagenesis brought about by a decrease in primary productivity in the overlying water, which lessened the amount of organic carbon reaching the sediment and so lowered the oxygen demand at or near the interface and set up a downward-migrating oxidation front (see Sec. 14.4.2) which eroded the Mn^{2+} interstitial-water profile.

From these various examples of Mn diagenesis it is apparent that much of the Mn remobilized in deep-sea sediments is trapped in the upper oxic layers and does not cross the sediment/water interface to yield a strong out-of-sediment flux, and any Mn that does get this far (e.g. in the absence of an oxic layer) is often incorporated into ferromanganese nodules (see Sec. 15.3.4.6). In general, therefore, Mn redox recycling in deep-sea sediments that have an upper oxic layer leads to a concentration of the element in the layer. Sawlan & Murray (1983) therefore identified two types of *upward* metal fluxes in oceanic sediments: (a) those to the base of the Mn oxidation zone, where they can become trapped, which are termed the **oxidation zone fluxes**; and (b) those to the sediment/water interface, from which they can diffuse into the overlying sea water, which are referred to as the **benthic fluxes**. In addition, *downward* metal fluxes can transport metals (e.g. Cu) to depth in the sediment. For Mn and Cu it is important to distinguish between diagenesis associated with oxic and sub-oxic processes.

(a) Oxic processes occur at or near the sediment surface and involve the

destruction of organic carbon by oxygen. This oxic release of metals from their organic carriers can lead to concentrations that are high in upper interstitial waters, relative to those in both the underlying interstitial waters and the overlying sea water, so that the concentration gradient set up can lead to a downward migration of the metals into the sediment and an upward migration into sea water. Thus, the metals released at this stage can follow a number of pathways: (i) they can diffuse out into sea water, (ii) they can be incorporated into solids close to the sediment surface, or (iii) they can diffuse downwards and be incorporated into solids at depth. The important point, however, is that the elements released during oxic diagenesis have a direct *seawater source* following their removal during biogeochemical processes within the ocean reservoir, and although they may have been recycled several times across the sediment/water interface they migrate downwards into the sediment from the surface.

(b) Sub-oxic processes usually occur at depth in the sediment column and involve the destruction of organic carbon via secondary oxidants, such as Mn oxides. During this process metals are released from the secondary oxidants and original carriers into interstitial waters at depth. As a result of this, the concentrations are greater here than higher up the sediment column, and the concentration gradients set up lead to an upward migration via diffusion through the interstitial waters. A large fraction of the metals released during sub-oxic diagenesis does in fact diffuse upwards via such concentration gradients to enter solid phases in the overlying oxic zone. However, sub-oxic diagenesis involves recycling within the sediment–interstitial water complex, and so the elements associated with this process have a direct *interstitial-water source* from reactions occurring at depth in the sediment reservoir, and mainly migrate upwards towards the surface.

A summary of the more recent data on the shallow depth diffusive fluxes of Mn, Cu and Zn is given in Table 14.5. For Cu and Mn there is a reasonable amount of data available, and for these two elements there is a remarkable degree of agreement on the magnitude of the fluxes that have been obtained from interstitial-water concentration gradients in *pelagic* sediments, those for Mn ranging from ~ 0.14 to $\sim 0.56 \times 10^{12}$ g yr^{-1} and those for Cu being in the range ~ 0.73 to $\sim 1.1 \times 10^{12}$ g yr^{-1}. However, it was shown above that the two elements behave differently with respect to their interstitial-water diffusive fluxes.

14.7 Interstitial-water inputs to the oceans: summary

(a) The interstitial waters of the most oceanic sediments originate as trapped sea water.

Table 14.5 Data on global shallow (0–50 cm) depth diffusive fluxes of Mn, Cu and Zn from marine sediments (units, 10^{12} g yr^{-1})

Element	Sediment type	Diffusive flux	Original data source
Mn	Estuarine	~189	a
	Hemi-pelagic mud	~0.88	b
	Pelagic sediments	~0.14	b
	"	~0.56	c
	"	~0.22	d
	"	~0.14	e
	Pelagic sediment range	≃0.1 - ≃0.6	
Cu	Estuarine	~11	a
	Hemi-pelagic mud	~2.3	b
	Pelagic sediments	~1.1	b
	"	~0.73	c
	"	~0.51	f
	"	~0.55	g
	"	~0.31	h
	Pelagic sediment range	≃0.3 - ≃1	
Zn	Estuarine	~3.4	a
	Pelagic sediments	~1.8	c
	"	~3.0	
	Pelagic sediment range	≃2 - ≃3	

a Elderfield & Hepworth (1975).
b Callender & Bowser (1980).
c Hartmann & Muller (1982).
d Elderfield (1976).
e Manheim (1976).
f Boyle et al. (1977).
g Chester (1981).
h Dymond in Callender & Bowser (1980).

(b) The external boundary conditions for the interstitial water–sediment complex are set by the basalt basement below and the water column above.

(c) Reactions take place in the sediment–interstitial water sandwich, during which changes are produced in the composition of the interstitial waters relative to the parent sea water, and diffusion gradients are set up via which elements migrate from high- to low-concentration regions.

(d) The most intense reactions usually take place in the upper ~ 30–50 cm of the sediment column. These reactions take place in response to the diagenetic environment, the intensity of the reactions generally decreasing in the order highly reducing shelf sediments > hemi-pelagic sediments > pelagic sediments.

(e) Data are now available on the diffusive interstitial water fluxes of a number of major and trace components. For some of these

components interstitial waters act as sinks for their removal from sea water; for others they act as sources for their addition to sea water.

(f) However, when considering interstitial water sources it is extremely important to make a distinction between primary and secondary fluxes. Interactions that take place between the basalt basement and interstitial waters, and between some types of dispersed volcanic material and interstitial waters, can lead to dissolved components being introduced into sea water for the first time. These are the **primary fluxes** in the same way as hydrothermal fluxes are primary in nature. In contrast, a large fraction of the trace metals that are mobilized into interstitial waters from particulate material via the diagenetic sequence has already been taken out of solution in sea water in the biogeochemical cycles that operate in the water column, and so is simply being returned to the dissolved state. These are the recycled or **secondary fluxes**. The dissolved trace metals associated with these fluxes can sometimes impose 'fingertips' on the water column if they escape recapture at the sediment surface. However, the important point is that they have been recycled *within* the ocean system, and as such do not represent an additional primary external source. Despite this, the diagenetic remobilization and release of elements that are initially removed from solution by incorporation into estuarine and coastal sediments can sometimes reverse the processes that occur in estuaries, and Bruland (1983) has suggested that for these elements such a diagenetic release can be regarded as an 'additional dissolved river input' to the oceans.

The diagenetic reactions that take place both within the sediment–interstitial water complex and at the sea water/sediment interface can strongly modify the composition of the material that reaches the sediment reservoir. The nature of these reactions has now been described, and in the following chapter we will consider the composition of the components that form the oceanic sediments in terms of their genetic histories, which, for some material, includes diagenetic modification.

References

Bender, M.L. & D.T. Heggie 1984. Fate of organic carbon reaching the deep sea flow: a status report. *Geochim. Cosmochim. Acta* **48,** 977–86.

Berner, R.A. 1980. *Early diagenesis: a theoretical approach.* Princeton, NJ: Princeton University Press.

Berner, R.A. 1981. A new geochemical classification of sedimentary environments. *J. Sed. Petrol.* **51,** 359–65.

Boyle, E.A., F.R. Sclater & J.M. Edmond 1977. The distribution of copper in the Pacific. *Earth Planet. Sci. Lett.* **37,** 38–54.

Bruland, K.W. 1983. Trace elements in sea water. In *Chemical oceanography*, J.P. Riley & R. Chester (eds), Vol. 8, 156–220. London: Academic Press.

Burdige, D.J. & J.M. Gieskes 1983. A pore water/solid phase diagenetic model for manganese in marine sediments. *Am. J. Sci.* **283,** 29–47.

Burdige, D.J. & C.S. Martens 1988. Biogeochemical cycling in an organic-rich coastal marine basin: 10. The role of amino acids in sedimentary carbon and nitrogen cycling. *Geochim. Cosmochim. Acta* **52,** 1571–84.

Callender, E. & C.J. Bowser 1980. Manganese and copper geochemistry of interstitial fluids from manganese nodule-rich pelagic sediments of the northeastern equatorial Pacific Ocean. *Am. J. Sci.* **280,** 1063–96.

Calvert, S.E. 1976. The mineralogy and geochemistry of near-shore sediments. In *Chemical oceanography*, J.P. Riley & R. Chester (eds), Vol. 6, 187–280. London: Academic Press.

Calvert, S.E. & N.B. Price 1970. Minor metal contents of Recent organic-rich sediments off South West Africa. *Nature* **227,** 593–5.

Chester, R. 1981. Regional trends in the distribution and sources of aluminosilicates and trace metals in recent North Atlantic deep-sea sediments. *Bull. Inst. Geol. Bassin d'Aquitaine* **31,** 325–35.

Degens, E.T. & K. Mopper 1976. Factors controlling the distribution and early diagenesis of organic materials in marine sediments. In *Chemical oceanography*, J.P. Riley & R. Chester (eds), Vol. 6, 59–113. London: Academic Press.

Drever, J.I. 1982. *The geochemistry of natural waters.* Englewood Cliffs, N.J.: Prentice-Hall.

Elderfield, H. 1976. Manganese fluxes to the oceans. *Mar. Chem.* **4,** 103–32.

Elderfield, H. & A. Hepworth 1975. Diagenesis, metals and pollution in estuaries. *Mar. Pollut. Bull.* **6,** 85–7.

Emmerson, S. & J. Dymond 1984. Benthic organic carbon cycles: toward a balance of fluxes from particle settling and pore water gradients. In *Global ocean flux study*, 285–304. Washington DC: National Academy Press.

Ertel, J.R. & J.I. Hedges 1985. Sources of sedimentary humic substances: vascular plant debris. *Geochim. Cosmochim. Acta* **49,** 2097–107.

Froelich, P.N., G.P. Klinkhammer, M.L. Bender, N.A. Luedtke, G.R. Heath, D. Cullen, P. Dauphin, D. Hammond, B. Hartman & V. Maynard 1979. Early oxidation of organic matter in pelagic sediments of the eastern equatorial Atlantic: suboxic diagenesis. *Geochim. Cosmochim. Acta* **43,** 1075–90.

Gagosian, R.B. 1986. The air–sea exchange of particulate organic matter: the sources and long-range transport of lipids in aerosols. In *The role of air–sea exchange in geochemical cycling*, P. Buat-Menard (ed.), 409–42. Dordrecht: Reidel.

Gagosian, R.B. & E.T. Peltzer 1986. The importance of atmospheric input of terrestrial material to deep sea sediments. In *Advances in organic geochemistry 1985*, D. Laythaeuser & J. Rullkotter (eds), Vol. 10, Part II, 661–9. Chichester: Wiley.

Gagosian, R.B., E.T. Peltzer & J.T. Merrill 1987. Long-range transport of terrestrially derived lipids in aerosols from the South Pacific. *Nature* **325,** 800–3.

Galoway, F. & M. Bender 1982. Diagenetic models of interstitial nitrate profiles in deep-sea suboxic sediments. *Limnol. Oceanogr.* **27,** 624–38.

Gieskes, J.M. 1983. The chemistry of interstitial waters of deep sea sediments: interpretations of deep-sea drilling data. In *Chemical oceanography*, J.P. Riley & R. Chester (eds), Vol. 8, 221–69. London: Academic Press.

REFERENCES

Grimalt, J. & J. Albaiges 1987. Sources and occurrence of C_{12}–C_{22} n-alkanes distributions with even carbon-nuclear preference in sedimentary environments. *Geochim. Cosmochim. Acta* **51,** 1379–84.

Hartmann, M. & P.J. Muller 1982. Trace metals in interstitial waters from central Pacific Ocean sediments. In *The dynamic environment of the ocean floor*, K.A. Fanning & F. Manheim (eds). Lexington, MA: Lexington Books.

Hawkesworth, C.J. & H. Elderfield 1978. The strontium isotopic composition of interstitial waters from Sites 245 and 336 to the Deep Sea Drilling Project. *Earth Planet. Sci. Lett.* **40,** 423–32.

Heath, G.R., T.C. Moore & J.P. Dauphin 1977. Organic carbon in deep-sea sediments. In *The fate of fossil fuel CO_2 in the oceans*, N.R. Anderson & A. Malahoff (eds), 605–25. New York: Plenum.

Henrichs, S.M. & J.W. Farrington 1987. Early diagenesis of amino acids and organic matter in two coastal marine sediments. *Geochim. Cosmochim. Acta* **51,** 1–15.

Jahnke, R.A., S.R. Emerson & J.W. Murray 1982. A model of oxygen reduction, denitrification, and organic matter mineralization in marine sediments. *Limnol. Oceanogr.* **27,** 610–23.

Klinkhammer, G., D.T. Heggie & D.W. Graham 1982. Metal diagenesis in oxic marine sediments. *Earth Planet. Sci. Lett.* **61,** 211–19.

Lawrence, J.R., J.M. Gieskes & W.S. Broecker 1975. Oxygen isotope and carbon composition of DSDP pore waters and the alteration of Layer II basalts. *Earth Planet. Sci. Lett.* **27,** 1–10.

Lerman, A. 1977. Migrational processes and chemical reactions in interstitial waters. In *The sea*, E.D. Goldberg, I.N. McCave, J.J. O'Brien & J.H. Steele (eds), Vol. 6, 695–738. New York: Interscience.

Lyle, M. 1983. The brown-green color transition in marine sediments: a marker of the Fe(II)–Fe(III) redox boundary. *Limnol. Oceanogr.* **28,** 1026–33.

Lynn, D.C. & E. Bonatti 1965. Mobility of manganese in diagenesis of deep-sea sediments. *Mar. Geol.* **3,** 457–74.

Manheim, F.T. 1976. Interstitial waters of marine sediments. In *Chemical oceanography*, J.P. Riley & R. Chester (eds), Vol. 6, 115–86. London: Academic Press.

Muller, P.J. & A. Mangini 1980. Organic carbon decomposition ratio in sediments of the Pacific manganese nodule belt dated by ^{230}Th and ^{231}Pa. *Earth Planet. Sci. Lett.* **51,** 96–114.

Murray, J. & R. Irvine 1895. On the chemical changes which take place in the composition of the seawater associated with blue muds on the floor of the ocean. *Trans. R. Soc. Edin.* **37,** 481–507.

Nissenbaum, A. & I.R. Kaplan 1972. Chemical and isotopic evidence for the *in situ* origin of marine substances. *Limnol. Oceanogr.* **17,** 570–82.

Oremland, R.S. & B.F. Taylor 1978. Sulfate reduction and methanogenesis in marine sediments. *Geochim. Cosmochim. Acta* **42,** 209–14.

Pederson, T.F., J.S. Vogel & J.R. Southon 1986. Copper and manganese in hemipelagic sediments at 21°N, East Pacific Rise: diagenetic contrasts. *Geochim. Cosmochim. Acta* **50,** 2019–31.

Peltzer, E.T. & R.B. Gagosian 1989. Organic geochemistry of aerosols over the Pacific Ocean. In *Chemical oceanography*, J.P. Riley & R. Chester (eds), Vol. 10, in press. London: Academic Press.

Sawlan, J.J. & J.W. Murray 1983. Trace metal remobilization in the interstitial waters of red clay and hemipelagic marine sediments. *Earth Planet. Sci. Lett.* **64,** 213–30.

Sayles, F.L. 1979. The composition and diagenesis of interstitial solutions – I. Fluxes across the seawater–sediment interface in the Atlantic Ocean. *Geochim. Cosmochim. Acta* **43,** 527–45.

Simoniet, B.R.T. 1978. The organic chemistry of marine sediments. In *Chemical oceanography*, J.P. Riley & R. Chester (eds), Vol. 7, 233–311. London: Academic Press.

Smith, K.L. & R.J. Baldwin 1984. Seasonal fluctuations in deep-sea sediment community oxygen consumption: central and eastern north Pacific. *Nature* **307,** 624–6.

Steinberg, S.M., M.I. Venkatesan & I.R. Kaplan 1987. Organic geochemistry of sediments from the continental margin off southern New England, U.S.A. – Part I. Amino acids, carbohydrates and lignin. *Mar. Chem.* **21,** 249–65.

Stumm, W. & J.J. Morgan 1981. *Aquatic chemistry*. New York: Wiley.

Tissot, B.P. & D.H. Welte 1984. *Petroleum formation and occurrence*. Berlin: Springer-Verlag.

Venkatesan, M.I. & I.R. Kaplan 1987. The lipid geochemistry of Antarctic marine sediments: Bromsfield Strait. *Mar. Chem.* **21,** 347–75.

Venkatesan, M.I., S. Steinberg & I.R. Kaplan 1988. Organic chemical characterization of sediments from the continental shelf south of New England as an indicator of shelf edge exchange. *Cont. Shelf Res.* **8,** 905–24.

Wallace, H.E., J. Thomson, T.R.S. Wilson, P.P.E. Weaver, N.C. Higgs & J.D. Hydes 1988. Active diagenetic formation of metal-rich layers in N.E. Atlantic sediments. *Geochim. Cosmochim. Acta* **52,** 1557–69.

Weaver, P.P.E. & A. Kuijpers 1983. Climatic control of turbidite deposition on the Madeira Abyssal Plain. *Nature* **306,** 360–63.

Wilson, T.R.S., J. Thompson, S. Colley, D.J. Hydes & N.C. Higgs 1985. Early organic diagenesis: the significance of progressive subsurface oxidation fronts in pelagic sediments. *Geochim. Cosmochim. Acta* **49,** 811–22.

Wilson, T.R.S., J. Thomson, J.D. Hydes, S. Colley, F. Culkin & J. Sørensen 1986a. Oxidation fronts in pelagic sediments: diagenetic formation of metal-rich layers. *Science* **232,** 927–75.

Wilson, T.R.S., J. Thomson, D.J. Hydes, S. Colley, F. Culkin & J. Sørensen 1986b. Metal-rich layers in pelagic sediments: reply. *Science* **234,** 1129.

15 The components of marine sediments

A number of the components that form the sediment building blocks will be described in the present chapter. However, it must be stressed again that no attempt will be made to adopt an all-embracing catalogue approach to the subject; rather, a limited number of individual components have been selected on the basis that they can provide information on the *processes* that control the mineralogical and chemical compositions of oceanic sediments. These sediment building-block components are described below in terms of a modification of the 'geosphere of origin' classification proposed by Goldberg (1954).

15.1 Lithogenous components

15.1.1 Definition

Following Goldberg (1954), lithogenous components are defined as those which arise from land erosion, from submarine volcanoes or from underwater weathering where the solid phase undergoes no major change during its residence in sea water.

A wide variety of solid products are mobilized on the continents and dispersed via river run-off, atmospheric deposition and glacial transport. Some of this mobilized material is trapped in continental environments, and some is brought to the oceans where it undergoes further dispersal. This material has a wide range of composition. Quantitatively, the most important of the land-derived components found in marine sediments are the clay minerals and quartz, together with generally smaller amounts of the feldspars. In addition, minor lithogenous minerals found in the oceanic sediments include amphiboles, pyroxenes, muscovite, biotite, haematite, goethite, anatase, rutile, zircon, kyanite, sillimanite, pyrophyllite, olivine, gibbsite, garnet, serpentine, tourmaline, calcite, dolomite and apatite. Even this is by no means a complete list and is meant only to show the range of minerals found in marine sediments, and in fact there is no reason why *any* continental mineral should not be found, albeit at small concentrations, in oceanic sediments. Some of these lithogenous minerals are deposited in nearshore sediments, but the finest fraction can reach open-ocean areas. The distributions of the fine-fraction lithogenous minerals in deep-sea sediments can therefore offer an insight into how

material derived from the continents is dispersed throughout the marine environment. This dispersion process is illustrated below with respect to the distribution of the clay minerals.

15.1.2 The distributions of the principal clay minerals in deep-sea sediments

The structure of the clay minerals consists of a combination of tetrahedral layers, which are made up of SiO_4 tetrahedra linked to form a sheet, and octahedral layers, which are made up of two layers of oxygen atoms or hydroxyl ions with cations of Al, Fe or Mg between them. Riley & Chester (1971) divided the principal clay minerals into two general types. In **type I** clays, the basic structure consists of a two-layer sheet of one tetrahedral and one octahedral layer (1:1 clays); in **type II** clays, the basic unit is a sandwich of two tetrahedral layers (in which there is usually some substitution of Si^{4+} by Al^{3+} in the SiO_4 tetrahedra) with one octahedral layer between them (2:1 clays). The clay minerals can be formed in a number of ways; for example some are stable weathering residues, some are metamorphic, some are hydrothermal and some are reconstituted during reverse weathering processes. A range of these clay minerals have been found in marine sediments, but the most common varieties belong to the **kaolinite**, **chlorite**, **illite** and **montmorillonite** groups. These clay minerals make up a large proportion of the < 2 μm land-derived (carbonate-free) fraction of deep-sea sediments, and since the members of the four major groups are sometimes formed under different geological conditions they are especially attractive for the study of the sources and dispersal patterns of solids in the oceans.

Much of the detailed, global-scale, work on the distributions of the clay minerals in deep-sea sediments was carried out in the 1960s by Russian and American scientists. In particular, the studies reported by Biscaye (1965) and Griffin *et al.* (1968), on the < 2 μm carbonate-free sediment fractions, provided a database that allowed major trends in the oceanic distributions of the clays to be established. The trends identified in these two studies are outlined below in terms of the principal clay mineral groups, and the distributions of the individual clays are illustrated in Figure 15.1. It is well documented that most clay minerals can be formed under a variety of geological conditions. However, in looking for major trends in the distribution patterns of the clays only their most important general sources will be identified, and although this will of necessity produce an oversimplified picture it is still a useful approach to adopt on an ocean-wide scale. Further, it must be stressed that not all the clay minerals found in deep-sea sediments are lithogenous. For example, it will be shown below that much of the montmorillonite in these deposits has a secondary hydrogenous origin. Nonetheless, it is convenient to group the clays together when using them as indicators of oceanic transport and dispersal processes.

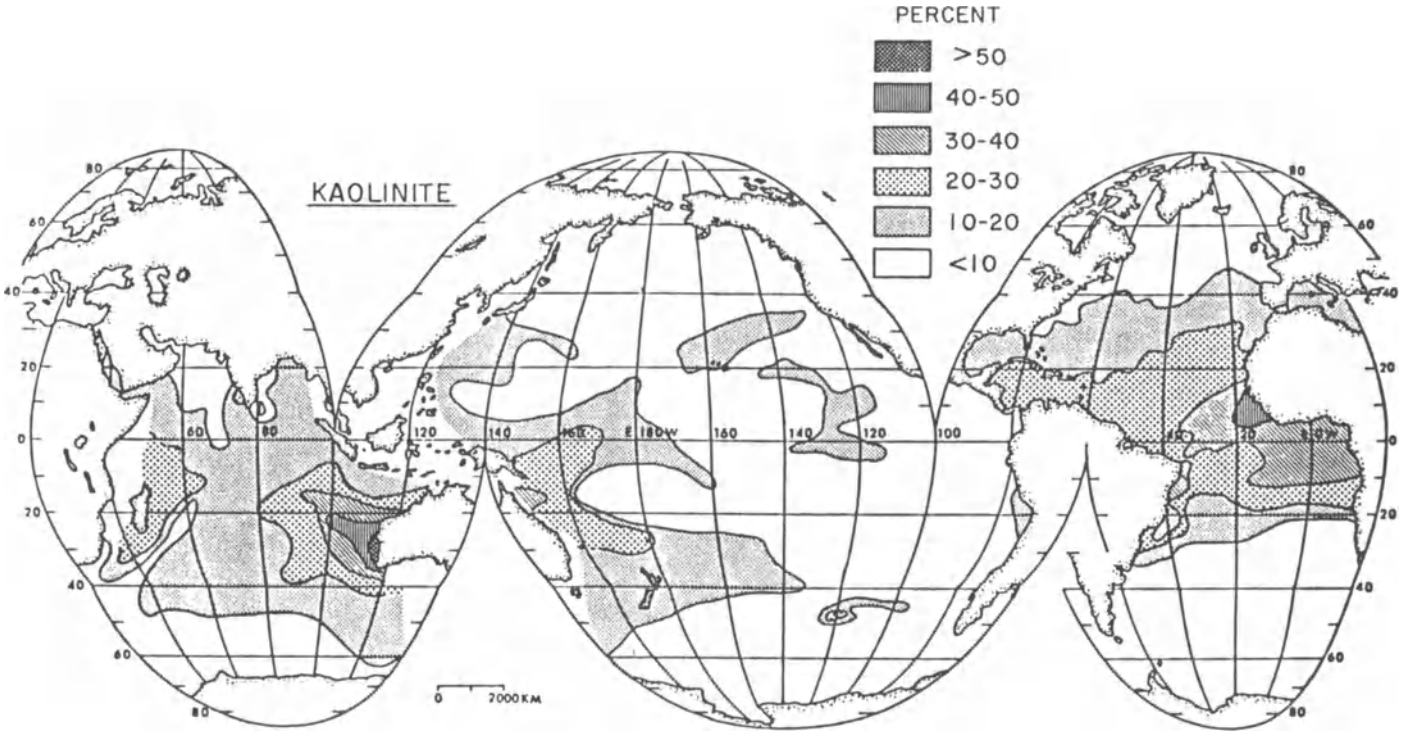

(a)

Figure 15.1a-d The concentration of clay minerals in the < 2 μm size fractions of deep-sea sediments (from Griffin *et al.* 1968); values expressed as percentages of a 100% clay sample.

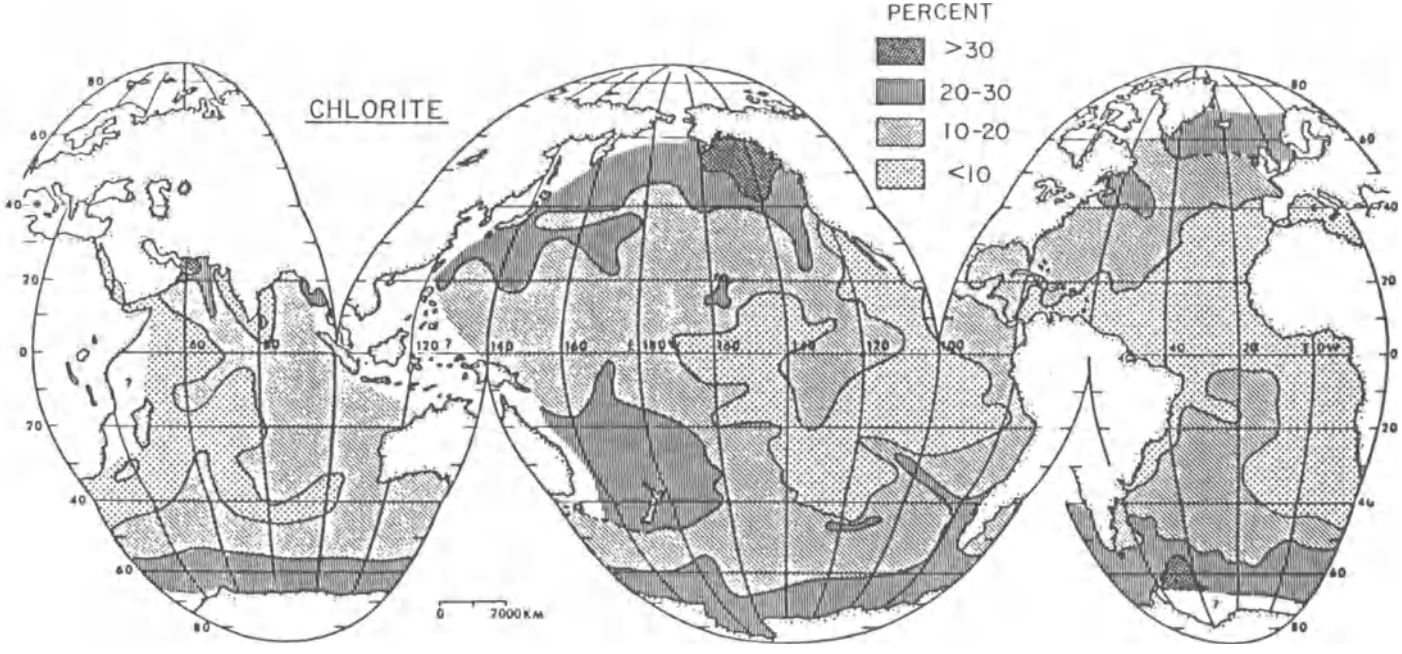

(b)

Figure 15.1b

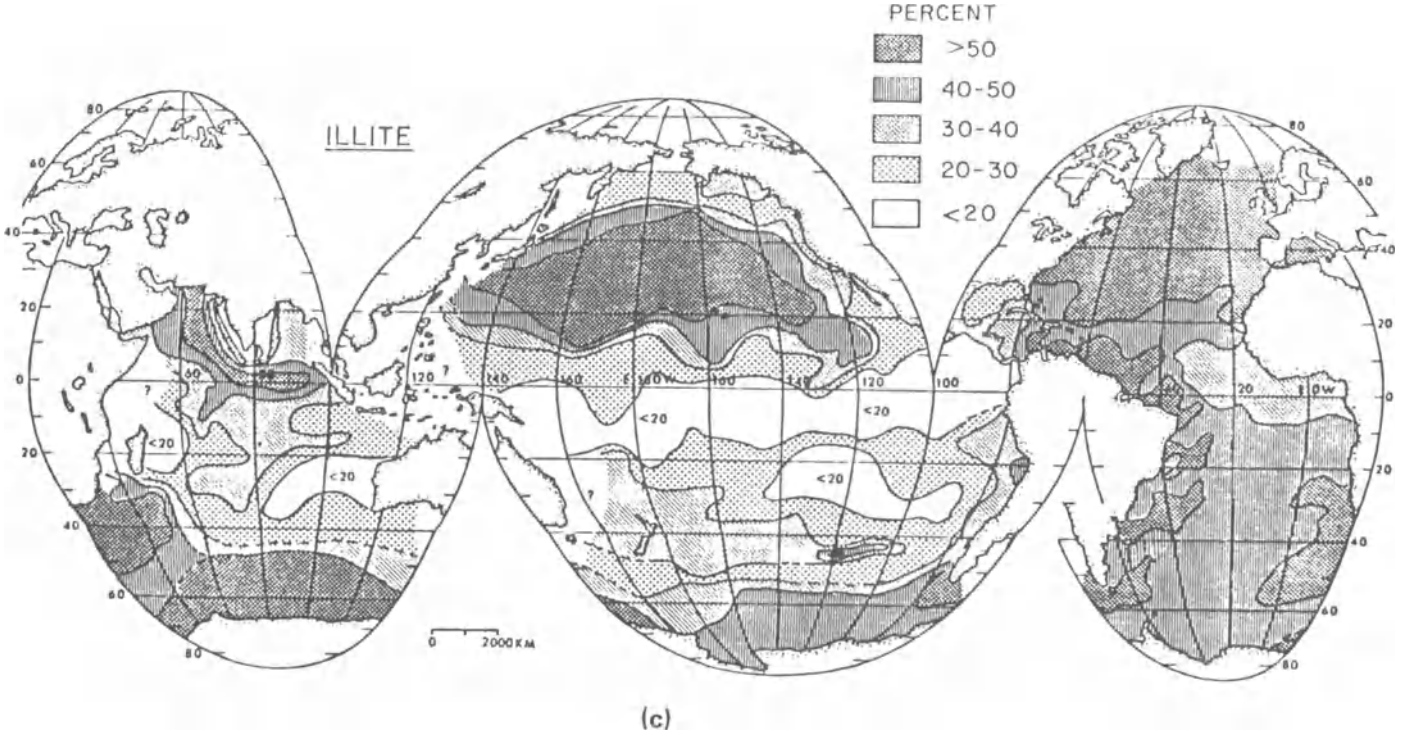

(c)

Figure 15.1c

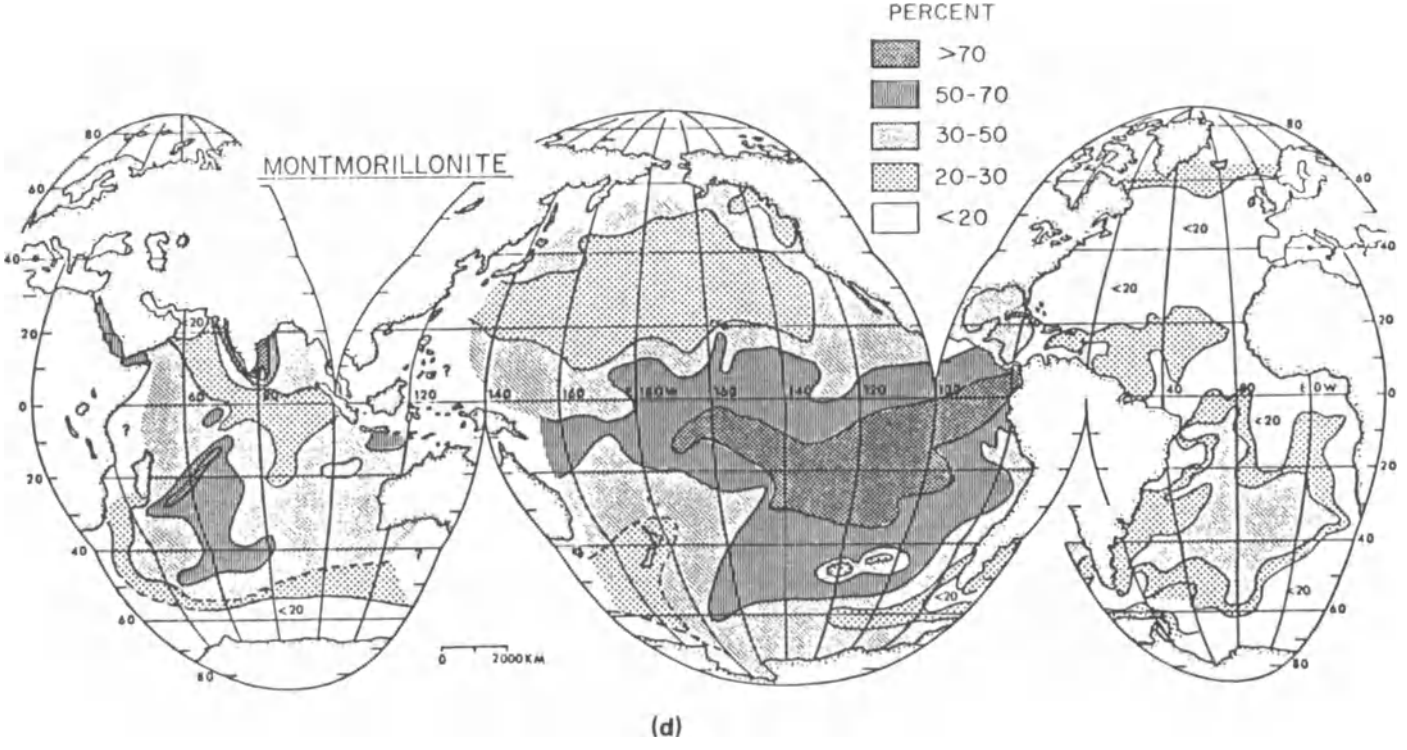

(d)

Figure 15.1d

KAOLINITE The formation of kaolinite, which is a type I clay, is characteristic of intense tropical and desert weathering, and it is clearly apparent from Figure 15.1a that the highest concentrations of the mineral are found in deep-sea sediments from equatorial regions. The mineral is transported to these regions from the surrounding arid and semi-arid land masses via fluvial and atmospheric pathways, and because of its distribution, Griffin *et al.* (1968) referred to kaolinite as the *low-latitude* clay mineral.

CHLORITE Chlorite is a type II clay mineral and has a brucite layer between the basic three-layer sandwich. It can be seen from Figure 15.1b that chlorite has its highest concentrations in sediments from the polar seas. The mineral is found in metamorphic and sedimentary rocks of the Arctic and Antarctic regions from which, in the general absence of chemical weathering, it is released by mechanical processes and is subsequently dispersed by ice rafting; the latter is confirmed by the sharp break-off in concentrations around 50°N and 50°S, which corresponds roughly to the iceberg transport limit. Thus, this chlorite is a primary mineral and not a weathering residue. Chlorite is also formed under a variety of other geological–climatic conditions, but because of its high concentrations in sediments from polar regions, Griffin *et al.* (1968) termed it the *high-latitude* clay mineral. In general, the overall distribution of chlorite in deep-sea sediments is therefore the inverse of that of the low-latitude clay mineral kaolinite.

ILLITE Members of the illite group are type II clays, which have K^+ ions lying between the three-layer basic sandwich. Illites are the most common of the clay minerals in deep-sea sediments. They are formed under a wide variety of geological conditions and, unlike kaolinites and chlorites, they are not confined to particular latitudinal bands. Most of the illites in deep-sea sediments are land-derived and their distributions are controlled by (a) the amount of land surrounding an oceanic area, and (b) the extent to which they are diluted by clays that have specific source regions (e.g. kaolinite and chlorite). As a result of a combination of these two factors, the highest concentrations of illite are found in deep-sea sediments from *mid-latitudes* (where there is less dilution from chlorite and kaolinite) in the Northern Hemisphere (which has a higher proportion of surrounding land areas than the Southern Hemisphere). This is particularly apparent in the North Pacific where the sediments have an average of 40% illite, compared with only 26% in the South Pacific – see Table 15.1. The distribution of illite in deep-sea sediments is illustrated in Figure 15.1c.

MONTMORILLONITE This is sometimes termed smectite or 'expanding-lattice' clay.) Montmorillonites are type II clays, in which water

Table 15.1 Average concentrations of the principal clay minerals in the < 2 μm carbonate-free fractions of sediments from the major oceans[a]

Oceanic area	Average % clay minerals[b]			
	Chlorite	Montmorillonite	Kaolinite	Illite
North Atlantic	10	16	20	55
South Atlantic	11	26	17	47
North Pacific	18	35	8	40
South Pacific	13	53	8	26
Indian	12	41	17	33

[a] Data from Griffin et al. (1968).
[b] Individual clay mineral percentages are expressed in terms of a 100% clay sample.

molecules are found lying between the basic three-layer sandwich units. According to Riley & Chester (1971) montmorillonites in deep-sea clays can be formed in at least three different ways: (a) as primary detrital weathering residues formed on the continents; (b) as secondary detrital degraded lattices of the illite or chlorite type which have had their inter-sheet K^+ ions replaced by water molecules; (c) as *in situ* products of the submarine weathering of volcanic material. The primary, and to a lesser extent the detrital, forms of the mineral may be regarded as providing a background supply of montmorillonite to deep-sea sediments. Superimposed on this background is the *in situ* formation of the mineral from volcanic material, and it is this form which imposes specific patterns on the distribution of montmorillonite in deep-sea sediments. As a result, the highest concentrations of this clay are found in areas that have a plentiful supply of parent volcanic debris, and in which the sedimentation rates are low enough to allow the transformation reactions to occur before the volcanic debris is buried. This is reflected in the sequence of increasing montmorillonite concentrations in deep-sea sediments, which are in the order: North Atlantic (16%) < South Atlantic (26%) < North Pacific (35%) < Indian Ocean (41%) < South Pacific (53%) – see Table 15.1. Thus, the deep-sea sediments from the South Pacific are richer in montmorillonite than those from the other oceanic areas. According to Griffin *et al.* (1968), the highest concentrations of montmorillonite in the South Pacific itself are found in sediments from mid-ocean areas, where the mineral is found in association with volcanic material, with concentration gradients decreasing towards the continents. This led the authors to propose that much of the montmorillonite in the mid-ocean sediments has an *in situ* origin from the alteration of volcanic material, and on this basis they characterized montmorillonite as being indicative of a *volcanic regime*. The distribution of montmorillonite in deep-sea sediments is illustrated in Figure 15.1d.

The North Pacific has more rivers draining into it, and a greater area of surrounding land, than the South Pacific, and this is reflected in the distributions of illite and montmorillonite in the deep-sea sediments from these two regions. That is, in the North Pacific, which receives a relatively large contribution of land-derived material, the sediments have some of the highest concentrations of the ubiquitous detrital clay mineral illite, whereas those in the South Pacific have the highest concentrations of the authigenic clay mineral montmorillonite. Griffin & Goldberg (1963) suggested therefore that the North Pacific is an area of mainly detrital deposition, but that in the South Pacific authigenic deposition is more important.

15.1.3 The chemical significance of the clay minerals in marine processes

Once they are brought into contact with saline waters the clay minerals can take part in ion-exchange reactions of the type

$$\begin{aligned}\text{Cation A (clay)} + \text{Cation B}^x \text{ (solution)} = \\ \text{Cation B (clay)} + \text{Cation A}^x \text{ (solution)}\end{aligned} \qquad (15.1)$$

where x is the charge on the cation. In addition to this normal ion exchange, the clay minerals can remove major cations from sea water during the reconstitution of degraded clay minerals, i.e. those which have had cations stripped from inter-sheet positions. According to Drever (1982), ion-exchange reactions between the clay minerals and sea water result in the *net* removal of Na, K and Mg from solution and the *net* addition of Ca to solution. Ion exchange with clay minerals can therefore affect the composition of sea water; however, according to Drever (1982), although they are probably important in the marine budgets of Na, and perhaps K, they are insignificant in that of magnesium.

A number of workers have attempted to model the composition of sea water on the basis of thermodynamic equilibria between components dissolved in the water and the mineral phases of marine sediments. This type of modelling was given a great impetus in the 1960s by Sillen. In his models, Sillen proposed that the composition of sea water was controlled by equilibria between individual minerals which would fix the ratios of the cations in solution. The removal of major ions supplied to the oceans from river run-off was then assumed to take place by the *transformation* of one clay mineral phase into another, and the equilibria were considered to operate betwen phases such as sea water–quartz–kaolinite–illite–chlorite–montmorillonite–calcite–zeolites as part of the overall atmosphere–sea water–sediment system (see e.g. Sillen 1961, 1963, 1965, 1967). In terms of these models, the coexistence of the various phases would fix the mutual ratios of all the cations, so that only the sum of their concentrations was variable, and this was assumed to be fixed by the

chloride concentration. The Sillen models offered a potentially attractive explanation for the composition of sea water. However, subsequent data (see above) showed that many of the clay minerals in deep-sea sediments are in fact land-derived in origin and are generally unreactive, at least to the extent that their source-controlled distribution patterns indicate that they do not appear to undergo significant inter-mineral transformations. In an attempt to overcome this particular objection to the equilibria model theory, Mackenzie & Garrels (1966) proposed that, rather than transformations between existing clay minerals, it was the transformation of either amorphous aluminosilicate material (formed during weathering) or degraded clays into new crystalline clay phases that controlled the reactions required by the equilibrium models. Thus

$$\text{X-ray amorphous Al silicate} + SiO_2 + HCO_3^- + \text{Cations} = \text{Cation Al silicate} + CO_2 + H_2O \qquad (15.2)$$

The normal weathering of aluminosilicates involves the uptake of CO_2 from the atmosphere and the release of bicarbonate. Thus

$$\text{Silicate} + CO_2 + H_2O = \text{Clay mineral} + HCO_3^- + H_4SiO_4 + \text{Cations} \qquad (15.3)$$

In effect, therefore, the processes occurring in the sea (i.e. in which cations, dissolved silica and bicarbonate are removed from solution) are the reverse of the weathering process on the continents; hence, they are often referred to as **reverse weathering**. There is no doubt that reverse weathering does take place within marine sediments; for example, in the formation of mixed-layer clays, zeolites, etc. However, according to Drever (1982) uptake during the formation of authigenic minerals of this type can account for only a small amount of the major ions supplied to the oceans via river input. To be effective, therefore, the clays must undergo alteration before burial in the sediments. In this context, Mackenzie & Garrels (1966) suggested that the alteration occurs during transport, and concluded that only a small fraction of the river suspended particulate load, i.e. the amorphous material, reacts to form new minerals, and that this may take place on the initial mixing of river and sea water. The amorphous silicates were thought to constitute between ~ 1 and $\sim 10\%$ of the river suspended material, and to have a composition similar to that of kaolinite. According to Mackenzie & Garrels (1966) the illite, chlorite and montmorillonite that are newly formed from this material would constitute only $\sim 7\%$ of the total mass of sediments at any one time. In view of this their contribution would be masked by the bulk input of land-derived clay minerals. Thus, their presence will be difficult to identify in deep-sea sediments.

The status of equilibria reactions between the clay minerals (and other sediment phases) in fixing the ionic composition of sea water remains a grey area. There is a tendency towards equilibria between the sediment phases and sea water, and although it is now accepted that the clay mineral transformations suggested by the Sillen equilibrium models do not take place, efforts have been made to replace them with reverse weathering type reactions. Other workers have suggested that the thermodynamic equilibria in the oceans cannot be approached fast enough to negate kinetic effects; for example, Broecker (1971) outlined a kinetic model to explain the composition of sea water. There is also another criticism that can be directed against the equilibrium model approach. The models involved propose that the cationic ratios in sea water are controlled by equilibria among the major solid phases present in marine sediments. It is now known, however, that basalt–sea water reactions can act as a sink for species such as Mg, and can in fact account for $\sim 50\%$ of the river flux of this element (see Sec. 17.2). The importance of these basalt–sea water reactions in controlling the chemistry of the oceans has been recognized by Holland (1978), who revised an earlier scheme presented by Mackenzie & Garrels (1966) for the mass-balance removal of river-derived constituents from sea water to take account of these reactions. The volume written by Holland (1978) is strongly recommended as a keynote work for students who wish to gain a deeper insight into the factors controlling the chemical compositions of the oceans and the atmosphere.

15.1.4 Clay minerals in deep-sea sediments: summary

The average concentrations of the four principal clay minerals in deep-sea sediments from the major oceans are listed in Table 15.1, and their origin–distribution trends may be summarized as follows.

(a) Illite, chlorite and kaolinite are largely land-derived, i.e. lithogenous, clays.
(b) Chlorite and kaolinite tend to be concentrated in surficial rocks and soils from particular latitudinal belts, and this is reflected in their distributions in oceanic sediments, chlorite being the *low-latitude* clay and kaolinite the *high-latitude* clay. These two clays therefore provide useful information on the origin and dispersal patterns of the < 2 μm land-derived fractions found in deep-sea sediments.
(c) Illite is also mainly land-derived, but because it is formed under a wide variety of weathering conditions it is not diagnostic of any particular supply region.
(d) The main features in the distribution of montmorillonite in deep-sea sediments arise from its transformation from volcanic debris. Thus, montmorillonite is characteristic of volcanic regimes.

15.2 Biogenous components

15.2.1 Definition

In the classification suggested by Goldberg (1954) biogenous components are defined as those produced in the biosphere, and as such include both organic matter and inorganic shell material. Organic matter in marine sediments has been discussed in Sections 14.1 and 14.3, and will not be considered here. Other biogenous components include phosphates (e.g skeletal apatite) and sulphates (e.g. barite). However, these usually make up only a few per cent of marine sediments, and in the present section attention will be focused on the major sediment-forming biogenic components, i.e. carbonate and opaline silica shell material.

15.2.2 Carbonate and opaline skeletal material in marine sediments

The most important carbonate-secreting organisms in the oceans are foraminifera, coccolithophorids and pteropods. **Forams** are animals. The planktonic forams have chambered shells (or tests) composed of calcite, which range in size from ~ 30 μm to ~ 1 mm. These planktonic forams, which are classified into a superfamily (the Globigerinacea), constitute the most common biogenous components in deep-sea sediments, evidenced by the fact that *Globigerina* oozes are the dominant type of pelagic sediment. **Coccolithophorids** are nanoplankton (plants) secreting calcite shells (generally ~ 10 μm in size), which after the death of the organism tend to break up into individual plates termed coccoliths. These coccoliths are a major component of many calcareous deep-sea sediments. **Pteropods** are pelagic molluscs which secrete large (millimetre-sized) shells of aragonite. These shells undergo dissolution at shallower depths than those composed of calcite (see below), and pteropod oozes have only a limited occurrence on the ocean floor.

The principal opal-secreting organisms in the marine environment are diatoms and radiolaria, with minor amounts of silica being produced by the silicoflagellates and the sponges. **Diatoms** are plants with frustules which range in size from a few micrometres to around 2 mm. **Radiolarians** are animals, with tests ranging in size from a few tens to a few hundred micrometres.

Both carbonate- and opal-secreting organisms contribute biogenous components to deep-sea sediments, calcareous oozes (which contain > 30% skeletal carbonate) covering ~ 50% of the deep-sea floor and siliceous oozes (which contain > 30% skeletal opal) covering ~ 15%. However, the oceanic distributions of the calcareous and siliceous oozes are very different. This is illustrated in Figure 15.2, from which it can be seen that, whereas the calcareous oozes are found mainly on topographic highs in mid-ocean areas, the siliceous oozes tend to be restricted to regions underlying coastal and equatorial upwelling, i.e. they are

correlated with high primary production in the surface waters. There are a number of reasons for this overall difference in the distributions of calcareous and siliceous oozes, and these can generally be related to the factors that control the output (production) of the organisms and the dissolution of their skeletal remains.

15.2.3 Shell production

The production of shells depends on the fertility of the ocean, which is measured by primary productivity. The two most striking features in the global distribution of primary production are (a) a ring of high-fertility zones in coastal areas around the edges of the ocean basins, and (b) a generally low fertility in the central gyres (see Sec. 9.2.2.2). Berger (1976) has identified a fundamental **biogeographical dichotomy** in the distribution of planktonic populations in the oceans between these two extreme fertility end-members. This dichotomy is represented by a coastal high-fertility regime, within a few hundred miles of the shore, which is characterized mainly by *diatoms*, and an oceanic low-fertility regime associated with a deep permanent thermocline (e.g. in the central gyres), which is characterized by *coccoliths*. This coastal–oceanic fertility dichotomy produces a geographical separation between opal-secreting and calcite-secreting organisms, and so imparts a major fingerprint on their distributions in deep-sea sediments.

15.2.4 Shell dissolution–preservation processes

After sinking from the surface layer of the ocean both calcareous and opaline skeletal remains undergo dissolution processes in response to physicochemical parameters. Sea water varies in the extent to which it is undersaturated with respect to carbonate, but it is always undersaturated with respect to opaline silica. As a result, dissolution affects carbonate and siliceous organisms to varying extents, and tends to strengthen the difference produced by the fertility dichotomy. For this reason it is convenient to treat the dissolution of calcareous and siliceous skeletal remains separately.

15.2.4.1 Carbonate shells From the time scientists first became interested in the oceans it was realized that the carbonate content of deep-sea sediments varies considerably from one location to another. Further, it soon became apparent that this was related to the depth of water under which the deposits had accumulated, with the higher carbonate contents being found in sediments located on topographic highs. There is, therefore, a first-order depth control on the occurrence of carbonate sediments in the World Ocean. In addition, there is a general depth that forms a boundary between the deposition of carbonate and non-carbonate sediments (or at least those containing only a few per cent of

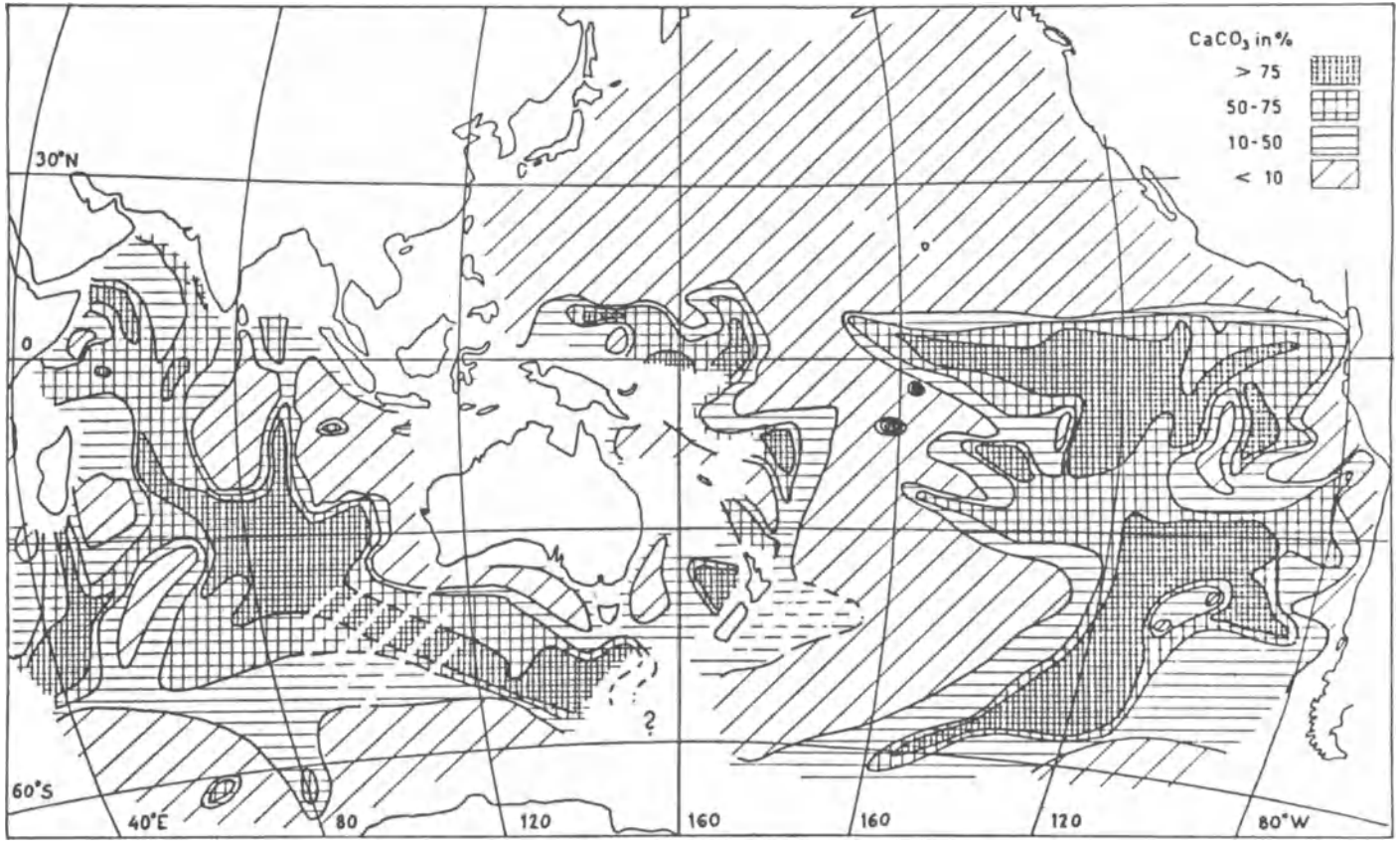

(a)

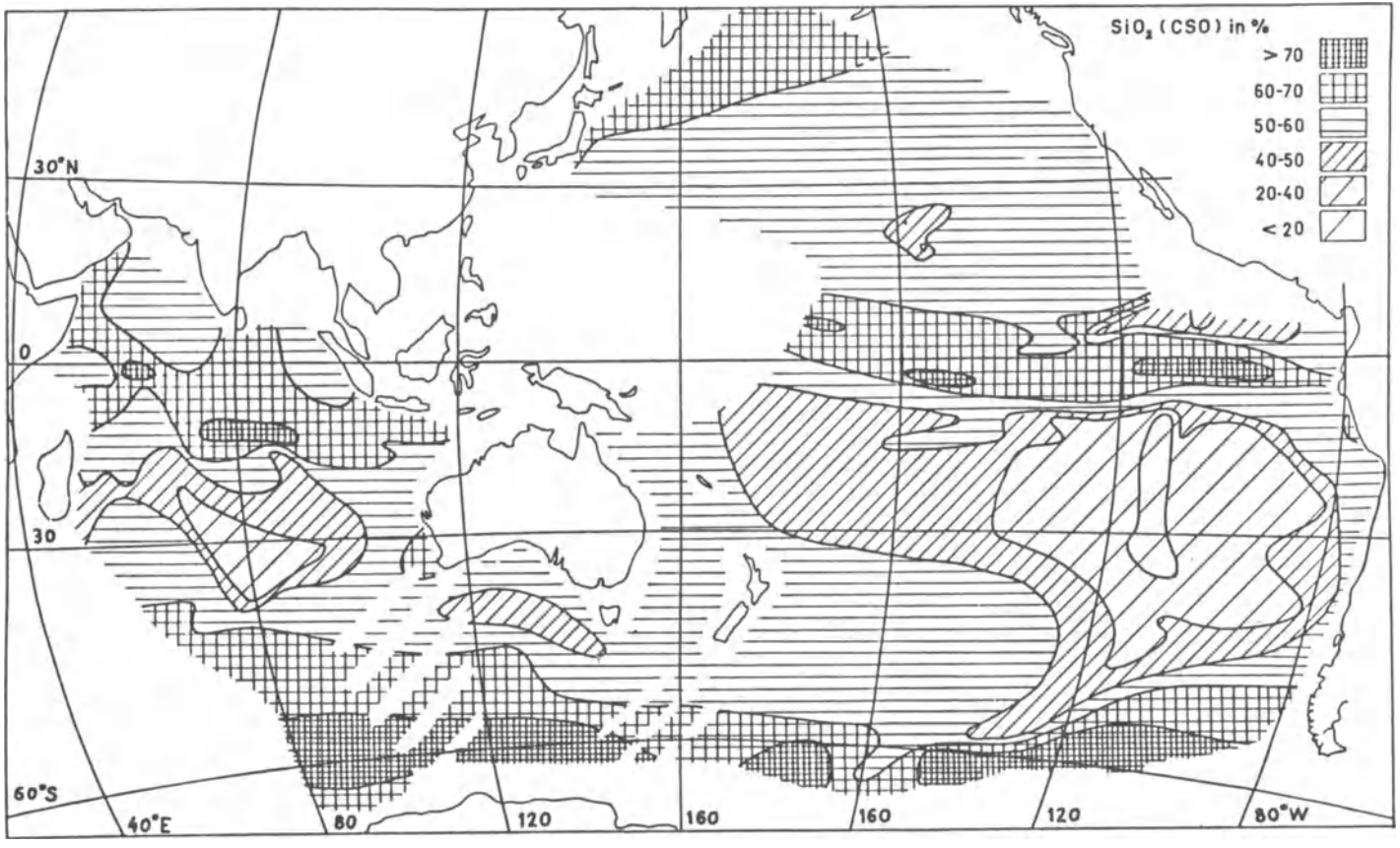

(b)

Figure 15.2 The distributions of calcium carbonate and opaline silica in deep-sea sediments. (**a**) The distribution of calcium carbonate in Indo–Pacific sediments (from Bostrom *et al.* 1973). (**b**) The distribution of opaline silica in Indo–Pacific sediments (from Bostrom *et al.* 1973); data on a carbonate-, salt- and organic matter-free basis.

carbonate). This is termed the **calcium carbonate compensation depth**. Above this depth, carbonate shells will accumulate in the sediments; at the depth itself, the rate of supply equals the rate of dissolution; at greater depths, dissolution exceeds supply and there is no *net* accumulation of significant amounts of carbonate material. The compensation depth differs for calcite and aragonite. For example, the calcite compensation depth (CCD) appears to be at ~ 4.5–5 km over much of the Atlantic, at ~ 5 km in the tropical Indian Ocean, and at ~ 3–5 km in the Pacific – see Figure 15.3. In contrast, the aragonite compensation depth (ACD) is much shallower, ranging from ~ 3 km in the western tropical North Atlantic, to between ~ 1 and ~ 2 km in the western tropical Pacific, and as low as a few hundred metres in the tropical North Pacific (Berger 1976). It is also important to recognize that in addition to the carbonate/non-carbonate deposition represented by the COD boundary, there is dissolution of shell material above this depth in the sediments. This leads to variations in the relative degrees to which carbonate shells have undergone dissolution, and there is a horizon in the sediment that separates well preserved from poorly preserved shell assemblages. Berger (1968) referred to this dissolution facies boundary, above which species are preserved more or less intact, as the sedimentary **lysocline**. In areas of low productivity the lysocline will be close to the level of the CCD, but there can be considerable separation of the two boundaries below fertile regions where there is an enhanced supply of carbonate. Berger (1976) pointed out that the lysocline surfaces are usually found at shallower depths in the Pacific than in the Atlantic, and suggested that this is the fundamental reason for the difference in the extent to which carbonates cover the sea floor in the two oceans, i.e. ~ 67.5% in the Atlantic as opposed to only ~ 36% in the Pacific.

The main feature in the distribution of calcium carbonate in deep-sea sediments is therefore its common occurrence on topographic highs. One of the keys necessary to understand how this depth control operates lies in the fact that the degree to which sea water is undersaturated with respect to calcium carbonate varies down the water column. The upper waters are always supersaturated with respect to calcium carbonate; however, the degree of saturation decreases by a factor of up to 10 with depth, leading to undersaturation at intermediate depths. It is this saturation–undersaturation depth pattern that can be regarded as being the driving force behind carbonate dissolution. Both calcite and aragonite are significantly soluble in sea water. The solubility increases with increasing pressure (and so depth) and decreasing temperature, with the result that carbonate shells are susceptible to dissolution both during their transit down the water column and when they reach the bottom sediment.

Shell dissolution in the sediments themselves appears to be the major process that produces the observed distribution of the carbonates in the

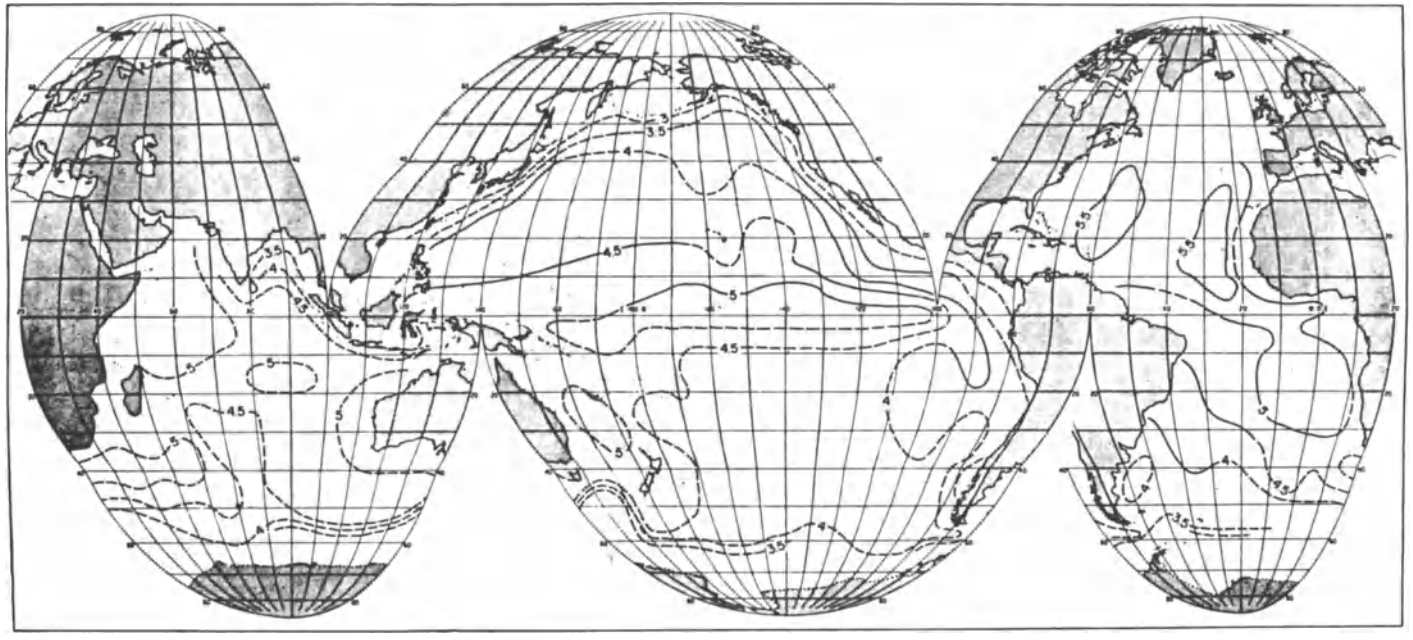

Figure 15.3 The distribution of the calcium carbonate compensation depth in the World Ocean (from Berger and Winterer 1974). This is the depth (km) of the level at which the carbonate content of deep-sea sediments decreases to a few per cent.

oceans, so that the degree to which the overlying waters are undersaturated with respect to calcium carbonate should exert a fundamental control on shell preservation. Because this undersaturation increases with depth, it has been suggested that **thermodynamic equilibrium** controls apply. Originally, it was thought that sea water was supersaturated with respect to calcite at depths above the CCD, although some doubt has been cast on this. However, Li *et al.* (1969) used measured values for the partial pressure of CO_2 and the total content of dissolved inorganic CO_2 to calculate the degree of saturation of calcium carbonate in the water column. Their results indicated that Atlantic waters become undersaturated with respect to calcite at depths of ~ 4–5 km and with respect to aragonite at depths of ~ 1–2.5 km, whereas those of the Pacific become undersaturated with respect to calcite at ~ 1.5–3.0 km and with respect to aragonite at ~ 0.3 km. The authors concluded that the CCD in both Atlantic sediments (~ 4.5 km) and Pacific sediments (~ 3.5 km) does therefore reflect a transition from saturation to undersaturation in the overlying waters, the differences in the depth of the CCD in the two oceans being a function of the differences in the dissolved CO_2 in the two water masses.

Broecker & Peng (1982) also considered the controls on the CCD and related them to reactions occurring in the seawater carbonate system (see Sec. 8.4.2). In doing this, they introduced the concept of a **saturation horizon**. When $CaCO_3$ undergoes dissolution, calcium ions and carbonate ions are formed, and since the calcium content of sea water is approximately constant Broecker & Peng (1982) simplified the degree of calcium carbonate saturation by expressing it in terms of carbonate ions only. Thus

$$D = \frac{[CO_3^{2-}]_{\text{sea water}}}{[CO_3^{2-}]_{\text{saturated sea water}}} \tag{15.4}$$

where D is the ratio of the carbonate ion content of a seawater sample to that of one saturated in the laboratory under the same temperature and pressure conditions. Thus, D is a measure of the degree to which the seawater sample is saturated with respect to calcite or aragonite, and so indicates the strength of the driving force for carbonate dissolution. The authors gave data on the distribution of carbonate ion in the oceans, and compared the values to those of the saturation carbonate ion content for calcite and aragonite. They then used the relationship $[CO_3^{2-}]_{in\ situ} - [CO_3^{2-}]_{sat}$ as a measure of the tendency for carbonate to dissolve, positive values indicating supersaturation and negative values undersaturation. In this terminology, the zero value is termed the *saturation horizon*. Broecker & Peng (1982) found that for calcite the saturation horizon was deepest in the western Atlantic Ocean (~ 4.5 km), intermediate in the

western Indian Ocean (~ 3.5 km) and least deep in the North Pacific (< 3 km). The saturation horizons for aragonite were much shallower than those for calcite, being ~ 3.5 km in the Atlantic and actually falling within the main thermocline in the Indian and Pacific Oceans. For calcite, the depth of the saturation horizon was about the same as that of the sedimentary lysocline, and it is here that the driving force for calcite dissolution is zero.

Drever (1982) sees the arguments over the nature of the factors that control the CCD as revolving around the central issue of whether it is the result of a transition from supersaturated to undersaturated conditions in the water column, or whether it is controlled by kinetic (rate) factors. In this context, the *kinetic* model proposed by Broecker (1971) for the composition of sea water is of special interest. In this model, it was suggested that the amount of carbon leaving the ocean is fixed by the phosphorus cycle, but that the presence of large amounts of calcium carbonate in deep-sea sediments proves that this organic removal is not adequate to cope with all the incoming carbon. The excess carbon is therefore precipitated by organisms as $CaCO_3$, but the rate at which this happens exceeds the rate at which the carbonate is removed into sediments, witnessed by the fact that shell dissolution, rather than preservation, occurs in deep waters. Broecker (1971) suggests, therefore, that organisms are generating more $CaCO_3$ than is necessary for the removal of carbon. This has caused the carbonate ion content of the sea to drop to a level low enough that a large area of the sea floor is covered by waters that are corrosive to $CaCO_3$; this area has a size sufficient to ensure that the overproduction of $CaCO_3$ is just balanced by deep water solution. The position of the CCD (or the lysocline, or the saturation horizon) is critical to this balance. For example, if it were too deep, more carbonate would accumulate and the removal of carbon would exceed its supply. As a result, the carbonate ion content of sea water would decrease, forcing the CCD upwards until the balance was again achieved. Broecker (1971) concludes that the carbonate ion content of sea water is therefore fixed by the requirement that carbon flows smoothly through the ocean system. There is evidence that the dissolution of calcium carbonate was greater in the last interglacial than during the last glacial period, so that the carbonate ion content of sea water must have been higher during the former time. Broecker (1971) believes that such a difference suggests that the ratio of $CaCO_3$ productivity to the dissolved $CaCO_3$ supplied by rivers was higher during the warm than the cold period. Thus, the relationship between the rate of production of $CaCO_3$ by plankton (controlled by the availability of phosphorus) to the rate of supply of dissolved $CaCO_3$ from rivers becomes critical in controlling the depth of the CCD. If the ratio is high, most of the carbonate must undergo dissolution to maintain the balance between the input and

removal of the calcium and carbonate species (otherwise the ocean would run out of Ca), and this will result in a shallow CCD. If the ratio is low, more of the carbonate will be preserved and the CCD will be found at greater depths (see also Drever 1982). Thus, the CCD acts to balance the calcium (and carbonate) input–output mechanisms by responding to changes in the ratio between them. In terms of the kinetic model, Broecker (1971) points out that although there is a calcite saturation horizon in the oceans, there are large gradients towards supersaturation and undersaturation on either side of it. The author concludes that since the position of the horizon is controlled by 'economic' factors, e.g. the necessity for carbon to flow smoothly through the system, the thermodynamic equilibrium restriction constrains only the order of magnitude of the carbonate ion content at any point in the sea.

Both the equilibrium and kinetic models have been the subject of criticism. In the equilibrium thermodynamic models the CCD is related to a saturation horizon, i.e. a depth below which sea water is undersaturated with respect to calcium carbonate. However, Edmond (1974) demonstrated that the saturation horizon is not in fact coincident with the CCD, but rather occurs everywhere at a shallower depth. This author also considered the validity of a chemical kinetic model in which, following Morse & Berner (1972), it was suggested that the destruction rate of carbonate sediments is controlled by an abrupt change in dissolution rate, which is related to a critical pH. Edmond (1974) mapped this **critical kinetic horizon**, but found that it was located at a depth several hundreds of metres shallower than the lysocline in the southwest Pacific and almost a kilometre deeper in the Antarctic. Edmond (1974) looked closely at the analogy between carbonate and silicate sedimentation in the deep ocean. Although sea water is always undersaturated to some degree with respect to opaline silica, siliceous sediments are preserved at all water depths, their major concentration at the ocean margins being dictated by the patterns of productivity. Thus, as Edmond (1974) points out, a steady-state situation operates for opaline shells, with dissolution being sufficiently slow to allow a significant fraction of the tests to survive long enough to be protected within the sediment. Edmond (1974) also demonstrated that there is a similarity in the distributions of alkalinity and silica in the oceans, and thus in the sites of dissolution of both calcite and opal. However, the solution chemistries of the two phases are very different, which led the author to suggest that the dissolution of calcite and opal is not particularly sensitive to equilibrium effects. He concluded, therefore, that the down-column transit of both opaline and calcareous tests through the water column is fast enough to make the contrasting influences of the two chemical regimes unimportant, and that the calcite compensation depth is best described by a steady-state *physical* model, rather than by a thermodynamic or a kinetic chemical model. At present,

the controversy over the nature of the factors controlling the CCD remains unresolved.

The distribution of calcium carbonate in deep-sea sediments from the major oceans is now known in some detail – see e.g. the Pacific Ocean (Berger *et al.* 1976), the Indian Ocean (Kolla *et al.* 1976) and the Atlantic Ocean (Biscaye *et al.* 1976). For example, Biscaye *et al.* (1976) used over 1700 data points to construct a map showing the areal distribution of calcium carbonate in surface sediments from the Atlantic Ocean and adjacent waters, and this is illustrated in Figure 15.4. The study confirmed the first-order relationship between the amount of calcium carbonate in deep-sea sediments and the water depth under which they were deposited, the highest concentrations being found on the Mid-Atlantic Ridge (MAR) and flanks, and on smaller topographic highs such as the Bermuda Rise, the Walvis Ridge and the Falkland Rise. However, this relationship was perturbed by several factors, which superimposed other controls on the concentrations of carbonate in the sediments. These included: (a) high surface productivity, where an enhanced supply of biogenic material can result in the accumulation of carbonate at depths greater than those under non-productive areas (e.g. in the Cape Verde Basin); (b) dilution by non-carbonate components, which can swamp the shell material; and (c) enhanced dissolution, e.g. under the influence of an influx of corrosive, CO_2-rich, bottom waters in the basins on the western side of the ocean, which results in dissolution being so effective that carbonate concentrations are low at all water depths (e.g. in the Argentine Basin). It may be concluded, therefore, that there is a general first-order relationship between calcium carbonate in the sediments and water depth in the Atlantic. However, the details in the carbonate distribution in the surface sediments are influenced by three rate processes associated with primary productivity, dilution of the carbonate components, and shell dissolution, all of which perturb the general carbonate–water depth relationship in the Atlantic. Thus, both *thermodynamic* and *kinetic* factors affect the distribution of carbonates in Atlantic deep-sea sediments.

15.2.4.2 Opaline shells Sea water is undersaturated everywhere with respect to opaline silica, and the distribution of opal in deep-sea sediments therefore mainly reflects the large-scale differences in the production of the silica-secreting organisms in the overlying waters. Silicate has a nutrient-type profile in the water column (see Sec. 9.1.2), with the consequence that much of the silica taken up in opaline shells is redissolved in the upper water layers. Most of the opaline silica that does escape from the upper waters appears to undergo dissolution on the sea floor rather than as it falls through the lower water column. Dissolution also continues in the sediment–interstitial water complex, and this can

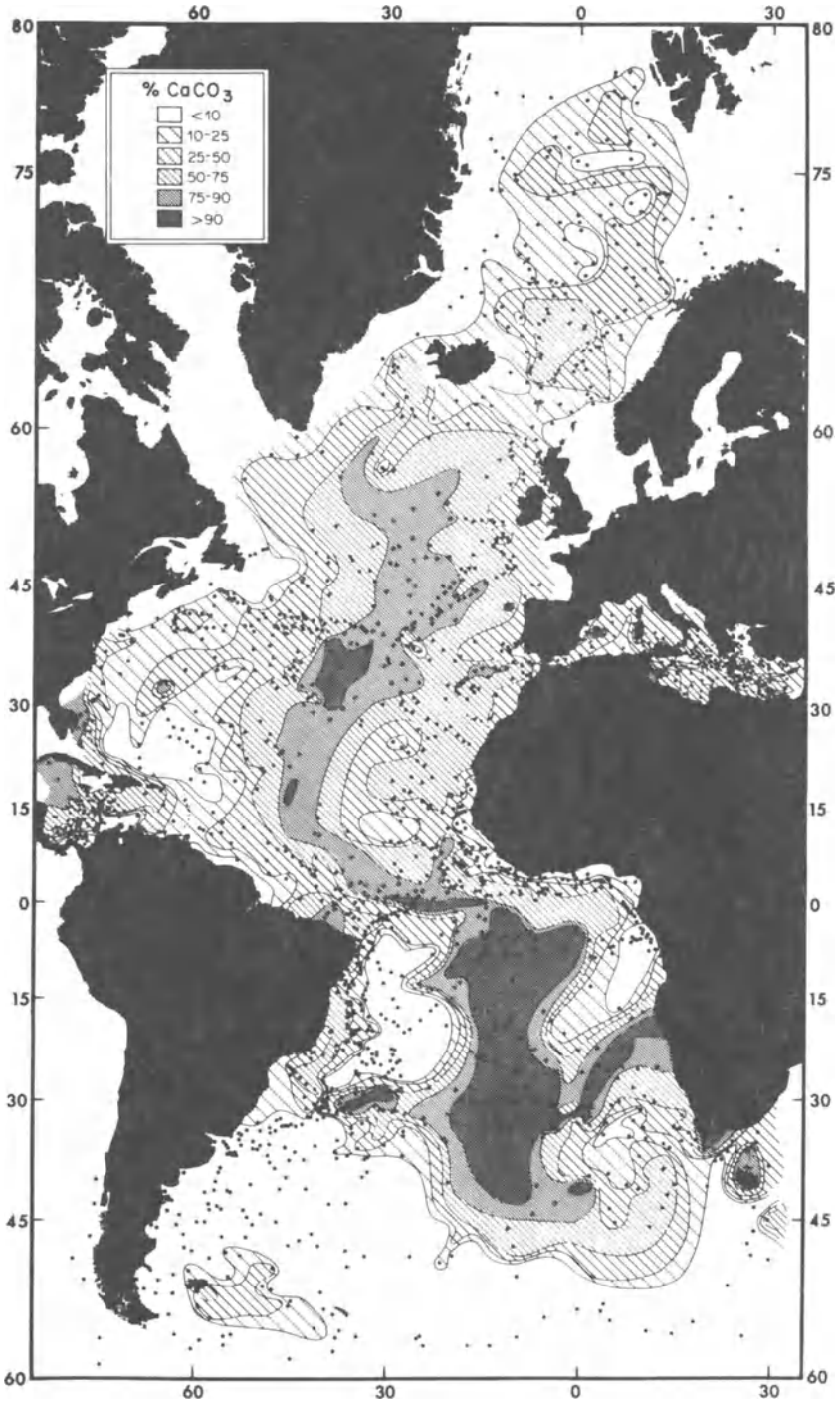

Figure 15.4 The present-day distribution of calcium carbonate in Atlantic Ocean surface sediments (from Biscaye *et al.* 1976).

result in the diffusion of dissolved silica out of bottom sediments.

The principal factors that control the distribution of opaline silica in deep-sea sediments can be summarized as follows. Since sea water is universally undersaturated with respect to opaline silica, the extent to which this component is preserved in deep-sea sediments ultimately depends on the degree to which it has undergone, or escaped, dissolution. The preservation of opaline silica in deep-sea sediments is therefore influenced by: (a) the thermodynamic driving force, which is a function of the temperature, pressure and H_4SiO_4 content of the bottom water; (b) the rate of production of opaline organisms in the overlying waters, i.e. the greater the amount of opal falling down the water column, the greater the chance it will be preserved in the sediment, with the result that the highest concentrations of opal are found in sediments under areas of coastal and equatorial upwelling; and (c) the extent to which the opaline remains are diluted with non-opaline material, which acts to decrease the rate at which the opal dissolves.

The overall effect of the various fertility (production), dissolution and preservation processes is a very restricted, but highly distinctive, distribution of siliceous oozes in the oceans – see Figure 15.2b. This distribution correlates with the high primary productivity upwelling areas, and as a result the distribution of sediments rich in siliceous organisms is concentrated into three major bands.

(a) A Southern Hemisphere polar band, or ring, which nearly circles the globe. The sediments here are mainly diatomaceous oozes, and according to Calvert (1968) they account for ~ 80% of the total silica accumulation in the oceans.
(b) A Northern Hemisphere polar belt, which is found in the Pacific Ocean but is absent from the Atlantic and Indian Oceans.
(c) An equatorial belt in the Pacific Ocean, in which the sediments are relatively rich in radiolaria.

In addition to these three major bands, siliceous sediments are found in a number of coastal regions where upwelling occurs (e.g. in the Gulf of California and off the coast of Namibia). In general, diatoms are the dominant organisms in high-latitude and coastal siliceous sediments, whereas radiolarians predominate in the equatorial sediments.

15.2.5 The chemical significance of carbonates and opaline silica in marine processes

15.2.5.1 Carbonates The production, dissolution and sediment preservation patterns of plankton-produced calcium carbonate in the ocean system have important effects on the chemistry of sea water, and on the

global CO_2 system (including climate); these have been discussed above and in Section 8.4.3.3. The formation of the skeletal carbonates, and their incorporation into deep-sea sediments, also regulates the marine budget of calcium, and carbonate sediments probably remove all of the element supplied to sea water from both river run-off and basalt–sea water reactions (Drever 1982). However, because the skeletal production of calcium carbonate exceeds the amount supplied via the inputs, the budget has to be interrupted by the dissolution of carbonates at depth in the water column. Carbonate sedimentation also removes carbon from the oceans. The production of skeletal carbonates does not appear to play a major role in the marine budgets of elements other than calcium and carbon. However, Sr, which can be found in the carbonate lattice, is an exception to this and much of the Sr in deep-sea sediments is associated with carbonate material. Skeletal carbonates probably contain a small amount of magnesium ($\sim 0.5\%$), but according to Drever (1974) carbonate formation can only account for $\sim 6\%$ of the Mg supplied to the oceans by fluvial transport. Carbonate skeletal material undergoes transit down the water column, but it does not appear to be a significant carrier for the nutrient-type trace metals (see Sec. 11.6.3.2). Overall, therefore, the carbonate skeletal material incorporated into deep-sea sediments tends to be relatively pure, and contains very low concentrations of trace metals other than Sr. However, the carbonate shells can absorb certain scavenging-type elements onto their surfaces; e.g. Martin & Knauer (1983) reported that Mn can undergo down-column transport adsorbed on $CaCO_3$ surfaces, and if the carbonate is dissolved the Mn could remain behind to become associated with other components in the sediment.

Because they contain information on the fertility, chemistry and climate of the oceans, carbonate deep-sea sediments have been of particular value in palaeo-oceanography. For example, data on water temperatures prevalent at the time of deposition have been obtained from ancient carbonates using temperature-dependent species distribution and $^{18}O : {}^{16}O$ ratios. Studies of this kind have played a large part in evaluating past oceanic environments in the CLIMAP programme; for a detailed treatment of the involvement of carbonates in palaeo-oceanography the reader is referred to the following key publications: Emiliani & Flint (1963), Broecker (1971), Luz & Shackleton (1975), Berger (1976), CLIMAP Project Members (1976), Schopf (1980), Vincent & Berger (1981), Shackleton (1982) and the volume edited by Hay (1974).

15.2.5.2 Opaline silica The marine budget of silicon is more complicated than that of calcium, and the role played by biogenous sediments in the removal of silica has proved difficult to assess. In fact, the topic has given rise to considerable controversy and two schools of thought have emerged in the literature regarding the factors that control the marine silica budget.

(a) **Biological removal**. Calvert (1968) proposed that biological processes involving the incorporation of opaline shell material into sediments are the most important pathway for the removal of silica from the oceans, with most of the removal (~ 80%) taking place around Antarctica. Calvert (1968) estimated that ~ 3.6×10^{14} g yr^{-1} of SiO_2 are taken out of sea water by biological processes, which amounts to ~ 83% of the generally accepted estimate for the river input of silica (i.e. 4.3×10^{14} g yr^{-1}).

(b) **Non-biological removal**. Some authors have proposed that the removal of silica by organisms, and the subsequent burial in the sediments of that fraction which escapes dissolution, can only account for a relatively small fraction of the input of silica to the ocean system (see e.g. Wollast 1974).

Between these two extremes, other authors have suggested that, while biological removal is certainly significant in the marine budget of silica, it is not the major control on it. For example, Burton & Liss (1968) estimated that biological processes remove SiO_2 at a rate of ~ 1.9×10^{14} g yr^{-1}, which is ~ 44% of the amount added by rivers each year. Because of this type of imbalance, other (i.e. inorganic) mechanisms have had to be sought to account for the removal of silica from the oceans. These have included: (a) reactions with clay minerals, including reverse weathering reactions between dissolved silicon and degraded silicates (see Sec. 15.1.3); (b) incorporation into quartz overgrowths, or into authigenic aluminosilicates such as palygorskite and sepiolite; and (c) reactions with particulate material during the early stages of estuarine mixing. In one of the most recent assessments of the marine silica budget, DeMaster (1981) critically examined the previous supply–removal estimates. He concluded that river run-off (~ $(4.1 \pm 0.8) \times 10^{14}$ g yr^{-1}) and hydrothermal emanations (~ $(1.9 \pm 1.0) \times 10^{14}$ g yr^{-1}) supply most of the silica brought to the marine environment. Although DeMaster (1981) was not able to construct an exact balance between supply and removal, he concluded that about two-thirds of the silica supplied to the oceans can be accounted for via the deposition of biogenic continental margin and deep-sea sediments, with > 25% of the total input being taken up by sediments depositing beneath the Antarctic Polar Front. Details of the marine silica budget outlined by DeMaster (1981) are given in Table 15.2. An interesting feature of this budget is that although coastal upwelling areas, such as those found in the Gulf of California and Walvis Bay, have some of the highest silica accumulation rates in the World Ocean, their relatively small areal extent means that the siliceous sediments deposited there take up < 5% of the total silica supplied to the marine environment.

From most of the budget estimates it is apparent, therefore, that

Table 15.2 The marine budget of silica (units, 10^{14} g yr^{-1})

	a	b
SUPPLY		
Rivers	4.2±0.8	4.3
Hydrothermal emanations	1.9±1.0	0.1
TOTAL	6.1±1.8	4.4
REMOVAL		
Deep sea		
Antarctic	2.5	2.5
Bering Sea	0.28	0.3
North Pacific	0.15	0.3
Sea of Okhotsk	0.14	-
Poorly siliceous Indian, Atlantic and Pacific sediments	<0.1	<0.1
Peripheral Antarctic basins	<0.02	-
Equatorial Pacific	0.01	0.01
SUB-TOTAL	3.1-3.2	3.1-3.2
Continental margins		
Estuaries	<0.8	
Gulf of California	0.10	
Walvis Bay	<0.11	
North America west coast basins	<0.10	
Peru and Chile coast	<0.06	
SUB-TOTAL	0.1-1.2	0.5-1.7
TOTAL DEEP SEA AND CONTINENTAL MARGIN REMOVAL	3.2-4.4	3.6-4.9

[a] From DeMaster (1981).

[b] From DeMaster (pers. comm).

biological processes involving the formation of opaline skeletal material, and its preservation in sediments, play an important, perhaps the major, role in the marine silica budget.

15.2.6 Carbonate and opaline shell material in marine sediments: summary

The oceanic fertility dichotomy in which diatoms are favoured in highly productive regions and coccoliths in poorly productive regions, combined with differences in the oceanic chemistries of the carbonate and silica systems, has led to distinct geographical patterns in the distributions of

calcareous and siliceous oozes. Thus, in general, the calcareous deposits are concentrated in relatively shallow open-ocean regions, whereas the siliceous deposits are found mainly at the edges of the oceans (with the exception of the radiolarian-rich band under the Equatorial Pacific high-productivity zone). In addition to these global distribution patterns, Berger (1976) has made the important observation that there is a distinct tendency for carbonates to accumulate in the Atlantic (where they cover ~ 67.5% of the deep-sea floor, compared to ~ 54% in the Indian Ocean and ~ 36% in the Pacific), and for siliceous oozes to be deposited in the Pacific and Indian Oceans (where they cover ~ 15% and ~ 20% of the deep-sea floor, respectively, compared to only ~ 7% in the Antarctic). The author ascribes these differences to the inter-ocean basin fractionation of silica and lime as a consequence of the global deep water circulation path. He points out that according to Redfield *et al.* (1963) the North Atlantic can be described as having an **anti-estuarine** type of circulation in which deep water flows outwards and is replaced at the surface sources, i.e. deep water is exchanged for shallow water. Vertical profiles of the nutrient elements exhibit higher concentrations at depth due to regeneration (see Sec. 9.1.2), so that an anti-estuarine system, which exchanges deep water for shallow water, becomes depleted in nutrients. Further, the bottom waters in such a system are young and oxygenated, and tend to be close to saturation with respect to calcite, thus allowing carbonate sediments to accumulate. In contrast, the North Pacific has an **estuarine** type of circulation, in which shallow water is exchanged for deep water, thus promoting upwelling. As a consequence, the waters of the North Pacific are enriched in nutrients and since they are older they are also enriched in CO_2. Thus, they tend to be undersaturated with respect to calcite even at shallow depths, which leads to enhanced calcite dissolution. In this type of system, therefore, both production and preservation processes favour the deposition of silica. The relationship between the North Atlantic anti-estuarine–carbonate-rich system and the North Pacific estuarine–silica-rich system are illustrated in Figures 15.5a and b.

15.3 'Hydrogenous' components: halmyrolysates and precipitates

15.3.1 Definition

There is some confusion in the literature over the terminology used to describe those components of marine sediments which have been formed inorganically from constituents dissolved in sea water. In the initial 'geosphere of origin' classification outlined by Goldberg (1954) **hydrogenous** components were defined as those which result from the formation of solid material in the sea by inorganic reactions, i.e. by non-biological

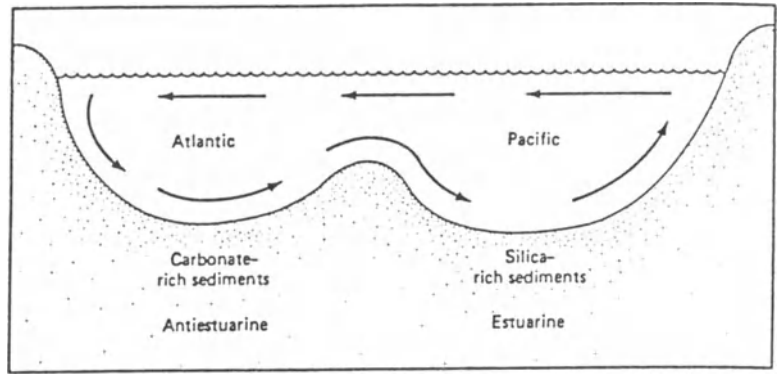

(a)

Figure 15.5 Water circulation patterns that influence the distributions of carbonate-rich and silica-rich sediments in the Atlantic and Pacific Oceans. (**a**) Schematic representation of the anti-estuarine and estuarine water circulation patterns in the Atlantic and Pacific Oceans (from Kennet 1982). In the Atlantic, young oxygenated bottom waters are formed at high latitudes, where deep water is exchanged for shallow water (anti-estuarine circulation type). The young oxygenated waters tend to be close to saturation with respect to calcite, which allows carbonate to accumulate over large parts of the ocean. In contrast, the Pacific receives older deep water at depth, i.e. it exchanges shallow water for deep water (estuarine circulation type). These older deep waters are rich in CO_2, i.e. they are relatively acidic, and as a result carbonate-poor sediments accumulate over much of the North Pacific. Silica-rich sediments accumulate in areas of upwelling.

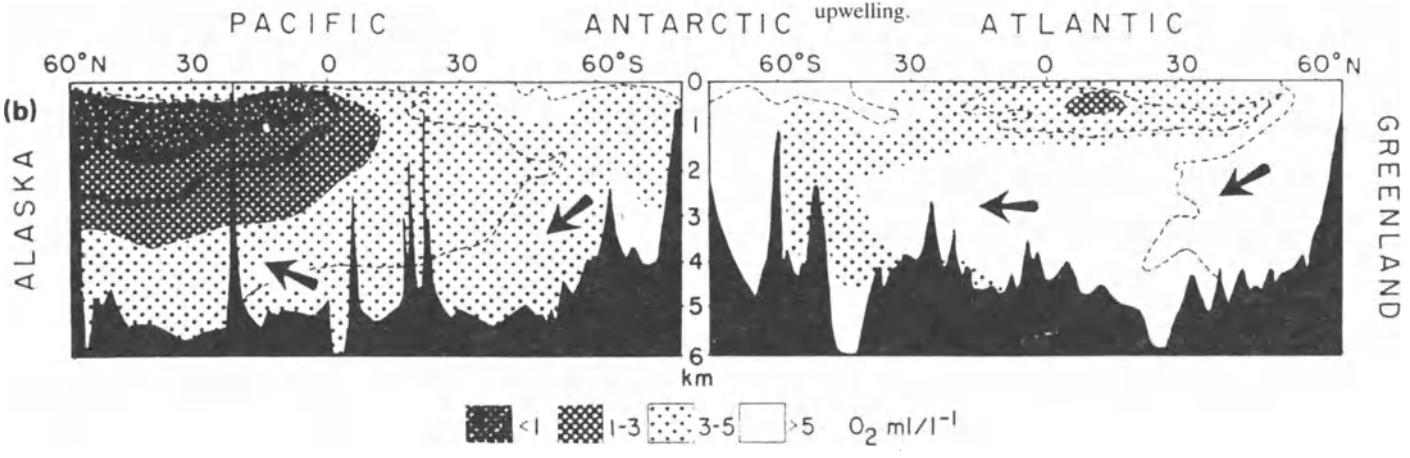

Figure 15.5b Oxygen concentrations along longitudinal profiles in the central Pacific and western Atlantic (from Berger 1970). The oxygen concentration pattern shows the formation of young oxygenated bottom waters in the high-latitude North Atlantic (anti-estuarine circulation), and a progressive decrease towards the North Pacific where shallow water is exchanged for deep water (estuarine circulation).

processes. However, these components have subsequently been reclassified into a number of separate types. For example, Chester & Hughes (1967) distinguished between (a) **primary hydrogenous material**, which is formed directly from material dissolved in sea water, and (b) **secondary hydrogenous material**, which results from the submarine alteration of pre-existing minerals. Thus, both the Goldberg (1954) and the Chester & Hughes (1967) classifications would include hydrothermal components in the general 'hydrogenous' category since they are also formed from sea water (modified by water–rock interactions) by inorganic reactions. In a more rigorous classification, Elderfield (1976) subdivided hydrogenous components into two basic categories, termed precipitates and halmyrolysates. **Precipitates** are primary inorganic components formed directly from sea water. **Halmyrolysates** are secondary components formed as a result of reactions between sediment components (usually silicates) and sea water subsequent to *in situ* weathering but prior to diagenesis. Elderfield (1976) then identified four main groups of hydrogenous material in marine sediments.

(a) Volcanic precipitates, which result from the introduction of elements into sea water from volcanic processes.
(b) Supergene precipitates, which are precipitated from sea water, or interstitial water, but are non-volcanic in origin.
(c) Lithogenous halmyrolysates, which are formed from the reaction of lithogenous components with sea water.
(d) Volcanic halmyrolysates, which are usually formed as a result of sea water-basalt reactions.

In his classification, therefore, (a) and (b) are primary components, and (c) and (d) are secondary.

Further complications arise when a closer look is taken at the origins of the dissolved elements that are involved in the formation of the precipitates and halmyrolysates. It is clear from Section 14.2 that diagenesis involving the destruction of organic carbon can release dissolved elements either at, or close to, the sediment surface (oxic diagenesis), or at depth in the interstitial waters from both the carbon carriers and from the components utilized as secondary oxidants (sub-oxic diagenesis). Oxic diagenesis therefore releases elements that have been removed from solution in sea water by their involvement in the oceanic biogeochemical cycles, and have been transported by the down-column vertical carbon-driven flux. In addition to this route for the transport of elements to the sediment surface, dissolved elements can also be removed directly from sea water, i.e. without undergoing a sediment surface-mediated carrier destruction process. In theory, therefore, these latter elements will be removed under conditions where there is no sediment

substrate to promote either oxic or sub-oxic diagenesis, e.g. on exposed rock surfaces.

For the present purposes an attempt will be made to classify the dissolved elements that take part in inorganic component-forming reactions by distinguishing between them on the basis of their sources. Thus, the following categories of elements are identified.

(a) **Direct seawater-derived** elements, which are further subdivided into (i) **hydrogenous** elements, i.e. those originating from the general background of elements dissolved in sea water, and (ii) **hydrothermal** elements, i.e. those originating from the debouching of hydrothermal solutions at the ridge crest spreading centres (see Sec. 5.1).
(b) **Oxic diagenetically derived** elements, i.e. those generated close to the sediment surface following their release on oxidative destruction of organic carbon.
(c) **Sub-oxic diagenetically derived** elements, i.e. those originating from interstitial waters at some depth in the sediment following the destruction of organic carbon by secondary oxidants.

The sediment components formed from these various types of elements can then be classified into **precipitates** (primary) and **halmyrolysates** (secondary) as proposed by Elderfield (1976). This hydrogenous–hydrothermal–diagenetic trinity offers a convenient framework within which to describe those components of marine sediments which are formed in the oceanic environment by inorganic reactions involving dissolved elements, and it is this inorganic origin that distinguishes them from the biogenous components. As the individual components are described, an attempt will be made to identify any coupling between the *processes* that utilize these genetically different elements.

The *precipitates*, or primary inorganic components, in marine sediments include oxyhydroxides, carbonates, phosphates, sulphides, sulphates and evaporite minerals; and the *halmyrolysates*, or secondary inorganic components, include glauconite, chamosite, palagonite, montmorillonite (smectite) and the zeolites. Thus, there is a wide range of halmyrolysates and precipitates in the marine environment. However, the influence they have on marine sedimentation varies from one component to another, both *quantitatively*, in their role as sediment-forming material, and *geochemically*, in the extent to which they influence chemical processes in the oceans. In both of these senses, the most important inorganically produced components found in marine sediments are (a) ferromanganese nodules, (b) ferromanganese oxyhydroxides, and (c) ridge-crest metal-rich sediments. Because of their geochemical importance, these ferromanganese deposits will therefore serve as prime example of process-orientated components formed inorganically in the marine environment.

15.3.2 Ferromanganese deposits in the oceans

The ferromanganese deposits include stains and encrustations on pebbles and rocks, nodules, sediment oxyhydroxides and sedimentary deposits of hydrothermal precipitates. Without assuming, at least at this stage, any genetic association in the sequence, the geochemical importance of these ferromanganese deposits will be considered in the order encrustations → ferromanganese nodules → sediment ferromanganese oxyhydroxides → hydrothermal precipitates. The sequence is set up in this way in order to consider first a hydrogenous end-member ferromanganese component (encrustations), then mixed hydrogenous–hydrothermal–diagenetic ferromanganese components (nodules), and finally a hydrothermal end-member ferromanganese component (hydrothermal precipitates). In this way it should be possible to identify how the pure hydrogenous and hydrothermal signals operate, and also how they combine with each other, and with the diagenetic signal, to form a variety of ferromanganese components.

15.3.3 Ferromanganese encrustations

Ferromanganese encrustations, or crusts, are relatively thin deposits on submarine rock outcrops, or on objects such as boulders or volcanic slabs. For example, on the Blake Plateau there is a manganese oxide crust 'pavement' that covers an area of ~ 5000 km^2 (Pratt & McFarlin 1966). Further, these crusts can be the typical ferromanganese deposit in seamount provinces. One particularly interesting feature of the crusts is that those which grow on exposed rock surfaces have acquired the elements necessary for their growth directly from the overlying sea water (*hydrogenous* supply) without receiving an input from sediment sources. In this sense, it will be shown below that they can be thought of as representing an end-member in the oceanic ferromanganese depositional sequence.

15.3.4 Ferromanganese nodules

15.3.4.1 Occurrence The first detailed description of the widespread occurrence of ferromanganese nodules in the oceans is usually attributed to Murray & Renard (1891) from collections made during the *Challenger Expedition* (1873–76). The nodules are found throughout the sediment column, but the highest concentrations are found on the surface. Here, they can cover vast areas of the sea floor in some regions; for example, ~ 50% of the sediment surface in the western Pacific has a blanket of nodules. They have been reported in association with many types of sediment, and Cronan (1977) identified two principal factors that control their abundance.

(a) Rate of accumulation of the host sediment. The highest number of nodules are found on those deep-sea sediments which are deposited at relatively slow rates of around a few millimetres per 1000 years ($mm/10^3\ yr^{-1}$); these include pelgaic clays and siliceous oozes. High concentrations of nodules can also occur where sedimentation is inhibited as a result of current action, e.g. on the tops of seamounts.
(b) The availability of suitable nuclei for oxide accretion. Various materials (e.g. a fragment of pumice, a shark's tooth, a foram skeleton, a piece of consolidated clay) can be utilized for this purpose, but volcanic nuclei are especially common, and this may explain the relatively high concentrations of nodules in areas of volcanism.

A generalized pattern of the distribution of ferromanganese nodules is illustrated in Figure 15.6.

15.3.4.2 Morphology The nodules can have a wide variety of shapes and sizes. When attempting to assess the role they play in marine geochemistry it is useful to make a distinction between **macronodules** and **micronodules**. This is a purely arbitrary division in which macronodules have diameters in the centimetre (or greater) range, and micronodules have diameters in the millimetre range. However, the distinction has some meaning in the sense that, while the macronodules may be considered to be foreign bodies on or in the sediment host, the micronodules are scattered throughout the deposits and are much more intimately associated with the other sediment-forming components, i.e. they are part of the general sediment. Further, the micronodules often do not have a nucleus, and may in fact be composed of oxides that have sedimented directly from the water column.

Some typical macronodules are illustrated in Figure 15.7. These macronodules have a wide variety of physical forms, and various schemes have been proposed for their morphological classification; for a detailed discussion of this topic see Raab & Meylan (1977). Perhaps the most widely used morphological framework is that in which the nodules are referred to as being some variant of a basic discoidal–ellipsoidal–spherical shape pattern. It is now recognized that the shape adopted by a macronodule is related to the matter in which it has grown, and in particular to whether it has received its component elements (mainly Mn and Fe) from overlying sea water or from underlying interstitial water. Manheim (1965) has described the two nodule end-member morphologies that might arise from these different element supply mechanisms – see Figures 15.8a and b.

(a) In Figure 15.8a, the nodule is formed on an oxidizing substrate and

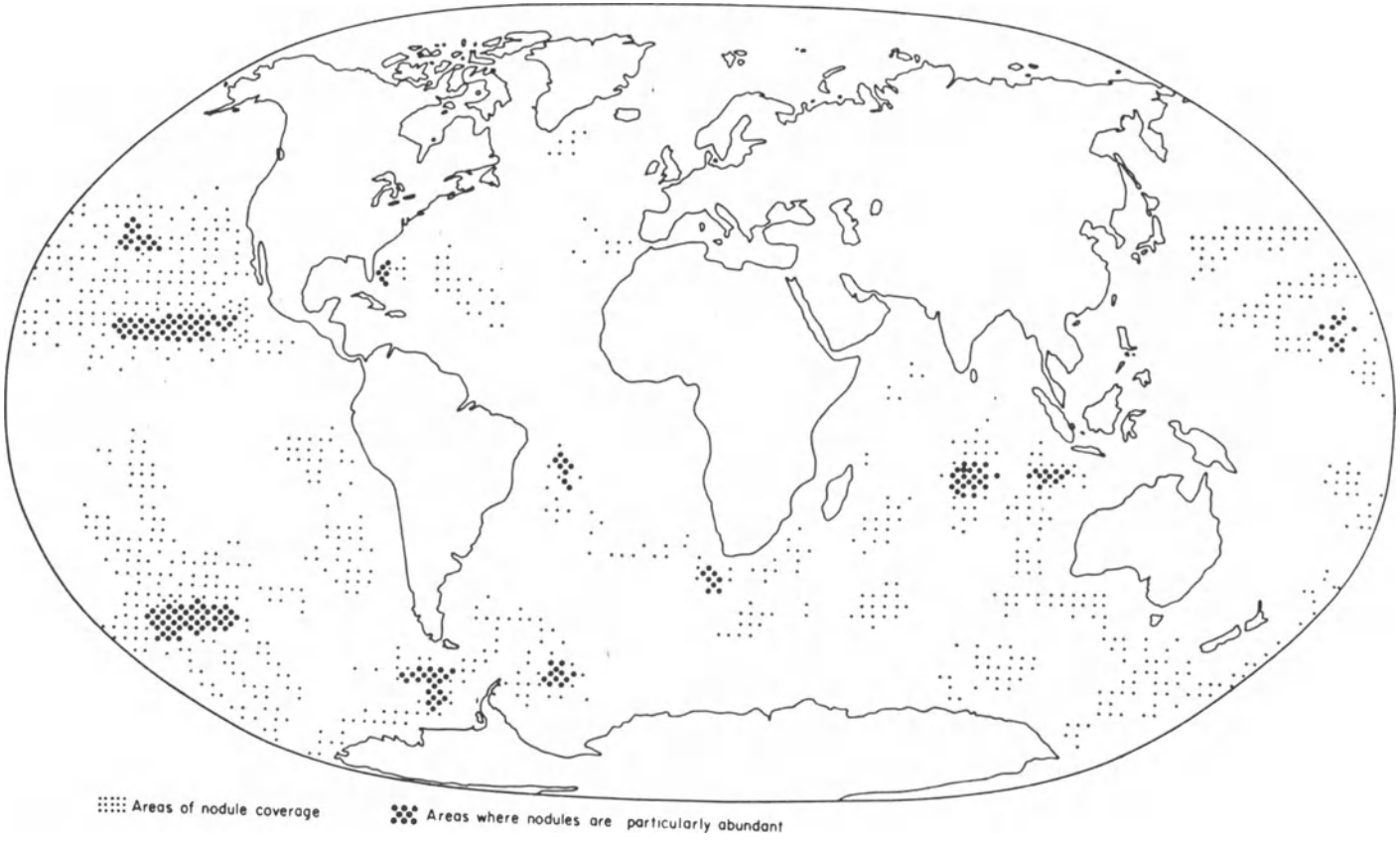

Figure 15.6 Generalized distribution of ferromanganese nodules in the World Ocean (from Cronan 1980).

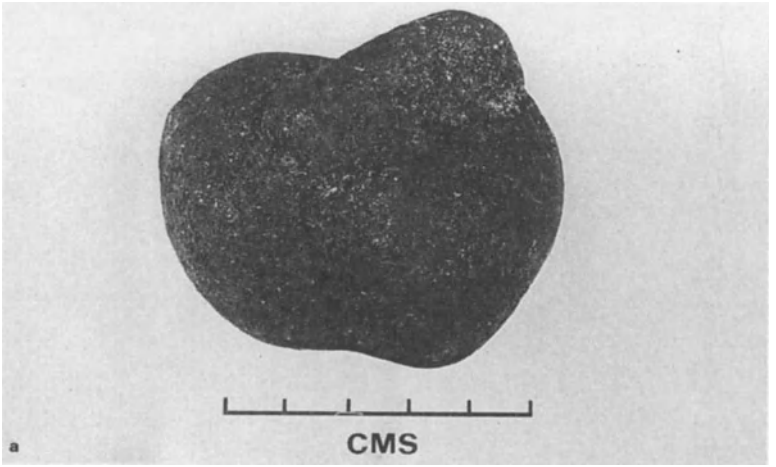

a

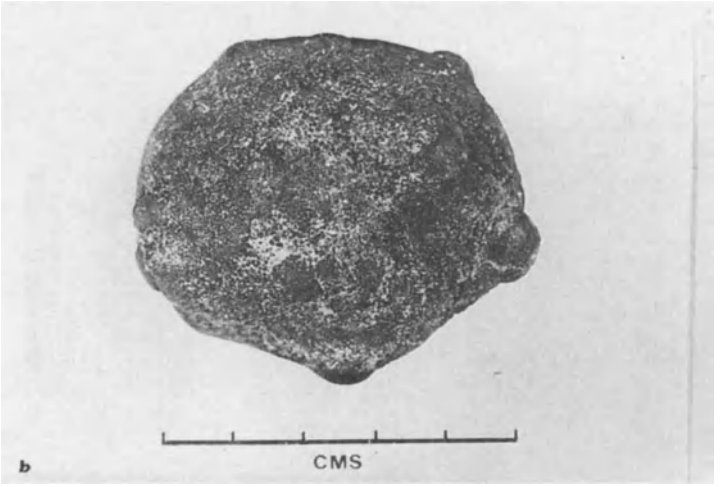

b

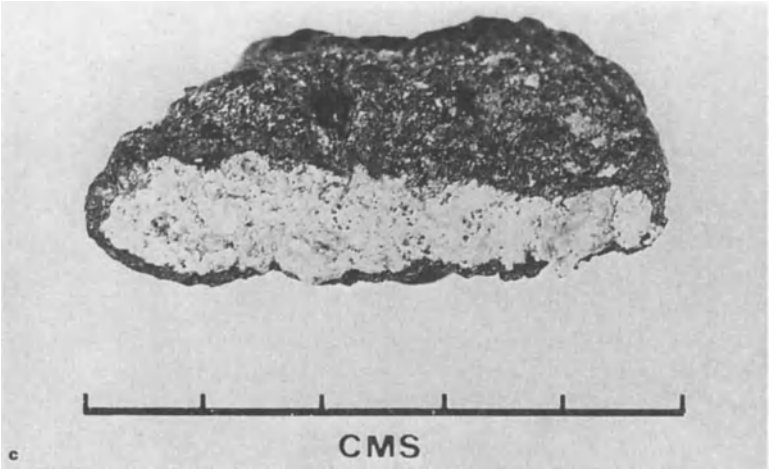

c

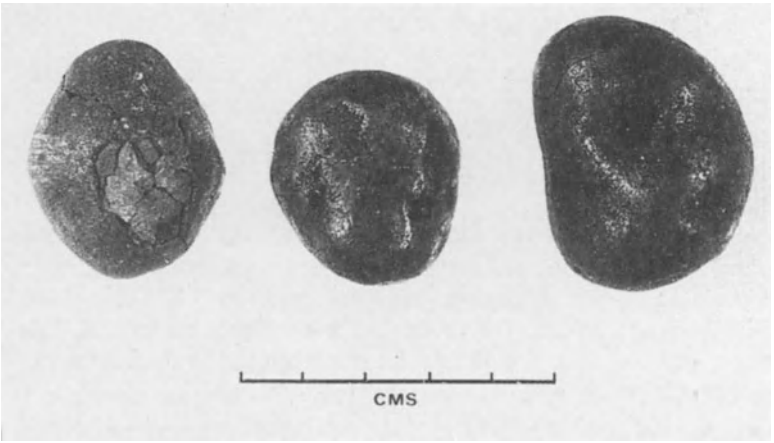

d

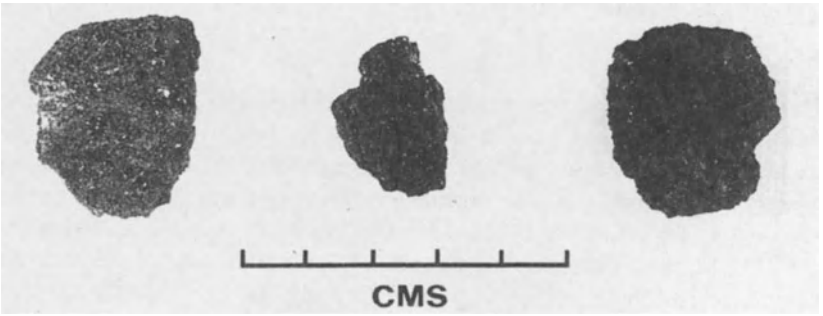

e

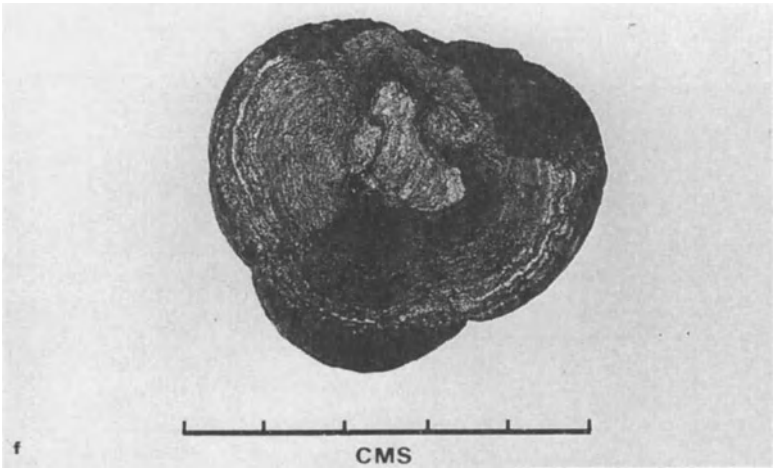

f

Figure 15.7 Typical morphologies of ferromanganese macro nodules from the Atlantic and Indian Oceans (photographs supplied by D.S. Cronan and S.A. Moorby; (**c**), (**e**) and (**f**) have also been reproduced in Cronan 1980). (**a**) (**b**) (**c**) Shapes include (**a**) and (**b**), semi-spherical shapes with 'knobbly' surface; (**c**), flattened nodule. (**d**) (**e**) Surface textures; (**d**) smooth; (**e**) granular. (**f**) A typical internal structure, showing concentric series of light and dark bands (see text).

has received only a minor supply of dissolved material from the underlying sediment. Most of the elements are therefore derived from the overlying sea water and the nodule grows slowly, with occasional overturning, so that it acquires a generally spherical shape.

(b) In Figure 15.8b, most of the elements are supplied from the interstitial waters below the sediment surface, following their sub-oxic release during the diagenetic sequence (see Sec. 14.2). They are then precipitated by oxidative processes at a suitable surface, in this case the nodule nucleus, which may be partly buried in the sediment. As the precipitation process continues, the sides nearest the source will take up the thickest layer of this bottom-derived metal input, while the upper sides will rely on a supply from the overlying sea water. As a result, nodules of this type will have a flattened discoidal shape.

These are, however, two extreme end-member morphologies, and a variety of intermediate nodule shapes can be found. In general, the extreme *sea water* end-member is really represented by encrustations on exposed rock surfaces, and the nodule (concretion) form closest to that of the sea water end-member is probably that found on the tops of current-washed seamounts. The extreme *diagenetic* end-member is best developed in nearshore and hemi-pelagic regions where the diagenetic sequence can proceed to a late stage. Between these two extremes, individual nodules

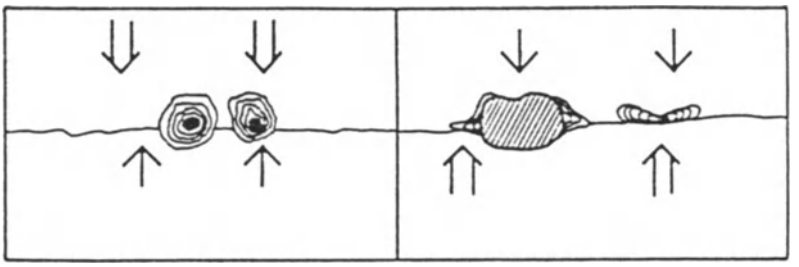

Figure 15.8 Schematic representation of ferromanganese nodule end-member morphologies (from Manheim 1965). The size of the arrows indicates the proportion and direction of metal supply. (**a**) This illustrates a typical situation in the open-ocean, with the nodules lying on an oxidized sediment substrate: here the dominant supply of metals is from the overlying sea water. (**b**) This illustrates a typical situation in nearshore and freshwater environments, with the nodules lying on a sediment substrate that is partly reducing in character: here the dominant supply of metals is via intersitial waters from below the substrate surface.

can have a supply of elements from both of the principal sources. Thus, the upper surfaces are supplied from the overlying sea water, whereas the lower surfaces are diagenetic in origin. This often results in morphological differences between the two surfaces of a single nodule, the upper surfaces being smooth and characteristic of the seawater type, and the lower surfaces being gritty and bumpy and characteristic of the diagenetic type (see e.g. Raab & Meylan 1977). On the basis of morphology, it is therefore possible to identify tentatively a sequence of formation that is related to the depositional environment in which the ferromanganese crusts and nodules grow. This is based on end-member sea water–diagenetic source types, and the general concept will be further expanded as the mineralogy and chemistry of the ferromanganese deposits are considered.

15.3.4.3 Growth rates The rate at which a ferromanganese nodule grows is intimately related to the environment within which it forms, the slowest accretion rates of a few millimetres per million years (mm/10^6 yr) being found for the hydrogenous end-member, intermediate rates of a few hundred millimetres per million years being characteristic of the diagenetic end-member, and the highest rates of a few thousand millimetres per million years being shown by the hydrothermal end-member crusts. There are, however, a number of uncertainties associated with the question of how fast the nodules do, in fact, grow. If it is accepted that at least some pelagic nodules do grow at an average rate of a few millimetres per million years, then this is considerably slower than the rates at which the host sediments accumulate, i.e. a few millimetres per thousand years. The question that then arises is 'What is the mechanism that keeps these nodules at the sediment surface and thus prevents them being buried?' Several mechanisms have, in fact, been proposed to explain this. These include: (a) the activity of worms, which are thought to lift the nodules through the sediment; (b) the winnowing of sediments, which sweeps the depositional surfaces clear; (c) rolling by currents; and (d) disturbance by earthquake activity. The difference in the rates at which Mn is accreted in the nodules and host sediments is also important in terms of other questions regarding the formation, and even the very existence, of the nodules. One of these questions was posed by Broecker & Peng (1982), i.e. 'Why do the nodules appear to attract more than their fair share of manganese and iron?' The answer, as the authors pointed out, is that of course they do not, since the sediments with which they are associated accumulate manganese at a much faster rate than do the nodules themselves (see e.g. Bender *et al.* 1970). Ku (1977) concluded, therefore, that the nodules do not grow because they have a special capability to attract manganese, but rather because some suitable nucleus escapes burial in the sediment. This suggests that, other factors being

equal, the growth of ferromanganese oxides will depend largely on the length of time the nucleus has been in contact with the sources of the metals, and the rate at which the metals themselves are supplied.

15.3.4.4 Mineralogy Much of our knowledge of the mineralogy of the manganese and iron phases in the nodules has bome from the pioneering work of Buser & Grutter (1956). Subsequently, many other studies have been carried out on the mineralogy of the nodules, and for a detailed review of this topic the reader is referred to Burns & Burns (1977). However, these later studies mostly served to confirm the original findings of Buser & Grutter (1956), and the nodule mineralogy may be summarized as follows.

There are at least four mineral phases found in ferromanganese nodules and crusts: δMnO_2, 7A and 10A manganite, and iron hydroxide. (a) δMnO_2 forms aggregates of randomly orientated sheets. (b) 7A manganite and (c) 10A manganite have a double layer structure consisting of ordered sheets of MnO_2 with disordered layers of metal ions, such as Mn^{2+} and Fe^{2+}, coordinated with O^{2-}, OH^- and H_2O, lying between them. In the 10A manganites the water and hydroxyls are probably present as discrete layers, whereas in the 7A manganites they form a single layer. (d) Amorphous iron hydroxide ($FeOOH{\cdot}nH_2O$) may be converted to goethite (α-FeOOH); other iron-rich phases, e.g. lepidocrocite, can also be present. The manganese phases have been related to known minerals, and in the most commonly adopted terminology 10A manganite is referred to as toderokite and 7A manganite is termed birnessite. Thus, the principal mineral phases in the nodules are δ**MnO$_2$**, **birnessite**, **toderokite** and some form of **hydrous iron oxide**.

There are various lines of evidence to suggest that, like the growth rate, the mineralogy of the manganese phases in the nodules (and crusts) is governed by the environment of formation, especially the prevailing oxidation conditions. For example, Arrhenius (1963) suggested that the degree of oxidation at formation decreases in the order δMnO_2 > birnessite > toderokite. This is reflected in the end-member nodule mineralogies; thus, nodules of the oxidized pelagic end-member type are relatively rich in δMnO_2, whereas the nearshore and hemi-pelagic end-members contain more toderokite. However, this is a very general distinction, and is by no means clear cut. Nonetheless, it is a useful first assumption to assign δMnO_2 to nodules that receive much of their Mn from sea water, and toderokite to those which have a diagenetic origin.

15.3.4.5 Chemistry Ferromanganese nodules are, as the name implies, rich in iron and manganese. However, they also contain relatively large concentrations of a variety of trace metals. Cronan (1976) assessed the

magnitudes of the enrichments of a series of elements in ferromanganese nodules relative to their average crustal abundances, and on this basis he was able to identify three groups of elements.

(a) The **enriched** elements, which were divided into a number of subgroups depending on the extent of their enrichment: (i) Mn, Co, Mo and Th, which are enriched in the nodules by a factor of more than 100; (ii) Ni, Ag, Ir and Pb, which are enriched by a factor of between 50 and 100; (iii) B, Cu, Zn, Cd, Yb, W and Bi, which have enrichments between 10 and 50; (iv) P, V, Fe, Sr, Y, Zr, Ba, La and Hg, which are enriched by less than a factor of 10.

(b) The **non-enriched–non-depleted** elements; these include Na, Mg, Ca, Sn, Ti, Ga, Pd and Au.

(c) The **depleted** elements, which include Al, Si, K, Sc, Cr; however, the depletions are only slight.

A compilation of the average abundances of elements in ferromanganese nodules from the major oceans is given in Table 15.3, together

Table 15.3 Average abundances of elements in ferromanganese oxide deposits from each of the major oceans (in wt.%), and enrichment factor for each element[a]

	Pacific Ocean	Atlantic Ocean	Indian Ocean	Southern Ocean	World Ocean Average	Crustal Abundance	Enrichment Factor
B	0·0277	—	—	—	—	0·0010	27·7
Na	2·054	1·88	—	—	1·9409	2·36	0·822
Mg	1·710	1·89	—	—	1·8234	2·33	0·782
Al	3·060	3·27	3·60	—	3·0981	8·23	0·376
Si	8·320	9·58	11·40	—	8·624	28·15	0·306
P	0·235	0·098	—	—	0·2244	0·105	2·13
K	0·753	0·567	—	—	0·6427	2·09	0·307
Ca	1·960	2·96	3·16	—	2·5348	4·15	0·610
Sc	0·00097	—	—	—	—	0·0022	0·441
Ti	0·674	0·421	0·629	0·640	0·6424	0·570	1·13
V	0·053	0·053	0·044	0·060	0·0558	0·0135	4·13
Cr	0·0013	0·007	0·0014	—	0·0014	0·01	0·14
Mn	19·78	15·78	15·12	11·69	16·174	0·095	170·25
Fe	11·96	20·78	13·30	15·78	15·608	5·63	2·77
Co	0·335	0·318	0·242	0·240	0·2987	0·0025	119·48
Ni	0·634	0·328	0·507	0·450	0·4888	0·0075	65·17
Cu	0·392	0·116	0·274	0·210	0·2561	0·0055	46·56
Zn	0·068	0·084	0·061	0·060	0·0710	0·007	10·14
Ga	0·001	—	—	—	—	0·0015	0·666
Sr	0·085	0·093	0·086	0·080	0·0825	0·0375	2·20
Y	0·031	—	—	—	—	0·0033	9·39
Zr	0·052	—	—	0·070	0·0648	0·0165	3·92
Mo	0·044	0·049	0·029	0·040	0·0412	0·00015	274·66
Pd	$0·602^{-6}$	$0·574^{-6}$	$0·391^{-6}$	—	$0·553^{-6}$	$0·665^{-6}$	0·832
Ag	0·0006	—	—	—	—	0·000007	85·71
Cd	0·0007	0·0011	—	—	0·00079	0·00002	39·50
Sn	0·00027	—	—	—	—	0·00002	13·50
Te	0·0050	—	—	—	—	—	—
Ba	0·276	0·498	0·182	0·100	0·2012	0·0425	4·73
La	0·016	—	—	—	—	0·0030	5·33
Yb	0·0031	—	—	—	—	0·0003	10·33
W	0·006	—	—	—	—	0·00015	40·00
Ir	$0·939^{-6}$	$0·932^{-6}$	—	—	$0·935^{-6}$	$0·132^{-7}$	70·83
Au	$0·266^{-6}$	$0·302^{-6}$	$0·811^{-7}$	—	$0·248^{-6}$	$0·400^{-6}$	0·62
Hg	$0·82^{-4}$	$0·16^{-4}$	$0·15^{-6}$	—	$0·50^{-4}$	$0·80^{-5}$	6·25
Tl	0·017	0·0077	0·010	—	0·0129	0·000045	286·66
Pb	0·0846	0·127	0·070	—	0·0867	0·00125	69·36
Bi	0·0006	0·0005	0·0014	—	0·0008	0·000017	47·05

[a] From Cronan (1976).

Note: Superscript numbers denote powers of ten, e.g. $^{-6} = \times 10^{-6}$.

with average elemental enrichment factors. The data in this table give an indication of how the composition of the nodules varies on an inter-oceanic basis. In addition, there are considerable variations in the compositions of the nodules within specific oceanic regions. For example, Mero (1962) showed that the nodules in the Pacific can be categorized into a number of Mn-, Cu-, Ni-, Fe-, and Co-rich 'ore provinces'. To some extent the variations in the chemical compositions of the nodules can be related to their mineralogy which, in turn, is a function of the depositional environment.

It may be concluded that ferromanganese nodules can be described in terms of two end-members, i.e. a diagenetic and a sea water end-member. It was shown in Section 14.2.3 that there is a lateral sequence of diagenetic environments on the deep-sea floor, from sub-oxic in marginal regions to oxic in the open ocean. This lateral sequence of environments exerts a control on the type of nodule formed. For example, Price & Calvert (1970) concluded that Pacific Ocean nodules have a continuous range of chemical and mineralogical compositions which extend between those of two end-members. One of these end-members, which is rich in δMnO_2, is characteristic of seamount tops. Nodules located on the pelagic sea floor and marginal seamounts are chemically and mineralogically intermediate between these two end-members.

(a) **Marginal end-member**. This has a disc-shaped morphology. Chemically, it is characterized by a high Mn : Fe ratio, and is relatively enriched in Mn, Cu, Ni and Zn. Mineralogically, it is composed of both δMnO_2 and toderokite, and some varieties also contain birnessite. This end-member is typically found in marginal and hemi-pelagic sediments, and is equivalent to the diagenetic nodule identified above.

(b) **Open-ocean end-member**. This has a generally spherical shape. Chemically it is typified by a low Mn : Fe ratio, and is relatively enriched in Fe, Co and Pb. Mineralogically, it consists mainly, or even exclusively, of δMnO_2. This end-member is best represented by ferromanganese crusts and nodules from seamounts, and is equivalent to the sea water nodule identified above.

15.3.4.6 Formation The two end-member nodules are formed by two end-member *processes*, the marginal nodules acquiring most of their component metals from the interstitial waters of the host sediments (**diagenetic nodules**) and the open-ocean varieties taking most of their metals from the overlying water (**seawater nodules**). It must be stressed, however, that there is a continuous spectrum of oceanic ferromanganese nodules between these two extreme end-members. This is evidenced by the fact that many nodules from abyssal regions have both a seawater

source (to their upper surfaces) and a diagenetic source (to their lower surfaces). Thus, many nodules are compositionally different on their seawater-facing and sediment-facing surfaces. Nonetheless, the basis differences are still related to the two different prime sources of metals to nodules.

According to Dymond *et al.* (1984), 'the compositions of ferromanganese nodules respond in a consistent manner to the sea floor environment in which they form'. In this respect the two end-member (i.e. sea water and diagenetic) nodule source concept provides a useful framework for a discussion of how the nodules formed. However, it was pointed out above that the components formed from both seawater and diagenetic sources can be subdivided into a number of genetic classes. For example, seawater sources can be either **hydrogenous** or **hydrothermal**, and diagenetic sources can be either **oxic** or **sub-oxic** in character. As a result, nodules having a seawater source can be subdivided into hydrogenous and hydrothermal types, and those having a diagenetic source can be subdivided into oxic and sub-oxic types. Hydrothermal processes will be considered separately in Section 15.3.6, and for the moment attention will be focused on the three nodule accretionary modes identified by Dymond *et al.* (1984). These are: (a) that resulting from hydrogenous precipitation from sea water; (b) that arising from oxic diagenetic processes; and (c) that associated with sub-oxic diagenetic processes. Dymond *et al.* (1984) then tested their three-mode accretionary model with reference to the formation of ferromanganese nodules at three contrasting MANOP sites in the Pacific (sites H, S and R). This study is an excellent example of modern thinking on the processes that control the genesis of ferromanganese deposits, and for this reason it will serve as a blueprint for a discussion of how the processes operate. To aid the discussion, model compositions of ferromanganese components arising from the three accretionary modes are given in Table 15.4.

THE SEAWATER (OR HYDROGENOUS) NODULE END-MEMBER This type of ferromanganese deposit is formed by the direct precipitation of colloidal metal oxides from sea water at the growth site, together with the accretion to the depositional surface of suspended Fe–Mn precipitates formed in the water column. The extreme example of a hydrogenous end-member ferromanganese deposit is provided by encrustations that are formed on exposed rock surfaces outside the direct influence of hydrothermal activity. Aplin & Cronan (1985a) described a series of such encrustations from the Line Islands (Central Pacific). The crusts have relatively low Mn : Fe ratios, and the principal minerals in them are δMnO_2 and amorphous $FeOOH{\cdot}nH_2O$; of these the δMnO_2 was the most important trace metal-bearing phase, containing Co, Mo, Ni, Zn and Cd, with only Ba appearing to be specifically associated with the iron

Table 15.4 Chemical composition of 'end-member' ferromanganese nodules (units, $\mu g\ g^{-1}$)

	Ferromanganese crusts		Ferromanganese nodules	
	HYDROGENOUS		OXIC	SUB-OXIC
Element	Line Islands, Pacific[a]	MANOP Site H, Pacific[b]	MANOP Site H, Pacific[b]	MANOP Site H, Pacific[b]
Mn	204000	222000	316500	480000
Fe	170000	190000	44500	4900
Co	5500	1300	280	35
Ni	3900	5500	10100	4400
Zn	590	750	2500	2200
Cu	-	1480	4400	2000
Al	16000	11800	27100	7500
Ti	12000	5300	1700	365
Si	-	52000	59000	16300
Na	-	10400	16100	32800
K	-	4900	8200	6200
Mg	-	10400	23000	13800
Ca	26000	26000	15200	12500
Mn:Fe	1.2	1.2	7.1	98
Co:Mn	0.027	0.006	0.0009	0.00007
Ni:Mn	0.019	0.024	0.032	0.0092
Cu:Mn	0.0075	0.0022	0.020	0.0024
Zn:Mn	0.0029	0.0034	0.0079	0.0046

[a] Data from Aplin & Cronan (1985a).
[b] Data from Dymond et al. (1984).

hydroxide phase. The authors concluded that the crusts had formed directly from the slow accumulation of trace metal-enriched oxides which had been deposited directly from the overlying water column, and that the trace metal–mineral associations had resulted from the different scavenging behaviours of Mn and Fe oxides in the water. Other influences on the composition of the hydrogenous end-member include variations in the concentrations of elements in mid-depth and bottom waters (see e.g. Aplin & Cronan 1985a). The transport, and subsequent deposition, of hydrothermal particulates can also affect the composition of the crusts

(see e.g. Dymond *et al.* 1984).

The accretion of the hydrogenous ferromanganese deposits is constrained by the concentration of Mn and the kinetics of its oxidation, and Piper *et al.* (1984) have reviewed the processes involved in the formation of marine manganese minerals. According to these authors the Mn oxide that forms initially may be a metastable hausmannite, which undergoes aging to δMnO_2 possibly by a disproportionation reaction as suggested by Hem (1978). Thus

$$3\ H_2O + 1/2\ O_2 + 3\ Mn^{2+} = Mn_3O_4 + 6\ H^+ \qquad (15.5)$$

and

$$Mn_3O_4 + 4\ H^+ = \delta MnO_2 + 2\ Mn^{2+} + 2\ H_2O \qquad (15.6)$$

Most Mn is present in sea water as Mn^{2+}, whereas the element is now thought to be found in nodules almost exclusively in the Mn(IV) state (Piper *et al.* 1984). Goldberg & Arrhenius (1958) suggested that ferric oxides might provide a catalytic surface for the oxidation of Mn^{2+} to MnO_2 and so initiate nodule formation. Once the process has started, usually around a nucleus, the nodule will continue to grow, being constrained by the length of time the catalytic surface is exposed to sea water and the rate of supply of the component elements. According to Dymond *et al.* (1984), it is the flux of dissolved Mn to the site of oxidation that controls the **accretion rate** of ferromanganese nodules, and it is the relative flux of Mn compared to other cations that determines their **composition**. The hydrogenous precipitation of ferromanganese components is a relatively slow process, and Dymond *et al.* (1984) estimated an accretion rate of 1–2 mm/10^6 yr for Pacific Ocean crusts, and the tops of nodules from MANOP site R.

Although the best end-member composition for the hydrogenous ferromanganese deposits is provided by crusts formed directly onto exposed rock surfaces, this type of accretion process also contributes to *all* nodule surfaces that are exposed to sea water, and it is evident that in addition to crusts, *nodules* having a large hydrogenous component can be found in the marine environment. However, once a sediment substrate is introduced the conditions for ferromanganese oxide formation change dramatically. In particular, the nodules can become partly buried and so can acquire a diagenetic input of dissolved metals. This can result in the distinct top–bottom compositional differences identified in Section 15.3.4.2, so that the hydrogenous end-member in concretions, as opposed to encrustations, is likely to be found on the upper surfaces of nodules, whereas their lower surfaces may reflect a diagenetic input. Although it is therefore convenient to treat diagenetic end-member nodules separately

from the point of view of the principal processes involved in their generation, it must be stressed that in a strict sense most marine nodules will be mixed-source types.

THE DIAGENETIC NODULE END-MEMBER The sea water–diagenetic metal supply system can result in nodules exhibiting top-bottom compositional differences. The extent to which these differences are found depends on how far the diagenetic sequence has proceeded. This, in turn, depends on the magnitude of the down-column carbon flux, which controls the sediment substrate depositional environment (see Sec. 14.3). In this respect, Dymond *et al.* (1984) distinguished between nodules formed under conditions of oxic and sub-oxic diagenesis.

(a) OXIC DIAGENESIS In oxic diagenesis, degradable organic matter is destroyed by dissolved O_2, and at this stage particulate MnO_2 is not broken down for utilization as a secondary oxidant (see Sec. 14.2.2).

(a)

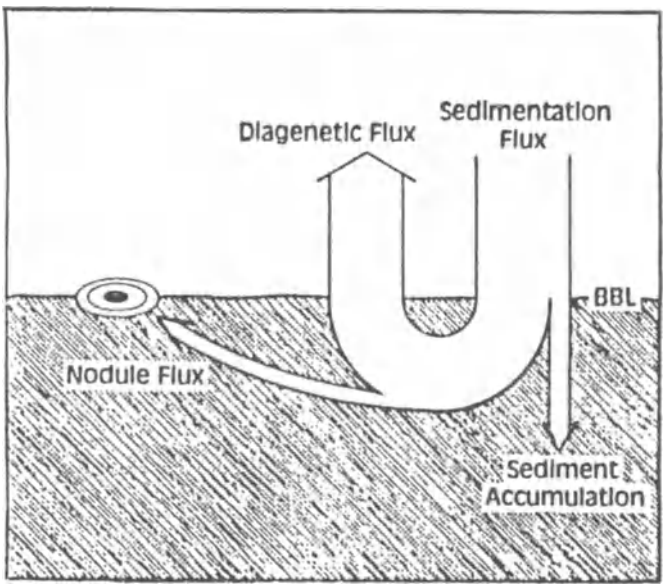

Figure 15.9 Models for the formation of ferromanganese nodules under conditions of oxic diagenesis. (**a**) General model for the early diagenetic release of trace metals (from Callender & Bowser 1980).

There is no doubt that nodules formed on *oxic* substrates receive a proportion of their metals directly from sea water (hydrogenous supply). However, *direct* precipitation from sea water is not the sole, or even the dominant, route by which Mn and associated elements are supplied to nodules accreting on oxic sediment substrates. There is still a problem, however, regarding the origin of the non-hydrogenous Mn and, to some extent, the other elements that are released during oxic (or early) diagenesis. This problem arises because MnO_2 is not broken down at this oxic stage. A number of mechanisms have been suggested to account for these early diagenetic metal sources, and in general these can be related to the processes involved in the down-column transport of the metals.

(i) Release from labile carriers. During oxic diagenesis, the dissolution of labile organic carriers will release biologically bound trace metals into solution. Some of these trace metals will be lost by diffusion out of the sediments, but a fraction will be retained and so become

(b)

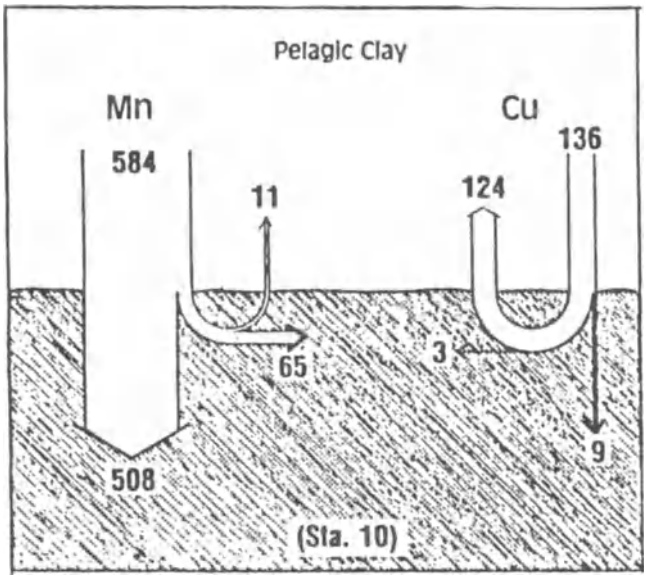

Figure 15.9b Fluxes involved in the early diagenetic release of Mn and Cu in sediments from the Equatorial Pacific (from Callender & Bowser 1980).

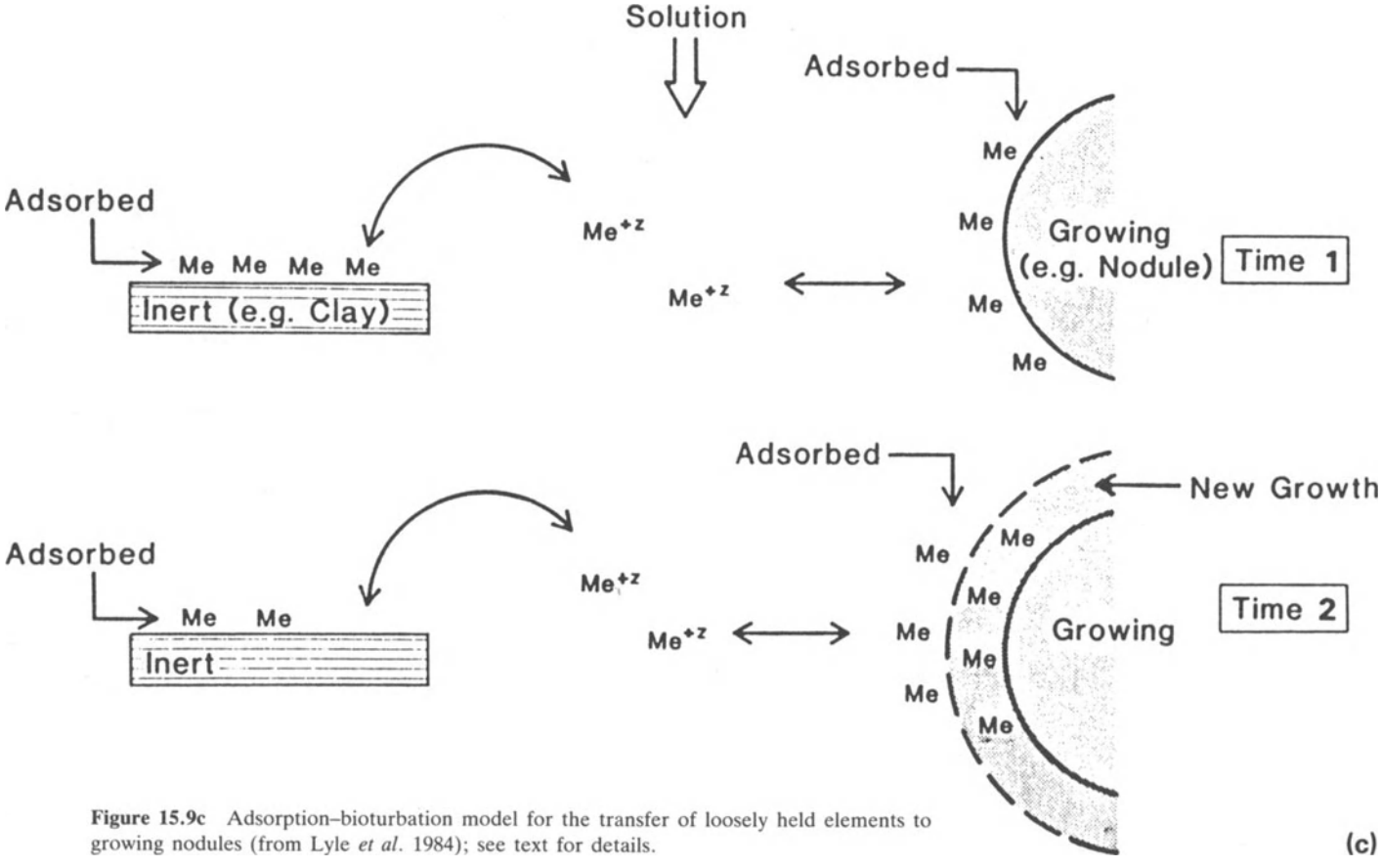

Figure 15.9c Adsorption–bioturbation model for the transfer of loosely held elements to growing nodules (from Lyle *et al.* 1984); see text for details.

available for incorporation into nodules that may form there. Callender & Bowser (1980) outlined a model for this; the general model is illustrated in Figure 15.9a and is applied to Cu and Mn in Figure 15.9b.

(ii) Adsorption–desorption reactions involving inorganic (non-labile) sediment phases. It is unlikely that labile carriers in (i) above will release sufficient Mn for nodule formation under all conditions of oxic diagenesis. Mn is a scavenging-type element (see Sec. 11.6.3.1), and is mainly transported down the water column either as discrete Mn oxides or in association with other inorganic particle surfaces. In view of the inability of oxic diagenetic processes to release Mn from its oxide hosts, Lyle *et al.* (1984) proposed an alternative mechanism for the supply of Mn, and associated elements, to the lower surface of nodules under oxic substrate conditions. Using a partitioning technique, the authors identified a loosely held sediment fraction in which the elements are present in carbonate-bound and sorbed associations. The technique was applied to sediments from two MANOP sites (M and H), and it was reported that between ~ 2 and $\sim 10\%$ of the total Mn, $\sim 10\%$ of the total Ni and Cu, but $< 1\%$ of the total Fe was present in these loosely held forms. The authors then outlined a two-stage adsorption–bioturbation model by which this pool of loosely held transition elements is transferred to nodules. In stage 1, the solid particles and sorbed pool are transported to a region of reaction around a growing nodule. In stage 2, there is desorption of the sorbed metals from their carrier particles. Some of the particles have inert surfaces in the sense that they sorb metals but do not take them in to their internal structures, so making them available for desorption and subsequent incorporation into the growing ferromanganese oxyhydroxide phases. The transfer is thought to be brought about by equilibrium between the metals in solution in the interstitial waters and those in the sorbed pool, in a manner similar to the equilibrium between particle-associated and dissolved elements in the water column, which can add metals to interstitial waters. However, growing surfaces, such as those of the nodules, will deplete the pool of sorbed metals by actively transferring them into their structures, thus taking them permanently out of solution. It is assumed that bioturbation brings fresh supplies of sorbed material to the reaction zones around growing nodules. The model is illustrated in Figure 15.9c.

(iii) Reactions between amorphous Fe–Mn oxyhydroxides and authigenic silicates. Dymond *et al.* (1984) identified two mechanisms of this type which might have the potential to release nodule-forming elements in oxic sediments. The first of these involves a reaction between the oxyhydroxides and dissolving opal, to yield the smectite mineral

nontronite. During this process SiO_2 and Fe are fixed in the silicate, but Mn (together with elements such as Ni, Cu and Co) is released. In the second mechanism, the alteration of volcanic glass to form the zeolite **phillipsite** raises the local pH and enhances the oxidation of Mn^{2+} which has been adsorbed from solution onto oxide surfaces, thus promoting oxide growth (see also Bischoff *et al.* 1981).

A number of mechanisms can therefore provide nodule-forming elements to sediments that are deposited under conditions of oxic diagenesis; in general, when the flux of biogenically associated labile elements is relatively high, mechanism (i) is operative, but when the flux is relatively low, mechanisms (ii) and (iii) become more important.

On the basis of data obtained during their investigation, Dymond *et al.* (1984) concluded that processes involving oxic diagenesis had operated during the formation of nodules at MANOP sites R and S. The nodules at these two sites provide an interesting example of how the influence of oxic diagenesis can vary according to the depositional environment. Nodules at both sites have a seawater (hydrogenous) component on their upper surfaces. At site R the flux of biogenic components was relatively low and the principal Mn mineral was δMnO_2. In contrast, there was a relatively strong biogenic flux to site S, and here oxic diagenesis becomes more important and a Cu- and Ni-rich toderokite was formed. The growth rates of the oxic nodules were estimated to be of the order of $\sim$ 10–50 mm/10^6 yr.

(b) SUB-OXIC DIAGENESIS In sub-oxic diagenesis, the diagenetic sequence is driven by the utilization of secondary oxidants for the degradation of organic carbon, usually at some depth in the sediment (see Sec. 14.4.2). MnO_2 can act as one of these secondary oxidants and in the process Mn^{2+} (and other trace elements associated with the oxides) is released into the interstitial waters where it can migrate upwards under concentration gradients to undergo reprecipitation to MnO_2 in the upper oxic zone, i.e. the elements reach the site of nodule formation from below. The depth at which this sub-oxic process takes place can be affected by the strength of the down-column carbon-mediated signal. For example, Dymond *et al.* (1984) reported the presence of sub-oxic diagenetic nodules at MANOP site H, but pointed out that Mn released from the utilization of MnO_2 was reprecipitated below the sediment surface on which the nodules were forming. To explain the formation of the sub-oxic diagenetic nodules, the authors therefore suggested that the site had received a supply of elements from pulses of biogenic debris, which had been sufficiently strong to decrease the depth at which sub-oxic diagenesis normally takes place. In oxic diagenesis, the destruction of labile material from the organic carriers results in the supply of relatively large amounts of metals

such as Cu, Ni and Zn, giving rise to the formation of Cu-, Ni- and Zn-rich toderokite. However, the sub-oxic diagenesis of Mn oxides from the organic matter pulses does not release large amounts of Cu and Ni, and the Mn-rich toderokite formed is less stable than the Ni-, Cu- and Zn-rich variety, and can collapse on dehydration to yield birnessite. Nodules containing Mn-rich toderokite and birnessite were reported at MANOP site H where they had grown in response to the biogenic pulses. Dymond *et al.* (1984) estimated the overall growth rates of the sub-oxic nodules to be of the order of ~ 100–200 mm/10^6 yr.

15.3.4.7 Ferromanganese nodules: summary There are three general modes by which non-hydrothermal ferromanganese crusts and nodules accrete: these are the *seawater* mode, the *oxic diagenetic* mode and the *sub-oxic diagenetic* mode. The crusts represent an individual end-member formed by the seawater mode, but the nodules are usually top–bottom mixtures of the seawater mode and one, or both, of the diagenetic modes. The signatures associated with each of the three modes are summarized below.

(a) Surface ferromanganese components formed by the seawater mode contain δMnO_2. They have low Mn : Fe ratios (~ 1), low Ni : Co ratios, and accrete at slow rates, which are probably in the order of ~ 1–2 mm/10^6 yr. Ferromanganese crusts on exposed rock surfaces and nodules formed on the tops of seamounts, and other swept sediment surfaces, are formed by this mode. In addition, the upper surfaces of all nodules have a component derived from the seawater accretion mode.
(b) Sediment surface ferromanganese components formed by the oxic diagenetic mode contain a Cu-, Ni- and Zn-rich toderokite. The growth-forming metals have been supplied by particulate matter via a variety of oxic diagenetic mechanisms, and the components have intermediate Mn : Fe rations (e.g. ~ 5–10) and accrete at rates of a few tens of millimetres per million years. These components are found on the lower surfaces of nodules that grow on sediment substrates where the diagenetic sequence has not progressed beyond the oxic stage.
(c) Sediment surface ferromanganese components formed by the sub-oxic diagenetic mode contain a Mn-rich toderokite which may undergo transformation to birnessite. The metals necessary for the formation of these components are released from particulate matter during sub-oxic diagenesis. In some instances they may arise from the oxidative utilization of MnO_2 at depth in the sediment. However, if the Mn^{2+} released in this manner is trapped below the sediment surface, a secondary source of sub-oxic Mn^{2+} may be provided by

pulses of biogenic material that are sufficiently strong to permit sub-oxic diagenesis to occur close to, or even at, the sediment surface. The components formed during sub-oxic diagenesis tend to have relatively high Mn : Fe ratios (often $\gtrsim 20$), and accrete episodically at rates that can be as high as several hundred millimetres per million years. Sub-oxic diagenetic components characterize the lower surfaces of nodules formed on marginal and hemi-pelagic sediments in which the diagenetic sequence has reached the MnO_2 oxidative utilization stage.

15.3.5 Sediment ferromanganese oxyhydroxides

In addition to macronodules, oceanic sediments contain micronodules and small-sized oxyhydroxides of a non-nodular origin. These are an intimate part of the sediment, and in the present section attention will be focused on the question 'Do they form part of a crust → nodule → sediment oxyhydroxide continuum, or is there a major decoupling between the nodule–sediment system?'

Aplin & Cronan (1985a, b) gave data on the chemical composition of a series of ferromanganese crusts, sediment oxyhydroxides, δMnO_2-rich macronodules and toderokite-rich macronodules from the central Pacific. The authors used a selective leaching technique to determine the compositions of the sediment oxyhydroxides, and then compared these to those of the crusts and nodules from the same sample suite. The data are summarized in Table 15.5, and two principal conclusions can be drawn from this investigation.

(a) The chemical compositions of the crusts, sediment oxyhydroxides and δMnO_2-rich nodules are generally similar. There are, however, some differences between the three phases; for example, the Mn : Fe, Cu : Mn and Co : Mn ratios varied, with those of the δMnO_2-rich nodules being intermediate between those of the crusts and the sediment oxyhydroxides. According to Aplin & Cronan (1985a, b) this can be explained in the following manner. The crusts derive their elements largely from sea water (*hydrogenous* supply). In contrast, the oxyhydroxides acquire most of their elements from processes occurring in the sediments, and in the region studied much of this elemental input arises from the decay of labile biologically transported material during early diagenesis (*oxic diagenetic* supply). The two phases therefore represent a seawater and an oxic diagenetic end-member, respectively. The δMnO_2-rich nodules, which grow at the sediment surface, receive elements from both the hydrogenous seawater and the oxic diagenetic sources; thus, they have a

Table 15.5 Elemental ratios in sediment oxyhydroxides, ferromanganese crusts, δMnO_2-rich nodules and toderokite-rich nodules from the Central Pacific[a]

Elemental ratio	Component			
	Sediment oxyhydroxide[b]	Fe-Mn crusts	δMnO_2-rich nodules	Toderokite-rich nodules
Mn:Fe	0.99	1.15	0.97	2.6
Cu:Mn	0.020	0.009	0.013	0.032
Ni:Mn	0.019	0.020	0.020	0.040
Co:Mn	0.012	0.026	0.019	0.009
Pb:Mn	0.004	0.006	0.0048	0.002
Zn:Mn	0.007	0.003	0.003	0.004

[a] Data from Aplin & Cronan (1985b).
[b] Leached fraction of sediment

composition that is intermediate between those of the seawater and the oxic diagenetic end-members. In this crust–δMnO_2-rich nodule–sediment oxyhydroxide sequence it is therefore oxic diagenetic reactions that perturb the composition of the seawater end-member.

(b) The chemical compositions of the toderokite-rich nodules were quite distinct from those of the members of the crust–δMnO_2-rich nodule–sediment oxyhydroxide sequence. For example, it can be seen from Table 15.5 that the Mn : Fe, Cu : Mn and Ni : Mn ratios are higher, and the Co : Mn ratio lower, in the toderokite-rich nodules than in the other components. These toderokite-rich nodules are indicative of more intense (i.e. sub-oxic) diagenesis, which involves the remobilization of Mn^{2+} from the breakdown of Mn oxides, and Aplin & Cronan (1985b) suggested that in the area under investigation the toderokite, which is a Cu-, Ni- and Zn-poor variety, had precipitated directly from the sediment interstitial waters.

It would appear, therefore, that although δMnO_2-rich nodules can have both a seawater and a diagenetic supply of trace metals, there is a general continuum of compositions in the sequence crusts–δMnO_2-rich nodules–sediment oxyhydroxides. A *major decoupling* is found, however, in the sediment–nodule system, at the sea water/diagenetic boundary, between the δMnO_2-rich and the toderokite-rich nodules. This results because sub-oxic diagenesis is a recycling process, which can release elements already incorporated into the sediments, and depends largely on the extent to which the diagenetic sequence has proceeded. Oxic diagenesis, e.g. when labile biologically transported elements are solubilized, can supply metals

to both sediment oxyhydroxides and nodules. However, the decoupling break is strongest at the point where sub-oxic diagenesis releases Mn^{2+}, which can replace Cu^{2+}, Ni^{2+} and Zn^{2+} in toderokite and can result in the formation of a Cu-, Ni- and Zn-poor toderokite variety, which may subsequently form birnessite (see Sec. 15.3.4.6).

15.3.6 Hydrothermal ferromanganese deposits

The convection of sea water through freshly generated oceanic crust at the centres of sea-floor spreading is now recognized as being a process of gobal geochemical significance (see Secs 5.1 and 6.4). The elements that are solubilized during hydrothermal activity are subsequently removed from solution via solid phases, and the processes involved can be described in terms of the Red Sea system, a system in which the complete sequence of metal-rich precipitates can be found in sediments surrounding the discharge points of the mineralizing solutions.

In the Red Sea system, hot highly saline brines gather in deeps in the central rift valley area. These brines have become enriched in a variety of metals by reacting at high temperatures with underlying evaporites, shales and volcanic rocks. On their discharge, the brines mix with sea water in the deeps. According to Cronan (1980), the Atlantis II Deep, which lies roughly in the centre of the Red Sea, and is an area of present-day metalliferous sediment deposition, can be used to describe the range of hydrothermal precipitates formed in the oceans. The sea water–discharging brine system in the Atlantis II Deep is complex, with two individual brine layers being present. However, it is possible to simplify the sedimentary sequence that is formed from the mineralized solutions in the following manner. The solutions debouch into sea water that has a restricted circulation, and the metals are precipitated from them in the general order: sulphides (e.g. sphalerite, pyrite, chalcopyrite, marcasite, galena) → iron silicates (e.g. smectite, chamosite, amorphous silicates) → iron oxides → manganese oxides. This fractionation of the precipitates manifests itself in their spatial separation from the venting source; for example, the iron and manganese oxides sometimes form separated haloes at a distance from the discharge point.

On the basis of the fractionation found in the Atlantis II Deep it is therefore possible to establish a general hydrothermal precipitation sequence, which occurs in the order: sulphides → iron silicates → iron oxides → manganese oxides. Thus, marine hydrothermal deposits can be thought of as representing various stages in this evolution of the mineralizing solutions. However, it was pointed out in Section 5.1 that the fractionation sequence may commence before the mineralizing solution actually reaches the hydrothermal venting outlet. In this context, two general types of plumbing systems were found to be associated with hydrothermal vents. In the **white smokers** the mixing of sea water and

hydrothermal fluids occurred at depth in the system, with the result that the sulphides had been removed within the vents before the fluids were debouched into sea water at a relatively low temperature. Here, therefore, the hydrothermal sequence had reached the sulphide precipitation stage under the sea floor. In the **black smokers**, however, the hydrothermal fluids, which were dark in colour, were vented directly onto the sea floor itself at a high temperature. Here, therefore, the early stages of the hydrothermal sequence were only reached at the venting outlet and sulphides were precipitated directly at the sea bed; some of the these sulphides were used to build the venting chimneys and some, together with other still dissolved hydrothermally derived elements, were dispersed to carry on the sequence around, and away from, the vents.

Lalou (1983) compiled a list of some 70 marine locations at which hydrothermal deposits have been reported, either at the sediment surface or close to the sediment/basement interface, and the reader is referred to that work for a description of the various types of hydothermal material found in the marine environment. However, some of the marine hydrothermal deposits have been studied in more detail than the others, and a number of these are described below.

EAST PACIFIC RISE The EPR was the classical area for the study of open-ocean hydrothermal deposits, and a wide variety of hydrothermal material has now been identified in this region. This material includes massive sulphide deposits, which have been found at a number of sites between ~ 21°N and ~ 20°S (see e.g. Hekinian *et al.* 1980). Sulphides are formed early in the hydrothermal sequence and are rare on the open-ocean sea bed; thus, the identification of the massive sulphide beds on the EPR was an important discovery. Hydrothermal deposits from the EPR also include Fe silicates (smectites) and a number of Fe, Mn and ferromanganese oxyhydroxides and micronodules; thus, the full hydrothermal precipitation sequence is represented at different locations on the EPR. Sediments from the crest and flank areas of the EPR are often rich in colloidal-sized grains of brown amorphous iron and manganese oxides, which have precipitated from hydrothermal solutions; analyses of such metal-rich sediments from the EPR are given in Table 15.6 (column a).

THE BAUER DEEP This is a small basin that lies between the EPR and the Galapagos Rise in the southeastern Pacific. Surface sediments in the Bauer Deep contain Fe-rich smectite and a wide variety of ferromanganese minerals. Analyses of Bauer Deep metalliferous sediments are included in Table 15.6 (column b).

THE GALAPAGOS REGION It was shown in Section 5.1 that hot springs of the white smoker type have been found on the Galapagos Rise and in the

Table 15.6 Chemical compositions of hydrothermal deposits[a] (units, μg g^{-1})

	a	b	c	d	e	f	g	h	i	j
Mn	60000	46000	39043	430000	550000	470000	40000	279000	410000	380000
Fe	180000	141000	587	1600	2000	6600	232900	10500	8000	27000
Al	5000	23000	-	1800	-	2000	7900	12700	9000	6900
Ti	200	-	-	-	-	28	-	-	400	1060
Co	105	64	19	24	39	13	10	82	33	30
Ni	430	820	353	880	180	125	80	371	310	400
Cu	730	910	43	450	50	80	76	206	120	80
Zn	380	330	-	540	2020	90	35	83	400	310
Mo	30	-	-	-	-	540	-	-	900	-
V	450	-	-	-	-	110	152	214	110	-

[a] Metal-rich sediment crest of East Pacific Rise, data on a carbonate-free basis (Bostrom & Peterson 1969).

[b] Metal-rich sediment, Bauer Deep, central Pacific, data on a carbonate-free basis (Dymond et al. 1974).

[c] Hydrothermal deposits, TAG area, Mid-Atlantic Ridge (Scott et al. 1974).

[d] Hydrothermal deposits, TAG area, Mid-Atlantic Ridge (Toth 1980).

[e] Hydrothermal deposits, Galapagos spreading centre (Moore & Vogt 1976).

[f] Hydrothermal deposits, Galapagos mounds (Moorby & Cronan 1983).

[g] Hydrothermal clay-rich deposit, FAMOUS area, Mid-Atlantic Ridge (Hoffert et al. 1978).

[h] Hydrothermal Fe-Mn concentrations, FAMOUS area, Mid-Atlantic Ridge (Hoffert et al 1978).

[i] Hydrothermal deposits, S.W. Pacific island arc system (Moorby et al. 1984).

[j] Hydrothermal deposits, Gulf of Aden (Cann et. al. 1977).

ridge valley. These springs, which discharge a milky white plume into the surrounding sea water, are examples of low-temperature hydrothermal activity in which the precipitation of hydrothermal material has commenced at depth in the venting system itself and the discharged solutions are enriched in Mn (characteristic of late-stage hydrothermal precipitation) relative to those exhaling from black smokers. The composition of hydrothermal deposits from the Galapagos area is given in Table 15.6 (columns e and f). Moore & Vogt (1976) described manganese crusts from two sites near the Galapagos spreading centre. The crusts, which consisted of toderokite and birnessite, had very high Mn : Fe ratios ($\gtrsim 10^3$) and were estimated to have grown at rates of (1–2) $\times$ 10^3 mm/10^6 yr, i.e. three orders of magnitude faster than the rates of accumulation for hydrogenous crusts.

THE TAG AREA The TAG (Trans-Atlantic Geotraverse) area is located on the Mid-Atlantic Ridge at 26°N. Scott *et al.* (1974) reported data on a number of Mn oxide crusts retrieved from the median valley in the TAG area. These crusts, which were almsot pure Mn oxides, and thus had very

high Mn : Fe ratios, had compositional similarities to those described by Moore & Vogt (1976) from the Galapagos region (see Table 15.6 (column c)). Radiochemical dating indicated that the TAG crusts had grown at the relatively fast rates of ~ 100–200 mm/10^6 yr. Toth (1980) also provided analysis of submarine crusts from the TAG area, and these are given in Table 15.6 (column d). More recently, both black smokers and massive sulphide deposits have been identified in the TAG area (Rona *et al.* 1986).

THE FAMOUS AREA The FAMOUS (French American Mid-Ocean Undersea Study) area is positioned on the Mid-Atlantic Ridge at 37°N, and Hoffert *et al.* (1978) have described a series of hydrothermal deposits that were found there. According to these authors, two types of hydrothermal material were present. (a) A green clay-rich material, consisting of hydromica, smectite and an amorphous Fe–Si mineral, is abundant near the hydrothermal vent. (b) Further away, black ferromanganese concretions, composed of rancieite and toderokite, are the principal hydrothermal components. Chemical compositions of examples of the two types of hydrothermal deposits are given in Table 15.6 (columns g and h).

In terms of the hydrothermal precipitation sequence, the deposits can be divided into sulphides, iron silicates, iron oxides and manganese oxides, and examples of these have been found in the open-ocean hydrothermal systems described above. In both the spatial and vertical precipitation–dispersion models, hydrothermal sulphides are generally restricted either to within the vents themselves or to the immediate vicinity of the venting system. In contrast, Fe and Mn dispersion haloes can cover much greater areas, and ferromanganese oxyhydroxides, nodules and crusts are the characteristic sedimentary components of much open-ocean hydrothermal activity. It is therefore of interest to compare the compositions of these end-member hydrothermal ferromanganese components with those which have a hydrogenous origin. Representative chemical and mineralogical analyses for a hydrogenous crust (column a), an oxic nodule (column b), a sub-oxic nodule (column c) and a ridge centre hydrothermal crust (column d) are given in Table 15.7. However, when hydrothermal crusts are considered it must be remembered that the parent hydrothermal activity is not confined to active centres of sea-floor spreading, but that it can also occur in other regions associated with volcanic activity. One such region can be found in island arcs and their associated marginal basins. For example, Moorby *et al.* (1984) described ferromanganese crusts recovered from several sites on the Tonga–Kermadec Ridge in the southwest Pacific island arc. The average chemical and mineralogical composition of these crusts is also included in Table 15.7 (column i).

Although most crusts are to some extent mixtures of end-member

Table 15.7 Some general characteristics of oceanic Fe–Mn deposits (units, $\mu g\ g^{-1}$)

Chemical composition ($\mu g\ g^{-1}$)	a Hydrogenous crust	b Oxic nodule	c Sub-oxic nodule	d Hydrothermal crust	e Hydrothermal crust
Mn	222000	316500	480000	410000	550000
Fe	190000	44500	4900	8000	2000
Co	1300	280	35	33	39
Ni	5500	10100	4400	310	180
Cu	1480	4400	2000	120	50
Zn	750	2500	2200	400	2020
Mn:Fe	1.2	7.1	98	51	275
Principal mineralogy of Fe-Mn phases	δMnO_2	δMnO_2, toderokite	toderokite	birnessite	birnessite, toderokite
Approximate growth rates ($mm/10^6 yr$)	1-2	10-50	100-200	500	1000-2000

a,b,c Data from Dymond et al. (1984), see Table 15.4.

d Data from Moorby et al. (1984); non-spreading centre hydrothermal deposit, S.W. Pacific island arc.

e Data from Moore & Vogt (1976); spreading centre hydrothermal deposit, Galapagos region.

sources, it is apparent from the various data in Table 15.7 that there are a number of important differences between the hydrothermal and hydrogenous crusts. These can be summarized as follows.

(a) **Growth rates**. In general, the hydrogenous crusts appear to accrete at relatively slow rates, which are of the order of a few millilitres per million years. In contrast, the hydrothermal crusts grow at much faster rates, which are of the order of several hundred millimetres per million years. The principal reason for this difference is probably related to the fact that the hydrothermal crusts are formed in the vicinity of localized pulses of Mn-rich mineralizing solutions, whereas hydrogenous nodules have to rely on a smoothed-out supply of Mn from normal sea water.

(b) **Mineralogy**. Hydrogenous crusts are usually dominated by δMnO_2 phases. However, the predominant minerals in the hydrothermal

crusts are often toderokite or birnessite, i.e. minerals with relatively high Mn : Fe ratios; however, a wide range of manganese minerals has in fact been reported in hydrothermal crusts.

(c) **Chemistry**. There are two principal differences between the chemical compositions of the hydrothermal and hydrogenous crusts. First, the hydrothermal crusts are generally depleted in Co, Ni and Cu compared with their hydrogenous counterparts; this is probably a result of the uptake of these elements in sulphides early in the hydrothermal sequence. Secondly, the hydrothermal crusts exhibit an extreme fractionation of Mn from Fe, evidenced in their relatively very high Mn : Fe ratios, which probably results from the removal of Fe in the sulphide, silicate and Fe oxide phases that precipitate before the Mn oxides in the hydrothermal pulses. Thus, the crusts, in which the constituent elements are derived directly from sea water, are enriched in Mn relative to Fe in hydrothermal regions; however, metal-rich sediments, which are found around active crestal regions, do not show this fractionation of Mn from Fe because they contain a variety of hydrothermal components, including Fe oxides.

Lalou (1983) attempted to establish a coupling between hydrothermal activity and the genesis of ferromanganese nodules on a global scale. To do this, two models for the formation of hydrogenous and hydrothermal deposits were considered. In model I, the two deposits were considered to have essentially independent elemental sources, ridge crest metalliferous material having a local hydrothermal source and abyssal plain nodules having a hydrogenous source – see Figure 15.10a. In this model, therefore, the hydrothermal influence on the formation of the nodules falls off with increasing distance from the source. In model II, an active coupling was suggested between the hydrothermal activity on the ridges and the formation of nodules on the abyssal plains, with both the metalliferous ridge deposits and the nodules receiving an input of hydrothermal Mn – see Figure 15.10b. To set up the second model, Lalou (1983) developed the theme that pulses of hydrothermal Mn are superimposed on a steady-state ocean, and pointed out that the pulsed Mn can be transported far from its source. This topic was considered in Section 6.3, where it was shown that under some conditions hydrothermal plumes are confined to within a relatively short distance of their vents. However, it was also pointed out that data were available to demonstrate that hydrothermal material can be transported for thousands of kilometres from its source, and that its distribution is controlled by mid-depth global oceanic circulation patterns. It would appear therefore that although *most* hydrothermally generated Mn probably accumulates close to the parent vents, at least some fraction of it can enter the major oceanic cycles. Lalou (1983) pointed out that this Mn, much of which is in

the form of small-sized hydroxide particles, is an excellent scavenger for trace metals dissolved in sea water, so that during its transport it will become enriched in elements such as Co, Cu and Ni. The author suggested that this hydrothermal Mn flux, which occurs episodically in the form of pulses, is transported over the abyssal plains and becomes the major source of Mn in many ferromanganese nodules – see Figure 15.10b. Using data available for currently active venting systems, Lalou (1983) attempted to construct a mass balance for the hydrothermal supply of Mn to ferromanganese nodules. The number of active vents necessary on this basis was unrealistic. However, the author suggested that the strength of the hydrothermal activity has varied with geological time, and that the present day is not a particularly active period. As a result, the current fluxes used in the mass-balance calculation will have underestimated past hydrothermal activity.

In model I it is proposed that the hydrothermal influence on the formation of ferromanganese nodules falls off with distance from the source, and this is only to be expected, of course, as the signal strength decreases. However, in model II, hydrothermal activity is envisaged as being episodic and the resulting non-steady-state pulses of Mn are thought to be sufficiently strong, and to be transported sufficiently far, to provide a supply of the element for the formation of ferromanganese nodules, which grow at considerable distances from the source. Clearly, hydrothermal activity is an important source for Fe and Mn (and some other elements) to sea water. The question of its ocean-wide importance over geological time must, however, remain unresolved for the moment.

15.3.7 Ferromanganese deposits in the oceans: summary

(a) Ferromanganese components in oceanic sediments consist of crusts, nodules and oxyhydroxides.
(b) The formation of these ferromanganese components can be related to a hydrogenous–hydrothermal–diagenetic Mn supply trinity.
(c) At the mid-ocean ridges the supply of Mn can be dominated by hydrothermal pulses. Away from the ridges, non-hydrothermal sources become more important, and there is an increasing contribution of elements to ferromanganese components from normal sea water, either directly (hydrogenous supply) or via diagenetic processes that involve a sediment substrate.
(d) In open-ocean areas, oxic diagenesis releases elements close to the sediment surface, but in marginal regions sub-oxic diagenesis drives the processes involved in the liberation of elements following recycling at depth in the sediment column.
(e) The ferromanganese components formed via this hydrogenous–hydrothermal–diagenetic trinity play an extremely important role in

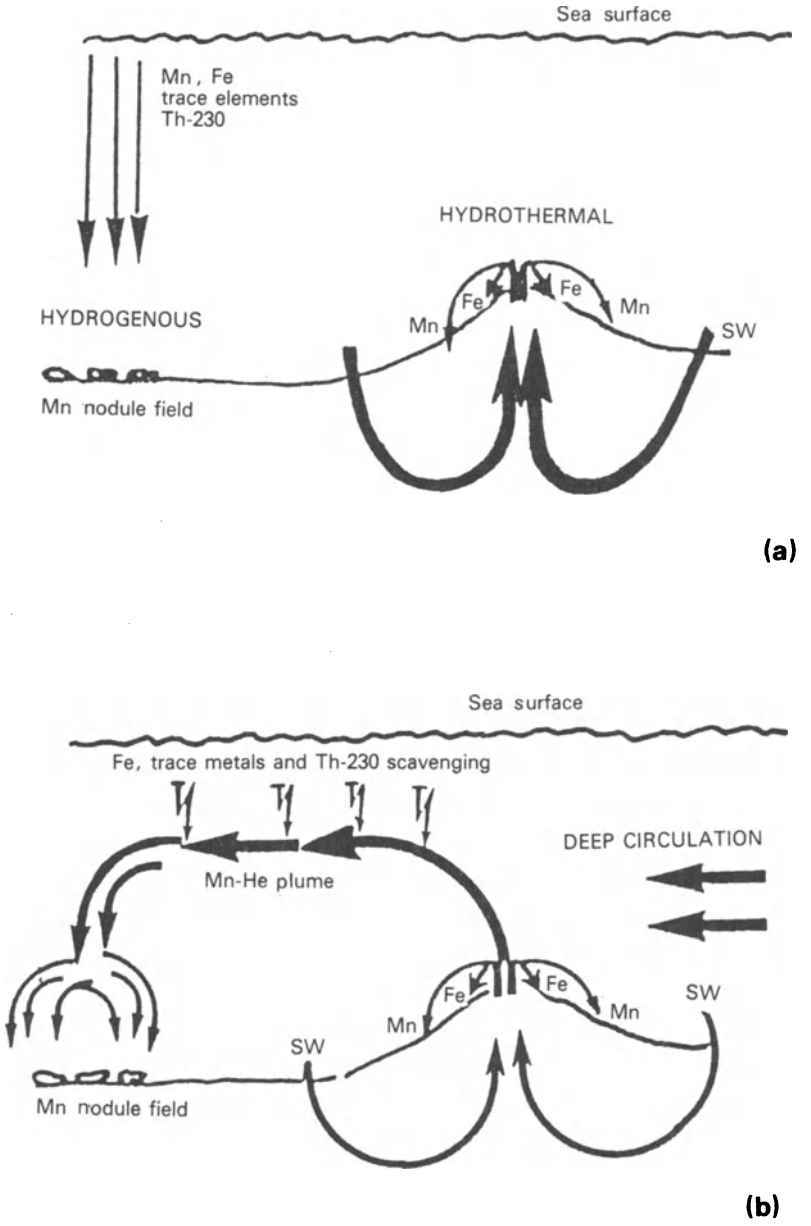

Figure 15.10 The sources for iron and manganese to nodules and hydrothermal deposits in the oceans (from Lalou 1983). (**a**) Model I: the independent formation of hydrothermal deposits on mid-ocean ridges and nodules on abyssal plains. (**b**) Model II: A coupling between the formation of hydrothermal deposits on mid-ocean ridges and nodules on abyssal plains.

removing a variety of dissolved elements from sea water and also exert a major influence on the composition of deep-sea sediments.

15.4 Cosmogenous components

15.4.1 Definition

These are components that have been formed in outer space and have reached the surface of the Earth via the atmosphere. According to Chester & Aston (1976) the extra-terrestrial material that has been identified in deep-sea sediments includes cosmic spherules and microtectites, together with cosmic-ray-produced radioactive and stable nuclides. However, these cosmic components form a very minor part of oceanic sediments, and for a detailed review of the topic the reader is referred to Brownlee (1981).

15.4.2 Cosmic spherules

Essentially, there are two kinds of spherules in deep-sea sediments, the iron and the stony types.

THE IRON SPHERULES Small black magnetic spherules have been found in sediments from all the major oceans (see e.g. Brunn *et al.* 1955, Crozier 1961, Millard & Finkelman 1970). They were first described by Murray & Renard (1891), and it was these authors who suggested that they had a cosmic origin. This type of spherule has a density of ~ 6 g cm^{-3}, and consists of a metallic (Fe–Ni) nucleus surrounded by a shell of magnetite and wüstite, the latter being an iron oxide that is virtually non-existent on Earth but is found in meteorite fusion crusts (see e.g. Murrell *et al.* 1980). According to Murray & Renard (1891), this type of cosmic spherule originated as molten droplets ablated from a meteorite. The droplets then underwent oxidation, during which the outer magnetite shell was formed, as they entered the Earth's atmosphere. In general, this theory is still accepted, and these spherules are considered to have a cosmic origin (see e.g. Parkin *et al.* 1967, Blanchard & Davies 1978, Blanchard *et al.* 1980). Estimates of the influx rates of the iron spherules to the Earth's surface vary widely, ranging from $> 10^6$ to $< 10^3$ ton yr^{-1}; in one of the most recent estimates, Esser & Turekian (1988) used osmium isotope systematics to derive a rate of 4.9×10^4 ton yr^{-1} for the accretion rate of C-1 carbonaceous chondrite material to the Earth's surface. However, it is thought by some workers that the accretion rates of the iron spherules may actually approach zero at certain times. For example, Parkin *et al.* (1967) sampled clean air at Barbados and reported that iron spherules with diameters > 20 μm were reaching the surface of the Earth at ~ 350 ton yr^{-1}, but that most of this could in fact be accounted for by

contamination effects. These authors suggested that variations in the accretion rates of the magnetic spherules, as recorded in deep-sea sediments and ice cores, result from the spasmodic availabiliy of suitable parent meteorites in outer space.

THE STONY SPHERULES These have a density of ~ 3 g cm^{-3} and diameters in the range $\sim$ 15–250 μm, although they often depart from a spherical shape. Essentially, they consist of fine-grained silicates (mainly olivine), magnetite and glass. It is generally thought that this type of spherule has originated from stony meteorites, although the actual mechanism involved in their formation is not clear. For example, Parkin *et al.* (1967) have suggested that they are in fact micrometeorites, which undergo relatively little physical alteration on passage through the atmosphere. However, Blanchard *et al.* (1980) showed that the stony spherules have similarities with chondrite fusion crusts, and concluded that they are products of the atmospheric heating of stony meteroids, a theory that would account for the presence of the magnetite in them. On the basis of their deep-sea sediment storage, Murrell *et al.* (1980) have estimated the accretion rate of the stony spherules to be $\sim$ 90 ton yr^{-1}. However, some of the stony spherules identified in deep-sea sediments may have a terrestrial origin (see e.g. Fredricksson & Martin 1963).

15.4.3 Microtectites

These are small bodies of green-black glass found in large numbers over a few restricted regions of the Earth's surface. They have been identified in bands in deep-sea sediments from the Indian Ocean and the equatorial Atlantic, and probably originate from locally associated strewn fields.

15.4.4 Cosmic-ray-produced nuclides

According to Chester & Aston (1976) cosmic-ray-produced stable and radioactive nuclides that have been identified in deep-sea sediments, and various ice deposits, include ^{36}Cl, ^{26}Al, ^{10}Be, ^{64}Fe, ^{3}He, ^{4}He, ^{40}Ar and ^{36}Ar.

We have now described the compositions and origins of the various components that are found in oceanic sediments. In the following chapter, we will attempt to show how the chemical signals associated with the formation of these components combine together to impose a control on the overall chemical composition of the sediments found in the oceans.

References

Aplin, A.C. & D.S. Cronan 1985a. Ferromanganese oxide deposits from the central Pacific Ocean, I. Encrustations from the Line Islands Archipelago. *Geochim. Cosmochim. Acta* **40,** 427–36.

Aplin, A.C. & D.S. Cronan 1985b. Ferromanganese oxide deposits from the central Pacific Ocean, II. Nodules and associated sediments. *Geochim. Cosmochim. Acta* **49,** 437–51.

Arrhenius, G. 1963. Pelagic sediments. In *The sea*, M.N. Hill (ed.), Vol. 3, 655–727. New York: Interscience.

Bender, M.L., T.-L. Ku & W.S. Broecker 1970. Accumulation rates of manganese in pelagic sediments and nodules. *Earth Planet. Sci. Lett.* **8,** 143–8.

Berger, W.H. 1968. Planktonic foraminifera: selective solution and paleoclimatic interpretation. *Deep-Sea Res.* **15,** 31–43.

Berger, W.H. 1970. Biogenous deep-sea sediments: fractionation by deep-sea circulation. *Geol. Soc. Am. Bull.* **18,** 1385–402.

Berger, W.H. 1976. Biogenous deep sea sediments: production, preservation and interpretation. In *Chemical oceanography*, J.P. Riley & R. Chester (eds), Vol. 5, 265–388. London: Academic Press.

Berger, W.H., C.G. Adelseck & L.A. Mayer 1976. Distribution of carbonate in surface sediments of the Pacific Ocean. *J. Geophys. Res.* **81,** 2617–27.

Berger, W.H. & E.L. Winterer 1974. Plate stratigraphy and the fluctuating carbonate line. *Spec. Publ. Int. Assoc. Sedimentol.* No. 1.

Biscaye, P.E. 1965. Mineralogy and sedimentation of Recent deep-sea clay in the Atlantic Ocean and adjacent seas and oceans. *Geol. Soc. Am. Bull.* **76,** 803–32.

Biscaye, P.E., V. Kolla & K.K. Turekian 1976. Distribution of calcium carbonate in surface sediments of the Atlantic Ocean. *J. Geophys. Res.* **81,** 2595–603.

Bischoff, J.L., D.Z. Piper & K. Leong 1981. The aluminosilicate fraction of North Pacific manganese nodules. *Geochim. Cosmochim. Acta* **45,** 2047–63.

Blanchard, M.B. & A.S. Davies 1978. Analysis of ablation debris from natural and artificial iron meteorites. *J. Geophys. Res.* **83,** 1793–808.

Blanchard, M.B., D.E. Brownlee, T.E. Bunch, P.W. Hodge & F.T. Kyte 1980. Meteor ablation spheres from deep-sea sediments. *Earth Planet. Sci. Lett* **46,** 178–90.

Bostrom, K. & M.N.A. Peterson 1969. The origin of aluminium-poor ferromanganoan sediments in areas of high heat flow on the East Pacific rise. *Mar. Geol. 7,* 427–47.

Bostrom, K., T. Kraemer & S. Gartner 1973. Provenance and accumulation rates of opaline silica, Al, Ti, Fe, Mn, Cu, Ni and Co in Pacific pelagic sediments. *Chem. Geol.* **11,** 123–48.

Broecker, W.S. 1971. A kinetic model for the chemical composition of sea water. *Quat. Res.* **1,** 188–207.

Broecker, W.S. & T.-H. Peng 1982. *Tracers in the sea.* Palisades, NY: Lamont-Doherty Geological Observatory.

Brownlee, D.E. 1981. Extraterrestrial components. In *The sea*, C. Emiliani (ed.), Vol. 7, 733–62. New York: Interscience.

Brunn, A.F., E. Langer & H. Pauly 1955. Magnetic particles found by raking the deep sea bottom. *Deep-Sea Res.* **2,** 230–46.

Burns, R.G. & V.M. Burns 1977. Mineralogy. In *Marine manganese deposits*, G.P. Glasby (ed.), 185–248. Amsterdam: Elsevier.

Burton, J.D. & P.S. Liss 1968. Processes of supply of dissolved silicon in the oceans. *Geochim. Cosmochim. Acta* **37,** 1761–73.

Buser, W. & A. Grutter 1956. Uber die Natur der Mangankollen. *Schweiz. Miner. Petrogr. Mitt.* **36,** 49–62.

REFERENCES

Callender, E. & C.J. Bowser 1980. Manganese and copper geochemistry of interstitial fluids from manganese-rich sediments of the northeastern equatorial Pacific Ocean. *Am. J. Sci.* **280,** 1063–96.

Calvert, S.E. 1968. Silica balance in the oceans and diagenesis. *Nature* **219,** 919–20.

Cann, J.R., C.K. Winter & R.G. Pritchard 1977. A hydrothermal deposit from the floor of the Gulf of Aden. *Mineralog. Mag.* **41,** 193–99.

Chester, R. & S.R. Aston 1976. The geochemistry of deep-sea sediments. In *Chemical oceanography*, J.P. Riley & R. Chester (eds), Vol. 6, 281–390. London: Academic Press.

Chester, R. & M.J. Hughes 1967. A chemical technique for the separation of ferro-manganese minerals, carbonate minerals and adsorbed trace elements from pelagic sediments. *Chem. Geol.* **3,** 199–212.

CLIMAP Project Members. 1976. The surface of the ice age earth. *Science* **191,** 1131–7.

Cronan, D.S. 1976. Manganese nodules and other ferromanganese oxide deposits. In *Chemical oceanography*, J.P. Riley & R. Chester (eds), Vol. 5, 217–63. London: Academic Press.

Cronan, D.S. 1977. Deep-sea nodules: distributon and geochemistry. In *Marine manganese deposits*, G.P. Glasby (ed.), 11–44. Amsterdam: Elsevier.

Cronan, D.S. 1980. *Underwater minerals.* London: Academic Press.

Crozier, D.S. 1961. Micrometeorite measurements – satellite and ground-level data compared. *J. Geophys. Res.* **66,** 2793–5.

DeMaster, D.J. 1981. The supply and accumulation of silica in the marine environment. *Geochim. Cosmochim. Acta* **45,** 1715–32.

Drever, J.I. 1974. The magnesium problem. In *The sea*, Vol. 5, E.D. Goldberg (ed.), 337–57. New York: Interscience.

Drever, J.I. 1982. *The geochemistry of natural waters.* Englewood Cliffs, NJ: Prentice-Hall.

Dymond, J., M. Lyle, B. Finney, D.Z. Piper, K. Murphy, R. Conrad & N. Pisias 1984. Ferromanganese nodules from MANOP Sites H, S and R – control of mineralogical and chemical composition by multiple accretionary processes. *Geochim. Cosmochim. Acta* **48,** 931–49.

Edmond, J.M. 1974. On the dissolution of carbonate and silicate in the deep ocean. *Deep-Sea Res.* **21,** 455–80.

Elderfield, H. 1976. Hydrogenous material in marine sediments: excluding manganese nodules. In *Chemical oceanography*, J.P. Riley & R. Chester (eds), Vol. 5, 137–215. London: Academic Press.

Emiliani, C. & R.F. Flint 1963. The Pleistocene record. In *The sea*, M.N. Hill (ed.), Vol. 3, 888–927. New York: Interscience.

Esser, B.K. & K.K. Turekian 1988. Accretion rate of extraterrestrial particles determined from osmium isotope systematics of Pacific pelagic clay and manganese nodules. *Geochim. Cosmochim. Acta* **52,** 1383–8.

Fredricksson, K. & L.R. Martin 1963. The origin of black spherules in Pacific islands, deep-sea sediments and Antarctic ice. *Geochim. Cosmochim. Acta* **27,** 241–51.

Goldberg, E.D. 1954. Marine geochemistry. Chemical scavengers of the sea. *J. Geol.* **62,** 249–55.

Goldberg, E.D. & G.O.S. Arrhenius 1958. Chemistry of Pacific pelagic sediments. *Geochim. Cosmochim. Acta* **13,** 153–212.

Griffin, J.J. & E.D. Goldberg 1963. Clay-mineral distribution in the Pacific Ocean. In *The sea*, M.N. Hill (ed.), Vol. 3, 728–41. New York: Interscience.

Griffin, J.J., H. Windom & E.D. Goldberg 1968. The distribution of clay minerals in the World Ocean. *Deep-Sea Res.* **15,** 433–59.

Hay, W.W. (ed.) 1974. *Studies in paleo-oceanography*. Soc. Econ. Paleontol. Min., Spec. Publ., no. 20.

Hekinian, R., M. Fevrier, J.L. Bischoff, P. Picot & W.C. Shanks 1980. Sulphide deposits from the East Pacific Rise near 21°N. *Science* **207,** 1433–44.

Hem, J.D. 1978. Redox processes at surfaces of manganese oxide and their effects on aqueous metal ions. *Chem. Geol.* **21,** 199–218.

Hoffert, M., A. Perseil, R. Hekinian, P. Choukroune, H.D. Needham, J. Francheteau & X. Le Pichon 1978. Hydrothermal deposits sampled by diving saucer in Transform Fault 'A' near 37°N on the Mid-Atlantic Ridge, FAMOUS area. *Oceanol. Acta* **1,** 73–86.

Holland, H.D. 1978. *The chemistry of the atmosphere and oceans*. New York: Wiley.

Kennet, J.P. 1982. *Marine geology*. Englewood Cliffs, NJ: Prentice-Hall.

Kolla, V.R., A.W.H. Be & P.E. Biscaye 1976. Calcium carbonate distribution in surface sediments of the Indian Ocean. *J. Geophys. Res.* **81,** 2605–16.

Ku, T.L. 1977. Rates of accretion. In *Marine manganese deposits*, G.P. Glasby (ed.), 249–67. Amsterdam: Elsevier.

Lalou, C. 1983. Genesis of ferromanganese deposits: hydrothermal origin. In *Hydrothermal processes at seafloor spreading centres*, P.A. Rona, K. Bostrom, L. Laubier & K.L. Smith (eds), 503–34. New York: Plenum.

Li, Y.-H., T. Takahashi & W.S. Broecker 1969. Degree of saturation of $CaCO_3$ in the oceans. *J. Geophys. Res.* **23,** 5507–25.

Luz, B. & N.J. Shackleton 1975. $CaCO_3$ solution in the tropical East Pacific during the past 130 000 years. In *Dissolution of deep-sea carbonates*, W.V. Sliter, A.W.H. Be & W.H. Berger (eds), 142–50. Spec. Publ. no. 13. Washington, DC: Cushman Foundation.

Lyle, M., G.R. Heath & J.M. Robbins 1984. Transport and release of transition elements during early diagenesis: sequential leaching of sediments from MANOP sites M and H, Part I. pH 5 acetic acid leach. *Geochim. Cosmochim. Acta* **48,** 1705–15.

Mackenzie, F.T. & R.M. Garrels 1966. Chemical mass balance between rivers and oceans. *Am. J. Sci.* **264,** 507–25.

Manheim, F.T. 1965. Manganese-iron accumulations in the shallow marine environment. In *Symposium on marine geochemistry*, D.R. Shrink & J.T. Corless (eds), 217–76. Narragansett Mar. Lab., Univ. Rhode Island, Occas. Publ. no. 3–1965.

Martin, J.H. & G.A. Knauer 1983. VERTEX: manganese transport with $CaCO_3$. *Deep-Sea Res.* **30,** 411–25.

Mero, J.L. 1962. Ocean-floor manganese nodules. *Econ. Geol.* **57,** 747–67.

Millard, H.T. & R.B. Finkelman 1970. Chemical and mineralogical compositions of cosmic and terrestrial spherules from a marine sediment. *J. Geophys. Res.* **75,** 2125–34.

Moorby, S.A. & D.S. Cronan 1983. The geochemistry of hydrothermal and pelagic sediments from the Galapagos Hydrothermal Mounds DSDP Leg 70. *Mineralog. Mag.* **47,** 291–300.

Moorby, S.A., D.S. Cronan & G.P. Glasby 1984. Geochemistry of hydrothermal Mn-oxide deposits from the S.W. Pacific island arc. *Geochim. Cosmochim. Acta* **48,** 433–41.

Moore, W.S. & P.R. Vogt 1976. Hydrothermal manganese crust from two sites near the Galapagos spreading axis. *Earth Planet. Sci. Lett.* **29,** 349–56.

Morse, J.W. & R.A. Berner 1972. Dissolution kinetics of calcium carbonate in seawater: II. A kinetic origin for the lysocline. *Am. J. Sci.* **272,** 840–51.

Murray, J. & A.F. Renard 1891. *Deep-sea deposits*. Sci. Rep. *Challenger* Exped., no. 3. London.

Murrell, M.T., P.A. Davies, K. Nishizumi & H.T. Millard 1980. Deep-sea spherules from Pacific clay: mass distribution and influx rate. *Geochim. Cosmochim. Acta* **44,** 2067–74.

REFERENCES

Parkin, D.W., A.C. Delany & A.C. Delany 1967. A search for airborne cosmic dust on Barbados. *Geochim. Cosmochim. Acta* **31,** 1311–20.

Piper, D.Z., J.R. Basler & J.L. Bischoff 1984. Oxidation state of marine manganese nodules. *Geochim. Cosmochim. Acta* **48,** 2347–55.

Pratt, R.M. & P.F. McFarlin 1966. Manganese pavements on the Blake Plateau. *Science* **151,** 1080–2.

Price, N.B. & S.E. Calvert 1970. Compositional variation in Pacific Ocean ferromanganese nodules and its relationship to sediment accumulation rates. *Mar. Geol.* **9,** 145–71.

Raab, W.J. & M.A. Meylan 1977. Morphology. In *Marine manganese deposits*, G.P. Glasby (ed.), 109–46. Amsterdam: Elsevier.

Redfield, A.C., B.H. Ketchum & F.A. Richards 1963. The influence of organisms on the composition of seawater. In *The sea*, M.N. Hill (ed.), Vol. 2, 26–77. New York: Interscience.

Riley, J.P. & R. Chester 1971. *Introduction to marine chemistry*. London: Academic Press.

Rona, P.A., G. Klinkhammer, T.A. Nelson, J.H. Trefry & H. Elderfield 1986. Black smokers, massive sulphides and vent biota at the Mid-Atlantic Ridge. *Nature* **321,** 33–7.

Schopf, T.J.M. 1980. *Paleoceanography*. Cambridge, MA: Harvard University Press.

Scott, M.R., R.B. Scott, P.A. Rona, L.W. Butler & A.J. Nalwak 1974. Rapidly accumulating manganese deposit from the median valley of the Mid-Atlantic Ridge. *Geophys. Res. Lett.* **1,** 355–8.

Shackleton, N.J. 1982. The deep-sea sediment record of climate variability. *Prog. Oceanogr.* **11,** 199–218.

Sillen, L.G. 1961. The physical chemistry of sea water. In *Oceanography*, M. Sears (ed.), 549–81. Am. Assoc. Adv. Sci. Publ. no. 67.

Sillen, L.G. 1963. How has sea water got its present composition? *Sven, Kem, Tidskr.* **75,** 161–77.

Sillen, L.G. 1965. Oxidation state of earth's ocean and atmosphere. I. A model calculation on earlier states. The myth of the 'probiotic soup'. *Arkiv Kemi* **24,** 431–44.

Sillen, L.G. 1967. Gibbs phase rule and marine sediments. In *Equilibrium concepts in natural water systems*, W. Stumm (ed.), 57–69. ACS Adv. Chem. Ser. no. 67. Washington, DC: American Chemical Society.

Toth, J.R. 1980. Deposition of submarine crusts rich in manganese and iron. *Geol. Soc. Am. Bull.* **91,** 44–54.

Vincent, E. & W.H. Berger 1981. Planktonic foraminifera and their use in paleoceanography. In *The sea*, C. Emiliani (ed.), Vol. 7, 1025–119. New York: Interscience.

Wollast, R. 1974. The silica problem. In *The sea*, E.D. Goldberg (ed.), Vol. 5, 359–92. New York: Interscience.

16 Unscrambling the sediment-forming chemical signals

In Chapter 3 it was suggested that rivers could be viewed as the carriers of chemical signals to the oceans. We are now attempting to understand the factors that control the chemical composition of marine sediments, and from the point of view of the present volume attention is focused on the upper portions of the sediment column since it is the material here that reacts directly with sea water. In a manner broadly similar to that used for rivers, the oceanic water column can therefore be viewed as a medium through which chemical signals, or *fluxes*, are transmitted to the upper portions of the marine sediment column. In addition, signals can be transmitted through interstitial water. However, there is a problem in identifying the various chemical signals that are actually transmitted through the water column. A number of authors have suggested that the overall elemental compositions of deep-sea sediments can be considered in terms of the contributions made by individual sediment *fractions*. For example, Krishnaswami (1976) postulated that the total concentration of an element in Pacific pelagic clays is the sum of the contributions made by the detrital and the authigenic fractions – see Equation 16.1. However, this is a very broad distinction and each of these fractions contains a number of individual sediment-forming *components*. In order to expand Krishnaswami's original concept it is therefore necessary to consider the individual components themselves. Taking an approach in which the formation of the components is viewed in terms of *chemical signals* offers a potentially attractive insight into the factors that control the overall composition of the marine sediments. In Section 13.6 the question of whether or not the components, or sediment building blocks, could be related to individual chemical signals was tentatively raised. However, now that the components have been described (Ch. 15) it has become apparent that the processes involved in the generation of some of them cannot in fact be related to single signals, but rather are a function of *signal coupling*. For example, ferromanganese nodules can receive elements transmitted by signals associated with hydrogenous, hydrothermal and both oxic and sub-oxic diagenetic processes. Thus, it is not possible to use a simple component-orientated signal framework. Despite this, it is still rewarding to follow the path suggested by Krishnaswami

(1976), and to consider the chemical composition of deep-sea sediments as being a function of contributions from individual fractions. The problem arises, however, when attempting to relate the components associated with the fractions to specific chemical signals. To expand Krishnaswami's original idea into one that considers component-forming signals or fluxes, a distinction must therefore be made between individual signals that are *potentially* able to give rise to individual components but more often combine together to form multi-source components. In the present approach, therefore, an attempt will be made to relate the chemistry of marine sediments to chemical signals that are associated with the *processes* involved in the generation of the sediment-forming components. It must be stressed, however, that this is a purely artificial approach and is adopted simply in order to provide a convenient framework within which to describe the factors that control the chemical compositions of the sediments.

16.1 Definition of terminology

To simplify the often confused terminology found in the literature, the chemical signals described here will be defined on the basis of the processes that have been shown to be operative in the formation of the sediment components, i.e. the *process-orientated* approach will be adopted. Initially, a distinction will be made between **detrital** (or lithogenous) and **non-detrital** (or non-lithogenous) components (see Sec. 3.1.4). This dual-component classification involves a fundamental geochemical division between two different types of elements.

(a) Detrital elements are part of the crystalline mineral matrix, usually in lattice-held associations, and have been carried through the mobilization–transportation cycle in a solid form.
(b) Non-detrital elements are not part of the mineral matrix, but have been removed from solution in association with either inorganic or organic hosts.

It should be stressed that this simple two-fold classification takes no account of non-lattice → lattice transformations that can affect some elements, e.g. during diagenesis. At this stage, therefore, only two general types of elements have been identified: those which have been transported within mineral lattices, and those which have been removed from solution at some time during the mobilization–transportation history of the host component.

In reality, of course, the signal associated with the formation of non-detrital components can be resolved into a number of individual signals

associated with the supply and removal of elements from the solution phase. The nature of these signals can be related to the processes involved in the generation of the sediment-forming components. These processes have been described in Chapter 15. In that chapter, the elements that were originally classified as 'hydrogenous' were related to a number of different processes and were defined as being oxic diagenetic, sub-oxic diagenetic, hydrogenous and hydrothermal in origin. When the formation of the sediment components was discussed it became apparent that there is a degree of **coupling** between some of the components formed via the non-detrital signal; for example, that between hydrogenous ferromanganese crusts, sediment ferromanganese oxy-hydroxides and δMnO_2-rich ferromanganese nodules. However, it was also shown that there was a major **decoupling** between these three components and toderokite-rich nodules. These toderokite-rich nodules are formed largely via elements supplied from within the sediment following their release at depth during sub-oxic diagenesis. Thus, a distinction could be made between elements supplied to the sediment surface from the sea water column *above*, and those supplied from the interstitial water column *below*. Elements can be supplied to the interstitial water either at the sediment surface, where they are released directly from material carried down the water column, or at depth, where some elements are released from secondary oxidants. To understand this, it is necessary to refer back to Section 14.2.1 in which the nature of the diagenetic process was described. *Oxic* diagenesis takes place in the presence of dissolved oxygen, and when this occurs at or near the sediment surface the elements released from the biogenic carriers will be available to sediment-forming components in much the same way as those derived directly from solution in sea water, although at different supply rates. In contrast, sub-oxic diagenesis occurs when all the dissolved oxygen has been exhausted and organic carbon is 'burned' by secondary oxidants. This usually takes place at some depth in the sediments and the elements mobilized are transported through the interstitial water column. Further, it has now been established that there is a major decoupling break between the processes involved in oxic and sub-oxic diagenesis. In terms of the identification of the chemical *signals* that result in the formation of sediment components, it is necessary to take account of this **decoupling break**, and for this reason a gross distinction will therefore be made between those signals transmitted via *sea water*, which will include the supply of elements released during oxic diagenesis at the sediment surface, and those transmitted via *interstitial water*, which are mainly released at depth during sub-oxic diagenetic mobilization. It is extremely important to differentiate between these two kinds of sediment diagenesis because elements released at the sediment surface from oxic processes represent a *primary* sediment supply, whereas sub-oxic mobilization at

depth can involve a *recycled* supply of elements associated with the secondary oxidants that are destroyed in the diagenetic process.

Up to this point, therefore, a distinction has been made between a sea water (primary) and an interstitial-water sub-oxic diagenetic (secondary) element-transmitting non-detrital signal. However, on the basis of the sediment components formed, the seawater signal can itself be subdivided into biogenous, hydrogenous, oxic diagenetic and hydrothermal types. In the process-oriented approach used here for the classification of the chemical signals transmitted to marine sediments the following signal types will therefore be identified.

(a) The **detrital** signal. This is a background signal, which transmits elements carried in the crystalline matrix of lithogenous minerals.

(b) The **non-detrital** signal. This transmits elements that have been removed from solution. It is subdivided into the following categories.

(i) The **biogenous** signal. In the present context, this refers mainly to biological shell material, and excludes the organic carbon involved in the down-column transport of trace elements to the sediment surface.

(ii) The **authigenic** signal. This term will be used here to describe the primary background signal transmitted through sea water, and as such includes both the hydrogenous and the oxic diagenetic signals. In an ocean-wide context, the hydrogenous signal receives contributions from *all* the sources that supply constituents to sea water, but in the present definition material from these sources is regarded as being smoothed out into a general background signal, i.e. one that excludes the effects of localized inputs from, for example, hydrothermal sources. The oxic diagenetic signal also involves the removal of elements from sea water followed by their release at or near the sediment surface. The *inorganic* processes that remove elements carried by both the hydrogenous and the oxic diagenetic signals are therefore linked together, and in the present context it is a combination of the two which is termed authigenic signal, i.e. the signal giving rise to components formed inorganically from material originating directly in the overlying *background* sea water.

(iii) The **hydrothermal** signal. This applies, in the sense used here, to the sea water signal resulting from the pulsed debouching of high-temperature solutions at the ridge crests.

(iv) The **diagenetic**, or sediment-recycled, signal. As used in the present context, this describes the signal transmitted through the interstitial water column following sub-oxic diagenetic mobilization, i.e. this is largely a recycled signal involving redox-sensitive elements (e.g. Mn).

(v) The **contaminant** signal. This arises from the introduction of anthropogenic material into the oceans.

The detrital and authigenic signals, both of which are transmitted via the water column, operate on an ocean-wide basis, and so may be regarded as carrying the background elements that have a direct sea water source. The biogenous signal principally involves carbonate and opaline shell material and, although siliceous sediments are restricted to certain environments, carbonates cover extensive areas of the deep-sea floor (see Sec. 15.2.1). In view of this, therefore, the biogenous signal, as defined here, is also considered to operate on an ocean-wide basis and to carry background elements. To establish a theoretical framework within which to unscramble the sediment-forming signals it is therefore convenient to envisage marine sediments as being formed by mixtures of these direct water column **background** signals, upon which are super-imposed perturbation **spikes** from more localized hydrothermal and contaminant sea water signals, and from the more widely occurring interstitial water sub-oxic diagenetic signals. However, it must be remembered that the elements associated with the diagenetic signal have been recycled and could have had a variety of primary sources. In the present context, however, any signal that is not **directly** associated with the water column background is regarded as a spike.

The question that must now be considered is 'How can these various signals be unscrambled?' A variety of techniques have been employed for this purpose, and these include the following.

(a) Interpretation of total sediment chemical analyses. These can be used, for example, to assess the relative amounts of major components such as clays, carbonates and opaline silica in oceanic sediments (see e.g. El Wakeel & Riley 1961).
(b) Spatial mapping of elemental concentrations. This can be employed, for example, to establish elemental source–transport patterns (see e.g. Turekian & Imbrie 1966).
(c) Elemental accumulation rate comparisons. These can be used to determine the rates at which different components are formed (see e.g. Bender *et al.* 1970).
(d) Factor analysis (see e.g. Krishnaswami 1976), isotope analysis (see e.g. Thompson *et al.* 1984) and chemical leaching techniques (see e.g. Chester & Hughes 1967). These can be utilized to assess the partitioning of elements between individual sediment phases.

Techniques such as those identified above will be introduced into the text as each of the individual chemical sediment-forming signals is described in the following sections.

16.2 The biogenous signal

The deposition of calcareous and siliceous organisms in marine sediments, and the degree to which they are preserved, plays a dominant role in controlling the major element chemistry of the deposits. Siliceous sediments have a generally restricted distribution and, with a few important exceptions, they are confined to the edges of the oceans (see Sec. 15.2.1). However, carbonate sediments are much more widespread and, in fact, the bulk composition of many deep-sea deposits may be considered to be made up of mixtures of carbonate and lithogenous end-members. The extent to which carbonate and siliceous components affect the overall major element composition of deep-sea sediments can be estimated from the proportions of Al (lithogeneous), Si (siliceous) and Ca (carbonate) present; see, for example, the major element analyses listed in Table 13.4. However, it was pointed out in Section 13.5 that, with the exception of Sr, which occurs in the carbonate lattice, both carbonate and siliceous sediments are generally impoverished in those excess trace metals that are concentrated in deep-sea clays. Further, neither of these shell phases act as significant carriers for the down-column transport of trace metals.

It may be concluded, therefore, that both carbonate and siliceous components can comprise large bulk fractions of many deep-sea sediments, and that the chemical signals involved can be unscrambled by relating them to the major element compositions of the deposits. These biogenous shell phases are not, however, important trace metal hosts, and indeed it is common practice to express trace metal sediment analyses on a carbonate-free basis to overcome the dilution effects of the shell matrix. Thus, in terms of trace metal transport, the biogeneous shell-associated signals can be generally ignored.

With respect to the background transport of trace metals to marine sediments, and the incorporation of the excess trace metal fractions into deep-sea clays, attention can therefore be focused largely on the detrital and authigenic signals. In a normal deep-sea clay, i.e. one that has not been perturbed by major hydrothermal, diagenetic or contaminant spikes, the total concentration (C_t) of an element may therefore be expressed in terms of the sum of the contributions from detrital and authigenic components:

$$C_t = C_d + C_a \tag{16.1}$$

where C is the concentration of the element and the suffixes t, d and a refer to the total, detrital and authigenic concentrations, respectively (see e.g. Krishnaswami 1976). In terms of this two-component framework, an attempt will now be made to unscramble the detrital and authigenic signals.

16.3 The detrital signal

In the definition used here, the detrital signal transmits elements carried in the crystalline matrix of lithogenous minerals. Crust-derived weathering products, together with continental and submarine volcanic debris, make up most of the lithogenous material transported to the oceans over geological time. This lithogenous material comprises the bulk of deep-sea clays; for example, the oxides of aluminium and silicon alone account for ~ 80% of the total sediments. This crust-derived material is brought to the open ocean mainly along the fluvial and atmospheric routes, but it is important to remember that the material carried by these forms of transport consists of both detrital and non-detrital components. For example, river particulate material removes elements from solution into the non-detrital phase, and some of the components of atmospheric particulates are found in loosely held, i.e. non-matrix, positions. Clearly, therefore, the *bulk* compositions of river and atmospheric particulates cannot be used to assess the composition of the detrital signal (C_d) transmitted to the oceans.

16.4 The authigenic signal

The geochemically important primary authigenic material in marine sediments consists mainly of ferromanganese crusts, nodules and sediment oxyhydroxides, which are formed by hydrogenous and oxic diagenetic processes, together with the population of elements associated with a wide variety of sediment components in inter-sheet and surface-adsorbed positions. The detailed chemistry of these primary authigenic components has been described in Section 15.3, and the average

Table 16.1 Typical compositions of primary authigenic components in deep-sea sediments[a] (units, μg g^{-1})

Elements	Hydrogenous crusts	Oxic nodules	Sub-oxic nodules	Pelagic clays
Mn	222000	316500	480000	65000
Fe	190000	44500	4900	12500
Co	1300	280	35	116
Ni	5500	10100	4400	293
Cu	1480	4400	2000	570
Zn	750	2500	2200	-
Al	11800	27100	7500	83000

compositions of the crusts and nodules are summarized in Table 16.1. It can be seen from this table that these authigenic components are rich in those elements which are present in deep-sea clays in excess concentrations (see also Table 13.5). Some of the authigenic components, such as micronodules and oxyhydroxides, are an intimate part of the sediment complex, and in certain regions they can have a major influence on the composition of the total sediments with respect to the excess trace elements.

16.5 Unscrambling the detrital and authigenic signals

In terms of the two-fold detrital–authigenic component classification, the bulk of the sediment-forming components in deep-sea clays are carried by the detrital signal, the major part of which is transported via fluvial and atmospheric pathways from continental crust sources. This detrital material is a major end-member component of multi-source deep-sea clays, but it cannot account for the presence of the excess trace metals in the deposits. Authigenic components are quantitatively much less important than the detrital material in most normal pelagic clays, but they are rich in the excess trace metals. However, the proportions in which the authigenic and detrital components are present in deep-sea sediments vary from one sediment suite to another, and it is therefore necessary to unscramble the signals associated with the two components. There are several ways which this can be done, and some of these are discussed below.

THE DIRECT APPROACH USING CHEMICAL LEACHING PROCEDURES In this approach, the detrital and authigenic fractions of a sediment are actually separated and one, or both, are analysed individually. For example, Chester & Hughes (1967) used a chemical leaching technique to establish elemental partitioning in a North Pacific pelagic clay core, and Chester & Messiha-Hanna (1970) applied the same technique to a series of North Atlantic deep-sea sediments. The data for the chemical compositions of the detrital and authigenic fractions of the sediments determined in this way are given in Table 16.2.

THE INDIRECT APPROACH Several routes can be employed when this approach is utilized.

(a) **Background correction**. When this route is adopted, it is assumed that the chemical composition of the detrital fraction can be estimated with respect to some reference material. For example, Krishnaswami (1976) used the compositions of (i) continental shale and (ii) nearshore sediments as being representative of that of crust-

Table 16.2 Estimated chemical compositions of the detrital and authigenic fractions of deep-sea clays (units, $\mu g\ g^{-1}$)

(a) Detrital fractions

Element	a	b	c	d	e	f	g	h
Mn	578	2087	770	605	550	740	850	850
Fe	42280	43300	51800	51240	-	51800	69900	47000
Cu	51	244	45	36	67	212	48	45
Co	24	48	24	23	12	16	13	19
Ni	65	92	56	65	63	46	55	68
Zn	111	-	117	124	-	-	95	95
V	158	-	153	-	120	92	130	130
Cr	-	-	-	-	72	91	100	90

[a] Nares Abyssal Plain red clays; estimated using background correction with respect to local grey clays (Thompson et al. 1984).

[b] Pacific pelagic clays; estimated using background correction with respect to continental shales (Krishnaswami 1976).

[c] Nares Abyssal Plain red clays; estimated using graphical procedure (Thompson et al. 1984).

[d] Bermuda Rise carbonates; estimated using graphical procedure (Bacon & Rosholt 1982).

[e] Atlantic deep-sea sediments; estimated using chemical leaching technique (Chester & Messiha-Hanna 1970).

[f] Pacific pelagic clay; estimated using chemical leaching technique (Chester & Hughes 1967)

[g] Average nearshore mud (Wedepohl 1960).

[h] Average shale (Wedepohl 1968).

derived material transported to the marine environment. In terms of Equation 16.1, values of C_t were therefore obtained by direct analysis, and C_d was assumed to be the same as that of either continental shales or nearshore muds. Thus, the composition of C_a could be obtained from $C_t - C_d$. The compositions of continental shales and nearshore sediments are given in Table 16.2a, and those for the derived authigenic fraction are listed in Table 16.2b. A different kind of background correction approach was employed by Thompson *et al.* (1984) for a suite of clays from the Nares Abyssal Plain in the northeast Atlantic. Two types of clay were found in this area, a **red clay** an a **grey clay**. On the basis of their total sediment analyses it was evident that the grey clays had only a negligible non-detrital fraction, and it was assumed that for these sediments $C_t \simeq C_d$. The data for the composition of the grey clays, which are

Table 16.2b

(b) Authigenic fraction

Element	a	b	c	d	e
Mn	4400	4380	3871	3112	7000
Fe	-	-	-	-	7500
Cu	110	101	110	128	225
Co	6	73	60	-	80
Ni	61	147	112	62	175
Zn	40	-	-	-	-

[a] Bermuda Rise carbonates; estimated using graphical procedure (Bacon & Rosholt 1982).

[b] Pacific pelagic clay; estimated using chemical leaching technique (Chester & Hughes 1967).

[c] Atlantic deep-sea sediments; estimated using chemical leaching technique (Chester & Messiha-Hanna 1970).

[d] Atlantic deep-sea sediments; estimated using chemical leaching technique (Thomas 1987).

[e] Pacific pelagic clays: best estimate using a variety of techniques (Krishnaswami 1976).

therefore representative of the detrital fraction, are given in Table 16.2a.

(b) **Graphical procedures**. Bacon & Rosholt (1982) used a graphical approach to estimate the compositions of the detrital and authigenic (pelagic) components in sediments from the Bermuda Rise in the North Atlantic. These authors assumed that the total trace metal content of the sediments could be expressed in terms of a two-component terrigenous (detrital) and pelagic (authigenic) system by the equation:

$$C_{tot} = f(C_{pel} - C_{ter}) + C_{ter} \qquad (16.2)$$

where C_{tot}, C_{pel} and C_{ter} are the metal concentrations in the total sediment, the pelagic and the terrigenous components, respectively, and f is the proportion of the pelgaic component in the sediment. If C_{ter} and C_{pel} are constant, then a plot of C_{tot} versus f will have a linear relationship. Bacon & Rosholt (1982) extrapolated this relationship to give estimates of the compositions of a pure terrigenous ($f = 0$) and a pure pelagic ($f = 1$) component. The

compositional data for the terrigenous (detrital) and pelagic (authigenic) end-member components obtained in this way are given in Tables 16.2a and b, respectively. In addition to their background correction method, Thompson *et al.* (1984) also used a graphical approach to estimate the detrital composition of their Nares abyssal plain sediments. The data obtained are included in Table 16.2a, and the graphical approach used is discussed in more detail later in this section.

(c) **Manganese nodule model**. Krishnaswami (1976) used this model, which is based on the assumption that the rates of precipitation for authigenic trace metals are the same in pelagic clays and ferromanganese nodules. Using compositional data obtained from nodules, Krishnaswami (1976) was then able to estimate the concentrations of a series of elements in the authigenic fractions of Pacific pelagic clays. These data are given in Table 16.2b.

Several different estimates are therefore available for the composition of the detrital and authigenic components present in deep-sea sediments (see Table 16.2). Perhaps the most striking feature to emerge from these data is that there is a generally good agreement between the estimates, especially for the composition of the detrital fraction in deep-sea sediments. Thus, it is possible, at least to a first-order approximation, to unscramble the detrital from the authigenic signal if the chemical composition of the total sediment is known. The signal strengths will, of course, be dependent on the relative rates at which the components associated with the detrital and authigenic signals accumulate. The manner in which the proportions of the two components vary in oceanic sediments can be illustrated with respect to the Atlantic Ocean.

Chester & Messiha-Hanna (1970) and Thomas (1987) used chemical leaching procedures to investigate the partitioning of a series of elements in samples from the present-day Atlantic sediment surface. A compilation of their data, expressed in terms of the two-component detrital–authigenic classification, is given in Table 16.3, and the data are illustrated in Figure 16.1. From Table 16.3 it can be seen that the average partitioning signatures of the elements vary considerably; for example, Al is ~ 80% detrital, whereas Mn is ~ 70% authigenic in character. However, these are ocean-wide averages, and the partitioning signatures of some elements vary with the environment of deposition of the host sediment. An example of this has been provided by Thomas (1987) who compared the partitioning signatures of a range of elements in a North Atlantic marginal (hemi-pelagic) sediment with those in a Mid-Atlantic Ridge sediment. The data are given in Table 16.4, and show that, whereas Al, Fe and Cr retain their detrital character (and Mn remains strongly authigenic) in sediments from both environments of deposition, Cu, Ni

Table 16.3 Average detrital-authigenic partitioning of elements in North Atlantic deep-sea sediments[a]

Element	% of total concentration	
	Detrital	Authigenic
Al	81	19
Fe	82	18
V	71	29
Cr	70	30
Ni	55	45
Cu	44	56
Co	42	48
Mn	32	68

[a] Data from Chester & Messiha-Hanna 1970) and Thomas (1987).

and Pb are considerably more authigenic in nature in the ridge than in the marginal sediments. Chester *et al.* (1988) used a six-stage sequential leaching technique, in which the non-detrital fraction was subdivided into a number of individual trace metal hosts, to investigate the partitioning of Cu in North Atlantic deep-sea surface sediments. The results are illustrated in Figure 16.2 in terms of an east–west, marginal → open ocean → marginal, sediment transect. The principal partitioning trends can be summarized as follows.

(a) There is a general decrease in the proportion of detrital Cu (stage 5) away from the margins to the mid-ocean regions, as the influence of continentally derived material decreases.
(b) The highest proportion of organically associated non-detrital Cu (stage 5) is found in marginal areas under regions of high surface water primary production; this is an important finding, since it suggests that in these regions significant amounts of non-detrital Cu can be stored in a relatively immobile form as the organic carriers escape oxic diagenetic destruction at the sediment surface.
(c) There is a clear trend in the distribution of Cu associated with the easily reducible oxides of stage 3 (mainly new manganese oxides), with the highest contributions being found in mid-ocean deposits around the Mid-Atlantic Ridge and ridge flanks and the lowest in sediments from the marginal areas. These mid-ocean sediments also contain enhanced concentrations of total Cu, and it is evident, therefore, that these mainly result from the element being incorporated into the stage 3 oxide hosts.

This type of spatial variation in elemental partitioning signatures is extremely important in relation to understanding the processes that

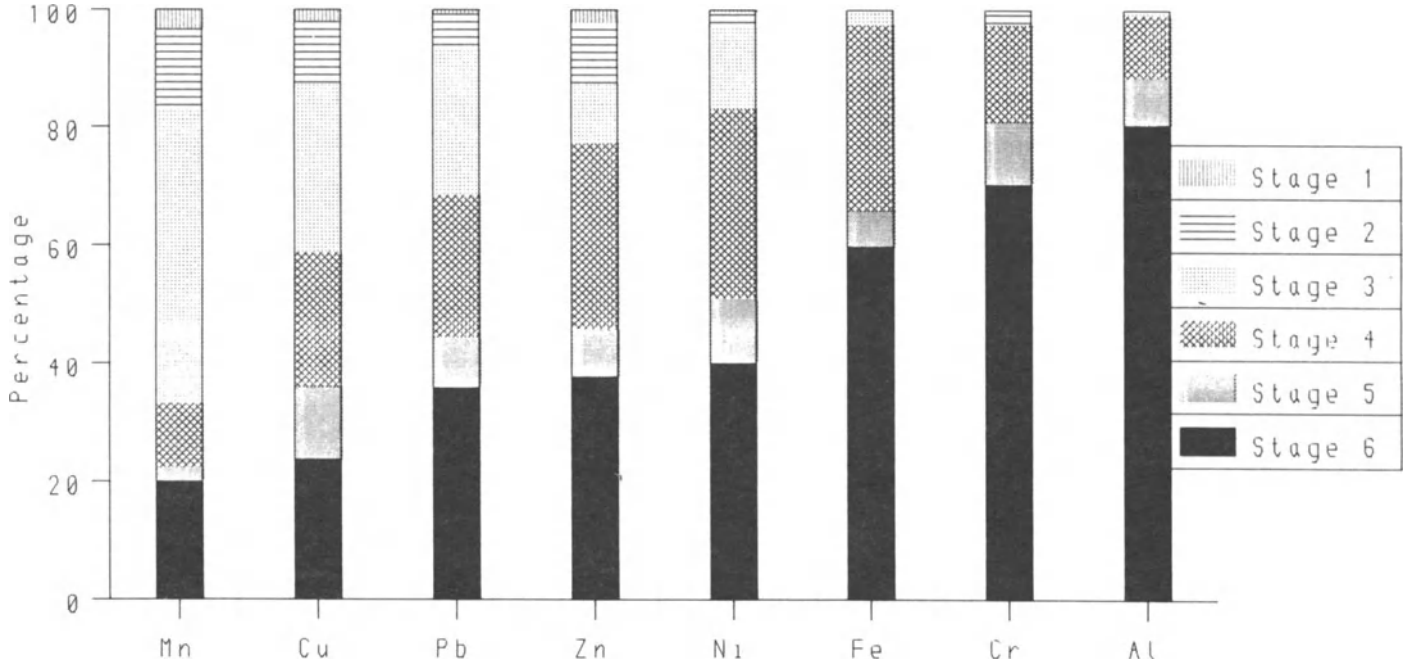

Figure 16.1 The average partitioning of some elements in North Atlantic surface deep-sea sediments (data from Chester & Messiha-Hanna 1970 and Thomas 1987). The diagram is intended to highlight the detrital–authigenic partitioning of the elements; stage 6 (black colour) represents the detrital fraction and stages 1–5 represent individual authigenic host fractions.

Table 16.4 Variations in the detrital-authigenic partitioning of elements in North Atlantic deep-sea sediments[a]

Element	Marginal sediment		Mid-Atlantic Ridge sediment	
	% of total concentration		% of total concentration	
	Detrital	Authigenic	Detrital	Authigenic
Al	93	7	76	14
Fe	77	23	68	32
Mn	18	82	14	86
Cu	55	45	23	67
Ni	64	36	17	83
Cr	63	37	88	12
Pb	85	15	38	62

[a] Data from Thomas (1987).

control the chemical compositions of deep-sea sediments. These spatial variations in elemental partitioning signatures can be explored further by considering Atlantic sediments in more detail, and then using them to illustrate how the detrital and authigenic signals operate on an ocean-wide basis.

In a classic paper, Turekian & Imbrie (1966) provided data on the spatial distributions of Mn, Co, Cu, Ni and Cr in surface sediments from the North and South Atlantic. When the concentrations of Mn, Co, Cu and Ni were expressed on a carbonate-free basis there were clear patterns in their spatial distributions, the highest values being found in sediments from remote mid-ocean areas of low clay accumulation, and the lowest in deposits from the continentally adjacent abyssal plains – this is illustated for Ni in Figure 16.3a. In contrast, there were no clear patterns in the spatial distribution of Cr, other than a number of high-concentration patches (e.g. around the Antilles), which are related to the supply of Cr-rich detrital minerals. Thus, the investigation identified a geographical fractionation between those elements which have excess concentrations in pelagic clays (e.g. Mn, Co, Cu and Ni) and those which do not (e.g. Cr).

Chester & Messiha-Hanna (1970) used a two-stage sequential chemical leaching technique to investigate the partitioning of a series of elements in North Atlantic deep-sea sediments. The technique distinguished between detrital (lattice-held) and authigenic (non-lattice-held) elements, the latter being associated with (a) ferromanganese phases, (b) carbonate phases and (c) inter-sheet and surface-adsorbed phases. A number of important conclusions can be drawn from the study carried out by Chester & Messiha-Hanna (1970), and these are summarized below.

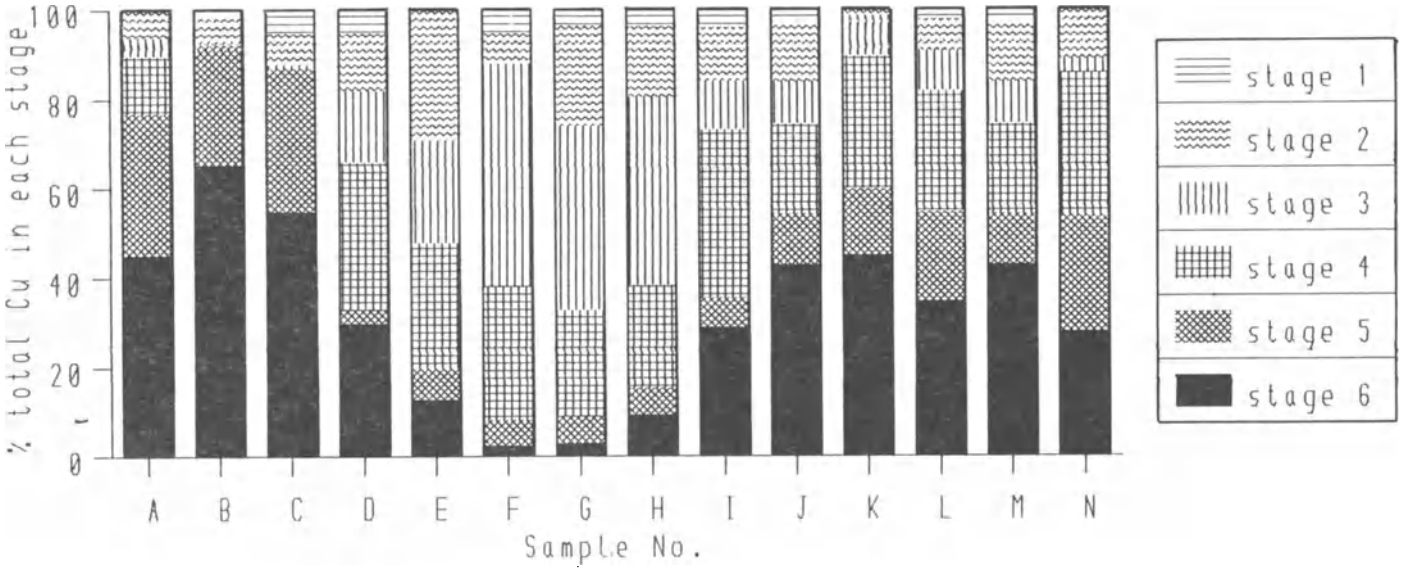

Figure 16.2 The partitioning signatures for ΣCu in Atlantic deep-sea sediments (from Chester *et al.* 1988). The samples were collected on an east–west equatorial transect: A–D, eastern margins; E–H, Mid-Atlantic Ridge and ridge flanks; I–N, western margins. The Cu host associations are as follows: stage 1, loosely held or exchangeable associations; stage 2, carbonate and surface oxide associations; stage 3, easily reducible associations, mainly with (new) oxides and oxyhydroxides of manganese and amorphous iron oxides; stage 4, moderately reducible associations, mainly with (aged) manganese oxides and crystalline iron oxides; stage 6, detrital, or residual, associations.

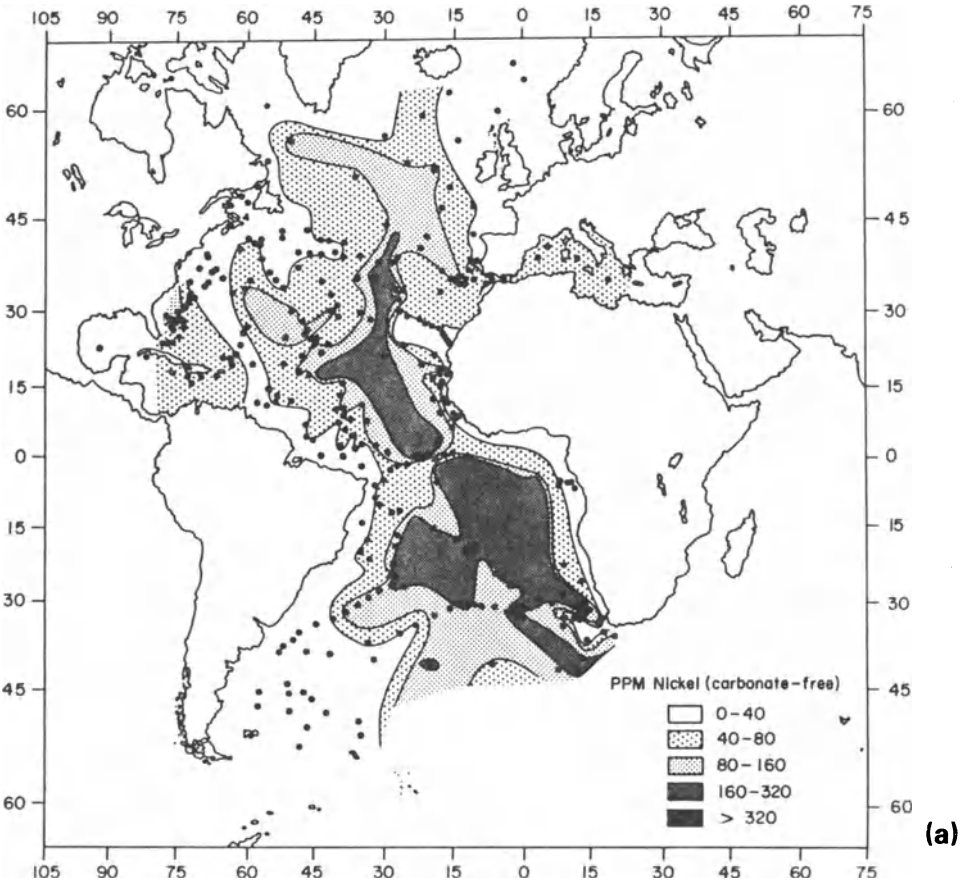

Figure 16.3 The distribution of Ni in Atlantic deep-sea sediments. (**a**) The distribution of total Ni (from Turekian & Imbrie 1966).

(a) Elements that have similar concentrations in pelagic clays and nearshore muds (see Table 13.5) are mainly associated with the detrital fractions of the sediments. For example, Fe, Cr, V and Al all have > 70% of their total concentrations in the detrital fractions.

(b) Elements such as Mn, Ni, Co and Cu, which are present in excess concentrations in pelagic clays, have a much higher proportion of their total concentrations in the authigenic associations. For example, > 70% of the total Mn is present in the authigenic fractions (see above). It may be concluded, therefore, that the elements that are enhanced in pelagic clays have been removed from solution at some time during their history.

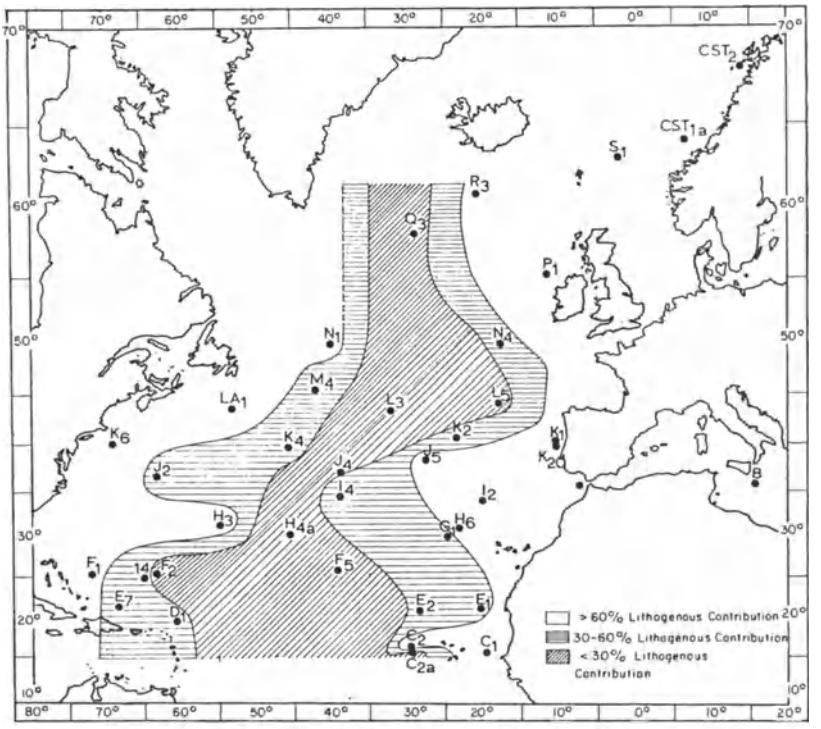

(b)

Figure 16.3b The distribution of lithogenous (detrital) Ni (from Chester & Messiha-Hanna 1970).

(c) There were clear trends in the spatial distributions of the excess authigenic elements. This is illustrated for Ni in Figure 16.3b, from which it is evident that the proportion of detrital Ni decreases from ~ 60% near to the continents to < 30% in the mid-ocean areas. Thus, the highest proportions of authigenic Ni are found in the remote regions. It may be concluded, therefore, that the enhanced total sediment concentrations of Ni reported by Turekian & Imbrie (1966) for the mid-ocean areas (Fig. 16.3a) are due to an increased contribution from authigenic Ni.

(d) The detrital fractions of the North Atlantic deep-sea sediments have a similar composition to those of the total samples of nearshore muds and continental shales – see Table 13.5. According to Chester & Aston (1976) these nearshore muds may be considered to represent an early stage in the adjustment of land-derived material to those processes which operate to produce trace metal enhancements in the

marine environment. This therefore supports their use as indicators of the composition of the detrital fraction of deep-sea sediments; e.g. in the background correction method (see above).

A number of techniques have been described that can be used to unscramble the detrital and authigenic sediment-forming signals, and in terms of the two-fold background signal classification it has also been demonstrated that the concentrations of the excess trace metals in deep-sea sediments result form the authigenic signal. It is now necessary to consider both the nature of the *driving force* behind this authigenic signal and the *manner* in which the signal itself operates in the oceans. Up to this point, spatial elemental distributions, together with a variety of unscrambling techniques, have been used to distinguish between the detrital and authigenic sediment components. In order to describe the various theories that have been proposed to explain how the authigenic signal itself operates, it is necessary to introduce another parameter into the system, and this is the rate at which the host sediments accumulate. The land-derived, or clay, fraction in deep-sea sediments has a relatively low accumulation rate, generally in the range of a few millimetres per thousand years (see Sec. 13.1). Within this low accumulation pattern, however, there are considerable variations between sediments deposited in different oceanic areas. In the two-component detrital–authigenic classification, the detrital material is equivalent to the clay fraction, and the rate at which it accumulates will obviously affect the authigenic signal, since the latter can be swamped out at very fast detrital accumulation rates.

Originally, two general theories were proposed to explain how the detrital–authigenic sediment-forming system operates on an ocean-wide basis.

THE TRACE ELEMENT VEIL THEORY This theory was proposed by Wedepohl (1960), and the rationale underlying it is that the excess trace elements in deep-sea clays have a *constant* independent supply to all parts of the World Ocean, which is superimposed on a *variable* clay accumulation rate. Thus, in this constant-flux model there is a **veil** of trace elements homogeneously distributed throughout the oceanic water column, from which the elements are removed by sediment components at rates which vary according to how fast the deposits accumulate; i.e. the longer the components are in contact with sea water, the higher the authigenic trace metal content of the sediment.

Turekian (1967) criticized the trace element veil theory on a number of grounds, the major criticism being directed at the fundamental underlying concept that the independent removal of trace metals from solution is essentially constant throughout the World Ocean. He pointed out that

this implies that there is a homogeneity in the trace element composition of sea water, whereas in fact variations occur in the geographical distributions of trace metals in both surface and deep waters (see Chap. 11). Turekian (1967) developed an alternative theory to explain the incorporation of the excess trace elements into deep-sea sediments, and this is described below.

THE DIFFERENTIAL TRANSPORT THEORY Turekian (1967) used the spatial trace metal distribution data for Atlantic sediments to develop this differential transport theory. It was shown above that the essential features in the spatial distributions of the excess trace metals in Atlantic deep-sea sediments are that they have their highest concentrations in open-ocean areas and their lowest values on the continentally adjacent abyssal plains. Turekian (1967) related these distribution patterns to the processes that govern sediment transport on a global-ocean scale. To do this, he distinguished between two principal transport mechanisms, which operate on material that escapes the coastal zone. These were (a) movement along the sea bed by bottom transport, and (b) movement down the water column by vertical transport; see e.g. the bottom transport and vertical transport flux study reported by Grousset & Chesselet (1986), which was described in Section 13.2.

(a) Relatively large-sized particulate material that escapes the estuarine environment is often dumped on the continental shelves, from which it can bleed out onto the deep-sea floor by processes such as turbidity current transport, which is largely responsible for the formation of the abyssal plains fringing the continental margins. These shelf sediment particles contain relatively high concentrations of lithogenous components, such as quartz, and generally have low trace metal concentrations, most of which are located in detrital material. Thus, Turekian (1967) identified a **trace metal-poor** particulate fraction, which is initially deposited on the shelves and may be transported to hemi-pelagic areas by bottom transport.
(b) The small-sized particles that escape the estuarine and coastal zones can be transported out into the open ocean by surface currents, where they are joined by particles transported directly via the atmospheric flux. Here, the particles enter the vertical flux and settle out down the water column to form pelagic deposits on remote topographic highs and other mid-ocean areas. These particles are composed of material such as manganese and iron oxyhydroxides, together with clay minerals that have oxide, or organic matter, coatings. Since they have relatively large specific surface areas, the particles are actively involved in the scavenging of trace metals from solution as they are transported along the river → estuarine → open

ocean → water column → sediment, or atmospheric → open ocean → water column → sediment, pathways. Thus, they form a **trace metal-rich** particulate fraction. Turekian (1967) therefore suggested that the deposition of the large-sized trace metal-poor particles around the continents by bottom processes, and the deposition of the small-sized trace metal-rich particles via water column settling in mid-ocean areas, was mainly responsible for the fractionation of the excess trace elements between hemi-pelagic and pelagic deep-sea sediments in the Atlantic.

On the face of it, there appears to be an essential conflict between the trace element veil and the differential transport theories with respect to the manner in which the excess trace elements are incorporated into pelagic deep-sea clays. That is, in the former theory the elements are thought to be removed directly out of sea water from the dissolved state by the sediment-forming components, whereas in the latter it is proposed that most of them are already in a particulate form when they are deposited. However, as Turekian (1967) pointed out, this confict can be reconciled if is assumed that for the differential transport theory the trace metal-rich population is associated with very fine particles having diameters $\lesssim 0.5$ μm since particles of this size are normally classified as being part of the dissolved trace metal population on the basis of the operationally defined dissolved–particulate cut-off at ~ 0.5 μm. In this sense, therefore, both theories assume that the excess trace elements in deep-sea clays have been removed from the dissolved state. The major difference between the two theories therefore revolves around the *rates* at which the excess elements accumulate in the sediments.

Turekian (1967) wrote a general equation for the accumulation rate of a trace element in a deep-sea sediment. Elderfield (1976) modified this equation into a form which, using the terminology employed in this volume, can be expressed in the following way:

$$\Sigma F_E = F_E + [E]_D F_D \tag{16.3}$$

where ΣF_E is the total accumulation rate of an element in a sediment, F_E is the constant rate of addition of E from solution in sea water to the sediment, and $[E]_D$ is the concentration of the element in the detrital component of the sediment, which accumulates at a rate F_D. Thus, a further step has been taken in defining the two-component detrital–authigenic concept for the distribution of trace elements in deep-sea sediments by linking the signals involved to sediment accumulation rates. Originally, in terms of the trace element veil theory, it was thought that the coupling between the two signals involved a *variable* detrital accumulation rate and a *constant* authigenic accumulation rate. This

constant-flux model for the accumulation of authigenic trace metals is based on the assumption of a uniform authigenic deposition rate over the entire ocean floor. If the rate of authigenic deposition is in fact uniform, and the detrital accumulation variable, then there will be a negative correlation between the authigenic concentration (C_a) and the sediment accumulation rate (S), since in clay sediments the latter is mainly dependent on the deposition of detrital material. Krishnaswami (1976) has expressed this relationship as

$$C_a = \frac{K}{S\rho_s} \tag{16.4}$$

and from this the total sediment concentration would be

$$C_t = C_a + C_d = \frac{K}{S\rho_s} + C_d \tag{16.5}$$

where K is the authigenic deposition rate (g $cm^{-2}yr^{-1}$), ρ_s is the *in situ* density of the sediment (g cm^{-3}) and S is the sedimentation rate (cm yr^{-1}). This constant-flux model will therefore apply to elements that have (a) a homogeneous distribution in the oceans and (b) residence times equal to or greater than the oceanic circulation times.

Krishnaswami (1976) used a variety of techniques to demonstrate that $\sim$ 90% of the Mn, $\sim$ 80% of the Ni and Co, and $\sim$ 50% of the Cu in Pacific pelagic clays are authigenic in origin. In contrast, $>$ 90% of the Sc, Ti and Th are detrital in character. The author then applied the constant-flux equations to his elemental concentration and sediment accumulation rate data and found, as predicted by the model, that there was a negative correlation between the detrital, or clay, sediment accumulation rates and the concentrations of Mn, Co, Ni, Fe and Cu in the Pacific pelagic sediments – see Figure 16.4. These negative correlations applied to a series of different sediments, and Krishnaswami (1976) concluded that this was consistent with the constant-flux model of a *uniform* authigenic deposition superimposed onto a *variable* background detrital input. In contrast, he found that the concentrations of the detrital elements Sc, Ti and Th were independent of sediment accumulation rates – see Figure 16.4. Krishnaswami (1976) also concluded that when the detrital sedimentation rate is high, i.e. $\gtrsim$ 10 mm/10^3 yr, the authigenic concentration will be small and $C_t \simeq C_d$. However, when the detrital sedimentation rate is small, a pure authigenic fraction will be formed and $C_t \simeq C_a$; for example, the extreme case for this would be found in hydrogenous ferromanganese crusts (see Sec. 15.3.3). From his data, Krishnaswami (1976) derived a best estimate of the authigenic deposition rate of a series of elements in the World Ocean,

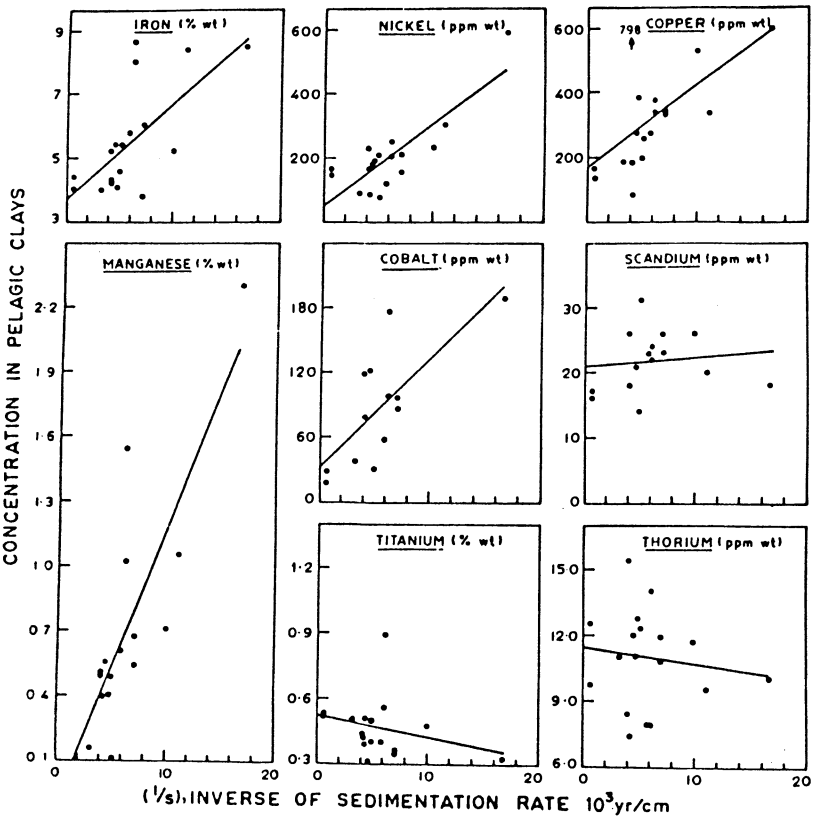

Figure 16.4 Scatter plots of elemental concentrations in Pacific pelagic clays against inverse sedimentation rates (from Krishnaswami 1976).

and these are given in Table 16.5. Bender *et al.* (1970) also found a generally similar rate for the authigenic deposition of Mn in a suite of 38 Pacific deep-sea sediments, and their data are included in Table 16.5.

Krishnaswami's data appeared to confirm the constant-flux model for the removal of authigenic trace metals from solution in sea water into pelagic clays, i.e. the trace element veil model was approximated. However, the past few years have seen a number of very important advances in our understanding of how oceanic trace metal cycles operate (see Chs 11 & 12), and these can be combined with sediment studies to assess the validity of the constant-flux model. Two recently reported investigations will serve to illustrate how modern trace metal scavenging concepts have been applied to this problem.

WORK OF BACON AND ROSHOLT: THE BERMUDA RISE Bacon and Rosholt

Table 16.5 Estimates of the accumulation rates of authigenic elements in sediments from the World Ocean (units, μg $cm^{-2}/10^3$ yr)

Element	a	b	c	d	e
Mn	500	4300 ± 1100	1220	1264 ± 110	100–3400
Fe	800	-	1560	2737 ± 503	-
Co	5	7.2 ± 5.7	14	13 ± 2.9	-
Ni	10	46 ± 16	20	17 ± 3.5	-
Cu	8	76 ± 26	28	26 ± 2.5	-
Zn	-	17 ± 20	5.1	7.2 ± 1.3	-
V	-	-	6.2	6.1 ± 2.5	-

[a] Estimated 'global' authigenic flux to deep sea (Krishnaswami 1976).

[b] Estimated authigenic flux to Bermuda Rise sediments (Bacon & Rosholt 1982).

[c] Estimated authigenic flux to Nares Abyssal Plain red clays; estimated using detrital background correction method (Thompson et al. 1984).

[d] Estimated authigenic flux to Nares Abyssal red clays; estimated using constant-flux method (Thompson et al. 1984).

[e] Estimated authigenic flux to Pacific deep-sea sediments (Bender et al. 1970) uncorrected for detrital input.

(1982) carried out a study of the accumulation rates of a series of radionuclides and trace metals in carbonate-rich sediments from the Bermuda Rise (North Atlantic), an area in which the sediment regime is characterized by a rapid deposition of material transported by abyssal currents. The authors employed a two-component sediment matrix, consisting of a terrigenous clay (detrital) component and a pelagic (authigenic) component, for the interpretation of their radionuclide and trace metal data. In terms of this matrix, it was assumed that the total metal content of the sediments was given by Equation 16.2, and the authors were able to show that the sediments in the region were formed by the deposition of (a) a terrigenous component transported to the North American Basin from continental sources (detrital), added to which was (b) a rain of biogenic debris produced in the surface waters, which had an associated flux of trace metals scavenged from the water column (pelagic). The sediments were therefore a mixture of these two end-member components. The magnitudes of the pelagic, or authigenic, fluxes to the sediments were estimated by relating the trace metal data to the excess ^{230}Th in the sediments. This ^{230}Th excess is defined as 'unsupported' ^{230}Th, and is obtained by subtracting the uranium-activity equivalent from the total ^{230}Th activity. The rationale behind this

approach is that ^{230}Th is known to be produced in the oceans at a constant rate determined by the amount of ^{234}U dissolved in sea water. If the decay of ^{234}U in sea water is the sole source of the unsupported ^{230}Th, or $^{230}Th_{ex}$, in the sediments it can be assumed that the ^{230}Th has been scavenged from the water column, and so it can be used to estimate the rates at which trace metals associated with the same sediment fractions have also been scavenged from the water column. A summary of the trace metal scavenging rates determined in this way by Bacon & Rosholt (1982) is given in Table 16.5, together with other authigenic flux estimates.

It is apparent from the data given in Table 16.5 that although the authigenic accumulation rate of Co on the Bermuda Rise is reasonably similar to that predicted as normal for the World Ocean by Krishnaswami (1976), those of Mn, Ni and Cu are considerably higher, thus throwing doubt on the constant-flux model. Bacon & Rosholt (1982) were unable to identify the reasons for the higher authigenic fluxes of Mn, Ni and Cu on the Bermuda Rise, but pointed out that if they are real they may have been affected by, among other factors, an enhanced trace metal scavenging by resuspended TSM, which is at a high level in this region of the North Atlantic (see Sec. 10.2). The authors also considered the important relationship between the residence time of an element and the magnitude of its authigenic flux. They pointed out that ^{230}Th has such a short oceanic residence time that it must be deposited almost entirely in the basin within which it is generated. However, trace metals having longer residence times might be expected to migrate greater distances from their source of supply, and perhaps accumulate preferentially in areas, such as the Bermuda Rise, that are particularly efficient **scavenging sinks**. Bacon & Rosholt (1982) suggested that this might explain the relatively high authigenic fluxes for Ni and Cu in their survey area, since both elements have residence times of several thousand years (see Sec. 11.2), and so could undergo large-scale oceanic migration. They concluded, however, that an inter-oceanic migratory hypothesis of this kind is unlikely to explain the differences in the magnitude of the Atlantic and Pacific authigenic Mn signals because this element has a relatively short residence time, which is similar to that of Th. On the basis of down-core data, Bacon & Rosholt (1982) concluded that the *concentrations* of trace metals in the sediments are controlled mainly by dilution of the authigenic fraction by varying inputs of the terrigenous (detrital) end-member; for example, the clay flux varied by a factor of around 4. However, the authigenic *fluxes* of the metals and radionuclides scavenged from the *water column* are not sensitive to this variation in the clay flux, and in fact they have remained almost constant from glacial to interglacial periods; i.e. in the region itself the constant-flux model was approximated over time. Thus, the authigenic fluxes are not associated with the

deposition of clay material, but are probably related to the deposition of biogenic carriers.

Three important overall conclusions can therefore be drawn from the study carried out by Bacon & Rosholt (1982).

(a) Regions that are large accumulators of sediment can also act as accumulators of scavenged trace metals.
(b) Although the authigenic fluxes of Mn, Ni and Cu on the Bermuda Rise differ from those in the Pacific, the constant-flux model appears to be approximated on a regional scale.
(c) The trace metal scavenging in the water column is controlled by biogenic rather than terrigenous phases.

WORK OF THOMPSON *ET AL.*: THE NARES ABYSSAL PLAIN Thompson *et al.* (1984) carried out an investigation into trace metal accumulation rates in a series of grey ($^{230}Th_{ex}$-poor) and red ($^{230}Th_{ex}$-rich) clays from the Nares Abyssal Plain (NAP) in the North Atlantic; the techniques they used to derive the composition of the detrital fractions of the clays have been described above. The sedimentation regime in the region was related to detrital material that had been rapidly deposited from distal turbidity currents to form the grey clays, and slowly deposited from nepheloid layers to give rise to the red clays. On the basis of the total sediment geochemistry the red clays were strongly enriched in Mn, Co, Cu, Ni, Zn and V relative to the grey clays. However, despite their colour differences, Sr isotope evidence showed that the clay fractions of both sediments had the same terrigenous origin, and the trace metal enhancement in the red clays was attributed to their scavenging from the water column; i.e. the slowly deposited red clays had received an additional trace metal supply from the overlying sea water. Thus, the chemical composition of the clays is controlled by the mixing of the detrital and authigenic components, which, in turn, is controlled by their relative accumulation rates. As a result, in the grey clays $C_t \simeq C_d$, which was the condition predicted by Krishnaswami (1976) when the detrital material accumulates at a sufficiently fast rate. For the red clays, however, the total metal flux (F_t) is the sum of the fluxes of the authigenic (F_a) and the detrital (F_d) components:

$$F_t = F_d + F_a \tag{16.6}$$

F_a is assumed to vary independently of F_d. Both F_t and F_d are the products of the total mean sediment accumulation rate (S) and the concentration of the metals in, respectively, the total sediment (C_t) and the detrital component (C_d). The net removal rate of the authigenic trace metals was then calculated by two routes:

(a) $$F_a = (C_t - C_d)S \quad (16.7)$$

where C_d is assumed to be equal to the total metal content of the grey clays, i.e. $C_t = C_d$ (the background correction method – see above); and

(b) $$F_t = F_a + C_dS \quad (16.8)$$

where a graphical procedure is employed in which the total metal fluxes ($F_t = C_tS$) are plotted against sedimentation rates to give a regression line that allows both F_a (the $S = 0$ intercept) and C_d (the gradient) to be evaluated. This approach does not assume a knowledge of C_d, but does assume that the authigenic flux is constant for each metal throughout the survey area, i.e. a constant-flux regional model.

The linearity of the plots confirmed the latter assumption, and the composition of the detrital fraction obtained from the gradients was generally similar to that obtained by assuming that it was equal to the total concentration of the grey clays. The form of the plots suggests that it is biogenic and not terrigenous (detritral) clays that control the authigenic fluxes, a conclusion similar to that reached by Bacon & Rosholt (1982) for the Bermuda Rise. These biogenic trace metal carriers have been destroyed at the sediment surface by oxic diagenesis, thus highlighting the importance of including oxic diagenetic processes in the authigenic signal.

The authigenic fluxes for the NAP derived from the two equations showed good agreement for Mn, Cu, Co, Ni and Zn – see Table 16.5. Although these authigenic fluxes are reasonably constant over the NAP survey area, comparison with data for other regions shows that the magnitudes of the fluxes do vary, both *within* ocean basins (cf. those for sediments of the Bermuda Rise, Atlantic) and *between* ocean basins (cf. those for the Pacific clays).

It is therefore becoming increasingly apparent from recent data that although the constant-flux model for the accumulation of authigenic elements in sediments can be approximated regionally, it does not apply on an ocean-wide basis. Despite this, however, Thompson *et al.* (1984) pointed out that the *relative magnitudes* of the authigenic fluxes are generally the same in different oceanic areas, and that there is a tendency for them to decrease in the order observed for the NAP, i.e.

$$\text{Fe} > \text{Mn} > \text{Cu} \simeq \text{Ni} > \text{Co} \simeq \text{V} \simeq \text{Zn}.$$

Thompson *et al.* (1984) identified two factors that might be expected to control the relative magnitudes of the authigenic metal fluxes. These were (a) the relative values of their input fluxes to the oceans, i.e. their

geochemical abundances, and (b) the relative efficiency of the **scavenging processes** that remove them from sea water. On the assumption that the oceanic inputs of the metals are dominated by fluvial sources, Thompson *et al.* (1984) used the data provided by Martin & Whitfield (1983) to show that the relative dissolved concentrations of the metals in river water are

$$Fe > Mn > Cu > Ni > Co.$$

This is the same order as that of their relative authigenic fluxes, although distortions by factors such as hydrothermal sources were not considered by the authors in their model. Thompson *et al.* (1984) concluded, therefore, that although there are large variations in the absolute magnitudes of the authigenic metal fluxes from one oceanic region to another, these do not fractionate the elements to an extent that removes the underlying pattern imposed by their geochemical abundances.

Transition metals that have relatively long residence times in sea water, e.g. Cu and Ni, will be expected to be transported further from their source areas before being removed from solution than would metals with shorter residence times, e.g. Fe and Mn. Despite the geochemical abundance control the authors were therefore able to identify differences in the magnitudes of the authigenic fluxes that do, in fact, reflect oceanic reactivities of the individual elements. To illustrate this, Thompson *et al.* (1984) made a direct comparison between the authigenic fluxes they derived for the NAP red clays and those estimated by Krishnaswami (1976) for a series of Pacific clays. To do this, the data for Mn, Cu and Ni from the two oceans were plotted in a graphical form – see Figure 16.5. The plots reveal that there is a wide range in the authigenic accumulation rates for Mn despite the narrow range in sediment accumulation rates. In contrast, the ranges in the authigenic accumulation rates for Cu and Ni are much smaller. The authors concluded that these features are consistent with the oceanic reactivities of the elements, Mn having a short oceanic residence time ($\sim$ 50 yr) resulting from rapid surface water scavenging, and Cu and Ni having longer residence times (several thousand years) due to their involvement in the biogeochemical assimilation–regeneration cycle and release from bottom sediments. Further, the authigenic fluxes for Cu and Ni in the Pacific clays are similar to those at the NAP site, whereas the fluxes for Mn are lower. Again, the authors related this to the residence times of the metals in sea water. Thus, it would be expected that because of their longer residence times, inter-oceanic concentration variations for Cu and Ni will be smaller than those for Mn, i.e. source strength effects will be smoothed out to a much greater degree for Cu and Ni than for Mn, so allowing the two former elements to be redistributed in both sea water and the authigenic fractions of deep-sea sediments.

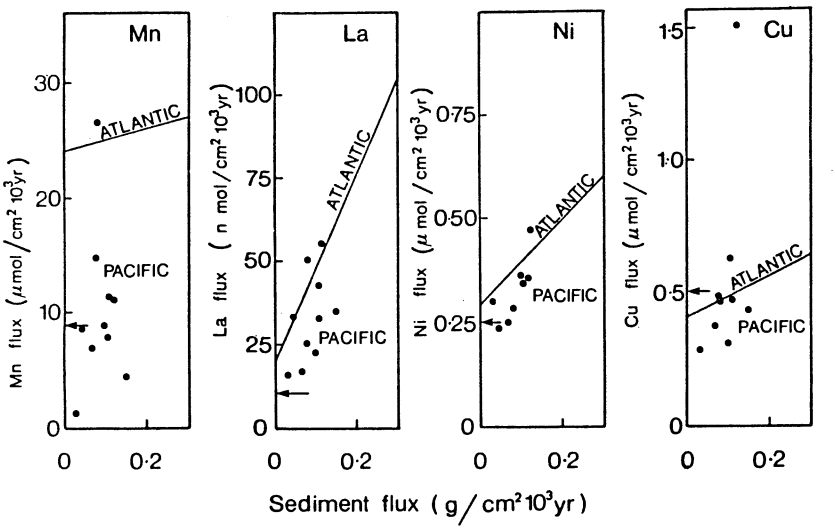

Figure 16.5 Comparison between the authigenic fluxes of elements in red clays from the Nares Abyssal Plain and those of Pacific pelagic clays (from Thompson *et al.* 1984).

It may be concluded, therefore, that the **geochemical abundances** of the metals are the principal factor governing their authigenic sediment fluxes, but that fractionation occurs in accordance with their **oceanic reactivities**. This results in the reactive elements (e.g. Mn) having higher fluxes in Atlantic relative to Pacific clays since the Atlantic has a greater fluvial input than the Pacific, and in the less reactive elements (e.g. Cu, Ni) having generally similar fluxes in the two oceans.

Bacon & Rosholt (1982) and Thompson *et al.* (1984) concluded that the settling of biogenic carriers in the form of organic aggregates is the main driving force behind the down-column transport of trace metals to the sediments on both the Bermuda Rise and the NAP. The carrier phases are destroyed by oxic diagenesis at the sediment surface and the associated metals are taken into authigenic components. The ocean-wide importance of these carriers has been demonstratedd by other workers. For example, Aplin & Cronan (1985) compared the magnitudes of the biogenic carrier down-column fluxes of a series of metals with the rates at which they accumulate in sediments from the southwest Equatorial Pacific. The relationship is illustrated graphically in Figure 16.6a, and demonstrates a close similarity between the down-column fluxes and sediment accumulation rates for Ni, Co, Ti, Mn and Fe; Cu is supplied in excess of its accumulation rate, which is in agreement with its release back into sea water across the sediment/water interface.

It is apparent, therefore, that down-column transport via biogenic

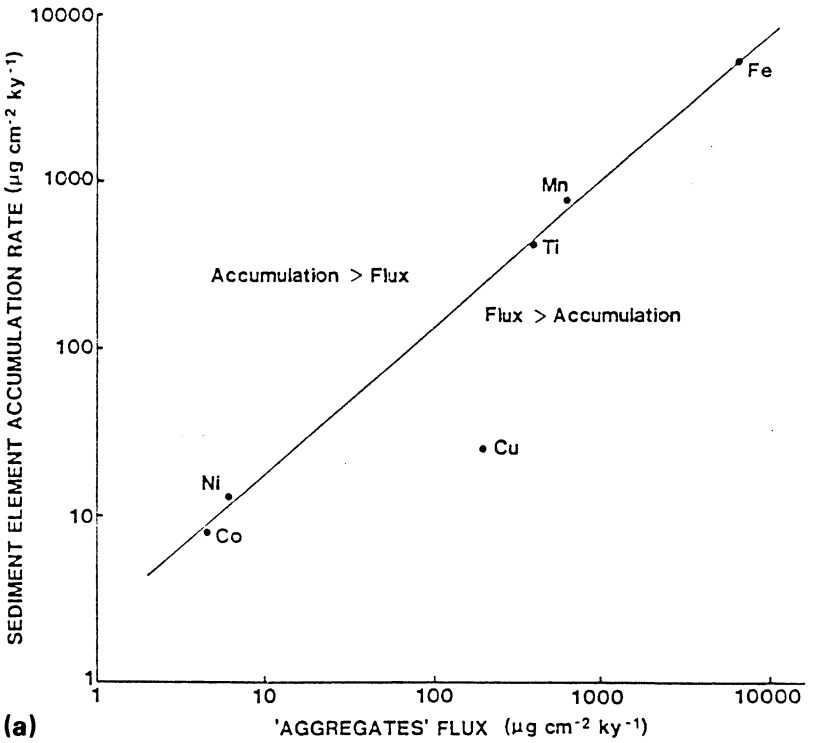

Figure 16.6 The rates of water column removal processes for trace elements. (**a**) Comparison between biogenic carrier down-column fluxes and accumulation rates of elements in sediments from the southwest Pacific (from Alpin & Cronan 1985).

carriers is the principal route by which authigenic trace metals reach the sediment surface. In view of this, it is not surprising that although the authigenic processes provide an ocean-wide background for the supply of non-detrital metals to sediments, the magnitudes of the authigenic fluxes of some elements vary both between and within ocean basins. These fluxes appear to be controlled mainly by geochemical abundances, but metal reactivities in the water column are superimposed on input source strengths. In terms of their oceanic reactivities, the scavenging-type elements have relatively short residence times and so undergo restricted transport between the major ocean basins. The nutrient-type elements have longer residence times, and so have a greater potential for inter-oceanic transfer. However, the down-column fluxes of these nutrient-type elements vary considerably throughout the oceans, depending largely on the magnitude of the down-column carbon-driven flux. For example, Collier & Edmond (1984) found a striking correlation between the scavenging rate of Cu in the water column and primary productivity in

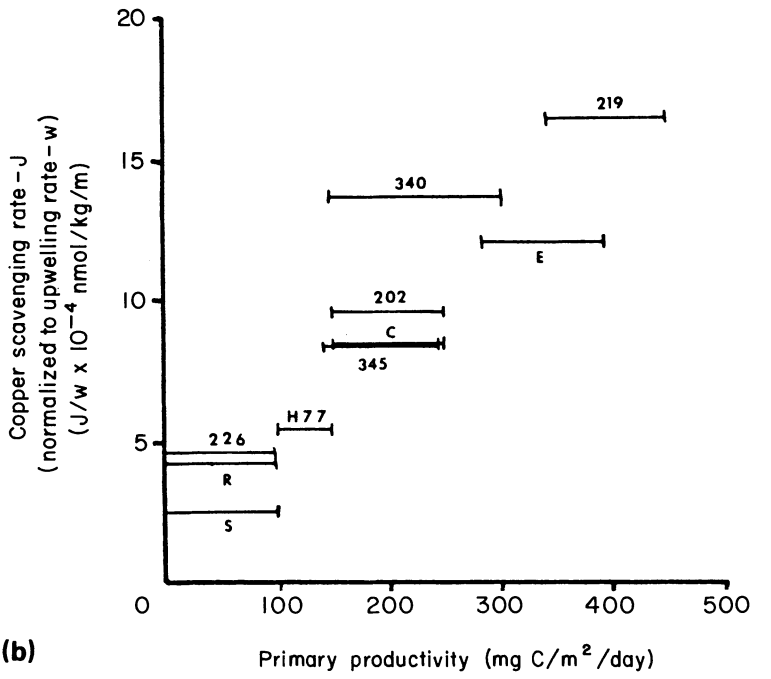

Figure 16.6b Estimates of the primary production of organic carbon in surface waters (^{14}C uptake) versus the relative scavenging rate of Cu in the deep ocean (from Collier & Edmond 1984).

surface waters – see Figure 16.6b. The authors concluded that this relationship emphasizes the importance of regions of high primary productivity in driving the vertical transport of elements in the oceans. As a result, nutrient-type elements *can* be removed from the water column on timescales that prevent their inter-oceanic transport, and this can lead to patches of high concentrations of these elements in sediments deposited under regions of intense primary production; for example, it will be shown in Section 16.7 that the authigenic fluxes of Cu in the Indo-Pacific Ocean are relatively high under the area of equatorial primary productivity, which leads to enhanced concentrations of the element in the underlying sediments in which the organic carriers are preserved (see e.g. Chester *et al.* 1988, and Sec. 14.4.2).

On the basis of recent evidence it may therefore be concluded that the authigenic signal does not operate in a manner that yields an ocean-wide

constant flux for those authigenic elements which have relatively short residence times. Authigenic elements that have longer residence times can, however, have their dissolved concentrations smoothed out between the major oceans, and may therefore approach the constant-flux model as originally proposed by Wedepohl (1960) and supported by data from Krishnaswami (1976). Thus, we have come full circle, and the distributions of the elements in deep-sea sediments can be linked to the processes controlling their oceanic residence times, and general sea water chemistries, discussed in Chapter 11.

16.6 Signal spikes

16.6.1 Introduction

In the previous sections, the sources of the excess trace metals found in deep-sea clays were assessed in terms of their background transport via the detrital and authigenic signals. This involved a two-component system in which (Eqn 16.1)

$$C_t = C_d + C_a.$$

However, within the ocean system a series of more localized signals can impose perturbation spikes on this background, such that

$$C_t = C_d + C_a + C_s \tag{16.9}$$

where C_s refers to the concentration of an element arising from the perturbation spikes. These spikes are transmitted through the water column mainly by the hydrothermal and contaminant signals, and through interstitial waters by the diagenetic signal.

16.6.2 The hydrothermal signal spike

The concepts underlying hydrothermal activity have been discussed in Chapter 5, and the processes involved in the generation of hydrothermal sediment-forming components have been described in Section 15.3.6. Attention will now be directed to considering the question 'How do these chemically specialized components affect the compositions of deep-sea sediments?' The hydrothermal emanations occur in the form of pulses, which are generated at the ridge crest spreading centres. These metal-rich pulses give rise to a variety of hydrothermal components, but as far as deep-sea sediments in general are concerned it is the ferromanganese precipitates that are the principal manifestations of hydrothermal activity.

It has been known for many years that metal-rich sediments are found in association with the mid-ocean ridge system. For example, Murray & Renard (1891) and Revelle (1944) reported the presence of such deposits

in the eastern Pacific, and El Wakeel & Riley (1961) gave details of a Mn- and Fe-rich calcareous ooze from the vicinity of the East Pacific Rise (EPR). The major boost to the study of these metalliferous deposits came in the mid-1960s following the work of Bostrom and coworkers. It was at this stage that the genesis of the deposits was linked to the formation of new crust at the ridge spreading centres, a theory that was given a firm foundation by the identification of hydrothermal venting systems on the ridge areas (see Sec. 5.1). Metal-rich deposits have subsequently been identified on, or in the vicinities of, the ridge system from various parts of the World Ocean. The locations where the deposits have been found included the Pacific Ocean (see e.g. Dasch *et al.* 1971, Bender *et al.* 1971, Sayles & Bischoff 1973, Piper 1973, Dymond *et al.* 1973, Sayles *et al.* 1975, Heath & Dymond 1977, Marchig & Grundlach 1982), the Indian Ocean (see e.g. Bostrom *et al.* 1969, Bostrom & Fisher 1971) and the Atlantic Ocean (see e.g. Bostrom *et al.* 1969, Cronan 1972, Horowitz 1974); compositional data for some of these metal-rich sediments are given in Table 16.6.

Metal-rich deposits are formed on newly generated crust. During the process of sea-floor spreading this crust moves away from ridges as the ocean basins are opened up, and the basement is covered by a blanket of normal deep-sea sediments. As a result, although surface outcrops of metal-rich sediments are usually found mainly at the ridge crests, Bostrom & Peterson (1969) predicted that they should also form a layer lying on top of the oceanic basement at all locations. A general model illustrating this process is shown in Figure 16.7. Confirmation that metalliferous sediments are the first material deposited on the basaltic basement was provided by cores obtained during the Deep Sea Drilling Project (DSDP), which showed that a Mn- and Fe-rich EPR analogue deposits was indeed found at the base of the sediment column at many oceanic locations (see e.g. von der Borch & Rex 1970, Cronan *et al.* 1972, Cronan 1973, Dymond *et al.* 1973, Cronan & Garrett 1973, Horder & Cronan 1981).

It may be concluded, therefore, that Fe- and Mn-rich metalliferous deposits are usually the first type of sediment to be laid down on the oceanic crust at the spreading centres, thus forming a bottom layer onto which other types of deep-sea sediments accumulate. Although the hydrothermal precipitates have their source at the ridge crest venting systems, the sediments formed there are rarely composed of pure hydrothermal material, but are usually mixtures of the metal-rich end-member precipitates and other sediment-forming components, mainly carbonate shells, which are preserved on the topographic highs. Marchig & Grundlach (1982) identified a *prototype* undifferentiated end-member formed at an initial stage in the evolution of hydrothermal material from the EPR. From the data given by these authors an estimate is therefore

Table 16.6 Chemical composition of some modern and ancient metalliferous sediments (units, μg g^{-1}; carbonate-free basis)

Element	East Pacific Rise; crest[a]	East Pacific Rise; flanks[a]	Pacific; Northwest Nazca Plate[b]			East Pacific Rise; basal sediments[c]	Mid-Atlantic Ridge[d]
			East Pacific	Bauer Deep	Central Basin		
Fe	180000	105000	302000	158300	121100	200700	76000
Mn	60000	30000	99200	57500	39600	60600	4100
Cu	730	960	1450	1171	985	790	-
Ni	430	675	642	1066	1307	460	-
Co	105	230	-	-	-	82	-
Pb	-	-	-	-	-	100	-
Zn	380	290	594	413	311	470	-
V	450	240	-	-	-	-	-
Hg	-	-	-	-	-	-	414
As	145	65	-	-	-	-	174
Mo	30	113	-	-	-	-	-
Cr	55	32	-	-	-	-	-
Al	5000	46300	5100	32400	67400	27300	57900

[a] Bostrom & Peterson (1969).

[b] Heath & Dymond (1977).

[c] Cronan (1976).

[d] Cronan (1972).

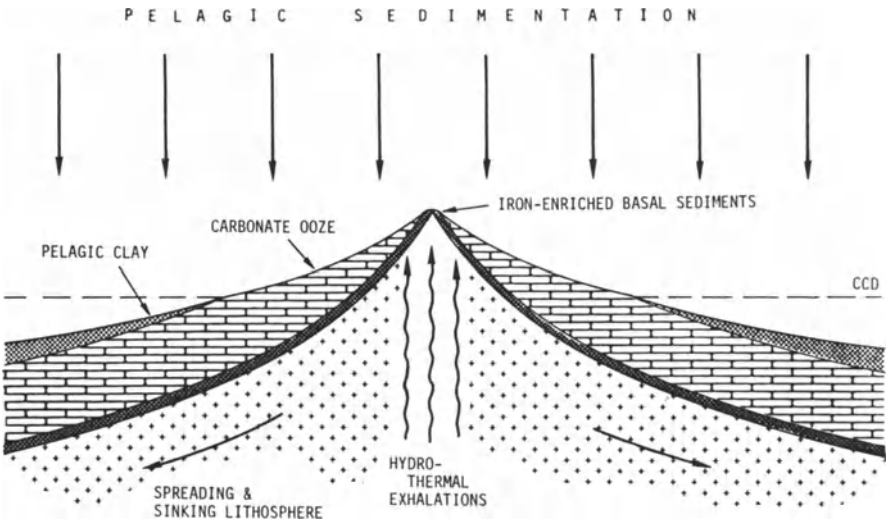

Figure 16.7 Schematic representation of a model for sediment accumulation at oceanic spreading ridge centres (from Davies & Gorsline 1976, after Broecker 1974 and Bostrom & Peterson 1969).

available of the composition of the Fe- and Mn-rich end-member that is precipitated from hydrothermal fluids on mixing with sea water (see Table 16.7). Some authors have suggested that pulses of these hydrothermal fluids can be dispersed on an ocean-wide basis (see e.g. Lalou 1983), and it is clear that hydrothermal manganese signals *can* be transmitted for long distances via the global mid-depth water circulation patterns (see Sec. 15.3.6). The question that arises, therefore, is 'How widespread is the Fe- and Mn-rich hydrothermal end-member that is generated from these pulses?' To answer this question, it is necessary to unscramble the effects of the hydrothermal pulse signal from those of other sediment-forming signals.

Bostrom *et al.* (1969) addressed the problem of unscrambling the hydrothermal signal on an ocean-wide basis. Various authors have identified a series of metal-rich deep-sea sediments associated with areas of high heat flow on the EPR. Relative to normal deep-sea sediments these deposits are enriched in elements such as Fe, Mn, Cu, Ni and Pb, which are associated with the colloidal-sized hydrothermal particles. Another important characteristic of the metalliferous sediments is that they are depleted in lithogenous elements such as Al and Ti – see Table 16.6. This enrichment–depletion patern was utilized by Bostrom *et al.* (1969) to characterize a **hydrothermal signature**. To quantify the signature, the authors employed the ratio Al : (Al + Fe + Mn) as an indicator of metalliferous sedimentation. In this way, the hydrothermal end-member was characterized as having A1 : (A1 + Fe Mn) ratios of

Table 16.7 Chemical composition of a prototype undifferentiated hydrothermal precipitate[a] (units, μg g^{-1}, carbonate-free basis)

Element	Concentration	Element	Concentration
Si	36000	Mo	134
Al	3600	Zr	73
Mn	91800	Nb	2
Fe	281000	Rb	9.3
Ti	300	Ce	13
Cu	1300	Th	61
Zn	393	V	1923
Co	111	W	21
Cr	30	Y	101
Ni	600	La	98

[a] Data for the <63μm fractions of sediment cores from the East Pacific Rise (Marchig & Grundlach 1982).

$< 10 \times 10^2$, and the normal deep-sea sediment end-member as having ratios $> 60 \times 10^2$. Sediments that are mixtures of the two end-members have intermediate ratios. The authors then plotted values of the hydrothermal ratio for deep-sea sediments, and showed that the metalliferous deposits are indeed characteristic of the mid-ocean ridge system throughout the World Ocean – see Figure 16.8. The lowest ratios, and the greatest coverage of hydrothermal sedimentation, was found in the Pacific Ocean around the EPR, and the influence of the hydrothermal material on surrounding sediments decreased in the order Pacific Ocean ridge system > Indian Ocean ridge system > Atlantic Ocean ridge system. This rank order correlates well with the relative rates of ocean-floor spreading, which can indicate the general degree to which a ridge is active; thus, the spreading rate in the Pacific is ~ 2.0–6.0 cm yr^{-1}, in the South Atlantic and Indian Oceans it is ~ 1.5–3.0 cm yr^{-1}, and in the North Atlantic it is ~ 1.0–1.4 cm yr^{-1}.

Bostrom *et al.* (1969) were thus able to identify the widespread occurrence of metalliferous deposits on the mid-ocean ridge system by unscrambling the hydrothermal signal in terms of the sediment Al : (Al + Fe + Mn) ratios. However, not all the elements associated with the metal-rich deposits have a hydrothermal origin, and other techniques have been used to unscramble hydrothermal signals for individual elements. These include metal accumulation rates, factor analysis and chemical leaching procedures, and isotopic analysis. In the

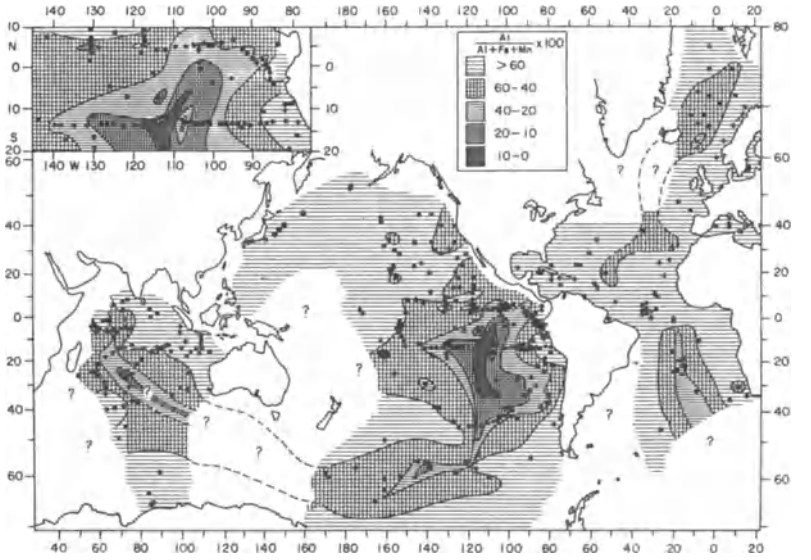

Figure 16.8 The distribution of the hydrothermal ratio, Al : (Al + Fe + Mn), in sediments from the World Ocean (from Bostrom *et al.* 1969). Note that low ratios are associated with spreading ridges.

context of the present discussion, metal accumulation rates are of particular interest. It was shown in Section 16.5 that, although there is not a constant ocean-wide authigenic deposition rate for Mn in deep-sea sediments, the rates do appear to be in the range ~ 1000–5000 μg $cm^{-2}/10^3$ yr for the Atlantic, and somewhat lower for the Pacific. For example, Krishnaswami (1976) estimated an authigenic deposition rate for Mn of ~ 500 μg $cm^{-2}/10^3$ yr for Pacific pelagic clays, and Bender *et al.* (1970) calculated an average total deposition area for Mn of ~ 1300 μg $cm^{-2}/10^3$ yr for Pacific deep-sea sediments from the same oceanic region. In contrast, Bender *et al.* (1970) used radiochemical data to estimate that the accumulation rate of Mn in a core from the crest of the EPR was ~ 35 000 μg $cm^{-2}/10^3$ yr, i.e. this Mn was accumulating almost 25 times faster than in normal deep-sea sediments. Dymond & Veeh (1975) gave data on the accumulation rates of Mn, Fe and Al in sediments on a transect extending west to east across the EPR, and clearly demonstrated enhanced accumulation rates for Mn and Fe in sediments deposited on the ridge crest. Mn accumulation rates on the crest reached values of ~ 28 000 μg $cm^{-2}/10^3$ yr, i.e. the same order of magnitude as those reported by Bender *et al.* (1970). The maximum rates for the accumulation of Fe on the EPR were ~ 82 000 μg $cm^{-2}/10^3$ yr. According to Dymond & Veeh (1975), the authigenic accumulation rate for Fe in normal deep-sea sediments from this region is ~ 200 μg

$cm^{-2}/10^3$ yr, and Krishnaswami (1976) estimated an average rate of $\sim$ 800 μg $cm^{-2}/10^3$ yr for the accumulation of Fe in Pacific pelagic clays. Clearly, therefore, the accumulation of Fe on the crest of the EPR is of the order of 100–400 times faster than it is in normal Pacific deep-sea sediments.

It may be concluded, therefore, that authigenic deposition cannot explain the enhanced accumulation rates of Mn and Fe on the crestal regions of the EPR. Rather, it would appear that the high accumulation rates are the result of an enhanced supply of the elements from a pulsed hydrothermal signal. However, as they form, hydrothermal precipitates can remove dissolved elements directly from sea water so that not all the elements that accumulate at fast rates around the ridge crests necessarily have a hydrothermal origin. For example, Froelich *et al.* (1977) reported that phosphorus was accumulating about 40 times faster on the crest of the EPR than in the adjacent Bauer Deep, and attributed this to the sorption of phosphate by hydrothermal iron oxyhydroxides; most of the phosphate was thought to have been derived from sea water, but a hydrothermal contribution may have been present. Thus, although accumulation rates are an indicator of the hydrothermal origin of Fe- and Mn-rich precipitates, they cannot be used to assign unequivocally a hydrothermal origin to all rapidly accumulating elements because the precipitates themselves can scavenge material directly from sea water (hydrogenous source) at enhanced rates. It is apparent, therefore, that a more refined degree of unscramblng is required in order to deconvolute the hydrothermal from the authigenic signal. One potentially rewarding way of achieving this is by using isotopic (see e.g. Dasch *et al.* 1971) and rare-earth element (see e.g. Bender *et al.* 1971) signatures to distinguish between elements derived from normal sea water origin and those having a magmatic origin. Another way of characterizing the hydrothermal source of an element is by making a direct comparison between the compositions of hydrothermal solutions and those of metalliferous sediments deposited in the same area. Such an approach was adopted by Von Damm *et al.* (1985). These authors determined the concentrations of Mn, Fe, Ni, Cu, Zn, Co, Cd, Ag and Pb in hydrothermal fluids vented from the high-temperature system at 21°N on the EPR, and compared the elemental ratios in the fluids to those in associated metalliferous sediments. Iron was used as an indicator of hydrothermal sources and a comparison was then made between element : Fe ratios in the fluids and the sediments. The results may be summarized as follows.

(a) For Co and Ni (which has an insignificant hydrothermal source), the ratios in the venting solutions were lower than in the sediments, implying that additional amounts of these elements are scavenged from sea water by the hydrothermal Fe–Mn precipitates.

(b) For Mn, Zn, Cu and Ag, the ratios in the hydrothermal solutions were greater than, or equal to, those in the sediments, indicating that although the hydrothermal input is the major source of the elements a proportion of them may be lost to sea water, i.e. may escape the immediate venting area.
(c) The Pb : Fe ratios were very similar in both the venting solutions and the metalliferous sediments, implying a predominantly hydrothermal origin for the Pb.

The hydrothermal signal results from the emanation of mineralizing solutions at the ridge crest spreading centres, which are delivered in the form of pulses. These metal-rich emanations impose spikes on the general background of biogenous, detrital and authigenic components which combine to form normal deep-sea sediments. The components derived from the hydrothermal pulses form an important class of metal-rich sediments. However, by unscrambling the hydrothermal signal it has been demonstrated that the metalliferous deposits themselves have only a relatively small areal extent and, with respect to the sediment surface, they are largely confined to regions around the mid-ocean ridge system.

16.6.3 The contaminant signal spike

There are a number of texts that offer an extensive treatment of pollution in the marine environment, and for this reason the subject is not covered as an individual topic in the present volume; for a state-of-the-art review of the subject, the reader is referred to Preston (1989). However, it is of interest at this stage to demonstrate how contaminant spikes can influence the elemental chemistry of marine sediments.

Contaminant, or anthropogenically generated, components are brought to the ocean reservoir by the same pathways that transport the naturally released material derived from crustal mobilization; for example, artificial radionuclides have been reported in the upper portions of deep-sea sediments (see e.g. Lapicque *et al.* 1987). At present, however, slowly accumulating deep-sea deposits have not yet recorded major inputs of most anthropogenically generated material to the extent that concentration spikes are apparent. But evidence is now beginning to appear that suggests the situation is changing, especially in respect to elements that have a strong anthropogenic signal to the oceans and a relatively short residence time in the water column. Lead is a prime example of such an element:

(a) It has a strong atmospheric anthropogenic signal to open-ocean surface waters (see Sec. 6.4).
(b) It is a scavenging-type element that is rapidly removed from surface waters within a few years (see Sec. 11.6.3.1).

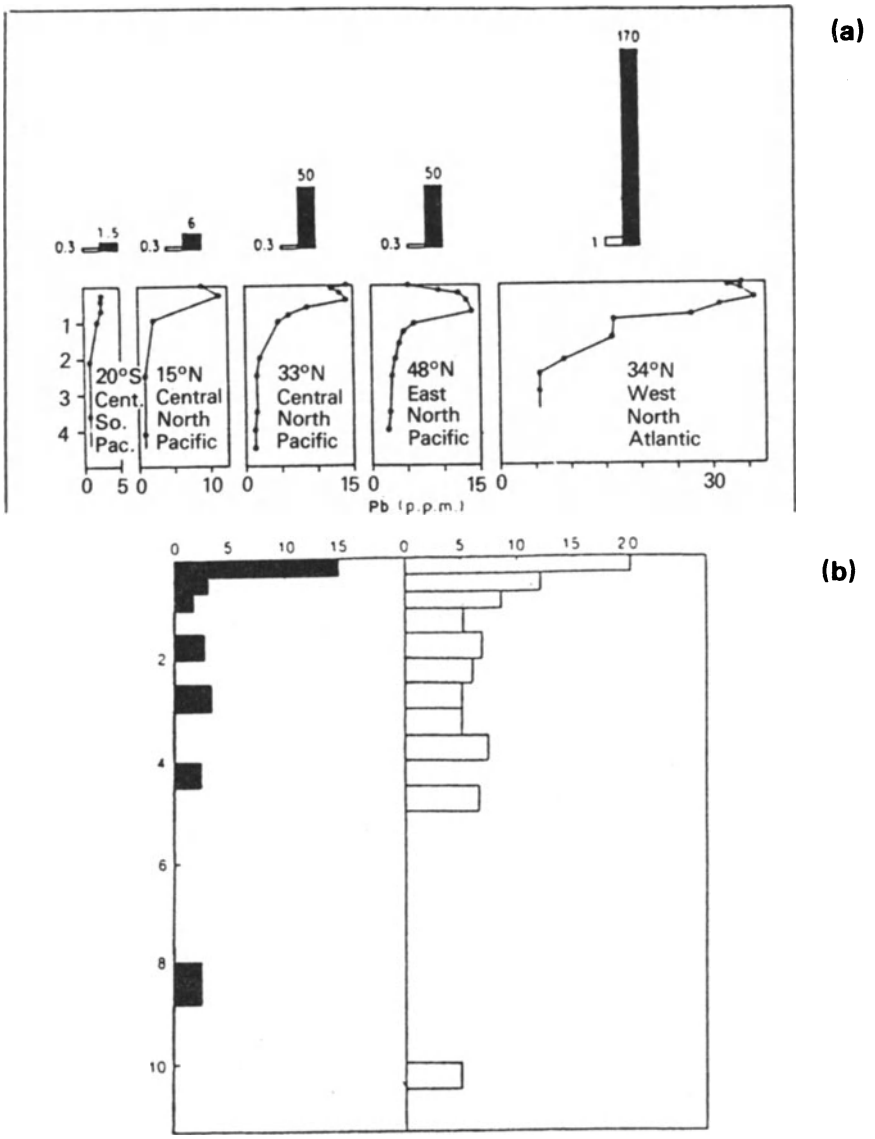

Figure 16.9 Anthropogenic effects on lead in the marine environment. (**a**) Comparisons of atmospheric lead inputs with lead concentration profiles in the open ocean (from Patterson 1987). The histograms display net atmospheric lead input fluxes (10^{-9} g cm^{-2} yr^{-1}), after correction for recycled sea spray; black columns, present-day fluxes; white columns, ancient fluxes. Graphs display the lead concentrations in sea water (10^{-9} g l^{-1}) against depth (km). The oceanic environments are ranked from the most pristine (central South Pacific) to the most anthropogenically contaminated (North Atlantic); this is reflected in the magnitudes of the atmospheric lead fluxes and the effect they have on the water column profiles, both of which are greatest in the North Atlantic. (**b**) Depth distributions of lead in two deep-sea sediment cores from the northeast Atlantic (from Veron *et al.* 1987); units in μg g^{-1}. The surficial samples in both cores contained excess Pb, which was attributed to an anthropogenic source.

(c) It has a relatively short overall residence time in the oceans of around 100 yr (see Sec. 11.2).

The relationship between the atmospheric input of Pb to surface ocean waters and its effect on the water column distribution of dissolved Pb is shown in Figure 16.9a. Most of the atmospheric Pb is anthropogenic in origin and has been delivered directly to open-ocean areas, thus by-passing the coastal sediment trap barriers (see Sec. 11.4). The highest anthropogenic input of Pb is to the North Atlantic, where it is reflected in the large 'bulge' of dissolved Pb concentrations in the upper 1–2 km of the water column (Patterson 1987). It is in the North Atlantic, therefore, that the effects of the input of anthropogenic Pb to surface waters are most likely to be recorded in surficial open-ocean sediments, and recently Veron *et al.* (1987) have reported data that do indeed offer evidence of recent Pb pollution in northeast Atlantic deep-sea sediments. These authors showed that Pb concentrations in the surficial sediments (21 and 15 $\mu g\ g^{-1}$ in the top 1 cm) of two short cores were higher than those in the underlying 10 cm (6.0 and 2.8 $\mu g\ g^{-1}$) – see Figure 16.9b. The amount of Pb stored in the surficial sediments was of the same order as the amount of Pb in the overlying water column, and the authors concluded that the surficial Pb spike was derived from anthropogenic sources.

It is apparent, therefore, that contaminant spikes are beginning to be identified in surficial deep-sea sediments, but it will be a considerable time before such spikes are recorded for elements that have relatively long oceanic residence times. The position is different, however, for some coastal sediments. There are two principal reasons for this: (a) coastal sediments are formed close to the major sources of pollution, and (b) they are deposited at relatively fast rates. As a result, some coastal deposits have recorded the fingerprints of anthropogenic inputs within both a spatial and temporal framework. Various techniques can be used to identify elements transmitted by contaminant signals, and to unscramble them from natural background inputs. Two examples will be used to illustrate how such techniques can assess the effects that contaminant spikes can have on these coastal sediments.

THE SPATIAL DISTRIBUTION OF POLLUTANT ELEMENTS IN COASTAL SEDIMENTS A large proportion of many of the elements associated with contaminant spikes have been removed from solution, and so are part of the non-detrital sediment fraction. In order to separate these non-detrital elements from the crystalline mineral matrix, i.e. the detrital or residual fraction, Chester & Voutsinou (1981) applied a chemical leaching technique to sediments from two Greek gulfs, one of which had received pollutant inputs and the other of which was reasonably pristine in character. By using the unpolluted gulf as a baseline, the authors were

able to identify contaminant trace metals, and to map their distributions in the sediments of the polluted Thermaikos Gulf. To illustrate this, the spatial distributions of non-detrital Zn and Pb in the Thermaikos Gulf are illustrated in Figure 16.10a and b, respectively. There is a heavily industrialized region at the head of this gulf, and it is evident from Figure 16.10 that the non-detrital concentrations of both Zn and Pb are highest in this region; thus local inputs have imposed fingerprints on the distributions of these two elements in the sediments of the gulf. Although they are very restricted in extent, these fingerprints do serve to show how contaminant spikes can modify the distributions of some elements in coastal sediments.

THE TEMPORAL DISTRIBUTION OF POLLUTANT ELEMENTS IN COASTAL SEDIMENTS

Because of their relatively fast rates of deposition, coastal sediments may provide a historical record of contaminant inputs. This was demonstrated by Chow *et al.* (1973) with respect to the deposition of Pb in coastal sediments off southern California. These authors carried out a survey of the distribution of Pb in dated sediment columns from a number of basins in the area. To aid their interpretation of the data, Al (which has a mainly natural origin) was used as a normalizing element to establish the background levels of Pb in the sediments, and isotopic ratios were employed to identify the sources of the Pb itself. Sediments were sampled from the following five localities.

(a) The Soledad Basin. This is remote from the prevailing winds blowing off southern California and is free from waste discharges, and was therefore used as a control area.
(b) The San Pedro, Santa Monica and Santa Barbara Basins. These are inner basins in the Los Angeles area.
(c) Whites Point. This is close to a waste outfall and provided sediments containing industrial and domestic wastes.

The Pb concentrations, and Pb : Al ratios, in the various basins are illustrated in Figure 16.11. The Pb concentrations in the Soledad Basin sediments are generally low (< 20 μg g^{-1}), and the surface deposits contain Pb which has an isotopic composition similar to that of weathered material from the Baja California province. The sediments in this basin were therefore used as a natural baseline against which to compare the Pb distributions in sediments from the other basins. In contrast to deposits in the Soledad Basin, those from White Point have Pb concentrations of several hundred micrograms per gram (μg g^{-1}), and Pb isotopic ratios that are similar to those in petrol (gasoline) sold in southern California. The sediments in the inner basins, which were anoxic and had not suffered bioturbation, had relatively high Pb concentrations

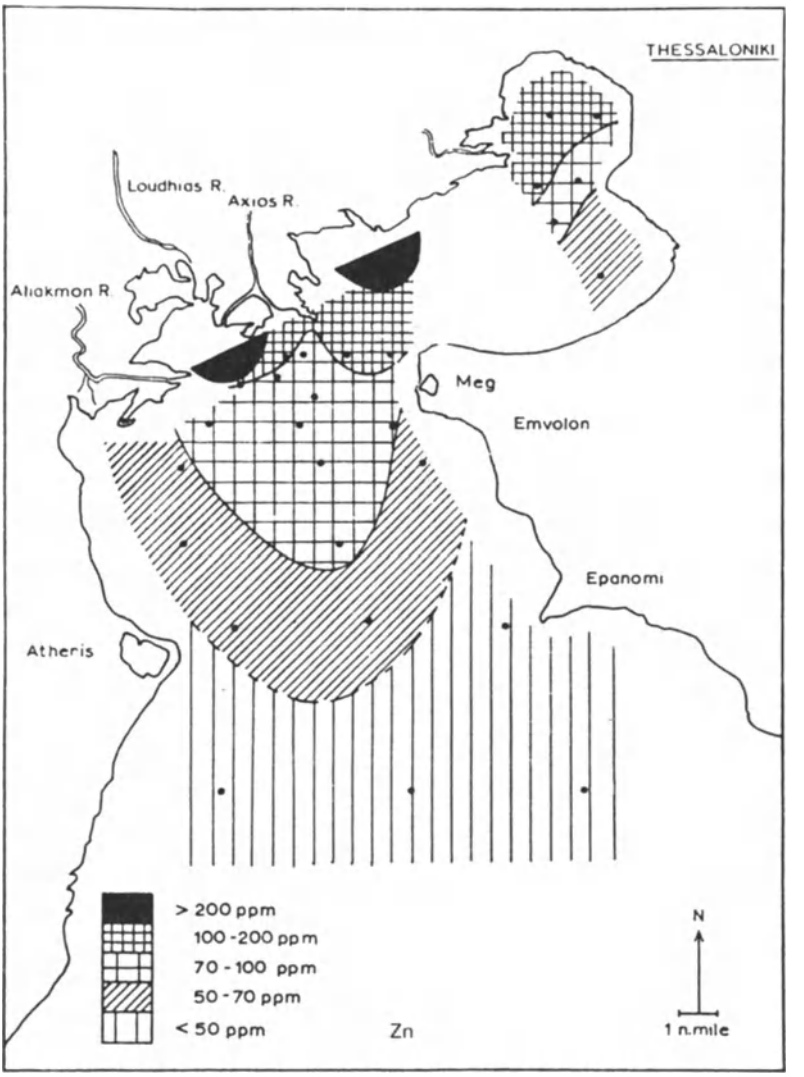

(a)

Figure 16.10 Distribution of non-detrital (**a**) Zn and (**b**) Pb in surface sediments from Thermaikos Gulf, Greece (from Chester & Voutsinou 1981).

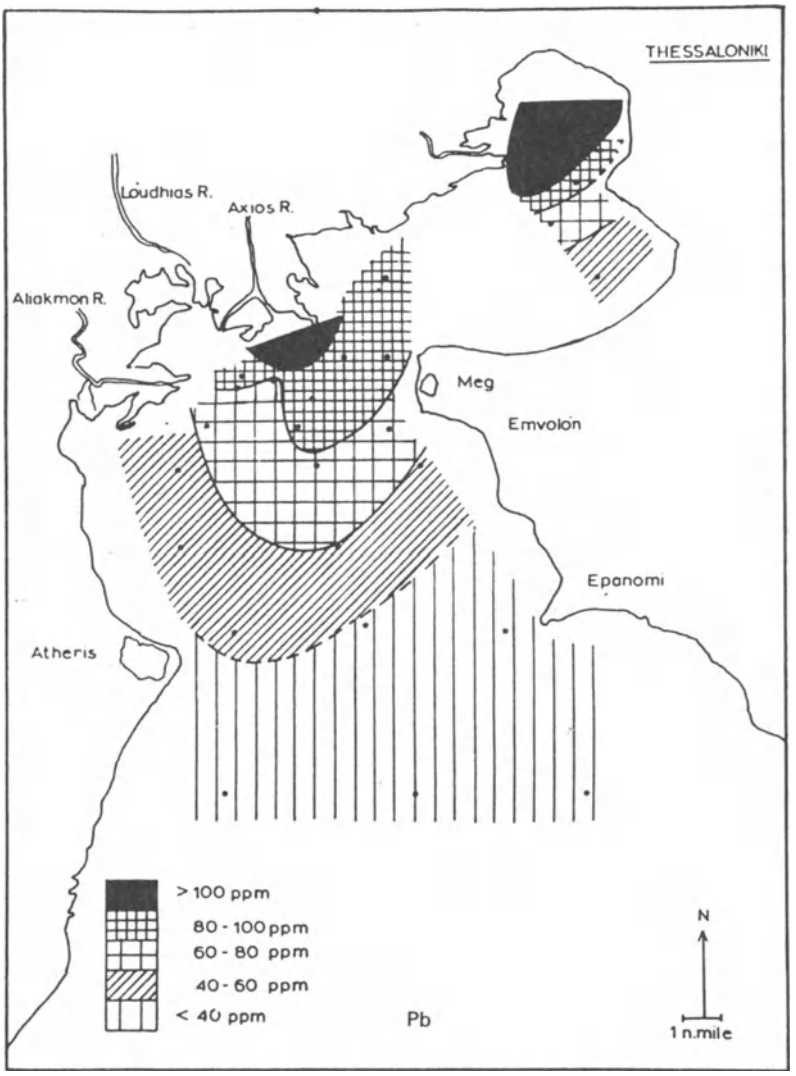
THESSALONIKI
Loudhias R.
Axios R.
Aliakmon R.
Meg
Emvolón
Epanomi
Atheris
> 100 ppm
80 - 100 ppm
60 - 80 ppm
40 - 60 ppm
< 40 ppm
Pb
N
1 n.mile

(b)

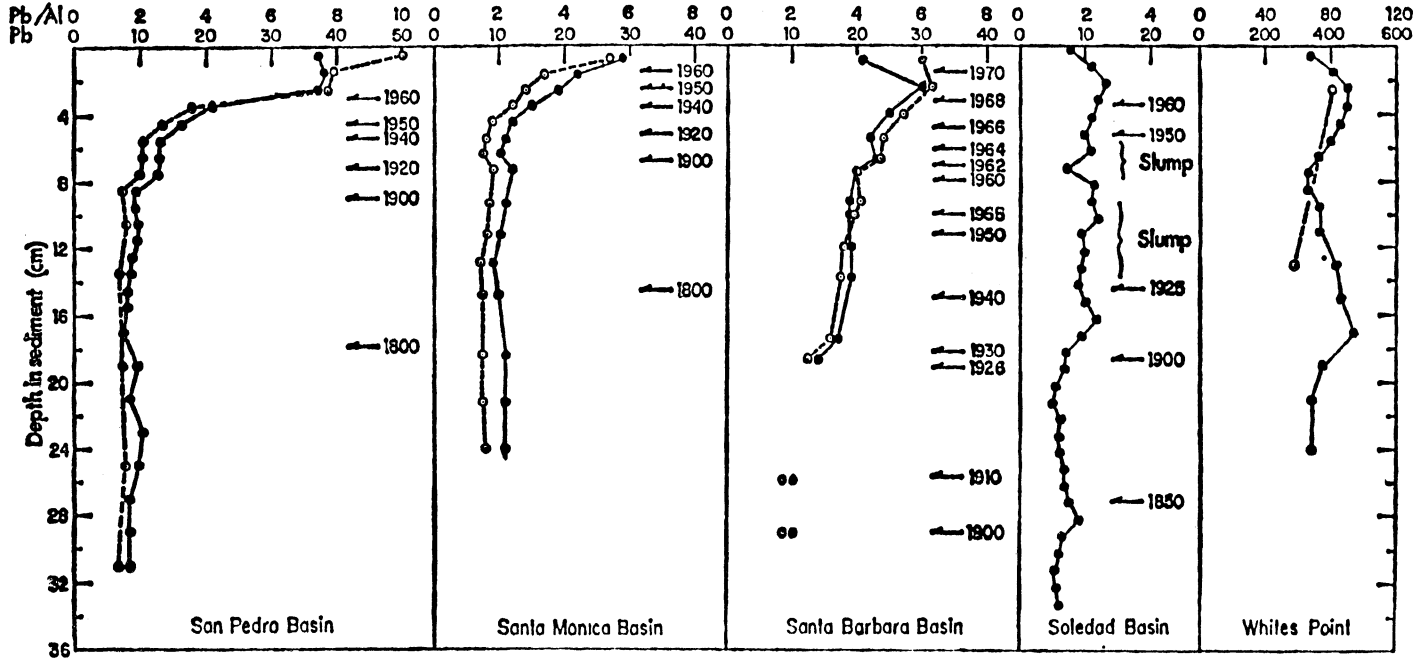

Figure 16.11 The down-column concentrations of Pb, and Pb : Al ratios, in sediments from basins off the coast of southern California (from Chow *et al.* 1973); concentration in μg g^{-1}.

in their upper portions, which decreased towards the baseline levels at ~ 8 cm. Below this depth, the isotopic ratios of the Pb were similar to those which represent the pre-pollution supply. The rates of contaminant Pb accumulation in the inner basins began to increase in the 1940s. This Pb could have been brought to the area via a number of transport pathways (e.g. atmospheric deposition, river run-off, sewage discharge), and the increased inputs are clearly reflected in contaminant spikes in the down-column profiles of the element in the inner basin sediments.

16.6.4 The diagenetic signal spike

Material is transported to the surface of the sediment reservoir via the primary sources. The sediment surface itself, together with the immediately overlying water, is a region of intense biogeochemical activity. Many of the changes that take place in this benthic boundary region are driven by the processes involved in oxic diagenesis, and because these affect elements that have been removed from sea water and subsequently transported down the water column, the processes themselves have been classified as part of the authigenic signal. Some of the processes associated with oxic diagenesis can lead to the transport of elements downwards into the sediment column via the interstitial water. This can be illustrated with respect to copper. Much of the copper reaching the sediment surface is transported via organic carriers. At the sediment surface the carriers are destroyed during oxic diagenesis, releasing the copper into the interstitial waters. The dissolved copper profiles in both pelagic and hemi-pelagic sediments display a maximum at the sediment surface and the shape of the profiles indicates that the element migrates both upwards, where it is lost into sea water, and downwards, where it is taken up in the sediment components at some depth within the oxic layer. The point is, however, that all this copper was originally transported down the seawater column. The authigenic signal is therefore the basic control on the lateral distribution of the chemical elements in surface deep-sea sediments, although this distribution can be perturbed by hydrothermal and contaminant spikes. The vertical distribution of elements added to the sediment column from primary sources can, however, be affected by remobilization and subsequent interstitial water transport, associated with sub-oxic diagenetic processes. These occur below the oxic layer, usually at some depth in the sediment column.

As defined in the present context, therefore, the diagenetic signal refers to that transmitted through the interstitial water column by mainly upward diffusion following *sub-oxic* diagenesis. This signal is generated, therefore, following the utilization of secondary oxidants for the destruction of organic carbon, during which elements are released (from both organic carriers and secondary oxidants) in a soluble form into interstitial waters through which they migrate under the influence of

concentration gradients (see Sec. 14.6.2). The elements may then be reprecipitated under suitable environmental conditions within the upper layers of the sediment, or they may escape into sea water. It is the elements that are trapped within the sediment complex that impose diagenetic fingerprints on oceanic deposits. Trapping at the sediment/sea water interface is especially important in the formation of diagenetic ferromanganese phases, either as discrete nodules or in the bottom portions of mixed nodules. This topic has been treated in detail in Section 15.3.4, and at present attention will be confined to the effects that the diagenetic signal has within the sediment column itself.

The diagenetic signal can manifest itself in down-column changes in elemental concentrations and in the formation of new, or altered, minerals. The post-depositional mobility and migration of elements in the diagenetic processes have been described in Section 14.6.2, in relation to interstitial water fluxes, and it was shown that post-depositional sub-oxic mobilization processes can affect elements such as Mn, Fe, Co, Ni, Cu, Zn, V, U and Mo. The release of elements into the interstitial waters via the sub-oxic diagenetic processes can lead to the setting-up of concentration gradients along which migration takes place, usually upwards towards the sediment surface. For redox-sensitive elements this often involves a recycling process in which release takes place at depth under sub-oxic conditions and is followed by reprecipitation at higher levels under oxic conditions. A large proportion of the elements released in sub-oxic diagenesis can be trapped in this way in the upper oxic layer of oceanic sediments. However, the extent to which this occurs depends on the presence, and thickness, of the oxic layer, which in turn is dependent on the surface redox environment. It was shown in Section 14.4.2 that there is a lateral, i.e. shelf $\rightarrow$ hemi-pelagic $\rightarrow$ pelagic, control on surface sediment redox conditions, and as a result there is also a lateral constraint on the fate of the elements released in sub-oxic diagenesis. This is apparent in the manner in which manganese responds to sub-oxic diagenesis. In pelagic deep-sea sediments, which have a thick oxic layer, the interstitial-water profiles do not generally display a zone of enriched dissolved Mn^{2+}. In most hemi-pelagic deep-sea sediments, where the surface oxic layer is thinner, manganese oxides are utilized as secondary oxidants in the reducing zone and dissolved manganese is liberated into the interstitial waters. This dissolved manganese then migrates upwards and a large fraction is reprecipitated as oxides in the oxic layer, thus operating a recycled manganese trap. In shelf and some hemi-pelagic sediments, however, the surface oxic layer can be absent and the dissolved manganese can escape into sea water via these windows (see Sec. 14.6.2.2). Other elements can be released into solution during the utilization of manganese oxides as secondary oxidants. These include elements that were removed from solution in association with the oxides

at the sediment surface; their subsequent interstitial water migration into the oxidation zone, and reprecipitation with new oxides, can influence their sediment distributions. For example, Sawlan & Murray (1983) showed that the upward diffusive flux of copper to the oxidation zone in hemi-pelagic sediments was of the same order of magnitude as the downward flux from the sediment surface. Clearly, therefore, recycling following sub-oxic diagenesis can affect the vertical distributions of elements brought to the sediments via the primary sources. In oceanic sediments such effects are perhaps most manifest in the distribution of the redox-sensitivie element manganese.

It has been known for many years that the concentration profiles of solid-phase manganese often display higher values close to the surface in *both* pelagic and hemi-pelagic sediments – see Figure 14.8. Manganese responds to redox changes, which can lead to an accumulation of the element in the upper oxic layers of sediments, and this obviously involves a major redistribution of manganese in the sediment column. The question which then arises is 'Do these diagenetic recycling processes operate on a sufficiently global-ocean scale to account for the depth depletion–subsurface enrichment of manganese found in all types of oceanic sediments?' A number of authors have attempted to address this question of whether sub-oxic diagenetic processes can supply sufficient Mn to account for the concentration of the element in the upper layers of marine sediments. For example, Bender (1971) applied a simple diffusive model to interstitial-water data and concluded that Mn^{2+} can only supply the Mn concentrated in the upper *pelagic* sediment column if it has to migrate through < 1 m of sediment. Thus, for those deep-sea sediments in which the Mn-rich zone can extend over tens of metres it would appear that post-depositional migration cannot supply the excess Mn requirement, although it can contribute Mn to the formation of ferromanganese nodules and individual Mn-rich bands (see also Sec. 14.6.2). Elderfield (1976) made a more detailed attempt to assess the influence of the diagenetic interstitial water transport of Mn^{2+} on the supply of non-detrital Mn to the upper layers of marine sediments, and reached the same overall conclusions as Bender (1971). To do this, Elderfield (1976) used a number of approaches to estimate how much Mn in excess of that provided by fluvial transport was required to maintain the non-detrital concentration of the element in the upper layers of the sediments. This fluvial-excess non-detrital Mn was found to be accumulating at a rate in the range $\sim$ 300–2000 $\mu g\ cm^{-2}/10^3$ yr. The author then used a vertical advection–diffusion model to assess the interstitial water transport of Mn in both nearshore and deep-sea sediments. For nearshore sediments, he concluded that the estimated diagenetic flux was in agreement with the known accretion rate of manganese deposits, thus supporting diagenetic theories for the origin of shallow water marine ferromanganese nodules.

For deep-sea sediments, however, the maximum value of the surface diagenetic flux of Mn was calculated to be $\sim$ 70 μg $cm^{-2}/10^3$ yr when the upper zone of the sediment was $\sim$ 20 cm thick, compared to the minimum estimate of 300 μg $cm^{-2}/10^3$ yr for the fluvial-excess Mn accumulation rate. Much smaller diagenetic fluxes will be found for deep-sea sediments in which the upper oxic zone extends over several metres, and Elderfield (1976) concluded that sub-oxic diagenesis cannot supply all the excess Mn in pelagic sediments and is, in fact, only likely to be significant for those deposits which have a thin (< 25 cm) oxic layer. However, this type of thin layer is characteristic of a number of hemi-pelagic sediments (see Sec. 14.4.1), and for these deposits diagenetic Mn fluxes can be important in supplying the element to the upper layers; this general conclusion has also been supported by Sawlan & Murray (1983) on the basis of detailed interstitial-water manganese profiles (see Sec. 14.6.2).

It may be concluded, therefore, that the extent to which upward sub-oxic diagenetic fluxes of Mn contribute to the total Mn in surface sediment layers varies in the sequence shelf > hemi-pelagic > pelagic deep-sea sediments, in relation to the lateral diagenetic sequence. In general, therefore, sub-oxic diagenetic recycling can only supply sufficient manganese to satisfy the upper layer enhancement in those sediments that have an oxic layer $\lesssim$ 25 cm in thickness. In the extreme case, Mn can be released from nearshore sediments directly into the water column from where it can be transported for incorporation into nodules and sediments in other regions. In less extreme hemi-pelagic environments, the remobilized Mn is trapped within the upper oxic layers of the sediment, and so imposes a diagenetic spike on the sediment column itself. However, in pelagic sediments, which have relatively thick surface oxic layers, diagenetic fluxes cannot supply the Mn required to generate the Mn-rich upper layer, and Elderfield (1976) concluded that in these deposits the fluvial-excess manganese probably has a hydrothermal origin; atmospheric sources also contribute to the fluvial-excess Mn. Nonetheless, hemi-pelagic sediments cover a significant area of the deep-sea floor, and here the top-loading of solid-phase manganese results from a major redistribution of the element in response to sub-oxic diagenetic recycling.

16.7 The ocean-wide operations of the sediment-forming signals

Most oceanic sediments are made up of a mixture of components of different origins, and so have received a variety of chemical signals. The nature of the individual chemical signals, and how they can be unscrambled from each other, has been described in the previous sections. In this way, it was possible, at least in a tentative manner, to

understand the chemical processes that are active in the formation of oceanic sediments. From this it has become apparent that the chemical compositions of the sediments are governed by a complex of interrelating controls in which the end-member components derived from the various signals are mixed together. The controls that govern the signal strengths are related to the overall pattern of sedimentation in a particular oceanic area. Thus, to understand fully how these interrelating controls actually operate, account must be taken of the physical processes that move material around the ocean reservoir.

To conclude the treatment of the factors that control the chemical composition of marine sediments, an attempt will therefore be made to draw together the various lines of evidence discussed earlier in order to establish how the signals interact on a global scale and so fix the overall chemical compositions of the sediments. To do this, attention will be focused on the deposits at the sediment surface.

For most deep-sea sediments, the contaminant signal can be ignored at the present day, and the sub-oxic diagenetic signal recycles elements most of which have already been deposited at depth in the sediment column. In order to determine how the element-carrying signals interact on a global scale to control the composition of the surface sediments, attention will therefore be concentrated on the *primary* signals, and for this purpose it will be assumed that

$$C_t = C_b + C_d + C_a + C_h. \tag{16.10}$$

Relatively few studies on the distributions and accumulation rates of elements in deep-sea sediments have been made on an ocean-wide basis; however, those carried out by Bostrom and coworkers are ideal for the present purpose. Bostrom *et al.* (1973) combined concentration patterns with sediment accumulation rate data to identify the factors that control the distributions of a series of elements in surface deep-sea sediments from the Indo-Pacific Ocean. This study, which included elements having a number of different geochemical characteristics, can therefore be used as a basis for assessing how chemical sediment-forming signals interact on a quasi-global scale.

16.7.1 Biogenous elements

Silicon in the form of opaline silica will serve as an example of a biogenous element in a deep-sea sediments. Bostrom *et al.* (1973) estimated the concentration of opaline silica from the total silica (ΣSiO_2) contents in the Indo-Pacific sediments by assuming that in crustal material $SiO_2 : Al_2O_3 = 3.0$, and then assigning any SiO_2 in excess of this to a biogenic source. The distribution of this biogenic silica in Indo-Pacific sediments is shown in Figure 16.12a(i), and clearly reflects the controls on

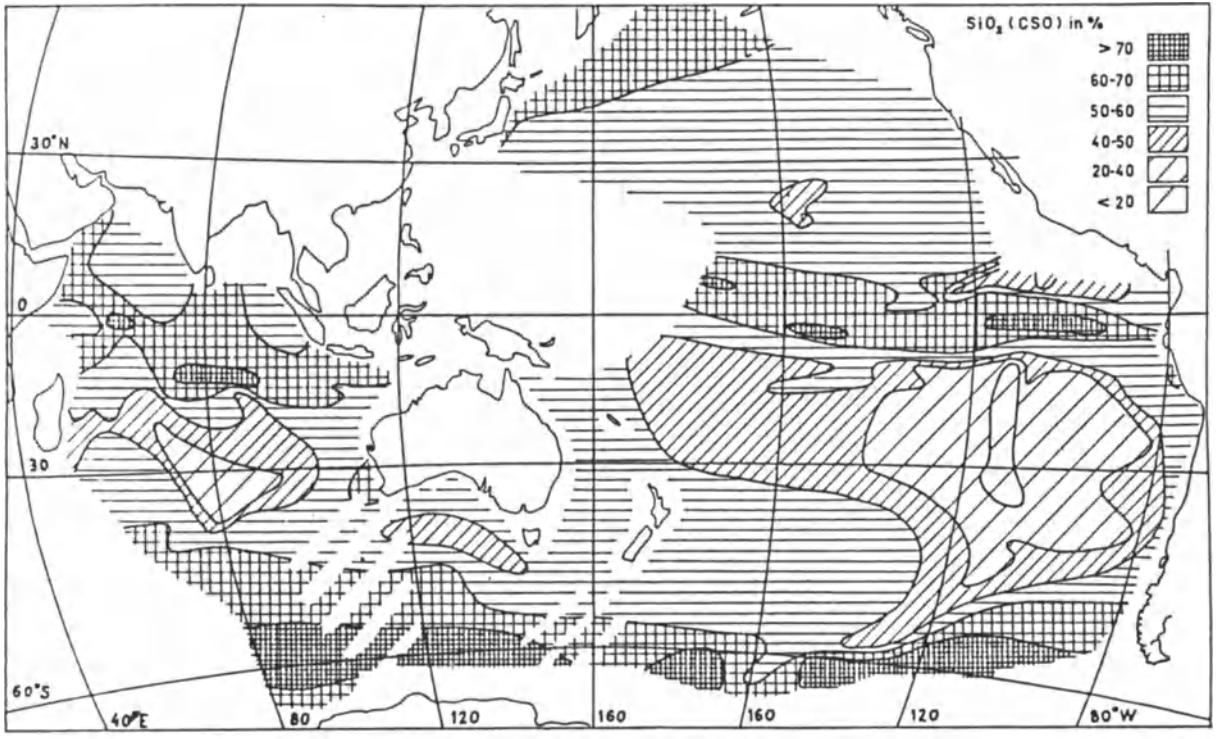

Figure 16.12 Distributions and accumulation rates of elements in Indo-Pacific sediments (from Bostrom *et al.* 1973); MB = minerogen basis. (**a**) (i) Distribution of SiO_2 in Indo-Pacific sediments (on a carbonate-, salt- and organic matter-free basis).

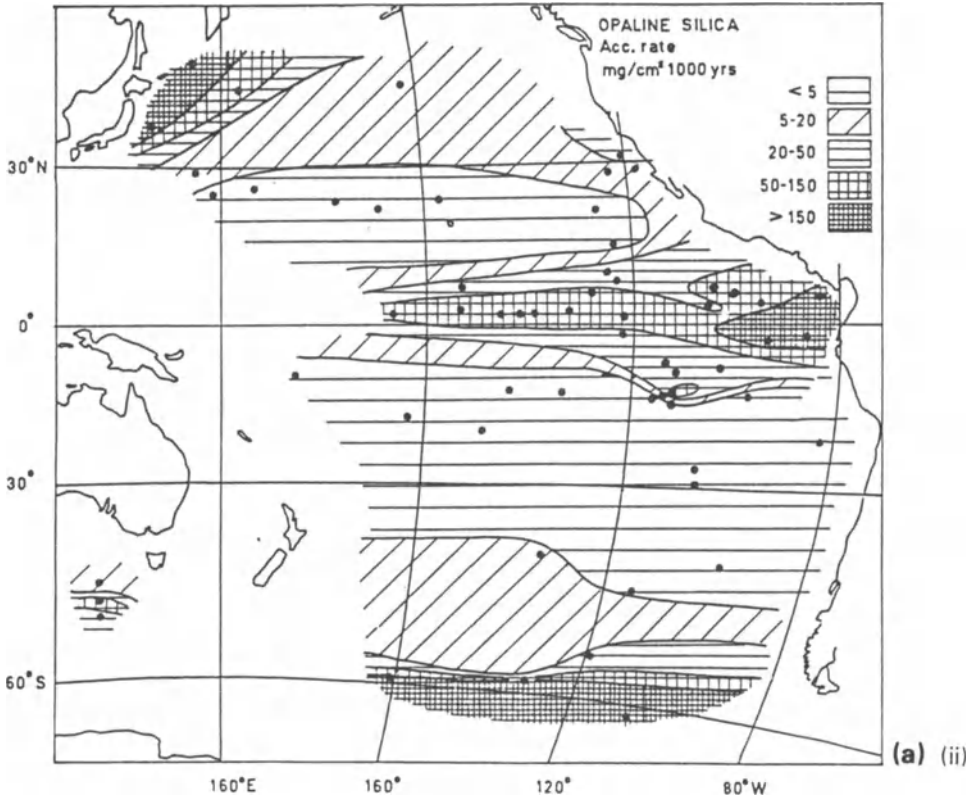

Figure 16.12a (ii) Accumulation rates of opaline silica in Pacific sediments.

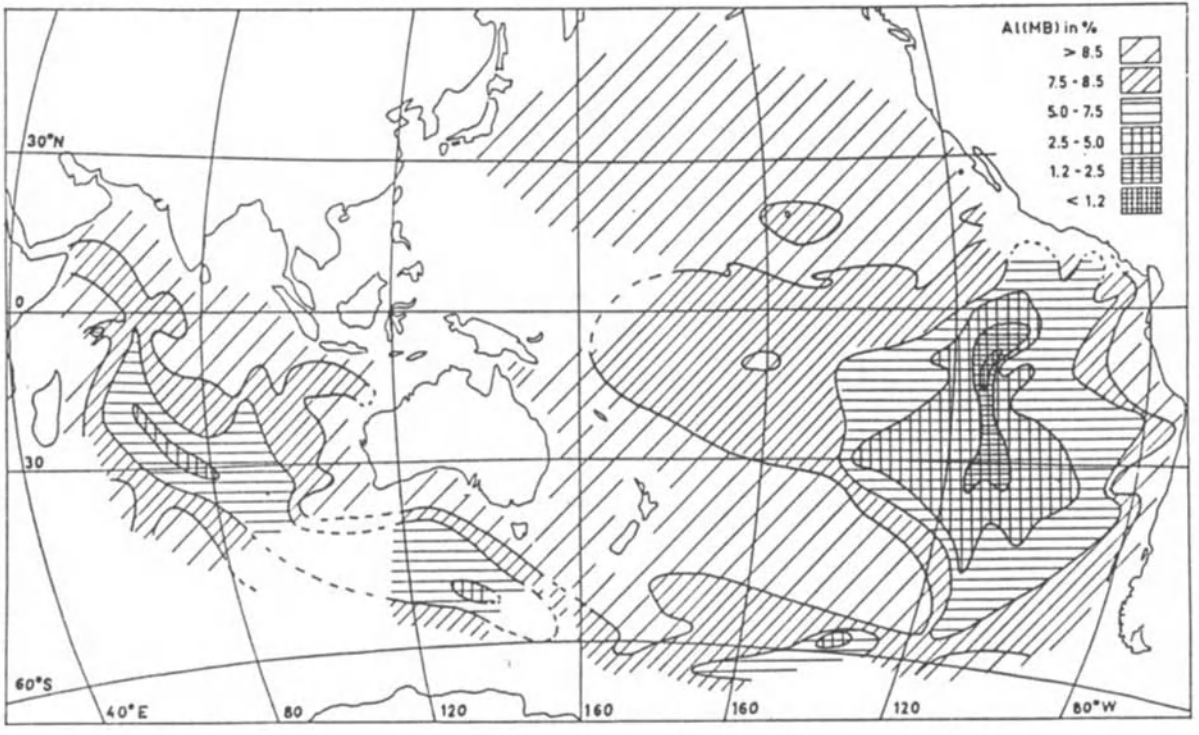

(b) (i)

Figure 16.12b (i) Distribution of Al in Indo-Pacific sediments (on a minerogen basis).

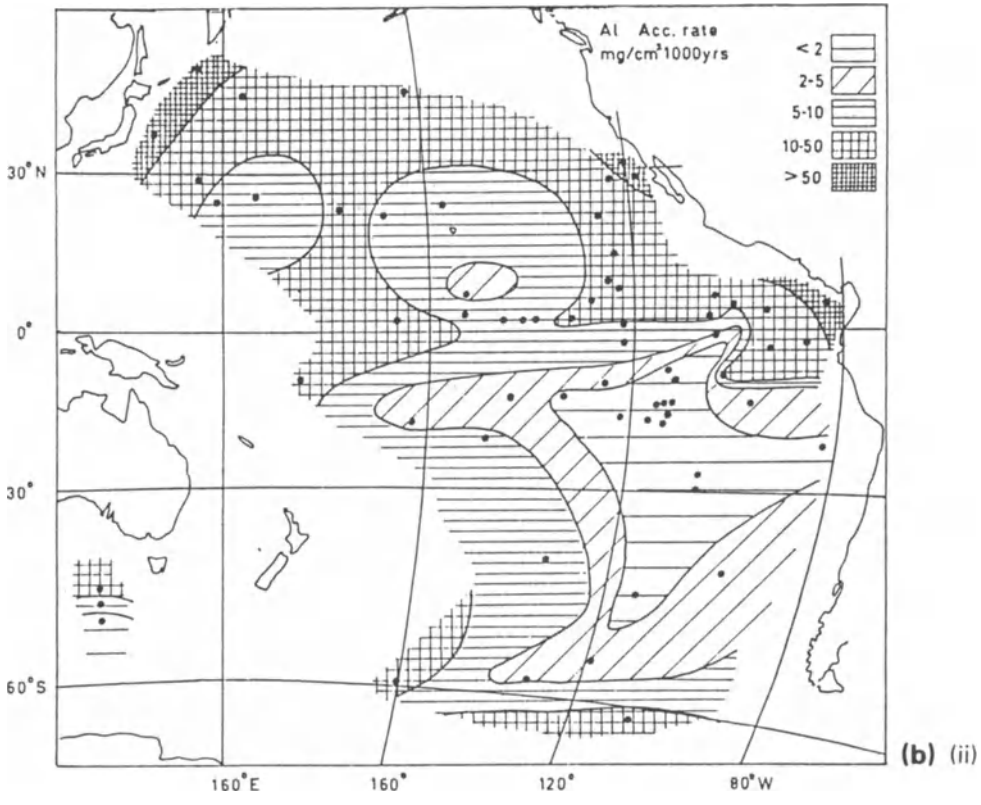

Figure 16.12b (ii) Accumulation rates of Al in Pacific pelagic sediments.

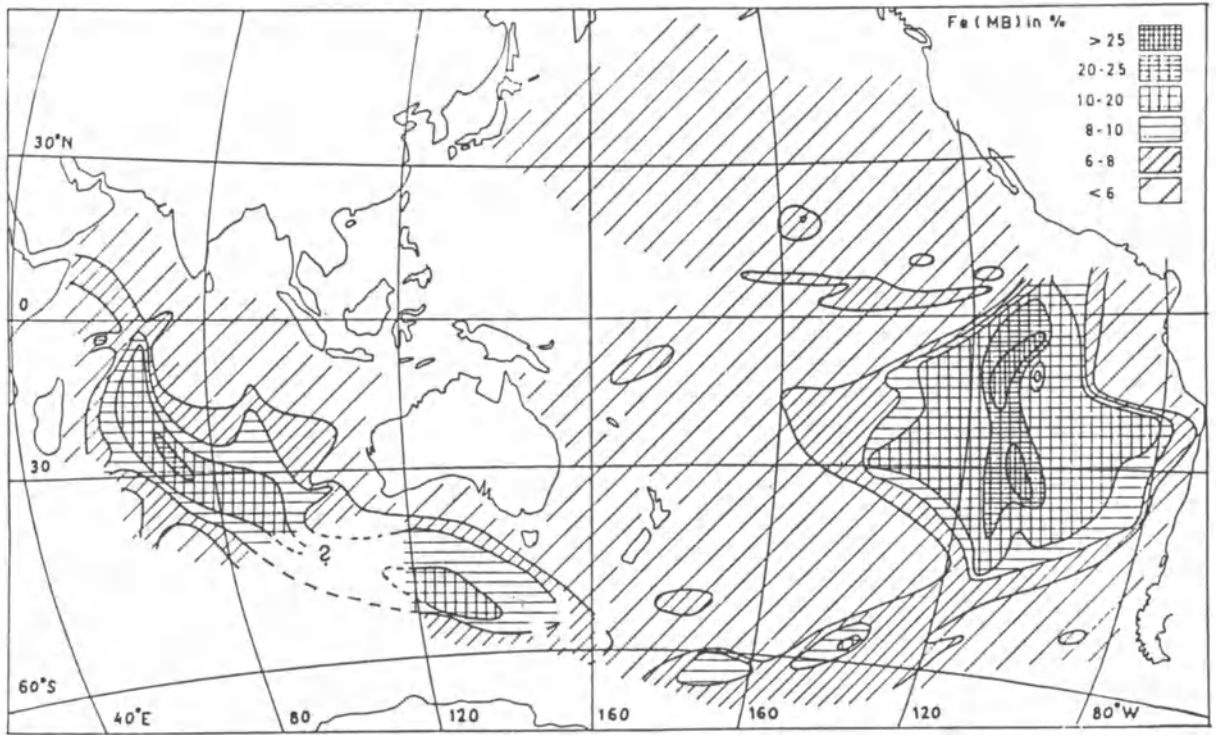

(c) (i)

Figure 16.12c (i) Distribution of Fe in Indo-Pacific sediments (on a minerogen basis).

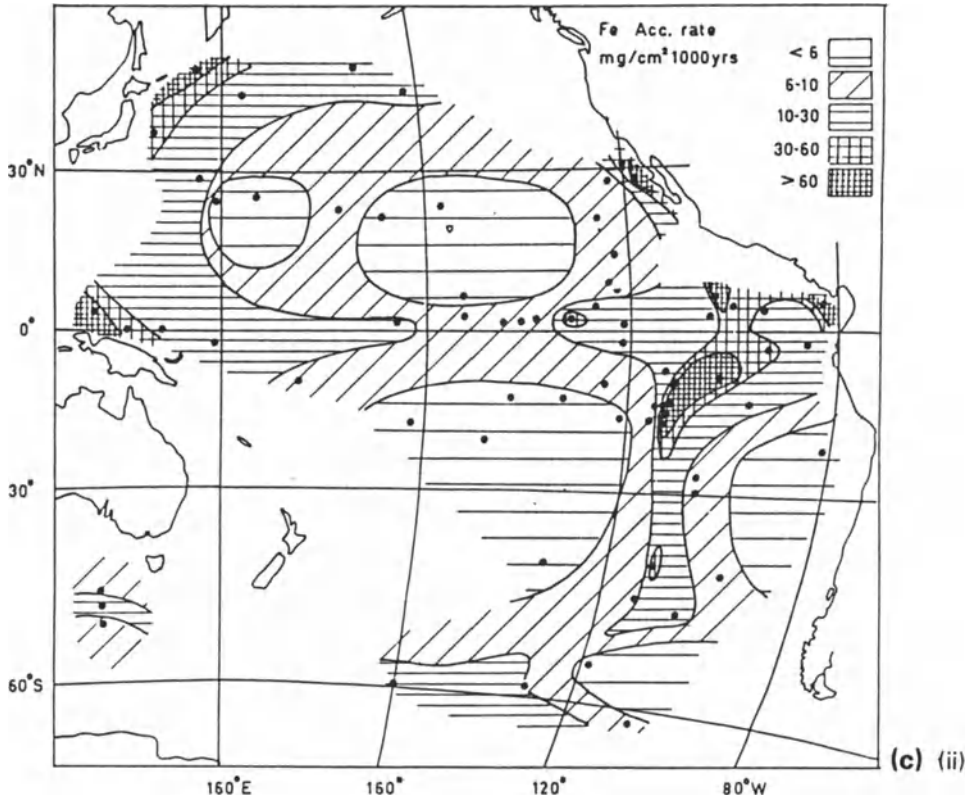

Figure 16.12c (ii) Accumulation rates of Fe in Pacific sediments.

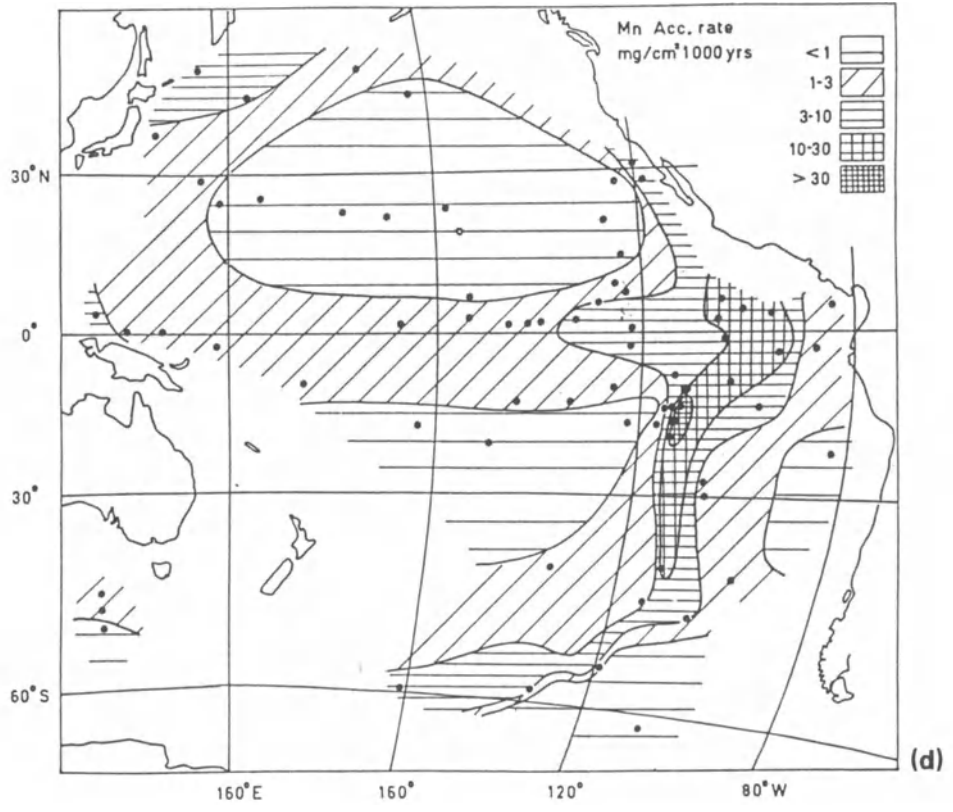

Figure 16.12d Accumulation rates of Mn in Pacific sediments.

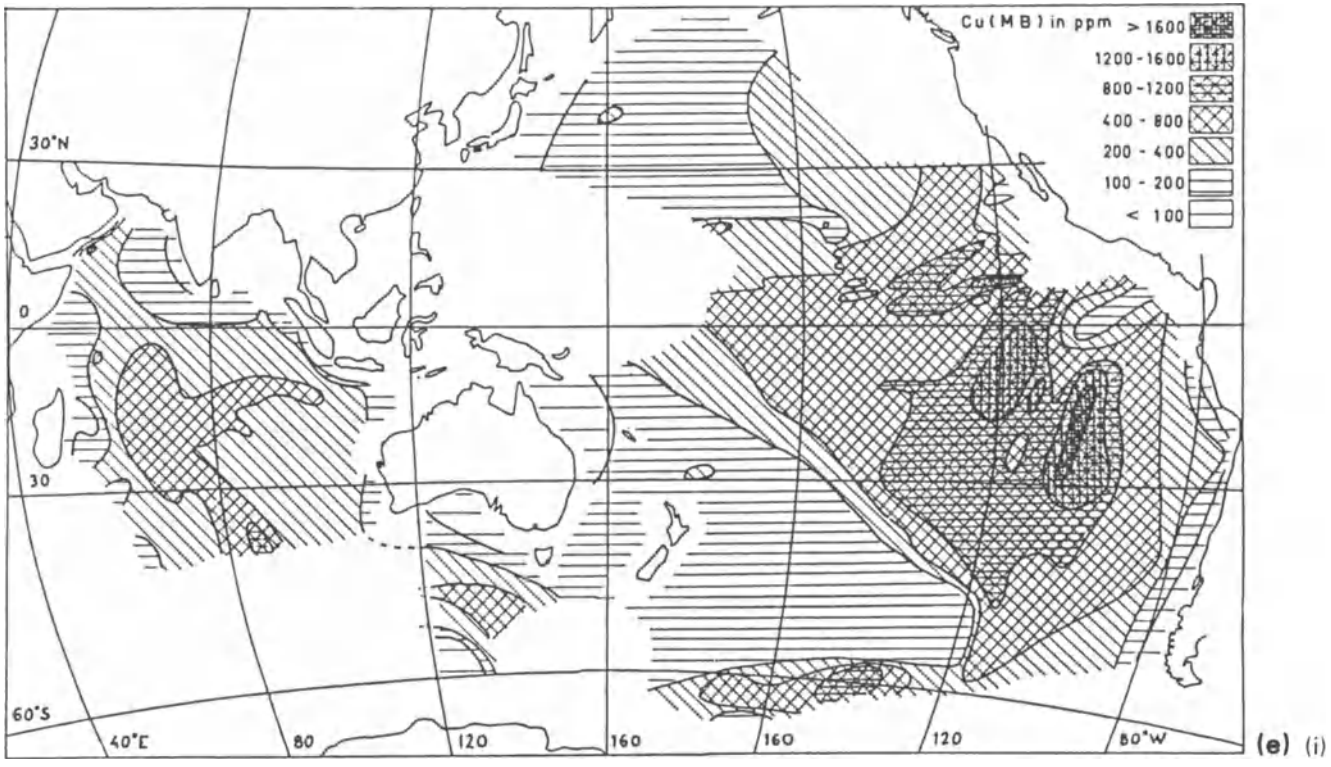

Figure 16.12e (i) Distribution of Cu in Indo-Pacific sediments (on a minerogen basis).

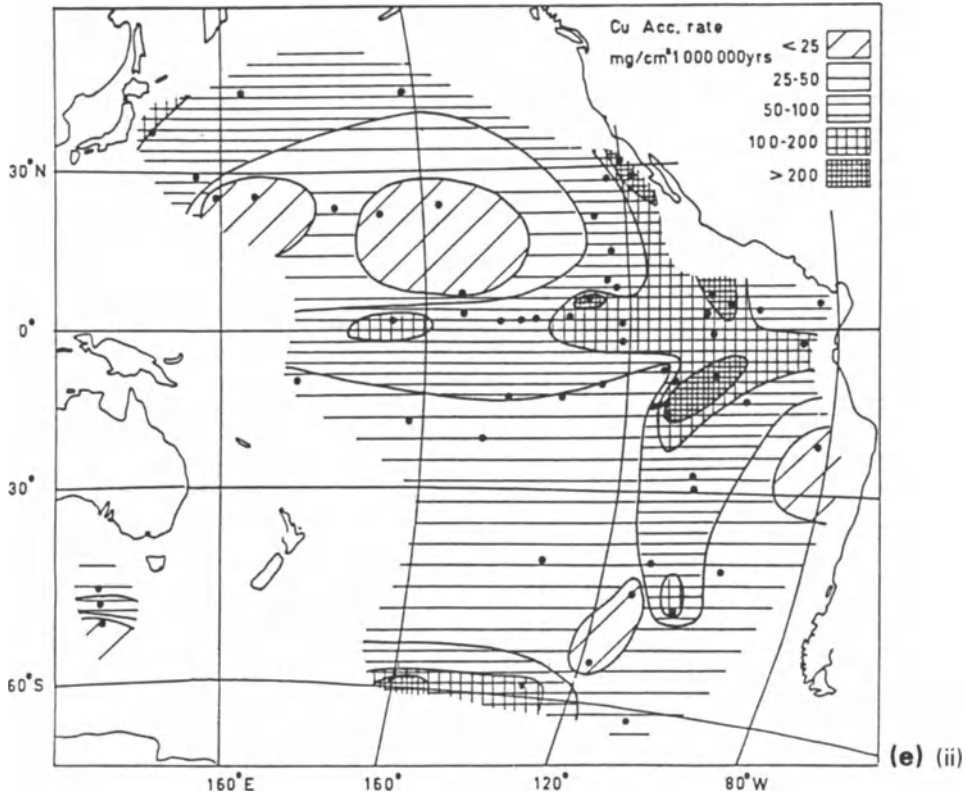

Figure 16.12e (ii) Accumulation rates of Cu in Pacific sediments.

the distribution of opaline silica that were discussed in Section 15.2.1. Thus, the greatest concentrations of biogenic silica are found in the high-latitude rings around Antarctica and in the northern Pacific, with enhanced concentrations in sediments under the equatorial high primary productivity zone also evident. The same general pattern can also be identified in the opaline silica accumulation rates (Fig. 16.12a(ii)), which demonstrates how the strength of the signal varies on an ocean-wide scale. It was shown in Section 15.2.3 that there is a fundamental oceanic dichotomy in which diatoms are favoured in highly productive regions and coccoliths in poorly productive regions, and that as a result siliceous deposits are found mainly at the edges of the oceans and calcareous deposits are concentrated in relatively shallow open-ocean regions. This dichotomy is evidenced when the distribution of opaline silica (Fig. 15.2b) is compared to that of calcium carbonate (Fig. 15.2a) in the Indo-Pacific deep-sea sediments. Thus, whereas opaline silica shows a pronounced 'ring' distribution around the ocean margins, calcium carbonate reaches its highest concentrations on mid-ocean topographic highs.

16.7.2 Non-biogenous elements

Bostrom *et al.* (1973) expressed the concentrations of non-biogenous elements on a **minerogen** basis. This procedure, in which the non-biogenic component is expressed in terms of a series of oxides, is more rigorous than those which simply express the data on a carbonate-free basis, since it compensates for the diluting effects of both carbonate and opaline silica shells. In relation to the primary chemical signals that contribute to the total concentration of the non-biogenic elements, therefore

$$C_t = C_d + C_a + C_h. \tag{16.11}$$

The factors controlling the distributions of a number of non-biogenic elements in the Indo-Pacific deep-sea sediments are discussed below in terms of this general equation.

ALUMINIUM The Al in deep-sea sediments is almost, but not entirely, associated with detrital material in which it is held in lattice positions within aluminosilicates; for example, > 80% of the total Al_2O_3 in deep-sea sediments is partitioned into the detrital phase (see Sec. 16.5). Thus, the distribution of the element is controlled mainly by the detrital signal, and the data provided by Bostrom *et al.* (1973) allow us to evaluate the manner in which this signal operates on a quasi-global scale. The distribution of total Al (ΣAl) in the Indo-Pacific is illustrated in Figure 16.2b(i), from which it can be seen that the highest concentrations are found in sediments close to the continents and the lowest around the spreading ridge system. The strength of the detrital signal is perhaps

better seen in the accumulation rate patterns for ΣAl in the Pacific sediments (Fig. 16.12b(ii)), and for this it is useful to treat the North and South Pacific separately. In the North Pacific, ΣAl accumulates at its highest rates around the continental margins, and decreases in a semi-regular manner towards the remote open-ocean areas. As a result, the strength of the detrital signal decreases in the order marginal sediments > hemi-pelagic sediments > normal open-ocean pelagic sediments. Bostrom *et al.* (1973) showed that over most of the North Pacific the detrital material in the sediments has a continental source, and the ΣAl accumulation rate pattern has clearly been established in response to the distance of the depositional environments from the surrounding source areas. Oceanic crust and active ridge sources complicate the situation in the South Pacific, and an area of relatively low ΣAl accumulation is found around the EPR.

IRON The distribution and accumulation rates of ΣFe in the Indo-Pacific sediments are illustrated in Figure 16.12c(i) and (ii), respectively. Like ΣA1, much of the ΣFe in normal deep-sea sediments is detrital in character (see Sec. 16.5), and this is apparent in the accumulation rates of the element in the North Pacific sediments, in which the patterns are very similar to those of ΣAl; i.e. high values adjacent to the continents, and a general decrease out towards open-ocean areas. It is apparent from Figures 16.12c(i) and (ii) that the open-ocean North Pacific is outside the major influence of the hydrothermal supply of Fe from the EPR, and here therefore

$$C_t(\mathrm{Fe}) \simeq C_d(\mathrm{Fe}) + C_a(\mathrm{Fe}). \qquad (16.12)$$

On the basis of the data given by Bostrom *et al.* (1973) (see Fig. 16.12c(ii)) it is apparent that in the open-ocean North Pacific, ΣFe (C_t) is accumulating at $\lesssim$ 6000–10 000 μg cm^{-2}/10^3 yr. According to Krishnaswami (1976), Fe_a accumulates at $\sim$ 800 μg cm^{-2}/10^3 yr in normal pelagic clays and so cannnot account for the accumulation of the ΣFe. Clearly, therefore, the detrital signal dominates the distribution of ΣFe in the open-ocean North Pacific sediments. This is consistent with the conclusions reached by Chester & Hughes (1969) that $\simeq$ 90% of the ΣFe in a North Pacific deep-sea clay was detrital in origin. Further, in the North Pacific, both the distribution and accumulation rates of Fe are similar to those of the detritally dominated ΣAl. In the South Pacific, however, the situation is very different, and here the patterns for ΣFe are almost a mirror image of those for the detrital element Al. Two features are apparent in the ΣFe accumulation patterns in this region.

(a) The dominant feature is the very high ΣFe accumulation rate around the

the EPR, where it can reach values of $> 60\,000$ μg cm^{-2}/10^3 yr, which agree well with those given in Section 15.3.6 for hydrothermal deposition.

(b) A less well developed feature is a band in the Equatorial Pacific in which the ΣFe accumulates at intermediate rates.

It would appear, therefore, that in the North Pacific the detrital signal is mainly responsible for the deposition of ΣFe, whereas in the South Pacific there is a very pronounced hydrothermal spike which dominates the accumulation of ΣFe.

MANGANESE The accumulation rates of ΣMn in the Indo-Pacific sediments are illustrated in Figure 16.12d. Manganese differes from both Al and Fe in that in deep-sea sediments an average of ~ 70–80% of the ΣMn is non-detrital in origin (see Sec. 16.5). This non-detrital character is seen in the accumulation rate pattern for ΣMn in the North Pacific, a region that is not strongly affected by hydrothermal inputs. Here, therefore

$$C_t(\mathrm{Mn}) \simeq C_d(\mathrm{Mn}) + C_a(\mathrm{Mn}). \qquad (16.13)$$

Although ΣMn does accumulate faster closest to the continents, the effect is much less apparent than that for either ΣAl of ΣFe, and over a very large area of the open-ocean North Pacific ΣMn accumulates at rates < 1000 μg cm^{-2}/10^3 yr. According to Krishnaswami (1976) Mn_a accumulates in normal Pacific clays at a rate of ~ 500 μg cm^{-2}/10^3 yr, which begins to approach that of the ΣMn accumulation rate in the sediments. In the North Pacific, therefore, the authigenic signal can supply a large fraction of the ΣMn accumulating in the sediments, thus highlighting the difference between this element and Fe, for which the authigenic signal supplies a very much smaller fraction of the ΣFe. However, in the South Pacific the accumulation rate patterns of the two elements are generally similar, each showing a very high accumulation rate patch around the EPR and a lesser one in the vicinity of the Equator. There is, however, a difference in the degree to which the hydrothermal spike influences the accumulation rates of ΣMn and ΣFe. Around the EPR, ΣMn accumulates at rates $> 30\,000$ μg cm^{-2}/10^3 yr, which is more than three times faster than over any other part of the entire Pacific; in contrast, the near-continental detrital accumulation rates for ΣFe are of a similar magnitude to the hydrothermal accumulation rates. For ΣMn, therefore, the detrital signal plays only a relatively minor role in the accumulation of the element. Thus, over much of the North Pacific the authigenic signal dominates the accumulation of ΣMn. In contrast, in the eastern South Pacific the hydrothermal signal is predominant, and results in accumulation rates that are at least three times greater than those found anywhere else in the ocean.

COPPER The distribution and accumulation rates of ΣCu in the Indo-Pacific deep-sea sediments are illustrated in Figure 16.12e(i) and (ii), respectively. Around 50% of the ΣCu in Pacific pelagic clays appears to be non-detrital in origin (see e.g. Krishnaswami 1976); i.e. the element has a partitioning signature that is intermediate between those of ΣFe and ΣMn. A number of features can be seen in the accumulation rate pattern of ΣCu in Pacific deep-sea sediments.

(a) There is a tendency for ΣCu to accumulate faster around the continents, which presumably reflects the near-source strength of the detrital Cu signal.
(b) In the North Pacific there is a general decrease in the accumulation rates of ΣCu towards mid-ocean areas as the influence of the detrital signal decreases. Here, ΣCu accumulates at rates of < 25 μg cm^{-2}/10^3 yr. From the data provided by Krishnaswami (1976), authigenic Cu accumulates in normal Pacific pelagic clays at ~ 8 μg cm^{-2}/10^3 yr, so that on this basis around one-third of the ΣCu arises from the authigenic signal; however, this is a minimum estimate, and the figure may well reach the 50% authigenic partitioning reported by Krishnaswami (1976).
(c) In the South Pacific, the accumulation of ΣCu, like those of ΣMn and ΣFe, is dominated by the hydrothermal signal, and around the EPR ΣCu accumulates at rates of > 200 μg cm^{-2}/10^3 yr, which is similar to the rate of accumulation associated with the detrital input from the US mainland in the North Pacific.
(d) There is a band of relatively high ΣCu accumulation around the Equator, which is considerably more well developed than those for either ΣMn or ΣFe. This band corresponds to a zone of high primary productivity in the surface waters, and the enhanced accumulation of ΣCu probably results from an accelerated down-column authigenic flux from the carbon-rich overlying waters (see Fig. 9.4). Bostrom *et al.* (1973) reported that the distribution and accumulation rate patterns of ΣNi and ΣCo in the Indo-Pacific were generally similar to those for ΣCu.

It may be concluded, therefore, that the distributions and accumulation rate patterns of elements in surface sediments from the Indo-Pacific can be used to illustrate how sediment-forming signals interact on a global scale. The main features in the distribution and accumulation rates of opaline silica in the sediments can be related to the biogenic signal, and those for ΣAl can be explained in terms of the predominance of the detrital signal. Patterns in the distributions and accumulation rates of ΣFe, ΣMn and ΣCu can be interpreted mainly in terms of the global interaction of the detrital, authigenic and hydrothermal signals. It must be

remembered, however, that within the sediment column the sub-oxic diagenetic signal can redistribute redox-sensitive elements such as manganese, the overall effect decreasing in the order: shelf > hemi-pelagic > pelagic sediments (see Sec. 14.4.2).

16.8 Unscrambling the sediment-forming chemical signals: summary

(a) The chemical composition of marine sediments can be interpreted within a framework in which the elements are envisaged as being transmitted to the deposits via a series of signals associated with a variety of geochemical processes. The components making up the sediments are formed by elements that are transmitted either by individual signals or, more usually, by signal couplings.
(b) Detrital, biogenous and authigenic signals operate on an ocean-wide scale. These are the background signals, which carry the elements having a direct seawater source.
(c) A series of perturbation spikes from more localized hydrothermal and contaminant seawater signals, and from interstitial-water diagenetic signals, are superimposed on the background signals.
(d) Sediments from different oceanic environments record varying signal strengths. For example: (i) authigenic signals have their greatest influence on pelagic sediments deposited in regions away from the spreading ridges; (ii) diagenetic signals are strongest in hemi-pelagic sediments, in which sub-oxic diagenesis takes place; (iii) hydrothermal signals can dominate in areas in the vicinity of spreading ridges, where metal-rich sediments can be formed; and (iv) the effects of contaminant signals are mainly confined to coastal deposits, but are starting to appear in deep-sea sediments.

References

Aplin, A.C. & D.S. Cronan 1985. Ferromanganese oxide deposits in the central Pacific Ocean, II. Nodules and associated elements. *Geochim. Cosmochim. Acta* **49,** 437–51.

Bacon, M.P. & J.N. Rosholt 1982. Accumulation rates of Th-230, Pa-231, and some transition metals on the Bermuda Rise. *Geochim. Cosmochim. Acta* **46,** 651–66.

Bender, M.L. 1971. Does upward diffusion supply the excess in manganese in sediments? *J. Geophys. Res.* **76,** 4212–15.

Bender, M.L., W. Broecker, V. Gornitz, W. Middel, R. Kay, S. Sun & P. Biscaye 1971. Geochemistry of three cores from the East Pacific Rise. *Earth Planet. Sci. Lett.* **12,** 425–33.

Bender, M.L., T.-L. Ku & W.S. Broecker 1970. Accumulation rates of manganese in pelagic sediments and nodules. *Earth Planet. Sci. Lett.* **8,** 143–8.

REFERENCES

Bostrom, K. & D.E. Fisher 1971. Volcanogenic uranium, vanadium and iron in Indian Ocean sediments. *Earth Planet. Sci. Lett* **11,** 95–8.

Bostrom, K. & M.N.A. Peterson 1969. The origin of aluminium-poor ferromanganoan sediments in areas of high heat flow on the East Pacific Rise. *Mar. Geol.* **7,** 427–47.

Bostrom, K., T. Kraemer & S. Gartner 1973. Provenance and accumulation rates of opaline silica, Al, Ti, Fe, Mn, Cu, Ni and Co in Pacific pelagic sediments. *Chem. Geol.* **11,** 123–48.

Bostrom, K., M.N.A. Peterson, O. Joensuu & D.E. Fisher 1969. Aluminium-poor ferromanganoan sediments on active oceanic ridges. *J. Geophys. Res.* **74,** 3261–70.

Broecker, W.S. 1974. *Chemical oceanography.* New York: Harcourt Brace Jovanovich.

Chester, R. & S.R. Aston 1976. The geochemistry of deep-sea sediments. In *Chemical oceanography*, J.P. Riley & R. Chester (eds), Vol. 6, 281–390. London: Academic Press.

Chester, R. & M.J. Hughes 1967. A chemical technique for the separation of ferro-manganese minerals, carbonate minerals and adsorbed trace elements from pelagic sediments. *Chem. Geol.* **3,** 199–212.

Chester, R. & M.J. Hughes 1969. The trace element geochemistry of a North Pacific pelagic clay core. *Deep-Sea Res.* **13,** 627–34.

Chester, R. & R.G. Messiha-Hanna 1970. Trace element partition patterns in North Atlantic deep-sea sediments. *Geochim. Cosmochim. Acta* **34,** 1121–8.

Chester, R. & F.G. Voutsinou 1981. The initial assessment of trace metal pollution in coastal sediments. *Mar. Pollut. Bull.* **12,** 84–91.

Chester, R., A. Thomas, F.J. Lin, A.S. Basaham & G. Jacinto 1988. The solid state speciation of copper in surface water particulates and oceanic sediments. *Mar. Chem.* **24,** 261–92.

Chow, T.J., K.W. Bruland, K. Bertine, A. Soutar, M. Koide & E.D. Goldberg 1973. Lead pollution: records in Southern California coastal sediments. *Science* **181,** 551–2.

Collier, R. & J.M. Edmond 1984. The trace element geochemistry of marine biogenic particulate matter. *Prog. Oceanogr.* **13,** 113–99.

Cronan, D.S. 1972. The Mid-Atlantic Ridge near 45°N, XVII: Al, As, Hg and Mn in ferruginous sediments from the median valley. *Can. J. Earth Sci.* **9,** 319–23.

Cronan, D.S. 1973. Basal ferruginous sediments cored during Leg 16, Deep Sea Drilling Project. In *Initial reports of the Deep-Sea Drilling Project*, Vol. XVI, 601–4. Washington DC: US Govt Printing Office.

Cronan, D.S. 1976. Basal metalliferous sediments from the eastern Pacific. *Geol. Soc. Am. Bull.* **87,** 929–34.

Cronan, D.S. & D.E. Garrett 1973. Distribution of elements in metalliferous Pacific sediments collected during the Deep Sea Drilling Project. *Nature* **242,** 88–9.

Cronan, D.S., Tj. H. van Andel, G.R. Heath, M.G. Dinkleman, R.W. Bennet, D. Buckry, S. Charleston, A. Kanaps, K.S. Rodolfo & R.S. Yeats 1972. Iron-rich basal sediments from the eastern equatorial Pacific: Leg 16, Deep Sea Drilling Project. *Science* **175,** 61–3.

Dasch, E.J., J. Dymond & G.R. Heath 1971. Isotopic analysis of metalliferous sediments from the East Pacific Rise. *Earth Planet. Sci. Lett.* **13,** 175–80.

Davies, T.A. & D.S. Gorsline 1976. Oceanic sediments and sedimentary processes. In *Chemical oceanography*, J.P. Riley & R. Chester (eds), Vol. 5, 1–80. London: Academic Press.

Dymond, J. & H.H. Veeh 1975. Metal accumulation rates in the southeast Pacific and the origin of metalliferous sediments. *Earth Planet. Sci. Lett.* **28,** 13–22.

Dymond, J., J.B. Corless, G.R. Heath, C.W. Field, E.J. Dasch & H.H. Veeh 1973. Origin of metalliferous sediments from the Pacific Ocean. *Geol. Soc. Am. Bull.* **84,** 3355–72.

Elderfield, H. 1976. Manganese fluxes to the oceans. *Mar. Chem.* **4,** 103–32.

El Wakeel, S.K. & J.P. Riley 1961. Chemical and mineralogical studies of deep-sea sediments. *Geochim. Cosmochim. Acta* **25,** 110–46.

Froelich, P.N., M.L. Bender & G.R. Heath 1977. Phosphorus accumulation rates in metalliferous sediments on the East Pacific Rise. *Earth Planet. Sci. Lett.* **34,** 351–9.

Grousset, F.E. & R. Chesselet 1986. The Holocene sedimentary regime in the northern Mid-Atlantic Ridge region. *Earth Planet. Sci. Lett.* **78,** 271–87.

Heath, G.R. & J. Dymond 1977. Genesis and transformation of metalliferous sediments from the East Pacific Rise, Bauer Deep and Central Basin, northwest Nazca Plate. *Geol. Soc. Am. Bull.* **88,** 723–33.

Horder, M.F. & D.S. Cronan 1981. The geochemistry of some basal sediments from the western Indian Ocean. *Oceanol. Acta* **4,** 213–21.

Horowitz, A. 1974. The geochemistry of sediments from the northern Reykjanes Ridge and the Iceland–Faroes Ridge. *Mar. Geol.* **17,** 103–22.

Krishnaswami, S. 1976. Authigenic transition elements in Pacific pelagic clays. *Geochim. Cosmochim. Acta* **40,** 425–34.

Lalou, C. 1983. Genesis of ferromanganese deposits: hydrothermal origin. In *Hydrothermal processes at seafloor spreading centres,* P.A. Rona, K. Bostrom, L. Laubier & K.L. Smith (eds), 503–34. New York: Plenum.

Lapicque, G., H.D. Livingston, C.E. Lambert, E. Bard & L.D. Labeyrie 1987. Interpretation of $^{239, 240}$Pu in Atlantic sediments with a non-steady state input model. *Deep-Sea Res.* **34,** 1841–50.

Marchig, V. & H. Grundlach 1982. Iron-rich metalliferous sediments on the East Pacific Rise: prototype of undifferentiated metalliferous sediments on divergent plate boundaries. *Earth Planet. Sci. Lett.* **58,** 361–82.

Martin, J.M. & M. Whitfield 1983. The significance of the river input of chemical elements to the oceans. In *Trace metals in sea water*, C.S. Wong, E. Boyle, K.W. Bruland, J.D. Burton & E.D. Goldberg (eds), 256–96. New York: Plenum.

Murray, J. & A.F. Renard 1891. *Deep-sea deposits.* Sci. Rep. *Challenger* Exped., no. 3. London.

Patterson, C. 1987. Global pollution measured by lead in mid-ocean sediments. *Nature* **326,** 244.

Piper, D.Z. 1973. Origin of metalliferous sediments from the East Pacific Rise. *Earth Planet. Sci. Lett.* **19,** 75–82.

Preston, M.R. 1989. Marine pollution. In *Chemical oceanography*, J.P. Riley (ed.), Vol. 9, 53–196. London: Academic Press.

Revelle, R.R. 1944. Scientific results of the cruise VII of the 'Carnegie'. *Publ. Carnegie Inst.* **556,** 1–180.

Sawlan, J.J. & J.W. Murray 1983. Trace metal remobilization in the interstitial waters of red clay and hemipelagic marine sediments. *Earth Planet. Sci. Lett.* **64,** 213–30.

Sayles, F.L. & J.L. Bischoff 1973. Ferromanganoan sediments in the equatorial east Pacific. *Earth Planet. Sci. Lett.* **19,** 330–6.

Sayles, F.L., T.-L. Ku & P.C. Bowker 1975. Chemistry of ferromanganoan sediments of the Bauer deep. *Geol. Soc. Am. Bull.* **86,** 1423–31.

REFERENCES

Thomas, A.R. 1987. Glacial–interglacial variations in the geochemistry of North Atlantic deep-sea deposits. *Ph.D. Thesis*, University of Liverpool.

Thompson, J., M.S.N. Carpenter, S. Colley, T.R.S. Wilson, H. Elderfield & H. Kennedy 1984. Metal accumulation in northwest Atlantic pelagic sediments. *Geochim. Cosmochim. Acta* **48,** 1935–48.

Turekian, K.K. 1967. Estimates of the average Pacific deep-sea clay accumulation rate from material balance considerations. *Prog. Oceanogr.* **4,** 226–44.

Turekian, K.K. & J. Imbrie 1966. The distribution of trace elements in deep-sea sediments of the Atlantic Ocean. *Earth Planet. Sci. Lett.* **1,** 161–8.

Veron, A., C.E. Lambert, A. Isley, P. Linet & F. Grousset 1987. Evidence of recent lead population in deep north-east Atlantic sediments. *Nature* **326,** 278–81.

Von Damm, K.L., J.M. Edmond, B. Grant, C.J. Measures, B. Walden & R.F. Weiss 1985. Chemistry of submarine hydrothermal solutions at 21°N, East Pacific Rise. *Geochim. Cosmochim. Acta* **49,** 2197–220.

von der Borch, C.C. & R.W. Rex 1970. Amorphous iron oxide precipitates in sediments cored during Leg 5, Deep Sea Drilling Project. In *Initial Reports of the Deep Sea Drilling Project*, Vol. 5, 541–4. Washington DC: US Govt Printing Office.

Wedepohl, K.H. 1960. Spurenanalytische Untersuchungen an Tiefseetonen aus dem Atlantik. *Geochim. Cosmochim. Acta* **18,** 200–31.

Wedepohl, K.H. 1968. Chemical fractionation in the sedimentary environment. In *Origin and distribution of the elements*, L. H. Ahrens (ed.), 999–1016. Oxford: Pergamon.

PART IV

THE GLOBAL JOURNEY: SYNTHESIS

17 Marine geochemistry: an overview

The 'global journey', which traced material from its sources, through the ocean reservoir, and to the sediment sink, has now been completed. In the present chapter the various strands will be brought together in an overview of the present state of the art in marine geochemistry.

17.1 How the system works

The question that was posed in the Introduction was 'How do the oceans work as a chemical system?' The route that was selected in an attempt to answer this question involved: (a) identifying the pathways followed by the material that entered the ocean reservoir from both external and internal sources, and quantifying the magnitudes of the fluxes associated with them; (b) describing the physical, biological and chemical processes that occur within the water column, and relating them to the fluxes that carry material to the sediment (and rock) sink; and (c) outlining the various processes that interact to control the composition of the sediments themselves. There is a wide variety of inorganic and organic components in sea water, but it was pointed out in the Introduction that in order to follow the route outlined above particular attention would be paid to a selected number of process-orientated trace elements, which could be used as tracers to establish how the ocean works as a chemical system. In order to summarize these processes, attention will again largely be focused on these process-orientated trace elements.

Essentially, the ocean system consists of two layers of water: a thin, warm, less dense surface layer, which caps a more dense, thick, cold, deep water layer. The two layers are separated by the thermocline and pycnocline mixing barriers. The primary global-scale sources of material to the oceans are river run-off, atmospheric deposition and hydrothermal exhalations, all of which supply both dissolved and particulate material to the ocean system. The system is therefore dominated by the large fluxes of material that enter it, and it has become apparent that the key to understanding the driving force behind many of the processes that operate in the water column lies in the particulate $\leftrightarrow$ dissolved interactions which take place during the throughput of material from its sources to the sediment sink. During this source $\rightarrow$ sink journey the dissolved

constituents encounter regions of relatively high particle concentrations; e.g. in estuaries (especially those having a turbidity maximum) and river plumes, in the sea surface microlayer, under conditions of high primary production, in the regions of hydrothermal venting systems and in nepheloid layers generated by boundary currents at the western edges of the ocean basins. All these high-particle regions became zones of enhanced dissolved $\leftrightarrow$ particulate reactivity. In addition, there is a background microcosm of particles dispersed throughout all the water column. The overall effect is that the ocean may be considered to be a particle-dominated system, and the composition of the seawater phase is controlled to a large extent by the 'great particle conspiracy'. It is this conspiracy that is the key to Forchhammer's 'facility with which the elements in sea water are made insoluble'.

Once they have reached the seawater system the dissolved and particulate elements are subjected to a complex series of transport–removal processes. Non-reactive elements will tend to behave in a generally conservative manner. Their distributions will be controlled by physical processes, such as water mass mixing, and their residence times in the ocean will be relatively long. As the degree of reactivity of an element increases it becomes progressively influenced by biogeochemical processes, and begins to behave in a non-conservative manner. The degree of reactivity exhibited by an element in sea water therefore exerts a basic control on how it moves through the ocean system. River run-off and atmospheric deposition both deliver dissolved and particulate material to the surface ocean via exchange across the estuarine/sea and air/sea interfaces. This surface ocean is a zone of relatively high particle concentration, the externally delivered particles being swamped in most areas by internally produced biological particles. These large-sized, biologically produced aggregates, which consist of a significant fraction of faecal material, sink from the surface layer. At relatively shallow depths a large fraction of the aggregates, usually $> 90\%$, undergoes destruction. However, it is the fraction that escapes destruction and falls to the sea bed which drives the principal transport of material to the sediment surface via the **global carbon flux**. The total oceanic particle population therefore consists of a wide particle size spectrum. However, it is convenient to divide it into fine particulate matter (FPM), i.e. the suspended population, and coarse particulate matter (CPM), i.e. the sinking population. The production coupling between the populations involves a continuous series of aggregation–disaggregation processes, the end-point of which is to produce a fine particle population, and the down-column transport coupling between them involves a piggy-back type of reversible FPM association with the large, fast-sinking CPM aggregates. Both the FPM and CPM particulate populations take part in a series of complex biologically and chemically mediated reactions, both in the

surface waters and at depth in the water column. These particle-driven reactions are the principal control on the chemical composition of sea water, which is regulated by a balance between the rate of addition of dissolved component and its rate of removal via sinking particulate material to the sediment sink; however, it must be remembered that uptake into the rock sink is important in the marine budgets of some elements.

Many trace elements in sea water have an oceanic residence time that is relatively short compared to both the rate at which they have been added to sea water over geological time and the holding time of the oceans. The controls on the short residence times of these dissolved elements are imposed by uptake reactions with the oceanic particle population, and a number of process-orientated trace elements were used in the text as examples of reactive oceanic components in order to illustrate how this 'great particle conspiracy' operates. Although it is difficult to distinguish between biologically dominated and inorganically dominated controls on dissolved trace elements in the water column, two general particle-assocation removal routes were distinguished. Both of these routes are ultimately driven by the global carbon flux, either directly, with carbon-associated carriers (**nutrient-type** trace metal removal reactions), or indirectly, via a coupling between the small-sized inorganic (FPM) and the large-sized carbon particles (CPM) (**scavenging-type** removal reactions). Although some trace metals do in fact exhibit mixed removal processes, the distinction does underline a fundamental dichotomy in the oceanic behaviour of a number of trace metals.

(a) Scavenging-type trace metals, which show a surface enrichment–depth depletion profile, undergo reactions with the fine (FPM) fraction of oceanic TSM, and although these reactions often involve reversible equilibria, in which there is continuous exchange between the dissolved and particulate states, their residence times in the oceans tend to be relatively short, i.e. of the order of tens to a few hundreds of years. These trace metals reach the sediment surface in association with their inorganic host particles.

(b) Nutrient-type trace metals become involved in the major oceanic biogeochemical cycles and undergo a surface depletion–subsurface regeneration enrichment at depth in the water column. This recycling results in the nutrient-type elements having residence times that are relatively long compared both to those of the scavenging-type elements and to the oceanic mixing time. For example, Bruland (1980) set a lower limit residence time for the nutrient-type elements of $\sim$ 5000 yr. The nutrient elements are carried to the sediment reservoir in association with the carbon fraction of the large-sized (CPM) oceanic TSM population. The fate of these elements depends

on the diagenetic environment in the upper part of the sediment column. (i) Under oxic conditions the carriers are rapidly destroyed to release their associated elements at the sediment surface. (ii) Under sub-oxic conditions, however, the carriers can be buried to release their associated elements at depth into the interstitial waters.

In addition to particle reactivity, water transport acts as a control on the distributions of dissolved elements in the ocean system. This has different effects on the nutrient-type and the scavenging-type elements. The trace element particulate carriers sink to deep water where the nutrient-type elements are released back into solution, and this imposes a fundamental control on their oceanic distributions. The oceanic deep water 'grand tour' transports water from the main deep water sources in the Atlantic through the Indian Ocean and finally to the North Pacific. As a result, components such as the nutrients and the nutrient-type trace elements, which have a deep water recycling stage, build up in concentration in the deep waters of the Pacific relative to those of the Atlantic. In contrast, the scavenging-type elements will become enriched in the deep Atlantic relative to the deep Pacific. Thus, the differences between the scavenging-type and nutrient-type elements are reflected not only in the manner in which they are taken out of solution but also in their water column residence times. Elements are introduced into the oceans from both continental and oceanic crustal sources, but for most elements the continental source dominates. The **geochemical abundances** of the elements in the continental crust source material will therefore exert a fundamental control on their oceanic distributions. However, because they are removed relatively rapidly from the water column the scavenging-type elements tend to be fractionated from the nutrient-type elements. In this way, therefore, the concentration of a specific dissolved element in sea water will depend in part on its geochemical abundance in the crust, and in part on the efficiency with which it is removed to the solid phase, i.e. its **oceanic reactivity**.

The down-column transport of components from the surface ocean is dominated by the carbon flux, which varies in relation to the extent of primary production in the surface waters; thus, the strength of the flux is greatest under the regions of intense productivity, which are located mainly at the edges of the ocean basins. However, it must be remembered that a series of lateral mid-water and bottom fluxes can also transport material in the oceans. These are coupled to the vertical flux, so that the throughput of material to the sea bed involves a coupling between the vertical flux and a series of these lateral fluxes. It is the removal of dissolved components via the particulates transported by this flux combination that control the elemental composition of sea water by delivering material across the benthic boundary layer to the sediment sink

and so taking it out of the water column.

The composition of oceanic sediments is therefore determined by the nature of the components transported by the various down-column and lateral fluxes, and by the relative strengths of the individual fluxes themselves. The overall result of these various factors is to set up a sediment regime in which the following general trends can be identified.

(a) During descent down the water column a large fraction of the organic matter from the surface layer is destroyed in the upper waters, but that which reaches the sediment surface is related to production so that the most organic-rich deposits are found fringing the continents under the areas of intense production.
(b) The major sediment-forming biogenic components are opaline silica and carbonate shell material. There is a fundamental biogeographical dichotomy in the distribution of planktonic populations that is evidenced in a coastal high-fertility regime, which is characterized by silica-secreting diatoms, and an oceanic low-fertility regime, which is characterized by carbonate-secreting coccoliths. The extent to which sea water is undersaturated with respect to calcium carbonate increases with depth so that away from the coastal regime its preservation is mainly restricted to mid-ocean topographic highs located above the carbonate compensation depth. In contrast, sea water is everywhere undersaturated with respect to silica and siliceous shells cán only accumulate in those regions where the supply exceeds the rate of dissolution, i.e. under areas of high primary production at the ocean margins. The overall result of these dissolution processes is that siliceous deposits are generally found mainly at the edges of the oceans, whereas carbonates are concentrated in mid-ocean areas. Thus, dissolution constraints on the preservation of shell material lead to an enhancement of the biogeographical open ocean (carbonate)–coastal ocean (silica) dichotomy.
(c) In open-ocean areas below the carbonate compensation depth the sediments are dominated by inorganic components and deep-sea clays are formed, which may be either lithogenous or hydrogenous in character.

A series of chemical signals are transmitted through the ocean system, and these combine together to control the composition of the bottom sediments. The background transport of material to sediments operates on a global ocean scale, and the signals involved can be subdivided into biogenous, detrital and authigenic types. The authigenic signal is the primary background signal, which carries elements derived from solution in sea water to the sediment surface. For elements that have relatively

short residence times in sea water, the authigenic signal does not operate on a constant-flux basis. However, dissolved elements that have a longer residence time can have their concentrations smoothed out between the major oceans, and their deposition may approach a constant-flux model. As a result, because they are removed relatively rapidly from the water column the scavenging-type elements tend to be fractionated from the nutrient-type elements in the sediments as well as in the water column (see above). Thus, Mn (a scavenging-type element) has an oceanic reactivity pattern imposed on its removal into sediments, with the result that the magnitude of its authigenic flux appears to be directly related to that of its input flux; for example, authigenic Mn is accumulating faster in the Atlantic, which has stronger fluvial and atmospheric fluxes, than in the Pacific. In contrast, less reactive elements, such as the nutrient-type Ni and the mixed-type Cu, have generally similar authigenic fluxes in the two oceans, i.e. the geochemical abundance versus oceanic reactivity control. In addition to the background signals, more localized signals, such as those associated with hydrothermal activity and anthropogenic effects, can transport components to the sediment surface from the overlying sea water.

Even when the components are actually incorporated into the sediments they have not simply been locked away in a static reservoir, but have in fact entered a diagenetically active and biogeochemically dynamic environment. The diagenetic reactions are controlled by the manner in which the sedimentary environment attempts to destroy organic carbon; i.e. even the small fraction of organic matter that survives the journey down the water column is subjected to further degradation in the sediment reservoir. The intensity of diagenesis is controlled by the amount of organic carbon that reaches the sediment surface, and there is a redox-driven diagenetic sequence in the sediments, in which a variety of oxidants are switched on as the previous one is exhausted, in the general order: oxygen $>$ nitrate $\simeq$ manganese oxides $>$ iron oxides $>$ sulphate. The extent to which this sequence progresses depends on the amount of organic matter reaching the sediment surface, and since this is related to the extent or primary production in the surface waters (supply rate) and the rate at which the sediments accumulate (burial rate), this results in a lateral diagenetic sequence, in which the diagenetic intensity decreases in the order: nearshore $>$ hemi-pelagic $>$ pelagic sediments. Components released in the diagenetic reactions are transported through the sediment interstitial waters. Some of these components are trapped in the solid phases and so can impose the diagenetic spike on the sediments. However, others can escape back into sea water, thus providing a secondary, i.e. recycled, oceanic source. Thus, rather than acting as a static sink, sediments can recycle some elements, either (a) retaining but redistributing them in the sediment column, or (b) losing them back to

sea water. Despite these recycling processes, the sediment reservoir remains the ultimate sink for particulate material that flows through the ocean system, and so also acts as the major sink for particle-reactive elements that are removed from the dissolved phase.

It is apparent, therefore, that the major process that controls the dissolved element composition of sea water is a balance between the rates at which the elements are added to the system and the rates at which they are removed by the throughput of particulate material, which delivers them to the sediment sink. During their residence time in sea water, dissolved elements are transported by physical circulation, and undergo a series of biogeochemical reactions by which they are ultimately taken up by particulate matter, which is also transported by vertical and horizontal movements. Overall, therefore, it may be concluded that the oceanic chemical system is driven by a physical–chemical–biological process **trinity**. This process trinity operates on both the particulate and dissolved material introduced into the ocean reservoir and controls their passage through the system to the sediment sink. It also continues to influence the fate of the elements within the sediment sink itself; e.g. physical processes resuspend sediments into the water column, and biogeochemical processes are active in diagenesis.

17.2 Balancing the books

A **process-orientated** approach to marine geochemistry has been adopted in an attempt to elucidate the oceanic cycles of various constituents, and one possible way of answering the question 'To what extent have we understood how the oceans work as a chemical system?' is to establish accounting procedures that can be used to assess the quantitative aspect of the cycles, e.g. by attempting to construct mass balances for the system. A variety of physical and biogeochemical processes control both the removal of a dissolved element from sea water and its transfer to the deposition sink(s). Although these processes work differently for different elements, if the oceans are assumed to be in a steady state, then there should be a balance for any constituent between its *input* and its *output* rates, i.e. if sufficient data are available it should be possible to construct a mass balance for the constituent.

Various authors have attempted to produce mass balances for the dissolved constituents found in sea water. However, a few examples will serve to illustrate how the mass-balance approach has evolved in terms of recent advances in our understanding of how the ocean system works.

MAGNESIUM Magnesium is a major, salinity-contributing element in sea water, and it offers an excellent example of how modern research has led

to the filling of gaps in the calculation of marine mass balances. Drever (1974) addressed what he called the magnesium problem in sea water. This problem was identified as follows. Dissolved Mg is being brought to the oceans by rivers, and other sources, at a rate of $\sim 1.3 \times 10^{14}$ g yr^{-1}, and if it is assumed that the oceans are in a steady state then this should be balanced by the output. However, when Drever (1974) attempted to make a mass balance for Mg he found that the then known removal processes could only account for $\sim 50\%$ of the river input. Significantly, one of the reasons postulated to explain this Mg imbalance was that perhaps there was a Mg^{2+} removal process that had not yet been studied intensely. We now know that basalt–sea water reactions can act as a Mg^{2+} sink (see Ch. 5), and according to Thompson (1983) the total flux taken up by the basalt sink in the various kinds of rock–sea water reactions is $\sim 0.6 \times 10^{14}$ g yr^{-1}; this is $\sim 45\%$ of the river flux, and approaches the imbalance of $\sim 0.72 \times 10^{14}$ g yr^{-1} found by Drever (1974). The old and new Mg marine mass balances are given in Table 17.1.

Table 17.1 The marine budget of magnesium (units, 10^{14} g yr^{-1})

SUPPLY OF Mg^{2+}			
Rivers	1.3		
TOTAL	1.3		
REMOVAL OF Mg^{2+}			
1. Original budget [a]			% river flux
Carbonate formation		0.075	
Ion exchange		0.097	
Glauconite formation		0.039	
Mg - Fe exchange		0.29	
Burial of interstitial water		0.11	
SUB TOTAL		0.61	47
2. Modified budget			
Hydrothermal activity		0.60	
SUB TOTAL		0.60	46
TOTAL REMOVAL		1.21	93

[a] After Drever (1974).

URANIUM is a trace element that also had gaps in its marine balance until it was proposed that ~ 50% of its sea water input was taken up by low-temperature sea water–basalt reactions (see e.g. Bloch 1980).

For examples of how the marine mass balances of other trace elements have been sharpened by recent advances in our understanding of oceanic biogeochemical processes, we can return to the combined experimental–modelling approach adopted by Collier & Edmond (1984) (see Sec. 11.6.3.2) and select examples of a nutrient-type element and a mixed nutrient-type–scavenging-type element.

CADMIUM Cd is a nutrient-type trace element that has a shallow water

Table 17.2 Maring geochemical cycle of cadmium[a]

Primary input fluxes	
Rivers	0.002 nmol cm^{-2} yr^{-1}
Atmosphere	0.004 - 0.017 nmol cm^{-2} yr^{-1}
Distribution of dissolved Cd	
Surface ocean	0.01 pmol cm^{-3}
Deep ocean	0.9 pmol cm^{-3}
Box model for surface particulate flux	0.34 nmol cm^{-2} yr^{-1}
Organic carrier model for surface particulate flux	0.5 - 1.0 nmol cm^{-2} yr^{-1}
Sediment trap fluxes	
California Current	
35m	0.6 nmol cm^{-2} yr^{-1}
1500m	0.05 nmol cm^{-2} yr^{-1}
Advection - diffusion model for deep water Cd distribution	
Regeneration of	0.02 - 0.5 nmol cm^{-2} yr^{-1}
Sediment accumulation	
Eastern tropical Pacific	0.0006 nmol cm^{-2} yr^{-1}

[a] After Collier & Edmond (1984).

regeneration cycle. The marine biogeochemical cycle of Cd as outlined by Collier & Edmond (1984) is given in Table 17.2, and reveals that the cyclic component completely dominates the total particulate flux. Thus, the particulate flux leaving the surface water, as estimated from a box model, is ~ 38 ng cm^{-2} yr^{-1}, whereas that passing into sediment traps at 1500 m depth is only ~ 5.6 ng cm^{-2} yr^{-1}, i.e. ~ 15% of the out-of-surface flux. The sediment accumulation rate for Cd given in the model is ~ 0·07 ng cm^{-2} yr^{-1}; this is ≪ 1% of the down-column particulate flux, but is reasonably close to that of the primary river flux (~ 0.23 ng cm^{-2} yr^{-1}); i.e. the fluxes in the cycle are moving towards a balance. It may be concluded, therefore, that recent advances in our understanding of the marine chemistry of Cd have allowed the main features in its cycle to be identified. In general terms, Cd is brought to the ocean mainly via river

Table 17.3 Marine geochemical cycle of copper[a]

Primary input fluxes		
	Rivers	0.3 nmol cm^{-2} yr^{-1}
	Atmosphere	0.01 - 0.15 nmol cm^{-2} yr^{-1}
Distribution of dissolved Cu		
	Surface ocean	1 - 1.5 pmol cm^{-3}
	Deep ocean	4.0 pmol cm^{-3}
Box model for surface particulate flux		1.2 - 1.5 nmol cm^{-2} yr^{-1}
Organic carrier model for surface particulate flux		1.5 - 1.8 nmol cm^{-2} yr^{-1}
Sediment trap fluxes		
	Eastern Pacific through 500m	0.3 - 1.7 nmol cm^{-2} yr^{-1}
Scavenging fluxes from advection - diffusion models		0.3 - 1.7 nmol cm^{-2} yr^{-1}
Pore water fluxes		
	Eastern tropical Pacific	1 - 6 nmol cm^{-2} yr^{-1}

[a] After Collier & Edmond (1984).

and atmospheric inputs to the surface ocean. Here, the element becomes involved in the major oceanic biogeochemical cycle in which it has a shallow regeneration phase similar to those of phosphate and nitrate. Cadmium enters this cycle via a labile carrier and the regeneration–recycling leads to the element having an oceanic residence time of the order of several thousand years.

COPPER Cu has an oceanic distribution that shows both nutrient-type and scavenging-type characteristics, and because of the complexity of its distribution pattern Collier & Edmond (1984) pointed out that its oceanic cycle is difficult to describe in terms of a simple two-box model. However, Cu *is* involved in removal by a biogenic carrier in surface waters and the authors attempted to relate this particulate flux to the overall cycle of the element in the oceans. The details of their marine biogeochemical cycle for Cu are given in Table 17.3. The main difference between the cycles of Cu and Cd is that although Cu is removed in surface waters it also undergoes scavenging in deep water, and according to Collier & Edmond (1984) this leads to an additional down-column particulate flux ($\sim$ 64 ng cm^{-2} yr^{-1} – see Table 17.3), the actual amount being related to the magnitude of the flux of organic particles through the water column – see Section 16.5 and Figure 16.6b. In general terms, the particulate down-column flux of Cu (i.e. the surface flux + the deep water scavenging flux) is $\sim$ 160 ng cm^{-2} yr^{-1}. As for Cd, this is considerably in excess of the surface water primary input of Cu, which is $\sim$ 20 ng cm^{-2} yr^{-1} for the Pacific and $\sim$ 29 ng cm^{-2} yr^{-1} for the Atlantic. However, a major difference between the cycles of Cu and Cd is that the main regeneration of Cu takes place at or close to the sediment surface. According to the data for the Pacific given in Table 17.3, the magnitude of this out-of-sediment Cu flux is in the range $\sim$ 60–380 ng cm^{-2} yr^{-1}. Clearly, therefore, much of the down-column particulate Cu flux is regenerated in the upper sediment column and escapes back into sea water (see Sec. 14.6.2.2). Thus, the vertical profiles of Cu in the water column involve the removal of the dissolved element via biogenic carriers in the surface waters and by scavenging in deep waters, and the marine biogeochemical cycle of the element, like that of Cd, is dominated by a large recycling component; however, for Cu this occurs in the sediment. The cycling involved in the shallow water biogenic regeneration of Cd led to the element having a residence time in sea water that may be as high as several tens of thousands of years. However, the deep water scavenging pulls down the residence time of Cu to around 4000–5000 years (see Sec. 11.2). The primary input of Cu to the Atlantic is $\sim$ 29 ng cm^{-2} yr^{-1}, and the removal of dissolved Cu in an authigenic form to the sediment surface in this ocean ranges from $\sim$ 25 to $\sim$ 75 ng cm^{-2} yr^{-1} (see Table 16.5). However, the higher end of the range was found for the Bermuda Rise

under conditions of enhanced particle reactivity, and the value for the Nares Abyssal Plain is probably more representative of the Atlantic as a whole. Here the authigenic sediment flux of Cu was $\sim$ 27 ng cm^{-2} yr^{-1}; this is very close to the estimated primary input of Cu to the Atlantic ($\sim$ 29 ng cm^{-2} yr^{-1}), so that again the magnitudes of the input and output fluxes in the Cu cycle begin to balance out.

17.3 Conclusions

The last few decades have seen a quantum leap in our understanding of how the oceans work as a chemical system. This has come about by a combination of various factors, which include the following.

(a) The design of improved collection and analytical techniques, which have allowed many fundamental properties of the system to be measured with an accuracy that was not possible in the past.
(b) The implementation of large-scale oceanographic programmes such as GEOSECS, TTO, HEBBLE, GOFS, VERTEX, MANOP, DSDP and SEAREX, which have allowed the new data to be collected on a global ocean scale.
(c) Advances in understanding the basic biogeochemical processes that drive the ocean system. These include those associated with particle surface reactions, hydrothermal activity, primary production, nutrient dynamics, biological cycling, the air–sea exchange of both gases and aerosols and diagenetic processes in sediments, and have allowed the new data to be interpreted within a more rigorous theoretical framework.
(d) The use of tracers, especially the radionuclide 'time clocks', which has provided information on the rates at which the system operates. Information such as this has allowed many aspects of the system to be modelled.

As a result of these improvements, marine geochemists are now beginning to have at least a first-order understanding of many of the processes that drive the chemistry of the ocean system. The present volume has described the manner in which these processes operate within a global ocean source–sink framework. The next step will be an attempt to describe the chemistry of the ocean system both in terms of underlying theoretical concepts and in relation to global geochemistry. This is perhaps the most exciting stage in marine geochemistry, and it has already begun. For example, over the past few years Whitfield and coworkers have attempted to find a rationale for the composition of sea water which is based on fundamental chemical principles.

It was suggested in Section 16.5 that the concentration of an element in sea water is controlled by a combination of its input strengths (geochemical abundance) and its output strengths (oceanic reactivity). Many of the elements present in sea water have been released from crustal rocks, transported to the oceans, and then become incorporated into marine sediments. However, these sediments are eventualy recycled back to the continents during the processes of sea-floor spreading and mountain building; these processes are illustrated in Figure 17.1, in which the dynamic nature of the structural and spatial relationships between large-scale geological phenomena are shown. Because of these large-scale recycling processes Whitfield & Turner (1979) concluded that the same material has been cycled through the ocean system several times during the history of the Earth, and suggested that it should therefore be possible to use the partitioning of the elements between the ocean and the crustal rocks to gain an insight into the nature of sea water itself. The ocean system is assumed to be in a steady state, such that the rate of input of an element balances its rate of removal. The time an element resides in sea water can be expressed in terms of its mean oceanic residence time (MORT), $\bar{t}_Y$ (Sec. 11.2), which may be defined as

$$\bar{t}_Y = Y_S^0/\bar{J}_Y^0 \tag{17.1}$$

where Y_S^0 is the total mass of the element Y dissolved in the ocean reservoir and $\bar{J}_Y^0$ is the mean flux of Y through the reservoir in unit time. The superscript zero emphasizes that the values refer to a system in steady state. The MORT is a measure of the reactivity of an element in the ocean system. This is because elements that are highly reactive will have low MORT values and a rapid throughput, whereas those which are unreactive will have high MORT values and will tend to accumulate in the system. The MORT values are therefore essential parameters which describe the steady-state composition of sea water, and Whitfield (1979) has suggestd that Forchhammer's 'facility with which the elements in sea water are made insoluble' has found a quantitative expression in the MORT concept. Thus, a MORT value is a direct measure of the ease with which an element is removed to the sediment sink by incorporation into the solid phase. This affinity of an element for the solid phase can be described by a coefficient that expresses its partitioning between the water and rock phases (partitioning coefficient, K_Y), which is calculated as the ratio between the mean concentration of the element in natural water to that in crustal rock. Whitfield & Turner (1979) found a linear relationship between the sea water–crustal rock partition coefficient (log K_Y(SW)) and the MORT (log t_Y) values of elements (see Fig. 17.2a). It was therefore demonstrated that the MORT value of an element is directly related to its partitioning between the oceans and crustal rocks.

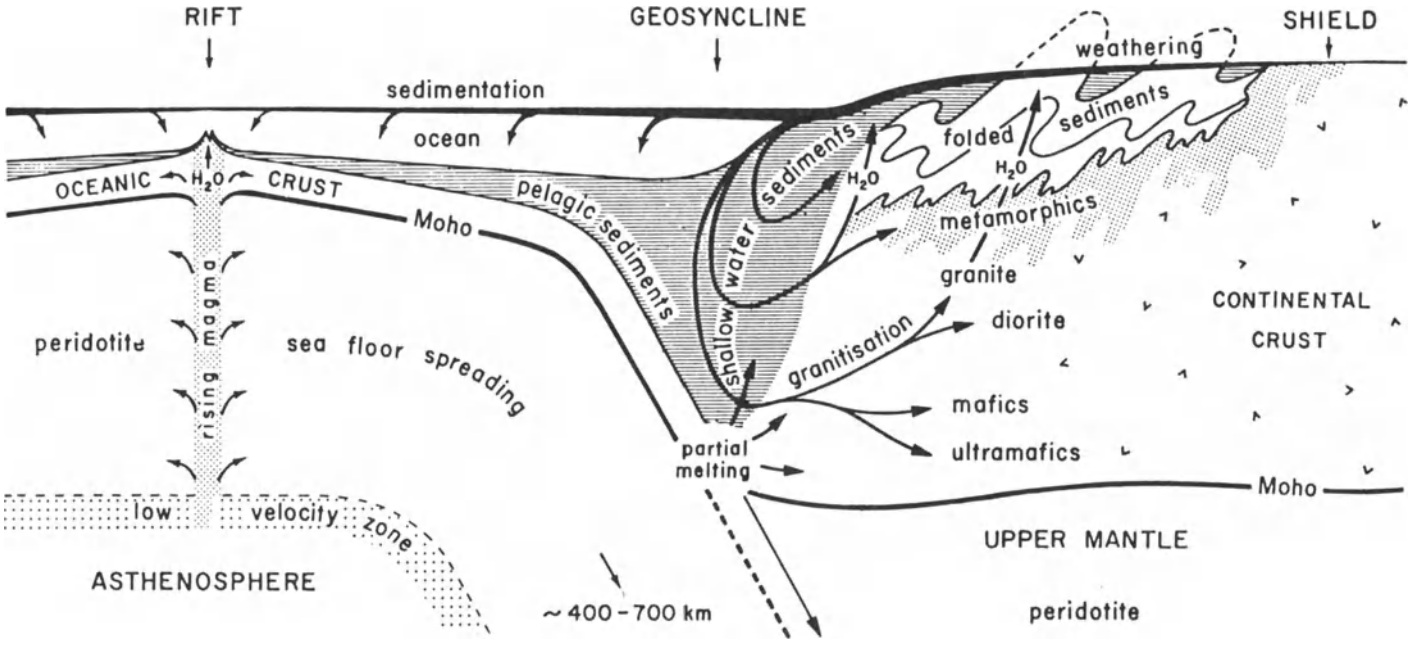

Figure 17.1 The recycling of oceanic sediments during the processes of sea-floor spreading and mountain building (from Degens & Mopper 1976).

Thus, a relationship was established between the reactivity of an element in the oceans (MORT) and its long-term recycling through the global reservoir system (K_Y).

Whitfield & Turner (1979) suggested that the partitioning of elements between solid and liquid phases in sea water (and river water) could be rationalized using a simple electrostatic model, in which the fundamental chemical control on the solid–liquid partitioning coefficients is related to the electronegativity of an element. This can be quantified by an electronegativity function (Q_{YO}), which is a measure of the attraction that an oxide-based mineral lattice will exert on the element. The authors then showed that the electronegativity function (Q_{YO}) of an element can be directly related to its partition coefficient (K_Y). The relationship between crustal rock–sea water partition coefficients and the electronegativity functions of the elements is illustrated in Figure 17.2b, from which it can be seen that the elements that are more strongly bound to the solid phase (high Q_{YO} values) have small partition coefficients (low K_Y values). It is apparent, therefore, that the manner in which an element is partitioned between crustal rock and sea water is dependent on the extent to which it is attracted to the oxide-based mineral lattice. The correlations between Q_{YO} and K_Y thus offer a theoretical explanation for variations in the partition coefficients of the elements, which is ultimately based on differences in their electronic structures, which themselves are a function of their atomic number and so their chemical periodicity. Whitfield & Turner (1983) drew attention to the fact that this chemical periodicity, which involves a link between electronic structure and chemical behaviour, provides a reationalization of the inorganic chemistry of all the elements. There is therefore a fundamental regularity in the organization of the elements which, as the authors pointed out, is sometimes forgotten when attempts are made to assess their behaviour in natural systems. For this reason, the correlation between the partition coefficients of the elements and their electronegativities represents an important step forward in our understanding of the chemistry of sea water. Further, the MORT–partition coefficient–electronegativity function relationships permit a number of the basic aspects of oceanic chemistry to be predicted on the basis of theoretical chemical concepts. For example, Whitfield (1979) derived a general equation relating to the MORT value and the electronegativity function of an element, and showed that MORT values derived from the electronegativity functions agreed with observed values within an order of magnitude; i.e. MORT values can be predicted reasonably well from a knowledge of the electrochemical properties of the elements. A second equation was proposed, which related the electronegativity function of an element to the global mean value of its river input, and this was used to estimate the composition of sea water. For most elements the estimated mean global composition of sea water

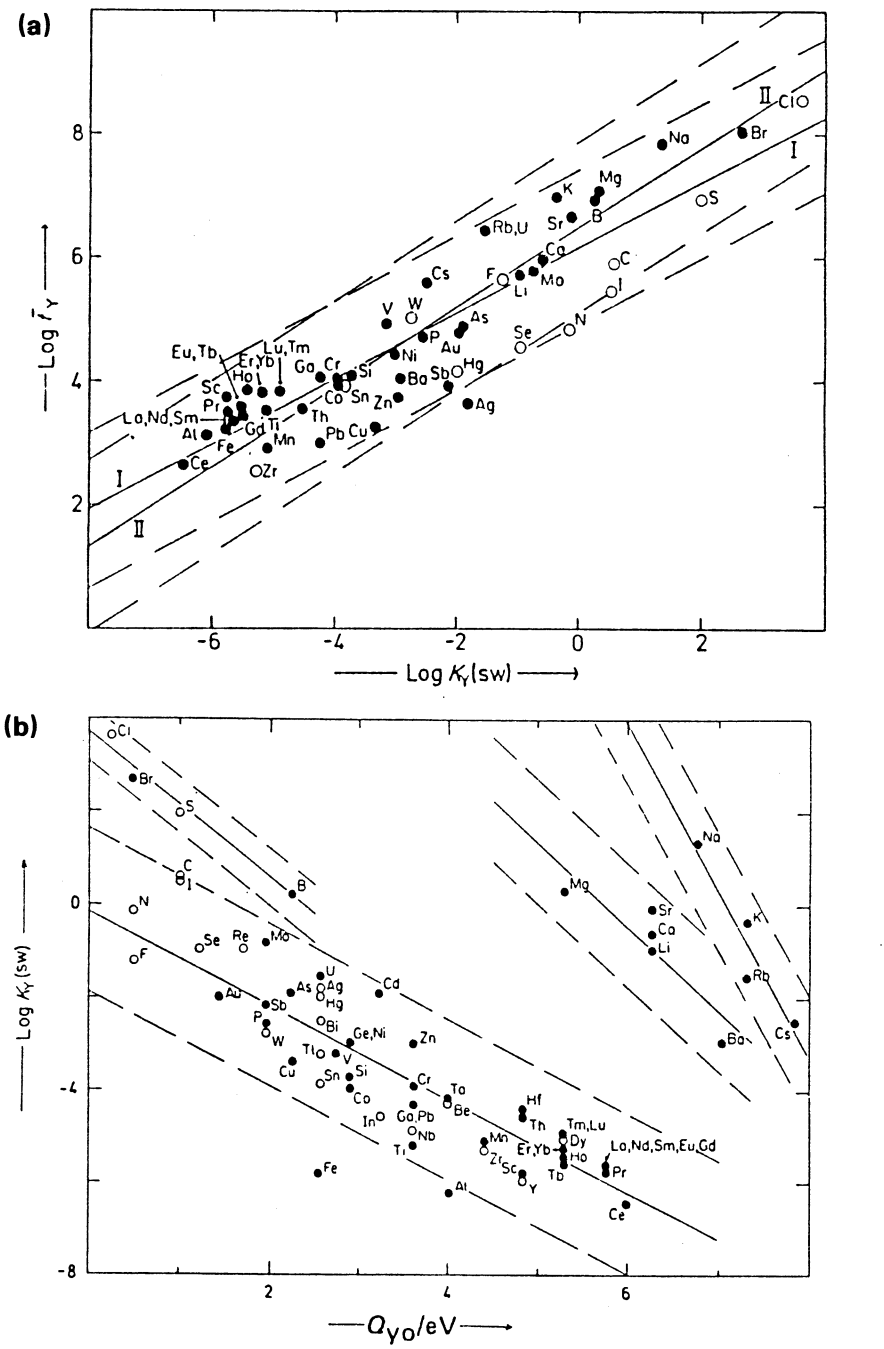

Figure 17.2 Relationships in the 'Whitfield ocean'. (**a**) The relationship between the mean oceanic residence the time (MORT, t_Y), and the sea water–crustal rock partition coefficient, K_Y(SW) (from Turner *et al.* 1980). (**b**) The relationship between the sea water–crustal rock partition coefficient, K_Y(SW), and the electronegativity function, Q_{YO} (from Turner *et al.* 1980).

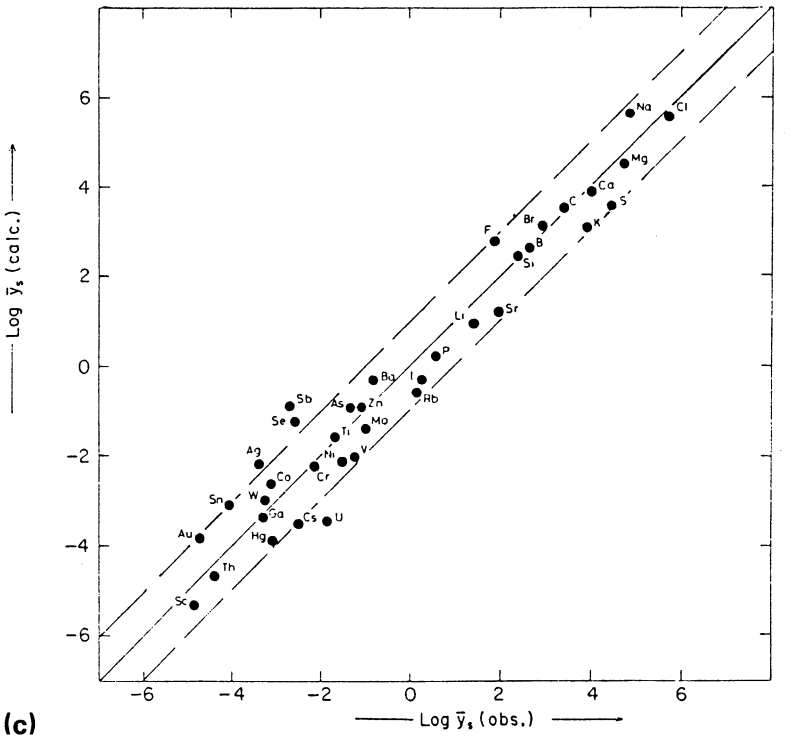

Figure 17.2c Comparison between the observed, Y_S(obs), and calculated, Y_S(calc), compositions of sea water (from Whitfield 1979).

again agreed with the observed values within an order of magnitude, even though the concentrations themselves range over 12 orders of magnitude; the predicted–observed seawater composition comparison is illustrated in Figure 17.2c.

The MORT–partition coefficient–electronegativity function relationships developed by Whitfield and coworkers therefore provide a series of theoretical chemical concepts which suggest that the overall composition of sea water is controlled by geological processes that are governed by relatively simple geochemical rules. As a result, the concentration of an element in sea water is controlled by its abundance in the crust (*geochemical abundance*) and by the ease with which it can be taken into solid sedimentary phases (*oceanic reactivity*). Thus, we now have a wider theoretical framework within which to interpret the factors that control the chemical composition of sea water.

To come full circle, therefore, it may be concluded that the overall *composition* of sea water is controlled by relatively simple geochemical rules. However, the *distribution* of the elements within sea water is

dependent on the physical–biological–chemical process trinity that drives the ocean system. The present volume has been concerned with the manner in which the processes involved in this process trinity operate on the throughput of material in the ocean system. The ultimate aim of marine geochemistry must be to produce a rationale for oceanic chemistry based on fundamental chemical principles, which can therefore provide a set of general rules enabling the concentrations and behaviours of elements in sea water to be described within a coherent pattern. It is apparent that such an approach is already gaining ground. The models produced will be refined in the future as marine geochemists struggle towards an explanation of Forchhammer's 'facility with which the elements in sea water are made insoluble'.

This future promises to be exciting.

References

Bloch, S. 1980. Some factors controlling the concentration of uranium in the World Ocean. *Geochim. Cosmochim. Acta* **44,** 373–7.

Bruland, K.W. 1980. Oceanographic distributions of cadmium, zinc, nickel and copper in the North Pacific. *Earth Planet. Sci. Lett.* **47,** 176–98.

Collier, R.W. & J.M. Edmond 1984. The trace element geochemistry of marine biogenic particulate matter. *Prog. Oceanogr.* **13,** 113–99.

Degens, E.T. & K. Mopper 1976. Factors controlling the distribution and early diagenesis of organic matter in marine sediments. In *Chemical oceanography*, J.P. Riley & R. Chester (eds), Vol. 5, 59–113. London: Academic Press.

Drever, J.I. 1974. The magnesium problem. In *The sea*, E.D. Goldberg (ed.), Vol. 5, 337–57. New York: Wiley.

Thompson, G. 1983. Hydrothermal fluxes in the ocean. In *Chemical oceanography*, J.P. Riley & R. Chester (eds), Vol. 8, 270–337. London: Academic Press.

Turner, D.R., A.G. Dickson & M. Whitfield 1980. Water–rock partition coefficients and the composition of natural waters: a reassessment. *Mar. Chem.* **9,** 211–18.

Whitfield, M. 1979. The mean oceanic residence time (MORT) concept – a rationalization. *Mar. Chem.* **8,** 101–23.

Whitfield, M. & D.R. Turner 1979. Water–rock partition coefficients and the composition of river and seawater. *Nature* **278,** 132–6.

Whitfield, M. & D.R. Turner 1983. Chemical periodicity and the speciation and cycling of the elements. In *Trace metals in sea water*, C.S. Wong, E. Boyle, K.W. Bruland, J.D. Burton & E.D. Goldberg (eds), 719–50. New York: Plenum.

Index

Explanatory note. Only the most important references are given for each subject. Chapter and Section numbers are given in bold type, figure numbers are given in italics.